

SEISMIC RETROFITTING MANUAL FOR HIGHWAY STRUCTURES: **PART 1-BRIDGES**

By

**Ian G. Buckle (Lead Author),
Ian Friedland, John Mander, Geoffrey Martin,
Richard Nutt and Maurice Power**

December 1, 2006 ■ MCEER-06-SP10





MCEER is a national center of excellence dedicated to establishing disaster-resilient communities through the application of multidisciplinary, multi-hazard research. Headquartered at the University at Buffalo, State University of New York, the Center was originally established by the National Science Foundation (NSF) in 1986, as the National Center for Earthquake Engineering Research (NCEER).

Comprising a consortium of researchers from numerous disciplines and institutions throughout the United States, the Center's mission has expanded from its original focus on earthquake engineering to address a variety of other hazards, both natural and man-made, and their impact on critical infrastructure and facilities. The Center's goal is to reduce losses through research and the application of advanced technologies that improve engineering, pre-event planning and post-event recovery strategies. Toward this end, the Center coordinates a nationwide program of multidisciplinary team research, education and outreach activities.

Funded principally by NSF, the State of New York and the Federal Highway Administration (FHWA), the Center derives additional support from the Department of Homeland Security (DHS)/Federal Emergency Management Agency (FEMA), other state governments, academic institutions, foreign governments and private industry.

This report was prepared by MCEER through a contract from the Federal Highway Administration. Neither MCEER, associates of MCEER, its sponsors, nor any person acting on their behalf makes any warranty, express or implied, with respect to the use of any information, apparatus, method, or process disclosed in this report or that such use may not infringe upon privately owned rights; or assumes any liabilities of whatsoever kind with respect to the use of, or the damage resulting from the use of, any information, apparatus, method, or process disclosed in this report.

The material herein is based upon work supported in whole or in part by the Federal Highway Administration, New York State and other sponsors. Opinions, findings, conclusions or recommendations expressed in this publication do not necessarily reflect the views of these sponsors or the Research Foundation of the State of New York.

Seismic Retrofitting Manual for Highway Structures: Part 1 - Bridges

by

Ian G. Buckle¹ (Lead Author), Ian Friedland², John Mander³,
Geoffrey Martin⁴, Richard Nutt⁵ and Maurice Power⁶

Publication Date: December 1, 2006

Technical Report MCEER-06-SP10

Task Number 106-G-2.2

FHWA Contract Number DTFH61-92-C-00106

Contract Officer's Technical Representatives: James Cooper, P.E. HRDI-03,
Wen-huei (Phillip) Yen, P.E., Ph.D., HRDI-07,
John O'Fallon, P.E. HRDI-07,
Federal Highway Administration

- 1 Center for Civil Engineering Earthquake Research, Department of Civil Engineering, University of Nevada-Reno
- 2 Federal Highway Administration; formerly Multidisciplinary Center for Earthquake Engineering Research, University at Buffalo, State University of New York
- 3 Department of Civil Engineering, University of Canterbury; formerly Department of Civil, Structural and Environmental Engineering, University at Buffalo, State University of New York
- 4 Department of Civil Engineering, University of Southern California
- 5 Structural Engineer Consultant, Orangevale, California
- 6 Geomatrix Consultants, Inc.

MCEER

University at Buffalo, The State University of New York
Red Jacket Quadrangle, Buffalo, NY 14261

Phone: (716) 645-3391; Fax (716) 645-3399

E-mail: mceer@buffalo.edu; WWW Site: <http://mceer.buffalo.edu>

PREFACE

This report is a major revision of the Federal Highway Administration publication ‘Seismic Retrofitting Manual for Highway Bridges,’ which was published ten years ago in 1995 as report FHWA/RD-94-052. This edition expands the coverage of the previous publication by including procedures for evaluating and retrofitting retaining structures, slopes, tunnels, culverts, and pavements, in addition to bridges. It is published in two parts as follows:

Part 1: Bridges

Part 2: Retaining Structures, Slopes, Tunnels, Culverts, and Pavements

Whereas Part 1 maintains the basic format of the retrofitting process described in the 1995 report, major changes have been made in this revision to include current advances in earthquake engineering, field experience with retrofitting highway bridges, and the performance of bridges in recent earthquakes in California and elsewhere. It is the result of several years of research with contributions from a multidisciplinary team of researchers and practitioners.

In particular, a performance-based retrofit philosophy is introduced similar to that used for the performance-based design of new buildings and bridges. Performance criteria are given for two earthquake ground motions with different return periods, 100 and 1000 years. A higher level of performance is required for the event with the shorter return period (the lower level earthquake ground motion) than for the longer return period (the upper level earthquake ground motion). Criteria are recommended according to bridge importance and anticipated service life, with more rigorous performance being required for important, relatively new bridges, and a lesser level for standard bridges nearing the end of their useful life.

Minimum recommendations are made for screening, evaluation and retrofitting according to an assigned Seismic Retrofit Category. Bridges in Category A need not be retrofitted whereas those in Category B may be assessed without a detailed evaluation, provided certain requirements are satisfied. Bridges in Categories C and D require more rigorous evaluation and retrofitting, as required. Various retrofit strategies are described and a range of related retrofit measures explained in detail, including restrainers, seat extensions, column jackets, footing overlays, and soil remediation.

This manual comprises 11 chapters and six appendices as follows:

Chapter 1 gives a complete overview of the retrofitting process including the philosophy of performance-based retrofitting, the characterization of the seismic and geotechnical hazards, the assignment of the Seismic Retrofit Category, and summaries of recommended screening methods, evaluation tools, and retrofit strategies. Topics in this chapter are described in greater detail in the following 10 chapters.

Chapters 2 and 3 describe the characterization of the seismic and geotechnical hazards.

Chapter 4 presents two screening and prioritization methods, with examples of each method.

Chapters 5, 6 and 7 describe six evaluation methods, of increasing rigor, for the detailed assessment of demand and capacity, using either a component-by-component approach, or a system approach for a complete bridge.

Chapters 8, 9, 10 and 11 describe retrofitting measures for bearings, seats, columns, piers, cap beams, column-to-cap joints, abutments, and foundations. Remedial techniques for hazardous sites are also addressed.

Appendices A through D provide supplementary material on conducting site-specific geotechnical investigations, the evaluation of geotechnical hazards, fragility curve theory, and the calculation of capacity/demand ratios for bridge components.

Appendices E and F present two examples illustrating the application of the component capacity/demand method (Method C) to multi-span concrete and steel highway bridges, respectively.

A glossary and lists of abbreviations, symbols, and references are also included.

It is noted that this manual was developed while the U.S. Department of Transportation was transitioning to metric units. As a consequence, example problems are presented in SI units. Future editions may however use Customary U.S. Units to reflect the current movement in many State DOTs back to customary units.

ACKNOWLEDGEMENTS

The authors are grateful for the financial support provided by the Federal Highway Administration (FHWA) during the preparation of this Manual. This assistance was provided through the Highway Project at the Multidisciplinary Center for Earthquake Engineering Research (formerly the National Center for Earthquake Engineering Research).

The authors also recognize the leadership taken by FHWA and other agencies, such as Caltrans, for the conduct of a comprehensive research and development program that has led to significant advances in the state-of-the-art of bridge retrofitting in the last decade. This Manual is based on many of the research findings and best practices developed during this time by these agencies.

Technical oversight by the FHWA Office of Infrastructure Research and Development was provided by James Cooper, John O'Fallon and Wen-huei Yen, who acted, at different times, as the Contracting Officer's Technical Representative. In addition, an external Highway Seismic Research Council (HSRC) provided critical advice and direction during the formative stages of the project. Members of the Council included Ralph Anderson, Roger Borchardt, James Gates, I.M. Idriss, Ayaz Malik, Jack Moehle, Joseph Nicoletti, Joanne Nigg, Joseph Penzien, James Roberts, Roland Sharpe, Arun Shirole, Carl Stepp and Bojidar Yanev.

Representatives from the four NEHRP Agencies (FEMA, NIST, NSF, and USGS) and the Transportation Research Board also served on this Council. The time and effort given by these experts to the success of the project is gratefully acknowledged.

The authors wish to recognize the valuable assistance given by MCEER staff and, in particular, the leadership of Center Director George Lee, the contributions of Senior Program Officers Michael Higgins and Jerry O'Connor, and the skill of Jane Stoyale and her staff editing and illustrating the Manual. The authors also recognize the technical assistance provided by Gokhan Pekcan in the early stages of the development of the Manual, and E.V. Leyendecker, formerly of the U.S. Geological Survey, for his review of the ground motion definitions presented in Chapter 2 and summarized in Chapter 1.

TABLE OF CONTENTS

	PAGE
CHAPTER 1: SEISMIC RETROFITTING OF HIGHWAY BRIDGES	1
1.1 General.....	1
1.2 Background.....	3
1.3 Philosophy.....	5
1.4 Seismic Performance Criteria	6
1.4.1 Performance Levels	6
1.4.2 Earthquake Ground Motion Levels.....	9
1.4.3 Bridge Importance	11
1.4.4 Anticipated Service Life	11
1.4.5 Selection of Performance Level.....	13
1.4.6 Retrofitting Process for Dual Level Ground Motions.....	13
1.4.7 Exempt Bridges.....	16
1.5 Seismic Hazard Level	16
1.5.1 Ground Motion Representation.....	16
1.5.2 Geotechnical Factors.....	17
1.5.2.1 Soil Amplification of Ground Motion	17
1.5.2.2 Geotechnical Hazards	17
1.5.3 Determination of Design Response Spectrum	20
1.5.4 Determination of Seismic Hazard Level.....	21
1.6 Performance-Based Seismic Retrofit Categories.....	21
1.7 Retrofitting Process for the Lower Level Ground Motion.....	23
1.7.1 Screening and Prioritization for the Lower Level Ground Motion.....	25
1.7.2 Evaluation for the Lower Level Ground Motion	25
1.7.3 Retrofitting for the Lower Level Ground Motion.....	26
1.8 Retrofitting Process for the Upper Level Ground Motion	26
1.9 Minimum Requirements for Upper Level Ground Motion.....	28
1.10 Screening and Prioritization for Upper Level Ground Motion.....	31
1.10.1 General.....	31
1.10.2 Factors to be Considered.....	32
1.10.3 Seismic Vulnerability Rating Methods	32
1.10.3.1 Minimum Screening Requirements	34
1.10.3.2 Seismic Inventory of Bridges.....	34
1.10.4 Indices Method.....	34
1.10.5 Expected Damage Method.....	37
1.11 Methods of Evaluation for Upper Level Ground Motion	38
1.12 Retrofit Strategies for Upper Level Ground Motion.....	42
1.12.1 General.....	42
1.12.2 Selecting a Retrofit Strategy	42
1.12.2.1 Objective of Retrofitting and Acceptable Damage.....	42
1.12.2.2 Cost Considerations of Seismic Retrofit.....	43
1.12.2.3 Other Considerations and Non-Seismic Issues	44

TABLE OF CONTENTS (Continued)

	PAGE
1.12.2.4 Identifying and Evaluating a Retrofit Strategy	45
1.12.2.5 Do-Nothing and Full-Replacement Options	47
1.12.3 Seismic Retrofit Approaches	47
1.12.3.1 Strengthening	48
1.12.3.2 Improvement of Displacement Capacity	48
1.12.3.3 Force Limitation.....	49
1.12.3.4 Response Modification	49
1.12.3.5 Site Remediation by Ground Improvement	50
1.12.3.6 Acceptance or Control of Damage to Specific Components	50
1.12.3.7 Partial Replacement	50
1.13 Retrofit Measures for Upper Level Ground Motion	51
1.13.1 General.....	51
1.13.2 Seismic Retrofit Matrix.....	52
 CHAPTER 2. SEISMIC GROUND MOTION HAZARD.....	 59
2.1 General.....	59
2.2 Basic Procedures for Characterizing Horizontal Seismic Ground Motion	63
2.3 Determination of Spectral Accelerations, S_s and S_1	63
2.3.1 USGS Probabilistic Ground Motion Maps	64
2.3.2 USGS Probabilistic Ground Motion Data Files from CD-ROM	68
2.4 Site Classes and Site Factors.....	77
2.4.1 Description of Site Classes and Site Factors.....	77
2.4.2 Considerations for Site Class F Soils.....	78
2.4.3 Effects of Site Class Variation Along a Bridge	83
2.4.4 Effect of Depth-of-Motion on Site Classification and Site Factors	83
2.5 Developing Horizontal Ground Motion Response Spectra Using National Ground Motion Maps and Site Factors	83
2.5.1 Two-Point Procedure for Constructing Response Spectra.....	83
2.5.2 Multi-Point Procedure of Response Spectrum Construction	85
2.5.3 Modification of Elastic Spectral Demand for Higher or Lower Damping	86
2.5.4 Obtaining Peak Ground Acceleration for Ground Failure Evaluations	88
2.6 Developing Site-Specific Response Spectra of Horizontal Ground Motions	88
2.7 Developing Vertical Ground Motion Response Spectra.....	91
2.8 Developing Acceleration Time Histories.....	92
2.8.1 General Requirements for Time Histories	92
2.8.2 Methods of Selecting and Developing Time Histories	94
2.8.3 Requirements for Compatibility of Time Histories with the Design Response Spectrum	96
2.8.4 Number of Time Histories	97
2.9 Spatial Variation of Ground Motions	98

TABLE OF CONTENTS (Continued)

	PAGE
CHAPTER 3. GEOTECHNICAL HAZARDS	99
3.1 General.....	99
3.2 Soil Liquefaction.....	99
3.2.1 Liquefaction Hazard Description.....	99
3.2.2 Initial Hazard Screening for Liquefaction	101
3.2.3 Earthquake Ground Motions for Liquefaction Analysis.....	104
3.2.4 Summary of Procedures for Detailed Liquefaction Evaluations	104
3.2.4.1 Evaluation of the Potential for Liquefaction Using Simplified Method	104
3.2.4.2 Numerical Modeling Methods and Laboratory Cyclic Testing for Evaluation of Potential for Liquefaction.....	105
3.2.4.3 Evaluation of the Potential for Liquefaction-Induced Flow Slides and Lateral Spreads.....	105
3.2.4.4 Other Evaluation Procedures	106
3.3 Soil Settlement.....	106
3.3.1 Settlement Hazard Description	106
3.3.2 Initial Hazard-Screening for Settlement	106
3.3.3 Summary of Procedures for Detailed Settlement Evaluations.....	107
3.4 Surface Fault Rupture	107
3.4.1 Surface Fault Rupture Hazard Description	107
3.4.2 Initial Hazard Screening for Surface Fault Rupture	107
3.4.3 Summary of Procedures for Detailed Surface Fault Rupture Evaluations	108
3.5 Flooding.....	108
3.5.1 Flooding Hazard Description.....	108
3.5.2 Initial Hazard Screening for Flooding	109
3.5.3 Summary of Detailed Evaluations for Flooding.....	109
CHAPTER 4. SEISMIC RATING METHODS FOR SCREENING AND PRIORITIZATION	111
4.1 General.....	111
4.2 Seismic Rating Method Using Indices.....	111
4.2.1 Calculation of Bridge Rank	113
4.2.1.1 Vulnerability Rating (V).....	113
4.2.1.1(a) Vulnerability Rating for Connections, Bearings, and Seat Widths, V_1	114
4.2.1.1(b) Vulnerability Rating for Columns, Abutments, and Liquefaction Potential, V_2	118
4.2.1.2 Seismic Hazard Rating (E).....	126
4.2.1.3 Examples.....	126
4.2.2 Calculation of Priority Index Based on Indices	126

TABLE OF CONTENTS (Continued)

	PAGE
4.3 Seismic Rating Method Using Expected Damage	127
4.3.1 Background	127
4.3.2 Database Requirements	133
4.3.3 Fragility Curves for Reference Bridges	133
4.3.4 Scaling Reference Bridge Fragility Curves to Account for Skew and Three-Dimensional Effects	135
4.3.4.1 Definition of Parameters: K_{skew} and K_{3D}	135
4.3.4.2 Scaling Relations for Damage States 3, 4, and 5	135
4.3.4.3 Scaling Relations for Damage State 2 (Slight Damage)	138
4.3.5 Economic Losses	139
4.3.5.1 Total Economic Losses	139
4.3.5.2 Direct Economic Losses	139
4.3.5.3 Indirect Economic Losses	141
4.3.5.4 Examples	141
4.3.6 Calculation of Bridge Rank Based on Expected Damage	142
4.3.7 Calculation of Priority Index Based on Expected Damage	142
 CHAPTER 5. EVALUATION METHODS FOR EXISTING BRIDGES	 147
5.1 General	147
5.1.1 Summary of Evaluation Methods	147
5.1.2 Demand Analyses	149
5.2 Method A: Connection Details and Seat Width Checks Only	150
5.2.1 Method A1	150
5.2.2 Method A2	151
5.3 Method B: Component Capacity Checks	152
5.3.1 Procedure for Method B	152
5.3.2 Restrictions on Use of Method B	153
5.4 Method C: Component Capacity/Demand Method	154
5.4.1 Approach	154
5.4.2 Selection of Elastic Analysis Method	157
5.4.2.1 Uniform Load Method	157
5.4.2.2 Multi-Mode Spectral Analysis Method	159
5.4.2.3 Elastic Time History Method	160
5.4.3 Procedure for Method C	160
5.4.4 Restrictions on Use of Method C	161
5.4.5 Examples	161
5.5 Method D1: Structure Capacity/Demand Method	161
5.5.1 Approach	161
5.5.2 Bridge Capacity	162
5.5.2.1 General	162
5.5.2.2 Calculation of Bridge Capacity Curve	163

TABLE OF CONTENTS (Continued)

	PAGE
5.5.3. Earthquake Demand.....	166
5.5.4. Capacity/Demand Spectrum	168
5.5.4.1 Calculation of Bridge Capacity/Demand (C/D) Ratios	168
5.5.4.2 Calculation of Bridge Response.....	170
5.5.5. Procedure for Method D1	171
5.5.6. Restrictions on Use of Method D1.....	174
5.6. Method D2: Structure Capacity/Demand (Pushover) Method.....	175
5.6.1 Approach.....	175
5.6.2 Displacement Capacity Evaluation	175
5.6.3 Demands	176
5.6.4 Procedure for Method D2	176
5.6.5 Restrictions on Method D2	177
5.7. Method E: Nonlinear Dynamic Procedure.....	177
5.7.1 Approach.....	177
5.7.2 Procedure for Method E.....	178
5.7.3 Restrictions on Method E.....	178
 CHAPTER 6. GEOTECHNICAL MODELING AND CAPACITY ASSESSMENT	179
6.1. General.....	179
6.2. Foundation Modeling.....	179
6.2.1 Soil-Foundation-Structure Interaction	179
6.2.1.1 Shallow Footings	180
6.2.1.2 Piles.....	181
6.2.2 Stiffness and Capacity of Foundation Components.....	182
6.2.2.1 Shallow Bearing Footing Foundations.....	183
6.2.2.1(a) Stiffness Parameters.....	184
6.2.2.1(b) Capacity Parameters.....	185
6.2.2.2 Pile Footing Foundations	191
6.2.2.2(a) Pile Cap – Lateral Stiffness and Capacity.....	191
6.2.2.2(b) Pile-Head Stiffness – Lateral Loading.....	191
6.2.2.2(c) Pile-Head Stiffness – Axial Loading	203
6.2.2.2(d) Pile Group Analysis	205
6.2.2.2(e) Pile Group Analyses – Moment-Rotation Capacity.....	206
6.2.2.3 Drilled Shafts	209
6.2.2.4 Abutments	211
6.2.2.4(a) Abutment Capacity – Longitudinal Direction.....	211
6.2.2.4(b) Calculation of Best-Estimate Passive Force, P_p	214
6.2.2.4(c) Abutment Stiffness – Longitudinal Direction.....	214
6.3. Ground Displacement Demands on Foundations	217
6.3.1 Sources of Demand.....	217
6.3.1.1 Earthquake-Induced Settlement	217

TABLE OF CONTENTS (Continued)

	PAGE
6.3.1.2 Liquefaction-Induced Lateral Spreads	217
6.3.1.3 Slope Stability	220
CHAPTER 7. STRUCTURAL MODELING AND CAPACITY ASSESSMENT	221
7.1 General	221
7.2 Load Path for Lateral Forces	221
7.3 Modeling Recommendations for Bridge Structures	224
7.3.1 Distribution of Mass	225
7.3.2 Distribution of Stiffness and Strength	225
7.3.2.1 Substructures	226
7.3.2.2 Superstructures	227
7.3.3 In-Span Hinges	228
7.3.4 Damping	228
7.3.5 Permanent Ground Movement	229
7.4 Combination of Seismic Force Effects	229
7.4.1 Seismic Loading in One Direction	229
7.4.2 Seismic Loading in Two or Three Orthogonal Directions	230
7.4.3 Combination of Response Quantities for Biaxial Design	231
7.4.4 Vertical Acceleration Effects	232
7.5 Member Strengths	233
7.6 Member Actions in Piers Using Capacity Principles	234
7.6.1 Single Column Piers	234
7.6.2 Multi-Column Piers	235
7.7 Strength Capacity of Bridge Members	236
7.7.1 Flexural Strength of Reinforced Concrete Columns and Beams	237
7.7.1.1 Expected Flexural Strength	237
7.7.1.2 Flexural Overstrength Capacity	238
7.7.1.3 Flexural Strength of Columns with Lap-Splices in Plastic Hinge Zones	241
7.7.2 Shear Strength of Reinforced Concrete Columns and Beams	242
7.7.2.1 Initial Shear Strength, V_i	242
7.7.2.2 Final Shear Strength, V_f	243
7.7.3 Shear Strength of Beam-Column Joints	244
7.7.3.1 Maximum Beam-Column Joint Strength, V_{ji}	244
7.7.3.2 Cracked Beam-Column Joint Strength, V_{jf}	244
7.8 Deformation Capacity of Bridge Members	245
7.8.1 Plastic Curvatures and Hinge Rotations in a Cantilever Beam	245
7.8.1.1 Deflections and Plastic Curvature, ϕ_p	245
7.8.1.2 Plastic Hinge Rotation, θ_p	247

TABLE OF CONTENTS (Continued)

	PAGE
7.8.2 Characterization of Deformation-Based Limit States.....	247
7.8.2.1 Compression Failure of Unconfined Concrete	249
7.8.2.2 Compression Failure of Confined Concrete	249
7.8.2.3 Buckling of Longitudinal Bars.....	250
7.8.2.4 Fracture of the Longitudinal Reinforcement.....	250
7.8.2.5 Low Cycle Fatigue of Longitudinal Reinforcement	250
7.8.2.6 Failure in the Lap-splice Zone	251
7.8.2.6(a) ‘Long’ or Confined Lap-splice, $l_{lap} > l_s$	251
7.8.2.6(b) ‘Short’ and Unconfined Lap-splice, $l_{lap} \leq l_s$	252
7.8.2.7 Shear Failure	252
7.8.2.7(a) Brittle Shear, $V_i \leq V_m$	253
7.8.2.7(b) Semi-ductile Shear, $V_f < V_m < V_i$	253
7.8.2.8 Joint or Connection Failure.....	253
7.8.2.8(a) Weak Joint and Strong Column, $V_{ji} \leq V_{jh}$	254
7.8.2.8(b) Semi-ductile Shear, $V_{jf} < V_{jh} < V_{ji}$	254
7.8.3 Neutral Axis Depth in Columns and Beams	254
 CHAPTER 8. RETROFIT MEASURES FOR SUPERSTRUCTURES, BEARINGS, AND SEATS	 257
8.1 General.....	257
8.2 Bridge Decks and Girders	257
8.2.1 Lateral Load Path Enhancement	257
8.2.1.1 Strengthening of Deck to Girder Connection	257
8.2.1.2 Diaphragm Strengthening or Stiffening.....	258
8.2.1.3 Energy Dissipating Ductile Diaphragms	259
8.2.1.4 Girder Strengthening.....	263
8.2.2 Providing Longitudinal Continuity	264
8.2.2.1 Web and Flange Plates.....	264
8.2.2.2 Superstructure Joint Strengthening.....	265
8.2.3 Reduction of Dead Load	267
8.2.4 Strengthening of Continuous Superstructures	267
8.3 Bearings, Anchorages and Pedestals.....	268
8.3.1 Strengthening of Existing Bearings	270
8.3.1.1 Expansion Bearings	270
8.3.1.1(a) Sole Plate to Girder.....	270
8.3.1.1(b) Bearing to Masonry Plate.....	271
8.3.1.1(c) Masonry Plate to Substructure.....	275
8.3.1.2 Fixed Bearings	276
8.3.1.2(a) Sole Plate to Girder.....	276

TABLE OF CONTENTS (Continued)

	PAGE
8.3.1.2(b) Masonry Plate to Substructure	276
8.3.2 Bearing Replacement	276
8.3.2.1 Conventional Bearings	276
8.3.2.2 Replacement with Seismic Isolation Bearings	281
8.3.3 Strengthening of Superstructure to Substructure Connections	285
8.4 Expansion Joint Retrofit	286
8.4.1 Bearing Seat Extensions	286
8.4.1.1 Concrete Seat Extensions and Catcher Blocks	286
8.4.1.2 Pipe Extenders	290
8.4.2 Restrainers	291
8.4.2.1 Longitudinal Joint Restrainers	292
8.4.2.1(a) Restrainer Cables	293
8.4.2.1(b) High Strength Bar Restrainers	295
8.4.2.1(c) Bumper Blocks	298
8.4.2.1(d) Anchorage of Restrainers	299
8.4.2.1(e) Design and Construction Issues	299
8.4.2.1(f) Evaluation of the Need for Restrainers for Simply Supported Spans	306
8.4.2.1(g) Restrainer Design Methods	310
8.4.2.2 Transverse Restrainers	316
8.4.2.2(a) General	316
8.4.2.2(b) Shear Keys	316
8.4.2.2(c) Keeper Brackets	317
8.4.2.2(d) Steel Pipe Restrainers	317
8.4.2.2(e) Design Forces	332
8.4.2.3 Vertical Motion Restrainers	332
8.4.3 Energy Dissipation Devices	333
8.4.4 Shock Transmission Units	333

CHAPTER 9. RETROFIT MEASURES FOR SUBSTRUCTURE COMPONENTS 337

9.1 General	337
9.2 Retrofit Measures for Piers	338
9.2.1 Reinforced Concrete Columns	339
9.2.1.1 Column Replacement	339
9.2.1.1(a) Total Replacement	340
9.2.1.1(b) Partial Column Replacement	340
9.2.1.1(c) Supplemental Columns	345
9.2.1.2 Column Flexural Strengthening	347
9.2.1.2(a) Concrete Overlays	347
9.2.1.2(b) Added Reinforcement in Conjunction with Steel Shell	348

TABLE OF CONTENTS (Continued)

	PAGE
9.2.1.2(c) Composite Steel Shell	348
9.2.1.3 Column Ductility Improvement and Shear Strengthening	352
9.2.1.3(a) Steel Jacketing	353
9.2.1.3(b) Fiber Composite Jacketing.....	364
9.2.1.3(c) External Prestressing Steel.....	371
9.2.1.3(d) Concrete Jacketing.....	375
9.2.1.4 Supplemental Column Shear Walls	378
9.2.1.5 Preservation of the Vertical Load Capacity of Columns	379
9.2.1.6 Limitation of Column Forces.....	380
9.2.1.6(a) Isolation Bearings	380
9.2.1.6(b) Flexural Strength Reduction	381
9.2.2 Steel Columns, Frames and Compression Members	382
9.2.2.1 Braced Frames	382
9.2.2.2 Built-up Compression Members.....	383
9.2.3 Concrete Wall Piers	387
9.3 Retrofit Measures for Cap Beams and Column-to-Cap Beam Joints	388
9.3.1 Pier Cap Replacement.....	390
9.3.1.1 Partial Replacement at a Joint.....	390
9.3.1.2 Total Replacement	390
9.3.2 Pier Cap Strengthening	390
9.3.3 Reduction of Pier Cap Forces	394
9.3.4 Strengthening of Column and Beam Joints	395
9.3.5 Supergirders	397
 CHAPTER 10. RETROFIT MEASURES FOR ABUTMENTS, FOOTINGS, AND FOUNDATIONS	 401
10.1 General.....	401
10.2 Retrofit Measures for Abutments.....	401
10.2.1 Approach Slabs	403
10.2.2 Anchor Slabs	405
10.2.3 Diaphragm Walls	408
10.2.4 Transverse Abutment Shear Keys.....	408
10.2.5 Transverse Abutment Anchors	408
10.2.5.1 Soil Shear Keys.....	409
10.2.5.2 Wingwall Strengthening	411
10.2.5.3 Cast-in-Drilled Hole Piles.....	414
10.2.6 Soil and Gravity Anchors.....	414
10.3 Retrofit Measures for Footings	418
10.3.1 Footing Replacement	418
10.3.2 Strengthening of Footings.....	418
10.3.3 Retrofit Design of Footings	420

TABLE OF CONTENTS (Continued)

	PAGE
10.3.4 Limiting Forces Transmitted to the Footings.....	433
10.4 Retrofit Measures for Piles and Pile-to-Footing Connections	433
10.4.1 Pile Type Considerations (New Piles)	435
10.4.2 Pile Tie-Downs	435
 CHAPTER 11. RETROFIT MEASURES FOR BRIDGES ON HAZARDOUS SITES	 437
11.1 General.....	437
11.2 Bridges Across or Near Active Faults	437
11.3 Bridges on or Near Unstable Slopes	438
11.4 Bridges on Liquefiable Soils.....	438
11.4.1 Structural Retrofitting of Piled Foundations.....	440
11.4.1.1 Simplified Analysis.....	443
11.4.2 Site Remediation using Ground Improvement	448
11.4.3 Superstructure Improvements	450
 APPENDIX A. GUIDELINES FOR CONDUCTING SITE-SPECIFIC GEOTECHNICAL INVESTIGATIONS AND DYNAMIC SITE RESPONSE ANALYSES.....	 453
A.1 Site-Specific Geotechnical Investigation.....	453
A.2 Dynamic Site Response Analysis	453
A.2.1 Modeling the Soil Profile.....	453
A.2.2 Selecting Input Rock Motion.....	454
A.2.3 Site Response Analysis and Results Interpretation.....	454
 APPENDIX B. EVALUATION OF GEOTECHNICAL HAZARDS.....	 455
B.1 General.....	455
B.2 Evaluation of Soil Liquefaction Hazard	455
B.2.1 Field Exploration for Liquefaction Hazard Assessment.....	455
B.2.1.1 Location of Liquefiable Soils	455
B.2.1.2 Location of Groundwater Level.....	456
B.2.1.3 Depth of Liquefaction.....	456
B.2.1.4 Field Exploration Methods	457
B.2.1.4(a) SPT Method	457
B.2.1.4(b) CPT Method.....	457
B.2.2 Evaluation of Liquefaction Potential	458
B.2.2.1 Simplified Procedure	459
B.2.2.1(a) Cyclic Resistance Ratio, CRR	459
B.2.2.1(b) Cyclic Stress Ratio, CSR	462
B.2.2.1(c) Liquefaction Potential.....	463
B.2.2.2 Numerical Modeling Methods	463

TABLE OF CONTENTS (Continued)

	PAGE
B.2.3 Liquefaction Hazards Assessment	464
B.2.3.1 Flow Failures	465
B.2.3.2 Lateral Spreading	467
B.2.3.2.1 Youd et al. Emprical Approach	468
B.2.3.2.2 Newmark Time History Analyses	468
B.2.3.2.3 Simplified Newmark Charts	469
B.2.3.2.4 Numerical Modeling	471
B.3 Evaluation of Soil Settlement Hazard	471
B.4 Evaluation of Surface Fault Rupture Hazard	474
B.4.1 Fault Location	476
B.4.1.1 Interpretation of Aerial Photographs	476
B.4.1.2 Contacting Knowledgeable Geologists	476
B.4.1.3 Ground Reconnaissance of Site and Vicinity	476
B.4.1.4 Surface Exploration	476
B.4.2 Fault Activity	477
B.4.2.1 Assess Fault Relationship to Young Deposits/Surfaces	477
B.4.2.2 Evaluate Local Seismicity	477
B.4.2.3 Evaluate Structural Relationships	477
B.4.3 Fault Rupture Characteristics	477
B.5 Evaluation of Flooding Hazard	479
 APPENDIX C. FRAGILITY CURVE THEORY	 481
 APPENDIX D. CAPACITY/DEMAND RATIOS FOR BRIDGE MEMBERS AND COMPONENTS	 485
D.1 General	485
D.2 Minimum Bearing or Restrainer Force Demands	485
D.3 Minimum Support Lengths	486
D.4 Capacity/Demand Ratios for Expansion Joints and Bearings	488
D.4.1 General	488
D.4.2 Displacement Capacity/Demand Ratios	490
D.4.3 Force Capacity/Demand Ratios	491
D.5 Capacity/Demand Ratios for Reinforced Concrete Columns, Walls and Footings	491
D.5.1 Anchorage of Longitudinal Reinforcement	496
D.5.2 Splices in Longitudinal Reinforcement	501
D.5.3 Column Shear	505
D.5.4 Transverse Confinement Reinforcement	511
D.5.5 Footing Rotation and/or Yielding	513
D.6 Capacity/Demand Ratios for Abutments	517
D.7 Capacity/Demand Ratios for Liquefaction Induced Foundation Failure	518
D.8 Summary	519

TABLE OF CONTENTS (Continued)

	PAGE
APPENDIX E. EXAMPLE PROBLEM 5.1: COMPONENT CAPACITY/DEMAND EVALUATION OF A 4-SPAN, REINFORCED CONCRETE BOX GIRDER BRIDGE	521
E.1 Introduction.....	521
E.2 Description of the Example Bridge.....	521
E.3 Seismic Rating	521
E.3.1 Vulnerability Rating, V.....	524
E.3.2 Seismic Hazard Rating, E	526
E.3.3 Bridge Rank, R.....	526
E.3.4 Priority Index	526
E.4 Detailed Evaluation.....	527
E.4.1 Capacity/Demand Ratios – Existing Bridge	527
E.4.2 Identification and Assessment of Potential Retrofit Measures	548
 APPENDIX F. EXAMPLE PROBLEM 5.2: COMPONENT CAPACITY/DEMAND EVALUATION OF A MULTISPAN SIMPLY-SUPPORTED STEEL GIRDER BRIDGE	 557
F.1 Introduction.....	557
F.2 Description of the Example Bridge.....	557
F.3 Bridge Evaluation	559
F.3.1 Seismic Retrofit Categories	559
F.3.2 Components for Capacity/Demand Ratio Evaluation.....	559
F.3.3 Analysis Procedure	559
F.3.4 Uniform Load Method for Case 2.....	560
F.3.4.1 Structural Data – Pier 2.....	560
F.3.4.2 Longitudinal Earthquake Loading	560
F.3.4.3 Transverse Earthquake Loading	561
F.4 Capacity/Demand Ratio for Bearings for Case 1.....	561
F.4.1 Displacement Capacity/Demand Ratio (Case 1).....	561
F.4.2 Force Capacity/Demand Ratio (Case 1)	562
F.5 Potential for Liquefaction in Case 1	562
F.6 Capacity/Demand Ratio for Bearings for Case 2.....	562
F.4.6.1 Displacement Capacity/Demand Ratio (Case 2).....	563
F.4.6.2 Force Capacity/Demand Ratio (Case 2)	564
F.7 Capacity/Demand Ratios for Pier 2 for Case 2.....	564
F.8 Potential for Liquefaction in Case 2	567
 GLOSSARY	 577
 REFERENCES	 583

LIST OF FIGURES

FIGURE	PAGE
1-1 Overview of the retrofitting process for highway bridges	2
1-2 Collapse of the link span at Tower E9 of the San Francisco Oakland Bay bridge due to inadequate seat lengths and anchor bolts	8
1-3 Collapse of the two-level Cypress Viaduct on I-880 in Oakland due to brittle shear failure at the connection between the upper and lower levels of the viaduct	8
1-4 Collapse of end spans in the Shi Wei bridge in Taichung, due to ground failure and nearby fault rupture	8
1-5 Diagonal shear crack in lightly reinforced concrete pier of the Wu Shu bridge in Taichung	8
1-6 Conceptual relationship between relative effort, increasing hazard and performance criteria implied in this manual	9
1-7 Retrofit process for dual level earthquake ground motions	15
1-8 Construction of the seismic design response spectrum	20
1-9 Determination of seismic retrofit category	23
1-10 Seismic retrofitting process for highway bridges subject to upper level ground motion	27
1-11 Relative effort to retrofit an (a) 'standard' and (b) 'essential' bridge with varying service life and hazard level	29
1-12 Screening and prioritization process	31
1-13 Evaluation methods for existing bridges showing relationship between demand analysis and capacity assessment	41
1-14 Identification and evaluation of a retrofit strategy	46
1-15 Selected retrofit measures	53
2-1 Variation in short- and long-period spectral acceleration with ground motion return period	61
2-2 Seismic hazard maps for the conterminous United States	65
2-3 Calculation of short- and long-period spectral accelerations for 100- and 1000-year ground motion return periods	73
2-4 Design response spectrum (five percent damping) construction using two-point procedure	85
2-5 Comparison of two-point method of five percent damped response spectrum construction with USGS multi-point mapping results for two percent probability of exceedance in 50 years	87
2-6 Time histories and horizontal response spectra (five percent damping) for the fault strike-normal and fault strike-parallel components of ground motion for the Rinaldi recording obtained 4.5 mi (7.5 km) from the fault rupture during the 1994 Northridge, California earthquake	90
2-7 Vertical/horizontal spectral ratios vs. period	92
2-8 Hazard deaggregation for 0.2 second response spectral acceleration (S_s) for ground motion with three percent probability of exceedance in 75 years (2500-year return period)	95

LIST OF FIGURES (Continued)

FIGURE	PAGE
4-1 Seismic rating method using indices.....	112
4-2 Calculation of bridge vulnerability, V	114
4-3 Seismically vulnerable bearings	115
4-4 Calculation of vulnerability rating for connections, bearings and seat widths (V_1)	119
4-5 Seismic rating method using expected damage	128
5-1 Capacity curve	163
5-2 Idealized capacity.....	164
5-3 Demand spectrum	167
5-4 Capacity/demand spectra	169
6-1 Uncoupled elasto-plastic spring model for rigid footings.....	183
6-2 Uncoupled winkler spring model.....	183
6-3 Upper and lower bound approach to define stiffness and capacity	184
6-4 Idealized concentration of stress at edge of rigid footings subjected to overturning moment.....	188
6-5 Rocking of shear wall on strip footing.....	189
6-6 Method for passive pressure capacity of footing or pile cap	190
6-7 Effect of boundary conditions on pile stiffness	193
6-8 Lateral pile-head stiffness (fixed-head condition)	194
6-9 Rotational pile head stiffness.....	195
6-10 Cross-coupling pile-head stiffness.....	196
6-11 Lateral pile-head stiffness (free-head condition)	197
6-12 Recommended coefficient of variation in subgrade modulus (f) with depth of sand...	198
6-13 Recommended coefficient of variation in subgrade modulus (f) with depth of clay....	199
6-14 Lateral embedded pile-head stiffness (fixed-head condition).....	200
6-15 Embedded pile-head rotational stiffness.....	201
6-16 Embedded pile cross-coupling pile-head stiffness.....	202
6-17 Axial load-displacement graphical solution.....	204
6-18 Modeling approaches for deep foundations.....	206
6-19 Pile footing configuration for moment-rotation study	207
6-20 Axial load-displacement curve for single pile	208
6-21 Cyclic moment-rotation and settlement-rotation solutions.....	209
6-22 Abutment types	212
6-23 Design passive pressure zone.....	213
6-24 Characterization of abutment capacity and stiffness	214
6-25 Trial wedge method for determining critical earthquake-induced active forces	216
6-26 Sketch of Magsaysay bridge showing earthquake damage.....	218
6-27 Landing Road bridge lateral spread	219
6-28 Site and damage characteristics for a precast concrete pile subjected to a lateral spread in the Kobe earthquake	220

LIST OF FIGURES (Continued)

FIGURE	PAGE
7-1 Evaluation methods for existing bridges showing relationship between demand analysis and capacity assessment.....	222
7-2 Confined strength ratio (K) for reinforced concrete members	241
8-1 Deck to girder connection retrofit.....	258
8-2 Steel girder diaphragm retrofit.....	260
8-3 Diaphragm free body diagram	261
8-4 Ductile end diaphragms	262
8-5 Girder bracing retrofit.....	264
8-6 Bearing stiffener retrofit	265
8-7 Methods for accommodating girder misalignment using web splice plates	266
8-8 Girders made continuous for live load.....	267
8-9 Retrofit of concrete box girder for flexural capacity	268
8-10 Steel bearing nomenclature.....	269
8-11 Bearing sole plate to girder connection retrofit	271
8-12 Bearing sole plate to girder with catcher bar retrofit	272
8-13 Expansion bearing retrofit.....	273
8-14 Retrofit to increase bearing transverse capacity	274
8-15 Retrofit to increase anchor plate capacity.....	275
8-16 Bearing retrofitting by encasement in steel shell.....	277
8-17 Bearing retrofitting by encasement in concrete	278
8-18 Bearing replacement retrofit using steel pedestal	279
8-19 Bearing replacement using concrete pedestal	280
8-20 Lead-filled elastomeric isolation bearing.....	282
8-21 Friction-pendulum isolation bearing.....	282
8-22 Eradiquake isolation bearing.....	283
8-23 Knock-off device in backwall of seat-type abutment	285
8-24 Freyssinet hinge	286
8-25 Pipe shear key	287
8-26 Concrete hinge retrofit	288
8-27 Abutment seat extension	289
8-28 Pipe seat extenders.....	291
8-29 Caltrans cable restrainer unit	294
8-30 Caltrans tests of restrainer cable	296
8-31 Multi-cable restrainer assembly	297
8-32 Bumper block retrofit.....	298
8-33 Restrainer anchorage schemes	300
8-34 <i>Undesirable</i> restrainer detail.....	301
8-35 Resistance of concrete wall to punching shear	302
8-36 Restrainer orientation for transversely rigid supports.....	303
8-37 Restrainer orientation for transversely flexible supports	303

LIST OF FIGURES (Continued)

FIGURE	PAGE
8-38	Restrainer at pier with a positive tie to pier 303
8-39	Required clearances for coring 304
8-40	Available seat width..... 305
8-41	SDOF model for end-span fixed bearing at abutment 307
8-42	SDOF model for an end-span fixed bearing at pier 308
8-43	Force displacement relationship for abutment..... 308
8-44	2DOF model for the iterative method..... 315
8-45	Transverse shear keys 317
8-46	Bearing keeper bracket retrofit 318
8-47	Steel pipe restrainers 318
8-48	Vertical hold down retrofit..... 332
8-49	Energy dissipation devices..... 335
8-50	Friction dampers 336
9-1	Column replacement on San Francisco viaducts 343
9-2	Column replacement using existing column reinforcement 344
9-3	Column anchorage using headed reinforcement..... 345
9-4	Replaceable plastic hinge with fuse bars 346
9-5	Supplemental column retrofit 347
9-6	Column strengthening by concrete overlay 349
9-7	Column strengthening by adding reinforcement within steel shell 350
9-8	Column strengthening by anchoring steel shell..... 351
9-9	Typical steel shell retrofit of round column..... 354
9-10	Typical steel shell retrofit of rectangular column 355
9-11	Free body diagram of column retrofitting with a steel shell 356
9-12	Geometry of an elliptically shaped jacket..... 360
9-13	Free body diagram of column retrofitting with a composite shell..... 367
9-14	Anchorage for prestress strand retrofit..... 371
9-15	Prestressing retrofit by wedging between column and strand 372
9-16	Semi-circular reinforcing bars with couplers..... 373
9-17	Free body diagram of column retrofitting with external prestressing..... 374
9-18	Infill shear wall in multi-column bents 379
9-19	Steel shell retrofit for vertical capacity preservation 380
9-20	Sierra Point overhead, US 101, near San Francisco, California 381
9-21	Column retrofit by flexural strength reduction 382
9-22	Retrofit of X-braced steel bent..... 384
9-23	Richmond-San Rafael bridge bent retrofit..... 385
9-24	Built-up steel columns stiffened by plates 386
9-25	Built-up steel column retrofitted with steel shell..... 387
9-26	Retrofit for wall pier with starter bars..... 388
9-27	Typical cap beam configurations for boxgirder bridges 389

LIST OF FIGURES (Continued)

FIGURE	PAGE
9-28 Pier cap strengthening.....	391
9-29 Flexural and shear retrofit of free standing multi-column bents.....	392
9-30 Pier cap retrofit tested at University at Buffalo	393
9-31 Flexural and shear retrofit of integral cap beams.....	393
9-32 Horizontal link beams for pier cap force reduction	394
9-33 Joint retrofit with external concrete jacket.....	395
9-34 Free body diagram of shear forces on a knee joint	396
9-35 Knee joint retrofit with steel plates.....	398
9-36 Retrofit of an integral cap beam joint for longitudinal loading	399
9-37 “Supergirders” added between piers to reduce torsion in pier caps.....	400
10-1 Abutment types	402
10-2 California style settlement slabs	404
10-3 New Zealand style settlement slabs	404
10-4 “Waffle” slabs.....	406
10-5 Anchor slabs with CIDH piles.....	407
10-6 Diaphragm abutment overlay.....	409
10-7 Concrete block abutment shear key	410
10-8 Pipe shear key at abutment	411
10-9 Abutment seismic shear walls.....	412
10-10 Wingwall overlay.....	413
10-11 Wingwall cross-tie	414
10-12 CIDH pile shear keys.....	415
10-13 Gravity or “Deadman” anchors.....	416
10-14 Abutment retrofit using soil anchors.....	417
10-15 Modified abutment friction anchor	417
10-16 Global footing strengthening	419
10-17 Footing retrofit with concrete overlay	421
10-18 Bottom reinforcing splice detail.....	422
10-19 Footing strengthening by horizontal prestressing	423
10-20 Footing shear strength retrofitting	424
10-21 Footing joint shear forces.....	425
10-22 Strut and tie model for joint design.....	427
10-23 Yield line analysis of footing overlay.....	433
10-24 Footing link beam retrofit	434
10-25 Prestressed tie-down anchor	436
11-1 Elevation view of a representative bridge on a liquefiable stratum.....	439
11-2 Pseudo-static stability analysis	440
11-3 Design flowchart.....	446
11-4 Corrections for P- Δ effects in piles with plastic hinges.....	447
11-5 Vibro-replacement equipment and process.....	448

LIST OF FIGURES (Continued)

FIGURE	PAGE
11-6 Vibro-system (stone column) treatment at toe of approach embankment	449
11-7 Vibro-system (stone column) treatment around a pile-supported bridge pier	450
11-8 Compaction grout bulb construction.....	451
11-9 Effect of restrainers at bent during liquefaction failure	452
 B-1 Simplified base curve recommended for determination of CRR from SPT data for magnitude 7.5 along with empirical liquefaction data	460
B-2 Magnitude scaling factors derived by various investigators.....	461
B-3 Robertson and Wride chart	462
B-4 Soil flexibility factor (r_d) versus depth curves developed by Seed and Idriss (1971) with added mean value lines	463
B-5 Relationship between residual strength (S_r) and corrected 'clean sand' SPT blowcount ($(N_1)_{60}$) from case histories	466
B-6 Simplified displacement chart for velocity-acceleration ratio of 30.....	470
B-7 Simplified displacement chart for velocity-acceleration ratio of 60.....	470
B-8 Relationship between cyclic stress ratio, blowcount ($(N_1)_{60}$), and volumetric strain for saturated clean sands and magnitude 7.5	473
B-9 Schematic diagram for determination of H_1 and H_2	474
B-10 Types of earthquake faults	475
B-11 Relationship between maximum surface fault displacement and earthquake moment magnitude for strike-slip faulting	479
 C-1 Capacity-demand acceleration-displacement spectra showing randomness and/or uncertainty in structural behavior and ground motion response	481
C-2 A normalized fragility curve based on a lognormal probability distribution with a coefficient of dispersion $\beta_c = 0.6$	482
 D-1 Minimum support length requirements.....	487
D-2 Effective seat width.....	489
D-3 Procedures for determining capacity/demand ratios for columns, piers and footings..	492
D-4 Effectiveness of poorly anchored transverse reinforcement as a function of ductility indicator	494
D-5 Effective anchorage length of longitudinal reinforcement	496
D-6 Procedure for determining capacity/demand ratios for anchorage of longitudinal reinforcement	499
D-7 Radial stresses developed due to bar anchorage	501
D-8 Procedure for determining capacity/demand ratios for splices in longitudinal reinforcement (mm and kPa)	503
D-9 Procedure for determining capacity/demand ratios for column shear	506

LIST OF FIGURES (Continued)

FIGURE	PAGE
D-10 Resolution of shear demand and shear capacity	509
D-11 Modes of failure for spread footings.....	515
D-12 Modes of failure for pile footings	516
E-1 Example bridge	522
E-2 Expansion joint detail	522
E-3 Column details	523
E-4 Positive sign convention for abutment, hinge and joint forces	528
E-5 Positive sign convention for column forces and moments	528
E-6 Bent 2 column and footing interaction diagrams.....	536
E-7 Bents 3 and 4 column and footing interaction diagrams.....	537
E-8 Development of footing interaction diagram at bent 2	538
F-1 Plan and elevation of example bridge.....	557
F-2 Pier 2 bent details.....	558
F-3 Column interaction diagram	565
F-4 Foundation interaction diagram	565
F-5 Foundation interaction diagram – transverse direction.....	566

LIST OF TABLES

TABLE	PAGE
1-1 Service life categories	12
1-2 Minimum performance levels for retrofitted bridges.....	14
1-3 Site classes	18
1-4 Site factors F_a and F_v	19
1-5 Seismic hazard level	21
1-6 Performance-based seismic retrofit categories	22
1-7 Minimum requirements.....	24
1-8 Sample bridge seismic inventory form	36
1-9 Evaluation methods for existing bridges.....	40
1-10 Cost of various retrofit strategies as percentage of new construction costs	43
1-11 Matrix of seismic retrofit approaches and section references to associated retrofit measures.....	56
2-1 Relationship between probability of exceedance of earthquake ground motion and return period.....	60
2-2 Site classes	79
2-3 Steps for classifying a site.....	80
2-4 Site factors F_a and F_v	82
2-5 Damping adjustment factors	88
2-6 Procedure for obtaining deaggregated seismic hazard from USGS web site	94
3-1 Estimated susceptibility of sedimentary deposits to liquefaction during strong ground motion	103
4-1 Values for P_R	122
4-2 Potential for liquefaction-related damage.....	125
4-3 NBI fields (attributes) used in determining bridge fragility	134
4-4 Fragility of bridges constructed before 1975 in California and 1990 elsewhere (non-seismic bridges).....	136
4-5 Fragility of bridges constructed since 1975 in California and 1990 elsewhere (seismic bridges)	137
4-6 Modification factors (K_{3D}) used to model 3D effects for multi-span bridges	138
4-7 Modified repair cost ratio for all bridges	140
4-8 Expected losses in two example bridges subject to similar earthquakes	141
5-1 Evaluation methods for existing bridges.....	148
5-2 Components for which capacity/demand ratios are required.....	155
5-3 Restrictions on the application of the uniform load method.....	157
5-4 Effective viscous damping ratios and damping factors, B_S and B_L	168

LIST OF TABLES (Continued)

TABLE	PAGE
6-1 Surface stiffnesses for a rigid plate on a semi-infinite homogeneous elastic half-space	186
6-2 Stiffness embedment factors for a rigid plate on a semi-infinite homogeneous elastic half-space.....	187
7-1 Component rigidities.....	226
7-2 Dead load multipliers (C_v) for bridges subject to vertical acceleration for rock sites.....	233
7-3 Values of plastic curvature corresponding to various limit states in reinforced concrete columns and beams	248
8-1 Basic characteristics of typical isolation bearings for bridges.....	283
8-2 Basic design properties for typical high strength bar sizes.....	297
9-1 Mechanical properties of fibers used in modern fiber-reinforced plastic composites ..	366
11-1 Summary of ground improvement methods for liquefaction remediation at existing bridges.....	441
D-1 Footing ductility indicators	513
D-2 List of capacity/demand ratios	520
E-1 Maximum elastic moment demands (kN m).....	535
E-2 Column and footing overstrength moments.....	537
E-3 Revised column and footing overstrength moments (iteration 1).....	539
E-4 Revised column and footing overstrength moments (iteration 2).....	540
E-5 Ultimate moment capacity/elastic moment demand ratios	541
E-6 Capacity/demand ratios for the as-built bridge.....	548
F-1 Seismic retrofit categories for upper level earthquake ($F_v = 1.0$, PL2)	559

LIST OF ABBREVIATIONS AND SYMBOLS

ABBREVIATIONS

AASHTO	American Association of State Highway and Transportation Officials
ASL	Anticipated Service Life
ASTM	American Society for Testing and Materials
ATC	Applied Technology Council
ATC/MCEER	Joint Venture of Applied Technology Council and Multidisciplinary Center for Earthquake Engineering Research
AVR	Abutment Vulnerability Rating
BHT	Becker Hammer Test
BSSC	Building Seismic Safety Council
BSTRUCT	Software for determining plastic deformation in piles
C/D	Capacity/Demand ratio
Caltrans	California Department of Transportation
CDMG	California Division of Mines and Geology
CD-ROM	Compact Disc-Random Access Memory
CEUS	Central and Eastern United States
CGS	California Geological Survey
CIDH	Cast-in-Drilled Hole
CPT	Cone Penetration Test or Cone Penetrometer Test
CQC	Complete Quadratic Combination
CRR	Cyclic Resistance Ratio
CSABAC	Caltrans Seismic Advisory Board Adhoc Committee
CSR	Cyclic Stress Ratio
CVR	Column Vulnerability Rating
DL	Dead Load
EBF	Eccentrically Braced Frames
FEMA	Federal Emergency Management Agency
FEX	Frequency of Exceedance

FHWA	Federal Highway Administration
FLPIER	Software for soil foundation interaction analysis
FRP	Fiber Reinforced Polymer composite material
FS	Factor of Safety
HAZUS	Software for estimation of earthquake losses in built environment, developed by FEMA (name derived from “Hazards - U.S.”)
HITEC	Highway Innovative Technology Evaluation Center
IBC	International Building Code
ICBO	International Conference of Building Officials
LL	Lower Level earthquake ground motion
LL	Live Load
LPILE	Software for lateral load analysis of piles
LRFD	Load and Resistance Factor Design
LVR	Liquefaction Vulnerability Rating
MCE	Maximum Considered Earthquake
MCEER	Multidisciplinary Center for Earthquake Engineering Research
MDOF	Multiple Degree of Freedom
NBI	National Bridge Inventory
NCHRP	National Cooperative Highway Research Program
NDP	Nonlinear Dynamic Procedure
NEHRP	National Earthquake Hazard Reduction Program
NSP	Nonlinear Static Procedure
NZS	Standards Association of New Zealand
PEX	Probability of Exceedance
PGA	Peak Ground Acceleration
PL	Performance Level
PTFE	Polytetrafluoroethylene (Teflon)
RCR	Repair Cost Ratio or Damage Ratio
SA	Spectral Acceleration
SCEC	South California Earthquake Center
SDOF	Single Degree of Freedom
SEISAB	Software for the seismic analysis of bridges

SHL	Seismic Hazard Level
SPC	Seismic Performance Category
SPS	Shear Panel System
SPT	Standard Penetration Test
SRA	Seismic Risk Assessment
SRC	Seismic Retrofit Category
SRSS	Square Root of the Sum of the Squares
SFSI	Soil-Foundation-Structure Interaction
SSI	Soil-Structure Interaction
STRAHNET	Strategic Highway Network, part of the National Highway System
STU	Shock Transmission Unit
TADAS	Triangular-plate Added Damping and Stiffness Device
UHM	Ultra High Modulus
UL	Upper Level earthquake ground motion
ULM	Uniform Load Method
USGS	United States Geological Survey
WUS	Western United States

SYMBOLS

CHAPTER 1: SEISMIC RETROFITTING OF HIGHWAY BRIDGES

F	=	Seismic demand or force.
F_L	=	Longitudinal seismic demand or force.
F_T	=	Transverse seismic demand or force.
F_a	=	Site factor in short-period range of design spectrum.
F_v	=	Site factor in long-period range of design spectrum.
\bar{N}	=	Average Standard Penetration Test (SPT) blowcount.
P	=	Priority index.
PI	=	Plasticity index.
R	=	Bridge rank.
S_1	=	Spectral acceleration at 1.0 sec period for reference site (Site Class B).
S_{D1}	=	Spectral acceleration at 1.0 sec period including site effects.

S_{DS}	=	Spectral acceleration at 0.2 sec period including site effects.
S_s	=	Spectral acceleration at 0.2 sec period for reference site (Site Class B).
\bar{s}_u	=	Average undrained shear strength.
\bar{v}_s	=	Average shear wave velocity for the upper 30 m (100 ft) of the soil profile.
W	=	Weight.
w	=	Moisture content.

CHAPTER 2: SEISMIC GROUND MOTION HAZARD

ξ	=	Viscous damping ratio.
ξ_{eff}	=	Effective viscous damping ratio.
v	=	Annual frequency of occurrence.
d_c	=	Total thickness of cohesive soil layers in the top 30 m (100 ft).
d_i	=	Thickness of a layer between 0 and 30 m (0 and 100 ft).
d_s	=	Total thickness of cohesionless soil layers in the top 30 m (100 ft).
F_a	=	Site factor in short-period range of design spectrum.
F_v	=	Site factor in long-period range of design spectrum.
i	=	Soil layer (ranges from 1 to n).
k	=	Number of cohesionless soil layers in the top 30 m (100 ft).
\bar{N}	=	Average Standard Penetration Test (SPT) blowcount (blows/0.30m or blows/ft).
N_{ch}	=	Blowcount for a cohesionless soil layer.
N_i	=	Standard penetration test blowcount of a layer.
P_E	=	Probability of exceedance.
PI	=	Plasticity index.
S_1	=	Spectral acceleration at 1.0 sec period for reference site (Site Class B).
S_{D1}	=	Spectral acceleration at 1.0 sec period including site effects.
S_{DS}	=	Spectral acceleration at 0.2 sec period including site effects.
S_s	=	Spectral acceleration at 0.2 sec period for reference site (Site Class B).
\bar{s}_u	=	Average undrained shear strength.
s_{ui}	=	Undrained shear strength for a cohesive soil layer.
T	=	Period of vibration.
t	=	Lifetime of bridge.

v_{si}	=	Shear wave velocity of i^{th} layer of soil.
\bar{v}_s	=	Average shear wave velocity for the upper 30 m (100 ft) of the soil profile.
w	=	Moisture content.

CHAPTER 4: SEISMIC RATING METHODS FOR SCREENING AND PRIORITIZATION

α	=	Angle of skew.
A_2	=	Modified median fragility curve parameter.
a_2	=	Median spectral acceleration (at 1.0 sec period).
B	=	Width of deck.
B_{LOSS}	=	Direct economic loss due to structural damage to a bridge.
b_{max}	=	Maximum transverse column dimension.
F	=	Framing factor.
H	=	Height.
H_{LOSS}	=	Indirect economic loss due to loss of life, injuries, business disruption, traffic congestion, and denied access.
K_{shape}	=	Factor relating to the shape of the design acceleration spectrum.
K_{skew}	=	Fragility modification factor to account for bridge skew.
L	=	Length of bridge deck
L	=	Available support length for superstructure
L_c	=	Effective column length.
N	=	Minimum recommended support length.
n	=	Number of spans in bridge.
np	=	Number of piers.
P	=	Priority index.
P_R	=	Total number of points to be deducted from Q for factors known to reduce susceptibility to shear failure.
P_s	=	Amount of main reinforcing steel expressed as a percent of the column cross-sectional area.
Q	=	Factor used to determine column vulnerability rating (equation 4-5b)
R	=	Bridge rank.
RCR_i	=	Repair cost ratio for the i^{th} damage state.
RCR_T	=	Total repair cost ratio.
S	=	Site factor.

S_{D1}	=	Spectral acceleration at 1.0 sec period including site effects (seismic coefficient).
T_{LOSS}	=	Total monetary loss to the economy.
U	=	Replacement cost of the bridge.
V	=	Bridge vulnerability rating.
V_L	=	Vulnerability to collapse or loss of access due to longitudinal movement.
V_T	=	Vulnerability to collapse or loss of access due to transverse movement.

CHAPTER 5: EVALUATION METHODS FOR EXISTING BRIDGES

α	=	Angle of skew.
Δ	=	Displacement of superstructure.
Δ_{max}	=	Maximum displacement.
Δ'_{max}	=	Displacement limit state.
Δ_y	=	Yield displacement.
μ	=	Displacement ductility factor.
ξ_{eff}	=	Effective viscous damping ratio.
ρ_t	=	Total area ratio of longitudinal reinforcement.
ϕ	=	Capacity reduction factor.
ω	=	Angular frequency.
ΣQ_{NSi}	=	Sum of the displacement or force demands on a component from non-seismic loads.
A_g	=	Gross area of the column section.
B	=	Width.
B_L	=	Damping factor used in the long-period range of the spectrum.
B_S	=	Damping factor used in the short-period range of the spectrum.
C_c	=	Capacity coefficient.
C_d	=	Seismic demand coefficient.
D	=	Smallest column dimension or diameter.
D_p	=	Pile dimension about the weak axis of bending.
F	=	Total horizontal force acting on the bridge.
F_y	=	Yield force.
f'_c	=	Compressive strength of concrete.
g	=	Acceleration due to gravity.

H	=	Height.
K	=	Lateral stiffness of the bridge.
k_1	=	Elastic stiffness in direction considered, transverse or longitudinal.
k_2	=	Equivalent post-yield stiffness in direction considered, transverse or longitudinal.
L	=	Total length of bridge
L	=	Distance between expansion joints.
M/V	=	Shear span length of an equivalent cantilever member where M is the end moment and V is the shear force.
M_n	=	Nominal column yield moment.
N	=	Minimum seat width.
N_0	=	Available seat width at an abutment or pier cap.
P	=	Axial load.
P_c	=	Axial capacity of a steel column or timber pile member in compression.
P_e	=	Axial load on the bridge column including both gravity and seismic effects.
p_e	=	Equivalent uniform static seismic loading per unit length of bridge.
p_o	=	Uniform load.
P_y	=	Axial capacity at yield of a steel column/pile member.
Q_{EQ}	=	Displacement or force demand for the earthquake loading under consideration.
R	=	Ratio of elastic force demand to lateral capacity of pier.
R_C	=	Nominal ultimate displacement or force capacity of the structural component being evaluated.
S_a	=	Spectral acceleration.
S_d	=	Spectral displacement.
T	=	Period, or wall thickness or the smallest cross-sectional dimension.
$v_{s,MAX}$	=	Maximum value of static displacement $v_s(x)$.
V_U	=	Lateral strength capacity at zero displacement.
W	=	Weight.
W'	=	Seismic weight per column.
$w(x)$	=	Unfactored dead load of the bridge superstructure and tributary substructure.

CHAPTER 6: GEOTECHNICAL MODELING AND CAPACITY ASSESSMENT

γ	=	Weight density of soil.
----------	---	-------------------------

γ_t	=	Total unit weight of soil.
γ_w	=	Unit weight of water.
δ_c	=	Axial displacement of the pile head due to compression of the pile under axial load but neglecting the surrounding soil.
λ	=	Characteristic length of a pile defined by $(EI_p/E_s)^{0.25}$.
ν	=	Poisson's ratio.
σ'_0	=	Effective vertical stress.
ϕ	=	Internal friction angle of a soil.
AE	=	Axial rigidity of pile.
B	=	Footing width.
c	=	Compressive strength of a soil.
D	=	Pile diameter.
D_g	=	Gap width.
d	=	Depth of sample.
d_w	=	Depth of water level.
E	=	Modulus of elasticity.
EI, EI_p	=	Flexural stiffness of pile.
E_s	=	Subgrade modulus of the soil.
e	=	Stiffness embedment factor (table 6-2).
F_v	=	Factor of safety.
f	=	Coefficient of variation of the inelastic subgrade modulus.
G_o	=	Initial or low strain shear modulus during cyclic loading.
g	=	Acceleration due to gravity.
H	=	Height.
I_x, I_y	=	Moments of inertia of a footing about the x and y axis, respectively.
K	=	Soil stiffness parameter (table 6-1).
L	=	Length.
M_c	=	Ultimate moment capacity.
$(N_1)_{60}$	=	Normalized corrected blowcount.
P	=	Vertical load on footing.
P_p	=	Total passive force per unit length of wall.
p_p	=	Passive pressure behind a wall.

Q	=	Axial load.
q	=	Vertical load on a footing (contact stress).
q_c	=	Ultimate strength of soil (capacity) per unit area.
v_s	=	Shear wave velocity at small strains.
Z	=	Displacement.
Z_c	=	Displacement when capacity is reached.
z	=	Depth below grade.

CHAPTER 7: STRUCTURAL MODELING AND CAPACITY ASSESSMENT

α	=	Corner-to-corner strut angle.
α	=	Ratio of average concrete stress in compression zone to confined concrete strength.
β	=	Stress block factor.
γ	=	Reinforcing steel configuration factor.
Δ_e	=	Elastic component of displacement.
Δ_p	=	Plastic component of displacement.
Δ_y	=	Nominal yield displacement.
ϵ_{ap}	=	Plastic strain amplitude.
ϵ_b	=	Buckling strain in the longitudinal reinforcing steel.
ϵ_{cu}	=	Ultimate compression strain of the confined core concrete.
ϵ_{su}	=	Strain at the maximum stress of the transverse reinforcement.
ϵ_y	=	Yield strain.
θ_p	=	Plastic hinge rotation.
θ_u	=	Ultimate (total) drift.
θ_y	=	Elastic drift at yield.
θ	=	Angle of the principal crack plane.
κ_o	=	Factor related to the centroid of the stress block.
Λ	=	Fixity factor.
$\mu_{lap\phi}$	=	Curvature ductility at the initial breakdown of bond in the lap-splice zone.
ρ_s	=	Volumetric ratio of transverse steel.
ρ_t	=	Volumetric ratio of the longitudinal reinforcement.
ρ_v	=	Volumetric ratio of transverse steel.

ρ_x, ρ_y	=	Volume ratio of transverse hoops or ties to the core concrete in x- and y- directions, respectively.
ϕ	=	Strength reduction factor.
ϕ_e	=	Expected strength factor.
ϕ_o	=	Overstrength factor.
ϕ_p	=	Plastic curvature.
ϕ_u	=	Ultimate (total) curvature.
ϕ_y	=	Nominal yield curvature.
A_{bh}	=	Area of one spiral or hoop bar.
A_{cc}	=	Area of confined concrete core.
A_e	=	Effective shear area.
A_g	=	Gross section area.
A_{jh}	=	Area of a beam-column joint in a horizontal plane.
A_{st}	=	Area of steel.
A_v	=	Area of transverse shear steel.
A_w	=	Shear area of beam or column.
b''	=	Width of column normal to y-direction.
b_w	=	Center-to-center spacing of transverse shear steel across width of rectangular column.
C_v	=	Dead load multiplier.
c	=	Depth from the extreme compression fiber to the neutral axis.
D	=	Overall depth of section.
D'	=	Distance between the outer layers of longitudinal steel in a rectangular section.
D''	=	Diameter of transverse hoop or spiral.
d	=	Depth to the outer layer of tension steel from the extreme compression fiber.
d'	=	Distance from the extreme compression fiber to the center of the nearest compression reinforcing bars.
d_b	=	Diameter of the longitudinal reinforcing bar.
E_c	=	Elastic modulus of concrete.
$E_c I_{eff}$	=	Effective flexural rigidity.
E_s	=	Elastic modulus of steel.
f_v	=	Average axial stress on the joint.
f'_{cc}	=	Confined concrete strength.

f'_c	=	Ultimate compressive strength of concrete.
f'_{ce}	=	Ultimate expected compressive strength of concrete.
f_h	=	Average horizontal axial stress on the joint.
f'_l	=	Confining stress supplied by the transverse reinforcement at yield in a circular column.
$f'_{\ell x}, f'_{\ell y}$	=	Confining stress in the x- and y- directions of a rectangular column, respectively.
f_{su}	=	Ultimate tensile strength of the longitudinal reinforcement.
f_y	=	Yield stress.
f_{ye}	=	Expected yield strength of longitudinal reinforcement.
f_{yh}	=	Yield stress of the transverse hoops.
h_b	=	Depth of the cap beam at the joint.
I_g	=	Moment of inertia of the gross uncracked section.
j_d	=	Internal lever arm of the concrete compression member.
K	=	Strength enhancement factor.
K_{shape}	=	Shape factor.
k_e	=	Confinement effectiveness coefficient for spirals and hoop steel.
L	=	Length.
L/D'	=	Slenderness ratio.
L_{gap}	=	Clear gap between edge of jacket and bottom of pier cap or top of footing.
L_p	=	Equivalent plastic hinge length.
l_s	=	Length of the lap splice.
M_D	=	Design moment.
M_e	=	Expected flexural strength (moment).
M_n	=	Nominal yield moment (theoretical yield strength) of the member.
M_p	=	Plastic strength capacity.
M_{po}	=	Flexural moment overstrength capacity.
M_S	=	Reduced moment.
N_f	=	Effective number of equal-amplitude cycles of loading that lead to fracture.
P	=	Axial load on member.
P_e	=	Axial load on the section.
p_t	=	Major principal tension stress.

S	=	Center-to-center longitudinal spacing of the transverse hoop steel.
S_d	=	Design strength.
S_n	=	Nominal strength.
S_o	=	Overstrength.
s	=	Spacing of spirals or hoops.
T_n	=	Natural period of vibration of the bridge.
V_{cf}	=	Final shear strength carried by the concrete.
V_{ci}	=	Contribution provided by diagonal tension field in the concrete.
V_f	=	Final shear strength.
V_i	=	Initial shear strength.
V_{jf}	=	Final (residual) joint shear strength.
V_{jh}	=	Horizontal shear in the joint.
V_{ji}	=	Initial shear strength of the beam-column joint.
V_m	=	Shear demand based on flexure.
V_p	=	Contribution provided arch (strut) action.
V_s	=	Contribution to the shear strength provided by rebar truss action.
v_j	=	Average joint shear stress acting on the joint.

CHAPTER 8: RETROFIT MEASURES FOR SUPERSTRUCTURES, BEARINGS AND SEATS

α	=	Angle of skew.
β	=	Frequency ratio.
ξ	=	Equivalent viscous damping ratio.
μ	=	Ductility capacity.
$\{\phi_i\}$	=	Mode shape for mode 'i'.
A_r	=	Area of one restrainer.
D_1	=	Maximum displacement of the span.
D_2	=	Maximum displacement at the top of the pier.
D_{as}	=	Available seat width.
D_{eq0}	=	Unrestrained relative expansion joint displacement.
D_r	=	Maximum permissible restrainer displacement.
D_{rs}	=	Restrainer slack.
D_y	=	Restrainer elongation at yield.

E	=	Modulus of elasticity.
F_h	=	Increase in longitudinal resistance resulting from wedging a rocker bearing.
f_y	=	Yield stress.
$[K]$	=	Stiffness matrix of a two frame system with restrainers.
K_{DED}	=	Stiffness of the ductile end diaphragm.
K_r	=	Restrainer stiffness.
K_{SUB}	=	Stiffness of the substructure.
L_r	=	Restrainer length.
$[M]$	=	Mass matrix of a two frame system.
N_r	=	Number of restrainers.
P	=	Dead load / bearing.
P_i	=	Participation factor for mode i .
R	=	Response modification factor (R-factor).
s	=	Restrainer slack.

CHAPTER 9: RETROFIT MEASURES FOR SUBSTRUCTURE COMPONENTS

α	=	Geometric aspect ratio of a column.
ϵ_{cu}	=	Ultimate strain of concrete column jacketed with composites.
ϵ_{du}	=	Ultimate design strain of the jacket material taking into account long-term environmental degradation.
ϵ_p	=	Maximum allowable passive strain.
ϵ_{su}	=	Ultimate strain in the shell steel.
θ	=	Shear crack angle.
ρ_l	=	Longitudinal reinforcement ratio (A_s/A_g).
ρ_s	=	Effective volumetric ratio.
A_b	=	Area of spliced longitudinal bar.
A_d	=	Area of dowel bar.
A_p	=	Wire cross-sectional area.
c	=	Cover over the main column reinforcing bars.
D	=	Diameter.
D'	=	Diameter of the pitch circle of the main column reinforcement; distance between the outermost reinforcing bars in the direction of shear.

d_b	=	Diameter of longitudinal reinforcement.
d_p	=	Diameter of wire.
E_a	=	Modulus of elasticity of active wrap.
E_j	=	Weighted average of the elastic moduli for the active and passive wraps.
E_p	=	Modulus of elasticity of passive wrap.
E_s	=	Modulus of elasticity for steel.
f_a	=	Active confining stress in the column.
f'_{cc}	=	Ultimate confined concrete stress capacity.
f_{du}	=	Ultimate design strength of the jacket material taking into account long-term environmental degradation.
f_i	=	Tensile stress in wire after losses.
f_ℓ	=	Required level of confinement stress.
f_{pu}	=	Ultimate design stress.
f_s	=	Stress induced in the jacket.
f_y	=	Yield stress.
f_{ys}	=	Jacket yield stress.
g	=	Gap between the retrofit measure and critical section.
L	=	Length.
ℓ_p	=	Length of plastic hinges.
ℓ_s	=	Splice length.
N	=	Number of main column reinforcing bars.
s	=	Spacing.
s_s	=	Gap between retrofit measure and critical section.
t	=	Steel jacket thickness.
t_a	=	Thickness of active wrap.
t_p	=	Thickness of passive wrap.
V_{sj}	=	Additional nominal shear capacity provided by a steel jacket.
v_i	=	Maximum interface shear stress.
v_{ih}	=	Horizontal interface shear stress.
v_{iv}	=	Vertical interface shear stress.

CHAPTER 10: RETROFIT MEASURES FOR ABUTMENTS, FOOTINGS, AND FOUNDATIONS

μ	=	Coefficient of friction between soil and concrete.
A_{eff}	=	Effective bearing area.
B_c	=	Column width.
b_{eff}	=	Column width plus depth for rectangular columns.
C_{in}	=	Column interior.
C_{ex}	=	Column exterior.
D	=	Column diameter.
D_c	=	Column depth.
DL_s	=	Dead load of slab and any overlaying fill.
d_f	=	Depth of the retrofitted footing.
F_D	=	Design force.
f_a	=	Effective axial compressive stress within the joint in the vertical direction.
f_t	=	Principle tensile stress in the joint region.
P	=	Axial load.
S_a	=	Spectral acceleration.
V_{jv}	=	Vertical joint shear stress.

CHAPTER 11: RETROFIT MEASURES FOR BRIDGES ON HAZARDOUS SITES

M_p	=	Plastic moment capacity of pile.
M_{pt}	=	Plastic moment capacity at head of pile.
V_{pass}	=	Passive force developed against end diaphragm.
V_{strut}	=	Force resisted by superstructure and other piers.

APPENDIX B: EVALUATION OF GEOTECHNICAL HAZARDS

$\tau_{\text{av}}/\sigma'_{\text{vo}}$	=	Average earthquake induced shearing stress divided by the effective overburden stress.
$\sigma_{\text{vo}}/\sigma'_{\text{vo}}$	=	Ratio of total overburden stress to effective overburden stress.
a_{max}	=	Peak ground acceleration in units of g.
r_d	=	Soil flexibility factor.

APPENDIX C: FRAGILITY CURVE THEORY

β_c	=	Normalized composite log-normal deviation.
Φ	=	Standard log-normal cumulative distribution function.
A_i	=	Median spectral acceleration necessary to cause the i^{th} damage state to occur.
DS_i	=	i^{th} damage state.
S_a	=	Spectral acceleration.

APPENDIX D: CAPACITY/DEMAND RATIOS FOR BRIDGE MEMBERS AND COMPONENTS

$\Delta_{eq}(d)$	=	Maximum calculated relative displacement due to earthquake loading.
$\Delta_i(d)$	=	Maximum possible movement resulting from temperature, shrinkage and creep shortening.
$\Delta_s(c)$	=	Available capacity of the expansion joint or bearing for movement.
μ	=	Ductility indicator.
$\rho(c)$	=	Volumetric ratio of existing transverse reinforcement.
$\rho(d)$	=	Required volumetric ratio of transverse reinforcement.
A_b	=	Area of the spliced bar.
A_g	=	Gross area of column.
$A_L(c)$	=	Effective peak ground acceleration at which liquefaction failures are likely to occur.
$A_L(d)$	=	Effective acceleration coefficient for the site.
$A_{tr}(c)$	=	Area of transverse reinforcing normal to potential splitting cracks.
B	=	Width of superstructure.
b_c	=	Width of the column.
b_{min}	=	Minimum width of the column cross section.
c	=	Lesser of the clear cover over the bar, or half the clear spacing between adjacent bars.
d_b	=	Diameter of longitudinal reinforcement.
f'_c	=	Concrete compression strength.
f_y	=	Yield stress of the longitudinal reinforcement.
f_{yt}	=	Yield stress of transverse reinforcement.
H	=	Height.

k_3	=	Effectiveness of transverse bar anchorage.
k_s	=	Constant for reinforcing steel with a yield stress of f_y .
L	=	Distance between joints.
$L_a(c)$	=	Effective anchorage length of longitudinal reinforcement.
$L_a(d)$	=	Required effective anchorage length of longitudinal reinforcement.
L_c	=	Height of the column.
L_s	=	Splice length.
$N(c)$	=	Actual support length provided.
$N(d)$	=	Minimum seat width.
P_c	=	Axial compressive load on the column.
s	=	Spacing of transverse reinforcement.
$V_b(c)$	=	Nominal ultimate capacity of the component in the direction under consideration.
$V_b(d)$	=	Seismic force acting on the component.
$V_e(d)$	=	Maximum calculated elastic shear force.
$V_f(c)$	=	Final shear resistance of the damaged column.
$V_i(c)$	=	Initial shear resistance of the undamaged column.
$V_u(d)$	=	Maximum column shear force resulting from plastic hinging at both the top and bottom of the column.

GREEK ALPHABET

A	α	alpha
B	β	beta
Γ	γ	gamma
Δ	δ	delta
E	ε	epsilon
Z	ζ	zêta
H	η	êta
Θ	θ	thêta
I	ι	iota
K	κ	kappa
Λ	λ	lamda
M	μ	mu
N	ν	nu
Ξ	ξ	xi
O	\omicron	omikron
Π	π	pi
P	ρ	rho
Σ	σ, ς	sigma
T	τ	tau
Y	υ	upsilon
Φ	ϕ	phi
X	χ	chi
Ψ	ψ	psi
Ω	ω	omega

CHAPTER 1: SEISMIC RETROFITTING OF HIGHWAY BRIDGES

1.1. GENERAL

Many bridges in the United States are inadequate for seismic loads and could be seriously damaged or suffer collapse in a relatively small earthquake. Major structural damage has occurred in Alaska, California, Washington and Oregon due to earthquake ground shaking. Some of these failures occurred at relatively low levels of ground motion and although the risk of bridge collapse is lower in the central and eastern United States, ground motions large enough to cause damage have a 10 percent chance of occurring within the next 50 years in 37 of the 50 states. In some states, this could lead to bridge collapse, and to remedy this situation, retrofitting or replacement of deficient structures is necessary. This is done by identifying bridges at risk, evaluating their vulnerability for collapse or major seismic damage, and initiating a program to reduce this risk.

Retrofitting is the most common method of mitigating risks; however, its cost may be so prohibitive that abandoning the bridge (total or partial closure with restricted access) or replacing it altogether with a new structure may be favored. Alternatively, doing nothing and accepting the consequences of damage is another possible option. The decision to retrofit, abandon, replace, or do-nothing requires that both the importance and degree of vulnerability of the structure be carefully evaluated. Limited resources will generally require that deficient bridges be prioritized, with important bridges in high risk areas being given the first priority for retrofitting.

This manual contains procedures for evaluating and upgrading the seismic resistance of existing highway bridges. Specifically, it contains:

- A screening process to identify and prioritize bridges that need to be evaluated for seismic retrofitting.
- A methodology for quantitatively evaluating the seismic capacity of a bridge and determining the overall effectiveness of alternative retrofitting measures, including cost and ease of installation.
- Retrofit approaches and corresponding techniques for increasing the seismic resistance of existing bridges.

This process is illustrated in figure 1-1. A bridge may be exempt from retrofitting if it is located in the lowest seismic zone, or has limited remaining useful life. Temporary bridges and those closed to traffic, may also be exempt. Details are provided in section 1.4.6.

This manual does not prescribe rigid requirements as to when and how bridges are to be retrofitted. The decision to retrofit a bridge depends on a number of factors, several of which are outside the realm of engineering. These include, but are not limited to, the availability of funding

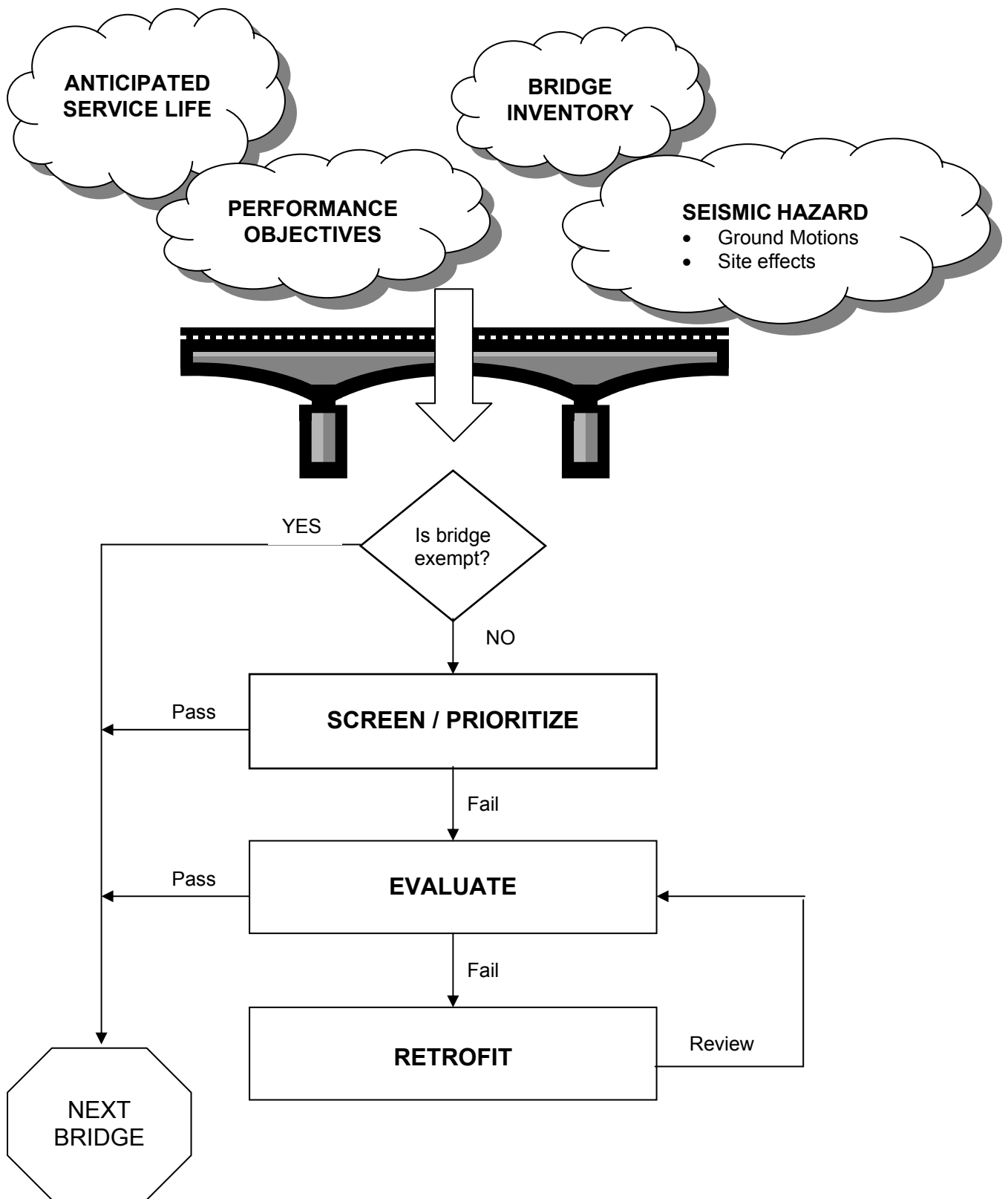


Figure 1-1. Overview of the retrofitting process for highway bridges.

and a number of political, social, and economic issues. This manual focuses on the engineering factors.

This manual is intended for use on conventional steel and concrete highway bridges with spans not exceeding 150 m (500 ft). Suspension bridges, cable-stayed bridges, arches, long-span trusses, and movable bridges are not covered. However, many of the procedures and techniques presented here can be applied to these types of structures, if appropriate judgment is used. This is particularly true for the substructures of truss bridges, for example. Although specifically developed for highway bridges, this manual may also be applicable to other types of bridges.

1.2. BACKGROUND

Within the United States, the first attempts to seismically retrofit bridges took place in the aftermath of the 1971 San Fernando earthquake in southern California. This earthquake has often been cited as a watershed event in bridge engineering since it demonstrated quite dramatically that the bridge design practices of the time did not guarantee that bridges would perform well during an earthquake, even if the earthquake was of moderate intensity.

Although bridge failures during this earthquake could be attributed to deficiencies in several types of structural components, initial retrofit measures focused on the potential for loss of support at bridge bearing seats. The principal retrofit strategy was to add restrainer cables or high strength bars within bridge superstructures in order to limit relative movements at expansion joints, and to tie individual spans to the bridge piers. A program was initiated in California to retrofit all bridges that had vulnerable expansion joints. Some believed at the time that this could prevent most, if not all, bridge failures at a minimum cost; however, this was not the case.

During the 1987 Whittier Narrows earthquake, a bridge that had been retrofitted with expansion joint restrainers suffered severe column damage, threatening the overall stability of the bridge (Wipf et al., 1997). This poor performance prompted renewed interest in column retrofitting, and research efforts were intensified to develop suitable methods for improving the seismic performance of existing reinforced concrete columns. Much of this research was conducted at the University of California at San Diego and was initially focused on the addition of steel shells (or jackets) to enhance confinement of the reinforcing steel within the columns (Chai et al., 1992). Unfortunately, the 1989 Loma Prieta earthquake occurred before Caltrans could begin a state-wide column retrofitting program. The most dramatic failure during this earthquake was the collapse of the Cypress Viaduct in Oakland due to column joint failures. Although this two-level structure had been retrofitted with expansion joint restrainers prior to the earthquake, large portions of the upper deck collapsed onto the lower deck, crushing vehicles and resulting in a number of deaths (Housner, 1990).

The Loma Prieta earthquake also demonstrated that the early restrainer designs were inadequate. Many of these designs relied on too few restrainers while others caused failures to occur elsewhere in the structure, such as in the diaphragms at either side of expansion joints (Yashinsky, 1997). Many of these deficiencies had been identified through research and refined

analysis (Selna and Malvar, 1987) and were not entirely unexpected. Still, it emphasized the need to review earlier bridge retrofits.

Since the Loma Prieta earthquake, there has been a major effort to perform comprehensive seismic retrofits on a large number of bridges in California. Initially, this effort was focused on bridges with single column piers, which were believed to be the most vulnerable to collapse. However, many bridges with multi-column piers collapsed or were severely damaged during the 1994 Northridge earthquake, and bridges of this type were subsequently added to the Caltrans retrofit program (Buckle, 1994).

Other states besides California now have active programs in seismic retrofitting. Washington and Nevada, for example, have sponsored research efforts and started seismic retrofit programs. Similarly, countries such as Japan and New Zealand have seismic retrofit programs. Due to these parallel efforts, significant progress has been made in the state-of-the-art of retrofitting bridge superstructures, columns, and foundations.

The Federal Highway Administration (FHWA) also became a major sponsor of bridge seismic research shortly after the 1971 San Fernando earthquake, including research on the retrofitting of existing bridges. An early research project dealing with the retrofitting of bridges was conducted at the Illinois Institute of Technology (Robinson et al., 1979). The first known guidelines for retrofitting highway bridges were published by FHWA in 1981, in a report titled *Seismic Design Guidelines for Highway Bridges*, FHWA-RD-81-081. This was followed in 1983 by the publication of the FHWA *Retrofitting Guidelines for Highway Bridges*, which contained recommendations intended for national use (FHWA-RD-83-007, ATC, 1983). In addition to providing formal screening and evaluation procedures, these guidelines presented retrofit concepts that in many cases had not been used in practice at that time. Concepts were provided for several different bridge components besides expansion joints including bridge columns, abutments and footings. Over the years, many of these concepts have been developed and refined into methods that are commonly used today. These procedures and techniques are also included in the *Seismic Design and Retrofit Manual*, FHWA-IP-87-6, published by FHWA in 1987.

Since 1992, FHWA has sponsored a multi-year research program to advance the state-of-the-practice in seismic retrofitting of bridges. This work was conducted at the National Center for Earthquake Engineering Research (NCEER), later to become the Multidisciplinary Center for Earthquake Engineering Research (MCEER). The project's first product was FHWA's *Seismic Retrofit Manual for Highway Bridges* that was published in 1995 (FHWA-RD-94-052, FHWA, 1995). This revision reflected advancements in the practice of seismic retrofitting that had occurred since 1983. Other products of this research program included improved methods for restrainer design (Randall et al., 1999; DesRoches and Fenves, 1998); methods for improving the performance of older steel bridge bearings (Mander et al., 1998a); improved methods of analysis and retrofit of reinforced concrete columns (Dutta et al., 1999); retrofit methods for multi-column reinforced concrete piers (Mander et al., 1996a and b); and a better understanding of the performance of retrofits that use both conventional and seismic isolation elastomeric bearings (Wendichansky et al., 1998). This program culminated in the preparation of this current FHWA

manual, which presents not only the results of FHWA research at MCEER, but also from throughout the United States and the world.

1.3. PHILOSOPHY

It has been common practice to design new bridges and buildings for a single-level of earthquake ground motion. This ground motion, often called the *design earthquake*, represents the largest motion that can be reasonably expected during the life of the bridge. Implied in such a statement is the fact that ground motions larger than the *design earthquake* may occur during the life of the bridge, but the likelihood of this happening is small. This likelihood is usually expressed as the *probability of exceedance*, and it may also be described by a *return period* in years. When setting the seismic hazard level, most design specifications that are intended for regions of varying seismicity use the same probability of exceedance from one region to another. This ‘uniform hazard’ approach is considered to be more rational than using the maximum historical event for each region.

The *Standard Specification for Highway Bridges* (AASHTO, 2002) in the United States adopted a uniform hazard approach following the 1989 Loma Prieta earthquake, and chose a level of hazard that had a 10 percent probability of exceedance in a 50-year exposure period (the assumed life of a bridge). This corresponded to a ground motion with a return period of about 500 years. During the development of the *AASHTO LRFD Specification* in the mid-nineties, the life of the average highway bridge was reassessed at 75 years and the exposure period was adjusted accordingly (AASHTO, 1998). The probability of exceedance was then raised to 15 percent to maintain (approximately) the same return period (500 years).

At the same time as adopting this uniform hazard approach, a corresponding set of performance standards was included in the philosophy of the 1992 *AASHTO Specifications* (AASHTO, 2002). These are given in Art. 1.1 of the Specification and summarized below:

- Small to moderate earthquakes should be resisted within the elastic range, without significant damage.
- Realistic seismic ground motion intensities and forces be used in the design procedures.
- Exposure to shaking from large earthquakes should not cause collapse of all or part of the bridge. Where possible, damage that does occur should be readily detectable and accessible for inspection and repair.

A set of basic concepts for seismic design was derived from this philosophy (Art. 1.3, AASHTO, 2002), and is summarized below:

- Hazard to life is minimized.
- Bridges may suffer damage but should have a low probability of collapse.
- Function of essential bridges is maintained.
- Ground motions used in design should have a low probability of being exceeded in the normal lifetime of the bridge.

While characterized by a lack of specificity, these criteria were a significant advance over the then prevailing requirements for seismic design.

In like manner, previous retrofit guidelines and manuals have also used a single-level of earthquake ground motion (a 500-year event) for representing the earthquake hazard, and adopted the same performance criteria as in the then current AASHTO Specifications for bridge design.

The assumption is made in single-level design and retrofit, that if performance under the *design earthquake* is satisfactory, it will be satisfactory at all other levels of ground motion, both smaller and larger. Such an assumption is generally not true as seen in recent earthquakes in California, Costa Rica, Japan, Turkey and Taiwan (figures 1-2 to 1-5). It would be true for a smaller event if elastic performance was required at the design ground motion, and it may also be true for a larger event, if it exceeded the design ground motion by only a small margin (i.e., less than 50 percent), and there was a sufficient reserve of strength in the bridge to accommodate this higher demand.

However, in many areas of the United States, these larger ground motions can be three or four times the design ground motions and may cause instability and collapse. Although such ground motions rarely happen, their occurrence should be explicitly considered in the design and retrofit process and a ‘multi-level’ rather ‘single-level’ design process should be used. In addition, performance requirements should be adjusted for ground motions of different sizes, with higher levels of performance being expected for smaller motions and lesser levels of performance for larger motions.

Performance-based design provides a format for addressing these needs in a rational manner. It explicitly allows for different performance expectations for bridges of varying importance while subject to different levels of seismic hazard. Accordingly, this manual recommends a performance-based approach to the seismic retrofitting of highway bridges in the United States.

This relationship is shown in figure 1-6. Representation of the hazard and performance expectations by discrete zones (or levels) is necessary given the current state-of-the-art, and this leads to the bar chart shown in this figure. Nevertheless, the trends are the same: high performance standards in high hazard zones imply higher costs.

1.4. SEISMIC PERFORMANCE CRITERIA

1.4.1. PERFORMANCE LEVELS

As noted in the previous section, this manual presents a performance-based approach to the seismic retrofitting of highway bridges. This means that the expected performance of the retrofitted bridge is explicitly recommended for different levels of earthquake ground motion. In this manual, performance criteria are defined for four performance levels. These are given as follows:

Performance Level 0 (PL0): No minimum level of performance is recommended.

Performance Level 1 (PL1): Life safety. Significant damage is sustained during an earthquake and service is significantly disrupted, but life safety is assured. The bridge may need to be replaced after a large earthquake.

Performance Level 2 (PL2): Operational. Damage sustained is minimal and full service for emergency vehicles should be available after inspection and clearance of debris. Bridge should be repairable with or without restrictions on traffic flow.

Performance Level 3 (PL3): Fully Operational. Damage sustained is negligible and full service is available for all vehicles after inspection and clearance of debris. Any damage is repairable without interruption to traffic.

The terms *negligible* damage, *minimal* damage, and *significant* damage are used in the above performance criteria. These terms are explained below:

- Minimal damage includes minor inelastic response and narrow flexural cracking in concrete. Permanent deformations are not apparent and repairs can be made under non-emergency conditions with the possible exception of superstructure expansion joints which may need removal and temporary replacement.
- Significant damage includes permanent offsets and cracking, yielded reinforcement, and major spalling of concrete, which may require closure to repair. Partial or complete replacement of columns may be required. Beams may be unseated from bearings but no span should collapse. Similarly, foundations are not damaged except in the event of large lateral flows due to liquefaction, in which case inelastic deformation in piles may be evident.
- Negligible damage includes evidence of movement, and/or minor damage to nonstructural components, but no evidence of inelastic response in structural members or permanent deformations of any kind.

Higher levels of performance may be specified by the owner. For example, the following criteria might be used for extremely important bridges:

- No damage is sustained and full service is available to all traffic immediately after the earthquake. No repairs are required.

Generally, the performance criteria vary with level of earthquake ground motion, bridge importance and anticipated service life. In this manual, these objectives are defined for two ground motion levels (a *lower* and an *upper* level), two importance classifications (*standard* and *essential*), and three service life categories (ASL 1, 2 and 3), as discussed below.

Figure 1-2 (right).
Collapse of the link span at Tower E9 of the
San Francisco Oakland Bay bridge due to
inadequate seat lengths and anchor bolts.



Loma Prieta earthquake, 1989



Loma Prieta earthquake, 1989

Figure 1-3 (left).
Collapse of the two-level Cypress Viaduct on
I-880 in Oakland due to brittle shear failure at
the connection between the upper and lower
levels of the viaduct.



Chi Chi earthquake, 1999

Figure 1-4 (right).
Collapse of end spans in the
Shi Wei bridge in Taichung,
due to ground failure and
nearby fault rupture.



Chi Chi earthquake, 1999

Figure 1-5 (left).
Diagonal shear crack in lightly
reinforced concrete pier of the Wu
Shu bridge in Taichung.

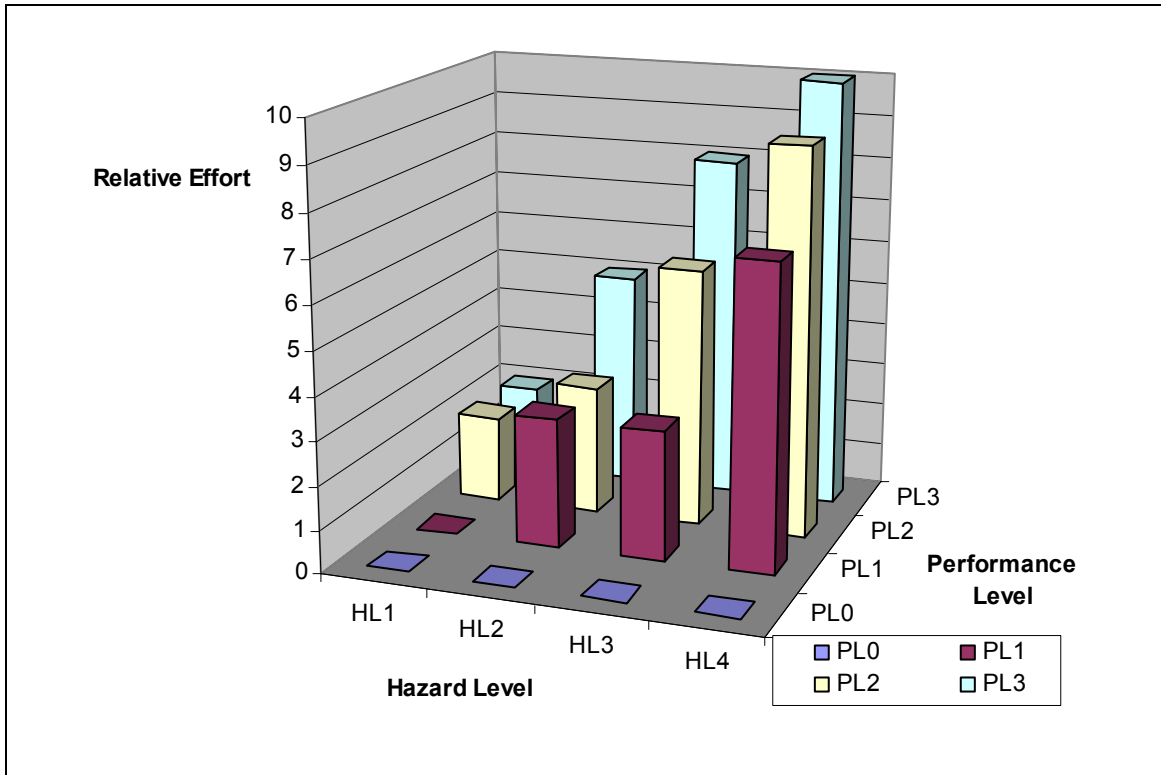


Figure 1-6. Conceptual relationship between relative effort, increasing hazard and performance criteria implied in this manual.

1.4.2. EARTHQUAKE GROUND MOTION LEVELS

The *lower level* (LL) earthquake ground motion is one that has a reasonable likelihood of occurrence within the life of the bridge (assumed to be 75 years), i.e., it represents a relatively small but likely ground motion¹. It is common practice to use a probability of exceedance to characterize the motion, as noted in section 1.3. Accordingly, the lower level motion has a relatively high probability of exceedance within the life of a bridge, and a figure of 50 percent is recommended for retrofit design. A 50 percent probability of exceedance in 75 years corresponds to a return period of about 100 years (table 2-1).

By contrast, the *upper level* (UL) earthquake ground motion has a finite, but remote, probability of occurrence within the life of the bridge; i.e., it represents a large but unlikely ground motion². Just as for the lower level motion, it is common practice to use a probability of exceedance to characterize this motion. Thus the upper level earthquake ground motion has a relatively low

¹ This ground motion is sometimes called the *frequent* earthquake. In the *NCHRP 12-49 Recommended LRFD Guidelines for Seismic Design* (ATC/MCEER, 2003) it is called the *expected* earthquake, and in the *Caltrans Seismic Design Methodology* (Caltrans, 1999) it is called the *functional evaluation earthquake (FEE)*.

² This ground motion is sometimes called the *rare* earthquake. In the *NCHRP 12-49 Recommended LRFD Guidelines for Seismic Design* (ATC/MCEER, 2003) it is the *maximum considered earthquake (MCE)*, and in the *Caltrans Seismic Design Methodology* (Caltrans, 1999) it is the *safety evaluation earthquake (SEE)*.

probability of exceedance within the life of a bridge. In this manual, the upper level motion has a 7 percent probability of exceedance in 75 years, which corresponds to a return period of about 1,000 years (table 2-1).

Spectral ordinates and peak ground accelerations for both the lower and upper level ground motions may be found using the CD-ROM included in this manual (inside back cover)³. Bridge sites may be identified by zip code or, more accurately, by latitude and longitude. However, values given on this CD are in terms of an exposure period of 50 years rather than the 75-year bridge life assumed above. Therefore, equivalent exceedance probabilities for a 50-year life are required to use this CD, as follows:

- The return period for an earthquake ground motion with a 50 percent probability of exceedance in 75 years is 108 years. However, this return period is only 72 years for a ground motion with a 50 percent probability of exceedance in 50 years. For the purpose of this manual, this lesser return period is considered to be close enough to the specified value of 100 years (table 1-2), and that values for the 50-year life may be used. Therefore, for the lower level ground motions, use data from the CD for 50 percent probability of exceedance in 50 years.
- The return period for an earthquake ground motion with a seven percent probability of exceedance in 75 years is approximately the same as that for a ground motion with five percent probability of exceedance in 50 years (both are about 1,000 years). Therefore, for the upper level ground motions, use data from the CD for five percent probability of exceedance in 50 years.

Alternatively, spectral ordinates and peak ground accelerations may be obtained for the upper level ground motion from the following web site maintained by the U.S. Geological Survey: <http://eqhazmaps.usgs.gov>. Mapped values are given for regions within the United States, and numerical values are given for specific locations according to zip code, or longitude and latitude. As with the CD-ROM, these values are expressed in terms of a 50-year bridge life and equivalent exceedance probabilities must be found to use this site, as described for the CD. At this time, this site does not give spectral ordinates and accelerations for the lower level ground motions (100 years) and the only known, readily available, source of this data is the CD-ROM included with this manual.

Some performance-based specifications for bridges and buildings have recommended a three percent probability of exceedance in 75 years for the upper level ground motions; but these specifications are for new construction and not necessarily appropriate for the retrofit of existing structures. Seismic resistance is much easier to provide in new structures than in existing ones. The selection of the reduced upper level motions for retrofitting is a compromise between the need to provide life safety and adequate performance for these less frequent motions and the limited resources of the owner. Keep in mind that these performance criteria are general recommendations and subject to change by the owner (or engineer) when specific circumstances of a particular bridge make it necessary.

³ This CD contains the seismic hazard maps and curves published by USGS in 1996. Updated maps were published in 2002 but not for the 1000-year return period. See section 2.3.

1.4.3. BRIDGE IMPORTANCE

Classification of bridge importance based on traffic counts and detour lengths has been proposed in the past and importance indices developed. But such quantitative methods do not usually include many non-technical issues that directly affect importance and are loosely called socio-economic factors. Instead, a broad classification based on engineering judgment is preferred, and in this manual two such classes are recommended: essential and standard. *Essential* bridges are those that are expected to function after an earthquake or which cross routes that are expected to remain open immediately following an earthquake. All other bridges are classified as *standard*. The determination of importance is therefore subjective and consideration should be given to societal/survival and security/defense requirements when making this judgment.

An *essential* bridge is, therefore, one that satisfies one or more of the following conditions:

- A bridge that is required to provide secondary life safety; e.g., one that provides access to local emergency services such as hospitals. This category also includes those bridges that cross routes that provide secondary life safety, and bridges that carry lifelines such as electric power and water supply pipelines.
- A bridge whose loss would create a major economic impact; e.g., one that serves as a major link in a transportation system, or one that is essential for the economic recovery of the affected region.
- A bridge that is formally defined by a local emergency plan as critical; e.g., one that enables civil defense, fire departments, and public health agencies to respond immediately to disaster situations. This category also includes those bridges that cross routes that are defined as critical in a local emergency response plan and those that are located on identified evacuation routes.
- A bridge that serves as a critical link in the security and/or defense roadway network. Security and defense requirements may be evaluated using the 1973 Federal-aid Highway Act, which required that a plan for defense highways be developed by each state. Now called STRAHNET, this defense highway network provides connecting routes to military installations, industries, and resources and is part of the National Highway System.

1.4.4. ANTICIPATED SERVICE LIFE

An important factor in deciding the extent to which a bridge should be retrofitted is the anticipated service life (ASL). Retrofitting a bridge with a short service life is difficult to justify for two reasons: it is not economical and the design earthquake is unlikely to occur during the remaining life of the structure. On the other hand, a bridge that is almost new or being rehabilitated to extend its service life, should be retrofitted for the longer remaining service life.

Estimating remaining life is not an exact science and depends on many factors such as age, structural condition, specification used for design, and capacity to handle current and future

traffic. Nevertheless, estimates can be made, at least within broad ranges, for the purpose of determining a bridge's remaining service life and, subsequently, a retrofit category. Three such categories are used in this manual, as defined in table 1-1. When setting these categories, it was noted that new bridges are assumed to have a service life of 75 years in the *AASHTO LRFD Specification* (AASHTO, 1998), and this life span was then divided into three categories for the purpose of assigning retrofit levels (retrofit categories) according to age and remaining life. It is recognized that many long-span bridges have service lives far greater than 75 years, but these are outside the scope of this manual. Bridges in benign climates and those located on low-density routes may also have service lives in excess of 75 years.

Bridges in category ASL 1 are considered to be near the end of their service life and retrofitting may not be economically justified. Thus, these bridges need not be retrofitted and are assigned to the lowest seismic retrofit category, i.e., category A (see section 1.6). Bridges in category ASL 3 are almost new, and retrofitting to the standard of a new design may be justified. Those in category ASL 2 fall between these two extremes and a lesser standard is acceptable. However, the owner may always choose to retrofit to a higher standard as circumstances permit.

Table 1-1. Service life categories.

SERVICE LIFE CATEGORY	ANTICIPATED SERVICE LIFE
ASL 1	0 - 15 yrs
ASL 2	16 - 50 yrs
ASL 3	> 50 yrs

Bridges are often rehabilitated toward the end of their service life to address deficiencies that have accumulated over time (e.g., deteriorated deck slabs, frozen bearings and damaged expansion joints), improve safety, and to accommodate increased traffic volume. As a consequence, a bridge with 15 years, or less, of life may, after rehabilitation, have a new service life of 35 years, and in so doing, the service life category (ASL) for the bridge has been lifted from ASL 1 to ASL 2 (table 1-1). The bridge should now be reevaluated for seismic performance, which should be done at the same time as planning the other rehabilitation. In this way, retrofit measures (if needed) can be implemented at the same time. By taking advantage of the contractor being on site, the cost of the seismic retrofit may be significantly reduced.

1.4.5. SELECTION OF PERFORMANCE LEVEL

Recommended minimum performance levels are given in table 1-2 according to the level of earthquake ground motion, bridge importance and service life category, as defined above. If retrofitting to these levels cannot be justified economically, the owner may choose a lower level. On the other hand, for certain classes of bridges, the owner may choose a higher level than that recommended here. An example of such a case is the bridges on STRAHNET, which are critically important to the operation of national or regional transportation routes. It is likely that some of these bridges are of sufficient importance to justify site-specific and structure-specific performance criteria. Such bridges may fall outside the scope of this manual.

1.4.6. RETROFITTING PROCESS FOR DUAL LEVEL GROUND MOTIONS

As noted in section 1.3, retrofitting is only one of several courses of action when faced with a bridge that is seismically vulnerable. Others include bridge closure, bridge replacement, and acceptance of the damage and its consequences. Bridge closure or replacement is usually not justified by seismic deficiency alone and will generally only be an option when other deficiencies exist. Therefore, for all practical purposes, a choice is made between strengthening and accepting the risk. This decision often depends on the importance of the bridge and on the cost and effectiveness of the proposed retrofit.

Budget constraints and limited resources prevent the simultaneous retrofit of all of the deficient bridges on the highway system, and the most critical bridges should be upgraded first. The selection and prioritizing of bridges for retrofitting requires an appreciation of not just the engineering issues but also the economic, social, and practical aspects of the situation.

Since it is recommended above that the seismic performance of a bridge be checked for two levels of earthquake ground motion (lower level and upper level) the overall retrofitting process has two distinct stages:

- Stage 1. Screening, evaluation and retrofitting for the lower level earthquake ground motion, and
- Stage 2. Screening, evaluation and retrofitting for the upper level earthquake ground motion.

It is not possible to combine these two stages into one, since the performance criteria for each is very different. For example, the criteria for the lower level ground motion includes no structural damage and no repair (i.e., elastic behavior is expected) whereas for the upper level ground motion, damage is acceptable provided collapse does not occur and, for some bridges, access for emergency vehicles is available (i.e., inelastic behavior is expected).

Each stage comprises the three steps discussed in section 1.1 and is shown schematically in figure 1-1, i.e., screening, evaluation, and retrofitting for the relevant ground motion. The breakdown of each stage into these steps is illustrated in figure 1-7, and discussed in sections 1.7 and 1.8.

Table 1-2. Minimum performance levels for retrofitted bridges.

EARTHQUAKE GROUND MOTION	BRIDGE IMPORTANCE and SERVICE LIFE CATEGORY					
	Standard			Essential		
	ASL 1	ASL 2	ASL 3	ASL 1	ASL 2	ASL 3
Lower Level Ground Motion 50 percent probability of exceedance in 75 years; return period is about 100 years.	PL0 ⁴	PL3	PL3	PL0 ⁴	PL3	PL3
Upper Level Ground Motion 7 percent probability of exceedance in 75 years; return period is about 1,000 years.	PL0 ⁴	PL1	PL1	PL0 ⁴	PL1	PL2
Notes: <ol style="list-style-type: none"> Anticipated Service Life categories are: <ul style="list-style-type: none"> ASL 1: 0 – 15 years ASL 2: 16 – 50 years ASL 3: > 50 years Performance Levels are: <ul style="list-style-type: none"> PL0: No minimum level of performance is recommended. PL1: Life safety. Significant damage is sustained and service is significantly disrupted, but life safety is preserved. The bridge may need to be replaced after a large earthquake. PL2: Operational. Damage sustained is minimal and service for emergency vehicles should be available after inspection and clearance of debris. Bridge should be repairable with or without restrictions on traffic flow. PL3: Fully Operational. Damage sustained is negligible and full service is available for all vehicles after inspection and clearance of debris. Damage is repairable without interruption to traffic. Spectral ordinates and peak ground accelerations may be found for the Upper Level earthquake ground motion from http://eqhazmaps.usgs.gov. Ordinates and ground accelerations may be found for <i>both</i> the Upper and Lower Level ground motions from the CD-ROM: <i>Seismic Hazard Curves and Uniform Hazard Response Spectra for the United States</i>, (Frankel and Leyendecker, 2001; see section 2.3). A copy of this CD is included with this manual (see inside back cover). Bridges assigned a Performance Level of PL0 have 15 years, or less, anticipated service life (ASL) and are candidates for replacement or rehabilitation. 						

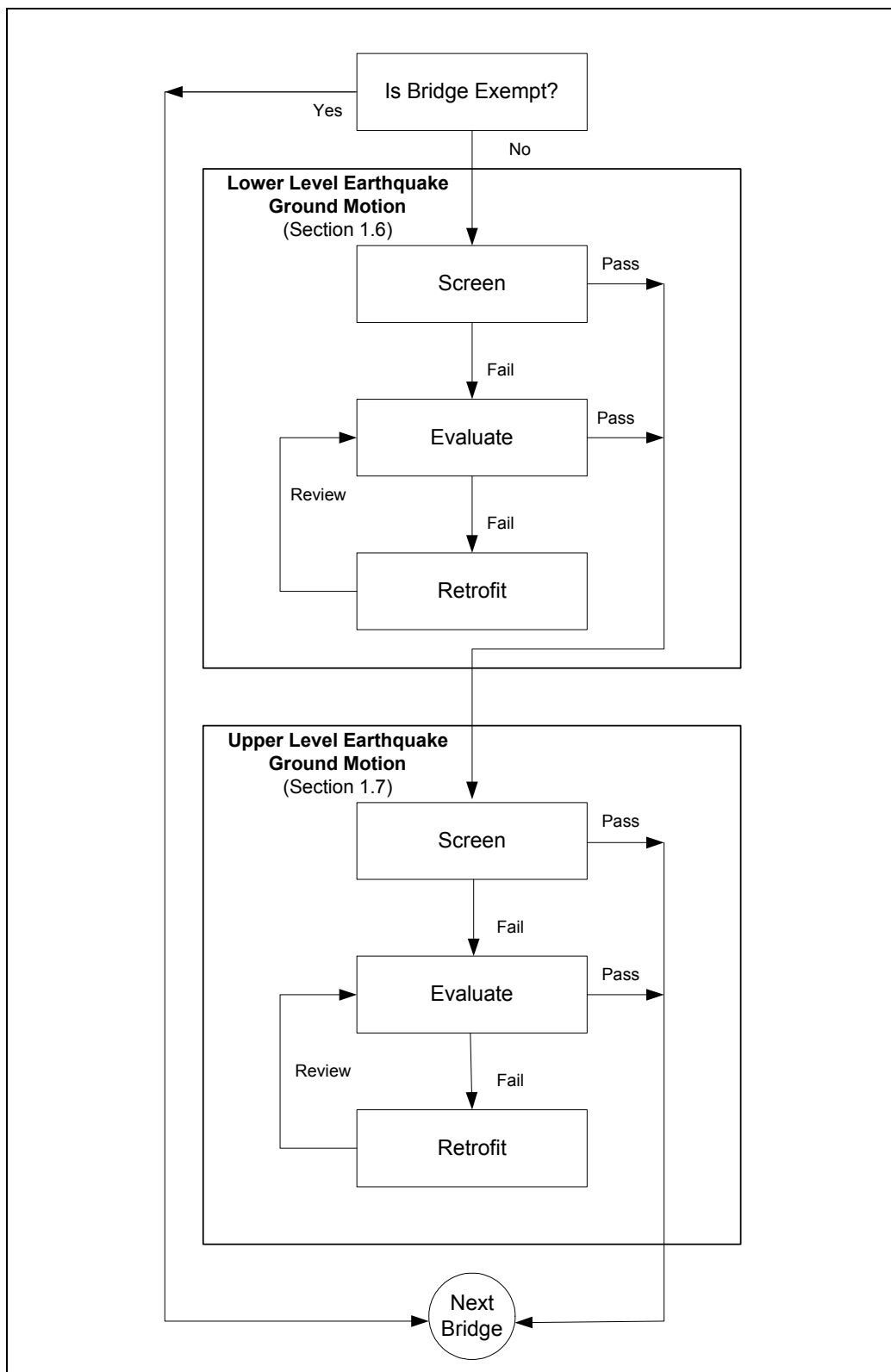


Figure 1-7. Retrofit process for dual level earthquake ground motions.

1.4.7. EXEMPT BRIDGES

A bridge is exempt from retrofitting for both levels of ground motion if it satisfies any one of the following criteria:

- The bridge has 15 years or less of anticipated service life (section 1.4.4).
- The bridge is ‘temporary’ (i.e., anticipated service life is 15 years or less).
- The bridge is closed to traffic and does not cross an active highway, rail or waterway.

A bridge is exempt from retrofitting for the upper level ground motion if it meets the criteria for Seismic Retrofit Category A (section 1.6) for this level of motion.

1.5. SEISMIC HAZARD LEVEL

The Seismic Hazard Level (SHL) at a bridge site is determined by the intensity of ground shaking in the rock below the site and the amplification of this motion by the overlying soils. Motions at the surface may be considerably greater than in the rock below. These two factors are treated separately below and then combined to define the SHL in section 1.5.4. Other geotechnical factors, such as liquefaction and fault rupture, can influence the hazard at a bridge site and these are also briefly described in this section.

1.5.1. GROUND MOTION REPRESENTATION

Earthquake ground motion may be characterized by either:

- a. The peak ground acceleration expected at a site in a given period of time, from which the design spectrum may be drawn based on several simplifying assumptions, or
- b. By two points on the design spectrum from which the remainder of the spectrum may be drawn using fewer, but more realistic, assumptions than in (a) above.

The earlier edition of this manual (FHWA, 1995) and the 1997 *AASHTO LRFD Bridge Design Specifications* (AASHTO, 1998) use the former method, whereas the NCHRP 12-49 provisions (ATC/MCEER, 2003) use the latter method, to take advantage of the improved accuracy that it offers. This edition of the retrofit manual also uses the latter two-point method.

The two points used to define the spectrum are *spectral ordinates* (peak structural accelerations) in bridges with periods of 0.2 and 1.0 second. For bridge sites on rock (site class B), these ordinates are identified as S_s and S_1 , respectively. The variation of these ordinates throughout the United States has been calculated for various return periods by the US Geological Survey (USGS), and the results are available (in both tabular and mapped formats) on the CD-ROM provided with this manual (inside back cover). Alternately, results for a selected number of return periods may be downloaded from the following web site: <http://eqhazmaps.usgs.gov>. Chapter 2 summarizes the development of these data and the method for constructing a design

spectrum from the given spectral ordinates. In lieu of using national ground motion maps, the spectral accelerations S_s and S_1 may be found from approved state ground motion maps.

1.5.2. GEOTECHNICAL FACTORS

Earthquake ground motions at a bridge site are not only dependent on the intensity of ground shaking in the rock below the site but also on the amplification of this motion by the overlying soils. The presence of one or more geotechnical hazards at the site, such as liquefaction and fault rupture, can also have a significant effect on the motion experienced by a bridge. These factors are discussed in this section.

1.5.2.1 Soil Amplification of Ground Motion

The behavior of a bridge during an earthquake is strongly related to the soil conditions at the site. Soils can amplify ground motions in the underlying rock, sometimes by factors of two or more. The extent of this amplification is dependent on the profile of soil types at the site and the intensity of shaking in the rock below. Sites are classified by type and profile for the purpose of defining the overall seismic hazard, which is quantified as the product of the soil amplification and the intensity of shaking in the underlying rock.

Site class definitions are given in table 1-3, where it is seen that sites are classified by their stiffness as determined by the shear wave velocity in the upper 30 m (100 ft). Standard Penetration Test (SPT) blowcounts and undrained shear strengths of soil samples from soil borings can also be used to classify sites as indicated in table 1-3. See chapter 2 for further details, including steps for classifying a site.

Site factors, for the site classes in table 1-3, are given in table 1-4. Site class B (soft rock) is taken to be the reference site category for the USGS and NEHRP MCE ground shaking maps. Site class B rock is therefore the site condition for which the site factor is 1.0. Site classes A, C, D, and E have separate sets of site factors for the short-period range (site factor F_a) and long-period range (site factor F_v), as indicated in table 1-4. These site factors generally increase as the soil profile becomes softer (in going from site class A to E). Except for site class A (hard rock), the factors also decrease as the ground motion level increases, due to the strongly nonlinear behavior of the soil. For a given site class, C, D, or E, these nonlinear site factors increase the ground motion more in areas having lower rock ground motions than in areas having higher rock ground motions. The levels of ground motion for use with table 1-4 are characterized by short-period (0.2 second) response spectral acceleration and long-period (1.0 second) response spectral acceleration on rock as mapped on USGS and NEHRP MCE national ground motion maps. Special considerations for site class F soils are discussed in chapter 2.

1.5.2.2 Geotechnical Hazards

Geotechnical hazards at bridge sites that can be triggered by earthquakes include soil liquefaction, soil settlement, slope failure (landslides and rock falls), surface fault rupture and flooding. In general, these hazards are examined independently of the rock ground motion and soil amplification effects described in the previous section.

Table 1-3. Site classes.

Site Class	Description
A	Hard rock with measured shear wave velocity, $\bar{v}_s > 1500$ m/sec (5,000 ft/sec)
B	Rock with $760 \text{ m/sec} < \bar{v}_s \leq 1500 \text{ m/sec}$ ($2,500 \text{ ft/sec} < \bar{v}_s \leq 5,000 \text{ ft/sec}$)
C	Very dense soil and soil rock with $360 \text{ m/sec} < \bar{v}_s \leq 760 \text{ m/sec}$ ($1,200 \text{ ft/sec} < \bar{v}_s \leq 2,500 \text{ ft/sec}$) or with either $\bar{N} > 50$ blows/0.30m (50 blows/ft) or $\bar{s}_u > 100$ kPa (2,000 psf)
D	Stiff soil with $180 \text{ m/sec} \leq \bar{v}_s \leq 360 \text{ m/sec}$ ($600 \text{ ft/sec} \leq \bar{v}_s \leq 1,200 \text{ ft/sec}$) or with either $15 \leq \bar{N} \leq 50$ blows/0.30m ($15 \leq \bar{N} \leq 50$ blows/ft) or $50 \text{ kPa} \leq \bar{s}_u \leq 100 \text{ kPa}$ ($1,000 \leq \bar{s}_u \leq 2,000$ psf)
E	Soil profile with $\bar{v}_s < 180$ m/sec (600 ft/sec) or with either $\bar{N} < 15$ blows/0.30m ($\bar{N} < 15$ blows/ft) or $\bar{s}_u < 150$ kPa (1000 psf), or any profile with more than 3 m (10 ft) of soft clay defined as soil with $PI > 20$, $w \geq 40$ percent and $\bar{s}_u < 25$ kPa (500 psf)
F	Soils requiring site-specific evaluations <ol style="list-style-type: none"> Peats or highly organic clays ($H > 3$ m [10 ft] of peat or highly organic clay where H = thickness of soil) Very high plasticity clays ($H > 8$ m [25 ft] with $PI > 75$) Very thick soft/medium stiff clays ($H > 36$ m [120 ft])
Exception: When the soil properties are not known in sufficient detail to determine the site class, site class D may be used. Site classes E or F need not be assumed unless the authority having jurisdiction determines that site classes E or F could be present at the site or in the event that site classes E or F are established by geotechnical data.	
Notes: <ol style="list-style-type: none"> \bar{v}_s is average shear wave velocity for the upper 30 m (100 ft) of the soil profile \bar{N} is the average Standard Penetration Test (SPT) blowcount (blows/0.30m or blows/ft) (ASTM D1586) for the upper 30 m (100 ft) of the soil profile \bar{s}_u is the average undrained shear strength in kPa (psf) (ASTM D2166 or D2850) for the upper 30 m (100 ft) of the soil profile PI is plasticity index (ASTM D4218) w is moisture content (ASTM D2216) The shear wave velocity for rock, Site Class B, shall be either measured on site or estimated for competent rock with moderate fracturing and weathering. Softer and more highly fractured and weathered rock shall either be measured on site for shear wave velocity or classified as Site Class C. The hard rock, Site Class A, category shall be supported by shear wave velocity measurements either on site or on profiles of the same rock type in the same formation with an equal or greater degree of weathering and fracturing. Where hard rock conditions are known to be continuous to a depth of 30 m (100 ft), surficial shear wave velocity measurements may be extrapolated to assess \bar{v}_s. Site classes A and B should not be used when there is more than 3 m (10 ft) of soil between the rock surface and the bottom of a spread footing. 	

Table 1-4. Site factors F_a and F_v .

(a) Values of F_a as a function of site class and short-period (0.2-sec) spectral acceleration, S_s

Site Class	Spectral Acceleration at Short-Period (0.2 sec), S_s^1				
	$S_s \leq 0.25$	$S_s = 0.50$	$S_s = 0.75$	$S_s = 1.00$	$S_s \geq 1.25$
A	0.8	0.8	0.8	0.8	0.8
B	1.0	1.0	1.0	1.0	1.0
C	1.2	1.2	1.1	1.0	1.0
D	1.6	1.4	1.2	1.1	1.0
E	2.5	1.7	1.2	0.9	0.9
F^2					
Notes: 1. Use straight-line interpolation for intermediate values of S_s . 2. Site-specific geotechnical investigation and dynamic site response analysis should be performed for class F soils.					

(b) Values of F_v as a function of site class and long-period (1.0-sec) spectral acceleration, S_1

Site Class	Spectral Acceleration at Long-Period (1.0 sec), S_1^1				
	$S_1 \leq 0.1$	$S_1 = 0.2$	$S_1 = 0.3$	$S_1 = 0.4$	$S_1 \geq 0.5$
A	0.8	0.8	0.8	0.8	0.8
B	1.0	1.0	1.0	1.0	1.0
C	1.7	1.6	1.5	1.4	1.3
D	2.4	2.0	1.8	1.6	1.5
E	3.5	3.2	2.8	2.4	2.4
F^2					
Notes: 1. Use straight-line interpolation for intermediate values of S_1 . 2. Site-specific geotechnical investigation and dynamic site response analysis should be performed for class F soils.					

Procedures for evaluating these hazards are presented in chapter 3. The consequences of these hazards in the free-field (e.g. ground settlement and fault displacements) are also addressed in that chapter. Methods for evaluating the effects of these hazards on the capacity and deformations of the bridge-foundation system are presented in chapter 6, and measures for mitigating them are described in chapter 11.

Assessing geotechnical hazards is a two-part procedure. In the first part, a quick screening evaluation is conducted. Generally, this can be accomplished using available information and field reconnaissance. If the criteria are satisfied, the risk is considered to be low and further evaluations of the hazard are not required. If a hazard cannot be screened out, more detailed evaluations are conducted in the second part of this procedure. This usually requires obtaining additional data to more rigorously assess the hazard and its consequences. Chapter 3 gives guidelines for initial hazard screening, together with a brief overview of methods for detailed hazard evaluation. Detailed methods for hazard evaluation are described in appendix B. Hazard screening and hazard evaluation should be carried out by geotechnical engineers, geologists, and seismologists, who have expert knowledge of these hazards and experience with their evaluation.

1.5.3. DETERMINATION OF DESIGN RESPONSE SPECTRUM

As noted in section 1.5.1, a two-point method is used to define the design response spectrum from which earthquake forces are calculated to determine seismic demand on a bridge due to a particular earthquake ground motion. Figure 1-8 shows how this spectrum is drawn from the two given points. It indicates that the S_s and S_1 ordinates are first scaled by the soil factors F_a and F_v and the resulting products S_{DS} and S_{D1} are used to plot the spectrum where:

$$S_{DS} = F_a \cdot S_s \quad \text{and} \quad S_{D1} = F_v \cdot S_1 \quad (1-1)$$

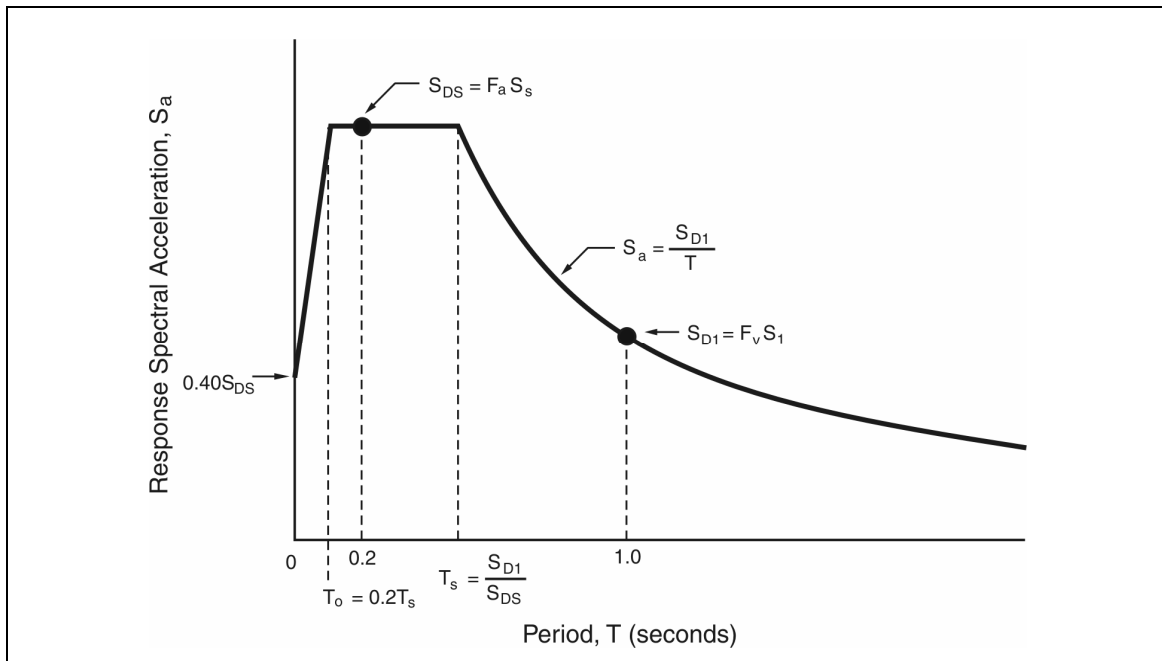


Figure 1-8. Construction of the seismic design response spectrum.

1.5.4. DETERMINATION OF SEISMIC HAZARD LEVEL

Each bridge is assigned a Seismic Hazard Level (SHL) as indicated in table 1-5, based on S_{DS} and S_{D1} , which are defined in section 1.5.3 to be the product of the spectral ordinates S_s and S_1 (section 1.5.1) and the soil factors F_a and F_v (section 1.5.2). In the event that two different hazard levels are indicated by table 1-5 for the same site, the higher level should be used.

The two footnotes to table 1-5 effectively limit boundaries for site classes E and F in Hazard Levels I and II to those of site class D. This is because of the greater uncertainty in the values of F_v and F_a for class E and F soils when ground shaking is relatively low ($S_1 < 0.10$ and $S_s < 0.25$).

Table 1-5. Seismic hazard level.

HAZARD LEVEL	Using $S_{D1} = F_v S_1$	Using $S_{DS} = F_a S_s$
I	$S_{D1} \leq 0.15$	$S_{DS} \leq 0.15$
II	$0.15 < S_{D1} \leq 0.25$	$0.15 < S_{DS} \leq 0.35$
III	$0.25 < S_{D1} \leq 0.40$	$0.35 < S_{DS} \leq 0.60$
IV	$0.40 < S_{D1}$	$0.60 < S_{DS}$
Notes: <ol style="list-style-type: none"> 1. For the purposes of determining the Seismic Hazard Level for Site Class E soils, the value of F_v and F_a need not be taken larger than 2.4 and 1.6 respectively, when S_1 is less than or equal to 0.10 and S_s is less than 0.25. 2. For the purposes of determining the Seismic Hazard Level for Site Class F soils, F_v and F_a values for Site Class E soils may be used with the adjustment described in Note 1 above. 		

1.6. PERFORMANCE-BASED SEISMIC RETROFIT CATEGORIES

Seismic retrofit categories (SRC) are used to identify minimum screening requirements, evaluation methods and retrofitting measures for deficient bridges. They are determined by the anticipated service life, importance, and the seismic hazard exposure of the bridge. There are four categories, A through D, in increasing order of rigor and complexity. SRC A is a default category, which means that bridges in this category do not need to be screened, evaluated or retrofitted. SRC D is the highest category requiring the most rigorous screening, evaluation, and retrofitting measures. SRC's perform a similar function to the SPC's (seismic performance categories) in the previous retrofit manual (FHWA, 1995). (The name has been changed to distinguish them from the SPC's used in the seismic design provisions of the *AASHTO Standard Specifications* (AASHTO, 2002), which are widely used for the seismic design of new bridges.)

Seismic retrofit categories are given in table 1-6 where they are determined by the performance level (PL) required, and the seismic hazard level (SHL) at the site.

Table 1-6. Performance-based seismic retrofit categories.

HAZARD LEVEL	PERFORMANCE LEVEL				
	During Upper Level Earthquake			During Lower Level Earthquake*	
	PL0: No Minimum Level	PL1: Life Safety	PL2: Operational	PL0: No Minimum Level	PL3: Fully Operational
I	A	A	B	A	C
II	A	B	B	A	C
III	A	B	C	A	C
IV	A	C	D	A	D

The steps required to determine an SRC are shown in figure 1-9 and are as follows:

Step 1. From the bridge records and other sources determine the:

- Importance of the bridge: either *standard* or *essential*,
- Anticipated service life of the bridge, and assign a service category: ASL 1 through ASL 3 (table 1-1), and
- Site class based on soil type and profile (table 1-3).

Step 2. Determine the performance level for the bridge (PL0 through PL3), based on the anticipated service life and bridge importance (table 1-2).

Step 3. Obtain the spectral accelerations S_s and S_1 , the soil factors F_a and F_v from table 1-4, and determine the hazard level using table 1-5. Determine the seismic retrofit category required to satisfy the performance objective for this event, using table 1-6. These steps are summarized as follows:

Step 3.1. Obtain the spectral ordinates, S_s and S_1 , from the CD-ROM in this manual or from the USGS web site: <http://eqhazmaps.usgs.gov>.

Step 3.2. Obtain the soil factors, F_a and F_v , for the site (table 1-4).

Step 3.3. Determine the seismic hazard level (SHL) based on $F_a S_s$ and $F_v S_1$ (table 1-5).

Step 3.4. Obtain the SRC for the required performance level from table 1-6.

This process is illustrated in example 1.1 in this chapter, and examples 4.1 and 4.2 in chapter 4.

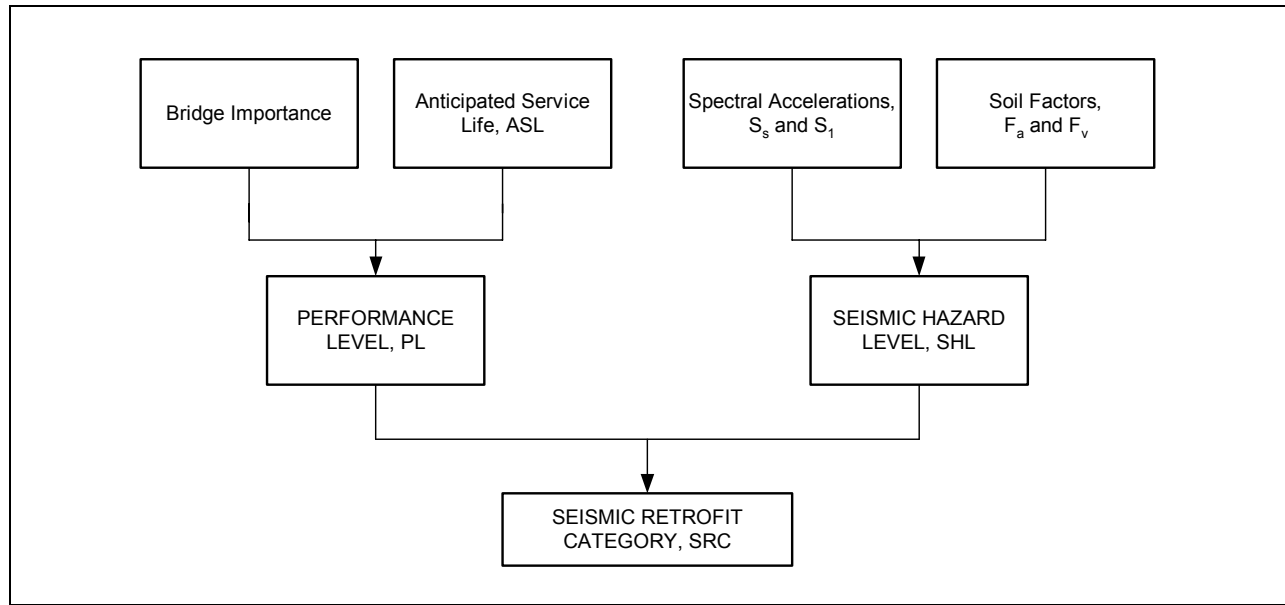


Figure 1-9. Determination of seismic retrofit category.

1.7. RETROFITTING PROCESS FOR THE LOWER LEVEL GROUND MOTION

The lower level earthquake ground motion has a return period of about 100 years and is therefore a relatively small motion. The performance required of any bridge for these motions (table 1-2) is elastic behavior, which is similar to the requirements for wind and braking loads. Indeed, in many parts of the United States, wind and braking loads may be larger than the earthquake loads for this return period and may govern for this stage.

The process of retrofitting bridges for the lower level earthquake ground motion is divided into three parts. These are:

- Preliminary screening of bridge inventory.
- Detailed evaluation of an existing bridge.
- Selection of retrofit strategy and design of retrofit measures.

Note that decisions are made at each step, based on the results obtained thus far, that determine the next step in the process. Bridges are passed through a series of checkpoints to assure that only those structures actually in need of retrofit will be strengthened.

As described in section 1.6, seismic retrofit categories (SRC) are used to recommend minimum requirements for evaluation and retrofitting. These requirements for the lower level ground motion are given in table 1-7.

Table 1-7. Minimum requirements.

ACTION	SEISMIC RETROFIT CATEGORY FOR THE LOWER LEVEL EARTHQUAKE				SEISMIC RETROFIT CATEGORY FOR THE UPPER LEVEL EARTHQUAKE			
	A	B ¹	C	D	A	B	C	D
Screening Components to be screened:	NR ²	-	seat widths, connections, columns, walls, footings and liquefaction	seat widths, connections, columns, walls, footings, abutments and liquefaction	NR	seat widths, connections and liquefaction	seat widths, connections, columns, walls, footings and liquefaction	seat widths, connections, columns, walls, footings, abutments and liquefaction
Evaluation Evaluation methods to be used ^{3,4} . See table 1-9.	NR	-	C	C	NR	A1/A2	B/C/D1/D2	C/D1/D2/E
Retrofitting Components to be retrofitted, if deficient:	NR	-	Yes	Yes	NR	Yes	Yes	Yes
	NR	-	Yes	Yes	NR	NR	Yes	Yes
	NR	-	NR	Yes	NR	NR	NR	Yes
	NR	-	Yes	Yes	NR	Yes	Yes	Yes
Notes:								
1. Seismic Retrofit Category B is not used when evaluating and/or retrofitting bridges for lower level ground motions.								
2. NR = Not Required.								
3. A1/A2 = No analysis; minimum capacity checks B = No analysis; component capacity checks C = Component C/D method using elastic dynamic analysis methods D1 = Capacity spectrum method.								
D2 = Structure C/D method; also called Nonlinear Static Procedure, or Displacement Capacity Evaluation								
E = Nonlinear dynamic method using inelastic time history analysis								
4. Selection of evaluation method also depends on bridge geometry: for irregular (complex) bridges, use Methods A, C, D2 and E as appropriate.								

The retrofitting process for this level of ground motion is described in the following sections where it will be seen to be a force-based approach. Displacements are not explicitly considered since they are assumed to be small and within the default capacity of the structure. This is a reasonable expectation provided yielding does not occur, bearing restraints do not fail, and soils do not soften at this level of ground motion.

1.7.1. SCREENING AND PRIORITIZATION FOR THE LOWER LEVEL GROUND MOTION

All bridges in the inventory should be checked for their lateral strength in both the transverse and longitudinal directions. This strength should be based on the elastic capacities of the members and foundations. Previous design calculations for wind and braking loads may be useful here. This capacity should then be checked against the seismic force (F) on the bridge, which can be conservatively estimated as:

$$F = S_{DS} W \quad (1-2)$$

where S_{DS} is defined in equation (1-1) and W is the weight of the superstructure. If the capacity is greater than the demand (F), the bridge passes the screen and the process moves to the second stage (section 1.8). If the capacity is less than the demand, the bridge should be considered for retrofitting at this earthquake level.

As noted above, a quick estimate of the elastic capacity of a bridge in the transverse direction is obtained by applying the factored wind load used in the design of the bridge. In the longitudinal direction, the factored braking load may be used for this purpose. If the seismic demand (F) is greater than either of these two service loads, a more detailed evaluation is necessary, as described in section 1.7.2.

1.7.2. EVALUATION FOR THE LOWER LEVEL GROUND MOTION

The seismic demand given by equation 1-2 is very conservative since it makes two simplifying assumptions. First, the period of the bridge is assumed to be very short (less than T_s , figure 1-8), in both the longitudinal and transverse directions, and second, the entire weight of the superstructure is assumed to be mobilized during an earthquake in both the longitudinal and transverse directions.

Therefore, a two-step process is recommended for the detailed evaluation of a bridge for the lower level ground motion. These steps are:

Step 1. Revise the estimate of the seismic demand using improved values for the period of vibration.

Step 1.1. Calculate the period of the bridge in both the longitudinal and transverse directions using any of the elastic methods described in Method C (section 1.11). These include the Uniform Load Method and the Multi-mode Spectral Method.

Step 1.2. Obtain the response spectral accelerations in the longitudinal and transverse directions (S_{aL} and S_{aT} , respectively), using the periods found in step 1.1 and figure 1-8.

Step 1.3. Calculate the longitudinal and transverse seismic demands (F_L and F_T) from:

$$F_L = S_{aL} W \quad (1-3a)$$

$$F_T = S_{aT} W \quad (1-3b)$$

Step 1.4. Compare F_L and F_T against total longitudinal braking load, and total transverse wind load respectively, and if either one is greater than the corresponding service load, a more rigorous evaluation is required. Go to step 2. If, however, both F_L and F_T are less than the corresponding service loads, no further evaluation is necessary and proceed to section 1.8.

Step 2. Revise the estimate of bridge capacity using explicit member strengths.

Use Method C (section 1.11 and section 5.4) to calculate capacity/demand ratios for each member and component in the lateral load path. Members and components with capacity/demand ratios less than unity are flagged for further consideration under section 1.7.3.

1.7.3. RETROFITTING FOR THE LOWER LEVEL GROUND MOTION

Once a bridge has been found to be vulnerable to the lower level ground motion, the next step is to decide what, if anything, should be done to correct the deficiencies. Decision-making may be formalized by exploring retrofit options and associated cost implications using the same process described for the upper level motion in section 1.12. In most instances, these deficiencies will be a lack of sufficient elastic strength, in which case component strengthening will be the most practical approach. The first column of table 1-11 lists a number of strengthening approaches that may be applicable. These approaches are described in chapters 8, 9 and 10.

However, before significant effort is devoted to retrofitting for the lower level earthquake, evaluate the structure for the upper level event. It is possible that the bridge is also inadequate for the upper level motion. Thus, while addressing the needs for the upper level earthquake, the deficiencies at the lower level may be eliminated, and retrofitting specifically for the lower level would no longer be necessary.

1.8. RETROFITTING PROCESS FOR UPPER LEVEL GROUND MOTION

The process of retrofitting bridges for the upper level earthquake ground motion involves an assessment of many variables and requires the use of considerable judgment. Just as for the lower level ground motion, it helps to divide the process into three parts. These are:

- Preliminary screening of bridge inventory.
- Detailed evaluation of an existing bridge.
- Selection of retrofit strategy and design of retrofit measures.

Figure 1-1 illustrates this three-step process and figure 1-10 shows the process in greater detail for the upper level ground motion. Note that decisions are made at each step, based on the results obtained thus far, that determine the next step in the process. Bridges are passed through a series

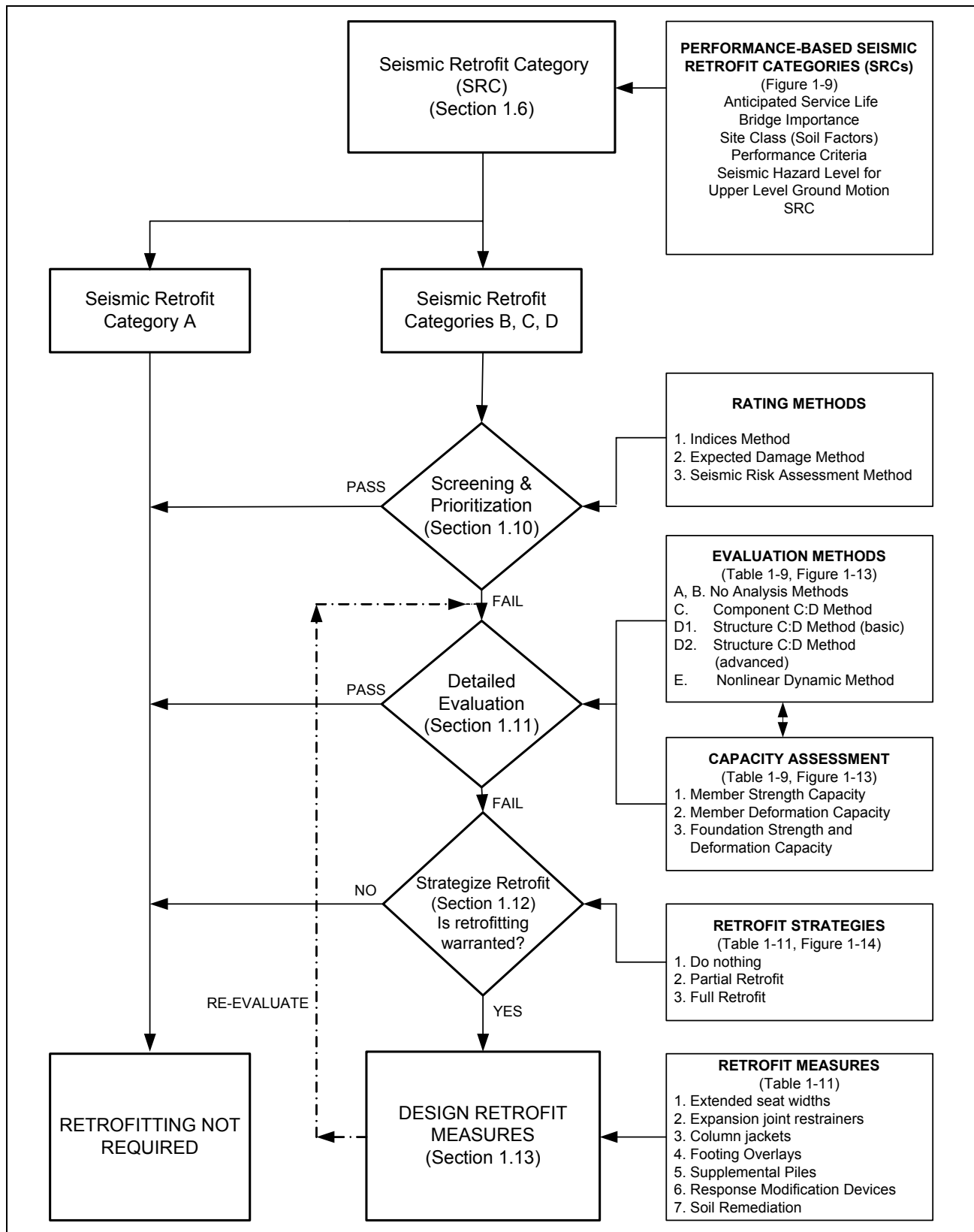


Figure 1-10. Seismic retrofitting process for highway bridges subject to

of checkpoints to assure that only those structures actually in need of retrofit will be strengthened.

As described in greater detail in sections 1.6 and 1.9, seismic retrofit categories (SRC) are used to recommend minimum requirements for evaluation and retrofitting. The SRC assigned to a bridge dictates the level of effort required to screen, analyze and retrofit a bridge, should strengthening be necessary. The SRC is determined by the importance of the bridge, its anticipated service life, and the seismic hazard level. Using these three factors, it is possible to schematically illustrate the relative effort required to retrofit bridges of different importance, in different hazard zones, and with different service lives. Figure 1-11 shows this relationship for both 'standard' and 'essential' bridges.

1.9. MINIMUM REQUIREMENTS FOR UPPER LEVEL GROUND MOTION

Minimum requirements for screening, evaluation and retrofitting are determined by the Seismic Retrofit Category (SRC), as recommended in table 1-7.

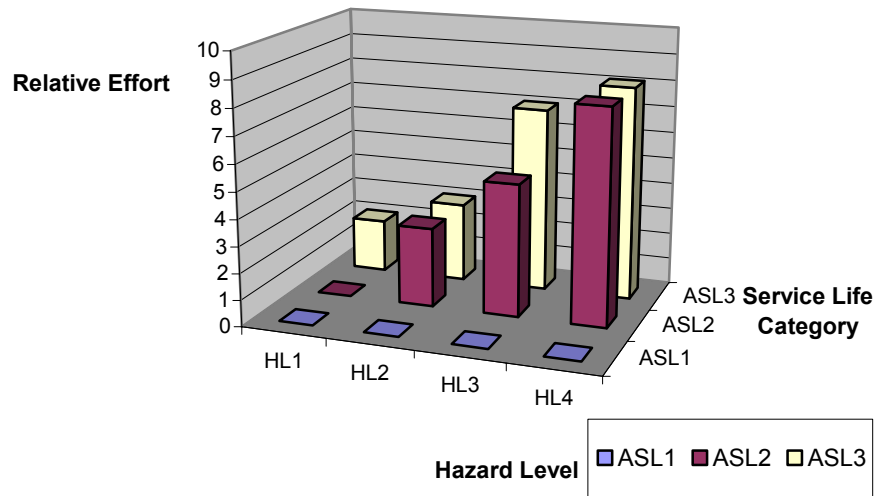
As noted above, bridges in SRC A need not be retrofitted due to their short anticipated service life, or the fact that they are located in the lowest seismic zone with minimum performance objectives (life safety only). Minimum screening, evaluation and retrofitting requirements are therefore given only for SRCs B, C and D. In general, the higher the category, the more rigorous the requirements, as seen in table 1-7

The screening requirements in table 1-7 list those components of a bridge that must be examined when setting priorities for retrofitting. Since insufficient seat width and inadequate connections are common reasons for bridge failures, the minimum screening requirements (SRC B) start with seats and connections. Other components are added in the higher categories.

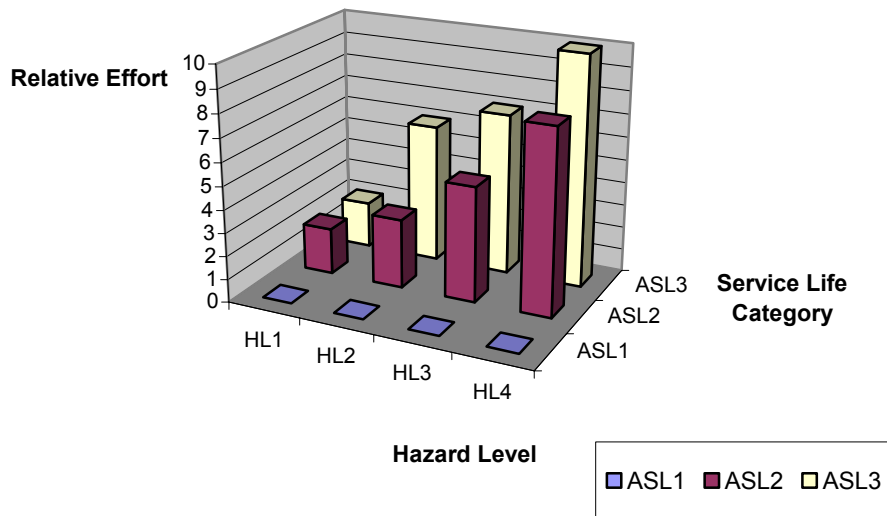
The evaluation requirements in table 1-7 give permissible methods of evaluation depending on the SRC. They range from the 'no analysis' option and simplified elastic methods for SRC B, up to the rigorous, nonlinear dynamic analysis methods for bridges in SRC D.

Table 1-7 lists those components of a bridge that should be retrofitted if found to be deficient. Inadequate seats and connections are common reasons for bridge failures and minimum requirements (SRC B) start with restrainers, seat width extensions and connection strengthening. More extensive retrofit measures such as column jacketing, footing overlays, cap beam prestressing, ground remediation and the like, are added in the higher categories.

Finally, it is noted that the requirements in table 1-7 are minima, and the owner may at any time impose more rigorous requirements.



(a) 'Standard' Bridge



(b) 'Essential' Bridge

Figure 1-11. Relative effort to retrofit an (a) 'standard' and (b) 'essential' bridge with varying service life and hazard level.

EXAMPLE 1.1: DETERMINATION OF SEISMIC RETROFIT CATEGORIES FOR BOTH UPPER AND LOWER LEVELS OF GROUND MOTION

An *essential* bridge in Salt Lake City, UT (zip code 84112) has an anticipated service life of 30 years, and is founded on very dense soils with an average shear wave velocity, in the upper 100 ft, of 1,350 ft/sec. Determine the seismic retrofit categories (SRC) for this bridge for both the upper and lower levels of ground motion.

Step 1. Importance, Anticipated Service Life, and Site Class

- 1.1 Bridge is stated to be *essential*.
- 1.2 For an anticipated service life of 30 years, the service life category is ASL 2 (table 1-1)
- 1.3 For the given soil description and shear wave velocity, the site class is C (table 1-3)

Step 2. Performance Criteria

- 2.1 From table 1-2, for the lower level ground motion, the performance level is PL3.
- 2.2 From table 1-2, for the upper level ground motion, the performance level is PL1.

Step 3. Seismic Retrofit Category for Upper Level Ground Motion

- 3.1 For zip code = 84112, the USGS CD-ROM gives $S_S = 1.11$ and $S_1 = 0.39$ (example 2.1)
- 3.2 For site class C and the values obtained for S_S and S_1 : $F_a = 1.0$ and $F_v = 1.4$ (table 1-4)
- 3.3 $F_a S_S = 1.0 (1.11) = 1.11$
 $F_v S_1 = 1.4 (0.39) = 0.55$
Seismic Hazard Level (SHL) = IV (table 1-5)
- 3.4 Seismic retrofit category for PL1 and SHL = IV, is C (table 1-6, upper level motion).
This is the SRC for the upper level ground motion.

Step 4. Seismic Retrofit Category for Lower Level Ground Motion

- 4.1 For zip code = 84112, the USGS CD-ROM gives $S_S = 0.18$ and $S_1 = 0.05$ (example 2.1)
 - 4.2 For site class C and the values obtained for S_S and S_1 : $F_a = 1.2$ and $F_v = 1.7$ (table 1-4)
 - 4.3 $F_a S_S = 1.2 (0.18) = 0.22$
 $F_v S_1 = 1.7 (0.05) = 0.09$
Seismic Hazard Level (SHL) = II (table 1-5)
 - 4.4 Seismic retrofit category for PL3 and SHL = II, is C (table 1-6, lower level motion).
This is the SRC for the lower level ground motion.
-

1.10. SCREENING AND PRIORITIZATION FOR UPPER LEVEL GROUND MOTION

1.10.1. GENERAL

Bridge inventories are screened to identify structures that are seismically deficient and to prioritize them in order of need for retrofitting. Such a process is intended to be rapid, easy to apply and conservative. Bridges found to be deficient at this stage are subject to detailed evaluation at the next step (section 1.11 and chapter 5), and any that are later found to be satisfactory are excluded from further study at that time. An overview of the recommended process for screening and prioritizing an inventory of bridges for retrofitting is illustrated in figure 1-12. Details are given in chapter 4.

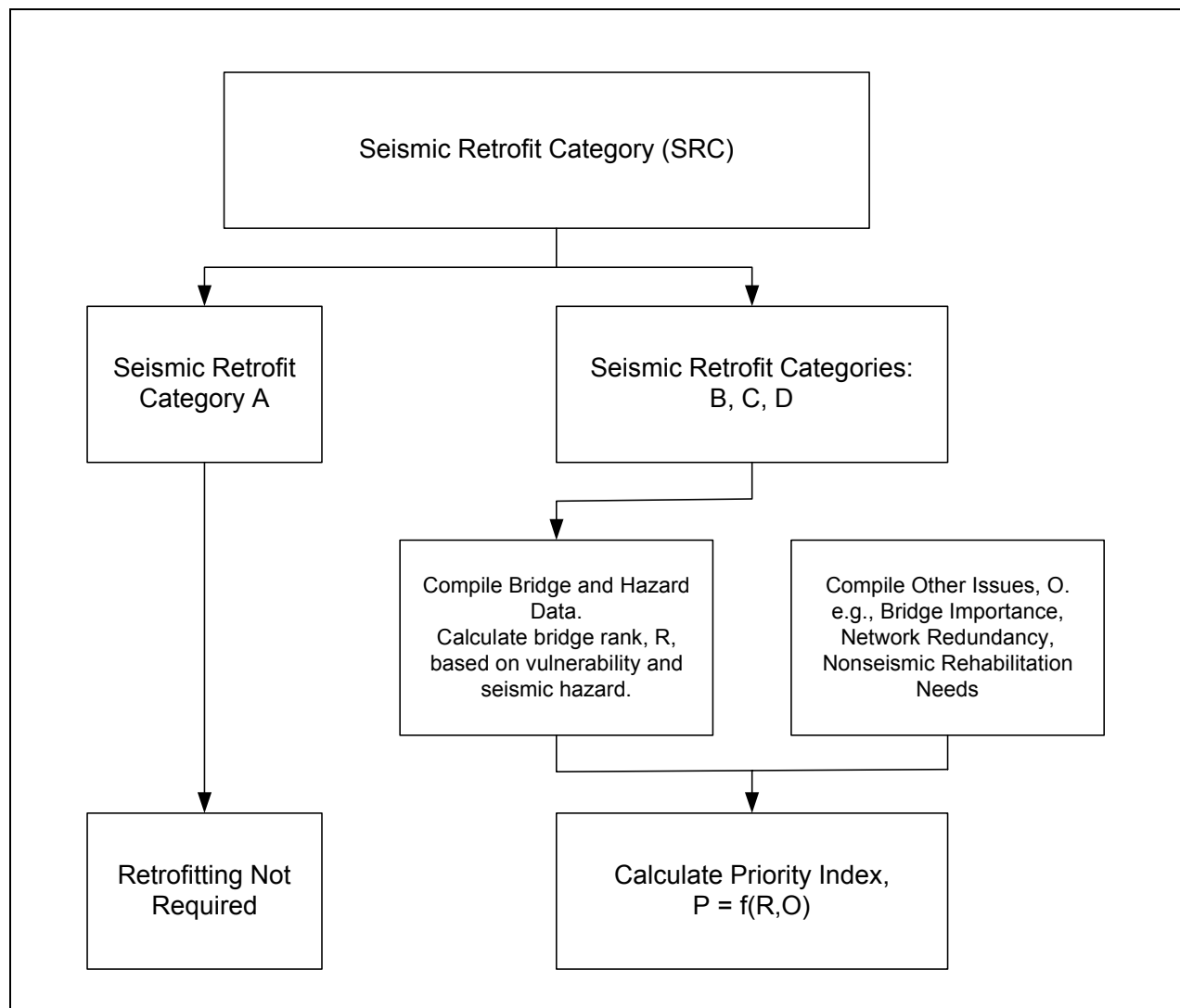


Figure 1-12. Screening and prioritization process.

Three screening and prioritization methods are described in this manual, two are presented in depth, and the third is only briefly noted. Screening programs for bridges in Seismic Retrofit Category A need not be conducted beyond the initial determination of SRC, since bridges in this category are not required to be retrofitted, regardless of their structural deficiencies or level of hazard.

Many screening and prioritization methods have been proposed in the past (Buckle, 1991). Most develop a Seismic Rating System first, and then use the results of this rating exercise to prioritize the inventory. Factors considered in the rating exercise usually include structural vulnerabilities, and prevailing seismic and geotechnical hazards. Some also include bridge importance and network redundancy at this stage, but others use these factors only when prioritizing the list of deficient structures. Another important factor to be considered is the political, social, and economic context in which the retrofit program is being conducted. Regardless of the process used to develop the final prioritized list, all bridges should be subject to detailed evaluation before actual retrofitting is undertaken, to confirm the identified structural deficiencies and determine the cost-benefits of retrofitting.

1.10.2. FACTORS TO BE CONSIDERED

The objective of a screening and prioritization program is to determine which bridge (or set of bridges) should be retrofitted first. Factors affecting such a program are the structural and soil vulnerabilities, the level of the seismic hazard and several other factors which include:

- Bridge importance. This has been discussed in section 1.4.3.
- Network redundancy. This is a measure of route availability and is used to calculate bridge importance. Whereas redundancy implies resiliency in the network, and should lessen the need for retrofitting, setting priorities based on redundancy alone is not so straightforward. For example, the likelihood that alternative routes will be damaged in the same earthquake must be considered. Suppose a freeway overpass is highly vulnerable but it can be bypassed using adjacent access ramps. Since a convenient detour is nearby, a lower seismic rating might be assigned. But this assumes that the ramps remain operational, which may not be the case if there is strong ground motion in the area. If, on the other hand, the structure is a vulnerable river crossing, and the nearest detour several miles away, the redundancy of the network will be low. However, the possibility of the alternate crossing being damaged will be low and an alternate route may be available. The length of the detour then becomes the issue when deciding priority for retrofitting. Other examples where network redundancy leads to unexpected results are given in example 1.2.
- Age and physical condition. It is generally not wise to spend a large sum retrofitting a bridge with relatively few years of service life remaining. This is one reason why bridges in SRC A do not need to be retrofitted. It is also true that an unusually high seismic vulnerability may be justification to accelerate closure or replacement of such a bridge. Also, a bridge in poor physical condition, or one that is already scheduled for structural or functional rehabilitation, may be given a higher priority for seismic retrofitting, since cost savings can be achieved by performing the non-seismic and seismic work simultaneously.

The above factors are not an exhaustive list, but illustrate some of the principles involved in assigning priorities. In most cases, seismic ratings are used to guide decision-making but are not the final word. Common sense and engineering judgment are necessary when weighing the actual costs and benefits of retrofitting against the risks of doing nothing.

1.10.3. SEISMIC VULNERABILITY RATING METHODS

Most vulnerability rating methods assign a structure vulnerability index (from 1-10) and a hazard index (1-10), and combine these in various ways to obtain an overall seismic rating. Some methods also develop an importance index (1-10) to address daily traffic flow, redundancy and the socioeconomic climate. Others use qualitative measures to include these factors. This last approach was recommended in the 1995 *FHWA Retrofitting Manual* (FHWA, 1995) and is also included in the current edition (section 1.10.4). Recent progress in seismic risk assessment methods has led to the development of fragility functions for specific classes of bridges. These in turn have led to loss estimation methodologies for highway systems. These methodologies have many potential applications in highway design and retrofitting, including planning for emergency response and recovery. They may be used for screening bridge inventories with more rigorous results than possible with the above methods, since they quantify the uncertainties surrounding bridge and site vulnerability, network redundancy and importance factors.

The three methods summarized below have increasing complexity, but decreasing conservatism. Two of these are further described in later sections of this chapter and in greater detail in chapter 4. These methods are differentiated by the manner in which structure vulnerability, seismic and geotechnical hazards, importance, redundancy and various socioeconomic factors are treated.

The methods are:

1. Indices Method (FHWA, 1995)

Indices are used to characterize the structure vulnerability and hazard level and are then combined to give a single rating for each bridge. Indices range from 0 to 10 and are based on conservative, semi-empirical rules. Prioritization is determined by this rating together with a qualitative assessment of importance, redundancy, non-seismic issues, and socioeconomic factors. This is the simplest of the three methods, but it is also the most conservative, since it uses arbitrary rules to allow for inherent uncertainties.

2. Expected Damage Method

This method compares the severity of expected damage for each bridge in the inventory, for the same earthquake. Severity of damage is measured either by sustained damage state(s) or by estimating direct economic losses. Bridges with the highest expected damage (and/or loss) are given the highest priority for retrofitting. Uncertainty in ground motions, and randomness in soil and structure properties, are explicitly addressed by using fragility functions to estimate damage-state probabilities (see chapter 4). A qualitative assessment of indirect losses, network redundancy, and non-seismic issues is required and the ranking, based on fragility, is modified accordingly.

3. Seismic Risk Assessment Method

Explicit analysis of the highway network is performed for a given hazard level and the resulting damage states used to estimate the effect on system performance as measured by

traffic flow (e.g., increased travel times). Sensitivity of this performance to bridge condition is subsequently used to determine bridge retrofit needs and priorities. Independent qualitative assessment of non-seismic issues and socioeconomic factors is required. This is the most complex of the three methods, but it is also the most rigorous with the least conservatism in the final result.

Methods 1 and 2 are summarized in sections 1.10.4 and 1.10.5 below and described in detail in chapter 4. Method 3 is considered outside the scope of this manual and is not discussed further. A full description may be found in Werner et al., 2000.

1.10.3.1. Minimum Screening Requirements

Minimum requirements for screening bridge inventories, based on Seismic Retrofit Categories, are recommended in table 1-7.

1.10.3.2. Seismic Inventory of Bridges

The first step in implementing any of the above methods is to compile a bridge inventory with the objective of obtaining the following basic information:

- The structural characteristics of each bridge to determine either the vulnerability rating or to select the fragility function as described in chapter 4, and
- The seismicity and soil conditions at each bridge site to determine the seismic hazard rating or select the fragility function as described in chapter 4.

This information may be obtained from the bridge owner's records, the National Bridge Inventory (<http://www.fhwa.dot.gov/bridge/nbi.htm>), "as-built" plans, maintenance records, the regional disaster plan, on-site bridge inspection records, and other sources. A form, such as the sample shown in table 1-8, should be used for recording this information and filed with the bridge records.

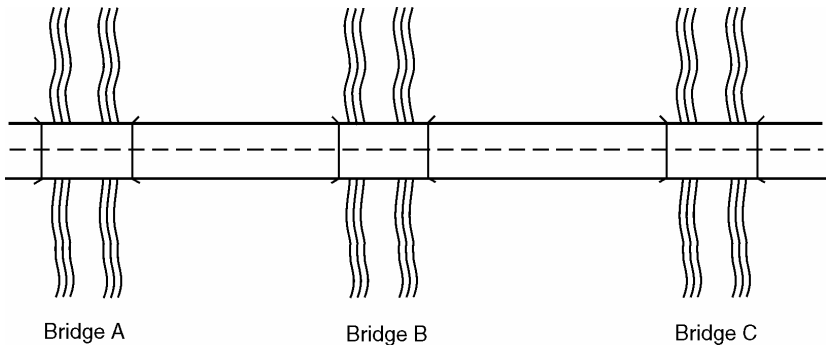
Much of the information used to assign the required performance level for the retrofitted bridge in section 1.4 will also be necessary when making assessments of importance, redundancy, and socioeconomic issues in the sections that follow.

1.10.4. INDICES METHOD

In this method, the seismic rating of a bridge is determined by its structural vulnerability, the seismic and geotechnical hazards at the site, and the socioeconomic factors affecting the importance of the structure. Ratings of each bridge are first found in terms of vulnerability and hazard, and then modified by importance (societal and economic issues) and other issues (redundancy and non-seismic structural issues) as necessary to obtain a final, ordered determination of retrofitting priority (Buckle, 1991; FHWA, 1995).

EXAMPLE 1.2: IMPACT OF NETWORK REDUNDANCY ON BRIDGE PRIORITIZATION

Example 1.2(a). In the figure at right, assume that Bridge A is a seismically vulnerable bridge and has a high seismic vulnerability rating. It is located on a major route in series with lower-rated Bridges B and C, which are also vulnerable to earthquakes, but to a lesser degree than Bridge A. Assume that no convenient detour to this route exists and that each bridge can be economically retrofitted. What priority should be given to Bridges B and C?

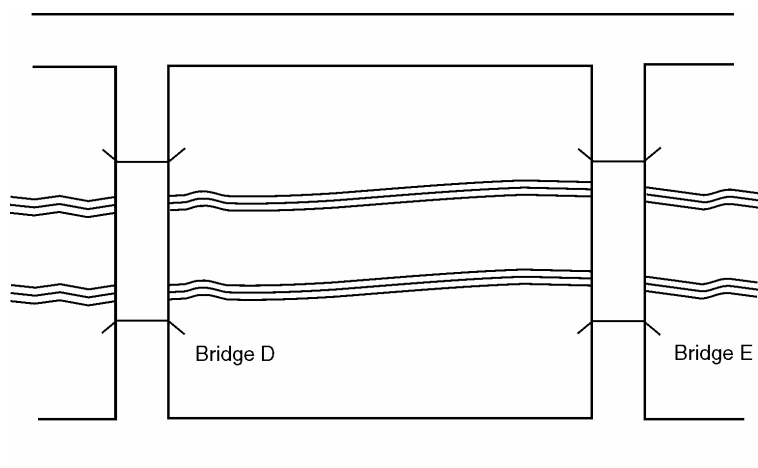


Answer: Since retrofitting Bridge A alone would improve only one point on the route and do nothing to prevent the failure of Bridges B or C, and because construction and administration savings can be realized by retrofitting more than one bridge in the same geographical area at a time, Bridges B and C, although lower rated than A, should also be considered for retrofitting.

Example 1.2(b). Suppose in the Example above, Bridge B has a high vulnerability rating but cannot be economically retrofitted. What priority should now be given to Bridges A and C?

Answer: Because Bridge B is in series with Bridges A and C, the route would be closed if Bridge B were to collapse. Therefore, unless Bridge B can be replaced at the same time, it may be advisable to give Bridges A and C a lower retrofit priority because strengthening of these two bridges alone may not prevent closure of the route.

Example 1.2(c). Consider two bridges that have parallel functions, such as Bridges D and E in the figure at right. If Bridge D has a lower vulnerability rating than Bridge E, which bridge should be retrofitted first?



Answer: Since Bridge D has the lower rating, it is possible that it could be more economically retrofitted than Bridge E, since less strengthening is required. If this is true, and the collapse of one bridge is preferred over the loss of both bridges, then it might be more logical to retrofit Bridge D before Bridge E, even though Bridge E had the higher vulnerability rating.

Table 1-8. Sample bridge seismic inventory form.

BRIDGE SEISMIC INVENTORY DATA FORM

GENERAL

Bridge Name _____ BIN Number _____

Location _____

Year Built _____ ADT _____ Detour Length _____

Total Length _____ Feature Carried _____

Overall Width _____ Feature Crossed _____

Importance: essential / standard Alignment: straight / skewed/ curved Geometry: regular / irregular

Seismic Hazard (100-year event): S_s = _____ g S_1 = _____ g Soil Site Class: A / B / C / D / E _____
(1000-year event): S_s = _____ g S_1 = _____ g Soil Site Class: A / B / C / D / E _____

SUPERSTRUCTURE

Material and Type _____

Number of spans _____ Continuous: yes / no Number of expansion joints _____

BEARINGS

Type _____ Condition: functioning / not functioning _____

Type of restraint: Longitudinal: _____ Transverse: _____

Actual support length _____ Minimum required length _____

COLUMNS AND PIERS

Material and Type _____

Cross-section: Min. transverse dimension _____ Min. longitudinal dimension _____

Height range (low – high): _____ Fixity: Top _____ Bottom _____

Longitudinal reinforcement (%) _____ Splices in end zones ? yes / no _____

Transverse confinement steel _____

FOUNDATIONS AND ABUTMENTS

Pier foundation type: spread footings / pile footings / pile bent / single shaft / other _____

Abutment type: seat / integral / other _____ On Piles: yes / no
other _____

Abutment height _____ Approach slabs: yes / no Slab length _____

Location: cut / fill Wingwalls: yes / no Liquefaction: susceptibility low / moderate / high _____

REMARKS _____

This rating system has two parts: quantitative and qualitative. The quantitative part produces a seismic rating ('bridge rank') based on structural vulnerability and site hazard. The qualitative part modifies the rank in a subjective way that accounts for importance, network redundancy, non-seismic deficiencies, remaining useful life, and similar issues to arrive at an overall priority index. Engineering and societal judgment are key to the second stage of the screening process. This leads to a priority index, P, which is a function of rank, importance, and other issues:

$$P = f(R, \text{importance, non-seismic, and other issues}) \quad (1-4a)$$

where P is the priority index, and R is the rank based on structural vulnerability and seismicity.

In summary, *bridge rank* is based on structural vulnerability and seismic hazard, whereas *retrofit priority* is based on bridge rank, importance, non-seismic deficiencies, and other factors such as network redundancy. A methodology for calculating bridge rank (R) and the assignment of the priority index (P) is given in chapter 4 (section 4.2).

1.10.5. EXPECTED DAMAGE METHOD

The Expected Damage Method compares the severity of expected damage for each bridge in the inventory for the same earthquake, and ranks each bridge accordingly. Severity of damage is measured either by the sustained damage state(s) or the estimated direct economic loss. Bridges with the highest expected damage (and/or loss) are given the highest priority for retrofitting.

In its present form, the method does not include indirect economic losses due to loss of life, injuries, business disruption, traffic congestion, denial of access to emergency responders and the like. These losses will probably exceed the direct losses (i.e., repair costs) but the state-of-the-art of loss estimation is currently unable to quantify these costs with any certainty.

As in the Indices Method, this method has two parts: quantitative and qualitative. The quantitative part is based on expected damage and direct economic losses, and is used to obtain a bridge rank, R. The qualitative part modifies the rank in a subjective way that takes into account such factors as indirect losses, network redundancy, non-seismic deficiencies, remaining useful life, and other issues, to obtain an overall priority index. As in the previous method, engineering and societal judgment are the key to the second stage of the process. This leads to a priority index, P, which is a function of rank, indirect losses, redundancy, and other issues, as follows:

$$P = f(R, \text{indirect losses, redundancy and various non-seismic issues}) \quad (1-4b)$$

where P is the priority index, and R is the rank based on expected damage and direct losses.

It is seen that *bridge rank* is based on expected damage and direct losses for a given earthquake, whereas *retrofit priority* is based not only on bridge rank, but also on expected indirect losses, network redundancy and non-seismic factors, estimated in a subjective way. Although equation 1-4b has the same form as equation 1-4a, the terms are calculated in different ways. A particular advantage of this method is that it provides a template by which indirect losses may be rationally included, as the state-of the art improves.

The estimation of expected damage is a critical step in this method and due to uncertainty in earthquake ground motions, and randomness in soil and structure properties, this step is a probabilistic one. Fragility functions are used to estimate the probability of a bridge being in one or more specified damage states, after a given earthquake. Appendix C summarizes the theory of fragility functions and briefly explains how they are obtained. It also describes the six damage states most commonly used to characterize expected damage.

As noted in section 1.10.3, fragility functions are also essential elements in the Seismic Risk Assessment Method for screening and prioritizing bridges. These functions are also used in most loss-estimation methodologies, including HAZUS, which is under development by the National Institute of Building Sciences for the Federal Emergency Management Agency (HAZUS, 1997). In order to simplify the method as much as possible, input data requirements are kept to a minimum. In particular, all structure attributes may be found in the NBI. Ground motions and soils data are based on spectral accelerations and soil types as described in section 1.5.

A methodology for calculating bridge rank (R) and the assignment of the priority index (P), based on expected damage, is given in chapter 4 (section 4.3).

1.11. METHODS OF EVALUATION FOR UPPER LEVEL GROUND MOTION

Bridges found to be deficient during screening and prioritization (section 1.10) are subject to detailed evaluation using one or more of the methods described in this section. Since the screening procedures described above are necessarily conservative, it is likely that a bridge identified as deficient during screening will be found satisfactory upon a more detailed evaluation.

The seismic evaluation of a bridge is explicitly or implicitly a two-part process. A demand analysis is first required to determine the forces and displacements imposed on the bridge by an earthquake; this is then followed by an assessment of capacity to withstand this demand. Most evaluation methods express their results as capacity/demand ratios calculated on a component-by-component basis, or for the bridge as a whole (i.e., as a single structural system).

Six evaluation methods are described in this manual, which are all based, to varying degrees, on capacity-demand principles. They are listed below in order of increasing sophistication and rigor, and are summarized in table 1-9. All six methods are described in detail in chapter 5. These methods emphasize the calculation of *demand* on a member or component of a bridge. Methods for calculating the *capacity* of a member or component are described in detail in chapters 6 and 7. The relationships between these methods for demand analysis and capacity assessment are shown schematically in figure 1-13.

Method A1/A2: Connection forces and seat width checks. Seismic demand analysis is not required but the capacity of connections and seat width adequacy is checked against minimum values (section 5.2). The method is suitable for all single span bridges and others in low hazard zones. The method is divided into two categories, A1 and A2. If the short-period spectral ordinate $S_s < 0.10$, Method A1 may be used. Otherwise, Method A2 must be used, which requires higher minimum connection capacities than Method A1.

Method B: Component capacity checks. Seismic demand analysis is not required, but the relative strength of the members and the adequacy of certain key details are checked against recommended minima. This method is suitable for regular bridges in SRC C, subject to restrictions on $F_v S_1$ (section 5.3).

Method C: Component capacity/demand method. Seismic demands are determined by an elastic analysis such as the uniform load method, multi-mode response spectrum method, or an elastic time history method. The uniform load method is adequate for bridges with regular configurations; otherwise, the multi-mode method is used as a minimum. Capacity/demand ratios are calculated for all relevant components. This method is suitable for all bridges in SRC C and D, but gives best results for bridges that behave elastically or nearly so (section 5.4).

Method D1: Capacity spectrum method. Seismic demands are determined by simple models such as the uniform load method, and capacity assessment is based on a simplified bilinear lateral strength curve. A capacity spectrum is used to calculate the capacity/demand ratio for the bridge, for each limit state. This method is suitable for regular bridges in SRC C and D (section 5.5).

Method D2: Structure capacity/demand method. Seismic demands are determined by elastic methods such as the multi-mode response spectrum method, or an elastic time history method. Capacity assessment is based on the displacement capacity of individual piers as determined by a ‘pushover’ analysis, which includes the nonlinear behavior of the inelastic components. A capacity spectrum is used to calculate the capacity/demand ratio for each pier, bearing, and foundation of the bridge, for each limit state. This method is suitable for all bridges in SRC C and D. It is also known as the *Pushover Method* or alternatively the *Nonlinear Static Procedure* (section 5.6).

Method E: Nonlinear dynamic procedure (time history analysis). Seismic demands are determined by a nonlinear dynamic analysis using earthquake ground motion records to evaluate the displacement and force demands. Capacities of individual components are explicitly modeled in the demand analysis. This method is suitable for irregular complex bridges, or when site specific ground motions are to be used for a bridge of major importance (section 5.7).

In summary, Methods A and B are based on default minima with no demand analysis required. Methods C and D are capacity-demand methods of varying rigor, and Method E is the most rigorous of all the methods and is based on inelastic time history analysis.

The choice of method to be used for an evaluation is determined by the minimum requirements in table 1-7 and the regular/irregular requirements summarized above and in table 1-9. The minima in table 1-7 are related to the Seismic Retrofit Category of the bridge under consideration, and are based on two principles. First, as the seismic hazard increases, improved modeling and analysis for the seismic demands is necessary, because bridge response is sensitive to increasing demand. Second, as the complexity of the bridge increases, more sophisticated models are required to capture both the demand and capacity with certainty. Note that a higher level of analysis may always be used in place of a lower-level method.

Table 1-9. Evaluation methods for existing bridges.

METHOD	CAPACITY ASSESSMENT	DEMAND ANALYSIS	APPLICABILITY		COMMENTS
			SRC-UL ¹	Bridge Type	
A1/A2	Uses default capacity due to non-seismic loads for connections and seat widths.	Not required	A – D	All single span bridges.	Hand method, spreadsheet useful.
B	Uses default capacity due to non-seismic loads for connections, seats, columns and foundations.	Not required	B	Bridges in low hazard zones.	
C	Uses component capacities for connections, seat widths, column details, footings, and liquefaction susceptibility (11 items).	Elastic Methods ² : • ULM • MM • TH	C	Regular bridges, but subject to limitations on $F_v S_1$.	Hand method, spreadsheet useful.
D1	Uses component capacities for connections, seat widths, column details, footings, and liquefaction susceptibility (11 items).	Elastic Methods ² : • ULM • MM • TH	C & D	Regular and irregular bridges that respond almost elastically, such as those in low-to-moderate seismic zones and those with stringent performance criteria.	Calculates C/D ratios for individual components. This is the C:D Method of previous FHWA highway bridge retrofitting manuals. Software required for demand analysis.
D2	Uses bilinear representation of structure capacity for lateral load, subject to restrictions on bridge regularity.	Elastic Methods ² : • ULM	C & D	Regular bridges that behave as single-degree-of-freedom systems and have 'rigid' in-plane superstructures.	Calculates C/D ratios for complete bridge, for specified limit states. Spreadsheet useful.
E	Uses pushover curve from detailed analysis of superstructure, individual piers and foundation limit states.	Elastic Methods ² : • ULM • MM • TH	C & D	Regular and irregular bridges.	Calculates C/D ratios for bridge superstructure, individual piers, and foundations. Also known as <i>Nonlinear Static Procedure</i> or <i>Displacement Capacity Evaluation Method</i> . Software required for demand and capacity analysis.
E	Uses component capacities for connections, seat widths, columns and footings.	Inelastic Methods ² : • TH	D	Irregular complex bridges, or when site specific ground motions are to be used such as for bridges of major importance.	Most rigorous method, expert skill required. Software essential.
Notes: 1. SRC = Seismic Retrofit Category for upper level earthquake; for the lower level earthquake, the recommended method of evaluation is Method C. 2. ULM = Uniform Load Method; MM = Multi-Mode Spectral Method; TH = Time History Method					

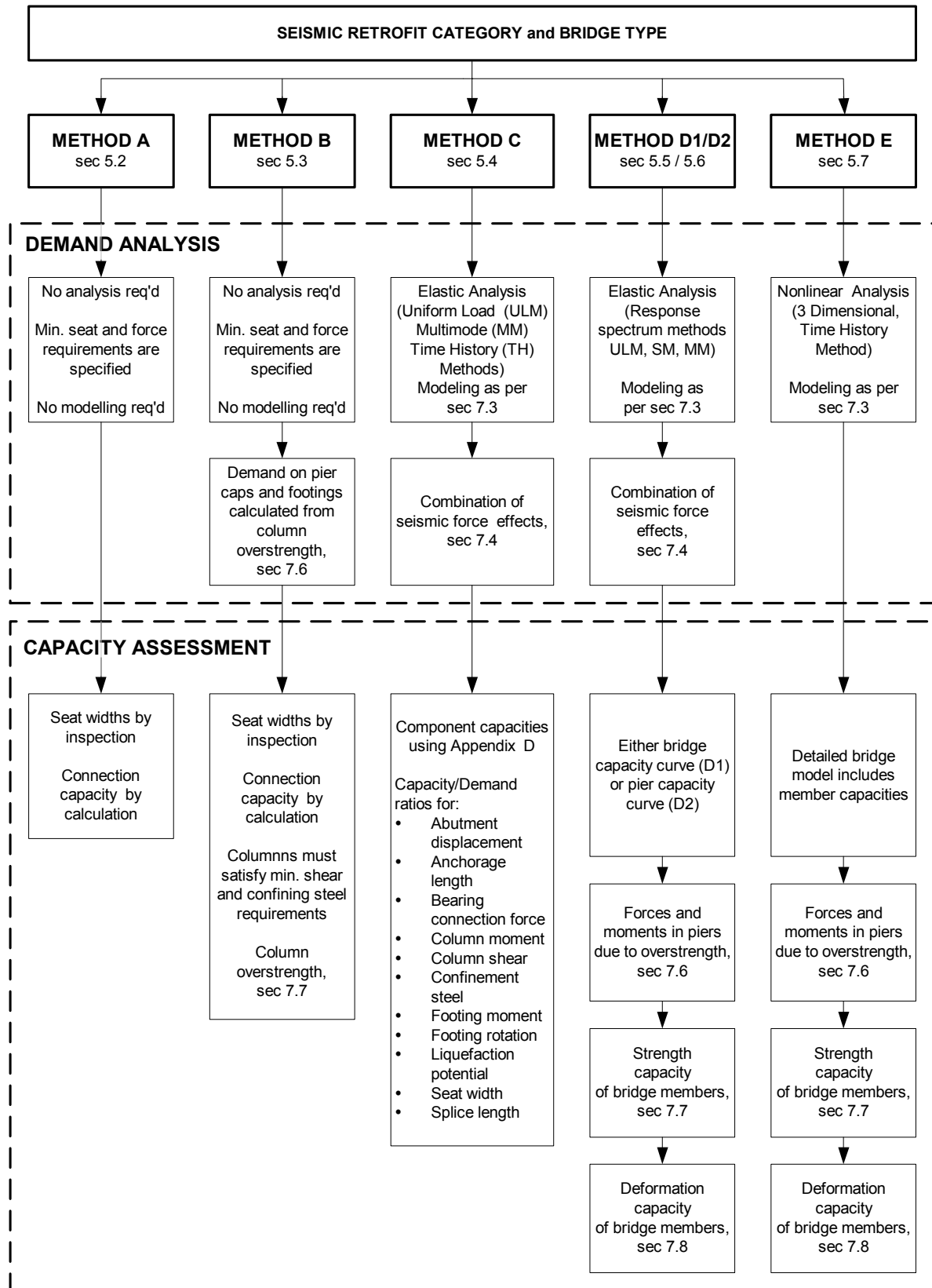


Figure 1-13. Evaluation methods for existing bridges showing relationship between demand analysis and capacity assessment.

1.12. RETROFIT STRATEGIES FOR UPPER LEVEL GROUND MOTION

1.12.1. GENERAL

Once a bridge is found to be seismically deficient, the next step is to decide what, if anything, should be done to correct the deficiencies. Decision-making may be formalized by exploring retrofit options and the associated cost implications. This section revisits the objectives of retrofitting and discusses the selection of a retrofit strategy (including cost considerations), developing a retrofit approach, and identifying retrofit measures.

A *Retrofit Strategy* is the overall plan for the seismic retrofit of a bridge. This plan can employ more than one retrofit approach and thus several different retrofit measures. Retrofit strategies are discussed in section 1.12.2.

A *Retrofit Approach* is the philosophy of seismic enhancement adopted for a bridge. Strengthening is an example of a retrofit approach. One or more retrofit approaches can be employed in the seismic retrofit of a bridge. Various approaches are discussed in section 1.12.3.

A *Retrofit Measure* is the physical modification of a component in a bridge for the purpose of upgrading overall seismic performance. For example, the addition of a steel shell to a reinforced concrete column is a retrofit measure. Retrofit measures for superstructure, substructure, and foundation components are briefly summarized in section 1.13, and described in detail in chapters 8, 9, and 10, respectively.

1.12.2. SELECTING A RETROFIT STRATEGY

1.12.2.1. Objective of Retrofitting and Acceptable Damage

The objective of retrofitting a bridge is to ensure that it will perform satisfactorily when subjected to the design earthquake. Specifically, bridges should be retrofitted to meet the performance criteria given in section 1.4 and table 1-2, which are determined by the importance of a bridge and its anticipated service life.

Performance criteria for both new and existing bridges permit considerable structural damage as long as collapse is prevented, and the amount of acceptable damage in existing bridges may be greater than for new designs.

There are at least two reasons why accepting some level of damage is an essential ingredient of almost all retrofit strategies. These are:

- Retrofitting is usually more complex and more expensive than providing adequate resistance in a new bridge. In some cases, the added cost of preventing damage could be as much, or more, than the cost of repairing the damage in the unretrofitted bridge (neglecting indirect losses).

- Existing bridges may have a reduced useful or remaining life due to normal ‘wear and tear,’ and increasing traffic volume and/or load capacity requirements. This shortened life reduces the likelihood that such a structure will experience a damaging earthquake, and increases the annualized cost of every dollar spent to prevent earthquake damage.

There are exceptions to this rule. These include very important bridges, and where the societal cost of any damage that disrupts serviceability, or reduces traffic capacity, is unacceptable.

1.12.2.2. Cost Considerations of Seismic Retrofit

Cost is a major consideration in seismic retrofitting. As noted above, the average cost of seismic retrofitting is much higher than of incorporating seismic resistance into the design of a new bridge. In fact, it has been estimated that in extreme cases, seismic retrofitting may be two to three times more expensive.

Data giving the actual cost of retrofitting is hard to find because very few States have completed extensive retrofit programs from which cost databases may be compiled. However, table 1-10 gives some data based on Caltrans’ experience in retrofitting 165 bridges during 1993 and 1994. In this table, retrofit costs are expressed as a fraction of the cost of new construction and the average cost is seen to be about 15 percent of the cost of building a new bridge in the same time period. Also, as might be expected, retrofit costs strongly depend on the strategy employed. When only the superstructure is retrofitted (cable restrainers and seat width extenders), the average construction cost is about 3.1 percent of new construction. When the substructure is also retrofitted, but not the foundation, the average cost rises to 15.4 percent. When the foundation is included, the average cost rises further to 28.8 percent. Table 1-10 also shows a significant variation in cost when the same strategy is applied to different bridges, due to differences in the extent of retrofitting required. Although this data reflects prevailing conditions in the California construction market at the time of these retrofits, the trends are believed applicable elsewhere in the country.

Table 1-10. Cost of various retrofit strategies as percentage of new construction costs ^{1,2}.

RANGE	RETROFIT STRATEGY			TOTALS (weighted sum all retrofits in California, 1993 and 1994)
	Superstructure Only ³	Superstructure and Substructure	Superstructure, Substructure and Foundations	
Low	1.3	0.7	2.3	0.7
Average	3.1	15.4	28.8	15.1
High	13.2	64.8	232.9	232.9
Notes: 1. Caltrans data for 165 bridges retrofitted in 1993 and 1994. 2. Costs expressed as percentage of new construction for same time frame. 3. Superstructure includes restrainers and seat width extensions.				

Engineering costs for retrofit design are also generally higher than for new construction. It is not unrealistic to expect that these costs will be twice the cost of the engineering required for a new bridge of similar value. This is because many bridges are unique and often require customized retrofit strategies. Standardization of design and retrofit details is therefore difficult to achieve. In addition, the detailed seismic evaluation of a bridge and identification of the most appropriate retrofit strategy is a time-consuming process that may involve a detailed dynamic analysis and potentially, many trial designs investigating possible strategies.

In addition to higher initial costs, the fact that the life of a retrofit should not exceed the remaining service life of the bridge means that the annualized cost of retrofitting is further increased over the cost of seismic resistance in new construction. This requires that the benefits of retrofitting, particularly for damage prevention, be weighed against these higher costs when selecting a retrofit strategy for the bridge.

1.12.2.3. Other Considerations and Non-Seismic Issues

Many existing bridges within the United States are either structurally deficient or functionally obsolete, in addition to being seismically vulnerable. Either one of these two conditions could result in a bridge being rehabilitated, which might present an opportunity for improving the seismic resistance of a bridge at the same time. If retrofitting is required immediately, it may be advisable for the designer to consider the additional demands that will be placed on the structure when the future widening is finally accomplished. A designer should therefore consider both the present condition and possible future service that will be required of the bridge.

Bridge inspection and maintenance needs should also be considered when designing a seismic retrofit. This includes access for inspection as well as maintenance activities. The retrofit measure itself should not become a maintenance problem. The designer should be aware of the needs of maintenance personnel and include them in the selection process of the retrofit strategy.

Retrofit measures can dramatically alter the appearance of the bridge. The designer should therefore be sensitive to the aesthetics of the retrofit design. This could be particularly important if the original design has notable aesthetic value or if it is desirable or required to preserve the appearance of the bridge for other reasons (e.g., if the bridge is a historic structure). There may be alternative retrofit measures that are just as effective, but more aesthetically acceptable.

It is often not possible to close a bridge to traffic while retrofitting is performed, but some retrofit measures require access to portions of the bridge that will disrupt traffic. Rerouting of traffic and staged construction will then be necessary, and when this is difficult to achieve, a strategy that limits disruption to traffic must be found. Similar constraints may exist with respect to utilities on or near the bridge. If they cannot be easily relocated, it may be necessary to redesign the retrofit to avoid damage or disruption to these utilities.

Constructability is always an issue for the bridge designer, but potentially more so in the case of seismic retrofitting. The main problem is access to the work area on and around the existing bridge and surrounding facilities. Some examples include driving or drilling piles under an existing structure with limited headroom, placing concrete under an existing horizontal surface,

and excavating near other adjacent facilities. The designer must carefully think through the steps required for construction, and verify that the proposed retrofit can indeed be built.

Political and environmental constraints often arise during retrofitting and should be identified as far ahead as possible during selection of the preferred strategy. For example, the bridge may be listed on an historical register, which could limit the types of modifications that can be performed. The bridge may be located in an environmentally sensitive area that limits access to certain critical elements such as columns or foundations. The bridge may be located in a highly urban or residential environment, which may limit certain types of construction activities such as pile driving because of vibration and noise. Hazardous wastes are likely to be present around bridges in urban environments and, if disturbed, will require remediation. Political opposition to certain solutions such as bridge replacement, may also limit the options of the designer. It is important that the designer be sensitive to these and other issues early in the retrofit process with a view to finding the best solution given the constraints.

1.12.2.4. Identifying and Evaluating a Retrofit Strategy

Selecting the preferred retrofit strategy can be complicated. Not only is it often a challenge to find the right technical solution, it is also a challenge to satisfy a multitude of socio-economic constraints. A systematic process should therefore be followed to assure an appropriate strategy is selected. A flowchart for such a process is shown in figure 1-14. The various steps are discussed below.

Step 1. Conduct a detailed as-built evaluation. The first step in seismic retrofitting is to perform a detailed analytical evaluation of the existing bridge, as it exists in the field. Procedures for this step are discussed in section 1.11 and chapters 5 through 7. The goal of this step is to assess the response of the bridge to the design earthquake and to identify weaknesses that can be addressed by retrofitting. A formal field review of the bridge should be performed as part of this step. This is needed to verify the as-built condition of the bridge and to identify any constraints on retrofitting. Structural and geotechnical specialists and the owner should be involved in this effort.

Step 2. Identify alternative retrofit strategies. Frequently, there is more than one way to improve the performance of an existing bridge, and it is important to identify as many options as possible. Many will be quickly eliminated because of excessive cost, constructability or other problems as noted in section 1.12.2.3. Solutions that appear viable should be further considered in Step 3. Table 1-11 (see section 1.13.2) identifies alternative retrofit approaches that might be used to address common deficiencies and directs the designer to possible retrofit measures for each approach. This table may therefore be helpful when looking for potential retrofit strategies.

Step 3. Evaluate alternative retrofit strategies. Detailed analytical evaluations of each viable retrofit strategy should be performed using the methods described in section 1.11 and chapters 5 through 7. This step should also include the preliminary design of the elements of the proposed retrofit so that a preliminary cost estimate may be prepared for each alternative.

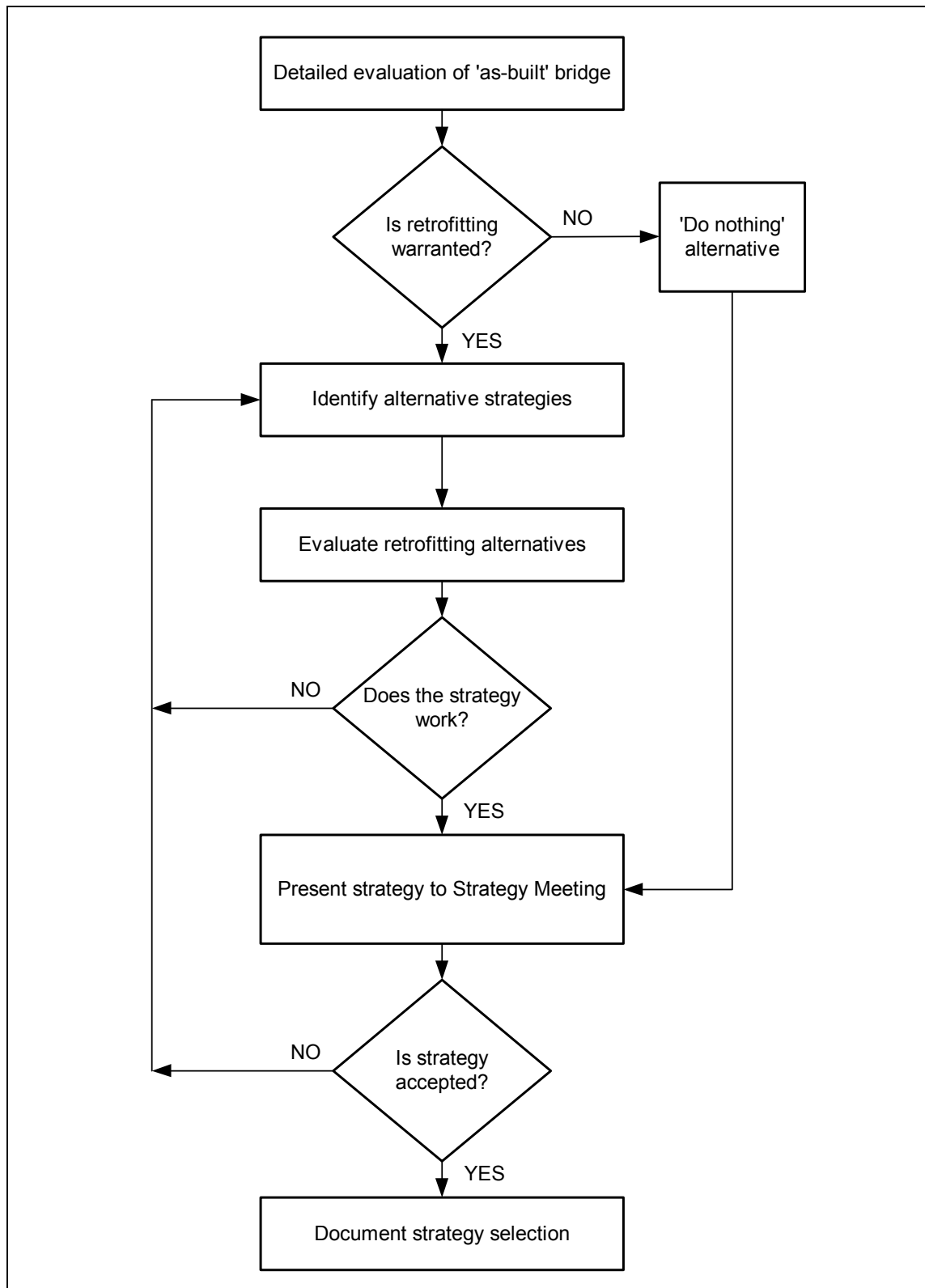


Figure 1-14. Identification and evaluation of a retrofit strategy.

Step 4. Conduct a strategy meeting. Since seismic retrofitting involves many complex issues, consensus must be achieved on the most appropriate strategy. This may be accomplished through a strategy meeting where the designer presents recommendations and cost estimates for retrofitting. Representatives of all agencies that have an interest in the project should attend this meeting, including the bridge owner, utility companies, Federal, state and local government agencies, structural and geotechnical engineering specialists, and environmental and citizens groups.

Step 5. Document the strategy selection. The retrofit decision should be documented in a strategy report that becomes part of the permanent record for the project. This report should include all the calculations of the as-built and as-retrofitted evaluations, preliminary plans and sketches showing the proposed retrofit, a summary of conclusions and recommendations, preliminary cost estimates, and a summary of the discussions from the strategy meeting.

1.12.2.5. Do-Nothing and Full-Replacement Options

When retrofitting a seismically deficient bridge, two possible solutions, at opposite ends of the spectrum, should be kept in mind: the ‘do-nothing’ and ‘full-replacement’ options.

The ‘do-nothing’ option requires the acceptance of damage during a future earthquake. This will be a relatively straightforward decision if life safety is the only performance requirement, and the expected damage is not a threat to life safety. The most likely cause of loss of life is total collapse of a span, but this is a relatively rare event. For example, the toppling or failure of individual bearings will not necessarily lead to collapse if the bearing seats are wide enough to catch the superstructure. Similarly, foundation failures are unlikely to cause collapse, unless the ground deformations are extremely large due to widespread liquefaction or massive ground failure such as fault rupture. Fortunately, these occurrences are rare. Nevertheless, judgment should be used when assessing collapse potential and, to the extent possible, this potential should be carefully evaluated using a detailed analysis.

The ‘full-replacement’ option may also be an attractive option, particularly when the cost of retrofit is on the same order of magnitude as the replacement cost of the bridge. Full replacement is generally considered whenever the retrofit costs approach 60 to 70 percent of a new bridge and may become even more attractive if the structure has non-seismic structural deficiencies and is functionally obsolete. However, in making this recommendation, the designer should also consider the cost of demolition and any costs associated with control and rerouting of traffic as part of the cost of the replacement alternative. These costs can be significant and may tip the scales back toward the retrofit alternative.

1.12.3. SEISMIC RETROFIT APPROACHES

Seismic retrofit approaches may be used alone or in combination to develop a seismic retrofit strategy for a given bridge. Some of the more common approaches are listed below and discussed in sections 1.12.3.1 through 1.12.3.7.

- Strengthening.
- Improvement of Displacement Capacity.
- Force Limitation.
- Response Modification.
- Site Remediation by Ground Improvement.
- Acceptance or Control of Damage to Specific Components.
- Partial Replacement.

1.12.3.1. Strengthening

Strengthening is intended to increase the force or moment capacity of one or more deficient elements of a bridge. This approach should also take into account any significant increase in stiffness due to the strengthening, and its likely effect on structural response.

It is generally not feasible to economically retrofit a bridge for a major earthquake within the elastic range of the members, and therefore, yield is to be expected in many locations. In cases where the force or moment demands on a structural element are limited by yielding elsewhere in the structure, the strength of the element should be sufficient to resist the demands placed on it without damage. Such is usually the case with superstructure and foundation elements where forces are controlled by column yielding. When these elements are not strong enough to resist the forces or moments generated by the existing or retrofitted column, they must then be strengthened.

Strengthening of a ductile component can reduce the ductility demand on the component and thus improve seismic performance. However, it will usually increase the forces or moments in adjacent components, which will then also need to be strengthened.

The addition of restrainer cables or high strength bars at hinges and seats is also considered to be a form of strengthening. The added strength and stiffness of restrainers will limit the relative movement between superstructure spans or frames, with the goal of preventing failure due to loss of support.

1.12.3.2. Improvement of Displacement Capacity

Displacement capacity is generally a better indicator of structural performance than member strength. A common retrofit approach, therefore, focuses on improving displacement capacity. This can be achieved in one of two ways.

The first technique extends the length of bearing seats to permit greater relative movement at bearing locations without loss of support. This is an alternative method to the use of restrainer cables or bars, which is a strengthening approach intended to reduce the displacement demand on the bearing seat. In many cases, both approaches are used in combination, i.e., both restrainers and seat extenders are used to prevent loss of support at the same location.

The second technique increases the ductility capacity of columns and piers. Large inelastic deformations may be required of columns and piers during a major earthquake and ductility

capacity is a measure of their ability to sustain this deformation without collapse or fracture. A ductile column or pier can therefore accommodate large imposed deformations, and any technique which increases this capacity is considered to be a form of displacement capacity enhancement.

1.12.3.3. Force Limitation

Forces in critical structural components can be limited by using yielding elements as a structural ‘fuse’, i.e., a sacrificial element. If one member in a bridge is deliberately designed to yield and thus limit the forces that can be transmitted to an adjoining member, the second member is ‘capacity-protected’ by the first member. If, for example, a column is intended to yield and develop plastic hinges, the maximum moment that can be transmitted from the column to the foundation is limited by the yield moment of the hinges. In such a case, the foundation is ‘capacity-protected’ by the column.

Although force limitation occurs naturally in many structures, several force-limiting retrofit methods have been developed to reduce the cost of strengthening of components, particularly those that are structurally difficult to implement.

One method of force limitation uses seismic isolation bearings. Although these bearings can be used to modify the dynamic response of a bridge, as discussed in section 1.12.3.4, they can also be used as ‘fuses’ that limit the amount of shear force that can be transmitted to a substructure or foundation.

Another example of force limitation is the link-beam concept that has been used for retrofitting multi-column piers. With this technique, shear forces are limited by plastic hinging in the beams, which in turn limits the magnitude of the moments that can be transmitted to bent caps and footings.

The ductile diaphragm method described in chapter 8 also utilizes the force limitation approach.

1.12.3.4. Response Modification

The dynamic response of a bridge to earthquake ground motion determines the force and displacement demands that will be placed on various components. It is often possible to retrofit the bridge in such a way that the dynamic response will be significantly altered. This could reduce force and displacement demands and thus eliminate or reduce the need for retrofitting by strengthening or enhancing displacement capacity. An example of this approach is seismic isolation, in which the fundamental period of the structure is deliberately increased to reduce the force demands. In this case, however, the displacement demands in the isolators may be very large and additional damping is usually provided to reduce these demands. Energy dissipators and dampers also modify dynamic response and may be used to reduce the need for strengthening or improving displacement capacity.

Another method of response modification is to modify the load path for horizontal inertia forces. Retrofitting to strengthen or stiffen an alternative load path may be used to attract forces away

from vulnerable components, and thus reduce or eliminate the need to retrofit them. An example is a continuous bridge in which the abutment stiffness and strength are increased. Inertial forces are then redistributed to the abutments, which relieve or reduce the forces on the interior columns or piers. This approach can be very effective for simply supported spans if the retrofit also includes provision for making the deck continuous for live load. Shock transmission units can also be used to modify a load path.

Response modification is a powerful retrofit approach but it requires careful consideration of possible side effects, such as changes in the way a bridge responds to service loads.

1.12.3.5. Site Remediation by Ground Improvement

Bridges can suffer significant damage when large permanent ground movements occur during an earthquake. Liquefaction, lateral spreading, landslides, and fault rupture are some of the more common causes of this damage. There are two possible approaches to this problem.

The first approach is to give the structure the capacity to resist the loading and/or accommodate the displacements created by the moving soil without collapse. A critical step in this approach is the quantification of the loads and/or the expected ground movement or fault rupture, which is a difficult problem to solve.

The second approach is to modify the soil using ground improvement techniques, such as those discussed in chapter 11. Site remediation often involves treatment of large areas of soil and can be expensive. In the case of river or stream crossings, improvements may be subject to flooding and require protection from scour. Nevertheless, there will be cases where this approach is a viable option and should be considered. It is not, however, applicable to sites where fault rupture is expected.

1.12.3.6. Acceptance or Control of Damage to Specific Components

When collapse prevention is the main goal of retrofitting, it is often acceptable to allow component damage as long as this does not jeopardize the overall stability of the structure. Often this will mean that no retrofit is required for the members in question. In some cases, however, damage must be controlled to prevent collapse. An example of this is the “P” column retrofit commonly used by Caltrans (Caltrans, 1996). This retrofit method is intended to preserve the vertical load carrying capacity of the column while the column sustains considerable damage. It is common to ignore the lateral load carrying capacity of such a retrofit when conducting an analysis of the structural response.

1.12.3.7. Partial Replacement

There are cases where the required retrofitting of a bridge component may be so extensive that partial replacement is the most economical solution. Partial replacement may have several goals, such as increasing strength and ductility when a column is replaced. In some cases, the type of retrofit performed on an adjacent element may mandate partial replacement. When load-bearing elements are replaced, temporary shoring will be required.

1.13. RETROFIT MEASURES FOR UPPER LEVEL GROUND MOTION

1.13.1. GENERAL

In the last decade, the range of available retrofit measures has increased markedly. Measures have now been developed for deficient superstructures, bearings, beam seats, piers and columns, including weak cap beams and column-to-cap beam joints. In addition, techniques for improving the behavior of abutments and foundations have been developed, including measures for bridges on hazardous sites. This progress is the result of an aggressive research program in California and elsewhere and field experience, mainly in California.

A partial list of these measures is as follows:

- Diaphragm strengthening.
- Energy dissipating ductile diaphragms.
- Provision of longitudinal continuity in simply supported spans.
- Replacement of bearings.
- Seismic isolation bearings.
- Energy dissipators.
- Seat width extensions and catcher blocks at girder supports and intermediate hinges.
- Restrainers at girder supports and intermediate hinges.
- Column replacement.
- Concrete shells, steel and fiber-composite jackets for columns.
- Infill shear walls in bents.
- Cap beam strengthening using prestressing.
- Supergirders.
- Anchor slabs behind abutments.
- Soil and gravity anchors.
- Abutment shear keys.
- Footing replacement.
- Footing overlays.
- Pile tie-down enhancement.
- Supplemental piles.
- Articulation for fault crossings.
- Site remediation for unstable slopes and liquefaction.
- Vibro-replacement of soils and stone columns.

Figure 1-15 illustrates some of the above measures; the details are discussed in chapters 8 through 11.

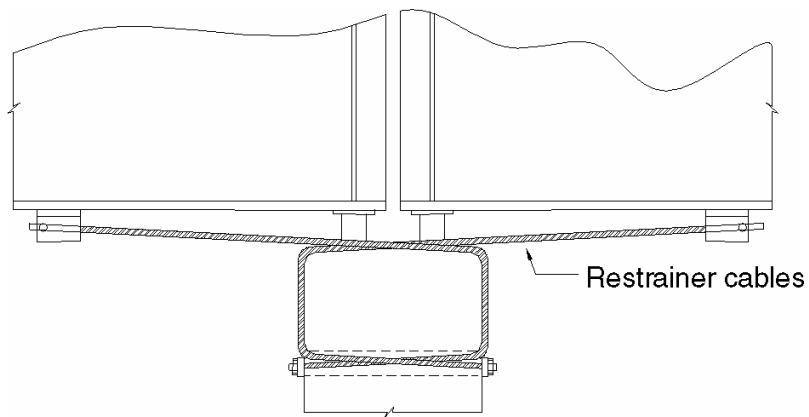
1.13.2. SEISMIC RETROFIT MATRIX

The matrix presented in table 1-11 is a roadmap for the above list of retrofit measures. It shows the relationship between the seven retrofit approaches in section 1.12.3 and the retrofit measures necessary to make them work.

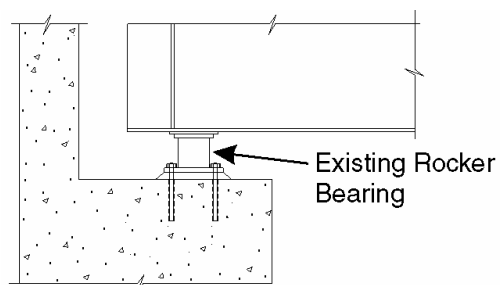
For example, if the *strengthening* approach is chosen to address *insufficient seat length*, then the following measures are recommended in table 1-11 for consideration:

- Section 8.2.2.1: Providing Longitudinal Continuity, Web and Flange Plates.
- Section 8.4.2.1: Longitudinal Joint Restrainers.

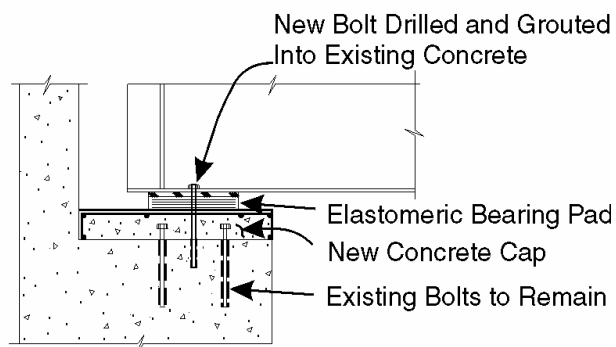
Although table 1-11 presents a comprehensive list of approaches and measures, it is not intended to preclude innovative retrofit approaches or measures that are not specifically mentioned in this manual.



(a) Restainers



Before

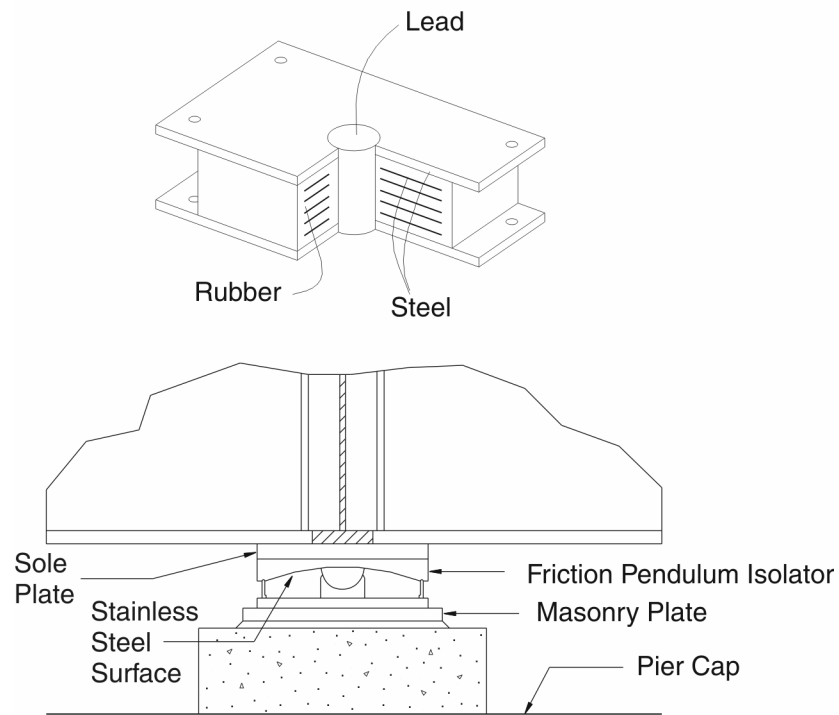


After

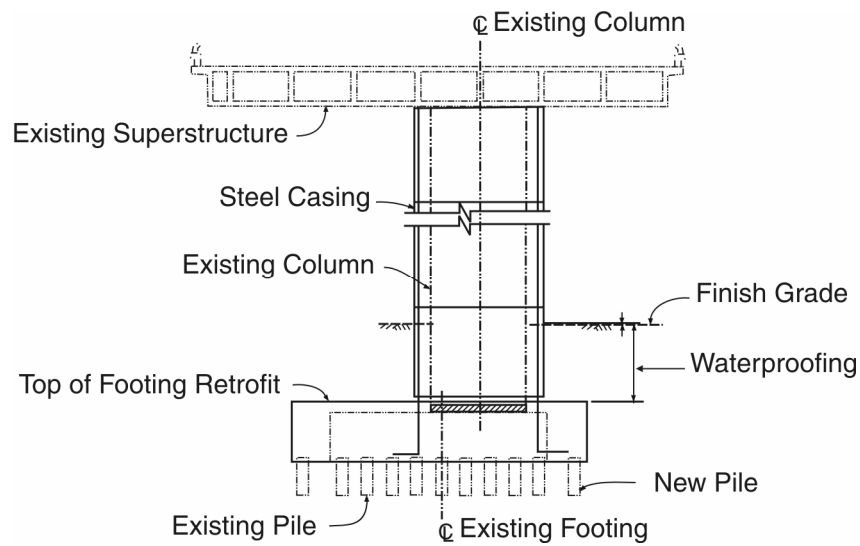
(b) New Bearings

(continued)

Figure 1-15. Selected retrofit measures.



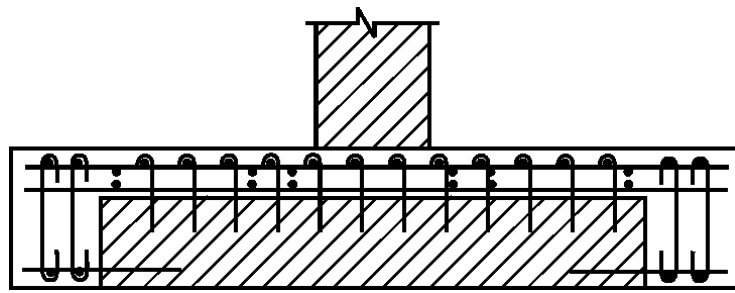
(c) Seismic Isolators



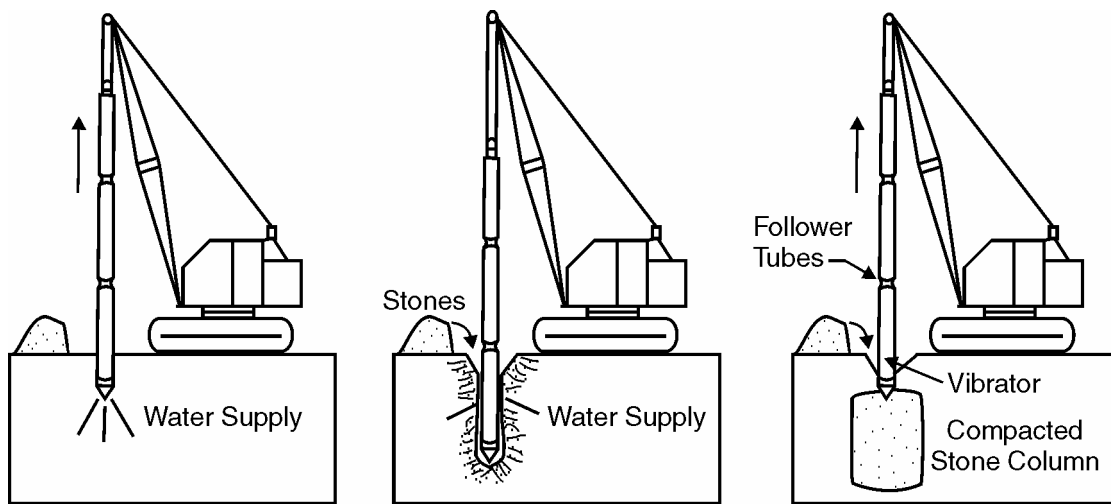
(d) Column Jacketing and Footing Overlay (Schematic)

(continued)

Figure 1-15 (continued). Selected retrofit measures.



(e) Footing Overlay (Detail)



(f) Vibro-Replacement Site Remediation

Figure 1-15 (continued). Selected retrofit measures.

Table 1-11. Matrix of seismic retrofit approaches and section references to associated retrofit measures.

SEISMIC DEFICIENCY	RETROFIT APPROACH						
	Strengthening	Displacement Capacity Enhancement	Force Limitation	Response Modification	Site Remediation	Damage Acceptance or Control	Partial Replacement
Superstructure deficiencies	8.2.1.1 Strengthening of Deck to Girder Connection 8.2.1.4 Girder Strengthening 8.2.4 Strengthening of Continuous Superstructures						
Structurally deficient diaphragms	8.2.1.2 Diaphragm Strengthening or Stiffening		8.2.1.3 Energy Dissipating Ductile Diaphragms				
Structurally deficient bearings/connections	8.3.1 Strengthening of Existing Bearings 8.3.3 Strengthening of Superstructure to Substructure Connections 8.4.2.2 Transverse Restrainers 8.4.2.3 Vertical Motion Restrainers			8.3.2.2 Replacement with Seismic Isolation Bearings 8.4.3 Energy Dissipation Devices 8.4.4 Shock Transmission Units			8.3.2.1 Conventional Bearings
Insufficient seat length	8.2.2.1 Web and Flange Plates 8.4.2.1 Longitudinal Joint Restrainers	8.4.1.1 Concrete Seat Extensions and Catcher Blocks 8.4.1.2 Pipe Extenders		8.2.2.2 Superstructure Joint Strengthening 8.2.3 Reduction of Dead Load			
Flexurally deficient columns or piers	9.2.1.2 Column Flexural Strengthening 9.2.1.4 Supplemental Column Shear Walls 9.2.2.1 Braced Frames 9.2.2.2 Built-up Compression Members 9.2.3 Concrete Wall Piers	9.2.1.3 Column Ductility Improvement and Shear Strengthening 9.2.2.2 Built-up Compression Members	9.2.1.6 Limitation of Column Forces 9.2.2.1 Braced Frames			9.2.1.5 Preservation of the Vertical Load Capacity of Columns	9.2.1.1 Column Replacement
Shear deficient columns or piers	9.2.1.3 Column Ductility Improvement and Shear Strengthening 9.2.1.4 Supplemental Column Shear Walls						

SEISMIC DEFICIENCY	RETROFIT APPROACH						
	Strengthening	Displacement Capacity Enhancement	Force Limitation	Response Modification	Site Remediation	Damage Acceptance or Control	Partial Replacement
Structurally deficient pier caps	9.3.2 Pier Cap Strengthening		9.3.3 Reduction of Pier Cap Forces	9.3.5 Supergirders			9.3.1.1 Partial Replacement at a Joint 9.3.1.2 Total Replacement
Structurally deficient column-to-cap joints	9.3.4 Strengthening of Column and Beam Joints			9.3.5 Supergirders			9.3.1.1 Partial Replacement at a Joint
Structurally deficient column-footing joints	10.3.2 Strengthening of Footings			10.3.4 Limiting Forces Transmitted to the Footings			10.3.1 Footing Replacement
Unstable footings	10.3.2 Strengthening of Footings 10.4.2 Pile Tie-downs			10.3.4 Limiting Forces Transmitted to the Footings	11.4.2 Site Remediation Using Ground Improvement		10.3.1 Footing Replacement
Structurally deficient footings	10.3.2 Strengthening of Footings			10.3.4 Limiting Forces Transmitted to the Footings			
Abutment fill settlement		10.2.1 Approach Slabs			11.4.2 Site Remediation Using Ground Improvement		
Unstable abutments	10.2.2 Anchor Slabs 10.2.5 Transverse Abutment Anchors 10.2.6 Soil and Gravity Anchors			10.2.2 Anchor Slabs			
Structurally deficient abutments	10.2.3 Diaphragm Walls 10.2.4 Transverse Abutment Shear Keys						
Excessive ground movement	8.2.2.1 Web and Flange Plates 8.4.2.1 Longitudinal Joint Restrainers 9.2.3 Concrete Wall Piers 10.3.2 Strengthening of Footings	8.4.1.1 Concrete Seat Extensions and Catcher Blocks 8.4.1.2 Pipe Extenders 9.2.1.3 Column Ductility Improvement and Shear Strengthening 9.2.2.2 Built-up Compression Members	9.2.1.6 Limitation of Column Force		11.4.2 Site Remediation Using Ground Improvement	9.2.1.5 Preservation of the Vertical Load Capacity of Columns	9.2.1.1 Column Replacement

CHAPTER 2: SEISMIC GROUND MOTION HAZARD

2.1. GENERAL

One of the first steps in retrofitting a bridge is to characterize the earthquake hazard at the bridge site. This is done by developing peak ground accelerations and response spectra for the site and, for some bridges, acceleration time histories with and without the effect of spatial variation. The following topics are covered in this chapter:

1. Developing horizontal ground motion response spectra using either:
 - A general procedure based on national ground motion maps and site factors, or
 - A site-specific procedure.
2. Developing vertical ground motion response spectra.
3. Developing acceleration time histories.
4. Assessing the spatial variation in the ground motion.

The estimation of ground motion at a site involves considerable judgment due to uncertainties in the location of seismic sources, the frequency of occurrence of earthquakes of different magnitudes, the maximum magnitude of an earthquake that could occur at a particular site, and the resulting site ground motions for any given earthquake. Since it is believed that these uncertainties are best addressed using a probabilistic approach, this methodology is typically used to obtain design ground motions for bridges and buildings.

As described in chapter 1, two levels of earthquake ground motion are used to determine the performance of an existing bridge and appropriate retrofit measures. They consist of a lower level ground motion and an upper level ground motion. The *lower level* motion has a probability of exceedance of 50 percent during the service life of the bridge (assumed to be 75 years), whereas the *upper level* motion has a probability of exceedance of seven percent in 75 years. As discussed below and shown in table 2-1, these two exceedance probabilities correspond to return periods of approximately 100 and 1000 years for the lower and upper level ground motions, respectively.

Using a Poisson probability model¹, the probability of exceedance (P_E) of a given amplitude of ground motion in the lifetime of the bridge (t) is related to the annual frequency of exceedance (v) of that ground motion amplitude, by the following equation:

¹ In a Poisson model, earthquakes of given magnitudes occur randomly in time at an average rate. The occurrence of an earthquake is assumed to have no influence on the timing or probability of a future earthquake.

$$P_E = 1 - e^{-vt} \quad (2-1)$$

Rewritten, equation 2-1 gives v as a function of P_E and t as follows:

$$v = \frac{-\ln(1 - P_E)}{t} \quad (2-2)$$

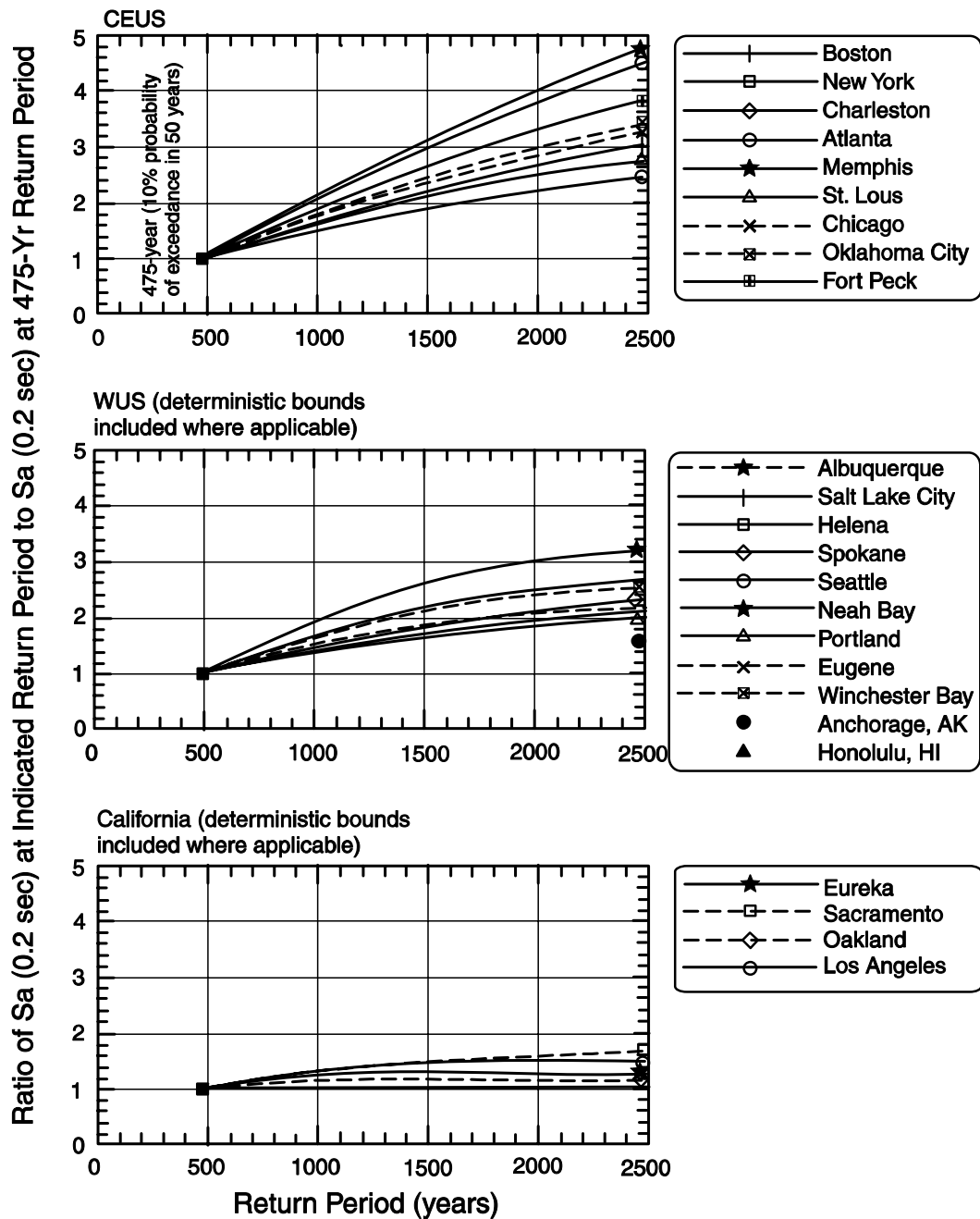
Return periods² corresponding to various probabilities of exceedance can be calculated using equation 2-2, as shown in table 2-1. For this table, the lifetime of a bridge (t) is taken as 75 years.

Table 2-1. Relationship between probability of exceedance of earthquake ground motion and return period.

Probability of Exceedance (P_E) in Bridge Life of 75 Years (%)	Annual Frequency of Exceedance, v	Return Period (years)	
		Actual	Rounded
50	0.009242	108	100
15	0.002167	461	500
7	0.000968	1033	1000
5	0.000684	1462	1500
3	0.000406	2462	2500

As described in section 1.5, two spectral accelerations (S_{DS} and S_{D1}) are used to determine the seismic loads for bridge screening and evaluation. These accelerations are obtained by modifying the spectral accelerations assuming a rock site (S_S and S_1), to account for the actual soil conditions at the site. Figure 2-1 shows the variation in these two accelerations with return period for different locations in the United States. Figure 2-1(a) gives the short-period (S_S) accelerations and figure 2-1(b) gives the long-period (S_1) values. These plots show that for bridge sites in the eastern United States, spectral accelerations for earthquake ground motions with very long return periods, such as 2500 years, may be three to four times higher than for the 500-year ground motions at the same site. This ratio varies considerably from state to state across the U.S., and is one of the primary reasons for adopting two different levels of earthquake ground motion for seismic retrofitting.

² The reciprocal of the annual frequency of exceedance is the return period of exceedance. In this manual, the reciprocal is simply called the 'return period'.

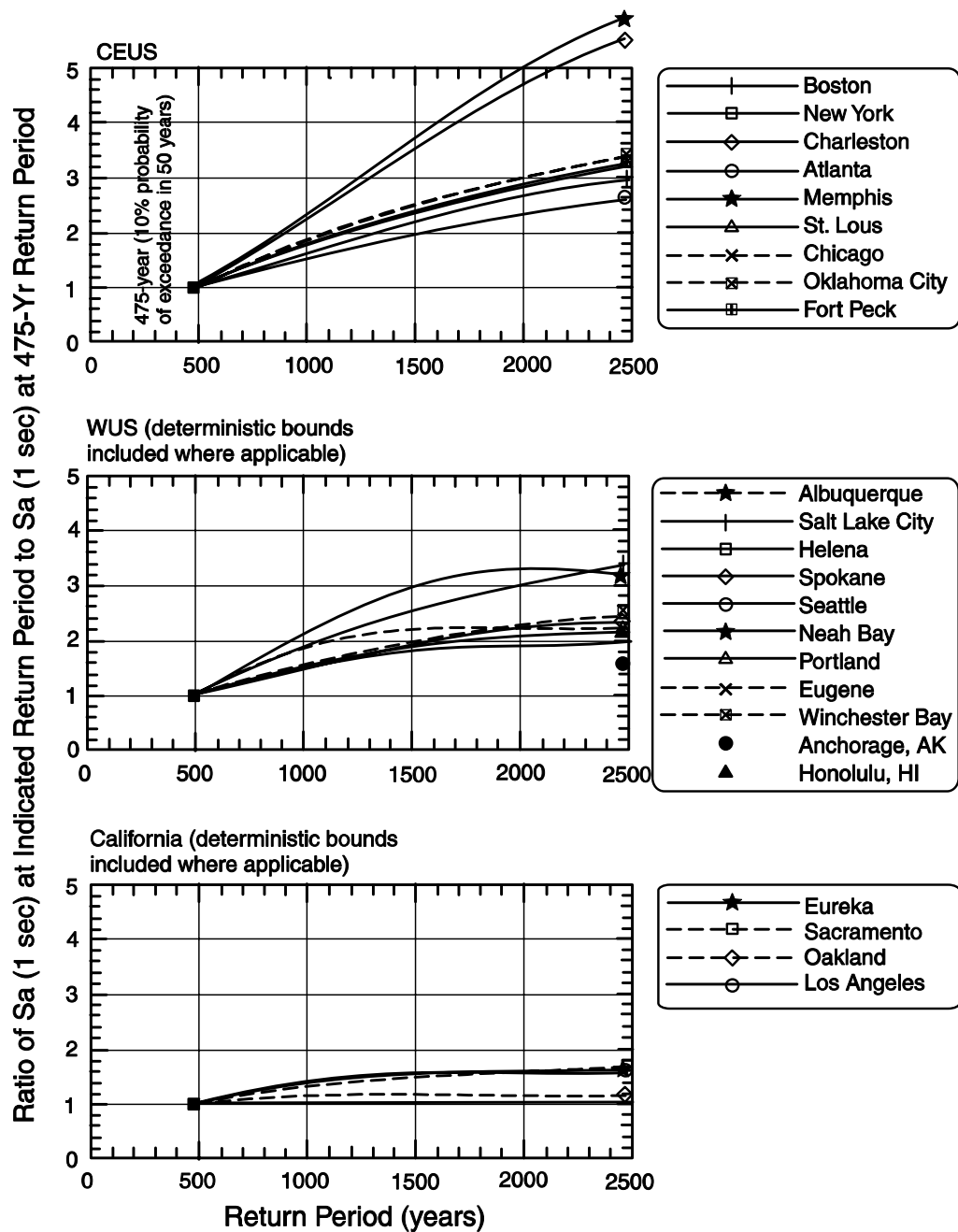


(a) Ratios of short-period (S_s) spectral acceleration at various return periods to short-period spectral acceleration at 475-year return period

ATC/MCEER, 2003

(continued)

Figure 2-1(a). Variation in short- and long-period spectral accelerations with ground motion return period.



(b) Ratios of long-period (S_L) spectral acceleration at various return periods to long-period spectral acceleration at 475-year return period

ATC/MCEER, 2003

Figure 2-1 (continued). Variation in short- and long-period spectral accelerations with ground motion return period.

2.2. BASIC PROCEDURES FOR CHARACTERIZING HORIZONTAL SEISMIC GROUND MOTION

The two basic procedures for developing response spectra and peak accelerations of horizontal ground motions are:

1. A general procedure using national ground motion maps and site factors as described in sections 2.3, 2.4 and 2.5.
2. A site-specific procedure as described in section 2.6.

The site specific procedure should be used if any of the following apply:

- Soils at the site require site-specific evaluation (i.e., site class F soils, as defined in section 2.4) unless a determination is made that the presence of such soils would not result in a significantly higher response of the bridge.
- The bridge is considered to be a major or very important structure by the owner.
- The site is located within 10 km (6 mi) of an active fault and its response would be significantly and adversely influenced by near-fault ground motions.

Examples of conditions for which site-specific evaluations would not be required for Type F soils are given in section 2.4. Section 2.6 describes the characteristics of near-fault ground motions that could lead to increased bridge response, but these effects might be considered for major bridges only.

2.3. DETERMINATION OF SPECTRAL ACCELERATIONS, S_s and S_1

Both the short-period (S_s) and long-period (S_1) spectral accelerations have been mapped by the U. S. Geological Survey (USGS) for the United States for various exceedance probabilities (return periods). The maps used with the general procedure are the 1996 edition of the probabilistic ground motion maps published by the USGS^{3, 4}. In California, these maps are produced jointly by the California Geological Survey (CGS), and the USGS. These maps are for a reference rock site condition (site class B). Procedures for adjusting the ground motions to other site conditions are described in section 2.4. However, maps are not available for all possible return periods and the USGS has provided ground motion hazard curves for selected longitudes and latitudes to provide for those cases not covered by the maps. These curves may be used to develop the relationship between the amplitude of a ground motion parameter and its annual frequency of exceedance, which allows spectral values to be found for any return period specified by the user. These curves are available on a CD-ROM published by the USGS; a copy of this CD is included in the manual (see inside back cover).

³ Updated maps were published by the USGS in 2002, but not for 1000-year return period. See sidebar. A new CD is expected in 2005 which will allow data to be automatically generated for any return period.

⁴ Frankel et al., 1996, 1997a, 1997b, 1997c, 2000; Klein et al., 1999; Peterson et al., 1996; Wesson et al., 1999a; 1999b

2.3.1. USGS PROBABILISTIC GROUND MOTION MAPS

The USGS probabilistic ground motion maps should be used to obtain horizontal response spectral accelerations and peak ground accelerations in rock. Large-scale paper maps are available for return periods of 500 (475), 1000 (975) and 2500 (2475) years, and give spectral accelerations at 0.0, 0.2, 0.3, and 1.0-second periods of vibration. The 0.0-second values are equivalent to peak ground accelerations. All mapped values are for five percent damping.

Maps can also be downloaded from the USGS web site at <http://eqhazmaps.usgs.gov>, but only for the return periods noted above. In addition to maps, ground motion values are also available from this site by entering the longitude and latitude coordinates of the site. If these coordinates are not available, the zip code for the region containing the site may be used. The same information is also available on a CD-ROM published by USGS (Frankel and Leyendecker, 2001). A copy of the CD is included in this manual (see inside back cover).

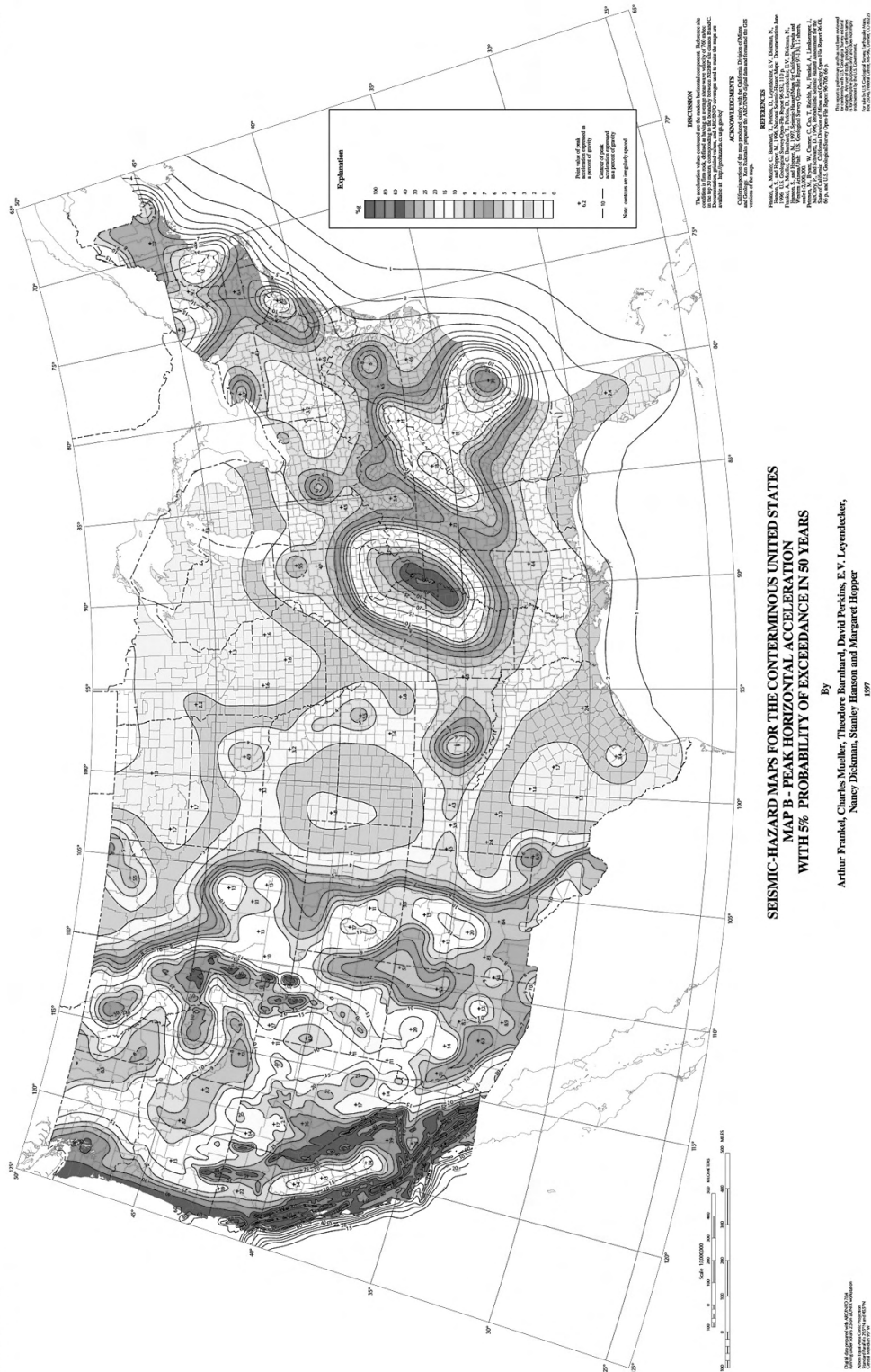
Note that the above sources of mapped and tabulated data do not include earthquakes with a 100-year return period. A methodology to obtain 100-year data is described in the next section.

Figure 2-2(a) is a map of the peak ground acceleration for the conterminous U.S. for the upper level earthquake (1000-year return period). This map was obtained from the CD-ROM noted above. Maps for Alaska, Hawaii, Guam and Puerto Rico are also available from this source. Figures 2-2 (b) and (c) are maps of the short-period (S_s) and long period (S_1) spectral accelerations, respectively, for the upper level earthquake (1000 years). These maps are from the same CD and are for the conterminous U.S. Maps for other states and regions are also available.

Available U.S. Geological Survey Seismic Hazard Maps and CDs

Maps of peak ground acceleration, and the short- and long-period spectral accelerations (S_s and S_1) for selected return periods are available from the US Geological Survey in either paper form or on CD as listed below. Seismic hazard curves are also available on CD from which accelerations and spectral ordinates may be found for any return period. Some of this data is also available on the USGS web site <http://eqhazmaps.usgs.gov>.

Year	Published Data
1996	Maps for 48 conterminous states, for return periods 500, 1000, and 2500 years.
1998	Maps for Alaska and Hawaii, for 500 and 2500 years.
2001	CD with maps and seismic hazard curves for 48 conterminous states, Alaska, and Hawaii based on 1996 data. This CD is provided inside back cover of this report.
2002	Maps for 48 conterminous states, for return periods 500 and 2500 years. Major difference between 1996 and 2002 Maps is in the hazard models used for New Madrid and Charleston regions.
2003	Maps for Puerto Rico and Virgin Islands, for return periods 500 and 2500 years.
2005 est.	Updated CD with 1996 and 2002 data; also automated means of generating data for any return period instead of manual method used in this report (section 2.3.2).



(a) Peak ground accelerations for the upper level ground motion (1000-year return period)

(continued)

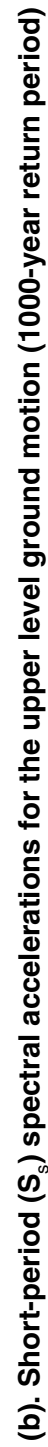
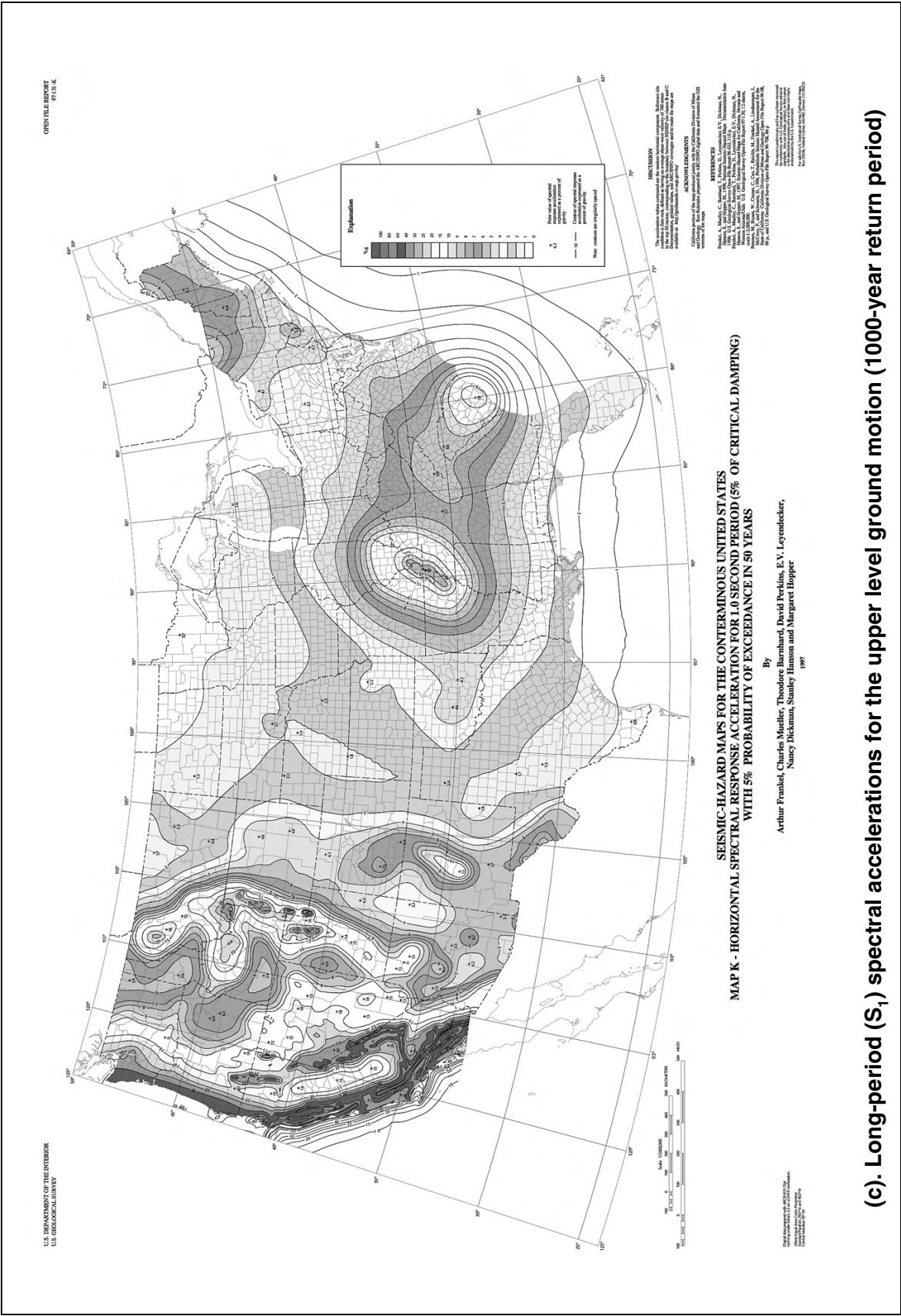


Figure 2-2 (continued). Seismic hazard maps for the conterminous United States.



(c). Long-period (S_1) spectral accelerations for the upper level ground motion (1000-year return period)

Figure 2-2 (continued). Seismic hazard maps for the conterminous United States.

2.3.2. USGS PROBABILISTIC GROUND MOTION DATA FILES FROM CD-ROM

Instead of using the USGS maps, the spectral accelerations S_s and S_1 may be obtained from the ground motion data files used to produce the maps which are available on the CD-ROM (Frankel and Leyendecker, 2001) included with this manual.

Spectral accelerations and peak ground motions may be found from this CD for both the lower and upper level earthquakes (100- and 1000-year return periods) for any site identified by either zip code or longitude and latitude coordinates. The procedure for these calculations is described in the following steps.

Step 1. Load CD titled *Seismic Hazard Curves and Uniform Hazard Response Spectra*, and using either Windows Explorer or Setup from the Start Menu, run “Probabilistic Hazard 3.10.” Display the window shown in figure 2-3(a).

Step 2. Click box labeled ‘Hazard Curves and Response Spectra for the United States’ and display the window shown in figure 2-3(b).

Step 3. Initialize:

- Check name box and enter identifier for results to be generated.
- Check box to include date and time on output file.
- Click box labeled ‘Open File Selection Menu’ and display window shown in figure 2-3(c).

Step 4. Setup files:

- Under heading ‘Select Directory for Data Files,’ select the drive letter for the CD-ROM and then choose ‘GM96-Data.’
- Under heading ‘Select Directory for Map Files,’ select the drive letter for the CD-ROM and then choose ‘GM96-Maps.’
- Click ‘OK’ if satisfied and display the window shown in figure 2-3(c); otherwise click ‘Cancel Selections’ and return to beginning of Step 3.

Step 5. Choose either ‘Latitude and Longitude’ or ‘5-Digit Zip Code’ to identify the bridge site as shown in figure 2-3(d)⁵.

⁵ Latitude and longitude coordinates are the most accurate way to locate a bridge but in the absence of these coordinates, a zip code may be used. In the latter case, the seismic hazard at the geographical center of the region covered by the zip code is presumed to be representative of that at the bridge site.

Step 6. To obtain values for S_S and S_1 for the upper level ground motion, go to the box labeled ‘Select Parameter,’ and select the line ‘U.H.S. for 5 percent PE in 50 years,’ then click ‘Calculate Spectrum’ (figure 2-3(d))⁶.

Step 7. Values for S_S and S_1 for the site specified in Step 5 and the return period selected in Step 6 are displayed in the box to the right of the screen under the heading ‘Output for All Calculations’ (figure 2-3(d)).

- Read S_S from the row with Period = 0.2 sec under column headed ‘PGA or S_a .’
- Read S_1 from the row with Period = 1.0 sec under column headed ‘PGA or S_a .’

Click box ‘Clear Selections’ and display screen shown in figure 2-3(e).

Step 8. To obtain values for S_S for the lower level ground motion, go to the box labeled ‘Select Parameter’ and select the line ‘Hazard Curve for 0.2 sec,’ then click ‘Calculate Hazard Curve’ (figure 2-3(e))⁷.

Step 9. Values for S_S for the site specified in Step 5 and for a range of frequencies of exceedance are displayed in the box to the right of the screen under the heading ‘Output for All Calculations’ (figure 2-3(e)). The value of S_S for a frequency of 0.01 (return period of 100 years) is obtained by linear interpolation from this table⁸. Alternatively, values may be read directly from a plot of frequency against acceleration, i.e., from the Hazard Curve, as described in Step 10.

Step 10. Click ‘View Hazard Curve’ to display plot shown in figure 2-3(f). Read S_S for annual frequencies of 0.01. Note that the value for S_S for the 1000-year return period may also be read from this same graph ($FEX = 0.001 = 1.0E-03$) and compared with the value obtained in Step 7. Return to the previous screen by clicking ‘Exit Viewer,’ and then click ‘Clear Selections’ to display the screen shown in figure 2-3(g).

Step 11. To obtain values for S_1 for the lower level ground motion, go to the box labeled ‘Select Parameter’ and select the line ‘Hazard Curve for 1.0 sec,’ then click ‘Calculate Hazard Curve’ (figure 2-3(g))^{7,8}.

Step 12. Values for S_1 for the site specified in Step 5 and for a range of frequencies of exceedance, are displayed in the box to the right of the screen under the heading ‘Output

⁶ The upper level ground motion is defined in chapter 1 (table 1-2) as having a seven percent probability of exceedance (PE) in 75 years, which is equivalent to a five percent PE in 50 years. Both probabilities of exceedance describe an earthquake with a return period of about 1,000 years.

⁷ The lower level event is defined in chapter 1 (table 1-2) as having a 50 percent probability of exceedance (PE) in 75 years, which is equivalent to a return period of about 100 years or an Annual Frequency of Exceedance (FEX) of about 0.01.

⁸ This table uses scientific notation to express frequencies of exceedance, and a frequency of 0.01 is therefore written as 1.0E-02.

for All Calculations' (figure 2-3(g)). The value of S_1 for a frequency of 0.01 (return period of 100 years) is obtained by linear interpolation from this table. Alternatively, values may be read directly from a plot of frequency against acceleration, i.e., from the Hazard Curve, as described in Step 13.

Step 13. Click 'View Hazard Curve' to display plot shown in figure 2-3(h). Read S_1 for annual frequencies of 0.01. Note that the value for S_1 for the 1000-year return period may also be read from this same graph ($FEX = 0.001 = 1.0E-03$) and compared with the value obtained in Step 7. Return to the previous screen by clicking 'Exit Viewer.'

Step 14. Click 'Exit Program' to end calculations.

Example 2.1 illustrates the above process for finding S_s and S_1 for both the lower and upper earthquake ground motions for a site identified by a zip code.

EXAMPLE 2.1: DETERMINATION OF S_s AND S_1 VALUES FROM CD-ROM

Calculate S_s and S_1 for a bridge site in Salt Lake City (zip code 84112) for both the lower and upper earthquake ground motions (100- and 1000-year return periods).

Steps 1, 2, 3, and 4. Initialize:

- Load CD and start 'Probabilistic Hazard 3.10'
- Click 'Hazard Curves and Response Spectra for the United States' (figure 2-3(a))
- Enter name 'Demonstration: SLC' (figure 2-3(b))
- Select 'Include Date and Time on Output' (figure 2-3(b))
- Select 'Open File Selection Menu on figure 2-3(b) and choose CD-ROM drive d: for both the Data Files and Map Files (figure 2-3(c))
- Select 'GM96-Data' and 'GM96-Maps' respectively (figure 2-3(c)), and
- Click 'OK'.

Step 5. Identify bridge site:

- Select '5-digit Zip Code' and enter '84112' (figure 2-3(d)).

Steps 6 and 7. Find S_s and S_1 for the Upper Level Ground Motion (1000-year return period):

- Go to 'Select Parameter' box and choose VHS '5 percent PE in 50 years' (figure 2-3(d))
- Click 'Calculate Spectrum' (figure 2-3(d))
- In panel at right read $S_a = 110.9$ percent $g = 1.109g$ at period = 0.2 sec (figure 2-3(d))
- In panel at right read $S_a = 38.6$ percent $g = 0.386g$ at period = 1.0 sec (figure 2-3(d)), and
- Click 'Clear Selections' (figure 2-3(d)).

Steps 8, 9, and 10. Find S_s for the Lower Level Ground Motion (100-year return period):

- Go to 'Select Parameter' box and choose 'Hazard Curve for 0.2 sec' (figure 2-3(e))
- Click 'Calculate Hazard Curve' (figure 2-3(e))
- Obtain S_s for frequency of exceedance (FEX) = 0.01 by linear interpolation as follows:

From the box at right of figure 2-3(e) labeled 'Output for All Calculations:'

Frequency of exceedance (FEX)		S_s (g)
1.448E-02	0.01448	0.128
8.551E-03	0.00855	0.192

Therefore, S_s at FEX = 0.01 is given by:

$$\begin{aligned} S_s &= 0.128 + (0.192 - 0.128) (0.01448 - 0.01000) / (0.01448 - 0.00855) \\ &= 0.176 \text{ g} \end{aligned}$$

Alternatively, S_s may be read directly from the Hazard Curve in figure 2-3(f) by selecting 'View Hazard Curve.' Here it can be seen that for a frequency of 0.01, the acceleration (S_s) is approximately 0.17g. Click 'Exit Viewer.'

- Click 'Clear Selections.'

Steps 11, 12, and 13. Find S_1 for the Lower Level Ground Motion (100-year return period):

- Go to 'Select Parameter' box and choose 'Hazard Curve for 1.0 sec' (figure 2-3(g))
- Click 'Calculate Hazard Curve' (figure 2-3(g))
- Obtain S_1 for frequency of exceedance (FEX) = 0.01 by linear interpolation as follows:

From the box at right of figure 2-3(g) labeled 'Output for All Calculations:'

Frequency of exceedance (FEX)		S_1 (g)
1.173E-02	0.01173	0.0427
7.146E-03	0.00715	0.0641

Therefore, S_1 at FEX = 0.01 is given by:

$$\begin{aligned} S_1 &= 0.0427 + (0.0641 - 0.0427) (0.01173 - 0.01000) / (0.01173 - 0.00715) \\ &= 0.0508 \text{ g} \end{aligned}$$

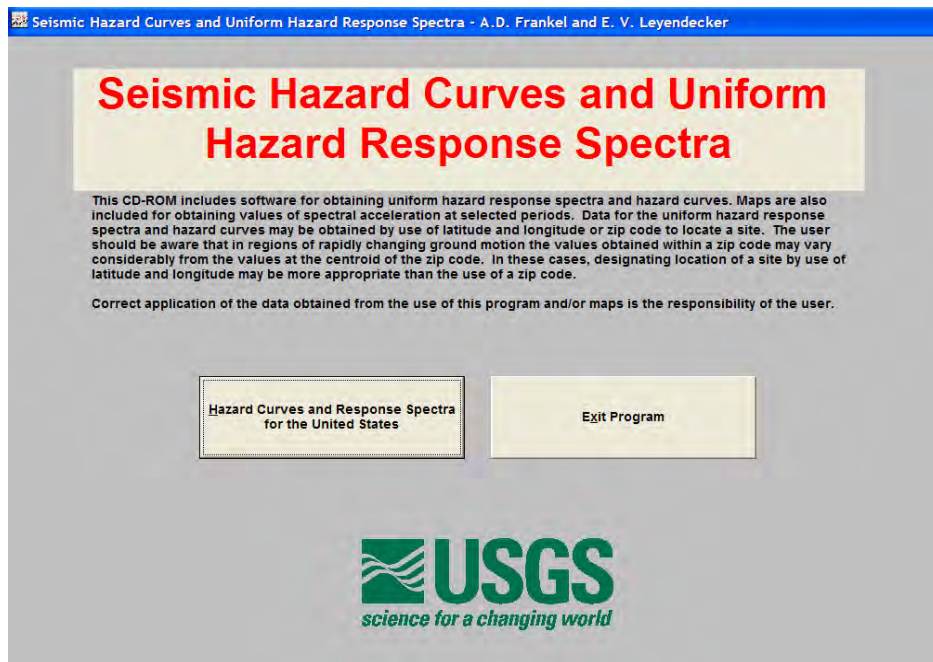
Alternatively, S_1 may be read directly from the Hazard Curve in figure 2-3(h) by selecting 'View Hazard Curve.' Here it can be seen that for a frequency of 0.01, the acceleration (S_1) is approximately 0.05g. Click 'Exit Viewer.'

Step 14. Click 'Exit Program.'

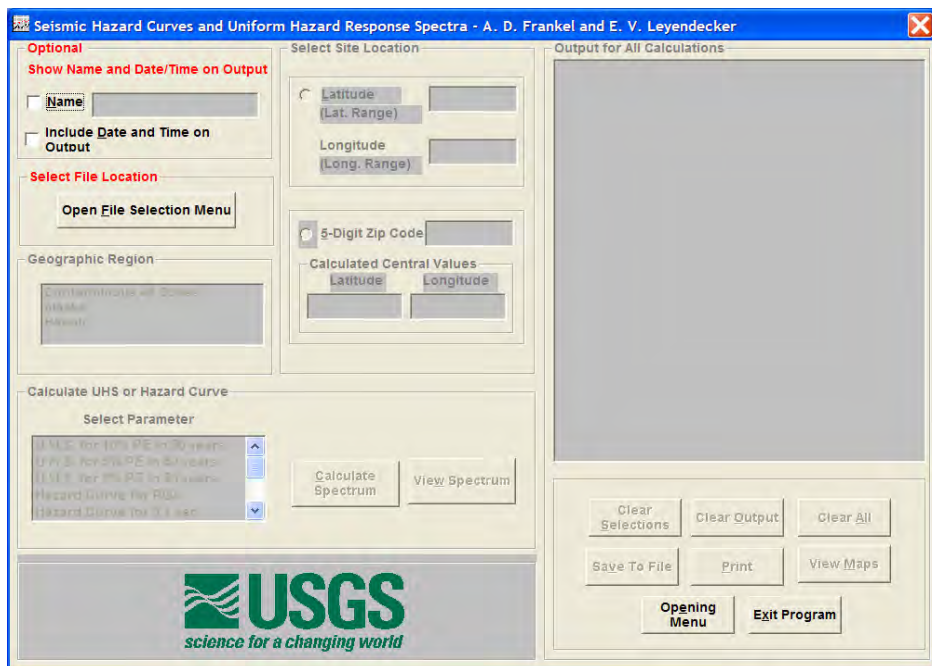
A summary of results obtained above is given in the table below.

Values of S_s and S_1 for Bridge Site in Zip Code 84112.

Ground Motion	S_s (g)	S_1 (g)
Lower Level: 100-year	0.176	0.051
Upper Level: 1000-year	1.109	0.386



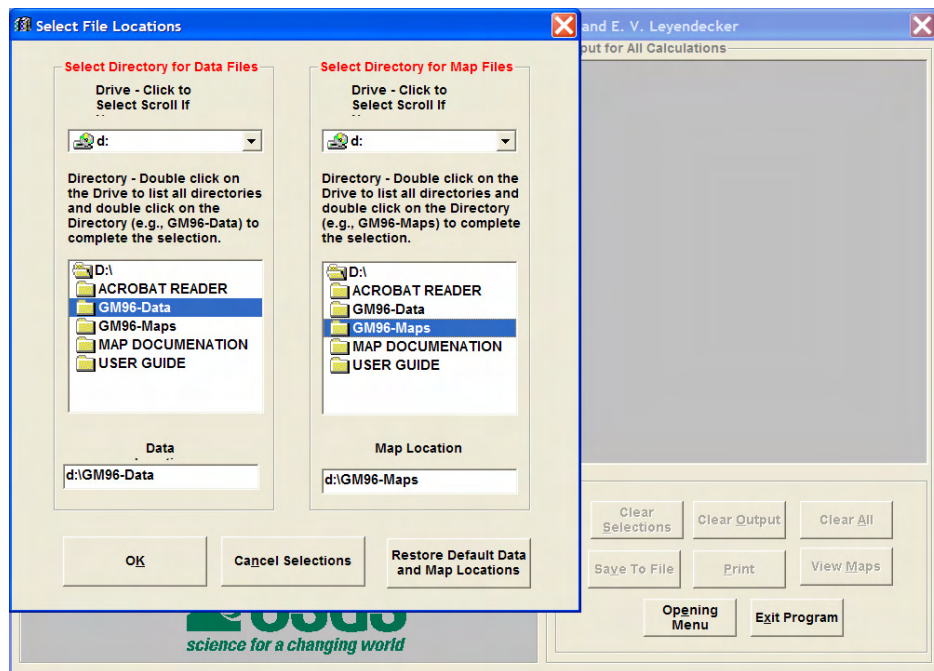
(a) Opening window for 'Probabilistic Hazard 3.10'



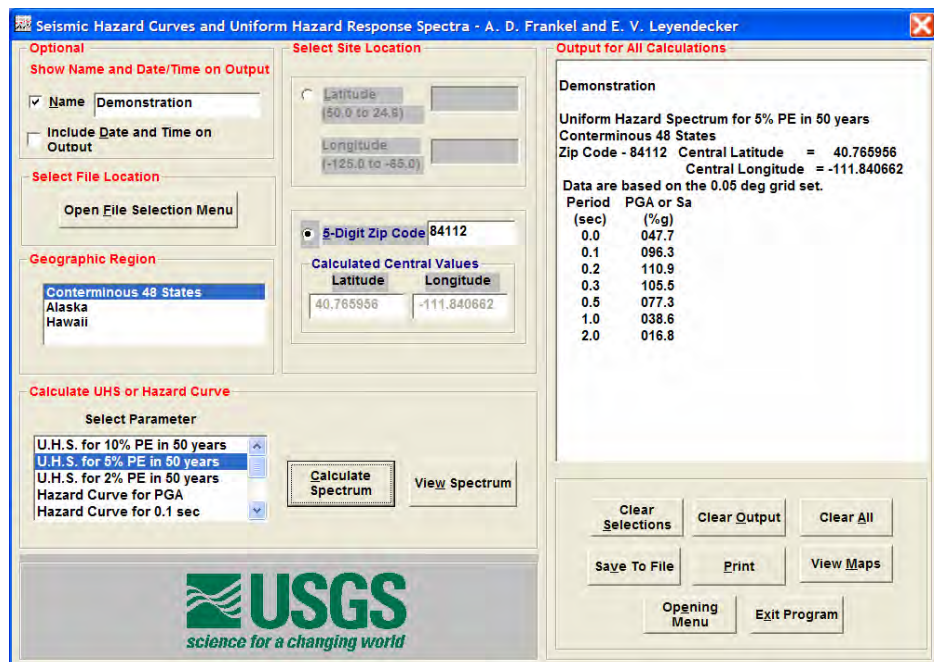
(b) Initialization window

(continued)

Figure 2-3. Calculation of short- and long-period spectral accelerations for 100- and 1000-year ground motion return periods.



(c) Setup window for data and map files



(d) Selection of 1000-year uniform hazard spectrum and result for given site

(continued)

Figure 2-3 (continued). Calculation of short- and long-period spectral accelerations for 100- and 1000-year ground motion return periods.

Seismic Hazard Curves and Uniform Hazard Response Spectra - A. D. Frankel and E. V. Leyendecker

Optional
 Show Name and Date/Time on Output
☒ Name: Demonstration
☐ Include Date and Time on Output

Select Site Location
 Latitude (50.0 to 24.8):
 Longitude (-125.0 to -85.0):
☒ 5-Digit Zip Code: 84112
 Calculated Central Values
 Latitude: 40.765956 Longitude: -111.840662

Select File Location
 Open File Selection Menu

Geographic Region
 Continental 48 States
 Alaska
 Hawaii

Calculate UHS or Hazard Curve
 Select Parameter
 U.H.S. for 2% PE in 50 years
 Hazard Curve for PGA
 Hazard Curve for 0.1 sec
 Hazard Curve for 0.2 sec
 Hazard Curve for 0.3 sec
 Calculate Hazard Curve View Hazard Curve

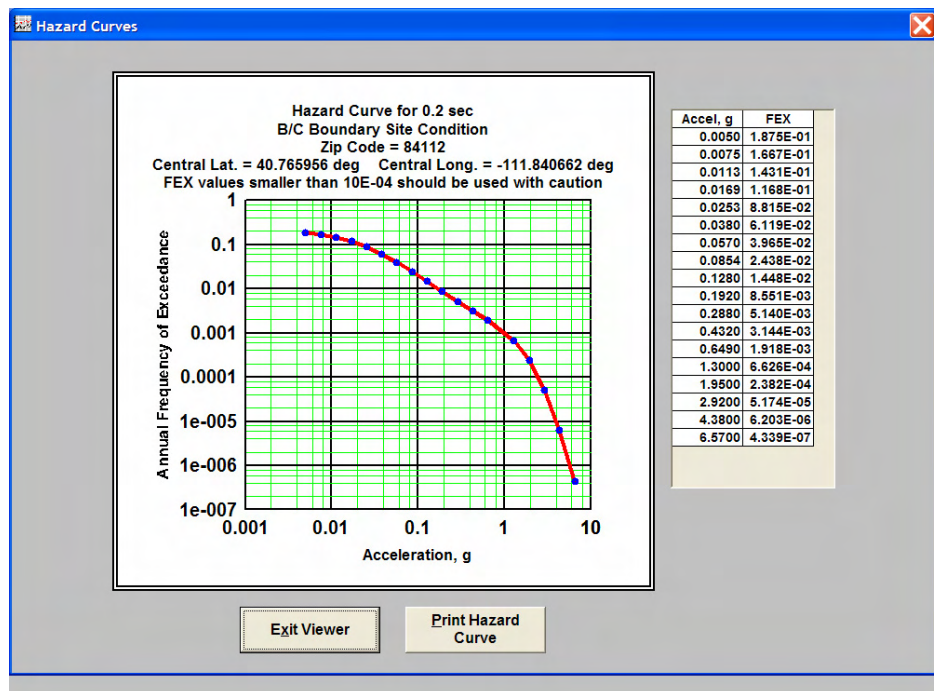
Output for All Calculations
 Hazard Curve for 0.2 sec
 Continental 48 States
 Zip Code - 84112 Central Latitude = 40.765956
 Central Longitude = -111.840662
 Data are based on the 0.05 deg grid set.
 Frequency of Exceedance values less than 10E-4 should be used with caution.

Frequency of Exceedance (per year)	Ground Motion (g)
1.875E-01	0.0060
1.667E-01	0.0075
1.431E-01	0.0113
1.168E-01	0.0169
8.815E-02	0.0253
6.119E-02	0.0380
3.965E-02	0.0570
2.438E-02	0.0854
1.448E-02	0.1280
8.551E-03	0.1920
5.140E-03	0.2880
3.144E-03	0.4320
1.918E-03	0.6490
6.626E-04	1.3000

Clear Selections Clear Output Clear All
 Save To File Print View Maps
 Opening Menu Exit Program

USGS
 science for a changing world

(e) Selection of S_s (0.2 sec) hazard curve and result for given site



(f) Example of S_s (0.2 sec) hazard curve for given site

(continued)

Figure 2-3 (continued). Calculation of short- and long-period spectral accelerations for 100- and 1000-year ground motion return periods.

Seismic Hazard Curves and Uniform Hazard Response Spectra - A. D. Frankel and E. V. Leyendecker

Optional
 Show Name and Date/Time on Output
☒ Name: Demonstration
☐ Include Date and Time on Output

Select File Location
 Open File Selection Menu

Geographic Region
 Continental 48 States
 Alaska
 Hawaii

Select Site Location
 Latitude (50.0 to 24.5)
 Longitude (-125.0 to -65.0)
 5-Digit Zip Code: 84112
 Calculated Central Values
 Latitude: 40.765956 Longitude: -111.840662

Calculate UHS or Hazard Curve
 Select Parameter
 Hazard Curve for 0.2 sec
 Hazard Curve for 0.3 sec
 Hazard Curve for 0.5 sec
 Hazard Curve for 1.0 sec
 Hazard Curve for 2.0 sec

Calculate Hazard Curve View Hazard Curve

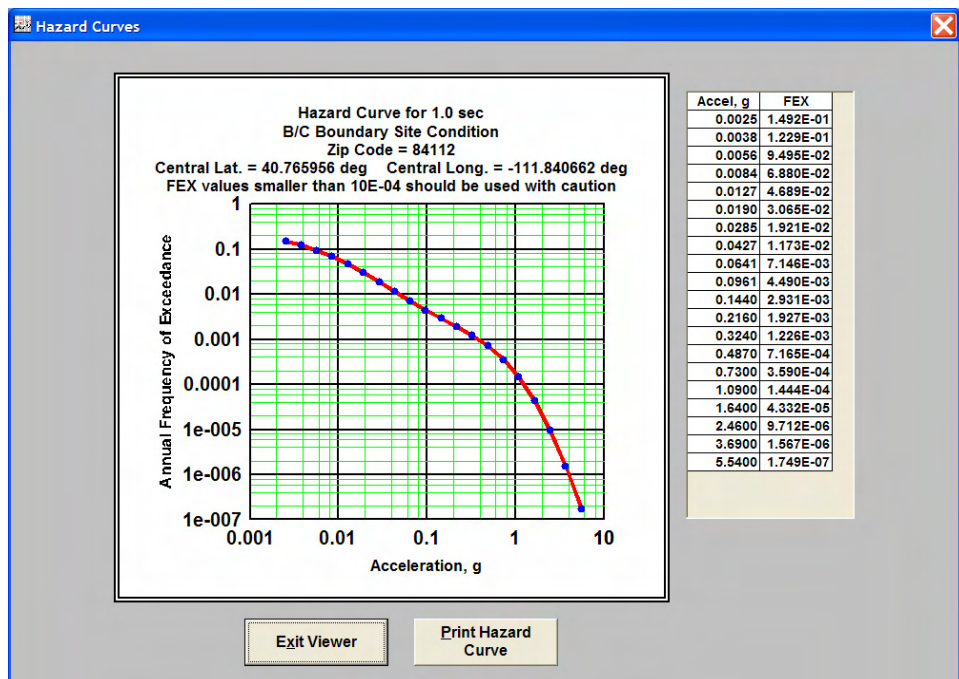
Output for All Calculations
 Hazard Curve for 1.0 sec
 Continental 48 States
 Zip Code - 84112 Central Latitude = 40.765956
 Central Longitude = -111.840662
 Data are based on the 0.05 deg grid set.
 Frequency of Exceedance values less than 10E-4 should be used with caution.

Frequency of Exceedance (per year)	Ground Motion (g)
1.492E-01	0.0025
1.229E-01	0.0038
9.495E-02	0.0056
6.880E-02	0.0084
4.689E-02	0.0127
3.065E-02	0.0190
1.921E-02	0.0285
1.173E-02	0.0427
7.146E-03	0.0641
4.490E-03	0.0961
2.931E-03	0.1440
1.927E-03	0.2160
1.226E-03	0.3240
7.165E-04	0.4870

Clear Selections Clear Output Clear All
 Save To File Print View Maps
 Opening Menu Exit Program

USGS
 science for a changing world

(g) Selection of S_1 (1.0 sec) hazard curve and result for given site



(h) Example of S_1 (1.0 sec) hazard curve for given site

Figure 2-3 (continued). Calculation of short- and long-period spectral accelerations for 100- and 1000-year ground motion return periods.

2.4. SITE CLASSES AND SITE FACTORS

2.4.1. DESCRIPTION OF SITE CLASSES AND SITE FACTORS

When using the general procedure, sites should be classified and site factors determined in accordance with this section. The development of response spectra using national ground motion maps (section 2.3) and site factors is described in section 2.5.

Recommended site classes and site factors are based on studies carried out following the 1989 Loma Prieta earthquake in California, which culminated in recommendations that have been adopted by the NEHRP Building Provisions (BSSC, 1994, 1998), the Uniform Building Code (ICBO, 1997), and the International Building Code (IBC) (ICC, 2000)⁹. Earthquake data obtained during the Loma Prieta earthquake confirmed the validity of these site factors and the improvement in accuracy compared to site factors in earlier bridge and building codes.

Site class definitions are given in table 2-2. Sites are classified according to their stiffness as determined by their shear wave velocity in the upper 30 meters (100 feet). Standard Penetration Test (SPT) blowcounts and undrained shear strengths of soil samples from soil borings can also be used to classify sites as indicated in table 2-2. Steps for classifying a site are given in table 2-3. Alternatively, SPT blowcounts and undrained shear strengths can be converted into estimated shear wave velocities and used for site classification. Procedures given in Kramer (1996) can be used for these conversions.

Shear wave velocities were used when conducting the original studies that defined the site classes and may be considered as the fundamental soil property. If the site profile consists of layered sands and clays or soil over rock within the upper 30 meters (100 feet), then it is particularly desirable to convert the profile to estimated shear wave velocities. If the resulting site class does not appear reasonable, or if the project involves special design issues, shear wave velocity measurements should be made at the site.

Site factors for the site classes in table 2-2 are given in table 2-4. Site class B rock (soft rock) is taken to be the site category for the USGS ground shaking maps. Type B rock is therefore the reference site condition for which the site factor is taken to be 1.0. Site classes A, C, D, and E have separate sets of site factors for the short-period range (site factor F_a) and long-period range (site factor F_v), as indicated in table 2-3. These site factors generally increase as the site profile becomes softer (in going from site class A to E). Except for site class A (hard rock), the site factors also decrease as the ground motion level increases, reflecting the nonlinear behavior of most soils. Therefore, for a given soil site class C, D, or E, these nonlinear site factors increase the ground motion more in areas having lower ground motions than in areas having higher ground motions. The levels of ground motion for use with table 2-4 are characterized by short-period (0.2-second) response spectral acceleration and long-period (1.0-second) response spectral acceleration on rock as shown on USGS national ground motion maps.

⁹ Martin and Dobry, 1994; Rinne, 1994; Dobry et al., 2000

2.4.2. CONSIDERATIONS FOR SITE CLASS F SOILS

As indicated in tables 2-2 and 2-4, a site class F is defined for types of soil for which site factors are not given and site-specific investigations are recommended to determine site response effects. Site class F is intended for soils for which site response effects may be very strong and not reliably quantified except by site-specific studies. Guidelines for determining the response of site class F soils by site-specific studies are given in appendix A.

Also per section 2.2, a site-specific investigation to determine site response for site class F soils is not required if a determination is made that the presence of such soils will not result in a significantly higher response of a bridge. Such a determination should be made jointly by the bridge engineer and the geotechnical engineer.

Examples of conditions that could lead to such a conclusion are the extent and depth of site class F soils. With regard to the extent of these soils, for short bridges with a limited number of spans and having earth approach fills, ground motions at the abutments will generally determine the response of the bridge. If site class F soils are found only at the piers and are not present at the abutments, it might be concluded that the response of the piers will not significantly affect overall bridge response. With regard to the depth of these soils, there may be cases where the effective depth of ground motion is in stiff soil below a soft surficial layer. If the surficial layer is site class F and the underlying soil profile is site class E or stiffer, the surficial soils are unlikely to significantly increase bridge response.

Note that in table 2-2, there is one less category of site class F soils than the four originally adopted in the 1994 NEHRP Provisions (BSSC, 1994). This category consists of soils vulnerable to potential failure or collapse under seismic loading, such as liquefiable soils, quick and highly sensitive clays, and collapsible weakly cemented soils. Such soils should be classified on the basis of tables 2-2 and 2-3 assuming that soil failure or collapse will not occur. Special analyses to define the amplification of site ground motion in these soils is too severe a requirement for ordinary bridge design because such analyses require utilization of either effective stress or strength-degrading, nonlinear analytical techniques that are difficult to apply even by experts. Also, limited case history data and analytical results indicate that liquefaction reduces spectral response rather than increases it, except in some cases at long periods.

However, in accordance with section 2.2, site-specific analyses should be considered for major or very important bridges and advanced analytical techniques, such as effective stress analysis, should be used if appropriate.

Since liquefaction generally reduces response spectral amplitudes, the engineer may wish to conduct special analyses of site response to avoid excessive over-estimation of bridge inertia loads when liquefaction occurs.

The deletion of ground-failure-susceptible soils from site class F only affects the requirement to conduct site-specific analyses for determining ground motion amplification by these soils. It is still necessary to evaluate their potential for failure and their effect on bridge performance as indicated in chapter 3.

Table 2-2. Site classes.

Site Class	Description
A	Hard rock with measured shear wave velocity, $\bar{v}_s > 1500$ m/sec (5,000 ft/sec)
B	Rock with $760 \text{ m/sec} < \bar{v}_s \leq 1500 \text{ m/sec}$ ($2,500 \text{ ft/sec} < \bar{v}_s \leq 5,000 \text{ ft/sec}$)
C	Very dense soil and soil rock with $360 \text{ m/sec} < \bar{v}_s \leq 760 \text{ m/sec}$ ($1,200 \text{ ft/sec} < \bar{v}_s \leq 2,500 \text{ ft/sec}$) or with either $\bar{N} > 50$ blows/0.30m (50 blows/ft) or $\bar{s}_u > 100$ kPa (2,000 psf)
D	Stiff soil with $180 \text{ m/sec} \leq \bar{v}_s \leq 360 \text{ m/sec}$ ($600 \text{ ft/sec} \leq \bar{v}_s \leq 1,200 \text{ ft/sec}$) or with either $15 \leq \bar{N} \leq 50$ blows/0.30m ($15 \leq \bar{N} \leq 50$ blows/ft) or $50 \text{ kPa} \leq \bar{s}_u \leq 100 \text{ kPa}$ ($1,000 \leq \bar{s}_u \leq 2,000$ psf)
E	Soil profile with $\bar{v}_s < 180$ m/sec (600 ft/sec) or with either $\bar{N} < 15$ blows/0.30m ($\bar{N} < 15$ blows/ft) or $\bar{s}_u < 150$ kPa (1000 psf), or any profile with more than 3 m (10 ft) of soft clay defined as soil with $PI > 20$, $w \geq 40$ percent and $\bar{s}_u < 25$ kPa (500 psf)
F	Soils requiring site-specific evaluations <ol style="list-style-type: none"> Peats or highly organic clays ($H > 3$ m [10 ft] of peat or highly organic clay where H = thickness of soil) Very high plasticity clays ($H > 8$ m [25 ft] with $PI > 75$) Very thick soft/medium stiff clays ($H > 36$ m [120 ft])
Exception: When the soil properties are not known in sufficient detail to determine the site class, site class D may be used. Site classes E or F need not be assumed unless the authority having jurisdiction determines that site classes E or F could be present at the site or in the event that site classes E or F are established by geotechnical data.	
Notes: <ol style="list-style-type: none"> \bar{v}_s is average shear wave velocity for the upper 30 m (100 ft) of the soil profile \bar{N} is the average Standard Penetration Test (SPT) blowcount (blows/0.30m or blows/ft) (ASTM D1586) for the upper 30 m (100 ft) of the soil profile \bar{s}_u is the average undrained shear strength in kPa (psf) (ASTM D2166 or D2850) for the upper 30 m (100 ft) of the soil profile PI is plasticity index (ASTM D4218) w is moisture content (ASTM D2216) The shear wave velocity for rock, site class B, shall be either measured on site or estimated for competent rock with moderate fracturing and weathering. Softer and more highly fractured and weathered rock shall either be measured on site for shear wave velocity or classified as site class C. The hard rock, site class A, category shall be supported by shear wave velocity measurements either on site or on profiles of the same rock type in the same formation with an equal or greater degree of weathering and fracturing. Where hard rock conditions are known to be continuous to a depth of 30 m (100 ft), surficial shear wave velocity measurements may be extrapolated to assess \bar{v}_s. Site classes A and B should not be used when there is more than 3 m (10 ft) of soil between the rock surface and the bottom of a spread footing. 	

Table 2-3. Steps for classifying a site.

Step	Description
1	Check for the three categories of site class F in table 2-2 requiring site-specific evaluation. If the site corresponds to any of these categories, classify the site as site class F and conduct a site-specific evaluation.
2	Check for existence of a soft layer with total thickness > 3m (10 ft), where soft layer is defined by $s_u < 25$ kPa (500 psf), $w \geq 40$ percent, and $PI > 20$. If these criteria are met, classify site as site class E.
3	<p>Categorize the site into one of the site classes in table 2-2 using one of the following three methods to calculate:</p> <ul style="list-style-type: none"> \bar{v}_s for the top 30 m (100 ft) (\bar{v}_s method) \bar{N} for the top 30 m (100 ft) (\bar{N} method) \bar{N}_{ch} for cohesionless soil layers ($PI < 20$) in the top 30 m (100 ft) and \bar{s}_u for cohesive soil layers ($PI > 20$) in the top 30 m (100 ft) (\bar{s}_u method) <p>To make these calculations, the soil profile is subdivided into n distinct soil and rock layers, and in the methods below the symbol i refers to any one of these layers from 1 to n.</p> <p>Method A: \bar{v}_s method</p> <p>The average \bar{v}_s for the top 30 m (100 ft) is calculated as follows:</p> $\bar{v}_s = \frac{\sum_{i=1}^n d_i}{\sum_{i=1}^n \frac{d_i}{v_{si}}}$ <p>where: $\sum_{i=1}^n d_i$ is equal to 30 m (100 ft), v_{si} is the shear wave velocity in m/sec (ft/sec) of a layer, and d_i is the thickness of a layer between 0 and 30 m (0 and 100 ft).</p> <p>Method B: \bar{N} method</p> <p>The average \bar{N} for the top 30 m (100 ft) is calculated as follows:</p> $\bar{N} = \frac{\sum_{i=1}^n d_i}{\sum_{i=1}^n \frac{d_i}{N_i}}$ <p>where: N_i is the Standard Penetration Test blowcount of a layer (not to exceed 100 blows/0.30m [100 blows/ft] in the above expression). Note that when using Method b, \bar{N} values are for cohesionless soils and cohesive soil and rock layers within the upper 30 m (100 ft). Where refusal is met for a rock layer, N_i should be taken as 100 blows/0.30m [100 blows/ft]</p>

(continued)

Table 2-3. Steps for classifying a site (continued).

Step	Description
<p>3 continued</p>	<p>Method C: \bar{s}_u method</p> <p>The average \bar{N}_{ch} for cohesionless soil layers in the top 30 m (100 ft) is calculated as follows:</p> $\bar{N}_{ch} = \frac{d_s}{\sum_{i=1}^m \frac{d_i}{N_{chi}}}$ <p>where: $\sum_{i=1}^m d_i = d_s$, m is the number of cohesionless soil layers in the top 30 m (100 ft), N_{chi} is the blowcount for a cohesionless soil layer (not to exceed 100 blows/0.30m [100 blows/ft] in the above expression), and d_s is the total thickness of cohesionless soil layers in the top 30 m (100 ft).</p> <p>The average \bar{s}_u for cohesive soil layers in the top 30 m (100 ft) is calculated as follows:</p> $\bar{s}_u = \frac{d_c}{\sum_{i=1}^k \frac{d_i}{s_{ui}}}$ <p>where: $\sum_{i=1}^k d_i = d_c$, k is the number of cohesive soil layers in the top 30 m (100 ft), s_{ui} is the undrained shear strength for a cohesive soil layer (not to exceed 250 kPa [5,000 psf] in the above expression), and d_c is the total thickness of cohesive soil layers in the top 30 m (100 ft).</p>
<p>Note:</p>	<p>When using Method C, if the site class resulting from \bar{N}_{ch} and \bar{s}_u differ, select the site class that gives the highest site factors and design spectral response in the period range of interest. For example, if \bar{N}_{ch} was equal to 20 blows/0.30m (20 blows/ft) and \bar{s}_u was equal to 38 kPa (800 psf), the site would classify as D or E in accordance with Method C and the site class definitions of table 2-2. In this example, for relatively low response spectral acceleration and for long-period motions, table 2-4 indicates that the site factors are highest for site class E. However, for relatively high short-period spectral acceleration ($S_s > 0.75g$), short period site factors, F_a, are higher for site class D.</p>

Table 2-4. Site factors F_a and F_v

(a) Values of F_a as a function of site class and short-period (0.2-sec) spectral acceleration, S_s

Site Class	Spectral Acceleration at Short-Period (0.2 sec), S_s^1				
	$S_s \leq 0.25$	$S_s = 0.50$	$S_s = 0.75$	$S_s = 1.00$	$S_s \geq 1.25$
A	0.8	0.8	0.8	0.8	0.8
B	1.0	1.0	1.0	1.0	1.0
C	1.2	1.2	1.1	1.0	1.0
D	1.6	1.4	1.2	1.1	1.0
E	2.5	1.7	1.2	0.9	0.9
F^2					
Notes: 1. Use straight-line interpolation for intermediate values of S_s . 2. Site-specific geotechnical investigation and dynamic site response analysis should be performed for class F soils.					

(b) Values of F_v as a function of site class and long-period (1.0-sec) spectral acceleration, S_1

Site Class	Spectral Acceleration at Long-Period (1.0 sec), S_1^1				
	$S_1 \leq 0.1$	$S_1 = 0.2$	$S_1 = 0.3$	$S_1 = 0.4$	$S_1 \geq 0.5$
A	0.8	0.8	0.8	0.8	0.8
B	1.0	1.0	1.0	1.0	1.0
C	1.7	1.6	1.5	1.4	1.3
D	2.4	2.0	1.8	1.6	1.5
E	3.5	3.2	2.8	2.4	2.4
F^2					
Notes: 1. Use straight-line interpolation for intermediate values of S_1 . 2. Site-specific geotechnical investigation and dynamic site response analysis should be performed for class F soils.					

2.4.3. EFFECT OF SITE CLASS VARIATION ALONG A BRIDGE

The procedures described above for assessing site effects on ground motions were originally developed for computing ground motions at the surface of relatively uniform soil conditions. However, soil conditions may differ significantly from one end of a bridge to the other; an example is where one abutment is on firm ground or rock and the other is on fill over soft soil. These variations are not handled well by simplified procedures and significant errors may result. As a general rule, when geotechnical conditions vary significantly along the length of a bridge, the site factors described above may be used to construct response spectra at key locations along the length. These spectra may then be used to construct an envelope of response spectra for design. For major or very important bridges, it may be necessary to use more rigorous numerical modeling to represent these conditions, as discussed in section 2.9.

2.4.4. EFFECT OF DEPTH-OF-MOTION ON SITE CLASSIFICATION AND SITE FACTORS

For short bridges with a limited number of spans, the motion at the abutment will generally be the primary mechanism by which energy is transferred from the ground to the bridge superstructure. If the abutment involves an earth fill, the site classification should be determined on the basis of the soil profile below the fill. The effects of the fill overburden pressure on the soil properties (e.g., change in shear wave velocity) should be included in the determination of site classification.

For some bridges, it will be necessary to determine the site classification at the piers. If a pier is supported on spread footings, then it is appropriate to define the site class for conditions extending below the ground surface. However, if deep foundations (e.g., piles or drilled shafts) are used to support the pier, then the input motion may effectively be at some depth below the surface, depending on the horizontal stiffness of the soil-pile-footing system relative to the horizontal stiffness of the soil-pile system. If the soil-pile-footing is the stiffer of the two, then the motion should be defined at the footing. If the soil-pile-footing provides little horizontal stiffness or if there is no footing (e.g., pile bents), then the effective input motion to the bridge will likely be applied at some depth below the surface. The determination of this depth and the effective motion requires considerable judgment and should be evaluated jointly by the geotechnical engineer and bridge engineer. If the effective input motion is defined at some depth, then it may be overly conservative to define the site class and site factors on the basis of the soil profile immediately below the ground surface. Instead, it may be more appropriate to define the site class for a soil profile extending 30 m (100 feet) below the depth at which the input motion is defined.

2.5. DEVELOPING HORIZONTAL GROUND MOTION RESPONSE SPECTRA USING NATIONAL GROUND MOTION MAPS AND SITE FACTORS

2.5.1. TWO-POINT PROCEDURE FOR CONSTRUCTING RESPONSE SPECTRA

The two-point procedure described in this section may be used to construct horizontal response spectra. Because the national ground shaking maps (section 2.3) give five percent damped

spectral accelerations, the spectra constructed from these maps are for five percent damping. In section 2.5.3, factors are provided for obtaining response spectra for other damping ratios.

The two-point response spectrum construction procedure uses response spectral accelerations of rock ground motion from national ground motion maps (section 2.3) for a short period of vibration (0.2 second) and a long period of vibration (1.0 second) along with site factors applicable to the short-period and long-period ranges (section 2.4). The following equations and figure 2-4 describe the response spectrum construction.

$$S_{DS} = F_a S_s \quad (2-3)$$

and

$$S_{D1} = F_v S_1 \quad (2-4)$$

Where S_{DS} is the short-period (0.2 sec) design spectral acceleration, S_{D1} is the long-period (1.0 sec) design spectral acceleration, S_s is the short-period (0.2 sec) spectral acceleration on rock (site class B) from national ground motion maps or CD-ROM, S_1 is the long-period (1.0 sec) spectral acceleration on rock (site class B) from national ground motion maps or CD-ROM, F_a is the short-period site factor interpolated for a given value of S_s using table 2-3, and F_v is the long-period site factor interpolated for a given value of S_1 using table 2-3.

The design spectral acceleration, S_a , of the plateau of the response spectrum is defined by:

$$S_a = S_{DS} \quad (2-5)$$

The design spectral acceleration of the long-period declining branch to the response spectrum is defined by:

$$S_a = \frac{S_{D1}}{T} \quad (2-6)$$

where T is the period of vibration.

The period of vibration, T_s , of the intersection of the plateau and the long-period branch of the spectrum is defined by:

$$T_s = \frac{S_{D1}}{S_{DS}} \quad (2-7)$$

At periods of vibration less than or equal to T_o , the design spectral acceleration is defined by:

$$S_a = 0.60 \frac{S_{DS}}{T_o} T + 0.40 S_{DS} \quad (2-8)$$

where $T_o = 0.2T_s$.

Note that for $T = 0$ seconds, the resulting value of S_a is equal to the peak ground acceleration (assumed equal to $0.40 S_{DS}$ based on equation 2-8).

For long periods of vibration ($T \geq 3$ seconds), the spectral acceleration S_a may decrease more rapidly with increasing period than implied by equation 2-6. However, there is considerable uncertainty as to the influence of very long-period motions and the effect of other factors such as earthquake magnitude on the rate of decrease. Therefore, the $1/T$ rate should be used unless a faster rate can be justified based on a site-specific study.

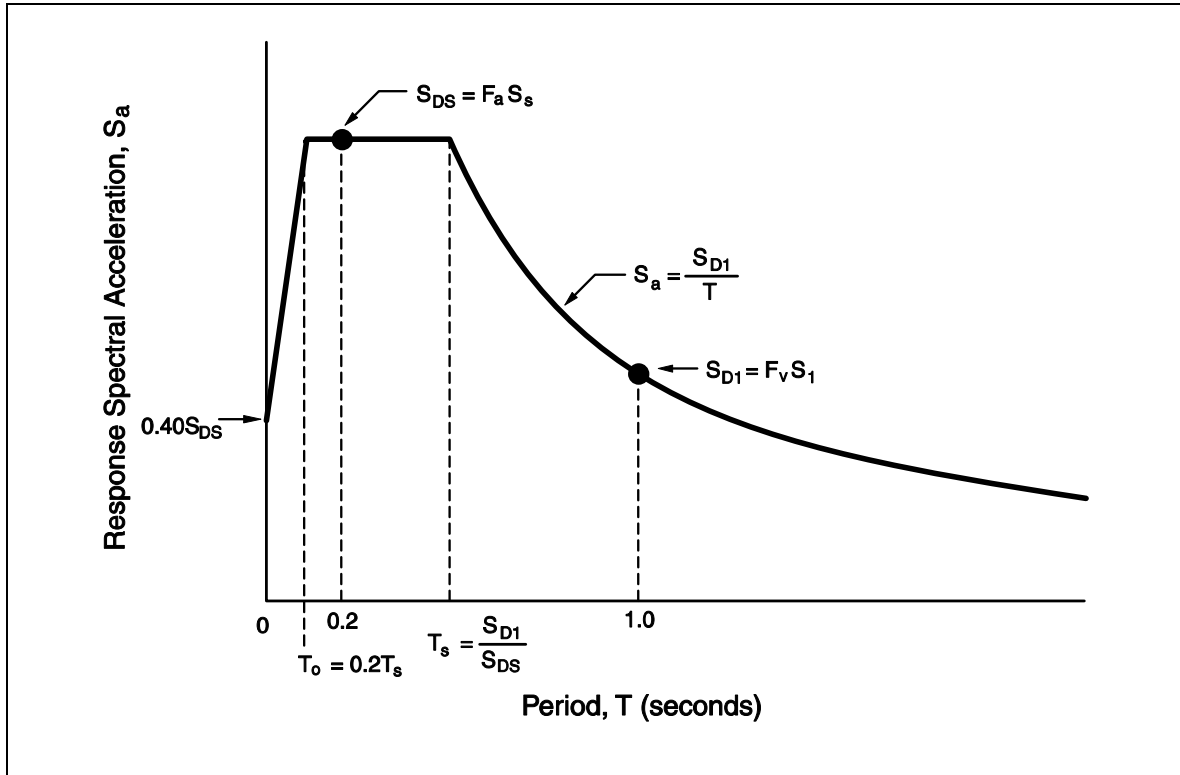


Figure 2-4. Design response spectrum (five percent damping) construction using two-point procedure.

2.5.2. MULTI-POINT PROCEDURE OF RESPONSE SPECTRUM CONSTRUCTION

Because the 1996 USGS national ground motion mapping provides spectral accelerations at several periods of vibration (section 2.3.1) in addition to the periods of 0.2 second and 1.0 second used for the two-point procedure described above, it is possible to use all of the spectral data directly rather than just the 0.2-second and 1.0-second values. This method of response spectrum construction is termed the multi-point method and can be used as an alternative to the two-point method. However, the multi-point method can lead to ambiguous results for sites other than rock (Power and Chiou, 2000). This is because only a short-period site factor and a long-period site factor are available (section 2.4) and it is not clear how the site factors vary when applied to spectral values at multiple periods. Therefore, judgment is required when applying the multi-point method for soil sites. Guidelines for applying site factors for soil sites using the multi-point method are:

1. Site factor F_a should be used for periods less than or equal to 0.2 second.
2. Site factor F_v should be used for periods greater than or equal to 1.0 second.
3. Between the 0.2 and 1.0 second periods, the resulting soil spectrum should be smooth and not contain spectral peaks higher than the larger of the spectral accelerations defined at 0.2 second and 1.0 second period.

Analysis of 1996 USGS mapping results indicates that the two-point method can be unconservative in comparison to multi-point data for periods longer than 1.0 second at some sites in the central and eastern United States (CEUS) having very low seismic ground motion hazard (Power et al., 1997, 1998). Therefore, for CEUS sites, it is desirable to check the rock spectrum constructed using the two-point method by comparing with map data for periods longer than 1.0 second.

Figure 2-5 illustrates differences between the two-point and multi-point method for a soft rock site (site class B) for two cities in the CEUS (New York City and Memphis) and a city in the western United States (WUS) (Seattle). As illustrated by the multi-period data in the figure, a typical difference in rock motion characteristics between the CEUS and WUS is the peaking of the CEUS spectrum at a shorter period (0.1 second for the CEUS spectrum and 0.2 second for the WUS spectrum). However, the moderate exceedance of the two-point plateau acceleration by the very short-period (0.1 second) spectral acceleration is probably not significant for most bridges.

In summary, use of the two-point method of response spectrum construction is a reasonable and acceptable approach for response spectrum construction. However, the following checks of the two-point-method spectrum at CEUS sites (east of 110° west longitude) are desirable:

1. If periods of vibration greater than 1.0 second are important to structural response, check the 2.0-second spectral acceleration to assure that the long-period response is not significantly underestimated.
2. If periods of vibration less than 0.2 second are important to structural response, check the 0.1-second spectral acceleration to assure that the short-period response is not significantly underestimated.

2.5.3. MODIFICATION OF ELASTIC SPECTRAL DEMAND FOR HIGHER OR LOWER DAMPING

Response spectra for structural damping ratios different than five percent can be obtained by multiplying the five percent damped spectra constructed using procedures in section 2.5.1 and 2.5.2 by the period-dependent factors in table 2-5. For spectra constructed using the two-point method, the factors for 0.2 second and 1.0 second can be used. The factors in table 2-5 are based on empirical studies of the variation of elastic response spectral amplitudes with damping ratio¹⁰.

¹⁰ Newmark and Hall, 1982; Abrahamson, 1993; Idriss, 1993

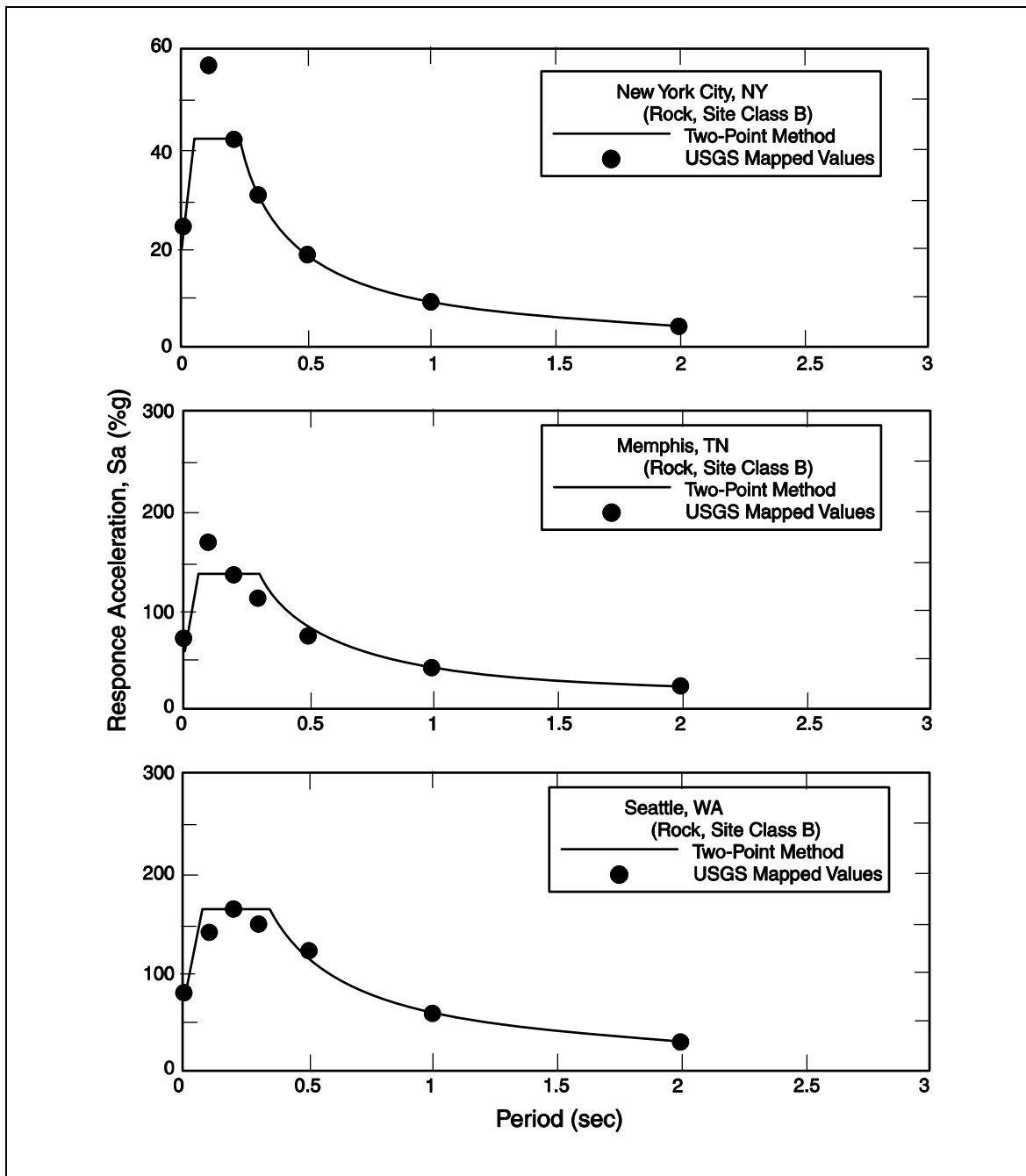


Figure 2-5. Comparison of two-point method of five percent damped response spectrum construction with USGS multi-point mapping results for two percent probability of exceedence in 50 years.

Table 2-5. Damping adjustment factors.

Period (seconds)	Ratio of Response Spectral Acceleration for Damping Ratio ξ to Response Spectral Acceleration for $\xi_{\text{eff}} = 5$ percent		
	$\xi_{\text{eff}} = 2$ percent	$\xi_{\text{eff}} = 7$ percent	$\xi_{\text{eff}} = 10$ percent
0.02	1.00	1.00	1.00
0.10	1.26	0.91	0.82
0.20	1.32	0.89	0.78
0.30	1.32	0.89	0.78
0.50	1.32	0.89	0.78
0.70	1.30	0.90	0.79
1.0	1.27	0.90	0.80
2.0	1.23	0.91	0.82
4.0	1.18	0.93	0.86

2.5.4. OBTAINING PEAK GROUND ACCELERATION FOR GROUND FAILURE EVALUATIONS

As noted in section 2.5.1, the peak ground acceleration is equal to the zero-period acceleration of a response spectrum. When peak ground acceleration is needed for an evaluation of the potential for soil failure, such as liquefaction or landsliding, it can be obtained as the zero-period acceleration from equation 2-8. Alternately, it can be directly obtained for rock site conditions from the 1996 USGS maps for peak ground acceleration for a selected probability of exceedance or return period. If obtained directly from the 1996 USGS maps, the corresponding soil-site acceleration for a given site class can reasonably be assumed to equal the mapped rock site acceleration multiplied by the short-period site factor (F_a) in table 2-4(a). In interpolating site factors as a function of peak rock acceleration level in table 2-4(a), it can be assumed that peak ground (rock) acceleration is equal to 0.4 times the short-period spectral acceleration on rock, S_s .

2.6. DEVELOPING SITE-SPECIFIC RESPONSE SPECTRA OF HORIZONTAL GROUND MOTIONS

In cases where a site-specific approach to developing response spectra is used, the overall objective is to develop ground motions that are more accurate for the local seismic and site conditions than can be determined from the general procedure using national ground motion maps and site factors (sections 2.3 through 2.5). Accordingly, site-specific studies must be comprehensive and incorporate current scientific interpretations for seismic sources and ground motion attenuation. It is also important to incorporate uncertainties in modeling in a site-specific probabilistic analysis. Examples of these uncertainties include seismic source location, extent, and geometry, maximum earthquake magnitude, earthquake recurrence rate, and ground motion

attenuation relationships. A site-specific analysis should be documented in detail and be subject to detailed peer review. When response spectra are determined from a site-specific study, the design spectra should not be lower than two-thirds of the spectra determined using the general procedure described in sections 2.3 through 2.5.

Where analyses to determine soil amplification are required by table 2-3 for site class F soils (see also section 2.4.2), the influence of the local soil conditions should be determined based on site-specific geotechnical investigations and dynamic site response analyses. Guidelines are presented in appendix A for conducting these investigations and analyses. These guidelines are applicable for site-specific determination of site response for any site class when the site response is determined on the basis of a dynamic site response analysis.

For sites located within 10 km (6 mi) of an active fault as defined in chapter 3, studies to quantify near-fault effects on ground motions should be conducted to determine if these could significantly influence bridge response. The USGS and state geological agencies may be contacted to determine the locations of known active faults.

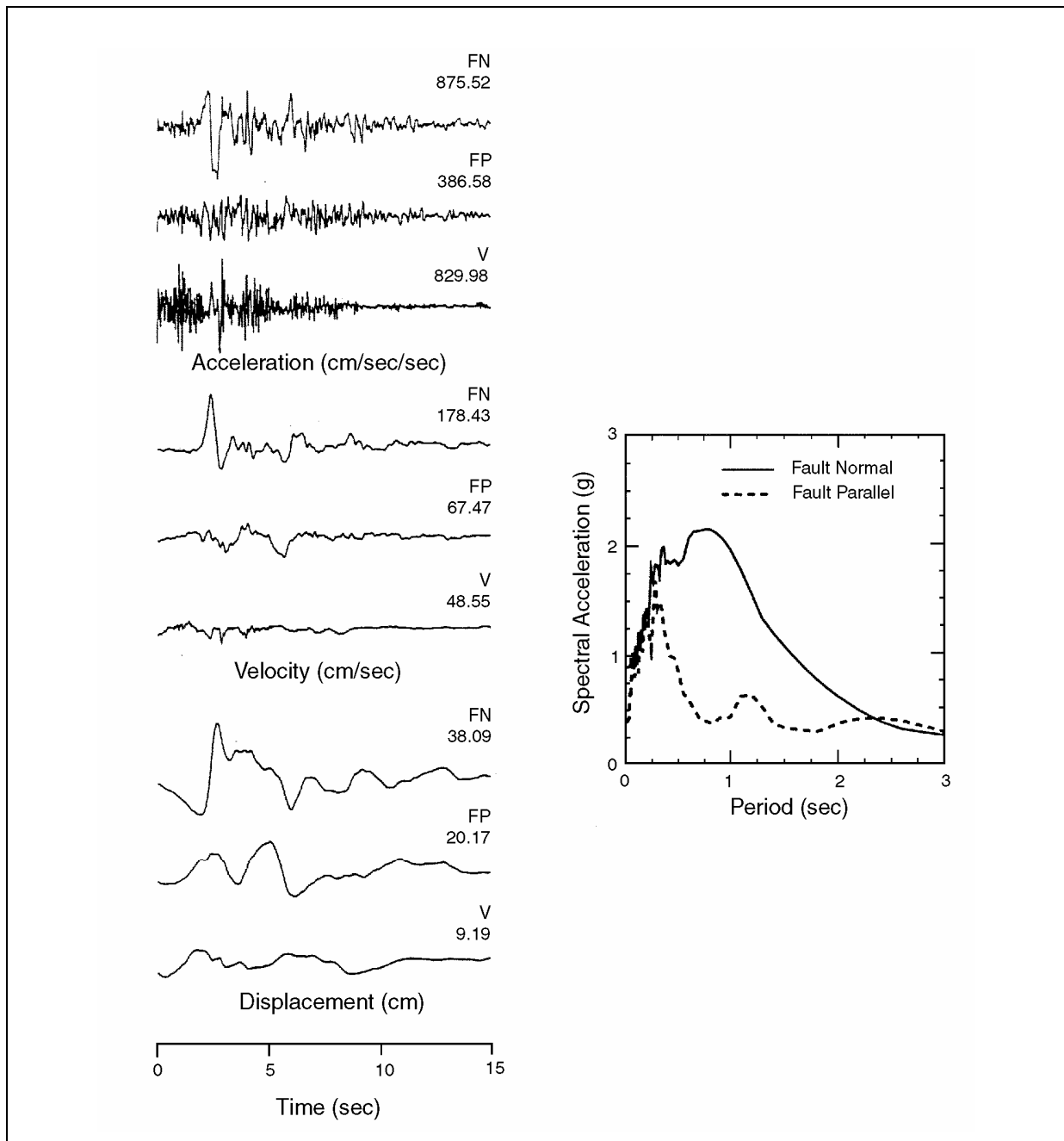
Near-fault effects on horizontal response spectra include:

1. Higher ground motions due to the proximity of the active fault,
2. Directivity effects that increase ground motions for periods greater than 0.5 second if the fault rupture propagates toward the site, and
3. Directionality effects that increase ground motions for periods greater than 0.5 second in the direction normal (perpendicular) to the strike of the fault.

If the active fault was included in the development of the national ground motion maps, then effect (1) is already included in the ground motions defined by national ground motion maps. Effects (2) and (3) are not included in the national maps. These effects are considered to be significant only for periods longer than 0.5 second. Normally these effects would be evaluated only for major or very important bridges having natural periods of vibration longer than 0.5 second (Somerville, 1997, and Somerville et al., 1997).

Figure 2-6 illustrates near-fault effects on both response spectra and time histories of horizontal ground motion. As seen in the time history plots, there is a significant long-period ground motion pulse that occurs in the direction perpendicular to the fault strike (i.e., fault-normal direction). As a result, the response spectrum at long periods is significantly increased in the fault-normal direction compared to the fault-parallel direction.

For purposes of developing deterministic spectra, subsurface faults as well as surface faults should be considered if (1) their location is known or can reasonably be inferred, and (2) the fault is an active fault as defined in chapter 3. The interfaces between tectonic plates in subduction zone regions are considered to be active faults.



Somerville, 1997

Figure 2-6. Time histories and horizontal response spectra (five percent damping) for the fault strike-normal and fault strike-parallel components of ground motion for the Rinaldi recording obtained 4.5 mi (7.5 km) from the fault rupture during the 1994 Northridge, California earthquake.

2.7. DEVELOPING VERTICAL GROUND MOTION RESPONSE SPECTRA

Recent studies¹¹ have shown that the ratio of the vertical response spectrum to the horizontal response spectrum of ground motions can differ substantially from the nominal two-thirds ratio commonly assumed in engineering practice. These studies show that the ratios of vertical to horizontal response spectral values are functions of the tectonic environment, subsurface soil or rock conditions, earthquake magnitude, earthquake source-to-site distance, and period of vibration. Whereas the two-thirds ratio may be conservative for longer periods of vibration (greater than about 0.2 second), at shorter periods the ratio of vertical to horizontal response spectra may exceed two-thirds and even substantially exceed 1.0 for close earthquake source-to-site distances and periods less than about 0.1 second.

Figure 2-7 illustrates vertical-to-horizontal response spectral ratios obtained in four studies for a moment magnitude 6.5 earthquake, source-to-site distance of 10 km, and for rock and soil site conditions. These results are from analysis of ground motion data from the western United States (WUS) and other regions having a similar shallow crustal faulting tectonic environment. Ground motion modeling analyses by Chiou et al. (2002) suggest that the ratios for the central and eastern United States (CEUS) are not greatly different from the ratios for the WUS.

At present, detailed procedures have not been developed for constructing vertical spectra having an appropriate relationship to the horizontal spectra constructed using the general procedure described in section 2.5. When developed, these procedures could be used in conjunction with deaggregation information on dominant earthquake source-to-site distance and earthquake magnitude (section 2.8.1), to construct vertical spectra at any location. For the present, when vertical response spectra are required and the horizontal response spectra are constructed using the general procedure of section 2.5, use of a vertical-to-horizontal spectral ratio of two-thirds throughout the period range is recommended unless the important vertical natural periods of vibration of the bridge are less than 0.2 second. In the latter case, analyses should be made to determine whether the short-period part of the vertical spectrum should be enriched. Such analyses should be made using results of current studies of vertical-to-horizontal spectral ratios, such as illustrated in figure 2-7.

In cases where site-specific horizontal spectra are developed (section 2.6) but vertical spectra are also required, results of current studies of vertical ground motions, such as those illustrated in figure 2-7, should be used. Vertical-to-horizontal spectral ratios less than two-thirds may be used if validated by site-specific vertical spectra but values less than 0.5 are not recommended.

¹¹ Abrahamson and Silva, 1997; Silva, 1997; Sadigh et al., 1993; Campbell, 1997; Bozorgnia et al., 1999; Campbell and Bozorgnia, 2000a, b; Chiou et al., 2002

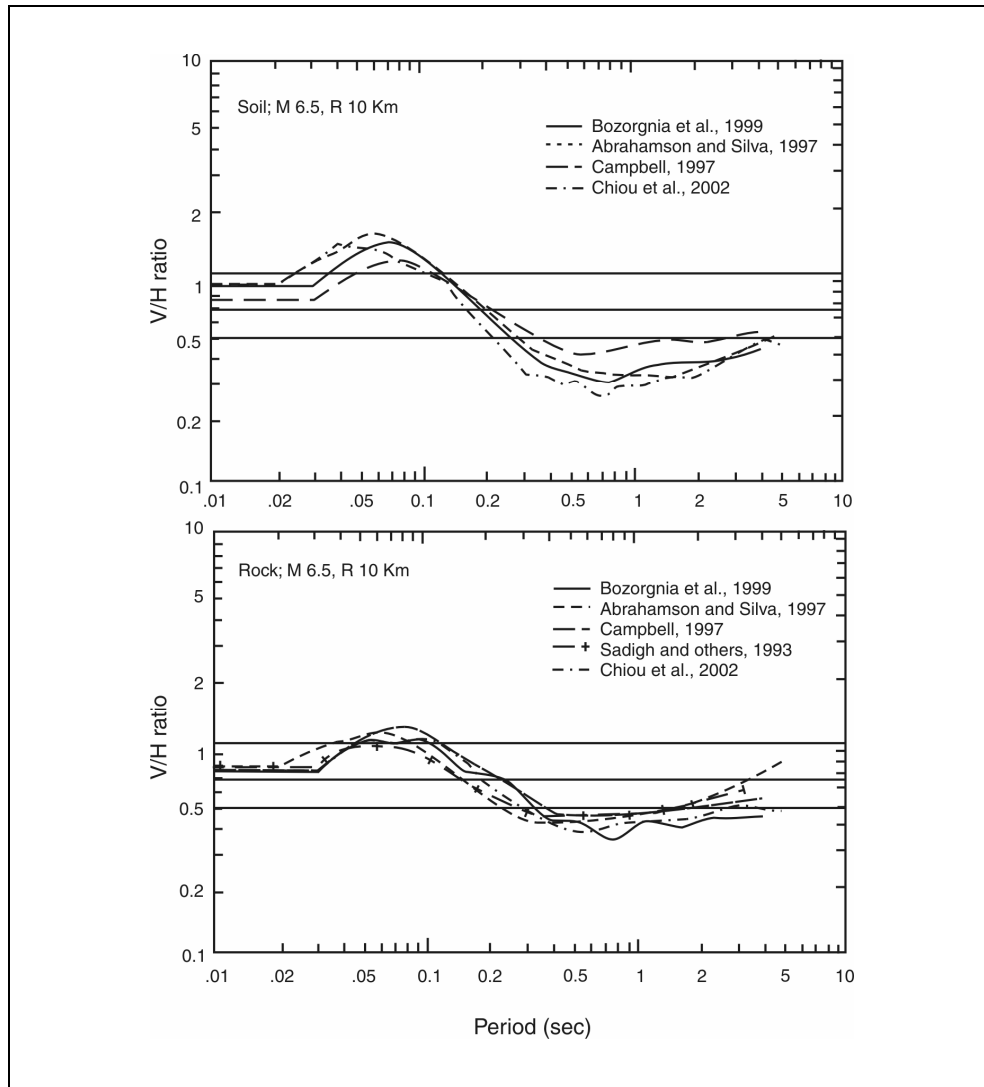


Figure 2-7. Vertical/horizontal spectral ratios vs. period

2.8. DEVELOPING ACCELERATION TIME HISTORIES

2.8.1. GENERAL REQUIREMENTS FOR TIME HISTORIES

When a time history analysis of a bridge is to be performed, the time histories of ground motions to be used in the analysis should represent the seismic environment of the site and local site conditions. Site characteristics to be considered include:

1. The tectonic environment, e.g., subduction zone, shallow crustal faults in western United States, or crustal environment in eastern United States.
2. Earthquake magnitude.
3. Type of faulting (e.g., strike-slip; reverse; normal).

4. Seismic source-to-site distance.
5. Local site conditions.
6. Design or expected ground motion characteristics (e.g., design response spectrum, duration of strong shaking, special ground motion characteristics such as near-fault characteristics).

Recorded time histories from sites with similar characteristics are preferred, but compromises are usually required because of the many characteristics defining the environment and the limited database of recorded time histories. Use of time histories having similar earthquake magnitudes and distances, within reasonable ranges, are especially important parameters because they have a strong influence on response spectral content, response spectral shape, duration of strong shaking, and near-source ground motion characteristics. The motions selected should be somewhat similar in overall ground motion level and spectral shape to the design spectrum to avoid using very large scaling factors for the recorded motions and very large changes in spectral content in the spectrum-matching approach discussed in section 2.8.3 below.

If the dominant earthquake is located within about 10 km (6 mi) of the site and has a magnitude equal to or greater than 6, then intermediate-to-long period ground motion pulses should be included, since these characteristics in the ground motion could significantly influence bridge response. Somerville et al. (2000, 2003) provides guidance on the time-domain characteristics of near-source ground motion pulses. The response spectral characteristics of near-source ground motions are described in section 2.6, and are illustrated in figure 2-6. Similarly, the high short-period spectral content of near-source vertical ground motions should be considered (section 2.7).

As indicated in figure 2-6, the amplitude of near-source horizontal ground motion pulses is dependent on the direction of the ground motion relative to the fault, being highest in the fault strike-normal (perpendicular) direction and lowest in the fault strike-parallel direction. Selected recorded near-source time histories should be transformed to fault-normal and fault-parallel directions. When used for a specific bridge, the time histories should be transformed to the principal bridge axes, depending on the orientation of the bridge relative to the fault strike.

When the design response spectrum is defined for a particular probability of exceedance or return period, a range of earthquake magnitudes and distances contribute to the spectrum. The ground motion hazard from a probabilistic ground motion analysis should be deaggregated to determine the predominant magnitude and distance contributions to the hazard to guide the selection and development of appropriate time histories. Hazard deaggregation of response spectral accelerations constructed using 1996 USGS ground motion maps can be obtained from the USGS website [<http://eqhazmaps.usgs.gov>]. Table 2-6 outlines the steps necessary to obtain these data from the web site.

Two examples of hazard deaggregation are shown in figure 2-8 for New York City and Seattle. The example is for 0.2-second spectral acceleration for three percent probability of exceedance in 75 years (2500-year return period). For this example, the hazard in New York City is dominated by small-to-moderate magnitude earthquakes occurring at close to moderate distances,

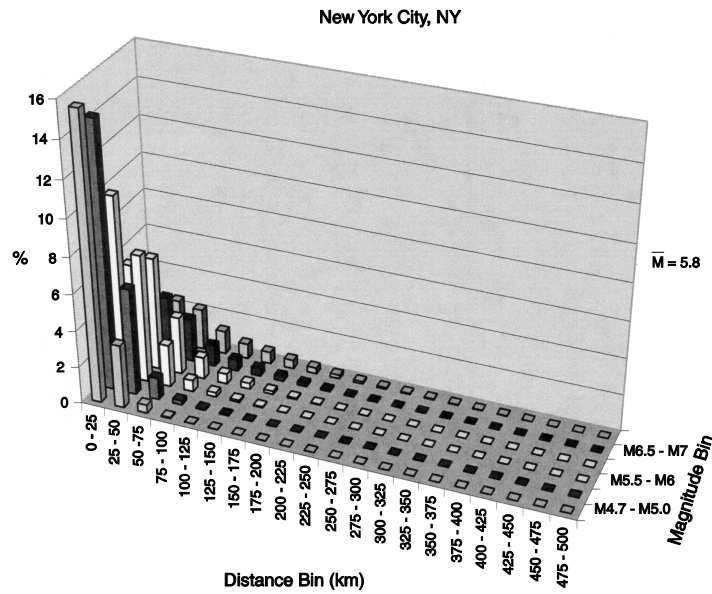
and the hazard at Seattle is dominated by moderate-to-large magnitude earthquakes occurring at close distances. The weighted average magnitude contribution to the hazard for each city is also shown. It should be noted that the relative magnitude and distance contributions for a particular location may vary with the ground motion parameters (e.g., relative contributions may differ for short-period and long-period motions) and with probability of exceedance. Also, at some sites, contributions may be more complex, such as a bi-modal contribution from nearby small-to-moderate magnitude earthquakes and distant large-magnitude earthquakes.

Table 2-6. Procedure for obtaining deaggregated seismic hazard from USGS web site.

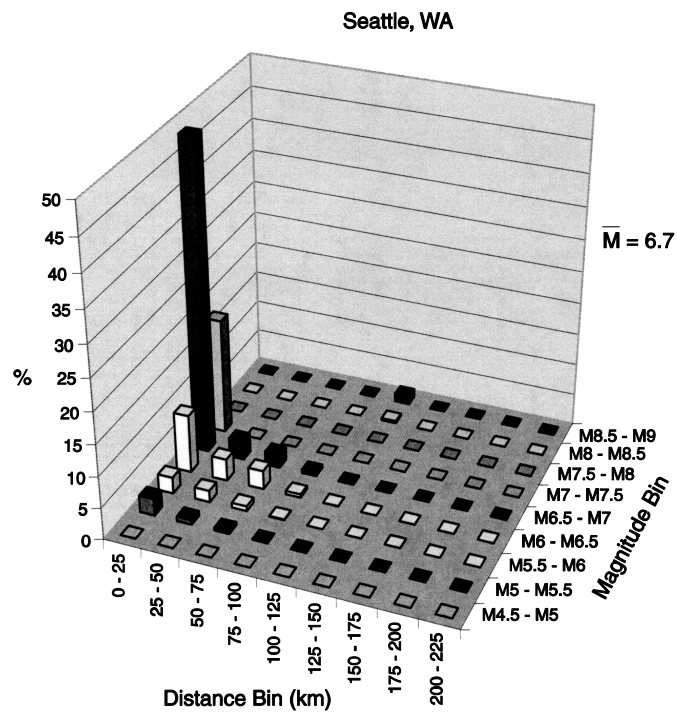
Step	Activity
1	Access http://eqhazmaps.usgs.gov with any recent browser and open home page.
2	Select 'Interactive Deaggregations, 1996'
3	On next screen: Enter site name and latitude and longitude coordinates for site. Select Return time from menu. For example: 5 percent PE 50 yrs for 1000-year return period. Select SA frequency from menu. For example: 1.0 Hz for S_1 (long-period spectral acceleration) or 5.0 Hz for S_s (short-period spectral acceleration). Choose 'Geographic Deaggregation.' Choose 'Mean' Seismograms.
4	Click 'Generate Plot(s) and Data.'
5	Select 'Hazard Matrices' to print tabulated data. Select 'Deaggregated Seismic Hazard Graph,' to print earthquake contribution to hazard by magnitude and distance. Choose desired format: gif, .pdf, .ps. Read mean (and modal) earthquake distance and magnitude. Select 'Geographic Deaggregated Seismic Hazard Map' and 'Seismograms for Modal or Mean Event' if required. Choose desired formats.
Note: Deaggregated seismic hazard data is not available on the CD-ROM provided with this manual. Use the website in step 1 to obtain this data.	

2.8.2. METHODS OF SELECTING AND DEVELOPING TIME HISTORIES

Time histories may be either recorded time histories that are scaled for the bridge location, or spectrum-matched time histories. For scaled time histories, the amplitudes of recorded ground motions are scaled by a constant factor so that the response spectrum of the time history (with its spectral peaks and valleys) is, on average, approximately at the level of the design response spectrum in the range of periods of structural significance. For spectrum-matched time histories, after simple scaling of recorded time histories as in the previous approach, a spectrum-matching procedure is then employed so that the frequency content of the scaled recorded time history is adjusted and the spectrum of the modified time history is a close fit or 'match' to the design response spectrum in the range of periods of structural significance.



(a) New York City, NY



(b) Seattle, WA

Figure 2-8. Hazard deaggregation for 0.2 second response spectral acceleration (S_s) for ground motion with three percent probability of exceedance in 75 years (2500-year return period).

If sufficient recorded motions are not available, simulations of recorded time histories may be developed using theoretical ground motion modeling methods that simulate the earthquake rupture process and wave propagation from source-to-site through the earth's crust. Analyses of soil column effects on time histories can be made using the methods of site response analysis described in appendix A.

If spectrum-matched time histories are developed, the initial time histories should be representative of recorded or simulated motions. The analytical techniques used for spectrum matching should be capable of achieving seismologically realistic time series that are similar to the time series of the initial time histories selected for spectrum matching. Response spectrum-matching approaches include methods in which time series adjustments are made in the time domain¹² and those in which the adjustments are made in the frequency domain¹³. Both of these approaches can modify existing time histories to achieve a close match to the design response spectrum while maintaining, fairly well, the basic time domain character of the recorded or simulated time histories. To minimize changes to the time domain characteristics, it is desirable that the overall shape of the spectrum of the recorded or simulated time history be similar to the shape of the design response spectrum and that the time history initially be scaled so that its spectrum is at the approximate level of the design spectrum before spectral matching.

If hazard deaggregation (section 2.8.1) indicates that different seismic sources dominate contributions to different period ranges of a design response spectrum (such as nearby small-to-moderate magnitude earthquakes dominating the short-period range and distant large-magnitude earthquakes dominating the long-period range), then it may be appropriate to develop two or more sets of time histories representing the different earthquakes and period ranges. In this way, individual time histories will be more realistic with respect to spectrum shape, duration, and energy.

2.8.3. REQUIREMENTS FOR COMPATIBILITY OF TIME HISTORIES WITH THE DESIGN RESPONSE SPECTRUM

When using recorded or simulated time histories that are not spectrum matched, they should be scaled to the approximate level of the design response spectrum in the period range of significance. For each component of motion, an aggregate match of the design response spectrum should be achieved for the set of acceleration time histories used for each component of motion. To evaluate the match, the mean of the spectra of the time histories should be calculated period-by-period. Over the range of periods of structural significance, the calculated mean spectrum should not be more than 15 percent lower than the design spectrum at any period, and the average of the ratios of the mean spectrum to the design spectrum should be equal to or greater than 1.0.

When developing spectrum-matched time histories, before the matching process, they should be scaled to the approximate level of the design response spectrum in the period range of significance. Thereafter, the set of time histories for each component should be spectrum-matched to achieve the same overall fit requirement as stated above for time histories that are not

¹² Lilhanand and Tseng, 1988; Abrahamson, 1992

¹³ Gasparini and Vanmarcke, 1976; Silva and Lee, 1987; Bolt and Gregor, 1993

spectrum-matched. Ordinarily this is easy to achieve because each spectrum-matched time history will have a spectrum close to the design spectrum.

When developing three-component sets of time histories by simple scaling rather than spectrum matching, it is difficult to achieve a comparable match to the design spectrum for each component when using the same scaling factor. It is desirable, however, to use the same scaling factor to preserve the relationship between the components. Approaches for dealing with this scaling issue include:

1. Increase the scaling factor to meet the minimum aggregate match requirement for one component of motion while exceeding it for the other two.
2. Use a scaling factor to meet the aggregate match for the most critical component of motion with the match somewhat deficient for other components.
3. Compromise on the scaling by using different factors as required for different components of a time history set.

All these approaches are acceptable, but the third approach is less desirable. The second approach requires careful examination and interpretation of the results and possibly dual analyses for application of the higher horizontal component in each principal horizontal direction.

Scaled or spectrum-matched time histories should be integrated to obtain corresponding time histories of velocity and displacement. All results should be examined for reasonableness.

2.8.4. NUMBER OF TIME HISTORIES

At least three time histories of either recorded, simulated-recorded, or spectrum-matched motions, should be used for each component of motion when performing nonlinear inelastic dynamic analyses. The design forces and displacements should be taken as the maximum response calculated for the three ground motions in each principal direction. However, if a minimum of seven recorded, simulated, or spectrum-matched time histories are used for each component of motion, the design forces and displacements may be taken as the mean of the forces and displacements calculated for each principal direction. These recommendations take into account the sensitivity of nonlinear response to both the response spectral content of the time histories and the time domain character of the time series (duration, pulse shape, pulse sequencing).

If linear elastic time history dynamic analysis is performed, fewer time histories could be used depending on the sensitivity of response to the time histories. Normally, for linear analysis, the response is not sensitive to the time domain character of the time series, and a sufficient number of time histories would be the number required to achieve an aggregate fit to the design spectrum. Using a spectrum-matching approach, this may be a single time history.

Additional guidance on developing acceleration time histories for dynamic analysis may be found in publications by the Caltrans Seismic Advisory Board Adhoc Committee on Soil-

Foundation-Structure Interaction (CSABAC, 1999) and the U.S. Army Corps of Engineers (2003).

2.9. SPATIAL VARIATION OF GROUND MOTIONS

Spatial variation in earthquake ground motion is principally due to:

1. Differences in arrival time of ground motions at bridge supports (out-of-phase motions). This is the so-called ‘traveling wave’ or ‘wave passage’ effect. Waves that propagate vertically do not show this effect..
2. Incoherence or dissimilarities in ground motions at bridge supports due to wave-scattering effects as seismic waves propagate through the earth’s crust.
3. Incoherence of ground motions due to variations in soil profiles at bridge supports.

Limited studies conducted to date indicate that spatial variation in the ground motion generally has little effect on bridge response and can be neglected in design. This is generally true for bridges less than 300 to 450 meters (1,000 to 1,500 feet) in total length and that have uniform soil conditions (Shinozuka et al., 2000). On the other hand, spatial variation can be significant for longer bridges or those with differential soil conditions and its effect should be included in design¹⁴. The effect of these differential soil conditions at bridge supports can be evaluated approximately using one-dimensional soil column analyses. Several computer programs that can be used for this purpose are identified in appendix A. These methods do not account for out-of-phase motions or incoherence due to crustal wave scattering. Shinozuka et al. (2000) presents a methodology for accounting for differential soil response in the development of out-of-phase, incoherent time histories.

Many bridge sites, especially those at river or valley crossings, are characterized by significant variations in both surface topography and subsurface soil stratigraphy (Martin, 1998a). In some cases, it may be warranted to use a two-dimensional, rather than one-dimensional, site response analysis to capture effects of the spatially varying soil and topographic conditions. Computer programs that can be considered for such analyses include the nonlinear analysis programs FLAC¹⁵ and TENSI-MUSC (Martin, 1998a) and the equivalent linear analysis programs FLUSH (Lysmer et al., 1975) and QUAD4M (Hudson et al., 1994). These methods capture two-dimensional interaction of the topographic and soil variations, but do not account for out-of-phase motions or incoherence due to crustal wave scattering.

¹⁴ Hao et al. (1989), Abrahamson (1985; 1992), Abrahamson et al. (1991), Shinozuka et al. (2000), and CSABAC (1999)

¹⁵ ITASCA, 1998; Wang and Makdisi, 1999

CHAPTER 3: GEOTECHNICAL HAZARDS

3.1. GENERAL

Geotechnical hazards at highway bridge sites that can be triggered by earthquakes include soil liquefaction, soil settlement, slope failure (landslides and rock falls), surface fault rupture, and flooding. In this chapter, liquefaction, settlement, fault rupture and flooding are described and their adverse consequences to highway bridges are discussed. Procedures for evaluating these hazards are also presented. Methods for screening and evaluating slope failure potential (landslides and rock falls) are given in Part 2 of this manual and are therefore not included in this chapter.

The consequences of these hazards in the free-field (e.g., ground settlement and fault displacements) are also addressed in this chapter. Methods for evaluating the effects of these hazards on the capacity and deformations of the bridge-foundation system are presented in chapter 6, and measures for mitigating them are described in chapter 11.

Assessing geotechnical hazards is a two-part procedure. In the first part, a quick screening evaluation is conducted. Generally, this can be accomplished using available information and field reconnaissance. If the criteria are satisfied, the risk is considered to be low and further evaluations of the hazard are not required. If a hazard cannot be screened out, more detailed evaluations are conducted in the second part of this procedure. This usually requires obtaining additional data to more rigorously assess the hazard and its consequences. In this chapter, guidelines for initial hazard screening are provided, and a brief overview of methods for detailed hazard evaluation is given. Detailed methods for hazard evaluation are described in appendix B. Hazard screening and hazard evaluation should be carried out by engineers and scientists (e.g., geotechnical engineers, geologists, and seismologists), who have expert knowledge of these hazards and experience with their evaluation.

3.2. SOIL LIQUEFACTION

3.2.1. LIQUEFACTION HAZARD DESCRIPTION

Soil liquefaction is a phenomenon in which a cohesionless soil deposit below the groundwater table loses a substantial amount of strength due to strong earthquake ground shaking. The reason for strength loss is that some types of cohesionless soil tend to compact during earthquake shaking and this tendency for compaction causes pore water pressures in the soil to increase. This, in turn, causes a reduction in soil strength. Recently deposited (i.e., geologically young) and relatively loose natural soils, and uncompacted or poorly compacted fills, are susceptible to liquefaction. Loose sands and silty sands are particularly susceptible. Loose silts and gravels also have potential for liquefaction. Dense natural soils and well-compacted fills have low susceptibility to liquefaction. Clay soils are generally not susceptible, except for highly sensitive clays found in some geographic locales.

Liquefaction has been perhaps the single most significant cause of damage to bridges during past earthquakes. Most of the damage has been related to the lateral movement of soil at bridge abutments. However, cases involving the loss of lateral and vertical bearing support of foundations for bridge piers have also occurred.

The potential consequences of liquefaction can be grouped into the following categories:

1. Flow slides. Flow failures are the most catastrophic form of ground failure that can occur due to liquefaction. These large slides occur when the downslope static (gravity) loads exceed the resistance provided by low shear strengths of liquefied soils (i.e., static factor of safety drops below 1.0 due to liquefaction). Because earthquake-induced inertial forces following liquefaction are not required to cause flow sliding (gravity forces being sufficient), these slides can occur even after the ground stops shaking. Flow slides commonly result in tens of meters (yards) of displacement and occur at relatively high velocities, up to tens of kilometers per hour (miles per hour).
2. Lateral spreads. Lateral spread is the most common form of landslide-type movements accompanying liquefaction. It can occur on very gently sloping ground (less than one percent slope in some cases) underlain by liquefied soil due to combined static forces plus seismically induced inertia forces in the soil mass. Lateral movements accumulate during the earthquake whenever the static plus seismically induced shear stresses exceed the strength of liquefied soil. The resulting lateral movements can range in magnitude from centimeters (inches) to several meters (yards) and are typically accompanied by severe ground cracking with horizontal and vertical offsets. The potential for lateral movements is increased if there is a 'free face,' such as a river channel or the sloping shoreline of a lake or bay, toward which movements can occur. Lateral spreading or 'embankment penetration' can occur beneath a bridge approach fill or any highway embankment if the underlying soil liquefies. Manifestations are settlements, lateral movements, and cracking of the embankment.
3. Reduction in foundation bearing capacity. The occurrence of liquefaction beneath, and/or laterally adjacent to, bridge foundations can greatly reduce foundation vertical and/or lateral capacity, resulting in unacceptable foundation settlements and/or lateral movements.
4. Ground settlement. Even in the absence of flow sliding, lateral spreading, or reduction in foundation bearing capacity due to liquefaction, ground settlements due to soil consolidation can occur as liquefaction-induced, excess pore water pressures in the soil dissipate. This consolidation occurs over time, perhaps for several days after the earthquake, and may result in the settlement and/or differential settlement of foundations located above the liquefied layer. Pile foundations extending through liquefied strata into stable ground may be subject to downdrag as soils overlying liquefied layers settle relative to the piles. In general, magnitudes of total and differential ground movements due to liquefaction-induced soil consolidation are less than those associated with flow slides, lateral spreading, or reduction in foundation bearing capacity.

5. Increased pressures on retaining walls. The occurrence of liquefaction in the backfill behind a retaining wall, such as an abutment backwall or wingwall, will increase pressures on the wall, potentially leading to wall failure or excessive deformations.

3.2.2. INITIAL HAZARD SCREENING FOR LIQUEFACTION

Prior to initiating screening and liquefaction evaluation procedures for soils that are susceptible to liquefaction, a check should be made as to whether liquefaction has previously occurred at the site (or in the near vicinity of the site in similar geotechnical conditions) during past earthquakes. This check may involve review of the earthquake history of an area and review of published post-earthquake reconnaissance reports. If there is evidence that liquefaction has previously occurred at the site, then it must be given further consideration.

In general, the requirement to conduct an evaluation of liquefaction potential is a function of the Seismic Hazard Level for the bridge, as described in chapter 1. For Seismic Hazard Levels I and II, the potential for liquefaction is generally low. In some cases (e.g., Type E and F soils for Seismic Hazard Level II), the peak ground acceleration may exceed 0.14 g ($F_a S_s$ in excess of 0.35 g). While this level of peak ground acceleration may cause liquefaction, the magnitude of the earthquake causing liquefaction at these hazard levels will generally be less than 6.0 and the duration of strong shaking will be relatively short. For magnitudes less than 6.0, liquefaction develops slowly at most sites, and affects the structure minimally during dynamic shaking. Therefore, the effects of liquefaction on dynamic response can be neglected. In addition, little potential exists for permanent movement of the ground, again because of the small size and limited duration of seismic events at these levels.

The potential for liquefaction at Seismic Hazard Levels III and IV is higher, and careful attention is needed to determine the potential for, and consequences of, liquefaction at sites with this classification. If the mean magnitude contributing to the peak ground acceleration is less than 6.0¹, then the discussion above with regard to duration is applicable for Seismic Hazard Levels III and IV. For magnitudes between 6.0 and 6.4, a liquefaction analysis may or may not be required depending on the combination of ground shaking and the blowcount values for the soils. For magnitudes above 6.4, a liquefaction analysis is required.

In summary, an evaluation of the potential for, and consequences of, liquefaction in soils near the surface should be made in accordance with the following requirements:

- Seismic Hazard Levels I and II: Not required.
- Seismic Hazard Levels III and IV: Required, unless one of the following two conditions is met:
 - Mean magnitude for the design event is less than 6.0.

¹ Mean earthquake magnitudes for a given bridge site and return period may be found on the USGS web site (<http://eqhazmaps.usgs.gov>), where results for the deaggregation of the seismic hazard are given (see section 2.8.1, table 2-6 and figure 2-8).

- Mean magnitude for the design event is less than 6.4 and equal to or greater than 6.0, and either the normalized Standard Penetration Test (SPT) blowcount $[(N_1)_{60}]$ is greater than 20, or $(N_1)_{60}$ is greater than 15 and $F_a S_s$ is less than 0.35 g.

If the mean magnitude is greater than or equal to 6.4, or if the above requirements are not met for magnitudes between 6.0 and 6.4, the potential for liquefaction and associated phenomena such as lateral flow, lateral spreading, foundation bearing capacity reduction, and settlement, should be evaluated.

In addition to the above criteria, it can be assumed that a significant liquefaction hazard does not exist for Seismic Hazard Levels III and IV if any of the following screening criteria are satisfied:

- The geologic materials underlying the site are either bedrock or have very low liquefaction susceptibility according to the relative susceptibility ratings shown in table 3-1, which are based on geologic age and general depositional environment (Youd and Perkins, 1978). Table 3-1 should be applied conservatively if there are uncertainties regarding geologic age or depositional environment.
- The soils below the groundwater table at the site are one of the following:
 1. Clayey soils which have a clay content (grain size < 0.005 mm) greater than 15 percent, liquid limit greater than 35 percent, or natural water content less than 90 percent of the liquid limit (Seed and Idriss, 1982). However, clayey soils that are highly sensitive, based on measured soil properties or local experience, should not be screened out. A highly sensitive soil possesses all of the following properties:
 - a. Liquid limit less than 40 percent.
 - b. Water content greater than 0.9 times the liquid limit.
 - c. Liquidity index greater than 0.6.
 - d. $(N_1)_{60}$ less than five or normalized cone penetration resistance, q_{c1} , less than 1 MPa (20 ksf).

Areas of the United States known to have highly sensitive soils include some coastal areas of Alaska, along the St. Lawrence River, some eastern and western coastal areas with estuarine soil deposits, near or within saline lakes in the Great Basin and other arid areas, and soils resulting from weathering of volcanic ash (Youd, 1998).

2. Sands with a minimum corrected Standard Penetration Test resistance, $(N_1)_{60}$ value of 30 blows/0.3m (30 blows/foot) or minimum corrected cone penetration test tip resistance, q_{CIN} , of 160 with a sufficient number of tests. The parameter $(N_1)_{60}$ is defined in Appendix B.
- The water table is deeper than 15 m (50 feet) below the existing ground surface or proposed finished grade at the site, whichever is lower, including considerations for seasonal, historic and possible future rises in groundwater level.

Table 3-1. Estimated susceptibility of sedimentary deposits to liquefaction during strong ground motion.

Type of Deposit	General Distribution of Cohesionless Sediments in Deposits	Likelihood that Cohesionless Sediments, When Saturated, Will be Susceptible to Liquefaction (by Age of Deposit)			
		<500 yr Modern	Holocene >11 ka	Pleistocene 11 ka - 2 Ma	Pre-Pleistocene >2 Ma
(a) Continental Deposits					
River channel	Locally variable	Very high	High	Low	Very low
Floodplain	Locally variable	High	Moderate	Low	Very low
Alluvial fan and plain	Widespread	Moderate	Low	Low	Very low
Marine terraces and plains	Widespread	---	Low	Very low	Very low
Delta and fan-delta	Widespread	High	Moderate	Low	Very low
Lacustrine and playa	Variable	High	Moderate	Low	Very low
Colluvium	Variable	High	Moderate	Low	Very low
Talus	Widespread	Low	Low	Very low	Very low
Dunes	Widespread	High	Moderate	Low	Very low
Loess	Variable	High	High	High	Unknown
Glacial till	Variable	Low	Low	Very low	Very low
Tuff	Rare	Low	Low	Very low	Very low
Tephra	Widespread	High	High	?	?
Residual soils	Rare	Low	Low	Very low	Very low
Sebka	Locally variable	High	Moderate	Low	Very low
(b) Coastal Zone					
Delta	Widespread	Very high	High	Low	Very low
Estuarine	Locally variable	High	Moderate	Low	Very low
Beach					
High wave-energy	Widespread	Moderate	Low	Very low	Very low
Low wave-energy	Widespread	High	Moderate	Low	Very low
Lagoonal	Locally variable	High	Moderate	Low	Very low
Fore shore	Locally variable	High	Moderate	Low	Very low
(c) Artificial					
Uncompacted fill	Variable	Very high	---	---	---
Compacted fill	Variable	Low	---	---	---

Youd and Perkins, 1978

If the above screening criteria are not satisfied, then the detailed evaluations described in appendix B should be used to evaluate a liquefaction hazard and its potential consequences. These evaluation approaches are briefly outlined in section 3.2.4.

3.2.3. EARTHQUAKE GROUND MOTIONS FOR LIQUEFACTION ANALYSIS

To perform analyses of the liquefaction potential, and some types of analyses to assess the consequences of liquefaction, an estimate of the peak ground acceleration and associated earthquake magnitude are needed. In addition, one type of evaluation for lateral spreading also requires earthquake source-to-site distance. These parameters can be obtained either by using the ‘general’ procedure based on national earthquake ground motion maps and site factors, or a ‘site-specific’ procedure, as described in sections 2.5 and 2.6, respectively.

Design ground motions are based on a probabilistic approach, except near highly active faults where ground motions are ‘bounded’ deterministically so as not to exceed levels associated with the occurrence of maximum magnitude earthquakes on these faults. When the design ground motions for a bridge are based on a probabilistic approach (i.e., developed for a certain probability of ground motion exceedance or return period), then it is necessary to deaggregate the peak ground acceleration hazard to determine ‘dominant’ magnitudes and distances contributing to the hazard, as described in section 2.8.1 and appendix A. The process of deaggregation is required because different seismic sources, earthquake magnitudes, and distances contribute to the probability of exceedance of a given ground motion in a probabilistic analysis.

When the deterministic approach is applied, design ground motions are estimated for a maximum earthquake magnitude occurring at a specific seismic source. It is assumed that the earthquake occurs on that portion of the source closest to the site. One or more earthquake sources, and associated magnitudes and distances, are selected on the basis of likelihood to cause liquefaction at the site.

3.2.4. SUMMARY OF PROCEDURES FOR DETAILED LIQUEFACTION EVALUATIONS

3.2.4.1. Evaluation of the Potential for Liquefaction Using Simplified Method

The procedure most widely used in engineering practice for the assessment of liquefaction potential is the ‘Simplified Procedure’². This procedure essentially compares the cyclic resistance ratio (CRR, the cyclic stress ratio required to induce liquefaction in a soil stratum at a given depth) with the earthquake-induced cyclic stress ratio (CSR) at that depth from the specified design earthquake, as defined by a peak ground surface acceleration and the associated earthquake moment magnitude.

The ratio of CRR to CSR should be greater than 1.0 to preclude the development of liquefaction. Even when the ratio of CRR to CSR is as high as 1.5, increases in pore water pressure in the soil

² Seed and Idriss (1982), Seed et al. (1983) and (1985), Seed and De Alba (1986), Seed and Harder (1990), Youd and Idriss (1997), Youd et al. (2001)

can occur. The potential consequences of these pore pressure increases in weakening the soil should be considered during design.

The most common application of the Simplified Procedure uses an empirically-based liquefaction criterion chart, or correlation, that describes the CRR as a function of SPT blowcounts from soil borings. However, variations of this procedure use other parameters as a measure of soil resistance to liquefaction, namely Cone Penetration Test (CPT) resistance, shear wave velocity, and Becker hammer penetration resistance. The use of CPT data and related correlations is becoming widely used as either a complementary or alternative method to the use of SPT data and correlations. The techniques of, and correlations with, shear wave velocity and Becker hammer penetration resistance are typically used for gravelly soils because of the difficulty of obtaining meaningful SPT or CPT measurements in these soils (Youd and Idriss, 1997; Youd et al., 2001).

3.2.4.2. Numerical Modeling Methods and Laboratory Cyclic Testing for Evaluation of Potential for Liquefaction

For critical projects, the use of numerical modeling of site response and/or the conduct of laboratory cyclic liquefaction tests may be appropriate to supplement the simplified method. The use of one- or two-dimensional effective stress site response analyses for acceleration time history inputs will provide increased understanding of the progressive development of pore water pressures during seismic shaking. Because of the great difficulty of obtaining and testing undisturbed cohesionless soil samples, a laboratory cyclic testing program to determine soil liquefaction resistance is seldom justified. However, such a program may be considered for certain soil types that are liquefiable but have liquefaction resistances that are less well quantified by the empirically-based correlations (e.g., cohesionless silts).

3.2.4.3. Evaluation of the Potential for Liquefaction-Induced Flow Slides and Lateral Spreads

For evaluation of the potential for flow sliding and magnitude of lateral spreading displacements, a critical parameter for analytical methods is the residual strength of the liquefied soil. The quantification of this parameter is described in appendix B.

The analysis of flow slide potential is essentially a static slope stability analysis in which the static factor of safety is evaluated considering the residual strength of the portion of the soil mass that has liquefied. Flow sliding is predicted to occur if the static factor of safety of the liquefied soil mass is less than 1.0. The estimation of displacements associated with flow sliding cannot be easily made. Sliding continues until geometric changes or increases in the strength of the liquefied soil cause the factor of safety to increase above 1.0.

For analysis of the potential for, and amount of, lateral spreading, empirically-based and analytical approaches may be used. Empirical approaches are based on observations of lateral spreading displacements during past earthquakes. The most widely used analytical approach is the simplified Newmark sliding block method in which displacements are estimated based on the amplitude of the induced accelerations in the soil mass, the amplitude of the ‘yield acceleration’

required to initiate movement of the soil mass considering the residual strength of the liquefied portion, and other parameters. The yield acceleration coefficient, k_y , is determined from a pseudo-static stability analysis as the acceleration required to cause the factor of safety to drop to 1.0. Two-dimensional nonlinear effective stress dynamic analysis approaches are now available as a complementary tool for evaluating lateral spreading.

3.2.4.4. Other Evaluation Procedures

The evaluation of the effects of liquefaction on vertical or lateral bearing capacity and foundation behavior and the effects on earth pressures behind retaining walls is addressed in chapter 6. The estimation of consolidation settlement due to liquefaction is considered in the following section.

3.3. SOIL SETTLEMENT

3.3.1. SETTLEMENT HAZARD DESCRIPTION

As noted in section 3.2.1, free-field settlements may accompany liquefaction. These settlements are associated with post-earthquake dissipation of pore water pressures induced by liquefaction and resulting soil consolidation and densification. If pore pressures develop during ground shaking, but not to a level high enough to cause liquefaction, their post-earthquake dissipation may also result in settlement, but less than that occurring due to liquefaction.

Settlements can also occur in dry or partially-saturated soils above the groundwater table and thus not be associated with pore pressure development and liquefaction. The mechanism in this case is densification during the period of ground shaking as the earthquake-induced cyclic shear stresses cause the soil grains to adjust into a denser state of packing. In the case of bridge approach embankment fills, a component of settlement may also be associated with small amounts of lateral yielding of the embankments, even in the absence of noticeable slope displacements or lateral spreading through weak foundation soils.

Loose natural soils, uncompacted and poorly compacted fills, are susceptible to densification. If densification does not occur uniformly over an area, the resulting differential settlements can be damaging to a bridge.

3.3.2. INITIAL HAZARD-SCREENING FOR SETTLEMENT

It can be assumed that a significant hazard due to differential compaction does not exist if both of the following screening criteria are satisfied.

1. The geologic materials underlying the foundations and below the groundwater table do not liquefy.
2. The geologic materials underlying the foundations and above the groundwater table are one or more of the following:
 - Pleistocene (geologic age older than 11,000 years),

- Stiff clays or clayey silts, or
- Cohesionless sands, silts, and gravels with a minimum $(N_1)_{60}$ of 20 blows/0.3 m (20 blows/ft).

Note that these criteria are not intended to be applied to embankment fills. The potential for settlement of fills is strongly dependent on the degree of compaction of the fill and settlements should be estimated as summarized in the next section.

3.3.3. SUMMARY OF PROCEDURES FOR DETAILED SETTLEMENT EVALUATIONS

Appendix B describes simplified procedures and empirical correlations for estimating seismically induced settlements in both saturated sands (below the groundwater table) and dry sands (applied to dry or partially saturated sands above the groundwater table). These procedures are based in part on case history data and in part on results of laboratory cyclic testing programs. Methods are also described for extending the evaluations for clean sands to silty sands and cohesionless silts. These procedures do not address cohesive soils (clays and clayey silts). In general, it is expected that stiff natural deposits of cohesive soils will not experience damaging settlements. However, cohesive or partially cohesive fills, including bridge approach embankment fills, may be susceptible to significant settlements if not adequately compacted.

3.4. SURFACE FAULT RUPTURE

3.4.1. SURFACE FAULT RUPTURE HAZARD DESCRIPTION

Surface fault rupture refers to the shearing displacements that occur along an active fault trace when movement on the fault extends to the ground surface, or the depth of the bridge foundation. Displacements can range from centimeters (inches) to several meters (yards). Because surface fault displacements tend to occur abruptly, often across a narrow zone, fault rupture can be very damaging to a bridge, particularly if it occurs directly below the structure. It is also difficult and often cost-prohibitive to mitigate. In the central and eastern United States, east of the Rocky Mountains, few active faults have been identified and the hazard of surface fault rupture is generally low in comparison to the western United States.

3.4.2. INITIAL HAZARD SCREENING FOR SURFACE FAULT RUPTURE

Surface fault ruptures generally are expected to occur along existing traces of active faults. Therefore, it can be assumed that a significant hazard of surface fault rupture does not exist if it can be established that either:

- There is no evidence of a fault trace traversing the bridge site, or
- If a fault trace does cross the bridge site, it has been established that the fault is not an active fault. Faults are generally considered to be active faults with a significant potential for future earthquakes and displacements if they have experienced displacements during the past approximately 11,000 years (Holocene time).

Hazard screening should involve, as a minimum, the following steps:

1. Review of geologic maps as well as discussions with geologists in government agencies who are knowledgeable about the geology of the area, and
2. Site reconnaissance and review of aerial photographs, looking for geomorphic expression of faulting. If there is uncertainty in the fault location or its activity, the screening criteria should be applied conservatively.

3.4.3. SUMMARY OF PROCEDURES FOR DETAILED SURFACE FAULT RUPTURE EVALUATIONS

If a surface fault rupture hazard cannot be screened out, the owner may decide to accept the risk or evaluate the hazard and consequences in detail. If detailed evaluations are carried out, they should be oriented toward:

1. Establishing the fault or fault zone location relative to the bridge if it is not clearly established in the screening stage,
2. Establishing the activity of the fault if it traverses the bridge, and
3. Evaluating fault rupture characteristics; i.e., amount of fault displacement, width of zone of displacement, and distribution of slip across the zone for horizontal and vertical components of displacement. A probabilistic assessment of the likelihood of different magnitudes of fault displacement during the life of the bridge may also be useful in decision-making.

3.5. FLOODING

3.5.1. FLOODING HAZARD DESCRIPTION

Phenomena that can result in earthquake-induced flooding include:

- Tsunami (large ocean waves generated by vertical displacements of the seafloor during offshore earthquakes,
- Seiche (waves induced in bays and lakes when the body of water is excited by ground shaking; e.g., sloshing),
- Waves generated by landslides within, or into, a body of water,
- Flooding caused by tectonic movements, such as uplift along a thrust fault damming a river, and
- Failure of an upstream dam and reservoir caused by an earthquake.

3.5.2. INITIAL HAZARD SCREENING FOR FLOODING

The hazard of flooding can be screened out for bridges that are not located near a body of water or in an area that could be inundated by the hazard. Tsunami potential is considered to be low in coastal regions of the eastern and southern United States and moderate to high along portions of the west coast of the United States, Alaska, and Hawaii. Seiche waves usually do not exceed several feet in height and would generally pose a potential hazard only to facilities within or immediately adjacent to a bay or lake. Many states and federal agencies have delineated inundation zones for failures of dams under their jurisdiction. The hazard of earthquake-induced flooding should also be viewed in the context of hazards of flooding from non-seismic causes.

3.5.3. SUMMARY OF DETAILED EVALUATIONS FOR FLOODING

If it appears that flooding could pose an unacceptable risk to the performance of a bridge immediately following an earthquake, detailed evaluations should be directed at assessing the potential, severity, consequences, and likelihood of the hazard.

CHAPTER 4: SEISMIC RATING METHODS FOR SCREENING AND PRIORITIZATION

4.1. GENERAL

Screening an inventory of bridges is done to identify seismically deficient bridges and prioritize them in order of need for retrofitting. Such a process is intended to be rapid, easy to apply and conservative. Bridges found to be deficient at this stage are subject to detailed evaluation at the next step, and any that are later found to be satisfactory are excluded from further study at that time.

As noted in section 1.10, two rating systems are identified in this manual for the purpose of screening and prioritizing bridges for seismic retrofitting. Both methods are described in detail in this chapter. The methods are:

- Seismic rating method using indices.
- Seismic rating method using expected damage.

4.2. SEISMIC RATING METHOD USING INDICES

In calculating the seismic rating of a bridge for prioritization, consideration should be given to structural vulnerability, seismic and geotechnical hazards, and the socioeconomic factors affecting importance. This is accomplished first, by making independent ratings of each bridge in the areas of vulnerability and seismic hazard, and second, by considering importance (societal and economic issues) and other factors (redundancy and non-seismic structural issues) to obtain a final, ordered determination of bridge retrofit priorities¹.

The rating system is therefore both quantitative and qualitative. The quantitative part produces a seismic rating (called the bridge rank, R) based on structural vulnerability and seismic hazard. The qualitative part modifies the rank in a subjective way that takes into account bridge importance, network redundancy, non-seismic deficiencies, anticipated service life, and similar factors for inclusion in an overall priority index. Engineering and societal judgment are thus the key to the second stage of the screening process. This leads to a priority index that is a function of rank, importance, and other factors as indicated below in equation 4-1.

$$P = f(R, \text{importance, non-seismic, and other factors...}) \quad (4-1)$$

where P is the priority index and R is the rank based on structural vulnerability and seismicity.

In summary, *bridge rank* is based on structural vulnerability and seismic hazard, whereas *retrofit priority* is based on bridge rank, importance, non-seismic deficiencies, and other factors such as network redundancy. This method is illustrated in figure 4-1.

¹ Buckle, 1991; Buckle and Friedland, 1995

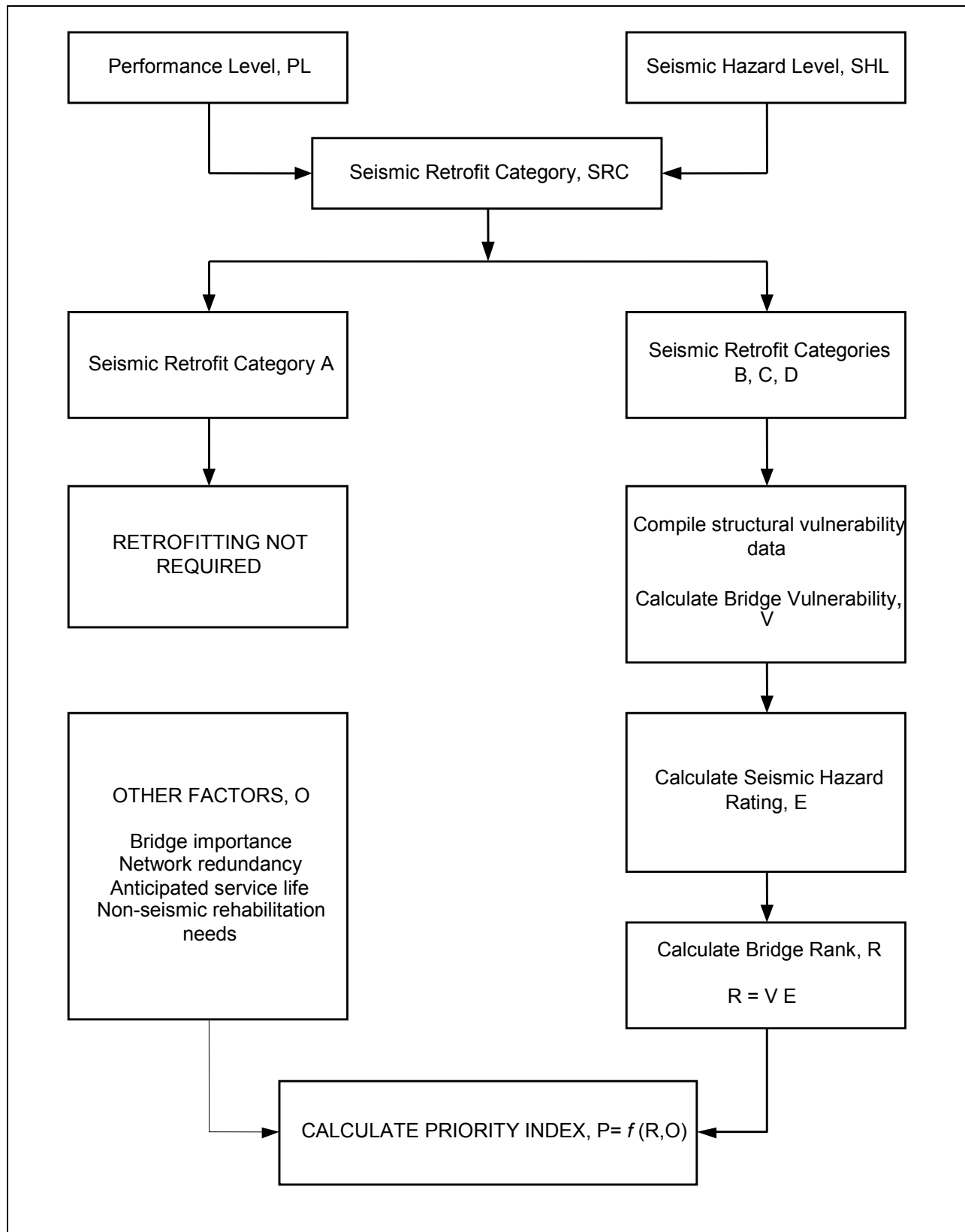


Figure 4-1. Seismic rating method using indices.

4.2.1. CALCULATION OF BRIDGE RANK

As noted above, the bridge rank, R , is based on a structural vulnerability rating, V , and a seismic hazard rating, E . Each rating lies in the range 0 to 10 and the rank is found by multiplying these two ratings together as shown in equation 4-2.

$$R = VE \quad (4-2)$$

Therefore, R can vary from 0 to 100, and the higher the score, the greater the need for the bridge to be retrofitted (ignoring at this time the other factors). Recommendations for assigning values for V and E are described below.

4.2.1.1. Vulnerability Rating (V)

Although the performance of a bridge is based on the interaction of all its components, certain bridge components are more vulnerable to damage than others. These are:

- Connections, bearings, and seats (support lengths).
- Piers, columns and foundations.
- Abutments.
- Soils.

Of these, connections, bearings and inadequate seat length are the most common reasons for bridge failure and the least costly to fix. For this reason, the vulnerability of these components is calculated separately from the rest of the structure and assigned a rating, V_1 . The vulnerability of the rest of the substructure, V_2 , is determined from the sum of the ratings for each of the other components that are susceptible to failure. The overall rating for the bridge is then given by the greater of V_1 and V_2 , as shown in the flowchart in figure 4-2.

The determination of these vulnerability ratings requires considerable engineering judgment. In order to assist in this process, a methodology for determining these ratings is given in sections 4.2.1.1(a) and 4.2.1.1(b).

Vulnerability ratings may range from 0 to 10. A rating of 0 means a very low vulnerability to unacceptable damage, a value of 5 indicates a moderate vulnerability to collapse or a high vulnerability to loss of access, and a value of 10 means a high vulnerability to collapse. This should not be interpreted to mean that the vulnerability rating must assume one of these three values.

For bridges classified in Seismic Retrofit Category (SRC) B (section 1.6 and table 1-6), the vulnerability ratings for bearings, transverse restraints, and support lengths need to be calculated along with a rating for liquefaction effects for bridges on liquefiable soils. Experience has shown that most connection, bearing, and seat deficiencies can be corrected economically.

For bridges classified as SRC C or D, vulnerability ratings are also required for the columns, abutments, and foundations. Experience with retrofitting these components is much more limited than for bearings. They are generally more difficult to retrofit and doing so may not be as cost-effective.

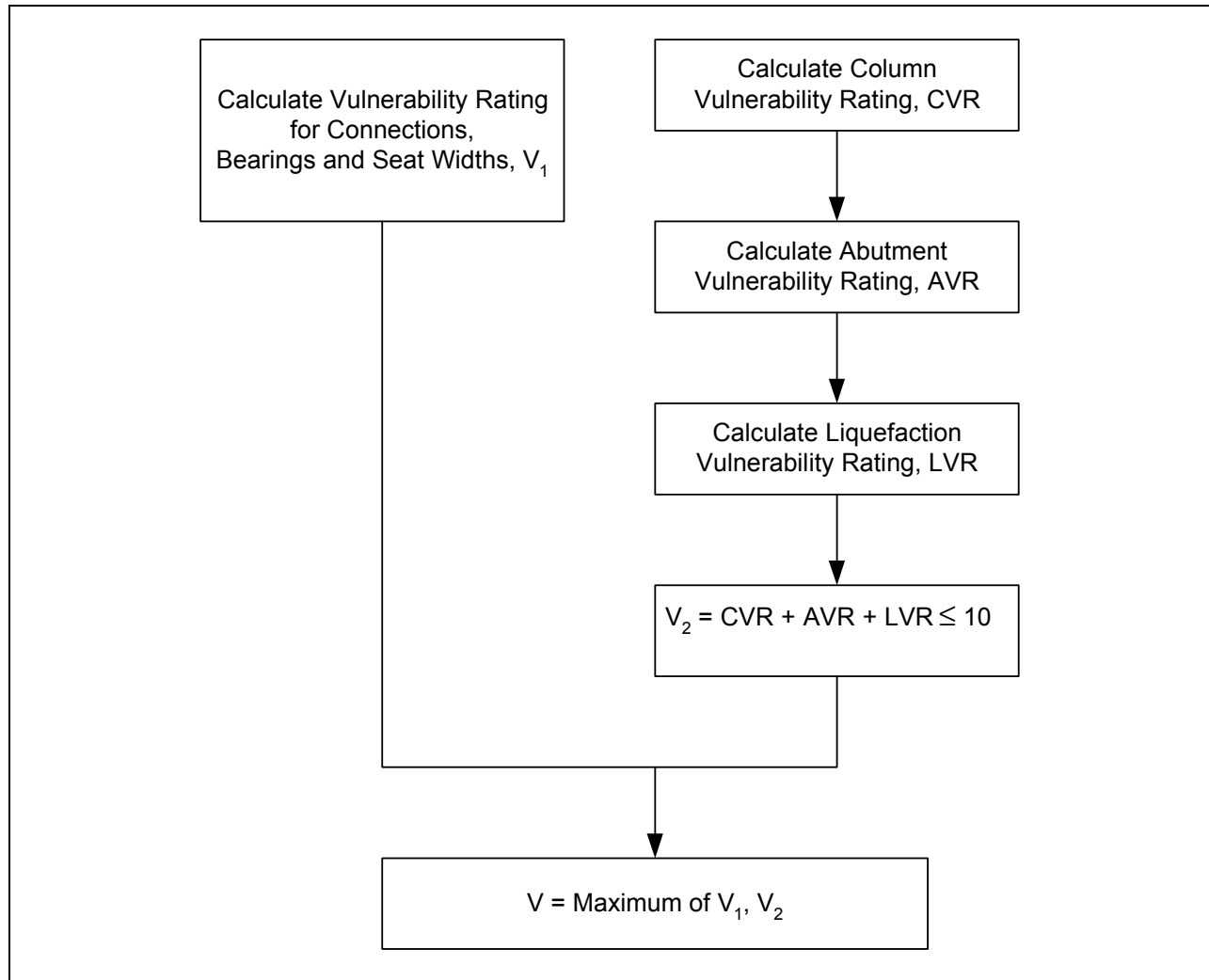


Figure 4-2. Calculation of bridge vulnerability, V .

A comparison of the above two vulnerability ratings, V_1 and V_2 , can be used to obtain an indication of the type of retrofitting needed. If the vulnerability rating for the bearings is equal to or less than the vulnerability rating of other components, simple retrofitting of only the bearings may be of little value. Conversely, if the bearing rating is greater, then benefits may be obtained by retrofitting only the bearings. A comparison of these two ratings during the preliminary screening process may be helpful in planning the type of comprehensive retrofit program needed, but should not serve as a substitute for the detailed evaluation of individual bridges as described in chapters 5, 6 and 7.

4.2.1.1(a). Vulnerability Rating for Connections, Bearings, and Seat Widths, V_1

Bearings are used to transfer loads from the superstructure to the substructure and between superstructure segments at hinge seats within the span. In this ranking system, bearings are considered to include shear keys, keeper bars and similar restraints. Bearings may be either fixed bearings, which do not provide for translational movement, or expansion bearings, which do

permit such movements, as shown in figure 4-3. An expansion bearing may provide for translation in one orthogonal direction, but not in the other.

There are five basic types of expansion bearings used in bridge construction. These are:

1. The rocker bearing, which is generally constructed of steel and permits translation and rotational movement. It is the most seismically vulnerable of all bridge bearings because it usually has a high aspect ratio, is difficult to restrain, and can become unstable and overturn after limited movement. Fixed bearings with high aspect ratios can also be very vulnerable to earthquakes.
2. The roller bearing, which is also usually constructed of steel. It is stable during an earthquake, except that it can become misaligned and horizontally displaced.
3. The elastomeric bearing pad is constructed of a natural or synthetic elastomer and is usually internally reinforced with steel shims. It relies on the distortion of the elastomer to provide for movement. This bearing is generally stable during an earthquake, although it has been known to 'walk out' under severe shaking due to inadequate fastening.
4. The sliding bearing, in which one surface slides over another and which may consist of almost any material from an asbestos sheet between two concrete surfaces to PTFE (Teflon) and stainless-steel plates.
5. High-load, multi-rotational bearings such as pot, disk, and spherical bearings. These bearings usually have adequate strength for earthquake loads, but their connections have failed in past earthquakes.

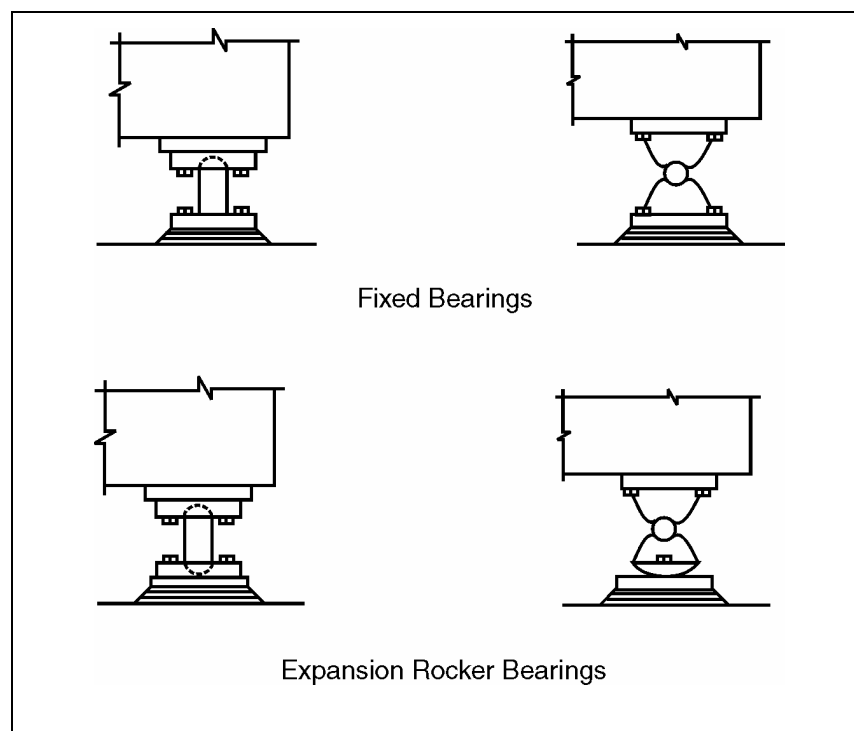


Figure 4-3. Seismically vulnerable bearings.

Transverse restraint of the superstructure is almost always provided at the bearings. Common types of restraint are shear keys, keeper bars, or anchor bolts. Restraints are usually not ductile, and are subjected to large seismically induced forces resulting from a redistribution of force from ductile components such as columns. In addition, when several individual bearings with keeper bars are present at a support, the bars do not resist transverse load equally because of slight variations in clearances. Therefore, individual bars may be subjected to very high forces which can lead to failure. Large transverse or longitudinal movements may then occur at the bearings, leading to loss of support and span collapse. The expected movement at a bearing is dependent on many factors and cannot be easily calculated. The AASHTO Specifications require a minimum support length at all bearings in new bridges.² This requirement is also in the NCHRP 12-49 provisions (ATC/MCEER, 2003). Because it is difficult to predict relative movement, the minimum support length, N , as given in the NCHRP 12-49 provisions, is recommended as the basis for checking the adequacy of longitudinal support lengths.

In metric units, this length is given by:

$$N = \left[100 + 1.7L + 7.0H + 50 \sqrt{1 + \left(2 \frac{B}{L} \right)^2} \right] \frac{(1 + 1.25F_v S_1)}{\cos \alpha} \quad (4-3a)$$

where: N is the recommended support length measured normal to the face of an abutment or pier (m),

L is the length of the bridge deck from the seat to the adjacent expansion joint, or to the end of the bridge deck (m). For hinges or expansion joints within a span, L is the sum of the distances on either side of the hinge (m); for single-span bridges, L is the length of the bridge deck (m).

H is the height. For abutment seats, H is the average height of piers or columns supporting the bridge deck between the abutment and the next expansion joint (m). For pier seats, H is the height of the pier (m); for hinge seats within a span, H is the average height of the two adjacent piers (m); for single-span bridges, $H=0$.

B is the width of deck (m),

α is the angle of skew (0° for a right bridge), and

$S_{D1} = F_v S_1$, is the product of the long-period soil factor (F_v) and the 1.0 second spectral acceleration (S_1) as in equation 1-1.

The ratio B/L need not be taken greater than $3/8$.

In U.S. customary units, this length is given by:

$$N = \left[4.0 + 0.02L + 0.08H + 1.1\sqrt{H} \sqrt{1 + \left(2 \frac{B}{L} \right)^2} \right] \frac{(1 + 1.25F_v S_1)}{\cos \alpha} \quad (4-3b)$$

² AASHTO, 1998; AASHTO, 2002

where N , L , H , B and α are as defined for equation 4-3a, but N is given in inches and L , H and B are expressed in feet. Again the ratio B/L need not be taken greater than $3/8$.

Since skew has a major effect on the performance of bridge bearings, rocker bearings may overturn at heavily skewed supports during only moderate seismic shaking. In such cases, it is necessary to consider the potential for collapse of the span, which will depend to a large extent on the geometry of the bearing seat. Settlement and vertical misalignment of a span due to an overturned bearing may be a minor problem, resulting in only a temporary loss of access that can be restored, in many cases, by backfilling with asphalt or other similar material. The potential for total loss of support should be the primary criteria when rating the vulnerability of the bearings.

A suggested step-by-step method for determining the vulnerability rating for connections, bearings, and seat widths (V_1) is detailed in the flowchart of figure 4-4 and is as follows:

Step 1. Determine if the bridge has satisfactory bearing details. Such bridges include:

- a. Continuous structures with integral abutments.
- b. Continuous structures with seat-type abutments where all of the following conditions are met:
 1. Either (a) the skew is less than 20° (0.35 rad), or (b) the skew is greater than 20° (0.35 rad) but less than 40° (0.70 rad) and the length-to-width ratio of the bridge deck is greater than 1.5.
 2. Rocker bearings are not used.
 3. The abutment's bearing seat under the end diaphragm is continuous in the transverse direction and the bridge has more than three beams.
 4. The support length is equal to, or greater than, the minimum required length (N) given in equation 4-3.

If the bearing details are determined to be satisfactory, a vulnerability rating, V_1 , of 0 may be assigned and the remaining steps for bearings omitted.

Step 2. Determine the vulnerability to structure collapse or loss of access to the bridge due to transverse movement, V_T .

Before significant transverse movement can occur, the transverse restraint must fail. In the absence of calculations showing otherwise, assume that the bearing keeper bars and/or the anchor bolts in bridges in SRC C and D will fail. Also assume that nominally reinforced, nonductile concrete shear keys will fail in bridges in SRC D.

When the transverse restraint is subject to failure, beams are vulnerable to loss of support if either of the following conditions exist:

- a. Individual beams are supported on individual pedestals or columns.
- b. The exterior beam in a 2- or 3-beam bridge is supported near the edge of a bearing seat regardless of whether the bearings are on individual pedestals or not.

In either of these cases, the vulnerability rating, V_T , should be 10.

Steel rocker bearings have been known to overturn transversely, resulting in a permanent superstructure displacement. All bridges in SRC D are vulnerable to this type of failure. Bridges in SRC C are vulnerable only when the skew is greater than 40° (0.70 rad). When bearings are vulnerable to a toppling failure but structure collapse is unlikely, the vulnerability rating, V_T , should be 5. Otherwise $V_T=0$.

Step 3. Determine the vulnerability of the structure to collapse or loss of access due to excessive longitudinal movement, V_L .

V_L is determined according to the available support length (L) measured in a direction perpendicular to the centerline of the support. This is done by comparing L with the minimum required length N , (equation 4-3), as follows:

If $L \geq N$ then $V_L = 0$ regardless of bearing type.

If $N > L \geq 0.5N$ and rocker bearings are not used, then $V_L = 5$.

If $N > L \geq 0.5N$ and rocker bearings are used, then $V_L = 10$.

If $0.5 N > L$ then $V_L = 10$ regardless of bearing type.

Step 4. Calculate vulnerability rating for connections, V_1 , from values V_T and V_L , with

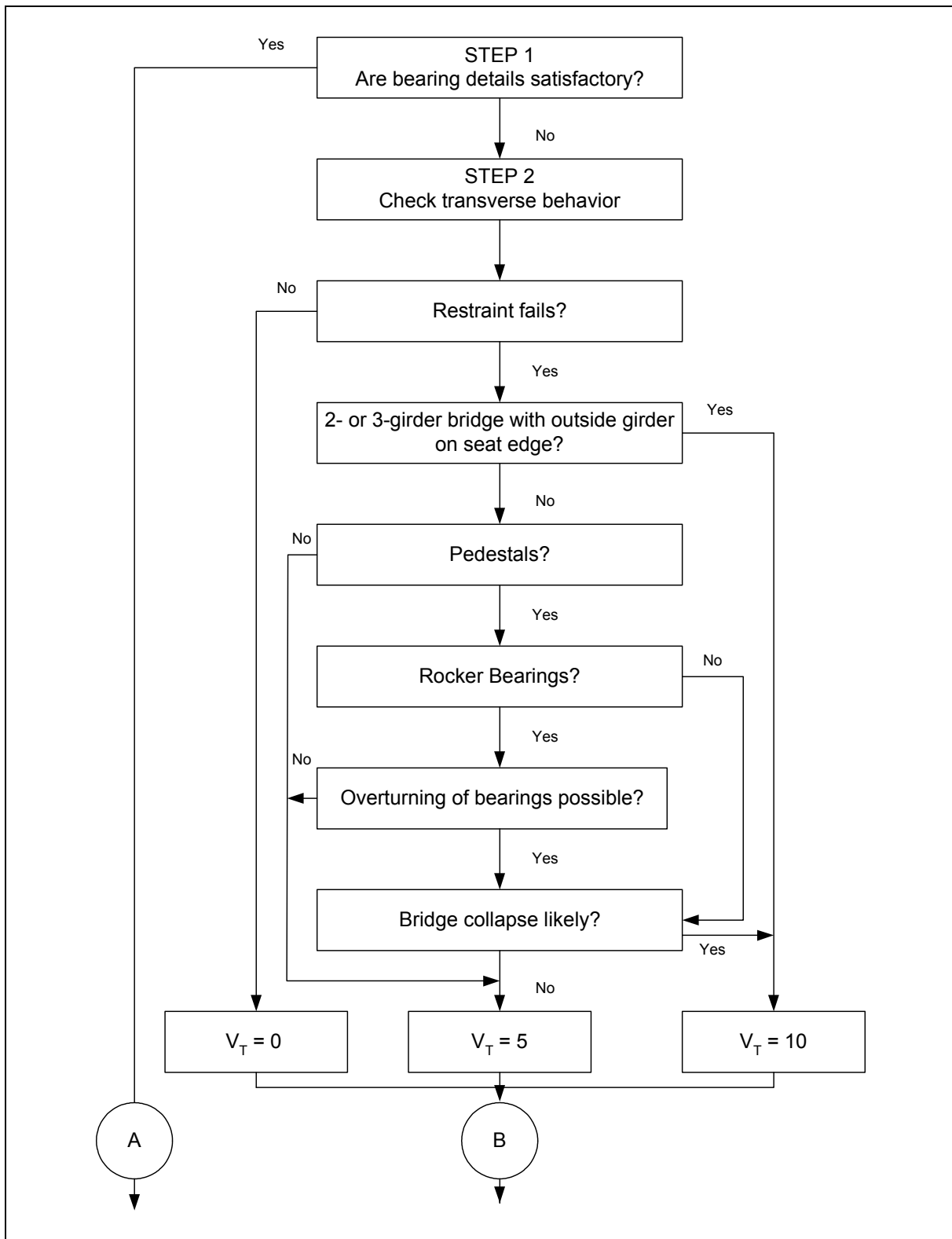
$V_1 = \text{greater of } V_T \text{ and } V_L$.

4.2.1.1(b). Vulnerability Rating for Columns, Abutments, and Liquefaction Potential, V_2

The vulnerability rating for the other components in the bridge that are susceptible to failure, V_2 , is calculated from the individual component ratings as follows:

$$V_2 = CVR + AVR + LVR \leq 10 \quad (4-4)$$

where CVR is the column vulnerability rating, AVR is the abutment vulnerability rating, and LVR is the liquefaction vulnerability rating.



(continued)

Figure 4-4. Calculation of vulnerability rating for connections, bearings and seat widths (V_1).

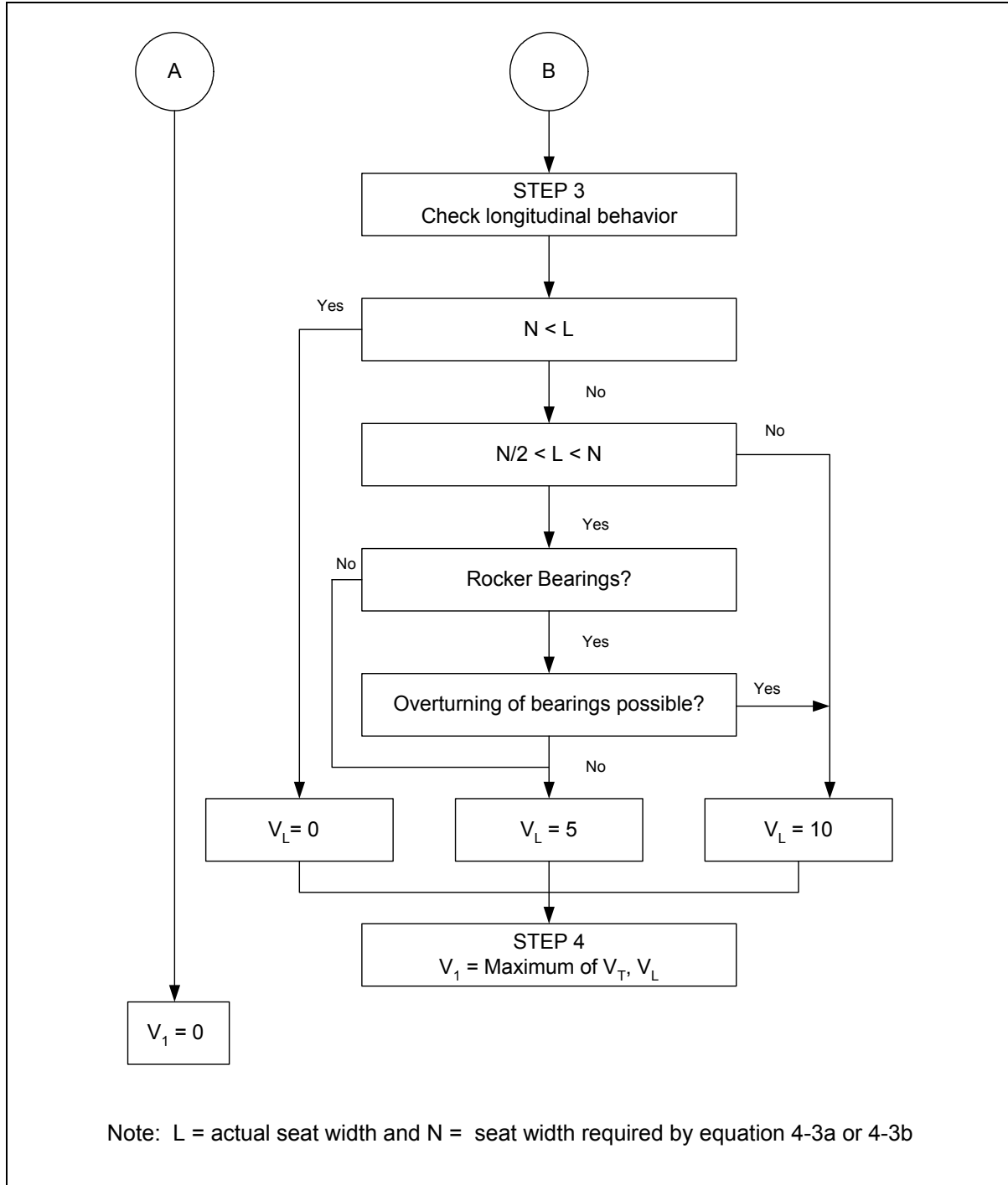


Figure 4-4 (continued). Calculation of vulnerability rating for connections, bearings and seat widths (V_1).

Suggested methods for calculating each of these component ratings are given in the following sections.

A. Column Vulnerability Rating, CVR

Columns have failed in past earthquakes due to lack of adequate transverse reinforcement and poor structural details. Excessive ductility demands have resulted in degradation of column strength in shear and flexure. In past earthquakes, columns have failed in shear, resulting in their disintegration and substantial vertical settlement. Column failure may also occur due to pullout of the longitudinal reinforcing steel, mainly at the footings. Fortunately, most bridge column failures occur during earthquakes that generate high ground accelerations of relatively long duration³.

The following step-by-step procedure may be used to determine the vulnerability of columns, piers, and footings.

Step 1. Assign a column vulnerability rating, CVR, of 0 to bridges classified as SRC B.

Step 2. Assign a vulnerability rating, CVR, of 0 if keeper bars or anchor bolts can be relied upon to fail (section 4.2.1.1(a), step 2), thereby preventing the transfer of load to the columns, piers, or footings.

Step 3. If columns and footings have adequate transverse steel as required by the current AASHTO Specifications, assign a column vulnerability rating, CVR, of 0.

Step 4. If none of the above apply (steps 1 through 3), check the column for shear, splice details, and foundation deficiencies, and give CVR the highest value calculated from the following steps:

Step 4a. Column vulnerability due to shear failure.

$$\text{CVR} = Q - P_R \quad (4-5a)$$

where:

$$Q = 13 - 6 \left(\frac{L_c}{P_s F b_{\max}} \right) \quad (4-5b)$$

L_c = effective column length,

P_s = amount of main reinforcing steel expressed as a percent of the column cross-sectional area,

F = framing factor:

2.0 for multi-column piers fixed top and bottom,

1.0 for multi-column piers fixed at one end,

³ This may not always be the case, as illustrated by the collapse of the Cypress Street Viaduct in Oakland, California, during the 1989 Loma Prieta earthquake. This short-duration earthquake generated peak rock accelerations of about 0.1g close to the bridge. Soft soils amplified this figure to approximately 0.25g at the surface, which is a relatively modest value. Nevertheless, the viaduct, designed before 1971, collapsed due to poor detailing and shear failures in the connections between the upper and lower decks.

1.5 for box girder superstructure with a single-column pier, fixed at top and bottom, and
 1.25 for superstructures other than box girders with a single-column pier, fixed at top and bottom.
 b_{\max} = maximum transverse column dimension, and
 P_R = the total number of points to be deducted from Q for factors known to reduce susceptibility to shear failure, as listed in table 4-1.

Table 4-1. Values for P_R .

Factor	P_R
Seismic coefficient, $S_{D1} < 0.5$	3
Skew $\leq 20^\circ$ (0.35 rad)	2
Continuous superstructure, integral abutments of equal stiffness and length-to-width ratio < 4	1
Grade 40 (or below) reinforcement	1

Values of CVR less than zero or greater than 10, should be assigned values of 0 and 10, respectively.

Equation 4-5b was derived empirically based on observations of column shear failure in bridges during the San Fernando earthquake in 1971. The derivation is given in appendix B of the 1983 retrofit guidelines (FHWA, 1983). This expression has since been checked against column failures in the 1994 Northridge earthquake and was found to be a reliable indicator of column damage (Buckle, 1994). However, the columns in this empirical data set are short to medium in height and equation 4-5b may not apply to tall and/or slender columns. In these cases, special studies should be undertaken to estimate Q, P_R , and CVR.

Step 4b. Column vulnerability due to flexural failure at splices.

To account for flexural failure when the column longitudinal reinforcement is spliced in a plastic hinge location, the following CVR should be used for columns supporting superstructures longer than 90 m (300 ft), or for superstructures with expansion joints:

$$CVR = 7 \quad \text{for } S_{D1} < 0.5 \quad (4-6a)$$

$$CVR = 10 \quad \text{for } S_{D1} \geq 0.5 \quad (4-6b)$$

where S_{D1} is the seismic coefficient defined in equation 1-1.

CVR need not be taken greater than seven unless microzoning confirms S_{D1} is greater than or equal to 0.5.

Step 4c. Column vulnerability due to foundation deficiencies.

The following CVR should be used for columns supported on pile footings that are not reinforced for uplift, or for poorly confined foundation shafts. This step is only applicable if microzoning yields values of S_{D1} greater than or equal to 0.5:

$$CVR = 5 \quad \text{for } 0.5 \leq S_{D1} \leq 0.6 \quad (4-7a)$$

$$CVR = 10 \quad \text{for } S_{D1} > 0.6 \quad (4-7b)$$

Step 4d. Assign overall column vulnerability rating, CVR.

Set the column vulnerability rating, CVR, to the highest value calculated for CVR in steps 4a, 4b, and 4c.

B. Abutment Vulnerability Rating, AVR

Abutment failures during earthquakes do not usually result in total collapse of the bridge. This is especially true for earthquakes of low-to-moderate intensity. Therefore, the abutment vulnerability rating should be based on damage that would temporarily prevent access to the bridge.

Fill settlements are generally of the order of three to five percent of fill height during moderate-sized earthquakes but may be as large as 10-15 percent⁴ in cases of poorly constructed approach fills or when spill-through abutments are used. Additional settlement may occur when the abutments are structurally damaged due to excessive earth pressures and/or forces transferred from the superstructure.

Certain abutment types, such as spill-through abutments and those without wingwalls, may be more vulnerable to this type of damage than others. Except in unusual cases, the maximum abutment vulnerability rating, AVR, need not exceed five. The following step-by-step procedure for determining the vulnerability rating for abutments is based on engineering judgment and the performance of abutments in past earthquakes.

Step 1. If bridges are classified as SRC B, assign a vulnerability rating, AVR, of 0.

Step 2. Determine the vulnerability of the structure to abutment fill settlement. The fill settlement in normally compacted approach fills may be estimated as follows:

- a. One percent of the fill height when $0.24 < S_{D1} \leq 0.39$.
- b. Two percent of the fill height when $0.39 < S_{D1} \leq 0.49$.
- c. Three percent of the fill height when $S_{D1} > 0.49$.

⁴ Fung et al., 1971; Elms and Martin, 1979

The above settlements should be doubled if the bridge is a water crossing. When fill settlements are estimated to be greater than 150 mm (6 in), assign a vulnerability rating, AVR, for the abutment of 5. Otherwise assign a value of 0 for AVR.

Step 3. Bridges classified as SRC D should be assigned a vulnerability rating, AVR, of 5 regardless of the estimated fill settlement, if all of the following conditions are present:

- Cantilever abutments.
- Skews greater than 40° (0.70 rad).
- Distance between the abutment seat and the underside of the footing exceeds 3 m (10 ft).

Otherwise, assign a value of 0 for AVR unless the fill settlement calculated in step 2 is greater than 150 mm (6 in), in which case AVR should be 5.

C. Liquefaction Vulnerability Rating, LVR

Although there are several possible types of ground failure that can result in bridge damage during an earthquake, instability resulting from liquefaction is the most significant. The vulnerability rating for foundation soil is therefore based on:

- A quantitative assessment of liquefaction susceptibility.
- The magnitude of the acceleration coefficient.
- An assessment of the susceptibility of the bridge structure itself to damage resulting from liquefaction-induced ground movement.

The vulnerability of different types of bridges to liquefaction has been illustrated by failures during past earthquakes, such as the 1964 Alaskan earthquake (Ross et al., 1973) and various Japanese earthquakes (Iwasaki et al., 1972). The damage observed has demonstrated that bridges with continuous superstructures and integral supports can withstand large translational displacements and usually remain serviceable (with minor repairs). However, bridges with discontinuous superstructures and/or substructures with little or no ductility, are usually severely damaged as a result of liquefaction. These observations have been taken into account in developing the vulnerability rating procedure described below. The procedure is based on the following steps:

Step 1. Determine the susceptibility of foundation soils to liquefaction.

High susceptibility is associated with the following conditions:

- a. Where the foundation soil, that is providing lateral support to piles or vertical support to footings, consists generally of saturated loose sands, saturated silty sands, or non-plastic silts.
- b. Where soils similar to a. (above) underlie the abutment fills or are present as continuous seams, which could lead to abutment slope failures.

Moderate susceptibility is associated with foundation soils that are generally medium dense soils, e.g., compact sands.

Low susceptibility is associated with foundation soils that are generally dense soils.

Step 2. Use table 4-2 to determine the potential for liquefaction-related damage where susceptible soil conditions exist.

For all sites where $S_{D1} > 0.49$, engineering judgment should be applied to determine the possibility of greater damage.

Table 4-2. Potential for liquefaction-related damage.

Soil Susceptibility To Liquefaction	Seismic Coefficient, S_{D1}				
	$S_{D1} \leq 0.14$	$0.14 < S_{D1} \leq 0.24$	$0.24 < S_{D1} \leq 0.39$	$0.39 < S_{D1} \leq 0.49$	$S_{D1} > 0.49$
Low	Low	Low	Low	Low	Low
Moderate	Low	Low	Moderate	Major	Severe
High	Low	Moderate	Major	Severe	Severe

Step 3. In general, bridges subject to severe liquefaction-related damage should be assigned a vulnerability rating, LVR, of 10. This rating may be reduced to 5 for single-span bridges with skews less than 20° (0.35 rad) or for rigid box culverts.

Step 4. Bridges subject to major liquefaction-related damage should be assigned a vulnerability rating, LVR, of 10. This rating may be reduced to between 5 and 9 for single-span bridges with skews less than 40° (0.70 rad), and for rigid box culverts and continuous bridges with skews less than 20° (0.35 rad), provided one of the following conditions exists:

- Reinforced concrete columns that are integral with the superstructure and have a CVR less than 5 and a height in excess of 8 m (25 ft).
- Steel columns (except those constructed of non-ductile material) that are in excess of 8 m (25 ft) high.
- Columns that are not integral with the superstructure, provided that large movements of the substructure will not result in instability.

Step 5. Bridges subjected to moderate liquefaction-related damage should be assigned a vulnerability rating, LVR, of 5. This rating should be increased to between 6 and 10 if the vulnerability rating for the bearings, V_1 , is greater than or equal to 5.

Step 6. Bridges subjected to low liquefaction-related damage shall be assigned a vulnerability rating, LVR, of 0.

4.2.1.2. Seismic Hazard Rating (E)

For the purpose of this rating, seismic hazard includes both the seismicity of the site and the geotechnical conditions. The seismic coefficient (S_{D1}) is used for this purpose, which, as defined in section 1.5.3, is the spectral acceleration at 1.0 sec modified by the site amplification factor for this period. This coefficient is then scaled to fit the range 0 – 10, so as to give the same weighting to the hazard as to the structural vulnerability. Hence the seismic hazard rating is given by:

$$E = 10 S_{D1} \leq 10.0 \quad (4-8)$$

where S_{D1} is the seismic coefficient at 1.0 sec period, and equals $F_v S_1$ (equation 1-1).

In locations where the soil properties are not known in sufficient detail to determine the soil profile type with confidence, or where the soil profile does not fit any of the specified types, the site coefficient (F_v) shall be based on engineering judgment.

4.2.1.3. Examples

Examples 4.1 and 4.2 are given to illustrate the process of calculating bridge rank, R , for two different bridges of the same length and soil conditions, subject to similar sized earthquakes. Additional examples are given in appendix E.

The results show that a greater vulnerability (higher bridge rank) has been calculated for the simply supported bridge ($R = 43$) than for the continuous bridge ($R = 33$), but this difference is not as great as might be expected. The reason is that, although the second bridge has continuous spans, they are supported on steel bearings, which in turn are mounted on pedestals. Although total span collapse is unlikely to occur, it is very possible that the beams will come off the pedestals despite the continuity.

These same bridges are also analyzed by the expected damage method (section 4.3) with similar results (section 4.3.5.4).

4.2.2. CALCULATION OF PRIORITY INDEX BASED ON INDICES

Once a rank has been calculated for each bridge based on equation 4-2, the bridges may be listed in numerical order of decreasing rank. This order now needs to be modified to obtain the Priority Index (equation 4-1) so as to include such factors as bridge importance, network redundancy, non-seismic deficiencies, remaining useful life, and other socioeconomic issues.

Guidance on assigning importance was given in section 1.4.3 and some discussion of network redundancy and non-seismic rehabilitation was provided in section 1.10.2. If a bridge is part of a highly redundant highway network with alternative bridges or routes, the likelihood that these alternative facilities may also be damaged must be considered. In general, it will not be possible to develop a single number by which to scale the seismic rank (equation 4-2) to obtain the

priority index (equation 4-1). Instead, reordering the rank by subjective means, using a combination of engineering and societal judgment, will be necessary. In this way, an attempt can be made to include all of the technical and societal issues that influence the prioritization of bridges for seismic retrofitting.

4.3. SEISMIC RATING METHOD USING EXPECTED DAMAGE

4.3.1. BACKGROUND

An alternative method for screening and prioritizing bridges is presented in this section. The method compares the severity of expected damage for each bridge in the inventory, for the same earthquake, and ranks each bridge accordingly. Severity of damage is measured by either the damage sustained or the direct economic losses. Bridges with the greatest expected damage (and/or loss) are given the highest priority for retrofitting.

Direct economic losses may be taken as the cost of repair or replacement of a damaged bridge. These losses do not include the so-called indirect costs or socioeconomic costs, which can be very significant and often exceed the direct costs. Indirect costs include loss of life, injuries, business disruption, delay due to traffic congestion, and denial of access. Estimation of these costs is a complex exercise and subject to great uncertainty.

As for the previous method, this method has both quantitative and qualitative parts. The quantitative part is based on expected damage and repair costs, and is used to obtain a bridge rank, R . The qualitative part modifies the rank in a subjective way that takes into account such factors as indirect losses, network redundancy, non-seismic deficiencies, remaining useful life, and other issues, to obtain an overall priority index. As in the previous method, engineering and societal judgment are the key to the second stage of the process. This leads to a priority index, which is a function of rank, indirect loss, redundancy, and other factors, including non-seismic rehabilitation needs. Thus the priority index is defined as

$$P = f(R, \text{indirect loss, redundancy and various non-seismic factors}) \quad (4-9)$$

where P is the priority index, and R is the rank based on expected damage and repair costs.

The *bridge rank*, R , is based on expected damage and direct losses for a given earthquake, whereas *retrofit priority* is based not only on bridge rank, but also on expected indirect losses, network redundancy and non-seismic factors, estimated in a subjective way. The method is illustrated by the flowchart in figure 4-5.

Although equation 4-9 has the same form as equation 4-1, the terms are calculated in different ways. A particular advantage of this method is that it provides a template by which indirect losses may be included, as the state-of-the-art improves.

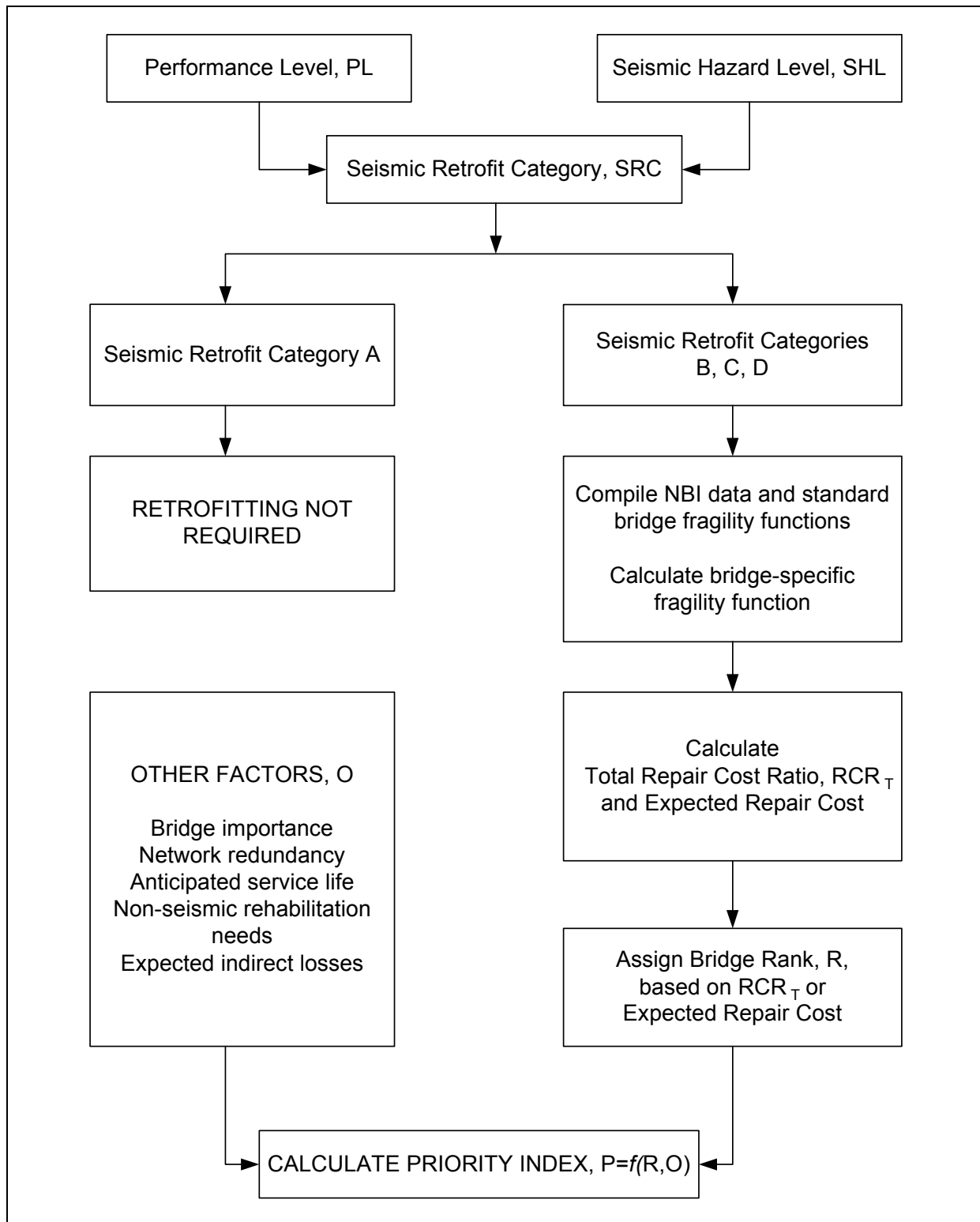


Figure 4-5. Seismic rating method using expected damage.

EXAMPLE 4.1: PRESTRESSED CONCRETE BRIDGE WITH SIMPLE SPANS – INDICES METHOD

A four-beam, prestressed concrete bridge is located on very dense soil and soft rock (site class C). Constructed in 1968, it has three simply-supported spans, each seated on elastomeric pads directly on the cap beams (no pedestals); seat widths are 450 mm (17 3/4"). The total length of the bridge is 56 m (183'- 8 3/4"), with an overall width of 10 m (32'- 9 3/4") and a skew of 32°. Abutment fill height is 7.6 m (24'- 11 1/4"). The bridge carries 65,000 ADT and is considered to be 'essential.'

Calculate the bridge rank R, for this bridge using the indices method (equation 4-2).

Step A. Determine seismic retrofit category, SRC, and minimum screening requirements

The anticipated service life, performance level, and seismic hazard level are required to find the SRC, as follows:

Anticipated service life (ASL):	Age of bridge = 2004-1968	= 36 years
	Assumed service life	= 75 years
	Anticipated service life	= 39 years
	Service life category	= ASL 2 (table 1-1)
Performance level (PL):	Bridge importance is 'essential' Therefore the performance level for the upper level earthquake is PL1 (table 1-2).	
Seismic hazard level (SHL):	Obtain S_s and S_1 from USGS CD-ROM (section 2.3) for upper level earthquake. Assume S_s and S_1 = 1.40 and 0.28. Obtain F_a and F_v from table 1-4 for site class C. Calculate S_{DS} and S_{D1} and obtain SHL from table 1-5 (Eq. 1-1). Results are summarized below:	
	Earthquake	S_s S_1 F_a F_v S_{DS} S_{D1} SHL
	Upper	1.40 0.28 1.0 1.52 1.4 0.43 IV
Seismic retrofit category (SRC):	Obtain SRC from table 1-6.	
	Earthquake	PL SHL SRC
	Upper	PL1 IV C

Minimum screening requirements are given in table 1-7: For SRC = C, minimum requirements are seat widths, connections, columns, walls, footings and liquefaction.

Step B. Vulnerability rating, V

Use the procedure in section 4.2.1.1 to find vulnerability rating, V:

- Step B.1 Bearing and seat width vulnerability, V_1 :
- Simple spans, elastomeric bearings, no pedestals, bearings are not vulnerable to toppling, Four-beam bridge, gives $V_T = 0$
Required longitudinal support, $N = 545$ (21 1/2") mm (equation 4-3a)
Available support, $L = 450$ mm (17 3/4"); hence $0.5 N < L < N$ and $V_L = 5$.
 $V_1 = \text{greater of } V_T \text{ and } V_L = \text{greater of } 0 \text{ and } 5 = 5$. $V_1 = 5$
Use procedure in section 4.2.1.1(b).
- Step B.2 Column, abutment, and liquefaction vulnerability, $V_2 = CVR + AVR + LVR < 10$

For the purpose of this example, assume elastomeric bearings do not fail and seismic loads are transferred to columns; assume columns are not vulnerable to shear failure but longitudinal steel is spliced in potential plastic hinge region.

Superstructure has expansion joints (three simple spans) and $S_{D1} = 0.43 < 0.5$; hence $CVR = 7$ (section 4.2.1.1 (b)).

Since $S_{D1} = 0.43$, fill settlement behind abutment is estimated at two percent $\times 7600 \text{ mm} = 152 \text{ mm}$ (6"); hence $AVR = 5$ (section 4.2.1.1 (b)).

The susceptibility of soils in site class C to liquefaction is low, and from table 4-2, the potential for liquefaction-related damage is 'low'; hence $LVR = 0$.

Therefore $V_2 = CVR + AVR + LVR \leq 10$ (equation 4-4) $= 7 + 5 + 0 = 12 > 10$

Hence $V_2 = 10$

Step B.3 Overall bridge vulnerability, V
Bridge vulnerability calculated as $V = \text{greater of } V_1 \text{ and } V_2$
 $= \text{greater of 5 and 10. } V = 10$

Step C Seismic hazard rating, E
Calculate $E = 10 S_{D1} \leq 10.0$ (equation 4-8) $= 10 \times 0.43 = 4.3$, for $S_{D1} = 0.43$.

Step D Bridge rank, R
Calculate $R = VE$ (equation 4-2) $= 10 \times 4.3 = 43$ Answer

EXAMPLE 4.2: STEEL GIRDER BRIDGE WITH CONTINUOUS SPANS – INDICES METHOD

A four-stringer, steel bridge is located on very dense soil and soft rock (site class C). Constructed in 1972, it has three continuous spans of equal length, each seated on steel bearings on pedestals (not rocker bearings); seat widths are 350 mm (13 3/4"). The total length of the bridge is 56 m (183'- 8 3/4"), with an overall width of 14 m (45'- 11") and a skew of 18°. Abutment fill height is 6 m (19'- 8 1/2"). The bridge carries 20,000 ADT and is considered to be 'standard.'

Calculate the bridge rank R, for this bridge using the indices method (equation 4-2).

Step A. Determine seismic retrofit category, SRC, and minimum screening requirements

The anticipated service life, performance level, and seismic hazard level are required to find the SRC, as follows:

Anticipated service life (ASL): Age of bridge = 2004-1972 = 32 years
 Assumed service life = 75 years
 Anticipated service life = 43 years
 Service life category = ASL 2 (table 1-1)

Performance level (PL): Bridge importance is 'standard'
 Therefore, the performance level for the upper level earthquake is PL1 (table 1-2).

Seismic hazard level (SHL): Obtain S_s and S_1 from USGS CD-ROM (section 2.3). Assume S_s and $S_1 = 1.50$ and 0.21 for upper level earthquake.
 Obtain F_a and F_v from tables 1-4a and b for site class C.
 Calculate S_{DS} and S_{D1} using Eq. 1-1 and obtain SHL from table 1-5.
 Results are summarized below:

Earthquake	S_s	S_1	F_a	F_v	S_{DS}	S_{D1}	SHL
Upper	1.50	0.21	1.0	1.59	1.50	0.33	IV

Seismic retrofit category (SRC): Obtain SRCs from table 1-6.

Earthquake	PL	SHL	SRC
Upper	PL1	IV	C

Minimum screening requirements are given in table 1-7: For SRC = C, minimum requirements are seat widths, connections, columns, walls, footings and liquefaction.

Step B. Vulnerability rating, V

Use the procedure in section 4.2.1.1 to find vulnerability rating, V:

- Step B.1 Bearing and seat width vulnerability, V_1 :
 Continuous spans, steel bearings, pedestals, bearings are not rocker bearings and therefore not vulnerable to toppling, 4-stringer bridge, gives $V_T = 10$
 Required longitudinal support, $N = 437$ mm (17 1/4") (equation 4-3a).
 Available support, $L = 350$ mm (13 3/4"); hence $0.5N < L < N$
 $0.5 (437 \text{ mm}) < 350 \text{ mm} < 437 \text{ mm}$; $V_L = 5$.
 $V_1 = \text{greater of } V_T \text{ and } V_L = \text{greater of } 10 \text{ and } 5$. $V_1 = 10$
- Step B.2 Column, abutment, and liquefaction vulnerability, $V_2 = \text{CVR} + \text{AVR} + \text{LVR} \leq 10$
 Assume failure of bearing keeper bars cannot be relied upon and seismic loads are transferred to columns; assume columns are not vulnerable to shear failure but longitudinal steel is spliced in potential plastic hinge region.

Superstructure has expansion joints at abutments and $S_{D1} = 0.33 < 0.5$; hence $CVR = 7$ (section 4.2.1.1 (b)).

Since $S_{D1} = 0.33$, use 1% of fill height for settlement.

Fill settlement behind abutment estimated at 1 percent x 6000 = 60 mm (2 3/8"); hence $AVR = 0$ (section 4.2.1.1 (b)).

The susceptibility of soils in site class C to liquefaction is low, and from table 4-2, the potential for liquefaction-related damage is 'low'; hence $LVR = 0$.

Therefore $V_2 = CVR + AVR + LVR \leq 10$ (equation 4-4) = 7 + 0 + 0 = 7

Hence $V_2 = 7$

Step B.3 Overall bridge vulnerability, V
Bridge vulnerability calculated as $V = \text{greater of } V_1 \text{ and } V_2$
= greater of 10 and 7. $V = 10$

Step C **Seismic hazard rating, E**
Calculate $E = 10 S_{D1} \leq 10.0$ (equation 4-8) = 10 x 0.33 = 3.3, for $S_{D1} = 0.33$.

Step D **Bridge rank, R**
Calculate $R = VE$ (equation 4-2) = 10 x 3.3 = 33 Answer

The estimation of expected damage is a critical step in this method. Due to uncertainty in earthquake ground motions, and randomness of soil and structure properties, this step is a probabilistic one. Fragility functions are used to estimate the probability of a bridge being in one or more specified damage states, after a given earthquake. Appendix C summarizes the theory of fragility functions and explains briefly how they are obtained. It also describes the six damage states most commonly used to characterize expected damage.

Fragility functions are also essential elements in the Seismic Risk Assessment Method for screening and prioritizing bridges as noted in section 1.10.3. These functions are also used in most loss estimation methodologies, including HAZUS, developed by the National Institute of Building Sciences for the Federal Emergency Management Agency (HAZUS, 1997).

To simplify the method as much as possible, input data requirements are kept to a minimum. In particular, all necessary attributes of the structure may be found in the National Bridge Inventory (NBI) or the bridge owner's bridge history file. Ground motions and soils data are again based on spectral accelerations and soil types as described in sections 1.5.1 and 1.5.2.

4.3.2. DATABASE REQUIREMENTS

The NBI database contains 116 fields that are used to describe structural and operational characteristics of a bridge, but there is still insufficient detail on each bridge to permit a detailed derivation of the required fragility curves. Therefore, for the purpose of screening and prioritization, bridge-specific fragility curves are obtained by taking the results for a *reference* bridge fragility curve and scaling them using selected data from the NBI.

A *reference* bridge is assumed to be a 'long' structure with no appreciable three-dimensional (3D) effects present. Such a bridge is identified for each major type of bridge, of which there may be five or six types (section 4.3.3). For each reference bridge, median spectral accelerations (a_2, a_3, a_4, a_5), at period $T=1.0$ sec, have been developed for each of the damage states (DS_i) described in appendix C. The results for these reference bridges are then modified by factors accounting for skew (K_{skew}) and three-dimensional arching⁵ effects within the plane of the superstructure (K_{3D}), using the NBI attributes in table 4-3. This table shows which fields of the NBI are used and for what purpose.

4.3.3. FRAGILITY CURVES FOR REFERENCE BRIDGES

As described in appendix C, fragility curves are constructed for each of five damage states, for each reference bridge. These five damage states are defined as follows:

- DS_1 = no damage (pre-yield)
- DS_2 = slight damage

⁵ 'Arching' refers to the ability of a bridge deck to distribute lateral loads to the abutments by the in-plane arching action of the deck spanning from one abutment to the other. If expansion joints occur within the superstructure, arching action cannot develop until all of these joints are closed.

Table 4-3. NBI fields (attributes) used in determining bridge fragility.

NBI Data Item	Definition	K_{skew}	K_{3D}	Other Use
1	State		X	To infer specification used in design
8	Structure number			General identification number
27	Year built		X	Infers whether seismic or conventional design
34	Skew	X		
42	Service type			To select highway bridges
43	Structure type		X	To infer base fragility curve from Tables 4-4 and 4-5
45	Number of spans in main unit		X	To infer whether single or multiple span
46	Number of approach spans (n)			To infer whether bridge is a major bridge (major bridge if $n > 6$)
48	Length of maximum span (L)			To infer whether bridge is a major bridge (major bridge if $L > 150$ m)

- DS_3 = moderate damage
- DS_4 = extensive damage
- DS_5 = collapse

Data for the construction of these fragility curves are presented in tables 4-4 and 4-5, where median fragility parameters are listed for non-seismic and seismic structures, respectively (see definitions below). In the development of the parameters in tables 4-4 and 4-5, certain assumptions have been made. These are listed in the rightmost column and are considered to be typical of bridge construction practice throughout the United States. Additional assumptions are noted below:

- The spectrum modification factors accounting for hysteretic energy dissipation (B_s , B_L) were taken as suggested in table 5-4.
- For large bridges, defined as those structures whose main span exceeds 150 m (500 ft), the above procedures do not apply. The values for such bridges presented in tables 4-4 and 4-5 are interpolations based on engineering judgment.

- Bridges built after 1990 (1975 in California), and designed in accordance with prevailing seismic provisions, are considered to have been seismically designed, i.e., they are ‘seismic’ structures. Bridges built prior to these dates are assumed to have not been designed for seismic loads and are called ‘non-seismic’ structures.
- For the sake of simplicity, and largely due to lack of details on regional pier construction practice in the NBI database, it is assumed that continuous bridges have weak bearings/strong piers. Anecdotally this appears to be the case, as relatively few continuous bridges were constructed in the eastern United States prior to the 1970's. In California, it is assumed that concrete bridges identified in the NBI as ‘continuous’ do not, in fact, have continuous superstructures but instead are reinforced concrete frames with in-span expansion joints.
- For the purpose of inferring what bearing types are matched with bridge deck types, it is assumed that steel and concrete (reinforced and prestressed) beam bridges possess steel and neoprene bearings, respectively.
- Site class B soils (table 1-3) were assumed when deriving the reference bridge fragility curves. The site factors described in section 1.5.2 and listed in table 1-4 are used to modify these curves for other site classes.

4.3.4. SCALING REFERENCE BRIDGE FRAGILITY CURVES TO ACCOUNT FOR SKEW AND THREE-DIMENSIONAL EFFECTS

4.3.4.1. Definition of Parameters: K_{skew} and K_{3D}

In order to convert the reference bridge fragility curves to a bridge-specific curve for a given spectral acceleration, the parameters K_{skew} and K_{3D} are used as scaling relations as described below.

The reference fragility curve is modified for skew by applying the correction factor, K_{skew} , which is calculated as follows:

$$K_{skew} = \sqrt{\cos \alpha} \quad (4-10)$$

where α is the angle of skew measured from a line normal to the bridge centerline to a line parallel to the centerline of bearing.

Likewise, the reference fragility curve is modified for 3D effects using the correction factor K_{3D} as tabulated in table 4-6. This factor converts the fragility curve for a long reference bridge to a specific right (no skew) bridge with a finite number of spans.

4.3.4.2. Scaling Relations for Damage States 3, 4, and 5

The modified median fragility curve parameter is given by

$$A_i = K_{skew} K_{3D} \frac{a_i}{S} \quad (4-11)$$

Table 4-4. Fragility of bridges constructed before 1975 in California and 1990 elsewhere.
(non-seismic bridges)

Classification	NBI Class	Damage State	Median Spectral Acceleration at T=1.0 sec		Assumptions ^{2,3}
			Non-California	California	
Multi-column piers, simply supported	101 - 106	2	0.26	0.33	D = 0.91 m (non-CA) D = 1.5 m (CA)
	301 - 306	3	0.35	0.46	
	501 - 506	4	0.44	0.56	
		5	0.65	0.83	
Single-column piers, box girders	205 - 206	2	Not applicable	0.35	D = 1.5 m
	605 - 606	3		0.42	
		4		0.50	
		5		0.74	
Continuous Concrete	201 - 206	2	0.60¹		F _b = 0.8 breakage F _b = 0.7 residual
	601 - 607	3	0.79		
		4	1.05		
		5	1.38		
Continuous Steel	402 - 410	2	0.76¹		F _b = 1.0 breakage F _b = 0.4 residual
		3	0.76		
		4	0.76		
		5	1.04		
Single-Span	All	2	0.80¹		F _b = 1.1 initial breakage F _b = 0.65 residual
		3	0.90		
		4	1.10		
		5	1.60		
Major Bridges		2	0.40		Interpolation from above categories
		3	0.50		
		4	0.60		
		5	0.80		
Notes: 1. Case I (section 4.3.4.3) applies for these cases, evaluate K _{shape} using equation 4-13 2. D = column diameter 3. F _b = bearing shear capacity as a fraction of dead load					

Table 4-5. Fragility of bridges constructed since 1975 in California and 1990 elsewhere.
(seismic bridges)

Classification	NBI Class	Damage State	Median Spectral Acceleration at T=1.0 sec	Assumptions ^{2,3}
Multi-column piers, simply-supported	101 - 106 301 - 306 501 - 506	2 3 4 5	0.45 0.76 1.05 1.53	D = 0.91 m
Single-column bents, box girders	205 - 206 605 - 606	2 3 4 5	0.54 0.88 1.22 1.45	D = 1.5 m
Continuous Concrete and Steel	201 - 206 402 - 410 601 - 607	2 3 4 5	0.91¹ 0.91 1.05 1.38	F _b = 1.2 initial breakaway F _b = 0.7 sliding value
Single-Span		2 3 4 5	0.8¹ 0.9 1.1 1.6	F _b = 1.1 initial breakaway F _b = 0.65 sliding value
Major bridges		2 3 4 5	0.6 0.8 1.0 1.6	Interpolation from above categories
Notes: 1. Case I (section 4.3.4.3) applies, evaluate K _{shape} using equation 4-13 2. D = column diameter 3. F _b = bearing shear capacity as a fraction of dead load				

Table 4-6. Modification factors (K_{3D}) used to model 3D effects for multi-span bridges.

Type	NBI Class	K_{3D} Non-seismic Bridges < 1990 (1975 in CA) ^{1,2}	K_{3D} Seismic Bridges > 1990 (1975 in CA) ¹
Concrete	101 – 106	$1 + 0.25 / n_p$	$1 + 0.25 / n_p$
Concrete Continuous	201 – 206	$1 + 0.33 / n_p$	$1 + 0.33 / n_p$
Steel	301 – 310	$1 + 0.09 / n_p$; $L \geq 20$ m (65ft) $1 + 0.20 / n_p$; $L < 20$ m (65ft)	$1 + 0.25 / n_p$
Steel Continuous	402 – 410	$1 + 0.05 / n_p$; $L \geq 20$ m (65ft) $1 + 0.10 / n_p$; $L < 20$ m (65ft)	$1 + 0.33 / n_p$
Prestressed Concrete	501 – 506	$1 + 0.25 / n_p$	$1 + 0.25 / n_p$
Prestressed Concrete Continuous	601 – 607	$1 + 0.33 / n_p$	$1 + 0.33 / n_p$
Notes: 1. n_p = number of piers = $n - 1$, where n = number of spans in bridge 2. L = length of maximum span (NBI Data Item 48, table 4-3)			

where a_i is the median spectral acceleration (at $T = 1.0$ sec) for the i^{th} damage state as listed in tables 4-4 and 4-5, and S is the site factor for the long-period range; that is $S = F_v$, the 1.0 second site factor given in section 1.5.2 and table 1-4 (note a rock site was assumed in deriving the reference bridge fragility curves, i.e., $S = 1$ for the reference curves).

4.3.4.3. Scaling Relations for Damage State 2 (Slight Damage)

Case I: When ‘short’ periods govern ($T < T_s$, figure 1-8):

$$A_2 = K_{\text{shape}} \frac{a_2}{S} \quad (4-12)$$

where:

a_2 = the median spectral acceleration (at $T = 1.0$ sec) for damage state 2, given in tables 4-4 and 4-5 and identified by superscript 1 in those tables,

S = site factor for the short period range; that is $S = F_a$, the 0.2 second site factor given in section 1.5.2 and table 1-4 (note a rock site was assumed in deriving the reference bridge fragility curves, i.e., $S = 1$ for the reference curves).

K_{shape} relates to the shape of the design acceleration spectrum and is defined as follows:

$$K_{\text{shape}} = 2.5 \frac{S_1}{S_s} \quad (4-13)$$

S_1 and S_s are the spectral accelerations defined in section 1.5.1.

In equation (4-13), the factor 2.5 is the ratio between the spectral amplitude at 1.0 second and 0.2 seconds for the standard code-based spectral shape from which the reference bridge fragility curves were derived. This equation is necessary to ensure all fragility curves possess a common format (either peak ground acceleration or spectral acceleration at $T = 1.0$ second). Note that for this case to govern, $K_{\text{shape}} \leq 1$.

Case II: When ‘long’ periods govern ($T \geq T_s$, figure 1-8):

$$A_2 = \frac{a_2}{S} \quad (4-14)$$

where:

- a_2 = the median spectral acceleration (at $T = 1.0$ sec) for damage state 2, given in tables 4-4 and 4-5 and identified without a superscript 1 in those tables, and
- S = site factor for the long-period range; that is $S = F_v$, the 1.0 second site factor given in section 1.5.2 and table 1-4 (note a rock site was assumed in deriving the reference bridge fragility curves, i.e., $S = 1$ for the reference curves).

Note that in equations (4-12) and (4-14) no modification is assumed for skew and 3D effects. The structural displacements that occur for this damage state are assumed to be small enough (generally less than 50 mm (2 ins)) so that the deck joints do not close and the 3D arching effect does not develop.

4.3.5. ECONOMIC LOSSES

4.3.5.1. Total Economic Losses

Economic losses may result from the combined effects of direct losses due to structural damage to the bridge (B_{LOSS}) and indirect losses resulting from a variety of causes such as loss of life, injuries, business disruption, traffic congestion, and denied access (H_{LOSS}). The total monetary loss to the economy (T_{LOSS}) may therefore be expressed as:

$$T_{\text{LOSS}} = B_{\text{LOSS}} + H_{\text{LOSS}} \quad (4-15)$$

Quantification of these losses is difficult to do at the present time, mainly because of the uncertainty with H_{LOSS} . Nevertheless B_{LOSS} can be found with some degree of confidence using the cost to repair or replace a damaged bridge. Such a methodology is described in the next section.

4.3.5.2. Direct Economic Losses

Direct economic losses are assumed to be due to the repair and replacement of damaged bridges alone and do not include other direct costs such temporary detours. Estimates of these losses may be obtained using the repair cost ratios listed in table 4-7⁶. These ratios (also known as damage

⁶ Basoz and Mander, 1999; Basoz and Kiremidjian, 1997

ratios) express repair costs as a proportion of bridge replacement costs. The mean repair cost ratio for ‘collapse’ ($RCR_{i=5}$ for damage state 5) may be expressed as a function of the number of spans. Since more than one span may collapse in this state, the assumption is made that no more than two spans collapse in any one event. Then RCR_5 is given as below:

$$RCR_{i=5} = \frac{2}{n} \text{ but not more than } 1.0 \quad (4-16)$$

where n is the number of spans in the main portion of the bridge.

Table 4-7. Modified repair cost ratio for all bridges.

Damage State, i	Range of Repair Cost Ratio	Mean Repair Cost Ratio, RCR
1: No damage (pre yield)	0	0
2: Slight damage	0.01 to 0.03	0.02
3: Moderate damage	0.02 to 0.15	0.08
4: Extensive damage	0.10 to 0.40	0.25
5: Collapse	0.1 to 1.0	equation (4-16)

If the repair cost ratio is multiplied by the replacement cost of the bridge, then the expected direct monetary dollar loss (B_{LOSS}) can be assessed, thus

$$B_{LOSS} = U RCR_T \quad (4-17)$$

where:

U = the replacement cost of the bridge.
 RCR_T = the total repair cost ratio that is the expected proportion of the total replacement cost of the entire bridge resulting from earthquake damage, or the *direct loss probability*, which is defined as follows:

$$RCR_T = \sum_{i=2}^5 (RCR_i P[DS_i | S_a]) < 1.0 \quad (4-18)$$

where:

$P[DS_i | S_a]$ = probability of being in damage state DS_i for a given spectral acceleration S_a at a structural period, $T = 1.0$ sec, using fragility curve data for this particular bridge and damage state, DS_i , and
 RCR_i = repair cost ratio for the i^{th} damage state.

4.3.5.3. Indirect Economic Losses

Earthquake related bridge damage may lead to indirect losses that may in many cases exceed the direct costs of the structural damage. These indirect costs may arise from any or all of the following: deaths and injuries, restricted access for emergency response and recovery, business disruption, loss of utility lines, and weakened security.

Quantifying these costs is extremely difficult and cannot be done without considering each bridge in its functional and societal context. Risk assessment models of complete highway systems are under development for this and other purposes, and are a promising tool for developing insight into the complex relationships that govern indirect costs (Werner et al, 2000).

4.3.5.4. Examples

Two examples, 4.3 and 4.4, are given which illustrate the process of calculating the expected losses for two different bridges of the same length and soil conditions, subject to similar sized earthquakes. The losses are expressed first, as the expected repair cost ratio (fraction of the replacement cost), and then as the repair cost assuming an actual replacement cost.

The results are summarized in table 4-8, where the greater vulnerability of the simply supported bridge (example 4.1) is illustrated by the higher loss ratios and repair costs for this bridge. It is noted that these two bridges were also evaluated by the indices method in section 4.2.1.3, where a similar result was obtained: the bridge rank for the simply supported bridge was found to be higher than for the continuous bridge (43 vs 33, respectively).

Table 4-8. Expected losses in two example bridges subject to similar earthquakes.

Example Bridge		RCR_T	B_{Loss}
1.	3-span, simply supported, prestressed, concrete bridge, total length: 56 m (180 ft), site class C	0.224	\$138,046
2.	3-span, continuous steel beam bridge, total length: 56 m (180 ft), site class C	0.039	\$ 33,258

However the difference between the two bridges is more marked in this case, possibly because the pedestal supports under the steel beams are not explicitly considered in this method, as they are in the indices method. Such data is not in the NBI files and its omission is a shortcoming of any method based solely on NBI data. As inventories improve over time (for bridge management purposes perhaps), this problem will be overcome and the usefulness of the method will likewise improve.

4.3.6. CALCULATION OF BRIDGE RANK BASED ON EXPECTED DAMAGE

Once the expected damage is known for each bridge in the inventory and expressed as a loss (RCR_T , or B_{LOSS}), the inventory may be ranked in descending order of expected losses and each bridge assigned a rank, R .

4.3.7. CALCULATION OF PRIORITY INDEX BASED ON EXPECTED DAMAGE

As defined in equation 4-9, the Priority Index is based on R , the bridge rank, calculated in section 4.3.6, and a qualitative assessment of the indirect losses, network redundancy and non-seismic factors, such as impending plans for bridge widening or deck replacement.

EXAMPLE 4.3: PRESTRESSED CONCRETE BRIDGE WITH SIMPLE SPANS – EXPECTED DAMAGE METHOD

A four-beam, prestressed concrete bridge is located on very dense soil and soft rock (site class C). Constructed in 1968, it has three simply-supported spans, each seated on elastomeric pads directly on the cap beams (no pedestals); seat widths are 250 mm (9 3/4"). The total length of the bridge is 56 m (183'- 8 3/4"), with an overall width of 10 m (32'- 9 3/4") and a skew of 32°. Piers are multi-column frames. Abutment fill height is 7.6 m (24'-11 1/4"). The bridge carries 65,000 ADT and is considered to be 'essential.' The table below lists data available from the NBI for this bridge. The estimated replacement cost of this bridge is \$616,000.

NBI field	Data	Remarks
27	1968	Year built
34	32°	Angle of skew
43	501	Prestressed concrete, simple span
45	3	Number of spans
48	23	Maximum span length (m)
49	56	Total bridge length (m)
52	10	Bridge width (m)
	65,000	ADT

Using only NBI data, calculate the expected total repair cost following the upper level earthquake for this site.

For the upper level event, spectral accelerations S_S and S_1 are taken to be 1.40 g and 0.28 g, respectively, for the bridge site. Corresponding values for site class C soil factors, F_a and F_v , are 1.00 and 1.52, respectively (table 1-4).

Since the bridge was constructed in 1968 and is located outside of California, the first row of table 4-4 and the fifth row of table 4-6 apply, respectively. From table 4-4 for type 501:

$$a_2 = 0.26g; a_3 = 0.35g; a_4 = 0.44g; a_5 = 0.65g$$

Note that the value for a_2 in table 4-4 is not superscripted to indicate Case I governs; thus the 'long-period' values govern for this bridge type; therefore $K_{shape} = 1$.

From table 4-6:

$$K_{3D} = 1 + \frac{0.25}{(n-1)} = 1 + \frac{0.25}{(3-1)} = 1.125$$

From equation 4-10:

$$K_{skew} = \sqrt{\cos \alpha} = \sqrt{\cos 32} = 0.92$$

From equation 4-14:

$$A_2 = \frac{a_2}{S} = \frac{0.26}{1.52} = 0.17 g$$

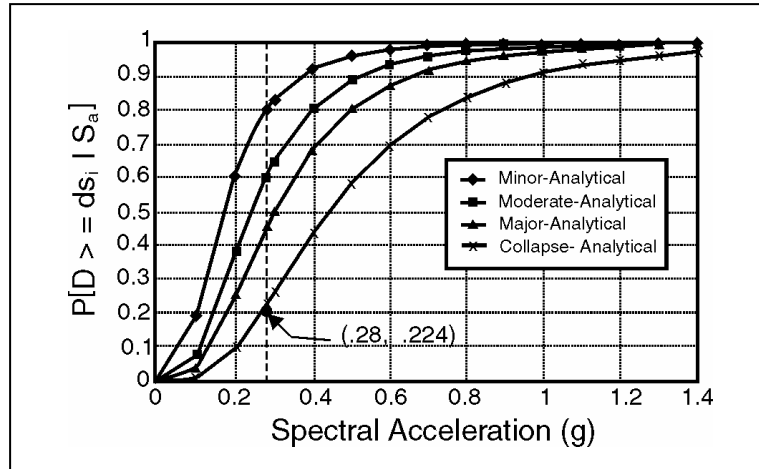
From equation 4-11:

$$A_i = K_{skew} K_{3D} \frac{a_i}{S} = \frac{(0.92)(1.125)}{1.52} a_i = 0.681 a_i$$

Hence:

$$A_3 = 0.24g; A_4 = 0.30g; A_5 = 0.44g$$

The figure presents the fragility curves for the prestressed concrete bridge with simply supported spans. As shown in the figure, the probability of being in a given damage state, when S_a ($T = 1$ sec) = 0.28g, is given in the table below. This table also presents the repair cost ratios from which the expected loss ratios are determined in terms of the total replacement cost for the entire bridge.



Damage State, i (1)	$P[D \geq DS_i S_a]$ (2)	$P[DS_i S_a]$ (3)	RCR_i (4)	Product (3) x (4) = (5)
1	1	0.203	0.00	0.00000
2	0.797	0.196	0.02	0.00392
3	0.601	0.147	0.08	0.01176
4	0.454	0.228	0.25	0.05700
5	0.226	0.226	0.67	0.15142
Total probabilities:		1.000	RCR_T	0.22410
Notes: 1. Column (2) is probability of being in a damage state (D) that is equal to, or greater than, damage state i (DS_i), and is read from the fragility curve for this bridge and damage state, for spectral acceleration = 0.28 g. 2. Column (3) is probability of being in damage state i, and is calculated by subtracting corresponding rows in column (2), e.g., row 1, col (3) = (row 1, col (2)) – (row 2, col (2)) Exception is last row, which is set equal to last row of col (2). Column (4) is read from table 4-7.				

The resulting value of total repair cost ratio ($RCR_T = 0.224$) is used to compute the expected repair cost in dollars from equation (4-17) as follows:

$$\begin{aligned}
 B_{Loss} &= U (RCR_T), \text{ where } U \text{ is the replacement cost of the bridge, estimated at } \$616,000. \\
 &= \$616,000 (0.224) \\
 &= \$138,046 \quad \text{Answer}
 \end{aligned}$$

EXAMPLE 4.4: STEEL GIRDER BRIDGE WITH CONTINUOUS SPANS – EXPECTED DAMAGE METHOD

A four-beam, steel bridge is located on very dense soil and soft rock (site class C). Constructed in 1972, it has three continuous spans, each seated on steel bearings on pedestals (not rocker bearings); seat widths are 250 mm (9 3/4"). The total length of the bridge is 56 m (183' 8 3/4"), with an overall width of 14 m (45' 11") and a skew of 18°. Abutment fill height is 6 m (19' 8 1/4"). The bridge carries 20,000 ADT and is considered to be 'standard.' Data available from the NBI for this bridge is given in the table below. The estimated replacement cost of this bridge is \$862,400.

NBI field	Data	Remarks
27	1972	Year built
34	18°	Angle of skew
43	402	Steel girder, continuous
45	3	Number of spans
48	23	Maximum span length (m)
49	56	Total bridge length (m)
52	14	Bridge width (m)
	20,000	ADT

Using only NBI data, calculate the expected total repair costs following the upper level earthquake for this site.

For the upper level event, spectral accelerations S_S and S_1 are taken to be 1.50 g and 0.21 g, respectively, for the bridge site. Corresponding values for site class C soil factors, F_a and F_v , are 1.00 and 1.59, respectively (table 1-4).

Since the bridge was constructed in 1972 and is located outside of California, a non-seismic structure is assumed. Therefore, the fourth row of both table 4-4 and table 4-6 applies. From table 4-4 for type 402:

$$a_2 = 0.76 \text{ g}; a_3 = 0.76 \text{ g}; a_4 = 0.76 \text{ g}; a_5 = 1.04 \text{ g}$$

Note that the value for a_2 in table 4-5 is superscripted, implying that short period values govern for small displacements for this bridge type; therefore K_{shape} applies.

From equation 4-13:

$$K_{\text{shape}} = 2.5 \frac{S_1}{S_S} = 2.5 \frac{0.21}{1.50} = 0.35 \leq 1$$

From equation table 4-6:

$$K_{3D} = 1 + \frac{0.05}{(n-1)} = 1 + \frac{0.05}{2} = 1.025$$

From equation 4-10:

$$K_{\text{skew}} = \sqrt{\cos \alpha} = \sqrt{\cos 18} = 0.98$$

From equation 4-12:

$$A_2 = K_{\text{shape}} \frac{a_2}{S} = 0.35 \frac{0.76}{1.00} = 0.27 \text{ g}$$

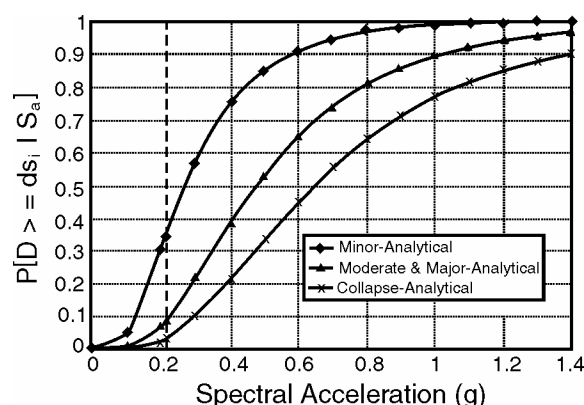
From equation 4-11:

$$A_3 = K_{\text{skew}} K_{3D} \frac{a_3}{S} = \frac{(1.025)(0.98)(0.76)}{1.59} = 0.48 \text{ g}$$

$$A_4 = K_{\text{skew}} K_{3D} \frac{a_4}{S} = \frac{(1.025)(0.98)(0.76)}{1.59} = 0.48 \text{ g}$$

$$A_5 = K_{\text{skew}} K_{3D} \frac{a_5}{S} = \frac{(1.025)(0.98)(1.04)}{1.59} = 0.66 \text{ g}$$

The figure presents fragility curves for the continuous steel girder bridge. It shows the probability of being in a given damage state as S_a ($T = 1$ sec) = 0.21 g for different damage states. These probabilities are used in the table to compute the expected loss ratio of the total replacement cost.



Damage State, i (1)	P[D>DS _i S _a] (2)	P[DS _i S _a] (3)	RCR _i (4)	Product (3) x (4) = (5)
1	1	0.662	0.00	0.00000
2	0.338	0.254	0.02	0.00508
3	0.084	0.000	0.08	0.00000
4	0.084	0.054	0.25	0.01350
5	0.030	0.030	0.67	0.02010
Total probabilities:		1.000	RCR _T	0.03868
Notes: <ol style="list-style-type: none"> Column (2) is probability of being in a damage state (D) that is equal to, or greater than, damage state i (DS_i), and is read from the fragility curve for this bridge and damage state, for spectral acceleration = 0.21 g. Column (3) is probability of being in damage state i, and is calculated by subtracting corresponding rows in column (2); e.g., row 1, col (3) = (row 1, col (2)) - (row 2, col (2)) Exception is last row, which is set equal to last row of col (2). Column (4) is read from table 4-7. 				

The resulting value of total loss ratio ($RCR_T = 0.03868$) is used to compute the expected direct loss in dollars from equation (4-17) as follows:

$$B_{\text{Loss}} = U \times RCR_T, \text{ where } U \text{ is the replacement cost of the bridge estimated at } \$862,400$$

$$B_{\text{Loss}} = \$862,400 \times 0.03868$$

$$= \$33,358 \text{ Answer}$$

CHAPTER 5: EVALUATION METHODS FOR EXISTING BRIDGES

5.1. GENERAL

5.1.1. SUMMARY OF EVALUATION METHODS

Six evaluation methods are described in this chapter. They are listed below in increasing order of sophistication and rigor. Table 1-9 summarizes the key features of these methods and is repeated here as table 5-1 for convenience.

Method A1/A2: Connection forces and seat width checks. Seismic demand analysis is not required but the capacity of connections details and seat width adequacy is checked against minimum values (section 5.2). The method is suitable for all single-span bridges and others in low hazard zones. The method is divided into two categories, A1 and A2.

Method A1: Connection forces and seat width checks ($S_s < 0.10$). Seismic demand analysis is not required but the capacity of the connections must exceed 10 percent of the vertical reactions at each connection, and seat width requirements are checked against minimum requirements. Suitable for all single-span bridges and others in low hazard zones. (section 5.2.1).

Method A2: Connection forces and seat width checks ($S_s \geq 0.10$). Seismic demand analysis is not required but the capacity of the connections must exceed 25 percent of the vertical reactions at each connection, and seat width requirements are checked against minimum requirements. Pile reinforcement must also meet minimum requirements. Suitable for all single-span bridges and other bridges in low hazard zones. (section 5.2.2)

Method B: Component capacity checks. Seismic demand analysis is not required, but the relative strength of the members and the adequacy of certain key details (including connection forces and seat widths) are checked against specified minima. Suitable for regular bridges in Seismic Retrofit Category (SRC) C, subject to restrictions on $F_v S_1$. (section 5.3).

Method C: Component capacity/demand method. Seismic demands are determined by an elastic analysis such as the uniform load method, multi-mode response spectrum method, or an elastic time history method. The uniform load method is adequate for bridges with regular configurations; otherwise, the multi-mode method is used as a minimum. Capacity/demand ratios are calculated for all relevant components. Suitable for all bridges in Seismic Retrofit Categories C and D, but gives best results for bridges that behave elastically or nearly so. (section 5.4)

Method D1: Capacity spectrum method. Seismic demands are determined by simple models such as the uniform load method, and capacity assessment is based on a simplified bilinear lateral strength curve for the complete bridge. A capacity spectrum is used to calculate the capacity/demand ratio for the bridge, for each limit state. Suitable for regular bridges in SRC C and D. (section 5.5)

Table 5-1. Evaluation methods for existing bridges.

METHOD	CAPACITY ASSESSMENT	DEMAND ANALYSIS	APPLICABILITY		COMMENTS
			SRC UL ¹	Bridge Type	
A1/ A2	Connection and Seat Width Checks	Not required	A – D B	All single-span bridges. Bridges in low hazard zones.	Hand method, spreadsheet useful.
B	Component Capacity Checks	Not required	C	Regular bridges, but subject to limitations on $F_y S_1$.	Hand method, spreadsheet useful.
C	Component Capacity/Demand Method	Elastic Methods ² : • ULM • MM • TH	C & D	Regular and irregular bridges that respond almost elastically, such as those in low-to-moderate seismic zones and those with stringent performance criteria.	Calculates C/D ratios for individual components. This is the C/D Method of previous FHWA Highway Bridge Retrofitting Manuals. Software required for demand analysis.
D1	Capacity Spectrum Method	Elastic Methods ² : • ULM	C & D	Regular bridges that behave as single-degree-of-freedom systems and have 'rigid' in-plane superstructures.	Calculates C/D ratios for complete bridge, for specified limit states. Spreadsheet useful.
D2	Structure Capacity/Demand Method	Elastic Methods ² : • ULM • MM • TH	C & D	Regular and irregular bridges.	Calculates C/D ratios for bridge superstructure, individual piers, and foundations. Also known as <i>Nonlinear Static Procedure</i> , <i>Pushover Method</i> or <i>Displacement Capacity Evaluation Method</i> . Software required for demand and capacity analysis.
E	Nonlinear Dynamic Method	Inelastic Methods ² : • TH	D	Irregular complex bridges, or when site specific ground motions are to be used such as for bridges of major importance.	Most rigorous method, expert skill required. Software essential.
Notes: 1. SRC = Seismic Retrofit Category for upper level earthquake; for the lower level earthquake, the recommended method of evaluation is Method C. 2. ULM = Uniform Load Method; MM = Multi-Mode Spectral Method; TH = Time History Method					

Method D2: Structure capacity/demand method. Seismic demands are determined by elastic methods, such as the multi-mode response spectrum method, or an elastic time history method. Capacity assessment is based on the displacement capacity of individual piers as determined by a ‘pushover’ analysis which includes the nonlinear behavior of the inelastic components. A capacity spectrum is used to calculate the capacity/demand ratio for each pier, bearing and foundation of the bridge for each limit state. Suitable for all bridges in SRC C and D. Method is also known as the *pushover method* or alternatively the *Nonlinear Static Procedure*. (section 5.6)

Method E: Nonlinear dynamic procedure (time history analysis). Seismic demands are determined by a nonlinear dynamic analysis using earthquake ground motion records to evaluate the displacement and force demands. Capacities of individual components are explicitly modeled in the demand analysis. Suitable for irregular complex bridges, or when site specific ground motions are to be used, as in the case of a bridge of major importance. (section 5.7).

5.1.2. DEMAND ANALYSES

Methods A and B simply check default capacities against minimum load requirements. No explicit demand analysis is required. Methods C, D1 and D2 are capacity/demand methods of varying sophistication, and Method E, which is based on inelastic time history analysis, is the most rigorous of all of these methods.

As noted above, no demand analysis is necessary for regular bridges in Method B. This is because the design strength for nonseismic loads should be sufficient for the hazard exposure. For regular bridges, a single-degree-of-freedom (SDOF) model is sufficiently accurate to represent the seismic response, and the capacity spectrum method (Method D1) combines the demand and capacity evaluations into one operation. This method is also appropriate for bridges with seismic isolation systems.

For bridges that do not satisfy the requirements of Method D1, an elastic response analysis, using either Methods C or D2, must be performed to determine the displacement and force demands in various members and components. Two elastic methods are presented in this chapter: the uniform load method and the multi-mode response spectrum method. The selection of a method is dependent on the configuration of the bridge.

The uniform load method is suitable for structures with regular configurations which can be modeled as SDOF structures. Long bridges, or those with significant skew or horizontal curvature, have dynamic characteristics that may prevent modeling in this way, and multi-modal methods should be used instead.

Elastic analyses use linear models which may not adequately represent the inelastic behavior of earthquake resisting members during strong ground motion. However, with the proper representation and interpretation of inelastic behavior, an elastic analysis can provide a reasonable estimate of seismic demand. The model should be based on cracked section properties for concrete components and secant stiffness coefficients for the foundations, abutments, and seismic isolators, that are consistent with the expected level of deformation. An elastic analysis should give superstructure displacements (usually at the center of mass), and the

forces in earthquake resisting members, such as the top and bottom bending moments in a column.

The nonlinear dynamic analysis method (Method E) is a powerful analytical tool because it is not restricted by geometry or nonlinearities in material behavior. The effect of inelastic behavior is included explicitly in the demand analysis. Depending on the mathematical model used, the deformation capacity of the inelastic members may also be included in the analysis. However, the data required to perform such an analysis is extensive and the corresponding mathematical model for the bridge is complex and time consuming to develop. Furthermore, a nonlinear dynamic analysis requires the selection of a set of time histories of ground motion that represents the local hazard and site conditions. For many bridge sites, this will be a significant effort requiring the advice of experts in the field. Because of the complexity involved in a nonlinear dynamic analysis, results should always be checked for reasonableness against those from other, but less rigorous, methods.

Nonlinear dynamic analysis should be used for bridges with earthquake protective systems (isolators and/or energy dissipators) that have long periods (> 3 sec) and/or high damping ratios (> 30 percent). This is because procedures that use effective stiffness and damping may not properly represent the effect of these properties when they reach such high values. In such cases, models for the isolators and dissipators should use explicit hysteretic properties and not equivalent linear values.

Regardless of the method of demand analysis used, it is essential that seat widths at abutments, piers, and in-span hinges be checked.

Note that the methods described below should be used in conjunction with the guidelines for bridge modelling and analysis given in chapters 6 and 7.

5.2. METHOD A: CONNECTION DETAILS AND SEAT WIDTH CHECKS ONLY

In areas of low seismicity, minimum seat widths and connection forces are usually adequate to ensure life safety. In such cases, design values are used as minimum requirements in lieu of rigorous analysis. For the operational objective, a check on the minimum shear reinforcement in concrete piles is also recommended. This same check is also recommended for the life safety objective when the Hazard Level is II and higher. To provide for these exceptions, Method A is divided into two categories, A1 and A2, as described below.

5.2.1. METHOD A1

In Method A1, the horizontal forces used to check the capacity of connections in their restrained directions, should not be less than 10 percent of the vertical reaction at that connection due to the tributary dead load. These loads are defined as follows:

- In the longitudinal direction, for each uninterrupted (continuous) segment of a superstructure, including simply supported spans, the tributary dead load at the fixed bearings is the total

dead load of the entire segment. The longitudinal capacity required at the expansion bearings in this segment is assumed to be zero.

- In the transverse direction, for each uninterrupted (continuous) segment of a superstructure, including simply supported spans, the tributary dead load is the dead load reaction at each bearing.

The connection detail between an elastomeric bearing and its masonry and sole plates should be able to resist the horizontal forces transmitted through the bearing. For all bridges evaluated with Method A1, and all single-span bridges, these shear forces should not be less than the connection force described above.

Seat widths should also be checked against the minimum requirements of equation 5-1 below (see also figure D-1).

$$N = \left[100 + 1.7L + 7.0H + 50\sqrt{H} \sqrt{1 + \left(2 \frac{B}{L} \right)^2} \right] \frac{(1 + 1.25F_v S_1)}{\cos \alpha} \quad (5-1a)$$

where N is the minimum seat width (mm), L is the distance between joints (m), H is the tallest pier between the joints (m), and B is the width of the superstructure (m).

Or, in U.S. customary units:

$$N = \left[4.0 + 0.02L + 0.08H + 1.1\sqrt{H} \sqrt{1 + \left(2 \frac{B}{L} \right)^2} \right] \frac{(1 + 1.25F_v S_1)}{\cos \alpha} \quad (5-1b)$$

where N is the minimum seat width (in), L is the distance between joints (ft), H is the tallest pier between the joints (ft), and B is the width of the superstructure (ft).

In both equations, α is the angle of skew (zero for a right bridge). The ratio of B/L need not be taken greater than 3/8.

5.2.2. METHOD A2

In Method A2, horizontal forces used to check the capacity of connections in their restrained directions, should not be less than 25 percent of the vertical reaction at that connection due to the tributary dead load. These loads are defined in Method A1.

The connection detail between an elastomeric bearing and its masonry and sole plates should be able to resist the horizontal forces transmitted through the bearing. For all bridges evaluated with Method A2, and all single-span bridges, these shear forces should not be less than the connection force described above.

Minimum seat widths should be checked against equation 5-1.

5.3. METHOD B: COMPONENT CAPACITY CHECKS

A seismic demand analysis is not required for bridges meeting the requirements of Method B, but capacity protection principles¹ and minimum detailing requirements must be satisfied. Method B permits the rapid evaluation of bridges complying with certain restrictions, without the need for full dynamic analysis. Each bridge is evaluated for non-seismic requirements and capacity protection requirements, then checked to determine the adequacy of certain details such as shear and confining reinforcement. Capacity protection principles are also used to check the adequacy of connection details between columns and footings; and between columns, pier caps and superstructure.

There are no evaluation requirements for abutments except that integral abutments need to be evaluated for passive pressure. This method will be mainly used in areas of low-to-moderate seismic hazard (SHL I and II) where superstructure displacements in the longitudinal direction are expected to be small. As a result, abutments are not expected to contribute to bridge response in any significant way, and may be omitted from further evaluation (in these low seismic zones). Earthquake loads for foundation design are determined from the column forces using an overstrength ratio of 1.0.

5.3.1. PROCEDURE FOR METHOD B

- Step 1. Check section 5.3.2 for restrictions on structural and site characteristics to determine if Method B is applicable. The hazard at the site must not exceed a limitation on $F_v S_1$, and the structure must meet certain geometric regularity requirements.
- Step 2. Check all connection and seat width requirements as for Method A2.
- Step 3. Reinforced concrete columns should be evaluated using non-seismic loading cases and checked for minimum longitudinal reinforcement of 0.8 percent.
- Step 4. Reinforced concrete columns should be checked to see whether the reinforcing details are adequate for column shear and confinement (check against minimum requirements specified in AASHTO, 2002 or AASHTO, 1998).
- Step 5. Steel columns should be evaluated using non-seismic loading cases and should be checked for compactness.
- Step 6. Members connecting to columns should be evaluated for their ability to resist the moments and shears caused by plastic hinging in the columns, using the principles of capacity protection, with an overstrength ratio of 1.4. See sections 7.6 and 7.7.

¹ Capacity protected design means that certain components and/or members of a bridge are protected from excessive forces during an earthquake by the yielding of components and/or members elsewhere in the bridge. For example, the maximum shear that can be transmitted to a footing by a column is determined by the flexural capacity of the column, i.e., the column's yield strength. Thus, the footing is protected by the capacity of the column.

Step 7. Foundations should be evaluated for their ability to resist the moments and shears caused by plastic hinging in the columns, using the principle of capacity protection, with an overstrength ratio of 1.0. See sections 7.6 and 7.7.

5.3.2. RESTRICTIONS ON USE OF METHOD B

Method B should be used only at sites where:

$$F_v S_1 < 0.3 \cos \alpha \quad (5-2)$$

where α is the skew angle of the bridge (zero for a right bridge).

Additionally, Method B should be used only on structures that comply with the following restrictions (notation is defined below):

- For bridges with concrete column and pile bents:

$$\begin{aligned} P_e &< 0.15 f'_c A_g \\ \rho_t &> 0.008 \\ D &\geq 300 \text{ mm (12 in)} \\ 2 &< M/VD < 7 \end{aligned}$$

- For bridges with wall piers with low percentages of longitudinal steel:

$$\begin{aligned} P_e &< 0.07 f'_c A_g \\ \rho_t &> 0.0025 \\ M/VT &< 7 \\ T &\geq 300 \text{ mm (12 in)} \end{aligned}$$

- For bridges with steel pile bents framing into reinforced concrete caps:

$$\begin{aligned} P_e &< 0.15 P_y \\ D_p &\geq 250 \text{ mm (10 in)} \\ M/VB &< 7 \end{aligned}$$

- For bridges with timber piles framing into reinforced concrete caps:

$$\begin{aligned} P_e &< 0.1 P_c \\ D_p &\geq 250 \text{ mm (10 in)} \end{aligned}$$

Notation used above is defined as follows:

P_e = axial load on the bridge column including both gravity and seismic effects,
 P_c = axial capacity of a steel column or timber pile member in compression,
 P_y = axial capacity at yield of a steel column/pile member,
 ρ_t = total area ratio of longitudinal reinforcement,
 f'_c = compressive strength of concrete,

A_g = gross area of the column section,
 D = smallest column dimension or diameter,
 D_p = pile dimension about the weak axis of bending,
 T = wall thickness or smallest cross-sectional dimension,
 B = flange width of a steel H-pile, and
 M/V = shear span length of an equivalent cantilever member (M is the end moment and V is the shear force).

Note that structures with lower axial loads or stronger columns (i.e., more reinforcement and larger column or pile sizes) have greater intrinsic strength. Thus, they are able to resist ground motions with less damage. However, the ductility of the details still needs to be checked.

Other restrictions on the use of Method B include the following:

- Stiffness of individual piers should not vary by more than a factor of two with respect to the average stiffness of all piers in the bridge.
- Maximum span length should not exceed 80 m (260 ft).
- Longest individual span should not exceed 150 percent of the average span length.
- Maximum skew angle should not exceed 30 degrees.
- For horizontally curved bridges, the subtended angle should not exceed 30 degrees.
- Columns must resist at least 80 percent of the horizontal load generated in the longitudinal direction by the tributary area of each column.
- Method B should not be used if the bridge site has a potential for liquefaction and the piers are seated on spread footings.
- Method B should not be used if the bridge site has a potential for liquefaction and the piers are on pile foundations, unless the piles possess ductile details over the length passing through the liquefiable soil layer plus an additional length of three pile diameters or 3 m (10 ft), whichever is larger, above and below this layer.

5.4. METHOD C: COMPONENT CAPACITY/DEMAND METHOD

5.4.1. APPROACH

Method C calculates capacity/demand ratios for bridge components that may be damaged during an earthquake. Ratios greater than one indicate sufficient capacity to resist the earthquake demand; ratios less than one indicate components in need of attention and possible retrofitting. Capacity/demand ratios are therefore used to indicate the need for retrofitting and may also be used to assess the effectiveness of various retrofit strategies.

One feature that distinguishes this method from Method D1, is that the demand is based on the elastic response of the structure calculated by either the uniform load method or a spectral modal analysis. Another difference is that this method focuses on individual component behavior rather than the response of a bridge as a complete structure. In this way, it gives a detailed view of the potential deficiencies of a bridge, but may overestimate the overall vulnerability of a bridge and imply a greater need for retrofitting than is actually necessary. This is because the method ignores ‘system’ response and the ability of a bridge, acting as a system, to redistribute loads from one member to another. The error here is small if the bridge responds elastically or nearly so. Method C gives conservative results and the degree of conservatism generally increases with the extent of plastic hinging in the bridge. If the indicated retrofit needs are high, it may be wise to use one of the more refined methods (D or E) to reassess the situation before committing to design and construction.

Components that should be evaluated will vary with the Seismic Retrofit Category of the bridge. Table 5-2 indicates components and failure modes that should be checked. For some bridge types, failure of certain components will not result in unacceptable damage, and capacity/demand (C/D) ratios for these components need not be calculated. For other bridge types, components, other than those listed, should be examined if their failure will result in unacceptable performance.

Table 5-2. Components for which capacity/demand ratios are required.

Component	Seismic Retrofit Category	
	B	C and D
EXPANSION JOINTS AND BEARINGS		
Support Length	X	X
Connection Forces	X	X
REINFORCED CONCRETE COLUMNS WALLS AND FOOTINGS		
Anchorage		X
Splices		X
Shear		X
Confinement		X
Footing Rotation		X
ABUTMENTS		
Displacement		X
LIQUEFACTION		
Lateral Spread	X	X

In addition to calculating elastic demands by spectral methods, some minimum requirements can be treated as demands. For example, minimum bearing connection forces and minimum support length requirements are useful indicators of demand when calculating C/D ratios for bearing forces and superstructure displacements

Seismic capacities are calculated at their nominal ultimate values without the use of capacity reduction factors, ϕ . In cases such as well-detailed reinforced concrete columns, where post-elastic behavior is acceptable, C/D ratios are modified by ductility indicators (see appendix D) to reflect the capacity of the column to withstand plastic deformation.

In general, the ability of a bridge to meet seismic demands will be determined by one of the following:

- Displacements at supports or intermediate hinges that result in a loss of support and collapse of one or more spans.
- Ultimate strength of fixed bearings and their anchorages.
- Ductile capacity of columns, piers, and foundations beyond which an unacceptable degradation in strength occurs.
- Abutment displacements which make the bridge inaccessible after an earthquake.
- Foundation movements which are excessive and will result in a collapse of the structure or loss of access to the bridge.

The basic equation for determining the C/D ratio, r , for a particular component is:

$$r = \frac{R_C - \Sigma Q_{NSi}}{Q_{EQ}} \quad (5-3)$$

where:

- R_C = nominal ultimate displacement or force capacity of the structural component being evaluated,
- ΣQ_{NSi} = sum of the displacement or force demands on a component from nonseismic loads, which are included in the group loading defined by equations 6-1, 6-2, 7-1 and 7-2 of the *AASHTO Standard Specifications* (AASHTO, 2002), or table 3.4.1-1 of the *AASHTO LRFD Specifications* (AASHTO, 1998), and
- Q_{EQ} = displacement or force demand for the earthquake loading under consideration.

C/D ratios should be calculated at the nominal ultimate capacity without the use of capacity reduction factors, ϕ , to account for possible understrength and/or undersize members. This is done because the objective of a C/D ratio is to determine the most likely level of failure.

Since C/D ratios reflect only component failures and not necessarily the state of the bridge as a whole, the global effect of one or more component failures must be assessed in a qualitative way using engineering judgment.

A methodology for calculating component C/D ratios is given in appendix D.

5.4.2. SELECTION OF ELASTIC ANALYSIS METHOD

The uniform load method may be used for structures satisfying geometric ‘regularity’ requirements of table 5-3. For structures not satisfying these requirements, the multi-mode method of dynamic analysis should be used, or alternatively an elastic time history method.

Table 5-3. Restrictions on the application of the uniform load method.

Parameter	Value				
	2	3	4	5	6
Number of spans	2	3	4	5	6
Maximum subtended angle for a curved bridge	20°	20°	30°	30°	30°
Maximum span length ratio from span to span	3	2	2	1.5	1.5
Maximum pier stiffness ratio from span-to-span, excluding abutments	—	4	4	3	2

5.4.2.1. Uniform Load Method

The uniform load method is described in Article 4.3 of the *Standard Specifications* (AASHTO, 2002) and Article 4.7.4.3.2c of the *LRFD Specifications* (AASHTO, 1998). It is based on the fundamental mode of vibration in the longitudinal or transverse direction, assuming an equivalent single mass-spring oscillator. The stiffness of this equivalent spring is calculated using the maximum displacement that occurs when an arbitrary uniform lateral load is applied to the bridge. The spectral acceleration, at the modal period T , is found from figure 1-8 and used to calculate the equivalent, uniform load from which design forces are determined.

This method may be used for both transverse and longitudinal earthquake motions. It is essentially an equivalent static method of analysis that uses a uniform lateral load to approximate the effect of seismic loads. The method is suitable for regular bridges that respond principally in their fundamental mode of vibration.

While all displacements and most member forces are calculated with satisfactory accuracy, the method is known to overestimate the transverse shears at the abutments by up to 100 percent. If such conservatism is undesirable, but a single mode representation is appropriate, then the single mode spectral analysis method (Article 4.4 of the *Standard Specifications* (AASHTO, 2002) and Article 4.7.4.3.2b of the *LRFD Specifications* (AASHTO, 1998)) is recommended. This method is a subset of the multi-mode spectral analysis method described in the next section.

The steps in the uniform load method are as follows:

Step 1. Calculate the static displacements $v_s(x)$ due to an assumed uniform load, p_o . The uniform loading p_o is applied over the length of the bridge; it has the dimensions of force/unit length, and may be arbitrarily set equal to 1.0. The static displacement $v_s(x)$ has the dimension of length.

Step 2. Calculate the lateral stiffness of the bridge, K , and total weight, W , from the following expressions:

$$K = \frac{p_o L}{V_{s, MAX}} \quad (5-4)$$

$$W = \int_0^L w(x) dx \quad (5-5)$$

where L is the total length of the bridge, $V_{s, MAX}$ is the maximum value of $v_s(x)$, and $w(x)$ is the unfactored dead load of the bridge superstructure and tributary substructure.

The weight should take into account structural elements and other relevant components including, but not limited to, pier caps, abutments, columns, and footings. Other loads, such as live loads, may also be included.

Step 3. Calculate the period of the bridge, T_m , using the expression:

$$T_m = 2\pi \sqrt{\frac{W}{gK}} \quad (5-6)$$

where g is the acceleration due to gravity.

Step 4. Calculate the equivalent static earthquake loading, p_e , from the expression:

$$p_e = \frac{C_s W}{L} \quad (5-7)$$

where $C_s = S_a/g$; g is the acceleration due to gravity; S_a is defined in figure 1-8 and equations 2-5, 2-6 and 2-8; and p_e is the equivalent uniform static seismic loading per unit length of bridge applied to represent the primary mode of vibration.

Step 5. Calculate the displacements and member forces for use in evaluation either by applying p_e to the structure and performing a second static analysis, or by scaling the results of Step 1 by the ratio p_e/p_o .

5.4.2.2. Multi-Mode Spectral Analysis Method

The elastic multi-mode spectral analysis method should be used for bridges in which coupling occurs in more than one of the three coordinate directions within each mode of vibration. As a minimum, linear dynamic analysis, using a three-dimensional model to represent the bridge, should be used. This method is described in Article 4.5 of the *Standard Specifications* (AASHTO, 2002) and Article 4.7.4.3.3 of the *LRFD Specifications* (AASHTO, 1998).

Ideally, all of the modes of vibration of a bridge will be included in a modal analysis but this may lead to excessive, and often unnecessary, computational effort. Instead, a reduced number is frequently used to reduce the effort while still maintaining accuracy. This number is usually determined by the relative size of the modal participation factors, which most dynamic analysis programs compute as contributions to the total base shear and express them as percentages of total bridge mass. For regular bridges, the total number of modes should be such as to include at least 90 percent of the modal mass. For irregular bridges, or large multi-segment bridges, it may be necessary to raise this figure to 95 percent, to ensure accurate results in all of the critical members and components.

The elastic response spectrum shown in figure 1-8 should be used for each mode, and should be scaled for damping ratios other than five percent. To scale the five percent spectrum for a damping ratio of ξ percent, multiply the spectral ordinates by $(0.2\xi)^{0.3}$ for periods greater than T_s , and by $(0.2\xi)^{0.5}$ for periods less than or equal to T_s , where T_s is defined as $\frac{S_{DI}}{S_{DS}}$ in figure

1-8. ξ should not be taken as greater than 30 percent. If a bridge is to be retrofitted using seismic isolation, scaling of the spectrum should only be done for periods greater than 80 percent of the effective isolated period.

Member forces and displacements may be estimated by combining the respective response quantities (moment, force, displacement, or relative displacement) from the individual modes by the Complete Quadratic Combination (CQC) method². Forces and displacements obtained using the CQC combination method are adequate for most bridge systems, especially if there is only one component to be considered in the ground motion. If the CQC method is not used, the square-root-of-the-sum-of-the-squares method (SRSS) may be used when the modal periods are well-separated. For modes that have closely spaced periods, the absolute sum of the modal responses may be used as an alternative.

Member forces and displacements due to two or three simultaneous components of ground motion should be estimated by the SRSS method. This method assumes these components are independent of each other (i.e., they are uncorrelated), which is an adequate assumption when evaluating a bridge because the spectrum in figure 1-8 is intended to represent the principal directions of ground motion. This assumption may not be valid for near-fault ground motions, which can exhibit strong correlation between the horizontal components.

² Newmark and Rosenblueth (1979); Der Kiureghian (1981)

5.4.2.3. Elastic Time History Method

Elastic time history methods provide displacements and member actions as a function of time, assuming all members remain elastic and no displacement limit is exceeded. These methods are more rigorous than the uniform load and multi-mode spectral methods described above, and may be used for irregular bridges with complex geometries and/or on poor foundations. They do, however, require the development of at least three sets of acceleration time histories for the bridge site and a minimum of three analyses is therefore performed, one for each set. Each set includes three components of the ground motion (two horizontal and one vertical). The maximum response for any single quantity (such as the transverse bending moment at the top of a particular column) from these three analyses, should be used for design. If more than seven sets of ground motions are used, the mean of the responses may be taken for evaluating the demand on the bridge.

In the absence of site-specific ground motions, time histories may be synthetically generated using the response spectrum for the site (figure 1-8). Procedures for developing these so-called spectrum-compatible time histories are discussed in section 2.8.

5.4.3. PROCEDURE FOR METHOD C

- Step 1. Decide whether the restrictions on the use of this method given in section 5.4.4 are satisfied. If so, an elastic force-based response spectrum analysis may be used. Based on the restrictions described below, determine the type of modal analysis to be undertaken.
- Step 2. Determine the capacity, Q_{ci} , for each of the relevant members in the structure.
- Step 3. Determine the sum of the non-seismic force and displacement demands, ΣQ_{NSi} , for each of the members in the structure, for each load combination in equations 6-1, 6-2, 7-1 and 7-2 of the *Standard Specifications* (AASHTO, 2002), or table 3.4.1-1 of the *LRFD Specifications* (AASHTO, 1998).
- Step 4. Determine the response spectrum parameters F_a , S_s , F_v and S_1 (section 2.5). Perform an elastic dynamic analysis (section 5.4.2) to determine the seismic demand, Q_{EQi} , on each of the members. The analysis should reflect the anticipated condition of the structure and the foundation during this earthquake.
- Step 5. For each member or component (i), determine the capacity/demand ratio from:

$$r_i = \frac{Q_{ci} - \Sigma Q_{NSi}}{Q_{EQi}} \quad (5-8)$$

If $r_i \geq 1.0$, the corresponding member has adequate capacity for the level of demand. Otherwise, devise retrofit measures that increase the displacement, strength, or ductility capacity, of the specific member or component.

Alternatively, reanalyze the bridge using a more rigorous approach where system behavior is accounted for explicitly and the beneficial effect of force redistribution due to inelastic action is included in the results. See Methods D1, D2 and E.

5.4.4. RESTRICTIONS ON USE OF METHOD C

This method is the same as the capacity/demand method described in the previous FHWA bridge retrofit manual (FHWA, 1995). As before, its use should be restricted to bridges that will behave in a ‘mostly elastic’ fashion, to ensure that the results are not overly conservative. This means that the method is mainly applicable to bridges in regions of low-to-moderate seismicity. It is also applicable to major structures in highly seismic zones, where a high level of operational performance is required which can only be satisfied by an ‘almost elastic’ design strategy. In such cases, the method of elastic analysis used for computing the C/D ratios should be the time history method described in section 5.4.2.3.

5.4.5. EXAMPLES

Two examples of the use of Method C are given in appendices E and F.

The first example is a four-span reinforced concrete, box-girder bridge similar to those used in California at the time of the San Fernando earthquake (1971). It has seat width deficiencies, and inadequate reinforcement details in the columns. This example is given in appendix E.

The second example is a multispan steel beam bridge with simple supports, constructed in Pennsylvania in 1968. It has vulnerable steel rocker bearings and concrete columns with potentially inadequate reinforcement details. This example is given in appendix F.

5.5. METHOD D1: CAPACITY SPECTRUM METHOD

5.5.1. APPROACH

This method of evaluation explicitly includes the inelastic behavior of members and other limit states due to bearing failure and unseated beams. It is a powerful technique that can be used to make a quick estimate of either the capacity of an existing bridge or the performance of a bridge during a given earthquake. The method may be used for either the design of a new bridge or the retrofit of an existing structure.

The method is restricted to bridges that vibrate as single-degree-of-freedom (SDOF) systems, i.e., to bridges with regular geometry and uniform distribution of weight and stiffness. It is also limited to bridges where the displacements at the tops of all the piers are the same, or nearly so, in both the longitudinal and transverse directions. This does not include piers with expansion bearings.

These limitations are described further in section 5.5.5.

A bridge that cannot be modeled as an SDOF structure or does not satisfy the equal displacement requirement, should be evaluated using a multi-modal method and a more advanced capacity assessment technique such as that described in Method D2.

5.5.2. BRIDGE CAPACITY

5.5.2.1. General

The capacity of a bridge to resist lateral loads may be expressed by a so-called pushover curve. Such curves show the total lateral load acting on the bridge plotted against the deflection of the center of mass of the bridge. This point is chosen because the center of mass is where the earthquake's inertial loads are assumed to act (in SDOF structures). In most highway bridges, the center of mass will be located within the superstructure. This curve is also a measure of the capacity of the bridge for lateral loads of increasing size and may be used to express force and displacement capacity for a number of potential limit states.

Figure 5-1(a) shows an idealized pushover curve for a flexurally ductile structure. It identifies several limit states that are important in characterizing the behavior of the bridge under increasing load or deformation. These are:

1. Pseudo-yield point, marking the end of essentially elastic behavior.
2. Point of maximum plastic deformation before softening (degradation) begins.
3. Onset of collapse (e.g., due to column rebar rupture in low cycle fatigue or $P-\Delta$ effects).
4. Collapse (e.g., due to the failure of a plastic hinge).

These limit states are characteristic of bridges with continuous superstructures on ductile columns that are capable of large inelastic deformation in well-detailed plastic hinges.

Bridges with simple spans may exhibit a different set of limit states and these are illustrated in figure 5-1(b). They are:

1. Pseudo-yield point, marking the end of essentially elastic behavior.
2. Expansion joint closure, followed by span lock-up, and limited plastic deformation.
3. Bearing failure (e.g., due to weld failures in keeper bars).
4. Collapse (e.g., due to the unseating of beams).

These limit states essentially describe brittle behavior and are likely to be found in older bridges with simple spans despite adequate column reinforcement details, particularly in regions of low-to-moderate seismicity.

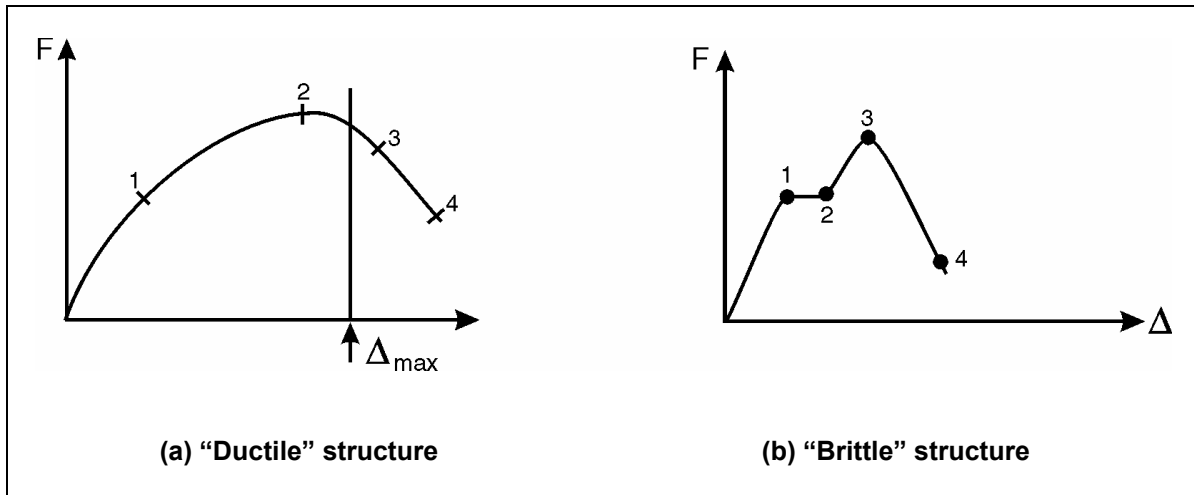


Figure 5-1. Capacity curve.

5.5.2.2. Calculation of Bridge Capacity Curve

In this method, the capacity curves shown in figure 5-1 are approximated by bilinear curves as in figure 5-2. Using the notation in these figures, a seismic capacity coefficient C_c is calculated at displacement Δ , as follows:

$$C_c = \frac{F}{W} \quad (5-9)$$

where:

- F = total horizontal force acting on the bridge
 = $F_y + k_2 (\Delta - \Delta_y)$ for $\Delta > \Delta_y$, and
 = $k_1 \Delta$ for $\Delta \leq \Delta_y$.
- W = weight of seismic mass, usually taken as the weight of the superstructure,
- F_y = yield force (see note 1 below),
- Δ_y = yield displacement corresponding to F_y and equals F_y / k_1 ,
- k_1 = elastic stiffness in direction considered, transverse or longitudinal (see note 2 below), and
- k_2 = equivalent post-yield stiffness in direction considered, transverse or longitudinal (see note 3 below).

The maximum displacement Δ_{max} , shown in figure 5-1, is set to the lesser of the following three displacement limit states, as appropriate:

1. Plastic hinge rotation: $\Delta_{max} \leq \theta_p H$

where $\theta_p = 0.035$ for reinforced concrete columns, and H is the clear height of the column.

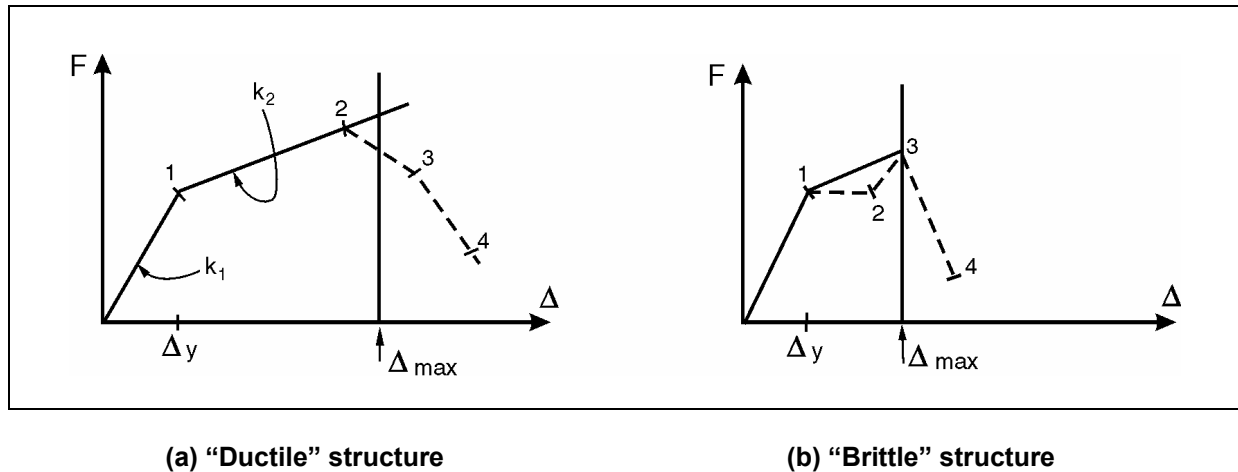


Figure 5-2. Idealized capacity.

2. P-delta ($P-\Delta$): $\Delta_{\max} \leq 0.25 C_c W' (H/P)$
 where W' is the seismic weight per column, and P is the axial load on the column due to gravity loads. See explanation in note 4 below and also a refinement for Δ_{\max} for short period bridges.
3. Seat length: $\Delta_{\max} \leq N_0$
 where N_0 is the existing seat width at an abutment or pier cap. See note 5 below.

Note 1. F_y is calculated from the sum of the individual column lateral strengths (V_{ui}) in the direction under consideration,

i.e.,

$$F_y = \sum V_{ui} = \sum \left(\frac{M_n}{H} \right)_i \quad (5-10)$$

where M_n is the column's nominal³ yield moment calculated from a moment interaction curve for column i , using column axial loads, dimensions and reinforcement details, and H is the clear height of column i .

This summation is made over all of the columns supporting the superstructure; abutments are excluded. Columns with expansion bearings in the direction being analyzed are also excluded from this calculation. Since the axial loads are not known at this stage, these loads may be taken equal to the gravity load values when calculating M_n .

Note 2. k_1 is the elastic stiffness of the bridge in a lateral direction and will generally be different in different directions (e.g., longitudinal and transverse) unless symmetrical, single-column piers are used. Cracked sections should be assumed for reinforced concrete columns and a moment of inertia equal to 50 percent of the uncracked moment of inertia is recommended. The uniform load method may be used to calculate this stiffness (equation 5-4, section 5.4.2.1).

³ See definition of nominal strength in section 7.5

Note 3. k_2 is the linearized post-yield stiffness used to approximate actual behavior in this part of the capacity curve. In the absence of rigorous analysis, k_2 may be taken equal to five percent of the elastic stiffness, i.e., $k_2 = 0.05 k_1$. If elastic-perfectly plastic behavior is assumed to occur in the column hinge, $k_2 = 0$. This assumption underestimates the capacity of the column once yielding begins and could be on the conservative side. But it will also underestimate the forces that the column can transmit to adjacent components (e.g., bearings above and footings below) which may lead to their unexpected failure. Setting $k_2 = 0$ is therefore not recommended. See the discussion of capacity-protected design in chapter 1.

Note 4. Bridges supported on slender piers that carry high axial loads are susceptible to instability due to so-called P- Δ effects. Inadequate strength can cause progressive ratcheting of a bridge sideways, eventually leading to collapse. Pier equilibrium equations show that P- Δ effects reduce the lateral stiffness of columns and may even cause this stiffness to become negative once yield occurs. Under these conditions, the post-yield stiffness is given by

$$\begin{aligned} k_2' &= k_2 - \frac{P}{H} \\ &= \frac{-P}{H} \quad \text{if } k_2 = 0 \end{aligned} \tag{5-11}$$

where k_2' is the post yield stiffness including P- Δ effects, k_2 is the post-yield stiffness excluding P- Δ effects (see Note 3 above), P is the axial load due to non-seismic sources, and H is the clear height of pier from point of fixity of piles, if any.

This decrease in stiffness leads to a reduction in strength with increasing displacement. The above displacement limit state is therefore chosen to limit this reduction to 25 percent of the capacity at zero displacement (V_U),
i.e.,

$$\Delta_{\max} \frac{P}{H} \leq 0.25V_U \tag{5-12}$$

Since the lateral strength (V_U) can be expressed as the product of the seismic coefficient (C_c) and the effective seismic weight on the pier (W'), the above equation can be rearranged to give:

$$\Delta_{\max} \leq 0.25C_c \left(\frac{W'}{P} \right) H \tag{5-13}$$

Note that the ratio W'/P should not be taken as greater than 2.0 for two-span bridges, or greater than 1.0 for other bridges. Note also that for bridges with periods less than $1.25 T_S$ (T_S is defined in figure 1-8), Δ_{\max} is reduced by the factor R_d to account for the possible underestimation of displacements by the equal-displacement theory of nonlinear response. For such bridges, the displacement limit state (Δ'_{\max}) is given by:

$$\Delta'_{\max} = \frac{\Delta_{\max}}{R_d} \quad (5-14)$$

where:

$$R_d = \left(1 - \frac{1}{R}\right) \frac{T^*}{T} + \frac{1}{R} \text{ for } R \geq 1 \text{ and } T < T^*,$$

$$R_d = 1.0 \text{ for } R \geq 1 \text{ and } T \geq T^*,$$

$$R_d = 1.0 \text{ for } R < 1 \text{ and any value of } T,$$

$$T^* = 1.25 T_s,$$

$$T_s = F_v S_1 / F_a S_s, \text{ as defined in figure 1-8,}$$

$$T = \text{period of vibration of bridge, and}$$

$$R = \text{ratio of elastic force on pier (F}_{el}\text{) to the lateral capacity of pier (V}_U\text{)}$$

$$= F_{el} / V_U.$$

Note 5. Ideally, the existing seat width (N_0) will be the greater of:

- $1.5 \Delta'_{\max}$ where Δ'_{\max} is the displacement of the superstructure at the seat, given by equation (5-14), or
- The minimum seat width given by equations 5-1a or 5-1b.

In retrofitting some bridges, satisfying this requirement may be very costly.

5.5.3. EARTHQUAKE DEMAND

The earthquake demand on a bridge may be represented by a response spectrum. Both acceleration and displacement spectra are used, but by far the most common is the acceleration spectrum. These spectra, when scaled by seismic mass, give the seismic forces acting through the center of mass of the bridge. Figure 1-8 shows the recommended acceleration spectrum for both seismic design and retrofit of highway bridges in the United States. This spectrum assumes five percent viscous damping in the bridge and should be modified for other damping values, as shown in figure 5-3. A value of five percent is appropriate for essentially elastic behavior but once yielding occurs, and other forms of damage begin to occur, the damping level increases. Two damping factors are introduced for this purpose, B_S and B_L , for use in the short and long period ranges of the spectrum respectively, as shown in figure 5-3. A procedure for calculating B_S and B_L is given in table 5-4, which shows that both factors depend on the displacement ductility factor μ , defined as follows:

$$\mu = \frac{\Delta}{\Delta_y} \quad (5-15)$$

where Δ is the displacement at which ductility is being calculated, and Δ_y is the yield displacement.

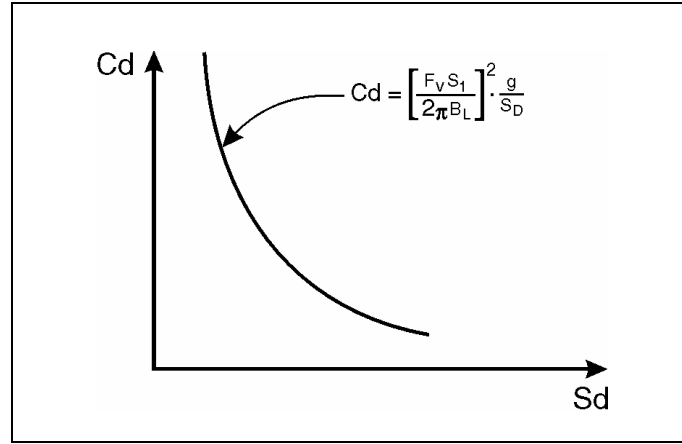


Figure 5-3. Demand spectrum.

A seismic demand coefficient, C_d , is defined as follows:

$$C_d = \frac{S_a}{g} \quad (5-16)$$

where:

$$S_a = \begin{aligned} &\text{spectral acceleration defined in figure 1-8,} \\ &= g [F_v S_1 / B_L T] \text{ for long period bridges, } T \geq T_s, \text{ and} \end{aligned} \quad (5-17a)$$

$$= g [F_a S_s / B_s] \text{ for short period bridges, } T < T_s. \quad (5-17b)$$

This is the traditional form of a demand spectrum (S_a vs period, T), but it is also convenient to express C_d in terms of S_d (spectral displacement) rather than period. To do so, S_d is first written as follows:

$$\begin{aligned} S_d &= \text{spectral displacement} \\ &= S_a / \omega^2 \\ &= S_a [T^2 / 4\pi^2] \\ &= [F_v S_1 / B_L] T g / 4\pi^2 \text{ (using equation 5-17a)} \end{aligned} \quad (5-18)$$

where ω is the angular frequency (rad/sec) and equals $2\pi/T$.

Combining equations 5-16, 5-17a and 5-18, to eliminate the period T , gives C_d for long period bridges as:

$$C_d = \left[\frac{g}{S_d} \right] \left[\frac{F_v S_1}{2\pi B_L} \right]^2 \text{ for } T \geq T_s \quad (5-19a)$$

Figure 5-3 shows C_d plotted against S_d for a particular value of damping factor B_L . This spectrum is seen to have a shape similar to that of the traditional, period-based spectrum and that C_d decreases as S_d increases.

Further, by combining equations 5-16 and 5-17b, C_d for short period bridges can be shown to be given by:

$$C_d = \frac{F_a S_s}{B_s} \quad \text{for } T < T_s \quad (5-19b)$$

Table 5-4. Effective viscous damping ratios and damping factors, B_s and B_L .

Substructure Type	Effective Viscous Damping Ratio, ξ_{eff}	Damping Factor, B_s	Damping Factor, B_L
Nonductile, conventionally-designed columns	$0.05 + 0.16(1-1/\mu)^1$	$[\xi_{\text{eff}}/0.05]^{0.5}$	$[\xi_{\text{eff}}/0.05]^{0.3}$
Ductile, sesimically-designed columns	$0.05 + 0.24(1-1/\mu)^1$		
Sliding bearings	0.20		
Note: 1. μ = displacement ductility factor			

5.5.4. CAPACITY/DEMAND SPECTRUM

It is possible to combine the capacity curve represented by equation 5-9 (and figure 5-2) and the demand spectrum represented by equation 5-19 (and figure 5-3) in a single plot. The result is known as a capacity/demand spectrum. There are many possible uses for such a plot, one of which provides capacity/demand ratios for a complete bridge subject to a given earthquake, and the other calculates bridge response (F , Δ) to a given earthquake. Both applications are described below. A step-by-step procedure is given in a subsequent section for the combination of both applications. This is Method D1.

5.5.4.1. Calculation of Bridge Capacity/Demand (C/D) Ratios

Figure 5-4 shows a capacity/demand spectrum in which three limit states are identified on the capacity curve. The displacements corresponding to these limit states are known and for the purpose of illustration, might be as follows:

- $\Delta_{LS1} = \Delta_y$ (yield displacement).
- $\Delta_{LS2} = \Delta_{\theta_p}$ (displacement corresponding to a given plastic hinge rotation $= \theta_p$, $H = 0.02H$ for $\theta_p = 0.02$; values of θ_p are given in sections 7.8.1 and 7.8.2 for a range of different column limit states).
- $\Delta_{LS3} = N_0$ (available seat width at abutment or pier cap).

Corresponding to each of these limit states there is capacity coefficient C_{CLS} .

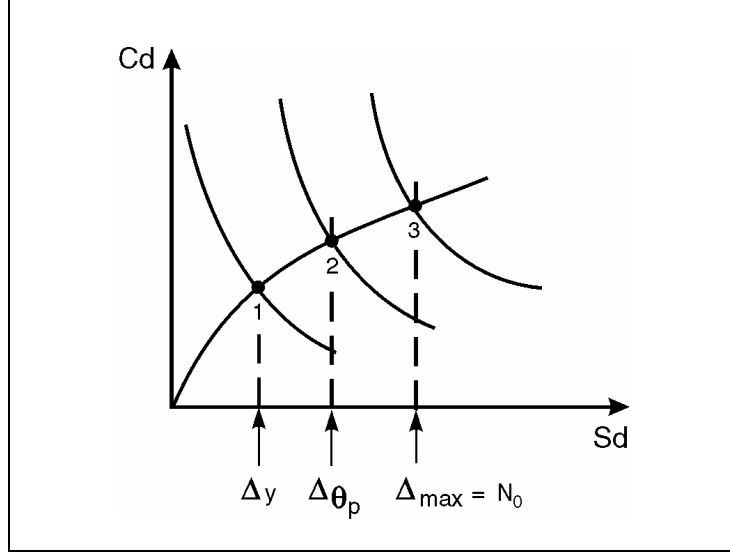


Figure 5-4. Capacity/demand spectra.

Also shown in the figure is a demand curve passing through each of the limit states. Equating C_d to C_{cLS} (and S_d to Δ_{LS}) at each limit state, and using equation 5-19a results in:

$$C_d = C_{cLS} \quad (5-20a)$$

$$\left[\frac{g}{\Delta_{LS}} \right] \left[\frac{F_v S_1}{2\pi B_L} \right]^2 = C_{cLS} \quad (5-20b)$$

from which

$$(F_v S_1)_{LS} = 2\pi B_L \sqrt{C_{cLS} \frac{\Delta_{LS}}{g}} \quad (5-21a)$$

The above result is applicable to bridges with long periods ($T \geq T_S$). By a similar process, it is possible to show that for short period bridges ($T < T_S$),

$$(F_a S_S)_{LS} = B_S C_{cLS} \quad (5-21b)$$

Note that B_L and B_S vary from one limit state to another since they are displacement dependent (table 5-4), but may be easily calculated because Δ_{LS} is known for each limit state.

The left hand side of equation 5-21a or 5-21b is a measure of the size of earthquake that would cause limit state LS to be reached. In other words, it is an indicator of the capacity of the bridge expressed in terms of the size of earthquake required to reach that capacity. This measure may be compared with the actual demand on the bridge using the same quantity, $(F_v S_1)$ or $(F_a S_S)$, expressed as a demand measure i.e., $(F_v S_1)_d$ or $(F_a S_S)_d$.

Accordingly, a capacity/demand ratio (r_{LSi}) may be defined for each limit state (i) as follows:

$$r_{LSi} = \frac{(F_v S_1)_{LSi}}{(F_v S_1)_d} \quad \text{for } T \geq T_s \quad (5-22a)$$

$$r_{LSi} = \frac{(F_a S_s)_{LSi}}{(F_a S_s)_d} \quad \text{for } T < T_s \quad (5-22b)$$

If $r_{LSi} \geq 1.5$, the limit state is not likely to be reached and no remedial action is required.

If $1.0 \leq r_{LSi} < 1.5$, the limit state may be reached and some remedial action may be required.

If $r_{LSi} < 1.0$, the limit state is likely to be reached and retrofit measures which increase deformability or ductility capacity of the bridge should be considered. These measures might include extending the seat widths at pier caps and/or abutments (to improve N_0), adding restrainers (to increase k_1 and F_y), and jacketing columns (to improve M_n and θ_p).

5.5.4.2. Calculation of Bridge Response

Capacity/demand spectra may be used to determine the response of a bridge with a known capacity spectrum (C_c vs Δ) during a given earthquake with a known demand spectrum (C_d vs S_d). The difficulty, however, is that the final displacement is unknown and both the capacity coefficient (C_c) and the damping factor (B_L) cannot be calculated in advance. Iteration is therefore used, starting with an initial estimate for displacement and iterating until the assumed value and the calculated value are in agreement. Basic steps in the method are listed below.

Step 1. Determine if the bridge has a long period of vibration by comparing the elastic period T with T_s (figure 1-8). If not, go to Step 8 (procedure for short period bridges).

Procedure for long period bridges:

Step 2. Start iteration by setting Δ equal to the displacement of the bridge assuming elastic behavior, and calculate ductility factor μ (equation 5-15).

Step 3. Calculate the damping factor B_L using table 5-4.

Step 4. Calculate the capacity coefficient C_c using equation 5-9.

Step 5. Set $C_d = C_c$ and solve for S_d in equation 5-19a.

$$\text{i.e.,} \quad S_d = \left[\frac{g}{C_c} \right] \left[\frac{F_v S_1}{2\pi B_L} \right]^2 \quad (5-23a)$$

Step 6. Compare S_d with value for Δ (see Step 2 or previous Step 6) and if in agreement, go to Step 7. Otherwise set $\Delta = S_d$, recalculate μ , and go to Step 3.

Step 7. Calculate forces in individual piers, bearings and foundations using Δ , and compare sum with total lateral force on bridge (base shear) F , using $F = C_c W$.

Procedure for short period bridges:

Step 8. Start iteration by setting Δ equal to the displacement of the bridge assuming elastic behavior, and calculate ductility factor μ (equation 5-15).

Step 9. Calculate the damping factor B_s using table 5-4.

Step 10. Calculate the capacity coefficient C_c using equation 5-9.

Step 11. Calculate effective stiffness from $K_{eff} = C_c W / \Delta$.

Step 12. From equation 5-19b, calculate $C_d = F_a S_s / B_s$.

Step 13. Calculate S_d from $S_d = C_d W / K_{eff}$ and by substituting results from Steps 11 and 12 obtain:

$$S_d = \left[\frac{\Delta}{C_c} \right] \left[\frac{F_a S_s}{B_s} \right] \quad (5-23b)$$

Step 14. Compare S_d with value for Δ (see Step 8 or value from previous Step 14) and if in agreement go to Step 15, otherwise set $\Delta = S_d$, recalculate μ , and go to Step 9.

Step 15. Calculate forces in individual piers, bearings and foundations using Δ , and compare sum with total lateral force on bridge (base shear) F , using $F = C_c W$.

5.5.5. PROCEDURE FOR METHOD D1

The two above applications (sections 5.5.4.1 and 5.5.4.2) may be combined into a single procedure as described in this section. Several checks are also introduced to assure that assumptions made above (both explicit and implicit) are satisfied. This is Method D1.

The procedure has three parts:

Part A : Initialization and calculation of bridge capacity.

Part B : Calculation of C/D ratios.

Part C : Calculation of bridge response (F, Δ).

Each part is described below.

PART A: Initialization and Calculation of Bridge Capacity

- Step A1. Obtain spectral ordinates (S_S and S_1) and site factors (F_a and F_v) for the earthquake under consideration from figure 2-2 and table 1-4. Calculate products $F_a S_S$ and $F_1 S_v$.
- Step A2. Calculate transition period T_S (figure 1-8) between short period and long period portions of the demand spectrum (see also equation 5-14).
- Step A3. Calculate weight of superstructure (W) and elastic stiffness (k_1) in both the longitudinal and transverse directions of the bridge. Estimate post-yield stiffness (k_2).
- Step A4. Calculate elastic period of structure (T) in each direction (longitudinal and transverse) using, for example, the uniform load method (section 5.4.2.1). Compare with T_S (Step A2) and determine whether bridge falls in the short or long period portion of the spectrum, in both directions.
- Step A5. If the bridge has a short period of vibration (Step A4), calculate elastic response from $F_{el} = F_a S_S W$ and $\Delta_{el} = F_{el}/k_1$. If the bridge has a long period (Step A4), calculate elastic response from $F_{el} = F_v S_1 W / T$ and $\Delta_{el} = F_{el}/k_1$.
- Step A6. Calculate F_y in each direction (longitudinal and transverse) from $F_y = \Sigma V_{ui}$ where V_{ui} is calculated from $(M_n/H)_i$ for column i , and M_n is nominal moment capacity of the column under axial gravity loads only. (See note 1, section 5.5.2.2.) This assumption (about axial column loads) may be refined using the procedure in section 7.6.2, once the overturning moments, due to earthquake loads acting through the superstructure, are known.
- Step A7. Calculate Δ_y from $\Delta_y = F_y/k_1$
- Step A8. Compare Δ_{el} (Step A5) with Δ_y . If $\Delta_{el} > \Delta_y$, the bridge will yield. Proceed to Step B1. If $\Delta_{el} \leq \Delta_y$ bridge remains elastic for earthquake described in Step A1. All C/D ratios are greater than 1.0, and bridge response (Part C) is the same as that calculated in Step A5. Set $\Delta = \Delta_{el}$, $F = F_{el}$ and go to Step C6.

PART B: Capacity/Demand Ratio Checks (r)

- Step B1. Determine the number of limit states to be considered and estimate or calculate the corresponding displacement(s) Δ_{LS} , for each state.
- Step B2. Calculate the capacity coefficient C_c , at each limit state
- Step B3. If bridge has a short period of vibration (Step A4), calculate the damping factor B_S , for each limit state using table 5-4. If bridge has a long period (Step A4), calculate the damping factor B_L , for each limit state using table 5-4.

Step B4. Calculate the size of the earthquake corresponding to each limit state, using equations 5-21a and 5-21b as follows:

$$(F_v S_1)_{LS} = 2\pi B_L \sqrt{\left[C_{eLS} \frac{\Delta_{LS}}{g} \right]} \quad \text{for } T \geq T_S \text{ (long period response)}$$

$$(F_a S_S)_{LS} = B_S C_{eLS} \quad \text{for } T < T_S \text{ (short period response)}$$

Step B5. Calculate the C/D ratio for each limit state using equations 5-22a and 5-22b as follows:

$$r_{LS} = \frac{(F_v S_1)_{LS}}{(F_v S_1)_d} \quad \text{for } T \geq T_S \text{ (long period response)}$$

$$r_{LS} = \frac{(F_a S_S)_{LS}}{(F_a S_S)_d} \quad \text{for } T < T_S \text{ (short period response)}$$

Step B6. Examine the C/D ratios and for those values equal to, or close to, unity; analytically explore potential retrofit measures that might lift these ratios above unity.

For example, if $r_{LS} \geq 1.5$, the limit state is not likely to be reached,
 if $1.0 \leq r_{LS} < 1.5$, the limit state may be reached, and some remedial action may be required, and
 if $r_{LS} < 1.0$, the limit state is likely to be reached and retrofit measures which increase the deformability or ductility capacity of the bridge should be considered. These measures might include extending the seat widths at pier caps and / or abutments (to improve N_0), adding restrainers (to increase k_1 and F_y), and jacketing columns (to improve M_n and θ_p).

PART C: Bridge Response (F, Δ)

Step C1. Start iteration by setting Δ equal to the displacement of the bridge assuming elastic behavior (Δ_{el} from Step A5) and calculate ductility factor μ (equation 5-15).

Step C2. Calculate the appropriate damping factor using table 5-4:

- B_L for $T \geq T_S$ (long period bridges), and
- B_S for $T < T_S$ (short period bridges).

Step C3. Calculate the capacity coefficient C_c using equation 5-9.

Step C4. Calculate S_d using equations 5-23a and 5-23b:

- $S_d = [g/C_c] [F_v S_1 / 2\pi B_L]^2$ for $T \geq T_S$ (long period bridges), and
- $S_d = [\Delta/C_c] [F_a S_S / B_S]$ for $T < T_S$ (short period bridges).

Step C5. Compare S_d with the assumed Δ (Step C1 or previous Step C5) and if in agreement, go to Step C6, otherwise set $\Delta = S_d$, recalculate μ , and go to Step C2.

Step C6. Calculate forces in individual piers, bearings and foundations using Δ , and compare sum with total lateral force on bridge (base shear) F , using $F = C_c W$.

5.5.6. RESTRICTIONS ON USE OF METHOD D1

The capacity spectrum method is restricted to bridges that:

1. Behave as single-degree-of-freedom structures, in both the transverse and longitudinal directions, and
2. Have equal displacements (or nearly equal) at the tops of all the piers in both the transverse and longitudinal directions, excluding piers with expansion bearings.

The first of these restrictions requires eligible bridges to have regular geometry and uniform distribution of weight and stiffness, and to conform to the requirements of table 5-3.

The second of these restrictions means that the method is limited to bridges with superstructures that either:

- Behave as nearly-rigid, in-plane diaphragms supported on seat-type abutments with bearings that are either elastomeric or have restraints (keeper bars) that can be assumed to fail, or
- Be of uniform geometry and weight, have sufficient length that the abutments have little influence on transverse response, and be supported on substructures of uniform stiffness.

In general, bridges which satisfy the following criteria will meet the equal-displacement requirement:

- Span length should not exceed 60 m (200 ft).
- The ratio of the longest to shortest span lengths in frame should not exceed 1.5.
- The maximum skew angle should not exceed 30° , and the skew of adjacent piers or bents should not differ by more than 5° .
- For horizontally curved bridges, the subtended angle of the frame should not exceed 20° .
- The ratio of maximum to minimum pier stiffness should not exceed 2.0, including the effect of foundation stiffness.
- The ratio of maximum to minimum pier lateral strength should not exceed 1.5.

These requirements are more stringent than the first set and take precedence for the application of Method D1. It is possible to check the equal-displacement requirement by an elastic analysis using, for example, the uniform load method (section 5.4.2.1).

5.6. METHOD D2: STRUCTURE CAPACITY/DEMAND (PUSHOVER) METHOD

5.6.1. APPROACH

This more advanced procedure for calculating structure capacity/demand ratios is also known as the nonlinear static procedure (NSP) or pushover method. As for Method D1, the NSP is a two-step approach. First, it requires a displacement capacity evaluation using a pushover analysis. Such an analysis considers each relevant limit state and level of functionality, including P- Δ effects. Second, it requires a response spectrum analysis to assess the displacement demands on the bridge.

5.6.2. DISPLACEMENT CAPACITY EVALUATION

The objective of a displacement capacity evaluation is to determine the displacement at which the earthquake resisting members of a bridge reach their inelastic deformation capacity. Damage states are defined by local deformation limits, such as plastic hinge rotation, footing settlement or uplift, and abutment displacement. Displacements may be limited by a loss of capacity such as the degradation of strength under large inelastic deformations, or P- Δ effects.

This evaluation should be applied to individual piers to determine their lateral load-displacement behavior. It should be performed independently in both the longitudinal and transverse directions, and should identify those components of a pier which are first to reach their inelastic capacities. The displacement at which the first component reaches its capacity defines the displacement capacity for the pier. The model used for this analysis should include all of the components providing resistance, and use realistic force-deformation relationships for these components, including abutments and foundations.

For piers with simple geometries (e.g., a single-column pier), the maximum displacement capacity can usually be found by hand calculation, using an assumed plastic hinge mechanism and a maximum allowable deformation capacity for the plastic hinges and foundations. If the interaction between axial force and moment is significant, iteration will be necessary to determine the capacity of the collapse mechanism.

For more complicated piers or foundations, displacement capacity can be evaluated by a nonlinear static analysis, commonly referred to as a pushover analysis.

As noted above, evaluation of the displacement capacity is conducted on individual piers. Although forces may be redistributed from pier-to-pier as the displacement increases and yielding begins to occur (particularly so for bridges with piers of different stiffness and strength), the objective of this evaluation is to determine the maximum displacement capacity of each pier. This capacity is then compared with the results from an elastic demand analysis, which does

consider the behavior of the bridge as a whole, and includes the effect of piers with different stiffnesses.

The structural model used for the evaluation should be based on the expected capacities of the inelastic components. The model for footings and abutments should include the nonlinear force–deformation behavior, including uplift, gap opening and closing. Stiffness and strength degradation of inelastic components, and the effects of loads acting through the lateral displacement (P- Δ), should be considered.

The maximum displacement of a pier is achieved when a component reaches maximum deformation. Maximum plastic hinge rotations for structural components are given in section 7.8.2. The maximum deformation for foundations and abutments are limited by geometric constraints on the structure.

Although this evaluation is based on monotonically increasing displacement, the effects of cyclic loading must be considered when selecting an appropriate model and establishing a maximum inelastic deformation. This includes strength and stiffness degradation and low-cycle fatigue.

5.6.3. DEMANDS

The uniform load method may be used for structures satisfying the ‘regularity’ requirements of table 5-3. For structures not satisfying these requirements, the multi-mode spectral analysis method of dynamic analysis should be used, or alternatively an elastic time history method. These methods are described in section 5.4.2.

5.6.4. PROCEDURE FOR METHOD D2

Step 1. Determine the strength and deformation capacity for each pier of the bridge.

Step 2. For each pier, carry out a nonlinear static pushover analysis until the structural displacement reaches the collapse limit state (limit state 5). Note the structural displacements, Δ_{ci} , at each of the limit states (i), namely at:

1. First yield,
2. Slight damage with cracking,
3. Moderate damage that is repairable,
4. Irreparable damage at the limit of life safety, and
5. Structural collapse.

Step 3. Determine the sum of the nonseismic displacement demands $\Sigma\Delta_{NSdi}$ for each of the load combinations given in equations 6-1, 6-2, 7-1 and 7-2 of the *Standard Specifications* (AASHTO, 2002), or table 3.4.1-1 of the *LRFD Specifications* (AASHTO, 1998).

Step 4. Determine the response spectrum parameters, S_s and S_1 and site factors, F_a and F_v (figure 1-8 and table 1-4). Perform an elastic dynamic analysis to determine the seismic displacement demands, Δ_{EQdi} , on each pier of the bridge. The analysis should reflect the anticipated condition of the structure and the foundation during this earthquake.

Step 5. Determine the capacity/demand ratio (r_{LSi}) for each limit state (i) from the following:

$$r_{LSi} = \frac{(\Delta_{ci} - \sum \Delta_{NSdi})}{\Delta_{EQdi}} \quad (5-24)$$

If $r_{LSi} \geq 1.5$, the limit state is not likely to be reached and no remedial action is required.

If $1.0 \leq r_{LSi} < 1.5$, the limit state may be reached and some remedial action may be required.

If $r_{LSi} < 1.0$, the limit state is likely to be reached and retrofit measures which increase deformability or ductility capacity of the bridge should be considered. These measures might include extending the seat widths at pier caps and/or abutments, adding restrainers, jacketing columns, and strengthening joints and foundations as needed.

5.6.5. RESTRICTIONS ON METHOD D2

This method is a general approach and has few restrictions. However, the capacity analysis is limited to a pier-by-pier evaluation which does not necessarily capture the capacity of the bridge as a whole. On the other hand, comparison of results with those from nonlinear time history analyses, shows this limitation is not significant for regular highway bridges. However, it would be wise to check the performance of a complex bridge with the potential for substantial inelastic behavior, or of a bridge of major importance, using a time history method and explicit modeling of bridge capacity, such as that described in the next section.

5.7. METHOD E: NONLINEAR DYNAMIC PROCEDURE

5.7.1. APPROACH

The nonlinear dynamic procedure (NDP) is also a two-step method. First, it requires an assessment of the seismicity at the site along with the development of a suite of earthquake ground motions (acceleration time histories) that represent this level of seismicity. The strength and displacement capacity of all members expected to function in a nonlinear fashion needs to be determined along with appropriate hysteretic rules to describe member behavior. Then, a nonlinear dynamic time history analysis is conducted for each ground motion. The hysteretic performance is evaluated and the expected limit state of the bridge assessed.

Nonlinear dynamic analysis provides displacements and member actions (forces and deformations) as a function of time for a specified earthquake ground motion. A minimum of

three ground motions representing the earthquake being considered, should be used in the analysis. Each ground motion should include two horizontal components and one vertical. The maximum response for the three ground motions should be used for evaluating performance. If more than seven ground motions are used, the mean of the responses may be used.

5.7.2. PROCEDURE FOR METHOD E

- Step 1 Determine the strength and deformation capacity for each member in the structure.
- Step 2 Determine the response spectrum parameters, S_s and S_1 , and site factors, F_a and F_v (figure 1-8 and table 1-4). Develop at least three earthquake acceleration time histories with spectra that are compatible with the design response spectrum. Site-specific ground motions may also be used, and these may be either derived from a site-specific spectrum, or developed directly from the seismicity and geotectonics of the site.
- Step 3 Conduct a nonlinear dynamic time history response analysis for each of the ground motions. Check the sensitivity of the results obtained to assumptions made in analysis, such as the size of the time step used in the analysis.
- Step 4 Compare the seismic demands with the member capacities and determine the degree of damage to the structure for both levels of earthquake. If the damage will be unacceptable, devise retrofit measures and reanalyze the bridge to assess the effectiveness of these improvements.

5.7.3. RESTRICTIONS ON METHOD E

This method is a general approach and has few restrictions. However, it requires considerable computational effort and a significant level of skill is needed in interpreting the results. The method is particularly useful for structures that have irregular geometry or large variations in mass and stiffness properties. Preliminary solutions from simpler methods should always be obtained before undertaking a nonlinear time history solution, to bound the results and check for meaningful results.

CHAPTER 6: GEOTECHNICAL MODELING AND CAPACITY ASSESSMENT

6.1. GENERAL

The behavior of a bridge during an earthquake is strongly dependent on the stiffness and strength of its foundation system, which includes the abutments and piers, footings, and piles. Dynamic response is determined by these two parameters, which in turn influence the earthquake demands on the bridge and the distribution of these loads to the structural and foundation components.

Because foundation retrofit work may be more costly than new construction, and often has to be conducted under difficult site conditions, there are significant advantages to be gained if the conservatism in normal foundation design can be minimized. To do this, a more detailed and higher level of analysis is usually required than for a new design. This may involve developing both a coupled linear stiffness-model for the foundation system to be used in elastic spectral analyses, and a nonlinear load-displacement relationship for time history solutions. Nonlinear solutions not only allow more rigorous models for stiffness to be used, but also permit the beneficial effect of hysteretic damping and soil yield to be studied.

Acceptable bridge performance is usually determined by satisfying certain displacement limit states (chapters 1 and 5). To verify that performance has been satisfied it may be necessary to use the displacement-based procedures described in chapter 5. If so, the nonlinear load-deformation characteristics of the foundation and the effects of mobilizing the ultimate capacity of the foundation system should be included in the calculations. Such consequences could include permanent foundation deformation. While transient foundation yielding will, in many cases, reduce structural displacement demands and reduce both the structural and foundation retrofit costs, permanent residual deformation needs to be very carefully assessed. To enable an integrated model of the complete bridge to be developed for system evaluation, as described in chapter 5, both linearized stiffness and foundation capacity models are needed. The nature and development of these foundation models are described in section 6.2.

In addition to the earthquake-induced inertial loads on the bridge, ground displacement demands may arise, due to liquefaction-induced lateral spreading or global instability of abutment slopes. Such demands have led to bridge failures and significant structural damage in past earthquakes. The problem entails both the estimation of the likely ground deformation, and the resulting soil-foundation interaction to assess the displacement demands on the bridge. Procedures for calculating such demands are discussed in section 6.3.

6.2. FOUNDATION MODELING

6.2.1. SOIL-FOUNDATION-STRUCTURE INTERACTION

The rigorous analysis of the dynamic response of a soil-foundation-bridge system in a fully-coupled manner is complex and difficult (Pecker and Pender, 2000). If the soil is idealized as an

elastic continuum, then a substructuring approach may be used. In this case, the problem is separated into three steps:

- Step 1. Analyze the influence of the stiffness and geometry of a massless foundation system on the free-field ground motion, leading to modified structural input motions at the foundation level (i.e., kinematic interaction).
- Step 2. Analyze the frequency-dependent impedance characteristics of the foundation system under cyclic loading, in the form of a foundation stiffness matrix.
- Step 3. Analyze the inertial response of the structure to the foundation input motions (from step 1), using the pile cap stiffness matrix to account for foundation compliance (i.e., inertial interaction).

Except for cases involving deep, and relatively stiff, foundations in soft soils and for large rigid shallow foundations, the effect of kinematic interaction is normally neglected in practice, and the foundation-input motions are assumed to be the same as the free-field motions. As a result, the inertial interaction of a bridge with its foundation is the major focus of the material presented in this chapter.

6.2.1.1. Shallow Footings

Procedures for evaluating soil-footing-bridge interaction have evolved over time from the theory of continuum mechanics. Frequency-dependent stiffness and damping parameters for low amplitude, machine-foundation vibration problems have been adapted to earthquake soil-foundation-structure interaction (SFSI) problems¹. But for practical modeling purposes, as described in section 6.2.2.1, the frequency dependence of the stiffness parameters may be ignored, and static or slow cyclic values for stiffness may be used instead. This is a reasonable assumption considering the range of frequencies in earthquake ground motions. Similarly, frequency-dependent radiation-damping due to wave propagation away from a footing is not considered. For most footing sizes, radiation damping values are small and difficult to quantify in a nonlinear soil.

In addition to developing secant stiffness parameters, the mobilization of the moment capacity of the footing is of concern in many retrofit applications, and is addressed in section 6.2.2.1. For practical modeling purposes, soil capacity may be evaluated assuming pseudo-static inertial loading on a footing from the bridge above. This is a reasonable assumption, considering normal factors of safety under static loading, the stiff or dense soils associated with spread footings, and the difficulties in determining phase relations between soil and foundation motions in a coupled problem².

¹ Mylonakis et al. (2002); Pecker and Pender (2000)

² *ibid*

6.2.1.2. Piles

Two distinct approaches to soil-pile-structure interaction under dynamic loading have been developed. One approach evolved from slow cyclic (long period) lateral loading tests on piles conducted in the 1970's, which were motivated originally by the need to develop pile design criteria for offshore structures subjected to wave loading. These studies led to analytical methods based on the use of nonlinear Winkler springs to model soil-pile interaction under cyclic lateral and axial loading. The second approach evolved from other studies conducted in the 1970's, originally motivated by machine foundation vibration problems, where the problem was driven by the need to develop frequency dependent stiffness and damping (i.e., impedance functions), to determine resonant frequency and amplitude characteristics of supporting pile foundations. In this approach, the model used was that of a vibrating mass supported by pile foundations in an elastic continuum.

Elastic impedance functions for piles and pile groups have been studied by numerous researchers and a large number of closed form analytical solutions are available³. Early research on this subject was stimulated by the need to establish analysis methods for vibrating machine foundations, where the higher frequencies of loading lead to radiation damping and foundation stiffness is strongly frequency dependent. In addition, amplitudes of vibration are generally small, and the assumption of an elastic soil is reasonable.

However, soil-pile interaction under larger earthquake-induced inertial loading can lead to strongly nonlinear soil behavior, particularly in the vicinity of the pile interface, and the use of the elastic approach becomes impractical for routine structural design under seismic loading. Fortunately, given the relatively low frequency range of earthquake inertial loading and the nature of representative pile foundation systems for bridges and buildings, stiffness functions are essentially frequency independent and static loading stiffness values are a reasonable approximation. In addition, the radiation damping component of energy loss arising from wave propagation away from the foundation is considerably reduced at lower frequencies, particularly in the presence of nonlinear soil behavior. Whereas fully coupled nonlinear solutions to the seismic loading problem, using finite element methods, are theoretically possible and have been used to a limited extent, the analytical complexity is daunting and impractical for routine design.

Given the complexity of nonlinear coupled models, the Winkler model, as represented by a series of independent or uncoupled lateral and axial springs (linear or nonlinear) simulating soil-pile interaction in the lateral and axial directions, provides the most convenient means of analyzing the response of pile foundation systems to earthquake loading. The pile is modeled by beam-column elements, supported by linear or nonlinear spring elements, and both kinematic and inertial interaction effects may be included (Matlock et al., 1978, 1981). Free-field earthquake ground motions determined from one-dimensional site response analyses may be used as displacement input motions for the spring elements. The analysis method is embodied in the computer program SPASM (Single Pile Analysis with Support Motion), as described by Matlock et al. (1978), and applications to bridges have been developed⁴ using this modeling concept.

³ Novak (1991); Pender (1993); Gazetas and Mylonakis (1998); Pecker and Pender (2000)

⁴ Lam and Law (2000); Gazetas and Mylonakis (1998)

Whereas the effects of the kinematic interaction can be significant for some pile-soil configurations (for example, larger diameter piles in soft soils or for sudden changes in soil stiffness with depth), piles may be assumed to deform in a compatible manner within the free-field. For such cases, free-field displacements are generally much less than those induced by inertial interaction. Hence, it can be assumed that inertial interaction dominates pile foundation response and that stiffness functions may be represented by values under static or slow cyclic conditions with foundation input motions assumed to be near surface free-field motions. This approach has had widespread application in the analysis of soil-pile-structure interaction analyses (Martin and Lam, 1995) and forms the basis for the stiffness and capacity modeling approaches described in section 6.2.2.2.

6.2.2. STIFFNESS AND CAPACITY OF FOUNDATION COMPONENTS

Load-deformation characteristics of foundations are required when the effects of foundations are to be taken into account in Evaluation Methods D and E (Capacity Spectrum and Structure Capacity/Demand Methods, and Nonlinear Dynamic Procedure), as discussed in chapter 5. Foundation load-deformation parameters, characterized by both stiffness and capacity, can have significant effects on both structural response and load distribution among structural elements.

Soil-structure systems for bridges can be complex in some cases, but for the purpose of simplicity, four foundation types are considered below: shallow footing foundations, pile foundations, drilled shafts, and abutments.

In addition to the load–deformation behavior of foundations being nonlinear, there are other difficulties in determining soil properties and static foundation loads for existing bridges. To account for the likely variability of the soils supporting the foundations, a best-estimate, equivalent, elasto-plastic representation of the load-deformation behavior is recommended.

In general, soils have considerable ductility unless their stiffness and strength are significantly degraded under cyclic action or large deformations. Degradable soils include cohesionless soils that are expected to liquefy or build up large pore pressures, and sensitive clays that may lose considerable strength when subject to large strains. Soils that are not subject to significant degradation will continue to sustain load, but with increasing deformations after reaching ultimate capacity. Such soils are necessarily assumed in the evaluation methods below.

If soils are susceptible to significant strength loss, due to either the direct effect of the earthquake vibration, or the foundation loading on the soil caused by the earthquake, then improvement of the soil should be considered or special analyses carried out to demonstrate that the loss of strength does not result in excessive structural deformations.

Acceptable levels of foundation deformation are determined by the consequences of these deformations on the structure, which in turn depend on the desired level of bridge performance. However, it should be recognized that foundation yielding may be accompanied by progressive, permanent foundation settlement or deformation during continued cyclic loading, but this settlement will probably be less than a few inches where the static factor of safety exceeds 2.5 to

3.0 (Martin and Lam, 2000). In general, foundation deformations will be small if the loads transmitted to the foundation do not exceed the ultimate capacity of the soil. Recommended procedures for determining the stiffness and capacity of various foundation types are given in sections 6.2.2.1 through 6.2.2.4.

6.2.2.1. Shallow Bearing Footing Foundations

Force-displacement relationships for soil foundations allow the designer to include their properties directly into the structural models used to determine earthquake response. Consider the spread footing shown in figure 6-1 with an applied vertical load, P , lateral load, H , and moment, M . The soil characteristics might be modeled as two translational springs and a rotational spring, each characterized by a linear elastic stiffness and a plastic capacity. However it is more common to use a Winkler spring model, acting in conjunction with the foundation, to eliminate the rotational spring, as shown in figure 6-2 (NEHRP, 1997a, 1997b). Conversion to Winkler springs uncouples the lateral action from the vertical and rotational actions. Springs with elasto-plastic properties are the simplest to use and give adequate results in most cases. More refined nonlinear models may be used if the importance of the project justifies it. A particular feature of the Winkler spring model is that it can capture progressive mobilization of plastic capacity during rotational rocking behavior relatively easily.

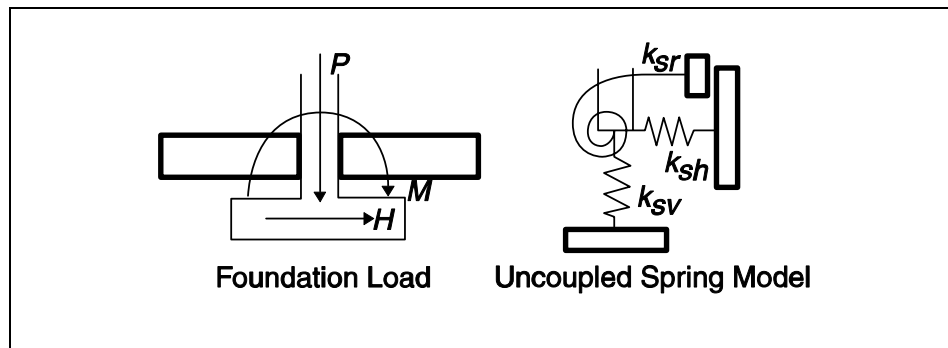


Figure 6-1. Uncoupled elasto-plastic spring model for rigid footings.

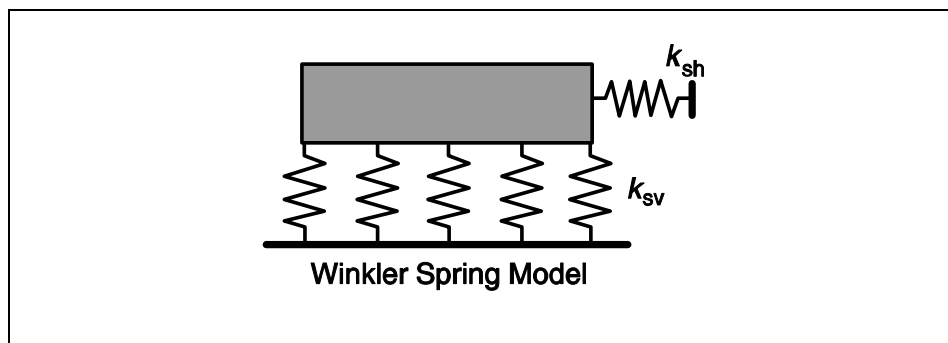


Figure 6-2. Uncoupled Winkler spring model.

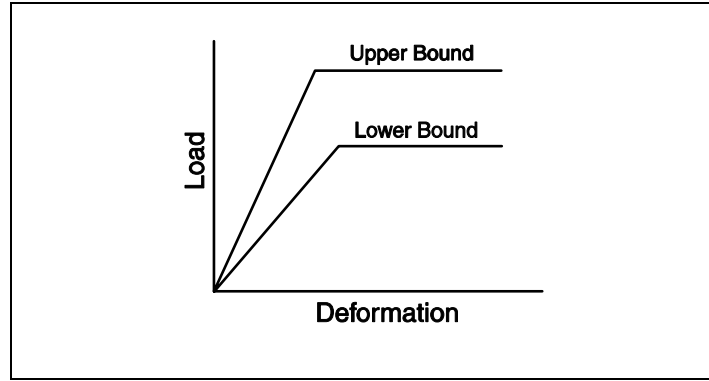


Figure 6-3. Upper and lower bound approach to define stiffness and capacity.

An upper and lower bound approach to defining stiffness and capacity is often suggested (as shown in figure 6-3) because of the uncertainties in the soil properties and the static loads on the foundations of existing bridges. Such an approach allows the sensitivity of the bridge to these properties to be determined. In such a case, the range of uncertainty represented by the upper and lower bounds should be jointly determined by the geotechnical and structural engineer. Otherwise, a best-estimate value may be chosen.

6.2.2.1(a). *Stiffness Parameters*

Most shallow spread footings are stiff relative to the soil on which they rest, and for analytical purposes, an uncoupled spring model as shown in figure 6-1 is sufficient. The three equivalent spring constants may be determined using theoretical static solutions for rigid plates embedded in an elastic medium. The solutions require knowledge of the average elastic modulus and Poisson's ratio of the soil in the vicinity of the foundation (say to a depth of 1.5 times the width of the footing below the base of the footing). The shear modulus, G , for a soil is then given by:

$$G = \frac{E}{2(1+\nu)} \quad (6-1)$$

where E is the modulus of elasticity, and ν is Poisson's ratio (0.35 for unsaturated soils and 0.5 for saturated soils).

The initial or low strain shear modulus during cyclic loading, G_0 , is given by

$$G_0 = \frac{\gamma}{g} v_s^2 \quad (6-2)$$

where v_s is the shear wave velocity at small strains, γ is the weight density (unit weight) of soil, and g is the acceleration due to gravity.

The initial shear modulus for granular soils may also be found from the normalized corrected blowcount, $(N_1)_{60}$, and the effective vertical stress as follows (Seed et al., 1986):

$$G_0 \equiv 20,000 \sqrt[3]{(N_1)_{60}} \sqrt{\sigma'_0} \text{ in psf} \quad (6-3)$$

where:

- $(N_1)_{60}$ = blowcount normalized for 1.0 ton per square foot confining pressure and 60 percent energy efficiency of hammer,
- σ'_0 = effective vertical stress in psf,
 $= \gamma_t d - \gamma_w (d - d_w)$,
- γ_t = total unit weight of soil,
- γ_w = unit weight of water,
- d = depth of sample, and
- d_w = depth of water level.

Either equation 6-2 or 6-3 may be used to calculate the modulus G_0 .

Most soils are very nonlinear, and the shear modulus decreases with increasing shear strain. The large-strain effective shear modulus, G , can be roughly estimated on the basis of the anticipated peak ground acceleration (PGA). For regions of low-to-moderate seismicity ($F_v S_1 \leq 0.3$), a value of $G = 0.5 G_0$ is recommended, while for regions of moderate-to-high seismicity ($F_v S_1 \geq 0.5$), a value of $G = 0.25 G_0$ is suggested. Interpolation should be used for intermediate values of $F_v S_1$.

The uncoupled stiffness parameters may be obtained from theoretical solutions for a rigid plate resting on a semi-infinite homogeneous elastic half-space. Tabular solutions are shown in tables 6-1 and 6-2 (Gazetas, 1991).

If the horizontal stiffness of the foundation is similar to, or less than, that of the bridge, the foundation properties should be included in the demand and capacity analyses. However, many foundation systems are relatively stiff and strong in the horizontal direction, due to the passive resistance of the soils on the sides of footings and the friction beneath the footings and may be several orders of magnitude greater than the bridge. In these cases, the foundations may be considered fixed in the horizontal directions, and foundation rocking will have the greater influence on bridge response.

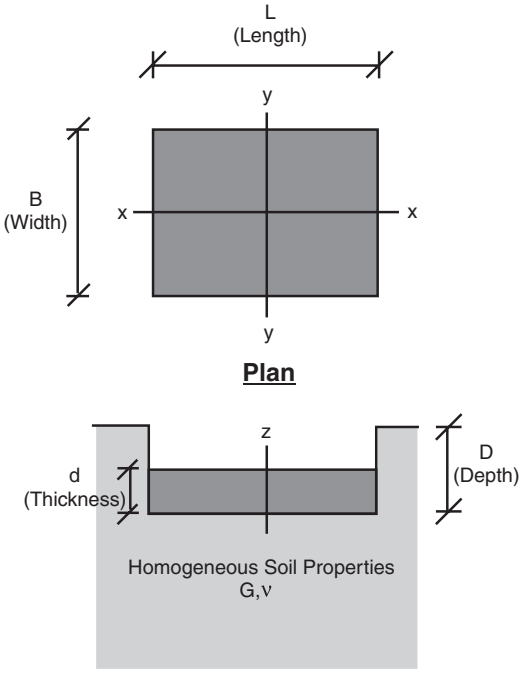
If the foundation capacity is exceeded during an elastic analysis based on initial estimates of foundation stiffness, softening will occur due to soil yield and it will be appropriate to reanalyze the bridge with an estimate of the degraded equivalent linear values. When nonlinear pushover analyses are used, initial estimates of elastic foundation stiffness should be used in conjunction with capacity estimates.

6.2.2.1(b). Capacity Parameters

Soil yield, rocking, and uplift of rigid footings under earthquake-induced moment loading can reduce the ductility demand in a bridge⁵. Accordingly, rotational yield could be allowed to occur

⁵ Taylor and Williams (1979); Taylor et al., (1981)

Table 6-1. Surface stiffnesses for a rigid plate on a semi-infinite homogeneous elastic half-space.

Stiffness Parameter	Rigid Plate Stiffness at Surface, K_i'
Vertical Translation, K_z'	$\frac{GL}{(1-\nu)} \left[0.73 + 1.54 \left(\frac{B}{L} \right)^{0.75} \right]$
Horizontal Translation, K_y' (toward long side)	$\frac{GL}{(2-\nu)} \left[2 + 2.5 \left(\frac{B}{L} \right)^{0.85} \right]$
Horizontal Translation, K_x' (toward short side)	$\frac{GL}{(2-\nu)} \left[2 + 2.5 \left(\frac{B}{L} \right)^{0.85} \right] - \frac{GL}{(0.75-\nu)} \left[0.1 \left(1 - \frac{B}{L} \right) \right]$
Rotation, $K_{\theta x}'$ (about x axis)	$\frac{G}{(1-\nu)} I_x^{0.75} \left(\frac{L}{B} \right)^{0.25} \left(2.4 + 0.5 \frac{B}{L} \right)$
Rotation, $K_{\theta y}'$ (about y axis)	$\frac{G}{(1-\nu)} I_y^{0.75} \left[3 \left(\frac{L}{B} \right)^{0.15} \right]$
<div style="display: flex; justify-content: space-between; align-items: flex-start;"> <div style="width: 45%;">  <p style="text-align: center;">Plan</p> <p style="text-align: center;">Section</p> </div> <div style="width: 50%;"> <ol style="list-style-type: none"> Determine the uncoupled total surface stiffnesses, K_i', of the foundation element by assuming it to be a rigid plate bearing at the surface of a semi-infinite elastic half-space (see above). Adjust the uncoupled total surface stiffnesses, K_i', for the effect of the depth of bearing by multiplying by embedment factors (see Table 6-2), e_i, to generate the uncoupled total embedded stiffnesses, K_i. $K_i = e_i K_i'$ </div> </div>	
<p>Note: I_x, I_y are moments of inertia of the footing about the x- and y-axes, respectively.</p>	

adapted from Gazetas, 1991

Table 6-2. Stiffness embedment factors for a rigid plate on a semi-infinite homogeneous elastic half-space.

Stiffness Parameter	Embedment Factors, e_i
Vertical Translation, e_z	$\left[1 + 0.095 \frac{D}{B} \left(1 + 13 \frac{B}{L} \right) \right] \left[1 + 0.2 \left(\frac{(2L + 2B)}{LB} d \right)^{0.67} \right]$
Horizontal Translation, e_y (toward long side)	$\left[1 + 0.15 \left(\frac{2D}{B} \right)^{0.5} \right] \left\{ 1 + 0.52 \left[\frac{\left(D - \frac{d}{2} \right) 16(L + B)d}{BL^2} \right]^{0.4} \right\}$
Horizontal Translation, e_x (toward short side)	$\left[1 + 0.15 \left(\frac{2D}{L} \right)^{0.5} \right] \left\{ 1 + 0.52 \left[\frac{\left(D - \frac{d}{2} \right) 16(L + B)d}{LB^2} \right]^{0.4} \right\}$
Rotation, $e_{\theta x}$ (about x axis)	$1 + 2.52 \frac{d}{B} \left(1 + \frac{2d}{B} \left(\frac{d}{D} \right)^{-0.20} \left(\frac{B}{L} \right)^{0.50} \right)$
Rotation, $e_{\theta y}$ (about y axis)	$1 + 0.92 \left(\frac{2d}{L} \right)^{0.60} \left(1.5 + \left(\frac{2d}{L} \right)^{1.9} \left(\frac{d}{D} \right)^{-0.60} \right)$

adapted from Gazetas, 1991

under earthquake loading, provided there is no serious loss of vertical load-bearing capacity and the vertical settlements induced are small. Footing yield and uplift are permitted in the FEMA 273 guidelines for the seismic retrofit of buildings (NEHRP 1997a, 1997b) and illustrated in figure 6-4.

In the absence of moment loading, the vertical load capacity of a rectangular footing (Q_c) is given by:

$$Q_c = q_c B L \quad (6-4)$$

where q_c is the ultimate strength of soil (capacity) per unit area, B is the footing width, and L is the footing length.

If moment loads are present in addition to the vertical load, contact stresses become concentrated at the edges of the footing, particularly as uplift occurs. The ultimate moment capacity, M_c , is dependent on the ratio of the vertical load to the vertical capacity of the soil. Assuming a rigid footing and that the contact stresses are proportional to vertical displacement and remain elastic until the vertical capacity is reached, a factor of safety, F_v , can be defined as follows:

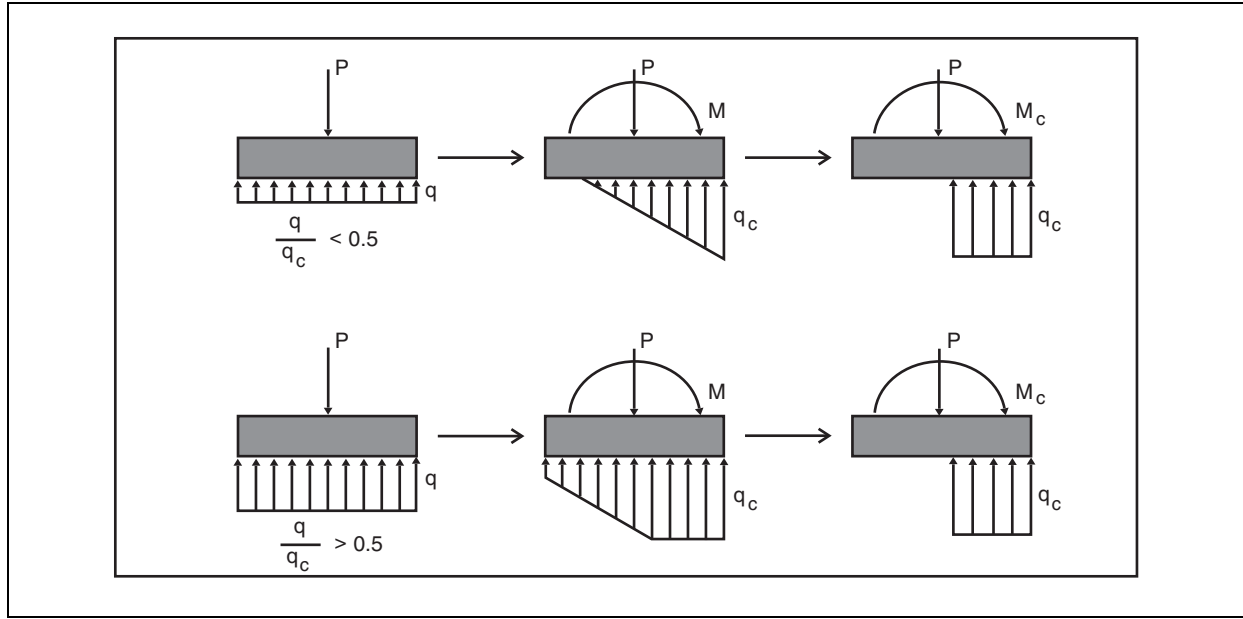


Figure 6-4. Idealized concentration of stress at edge of rigid footings subjected to overturning moment.

$$F_v = \frac{q_c}{q} \quad (6-5)$$

where q is the vertical load on footing (contact stress).

If F_v is greater than 2, uplift will occur prior to plastic yielding of the soil, but if F_v is less than or equal to 2, the soil at the toe yields before uplift begins.

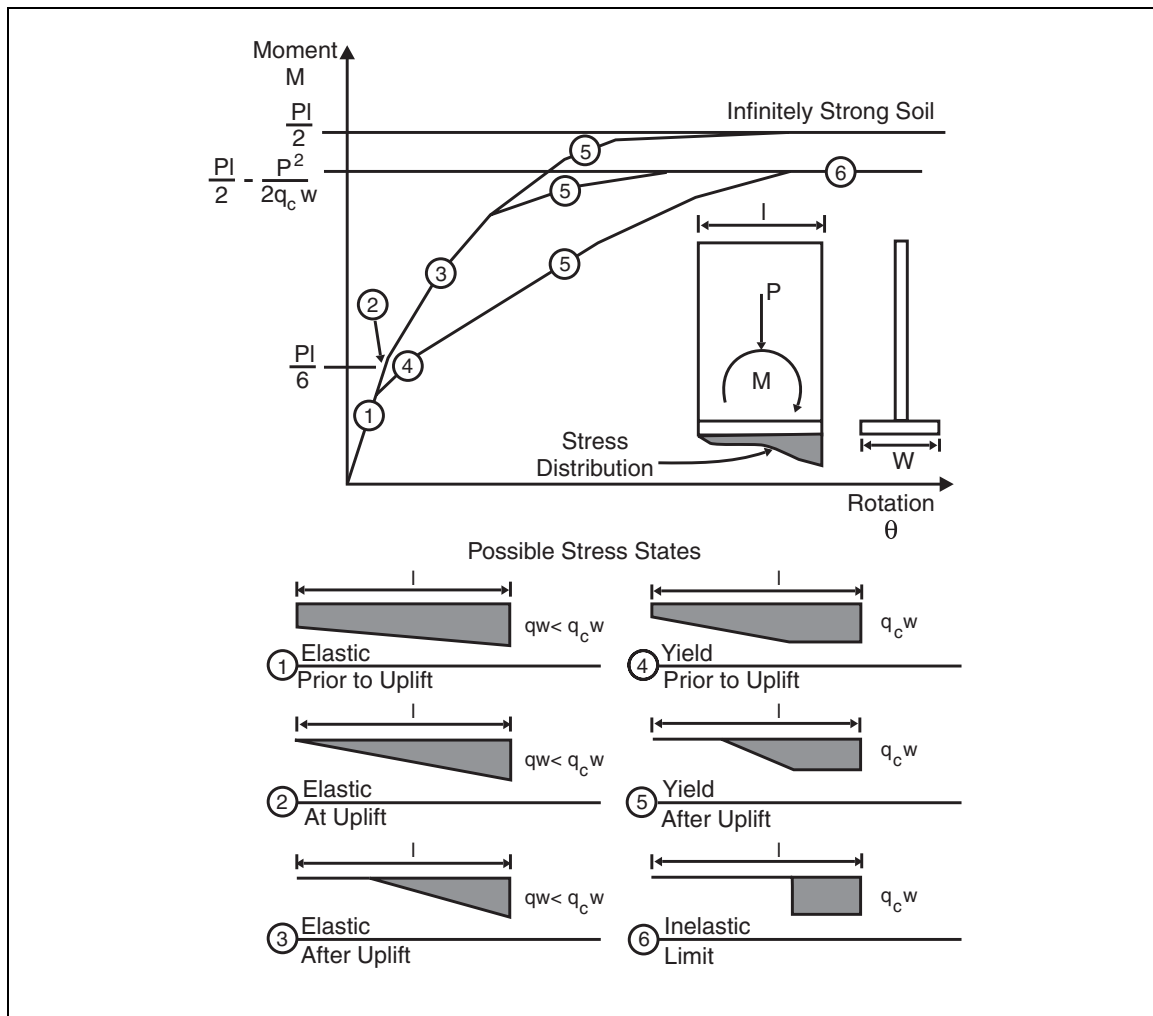
With these assumptions, the moment capacity of a rectangular footing may be expressed as:

$$M_c = \frac{LP}{2} \left(1 - \frac{q}{q_c} \right) = \frac{LP}{2} \left(1 - \frac{1}{F_v} \right) \quad (6-6)$$

where P is the vertical load on footing, q equals P/BL , B is the footing width, and L is the length of footing in direction of bending.

The nonlinear moment-rotation behavior generated by yield and uplift corresponding to this model is illustrated graphically in figure 6-5.

Rocking behavior has several important consequences on the seismic response of a structure. First, rocking results in a decrease in stiffness and lengthening of the fundamental period of the bridge. This effect is amplitude dependent and very nonlinear. The result is generally a reduction in the maximum seismic response as previously noted. Depending on the ratio of initial bearing pressure to the ultimate capacity of the soil, significant amounts of energy may be



after NEHRP, 1997b

Figure 6-5. Rocking of shear wall on strip footing.

dissipated by soil yielding. This behavior also can result in decreased ductility demand on bridge piers.

When plastic yielding of the soil under the footings is permitted, the magnitude of accumulated settlement, induced by the static vertical load, must be considered. Model tests and analytical studies (Martin and Lam, 2000) suggest that, provided the initial static factor of safety, F_v , is greater than 2.5, expected settlements will be small (say a few centimeters or inches) and may be acceptable for retrofit purposes.

Column shear forces are resisted by friction at the base and sides of footings and by passive resistance at the face of the footing. For simplicity, it may be assumed that the maximum total resistance develops at a deformation equal to two percent of the embedded depth of the footing. For most cast-in-place concrete foundations, a value of interface friction of 80 percent of the friction angle of the soil is appropriate for evaluating base and side friction. Classical earth

pressure theory can be used to calculate the ultimate passive pressure capacity. A simplified approach based on log spiral solutions for granular soils is shown in figure 6-6.

If foundation forces are calculated from an equivalent elastic analysis using the shear stiffness parameters in tables 6-1 and 6-2, and they exceed the horizontal shear capacity of the footing, the consequential yield may be approximated by reducing the stiffness parameters and reanalyzing the bridge.

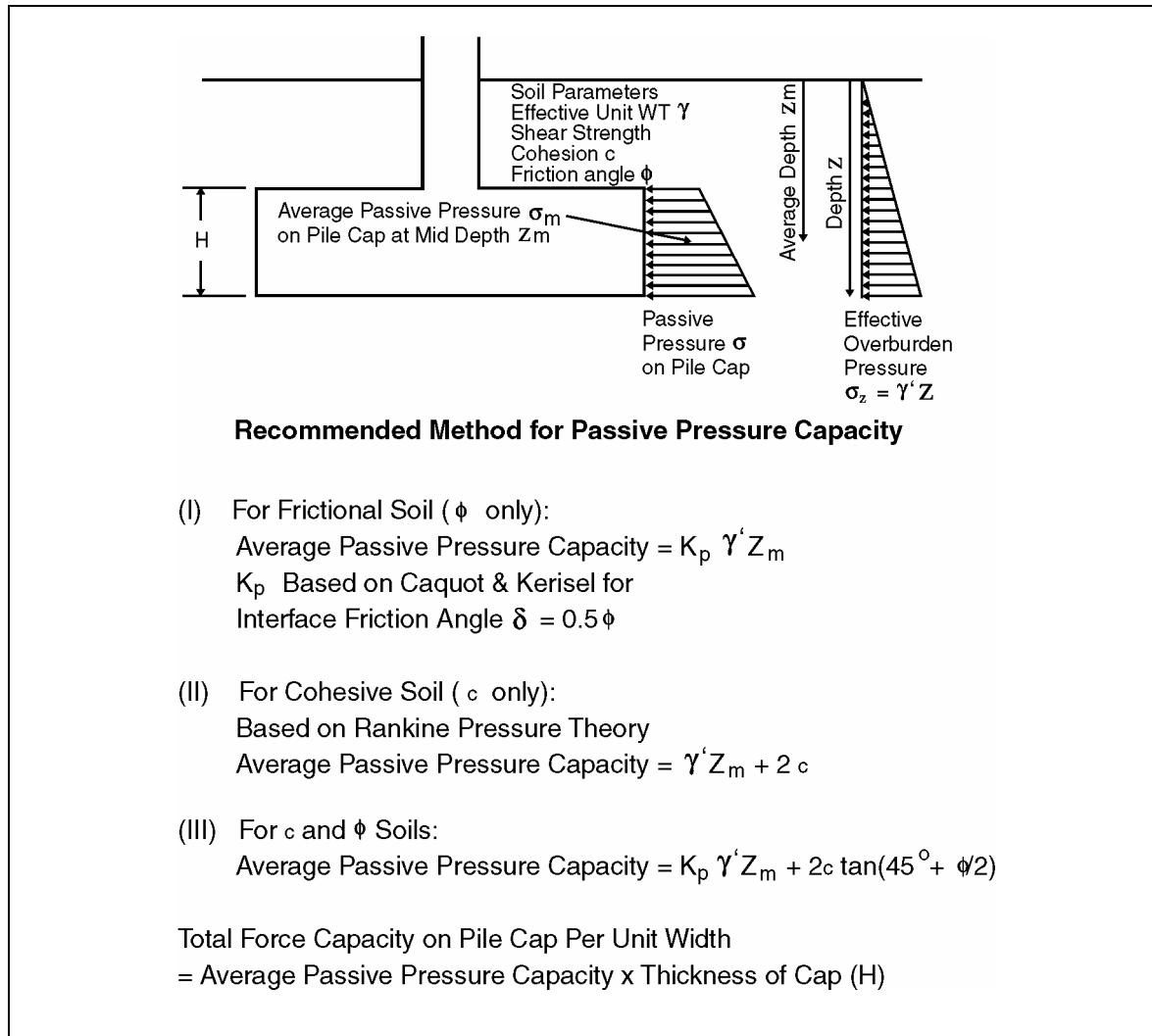


Figure 6-6. Method for passive pressure capacity of footing or pile cap.

6.2.2.2. Pile Footing Foundations

Pile foundations generally comprise pile groups connected to a footing or pile cap, with pile diameters (normally driven piles) usually less than 0.6 m (2 ft) in diameter. These types of foundations are the most typical and are found on a variety of bridge types, including those with single-columns, multiple-columns, and wall piers. Connection details at the pile cap can also vary from pinned to fixed conditions. In general, bridges that are stiff under lateral loading will be more sensitive to foundation flexibility and the careful characterization of foundation stiffness becomes more important in these circumstances. In other words, foundation stiffness should be explicitly included when the foundation is flexible compared to the bridge, such as in soft soil conditions, or in the transverse direction under walls and single-column piers.

The overall seismic response of a pile group foundation depends on the response of individual piles under both axial and lateral loading and on the lateral response of the pile cap. The stiffness and capacity characteristics of the various components are discussed below.

For the purpose of computing stiffness and capacity for analyses, the footing or pile cap is normally uncoupled from the piles, and contributions from the two components are evaluated separately. Based on centrifuge tests (Gadre, 1997), this appears to be a reasonable solution. The stiffness and capacity of the pile cap in the lateral direction is normally much higher than the contributions from the piles, while rotational stiffness and capacity is usually governed by axial loading in the piles due to moments in the columns.

6.2.2.2(a). Pile Cap – Lateral Stiffness and Capacity

Because of the possibility of soil settlement, and the uncertain interaction between the footing and the piles, contributions to soil stiffness and capacity from the footing's base and side shear are neglected. Hence the primary source of lateral resistance is the mobilization of passive pressure on the vertical face of the pile cap. Maximum passive pressures can be computed using the same procedure described for shallow footing foundations, as illustrated in figure 6-6. As the ultimate capacity is reduced at small deflection values (about two percent of the embedment depth), an initial elastic stiffness or lateral load-deflection stiffness may be defined using this assumption. A softened secant stiffness may be used if displacement demands are greater than this deflection value.

6.2.2.2(b). Pile-Head Stiffness – Lateral Loading

In practice, the lateral load-deflection characteristics of a pile are determined by a pushover analysis, assuming a beam supported on Winkler springs that are characterized by nonlinear p-y curves. This type of pseudo-static soil foundation interaction problem can be analyzed using a variety of methods, including discrete beam-column and finite-element analyses. Various authors have developed empirical deflection-dependent lateral soil resistance curves for sand and clays based on small-diameter pile load tests. The most commonly used p-y curves are those by Reese et al. (1974) for sands and by Matlock (1970) for clays. These curves should be linearized to develop a consistent set of lateral, rotational, and coupled stiffness values, if a full, 6 x 6 stiffness matrix is used to represent the pile group in an elastic structural demand analysis (Lam

et al., 1998). Programs such as LPILE (Reese et al., 1997) and FLPIER (Hoit and McVay, 1996) may be used if a nonlinear load-deflection relationship for the pile-head is required, based on the nonlinear p-y curves. However such curves are very sensitive to pile-head fixity conditions (figure 6-7) and the value of the cracked section modulus for the piles.

In choosing an equivalent secant modulus for such curves for demand analyses, compatibility with displacement demand, which would normally be less than a few centimeters or inches in a strong earthquake, should be provided. However, given the many uncertainties in site conditions, a simplified procedure to develop a linear stiffness for retrofit evaluations is recommended below.

Lam and Martin (1986) found that lateral load-deflection characteristics representing the overall stiffness of the soil-pile system is only mildly nonlinear because the elastic pile usually dominates the nonlinear soil stiffness. Furthermore, the significant soil-pile interaction zone is usually confined to a depth equal to the upper 5 to 10 pile diameters. Therefore, simplified single-layer pile-head stiffness design charts are appropriate for lateral loading.

Single-layer linear design charts are presented in figures 6-8 to 6-11. These charts use a discrete Winkler spring soil model in which stiffness increases linearly with depth, from zero at grade level where the location of the pile-head is assumed to be located. A linear representation of subgrade stiffness is a good first approximation to test data for pile-caps in both sand and clay soil conditions. Two parameters may then be used to define this soil-pile system: the pile bending stiffness, EI, and the coefficient of variation of the inelastic subgrade modulus, f , as defined in equation 6-7:

$$f = \frac{E_s}{z} \quad (6-7)$$

where E_s is the subgrade modulus (soil stiffness per unit length of pile) at a particular depth, and z is the depth below grade.

Values of the coefficient f , which has units of force/unit volume, have been published for piles embedded in sand carrying normal working loads⁶, as a function of corrected Standard Penetration Test (SPT) blowcount or relative density (see figure 6-12). Values for piles in clay soils are given in figure 6-13 (Lam et al., 1991). Average soil conditions for the upper five pile diameters should be used when reading values from these charts, which are applicable for piles up to 0.6 m (24 in) in diameter.

Given the coefficient f , and the bending stiffness of the pile, EI, lateral and rotational stiffness can be read directly from the charts in figures 6-8 through 6-11 (Lam et al., 1991). Although the charts assume no pile embedment, they do provide reasonable estimates of stiffness for shallow embedments up to say 1.5 m (5 ft), in which case the soil above the pile top is neglected. An additional set of design charts for piles with pinned heads (i.e., zero bending moment) is given in figure 6-11. If the coefficient of variation in subgrade modulus, as shown in figures 6-12 and

⁶ Terzaghi (1955); Murchison and O'Neill (1984)

6-13, is used to derive the pile-head stiffness matrix from figures 6-8 through 6-11, the resulting pile cap stiffness matrix is appropriate for cap deflections between 6 and 50 mm (0.25 and 2 in).

Deeper embedment increases the stiffness coefficients. Figures 6-14 through 6-16 give pile cap stiffness coefficients for pile embedment depths of 1.5 m and 3 m (5 and 10 ft), based on a subgrade modulus that increases linearly with depth. It can be seen from these figures that the embedment effect on stiffness is larger for slender piles, and tends to diminish for stiffer piles. The lateral stiffness is affected the most. For example, for a pile cap embedded in slightly compact sand ($f = 2.7 \text{ MN/m}^3 [10 \text{ lb/in}^3]$), figure 6-14 shows an increase in embedment depth from 0 to 1.5 m (0 to 5 ft) can increase the lateral pile cap stiffness by 130 percent for rigid piles and 230 percent for slender piles. For a depth increase from 0 to 3 m (0 to 10 ft), the stiffness increases by 150 percent for rigid piles and 350 percent for slender piles.

These figures also illustrate that the effect of the embedment depth is greater in dense sands. For example, for a 0.3 m by 0.3 m (12 in by 12 in) concrete pile ($EI = 43 \times 10^6 \text{ MPa} [6.22 \times 10^6 \text{ ksi}]$) embedded 1.5 m (5 ft), the lateral stiffness increases by a 160 percent in slightly compact sand ($f = 2.7 \text{ MN/m}^3 [10 \text{ lb/in}^3]$) and 260 percent in dense sand ($f = 270 \text{ MN/m}^3 [100 \text{ lb/in}^3]$).

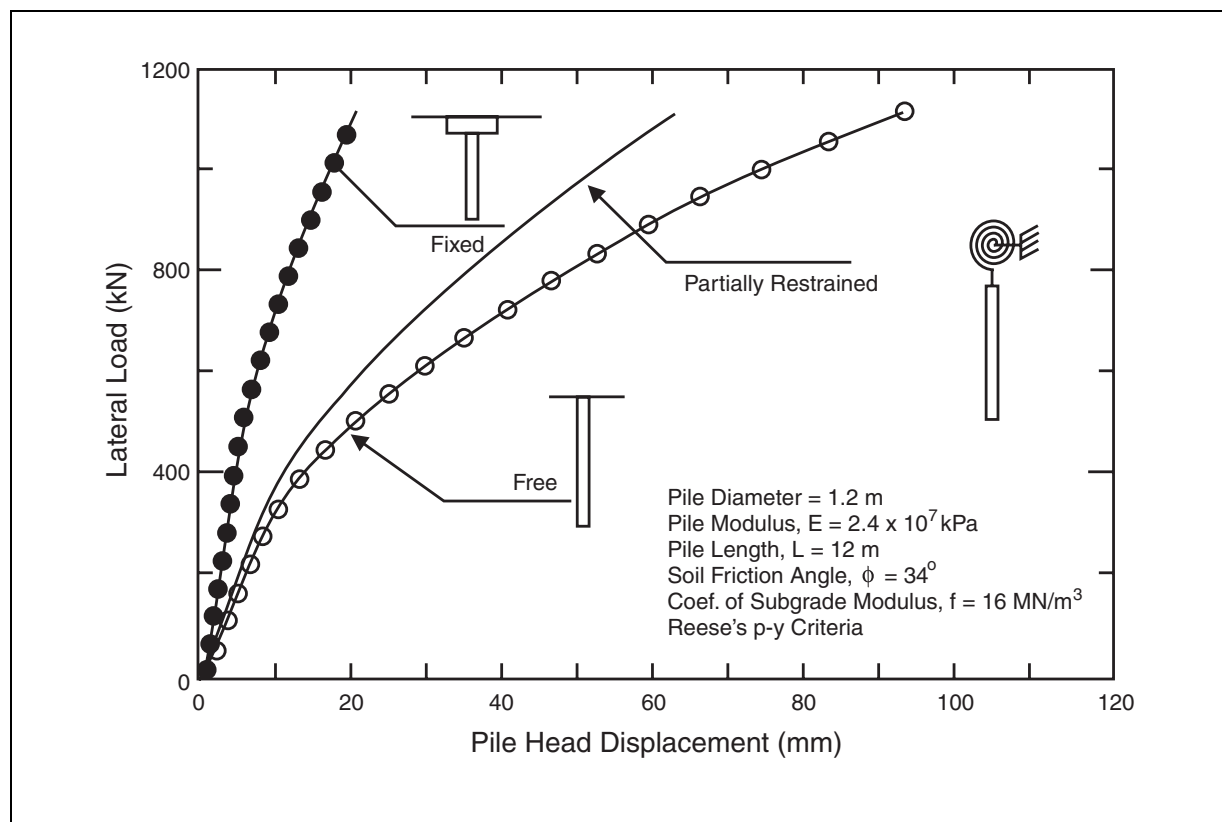


Figure 6-7. Effect of boundary conditions on pile stiffness

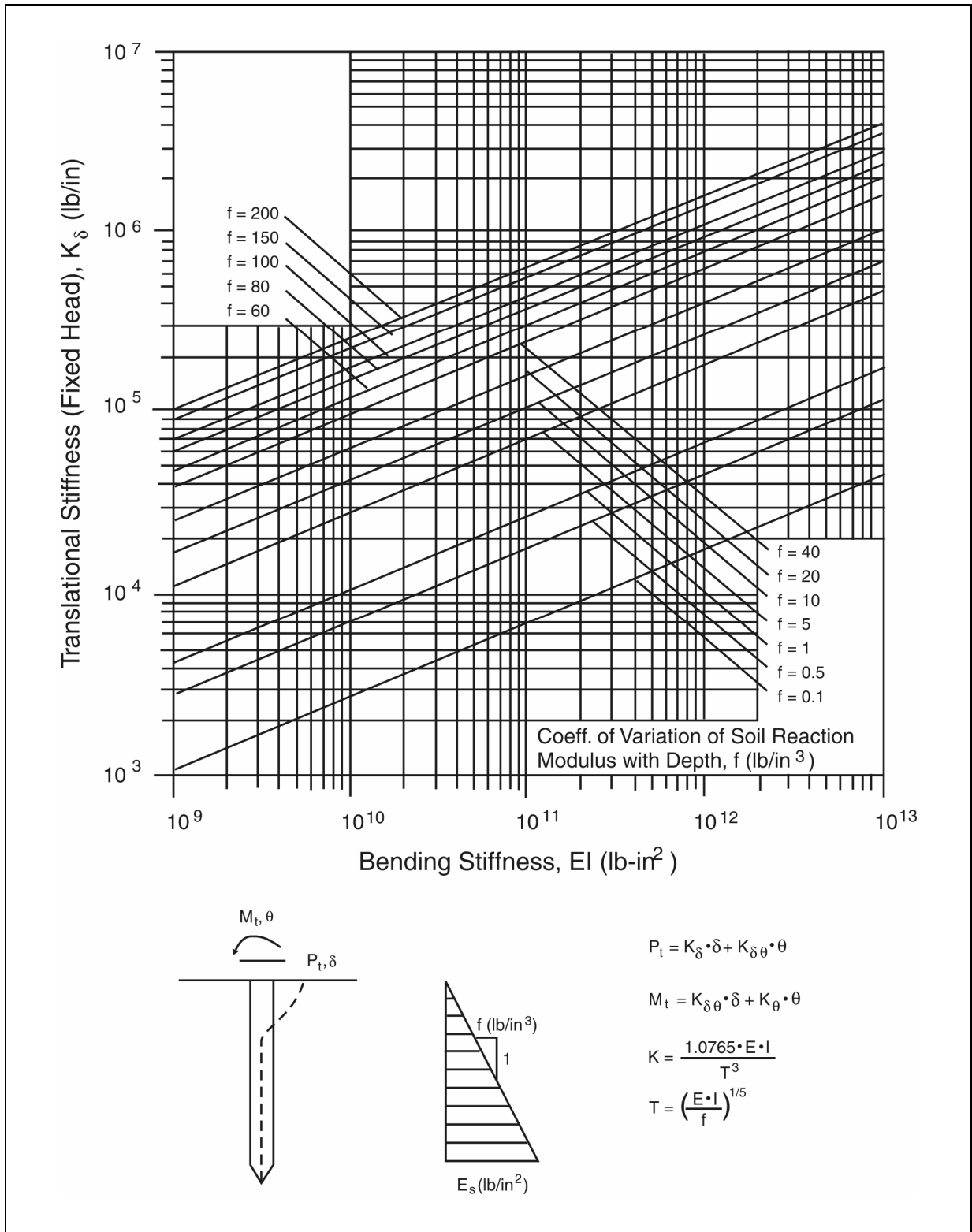


Figure 6-8. Lateral pile-head stiffness (fixed-head condition).

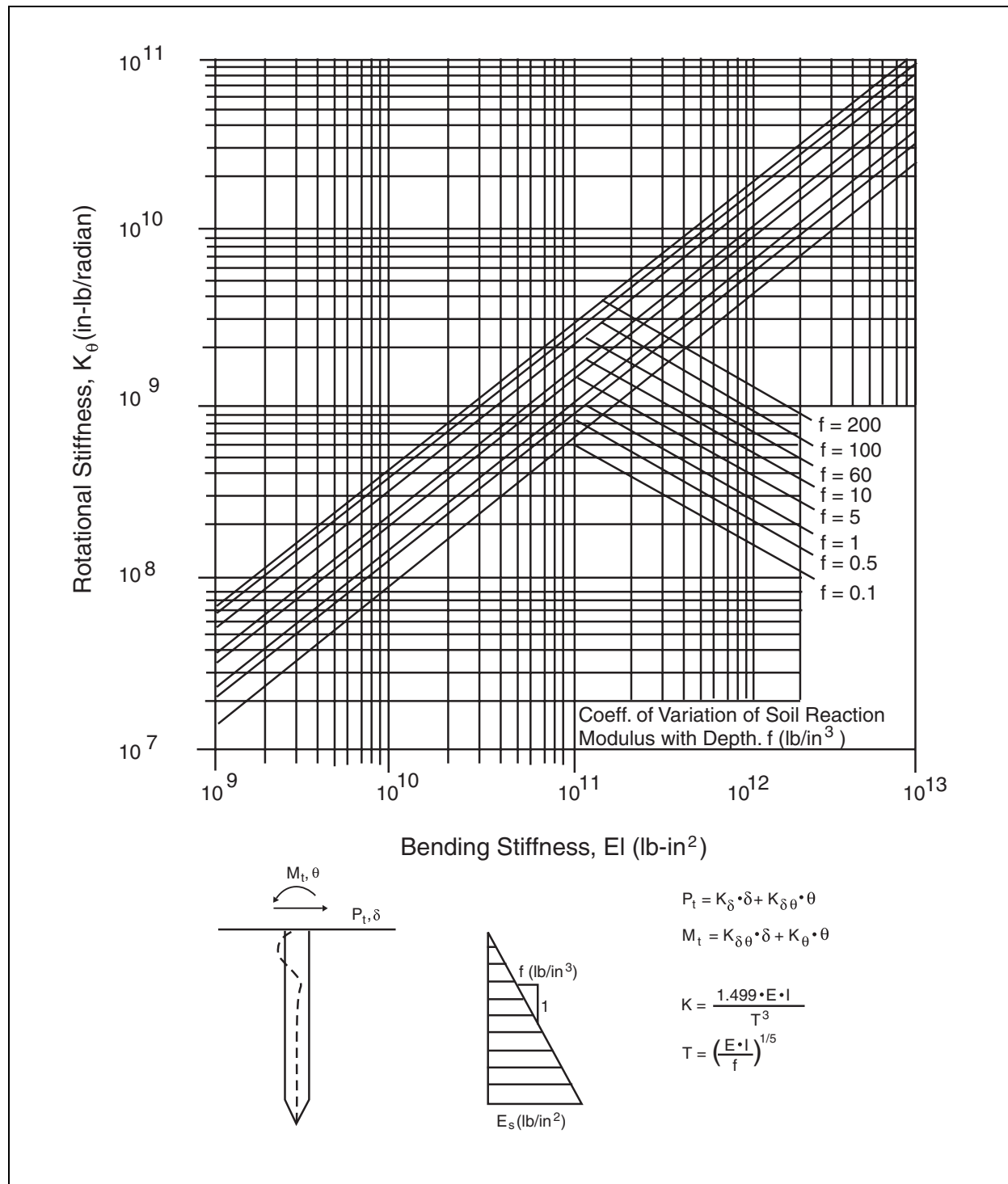


Figure 6-9. Rotational pile-head stiffness.

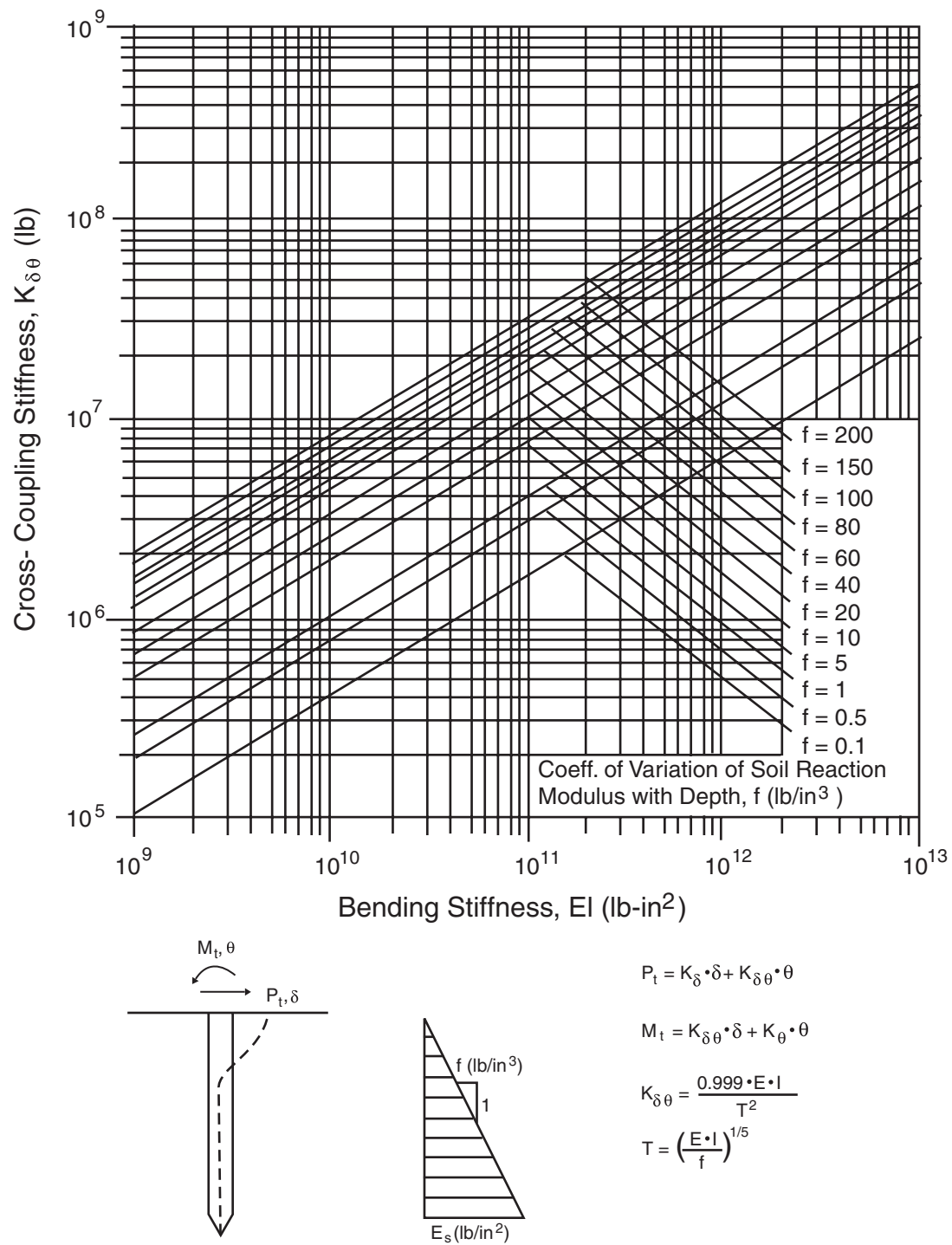


Figure 6-10. Cross-coupling pile-head stiffness.

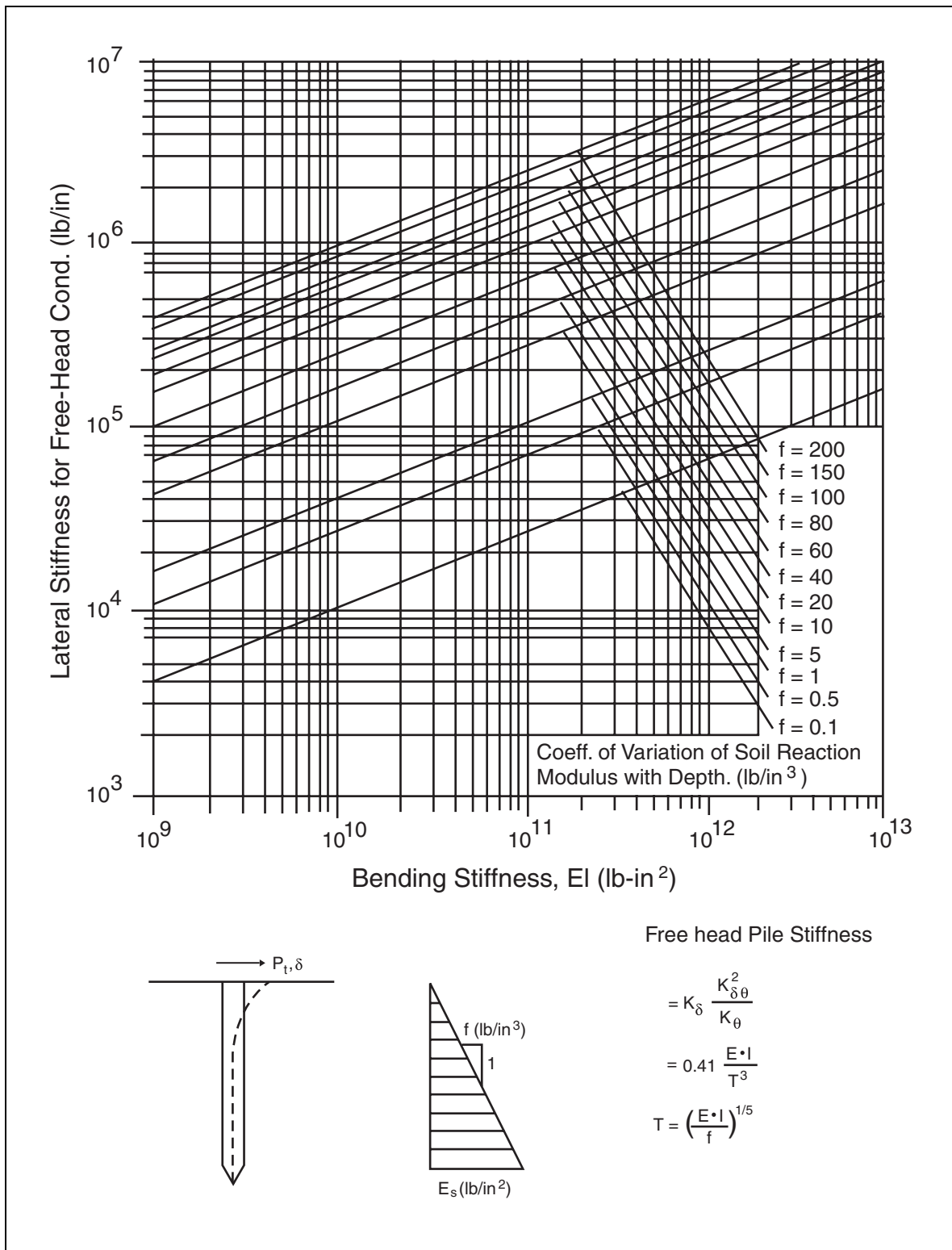


Figure 6-11. Lateral pile-head stiffness (free-head condition).

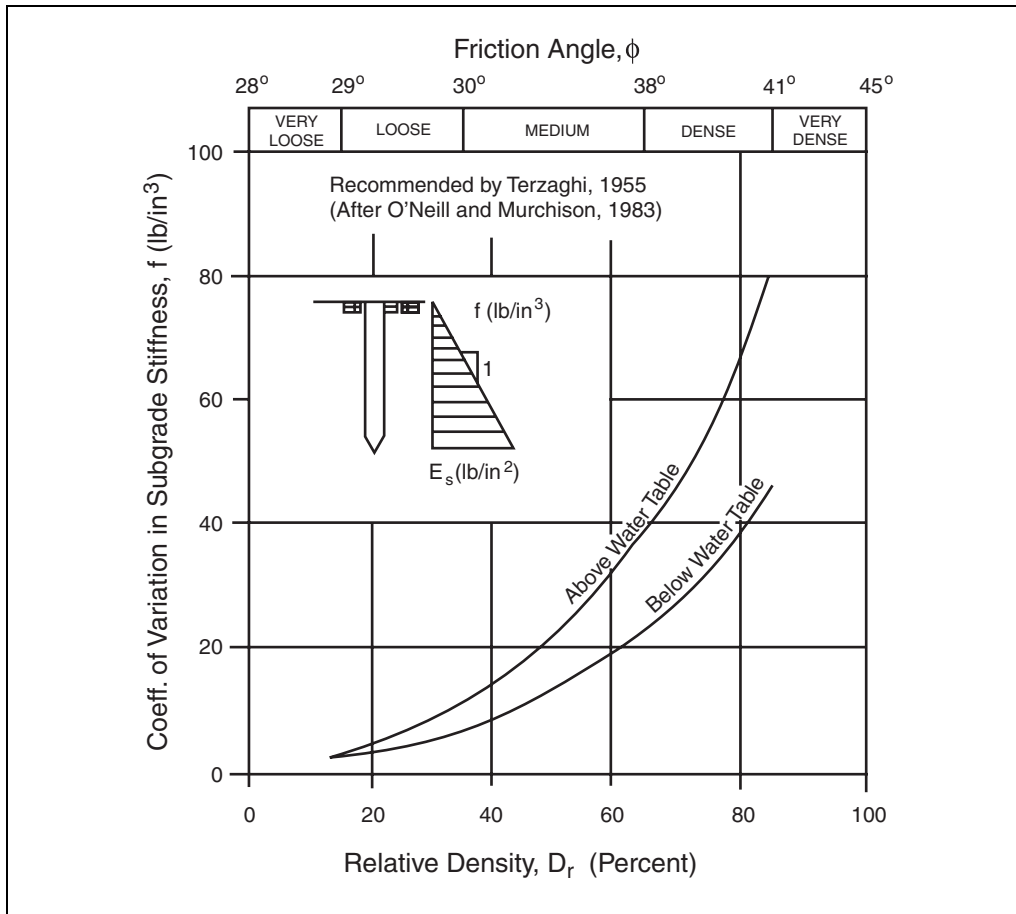


Figure 6-12. Recommended coefficient of variation in subgrade modulus (f) with depth of sand.

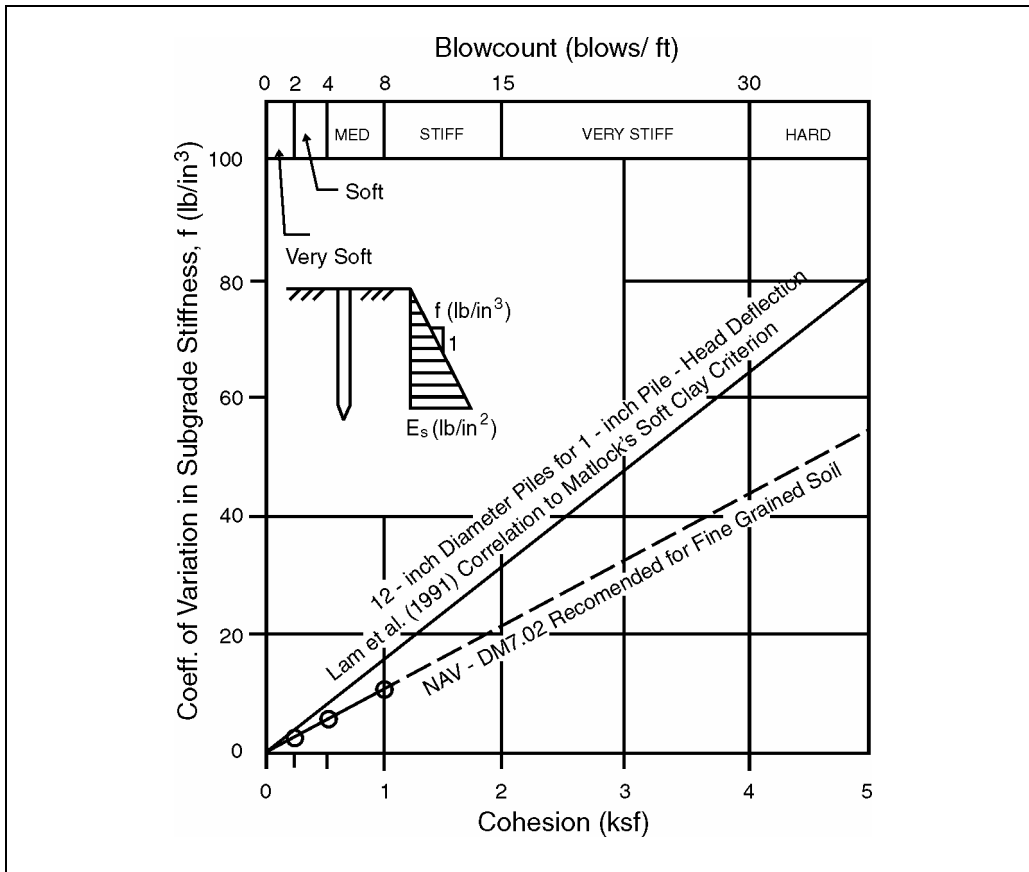


Figure 6-13. Recommended coefficient of variation in subgrade modulus (f) with depth of clay.

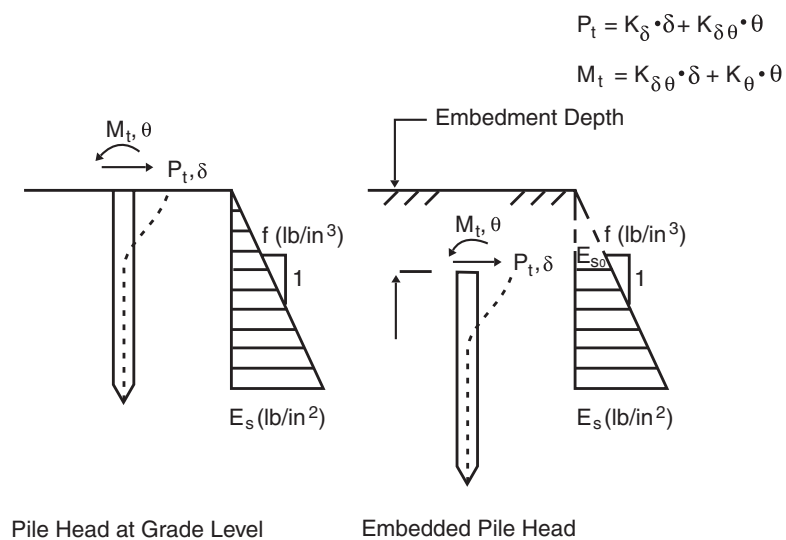
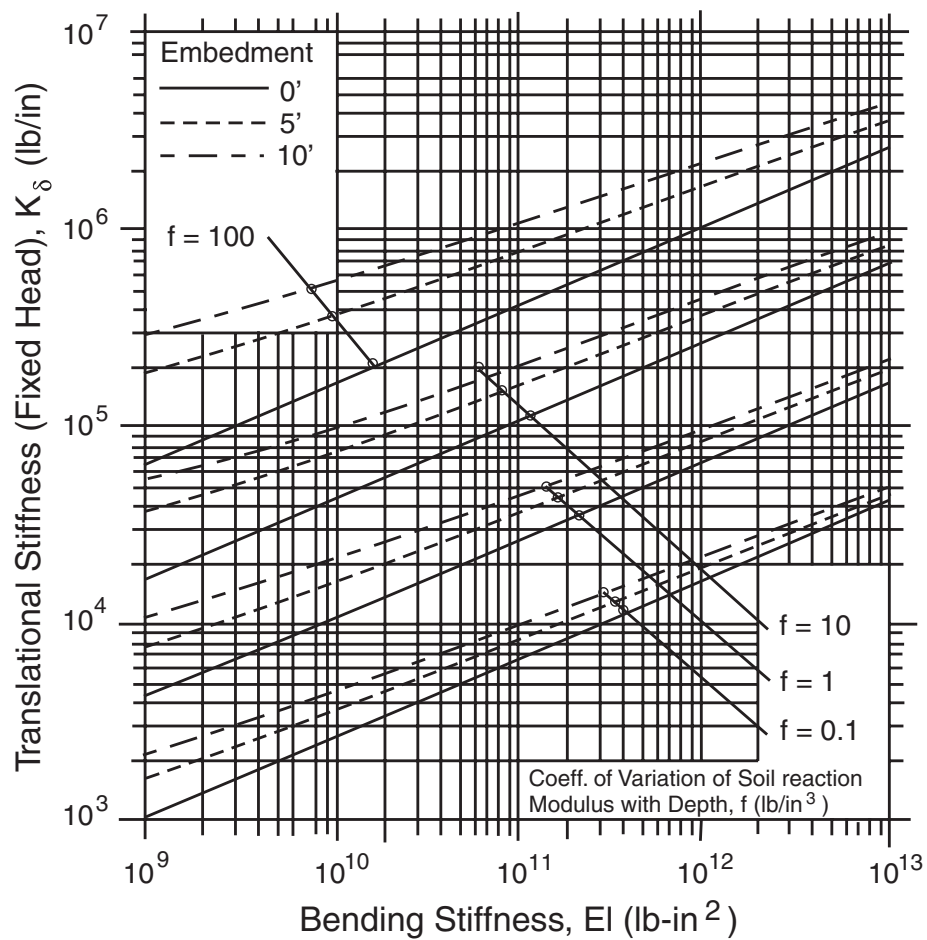
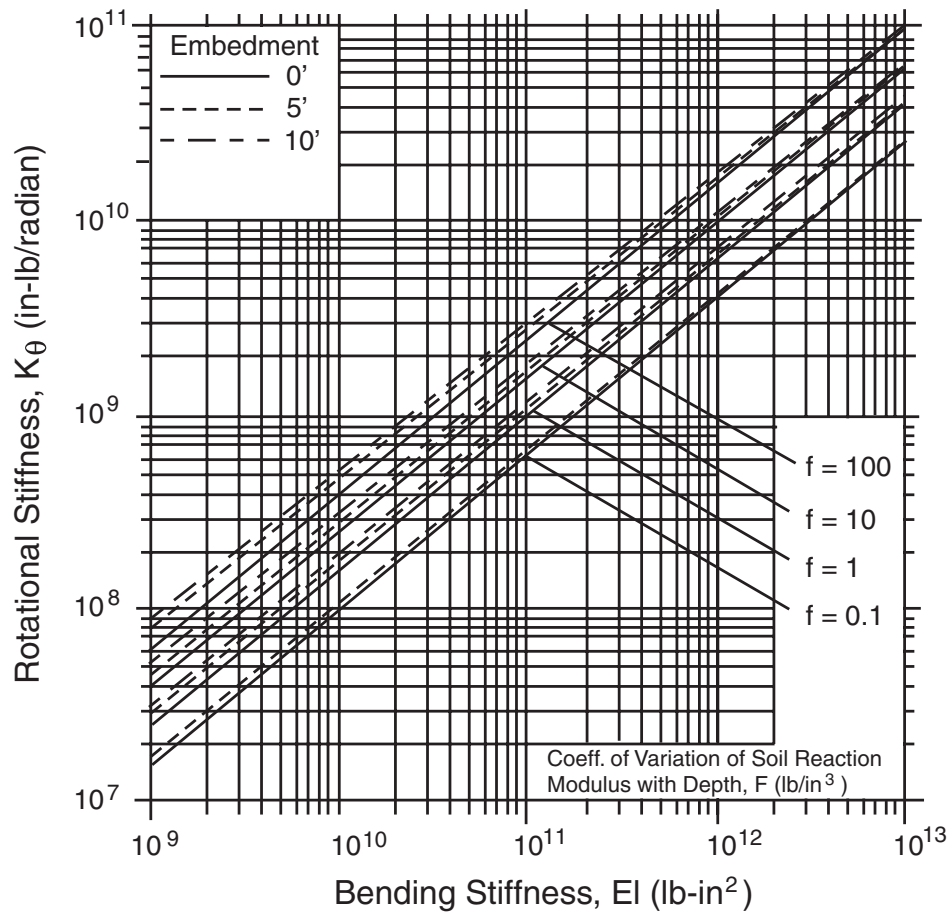


Figure 6-14. Lateral embedded pile-head stiffness (fixed-head condition).



$$P_t = K_\delta \cdot \delta + K_{\delta\theta} \cdot \theta$$

$$M_t = K_{\delta\theta} \cdot \delta + K_\theta \cdot \theta$$

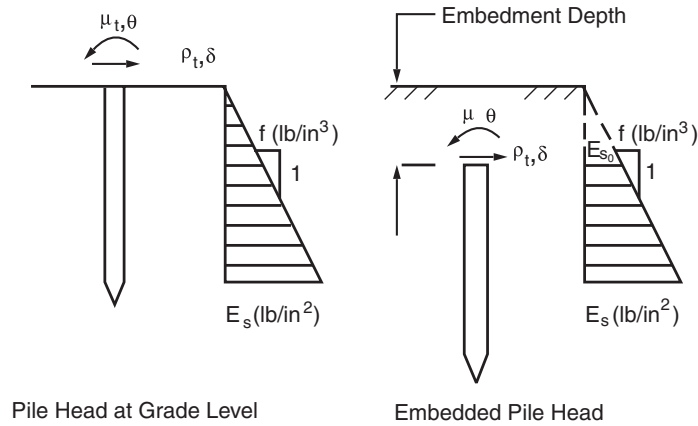


Figure 6-15. Embedded pile-head rotational stiffness.

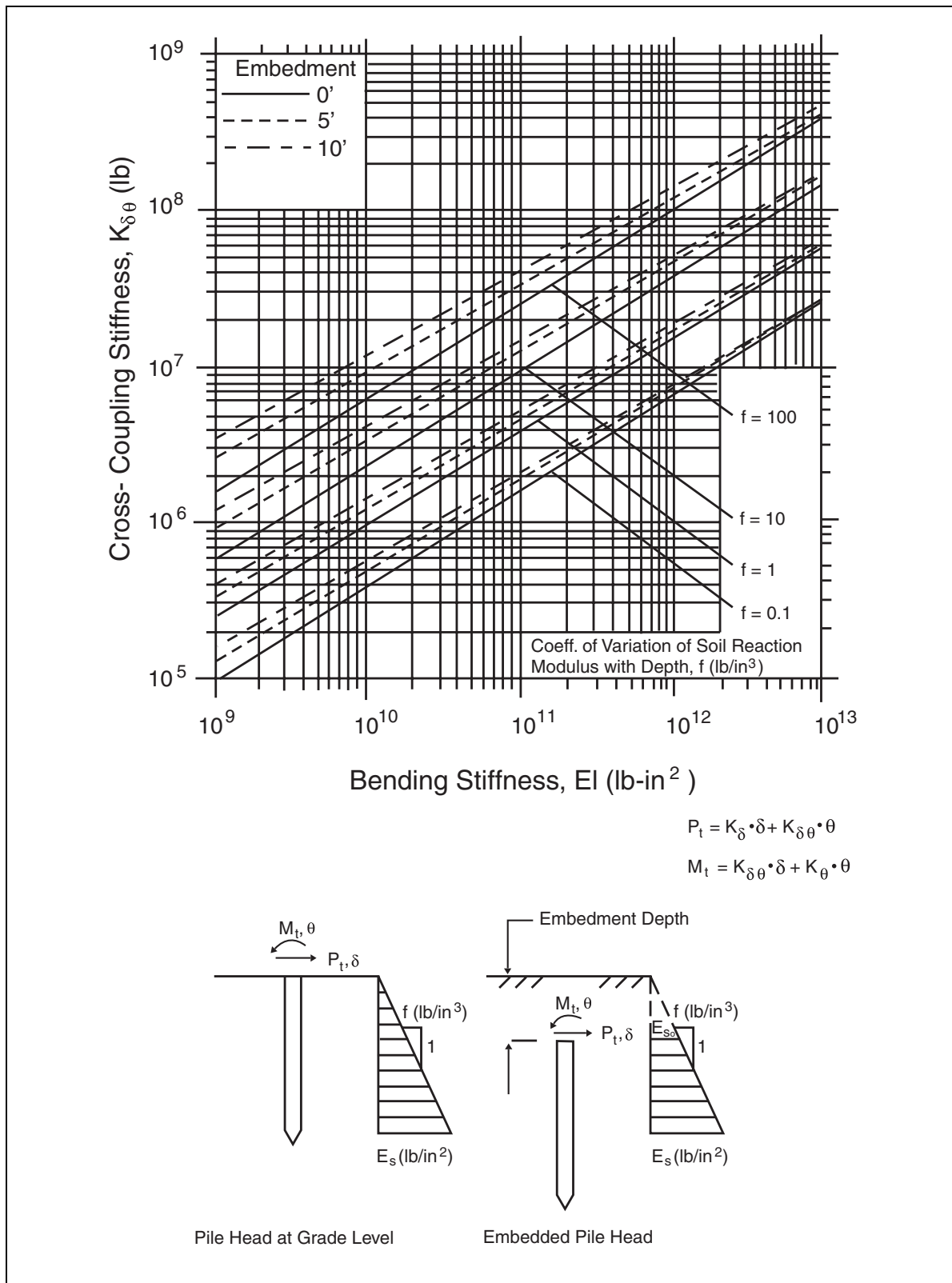


Figure 6-16. Embedded pile cross-coupling pile-head stiffness.

6.2.2.2(c). *Pile-Head Stiffness – Axial Loading*

The axial stiffness of a pile head is generally assumed to be uncoupled from the stiffnesses in the lateral and rotational directions. Axial load-displacement characteristics are also assumed to be uncoupled from the lateral load-displacement behavior because much of the soil resistance to axial loading comes from relatively deep elevations. As a result, these properties are relatively insensitive to the characteristics of the shallower, soil-structure-interaction zone that influences lateral loading. However, since the overall resistance to axial loading is derived along a significant length of the pile (especially in the deeper soil strata), and the pile is under a relatively large static dead load prior to the earthquake, a realistic determination of axial properties requires an ability to account for heterogeneous soil layering as well as plastic slippage in the upper part of the pile. As a result, linear, homogeneous analytical solutions should not be used for axial loading calculations. Instead methods that account for both soil layering and plastic slippage at the soil-pile interface should be used, such as the one described below.

A graphical procedure that gives the axial stiffness coefficient and includes layering and slippage (Lam and Martin, 1986), is illustrated in figure 6-17 for a 21.3-m (70-ft) long 0.3-m (1-ft) diameter pipe pile embedded in sand with $\phi = 30^\circ$ and consists of the following steps:

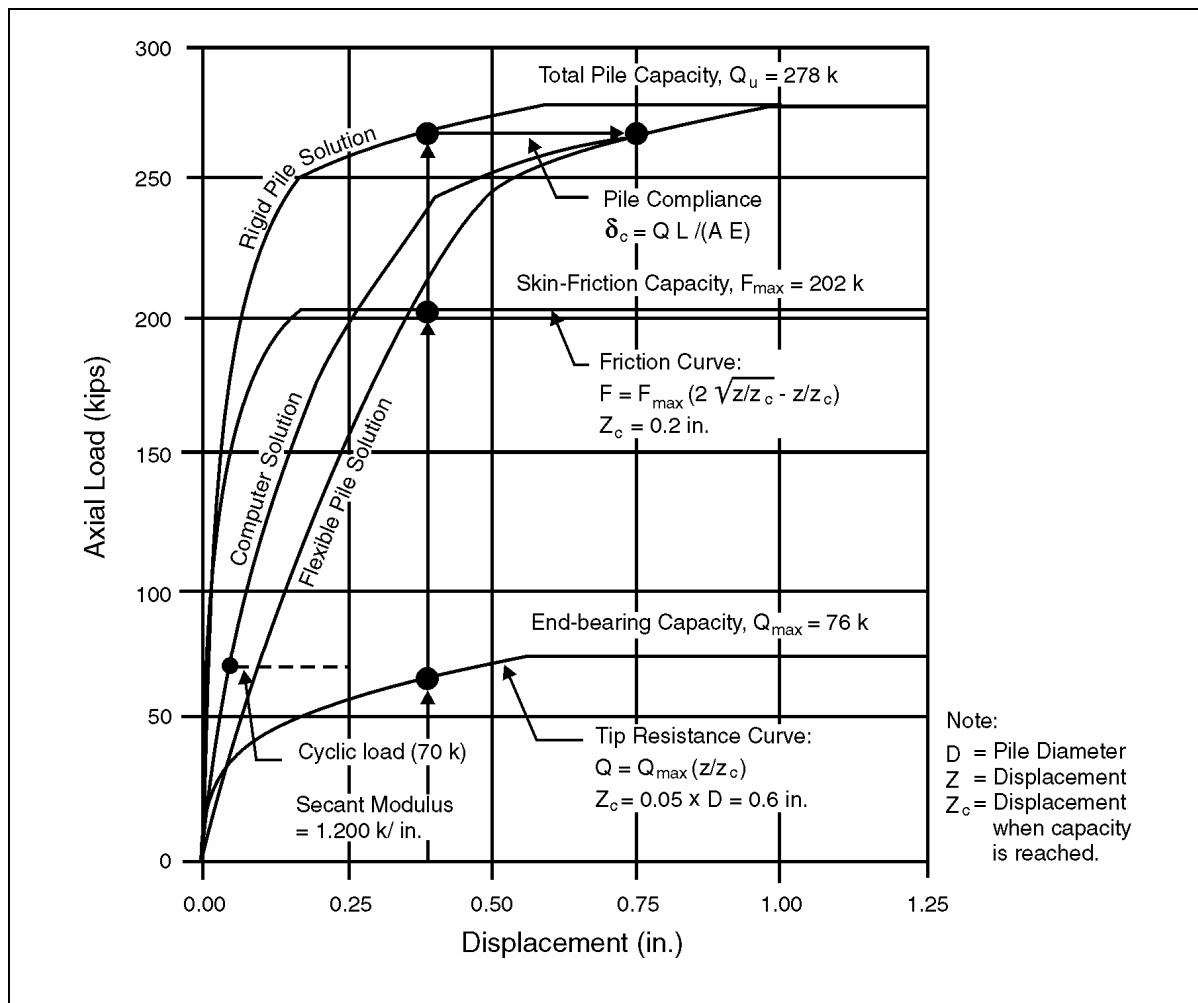
- Step 1. Ultimate compressive capacity.** Calculate the ultimate pile capacity from a site-specific pile capacity analysis using conventional procedures for skin-friction and end-bearing capacities for the different soil layers. When assigning values to the skin-friction and end-bearing capacities, make allowance for the construction method (e.g., pre-drilling, driving), special conditions (e.g., consolidation due to surcharging, corrosion), and dynamic soil behavior (e.g., cyclic strength degradation, soil liquefaction).
- Step 2. Rigid pile load–displacement curve.** Develop the pile load-displacement curve based on the estimated ultimate capacity and published skin-friction and end-bearing pile displacement relationships. The resulting load-displacement curve in figure 6-17, which was obtained from the sum of the skin friction and end-bearing capacities at each axial displacement, will result in a pile-head load–displacement relationship for a pile that is axially-rigid. This curve is a lower bound on the actual pile displacements.
- Step 3. Flexible pile load-displacement curve.** Calculate the axial displacement at the pile head due to the compression of the pile under axial load but neglecting the surrounding soil. This displacement is given by:

$$\delta_c = \frac{QL}{AE} \quad (6-8)$$

where Q is the axial load, L is the length, and AE is the axial rigidity of pile.

Obtain the flexible pile solution by adding δ_c from equation 6-8, to the rigid-pile load-displacement curve in figure 6-17, at pile loads that correspond to the rigid pile load-displacement curve. This curve is an upper bound on the actual pile displacements.

Step 4. Actual load-displacement curve. As a first approximation, obtain the actual axial load-displacement curve by averaging the curves from steps 2 and 3. The actual solution is bounded by the rigid and flexible load-displacement solutions derived in steps 2 and 3 and depends on the nature of the soil-pile system. Averaging the results is a good place to start. For an end-bearing pile, the actual curve may be closer to the flexible-pile solution. For a friction pile at small load levels, the upper portion of the pile is compressed first, and thus the load-displacement curve will be closer to the rigid-pile curve. At higher loads, slippage occurs along most of the pile and the solution moves towards the flexible-pile curve.



after Lam and Martin, 1986

Figure 6-17. Axial load-displacement graphical solution.

Step 5. Axial pile stiffness. Calculate a value for the pile secant stiffness from the load-displacement curve over the range of expected displacements, and use it to find the equivalent axial stiffness coefficient for inclusion in the pile stiffness matrix. Expected displacements may be found from the expected range of axial loads, which for a regular highway bridge foundation would be in the range of 50 to 70 percent of the ultimate pile capacity.

The above procedure may be used to obtain the corresponding *uplift* load-displacement curve by ignoring end-bearing and using only skin-friction to evaluate capacity.

In an even simpler approximation, values for pile-head stiffness under normal loading (not exceeding the capacity) may be expressed as a multiple of AE/L , with the constant, α , depending on the relative amounts of skin friction and end bearing resistance that are mobilized (Gohl, 1993). For example, a value of $\alpha = 1$ gives a lower bound to the stiffness (i.e. AE/L), and would be appropriate for an end-bearing pile on rock with negligible skin friction. Values of α close to 2.0 would be reasonable for friction piles with negligible end tip resistance.

6.2.2.2(d). *Pile Group Analysis*

A group of piles may be modeled in a dynamic analysis of a bridge by either a series of uncoupled springs or a fully coupled foundation stiffness matrix, as shown in figure 6-18. The latter model is the most general and rigorous approach, and requires the determination of the stiffness coefficients in a generalized 6 x 6 stiffness matrix for each pile. The matrix represents the lateral and rotational (rocking) stiffnesses for and about the two horizontal axes, and their cross-coupling terms. The vertical and rotational stiffnesses for and about the vertical axis, are also included (Lam et al., 1998).

The buried pile cap represents an additional but very important component. As previously noted, the pile cap is uncoupled from the piles to determine the lateral stiffness coefficients, which are then added to the pile stiffness matrix. In many cases, the pile cap stiffness will be significantly greater than the lateral stiffness of the pile group.

For a vertical pile group, the stiffness for the translational displacement terms (the two horizontal and one vertical displacement terms) and the cross-coupling terms can be obtained by merely multiplying the corresponding stiffness components of a single pile by the number of piles. However, the rotational stiffness terms (the two rocking and torsional rotations) require consideration of an additional stiffness component. In addition to individual pile-head bending moments, a unit rotation at the pile cap will introduce displacements and corresponding forces at each pile head (e.g., vertical forces for rocking rotation and lateral pile forces for torsional rotation). These pile-head forces will work together among the piles and will result in an additional moment reaction on the overall pile group. In most cases, the axial stiffness of the piles will dominate the rotational or rocking stiffness of the group.

The above procedure does not account for ‘group effects’, which relate to the interaction between closely spaced piles and the properties of the surrounding soil, particularly if nonlinear behavior occurs. In general, pile spacings of less than three to five pile diameters are necessary

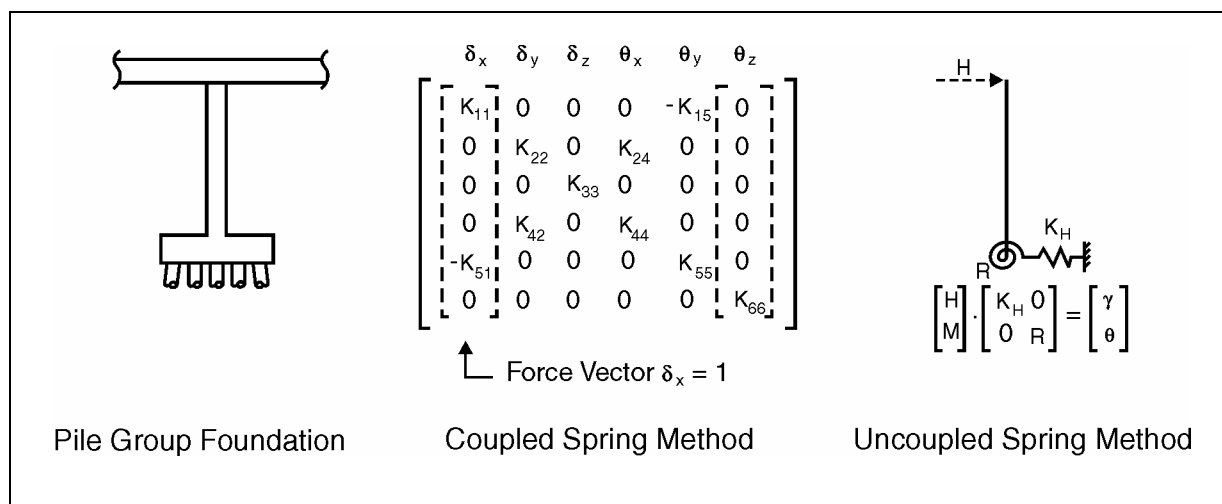


Figure 6-18. Modeling approaches for deep foundations.

before the effects of pile interaction become significant in practical terms. Experimental data on p-y multipliers for closely spaced piles in sand, indicate about a 20 percent loss for pile spacings of three diameters⁷. Detailed discussion on group effects is given by Lam et al. (1998).

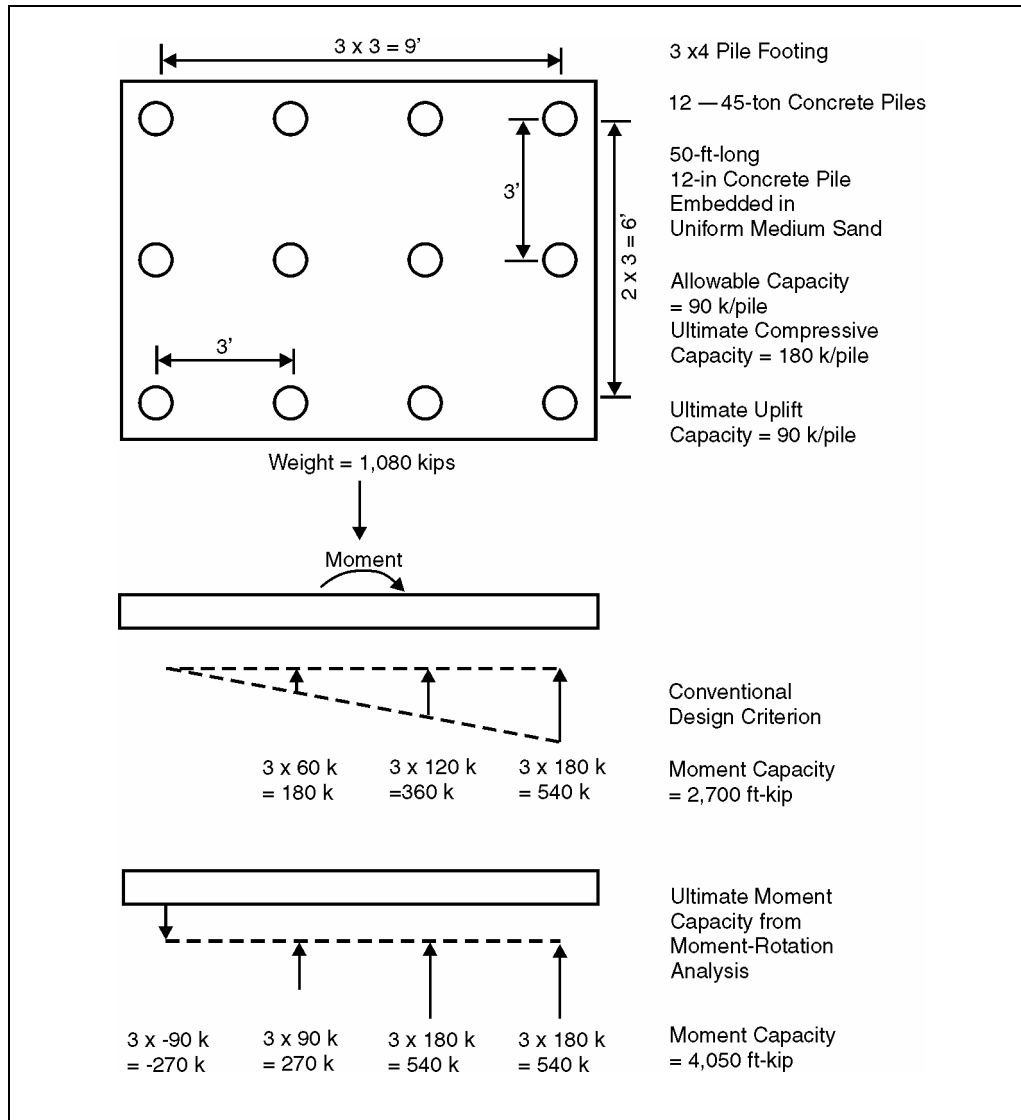
6.2.2.2(e). Pile Group Analyses – Moment-Rotation Capacity

The moment-rotation characteristics and the capacity of a pile footing depend on the following factors:

- Configuration of the pile footing, including the number of piles and spatial dimensions, and
- Capacity of each pile for both compression and uplift loading.

This is illustrated in figure 6-19 by way of an example problem involving a typical pile footing (Lam, 1994). The load-displacement curves for each individual pile in the pile group are shown in figure 6-20. The pile is modeled as an elastic beam-column, and nonlinear axial soil springs are distributed along the pile to represent the soil resistance in both compression and uplift. The pile cap is assumed to be rigid. It can be seen from the figure that the ultimate soil capacities of the pile for compression and tension are 800 and 400 kN (180 and 90 kips) per pile, respectively. This assumes that the connection details and the pile member have sufficient strength to ensure that the failure takes place in the soil. The pile is assumed to be 15 m (50ft) long, and have a diameter of 0.3m (12in). It is a concrete pile, driven into a uniform medium sand, which has a design load capacity of 400 kN (45 tons) per pile. The adopted ultimate capacity values (800 kN [180 kips] compression and 400 kN [90 kips] uplift) are default values commonly assumed in seismic retrofit projects for the 400 kN (45 ton) class pile. In the example, it is assumed that the footing has been designed for a static factor of safety of 2.0, and the piles are loaded to 50 percent of the ultimate compression capacity before the earthquake.

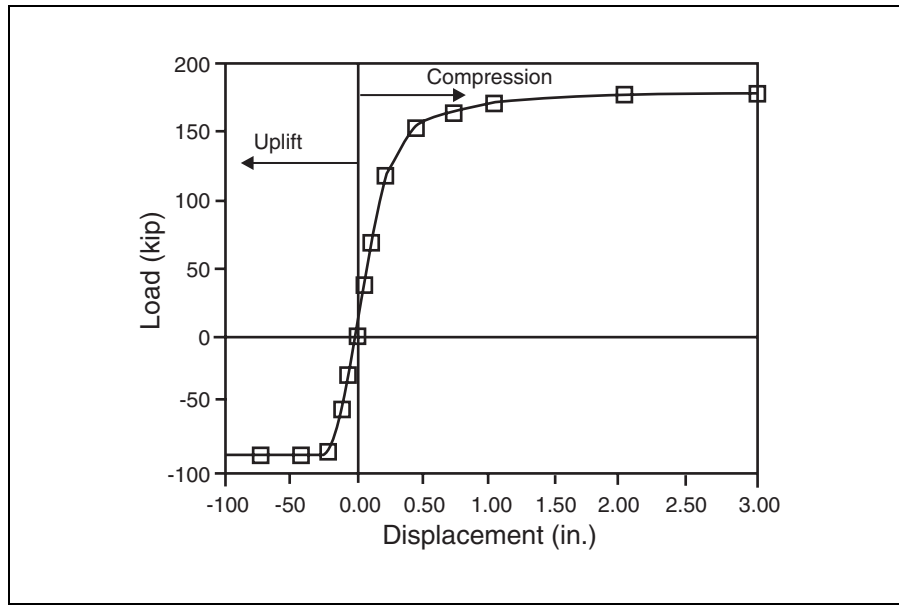
⁷ Brown et al. (1988); McVay et al. (1995)



Lam, 1994

Figure 6-19. Pile footing configuration for moment-rotation study.

Figure 6-19 presents various capacity criteria for the pile footing. Under conventional practice, the moment capacity of the pile footing would be 3,665 kNm (2,700 kip/ft). This capacity is due to the assumption of a linear distribution of the pile reaction across the footing. The moment capacity of 3,665 kNm (2,700 kip/ft) is limited by the ultimate compressive capacity value of the most heavily loaded pile (800 kN [180 kip] per pile) while maintaining vertical equilibrium of the overall pile group (i.e., for a static load of 4,800 kN [1,080 kips]). The lowest part of figure 6-19 presents the moment capacity that can be achieved from a nonlinear moment-rotation analysis of the pile footing, in which the moment increases above the conventional capacity. Nonlinear load-displacement characteristics of the pile are included to allow additional load be distributed to the other less-loaded piles in the pile group. As shown, a maximum ultimate capacity of 5,500 kNm (4,050 kip/ft), which is 50 percent above the conventional capacity, is estimated by this nonlinear analysis.

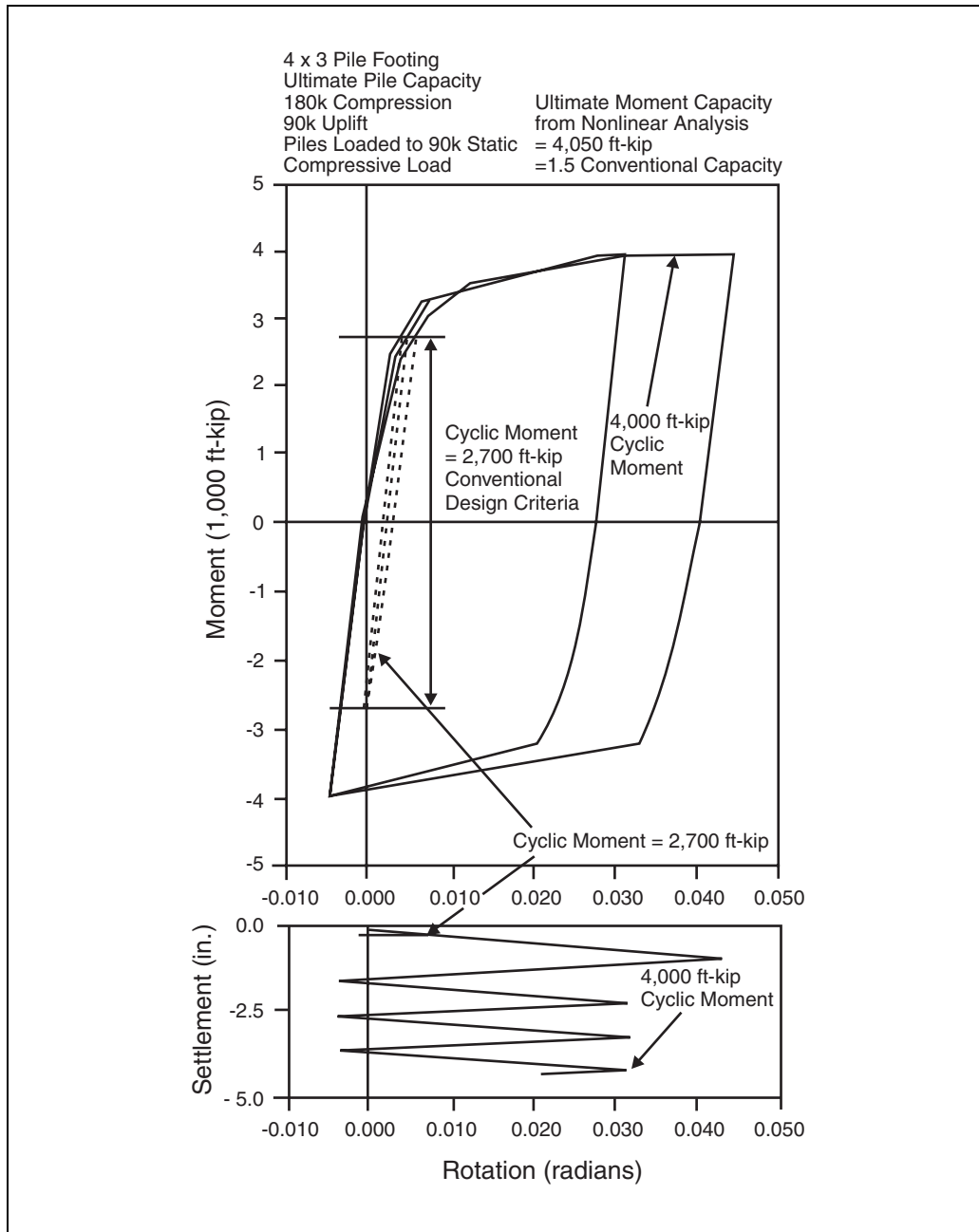


Lam, 1994

Figure 6-20. Axial load-displacement curve for single pile.

Figure 6-21 presents the cyclic moment-rotation solutions for the example discussed above. The dotted line on the moment-rotation plot defines the monotonic loading path of the moment-rotation relationship. Solutions for two uniform cyclic moment loads are presented: a lower cyclic moment level of 3,665 kNm (2,700 kip/ft) corresponding to the conventional design capacity, and a higher cyclic moment load of 5,500 kNm (4,050 kip/ft). As shown in the figure, at the lower cyclic moment of 3,665 kNm (2,700 kip/ft), the moment-rotation characteristic is almost linear, and both the moment-rotation characteristics and settlement will equilibrate to a final value very quickly, i.e. within a few cycles of loading. However, at the higher cyclic moment load of 5,500 kNm (4,050 kip/ft), progressive settlement of the footing is occurring and, within about four cycles of loading, the footing settles almost 125 mm (5 in). The moment-rotation relationship also indicates that some level of permanent rotation of the footing will likely occur even if the load is symmetric between positive and negative cyclic moments. The potential for the permanent rotation is associated with the change in the state of stress in the soil from a virgin (unstressed) condition to the equilibrated state after cyclic loading, unloading, and reloading. A similar analysis, using a static factor of safety of 3.0 (rather than 2.0) corresponding to a dead load of 3,200 kN (720 kips), resulted in an ultimate moment capacity of 130 percent of the conventional capacity, and a reduced settlement of about 6 mm (0.25 in) under loading cycles at the increased ultimate capacity level.

Considering the conservatism in the estimates of pile capacity (especially for compressive loading), most existing pile footings probably have an static factor of safety for dead load greater than 3.0. Hence, it can be speculated that, the potential for significant settlement or rotation of a pile footing is not high, except on poor soil sites where cyclic degradation of soil strength can be significant. Instead, the most likely cause of foundation failure will be some form of permanent rotation of the pile group, if the size of the footing and the number of piles are inadequate.



Lam, 1994

Figure 6-21. Cyclic moment-rotation and settlement-rotation solutions.

6.2.2.3. Drilled Shafts

Drilled shafts are large diameter piles (normally greater than 600 mm [2.0 ft] in diameter) that are used to support high axial loads and overturning moments. They are constructed by drilling, or auguring, a hole in the ground, which may then be lined to support the sides of the excavation. When drilling is complete, a reinforcement cage is placed and the cavity filled with concrete. Because installation is straightforward, with minimum disturbance to the site, and they have high

load carrying capacity, drilled shafts are often advantageous over conventional small diameter piles for many bridge configurations.

The analysis and design of a drilled shaft is, for the most part, similar to that for a conventional-driven pile. Important differences exist, however, due to installation procedure, larger diameter, and a small length-to-diameter ratio compared to typical smaller driven piles. Also, for bridges, the structural arrangement of drilled shaft foundations can be different from that of a more conventional foundation. Most bridges supported on drilled shafts are pile-extension type structures involving a single shaft, rather than a group of shafts, as in the case of driven piles. The lateral loads that act on the bridge deck are resisted by the induced shear and bending moment on the drilled shafts, and the overall bridge response is relatively insensitive to axial effects in contrast to pile footings. Where a drilled shaft foundation system consists of a single shaft supporting a column, compressive and uplift loads on these shafts during seismic loading will normally be within limits of load factors used for gravity loading. However, checks should be performed to confirm that any changes in axial load do not exceed ultimate capacities in uplift or compression. In contrast to driven piles in a group, no reserve capacity exists for a single shaft; i.e., if ultimate capacity is exceeded, large deformation can occur. For a pile-extension type structure, the cross-coupling between the lateral and rotational stiffnesses is significant and, therefore, an uncoupled foundation spring model is not appropriate and a cross-coupled matrix formulation should be used instead.

Various studies (Lam et al., 1998) have found that conventional p-y stiffnesses derived for driven piles are too low (soft) for drilled shafts. This stiffer response is attributed to a combination of higher unit side friction, base shear at the bottom of the shaft, and the rotation of the shaft. The rotation effect is often implicitly included in the interpretation of lateral load tests, as most lateral load tests are conducted in a free-head condition. A scaling factor to stiffen the p-y curves equal to the ratio of shaft diameter to 600 mm (2.0 ft) is generally applicable (Lam et al., 1998). The scaling factor is applied to either the linear subgrade modulus or the resistance value in the p-y curves. This adjustment is thought to be also dependent on the construction method.

A drilled shaft may be represented by an equivalent cantilever beam in a dynamic analysis. The beam is founded at a point of fixity, which is located by matching the beam stiffness to that of the shaft (Lam et al., 1998). If a static pushover analysis is to be used for capacity evaluations, a p-y curve analysis approach will provide more reliable estimates of moment and shear distribution and the location of the depth to fixity may need to be revised.

Because the elastic modulus and effective cross-section of a concrete pile change with strain, the flexural rigidity changes with applied load level. For large diameter concrete piles, minor cracking develops at a relatively small moments and effective section properties should be used when evaluating pile stiffness. In the absence of detailed information regarding steel reinforcement and applied axial load, equivalent properties for the cracked section can be taken at 50 percent of those for the uncracked section. This will be sufficiently accurate for most pile analyses.

The depth of maximum moment for a drilled shaft will often be located 2 to 3 diameters below the ground surface for dense and loose soils, respectively, if the shaft diameter and stiffness are

the same as the column (Lam et al., 1998). For a cracked section with flexural rigidity equal to 50 percent of the uncracked section, the depth to the maximum moment is shallower, being on the order of 1.5 to 2 diameters.

For most piles, the boundary conditions at the pile tip do not affect the pile performance because they are sufficiently far from the structure and the piles can be considered as infinitely long piles when the pile length is larger than 3 times a characteristic length, λ , defined as (Lam et al., 1998):

$$\lambda = \left(\frac{EI_p}{E_s} \right)^{0.25}$$

where EI_p is the flexural rigidity of the pile, and E_s is the subgrade modulus of the soil.

For large diameter shafts, it is important to check the pile length, especially for soft soil conditions, to determine the need to include the boundary conditions at the pile tip in the analyses. Lower lengths are acceptable if the drilled shaft provides sufficient lateral stiffness. Lateral load analyses using programs such as LPILE or the FHWA program COM624P would be needed for such determinations.

In many instances, concrete pavement or traffic barriers are constructed around drilled shafts at the ground level. Unless a gap is maintained around the shaft, the pavement can provide lateral support to the pile, which may in turn influence the pile-head stiffness.

6.2.2.4. Abutments

Abutment walls and wingwalls can play a very beneficial role in the performance of a bridge during an earthquake, because the back fills behind these walls can resist large inertial loads and thus reduce ductility demands elsewhere in the bridge. The extent of this reduction depends on the structural configuration (e.g. simple or continuous spans), load-transfer mechanism from the bridge to the abutment system (e.g. integral or seat type abutments), effective stiffness and force capacity of the wall-soil system, and the level of acceptable damage to the abutment that is consistent with the performance criteria. The capacity of the abutments for the inertial load is determined by the structural design of the abutment wall and the shear keys, if any, as well as the resistance of the soil that can be mobilized.

6.2.2.4(a). Abutment Capacity – Longitudinal Direction

Under earthquake loading, the earth pressure action on abutment walls changes from a static condition to one of two possible conditions, depending on the movement of the abutment walls, the bridge superstructure, and the bridge/abutment configuration.

For seat-type abutments where the expansion joint is sufficiently large to accommodate the movement between the abutment wall and the bridge superstructure (i.e., the superstructure does not strike the wall), the earthquake-induced earth pressure on the abutment wall will be the active pressure condition. However, when the gap at the expansion joint is too small to accommodate

the relative movements, there will be a transfer of forces from the superstructure to the abutment wall. As a result, the active earth pressure condition is no longer valid and the earth pressure behind the wall approaches a passive pressure condition due to loading from the bridge superstructure.

For integral or diaphragm abutments as shown in figure 6-22, the abutment stiffness and capacity under passive pressure must be defined as described below.

However, for high, seat-type abutment walls, earthquake-induced active earth pressures will continue to act below the backwall if the backwall fails. These active pressures need to be considered in checking wall stability. In these circumstances, backwall failure may be a desirable condition so as to avoid backward tilt of the wall. This technique is commonly deployed for new design and for the same reason, the backwalls of existing abutments might be modified to encourage their 'early' failure. This retrofit measure is strongly recommended for bridges in Seismic Hazard Levels III and IV.

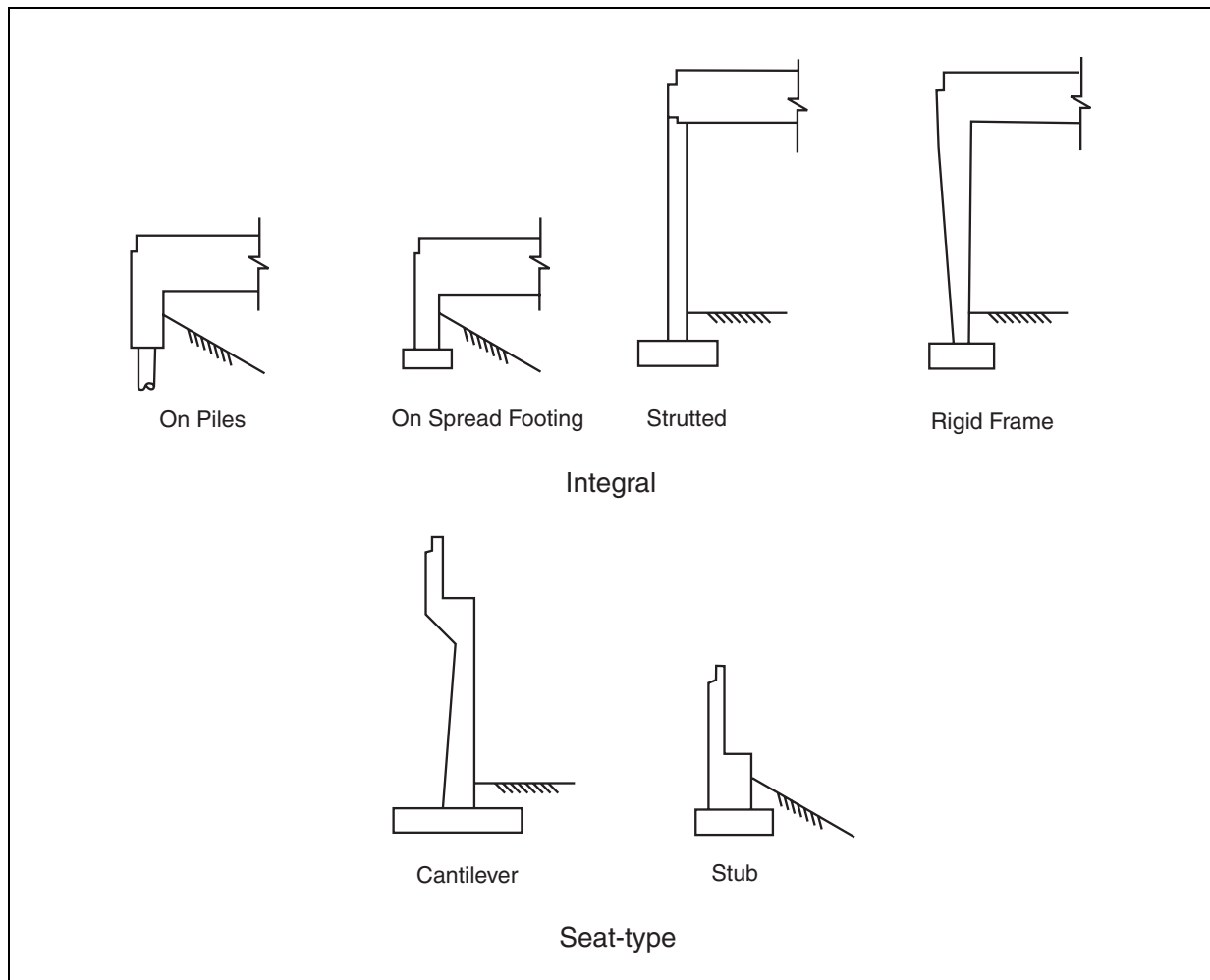


Figure 6-22. Abutment types.

For Seismic Hazard Levels III and IV, the resistance due to passive pressure in the soils behind the abutment walls, will usually be mobilized by large longitudinal superstructure displacements. For design purposes, static passive pressures may be used without reduction for inertial loading effects in the abutment backfill. The passive pressure zone that is mobilized by the displacement of the abutment, extends beyond the active pressure zone normally adopted for static service-load design, as illustrated schematically in figure 6-23. Hence, the soil properties (compressive strength, c , and internal friction angle, ϕ) in the zone will control passive pressures.

Abutment stiffness and passive pressure capacity should be characterized by a bi-linear relationship as shown in figure 6-24. For seat-type abutments, knock-off backwall details should be used with superstructure diaphragms that are designed to accommodate passive pressures. Passive pressures may be assumed uniformly distributed over the height of the backwall or diaphragm. Thus, the total passive force per unit length of wall, P_p , is:

$$P_p = p_p H \quad (6-9)$$

where p_p is the passive pressure behind the backwall, and H is the wall height.

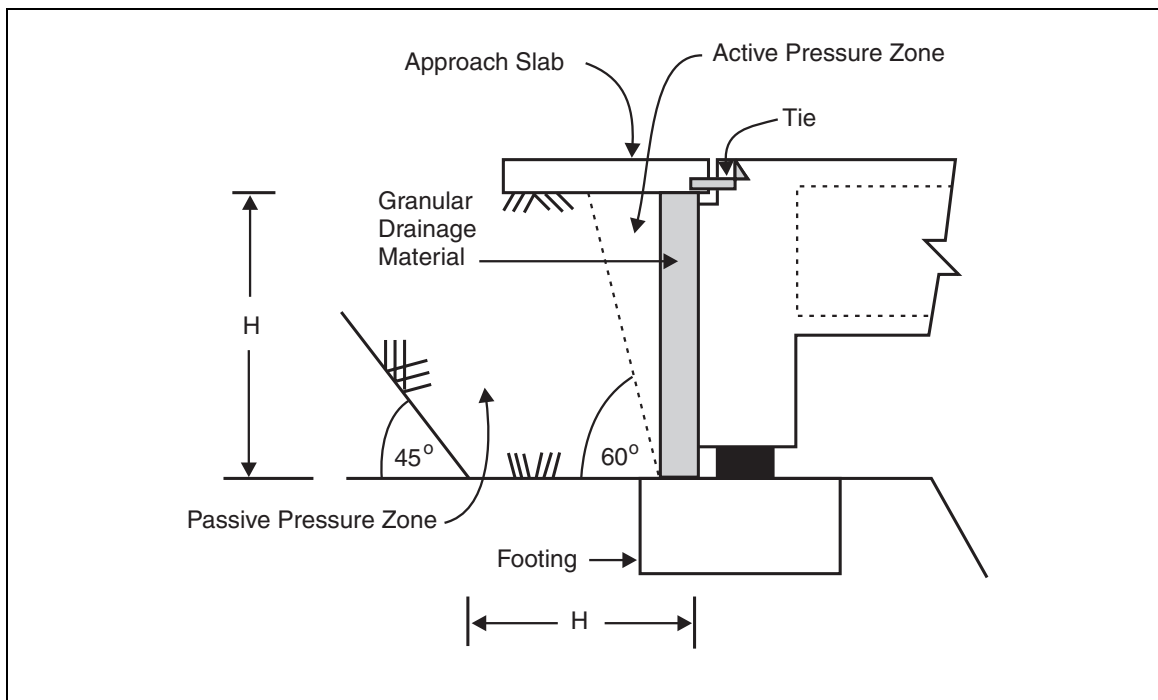


Figure 6-23. Design passive pressure zone.

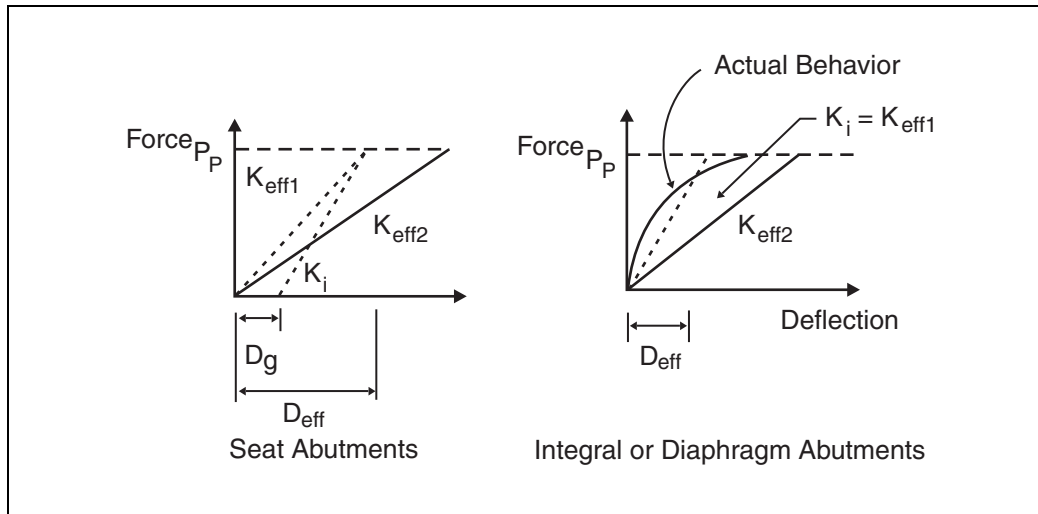


Figure 6-24. Characterization of abutment capacity and stiffness.

6.2.2.4(b). Calculation of Best-Estimate Passive Force, P_p

If the strength characteristics of compacted or natural soils in the passive pressure zone (total stress strength parameters c and ϕ) are known, then the passive force for a given height, H , may be calculated using accepted procedures. These procedures should account for the interface friction between the wall and the soil. (A conservative value equal to 50 percent of the friction angle of the backfill adjacent to the wall is recommended.) The strength properties used shall be indicative of the entire passive pressure zone as indicated in figure 6-23. Therefore, backfill properties adjacent to the wall in the active pressure zone may not be appropriate.

If default passive pressures are to be used for design, then the following values might be used:

1. For cohesionless, non-plastic backfill (fines content less than 30 percent), the passive pressure, p_p , may be assumed equal to $H/10$ MPa (H in meters) or $2H/3$ ksf (H in feet).
2. For cohesive backfill (clay fraction > 15 percent), the passive pressure, p_p , may be assumed equal to 0.25 MPa (5 ksf) provided the estimated unconfined compressive strength is greater than 0.20 MPa (4 ksf).

Alternatively, the approximate approach shown in figure 6-6 may be adopted.

6.2.2.4(c). Abutment Stiffness – Longitudinal Direction

For integral or diaphragm abutments, an initial secant stiffness, K_{eff1} as shown in figure 6-24, may be calculated as follows:

$$K_{eff1} = \frac{P_p}{0.02H} \quad (6-10)$$

where it is assumed that the displacement D_{eff} where P_p is mobilized equals $0.02H$.

If computed abutment forces exceed the capacity, the stiffness should be reduced iteratively (K_{eff1} to K_{effn}) until abutment displacements are consistent (within 30 percent) with the assumed stiffness. For seat-type abutments, the expansion gap should be included in the calculation of secant stiffness. Thus:

$$K_{eff} = \frac{P_p}{(0.02H + D_g)} \quad (6-11)$$

where D_g is the gap width.

Where nonlinear or pushover analyses are conducted, values of P_p and the initial estimate of K_{eff} should be used to define the bilinear load-displacement behavior of the abutment for the assessment of capacity.

For partial- or full-depth seat abutment walls, where knock-off backwalls are activated, the design of the remaining portion of the wall, and a stability check under the action of continuing earthquake-induced active pressures, should be evaluated. For the ‘no collapse’ performance criteria, and assuming conventional cantilever retaining wall construction, horizontal wall translation under dynamic active pressure loading is acceptable. However, rotational instability may lead to collapse and thus should be prevented.

The design approach is similar to that of a free-standing retaining wall, except that lateral forces from the bridge superstructure should be included in equilibrium evaluations, as the superstructure moves away from the wall. Earthquake-induced active earth pressures should be computed using horizontal accelerations that are at least equal to 50 percent of the site peak ground acceleration, which assumes that limited sliding of the wall has occurred during the earthquake. A limiting equilibrium condition should be checked in the horizontal direction. To ensure safety against potential overturning about the toe, a restoring moment of at least 50 percent more than the overturning moment should exist. If necessary, wall design (initially based on a static loading condition) should be modified to meet the above condition.

For the case of seismic active earth pressures, the Mononobe-Okabe equations are often used. These are based on Coulomb failure wedge assumptions and a cohesionless backfill. For high accelerations and/or for backslopes, these equations lead to excessively high pressures that tend to infinity at critical acceleration levels or backslope angles. For the latter conditions, no real solution to the equations exist, implying that equilibrium is not possible (Das, 1999). For example, in a horizontal backfill of sand with a friction angle of 40 degree, a wall friction of 20 degrees, and a peak acceleration of $0.4g$, the failure surface angle is 20 degrees to the horizontal. For a peak acceleration of $0.84g$, the active pressure becomes infinite, implying a horizontal failure surface.

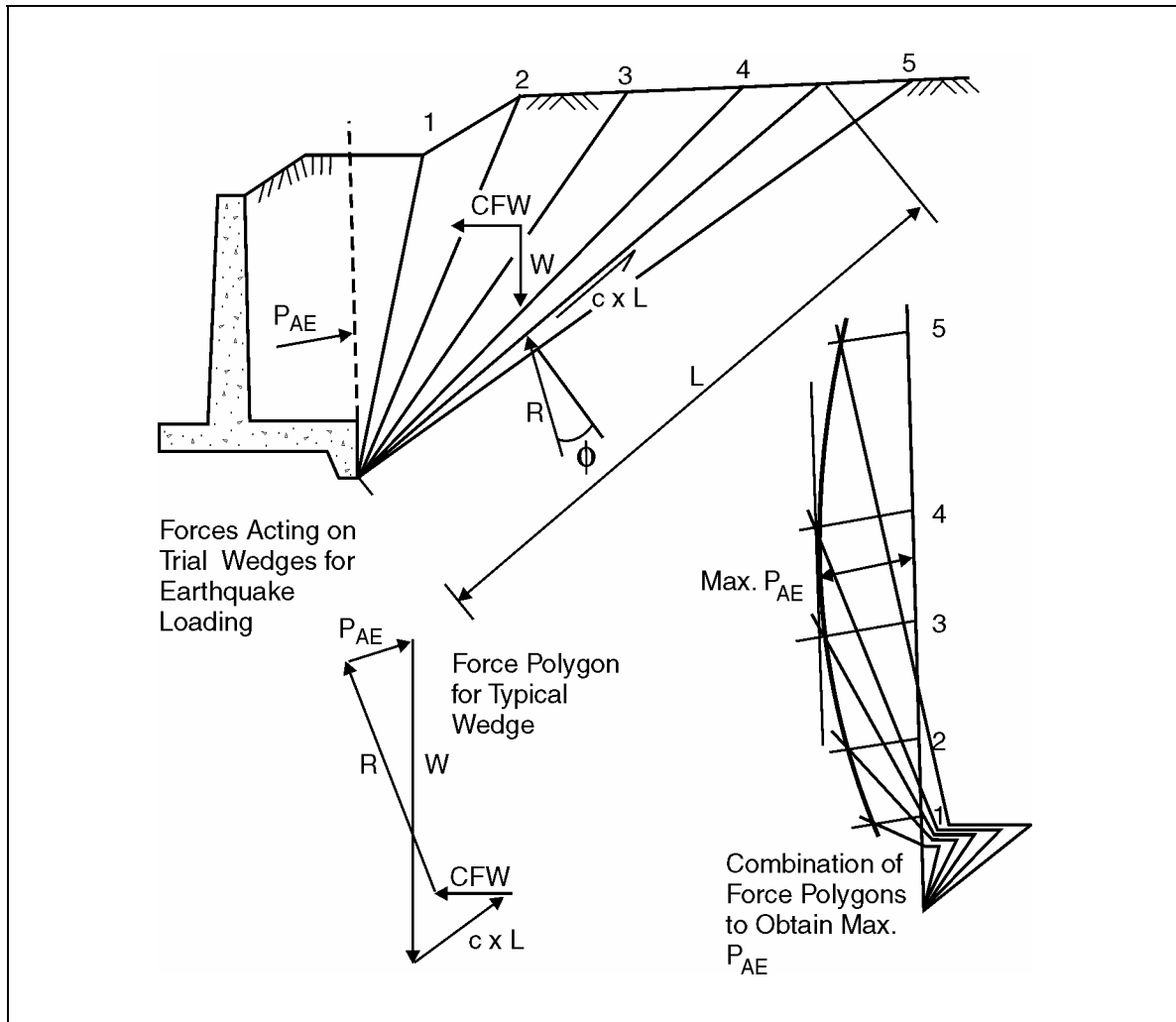


Figure 6-25. Trial wedge method for determining critical earthquake-induced active forces.

Clearly, for practical situations, cohesionless soil is unlikely to be present for a great distance behind an abutment wall and encompass the entire failure wedge under seismic conditions. In some cases, free-draining cohesionless soil may only be placed in the static active wedge (say at a 60° angle) with the remainder of the soil being cohesive embankment fill or even rock. Under these circumstances, the maximum earthquake-induced active pressure should be determined using trial wedges as shown in figure 6-25, with the strength on the failure planes determined from the strength parameters for the soils through which the failure plane passes. This approach will provide more realistic estimates of active pressure.

6.3. GROUND DISPLACEMENT DEMANDS ON FOUNDATIONS

6.3.1. SOURCES OF DEMAND

The two principal sources of ground displacement demands on foundations are due to ground settlement and lateral spreading during liquefaction. Both are discussed below.

6.3.1.1. Earthquake-Induced Settlement

Procedures for calculating the magnitude of earthquake-induced settlement in both saturated and unsaturated sands are described in section 3.3 and appendix B, and are based primarily on the Tokimatsu and Seed (1987) procedures. A methodology for estimating settlements of highway embankment fills is also available in Part 2 of this manual.

Settlements should be estimated for each foundation component. However, the force demands on the bridge due to settlement will be a function of size of the relative settlement between adjacent piers and/or abutments, and the flexibility and/or articulation of the bridge. Displacement demands will determine collapse potential due to the possible unseating of the superstructure. The minimum seat widths defined in equations 5-1a and 5-1b, include an allowance for possible ground rotation due to settlement, which may lead to unseating at the top of the pier. Computed demands on the seats, due to footing rotation, should be checked against these minima. Additional demands due to lateral spreading are discussed in the following section.

Even though collapse may have been prevented due to adequate seat widths, differential settlements may adversely affect performance criteria, and these should be assessed against recommended tolerable limits.⁸

6.3.1.2. Liquefaction-Induced Lateral Spreads

Large rigid-body movements of abutments and piers (both sliding and tilting) can occur when a bridge site liquefies and lateral spreading takes place. Such movements may cause catastrophic damage to the piers and foundations and/or unseat the superstructure.

The Magsayay Bridge was damaged in the 1990 Luzon, Philippines earthquake due to liquefaction (Hall and Scott, 1995). Figure 6-26 shows the collapse mode of four simply supported spans, which was caused by about 2 m (6.5 ft) of lateral spread at the west abutment. As the east abutment did not move, it is possible that a continuous deck may have prevented collapse due to strut action.

⁸ Cooke and Mitchell (1999); Part 2 of this manual

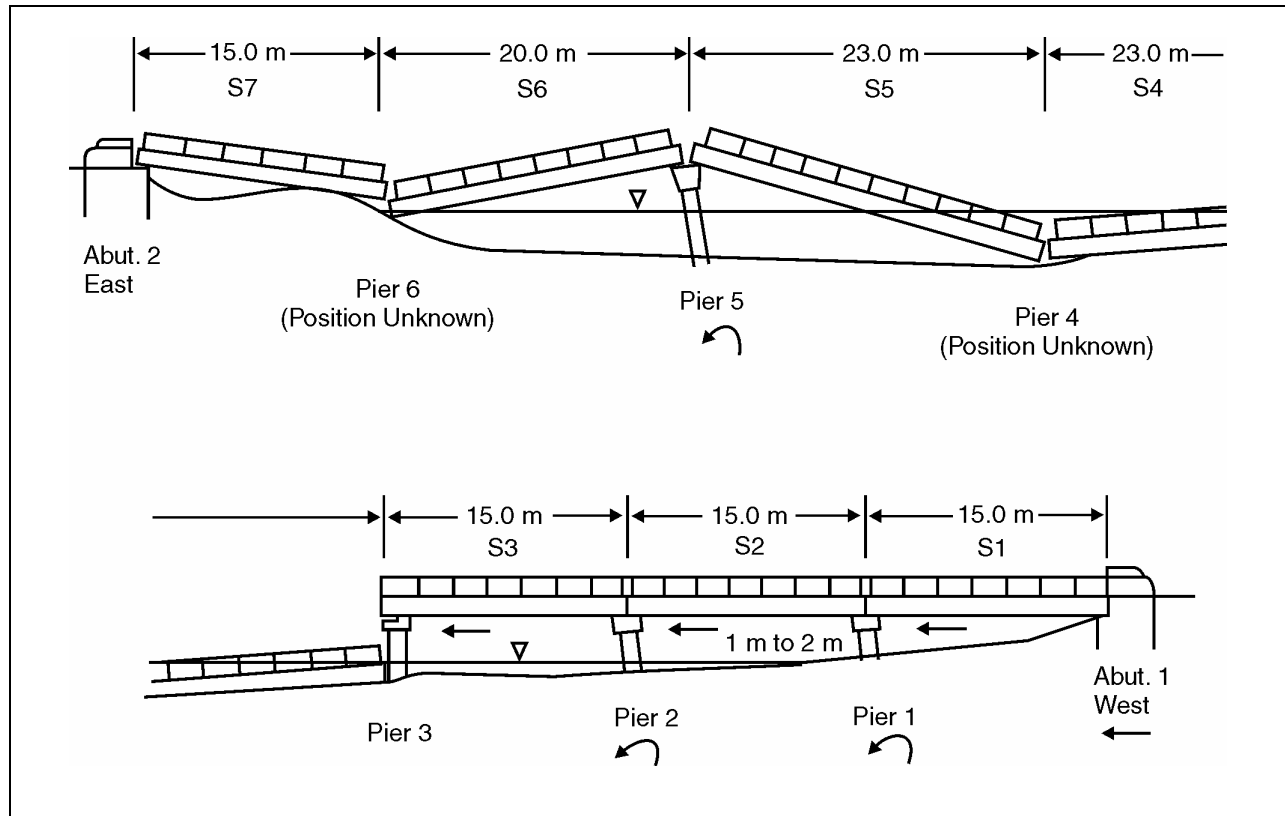
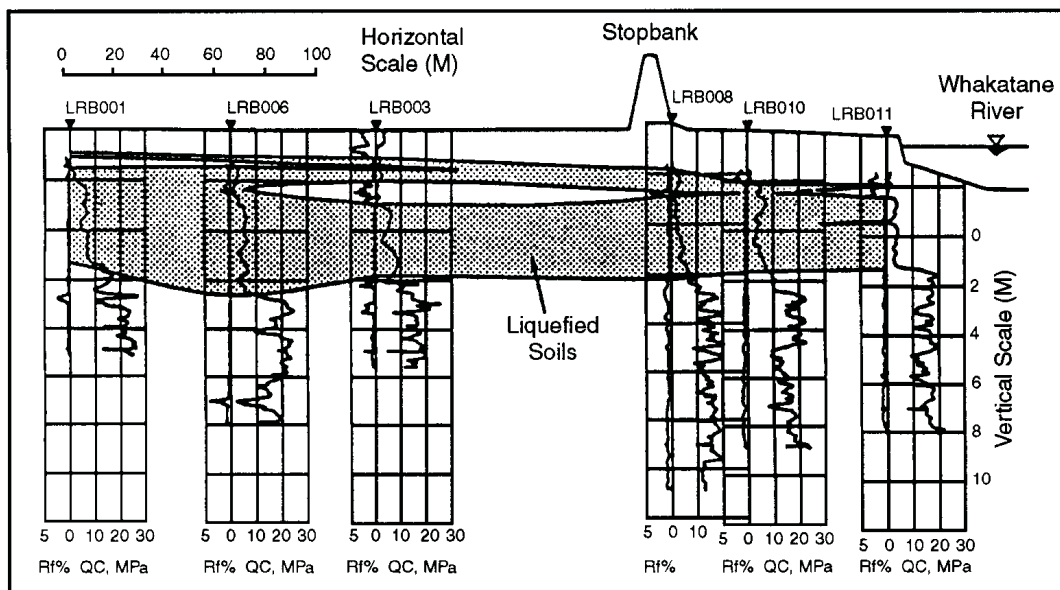


Figure 6-26. Sketch of Magsaysay bridge showing earthquake damage.

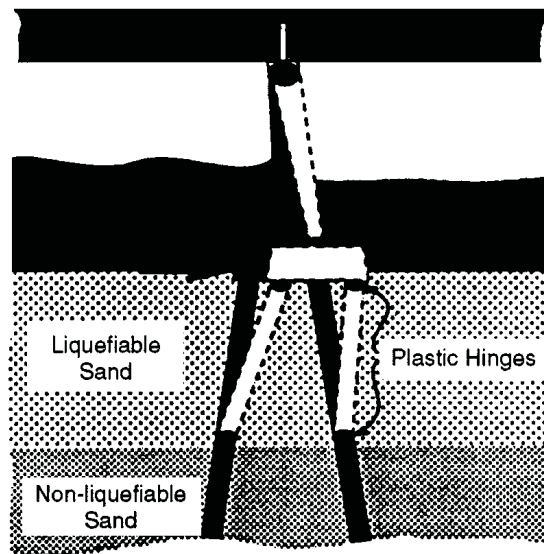
Liquefaction also occurred at the Landing Road Bridge during the 1987 earthquake in Edgecumbe, New Zealand (Berrill et al., 1997). In this case, the approach spans over the riverbank were supported on concrete wall piers founded on battered prestressed concrete piles, as shown in figure 6-27. Liquefaction-induced lateral spreads in the liquefiable sand layer were of the order of 2 m (6.5 ft). Back analyses and observations from site excavations indicated that the piles successfully resisted the passive pressures mobilized against the piers, although cracks in the piles suggested that plastic hinges were on the verge of forming, as shown schematically in figure 6-27.

In the 1995 earthquake in Kobe, Japan, widespread liquefaction occurred and field investigations using borehole cameras and slope indicators showed that failures of piles in lateral spread zones were concentrated at the interfaces between liquefied and non-liquefied layers, as well as near pile heads. Lateral pile analyses using p-y interface springs together with pile deformations induced by estimated ground displacement profiles were consistent with observed pile performance, as can be seen in figure 6-28 (Tokimatsu and Asaka, 1998).

When the potential for liquefaction is identified and significant lateral spreading is expected, the ability of the bridge to accommodate these movements needs to be assessed. This may require a soil-foundation-structure-interaction analysis to be performed. If the bridge is unable to meet the required performance criteria, retrofitting will be necessary assuming it is not feasible to relocate the bridge to a less vulnerable site. Two retrofit options may be considered:



Cross Section AA at Landing Road Bridge showing the estimated liquefied strata
 Cross Section BB is generally similar, with the loose sand layer slightly thicker

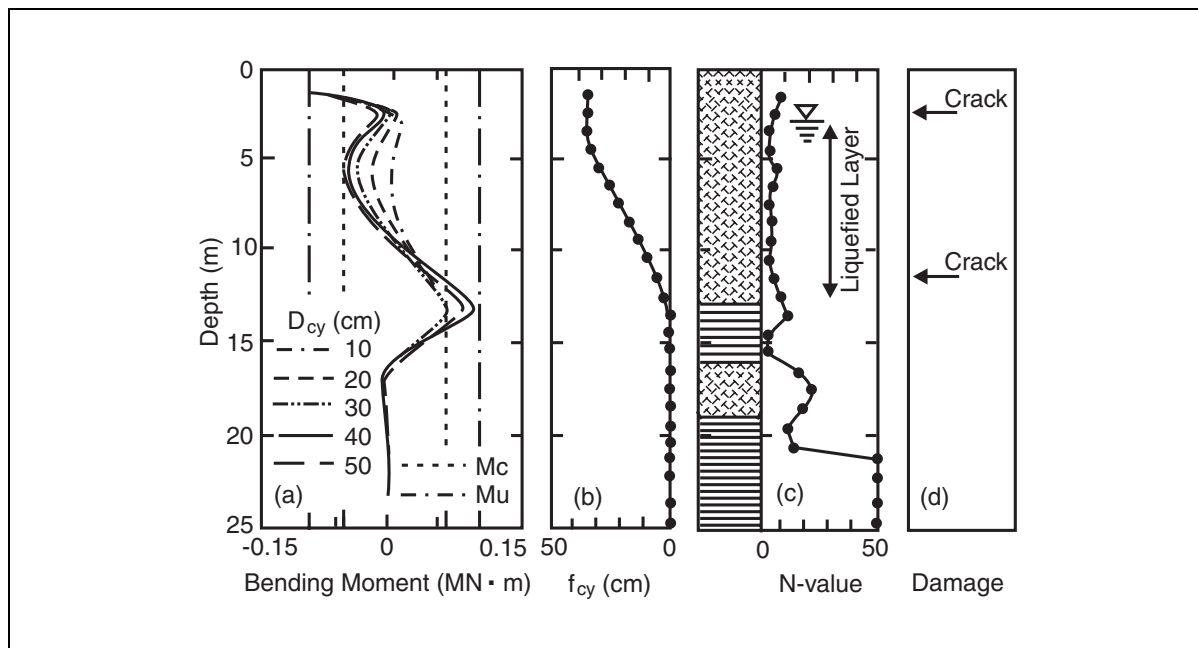


Substructure Collapse Mechanism

Berrill et al., 1997

Figure 6-27. Landing Road bridge lateral spread.

1. Retrofit the foundation / bridge structural system to accommodate the estimated ground movements. This may involve strengthening the foundation system and providing articulation in the superstructure to accommodate the movements. The cost of this work may be compared with the cost of the ground remediation option below.
2. Remediate the site to prevent liquefaction or minimize ground displacement demands. Such methods are also discussed in chapter 11.



after Tokimatsu and Asaka, 1998

Figure 6-28. Site and damage characteristics for a precast concrete pile subjected to a lateral spread in the Kobe earthquake.

6.3.1.3. Slope Stability

The potential for earthquake-induced slope failures or landslides next to a bridge (where landslide debris could damage the structure) or due to the instability of the bridge site itself should be evaluated. Such failures may occur in rock or soil slopes, and may take the form of a major landslide or limited slope movement. Methods of stability analysis and retrofit measures are briefly summarized in chapter 11. Liquefaction-induced instability is addressed in section 6.3.1.2.

CHAPTER 7: STRUCTURAL MODELING AND CAPACITY ASSESSMENT

7.1. GENERAL

As noted in section 1.11 and again in chapter 5, bridge evaluation is essentially a two-part process. A demand analysis is first required to determine the forces and displacements imposed on a bridge by an earthquake. This is followed by an assessment of the capacity to withstand the demand. This process is illustrated in figure 7-1. If the bridge has the capacity to withstand the demand, retrofitting is not required, but if the capacity is less than the demand, a decision needs to be made as to the extent of retrofitting that will be undertaken. Many evaluation methods express their results as capacity/demand ratios; a ratio less than one indicates a need for retrofitting.

Five evaluation methods (A - E) are presented in chapter 5, and several demand analysis methods are also discussed. This chapter continues this discussion with sections on load path, bridge modeling (stiffness, mass and damping), and combination of seismic force effects.

The remainder of this chapter describes methods for assessing the strength and deformation capacities of bridge members (principally columns) for use in the evaluation methods described above. The focus is on individual member behavior. Chapter 5 describes how this information is used to assess the overall capacity of a bridge (Methods D1, D2 and E).

In some instances, preset rules are given as a pragmatic way of providing the required member properties that are necessary for both *capacity* and *demand* analyses for an entire bridge. Where simplified rules are given, it is with the intent to be reasonably (but conservatively) accurate and simple (and thus economical) to apply. For new or unusual situations not covered by these guidelines, member behavior models should be verified by experimental studies.

7.2. LOAD PATH FOR LATERAL FORCES

For a bridge to survive a major earthquake without collapse, a clear and straightforward load path must exist from the superstructure (where the inertia forces act) to the substructure and foundations. Furthermore, all members and components, including connections, in that load path must be capable of resisting the imposed forces and deformations. These members and components include slab-to-beam connections, beam flanges and webs, diaphragms, cross-frames, bearing assemblies, anchor bolts, masonry and sole plates, columns, abutments, footings and foundations.

Members and components in the load path form an earthquake resisting system in which the load is attracted to each element, and its performance is determined by the strength and stiffness characteristics of other elements in the path. Past earthquakes have shown that, when one of these elements responds in a ductile manner, or allows movement, damage is limited. Most

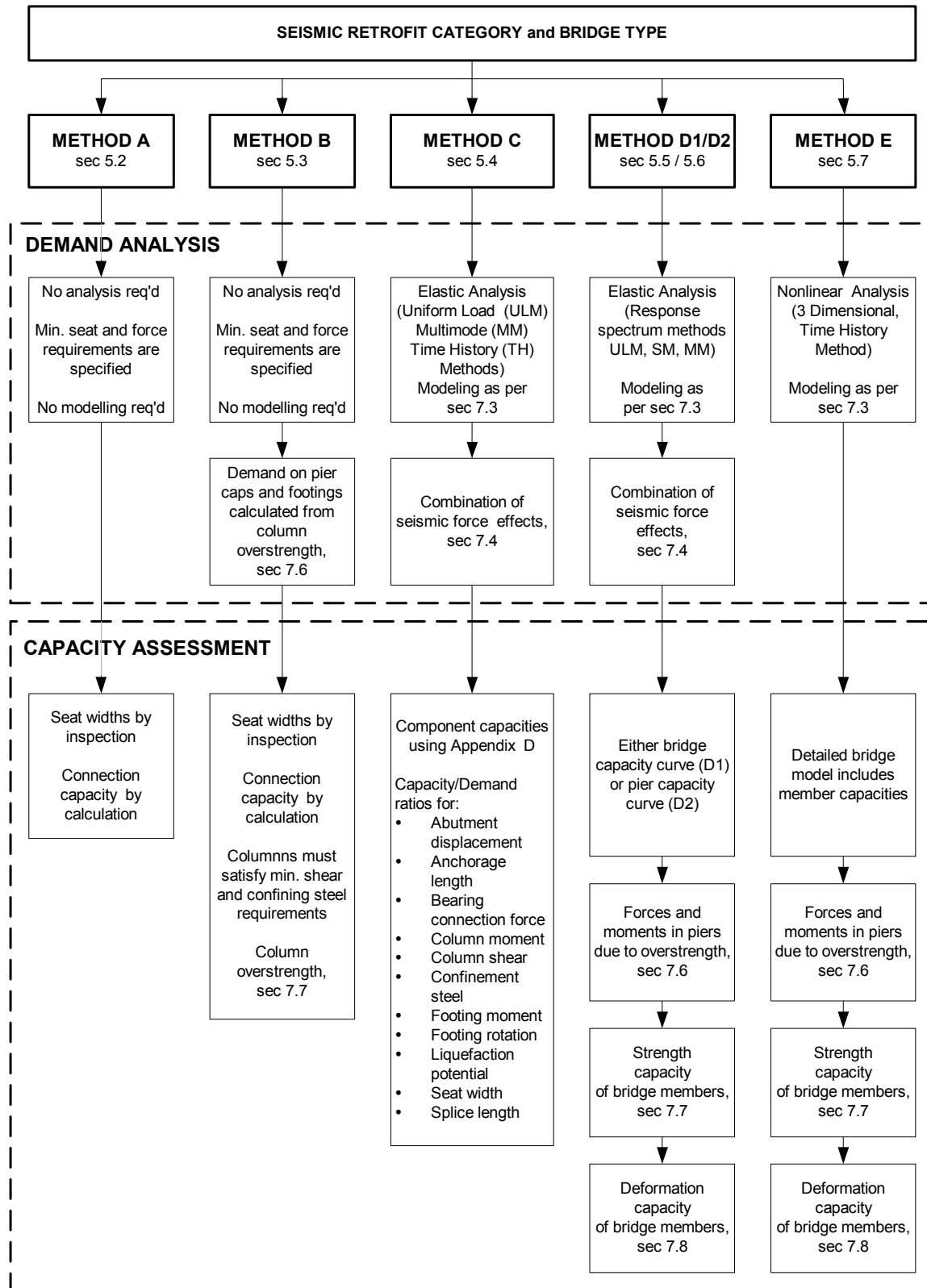


Figure 7-1. Evaluation methods for existing bridges showing relationship between demand analysis and capacity assessment.

retrofit approaches deliberately introduce ductility into selected substructure members (usually columns) for this reason.

Elastic methods of analysis may be used to calculate the forces in the load path; but if extensive yielding occurs, the actual distribution of forces may be quite different from that calculated. A more refined distribution may be found by calculating the forces in the columns and other substructure elements assuming a sufficient number of hinges have formed to allow a collapse mechanism to develop. Superstructure forces are then calculated from the substructure values, including an allowance for overstrength (section 7.6).

However, in lieu of this, the simpler elastic distribution of forces may be used, so long as the applied forces are in equilibrium with the inelastic substructure forces. The eccentricity of the superstructure inertia force from the center of substructure resistance should be considered in this analysis.

The analysis and seismic evaluation of the diaphragms and cross-frames should consider horizontal supports at an appropriate number of bearings. Slenderness and connection requirements of bracing members that are part of the lateral force resisting system should comply with the recommendations given for main members.

Elements not in the seismic load path will also deform during an earthquake, and should be checked to ensure they have sufficient capacity to maintain their load resistance.

In lieu of refined analysis, a conservative load path should be assumed. For example, in bridges with concrete decks that provide horizontal diaphragm action, or with a horizontal bracing system in the plane of the top flange, the lateral loads applied to the deck may be assumed to be transmitted directly to the bearings through the end cross-frames. The development and analysis of the load path is then similar to that used for wind loading.

Where the bridge deck cannot provide horizontal diaphragm action and there is no lateral bracing in the plane of the top flange, lateral loads applied to the deck should be distributed through the intermediate cross-frames to the bottom lateral bracing or the bottom flange, and then to the bearings under the end cross-frames, in proportion to their relative rigidity and the respective tributary mass of the deck.

A continuous load path is necessary for the transmission of the superstructure's inertial forces to the substructure. Concrete decks have significant rigidity in their horizontal plane, and in short-to-medium span slab-on-beam bridges, their response approaches rigid body motion. Therefore, the lateral loading of the intermediate cross-frames is minimal, consisting primarily of local tributary inertia forces from the beams themselves.

It is unlikely that all bearings will see their peak load simultaneously, particularly in the transverse direction. Uneven engagement of side-bar restraints in steel bearings is likely to occur and, if so, some bearings will attract high concentrations of transverse load and others will see negligible loads. Member loads within the cross-frames will then be significantly different from those assumed, and this redistribution should be considered when evaluating cross-frame

members. For the same reason, caution should be exercised when evaluating bearing details including transverse restraints and anchor bolts. This problem is less likely to occur with elastomeric bearings that are bolted to their masonry and sole plates.

7.3. MODELING RECOMMENDATIONS FOR BRIDGE STRUCTURES

Mathematical models used for dynamic analysis should include the strength, stiffness, mass, and energy dissipation characteristics of the structural members and components of the bridge.

Depending on the method of dynamic analysis, different approximations may be used for modeling these quantities. One-dimensional, beam-column members are sufficient for the earthquake analysis of most regular bridges,¹ and grid or finite element models are usually not necessary. Joint size should be included in these models. The advantage of these simple models (sometimes referred to as *spine* models or *stick* models) is that they permit rapid interpretation of results and a quick check on load path and equilibrium.

Irregular bridges¹ include those with skew and horizontal curvature, and three-dimensional models should be used in these cases to more carefully represent the load path, particularly at piers and abutments. Short columns or piers may be modeled as a single element, but tall columns should have two or more elements. This is particularly true if the piers have significant mass as in the case of a concrete bridge, or are framed systems as in the case of a steel tower.

It is not necessary to model bridges with multiple segments as one complete bridge. Each segment (also called a *longitudinal frame* or simply a *frame*) should have sufficient capacity to resist the inertial loads generated within that segment and may be analyzed as a freebody or stand-alone structure. However when the segments have large differences in their modal periods, out-of-phase motion may occur and the frames may adversely interact with each other, causing impact and/or unseating at the hinges.

To account for these effects, the number of segments that should be included in a model depends on the ratio of the fundamental periods. For bridges in which the period ratio of adjacent frames is less than 0.70 (shorter period divided by longer period), it is recommended that the model be limited to five frames. The first and fifth frames in the model are considered to be boundary frames, representing the interaction with the remainder of the structure. The response of the three interior frames can then be used for evaluation. For bridges with frames that have period ratios between 0.70 and 1.0, less than five frames may be used in the model if desired. For a bridge with more than five frames, several different models are required to be analyzed.

Response of a bridge in two orthogonal horizontal directions should be determined in the seismic analysis and the results combined to determine demand forces and deformations (see section 7.4).

If the bridge is located within 10 km (6 mi) of a known active fault, the response in the vertical direction should also be determined and combined with the horizontal response. These bridges should also be subjected to a site-specific study to determine both the horizontal and vertical

¹ *Regular* and *irregular* bridges are as defined in AASHTO, 1998 and 2002.

ground motions for use in the above analyses. Explicit analysis for vertical motions need not be carried out for regular bridges located more than 10 km (6 mi) from an active fault. For irregular bridges, such as those with long flexible spans, C-shaped piers, or with other large eccentricities in the load path for vertical loads, an analysis in the vertical direction should be included (see section 7.5).

7.3.1. DISTRIBUTION OF MASS

Modeling the mass of a bridge should consider the degree of discretization and the expected motion during an earthquake. The number and location of the displacement degrees of freedom in a bridge model determine the way mass is represented and distributed throughout the structure. As most of the mass of a bridge is in the superstructure, four to five elements per span are generally sufficient to represent the superstructure. For *spine* models of superstructures, the beam elements have the same neutral axis as the superstructure and rigid links are then used to locate the mass centroid relative to the neutral axis of these elements.

For single column piers, C-shaped piers, or other unusual configurations, the rotational mass moment of inertia of the superstructure about the longitudinal axis should be included.

The inertia of live loads need not be included in the seismic analysis. However, the probability of a large live load being on the bridge during an earthquake should be considered when evaluating bridges with high live-to-dead load ratios, including those bridges which are located in metropolitan areas where traffic congestion is likely.

7.3.2 DISTRIBUTION OF STIFFNESS AND STRENGTH

The mathematical model should represent the stiffness of individual structural elements considering material properties and section dimensions. When an elastic analysis is used to determine the response of an inelastic structure, significant approximations are necessary. The most important assumption is that stiffness may be based on an equivalent linearized value. For inelastic columns, common practice is to use cracked section properties for concrete members and full section properties for steel members. This value for stiffness is sometimes called a tangential stiffness. However, for seismic isolators, abutments, and foundation soils, stiffness is calculated from the maximum expected deformation. This value is then known as a secant stiffness. The distribution of forces from an elastic analysis should be carefully reviewed to verify that the results are consistent with the expected nonlinear behavior of the earthquake resisting elements.

For Method D2, the Structure Capacity/Demand Method (Pushover or Nonlinear Static Method) described in section 5.6, the mathematical model should use strength values based on expected material properties. For nonlinear dynamic analysis, the model should use the actual stiffness and strength values of the hysteretic elements under seismic loads.

7.3.2.1. Substructures

The stiffness of structural steel members should be based on elastic properties. For reinforced concrete piers, stiffness should be based on cracked section properties, as explained in this section.

Analytical methods for seismic demand generally use stiffness values that are representative of deformations close to the deformations at yield. At these levels of deformation, even prior to yield, reinforced concrete elements crack. The effect of cracking on stiffness depends on the cross-section, longitudinal reinforcement ratio, axial load, and amount of bond slip. The cracked flexural stiffness of a reinforced concrete member can be obtained by moment–curvature analysis of the cross-section, with modifications for bond-slip. In many cases, it is impractical to compute the effective stiffness in this manner, and instead, effective stiffness quantities are assumed based on component rigidity values such as those shown in table 7-1.

Table 7-1. Component rigidities.

Component	Flexural Rigidity	Shear Rigidity	Axial Rigidity
Reinforced concrete columns, beams and caps where cracking (but not hinging) is expected	$0.5 E_c I_g$	$0.4 E_c A_w$	$E_c A_g$
Prestressed concrete beams, caps and piles where cracking is not expected	$E_c I_g$	$0.4 E_c A_w$	$E_c A_g$
Concrete columns, piles and walls where plastic hinging is expected	$\frac{M_n D'}{2\varepsilon_y}$	$0.2 E_c A_g$	$0.5 E_c A_g$
Note: E_c = elastic modulus of concrete, I_g = moment of inertia using gross dimensions, A_w = shear area of column or beam, A_g = cross-sectional area of column or beam using gross dimensions, M_n = nominal moment capacity of column or beam, D' = distance between outer layers of longitudinal reinforcement, and ε_y = yield strain of steel reinforcement.			

From table 7-1 it is noted that for flexurally-dominated regions, where plastic hinging is expected to occur at the ends of the member, the effective flexural rigidity, $E_c I_{eff}$, may be determined from the ‘theoretical’ yield curvature given by:

$$\phi_y = \frac{2\varepsilon_y}{D'} = \frac{M_n}{E_c I_{eff}} \quad (7-1)$$

where:

$$\begin{aligned} \varepsilon_y &= \text{yield strain} = f_y / E_s, \\ f_y &= \text{yield stress (theoretical value, i.e., specified value),} \end{aligned}$$

- E_s = elastic modulus of steel,
- D' = center-to-center distance between the outer layers of longitudinal reinforcement in a rectangular section normal to axis of bending, or pitch circle diameter of the longitudinal reinforcement in a circular section, generally assumed to be 80 percent of overall beam depth or overall column diameter, and
- M_n = nominal yield moment (theoretical yield strength) of the member (see section 7.5).

Thus the effective flexural rigidity of a severely cracked structural concrete column is:

$$E_c I_{\text{eff}} = \frac{M_n D'}{2\epsilon_y} \quad (7-2)$$

This rigidity will generally be somewhat less than $0.5 E_c I_g$ (I_g is the moment of inertia of the gross, uncracked section), which is a commonly assumed value for reinforced concrete members, when only a moderate amount of cracking and no plastic hinging is expected.

Table 7-1 also lists effective values for the shear and axial rigidity of cracked and uncracked reinforced concrete beams and columns with and without plastic hinges. In addition, the torsional stiffness of a cracked reinforced concrete column may be taken as 20 percent of the uncracked value.

For a displacement capacity assessment (pushover method), the strength of structural steel components in the model should be based on their expected plastic capacity. The flexural strength of reinforced and prestressed elements should be based on the expected material properties of the steel and concrete. The objective here is to determine the displacement at which the inelastic components reach their deformation capacity. The deformation capacity is usually expressed in terms of a maximum plastic rotation of hinge zones. The maximum deformation capacity is the sum of the deformation at yield and the plastic deformation (see equation 7-31).

The stiffness of other elements that are not subjected to inelastic response and damage should be based on elastic properties, including the effects of concrete cracking. The stiffness of pier caps should be included in the model. Pile caps and joints in reinforced concrete substructures may be assumed to be rigid.

7.3.2.2. Superstructures

The stiffness of the superstructure should be consistent with the load path (section 7.2) including consideration of composite behavior between girders and decks, and effective width of the superstructure components that are monolithic with piers.

For a stick model of the superstructure, the stiffness can be represented by equivalent section properties for axial deformation, flexure about two axes, torsion, and possibly shear deformation in two directions. The calculation of the section stiffness should represent reasonable assumptions about the three-dimensional flow of forces in the superstructure, including composite behavior.

The effects of skew can be neglected in the model of the superstructure. However, for large skew angles, the geometry of the connection between superstructure and piers must be included.

For reinforced concrete box girders, the effective stiffness may be based on 75 percent of the gross stiffness to account for cracking. For prestressed concrete box girders, the full gross stiffness should be used. The torsional stiffness may be based on a rational shear flow without reduction due to cracking.

The flexural stiffness of the superstructure taken about a transverse axis should be reduced near piers when there is a moment transfer between the superstructure and pier because of shear lag effects. The reduced stiffness should be used in modeling the superstructure.

7.3.3. IN-SPAN HINGES

Two different models are used to represent expansion bearings and in-span hinges. First, a compression model is used that assumes the joint at the bearing or hinge is closed and can transfer longitudinal forces. Then, a tension model is used that assumes the joint or hinge is open and cannot transfer longitudinal forces. The stiffness of restraining devices, such as cable restrainers or shock transmission units, is included in the tension model. Two separate analyses are run, one for each model, and the larger value for a particular force or deformation is used in design.

The use of compression and tension models is expected to provide a reasonable bound on forces (compression model) and displacements (tension model). A compression model need not be considered for expansion bearings if calculations show that longitudinal forces cannot be transferred through the superstructures at the bearing.

7.3.4. DAMPING

Energy dissipation in a bridge, including that developed by the footings and abutments, may be represented with sufficient accuracy by viscous damping. The selection of an effective viscous damping ratio depends on the type of dynamic analysis and the configuration of the bridge. In an elastic response spectrum analysis, this ratio is based on the energy dissipation due to small-to-moderate deformations of the members and soil.

Damping may be neglected in the calculation of natural frequencies and associated mode shapes. The effects of damping should be considered when the dynamic response for seismic loads is considered. This is usually done by scaling the earthquake response spectrum for the correct amount of damping.

Suitable damping values may be obtained from field measurements of induced free vibrations or from forced vibration tests. In lieu of measurements, the following values may be used for the equivalent viscous damping ratio:

- Concrete bridges: five percent.
- Welded and bolted steel bridges: two percent.
- Timber bridges: five percent.

For a single-span or two-span bridge with abutments that are expected to develop significant passive pressure in the longitudinal direction, a damping ratio of up to 10 percent may be used for the longitudinal vibration modes.

Equivalent viscous damping may be used to represent the energy dissipated in the cyclic loading of members beyond yield, but only when a secant stiffness model is used for the entire bridge. For single-degree-of-freedom models, the equivalence can be established within a satisfactory degree of accuracy. For bridges with seismic isolation or with fuses and knock-off walls, only an approximate equivalence can be established. Equivalent viscous damping should not be used to represent inelastic energy dissipation for any other model or method of dynamic analysis.

7.3.5. PERMANENT GROUND MOVEMENT

In general, the effect of gross soil movement and liquefaction should be included in the analysis. However, the need for sophisticated modeling of foundations and abutments depends on the sensitivity of the structure to foundation movements and the degree of conservatism that can be tolerated in the calculated forces. When gross soil movement or liquefaction is possible, and an analysis is required, the model should represent the change in support conditions and additional loads imposed on the substructure due to soil movement.

When the results of a seismic analysis are expected to be sensitive to foundation properties, these properties should be bounded between upper and lower limits of strength and stiffness and multiple analyses carried out. Strength and stiffness values should, however, be consistent with the expected deformations of the soil and the goals of the analysis. The sensitivity of results to the assumptions made about these properties may then be used to direct site investigations for the bridge under consideration.

See also chapter 11, which describes retrofitting measures for bridges on hazardous sites.

7.4. COMBINATION OF SEISMIC FORCE EFFECTS

7.4.1. SEISMIC LOADING IN ONE DIRECTION

Maximum response quantities for use in design, due to seismic loading in one direction, should be based on a combination of modal responses in that direction. The preferred method for this combination is the Complete Quadratic Combination (CQC) method (section 5.4.2.2), because it combines modes with closely-spaced periods more rigorously than other modal combination rules.

7.4.2. SEISMIC LOADING IN TWO OR THREE ORTHOGONAL DIRECTIONS

When combining the responses of two or three orthogonal directions, the design value of any quantity of interest (displacement, bending moment, shear or axial force) should be obtained either by the ‘square root of the sum of the squares’ (SRSS) rule or the 100-40 percent combination rule.

The SRSS rule is the most appropriate one for combining the contribution of orthogonal and uncorrelated ground motion components into a single design force. The method is especially recommended if the vertical components of the ground motion are being used in combination with the horizontal components (Button et al., 1999). However, the familiar 100-30 percent combination rule is also suitable, particularly if the second component is increased from 30 to 40 percent. This option is, however, more conservative than the SRSS combination rule.

These two alternative combination rules may be summarized as follows.

- SRSS Combination Rule – the design value is the SRSS combination of the response quantity from each of the orthogonal directions:

$$M_x = \sqrt{(M_x^T)^2 + (M_x^L)^2 + (M_x^V)^2} \quad (7-3)$$

where M_x^T , M_x^L , M_x^V are the x-components of moment calculated from a transverse, longitudinal and vertical analysis, respectively.

- 100–40 percent Combination Rule – the design value is obtained from the largest value given by the following three load cases.

Load Case 1 (LC1) – 100 percent of the absolute value of the response resulting from the analysis in one orthogonal direction (transverse) is added to 40 percent of the responses resulting from analyses in the other two orthogonal directions (longitudinal and vertical):

$$M_x^{LC1} = M_x^T + 0.4M_x^L + 0.4M_x^V$$

Load Case 2 (LC2) – 100 percent of the absolute value of the response resulting from an analysis in one of the other orthogonal directions (longitudinal) added to 40 percent of the responses resulting from analyses in the other two orthogonal directions (transverse and vertical):

$$M_x^{LC2} = 0.4M_x^T + M_x^L + 0.4M_x^V$$

Load Case 3 (LC3) – 100 percent of the absolute value of the response resulting from an analysis in one of the other orthogonal directions (vertical) added to 40 percent of the response values resulting from analyses in the other two orthogonal directions (transverse and longitudinal):

$$M_x^{LC3} = 0.4M_x^T + 0.4M_x^L + M_x^V$$

The response to be used in design is given by the largest value from these three load cases,

$$\text{i.e., } M_x = \text{maximum of } [M_x^{LC1}, M_x^{LC2}, M_x^{LC3}] \quad (7-4)$$

If the seismic loading is applied in only two orthogonal directions (longitudinal and transverse), the above rules still apply, but M_x^V is set equal to zero, and Load Case 3 need not be calculated i.e., $M_x^{LC3} = 0$.

7.4.3. COMBINATION OF RESPONSE QUANTITIES FOR BIAXIAL DESIGN

When the biaxial response of a member is important (e.g., for circular columns), it is necessary to find the maximum resultant moment on the column section and the corresponding axial load. This is not easy because the maxima of the three components (i.e., axial force, P , and bending moments about two local axes, M_x and M_y) are not likely to occur at the same time. A sophisticated approach to finding the critical combination is difficult to justify for most bridges, and a simpler approach may be used. Again two choices, based on the SRSS combination rule and the 100-40 percent rule, are available. They are as follows.

For the SRSS combination, the two components to be combined, M_x and M_y , are first found from equation 7-3 and then a 100-40 percent rule is used to find a vector sum. There are two possible vector sums and the maximum is taken as the moment resultant M_R . This moment is then used with the maximum positive or negative axial force to evaluate the column.

i.e.,

$$M_R = \text{maximum of } \left[\sqrt{M_x^2 + (0.4M_y)^2}, \text{ or } \sqrt{(0.4M_x)^2 + M_y^2} \right] \quad (7-5)$$

and M_R is used with the maximum axial load of $\pm P$ to evaluate the column.

For the 100-40 percent combination rule, the M_x and M_y components from each load case are combined to obtain the vector sum, and the maximum moment of the three load cases is taken as the moment resultant M_R . This moment is then used with the maximum positive or negative axial load to evaluate the column.

i.e.,

$$M_R = \text{maximum of } \left[\sqrt{(M_x^{LC1})^2 + (M_y^{LC1})^2}, \sqrt{(M_x^{LC2})^2 + (M_y^{LC2})^2}, \text{ or } \sqrt{(M_x^{LC3})^2 + (M_y^{LC3})^2} \right] \quad (7-6)$$

and M_R is used with the maximum axial load of $\pm P$ to evaluate the column.

7.4.4. VERTICAL ACCELERATION EFFECTS

A limited study of the effect of vertical accelerations on the behavior of bridges indicates that these effects can be significant (Button et al., 1999). This is particularly true for some response parameters (such as superstructure moments and shears, and column axial forces) and certain bridge types (such as those with long flexible spans, C-shaped piers, or with other large eccentricities in the load path for vertical loads). The study was based on vertical response spectra developed from recorded ground motions in the western United States (Silva, 1997). Response spectra for vertical ground motions are discussed further in section 2.7.

Until more is known about the characteristics of vertical ground motions in the eastern United States and those areas affected by subduction zones, such as in the Pacific Northwest, recommendations for design should be primarily cautionary and optional. However, vertical acceleration effects may be significant and should be assessed for important bridges. For this purpose, the following recommendations may be helpful.

The impact of vertical ground motion may be ignored if the bridge is greater than 50 km (30 mi) from an active fault. If the bridge site is within 10 km (6 mi) of an active fault, then a site-specific study is required if the response of the bridge could be significantly and adversely affected by vertical ground motions. In such cases, response spectra and acceleration time histories should be developed for use in the response analysis of the bridge. For vertical response forces, the linear analysis should use the CQC modal combination method and the SRSS directional combination method.

If the bridge is more than 10 km (6 mi) but less than 50 km (30 mi) from an active fault, a site-specific study should be performed to evaluate the effects of vertical ground motion.

In lieu of a dynamic analysis that explicitly includes the effect of vertical ground motion, the following variations in column axial loads and superstructure moments and shears should be included in the evaluation of the columns and superstructure to account for the effects of vertical ground motion.

- Column axial loads = $(1 \pm C_V)$ axial forces due to dead load.
- Superstructure bending moments = $(1 \pm C_V)$ bending moments due to dead load.
- Superstructure shears = $(1 \pm C_V)$ shear forces due to dead load.

In the above bullets, C_V is a dead-load multiplier and recommended values are given in table 7-2. For superstructures, C_V is specified at both a mid-span location and a pier. Linear interpolation may be used to determine values of C_V for points between these two locations.

Table 7-2. Dead load multipliers (C_v) for bridges subject to vertical acceleration for rock sites.

Member Force / Moment	Distance from Fault (km), D				
	$0 \leq D < 10$	$10 \leq D < 20$	$20 \leq D < 30$	$30 \leq D < 40$	$D \geq 40$
Pier axial force	0.7	0.3	0.2	0.1	0.1
Superstructure shear force at pier	0.7	0.4	0.2	0.1	0.1
Superstructure bending moment at pier	0.6	0.3	0.2	0.1	0.1
Superstructure shear force at mid-span	0.1	0.1	0.1	0.1	0.1
Superstructure bending moment at mid-span	1.4	0.7	0.4	0.3	0.2
Note: The dead load multipliers given above are in addition to the dead load. Thus the actual 'load factor' is 1.0 plus/minus the tabulated values.					

Button et al., 1999

7.5. MEMBER STRENGTHS

It is difficult to calculate the precise capacity of a bridge because the actual strength of concrete and steel may vary considerably from their specified values. Furthermore, deviations from specified dimensions due to construction tolerances and simplifying assumptions made in design can lead to both under- and over-capacity in the field. However, it is possible to define different levels of member strength, which are then used in various types of calculations for capacity assessment of a complete bridge. Four strength levels are defined as follows:

- *Nominal* strength, S_n
The nominal strength of a member is obtained from failure theory for a section of the member and is based on assumed section geometry and specified material strengths. Other strength levels are usually related to the nominal strength.
- *Design* strength, S_d
The design strength of a member allows for approximations in calculations and variations in material strengths, workmanship, and dimensions. Each of these may be within tolerable limits, but in combination, they may result in a capacity that is less than the nominal strength. A strength reduction factor (ϕ) is used to relate the design strength to the nominal strength, where ϕ is always less than unity. (The resistance factors in the *AASHTO LRFD Specifications* (1998) or the current LRFD specification may be used here.)

$$\text{i.e.,} \quad S_d = \phi S_n \quad (7-7a)$$

- *Expected strength, S_e*

The expected strength takes into account the fact that the material strengths are generally greater than the specified strengths. Expected strengths can be found from routine testing of material samples taken from existing bridges, but if these are not available, they are based on previous experience with the same materials in other bridges. An expected strength factor (ϕ_e) is used to relate the expected strength to the nominal strength, where ϕ_e is always greater than unity.

i.e.,
$$S_e = \phi_e S_n \quad (7-7b)$$

Values for ϕ_e may be obtained by taking material samples in the field and testing for actual strength, or by taking values from the mill certificates provided by the supplier at the time of construction, if these are still available in the bridge file. In the absence of such data, ϕ_e may be taken as 1.2 and 1.3 for steel and concrete, respectively.

- *Overstrength, S_o*

Overstrength takes into account all possible factors contributing to a strength increase above the nominal value. These include but are not limited to:

- Steel strength higher than the specified yield strength,
- Additional steel strength due to strain hardening at large deformations,
- Concrete strength higher than specified,
- Section sizes larger than assumed,
- Axial compression in flexural members due to lateral restraint,
- Additional reinforcement placed for construction purposes and unaccounted for in design,
- Conservative assumptions made in the derivation of the equations for nominal strength.

An overstrength factor (ϕ_o) is used to relate the overstrength to the nominal strength, where ϕ_o is always greater than unity.

i.e.,
$$S_o = \phi_o S_n \quad (7-7c)$$

7.6. MEMBER ACTIONS IN PIERS USING CAPACITY PRINCIPLES

Capacity design principles are used to calculate member actions in bridge piers due to plastic hinging. This process is described in this section for both single-column and multi-column piers and for extensions to drilled shafts and piled bents are also given. These procedures are the same as those given in Article 7.2.2 of the *AASHTO Standard Specifications* (AASHTO, 2002). A worked example may be found in appendix A of the *AASHTO Guide Specifications for Seismic Design of Highway Bridges* (AASHTO, 1983).

7.6.1 SINGLE COLUMN PIERS

Column shear forces and moments in the superstructure, pier caps, and footings should be calculated for the two principal axes of a column and in the weak direction of a pier as follows:

Step 1. Determine the column overstrength moment capacities (sections 7.5 and 7.7.1.2). For reinforced concrete or structural steel columns, apply an overstrength factor (ϕ_o) of 1.4 to the nominal moment, and use a column axial load equal to the sum of the axial load calculated from an elastic analysis and the column dead load. Column overstrength moments should be distributed to the connecting structural elements.

Step 2. Using the column overstrength moments, calculate the corresponding column shear force(s) that satisfy static equilibrium. For columns that have flares that are integral with the superstructure, the shear should be calculated as the larger of:

1. The value obtained from the overstrength moments at the top of the flare and bottom of the column immediately above the top of the footing, using the clear height from top of footing to underside of pier cap, and
2. The value obtained from using the overstrength moments at the bottom of the flare and top of the footing, with the column height reduced to the distance between them.

This method is satisfactory for most columns, but may be unconservative for shear when the column contributes a significant portion of the total mass of the bridge.

If the footing of a column is significantly below ground level, consideration should be given to the possibility of a plastic hinge forming below ground level. In such a case, the hinge may not form directly above the footing as assumed in Step 2 above, due to restraint provided by the overlying soil. If this can occur, the estimated length of the column between plastic hinges should be used in Step 2 to calculate the shear force.

For pile bents or drilled shafts, the length of the column between plastic hinge locations should again be used. Assume that hinges below ground level occur no lower than two pile/shaft diameters below the mud line.

In summary, column forces corresponding to plastic hinging in a single column are:

- Axial forces using unreduced maximum and minimum axial load from elastic analyses, plus dead load.
- Bending moments as calculated in Step 1.
- Shear forces as calculated in Step 2.

7.6.2. MULTI-COLUMN PIERS

The forces in piers with two or more columns should be calculated both in the plane of the pier and perpendicular to the plane of the pier. Forces perpendicular to the plane of the pier should be calculated as for single columns in section 7.6.1 above. Forces in the plane of the pier should be calculated as follows:

- Step 1. Determine the column overstrength moment capacities. Use an overstrength factor (ϕ_o) of 1.4 for both reinforced concrete and structural steel to obtain these moments. Set the axial load equal to the dead load.
- Step 2. Using the column overstrength moment capacities, calculate the corresponding column shear forces. Sum the column shears in the pier to determine the maximum shear force for the pier. Note that if a partial-height wall exists between the columns, the effective column height is taken from the top of the wall. For flared columns and foundations below ground level, see Step 2 in section 7.6.1. For pile bents, the portion of pile from the pile cap to a length of two diameters below the mud line should be used to calculate the shear force.
- Step 3. Apply the pier's shear force to the center of mass of the superstructure above the pier, and, using static equilibrium, calculate the axial forces in the columns due to this force when the column overstrength capacities are reached.
- Step 4. Combine these column axial forces with the dead load axial forces, and calculate revised column overstrength moments. With the revised overstrength moments, calculate the column shear forces and the maximum shear force for the pier. If the maximum shear force for the pier is not within 10 percent of the value determined in Step 2, use this maximum pier shear force and return to Step 3.

In summary, column forces corresponding to plastic hinging in individual columns in the plane of a pier are:

- Axial forces using the maximum and minimum axial load and dead load, plus or minus the axial load determined from the final iteration of Step 3.
- Column overstrength moment capacities corresponding to the maximum compressive axial load specified in Step 1 with an overstrength factor of 1.4 for reinforced concrete and structural steel.
- Shear forces corresponding to the final column overstrength moments in Step 4 above.

7.7. STRENGTH CAPACITY OF BRIDGE MEMBERS

Guidelines for determining the *capacity* of bridge members in terms of strength are given in this section for use when assessing the strength capacity of complete bridges or bridge substructures as required in Methods D1 and D2 of chapter 5. Guidelines for determining *displacement capacity* are given in the following section (section 7.8).

In particular, procedures are given for calculating the following:

- Flexural strength of reinforced concrete columns and beams (section 7.7.1):
 - Expected flexural strength (7.7.1.1),
 - Flexural overstrength capacity (7.7.1.2), and

- Flexural strength of columns with lap-splices in plastic hinge zones (7.7.1.3).
- Shear strength of reinforced concrete columns and beams (section 7.7.2):
 - Initial shear strength (7.7.2.1), and
 - Final shear strength (7.7.2.2).
- Shear strength of reinforced concrete beam-column joints (section 7.7.3):
 - Maximum beam-column joint strength (7.7.3.1), and
 - Cracked beam-column joint strength (7.7.3.2).

7.7.1. FLEXURAL STRENGTH OF REINFORCED CONCRETE COLUMNS AND BEAMS

Several types of member flexural strength are required for a detailed capacity assessment of a bridge. These include the:

- *Expected flexural strength* based on material expected strength factors and equation 7-7b.
- *Flexural overstrength* based on member overstrength factors and equation 7-7c.
- *Expected flexural strength* of columns with lap-splices located in potential plastic hinge zones, based on expected strength factors.

7.7.1.1. Expected Flexural Strength

The flexural strength of members (either with or without axial loads) is determined based on monotonic behavior, where strains are assumed to vary linearly across the section, and the stresses are related to strains through material property laws. If a moment-curvature analysis is undertaken, then it is possible to define the expected yield strength and determine the maximum overstrength capacity and deformation capacity. However, for most situations, this effort is not justified and simplified methods, as described below, are used.

The expected flexural strength (at theoretical yield) should be based on a modified form of the nominal strength calculations required in the *AASHTO LRFD Specification* (AASHTO, 1998). A rectangular stress block for unconfined concrete and elasto-plastic behavior for steel is assumed. The following assumptions are made:

- Maximum concrete strain at the outermost concrete fiber is 0.003.
- Average concrete stress in the effective compression zone is $0.85f'_{ce}$, where f'_{ce} is the expected concrete strength.
- Expected yield stress of the longitudinal reinforcement (f_{ye}) is 300 MPa (43.5 ksi) and 450 MPa (65.3 ksi) for Grade 40 and Grade 60 steel respectively, in lieu of material tests on samples taken from the bridge.
- Effective depth of the concrete stress block is $a = \beta_1 c$,

where c is the neutral axis depth, and $\beta_1 = 0.85$ for $f'_{ce} \leq 30$ MPa (4.3 ksi) and $\beta_1 = 0.65$ for $f'_{ce} \geq 60$ MPa (8.7 ksi). Linear interpolation is used for β_1 if $30 \text{ MPa} < f'_{ce} < 60 \text{ MPa}$ (4.3 ksi $< f'_{ce} < 8.7$ ksi).

The expected flexural strength (M_e) is calculated using a plastic analysis approach as given below (Mander et al., 1998b):

$$\frac{M_e}{f'_{ce} A_g D} = \left(\frac{M_b}{f'_{ce} A_g D} \right) \left[1 - \left(\frac{\frac{P_e}{f'_{ce} A_g} - \frac{P_b}{f'_{ce} A_g}}{\frac{P_t}{f'_{ce} A_g} - \frac{P_b}{f'_{ce} A_g}} \right)^2 \right] \quad (7-8)$$

where:

$\frac{P_e}{f'_{ce} A_g}$ = axial stress ratio based on gravity load and seismic actions,

$\frac{P_t}{f'_{ce} A_g} = -\rho_t \frac{f_{ye}}{f'_{ce}}$ = axial tensile capacity ratio of the column based on the expected material properties,

$\frac{P_b}{f'_{ce} A_g} = 0.425 \beta_1$ = axial load capacity ratio at the maximum nominal (balanced) moment on the section,

$$\frac{M_b}{f'_{ce} A_g D} = \left(K_{\text{shape}} \rho_t \frac{f_{ye}}{f'_{ce}} \frac{D'}{D} + \frac{P_b}{f'_{ce} A_g} \frac{1 - \kappa_o}{2} \right),$$

β_1 = stress block factor (≤ 0.85),

D' = pitch circle diameter of the reinforcement in a circular section, or the out-to-out dimension of the reinforcement in a rectangular section, generally assumed to be equal to 80 percent of overall diameter of column, D ,

K_{shape} = shape factor:

= 0.32 for circular sections,

= 0.375 for square sections with 25 percent of the reinforcement placed in each face,

= 0.25 for walls with strong axis bending, and

= 0.50 for walls with weak axis bending.

κ_o = factor related to the centroid of the stress block:

= 0.6 for circular sections, and

= 0.5 for rectangular sections.

7.7.1.2. Flexural Overstrength Capacity

In any method of capacity assessment that is based on a collapse mechanism, it is necessary to know the upper bound on flexural capacity, i.e., the flexural moment overstrength capacity, M_{po} , of the

columns, piers, and piles that form the primary load resisting mechanism. Three different approaches are described below for the calculation of M_{po} .

Method 1. A compatibility section analysis is made to calculate the flexural overstrength capacity, M_{po} , taking into account the expected strengths of the materials, the properties of confined concrete, and the strain hardening effects of the longitudinal reinforcement.

Method 2. The flexural overstrength capacity, M_{po} , is estimated by scaling the expected strength using an empirical factor, e.g., $M_{po} = 1.4 M_e$, where M_e is the expected flexural strength.

Method 3. The flexural overstrength capacity, M_{po} , is estimated from a sectional plastic analysis using the properties of confined concrete and the ultimate tensile strength for the stress in the longitudinal reinforcement. (Mander et al., 1998a). In this method, M_{po} is given by

$$\frac{M_{po}}{f'_c A_g D} = \left(\frac{M_{bo}}{f'_c A_g D} \right) \left[1 - \left(\frac{\frac{P_e}{f'_c A_g} - \frac{P_{bcc}}{f'_c A_g}}{\frac{P_{to}}{f'_c A_g} - \frac{P_{bcc}}{f'_c A_g}} \right)^2 \right] \quad (7-9)$$

where:

$\frac{P_e}{f'_c A_g}$ = column axial stress ratio based on gravity loads and seismic actions,

$\frac{P_{to}}{f'_c A_g} = -\rho \frac{f_{su}}{f'_c}$ axial tensile capacity ratio of the column,

$\frac{P_{bcc}}{f'_c A_g} = 0.5\alpha\beta \frac{A_{cc}}{A_g}$ = axial load capacity ratio at the maximum confined (balanced) moment on the section,

$$\frac{M_{bo}}{f'_c A_g D} = \left(K_{shape} \rho_t \frac{f_{su}}{f'_c} \frac{D'}{D} + \frac{P_{bcc}}{f'_c A_g} \frac{1 - \kappa_o}{2} \right),$$

D' = pitch circle diameter of the reinforcement in a circular section, or the out-to-out dimension of the reinforcement in a rectangular section (normal to the axis of bending), generally assumed to be equal to 80 percent of overall diameter of column, D (or overall depth of beam),

f_{su} = ultimate tensile strength of the longitudinal reinforcement
= $1.5 f_{ye}$ unless determined otherwise by coupon tests,

α, β = stress block factors for confined concrete defined below,

A_{cc} = area of confined concrete core, and

A_g = gross section area.

Stress block factors α, β are as follows:

α = ratio of average concrete stress in compression zone to confined concrete strength

$$\begin{aligned}
K &= 0.85 + 0.12(K - 1)^{0.4}, \\
K &= \text{strength enhancement factor due to the confining action of the transverse reinforcement, and is given below for circular and rectangular sections} \\
&= f'_{cc} / f'_{ce}, \\
f'_{cc} &= \text{confined concrete strength, and} \\
\beta &= \text{depth of stress block} \\
&= 0.85 + 0.13(K - 1)^{0.6}.
\end{aligned}$$

For *circular* sections, the confined strength parameter (K) is given by Mander et al. (1988):

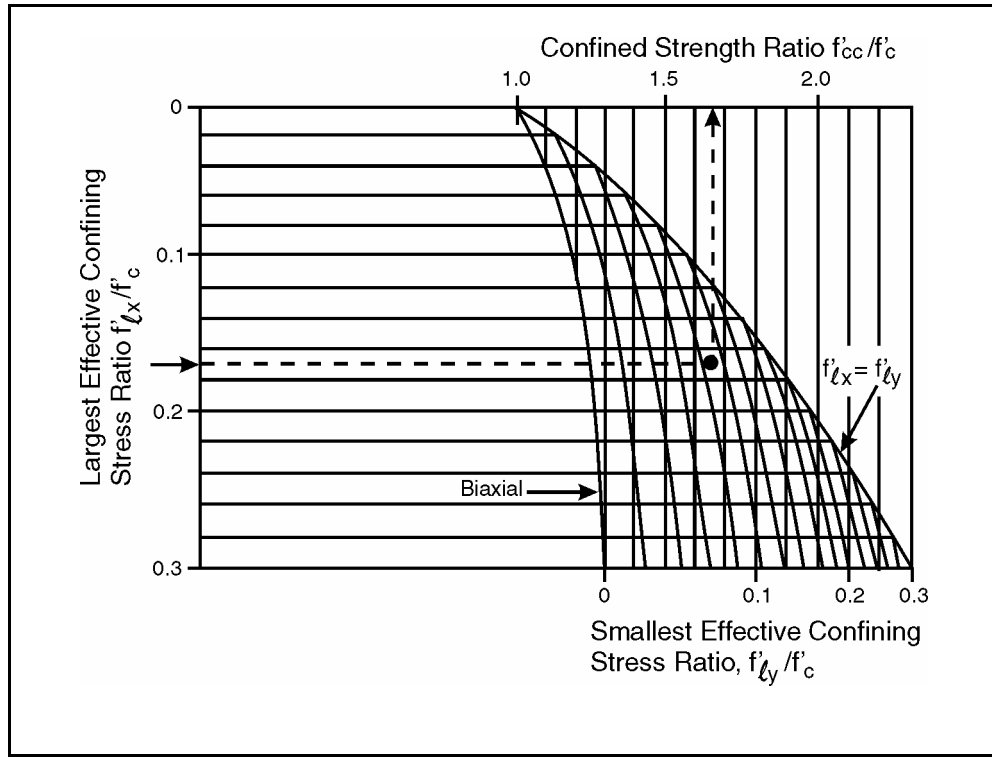
$$K = 2.254 \sqrt{1 + 7.94 \frac{f'_\ell}{f'_{ce}}} - 2 \frac{f'_\ell}{f'_{ce}} - 1.254$$

where:

$$\begin{aligned}
f'_\ell &= \frac{1}{2} k_e \rho_s f_{yh} = \text{lateral stress supplied by the transverse reinforcement at yield,} \\
\rho_s &= \frac{4 A_{bh}}{s D''} = \text{volumetric ratio of spirals or circular hoops to the core concrete,} \\
k_e &= \frac{(1 - \chi s / D'')}{(1 - \rho_{cc})} = \text{confinement effectiveness coefficient for spirals and hoop steel,} \\
\chi &= \text{coefficient with values of 0.5 and 1.0 for spirals and hoops, respectively,} \\
s &= \text{spacing of spirals or hoops, and} \\
D'' &= \text{diameter of transverse hoop or spiral (measured to the centerline of the hoop).}
\end{aligned}$$

For *rectangular* sections, the confined strength parameter (K) is obtained from figure 7-2 which uses the x- and y- confining stresses ($f'_{\ell x}$ and $f'_{\ell y}$ respectively) to give K (Mander et al., 1988; Paulay and Priestley, 1991). Stresses $f'_{\ell x}$ and $f'_{\ell y}$ are defined as follows:

$$\begin{aligned}
f'_{\ell x} &= k_e \rho_x f_{yh} \text{ is the lateral confining stress in the x-direction,} \\
f'_{\ell y} &= k_e \rho_y f_{yh} \text{ is the lateral confining stress in the y-direction,} \\
\rho_x &= \frac{A_{sx}}{s D''} \text{ is the volume ratio of transverse hoops or ties to the core concrete in x-direction,} \\
\rho_y &= \frac{A_{sy}}{s b''} \text{ is the volume ratio of transverse hoops or ties to the core concrete in y-direction, and} \\
k_e &= \text{confinement effectiveness coefficient for rectangular sections with hoops or ties:} \\
&= 0.75 \text{ for rectangular columns, and} \\
&= 0.6 \text{ for rectangular wall sections.} \\
f_{yh} &= \text{yield stress of the transverse hoops,} \\
D'' &= \text{width of column normal to x-direction (measured to the centerline of hoops or ties),} \\
&\text{and} \\
b'' &= \text{width of column normal to y-direction (measured to the centerline of hoops or ties).}
\end{aligned}$$



Paulay and Priestley, 1991

Figure 7-2. Confined strength ratio (K) for reinforced concrete members.

7.7.1.3. Flexural Strength of Columns with Lap-Splices in Plastic Hinge Zones

The flexural strength of a column is reduced when the longitudinal steel is lapped in the plastic hinge zone, which is a common occurrence near the base of columns in older bridges. As a first approximation, the reduction in strength is assumed to depend solely on the length of the splice, l_{lap} , compared to the minimum required value. The reduced moment (M_s) is then given by:

$$M_s = M_e (l_{lap} / l_s) \quad \text{but not greater than } M_e \quad (7-10)$$

where:

- M_e = expected flexural strength defined in section 7.5,
- l_s = theoretical lap-splice length and is determined from:

$$l_s = 0.4 \frac{f_{ye}}{\sqrt{f'_{ce}}} d_b, \quad (7-11)$$

- d_b = diameter of the longitudinal reinforcing bar in the lap,
- f_{ye} = expected yield strength (MPa) of the longitudinal reinforcement in the lap-splice zone, and
- f'_{ce} = expected strength (MPa) of concrete surrounding the lap-splice zone.

7.7.2. SHEAR STRENGTH OF REINFORCED CONCRETE COLUMNS AND BEAMS

The shear resistance of cracked structural concrete members is reduced by load reversals and increasing plastic hinge rotations. As a consequence, two shear strength states are defined:

1. V_i the initial shear strength, and
2. V_f the final shear strength.

The difference between the two states is due to deterioration in the concrete as the cyclic loading progresses with a corresponding reduction in the concrete contribution, V_c , to the shear capacity. This contribution diminishes due to the presence of widely-spaced tensile cracks and yielding of the longitudinal bars. Expressions for the initial and final shear strengths are given in the following sections.

7.7.2.1. Initial Shear Strength, V_i

Initial shear strength, V_i , is given by:

$$V_i = V_s + V_p + V_{ci} \quad (7-12)$$

where:

- V_s = contribution to the shear strength provided by rebar truss action,
- V_p = contribution provided arch (strut) action, and
- V_{ci} = contribution provided by diagonal tension field in the concrete.

Each of these contributions is described below.

The shear resistance provided by truss action in the reinforcing steel is given by:

$$V_s = A_v f_{yh} \frac{D''}{s} \cot \theta \quad (7-13)$$

where:

- A_v = shear area provided by the transverse hoops:
 - = $2 A_{bh}$ for rectangular columns, and
 - = $\pi A_{bh} / 2$ for circular columns.
- A_{bh} = area of one spiral or hoop bar,
- f_{yh} = yield stress of the transverse hoops or spirals,
- D'' = diameter of transverse hoop or spiral (measured to the centerline of the hoop),
- s = center-to-center longitudinal spacing of the transverse hoop steel,
- θ = angle of the principal crack plane (Kim and Mander, 1999) and given by

$$\tan \theta = \left(\frac{1.6 \rho_v A_e}{\Lambda \rho_t A_g} \right)^{0.25} \geq \tan \alpha, \quad (7-14)$$

- Λ = fixity factor:
 = 2 for fixed-fixed column conditions, and
 = 1 for fixed-pinned conditions.
- A_e = effective shear area (assumed as 80 percent of the gross area, A_g , for rectangular and circular sections),
- ρ_t = ratio of the total area of longitudinal reinforcement to the gross section area
 = A_{st} / A_g ,
- ρ_v = volumetric ratio of transverse steel:
 = $A_v / b_w s$ for rectangular columns, and
 = $\rho_s / 2 = 2 A_{bh} / s D$ for circular columns.
- A_v = area of transverse shear steel,
- b_w = center-to-center spacing of transverse shear steel across width of rectangular column,
- $\tan \alpha$ = corner-to-corner strut angle:
 = jd / L ,
- jd = internal lever arm of the concrete compression member, and
- L = length of the column.

The shear resistance provided by the arch (strut) action is given by:

$$V_p = \frac{\Lambda}{2} P \tan \alpha \quad (7-15)$$

where Λ is the fixity factor defined above, P is the axial load on member (compression only), and $\tan \alpha$ is the corner-to-corner strut angle defined above.

The shear resistance provided by the diagonal tension field in the concrete is:

$$V_{ci} = 0.3 \sqrt{f'_{ce}} A_e \quad (7-16)$$

where A_e is the effective shear area equal to $0.8A_g$.

7.7.2.2. Final Shear Strength, V_f

The final shear strength is given by:

$$V_f = V_s + V_p + V_{cf} \quad (7-17)$$

In this equation, V_s and V_p are as defined above, while V_{cf} is the final shear strength carried by the concrete, which is reduced to allow for plastification, cracking, and cyclic loading effects. This is given by:

$$V_{cf} = 0.05 \sqrt{f'_{ce}} A_e \quad (7-18)$$

7.7.3. SHEAR STRENGTH OF BEAM-COLUMN JOINTS

The shear strength of beam–column joints can be assessed in a manner similar to column elements. A principal stress approach is usually adopted, as this is a major determinant in joint performance. A beam–column joint will remain essentially elastic and uncracked, providing that the principal tensile stress in the joint is less than $0.29\sqrt{f'_{ce}}$ MPa. When the principal tensile stress exceeds this level, diagonal cracking of the joint can be expected. The joint strength will be limited to a maximum principal stress of $0.42\sqrt{f'_{ce}}$ MPa, at which point, full diagonal cracking of the joint will have developed. If the joint shear demand arising from the flexural overstrength capacity exceeds this limit, then the joint is said to be shear-critical and the structural performance will be governed by the reduced joint strength. The shear strength of the beam-column joint is therefore given by:

$$V_j = v_j A_{jh} \quad (7-19)$$

in which A_{jh} is the area of the beam-column joint in a horizontal plane, and v_j is the average joint shear stress acting on the joint. The latter can be found from a Mohr's circle analysis for principal stresses in a joint subject to the combined actions of f_v , f_h and v_j as follows:

$$v_j = \sqrt{p_t^2 - p_t(f_v + f_h) + 2f_v f_h} \quad (7-20)$$

where:

- f_v = average axial stress on the joint (compression is negative),
- f_h = average horizontal axial stress on the joint (has a zero value unless the joint has horizontal prestress, or similar, applied), and
- p_t = major principal tension stress (tension is positive). This term dominates performance of the joint; recommended values are given in following sections.

7.7.3.1. Maximum Beam-Column Joint Strength, V_{ji}

The maximum joint shear capacity is achieved when full diagonal cracking develops. This occurs when the principal tensile stress in the joint is given by:

$$p_t = 0.42 \sqrt{f'_{ce}} \text{ MPa} \quad (7-21)$$

where f'_{ce} is the expected concrete strength in MPa. This principal stress is used to calculate V_{ji} using equation 7-20.

7.7.3.2. Cracked Beam–Column Joint Strength, V_{jr}

The residual joint shear capacity is maintained after the strength has deteriorated. This occurs when the principal tensile stress in the joint is given by:

$$p_t = 0.29\sqrt{f'_{ce}} \text{ MPa} \quad (7-22)$$

where f'_{ce} is the expected concrete strength in MPa. This principal stress is used to calculate V_{jf} using equation 7-20.

7.8. DEFORMATION CAPACITY OF BRIDGE MEMBERS

A displacement capacity evaluation of a bridge, or pushover analysis (Method D2, chapter 5), should be able to track the nonlinear relationship between load and deformation for the columns and beams as the lateral load is monotonically increased from an initial elastic condition to failure. This requires the estimation of the capacity of each of the critical structural members, from first yield until collapse, and at intermediate limit states. Therefore, member performance needs to be found in terms of force versus deformation, moment versus rotation, or shear force versus distortion.

Cap beams, columns, footings and piles may be modeled as line elements with concentrated plastic hinges at their ends. Other models, such as those with distributed plasticity, distributed flexibility, or general-purpose nonlinear finite element approaches may also be used, provided it can be demonstrated that their theoretical response agrees with experimental results from members similar to those being modeled.

Guidelines for determining the deformation capacity of bridge components are given in this section for use in calculating the strength-deformation capacity of bridge members as required in the structure capacity/demand methods described in chapter 5 (Methods D1 and D2).

In particular, procedures are given for calculating the following:

- Plastic curvatures, rotations and drift angles (section 7.8.1).
- Deformation-based limit states (section 7.8.2). There are eight of these.
- Neutral axis depth in columns and beams (section 7.8.3).

7.8.1 PLASTIC CURVATURES AND HINGE ROTATIONS IN A CANTILEVER BEAM

7.8.1.1. Deflections and Plastic Curvature, ϕ_p

The ultimate displacement, Δ_u , of a cantilever column under a lateral (shear) load, F , is given by:

$$\Delta_u = \Delta_e + \Delta_p \quad (7-23)$$

where Δ_e is the elastic component of displacement, and Δ_p is the plastic component of displacement.

Each of these two components is described below.

For the elastic component, Δ_e :

$$\Delta_e = \frac{F L^3}{3E_c I_{eff}} \quad (7-24)$$

where L is the length from the fixed end to the free tip (or the inflection point of a fixed-fixed beam-column element), and $E_c I_{eff}$ is the effective flexural rigidity (equation 7-2) that reflects the degree of cracking in the member.

When the plastic strength of the member (F_p , M_p), is reached $\Delta_e = \Delta_y$, and the nominal yield displacement is given by:

$$\Delta_y = \frac{F_p L^3}{3E_c I_{eff}} = \frac{M_p L^2}{3E I_{eff}} = \frac{1}{3} \phi_y L^2 \quad (7-25)$$

where M_p is the plastic moment capacity and ϕ_y is the nominal yield curvature given by modifying equation 7-1 such that:

$$\phi_y = \frac{2\varepsilon_y}{D'} = \frac{2 f_y}{E_s D'} \quad (7-26)$$

For the plastic component, Δ_p :

$$\Delta_p = \phi_p L_p (L - 0.5L_p) \quad (7-27)$$

where L_p is the equivalent plastic hinge length, and ϕ_p is the plastic curvature as defined below.

The equivalent plastic hinge length is given by the semi-empirical equation:

$$L_p = 0.08L + 4400 \varepsilon_y d_b \quad (7-28)$$

where d_b is the diameter of the longitudinal tension reinforcement, and L is the shear span or effective height (i.e., $L = M/V$).

If the column has been jacketed as part of the retrofitting process, then the equivalent plastic hinge length is modified to give:

$$L_p = L_{gap} + 8800 \varepsilon_y d_b \quad (7-29)$$

where L_{gap} is the clear gap between the edge of the jacket and the bottom of the pier cap or top of the footing.

The plastic curvature capacity depends on the failure mode and is highly dependent on the quantity of transverse reinforcement that is present. Values of ϕ_p for several deformation-based limit states are given in section 7.8.2. ϕ_p can be expressed in terms of the ultimate (total) curvature ϕ_u as follows:

$$\phi_p = \phi_u - \phi_y \quad (7-30)$$

7.8.1.2. Plastic Hinge Rotation, θ_p

The analysis in section 7.8.1.1 for deformation is in terms of absolute displacement quantities. It is often more convenient to express deformation behavior in relative terms, i.e., drift which is the ratio of lateral displacement to column height, and is the same as the angular rotation of the member chord. Thus, in terms of drifts (or rotations):

$$\theta_u = \theta_y + \theta_p \quad (7-31)$$

where the elastic drift at yield is given by:

$$\theta_y = \frac{\Delta_y}{L} = \frac{1}{3} \phi_y L = \frac{2}{3} \epsilon_y \frac{L}{D'} \quad (7-32)$$

and the plastic drift is given by:

$$\theta_p = \phi_p L_p \quad (7-33)$$

The elastic component of the total drift is related to the member slenderness (L/D') and the plastic drift is given by the plastic hinge rotation, which in turn is related to the plastic curvature within the hinge zone.

7.8.2. CHARACTERIZATION OF DEFORMATION-BASED LIMIT STATES

The plastic rotational capacity of a member should be based on the governing limit state for that member. As shown in the previous section, this rotation may be found using equation 7-33. The governing limit state is the state that has the least plastic rotational (or plastic curvature) capacity. Plastic curvatures (and therefore plastic rotations) for the following limit states are developed in this section and summarized in table 7-3:

- Compression failure of unconfined concrete.
- Compression failure of confined concrete.
- Compression failure due to buckling of the longitudinal reinforcement.
- Longitudinal tensile fracture of reinforcing bar.

- Low cycle fatigue of the longitudinal reinforcement.
- Failure in the lap-splice zone.
- Shear failure of the member that limits ductile behavior.
- Failure of the joint.

Table 7-3. Values of plastic curvature corresponding to various limit states in reinforced concrete columns and beams.

Column or Beam Limit State	Plastic Curvature, $\phi_p^{1,2}$	Equation
Compression failure, unconfined concrete	$\phi_p = \frac{\epsilon_{cu}}{c} - \phi_y$	7-34
Compression failure, confined concrete	$\phi_p = \frac{\epsilon_{cu}}{(c-d'')} - \phi_y$	7-35
Buckling of longitudinal bars	$\phi_p = \frac{\epsilon_b}{(c-d')} - \phi_y$	7-37
Fracture of longitudinal reinforcement	$\phi_p = \frac{\epsilon_{s\max}}{(d-c)} - \phi_y$	7-39
Low-cycle fatigue of longitudinal reinforcement	$\phi_p = \frac{2 \epsilon_{ap}}{(d-d')} = \frac{2 \epsilon_{ap}}{D'}$	7-40
Lap-splice failure: (a) long / confined lap-splices (b) short / unconfined lap-splices	See low cycle fatigue $\phi_p = (\mu_{lap} + 7) \phi_y$	Section 7.8.2.6a 7-46
Shear failure: (a) brittle (b) semi-ductile	$\phi_p = 0$ $\phi_p = \left(5 \left(\frac{V_m - V_f}{V_i - V_f} \right) + 2 \right) \phi_y$	7-48 7-49
Joint or connection failure: (a) weak joint / strong column (b) semi-ductile	$\theta_p = 0.04 \text{ rad}$ $\phi_p = \left(4 \left(\frac{V_{jh} - V_{jf}}{V_{ji} - V_{jf}} \right) + 2 \right) \phi_y$	Section 7.8.2.8a 7-51
Notes: 1. Hinge rotation $\theta_p = \phi_p L_p$ where L_p is length of plastic hinge 2. Notation is defined in section 7.8.2.		

7.8.2.1. Compression Failure of Unconfined Concrete

The plastic curvature corresponding to compression failure in unconfined concrete is given by:

$$\phi_p = \frac{\epsilon_{cu}}{c} - \phi_y \quad (7-34)$$

where ϵ_{cu} is the ultimate concrete compression strain for concrete, which should be limited to 0.005 for unconfined concrete, and c is the depth from the extreme compression fiber to the neutral axis. The location of the neutral axis is defined in section 7.8.3.

7.8.2.2. Compression Failure of Confined Concrete

For concrete confined by transverse hoops, cross-ties, or spirals, the compression strain is limited by first fracture within the confining steel. While this type of failure depends on the cyclic load history, a conservative estimate of the plastic curvature can be obtained from:

$$\phi_p = \frac{\epsilon_{cu}}{(c - d'')} - \phi_y \quad (7-35)$$

where:

- c = depth from the extreme compression fiber of the cover concrete (which is expected to spall) to the neutral axis,
- d'' = distance from the extreme compression fiber of the cover concrete to the centerline of the perimeter hoop (thus, $c - d''$ is the depth of confined concrete under compression), and
- ϵ_{cu} = ultimate compression strain of the confined core concrete, as given by:

$$\epsilon_{cu} = 0.005 + \frac{1.4 \rho_s f_{yh} \epsilon_{su}}{f'_{cc}} \quad (7-36)$$

- ϵ_{su} = strain at the maximum stress of the transverse reinforcement,
- f_{yh} = yield stress of the transverse steel,
- ρ_s = volumetric ratio of transverse steel, and
- f'_{cc} = confined concrete strength.

For bridge columns that have confined concrete details, it is unlikely that this failure mode will govern, as low cycle fatigue is a more likely controlling mechanism. This is because the axial load in bridge columns is relatively low, and the transverse reinforcement is primarily required to provide restraint against buckling of the longitudinal reinforcement.

7.8.2.3. Buckling of Longitudinal Bars

If a compression member has inadequate transverse reinforcement and the spacing of the spirals, hoops, or cross-ties, s , in potential plastic hinge zones exceeds six longitudinal bar diameters (i.e., $s > 6d_b$), then local buckling at high compressive strains in the longitudinal reinforcement is likely. The plastic curvature of this failure mode can be determined from:

$$\phi_p = \frac{\epsilon_b}{(c - d')} - \phi_y \quad (7-37)$$

where d' is the distance from the extreme compression fiber to the center of the nearest compression reinforcing bars, and ϵ_b is the buckling strain in the longitudinal reinforcing steel. If $6d_b < s < 30d_b$, the buckling strain may be taken as twice the yield strain of the longitudinal steel, i.e.,

$$\epsilon_b = \frac{2f_y}{E_s} \quad (7-38)$$

7.8.2.4. Fracture of the Longitudinal Reinforcement

Tensile fracture occurs when the tensile strain reaches a critical level, as given by ϵ_{smax} . This failure mode is only likely under near-field impulse-type ground motions where there is essentially a monotonic (pushover) response. The plastic curvature in this case is given by:

$$\phi_p = \frac{\epsilon_{smax}}{(d - c)} - \phi_y \quad (7-39)$$

where d is the depth to the outer layer of tension steel from the extreme compression fiber, and c is the depth to the neutral axis.

The tensile strain ϵ_{smax} should be limited to a value less than or equal to 0.10.

7.8.2.5. Low Cycle Fatigue of Longitudinal Reinforcement

Since earthquakes induce cyclic loads in bridges, low cycle fatigue failure of the longitudinal reinforcement is possible. This is especially so if the column is well confined and other types of failure, as described above, are prevented. The plastic curvature that leads to a low cycle fatigue failure is given by:

$$\phi_p = \frac{2\epsilon_{ap}}{(d - d')} = \frac{2\epsilon_{ap}}{D'} \quad (7-40)$$

where:

D' = distance between the outer layers of longitudinal steel in a rectangular section ($d - d'$), or the pitch circle diameter of the longitudinal reinforcement in a circular section,

ϵ_{ap} = plastic strain amplitude, as given by:

$$\epsilon_{ap} = 0.08 (2N_f)^{-0.5} \quad (7-41)$$

N_f = effective number of equal-amplitude cycles of loading that lead to fracture, which can be approximated by:

$$N_f = 3.5 (T_n)^{-1/3} \quad (7-42)$$

provided that: $2 \leq N_f \leq 10$, and

T_n = natural period of vibration of the bridge.

7.8.2.6. Failure in the Lap-splice Zone

It is common to have a lap-splice zone at the base of a column where the starter bars from the footing or pile cap are lapped with the flexural reinforcement of the column. This is generally also the location of the plastic hinge zone. The presence of the lap-splice within the plastic hinge may lead to two different behavior modes, which depend on the length of the lap-splice that is provided, l_{lap} , compared to the required length, given by:

$$l_s = 0.4 \frac{f_{ye}}{\sqrt{f'_{ce}}} d_b \quad (7-43)$$

where d_b is the diameter of the longitudinal reinforcing bar in the lap, f_{ye} is the expected yield strength of the longitudinal reinforcement in the lap-splice zone, and f'_{ce} is the expected strength of concrete surrounding the lap-splice zone (MPa).

7.8.2.6(a). 'Long' or Confined Lap-splice, $l_{lap} > l_s$

Some lap-splice zones in existing bridge columns were designed as tension splices and generous lap lengths were provided by some 40 bar diameters or more. It is possible that if the bond between the reinforcing steel and column concrete is satisfactory, the effective plastic hinge is reduced in length and behavior is then governed by low cycle fatigue of the longitudinal bars. From equation 7-28, it follows that the effective plastic hinge is concentrated at the beginning of the lap and is given by:

$$L_p = \text{the minimum of } \left[(8800\epsilon_y d_b) \text{ or } (0.08L + 4400\epsilon_y d_b) \right] \quad (7-44)$$

Equation 7-33 may be used to assess the rotational capacity of a long lap-splice.

7.8.2.6(b). 'Short' and Unconfined Lap-splice, $l_{lap} \leq l_s$

Many lap-splices in bridge columns were designed as compression splices with a lap of 20 bar diameters or less. Initially, such a lap-splice may function quite well and be capable of sustaining the flexural strength capacity of the column. However, under the effect of earthquake-induced cyclic loading, the bond in the lap-splice zone deteriorates and the moment capacity of the hinge is reduced.

For a short and unconfined lap-splice zone where $l_{lap} \leq l_s$, the component has a reduced ductility that depends on the curvature ductility of the member. The effective plastic hinge length can be taken as:

$$L_p = L_{lap} \quad (7-45)$$

The lap-splice-limited plastic curvature capacity is given by:

$$\phi_p = (\mu_{lap\phi} + 7) \phi_y \quad (7-46)$$

where:

- ϕ_y = yield curvature, and
- $\mu_{lap\phi}$ = curvature ductility at the initial breakdown of bond in the lap-splice zone:
 - = 0 when $M_s < M_e$, where M_s is given by equation 7-10; i.e., when the lap-splice strength (M_s) is less than the expected flexural strength (M_e), the deterioration in strength commences as soon as the moment reaches M_s and
 - = curvature ductility in the member when it reaches an ultimate strain of 0.002, when $M_e < M_s < M_{po}$, i.e., when the strength of the lap-splice (M_s) exceeds the expected flexural strength (M_e), but is less than the flexural overstrength (M_{po}), strength deterioration can still be expected but will be delayed.

7.8.2.7. Shear Failure

If the shear strength of the member is less than the shear demand (based on its flexural strength), the plastic rotation will be limited. Two limiting cases are: (a) brittle shear, and (b) semi-ductile shear. These cases are based on the shear strength relative to the flexural strength. The shear demand (V_m), based on flexure, is given by:

$$V_m = M_p / L \quad (7-47)$$

where M_p is the expected plastic moment capacity, and L is the distance to the inflection point from the point of maximum moment in the member.

7.8.2.7(a). Brittle Shear, $V_i \leq V_m$

When the initial shear strength (V_i) is less than or equal to the shear demand (V_m), the member is considered to be 'shear-critical' and will fail in shear in a brittle manner. Since the member has no ductility capacity,

$$\phi_p = 0 \quad (7-48)$$

7.8.2.7(b). Semi-ductile Shear, $V_f < V_m < V_i$

If the shear demand, based on flexure, lies between the initial (V_i) and final shear strength (V_f) of the member, the member has limited ductility capacity given by:

$$\phi_p = \left(5 \left(\frac{V_m - V_f}{V_i - V_f} \right) + 2 \right) \phi_y \quad (7-49)$$

where ϕ_y is the yield curvature, V_i is the initial shear strength (as defined previously) which is maintained until a curvature ductility of three is reached after which deterioration commences, and V_f is the final (residual) shear strength that is maintained when the curvature ductility exceeds eight.

However, if $V_m < V_f$, the shear demand is less than the final shear strength of the member and the rotational capacity is limited by flexure and not shear.

7.8.2.8. Joint or Connection Failure

If the shear induced in a joint between a beam and a column is less than the shear strength of the joint, the joint will remain elastic, and the ductility of the beam-column system will be governed by the plastic hinges in the beam and column.

Conversely, if the shear demand exceeds a certain critical level of principal stress in the joint, the joint may fail and the ductility of the beam-column system will be limited.

Although damage (in the form of plastic rotations) will take place in the joint itself, it is difficult to model such behavior. Instead, it is more convenient to modify the response of the adjoining plastic hinges in the columns. The analysis therefore can proceed in a manner similar to the case of a shear-critical column, as described earlier.

The horizontal shear in the joint (V_{jh}) is caused by flexure in the column and is given by:

$$V_{jh} = M_p / h_b \quad (7-50)$$

where M_p is the expected plastic moment flexural strength of the column, and h_b is the depth of the cap beam at the joint.

7.8.2.8(a). Weak Joint and Strong Column, $V_{ji} \leq V_{jh}$

When the joint shear strength (V_{ji}) is less than the horizontal shear in the joint due to flexure in the column (V_{jh}), joint performance will influence column behavior. The joint strength will deteriorate at the onset of full cracking (i.e., when the principal tensile stress in the joint reaches or exceeds $0.42\sqrt{f'_c}$) until a plastic rotation of $\theta_p = 0.04$ rad occurs (i.e., when the principal tensile stress in the joint is $0.29\sqrt{f'_c}$). The plastic rotation, which actually occurs in the joint, may be assumed to occur within the column's plastic hinge zone.

7.8.2.8(b). Semi-ductile Shear, $V_{jf} < V_{jh} < V_{ji}$

When the column causes a shear demand that lies between the initial and final shear strength of the joint (i.e., $V_{jf} < V_{jh} < V_{ji}$), the joint has limited ductility capacity, which can be calculated from the curvature ductility of the member as follows:

$$\phi_p = \left(4 \left(\frac{V_{jh} - V_{jf}}{V_{ji} - V_{jf}} \right) + 2 \right) \phi_y \quad (7-51)$$

where ϕ_y is the yield curvature, V_{ji} is the initial shear strength of the beam-column joint (as defined previously) which is sustained until a curvature ductility of three is reached after which deterioration commences, and V_{jf} is the final (residual) joint shear strength that is sustained when the curvature ductility exceeds seven.

However, if $V_{jf} > V_{jh}$, the shear strength is greater than the flexural demand, and the rotational capacity is limited by beam or column flexure and not joint shear.

7.8.3. NEUTRAL AXIS DEPTH IN COLUMNS AND BEAMS

In several of the above failure modes, it is necessary to find the neutral axis depth for a given value of strain, usually in an extreme fiber. This can be done either by a moment-curvature analysis, or by a plastic section analysis. The moment-curvature analysis generally requires detailed computational modeling of the entire section and is more exact. The plastic section analysis is based on equilibrium of the section and several simplifying assumptions, however, its accuracy is adequate for purposes of this manual.

For rectangular sections that are doubly reinforced, the neutral axis depth ratio is given by:

$$\frac{c}{D} = \frac{\left(\frac{P_e}{f'_c A_g} \right) + \left(\frac{\gamma \rho_t f_y / f'_c}{1 - 2d'/D} \right)}{\alpha \beta + \frac{2 \gamma \rho_t f_y / f'_c}{1 - 2d'/D}} \quad (7-52)$$

For circular sections, the neutral axis depth ratio is given by:

$$\frac{c}{D} = \frac{1}{\beta} \left[\frac{\frac{P_e}{f'_c A_g} + 0.5 \rho_t \frac{f_y}{f'_c} \left(\frac{1 - 2c/D}{1 - 2d'/D} \right)}{1.32 \alpha} \right]^{0.725} \quad (7-53)$$

where:

- c = depth to neutral axis,
- D = overall depth of section,
- P_e = axial load on the section,
- f'_c = expected concrete strength,
- f_y = expected yield strength of the longitudinal reinforcement,
- A_g = gross cross-section area,
- d' = depth from the extreme compression fiber to the center of the compression reinforcement,
- ρ_t = volumetric ratio of the longitudinal reinforcement,
- α, β = concrete stress block parameters as previously defined in section 7.7.1.2, and
- γ = reinforcing steel configuration factor:
 - = 0.5 for square sections with steel placed symmetrically around the perimeter,
 - = 0.0 for rectangular beam sections with steel lumped at the outer (top and bottom) faces,
 - = 0.0 for wall section bending about the weak (out-of-plane) axis, and
 - = 1.0 for wall sections bending about the strong (in-plane) axis.

CHAPTER 8: RETROFIT MEASURES FOR SUPERSTRUCTURES, BEARINGS, AND SEATS

8.1. GENERAL

This chapter discusses measures for retrofitting a bridge from the bearing seats up to and including the superstructure. The most common and serious seismic deficiencies are often at the bearings and bearing seats, and can potentially lead to a loss of support and collapse of the bridge. The focus of early seismic retrofitting efforts was on correcting these deficiencies, and this continues to be a significant part of current retrofitting practice. Retrofit measures include restraining devices, bearing seat extensions, bearing strengthening, and bearing replacement. Other weaknesses in the superstructure are also of concern. For example, the superstructure must be capable of transferring its inertial load to the substructure without compromising the stability of the beams. Control of plastic hinging in the superstructure will also be a concern in some cases. In addition, there are several retrofit measures for superstructures that can be used to reduce or redistribute load to the substructure. These methods include the use of special energy dissipating devices or isolation bearings, reduction of superstructure dead load, and provisions for superstructure continuity.

The following sections discuss some of the most common retrofit measures in greater detail. Many of these measures have been used extensively and have evolved to their current state over time, while others have had only limited use or are concepts developed as part of recent research efforts. The measures presented are not intended to cover all possible situations, and variations of these concepts may be possible and, perhaps, necessary for some applications.

8.2. BRIDGE DECKS AND GIRDERS

This section discusses retrofitting measures that are applicable to bridge decks and girders. It does not include a discussion of cable and bar restrainers, which are covered in section 8.4.

8.2.1. LATERAL LOAD PATH ENHANCEMENT

Retrofitting may be required to assure that inertial forces in the superstructure are effectively transmitted to the bearings and substructure. These measures are particularly applicable to steel girder bridges where a substantial portion of the mass is in the concrete deck slab and the girders and cross frames of the superstructure that may be inadequate to transmit the corresponding inertial forces to the substructure. In many cases, they are also applicable to pre-cast concrete girder bridges, which can experience the same deficiencies.

8.2.1.1. Strengthening of Deck to Girder Connection

Many older steel girder bridges are not designed for composite action and therefore do not have a positive connection between the deck slab and the girders. This could result in a separation of the deck from the girders during a strong earthquake. In many cases, this may be tolerable if it does

not result in the formation of a collapse mechanism, and may improve overall performance if it protects other vulnerable structural elements from damage. In other cases, however, it may be desirable to strengthen the deck-to-girder connection. This situation could occur when unacceptable movement of the deck is expected, when a higher level of seismic performance is required, or when a positive deck-to-girder connection is a component of a larger seismic retrofit strategy. Figure 8-1 shows one method that has been used in the past to improve the deck-to-girder connection.

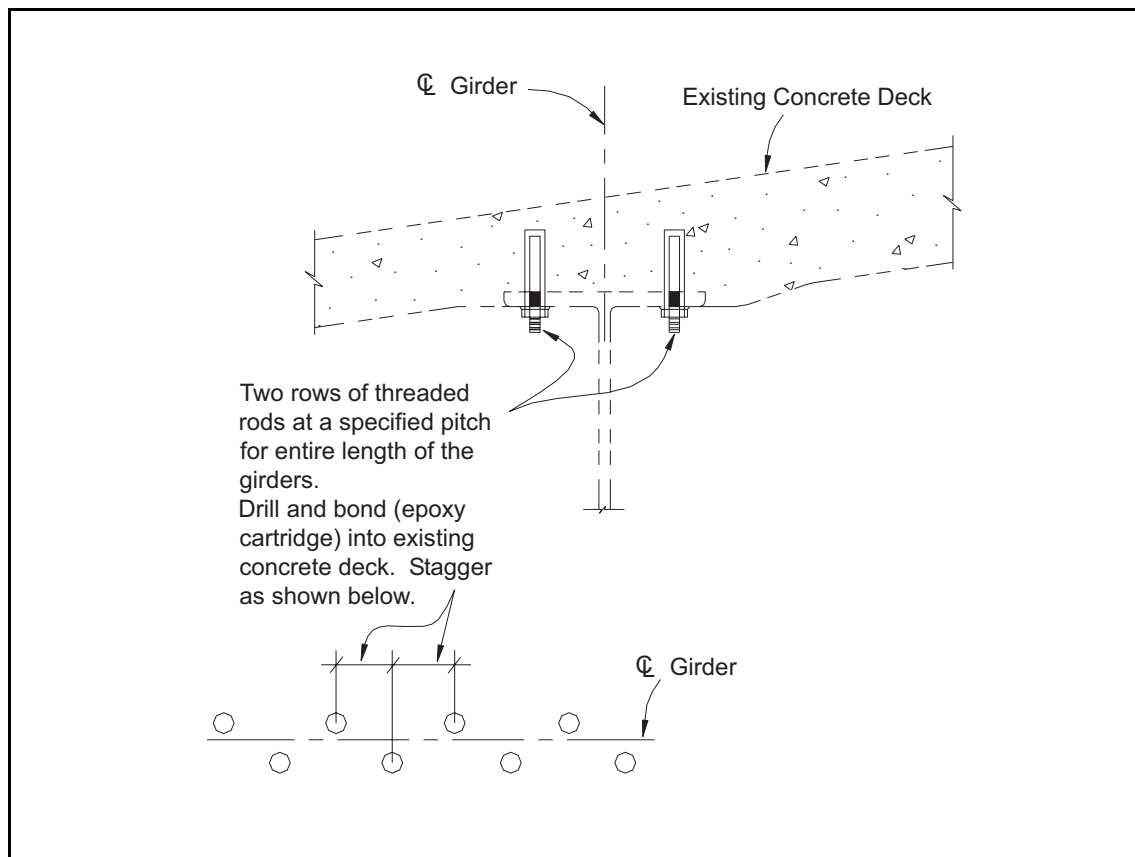


Figure 8-1. Deck to girder connection retrofit.

8.2.1.2. Diaphragm Strengthening or Stiffening

Many existing diaphragms in steel or pre-cast concrete beam bridges were not designed for high seismic loads and are not strong enough, or sufficiently ductile, to transfer the inertial forces from the deck into the bearings. This may protect the bearings from damage, but could also jeopardize the transverse stability of the beams if deformation of the diaphragm is large enough. If it is not practical to make diaphragms strong enough to resist loads elastically, brittle or non-ductile diaphragm failure modes could occur. This would include shear failure of bolted or riveted connections or inelastic buckling of compression members within the diaphragm. Generally, this will require strengthening or bracing of the diaphragm in such a way as to make axial yielding in a diaphragm member the principle mode of failure.

If existing riveted or bolted connections are not strong enough to resist the loads applied to them, then retrofitting might include removal of the existing rivets or bolts and replacement with stronger connectors (e.g., higher grade material or larger diameter bolts). When only bolts are used in a connection, their ultimate strength as bearing connectors may be used. The use of welds should also be considered if the weldability of the existing steel is acceptable and the direction of applied stress is conducive to a welded connection. Welds may be considered to complement the strength of existing rivets and bolts if capacity design principles are used to design the connection, and the rivet or bolt design strength is strain-compatible with the welds. This could be the case if the design capacity of the existing bolts is limited to that of a friction-type connection.

A method of increasing the inelastic buckling strength of a diagonal member is shown in figure 8-2. This method involves the addition of a relatively stiff member, such as a steel tube, to brace the existing diaphragm member against buckling. Slotted bolt holes are used to connect the bracing member so that it does not add to the yield strength of the existing diaphragm member. This is important, because the diaphragm will be subject to load reversals during the earthquake, and some members will act in both tension and compression. Yielding of these members will limit forces in other elements of the diaphragm and result in ductile behavior. This phenomenon is illustrated in the free body diagram for a typical diaphragm shown in figure 8-3.

Axial yielding of mild steel members in the diaphragm can be relatively ductile if inelastic buckling is prevented. However, it is important to consider the displacement ductility of the entire lateral force resisting system (diaphragms, girders, bearings, piers and foundations) in determining the adequacy of the critical diaphragm member. This can be accomplished by performing a two-dimensional, nonlinear, static 'pushover' analysis of the system with a target displacement equal to 150 percent of the displacement from an elastic analysis in which the stiffness of all elements is considered. With this analysis, it is suggested that the design may be considered satisfactory for collapse prevention if no brittle or non-ductile failures are indicated (e.g., fracture of the net section at the connections) and axial elongations of diaphragm components limit relative transverse displacement at the top of the girder to two percent of the girder height.

8.2.1.3. Energy Dissipating Ductile Diaphragms

A seismic retrofit strategy that replaces existing end diaphragms in the steel superstructure with specially detailed *ductile* end diaphragms may provide a desirable energy dissipation mechanism in the structure in the transverse direction. These ductile diaphragms can be specially designed and calibrated to yield before the substructure elements (foundation and bearings). This strategy may be adopted when the substructure elements have limited ductility and cannot be relied upon to achieve a stable ductile response (e.g., stiff wall piers). Ductile diaphragms should be capable of dissipating energy in a stable manner without strength degradation during cyclic deformation. Various types of systems capable of stable passive seismic energy dissipation may be adopted for this purpose. Among these are eccentrically braced frames (EBF)¹, shear panel systems (SPS)²,

¹ Malley and Popov, 1983; Kasai and Popov, 1986

² Fehling et al., 1992; Nakashima, 1994

and steel triangular-plate added damping and stiffness devices (TADAS)³. TADAS devices are popular in building applications and have been studied for bridge applications⁴. Although concentrically braced frames can also be ductile, they may not be desirable because they may be stronger than calculated, and their hysteretic curves may exhibit pinching and some strength degradation. Typical energy dissipating, ductile diaphragms are shown in figure 8-4.

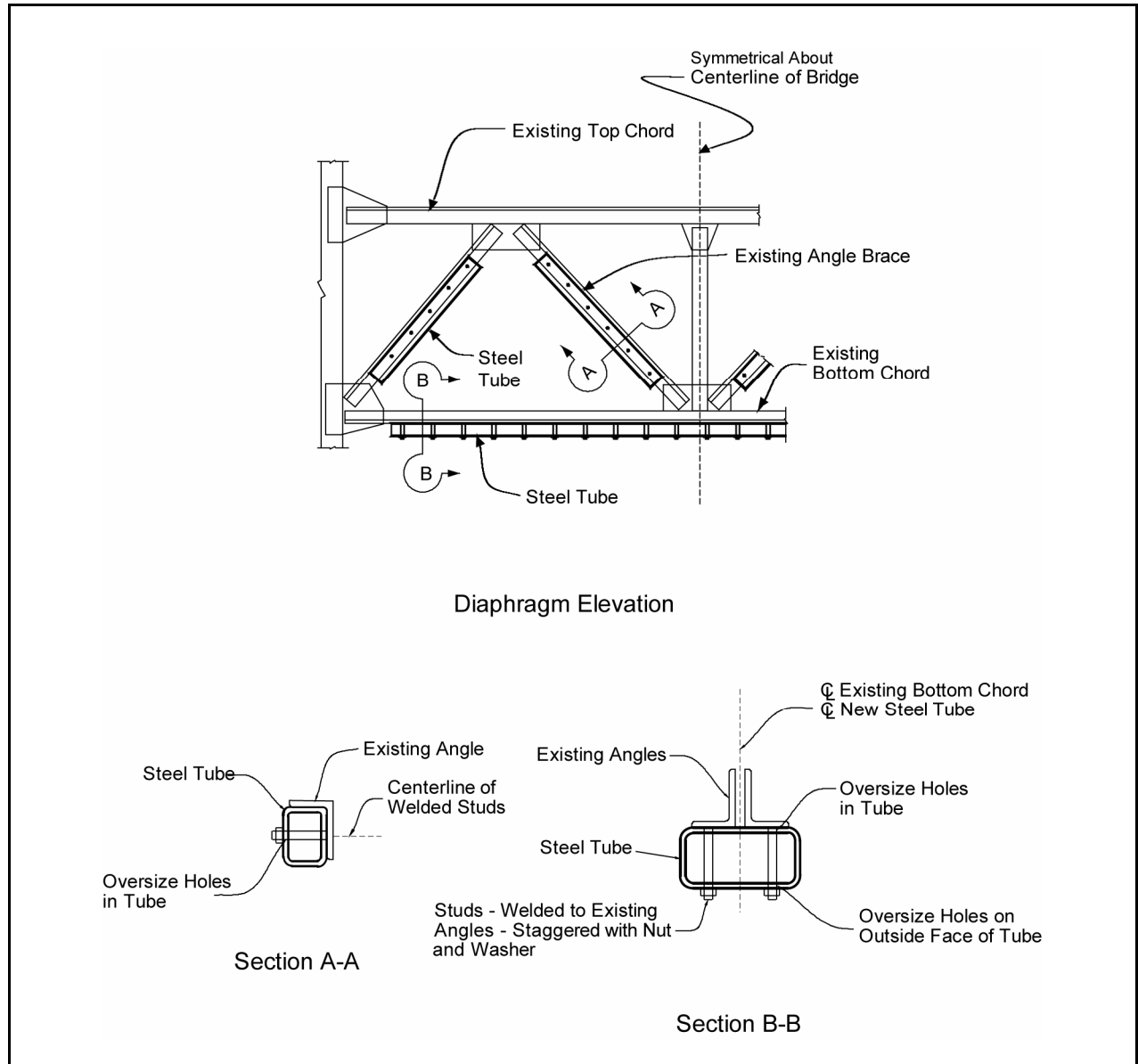


Figure 8-2. Steel girder diaphragm retrofit.

³ Tsai et al., 1993

⁴ Zahrai and Bruneau, 1998, 1999

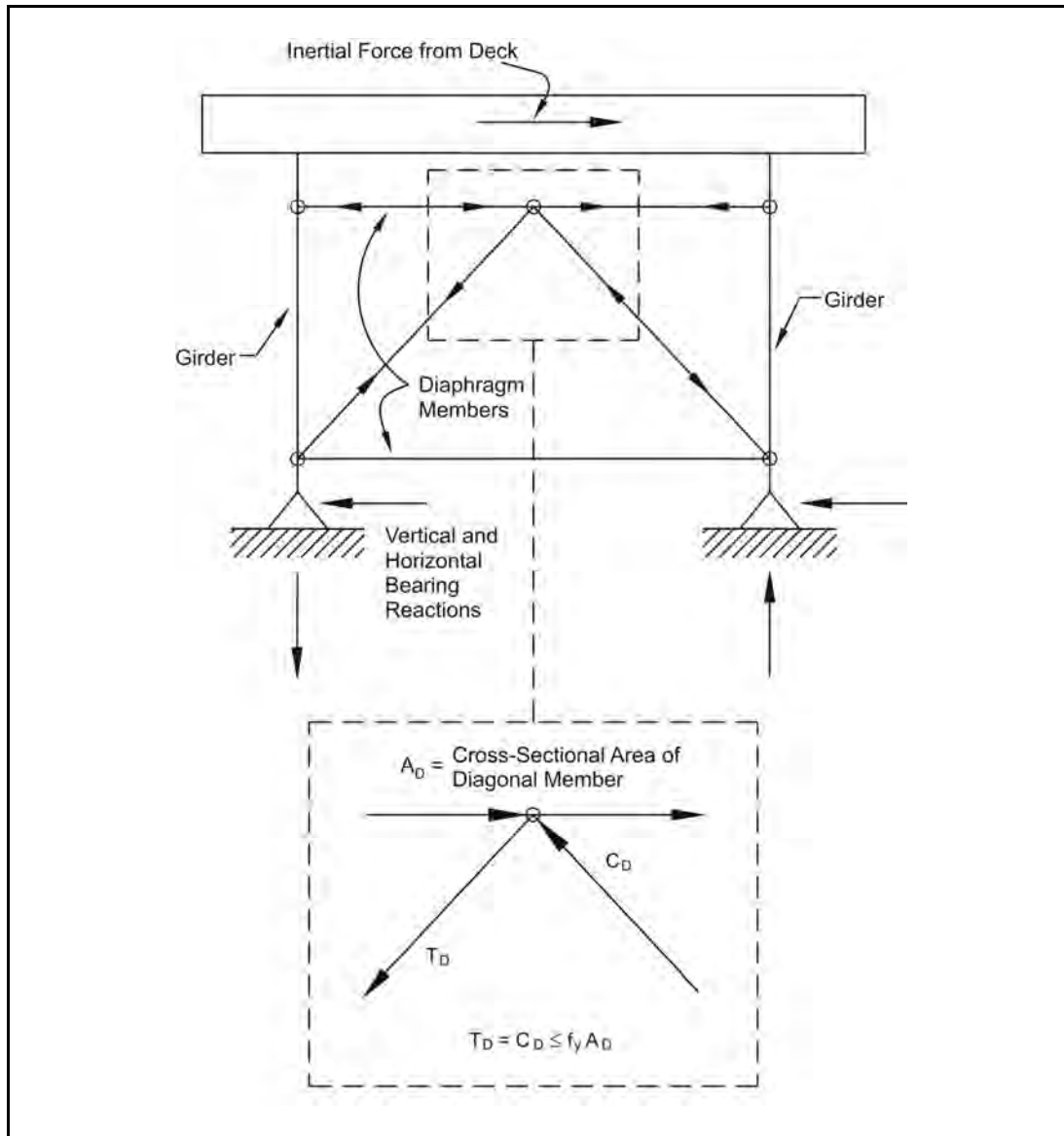


Figure 8-3. Diaphragm free body diagram.

The ductile diaphragm approach may not be effective when the substructure is significantly more flexible than the superstructure. Therefore, bridges with wide piers, wall piers, or other stiff substructure elements of similar limited ductility, are candidates for the implementation of this system. Ductile diaphragms can also be designed to yield before the bridge piles, thus preventing the development of damage below ground where it is difficult to inspect following an earthquake. Recent studies have provided methods to account for the effect of substructure flexibility⁵ on the ductility demands of ductile diaphragms. This is reflected in the recommended response modification factor (i.e., R-factor) for design of ductile end diaphragms recommended by equation 8-1:

⁵ Alfawakiri and Bruneau, 2000

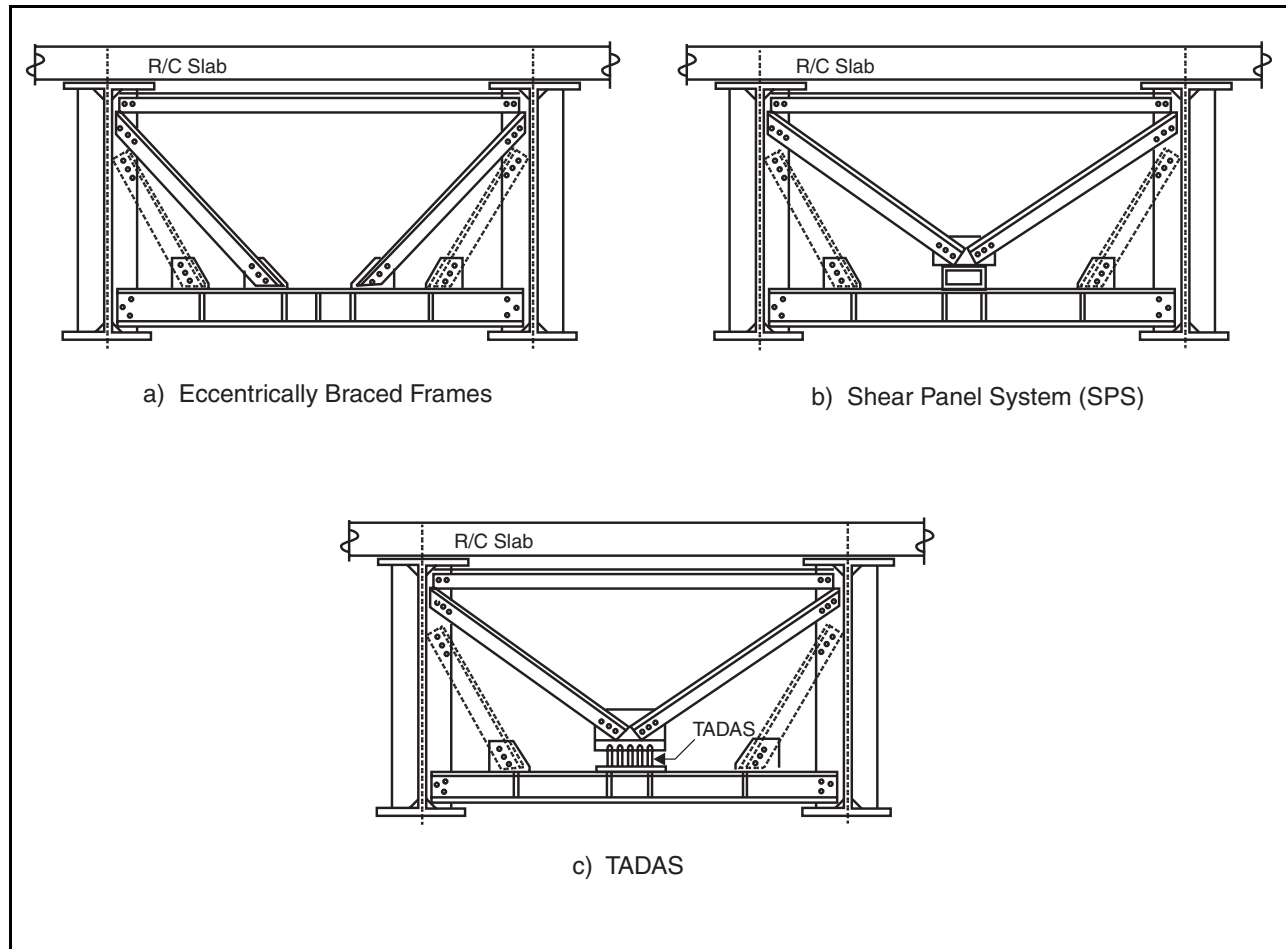


Figure 8-4. Ductile end diaphragms.

$$R = \left(\frac{\mu + \frac{K_{DED}}{K_{SUB}}}{1 + \frac{K_{DED}}{K_{SUB}}} \right) \quad (8-1)$$

where μ is the ductility capacity of the end diaphragm itself, which should not be taken to be greater than four, K_{DED} is the stiffness of the ductile end diaphragm, and K_{SUB} is the stiffness of the substructure.

Typically, increased substructure flexibility results in higher ductility demands in ductile end diaphragm systems. The capacity of the ductile system, or device, should not be exceeded for the maximum expected lateral drift of the bridge at the diaphragm location. A drift limit of two percent of the girder height is recommended until further experimental evidence is provided to demonstrate that higher values may be acceptable.

Inertia forces due to the mass of the pier cap will not be reduced by ductile end diaphragms, and must be resisted by the substructure. Refined analyses should consider this condition if the mass of the pier cap is a significant portion of the total superstructure mass.

Ensuring an adequate load path within the superstructure can enhance the effectiveness of ductile end diaphragms. In general, a continuous path is necessary for the transmission of the superstructure inertia forces to the substructure. Concrete decks have significant rigidity in their horizontal plane, and in short-to-medium steel beam spans, their response approaches rigid-body motion. Therefore, the lateral loads resisted by the intermediate diaphragms are minimal, and the load path for seismic loads is effectively through the deck and the end diaphragms to the bearings.

It is important to note that the contribution of girders to lateral stiffness at the end diaphragms can be significant and should not be neglected. For this reason, ductile diaphragms are typically more effective in longer span bridges, and may be of limited benefit for very short span bridges. The retrofit design should consider the combined stiffness and strength of end diaphragms acting in conjunction with the girders (including the effect of the girder's bearing stiffeners) in establishing the diaphragm's strength and therefore the design forces for capacity protected elements such as bearings.

Ductile energy dissipating elements in the end diaphragms should be laterally braced at their ends to prevent out-of-plane instability. It is recommended that these lateral supports and their connections be designed to resist six percent of the nominal strength of the beam flange. To prevent lateral torsional buckling of beams in the end diaphragms, the unsupported length of these beams should be typically limited to $200 \frac{b_f}{\sqrt{f_y}}$, where b_f is the width of beam flange in meters and f_y is the yield strength of steel in MPa.

The energy dissipating ductile end diaphragm concept is relatively new and has yet to be implemented in practice. However, considerable research related to these members has been conducted⁶, which has demonstrated the effectiveness and validity of the design methods described above. Further information is given in the recommended provisions for seismic design developed for the NCHRP 12-49 project (ATC/MCEER 2003).

8.2.1.4. Girder Strengthening

Girders may be subjected to high transverse bending stresses in the vicinity of the bearings during an earthquake. This will be most critical when diaphragms are not provided or when diaphragms consist of horizontal beam type elements located some distance above the bearings. In these cases, the principal resistance to transverse bending is that provided by web stiffeners at the bearings, which may be inadequate for this purpose. If stresses and distortions are too high, the ability of the girder web to support dead load may be compromised. Supplemental braces as shown in figure 8-5 may be used to prevent transverse distortion of the girders, or bearing stiffeners may be strengthened as shown in figure 8-6.

⁶ Zahrai and Bruneau, 1998 and 1999; Sarraf and Bruneau, 1998a and 1998b

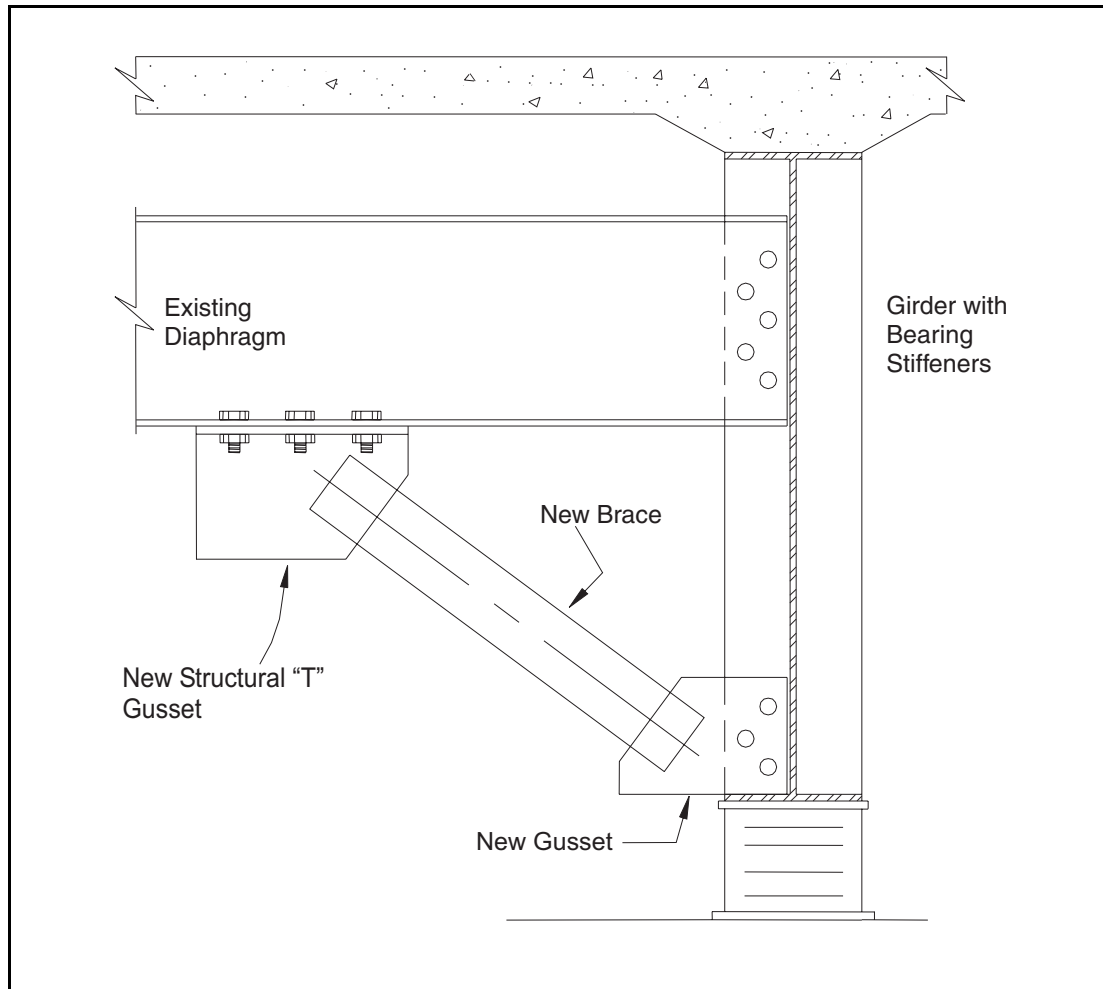


Figure 8-5. Girder bracing retrofit.

8.2.2. PROVIDING LONGITUDINAL CONTINUITY

Several retrofit measures other than cable or bar restrainers are available for providing superstructure continuity in the longitudinal direction during an earthquake so that seismically induced forces can be better shared between the supports. Some of these methods are discussed below.

8.2.2.1. Web and Flange Plates

It is often possible to tie steel beams together using web plates as shown in figure 8-7. It may be necessary to use shims to get the web splice plates to align properly with the beam webs. If the plates are located at an expansion joint, bolt holes may be slotted to provide for thermal expansion and contraction of the superstructure. This retrofit measure also provides for vertical support of one of the girders if it becomes unseated. To prevent bolt failure due to vertical and horizontal impact loading and misalignment or slotting of the bolt holes, bolts should be designed as bearing

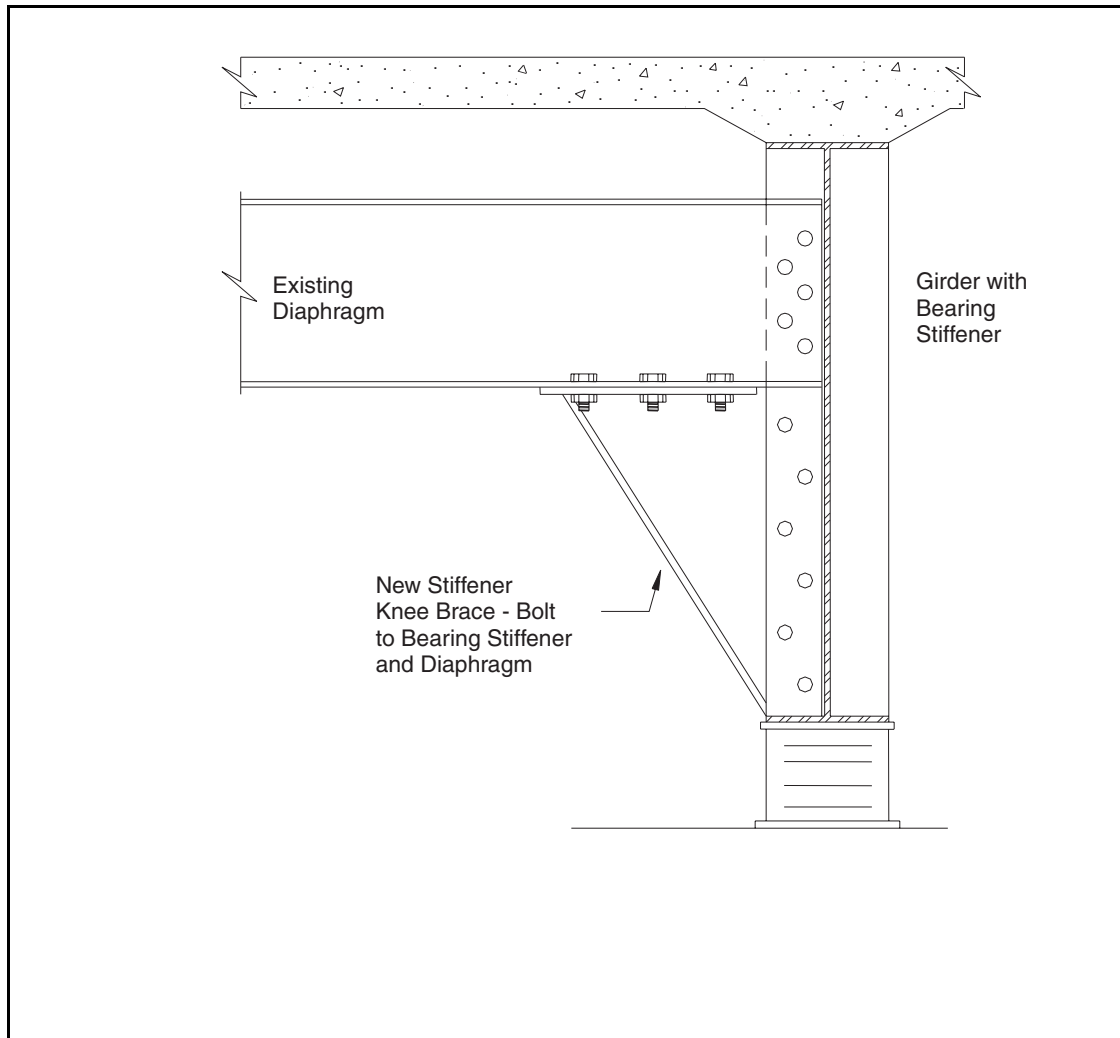


Figure 8-6. Bearing stiffener retrofit.

connectors with large factors of safety (i.e., two or greater). Also, relative transverse movement of the beams should be restrained to prevent tearing of the web.

8.2.2.2. Superstructure Joint Strengthening

It is often possible to make a structure continuous for live load across existing joints without significantly affecting its ability to accommodate changes in temperature. This is true if the bridge is relatively short or if the joint in question involves fixed bearings on both sides of the joint. This can be done by removing a portion of the deck on either side of the existing joint, connecting the girders together with splice plates at the flanges, and reconstructing the deck so as to be continuous. This retrofit method is illustrated in figure 8-8. This method requires verification of the ability of the girders to accommodate the resulting negative moments that will occur under service load conditions.

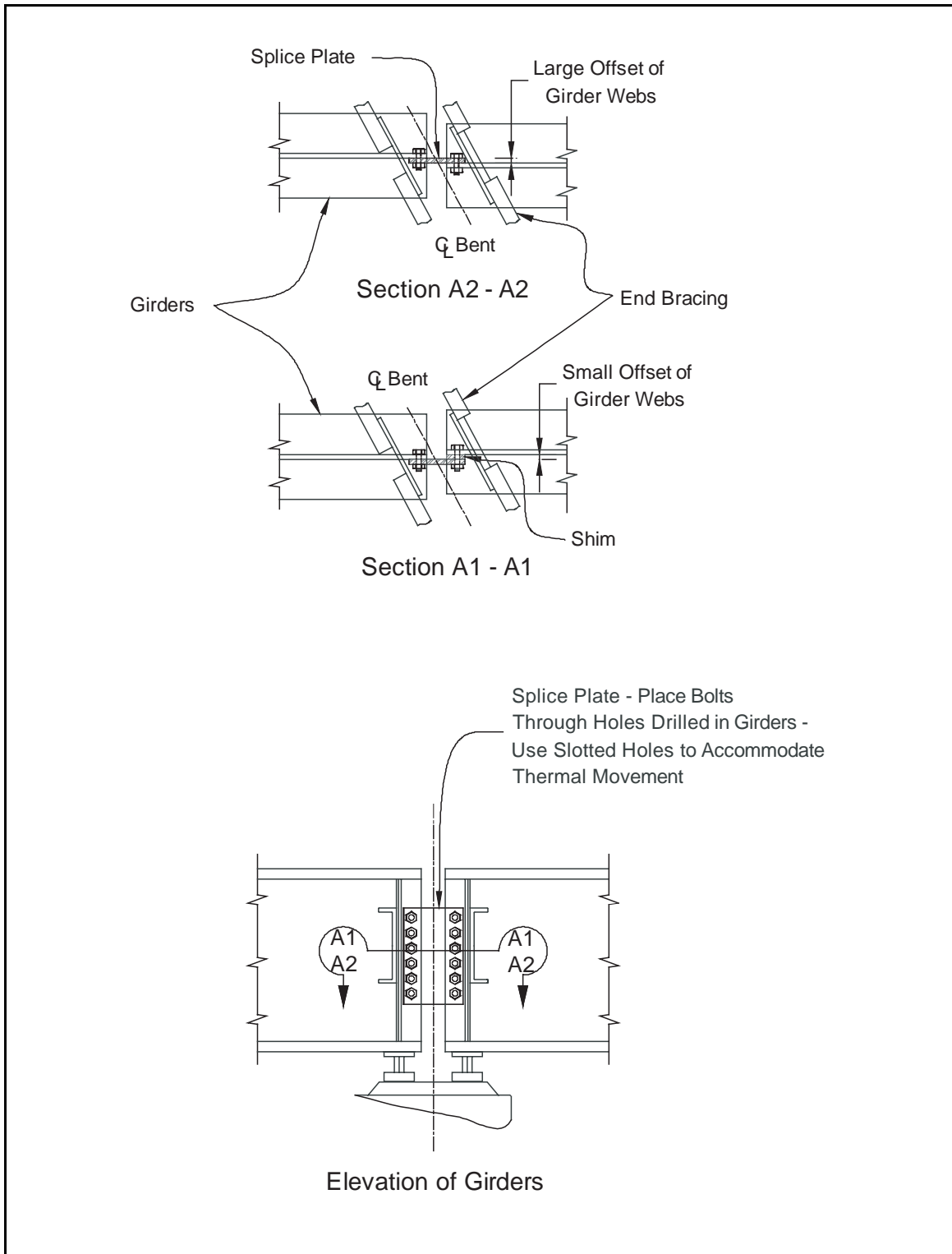


Figure 8-7. Methods for accommodating girder misalignment using web splice plates.

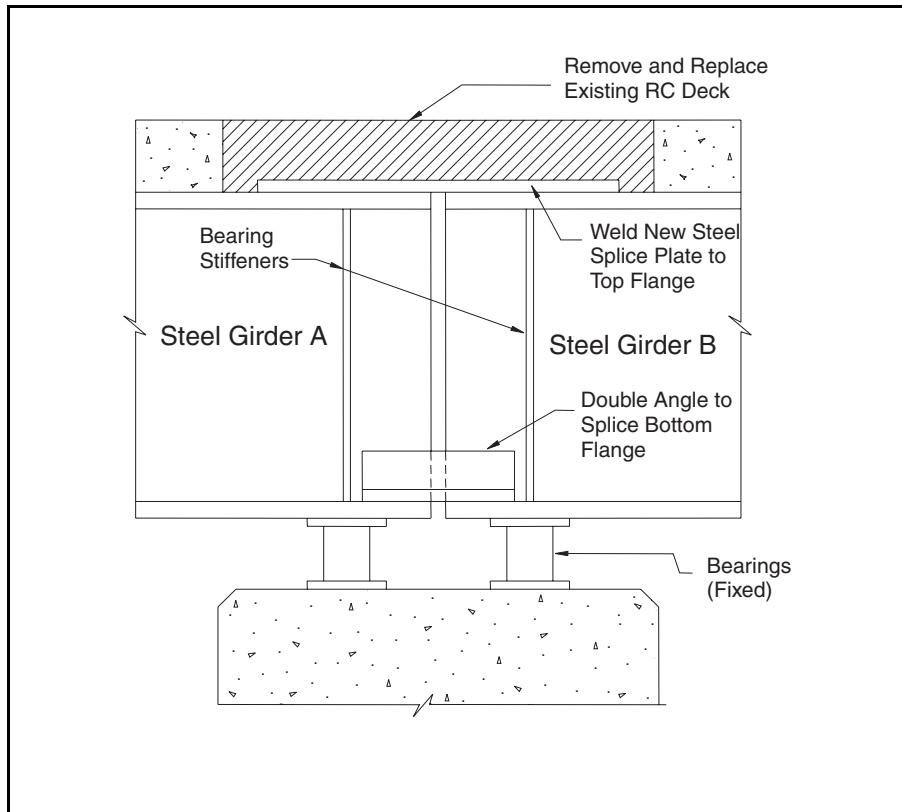


Figure 8-8. Girders made continuous for live load.

8.2.3. REDUCTION OF DEAD LOAD

It is sometimes possible to reduce dead load on a bridge superstructure. Although this will often decrease the natural period of vibration, and therefore result in a slight increase in the spectral acceleration, the net effect will be to reduce the displacement and ductility demands on the bridge. This reduction in seismic demand may be enough to improve seismic performance. Removal of heavy concrete barrier rails and accumulated overlays of asphalt concrete or other materials, or replacement of a heavy concrete deck with light weight concrete or other material, are some of the options that may be considered.

8.2.4. STRENGTHENING OF CONTINUOUS SUPERSTRUCTURES

It is generally not desirable to allow extensive plastic hinging to occur in a superstructure that is integral with the substructure, since the superstructure is usually not designed to behave in a ductile manner. To prevent this, the superstructure can be strengthened to restrict plastic hinging to the piers. This is preferable since piers are more easily retrofitted for ductility enhancement. Figure 8-9 illustrates how this can be done for a concrete box girder structure that lacks significant positive moment capacity near a support. Additional retrofitting would be required if the negative moment capacity of the superstructure was also inadequate. To prevent excessive torsion from developing in the pier cap near the column, retrofitting should be done symmetrically about a column within a width equal to the width of the column plus twice the

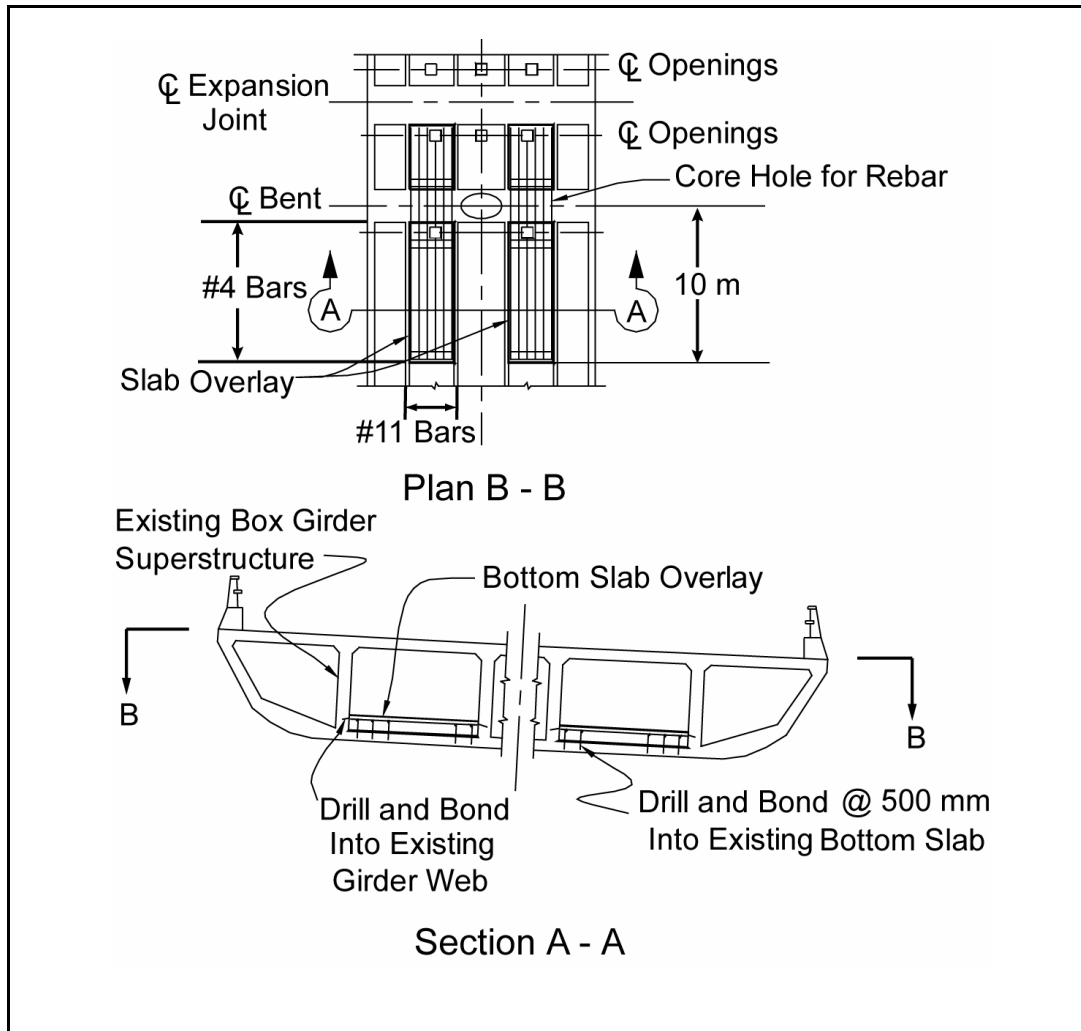


Figure 8-9. Retrofit of concrete box girder for flexural capacity.

depth of the superstructure for box girders and solid superstructures, or the width of the column plus the depth of the superstructure for stringer-type superstructures.

8.3. BEARINGS, ANCHORAGES AND PEDESTALS

When the superstructure can become dislodged from its bearings, the designer has several options to consider. If the seat that supports the bearings is wide enough and the superstructure can drop only a short distance, it may acceptable to allow the bearings to fail as long as a collapse mechanism is avoided and the resulting level of performance is acceptable. If the height of the vulnerable bearings is large, it is usually advisable to retrofit the structure. This can be done by strengthening the existing bearings, replacing them with new bearings, or providing an elevated seat extension (i.e., a catcher block) that will maintain the grade of the superstructure in the event of bearing failure. This section deals with bearing strengthening and replacement. Catcher blocks are discussed in section 8.4

Bearing types that have fared poorly in past earthquakes are shown in figure 4-3. Although different bearings have different configurations, failure will usually occur at the connection between the bearing and the girder, at keeper plates, at the connection between the bearing and the masonry plate, or at the anchor bolts that connect the masonry plate to the support. In some cases, bearings will be mounted on concrete pedestals that must also be considered as a possible cause for bearing failure. Steel rocker bearings are particularly vulnerable to damage during an earthquake. Figure 8-10 shows the nomenclature for two typical steel bearing types.

New or strengthened bearings and their restraining components should be capable of resisting the longitudinal, transverse, and vertical forces obtained by analysis.

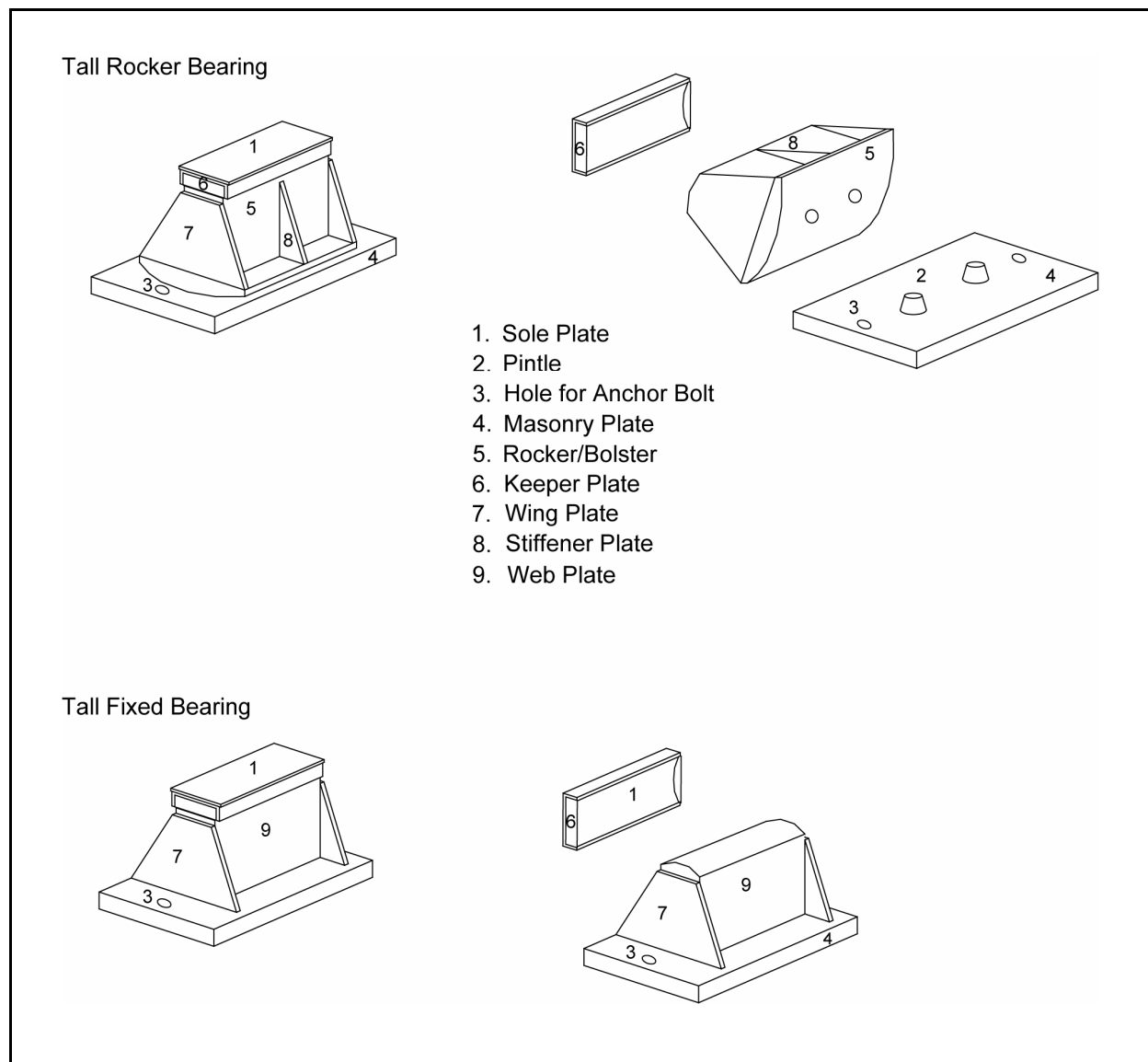


Figure 8-10. Steel bearing nomenclature.

8.3.1. STRENGTHENING OF EXISTING BEARINGS

Strengthening is not usually the preferred retrofit measure for steel rocker bearings because of their poor maintenance history, and replacement may be preferred instead. But there may be cases where strengthening is the best option, in which case the focus should be on those components of the bearing that are most likely to fail. Note that if bearings are strengthened, failure and/or yielding may shift to other locations within the structure - usually the piers. The designer should verify that yielding at this new location is acceptable, and that there is sufficient strength and/or ductility to achieve the desired performance of the bridge.

8.3.1.1. Expansion Bearings

Expansion bearings are intended to allow free movement in the longitudinal direction and usually have keeper plates, pintels, anchor bolts, or some other mechanism, to prevent transverse movement and resist transverse loads. Retrofitting to increase the strength of these connections is frequently necessary to meet minimum force requirements and prevent loss of support in the transverse direction. Care should be taken that these measures do not impede the longitudinal movement of the bearing and inadvertently restrict longitudinal expansion.

8.3.1.1(a). Sole Plate to Girder

Sole plates are usually connected to girders with bolts or rivets, which often lack the shear capacity required to prevent the sole plate from breaking loose from the girder during an earthquake. This deficiency can be overcome by replacing existing bolts and rivets with stronger bolts. If this does not provide sufficient strength, it may be possible to use a supplemental connector plate that will put the bolts in double shear as shown in figure 8-11. These new bolts must be designed to resist both tension and shear simultaneously, and the flange and sole plates must be capable of resisting these forces.

Another retrofit measure is to provide for an extended range of transverse movement of the beam on the bearing. The details used for this retrofit will depend on the details of the bearing, but one method that was proposed for bearings tested in the laboratory is shown in figure 8-12 (Mander et al., 1996a). In this case, keeper plates are allowed to fail. The steel catcher bars that are welded to the sole plate would accommodate the resulting sliding of the bearing on the sole plate. Transverse movement is limited to half the width of the bearing. In this case, vertical legs extending downward from the catcher bars resist extreme movement provided vertical accelerations are not excessive.

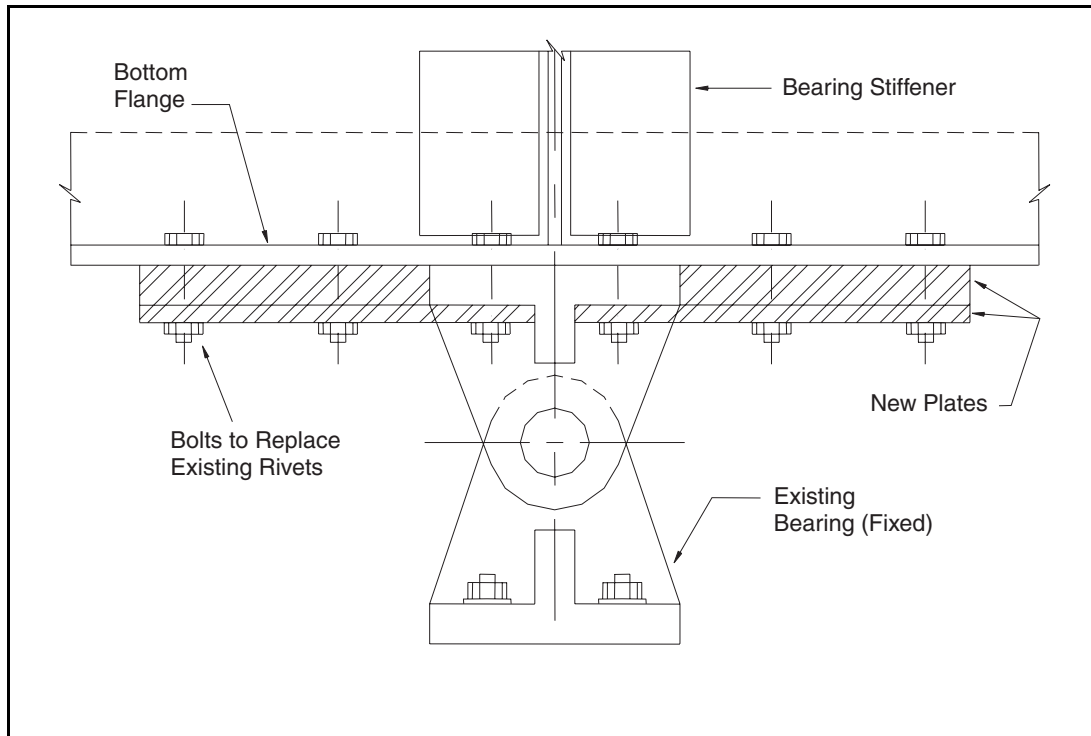


Figure 8-11. Bearing sole plate to girder connection retrofit.

8.3.1.1(b). Bearing to Masonry Plate

Steel rocker bearings provide very little resistance to movement in the longitudinal direction. Recent laboratory testing has shown that it is possible to retrofit this type of bearing to increase resistance to displacement beyond a predetermined range (Mander et al., 1996c). This allows freedom of movement for thermal expansion and contraction of the superstructure, but resists excessive movement due to an earthquake. This is done by welding steel wedges to the bearing plate as shown in figure 8-13. The edges of the wedge plate should be sealed to prevent the entry of moisture and thus eliminate potential corrosion between the wedges and the bearing plate. The resulting increase in longitudinal resistance, F_h , is given as a function of the bearing dead load reaction, P , and the angle of the wedges, α , per equation 8-2.

$$F_h = P \tan \alpha \quad (8-2)$$

In the transverse direction, the connection between bearing and bearing plate is sometimes provided by pintles that engage holes in the rocker. In other cases, keeper bars or anchor bolts provide resistance to transverse force. Any of these transverse force-resisting devices can fail in shear and result in unacceptable transverse movement of the superstructure. The type of retrofit selected to prevent excess transverse movement will depend on the configuration of the bearing. One possible method is shown in figure 8-14.

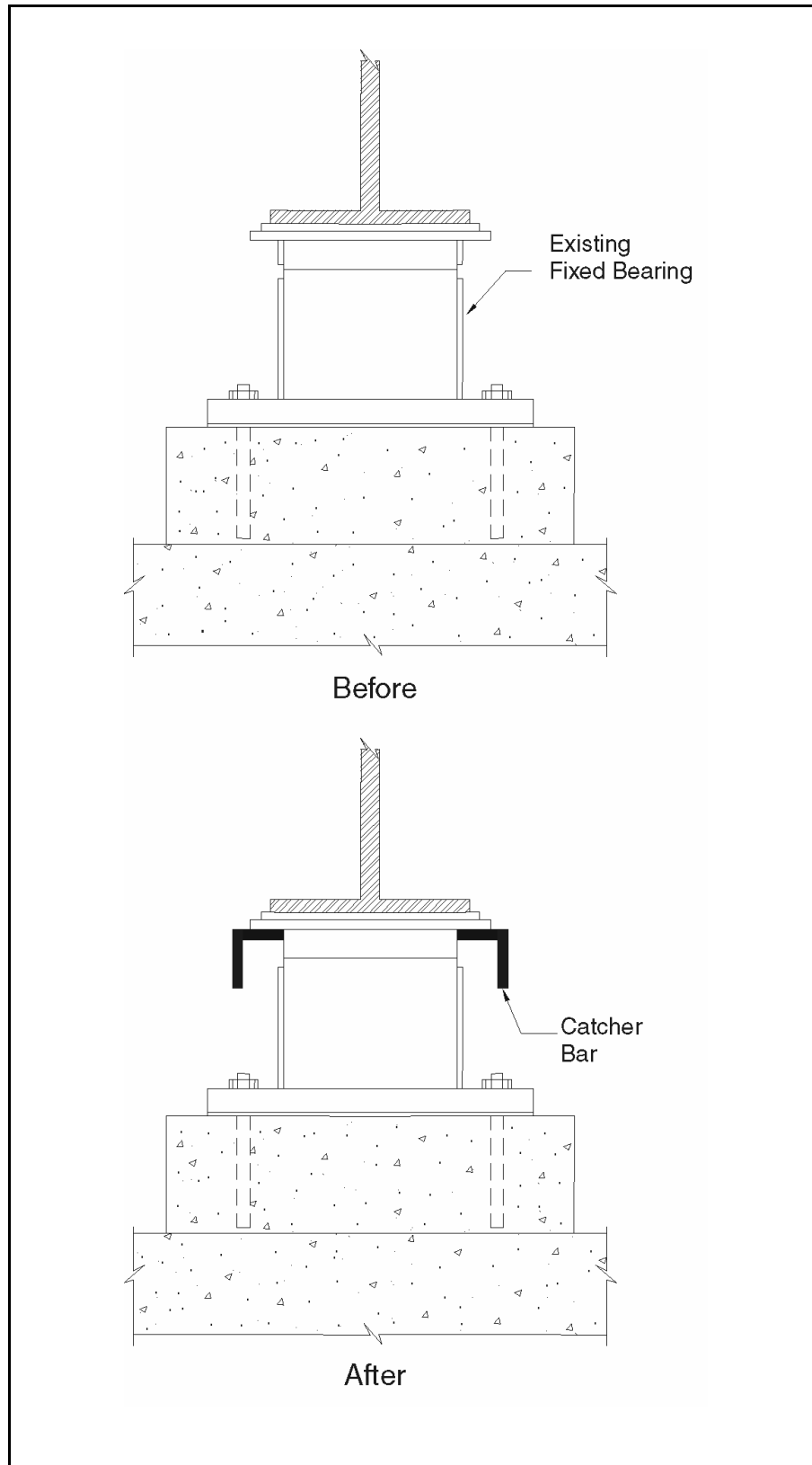


Figure 8-12. Bearing sole plate to girder with catcher bar retrofit.

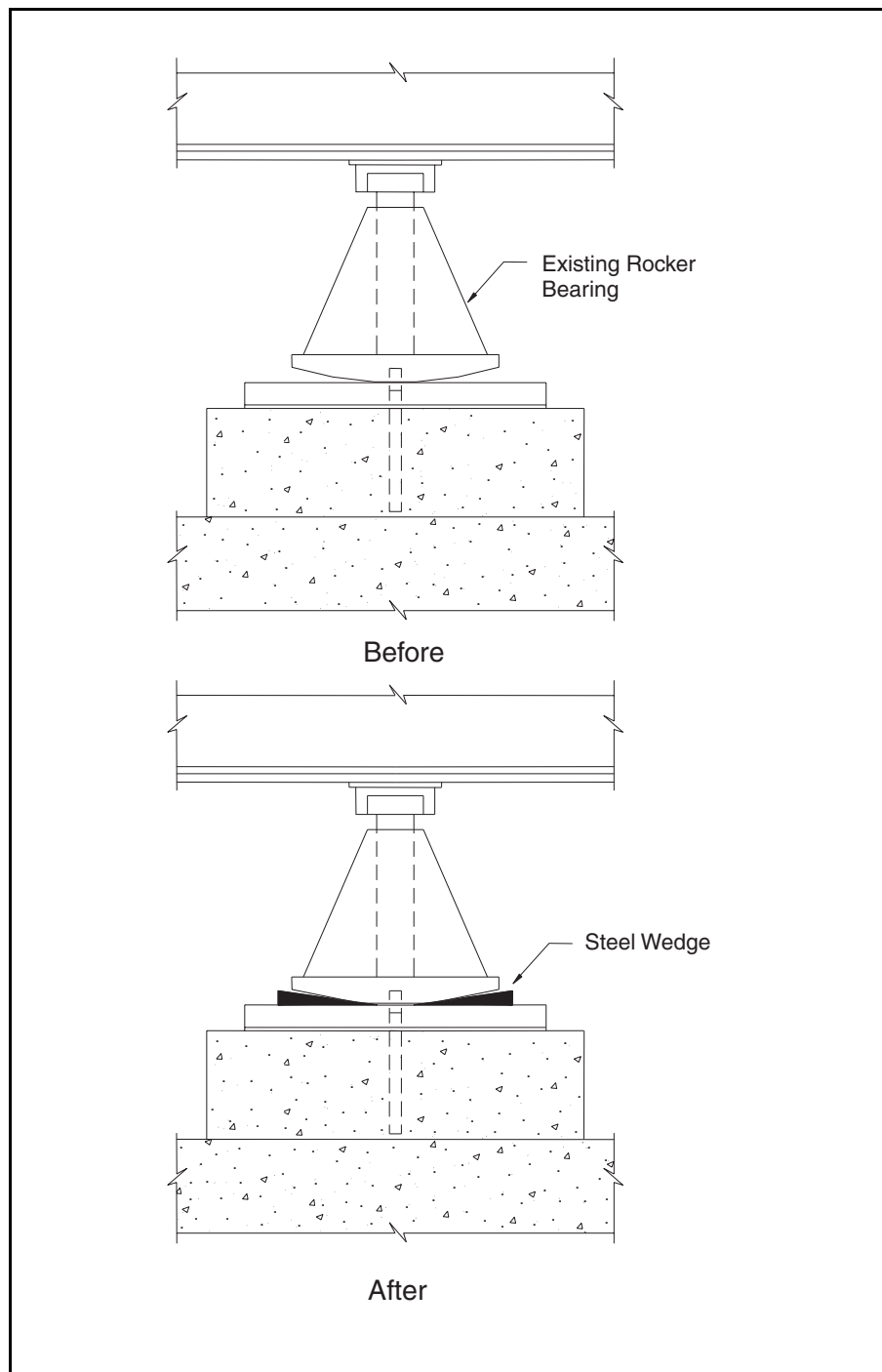


Figure 8-13. Expansion bearing retrofit.

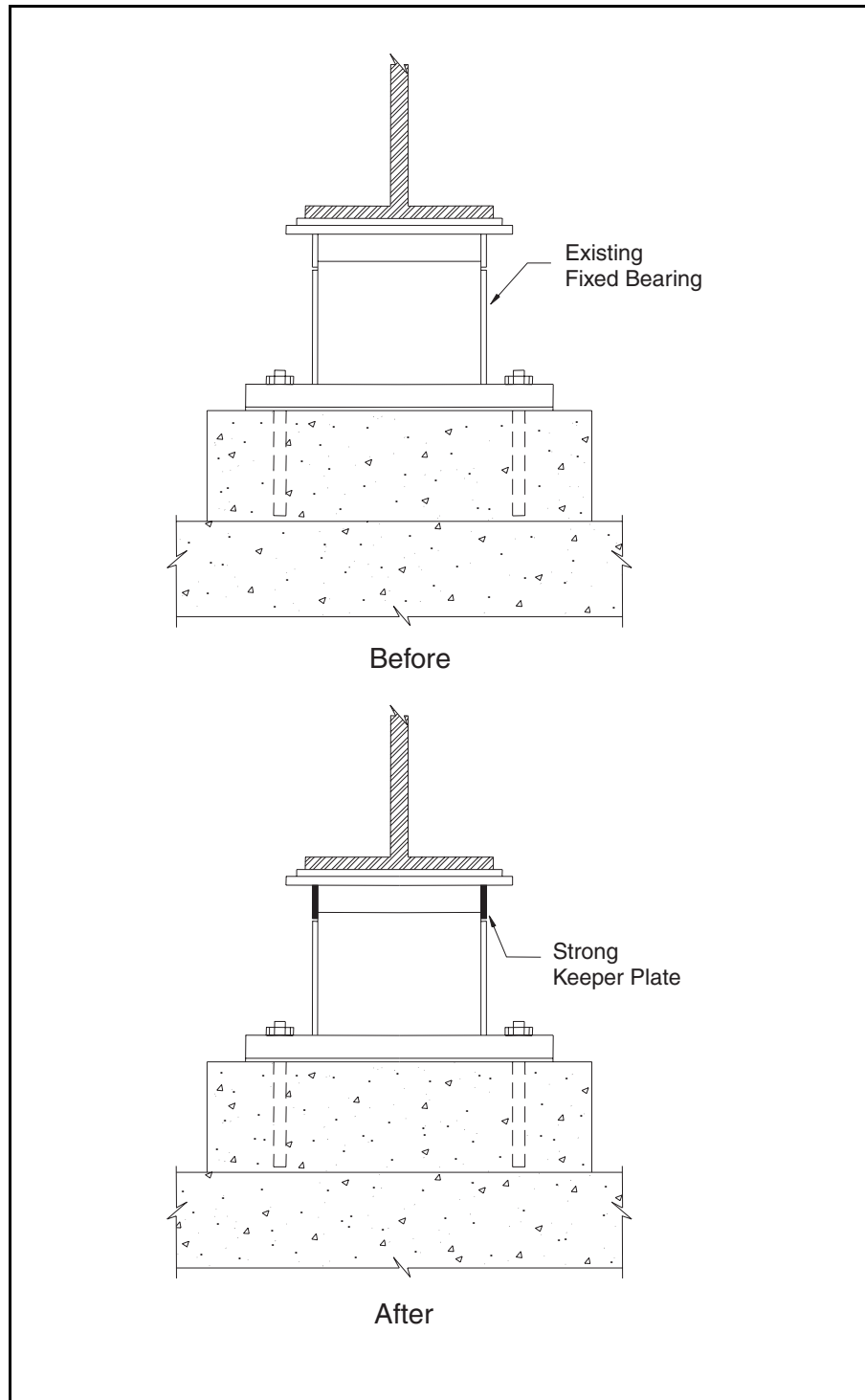


Figure 8-14. Retrofit to increase bearing transverse capacity.

8.3.1.1(c). Masonry Plate to Substructure

Masonry plates are usually connected to the substructure with anchor bolts cast into concrete bearing seats. These bolts must resist both shear and tension when the bearing is subjected to transverse forces, and if they should fail, the resulting sliding of the bearing may cause excessive displacement of the superstructure. The capacity of the masonry plate to resist these forces can be increased by adding more anchor bolts, which may require making the plate larger. This can be done by drilling and grouting new anchor bolts into the concrete bearing seat and connecting these new anchor bolts to the existing masonry plate. One method for doing this is shown in figure 8-15.

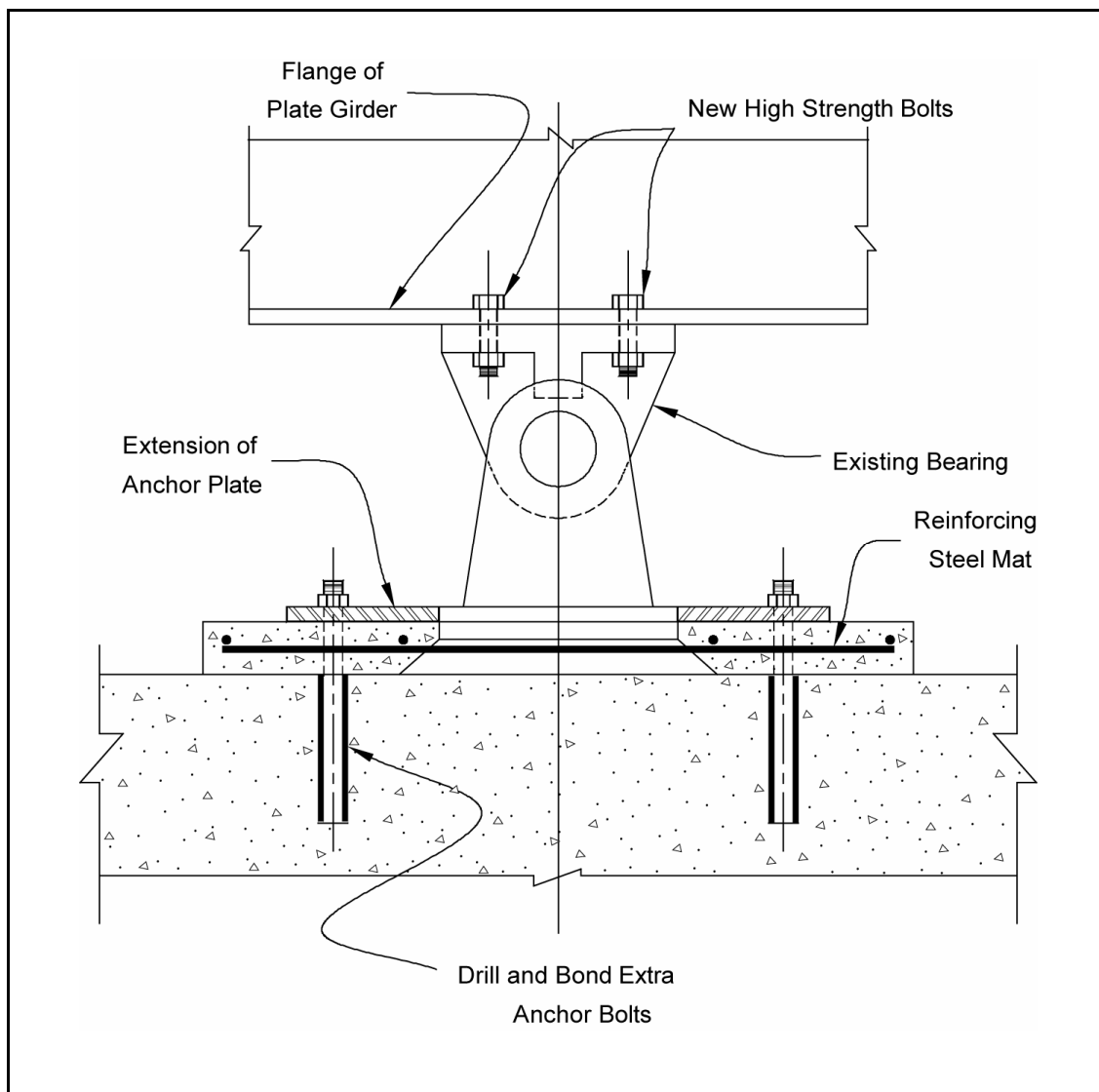


Figure 8-15. Retrofit to increase anchor plate capacity.

8.3.1.2. Fixed Bearings

In the case of fixed bearings, horizontal forces are resisted in both the longitudinal and transverse direction. There are several locations within a bearing assembly where failure can occur. Usually, the sole plate-to-beam connection, keeper bars, and masonry plate-to-substructure connection are the weakest points. In some cases, bearings are mounted on concrete or masonry pedestals that may fail during an earthquake.

8.3.1.2(a). Sole Plate to Girder

There is very little difference between retrofitting a sole plate-to-beam connection for a fixed bearing than for an expansion bearing. The primary difference is that the connection in a fixed bearing must carry large longitudinal as well as transverse forces. See section 8.3.1.1(a) and figures 8-11 and 8-12 for suggested retrofit measures.

8.3.1.2(b). Masonry Plate to Substructure

Anchor bolts on fixed bearings are usually subjected to simultaneous tension and shear during an earthquake. This makes it more difficult to retrofit the masonry plates by simply adding more anchor bolts. An alternative method is bearing encasement, which can also be used to increase the strength of concrete and masonry pedestals. One approach (Mander et al., 1996c) is to place a steel shell around the portion of the bearing to be encased, up to the pivot point of the bearing. The concrete within the shell is anchored to the bearing seat by dowels that are drilled and bonded into the existing concrete. If insufficient length exists to fully develop the dowels in the new concrete encasement, they may be welded to the steel shell. A typical retrofit detail is shown in figure 8-16.

Another method of bearing embedment is shown in figure 8-17. This will prevent shear failure and toppling of the bearings. In addition, if the spans are unseated from the bearings, the concrete cap will limit the vertical drop. The concrete cap can also act as a shear key and an anchorage for vertical motion restrainers.

8.3.2. BEARING REPLACEMENT

8.3.2.1. Conventional Bearings

Replacement is the preferred retrofit measure for bearing types that have performed poorly in past earthquakes. This is because seismically vulnerable bearings also have a history of maintenance problems. But many of the newer bearings have smaller vertical dimensions than the ones they are replacing, and it will be necessary to compensate for the difference in height as part of the retrofit. This may be done by using either a steel pedestal (figure 8-18) or a concrete pedestal (figure 8-19). In the latter case, the pedestal can be constructed to a higher elevation between beams to provide a transverse shear key and vertical motion restrainers may be anchored into the pedestal.

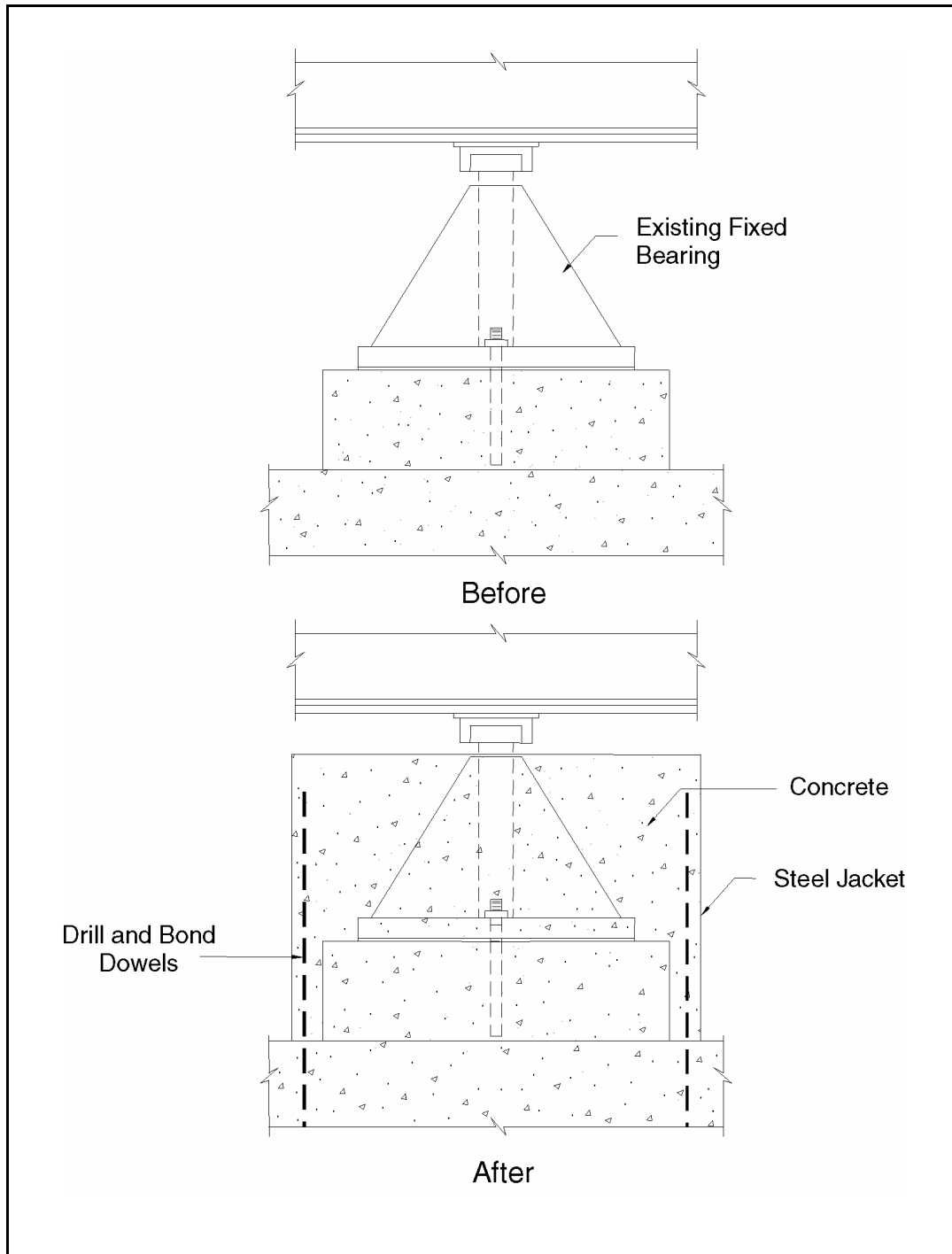


Figure 8-16. Bearing retrofitting by encasement in steel shell.

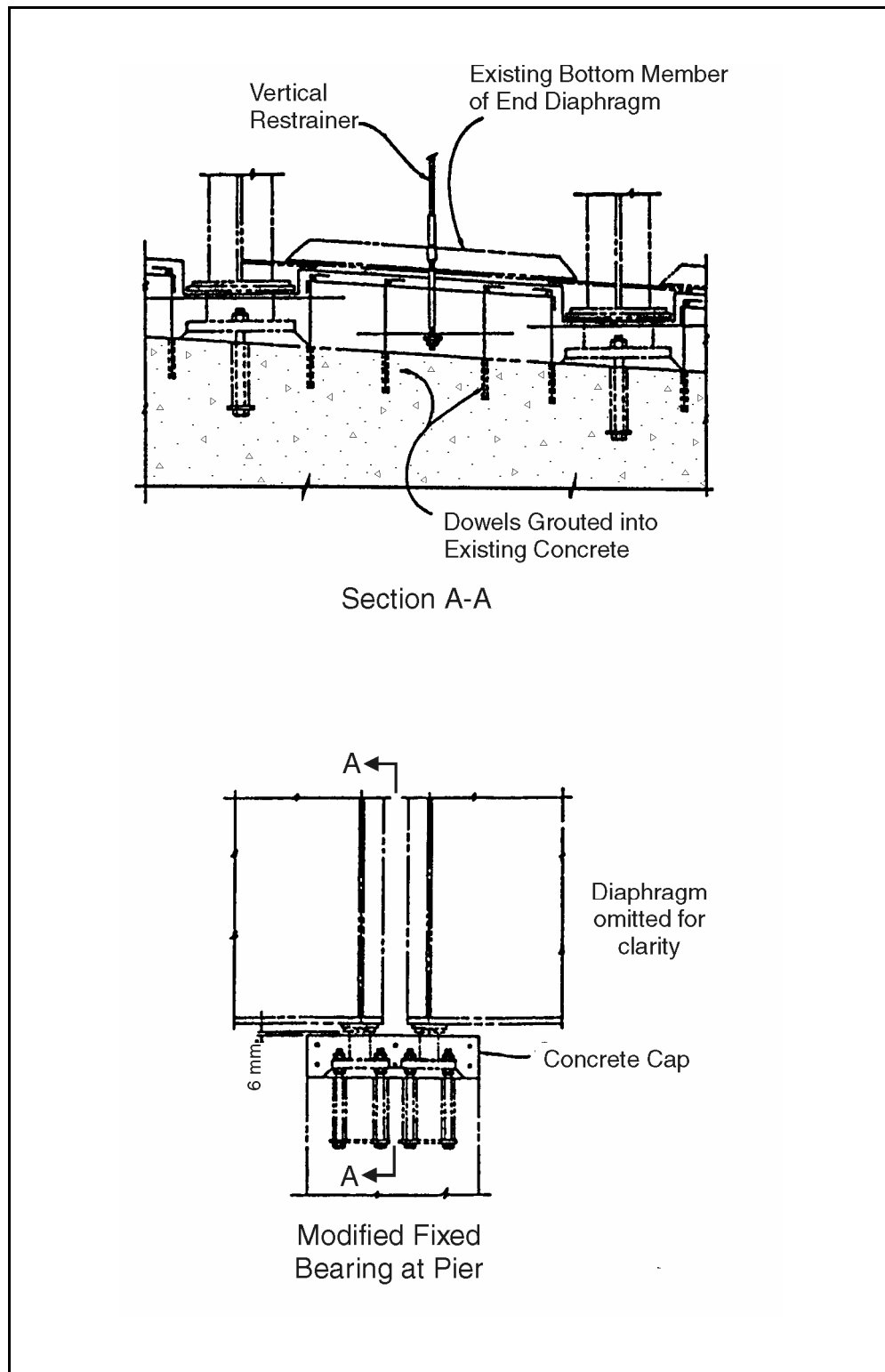


Figure 8-17. Bearing retrofitting by encasement in concrete.

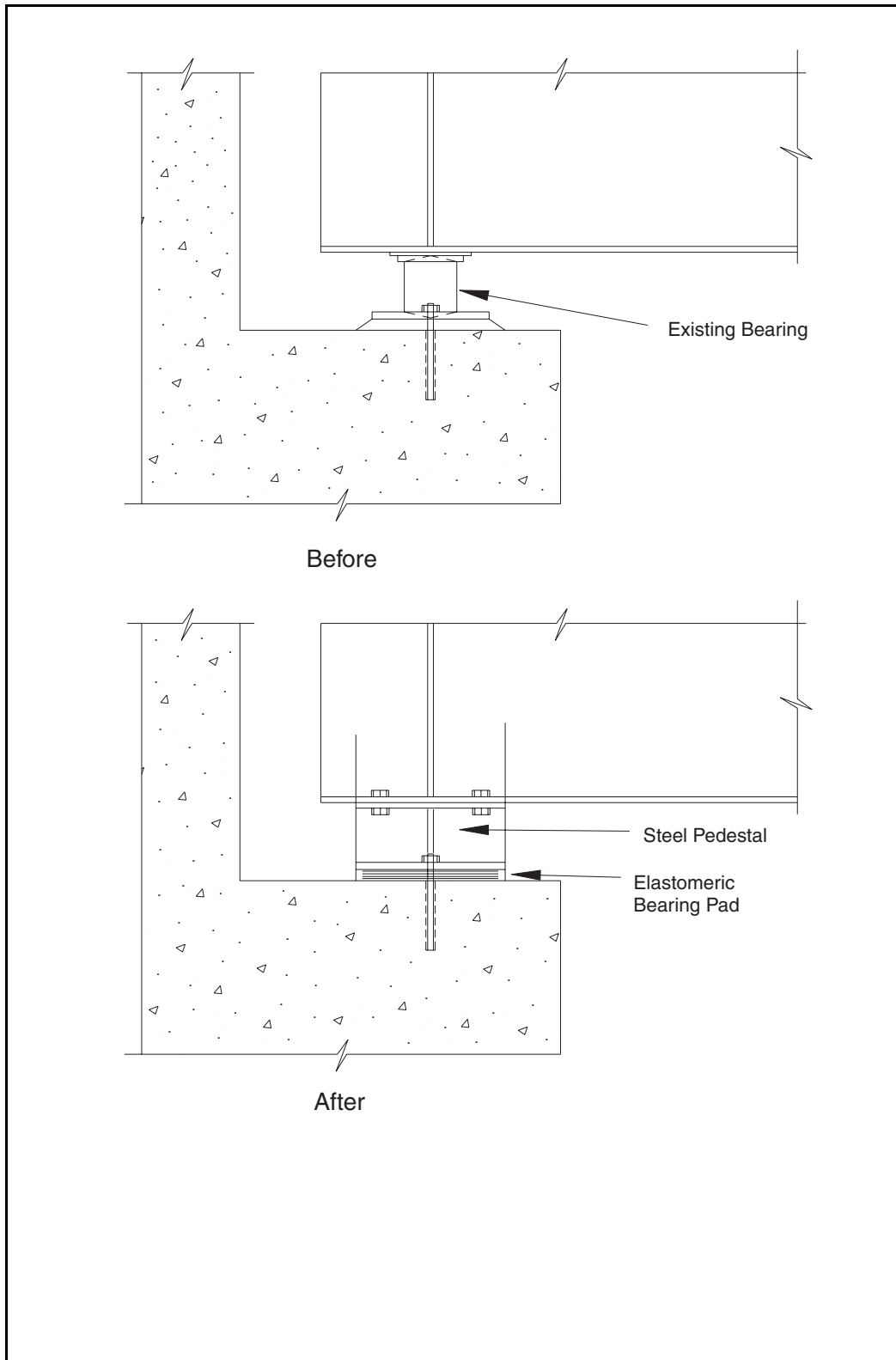


Figure 8-18. Bearing replacement retrofit using steel pedestal.

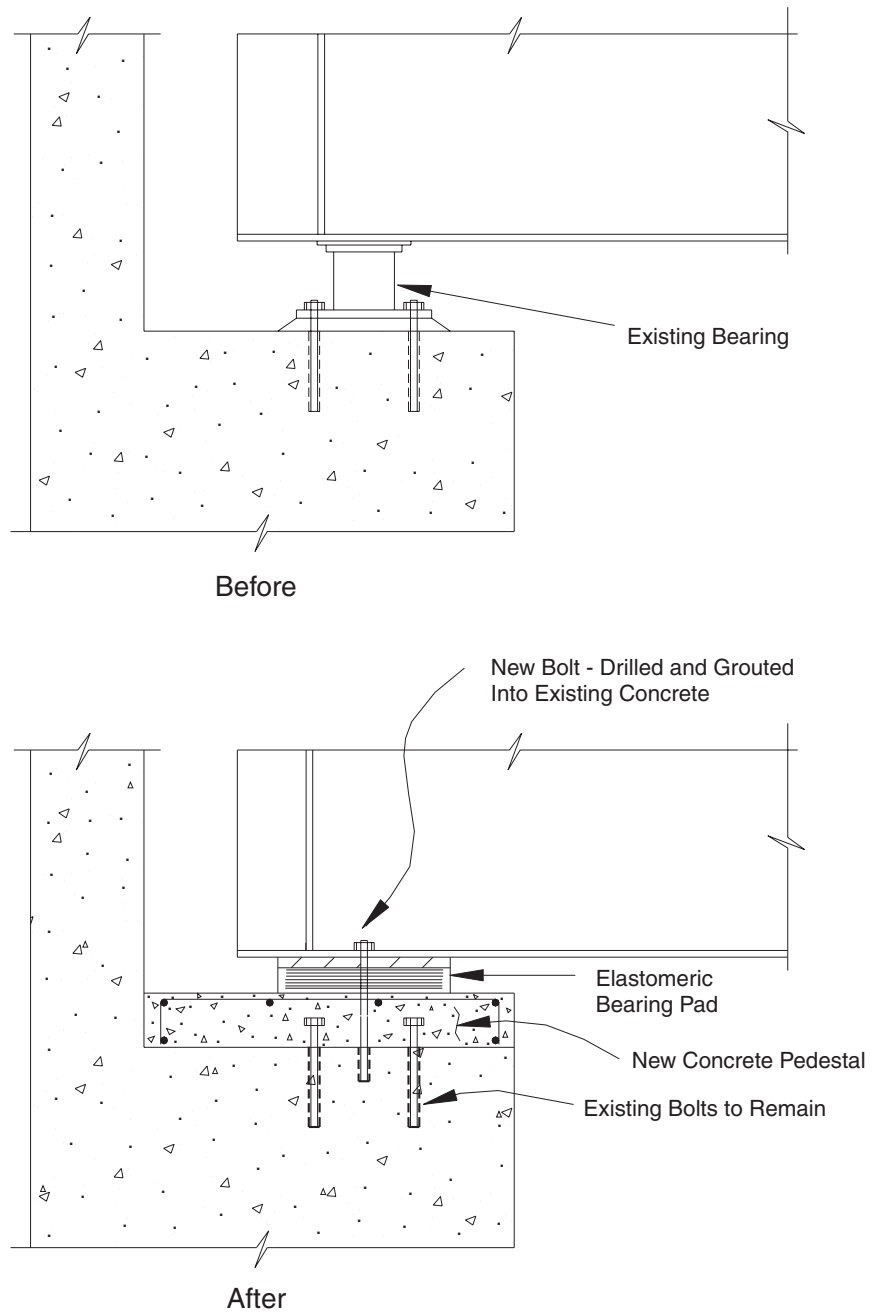


Figure 8-19. Bearing replacement using concrete pedestal.

Wherever possible, the replacement bearings at expansion and fixed ends of a girder should be of the same type so that the girder end rotations are similar and symmetry is preserved.

8.3.2.2. Replacement with Seismic Isolation Bearings

Use of isolation bearings as a seismic retrofit measure may have the dual benefit of replacing a vulnerable bearing while also protecting other structural components from damage. More than 150 bridges in the U.S. have been successfully retrofitted using this method.

Seismic isolation bearings may be used to reduce the response of a bridge during an earthquake. This is done by increasing the fundamental period of vibration of the bridge, which in most cases will reduce the accelerations in the superstructure and the inertia forces transmitted to the substructure. At the same time, the relative displacements between the superstructure and the substructure increase; these are kept to acceptable levels by the energy dissipating characteristics of the bearing. An analysis should be performed to determine the magnitude of these forces and displacements to assure that the capacity of the bridge will not be exceeded.

Isolation bearings should be stiff under service conditions, and flexible under seismic loads. This is because the isolators should be able to resist service loads with only a minimum amount of movement, but soften at higher amplitudes to give the required flexibility that will effectively isolate the bridge during an earthquake. This usually means that the force-deflection characteristics of these devices will be nonlinear. In most isolators, these nonlinear characteristics are also used to provide hysteretic energy dissipation.

Isolators currently being used for bridges include both rubber- and friction-based systems. The majority of bridge applications in the United States are rubber-based and the principal type is the lead-filled elastomeric bearing⁷. Friction-based systems, principally the friction pendulum bearing, have also been used in a number of bridge applications and are gaining in popularity. Both rubber- and friction-based isolation bearings have been used extensively in other countries. Seismic isolation can be provided by conventional elastomeric or sliding bearings, when used in conjunction with separate energy dissipation devices. An example of such an isolator is the EradiQuake bearing. Examples of isolation bearings are listed in table 8-1 and illustrated in figures 8-20 through 8-22. Energy dissipating devices are discussed further in section 8.4.3.

A number of these isolation systems have been evaluated in the HITEC⁸ program on behalf of Caltrans and FHWA (HITEC, 1999a). These include elastomeric, sliding and rolling bearings that are capable of resisting the types of loadings experienced in bridges. Summaries of test results for eight of these systems are available through HITEC (HITEC, 1998a through h, inclusive).

⁷ Buckle 2003

⁸ Highway Innovative Technology Evaluation Center, ASCE Civil Engineering Research Foundation, Washington DC

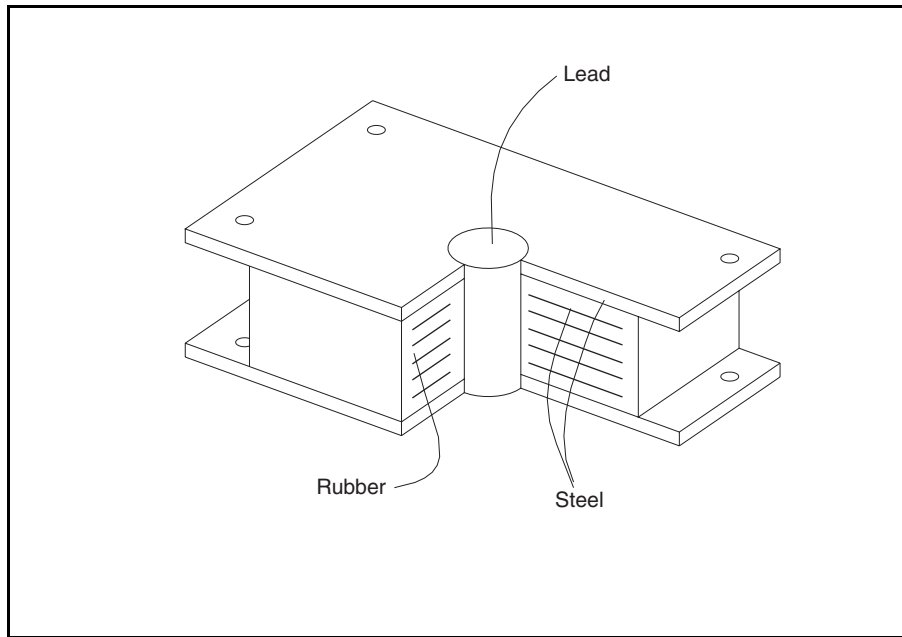


Figure 8-20. Lead-filled elastomeric isolation bearing.

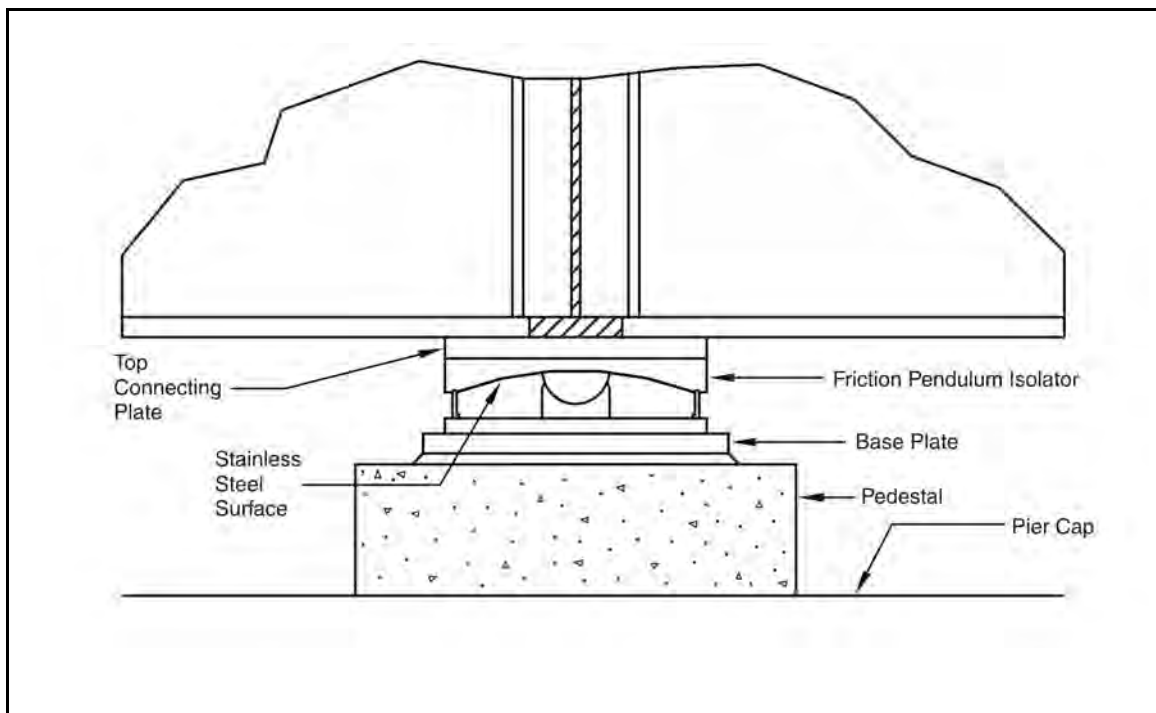


Figure 8-21. Friction-pendulum isolation bearing.

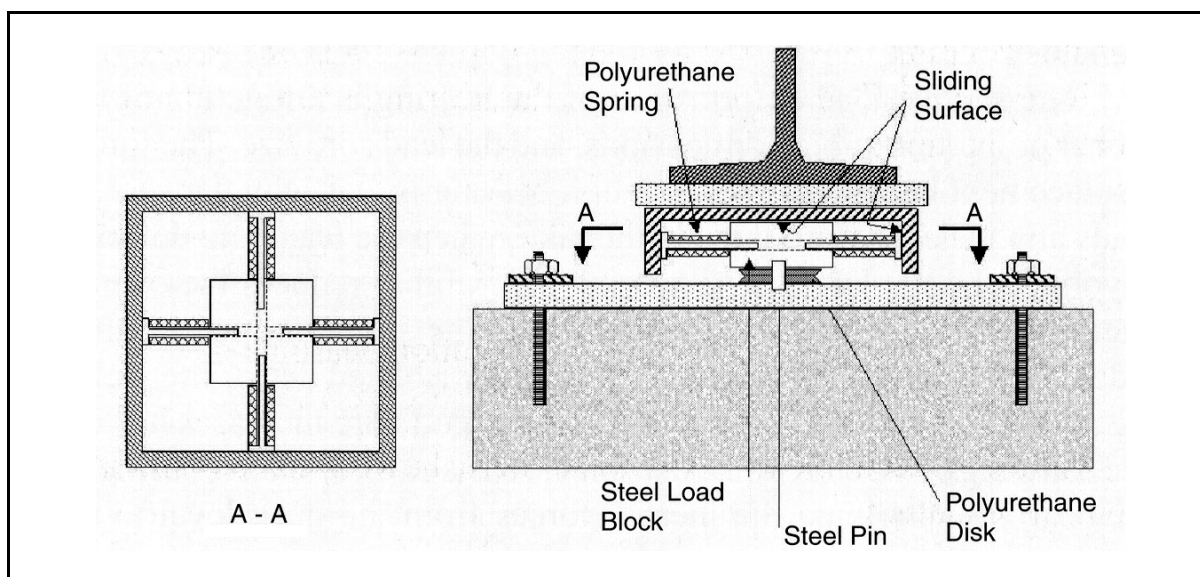


Figure 8-22. Eradiquake isolation bearing.

Table 8-1. Basic characteristics of typical isolation bearings for bridges.

Bearing Type	Flexible Element	Energy Dissipation	Rigidity for Service Loads
Lead-filled elastomeric bearings	Standard elastomeric bearing	Plastically deformed lead core	Elastic stiffness of lead core
Eradiquake bearings	Flat slider with low friction coefficient and uniaxial polyurethane springs	Friction	No slip until friction coefficient exceeded
Friction-pendulum bearings	Spherical slider with low friction coefficient	Friction	No slip until friction coefficient exceeded
Note: Some of the above hardware is patented or proprietary and is only available through licensed suppliers.			

The selection of isolator type is an important decision, since both short-term and long-term performance characteristics are important. In the short-term, resistance to wind and braking loads without excessive displacement requires rigidity at small deformations, as noted above. However, the same device must also permit thermal expansion to occur in the superstructure without overstressing the substructure. In the long-term, reliability of performance is essential. It may be decades before the design earthquake occurs, and over this period of time, the isolator properties must remain stable. In this regard, the ideal isolator is maintenance free, does not require precise field tolerances to operate successfully, and is constructed from materials that are chemically inert and resistant to atmospheric pollutants and de-icing salts.

All isolation systems should satisfy rigorous testing requirements and quality control standards. The physical properties of many isolators vary with temperature and this can be important in areas subject to low temperatures. Guidance on suitable testing requirements, including low-temperature performance testing, is provided in AASHTO, 1999. Properties likely to exist under field conditions should be used in analysis.

Bridges that already have bearings at every pier and abutment are good candidates for seismic isolation because isolator installation is relatively straightforward. In cases where a shallow-profile bearing such as an elastomeric pad is being replaced, there may be insufficient headroom to make a direct exchange with an isolator. Extra effort will then be required to create the necessary space to install the device. This is unlikely to be the case when replacing steel bearings, and in some cases, the reverse situation will be true, requiring the use of a pedestal (see section 8.3.2.1).

Isolation may also be used to retrofit an integral bridge, since the columns may be cut directly under the pier cap to create a space for the isolators.

When a bridge is isolated, it must be free to move in any horizontal direction in order for the isolation to be effective. This is not usually a problem in the transverse direction; but in the longitudinal direction, special care is necessary at the abutments. This is because the clearance at existing expansion joints for most abutments will be insufficient to accommodate the expected movements under seismic loads. If the clearance is not increased, impact between the superstructure and the backwall will most likely occur. The resulting damage to the backwall is unlikely to cause collapse or close the bridge for any period of time since temporary repairs can be implemented quickly and access restored. This leads to an approach of not providing the required clearance at the time of retrofitting, but waiting until the wall is damaged in an earthquake. When the wall is repaired, adequate clearances can be provided for future earthquakes. While this approach is not recommended for new bridges, it has merit in retrofit situations.

The backwall can also be modified at the time of retrofit. One way to do this is shown in figure 8-23. A sacrificial knock-off element is incorporated into the top of the wall, and can be replaced if dislodged in an earthquake. Impact is still likely to occur in the longitudinal direction, but the consequences are minor. Another option is to provide for a much larger clearance so that impact does not occur. In this case, the gap must be bridged with an expansion joint. This may be the ideal solution from a structural response point-of-view, but may not be the most economical one since road joints that can accommodate large opening and closing movements are expensive and difficult to maintain.

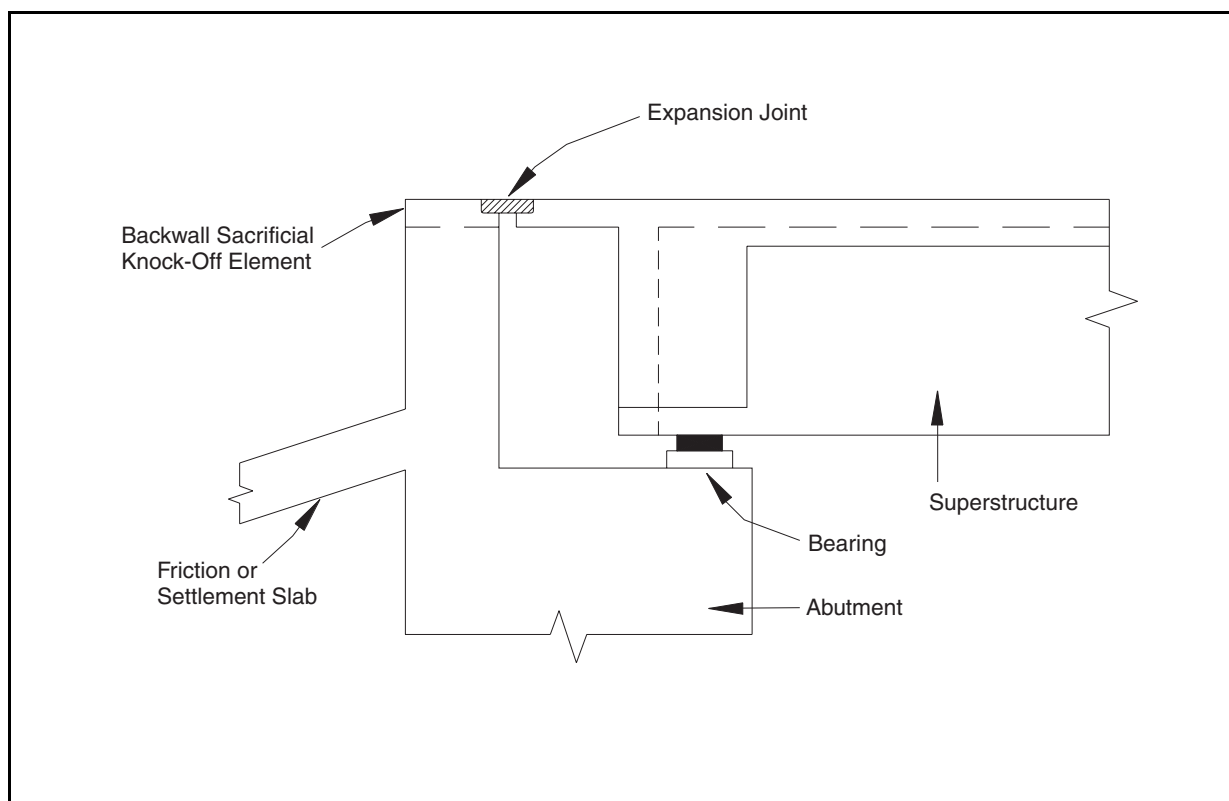


Figure 8-23. Knock-off device in backwall of seat-type abutment.

8.3.3. STRENGTHENING OF SUPERSTRUCTURE TO SUBSTRUCTURE CONNECTIONS

Some integral bridges employ concrete hinges (also called Freyssinet hinges) for the connection between the superstructure and the substructure. These hinges allow rotational movement in the longitudinal direction, but resist transverse rotation. They also generally resist shear forces in both directions. These hinges may be located either at the top or bottom of piers and abutments as is shown in figure 8-24. When the steel reinforcing is inadequate to resist the shear forces in either direction, or the moments in the transverse direction, retrofitting may be necessary. A method that can be used to increase the shear resistance of these hinges is shown in figure 8-25. It involves coring a hole through the joint and inserting a steel pin such as a thick-walled pipe.

Another method of increasing the transverse moment resistance of a hinge is shown in figure 8-26. This method uses supplemental tie-down piles and a prestressed concrete cap beam to strengthen a concrete hinge at the bottom of a single column pier that is deficient in transverse overturning capacity.

Methods used to strengthen these types of hinges will vary based on the configuration of the bridge being retrofitted. The design forces should be determined from an analysis of the structure. In many cases, these forces are dictated by plastic capacity elsewhere in the bridge, for example, the moment capacity at the opposite end of the column to the hinge. The designer must also check that the retrofit allows the bridge to perform adequately under service conditions.

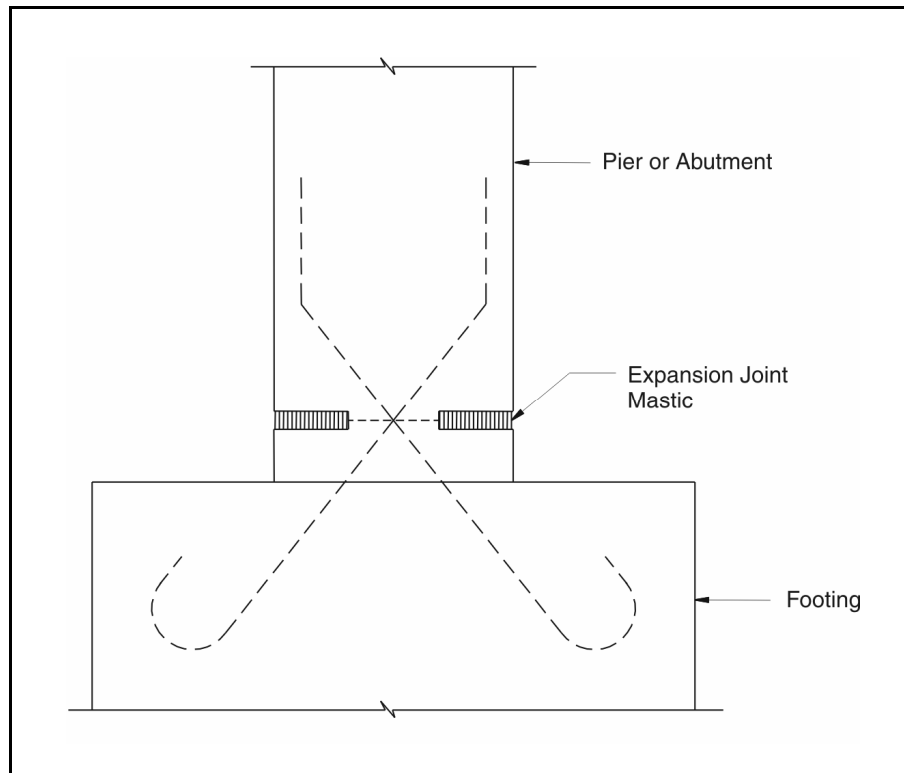


Figure 8-24. Freyssinet hinge.

8.4. EXPANSION JOINT RETROFIT

This section presents several methods for preventing loss of support at expansion joints during earthquakes. Two basic retrofitting approaches are discussed. The first provides additional displacement capacity, and the second reduces the displacement demand. These approaches may be used alone or in combination to prevent failure due to loss of support.

8.4.1. BEARING SEAT EXTENSIONS

Increasing the seat width increases the displacement capacity at an expansion joint, often without affecting the dynamic characteristics of the bridge. Two ways of doing this are discussed below.

8.4.1.1. Concrete Seat Extensions and Catcher Blocks

Seat extensions are used when too many restrainers would be required to limit movement at an expansion joint to 67 percent of the available seat width (see section 8.4.2.1 (f)). By using seat extensions to increase the range of movement, a smaller number of restrainers can be used. If installed at abutments, these extensions should preferably be supported directly on the footing, as shown in figure 8-27.

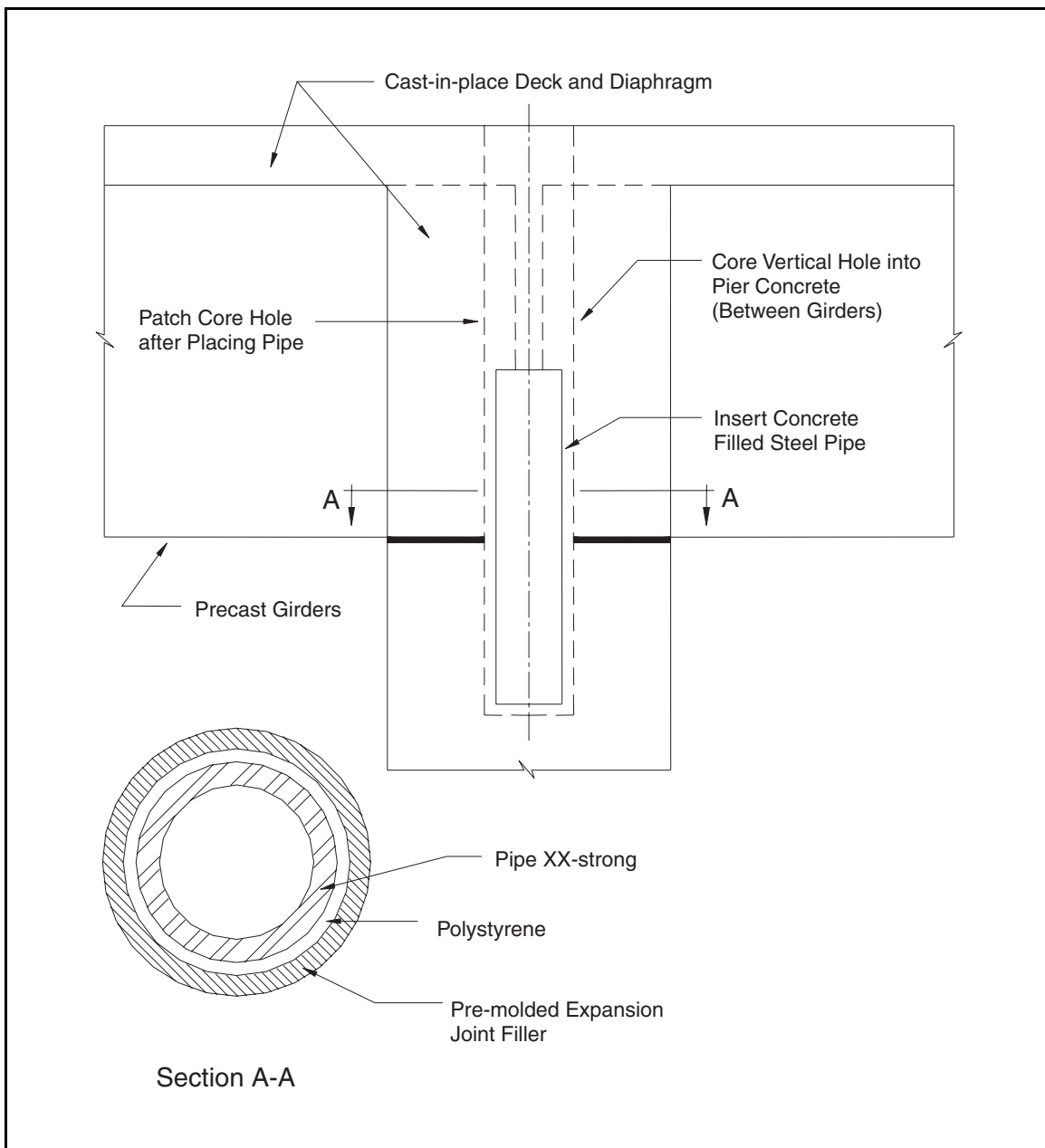


Figure 8-25. Pipe shear key.

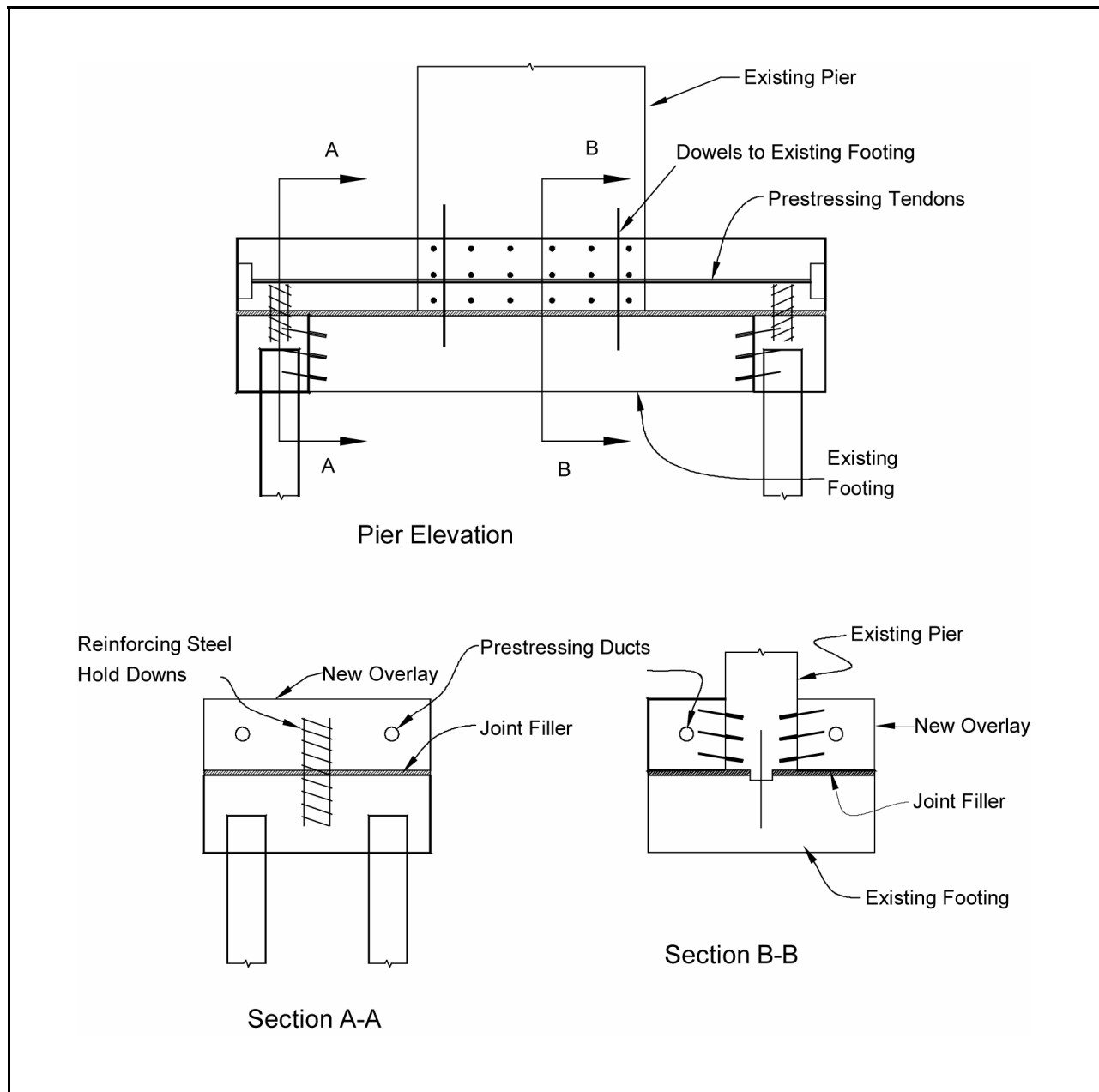


Figure 8-26. Concrete hinge retrofit

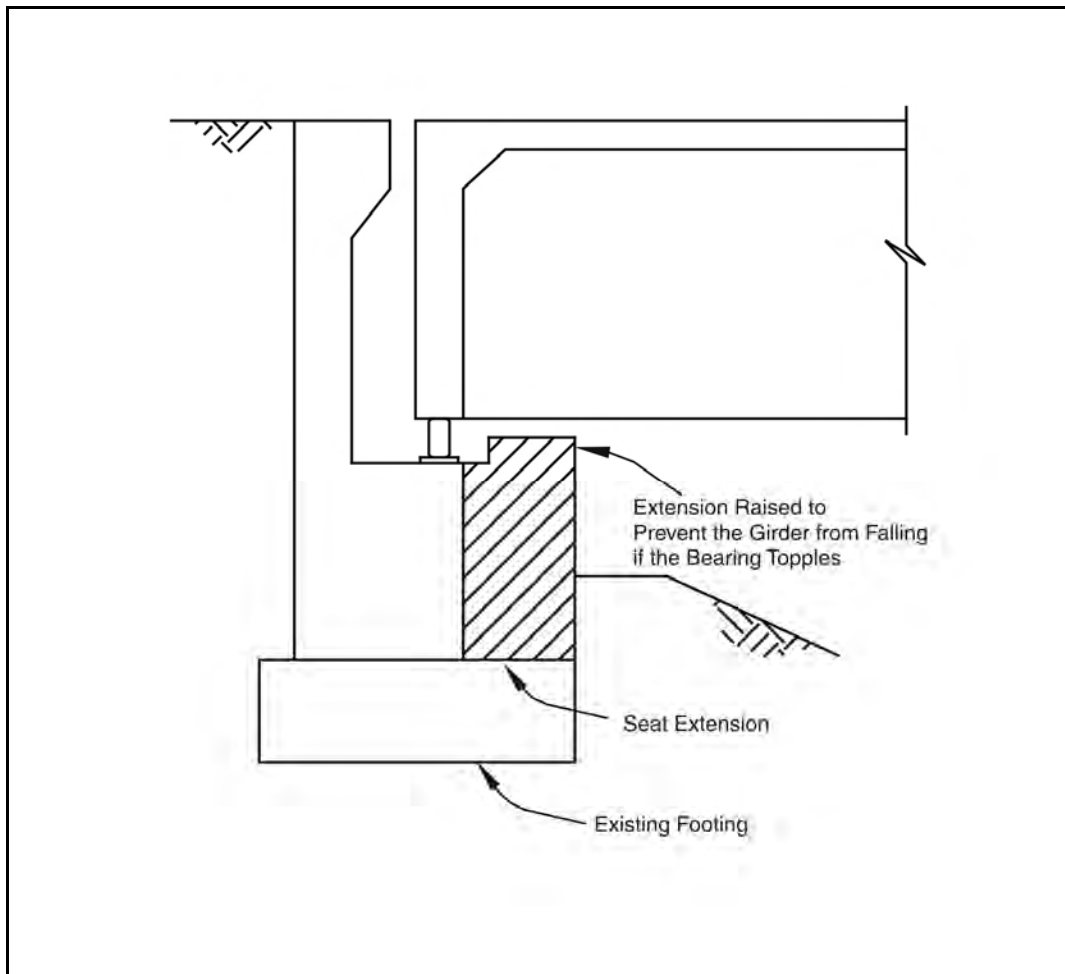


Figure 8-27. Abutment seat extension.

Extensions that are anchored to the vertical face of a concrete abutment or pier, with dowels or anchor bolts, must be designed to carry the large vertical and horizontal forces that will be imposed if the bearings fail. These include the impact of the falling superstructure and the horizontal forces from the earthquake. When these forces are eccentric to the dowels and anchor bolts, the resulting moments must be considered in designing the anchorage to the abutment or pier. When feasible, post-tension the seat extensions to the substructure.

When the bridge is supported on high bearings, the seat extension should be elevated to just below the level of the beams. If these so-called ‘catcher blocks’ are used, consideration should be given to future inspection and maintenance of the bearings. One approach is to use a removable steel assembly for the raised portion of the seat extension. An oversized sole plate that is fastened below the bottom flange of the girder has also been used with some older bearings. There must be sufficient clearance for this plate to avoid impact or interference with the seat extension.

If bearing seats are extended, their width should be increased to the minimum seat width recommended in section 5.2.1. These widths reflect the possibility of large relative movements at the bearings resulting from the overall inelastic response of the bridge, possible independent movement of different parts of the substructure, and out-of-phase rotation of abutments and piers resulting from traveling surface wave motion.

The following load cases should be used to design the seat extensions:

1. Vertical load equal to twice the dead load reaction.
2. Vertical load equal to the dead load reaction plus a horizontal load due to the earthquake.

The first case considers vertical forces only and is intended to account for the large impact forces that can result when the superstructure drops from the bearings onto the seat. The second case considers both the horizontal and vertical loads that can develop when the superstructure is resting on the bearing seat extension and is still being subjected to earthquake ground motions. Depending on the type and amount of traffic likely to be present on the bridge at any time, consideration should also be given to including a portion of the live load in the vertical load for both of these load cases. The horizontal earthquake loading should be equal to the lesser of the dead load reaction times, the spectral acceleration coefficient, or the dead load times the maximum feasible coefficient of friction between the girder and seat extension.

8.4.1.2. Pipe Extenders

For seats at in-span expansion joint hinges, pipe extenders may be used to increase seat width capacity. A typical detail is shown in figure 8-28. These extenders may also be used as transverse shear keys.

As for seat extensions, pipe extenders are used when too many restrainers are required at an in-span hinge to limit movement to 67 percent of the available seat width (see section 8.4.2.1 (f)). By using pipe extenders to increase the range of movement, a smaller number of restrainers can be used.

Pipe extenders will be subjected to both vertical gravity loading and transverse earthquake loading. This will result in both flexural and shear stresses within the pipe as well as complex stresses within the concrete diaphragm in which the pipe is anchored. Caltrans has conducted field tests of 200 mm (8 in) diameter double extra strong pipe extenders and found that failure occurs in the pipe at an ultimate load of approximately 1070 kN (240 kips) and an extension of 200 mm (8 in). Based on these findings, it is recommended that shear capacity be limited to 930 kN (210 kips) for resolved vertical and horizontal shear and 800 kN (180 kips) for shear in either of the orthogonal directions. These values are for a normal joint, and horizontal shear capacity will be reduced in skewed joints. Despite these findings, it is good practice to limit seat extender capacity to 445 kN (100 kips) unless space limitations prevent it (Caltrans, 1996).

Calculated shear demands on multiple pipe extenders should be increased by 130 percent to account for potential misalignment of the extenders. Consideration should also be given to the

participation of existing concrete shear keys in resisting transverse shear. For the load case in which transverse shears are high and the expansion joint opening is relatively low, existing transverse shear keys can be engaged. If the pipe extenders engage before the concrete shear keys, then the ductility of the pipe extenders will permit the eventual participation of the shear keys during a strong earthquake. If the shear keys engage first, they are likely to experience brittle failure before the pipe extenders take up load, and therefore would not contribute to the ultimate shear resistance at the expansion joint.

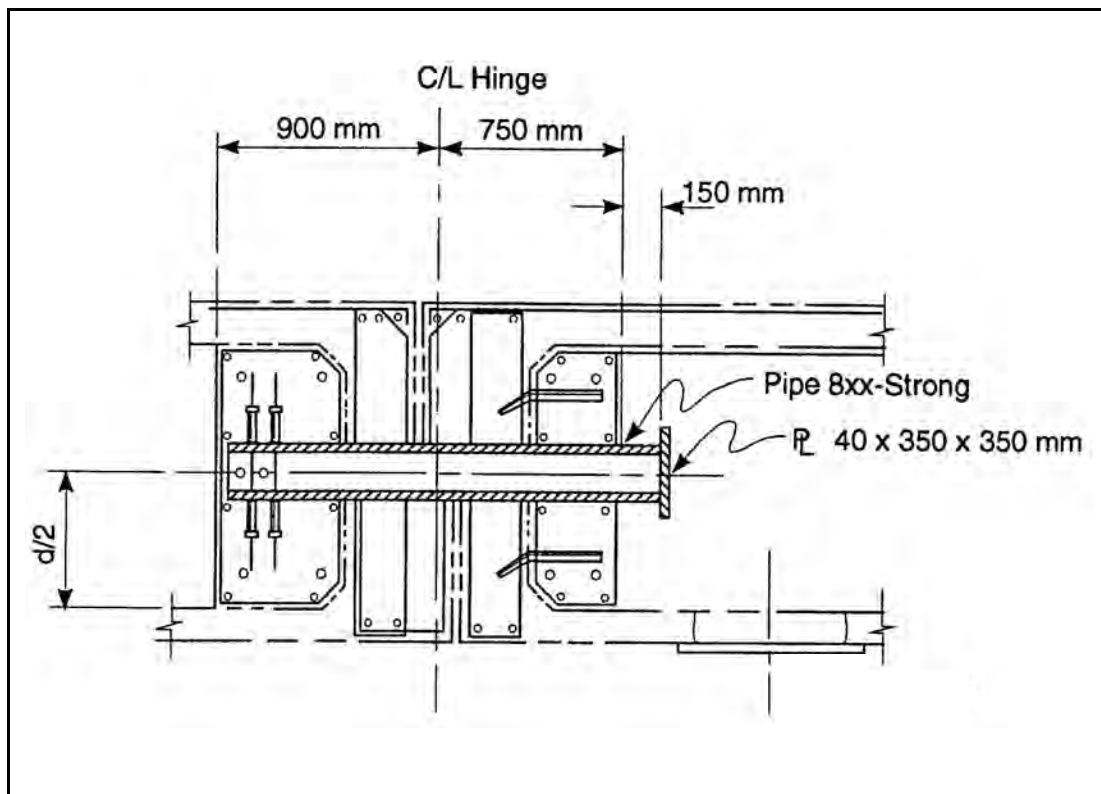


Figure 8-28. Pipe seat extenders.

8.4.2. RESTRAINERS

Many of the bridge failures observed in earthquakes prior to and including the 1971 San Fernando earthquake in southern California resulted from loss of support of the superstructure at the bearing seats. Such failures usually cannot be repaired and result in the demolition and reconstruction of the collapsed spans. Because of the catastrophic consequences of loss of support, and the perception that they could be easily prevented at relatively low cost, early retrofitting programs focused on preventing such failures. These programs, which were first undertaken by Caltrans, involved the addition of longitudinal restrainer cables and bars to limit relative movements at expansion joints.

Subsequent earthquakes showed that longitudinal restrainers may have prevented loss of support at expansion joints in some cases, but were unable to prevent serious damage or even collapse in many others. Bridges that had been retrofitted with restrainer cables failed in both the 1989

Loma Prieta and 1994 Northridge earthquakes. Many of these failures resulted from flaws in the design of the restrainer assemblies themselves. Restrainers ruptured, anchorage plates pulled through concrete diaphragms, swaged fittings pulled away from cables, and anchorage nuts had apparently worked loose from the ends of cable units. Similar failures of Japanese restraining devices were observed during the 1995 Kobe earthquake.

Restrainer failures drew attention to the need to carefully design restrainer systems. Restrainers must not only be stiff enough and strong enough to prevent joints from separating, but the remainder of the bridge must be able to resist the forces developed in restrainers (Selna and Malvar, 1987). The number of restrainers in a typical Caltrans multi-cable unit was subsequently limited and strengthening was required to prevent punching shear failures of concrete diaphragms in the expansion joints of continuous box girder bridges. Restraining devices may also transmit higher forces to other bridge components such as bearings and columns, and may cause their failure if not properly designed.

On the other hand, dynamic analysis of bridge and restrainer systems has demonstrated that a large number of restrainers is often required to limit joint movement to acceptable levels, particularly for high seismic loadings. In some of these cases, it is almost physically impossible to place the required number of restrainers in the bridge. In other cases, the required number of restrainers could severely overstress components elsewhere in the bridge.

Due to the need to limit restrainer forces to protect other structural elements on the one hand, and the need to increase restrainer forces to accomplish their intended purpose on the other, restrainers alone may not be the best retrofitting solution in many cases. Alternatives that should be considered, either alone or in conjunction with restrainers when a loss of support failure is possible, include seat extensions, bearing strengthening, and bearing replacement with conventional or isolation bearings.

8.4.2.1. Longitudinal Joint Restrainers

Longitudinal joint restrainers are intended to limit the relative displacement at expansion joints and thus decrease the chance of a loss of support at these locations. When bearing anchor bolts and similar details are inadequate to prevent a loss of support at fixed bearings, longitudinal restrainers can also be used to transfer the longitudinal inertia force of the superstructure into the substructure. Because most restrainers can carry only tension forces, it will be necessary to provide restrainers at both ends of the span in such cases.

Restrainers should be designed to resist the maximum calculated force within their elastic range. Two symmetric restrainers per joint will minimize eccentric movement of the joint. An adequate gap should be provided to permit normal in-service movements. For joints located at piers, restrainers should provide a direct and positive connection between the superstructure and the pier, unless the pier caps are wide enough to prevent a loss of support at the end of the span *and* the anticipated maximum movement of the superstructure will not cause excessive damage.

Steel cables and bars acting in direct tension have been the most frequently used method for restraining expansion joints against excessive movements. These devices do not dissipate

significant amounts of energy because they are intended to remain elastic. Cable and bar restrainers may allow the ends of girders to be damaged by pounding, but the damage will usually be repairable and not extensive enough to allow the spans to lose support. Although cables and bars are not ideal restrainers, they are relatively simple to install and are an economical means of preventing a catastrophic failure during an earthquake.

There is no established rule for choosing between cables and bars. Often cables have the economic advantage, since shorter lengths are possible for a given amount of joint movement. In addition, cables are flexible and able to accommodate transverse and vertical movements. If bars are used, transverse and vertical restrainers may be required to prevent shear and flexural distortion in the bars.

8.4.2.1(a). Restrainer Cables

The single restrainer cable unit is the fundamental component used in most restrainer cables. The most commonly used restrainer cable consists of a galvanized 19 mm (0.75 in) diameter steel cable that is identical to the type commonly used to anchor guard railing. The cable has galvanized, cold-swaged fittings and 25 mm (1 in) diameter ASTM A-449 threaded studs at each end. Washers and nuts use a special thread locking system consisting of a cleaner, primer, and anaerobic adhesive to prevent the nuts from working loose over time.

Spring washers and cable yield indicators can be added to the basic restrainer cable unit. The washers are designed to keep tension in the cable while allowing movement due to temperature effects. The yield indicators provide post-earthquake evidence that the cables have been stressed. Once these indicators have yielded, there will be additional restrainer slack, or free movement, before they become effective again. Details of a typical Caltrans restrainer cable unit are shown in figure 8-29.

An individual restrainer cable has a cross-sectional area of 143 mm^2 ($.222 \text{ in}^2$) and a minimum breaking strength of 205 kN (46 kips). For load and resistance factor design purposes, cables are assumed to have a tensile capacity of 174 kN (i.e., $0.85 \times 205 \text{ kN}$) (39.1 kips; i.e., $0.85 \times 46 \text{ kips}$). A cable is more flexible than a steel bar of equivalent length and cross-sectional area. When cables are initially tensioned, they undergo a conditioning in which individual wires within the cable shift to form a more compact shape. In the case of restrainer cables, this results in an effective modulus of elasticity of approximately 69,000 MPa (10,000 ksi). Once this conditioning has taken place, a modulus of elasticity of 124,000 MPa (18,000 ksi) can be used.

Cable length is defined as the distance between the anchored end of a cable unit and the point of no movement on the cable. In the case of looped restrainers, this point will be near the center of the loop.

A complete description of these cable units is given in the *Caltrans Standard Specifications*, section 75-1.035 – Bridge Joint Restrainer Units (Caltrans, 1995).

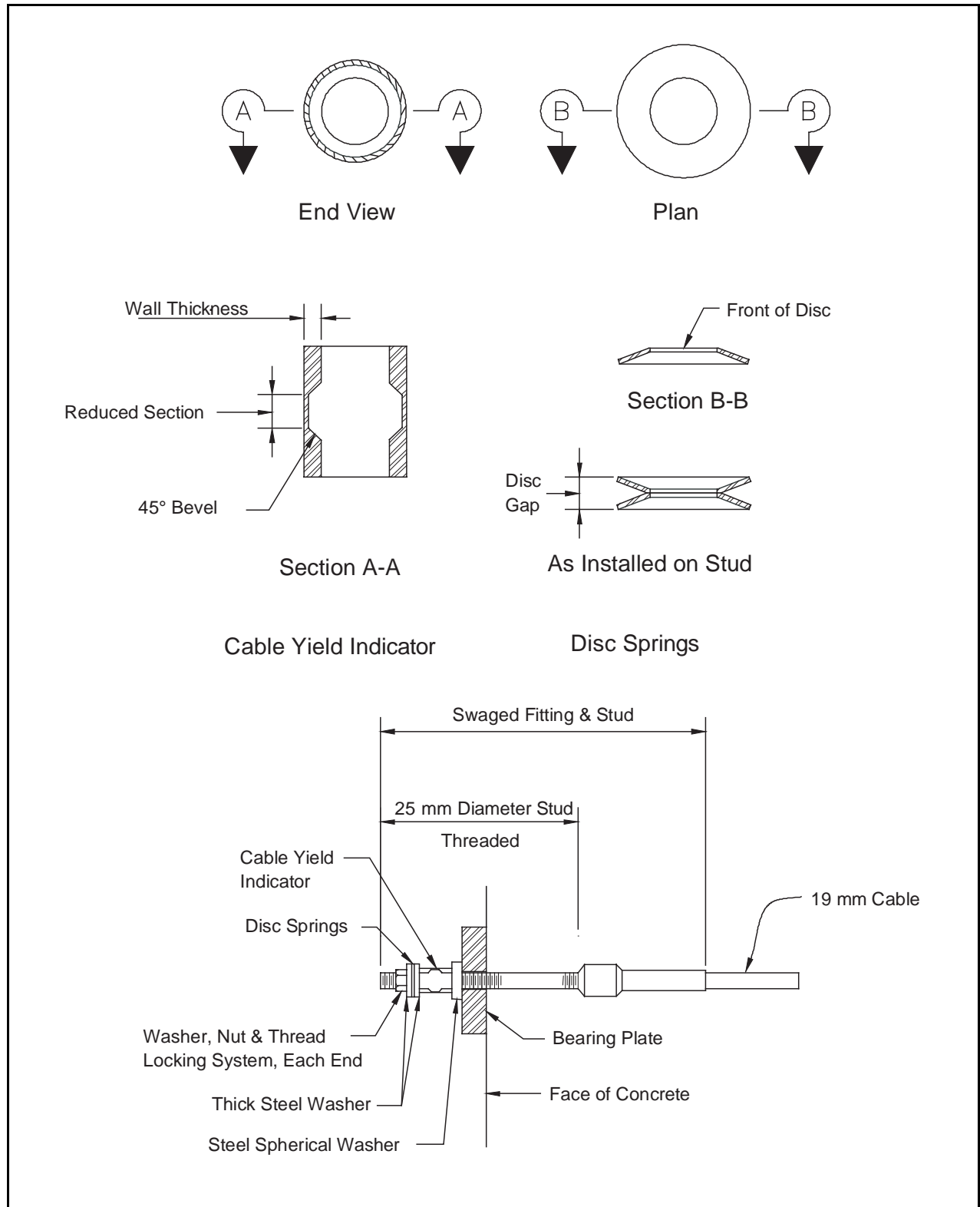


Figure 8-29. Caltrans cable restrainer unit.

Caltrans has conducted research to study the performance of cable under repeated cycles of loading near or beyond the yield stress. The graph shown in figure 8-30(a) was developed by loading 2.9 m (9.5 ft.) long specimens to $0.85f_{ult}$ for 15 cycles, and then to failure. On the first cycle of loading, the cable underwent a conditioning in which slack in the strands was taken up. On subsequent loadings, the specimen elongated approximately 38 mm (1.5 in) before yield. Total elongation after the initial conditioning was approximately 115 mm (4.5 in) prior to failure.

In a second series of tests, specimens were loaded by applying 25 mm (1 in) increments of displacement up to failure. Between each displacement increment, the specimen was unloaded to zero tension. Typical results from these tests are shown in figure 8-30(b). The wire rope failed at 127 mm (5 in) of elongation, which is slightly less than that demonstrated by the first series of tests.

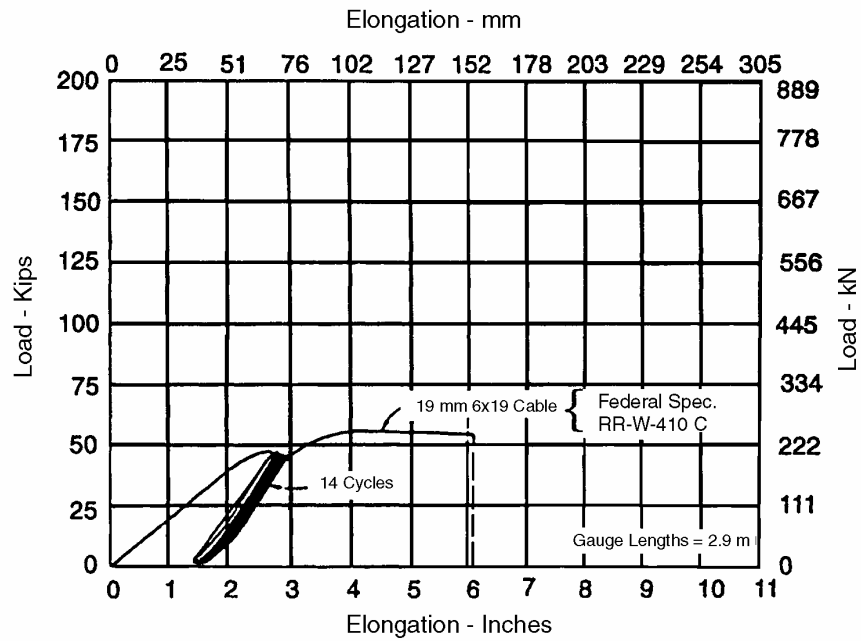
When a large number of cables are required to limit displacements to an acceptable level, it is usually necessary to use multi-cable assemblies. These assemblies simplify the anchorage of a large number of restrainers and minimize congestion at the joint. Caltrans has used a standard multi-cable unit in many retrofitting projects involving concrete box girder bridges. A detail of this restrainer assembly is shown in figure 8-31. Installation requires access to the interior cells of the box girder on both sides of an in-span expansion joint. It is generally preferable to cut access openings through the soffit slab since this will have the least effect on traffic during construction. These access holes are typically left in place and covered with a metal plate that can be removed if access to the restrainers is necessary at some time in the future. Access through the deck slab is possible, but will interfere with traffic.

Laboratory testing of the early designs of these restrainer assemblies demonstrated that the ultimate capacity of multi-cable assemblies was limited by a punching shear failure of the anchor plates through the concrete diaphragm. To prevent this type of failure, it is often necessary to strengthen the diaphragms using cast-in-place concrete bolsters.

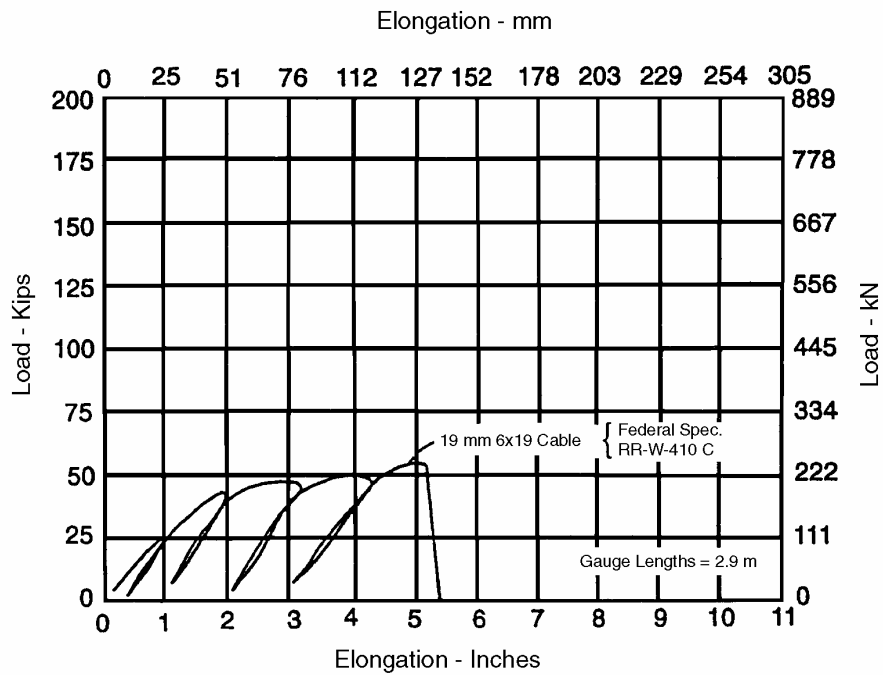
8.4.2.1(b). High Strength Bar Restrainers

Galvanized ASTM-A 722 high strength bars have also been used as longitudinal earthquake restrainers. These bars are less flexible, but more ductile, than standard restrainer cables.

Because the goal of restrainer design is to keep restrainers within the elastic range, the added ductility is not considered a major advantage, and the reduced flexibility requires the use of longer bars or a larger restrainer slack to provide for the same range of movement as cables. If this is not done, then a larger restrainer design force is required and this in turn leads to a greater number of bars. Therefore, bars are used far less frequently than cables.



a. Test One



b. Test Two

Figure 8-30. Caltrans tests of restrainer cable.

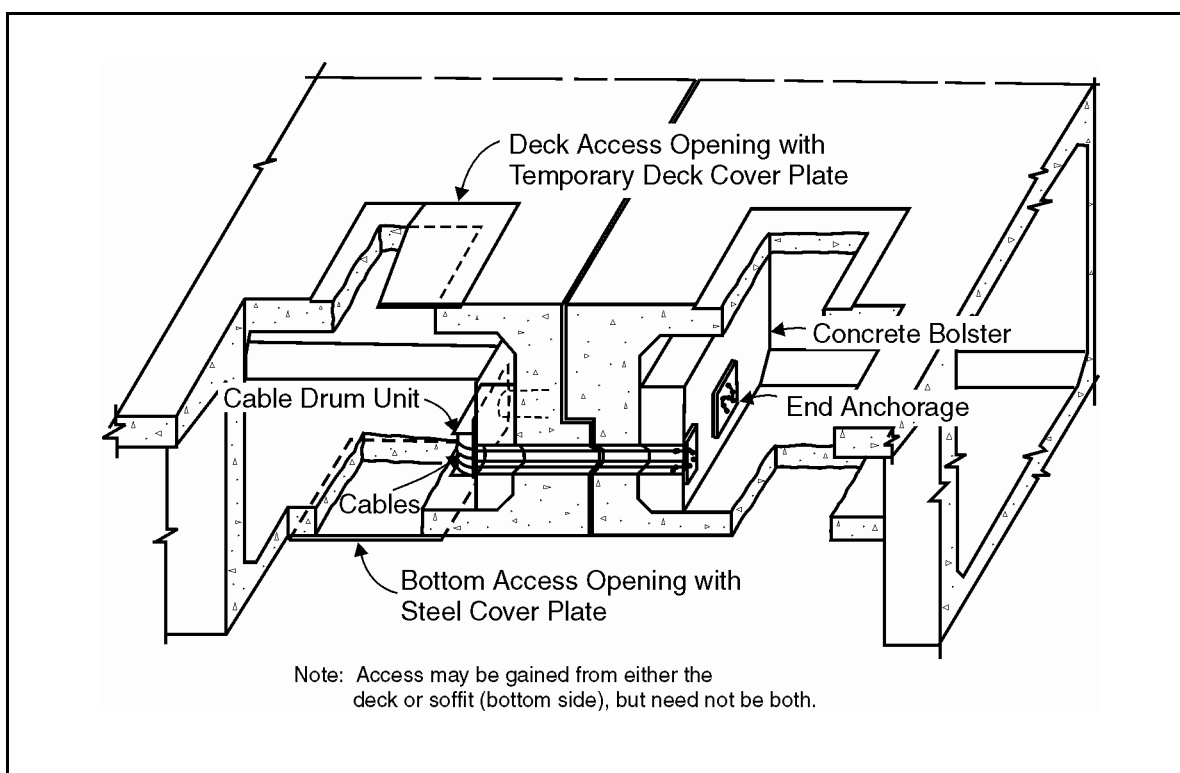


Figure 8-31. Multi-cable restrainer assembly.

Bars should also comply with ASTM A-722 supplementary requirements, which require a minimum elongation of seven percent in 10 bar diameters. The modulus of elasticity of high strength bars may be assumed to be 200,000 MPa (29,000 ksi). Table 8-2 provides other basic design properties for a number of standard bar sizes.

Table 8-2. Basic design properties for typical high strength bar sizes.

Diameter mm (in)	Area mm ² (in ²)	Ultimate Strength MPa (ksi)	Yield Strength MPa (ksi)	Yield Force kN (kips)
25 (1)	549 (0.85)	1030 (150)	827 (120)	703 (102)
32 (1¼)	807 (1.25)	1030 (150)	827 (120)	1030 (150)
35 (1½)	1020 (1.58)	1030 (150)	827 (120)	1310 (190)

Galvanizing can cause field problems during the installation of high strength bars. Both threaded bars and smooth bars with threaded ends have been used in the past. Threaded bars are galvanized after being threaded. Therefore, the bar ends must be hot-brushed immediately after galvanizing. Even then, placement of end nuts can be difficult. Smooth bars are usually threaded after being galvanized. After installation, the ends are coated with zinc-rich paint.

Neither galvanizing nor threading compromise the strength or the anchorage requirement of either type of bar. If any damage to the galvanizing occurs, zinc-rich paint must be applied to the affected area.

Another problem is that standard locking devices are not always effective on threaded bars. Steps must be taken to prevent lock nuts from vibrating off such bars. Restrainer devices used in easily accessible areas should have bolt threads peened after installation, to prevent loss of components to vandalism.

Bars longer than 9 m (30 ft) should be avoided for two reasons: stock lengths are usually 9 m (30 ft), and it is difficult to galvanize bars longer than this length.

8.4.2.1(c). *Bumper Blocks*

An alternative method for restricting the relative longitudinal movement of the superstructure is to use bumper blocks. These devices are usually connected to the bottom flanges of girders and project downward to engage the substructure and thus restrict movement. This retrofit method is illustrated in figure 8-32.

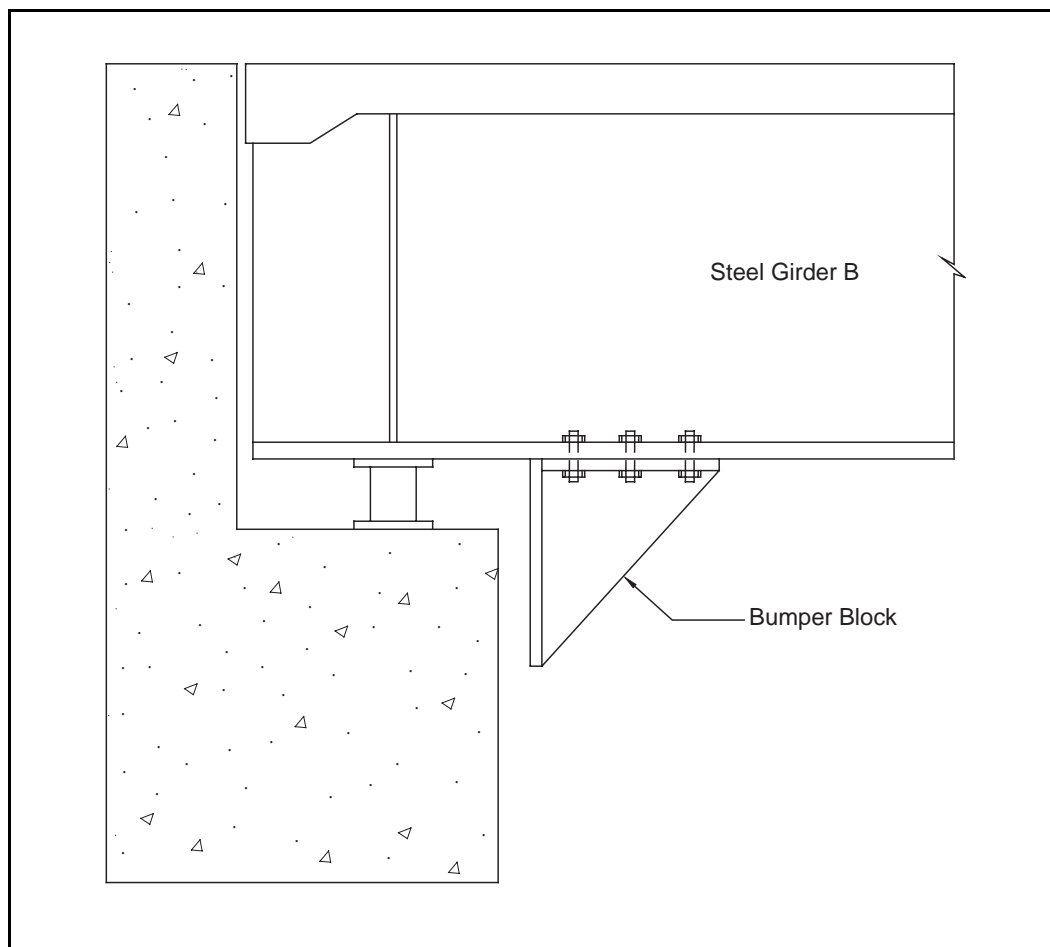


Figure 8-32. Bumper block retrofit.

8.4.2.1(d). Anchorage of Restrainers

Restrainers must be physically attached to the existing bridge and care should be taken that, in doing so, critical components are not weakened or overloaded. Anchorage takes the form of steel brackets, anchor plates and looping of the cable through holes drilled or cored into existing members. To prevent damage to the cables, they should not be bent to a radius less than 100 mm (4 in). A number of restrainer anchorage schemes are shown in figure 8-33. All of these connections should be designed for a force equal to 125 percent of the nominal breaking strength of the restrainers. In addition, structural members subject to brittle failure should be capable of resisting this same force. Restrainers should be placed symmetrically to minimize the introduction of eccentricities. The consequences of a premature restrainer failure should also be carefully considered. For example, the restrainer detail shown in figure 8-34 may be undesirable because, in the event of a premature failure of one of the cables, the resulting eccentric load could tear the web out of the girder and cause a serious loss of structural capacity, unless the web has been adequately reinforced to prevent such a failure. Both restrainer connections and existing structural elements should be capable of resisting the eccentricities caused by variations in the restrainer forces of at least 10 percent of the nominal ultimate restrainer capacity.

Concrete diaphragms or walls that provide anchorage for restrainers should be capable of resisting a punching failure. If not, they should be strengthened to resist a force equal to 125 percent of the nominal breaking strength of the restrainers. As previously mentioned, this type of strengthening is often required at expansion joint diaphragms. The size of plates to resist punching shear can be selected from the chart in figure 8-35.

8.4.2.1(e). Design and Construction Issues

Longitudinal restrainers should be oriented along the direction of expected movement. If piers are rigid in the transverse direction, as shown in figure 8-36, the superstructure will move primarily along the longitudinal axis of the bridge and restrainers should be placed accordingly. However, in a skewed bridge with transversely flexible supports, significant superstructure rotation can occur. In this case, restrainers will be more effective if placed normal to the expansion joint, as shown in figure 8-37. This arrangement should only be used when movements that could shear the restrainers are minimal.

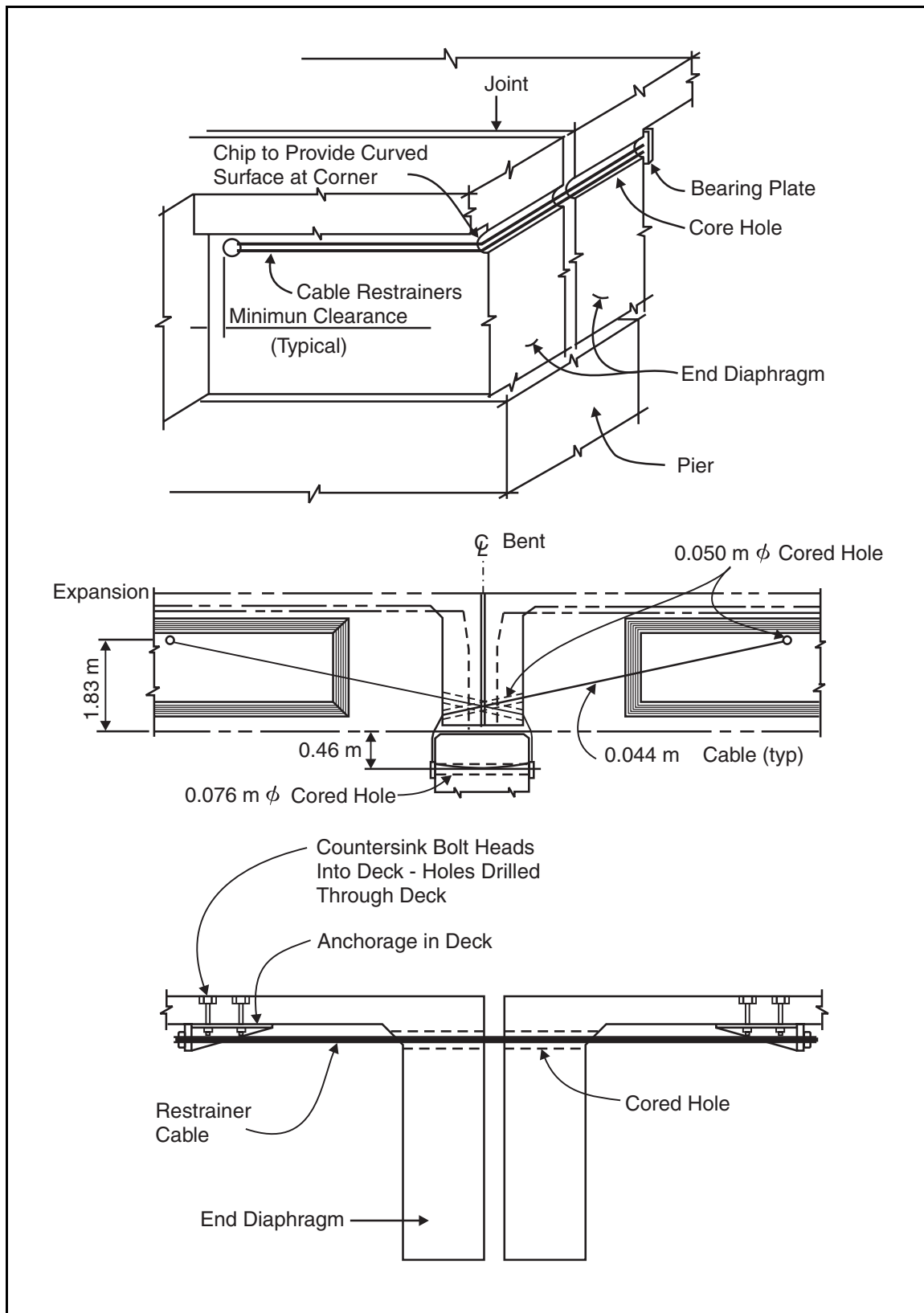


Figure 8-33. Restrainer anchorage schemes.

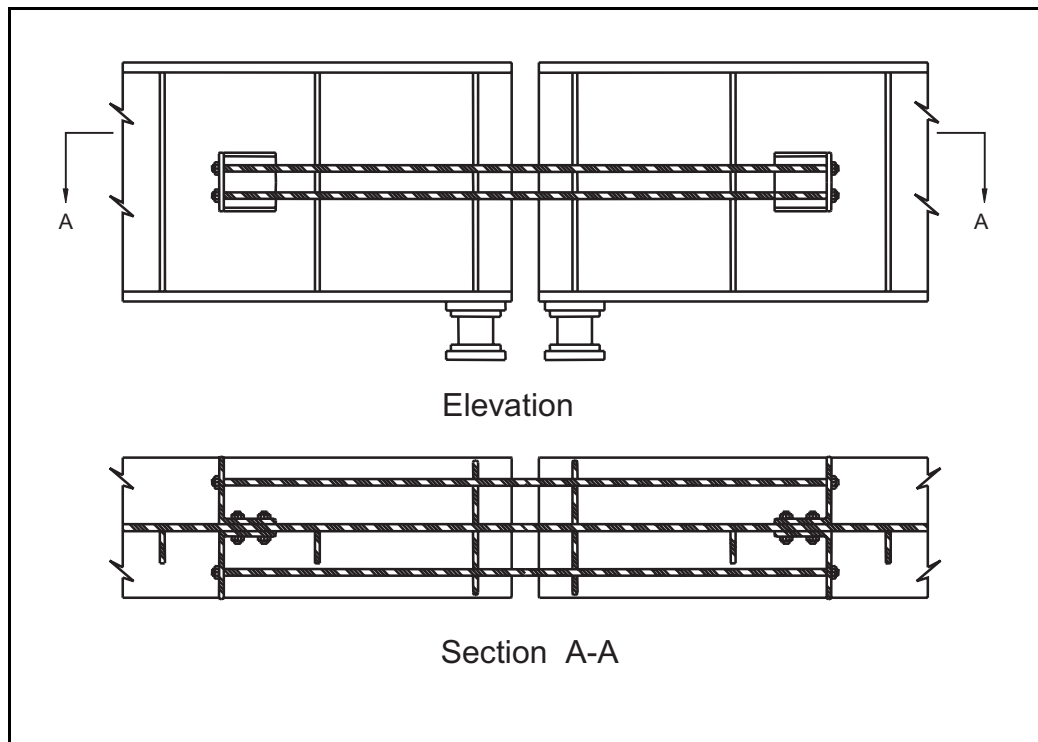


Figure 8-34. *Undesirable* restrainer detail.

When an expansion joint exists at a pier, restrainers at the expansion joint should provide a positive connection to the pier, as shown in figure 8-38. This detail will tend to prevent the bearings from becoming unseated. Since each of the restrainers can only resist movement in one direction, and because closure of the expansion joint will transfer the inertia forces of one span to the adjacent span, each restrainer must resist the inertia forces of both spans in conjunction with other load-resisting elements. Depending on the configuration of the restrainers at adjacent expansion joints, it is possible that the inertia forces of other spans should also be included. Note that the restrainers are connected to the bottom flange in figure 8-38. While this will prevent the possibility of tearing the web, it will also reduce vertical clearance under the bridge.

Consideration should also be given to minimizing access difficulties during construction and maintenance. For example, in box girders, the number of bays in which restrainers are placed should be kept to a minimum.

Many retrofit techniques for bearing and expansion joints will require coring of existing concrete. When coring is to be used, there are at least two issues that should be considered. The first is the clearance required for coring equipment. The minimum distance between the center of a cored hole and an adjacent surface should be 75 mm (3 in). For holes larger than 150 mm (6 in), the edge of the hole may be flush against the adjacent surface. In addition, cored holes should be located so that a minimum of 1.2 m (4 ft) of clearance exists on at least one side from the centerline of the hole. These clearances are shown in figure 8-39.

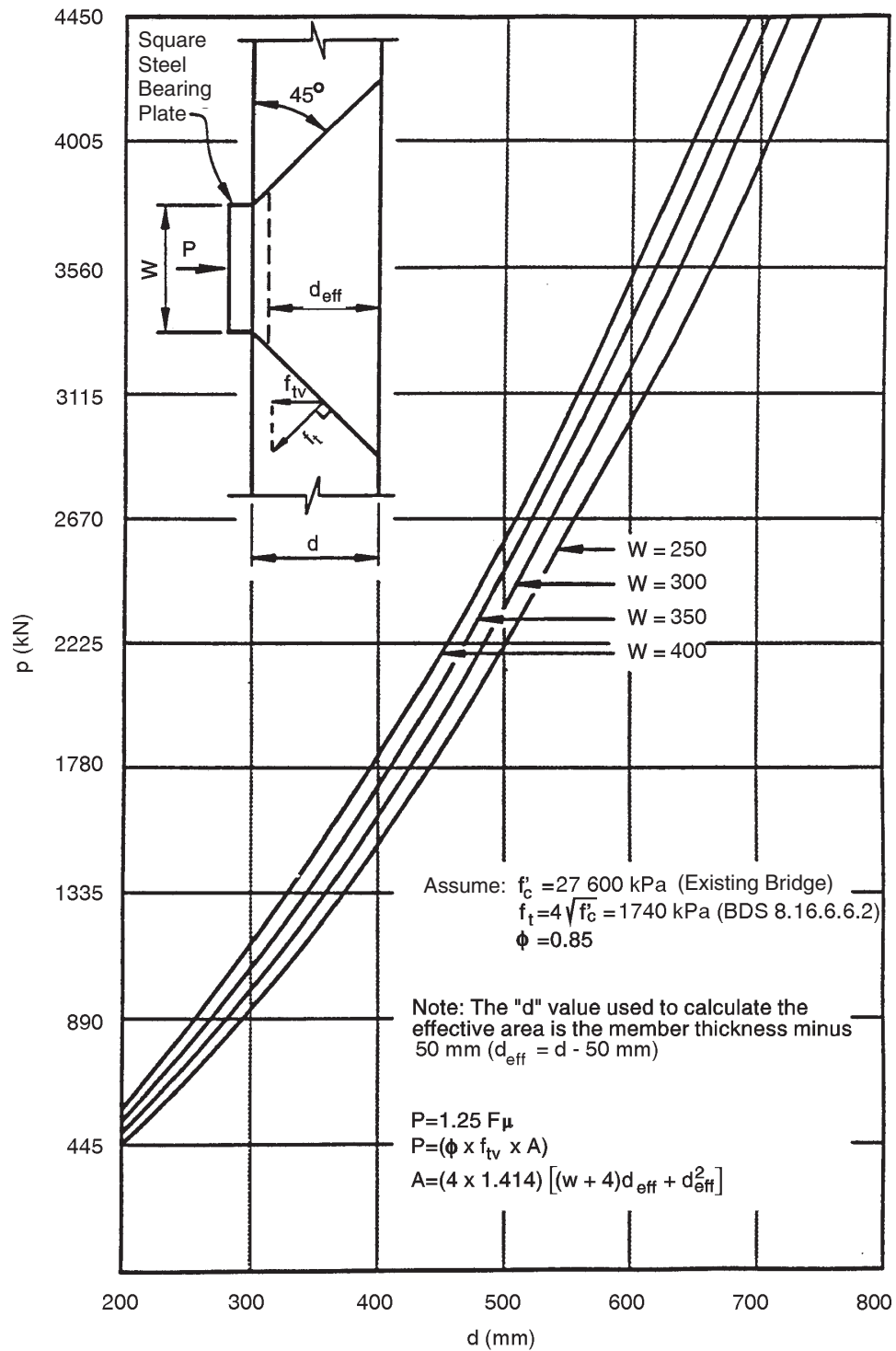


Figure 8-35. Resistance of concrete wall to punching shear.

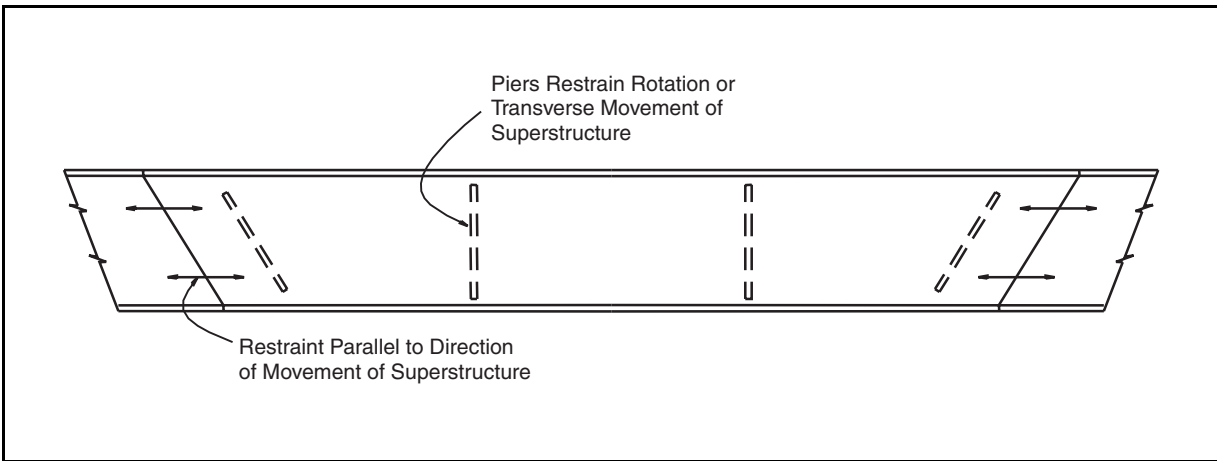


Figure 8-36. Restrainer orientation for transversely rigid supports.

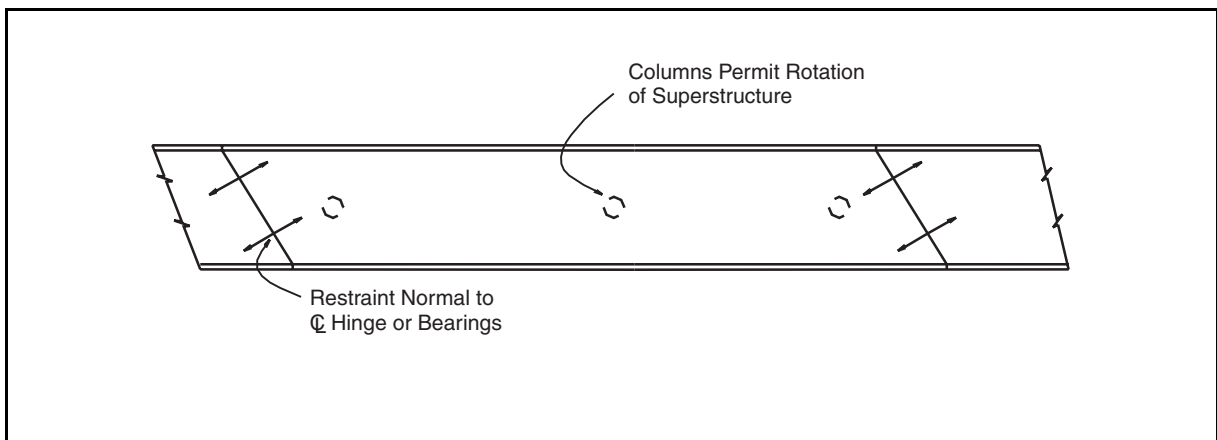


Figure 8-37. Restrainer orientation for transversely flexible supports.

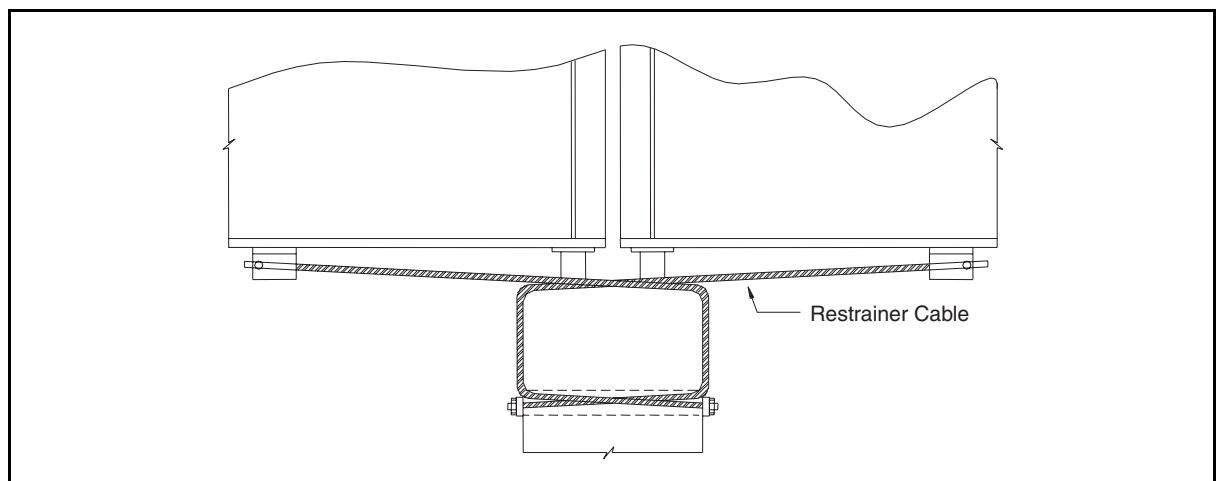


Figure 8-38. Restrainer at pier with a positive tie to pier.

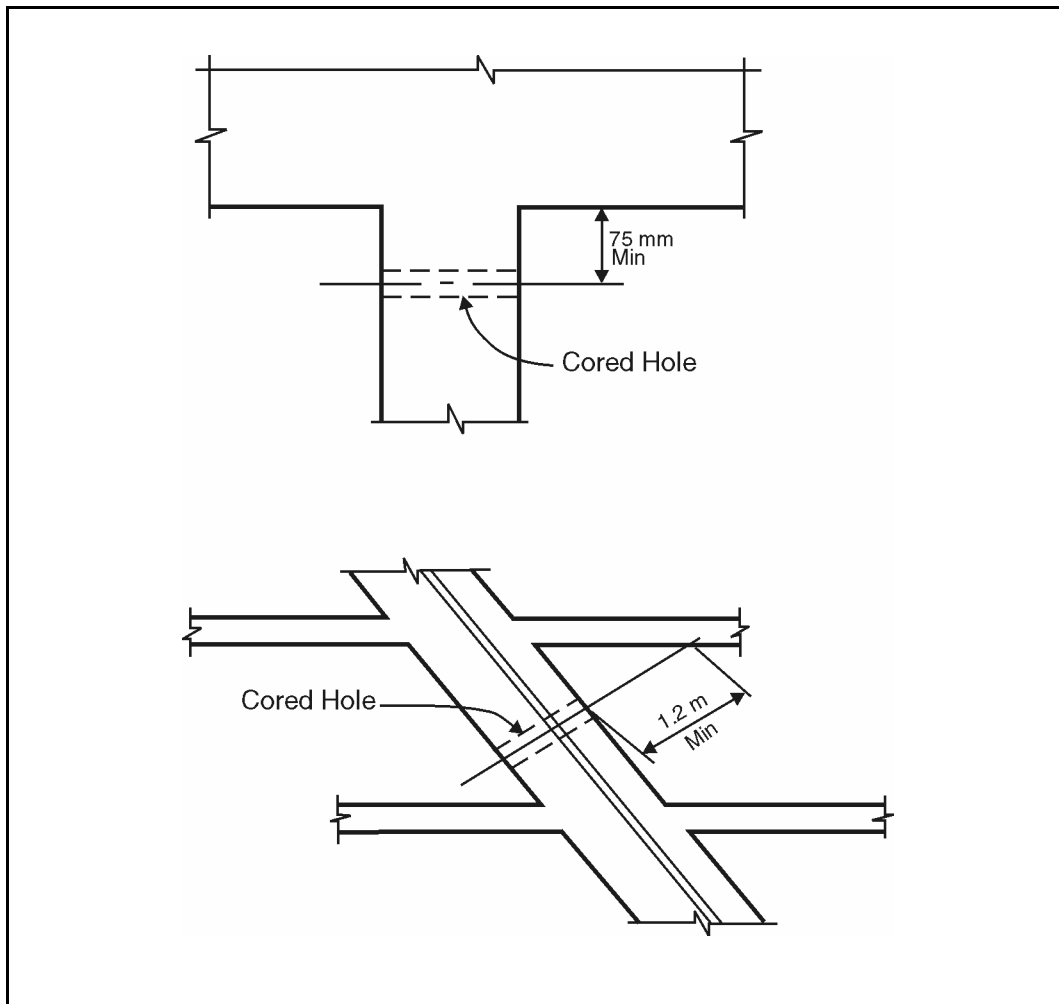


Figure 8-39. Required clearances for coring.

The second issue is the potential for interference with primary reinforcing steel, expansion joint hardware, and prestressing tendons. Special care should be taken to avoid cutting structurally-critical reinforcement and prestressing bars, or large multi-wire or multi-strand tendons, in post-tensioned bridge components. If the type of prestressing system used cannot be determined from the “as built” plans or construction records, bars and large tendons should be assumed. Construction personnel should be alerted to the presence of these elements so that appropriate precautions can be taken in the field. When possible, drilling should be specified instead of coring, since there is less potential for damaging reinforcing or prestressing steel.

The response of a bridge that has been retrofitted with restrainers is nonlinear, even if the columns and foundations remain elastic. This is because restrainers at expansion joints are initially slack and intended to engage only after some movement has taken place. The restrainers are also essentially tension-only devices and are ineffective while the joints are closing. Furthermore, the impact that occurs at joint closure is a highly nonlinear problem that cannot be solved rigorously by simplified means.

Because restrainer behavior is very nonlinear, an accurate analysis of restrainer forces can only be obtained from a nonlinear dynamic analysis of the entire bridge. Since this is impractical in most cases, approximate static analysis procedures are commonly used to evaluate the need for, and design of, restrainers. These procedures generally yield better results than those obtained from an elastic dynamic analysis. When restrainers are required, the restrainer force capacity should be determined according to the procedures described in section 8.4.2.1(g).

For all single span bridges and bridges in Seismic Retrofit Category B (section 1.10), a dynamic analysis is not necessary and the design force is given by Methods A1 and A2 (section 5.2). Restrainers should develop this force capacity before movement, equal to 67 percent of the available seat width as shown in figure 8-40, is exceeded. In areas of low seismicity, it may be desirable to restrain joints having narrow seats by using short, stiff restrainers designed to function below their yield capacity. The stiffness of the restrainers will result in small joint movements, while restrainer forces will be kept to reasonable levels because of the low seismicity. However, for the purpose of designing restrainer anchorages and evaluating the effect of restrainers on other structural members, design forces should be assumed to be 125 percent of the nominal restrainer breaking strength.

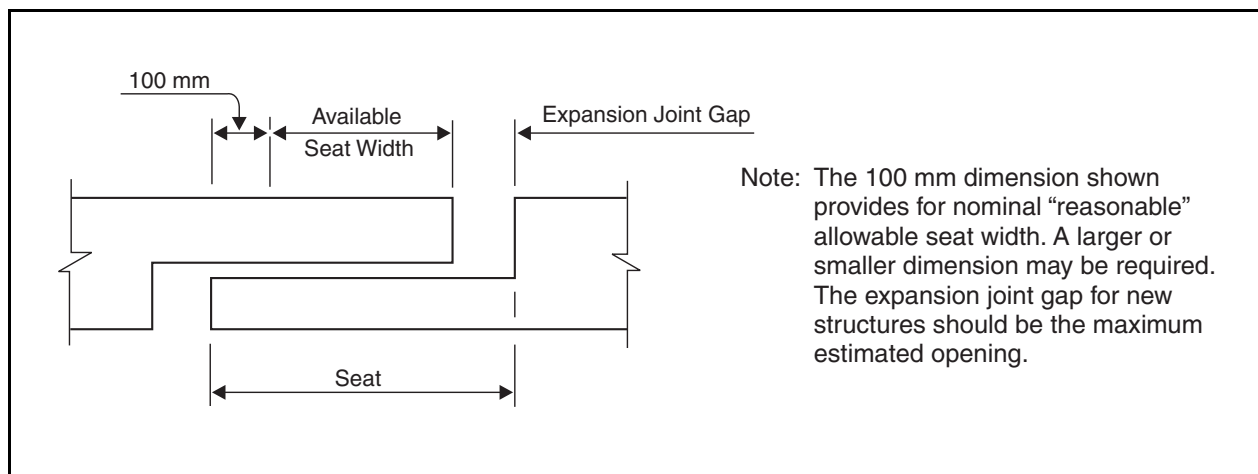


Figure 8-40. Available seat width.

Section 8.4.2.1(f) describes a simplified method for evaluating the need for restrainers in multi-span simply supported bridges. Simplified methods for verifying the number, size, and length of restrainers is presented in section 8.4.2.1(g). Both iterative and non-iterative methods are described. Although these methods are not rigorously correct, they yield acceptable results in most cases. The two restrainer design methods given below were developed principally for restrainers at in-span expansion joints in continuous superstructures, but can be adapted to simply-supported spans by considering every span to be a 'frame' (DesRoches and Fenves 1998).

Both restrainer design methods are based on limiting joint movement to 67 percent of the available seat width, as shown in figure 8-40, which may call for a large number of restrainers in some cases. When this occurs, increasing the available seat width and allowable restrainer

displacement will reduce the number of restrainers. Seat extenders may be used to increase the available seat width. Increasing the length of restrainers or increasing the restrainer slack will increase the allowable restrainer displacement.

8.4.2.1(f). Evaluation of the Need for Restrainers for Simply Supported Spans

The following procedure may be used to determine the adequacy of the connection between the span and substructure, and to determine the unrestrained displacements of the structure. If the connection is adequate and the unrestrained displacements are less than 67 percent of the available seat width, no restrainers are required. If the connection is not adequate and the unrestrained displacements are more than 67 percent of the available seat width, restrainers should be designed using the procedures described in section 8.4.2.1(g).

In this evaluation, it is necessary to distinguish between fixed and expansion bearings, and to consider the location of the bearing. The evaluation procedure varies for bearings located at abutments, end-span piers, and the remaining piers. In all cases, an equivalent single degree of freedom (SDOF) system is analyzed to determine bearing forces and bearing displacements. The following paragraphs define the procedures for determining the adequacy of the connection and bearing seat for each case in which one of the spans supported at a pier has fixed bearings while the other span at this pier has expansion bearings. These procedures could be adapted to interior piers with two sets of expansion bearings or two sets of fixed bearings by modifying the participating masses and stiffness of the equivalent SDOF system, as required.

Fixed Bearings at Abutments – The SDOF system for this case assumes the span is moving away from the abutment. Therefore, the stiffness of the unrestrained system is derived from the nonlinear behavior of the bearing. The bearing is initially very stiff and, therefore, the equivalent maximum elastic force applied to the bearing is simply the weight of the span multiplied by the peak ground acceleration, which may be assumed to be given by $0.4 F_a S_s$ (see figure 1-8). If the equivalent elastic force exceeds the capacity of the bearings, then the bearings are assumed to fail and it will be necessary to check the resulting bearing displacement. This is done using an iterative procedure in which the bearing is assumed to have a perfectly elastoplastic force-displacement relationship. Therefore, the effective bearing stiffness in the SDOF model is reduced until the resulting bearing force equals the capacity of the bearing. This stiffness represents the secant stiffness on the force displacement diagram of the bearing at maximum displacement. No corresponding increase in damping should be assumed. The resulting maximum displacement is compared to the available seat width to determine whether or not restrainers are required. This case and procedure are illustrated in figure 8-41.

End-Span Fixed Bearings at Piers – In this case, the SDOF system is derived by assuming the unrestrained span is moving toward the abutment. Therefore, in addition to the stiffness of the bearing, the stiffness of the column and foundation must be considered. If displacements are large enough to close the gap between the span and the abutment, then the abutment stiffness will also play a role in the seismic response of the bearing. This case and a model of the assumed SDOF system is shown in figure 8-42.

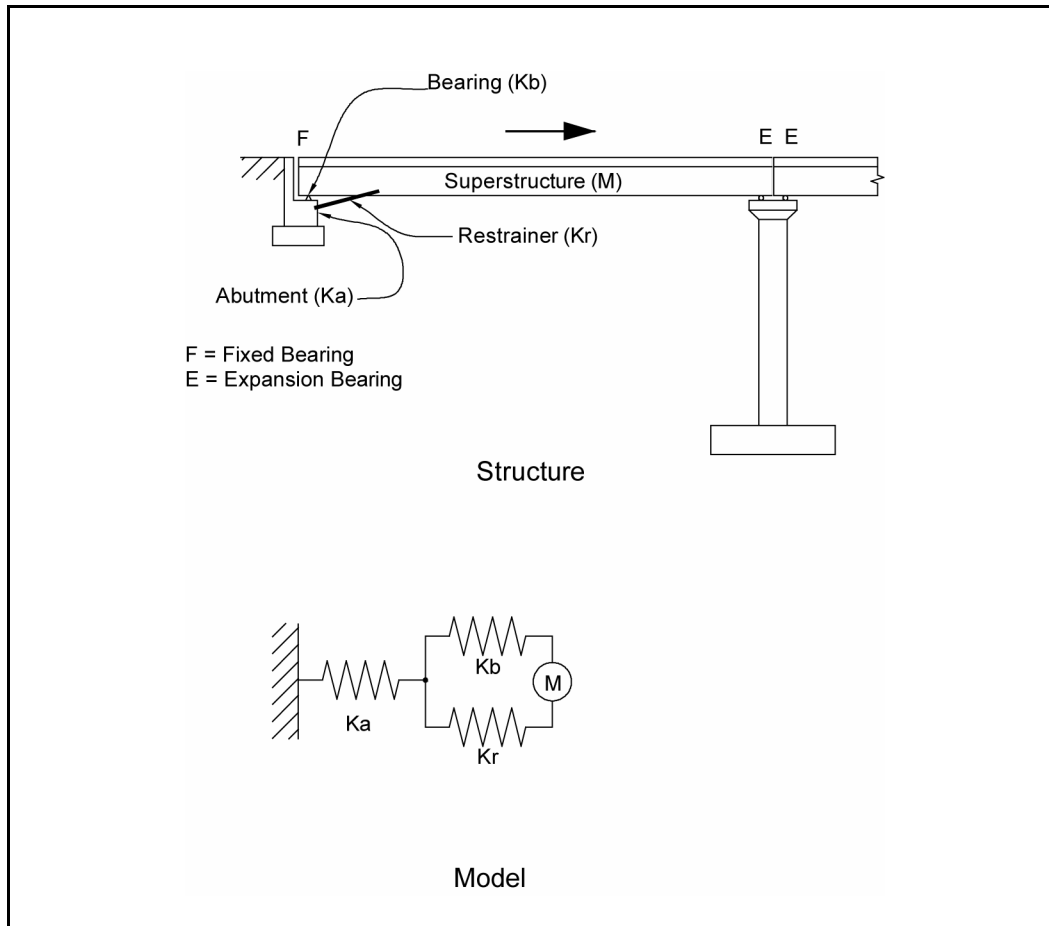


Figure 8-41. SDOF model for end-span fixed bearing at abutment.

As previously described, the procedure first involves finding the maximum equivalent elastic force in the bearing to determine if the bearing will fail. Initially, only the stiffness of the column and foundation is considered. If the resulting displacements are smaller than the gap at the abutment, bearing forces are compared with bearing capacity to determine if a bearing failure will occur. If the displacement at the abutment is larger than the gap, the stiffness of the SDOF system must be adjusted to consider the stiffness of the abutment. This is done iteratively by first assuming a value for the abutment stiffness and adjusting that stiffness until there is force and displacement compatibility at the abutment. The force displacement curve for the abutment is assumed to be bilinear once the gap is closed, as shown in figure 8-43. Abutment stiffness in the SDOF model is assumed to correspond to a chord from the at-rest point to the point of force and displacement compatibility on this curve (Point A). Once the correct abutment stiffness has been identified, the bearing force is compared with bearing capacity to determine if yielding of the bearing will occur.

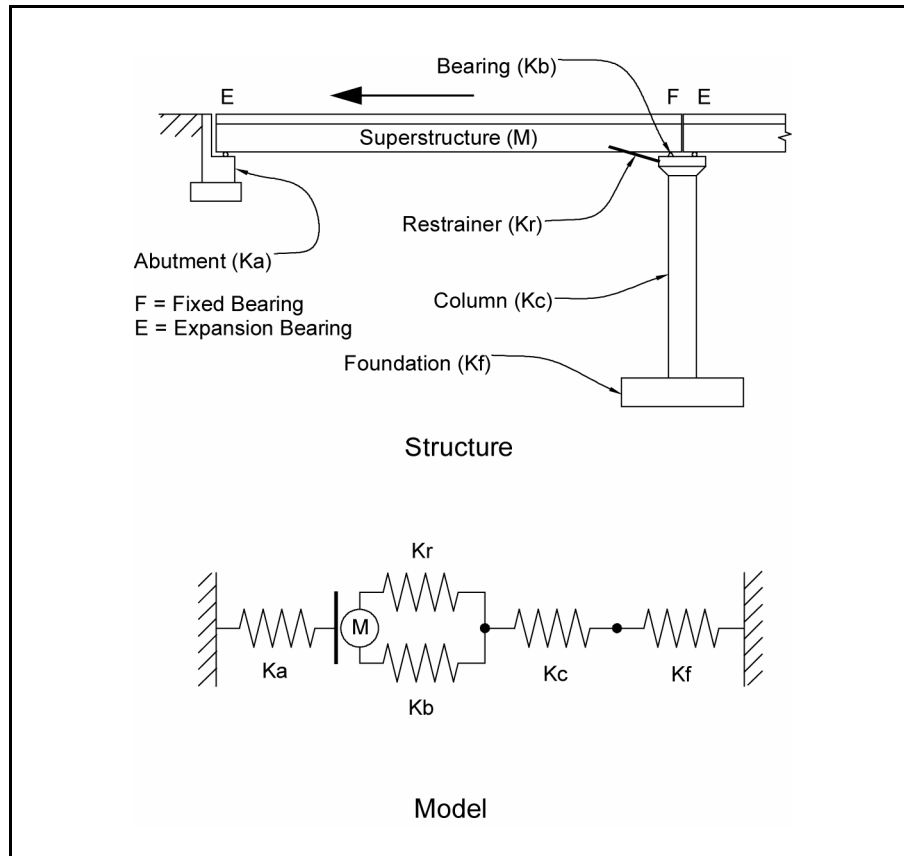


Figure 8-42. SDOF model for an end-span fixed bearing at pier.

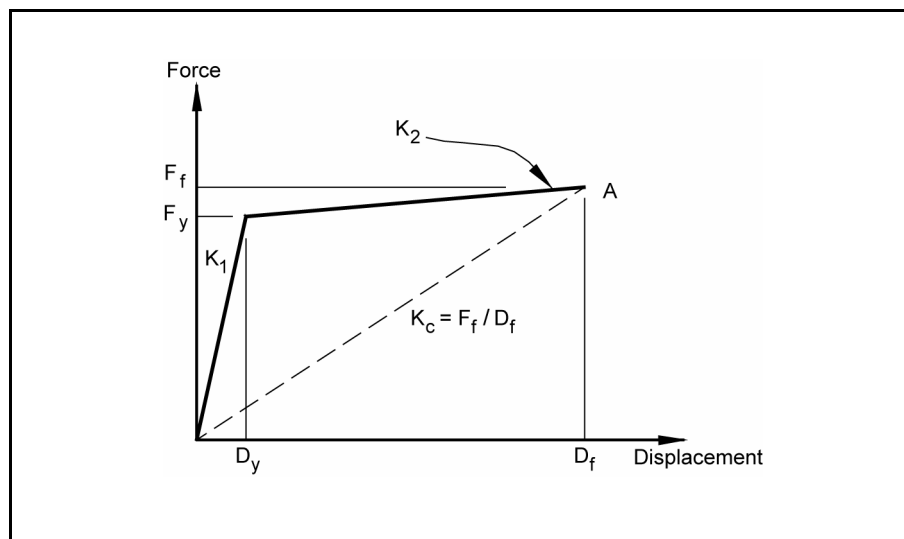


Figure 8-43. Force displacement relationship for abutment.

If the bearing yields, it will be necessary to perform a new analysis to assess whether the bearing seat is adequate to prevent unseating of the span. In this case, the equivalent bearing stiffness will be included in the SDOF system (see figure 8-42). Because of the nonlinear behavior of the bearings and the abutment, a trial and error procedure will be required to determine the combined secant stiffness of the two elements. Since force and displacement compatibility must be achieved in both the bearings and the abutment simultaneously, it will be necessary to adjust the combined stiffness of both elements until such compatibility is achieved. To accomplish this, the forces and displacements in each element derived from the SDOF analysis must be tracked and their combined stiffness adjusted accordingly. The analysis converges on the correct solution when these forces correspond to the combined forces from the assumed force and displacement curves at the displacement derived from the same analysis. Once this has been achieved, the relative displacement at the pier bearing seat may be calculated as the force in the bearing divided by the assumed bearing stiffness. This relative displacement must be less than 67 percent of the available bridge seat to provide an adequate factor of safety against unseating of the span.

Fixed Bearings at Interior Spans – The SDOF model and analysis procedures used for this case are similar to those used for an end span fixed bearing at a pier, except that the participation of the abutment is not included. It is recommended that the mass include the pier cap mass and tributary column mass (may be assumed to be one-third of the column mass), in addition to the mass of the span.

Expansion Bearings at Abutments – The analysis of expansion bearings is limited to determining relative displacements. At abutments, this displacement is determined by considering the displacement of the end span. Since the critical response occurs when the span moves away from the abutment, only the mass of the span and the effective stiffness of the adjacent pier, foundation, and fixed bearing are considered. The methods for determining effective stiffness are similar to those used in previous cases. Because the abutment in this case is assumed not to move with respect to the ground, the movement of the span and the relative movement at the abutment are assumed to be equal.

End Span Expansion Bearings at Piers – For the case of an expansion bearing located at a pier that supports an end span, the critical response involves the pier moving out from under the bearing. Because the abutment end of the span is assumed to remain fixed relative to the ground, the maximum relative displacement at the pier can be determined by finding the maximum relative displacement at the top of the pier. In this case, it is assumed that the adjacent span has fixed bearings at the pier in question. The displacement at the top of this pier is determined by considering the response of a SDOF system consisting of the mass of the adjacent span and the equivalent stiffness of the pier, foundation, and fixed bearing system. The relative displacement at the top of the pier is determined by dividing the inertia force at the top of the column by the stiffness of the column and foundation system.

Expansion Bearings at Interior Spans – This case differs from the previous case in that the span with the expansion bearings can move independently of the pier supporting it. Therefore, in addition to calculating the movement at the top of the pier, it is also necessary to determine the movement of the span. This is done by modeling the span as a SDOF system with a mass equal to the span and an equivalent stiffness equal to the adjacent pier, foundation, and fixed bearing

system. The displacement at the top of the supporting system is determined as in the previous case.

Once these displacements are determined, they are combined using the Complete Quadratic Combination (CQC) rule (section 5.4.2.2) to find the maximum relative displacement. The application of the CQC rule is given in equation 8-3:

$$D_r = \sqrt{D_1^2 + 2\rho_{12} D_1 D_2 + D_2^2} \quad (8-3a)$$

where:

D_1 is the maximum displacement of the span,
 D_2 is the maximum displacement at the top of the pier,

$$\rho_{12} = \frac{8\xi^2(1+\beta)\beta^{3/2}}{(1-\beta^2)^2 + 4\xi^2\beta(1+\beta)^2}, \quad (8-3b)$$

ξ is the equivalent viscous damping ratio, and
 β is the ratio of the vibration frequencies (mode 1 to mode 2).

Whenever the above analyses indicate the need for restrainers, the restrainers should be designed (i.e., number, size, length, and slack) using the methods described in section 8.4.2.1(g). This should be done by assuming that the bearings have failed and can no longer resist horizontal forces. Only the restrainers should be assumed to contribute to the lateral strength and stiffness of the system. In addition, restrainer design forces should be modified by a skew factor of $1/\cos\alpha$, where α is the skew angle.

8.4.2.1(g). Restrainer Design Methods

The number of 19 mm (0.75 in) diameter restrainer cables required to limit the relative displacement of expansion joints is dependent on many factors (DesRoches and Fenves, 1998). One of the most critical parameters is the ratio between the longitudinal periods of vibration of adjacent frames or spans that are being restrained. Simplified methods are valid only within specific ranges of this parameter.

When the ratio of the periods (smallest period to largest period) is 0.3 or less, a rigorous nonlinear dynamic analysis of the bridge must be used to reliably calculate the number and length of restrainers that are required. This procedure requires computer software that is not readily available, nor is it easy to use. In addition, the number of restrainers required is often so large that it is difficult or impossible to fit them into the bridge. Therefore, restrainers are not recommended for bridges with small seat widths when the ratio of the periods of adjacent frames or spans is less than 0.3. Other retrofit measures should be considered in this case.

Comparison of simplified methods with nonlinear dynamic analysis results show that many of the existing design methods are not reliable at low period ratios. For example, the current Caltrans method (Caltrans, 1989) underestimates the required number of restrainers for period ratios below approximately 0.6, but grossly overestimates the number of restrainers required for

period ratios above this level. The current AASHTO method estimates a number of restrainers that is independent of the period ratio. This is less than the number of restrainers estimated by nonlinear dynamic analysis for period ratios under approximately 0.5, and more than the number of restrainers estimated for higher ratios of the periods.

Two new design methods have recently been developed (DesRoches and Fenves, 1998) which are more applicable to retrofitted structures than the previous methods. For ratios of periods between 0.3 and 0.6, an iterative method is recommended. This procedure may require several iterations to converge to the correct solution. For ratios greater than 0.6, a single-step simplified method is available that requires less design effort than the first. Both methods are described below and illustrated in examples 8-1 and 8-2.

The Iterative Method

This method utilizes the substitute structure method (Gulkan and Sozen, 1974) to determine the required number of restrainers. The span or frame properties that are used in this procedure are the frame stiffnesses, K_1 and K_2 , frame masses, m_1 and m_2 , and target displacement ductility of the frames, μ . The properties of the restrainers are the length L_r , modulus of elasticity E , yield stress f_y , and restrainer slack D_{rs} . All analysis is performed using the applicable design spectra. The procedure includes the following steps:

Step 1. Calculate Maximum Allowable Expansion Joint Displacement

Step 1a. Calculate the elongation capacity of a restrainer, D_r , as follows:

$$D_r = D_y + D_{rs} \quad (8-4)$$

where D_r is the maximum permissible restrainer elongation, D_y is the restrainer elongation at yield (equation 8-5), and D_{rs} is the slack in the restrainer system.

The yield elongation is given by:

$$D_y = f_y L_r / E \quad (8-5)$$

where f_y is the yield stress of restrainer, L_r is the restrainer length, and E is the initial modulus of elasticity of restrainer (before initial stretching).

The restrainer slack, D_{rs} , is the clearance provided to accommodate thermal expansion and other non-seismic effects.

Step 1b. Compare the available expansion joint seat width with the maximum permissible restrainer elongation, D_r .

If the maximum permissible restrainer displacement, D_r , is greater than 67 percent of the available seat width D_{as} (see figure 8-40), there is an insufficient safety factor against the expansion joint becoming unseated before the restrainer capacity is reached. In this case,

either the seat width must be increased or D_r must be reduced by one or more of the following:

- Shortening the restrainers.
- Decreasing the restrainer slack.
- Reducing the stress in the restrainers to a value less than yield.

Step 2. Compute the Unrestrained Relative Expansion Joint Displacement, D_{eq0}

The unrestrained relative expansion joint displacement (D_{eq0}) can be obtained using the CQC rule defined in equation 8-3. The frame displacements, D_1 and D_2 , are determined from the following, based on the design spectrum corresponding to the effective damping coefficient given by equation 8-7:

$$D_i = \left(\frac{T_{eff_i}}{2\pi} \right)^2 F_v S_1 (T_{eff}, \xi_{eff}) \quad (8-6)$$

$$\text{where } T_{eff_i} = 2\pi \sqrt{\frac{m_i}{K_{eff_i}}} = 2\pi \sqrt{\frac{w_i}{gK_{eff_i}}} \text{ and } K_{eff_i} = \frac{K_i}{\mu}.$$

The effective damping coefficient, ξ_{eff} , may be estimated as:

$$\xi_{eff} = 0.05 + \frac{1 - \frac{0.95}{\sqrt{\mu}} - 0.05\sqrt{\mu}}{\pi} \quad (8-7)$$

When design spectra are not available for ξ_{eff} , the value of $F_v S_1$ for five percent damping, $[F_v S_1]_{0.05}$, may be modified by a coefficient c_d to obtain values at ξ_{eff} .

That is

$$[F_v S_1]_{\xi_{eff}} = c_d [F_v S_1]_{0.05} \quad (8-8a)$$

where:

$$c_d = \frac{1.5}{40\xi_{eff} + 1} + 0.5. \quad (8-8b)$$

If $D_{eq0} \leq 0.67$ of the available seat width (D_{as}), no restrainers are required.

If $D_{eq0} > 0.67D_{as}$, restrainers must be provided, in accordance with step 3.

Step 3. Estimate the Initial Restrainer Stiffness

The initial estimate of restrainer stiffness required to limit expansion joint displacement is obtained from the incremental stiffness expression given in equation 8-9:

$$K_r = \frac{K_{\text{eff}_{\text{mod}}} (D_{\text{eq}_0} - D_r)}{D_{\text{eq}_0}} \quad (8-9)$$

where:

$$K_{\text{eff}_{\text{mod}}} = \frac{K_{\text{eff}_1} K_{\text{eff}_2}}{K_{\text{eff}_1} + K_{\text{eff}_2}} = \frac{K_1 K_2}{\mu (K_1 + K_2)} \quad (8-10)$$

Step 4. Calculate Relative Expansion Joint Displacement from Modal Analysis

The maximum relative expansion joint displacement is determined from a two-degree-of-freedom (2DOF) modal analysis of the frames using the restrainer stiffness determined in step 3. This 2DOF system is shown in figure 8-44. The relative displacement of the expansion joint is obtained from the CQC, and is given by:

$$D_{\text{eq}} = \sqrt{D_{\text{eq}_1}^2 + D_{\text{eq}_2}^2 + 2\rho_{12} D_{\text{eq}_1} D_{\text{eq}_2}} \quad (8-11)$$

where:

$$\rho_{12} = \frac{8\sqrt{\xi_1 \xi_2} (\xi_1 + \beta \xi_2) \beta^{3/2}}{(1 - \beta^2)^2 + 4\xi_1 \xi_2 \beta (1 + \beta^2) + 4(\xi_1^2 + \xi_2^2) \beta^2} \quad (8-12)$$

$$D_{\text{eq}_i} = P_i S_a(T_{\text{eff}_i}, \xi_{\text{eff}_i}) \quad (8-13)$$

$$P_i = \frac{\{\phi_i\}^T [M] \{1\}}{\{\phi_i\}^T [K] \{\phi_i\}} \left(\{a\}^T \{\phi_i\} \right) = \text{participation factor for mode "i"} \quad (8-14)$$

$$\begin{aligned} \beta &= \text{frequency ratio (mode 1 to mode 2),} \\ \{\phi_i\} &= \text{mode shape for mode 'i',} \\ [M] &= \text{mass matrix of a two frame system,} \\ [K] &= \text{stiffness matrix of a two frame system with restrainers, and} \\ \{a\}^T &= [-1 \quad 1], \\ \{1\} &= \begin{Bmatrix} 1 \\ 1 \end{Bmatrix}. \end{aligned}$$

Note that in equation 8-12, ρ_{12} may be calculated using the formula provided in equation 8-3b if the effective damping coefficient, ξ , is equal for both frames.

Solution of the above equations first requires that the equations of motion for the 2DOF system be solved. This can be accomplished by computer analysis or by hand calculations.

If $D_{eq} > D_r$, go to step 5 and then back to step 4. Otherwise, go to step 6 and calculate the required number of restrainers.

Step 5. Calculate the Incremental Restrainer Stiffness Required to Limit Expansion Joint Displacement

The incremental restrainer stiffness is:

$$K_{r_{j+1}} = K_{r_j} + \left(K_{eff_{mod}} + K_{r_j} \right) \frac{(D_{eq_j} - D_r)}{D_{eq_j}} \quad (8-15)$$

Steps 4 and 5 are repeated until $D_{eq} \leq D_r$.

Step 6. Calculate the Number of Restrainers

Once the required restrainer stiffness is calculated, the number of restrainers is determined by:

$$N_r = \frac{K_r D_r}{f_y A_r} \quad (8-16)$$

where A_r is the area of one restrainer, which for typical 19 mm (0.75 in) diameter cables is 143 mm^2 (0.22 in^2).

A restrainer design example using the iterative method is given in example 8-1.

The Single Step (Simplified) Method

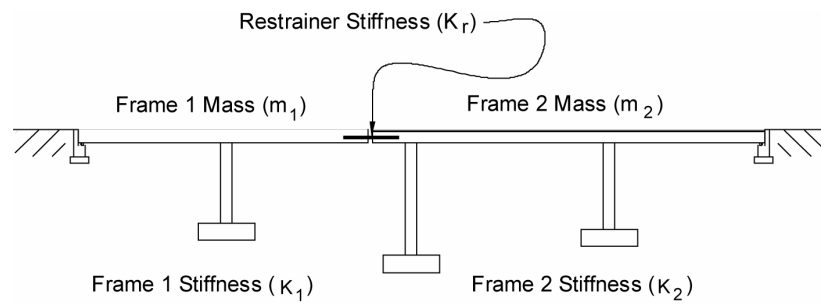
The single step method is reliable only when the ratio of the periods is greater than 0.60 and the ratio of restrainer displacement capacity to initial unrestrained displacement, (η , where $\eta = D_r/D_{eq0}$), is between 0.20 and 0.50. If these criteria are not met, the iterative method should be used. The following steps are required in the single-step method.

Step 1. Calculate Maximum Allowable Expansion Joint Displacement

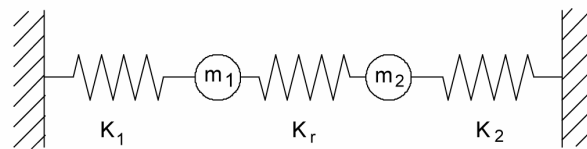
Same as Step 1 for the iterative method.

Step 2. Compute Unrestrained Relative Expansion Joint Displacement

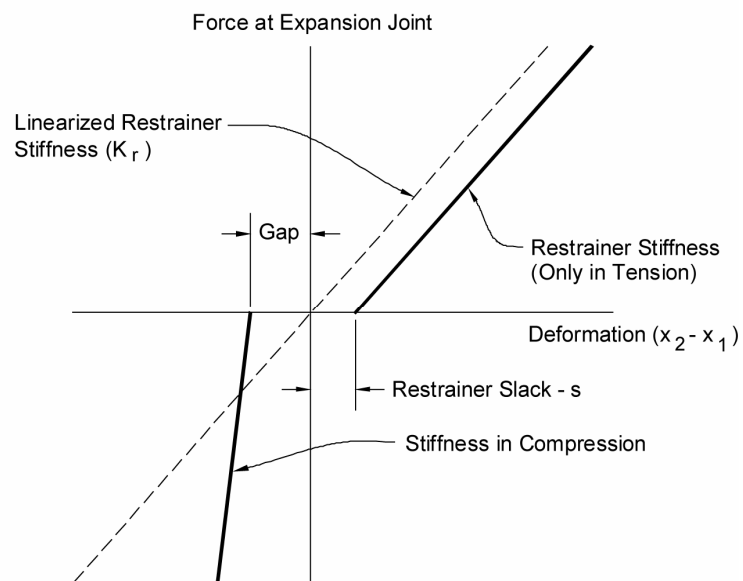
Same as Step 2 for the iterative method.



Structure



Model



Linearization of Hinge

Figure 8-44. 2DOF model for the iterative method.

Step 3. Calculate Required Restrainer Stiffness

$$K_r = K_{\text{eff}_{\text{mod}}} \left[0.50 + \frac{0.50 - \eta^2}{\eta} \right] \quad (8-17)$$

where $K_{\text{eff}_{\text{mod}}}$ is given by equation 8-10 and $\eta = \frac{D_r}{D_{\text{eq0}}}$.

Step 4. Calculate Number of Restrainers

$$N_r = \frac{K_r D_r}{f_y A_r} \quad (8-18)$$

Examples of restrainer design using the single step method are given in examples 8-2 and 8-3.

8.4.2.2. Transverse Restrainers

8.4.2.2(a). General

Transverse restrainers are necessary in many cases to keep the superstructure from sliding off its supports should the bearings fail in the transverse direction. Particularly vulnerable conditions exist when any of the following conditions exist:

- High concrete pedestals are used as bearing seats under individual beams.
- Bearing seats are narrow and highly skewed.
- Steel rocker bearings are relatively tall.
- Transverse distance between the edge bearing and the edge of the seat is small.

Whenever transverse movement might lead to a loss of support, transverse restraint should be provided as a retrofit measure.

8.4.2.2(b). Shear Keys

Concrete shear keys that are doveled into the bridge seats can be used to resist transverse movement at supports. These keys may be placed between beams and outside the edge beams if there is sufficient room, and should be designed to carry the expected forces elastically. Transverse diaphragms or cross frames at these locations should be strong enough to transmit the design force. Shear keys can sometimes be incorporated in new bearing pedestals. An example of a transverse concrete shear key is shown in figure 8-45.

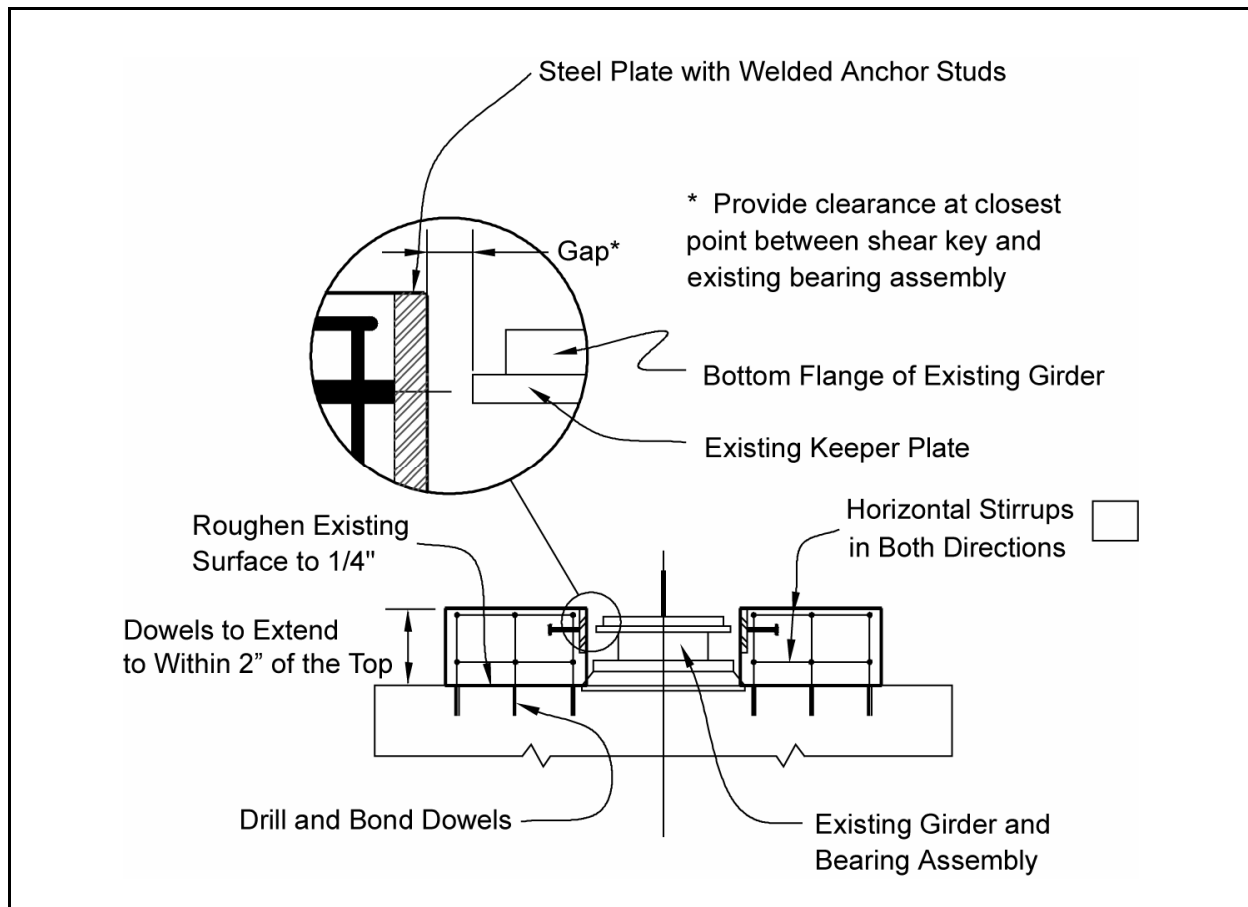


Figure 8-45. Transverse shear keys.

8.4.2.2(c). Keeper Brackets

Transverse restrainers can sometimes be added as part of a bearing retrofit. These restrainers take the form of supplemental keeper brackets that must be designed to carry loads elastically. If sufficient deformation of the beams can take place to engage all of the brackets, they may be considered to be 100 percent effective. If not, some engineering judgement must be used to allow for variable gaps that could cause one bracket to be overloaded with respect to others at the same support. An example of a keeper bracket used in a bearing retrofit is shown in figure 8-46.

8.4.2.2(d). Steel Pipe Restrainers

Another method that has been used to provide transverse restraint in concrete structures employs a double extra-strong steel pipe filled with concrete that passes through the joint (see figure 8-47). This design assumes that the pipe bears against the walls of the cored hole. The full concrete compressive strength may be used in well-reinforced expansion joint diaphragms. However, the full strength of acute corners at highly skewed joints should not be relied upon to resist the full shear force, because such corners can easily break off.

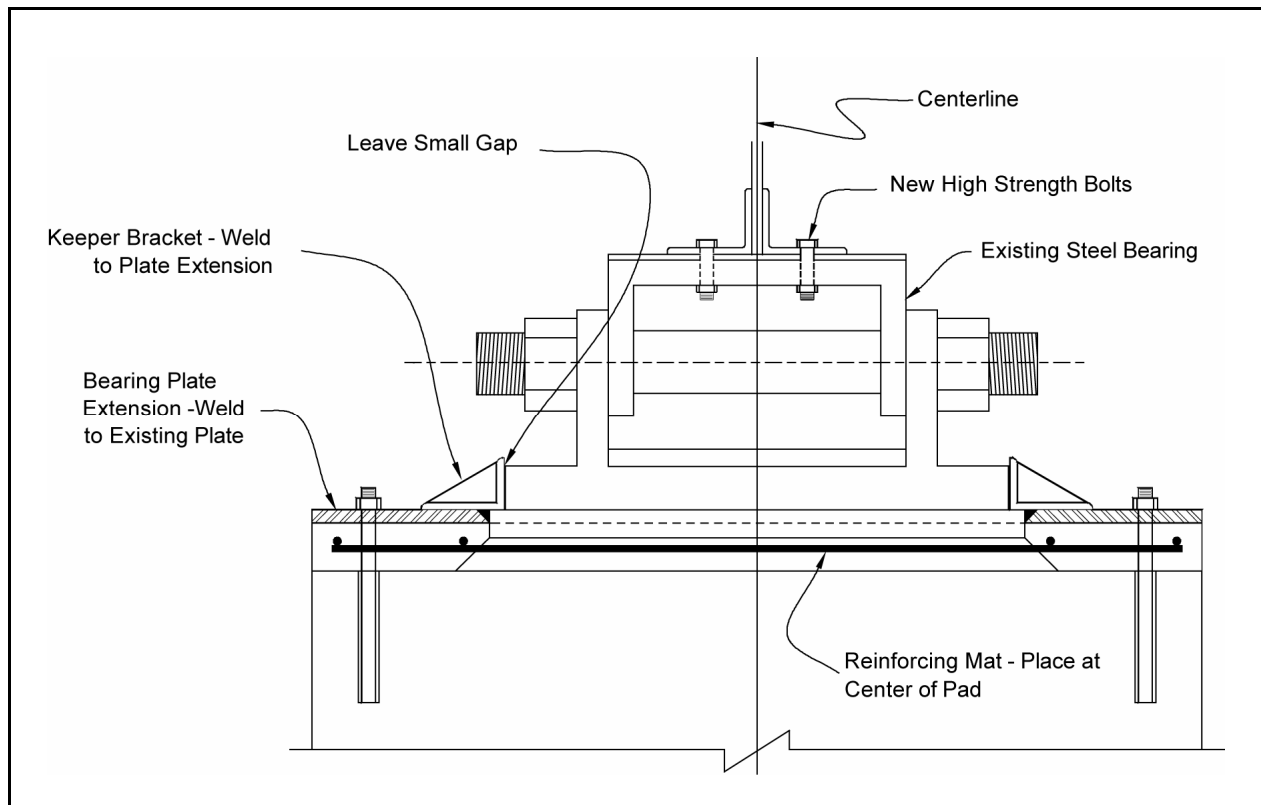


Figure 8-46. Bearing keeper bracket retrofit.

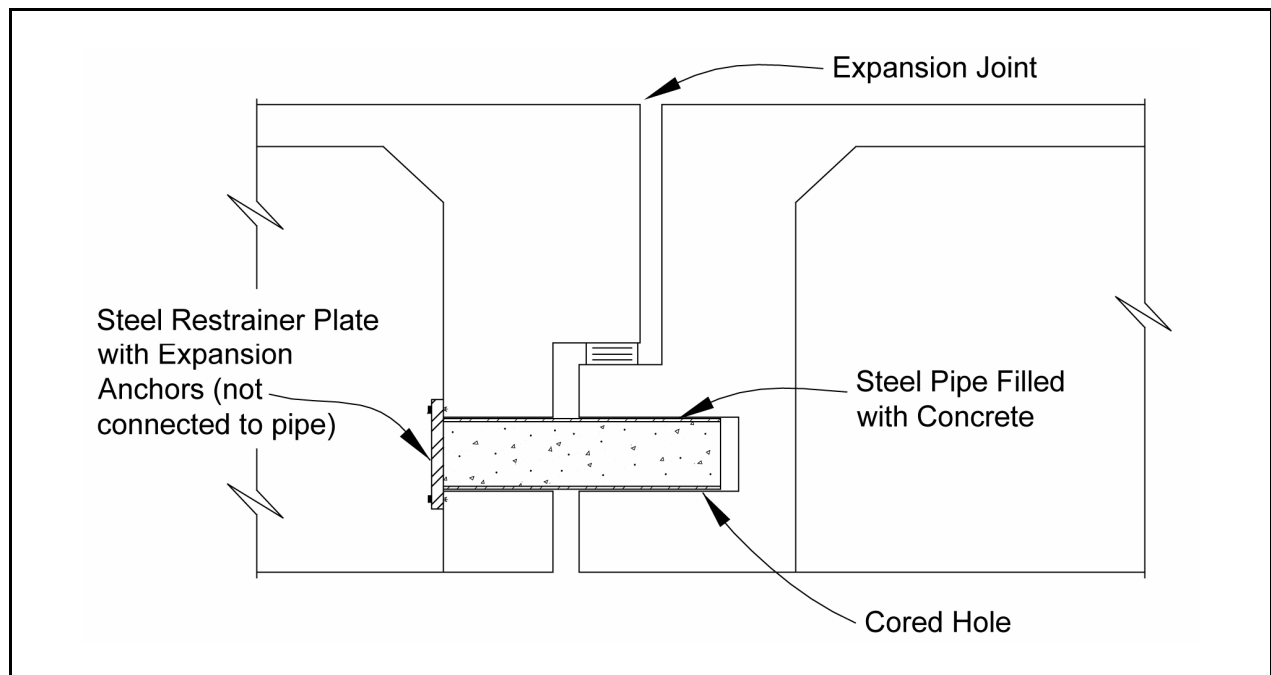


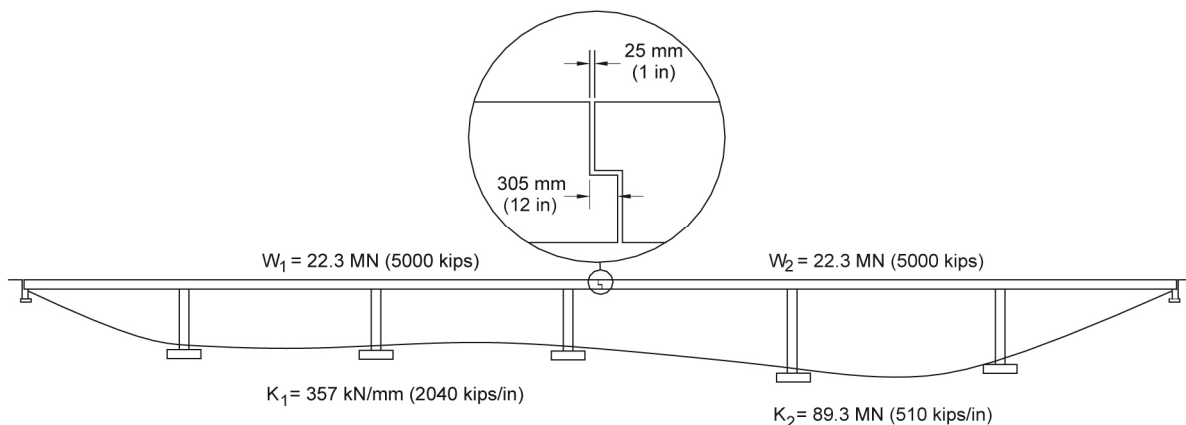
Figure 8-47. Steel pipe restrainers.

EXAMPLE 8.1: RESTRAINER DESIGN BY ITERATIVE METHOD

A six-span bridge divided into two, three-span segments as shown in the figure below. Design restrainers for the expansion-joint seat where the two segments meet. Calculate the number and size of the restrainers required using the iterative method.

Assume the following:

Seat width, N	= 305 mm (12 in)
Concrete cover on vertical faces at seat, d_c	= 50 mm (2 in)
Restrainer yield stress, f_y	= 1,214 MPa (176 ksi)
Restrainer modulus of elasticity, E	= 69,000 MPa (10,000 ksi)
Restrainer length, L_r	= 5.4 m (18 ft)
Restrainer slack, D_{rs}	= 25 mm (1 in)
Response spectrum for site:	figure 1-8
Short period coefficient, $F_a S_s$	= 1.75
Long period coefficient, $F_v S_l$	= 0.70
Target displacement ductility of the frames, μ	= 4
Frame stiffnesses, K_1 and K_2	= 357 and 89.3 kN/mm, respectively (2040 and 510 K/in, respectively)
Frame weights, $W_1 = W_2$	= 22.3 MN (5000 K)



STEP 1. CALCULATE ALLOWABLE EXPANSION JOINT DISPLACEMENT

$$D_r = 95 + 25 = 120 \text{ mm (4.7 in)}$$

$$D_{as} = 305 - 25 - 100 = 180 \text{ mm (7.1 in)}$$

$$2/3 D_{as} = D_r \quad \text{OK}$$

STEP 2. COMPUTE EXPANSION JOINT DISPLACEMENT WITHOUT RESTRAINERS

The effective stiffness of each frame modeled as a substitute structure is:

$$K_{\text{eff}_1} = K_1/\mu = 357/4 = 89.3 \text{ kN/mm (510 kips/in)}$$

$$K_{\text{eff}_2} = K_2/\mu = 89.3/4 = 22.3 \text{ kN/mm (128 kips/in)}$$

Therefore, the effective natural period of each frame is given by:

$$T_{\text{eff}_1} = 2\pi \sqrt{\frac{W_1}{gK_{\text{eff}_1}}} = 2\pi \sqrt{\frac{22.3 \cdot 1000}{9800 \cdot 89.3}} = 1.0 \text{ sec}$$

$$T_{\text{eff}_2} = 2\pi \sqrt{\frac{W_2}{gK_{\text{eff}_2}}} = 2\pi \sqrt{\frac{22.3 \cdot 1000}{9800 \cdot 22.3}} = 2.0 \text{ sec}$$

The effective damping and design spectrum correction factor is:

$$\xi_{\text{eff}} = 0.05 + \frac{1 - \frac{0.95}{\sqrt{\mu}} - 0.05\sqrt{\mu}}{\pi} = 0.05 + \frac{1 - \frac{0.95}{2} - 0.05 \cdot 2}{3.142} = 0.19$$

$$c_d = \frac{1.5}{40\xi_{\text{eff}} + 1} + 0.5 = 0.67$$

Therefore, the frame deflections are calculated as follows:

$$D_1 = \left(\frac{T_{\text{eff}_1}}{2\pi} \right)^2 gc_d S_a(T_{\text{eff}_1}, 0.05) = \left(\frac{1.0}{2 \cdot 3.142} \right)^2 \cdot 9800 \cdot 0.67 \cdot 0.7 = 116 \text{ mm (4.6 in)}$$

$$D_2 = \left(\frac{T_{\text{eff}_2}}{2\pi} \right)^2 gc_d S_a(T_{\text{eff}_2}, 0.05) = \left(\frac{2.0}{2 \cdot 3.142} \right)^2 \cdot 9800 \cdot 0.67 \cdot 0.35 = 232 \text{ mm (9.2 in)}$$

The relative displacement of the two frames can now be calculated using the CQC combination of the two frame displacements as given by equation 8-3. In this case the frequency ratio, β , is 2.0.

$$\rho_{12} = \frac{8\xi^2(1+\beta)\beta^{3/2}}{(1-\beta^2)^2 + 4\xi^2\beta(1+\beta)^2} = \frac{8 \cdot (0.19)^2 \cdot (1+2) \cdot 2^{3/2}}{(1-2^2)^2 + 4 \cdot (0.19)^2 \cdot 2 \cdot (1+2)^2}$$

Because D_1 and D_2 are of opposite sign, equation 8-3 becomes

$$D_{eq_0} = \sqrt{D_1^2 - 2\rho_{12}D_1D_2 + D_2^2} = \sqrt{116^2 - 2 \cdot 0.21 \cdot 116 \cdot 232 + 232^2} = 237 \text{ mm (9.3 in)}$$

$$> 2/3 D_{as} = 120 \text{ mm.}$$

Therefore, restrainers are needed.

STEP 3. DETERMINE FIRST ESTIMATE OF RESTRAINER STIFFNESS

$$K_{eff_{mod}} = \frac{K_{eff_1} K_{eff_2}}{K_{eff_1} + K_{eff_2}} = \frac{89.3 \cdot 22.3}{89.3 + 22.3} = 17.9 \text{ kN/mm (102 kips/in)}$$

$$K_{r_0} = \frac{K_{eff_{mod}} (D_{eq_0} - D_r)}{D_{eq_0}} = \frac{17.9 \cdot (237 - 120)}{237} = 8.84 \text{ kN/mm (53.5 kips/in)}$$

STEP 4. CALCULATE RELATIVE EXPANSION JOINT DISPLACEMENT FROM MODAL ANALYSIS

Solve Modal Equations:

$$\begin{bmatrix} K_{eff_1} + K_{r_0} & -K_{r_0} \\ -K_{r_0} & K_{eff_2} + K_{r_0} \end{bmatrix} \{\phi\} = \omega_{eff_i}^2 \begin{bmatrix} m_1 & 0 \\ 0 & m_2 \end{bmatrix} \{\phi\}$$

$$\begin{bmatrix} 98.1 & -8.84 \\ -8.84 & 31.1 \end{bmatrix} \{\phi\} = \omega_{eff_i}^2 \begin{bmatrix} 2.28 & 0 \\ 0 & 2.28 \end{bmatrix} \{\phi\}$$

$$\omega_{eff_1}^2 = 13.2 \frac{1}{\text{sec}^2}, \quad \omega_{eff_2}^2 = 43.9 \frac{1}{\text{sec}^2}$$

$$T_{eff_1} = 2\pi / \sqrt{13.2} = 1.73 \text{ sec}, \quad T_{eff_2} = 2\pi / \sqrt{43.9} = 0.95 \text{ sec}$$

$$\{\phi_1\} = \begin{Bmatrix} 0.13 \\ 1.00 \end{Bmatrix}, \quad \{\phi_2\} = \begin{Bmatrix} 1.00 \\ -0.13 \end{Bmatrix}$$

Calculate Participation Factors:

$$P_1 = \frac{\{\phi_1\}^T [M] \{1\}}{\{\phi_1\}^T [K] \{\phi_1\}} \left(\{a\}^T \{\phi_1\} \right) = \frac{\begin{Bmatrix} 0.13 & 1.00 \end{Bmatrix} \begin{bmatrix} 2.28 & 0 \\ 0 & 2.28 \end{bmatrix} \begin{Bmatrix} 1 \\ 1 \end{Bmatrix}}{\begin{Bmatrix} 0.13 & 1.00 \end{Bmatrix} \begin{bmatrix} 98.1 & -8.84 \\ -8.84 & 31.1 \end{bmatrix} \begin{Bmatrix} 0.13 \\ 1.00 \end{Bmatrix}} \left(\begin{Bmatrix} -1 & 1 \end{Bmatrix} \begin{Bmatrix} 0.13 \\ 1.00 \end{Bmatrix} \right) = 0.074 \text{ sec}^2$$

$$P_2 = \frac{\{\phi_2\}^T [M] \{1\}}{\{\phi_2\}^T [K] \{\phi_2\}} \left(\{a\}^T \{\phi_2\} \right) = \frac{\begin{Bmatrix} 1.00 & -0.13 \end{Bmatrix} \begin{bmatrix} 2.28 & 0 \\ 0 & 2.28 \end{bmatrix} \begin{Bmatrix} 1 \\ 1 \end{Bmatrix}}{\begin{Bmatrix} 1.00 & -0.13 \end{Bmatrix} \begin{bmatrix} 98.1 & -8.84 \\ -8.84 & 31.1 \end{bmatrix} \begin{Bmatrix} 1.00 \\ -0.13 \end{Bmatrix}} \left(\begin{Bmatrix} -1 & 1 \end{Bmatrix} \begin{Bmatrix} 1.00 \\ -0.13 \end{Bmatrix} \right) = -0.022 \text{ sec}^2$$

Calculate new relative displacement at expansion joint:

$$D_{eq_1} = P_1 g c_d S_a (1.73, 0.05) = 0.074 \cdot 9800 \cdot 0.67 \cdot 0.405 = 197 \text{ mm (7.7 in)}$$

$$D_{eq_2} = P_2 g c_d S_a (0.95, 0.05) = -0.022 \cdot 9800 \cdot 0.67 \cdot 0.737 = -106 \text{ mm (4.2 in)}$$

$$\beta = 1.73 / 0.95 = 1.8$$

$$\rho_{12} = \frac{8(0.19)^2 \cdot (1+1.8) \cdot 1.8^{3/2}}{(1-1.8^2)^2 + 4 \cdot (0.19)^2 \cdot (1.8) \cdot (1+1.8)^2} = 0.27$$

$$D_{eq} = \sqrt{(197)^2 + (-106)^2 + 2(0.27)(197)(-106)} = 197 \text{ mm (7.8 in)}$$

Because $D_{eq} > D_r$, Continue to Step 5

STEP 5. CALCULATE NEW RESTRAINER STIFFNESS

$$K_{r1} = K_{r_0} + (K_{eff_{mod}} + K_{r_0}) \frac{(D_{eq} - D_r)}{D_{eq}} = 8.84 + (17.9 + 8.84) \frac{(196 - 120)}{196} \\ = 19.2 \text{ kN/mm (110 kips/in)}$$

STEP 4. SECOND ITERATION

$$\omega_{eff_1}^2 = 15.4 \frac{1}{\text{sec}^2}, \quad \omega_{eff_2}^2 = 48.1 \frac{1}{\text{sec}^2}$$

$$T_{\text{eff}_1} = 1.60 \text{ sec}, \quad T_{\text{eff}_2} = 0.91 \text{ sec}$$

$$\{\phi_1\} = \begin{Bmatrix} 0.27 \\ 1.00 \end{Bmatrix}, \quad \{\phi_2\} = \begin{Bmatrix} 1.00 \\ -0.27 \end{Bmatrix}$$

$$P_1 = 0.054 \text{ sec}^2, \quad P_2 = -0.017 \text{ sec}^2$$

$$D_{\text{eq}_1} = 0.054 \cdot 9800 \cdot 0.67 \cdot 0.438 = 156 \text{ mm (6.1 in)}$$

$$D_{\text{eq}_2} = -0.017 \cdot 9800 \cdot 0.67 \cdot 0.769 = -88 \text{ mm (3.5 in)}$$

$$\beta = 1.60/0.91 = 1.77$$

$$\rho_{12} = \frac{8(0.19)^2 \cdot (1+1.77) \cdot 1.77^{3/2}}{(1-1.77^2)^2 + 4 \cdot (0.19)^2 \cdot (1.77) \cdot (1+1.77)^2} = 0.29$$

$$D_{\text{eq}} = \sqrt{(156)^2 + (-88)^2 + 2 \cdot 0.29 \cdot 156 \cdot (-88)} = 155 \text{ mm (6.1 in)}$$

Since $D_{\text{eq}} > D_r$, Continue to Step 5

STEP 5. CALCULATE REQUIRED RESTRAINER STIFFNESS

$$K_{r2} = 19.2 + (17.9 + 19.2)(155 - 120)/155 = 27.6 \text{ kN/mm (158 kips/in)}$$

STEP 4. THIRD ITERATION

$$\omega_{\text{eff}_1}^2 = 16.5 \frac{1}{\text{sec}^2}, \quad \omega_{\text{eff}_2}^2 = 52.3 \frac{1}{\text{sec}^2}$$

$$T_{\text{eff}_1} = 1.55 \text{ sec}, \quad T_{\text{eff}_2} = 0.87 \text{ sec}$$

$$\{\phi_1\} = \begin{Bmatrix} 0.36 \\ 1.00 \end{Bmatrix}, \quad \{\phi_2\} = \begin{Bmatrix} 1.00 \\ -0.36 \end{Bmatrix}$$

$$P_1 = 0.044 \text{ sec}^2, \quad P_2 = -0.014 \text{ sec}^2$$

$$D_{eq_1} = 0.044 \cdot 9800 \cdot 0.67 \cdot 0.452 = 131 \text{ mm (5.2 in)}$$

$$D_{eq_2} = -0.014 \cdot 9800 \cdot 0.67 \cdot 0.805 = -73 \text{ mm (2.9 in)}$$

$$\beta = 1.60/0.91 = 1.78$$

$$\rho_{12} = \frac{8(0.19)^2 \cdot (1+1.78) \cdot 1.78^{3/2}}{(1-1.78^2)^2 + 4 \cdot (0.19)^2 \cdot (1.78) \cdot (1+1.78)^2} = 0.29$$

$$D_{eq} = \sqrt{(131)^2 + (-73)^2 + 2 \cdot 0.29 \cdot 131 \cdot (-73)} = 130 \text{ mm (5.1 in)}$$

Since $D_{eq} > D_r$, Continue to Step 5

STEP 5. CALCULATE REQUIRED RESTRAINER STIFFNESS

$$K_{r3} = 27.6 + (17.9 + 27.6)(130 - 120)/130 = 31.1 \text{ kN/mm (178 kips/in)}$$

STEP 4. FOURTH ITERATION

$$\omega_{eff_1}^2 = 16.8 \frac{1}{\text{sec}^2}, \quad \omega_{eff_2}^2 = 54.1 \frac{1}{\text{sec}^2}$$

$$T_{eff_1} = 1.53 \text{ sec}, \quad T_{eff_2} = 0.85 \text{ sec}$$

$$\{\phi_1\} = \begin{Bmatrix} 0.39 \\ 1.00 \end{Bmatrix}, \quad \{\phi_2\} = \begin{Bmatrix} 1.00 \\ -0.39 \end{Bmatrix}$$

$$P_1 = 0.041 \text{ sec}^2, \quad P_2 = -0.013 \text{ sec}^2$$

$$D_{eq_1} = 0.041 \cdot 9800 \cdot 0.67 \cdot 0.458 = 122 \text{ mm (4.8 in)}$$

$$D_{eq_2} = -0.013 \cdot 9800 \cdot 0.67 \cdot 0.824 = -68 \text{ mm (2.7 in)}$$

$$\beta = 1.53/0.85 = 1.8$$

$$\rho_{12} = \frac{8(0.19)^2 \cdot (1+1.8) \cdot 1.8^{3/2}}{(1-1.8^2)^2 + 4 \cdot (0.19)^2 \cdot (1.8) \cdot (1+1.8)^2} = 0.28$$

$$D_{eq} = \sqrt{(122)^2 + (-68)^2 + 2 \cdot 0.28 \cdot 122 \cdot (-68)} = 122 \text{ mm (4.8 in)}$$

$D_{eq} \approx D_r$, Say OK - Continue to Step 6

STEP 6. CALCULATE NUMBER OF RESTRAINERS

$$K_r = 31.1 \text{ kN/mm (178 kips/in)}$$

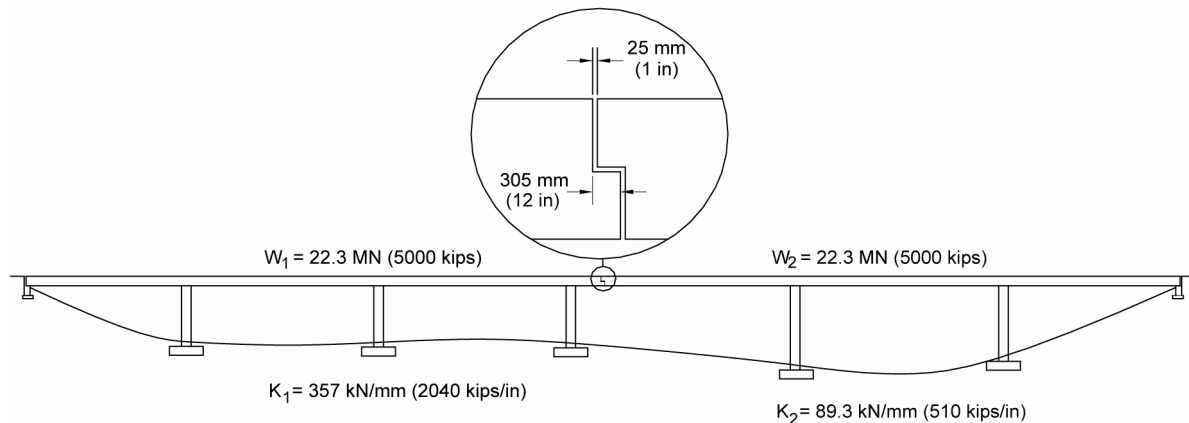
$$N_r = \frac{K_r D_r}{F_y A_r} = \frac{31.1 \cdot 0.120}{1214 \cdot 0.000143} = 21.5 \quad \text{Use 22 – 19 mm restrainer cables}$$

EXAMPLE 8.2: RESTRAINER DESIGN BY THE SINGLE-STEP (NON-ITERATIVE) METHOD (SIMPLIFIED)

A six-span bridge has two, three-span segments as shown in the figure below. Restrainers are to be designed for the hinge seat where the two segments meet. This is the same bridge as in example 8-1. Calculate the number and size of the restrainers required using the single step (simplified) method.

Assume the following:

Seat width, N	= 305 mm (12 in)
Concrete cover on vertical faces at joint, d_c	= 50 mm (2 in)
Restrainer yield stress, f_y	= 1,214 MPa (176 ksi)
Restrainer modulus of elasticity, E	= 69,000 MPa (10,000 ksi)
Restrainer length, L_r	= 5.4 m (18 ft)
Restrainer slack, D_{rs}	= 25 mm (1 in)
Response spectrum for site:	figure 1-8
Short period coefficient, $F_a S_s$	= 1.75
Long period coefficient, $F_v S_l$	= 0.70
Target displacement ductility of the frames, μ	= 4
Frame stiffnesses, K_1 and K_2	= 357 and 89.3 kN/mm, respectively (2040 and 510 K/in, respectively)
Frame weights, $W_1 = W_2$	= 22.3 MN (5000 K)



STEP 1. CALCULATE ALLOWABLE EXPANSION JOINT DISPLACEMENT

Restrainer elongation at yield.

$$D_y = f_y L_r / E = 1,214 \text{ MPa (5,400 mm)} / 69,000 \text{ MPa} = 95 \text{ mm (3.7 in)} \quad (\text{Eq. 8-5})$$

$$D_r = D_y + D_{rs} = 95 \text{ mm} + 25 \text{ mm} = 120 \text{ mm (4.7 in)}$$

$$D_{as} = N - \text{gap} - 2d_o = N - 25 - 2d_c = 305 \text{ mm} - 25 \text{ mm} - 2(50 \text{ mm}) = 180 \text{ mm (7.1 in)}$$

$$\text{Therefore } D_r = 2/3 D_{as} = (180 \text{ mm}) = 120 \text{ mm}$$

$$D_r = 120, \quad 2/3 D_{as} = 120$$

And if $D_r \leq 2/3 D_{as} \Rightarrow$ restrainer design is feasible for given properties.

$$D_r = 100 \frac{2}{3} D_{as} = 120$$

STEP 2. COMPUTE EXPANSION JOINT DISPLACEMENT WITHOUT RESTRAINERS, D_{eq0}

The effective stiffness of each frame is:

$$K_{eff_1} = K_1/\mu = 357 \text{ kN/mm}/4 = 89.3 \text{ kN/mm} \quad (510 \text{ k/in})$$

$$K_{eff_2} = K_2/\mu = 89.3 \text{ kN/mm}/4 = 22.3 \text{ kN/mm} \quad (128 \text{ k/in})$$

Therefore, the effective natural period of each frame is given by:

$$T_{eff_1} = 2\pi \sqrt{\frac{W_1}{gK_{eff_1}}} = 2\pi \sqrt{\frac{22.3 (1000) \text{ KN}}{9800 \text{ mm/sec}^2 (89.3 \text{ kN/mm})}} = 1.0 \text{ sec} \quad \text{See STEP 2 in the Iterative Method}$$

$$T_{eff_2} = 2\pi \sqrt{\frac{W_2}{gK_{eff_2}}} = 2\pi \sqrt{\frac{22.3 \text{ MN} (1000)}{9800 \text{ mm/sec}^2 (22.3 \text{ kN/mm})}} = 2.0 \text{ sec}$$

The effective damping coefficient is:

$$\xi_{eff} = 0.05 + \frac{1 - \frac{0.95}{\sqrt{\mu}} - 0.05\sqrt{\mu}}{\pi} = 0.05 + \frac{1 - \frac{0.95}{2} - 0.05 \cdot 2}{3.142} = 0.19 \quad (\text{Eq. 8-7})$$

The design spectrum correction factor is:

$$c_d = \frac{1.5}{40\xi_{eff} + 1} + 0.5 = 0.67 \quad (\text{Eq. 8-8b})$$

Therefore, the frame deflections are calculated as follows:

$$D_1 = \left(\frac{T_{eff_1}}{2\pi} \right)^2 g c_d F_v S_1 (T_{eff_1}, 0.05) = \left(\frac{1.0 \text{ sec}}{[2] \cdot 3.142} \right)^2 9800 \text{ mm/sec}^2 (0.67)(0.7) = 119 \text{ mm} \quad (4.6 \text{ in}) \quad (\text{Eq. 8-6})$$

$$\text{For } T_{eff_2} = 2; S_a = \frac{F_v S_1}{T_{eff_2}} = \frac{0.7}{2} = .35g$$

$$D_2 = \left(\frac{T_{eff_2}}{2\pi} \right)^2 g c_d S_a (T_{eff_2}, 0.05) = \left(\frac{2.0 \text{ sec}}{2(3.142)} \right)^2 9800 \text{ mm/sec}^2 (0.67) 0.35 = 236 \text{ mm} \quad (9.3 \text{ in})$$

The relative displacement of the two frames can now be calculated using the CQC combination of the two frame displacements, as obtained from equation 8-3a. In this case, the frequency ratio, β , is 2.0.

$$\rho_{12} = \frac{8\xi_{\text{eff}}(1+\beta)\beta^{3/2}}{(1-\beta^2)^2 + 4\xi_{\text{eff}}\beta(1+\beta)^2} = \frac{8 \cdot (0.19)^2 \cdot (1+2) \cdot 2^{3/2}}{(1-2^2)^2 + 4 \cdot (0.19)^2 \cdot 2 \cdot (1+2)^2} = .203 \quad (\text{Eq. 8-3b})$$

$$D_{\text{eq0}} = \sqrt{D_1^2 + 2\rho_{12}D_1D_2 + D_2^2} = \sqrt{119^2 + 2(0.203) \cdot 119(236) + 236^2} = 285 \text{ mm (11.2 in)} \quad (\text{Eq. 8-3a})$$

Since $2D_{\text{as}} = 120 \text{ mm}$ and $D_{\text{eq0}} > 2/3 D_{\text{as}} = 120 \text{ mm (4.7 in)}$, restrainers are needed.

But $T_{\text{eff1}}/T_{\text{eff2}} = 1.0 / 2.0 = 0.5$ is less than 0.6

$\eta = D_r/D_{\text{eq0}} = 120 / 285 = 0.421$ is within range 0.2 and 0.5,

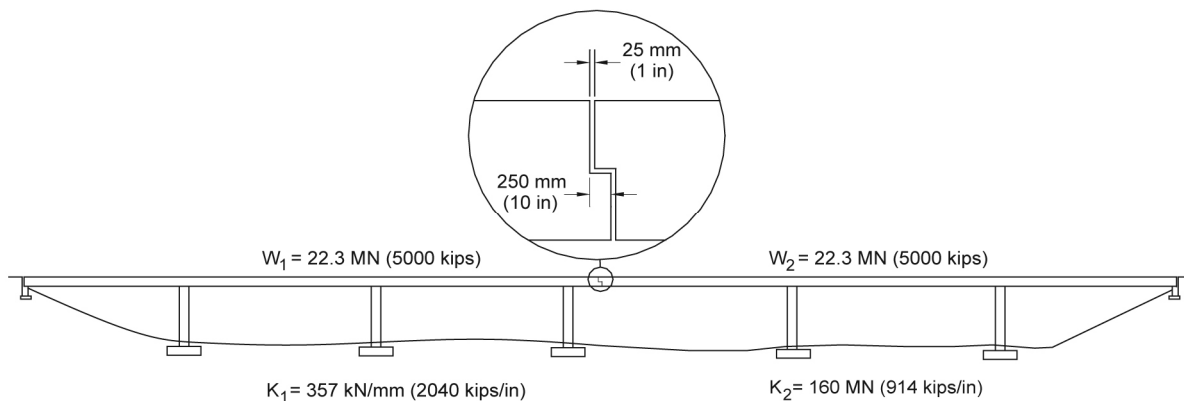
and therefore the single step (non-iterative) method cannot be used for this bridge, since the ratio of the periods exceeds the allowable range.

EXAMPLE 8.3: RESTRAINER DESIGN BY THE SINGLE-STEP (NON-ITERATIVE) METHOD

A six-span bridge has two, three-span segments as shown in the figure below. Restrainers are to be designed for the hinge seat where the two segments meet. This is the not same bridge as in example 8-2; frame stiffnesses have been changed, the hinge seat is smaller and the restrainer cables are shorter. Calculate the number and size of the restrainers required using the single step (non-iterative) method.

Assume the following:

Seat width, N	= 250 mm (10 in)
Concrete cover on vertical faces at joint, d_c	= 50 mm (2 in)
Restrainer yield stress, f_y	= 1,214 MPa (176 ksi)
Restrainer modulus of elasticity, E	= 69,000 MPa (10,000 ksi)
Restrainer length, L_r	= 2.0 m (9.8 ft)
Restrainer slack, D_{rs}	= 25 mm (1 in)
Response spectrum for site:	figure 1-8
Short period coefficient, $F_a S_s$	= 1.75
Long period coefficient, $F_v S_l$	= 0.70
Target displacement ductility of the frames, μ	= 4
Frame stiffnesses, K_1 and K_2	= 357 and 150 kN/mm, respectively (2040 and 914 K/in, respectively)
Frame weights, $W_1 = W_2$	= 22.3 MN (5000 K)



STEP 1. CALCULATE ALLOWABLE EXPANSION JOINT DISPLACEMENT

$$D_r = 53 + 25 = 78 \text{ mm (3.1 in)}$$

$$D_{as} = 250 - 25 - 100 = 125 \text{ mm (4.9 in)}$$

$$2/3 D_{as} > D_r \quad \text{OK}$$

STEP 2. COMPUTE UNRESTRAINED EXPANSION JOINT DISPLACEMENT

The effective stiffness of each frame modeled as a substitute structure is:

$$K_{\text{eff}_1} = K_1/\mu = 357/4 = 89.3 \text{ kN/mm (510 kips/in)}$$

$$K_{\text{eff}_2} = K_2/\mu = 160/4 = 40.0 \text{ kN/mm (228 kips/in)}$$

Therefore, the effective natural period of each frame is given by:

$$T_{\text{eff}_1} = 2\pi \sqrt{\frac{W_1}{gK_{\text{eff}_1}}} = 2\pi \sqrt{\frac{22.3 \cdot 1000}{9800 \cdot 89.3}} = 1.0 \text{ sec}$$

$$T_{\text{eff}_2} = 2\pi \sqrt{\frac{W_2}{gK_{\text{eff}_2}}} = 2\pi \sqrt{\frac{22.3 \cdot 1000}{9800 \cdot 40.0}} = 1.5 \text{ sec}$$

The effective damping and design spectrum correction factor is:

$$\xi_{\text{eff}} = 0.05 + \frac{1 - \frac{0.95}{\sqrt{\mu}} - 0.05\sqrt{\mu}}{\pi} = 0.05 + \frac{1 - \frac{0.95}{2} - 0.05 \cdot 2}{3.142} = 0.19$$

$$c_d = \frac{1.5}{40\xi_{\text{eff}} + 1} + 0.5 = 0.67$$

Therefore, the frame deflections are calculated as follows:

$$D_1 = \left(\frac{T_{\text{eff}_1}}{2\pi} \right)^2 g c_d S_a(T_{\text{eff}_1}, 0.05) = \left(\frac{1.0}{2 \cdot 3.142} \right)^2 \cdot 9800 \cdot 0.67 \cdot 0.7 = 116 \text{ mm (4.6 in)}$$

$$D_2 = \left(\frac{T_{\text{eff}_2}}{2\pi} \right)^2 g c_d S_a(T_{\text{eff}_2}, 0.05) = \left(\frac{1.5}{2 \cdot 3.142} \right)^2 \cdot 9800 \cdot 0.67 \cdot 0.47 = 176 \text{ mm (6.9 in)}$$

The relative displacement of the two frames can now be calculated using the CQC combination of the two frame displacements as given by equation 8-3. In this case the frequency ratio, β , is 1.5.

$$\rho_{12} = \frac{8\xi^2(1+\beta)\beta^{3/2}}{(1-\beta^2)^2 + 4\xi^2\beta(1+\beta)^2} = \frac{8 \cdot (0.19)^2 \cdot (1+1.5) \cdot 1.5^{3/2}}{(1-1.5^2)^2 + 4 \cdot (0.19)^2 \cdot 1.5 \cdot (1+1.5)^2} = 0.45$$

$$D_{\text{eq}_0} = \sqrt{D_1^2 - 2\rho_{12}D_1D_2 + D_2^2} = \sqrt{116^2 - 2 \cdot 0.45 \cdot 116 \cdot 176 + 176^2} = 161 \text{ mm (6.4 in)}$$

$> 2/3 D_{\text{as}} = 83 \text{ mm}$. Therefore, restrainers are needed. Because $T_{\text{eff}_1}/T_{\text{eff}_2}$ is greater than 0.6 and because D_r/D_{eq_0} is between 0.2 and 0.5, the non-iterative method is applicable.

STEP 3. CALCULATE RESTRAINER STIFFNESS

$$K_{\text{eff}_{\text{mod}}} = \frac{K_{\text{eff}_1} K_{\text{eff}_2}}{K_{\text{eff}_1} + K_{\text{eff}_2}} = \frac{89.3 \cdot 40.0}{89.3 + 40.0} = 27.6 \text{ kN/mm (158 kips/in)}$$

$$\eta = \frac{D_r}{D_{\text{eq}_0}} = \frac{78}{161} = 0.484$$

$$K_r = K_{\text{eff}_{\text{mod}}} \left[0.50 + \frac{0.50 - (\eta)^2}{\eta} \right] = 27.6 \cdot \left[0.50 + \frac{0.50 - 0.235}{0.484} \right] = 28.9 \text{ kN/mm (165 kips/in)}$$

STEP 4. CALCULATE NUMBER OF RESTRAINERS

$$N_r = \frac{K_r D_r}{F_y A_r} = \frac{28.9 \cdot 0.078}{1214 \cdot 0.000143} = 13.0 \quad \text{Use 14 – 19 mm restrainer cables}$$

8.4.2.2(e). Design Forces

Transverse bearing restrainers are usually designed to resist load elastically. Studies have shown that when columns yield, additional forces will be transferred to elements that are not designed to yield. In addition, transverse restrainers will be installed with slightly different construction tolerances that will cause them to engage and resist load unevenly. To account for possible increased load due to these effects, the elastic forces derived from an analysis should be increased by 25 percent for design.

Although a dynamic analysis is not necessary for any single span bridge or a bridge in Seismic Retrofit Category B, transverse restrainers in these bridges are required to resist a minimum horizontal load as described in Methods A1 and A2 (section 5.2).

8.4.2.3. Vertical Motion Restrainers

Vertical hold-down devices may be used at bearings to prevent uplift that, if free to occur, could result in damage or loss of stability. Although uplift by itself is unlikely to result in the collapse of a span, vertical hold-down devices should be considered whenever the vertical seismic forces exceed the dead load reaction. Vertical motion restrainers are usually not economically justified unless some additional bearing retrofit is being performed and the bridge is in Seismic Retrofit Category D. An example of a possible hold-down detail is shown in figure 8-48.

Vertical accelerations are often not included in a dynamic response analysis, but if uplift is an issue, an analysis which includes the vertical component of the ground motion should be used.

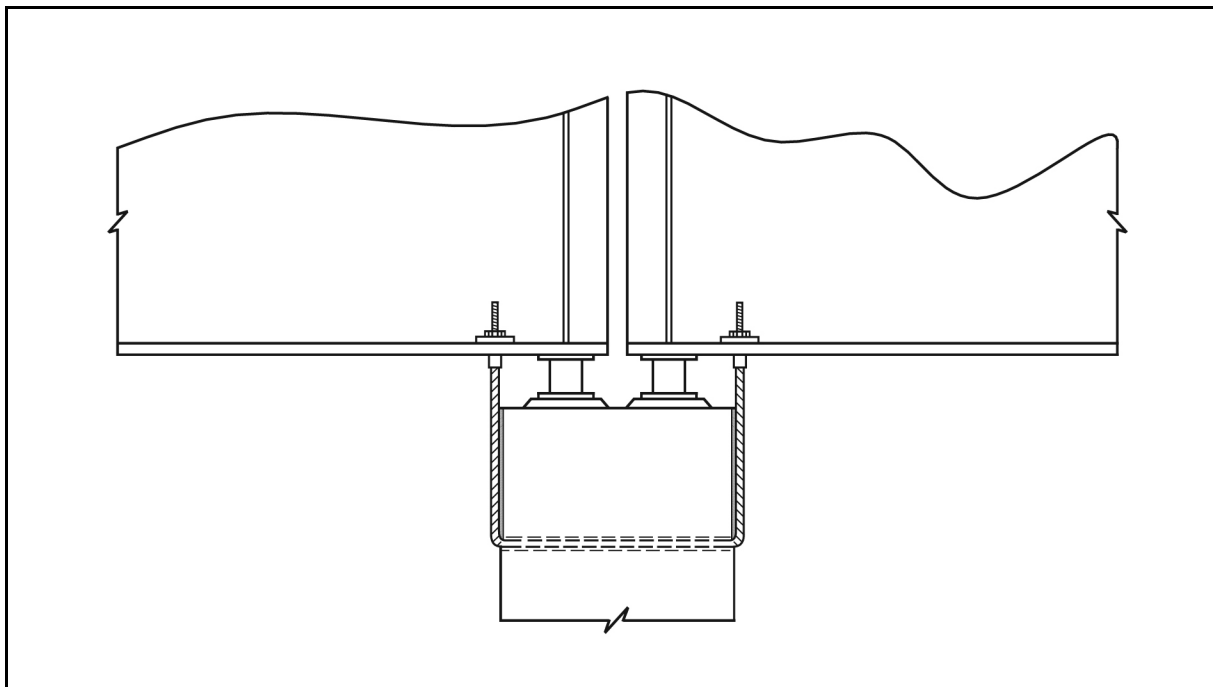


Figure 8-48. Vertical hold down retrofit.

8.4.3. ENERGY DISSIPATION DEVICES

Conventional expansion bearings, such as elastomeric bearing pads or sliding bearings, are natural isolators. However, these bearings do not generally dissipate much energy, and differential displacements at bearing locations may therefore be unacceptably large. In these cases, the retrofit designer can obtain functional performance similar to that provided by seismic isolation bearings by adding separate energy dissipating devices alongside conventional bearings. Energy dissipation devices may also be used at other structural locations where relative movement of the structural components is expected during an earthquake. Over the years there have been many proposals for energy dissipating devices including steel cantilever or beam elements that can deform plastically, lead extrusion devices, viscous dampers, and friction dampers. Each of these devices relies on dissipation of energy during movement to keep movements to acceptable levels.

Rigidity under service loads is provided by the initial stiffness of these devices. Some of the mechanisms used by these devices, such as lead extrusion, and viscous or friction damping, are able to accommodate service load movements if properly designed. However, devices that rely on the plastic deformation of steel are likely to experience fatigue failure over time if they are allowed to yield under service loads. Many of these devices will also have difficulty accommodating orthogonal movements. These issues should be given careful consideration during design.

Energy dissipation devices have been developed and implemented for seismic applications for a number of years. Figure 8-49 shows a number of energy dissipation devices that were originally developed in Japan and New Zealand. Most of these rely on the plastic deformation of steel elements, but one device uses lead extrusion to dissipate energy. Figure 8-50 shows two friction dampers.

A number of energy dissipators have also been developed and tested in the U.S., specifically for bridge applications⁹. Several of these devices were evaluated in the HITEC program on behalf of Caltrans and FHWA (HITEC, 1999a). These included large piston and cylinder type shock absorbers that are capable of resisting the types of loadings experienced in bridges. Summaries of test results for three damper technologies are available through HITEC (HITEC, 1999b,c,d).

8.4.4. SHOCK TRANSMISSION UNITS

Shock transmission units (STUs) are specially fabricated devices that allow very slow movement to occur, such as that caused by temperature change, but become rigid under rapid motion, such as would occur during an earthquake. This characteristic allows these devices to be placed at the expansion joints between superstructure segments, or between the superstructure and substructure at expansion bearings. A typical application would be a continuous bridge where only one line of bearings is designed to take longitudinal loads at a fixed bearing, and the remaining supports are expansion bearings. By placing STUs at the expansion bearings, longitudinal load is shared by all supports, thus reducing the load at the fixed bearing.

⁹ Whittaker et al., 1989; Richter et al., 1990; Constantinou et al., 1992; Aiken et al., 1993; Bergman and Hanson, 1993; Tsai et al., 1993; Grigorian et al., 1993

STUs which are typically composed of a piston and cylinder filled with a viscous fluid, are usually custom manufactured for each application. The designer should specify the required maximum load capacity of the device, maximum range of movement, and maximum rate of movement or acceptable drag forces that can result from this movement. It is difficult for most manufacturers to achieve a drag force of less than two percent of the rated capacity of the unit. The rated capacity may therefore be limited by the fatigue strength of the structural elements of the bridge. When unknown, the rate of movement of an STU can be assumed to be 0.0001 L per hour, which corresponds to a temperature change of 25 degrees Celsius in one hour. The distance, L, is the effective bridge length subject to thermal movement and is limited to 150 m (500 ft) for the above rule of thumb to apply. The designer should also specify the temperature range in which the STU will operate, since their performance may be temperature dependent.

STUs are unidirectional devices that must be mounted in such a way as to accommodate out-of-plane movement. One method of doing this is to use ball joints at either end of the unit where it is mounted to the structure. Generally, the designer will also specify or design the mounting hardware. The structure and brackets must be able to resist drag forces without fatigue. During an earthquake, STUs may be assumed to be rigid even though they may experience a small movement prior to 'locking up.' This small movement can create impact forces, so it is recommended that the STU, brackets, and non-ductile structural elements be designed for 125 percent of the calculated required forces.

Because these are custom-manufactured devices, it is strongly recommended that they be prequalified for use in a retrofit project. This includes satisfying the requirements of a series of performance tests such as:

- Seal wear test.
- Cyclic load test.
- Crag force test.
- Overload test at 150 percent of the rated capacity.
- Fatigue load test.

Units should also be proof-tested using the overload test.

Because of the small number of moving parts, these devices should require relatively low levels of maintenance. Nevertheless, it is recommended that they receive periodic inspection. Of particular concern are the seals, which could potentially leak. It is recommended that STU installations be designed in such a way that they can be easily inspected and replaced if they become worn during the life of the bridge. These devices should be protected from a corrosive environment by painting or galvanizing exposed components.

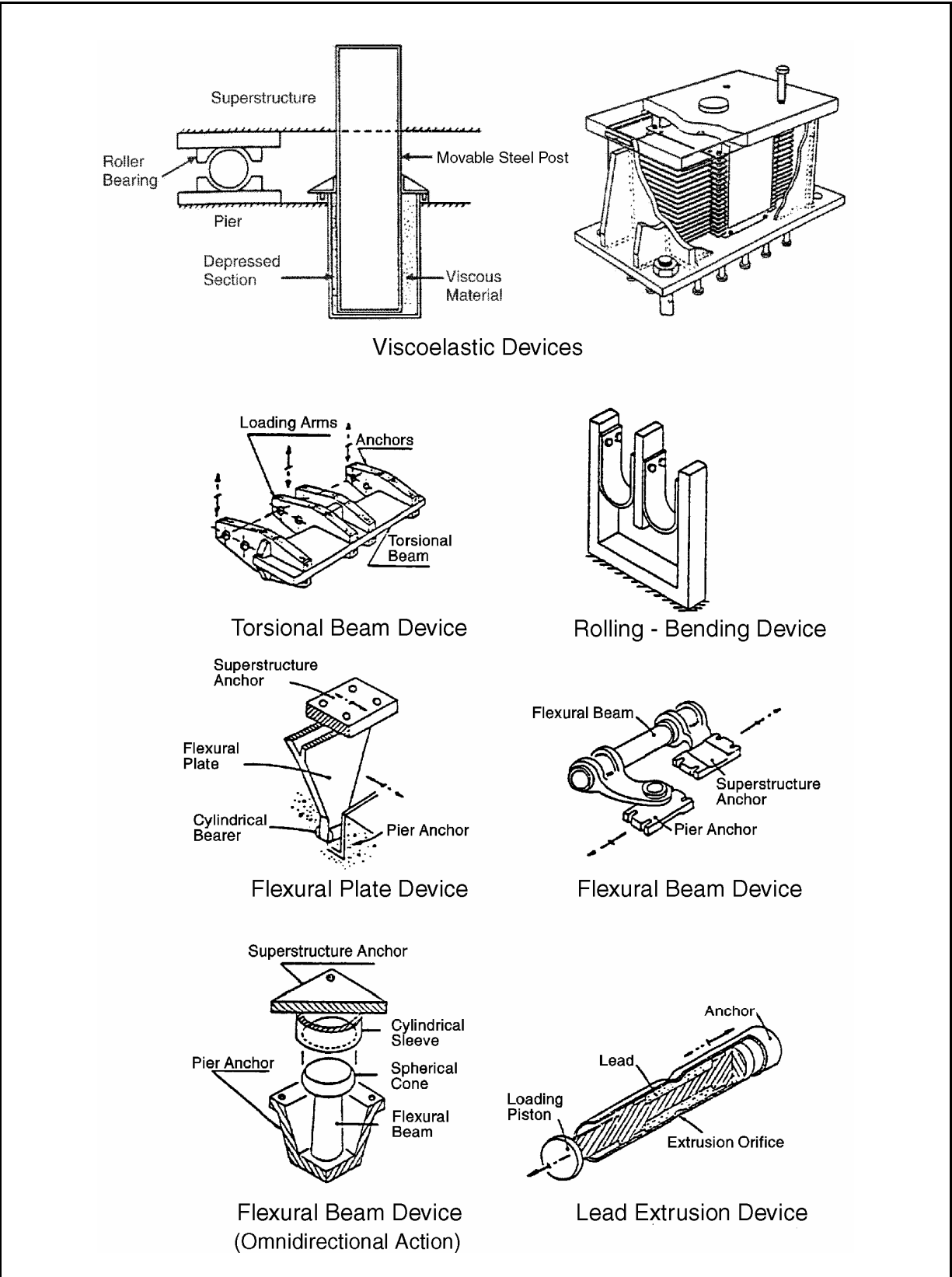
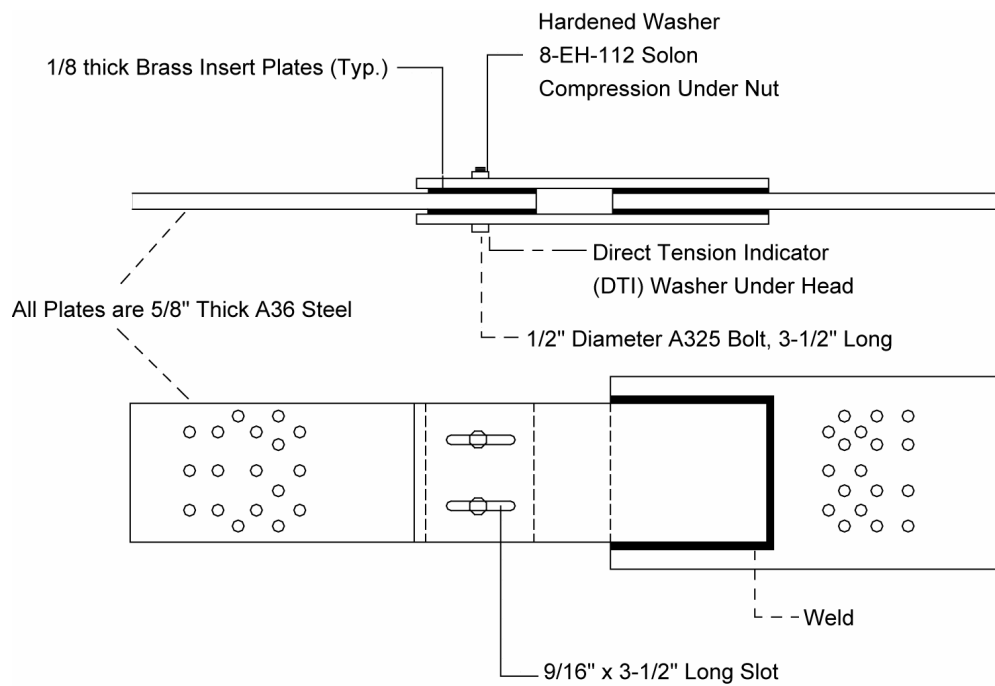
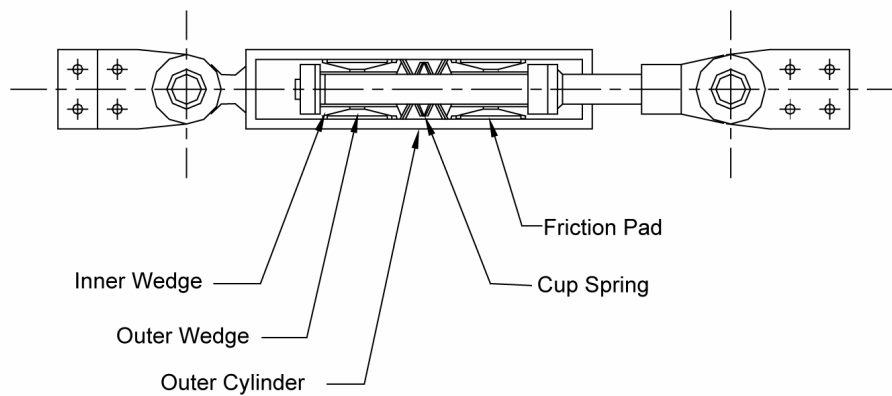


Figure 8-49. Energy dissipation devices.



Slotted Hole Friction Damper



Conical Wedge Friction Damper

Figure 8-50. Friction dampers.

CHAPTER 9: RETROFIT MEASURES FOR SUBSTRUCTURE COMPONENTS

9.1. GENERAL

Although retrofit measures for improving the seismic resistance of existing bridge substructures (columns, cap beams, and foundations) were proposed in early bridge retrofitting manuals (FHWA, 1983), very little actual work of this type was done until the 1990's. Some bridges that had been retrofitted with hinge restrainers alone failed in both the 1987 Whittier Narrows earthquake and the 1989 Loma Prieta earthquake, demonstrating the need to also retrofit the substructures of many bridges (Housner, 1990).

A significant portion of the initial column research provided insight into the effectiveness of different retrofit measures to improve both flexural and shear strength, and flexural ductility of reinforced concrete bridge columns (Chai et al., 1992). As a result, standards were developed for evaluating bridge columns and standard techniques were adopted for improving their ductility and shear resistance (Caltrans, 1996). This was accomplished by encasing reinforced concrete columns in circular or elliptical steel shells or by wrapping them with fiber composite materials. These methods were shown in the laboratory to improve flexural ductility and shear strength and to prevent the failure of starter bar splices located within potential plastic hinge zones. These methods, which have now been implemented on a large number of California bridges, proved to be effective in practice by preventing several bridge failures during the 1994 Northridge earthquake (Buckle, 1994).

The marketplace also responded to the need for column retrofitting, through the development of other retrofitting systems aimed at improving column ductility. Some of these have been successfully tested in the laboratory and have been used in retrofitting demonstration projects¹.

Caltrans' research has added to the body of knowledge about substructure retrofitting. In addition to addressing other topics related to the retrofit of reinforced concrete columns, this research has investigated the retrofitting of wall piers², bent caps³, and column footings⁴. Significant research has also been conducted by other State Departments of Transportation, and the Federal Highway Administration.

Concurrent with the relatively large amount of research relating to the seismic retrofitting of bridges, there has been a major acceleration of seismic retrofitting programs throughout the country. In California alone, this has involved the seismic evaluation and retrofitting of approximately 2,200 bridges (Roberts, 1998). Many economical and effective retrofit measures

¹ Fyfe, 1994; Seible et al., 1995; Xiao et al., 1995

² Haroun et al., 1994

³ Ingham et al., 1993; Lowes and Moehle, 1994; Thewalt and Stojadinovic, 1995; Zayati et al., 1993

⁴ Xiao et al., 1994

have been developed and implemented in the course of this work, and retrofitting techniques and procedures have been refined.

This chapter summarizes the current state of practice related to the seismic retrofitting of bridge substructures. It contains sections on bridge columns, pier caps, and column-to-cap beam joints. These components have been found to be particularly vulnerable during recent damaging earthquakes.

The use of an earthquake protective system, such as seismic isolation, might be an acceptable alternative, or supplement, to many of the approaches described in this chapter (see the overview of different retrofitting approaches in section 1.13). Note that the optimal retrofit approach for a given bridge may well be a combination of more than one measure. For example, if isolation cannot reduce the seismic demand to a level below the existing column capacity, then column retrofitting may appear to be the only option. However, the required amount of conventional retrofitting (e.g., column wrapping) may be significantly less if isolation is used, and the optimal strategy may be a combination of both measures.

9.2. RETROFIT MEASURES FOR PIERS

Reinforced concrete columns constructed before 1971 are commonly deficient in flexural ductility and shear strength. Reduced column ductility, which results in a rapid loss of flexural strength, is likely to occur when lap splices exist within potential plastic hinge zones at the base of columns. Even when starter bars are not used, inadequately confined plastic hinge zones will lose flexural strength due to the crushing of concrete and the buckling of longitudinal reinforcement. The shear strength of an inadequately reinforced plastic hinge will also degrade, leading to the potential for shear failure. If the existing reinforcement within the zone of a potential plastic hinge is adequate, or the ductility of that zone is enhanced through retrofitting, plastic hinging may still occur, but outside the intended plastic hinge zone. This may be due to premature termination of longitudinal bars, the presence of architectural flares, or the unintended stiffening effect of median barriers, sidewalks, or pavement. Designers should be aware of this possibility.

In most cases, it will not be necessary (or even desirable) to increase the flexural strength of columns, provided the ductility of the column can be assured or improved. Even though smaller seismic design loads were used in the past, adequate flexural strength often exists because of the conservatism inherent in working stress design widely used in the past. In fact, excess existing flexural strength is often undesirable because it leads to higher plastic shear forces within the column and larger foundation forces. When it is necessary to increase column flexural strength as part of a retrofit, corresponding increases in shear strength and the strength of foundations are usually required.

Wall piers usually perform better than multi-column or single-column piers during an earthquake. In most cases, sufficient horizontal and vertical reinforcement is present to withstand earthquake loading along the strong axis of the pier, although excessive forces in foundation piles may result if the wall does not yield in its strong direction. In the weak direction however, walls behave much like columns, except that these walls possess significant

ductility even when the amount of transverse reinforcement is less than that specified for a new bridge. This is particularly the case when there are no starter bar splices in the main vertical reinforcement⁵. Therefore, retrofitting of wall piers is less common than it is for conventional reinforced concrete columns.

Methods of retrofitting reinforced concrete columns include:

- Complete or partial replacement.
- Addition of supplemental columns.
- Shear or flexural strengthening.
- Improvement of column ductility.

The most popular of these methods is ductility improvement, which is possible using one or more of the following techniques:

- Steel jacketing.
- Active confinement by prestressing wire.
- Active or passive confinement by a composite fiber/epoxy jacket.
- Reinforced concrete jacketing.

Of these techniques, the steel jacket and composite fiber/epoxy jacket are the most widely used. The following sections describe these methods in greater detail.

9.2.1. REINFORCED CONCRETE COLUMNS

9.2.1.1. Column Replacement

Total or partial column replacement will require placement of temporary shoring to carry the weight of the bridge while the column is being removed and replaced. This shoring must generally be capable of resisting the horizontal loads produced by small earthquakes and, in some cases, must support live loads in addition to the weight of the bridge. In general, shoring must be capable of carrying at least 50 percent of the shear capacity of the column being removed, but not less than the shear given by 50 percent of the spectral value for the lower level event for the site (section 1.4.2 and figure 1-8).

⁵ Haroun et al., 1994; Abo-Shadi et al., 2000

9.2.1.1(a). Total Replacement

Total column replacement will sometimes be the most appropriate method for retrofitting the bridge substructure. It will usually be necessary to modify or replace both the footing supporting the column and the pier cap to which the column is connected. In fact, it is often the need to replace the foundation, or strengthen the pier cap, that mandates column replacement in the first place. Replacement should also be considered when the column is damaged or deteriorated, column flexural capacity is grossly inadequate, or where space limitations or architectural considerations preclude other retrofitting alternatives.

Column replacement was used extensively in San Francisco following the 1989 Loma Prieta earthquake (figure 9-1). Some of these columns were damaged during the earthquake, but most were replaced as part of a seismic upgrading program for these structures. Because of a lack of alternative routes and the fact that many of these structures were two-level viaducts, carefully designed shoring systems were required to avoid interference with traffic.

A key issue in column replacement is the connection of the column to the existing structural members. An example of a column replacement illustrating this point is shown in figure 9-2. Note that the existing column steel was left in place and allowed to extend into the new column, thus forming a moment-resistant connection with sufficient ductility to withstand large earthquake loads. Anchoring column reinforcement by drilling and grouting is not desirable unless a considerable embedment length is provided. This method should be used with caution when the reinforcement will be subjected to several cycles of loading beyond the yield strain of the steel. It may be possible to add new 'headed' reinforcement in the column by drilling through connecting members such as pier caps. In this case, the headed steel is anchored on the opposite side of the column, as shown in figure 9-3. In all cases, the structural adequacy of the pier cap-to-column joint must be considered.

When a concrete column is replaced below an existing bridge, it will usually be necessary to create a seal between the top of the column form and the soffit of the pier cap so that concrete can be placed under pressure, thus assuring full contact between existing and new concrete. It may sometimes be necessary to provide cored vent holes in the overlaying member to prevent the formation of air pockets. Roughening of the concrete contact surface is also recommended.

9.2.1.1(b). Partial Column Replacement

Partial column replacement involves the removal of surface concrete in the region of the potential plastic hinge zone. The main vertical column reinforcement is cut and replaced by machined 'fuse bars' that are, in turn, connected to the existing main steel outside of the plastic hinge zone (see figure 9-4). The connection is made by welded splice plates to which threaded couplers are welded so that the fuse bars can be replaced in the future. This requires knowledge of the weldability of the existing reinforcement so that the correct welding procedures can be developed. The connections are designed to assure that yielding occurs in the fuse bars. The new hinge is then wrapped with high strength cable to provide the necessary confinement. High performance concrete is then used to cover the fuse bars and cable. The procedure is described in greater detail in example 9-1.

EXAMPLE 9.1: REPLACEABLE HINGE

A column plastic hinge zone with lap splices is to be retrofitted with a replaceable hinge constructed with high strength fuse bars that can be removed and replaced after an earthquake.

Connector plates are welded to the existing longitudinal rebar such that each connector plate engages two existing rebar. This is done on the starter bars in the footing and on the column bars. Threaded studs are welded to the plates, to which threaded couplers are attached. Machined fuse bars are connected between the threaded studs by means of the couplers.

The existing column is 1.22 m (4 ft) in diameter with 50 mm cover and contains 20 #35 (metric) (#11, cus) reinforcing bars. The concrete strength is 35 MPa (5000 psi) and the yield stress of the reinforcing steel is 276 MPa (40 ksi). Fuse bars are made of steel that has a yield stress of 855 MPa (124 ksi) and an ultimate strength of 990 MPa (144 ksi). The structure has a longitudinal period = 0.7 seconds.

Calculate the fuse bar area and length, size of connector plate, and transverse reinforcement details.

STEP 1. DETERMINE FUSE BAR AREA

To assure that the fuse bars yield before the existing main reinforcing bars:

$$d_f < d_b \sqrt{\frac{2f_y}{f_{su}}} = 0.035 \text{ m} \sqrt{\frac{2(276)}{990}} = 0.035(0.747) = 0.026 \text{ m} \quad (1.0 \text{ in})$$

Therefore, the fuse bars will be machined to a diameter of 26 mm (1 in).

STEP 2. DETERMINE FUSE BAR LENGTH

The length of the fuse, L_f , is determined so that steel strains remain below levels that will result in low cycle fatigue during the design earthquake (Dutta and Mander, 1998). Therefore:

$$L_f = \frac{\theta_p}{0.16} D' (2N_f)^{0.5}$$

where

θ_p = plastic hinge rotation determined from an analysis; in this case assume $\theta_p = 0.03$

D' = distance between extreme tension and compression bars = (Diameter – cover – spiral ties – $\frac{1}{2} d_b$)

$$= 1.22 \text{ m} - 2(0.05 + 0.019 + 0.018 \text{ m}) = 1.046 \text{ m}$$

N_f = effective number of cycles imposed by the seismic event $\approx \frac{7}{\sqrt[3]{T}}$ where in this case $T = 0.7 \text{ sec}$.

$$N_f \approx 8$$

Therefore:

$$L_f = \frac{0.03 \text{ rad}}{0.16} 1.046 \text{ m} (2[8])^{0.5}$$

$$= 0.785 \text{ m} \quad (31 \text{ in}) \Rightarrow 0.8 \text{ m} \quad (31.5 \text{ in})$$

STEP 3. DETERMINE SIZE OF CONNECTOR PLATE AND WELD

For E70XX electrodes and a 4.8 mm (0.19 in) weld size:

$$l_w = 0.56 \frac{d_f^2}{s_w} \frac{f_{su}}{217} = 0.56 \frac{0.026^2}{0.0048} \frac{990}{217} = 0.327 \text{ m} \quad (13 \text{ in})$$

Based on AISC LRFD, the minimum plate thickness is:

$$t_{\text{plate}} = \text{size of weld} + 1.6 \text{ mm} = 4.8 \text{ mm} + 1.6 \text{ mm} = 6.4 \text{ mm} \quad (0.25 \text{ in})$$

STEP 4. DETERMINE TRANSVERSE REINFORCEMENT

For concrete confinement:

ρ_s = effective volumetric ratio

$$\rho_s = 0.008 \frac{f'_c}{U_{sf}} (12) \frac{P_e}{f'_c A_g} + \rho_t \frac{f_y}{f'_c} \left(\frac{A_g}{A_{cc}} \right)^2 - 1 \quad \text{where } \rho_t = \frac{A_s}{A_g} = 20 \frac{(0.000962 \text{ m}^2)}{1.17 \text{ m}^2} = 0.0164$$

$$\rho_s = 0.008 \frac{35}{110} (12) \frac{4.45}{35(1.17)} + 0.00455 \frac{855}{35} (0.735)^2 = 0.0011$$

For antibuckling:

$$\rho = 0.025 \frac{D}{s} \frac{s}{d} \rho \frac{f}{f} = 0.025 \left(\frac{1.22 \text{ m}}{0.026 \text{ mm}} \right) \frac{1.22}{0.026} \cdot 0.00455 \left(\frac{855}{1489} \right) = 0.0031$$

For shear resistance:

$$\rho_s = 0.75 \Lambda \frac{\rho_t}{\phi} \frac{f_{su}}{f_{yh}} \frac{A_g}{A_{cc}} \left[1 - \left(\frac{0.65 - P_e / \phi f'_c A_g}{0.65 + 1.2 \rho_t f_{su} / f'_c} \right) \right]$$

$$= 0.75(1.0) \frac{0.00455}{0.85} \frac{990}{1489} \cdot 0.735 \cdot 0.351 = 0.0007$$

Antibuckling therefore controls, and $\rho_s = 0.0031$. This requires 13 mm (0.5 in) strand @ 100 mm (4 in) spacing.

LEGEND

- (A) Lower bent (pier) cap retrofit
- New prestressed concrete beam
- (B) Column replacement
- Remove existing columns and construct new reinforced concrete column
- (C) New "super" girder (see Fig. 9-37)
- (D) Footing retrofit or replacement
- (E) Barrier replacement
- (F) Upper bent cap retrofit
- New prestressed concrete beam
- (G) New concrete diaphragm overlays

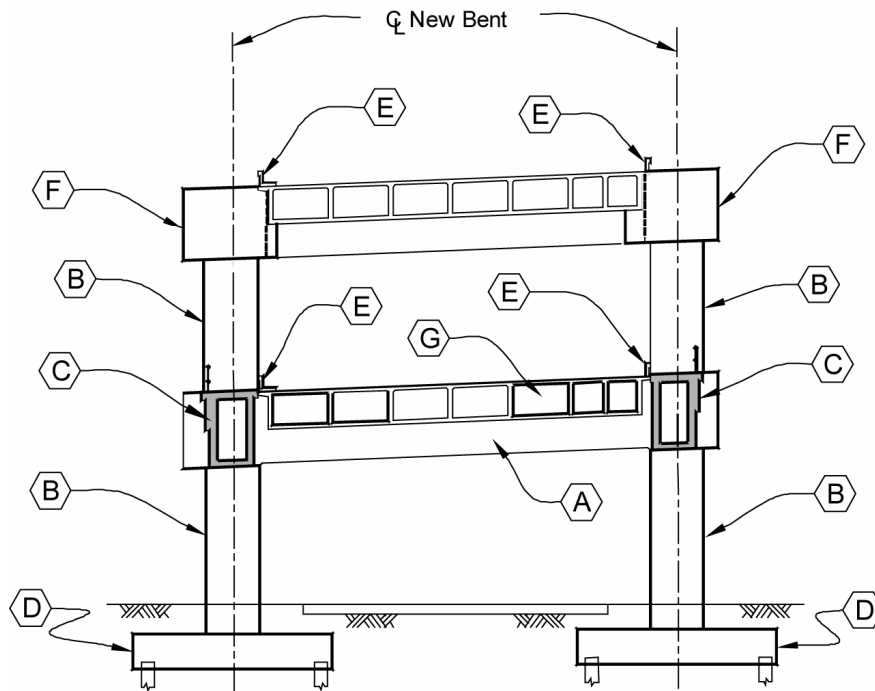


Figure 9-1. Column replacement on San Francisco viaducts.

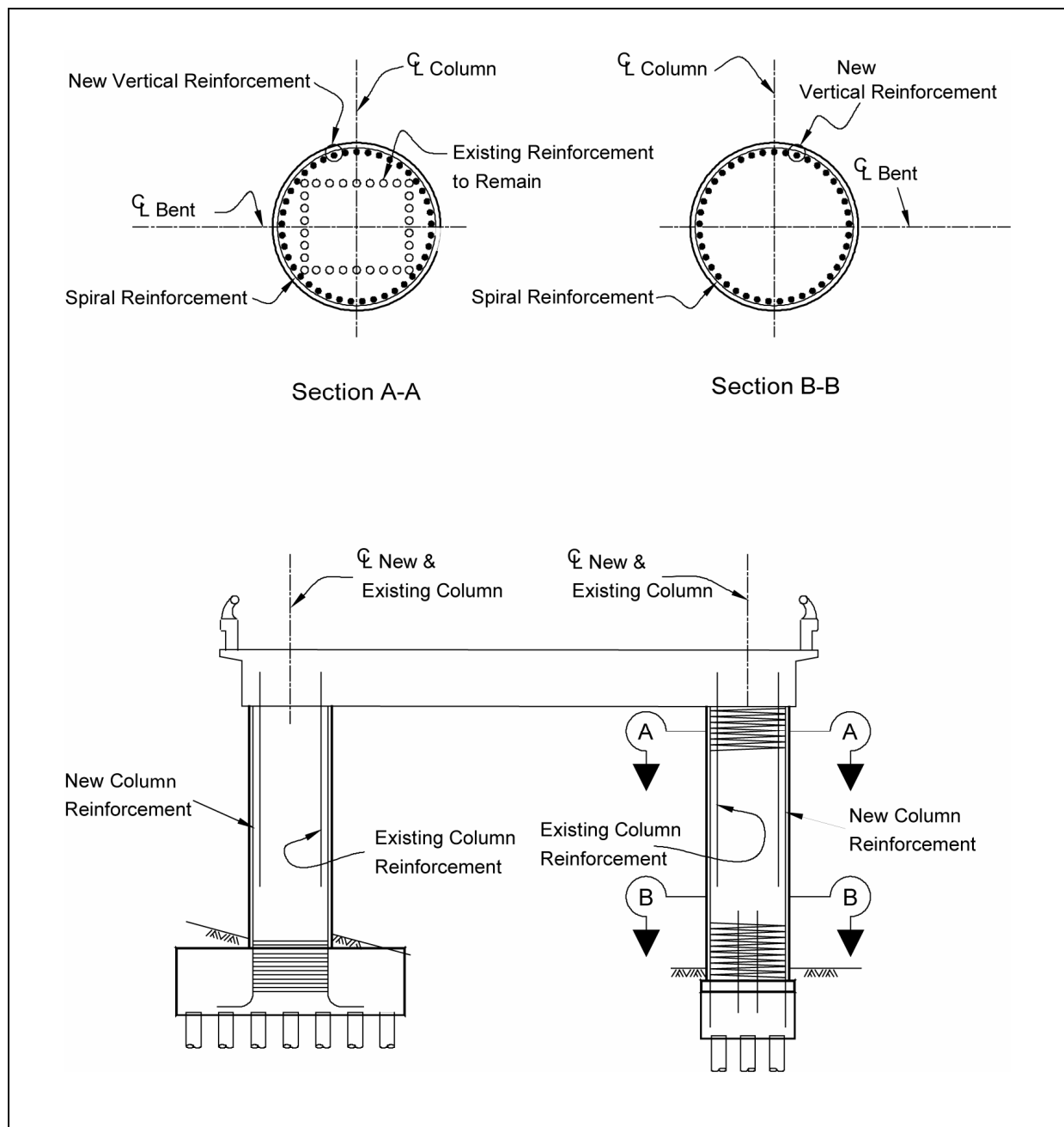


Figure 9-2. Column replacement using existing column reinforcement.

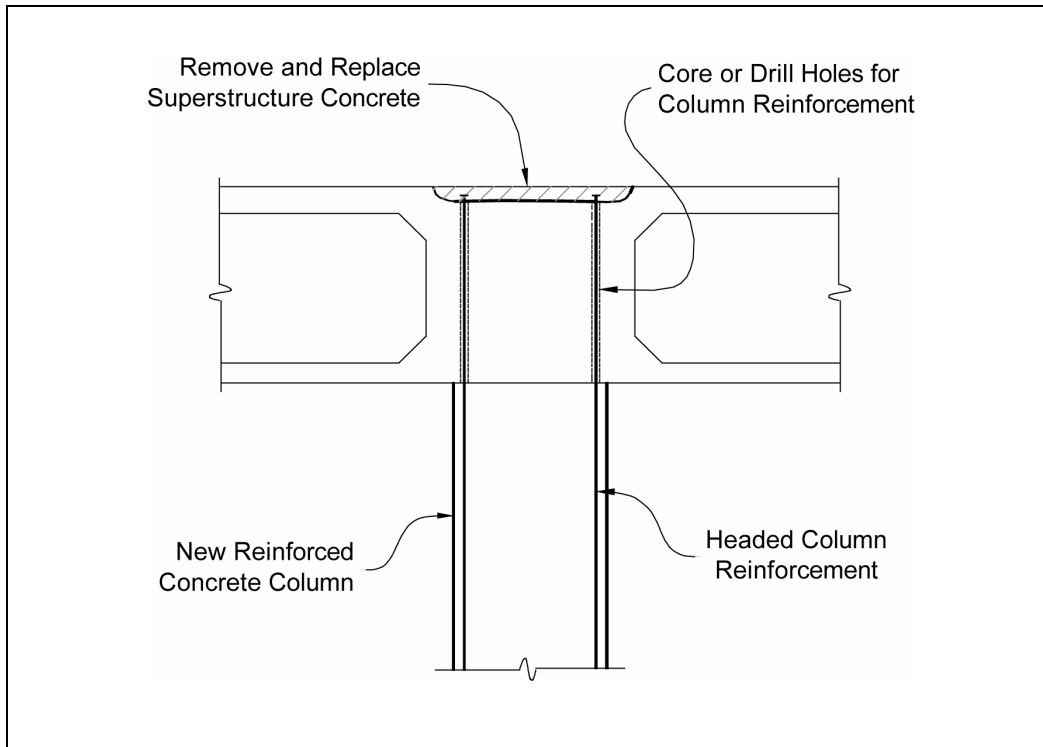


Figure 9-3. Column anchorage using headed reinforcement.

This retrofit method is intended to provide ductile response during an earthquake while effectively protecting other structural components. Capacity design principles (see Chapter 5) are employed to assure yielding in the fuse bars before damage occurs elsewhere in the column. The method has the advantage that the fuse bars are replaceable following an earthquake. An alternative design approach, in which these replaceable hinges are constructed as part of new precast columns, has also been proposed.

9.2.1.1(c). *Supplemental Columns*

New supplemental outrigger columns to provide ductile resistance to horizontal loads have also been used when space is available, or when column replacement, with its required shoring, is an undesirable solution. These columns are usually tied into existing or new pier caps. This is accomplished by welding or mechanically splicing to existing pier cap reinforcement, or by prestressing through concrete overlays tied to the sides of existing pier caps. Because of the potential for introducing high torsion forces into these pier caps, supplemental outrigger columns are often ‘pinned’ at the top to minimize moment transfer.

Another design issue is displacement compatibility between the existing columns, which must continue to support the weight of the bridge, and the new, more ductile, supplemental columns. This often requires that existing columns be retrofitted to preserve a column’s vertical capacity, as described in section 9.2.1.5. An example of a retrofit using supplemental columns is shown in figure 9-5.

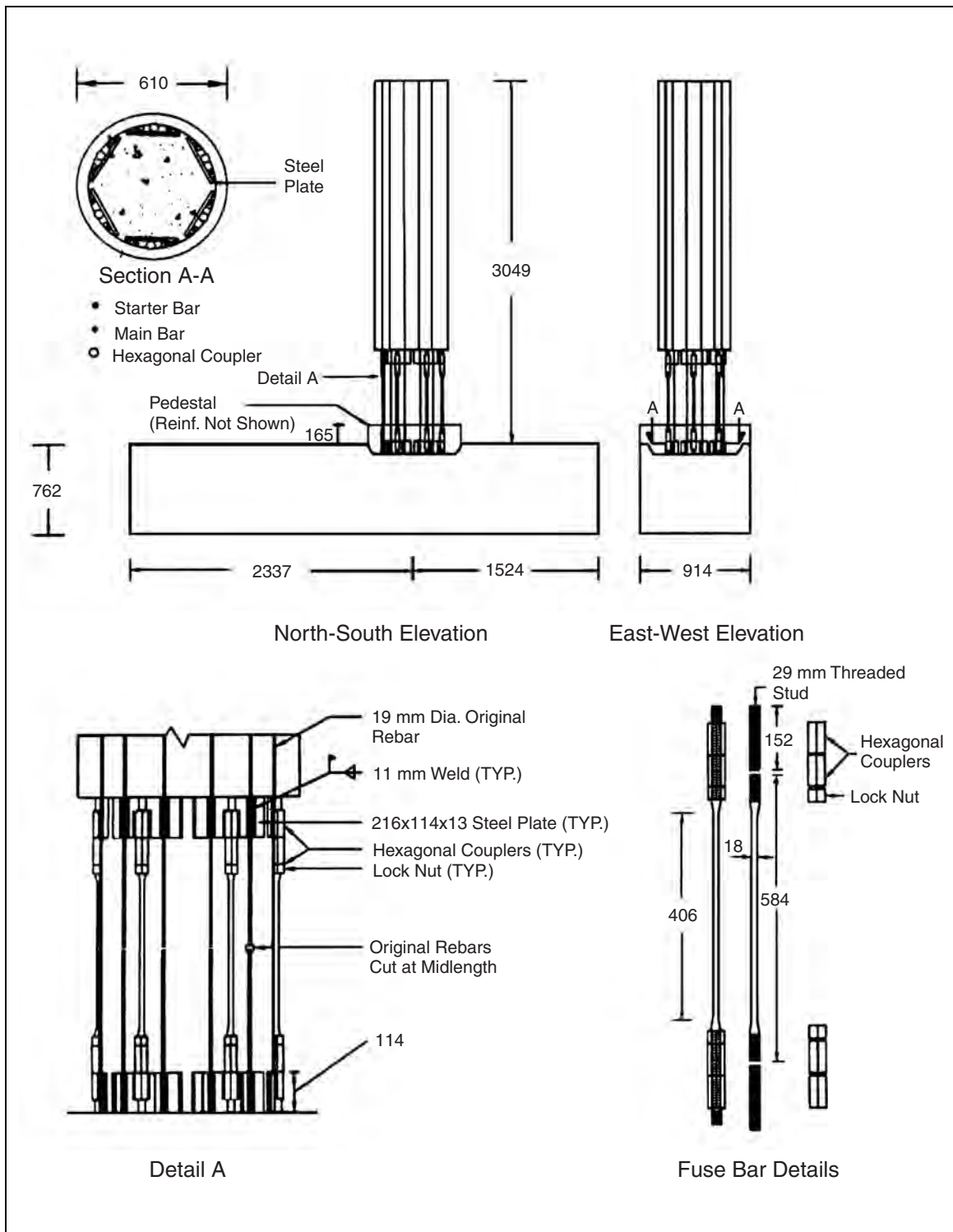


Figure 9-4. Replaceable plastic hinge with fuse bars.

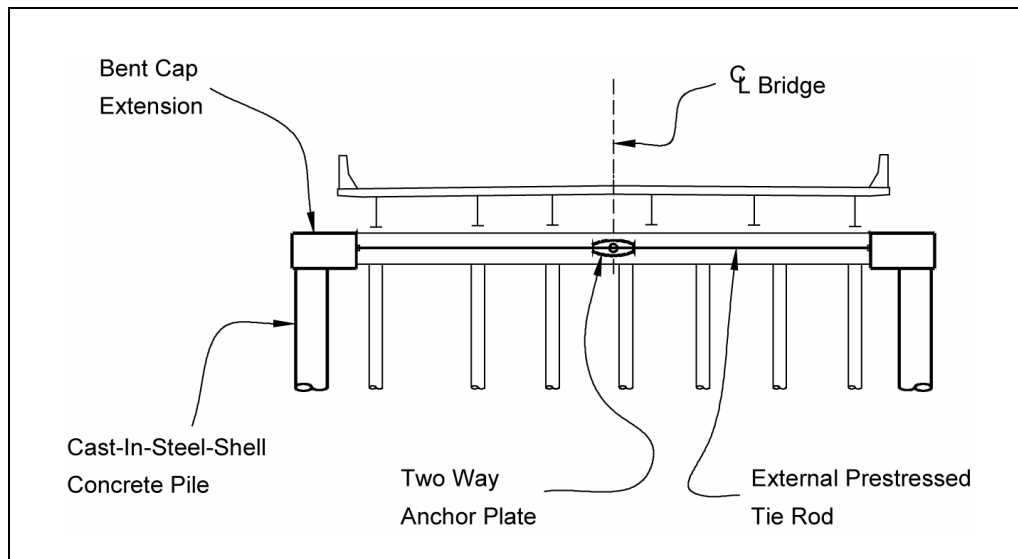


Figure 9-5. Supplemental column retrofit.

9.2.1.2. Column Flexural Strengthening

In general, it is not necessary or even desirable to increase the flexural strength of a reinforced concrete bridge column. Increased column strength results in increased shear capacity, which in turn attracts increased forces to foundations and pier caps. However, it will occasionally be necessary to increase the flexural strength of a column. For example, increasing column strength at a lap splice in the reinforcement will force the plastic hinge to form in a region of the column away from the splices.

Three methods for increasing column strength are discussed below.

9.2.1.2(a). Concrete Overlays

Applying full or partial height concrete overlays to the face of an existing column can increase a column's flexural strength. A sufficient number of dowels must be provided for shear transfer between the overlay and the existing column and a roughened contact surface can also help in this regard.

The extra concrete itself will add some flexural strength because of the increased moment arm between the vertical column reinforcement and the compression block in the new concrete. To provide additional flexural strength, it will be necessary to add vertical reinforcement in the overlays. The additional reinforcing steel must be anchored into existing structural members, which presents some of the same problems encountered with column replacement. It may be possible to anchor this reinforcing into newly constructed portions of the pier cap or footing, or use the headed reinforcement approach discussed earlier and shown in figure 9-3.

The flexural ductility of concrete overlays is also an issue. This is most easily and effectively done when the existing column is circular or nearly circular in cross-section. Providing

continuous transverse hoops that are connected with mechanical couplers will generally provide sufficient confinement for ductility. When the column cross-section is rectangular, closed ties will effectively support only the corner bars and it will be necessary to provide lateral support for other bars by drilling and grouting adequate transverse reinforcement through the existing column. In designing this transverse reinforcement, due consideration should be given to its anchorage and its effectiveness in providing confinement. An example of column flexural strengthening by concrete overlays is shown in figure 9-6. This retrofit method is discussed further in section 10.3.2

9.2.1.2(b). Added Reinforcement in Conjunction with Steel Shell

The strength of an existing column can also be increased by adding extra longitudinal reinforcement in the grout space between a steel shell and the column. This will require adequate shear transfer between the grout and the existing column, which can generally be assured by roughening the existing concrete surface or providing drilled and grouted dowels on the surface of the existing column. A detail of an application of this retrofit method is shown in figure 9-7. In this case, a pinned column base was made fixed through this technique. Most of the additional column steel was anchored into a newly cast concrete footing, but some was anchored by drilling and grouting into the existing footing concrete. If the new steel is anchored into existing concrete, it is necessary to provide sufficient embedment length to assure that the reinforcement can achieve high levels of plastic strain.

9.2.1.2(c). Composite Steel Shell

A steel shell can also contribute to flexural strength if sufficient shear transfer is provided between the shell and the grout. This is done by coating the inside of the steel shell with an epoxy adhesive impregnated with grit. Steel shear rings, on the inside of the shell, consisting of welded reinforcing bar hoops, steel bars, or weld beads can also be used for this purpose. High strength adhesives can be used to bond steel plates to the surface of the existing column. Because it is difficult to develop full flexural capacity at the ends of these shells or overlays, this retrofit method is best used to force yielding of the rebar to occur away from a vulnerable column region, such as at a splice location or where reinforcing steel has been prematurely terminated.

Some development of strength at the ends of steel shells is also possible. Anchor bolts may be used to connect the steel shell at the base of a column to the footing. Tests have demonstrated the effectiveness of this retrofitting technique for increasing both flexural strength and ductility, and have shown that flexural yielding of the anchor plate was an efficient means of dissipating energy, provided that the anchor bolts themselves could be capacity-protected. A detail of this retrofit method is shown in figure 9-8.

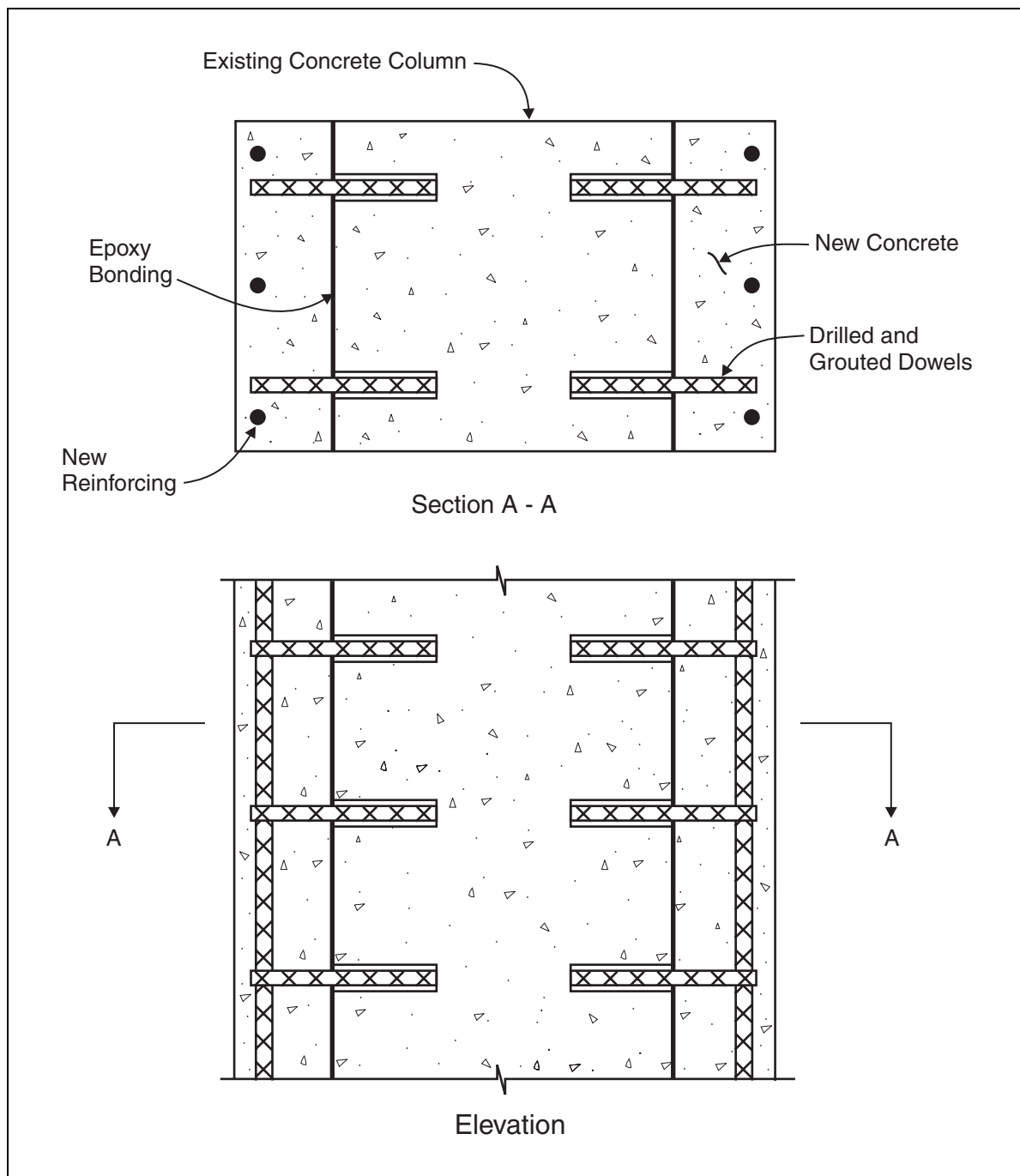


Figure 9-6. Column strengthening by concrete overlay.

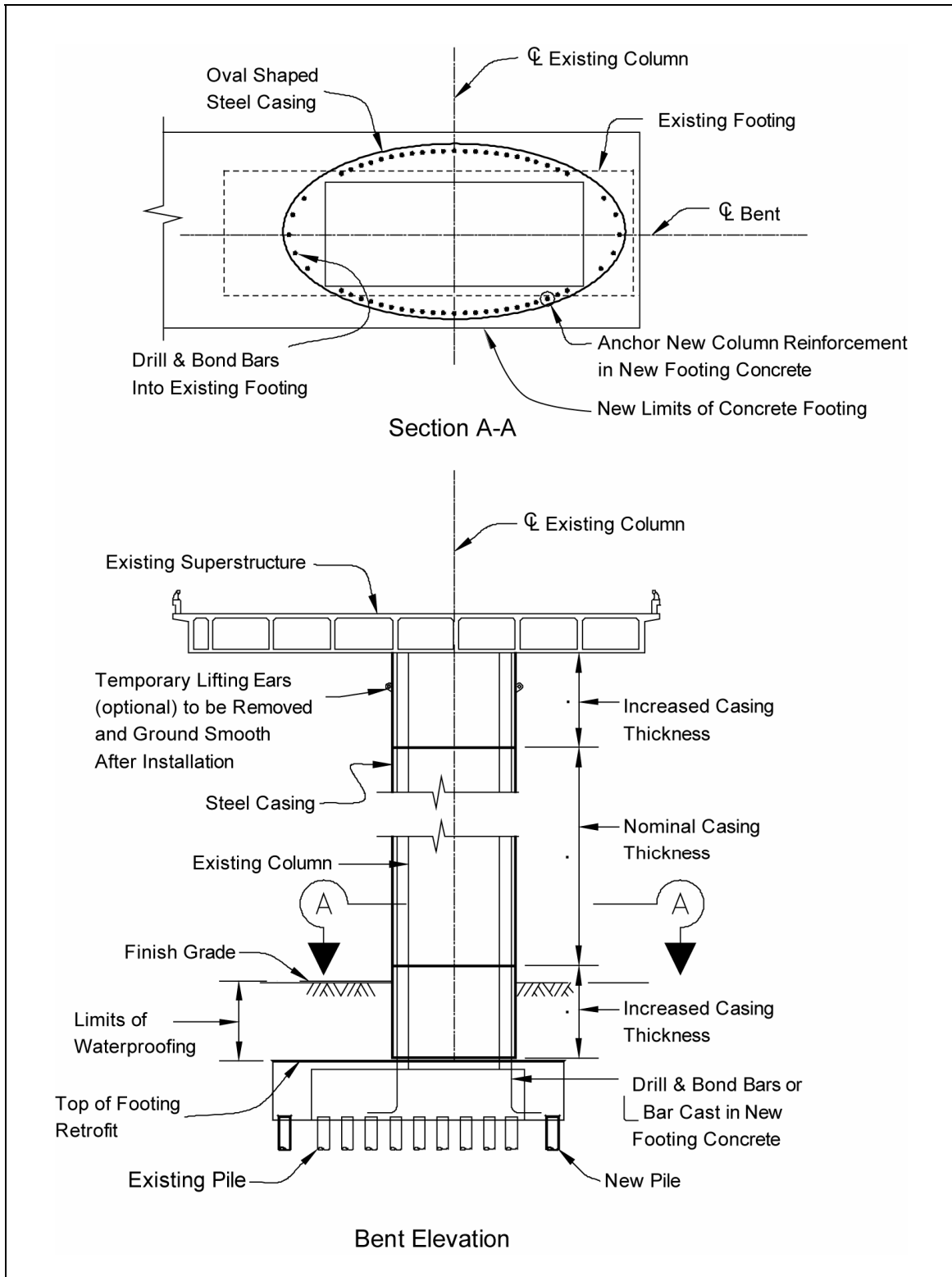


Figure 9-7. Column strengthening by adding reinforcement within steel shell.

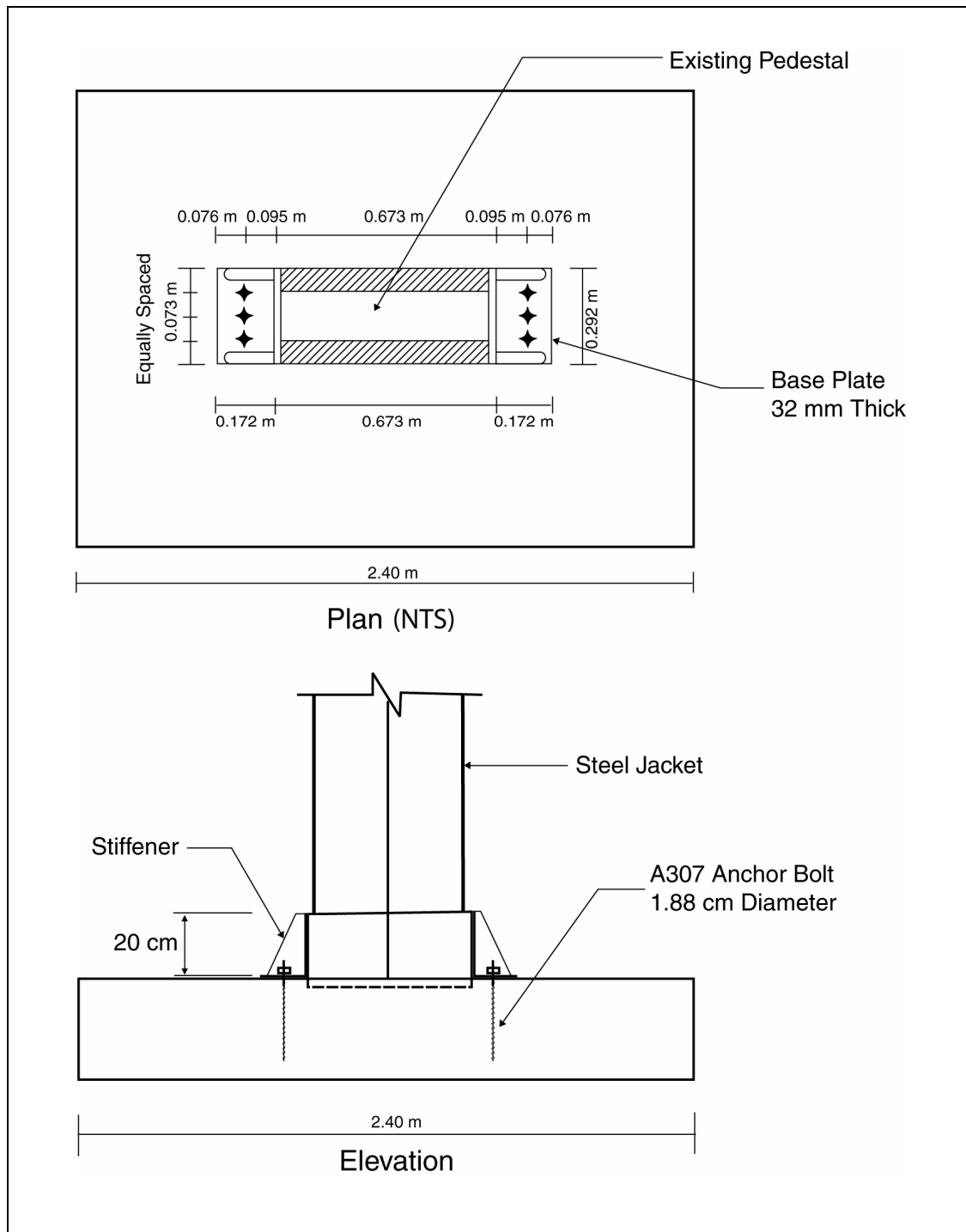


Figure 9-8. Column strengthening by anchoring steel shell.

9.2.1.3. Column Ductility Improvement and Shear Strengthening

One of the principal reasons for the low ductility of existing reinforced concrete columns was the practice of using starter bars at the base of columns where plastic hinges are likely to form. Failure in the splice between the starter bars and the longitudinal reinforcement generally occurs when the concrete surrounding the reinforcing bars splits due to radial stresses that are produced as the deformed bar tries to pull out of the concrete socket into which it is cast. Once split, the concrete socket dilates and allows the bar to pull free. Tests have indicated that the critical radial dilation strain, ϵ_d , is on the order of 0.001 for splice lengths of $20 d_b$ and reinforcement yield strengths of 276 MPa (40 ksi). If the column has enough confinement at a radial strain of 0.001, then splice failures can be prevented. Because existing columns usually have either insufficient or poorly detailed transverse reinforcement that cannot reliably provide this level of confinement, it is necessary that a retrofit method be employed to do so. The required level of confinement stress, f_ℓ , is given by Priestley and Seible, 1991, as:

$$f_\ell \geq \frac{A_b f_y}{\left(\frac{\pi D'}{2n} + 2(d_b + c) \right) \ell_s} \quad (9-1)$$

where d_b is the diameter of spliced longitudinal bar, A_b is the area of spliced longitudinal bar, f_y is the yield stress of splice longitudinal bar, D' is the diameter of the pitch circle of the main column reinforcement, N is the number of main column reinforcing bars, c is the cover over these bars, and ℓ_s is the splice length.

Equation 9-1 assumes that no slippage of the splice will occur when the stress in the main reinforcing steel is less than $1.4 f_y$, which is typically the ultimate stress for this steel. The splice length must be at least long enough to prevent the shearing of concrete between bar deformations, which can also cause a splice bar to pull out. Extra confinement cannot prevent this type of failure. The minimum splice length required is:

$$\ell_s \geq \frac{0.25 d_b f_y}{\sqrt{f'_c}} (\text{MPa units}) = \frac{0.021 d_b f_y}{\sqrt{f'_c}} (\text{psi units}) \quad (9-2)$$

Flexural retrofit measures should extend from the critical section to the location where the moment has decreased to 75 percent of the maximum moment, but not less than a distance equal to the column diameter. The higher level of confinement required for lap splices needs to be provided only over the length of the lap splice.

A relaxation of the requirements of equation 9-1 is allowed if slip is permitted at moderate displacement ductilities. In this case, the maximum tensile stress in the reinforcement could be assumed to be $1.0 f_y$, which assumes no strain hardening of the longitudinal reinforcement. Bond slip will occur at moderate ductilities (typically in the range of three to five), but the constant confining stress will provide a rather ductile response with only gradual degradation of performance as a result of dependable friction across the displacing surfaces of the fracture

plane. The required confining stress would then be 28.5 percent less than that given by equation 9-1, where the value 0.285 is calculated from $(1.4 - 1.0)/1.4$.

The ductility of existing columns is less than that of new columns even if there are no starter bar splices near the footing. Excessive flexural deformations in a plastic hinge will subject concrete and steel to excessive levels of strain. When concrete strains reach a level of about 0.005, cover concrete begins to spall. When this occurs, inadequate or poorly detailed transverse column reinforcement will be subjected to increased stresses, which may cause ties, hoops, and discontinuous spirals to stretch, slip, or pull free from the column, thus becoming ineffective in providing passive confinement of the column core. This in turn will cause the column core concrete to crush and vertical reinforcing steel to buckle. Eventually, the core concrete will fracture badly and lose its capacity to resist axial, flexural, and shear forces. When this occurs, the column will disintegrate and collapse of the bridge may occur.

Retrofitting will probably affect a column's elastic (cracked-section) stiffness, and this should be taken into consideration when analyzing the bridge for design forces. For a steel jacket retrofit, average increases in stiffness between 10 and 15 percent for a partial height retrofit and 30 percent for a full height retrofit may be expected (Priestley and Seible, 1991). External prestressed confinement steel and fiber composite jacket retrofits have a negligible influence on the column stiffness (Wipf et al., 1997).

9.2.1.3(a). Steel Jacketing

This technique was originally developed for circular columns, as shown in figure 9-9 and is currently the preferred method used by Caltrans for the seismic retrofits of bridge columns (Caltrans, 1996). Two steel plate half-shells, which have been rolled to a radius equal to the column radius plus 13 to 25 mm (0.5 to 1 in) for clearance, are positioned over the portion of the column to be retrofitted, and the vertical seams are then welded. The gap between the jacket and the column is grouted with a pure cement grout, after flushing with water. A vertical space of about 50 mm (2 in) is typically provided between the end of the jacket and any supporting member (i.e., the footing or cap beam) to avoid the possibility of the jacket acting as compression reinforcement by bearing against the supporting member at large drift angles. Significant increases in flexural strength are possible from this source, which may then result in undesirable overload of the adjacent members.

The construction and fabrication procedures typically used for steel jackets place constraints on their design. Limitations on handling stresses require that the shells have a minimum thickness of 10 mm (0.375 in), and restrictions on bending thick plates require a maximum thickness of 25 mm (1 in) (Caltrans, 1996).

A steel jacket is effective as passive confinement, but confinement is not provided until the radial expansion of the concrete column induces circumferential stresses in the steel shell. This radial expansion occurs as a result of bulging caused by high axial compression strains in the concrete and dilation around longitudinal reinforcement caused by vertical cracking near the bar splices. Similar radial dilation occurs with the development of diagonal shear cracks in the concrete of the column.

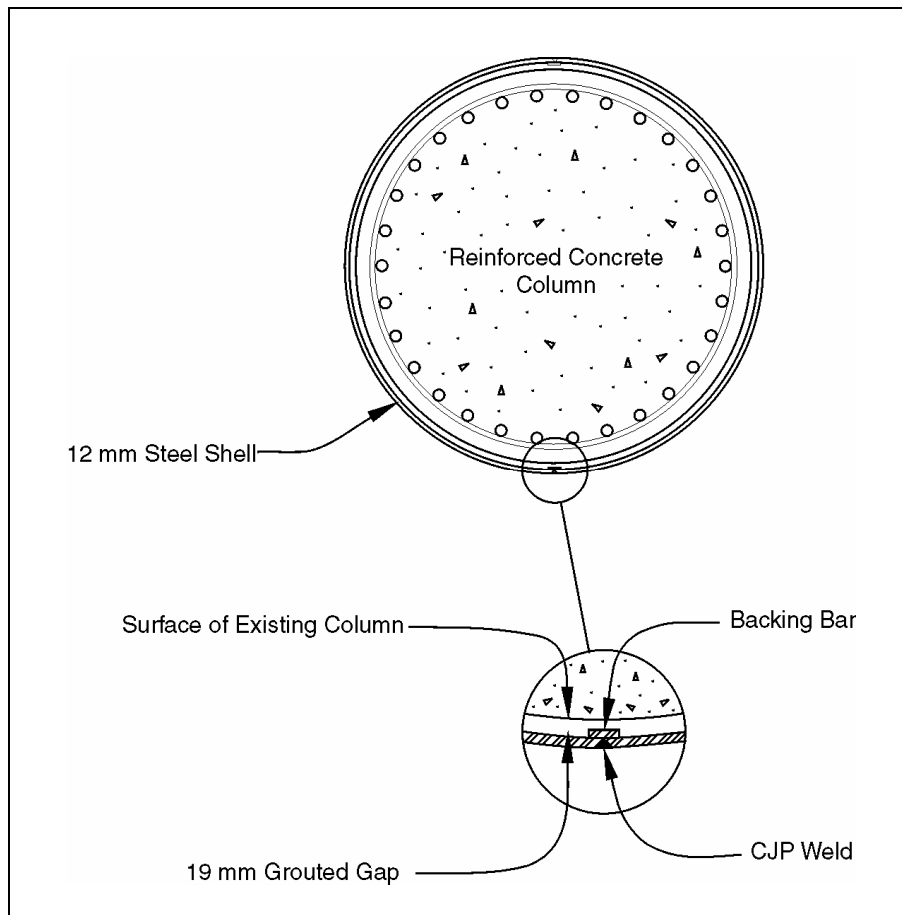


Figure 9-9. Typical steel shell retrofit of round column.

For rectangular columns, the recommended procedure is to use an oval jacket, which provides continuous confining action similar to that for a circular column. Because of increased space between the shell and the existing column, small sized aggregate is added to the grout that is placed in the gap between the column and the shell, as shown in figure 9-10. Rectangular columns retrofitted in this manner perform very well in flexure and shear. Attempts to retrofit rectangular columns with rectangular jackets have been less successful, even when the jackets have been extensively stiffened. This is because the confining action of the rectangular jackets can only be developed as a consequence of lateral bending of the jacket sides, which is a very flexible action, compared to the membrane action developed in an oval or circular jacket. However, if the radius of a portion of the oval is very large, it may be necessary to stiffen it with braces or to support it at interim locations with bolts drilled through the column, which will help achieve the required confinement.

Rectangular steel jackets are effective in enhancing the performance of 'shear critical' columns. These jackets can improve column ductility by eliminating the brittle shear mode of failure, but the failure mode may then shift to a flexural one for which the rectangular jacket can provide only limited assistance, for the reasons described above.

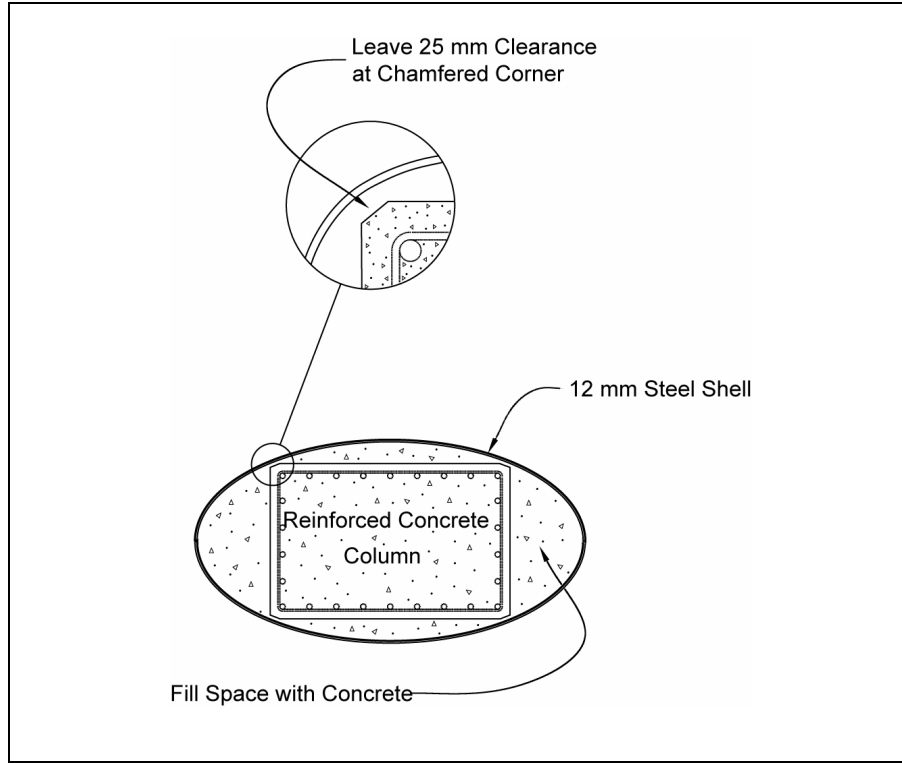


Figure 9-10. Typical steel shell retrofit of rectangular column.

The designer should also consider the potential distortion of a steel shell due to the hydrostatic pressures created as concrete is poured into the space between the shell and the column. This is particularly important for large oval-shaped shells placed around rectangular columns. Because the clearances between the shell and existing concrete at the corners of the column are small and may prevent the flow of the concrete, it may be necessary to provide grouting ports at all four lobes of the ellipse and to require that the concrete be placed in nearly equal lifts.

Performance of Lap Splices – For a circular column, the required confinement stress, f_ℓ , can be related to the characteristics of this retrofit concept by reference to figure 9-11, which shows a free body diagram of a half-column section. Equilibrium requires that:

$$2 t f_s = f_\ell D \quad (9-3)$$

where t is the steel jacket thickness, f_s is the stress induced in the jacket, and D is the diameter of the column.

For a steel modulus of elasticity E_s , equal to 200 GPa (29,000 ksi), f_s will be 200 MPa (29 ksi) at a strain of 0.001. Substituting this result into eq. 9-3 and rearranging terms gives the following:

$$t \geq \frac{f_\ell D}{2 f_s} = \frac{f_\ell D}{400} (\text{mm}) = \frac{f_\ell D}{58} (\text{in}) \quad (9-4)$$

where the confinement stress, f_ℓ , is expressed in MPa or ksi, as appropriate.

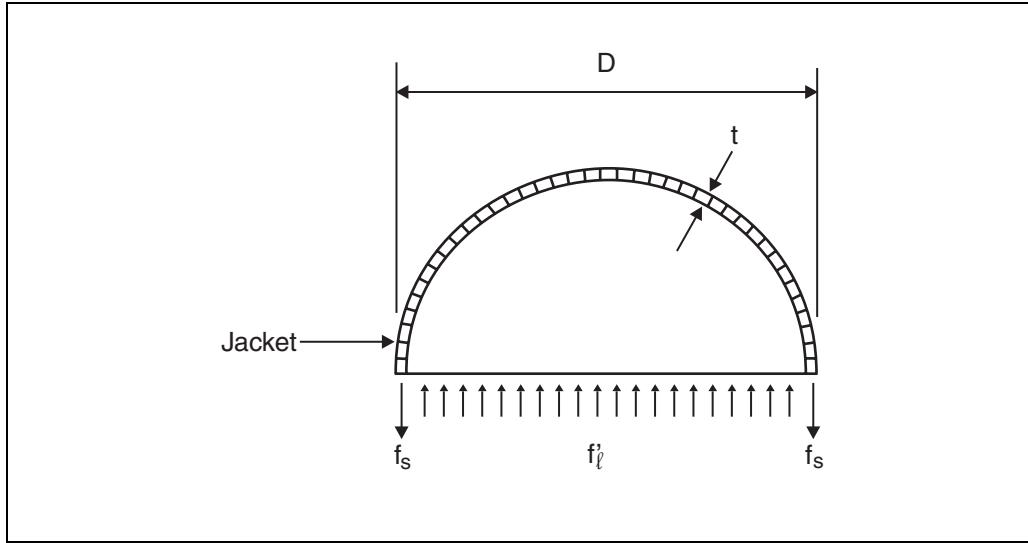


Figure 9-11. Free body diagram of column retrofitting with a steel shell.

Equation 9-4 may be simplified by assuming that f_t is approximately 2.07 MPa (300 psi), which is the value used in the development of this method (Chai et al., 1991). This assumption will provide satisfactory performance where volumetric ratios of longitudinal reinforcement are less than 2.5 percent and axial loads, P , are less than $0.15f'_cA_g$.

Columns satisfying the above requirements will sustain drift angles of four percent with an adequate reserve of displacement capacity. Such retrofitting generally provides sufficient ductility to allow the retrofitted column to be designed using a response modification (R-factor) method. In this case, R-factors of four for single column piers, and six for multi-column piers, may be used. Higher R-factors can be justified in some cases (Caltrans, 1996).

Flexural Confinement – Increasing flexural confinement by retrofitting is often done by simplified means that yield conservative results. For example, only 83.3 percent of the steel shell thickness given by equation 9-4 is needed when lap splices are not present. This corresponds to a passive confinement of 1.72 MPa (250 psi) at radial strains of 0.001. The R-factor approach described above is then used for columns retrofitted in this manner.

A more rigorous and less conservative design approach relies on determining material strains that will occur under seismic loading, and then designing the steel shell to provide the confinement necessary to achieve these strain levels. By equating the strain energy in confined concrete to the strain energy in the confining steel, it is possible to determine ultimate strains in the concrete based on the ultimate achievable strains in the confining steel (Mander et al., 1988). Applying this principle to a circular steel shell of constant thickness, t , leads to the following equation for ultimate concrete strain capacity:

$$\epsilon_{cu} = 0.004 + \frac{5.6tf_{ys}\epsilon_{su}}{Df'_{cc}} \quad (9-5)$$

where f_{ys} is the yield stress in the shell steel, ϵ_{su} is the ultimate strain in the shell steel (a value of 0.10 is recommended for A36 steel), D is the diameter of the steel shell, and f'_{cc} is the ultimate confined concrete stress capacity.

The value of f'_{cc} can be related to the lateral confinement stress, which equation 9-3 shows is related to the shell thickness, t .

Therefore:

$$f'_{cc} = f'_c \left(-1.254 + 2.254 \sqrt{1 + \frac{15.88 t f_s}{D f'_c}} - \frac{4 t f_s}{D f'_c} \right) \quad (9-6)$$

By reorganizing equation 9-5 and solving for the shell thickness, t :

$$t \geq \frac{(\epsilon_{cu} - .004) D f'_{cc}}{5.6 f_{ys} \epsilon_{su}} \quad (9-7)$$

Equation 9-7 is solved for t for known values of ϵ_{cu} and f'_{cc} . An initial, but conservative, value for t may be obtained by assuming concrete strain demands of 0.02 and confined concrete stress demands of $1.7 f'_c$.

Once an initial value for t is determined, a more accurate value of ϵ_{cu} for a given earthquake response can be determined using a computer program to perform moment-curvature analysis of the retrofitted section. This analysis relates concrete and reinforcing steel strains to various degrees of plastic curvature of the column. Several computer programs are commercially available for this purpose. This analysis also allows the development of a simplified inelastic moment-curvature relationship for use in an inelastic static analysis. In this analysis, the frame containing the subject column(s) is incrementally deformed (or 'pushed over') to a target displacement equal to a multiple of the displacement obtained from an elastic analysis (a factor of 1.5 is suggested to provide an adequate factor of safety). At each increment of deformation, the plastic hinges, which are assumed to have a length ℓ_p , are allowed to deform according to the assumed moment-curvature relationship, which will vary with the column's axial load. At the target displacement, it will be possible to identify the plastic hinges and determine the corresponding plastic rotation at each location. The plastic curvature at a section is determined by dividing the plastic rotation by the effective plastic hinge length, ℓ_p . The revised target concrete strain, ϵ_{cu} , is then determined from the moment-curvature analysis. If necessary, the shell thickness can be adjusted and the procedure repeated until the solution converges to an acceptable value for shell thickness. An example of a steel shell design using both the simplified procedure and this iterative procedure is given in example 9-2.

The plastic hinge length will be shortened due to the clamping action of the retrofit measure, particularly if the plastic hinge contains lap-spliced longitudinal reinforcement. For example, the hinge length for a column with a steel shell retrofit is given by

$$\ell_p = s_g + 2\chi d_b \quad (9-8)$$

where s_g is the gap between the retrofit measure and critical section (typically about 50 mm (2 in)), d_b is the diameter of longitudinal reinforcement, and χ equals 6 for grade 40 reinforcing bars (i.e., $f_y = 275$ MPa (40 ksi)) or 9 for grade 60 reinforcing bars (i.e., $f_y = 414$ MPa (60 ksi)).

Equation 9-8 has been developed for steel-jacketed columns, both with and without lap splices. It is expected to give conservative estimates of hinge length for columns that have externally prestressed confinement systems or fiber composite jacket retrofits where there are no lap-spliced reinforcing bars in the plastic hinge region.

Shear Strength Enhancement – The shear resistance of a passive circular steel jacket may be found by analogy to hoop or spiral reinforcement. The jacket is considered to act like a spiral bar of area A_v at spacing s , equal to A_v/t . The additional nominal shear capacity V_{sj} , provided by the jacket, is given by:

$$V_{sj} = \frac{\pi}{2} t f_{ys} D \cot \theta \quad (9-9)$$

where f_{ys} is the jacket yield stress, and θ is the shear crack angle measured from the vertical, and is given by the equations 9-10 or 9-11 below, provided that the longitudinal reinforcement is not terminated in the length of column encompassed by the failure plane defined by the angle.

$$\theta = \tan^{-1} \left(\frac{\rho_v n + 1.26 \frac{\rho_v}{\rho_\ell}}{1 + \rho_v n} \right)^{\frac{1}{4}} > \alpha \quad \text{for fixed-pinned columns} \quad (9-10)$$

$$\theta = \tan^{-1} \left(\frac{\rho_v n + 0.46 \frac{\rho_v}{\rho_\ell}}{1 + \rho_v n} \right)^{\frac{1}{4}} > \alpha \quad \text{for fixed-fixed columns} \quad (9-11)$$

where:

- $\rho_v = 2t/r$,
- $\rho_\ell = A_s/A_g$ (longitudinal reinforcement ratio),
- $n = E_s/E_c$,
- $\alpha = D'/L$ (geometric aspect ratio of the column),
- $D' =$ distance between the outermost reinforcing bars in the direction of shear, and
- $L =$ twice the distance from the point of fixity to the point of zero moment within the column.

Retrofit Design Criteria for Rectangular Columns – The principles developed above can be extended to rectangular columns. At this time, only the elliptical-steel jacket method of retrofit, as shown in figure 9-10, has been demonstrated in the laboratory to have adequate confinement due to hoop action in the shell (Sun et al., 1993). Stiffened flat steel plates have also been used

in the field and tested in the laboratory (Priestley et al., 1992) but their performance under cyclic loads is inferior to the elliptical jacket. In some cases, flat plates may be desirable on wide (or architecturally flared) columns for aesthetic reasons. In these cases, the required confining pressure will need to be provided by plate bending. A thicker or a stiffened plate, in conjunction with bolts placed in holes drilled through the column, may be required to accomplish this.

Rectangular columns that are not square generally have greater stiffness, and thus greater ductility demand, in the direction of the longer side (usually the transverse direction). Square columns or those that are almost square, can be retrofitted with a circular shell, but those that have significant plan aspect ratios should be fitted with elliptical jackets. As a consequence, the curvature of the shell surface for a rectangular column varies continuously.

The equation of an ellipse may be expressed as:

$$\frac{x^2}{B_x^2} + \frac{y^2}{B_y^2} = 1 \quad (9-12)$$

where B_x and B_y are defined in figure 9-12. The extreme radii of an elliptical jacket in the two principal directions are:

$$r_1 = \frac{B_y^2}{B_x} \quad \text{and} \quad r_3 = \frac{B_x^2}{B_y} \quad (9-13)$$

The jacket radius at the corner of the column section, r_2 , may be taken as the average of r_1 and r_3 . In practice, it simplifies shell fabrication if two constant radius segments are joined to approximate an ellipse. Standard shapes have been developed for various cross-section dimensions (Caltrans, 1996).

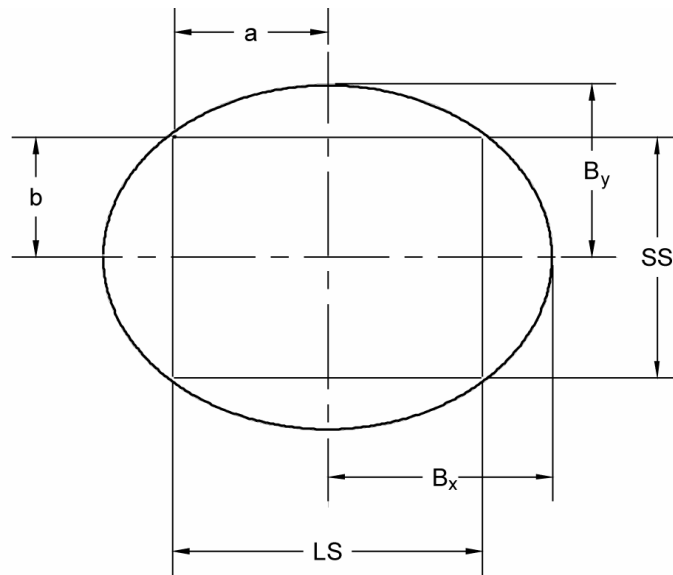
The design equations for flexural integrity and ductility capacity may be adapted from design equations for circular columns using an average radius of the ellipse over the extent of the compression zone. A reasonable approximation to this could be obtained by taking the average of the jacket radius at the column section corner, r_2 , and at the principal axis under consideration. With reference to figure 9-12 for a rectangular column with cross-sectional dimensions of $2a$ in the x -direction, and $2b$ in the y -direction, the average radius for the shell in the x direction is:

$$r_x = (r_1 + r_2) / 2 \quad (9-14)$$

and in the y -direction is:

$$r_y = (r_3 + r_2) / 2 \quad (9-15)$$

The appropriate confinement equations can now be used to determine the required shell thickness by substituting $D = 2r_x$ or $D = 2r_y$.



$$B_y = \sqrt{b^2 + \frac{a^2}{(A_{SR})^2}}$$

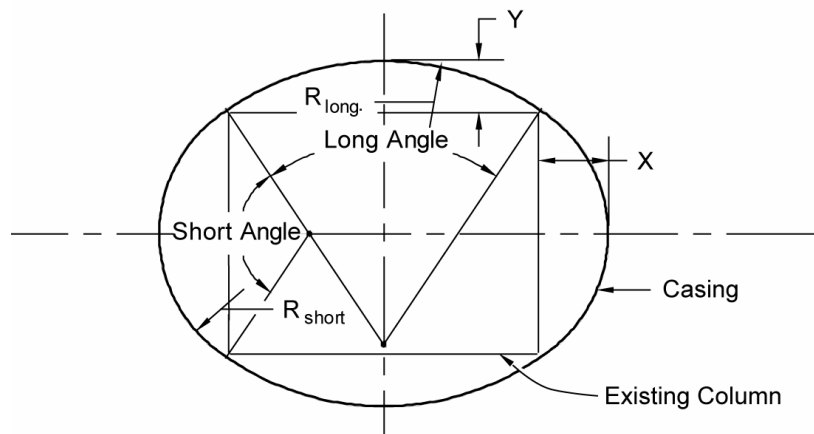
$$A_{SR} = \frac{LS}{SS} = \text{Aspect Ratio}$$

$$B_x = B_y \times A_{SR}$$

LS = Long Side

SS = Short Side

Geometry of Ellipse



Fabrication of Shell Using Two
Curves to Simulate Ellipse

Figure 9-12. Geometry of an elliptically shaped jacket.

EXAMPLE 9.2: STEEL SHELL RETROFIT

Given: a 9.15 m (30 ft) high single column pier that is 1.22 m (4.0 ft) in diameter. It is assumed to be rigidly connected to a footing and unrestrained at the top. The dead load of the superstructure is 4.45 MN (1000 kips). The structure is located at a site where $F_v S_1 = 0.6$.

The main reinforcement in the column is 20 #35 (metric) (#11 cus) grade 40 reinforcing bars that are not lap-spliced and are confined by #13 (#4 cus) hoops at 305 mm (12 in) spacing. There is 50 mm (2 in) cover over the #13 (#4 cus) hoops. The concrete strength is assumed to be approximately 35 MPa (5000 psi) and the effective moment of inertia of the section is 0.0544 m^4 (6.3 ft^4).

Moment capacity $M_n = 4.5 \text{ MNm}$ (3317 k/ft)

Shear capacity $V_n = 0.492 \text{ MN}$ (110.6k)

The column details are non-ductile and it is proposed to use a circular steel shell to increase the ductile capacity of the column. Calculate the thickness of the shell required for flexural confinement and check shear strength requirements.

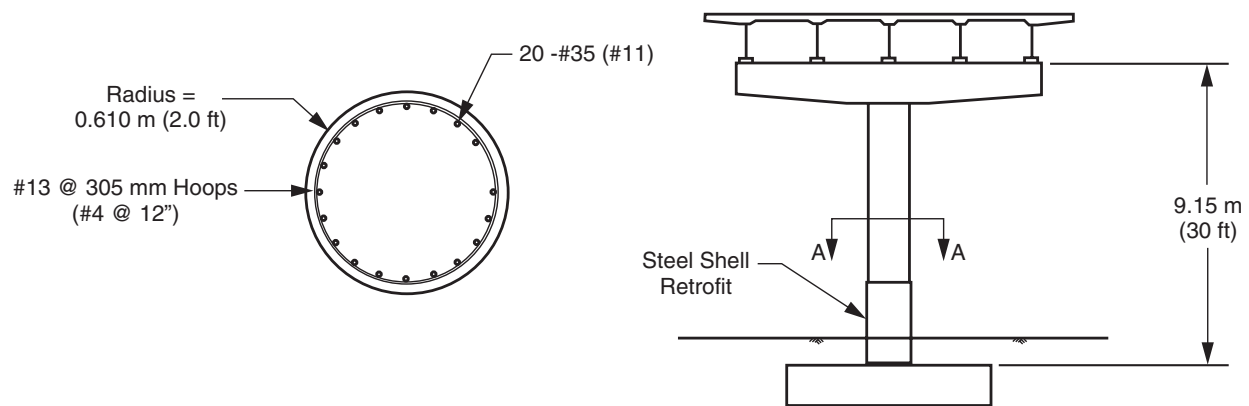
STEP 1. SIMPLIFIED DYNAMIC ANALYSIS

Stiffness for single curvature.

$$\text{Stiffness } k_c = \frac{3EI_{\text{eff}}}{L^3} = \frac{3 \cdot (27800 \text{ MPa}) (0.0544 \text{ m}^4)}{9.15^3 \text{ m}^3} = 5.93 \text{ MN/m} \quad (406 \text{ k/ft})$$

$$\text{Mass } m = \frac{W}{g} = \frac{4.45 \text{ MN}}{9.8 \text{ m/sec}^2} = 0.454 \text{ MNsec}^2/\text{m} \quad (31.0 \text{ k} \cdot \text{sec}^2 / \text{ft})$$

$$\text{Period } T = 2\pi \sqrt{\frac{m}{k_c}} = 2\pi \sqrt{\frac{0.454 \text{ MNsec}^2}{5.93 \text{ MN/m}}} = 1.74 \text{ sec}$$



Single Column Pier

$$S_a = \frac{F_v S_1}{T} = \frac{0.6}{1.74 \text{ sec}} = 0.345$$

$$V_{EQ} = S_a M_g = 0.345 (0.454 \times 9.8) = 1.54 \text{ MN (346 k)}$$

$$M_{EQ} = V_{EQ} L = 1.54 \text{ MN (9.15 m)} = 14.05 \text{ MN/m (10,360 k/ft)}$$

$$\Delta_{EQ} = \frac{V_{EQ}}{k_c} = \frac{1.54 \text{ MN}}{5.93 \text{ MN/m}} = 0.26 \text{ m (0.85 ft)}$$

STEP 2. SIMPLIFIED SHELL DESIGN

$$\text{Plate thickness: } t_j \geq \frac{f_c D}{400} = \frac{2.07 \text{ MPa (1220) mm}}{400} = 6.3 \text{ mm (0.25 in)} \Rightarrow \text{say 6 mm (0.25 in) (Eq 9-4)}$$

F_s was taken as 100 MPa.

Ductility factor:

$$\text{R-factor: } R_{\text{eff}} = \frac{M_{EQ}}{M_n} = \frac{14.05 \text{ MNm}}{4.50 \text{ MNm}} = 3.12 < 4 \Rightarrow \text{OK (for } M_n \text{ derived from section analysis)}$$

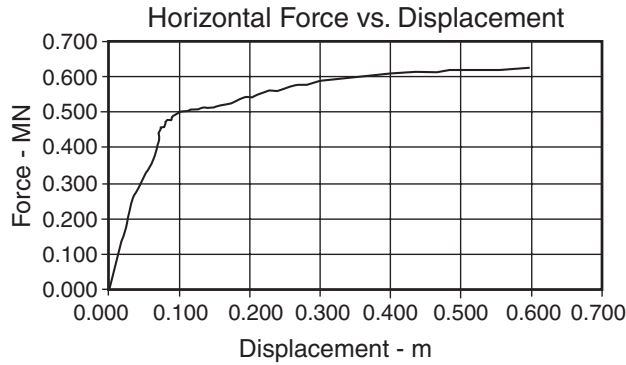
Using $t = 10 \text{ mm (0.4 in)}$ as the minimum thickness required for field handling:

Length of plastic hinge zone:

$$\ell_p = 0.25L = 0.25 (9.15 \text{ m}) = 2.29 \text{ m (7.5 ft)} \Rightarrow \text{use 2.5 m (8.2 ft)}$$

STEP 3. RIGOROUS DESIGN CHECK

The first step in a rigorous design check is to perform a computer based moment-curvature analysis that considers the concrete stress and strain enhancement resulting from shell confinement and the strain hardening of the steel. Such programs may model the column section as a series of concrete and steel elements with these enhanced stress-strain properties. The shell is only considered effective as confining reinforcement. Plane sections are assumed to remain plane as the section is rotated incrementally while maintaining force equilibrium. The results can be presented as force-displacement curves at the top of the column. The following plot, obtained from a Caltrans in-house program, reflects the force-displacement curve for this column retrofitted with a 10 mm (0.4 in) thick steel shell.



The following values were obtained from the moment-curvature analysis:

$$\theta_p = 0.0591 \text{ radians} \quad (\text{plastic rotation capacity})$$

$$\epsilon_{cu} = 0.03211$$

$$\Delta_Y = 0.10 \text{ m} \quad (4 \text{ in}) \quad (\text{idealized yield displacement – see plot})$$

The next step is to perform a pushover analysis of the bent to the following target displacement, and to calculate the plastic rotation demand at the critical section of the column. In this case, the pushover analysis can be calculated by hand, but in a more complicated structure, a nonlinear computer program must be used.

$$\Delta_T = 1.5\Delta_{EQ} = 1.5 (0.26) \text{ m} = 0.39 \text{ m} \quad (1.3 \text{ ft}) \quad (\text{target displacement derived from elastic analysis})$$

$$\Delta_P = \Delta_T - \Delta_Y = 0.39 \text{ m} - 0.10 \text{ m} = 0.29 \text{ m} \quad (0.95 \text{ ft})$$

$$\theta_p = \frac{\Delta_P}{L} = \frac{0.29 \text{ m}}{9.15 \text{ m}} = 0.0317 \text{ radians} \quad (\text{plastic rotation demand from “pushover”})$$

$$\theta_p < 0.0591 \text{ radians} \Rightarrow \text{OK}$$

Notice that, based on rigorous analysis, the retrofitted column can accommodate nearly twice the plastic rotation demand that would be imposed on it during the design earthquake. There would be a case for reducing the shell thickness if constructability were not an issue. Out of curiosity, the above process was repeated until the shell thickness converged on a value that was just sufficient to resist the plastic rotational demands. The value obtained was approximately 4 mm (0.16 in), even less than obtained by the simplified approach.

STEP 4. SHEAR DESIGN CHECK

$$V_p = 1.5V_N = 1.5 (0.492) \text{ MN} = 0.74 \text{ MN} \quad (166 \text{ k})$$

$$V_c = \phi 0.8 A_g (0.083) 2\sqrt{f'_c}$$

$$= 0.85(0.8) 1.17\text{m}^2 (0.083) 2\sqrt{35\text{MPa}} = 0.78 \text{ MN} \quad (175.3 \text{ k}) > 0.74 \text{ MN} \quad (166 \text{ k}) \Rightarrow \text{OK}$$

Shear does not control outside the plastic hinge region.

The effective confinement will thus be less in the direction of the shorter side (usually the longitudinal direction), which will therefore be the weak direction of the column and may govern design. In piers with large plan aspect ratios, it may be impossible to obtain adequate confinement in the direction of the shorter side. In these cases, it will be necessary to add stiffeners or tie rods to assist the shell in providing the required confinement. However, it will frequently be found that a realistic assessment of displacement capacity in the weak (longitudinal) direction of the bridge will indicate that no retrofit is necessary, and the design of the jacket will be governed by the requirements in the strong (transverse) direction.

9.2.1.3(b). Fiber Composite Jacketing

There are a number of proprietary techniques for jacketing or wrapping deficient concrete columns that use advanced fiber composites to increase the flexural ductility and shear strength, and to correct lap splice length deficiencies at ends of columns. These composites are usually high strength glass (E-glass), carbon, or aramid fibers oriented primarily in the circumferential direction of the column, and bound in a polyester, vinyl ester, or epoxy resin matrix. The resulting material has anisotropic properties, which allows the flexural ductility, splice strength and shear strength of a column to be improved without significantly affecting flexural strength and stiffness. Since the properties of a cured composite laminate depend on the particular fiber and resin combination, it is advisable to use only components that have been developed for use as part of a system and thoroughly tested. Detailed guidance on the use of composites for column wraps is available in ACI's *Design and Construction of Externally Bonded FRP Systems for Strengthening Concrete Structures* (ACI, 2002).

Current design philosophy is to install column confinement as a passive system that is engaged only when the concrete column is loaded and dilates. In the past, there has been some experimentation with active systems where the fibers are loaded or prestressed during installation. However, extreme caution must be taken with an active system because of the natural tendency of composite materials to creep under sustained loading, which can lead to rupture of the wrap. This can occur even at relatively low stresses and is exacerbated by the difficulty in obtaining uniform stresses in the wrap. Exterior steel prestressed cables, used in a similar fashion to steel hoops, have been used successfully by Illinois DOT to retrofit inadequate length lap splices.

One of the first fiber composite wrapping systems to be developed consisted of glass and aramid fibers in an epoxy matrix (Fyfe, 1994). The fibers were woven into a fabric, which was saturated in an epoxy resin in the field and then hand wrapped around an existing column. Additional confinement may be provided in critical regions, such as the bottom of columns. This approach has been successful in enhancing the flexural ductility and shear strength of circular columns in the laboratory (Priestley et al., 1994).

In the past, another form of passive confinement involved the use of a special wrapping machine that placed epoxy impregnated carbon fiber 'tows' (a tow is a series of straight-laid fibers) directly onto the column (Seible et al., 1995). The tows were wound up the column at 6 rpm and heat cured for at least two hours at temperatures up to 121 degrees centigrade. After curing, the jacket was protected with an acrylic emulsion spray coating. This proprietary system is no

longer in use. However, carbon systems can be effective when applied in the same manner as E-glass systems.

Rectangular columns have also been tested with fiber composite shell retrofits (Seible and Priestley, 1993; Seible et al., 1995). One approach, which utilizes an elliptical jacket placed over a section of the column that has been built up into an elliptical shape, has been shown to increase both the ductility and shear strength of the column. Another approach allows jacketing to be placed directly on the surface of a rectangular column. This method will increase the shear resistance of the column and force a flexural failure with increased, but limited, ductility provided that the cross-sectional dimensions of the column are not too large.

At least two systems now available use prefabricated fiber composite shells (Xiao et al., 1995; Steckel et al., 1998). One of these systems uses a series of shells comprised of high strength fibers in a polymer matrix similar to field-installed systems, except that they are manufactured under factory controlled conditions. Field installation of this passive confinement system involves bonding an initial prefabricated shell to the existing column. Subsequent shells are placed over the first shell, with the shell seams rotated around the column so that they are overlapped, until the desired jacket thickness is achieved. These shells are clamped to the existing column using straps, until the bond has fully cured. This system can be quickly installed without the need for heavy equipment or skilled labor.

Fiber composite column jacketing systems have been developed and tested (Matsuda et al., 1990; Ogata et al., 1993). In addition to using fiber composites to increase flexural ductility and shear strength, some of the fibers may be placed along the axis of the column to increase flexural strength.

Designers should be aware of potential freeze-thaw problems when considering column jacketing in cold regions. A potential problem exists when retrofitting using continuous fiber composite jackets. Moisture can collect between the jacket and the concrete column and freeze, resulting in expansive pressures that can cause a rapid deterioration of the concrete or damage to the wrap. The potential for this deterioration can be reduced by applying the jacket in relatively narrow bands (e.g., 150 mm (6 in)) with an epoxy-free gap between bands equal to or greater than the width of the bands, but not greater than six times the main reinforcing bar diameter plus the clear cover over the bar (Aquino et al., 2004). Tests (Jin et al., 1994) have also shown that discrete fiber composite straps placed around an existing column could increase its flexural ductility and shear strength. If a continuous wrap is used, precaution should be taken to prevent water ingress from the top. Repair of leaking joints at piers and/or waterproofing at the top of the column is very important.

Another drawback of fiber composite systems is their susceptibility to absorbed moisture (Steckel et al., 1998). Glass fibers can lose significant strength due to moisture absorption, which can be accelerated by temperature variation. The polyester epoxy matrix used in glass fiber composites can provide a measure of protection against this type of damage, but is very sensitive to the type of material used and the manner in which the composite is fabricated and installed.

Carbon fibers themselves are not affected by moisture, but the quality of the polyester epoxy matrix is critical to the performance of the composite. Carbon fiber systems have shown loss of tensile strength at high temperatures due to moisture absorption. This may require redesign of the epoxy matrix component in order to satisfy design and performance requirements. Collaboration between the designer and composite material supplier is encouraged.

These types of problems can be addressed by careful testing of prospective systems under extreme or accelerated service conditions, good quality control during construction and application in the field, and design with sufficient safety factors to account for prospective strength loss. It is important to note that although the strength of fiber composite systems is susceptible to environmental factors, the stiffness of these systems remains constant. This is encouraging since their effectiveness is stiffness sensitive.

Table 9-1 shows mechanical properties for a number of different fiber types. This is provided for reference only and it should be noted that the properties of the cured laminate may differ from the fiber properties.

Table 9-1. Mechanical properties of fibers used in modern fiber-reinforced plastic composites.

Type of Fiber	Ultimate Strength, MPa (ksi)	Ultimate Strain	Modulus of Elasticity, GPa (ksi)
E-Glass	2410 (350)	0.020	41 (6,000)
S-Glass	3450 (500)	0.030	41 (6,000)
CF-Pan	4140 (600)	0.020	228 – 345 (33,000 – 50,000)
C-Pitch-GP	1380 (200)	0.003	41 (6,000)
Pitch UHM	2760 (400)	0.005	483 – 827 (70,000 – 120,000)
Aramid	3450 (500)	0.020	69 – 138 (10,000 – 20,000)
Ceramic	690 (100)	0.020	69 – 276 (10,000 – 40,000)
Nylon	345 (50)	0.050 – 0.500	3.5 (500)

A procedure for the design of fiber-composite column jackets is described below.

Performance of Lap Splices – In the active/passive confinement system of figure 9-13, an active wrap is stressed to produce a reliable, after-creep, active confining stress in the column, and an additional passive wrap is also provided. Both layers develop (additional) hoop stress as the jacket expands to a strain of 0.001. Wrap thicknesses can be found from equilibrium as follows:

$$2 (t_a E_a + t_p E_p) (0.001) = D (f_l - f_a) \quad (9-16)$$

where t_a is the thickness of active wrap, E_a is the modulus of elasticity of active wrap, f_a is the active confining stress in the column, t_p is the thickness of passive wrap, and E_p is the modulus of elasticity of passive wrap.

Rearranging equation 9-16 gives:

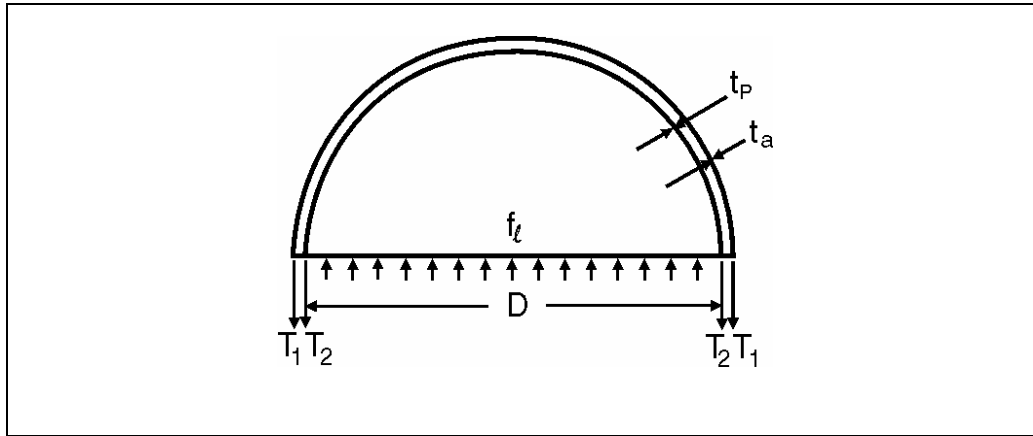
$$t_a E_a + t_p E_p \geq 500 D (f_\ell - f_a) \quad (9-17)$$

In a passive system, the active layer is eliminated and equation 9-17 becomes:

$$t_p E_p \geq 500 D f_\ell \quad (9-18)$$

As with steel jackets, the required confinement stress, f_ℓ , can be determined from equation 9-1, or a simplified approach can be used in which f_ℓ is set equal to 2.07 MPa (300 psi) for a typical column with Grade 40 starter bars and splice lengths of 20 d_b .

It is likely that columns with bars that have inadequate lengths of lap-splices can be safely retrofitted with thinner jackets than those determined by the above design procedure, since there is good experimental evidence that columns can tolerate jacket dilation strains up to 0.003 without a loss in strength (Hawkins, 2000). The Illinois DOT uses this higher value for column composite jackets, but requires that any circumferential crack in the lap-splice zone be limited to 0.8 mm (0.03 in) in width. This width may be exceeded if the shear capacities along the crack are calculated and found to be otherwise acceptable. The advantage of a thinner jacket is that it will allow the development of a greater plastic hinge length, and thus there will be less chance of bar fracture than with a thicker jacket subject to the same plastic rotation.



after Priestley et al., 1992

Figure 9-13. Free body diagram of column retrofitting with a composite shell.

Flexural Confinement – The jacket thickness requirements for fiber composites can be determined using moment-curvature analysis of the retrofitted column in conjunction with a nonlinear static (‘pushover’) analysis. This approach, which is described in section 9.2.1.3(a) for steel jacketing, is also applicable for fiber composites. Because the stress-strain curves for high strength fiber composites used for column retrofitting are essentially linear up to failure, the ultimate strain in concrete (ϵ_{cu}) confined by these jackets is given in equation 9-19:

$$\epsilon_{cu} = 0.004 + \frac{2.5 \rho_s f_{du} \epsilon_{du}}{f'_{cc}} \quad (9-19)$$

where f_{du} is the ultimate design strength of the jacket material taking into account long-term environmental degradation, ϵ_{du} is the ultimate design strain of the jacket material taking into account long-term environmental degradation, and ρ_s is the effective volumetric ratio.

$$\rho_s = \frac{4(t_a + t_p)}{D} \quad (9-20)$$

Equations 9-19 and 9-20 may be used to solve for the required combined thickness of both active (t_a) and passive (t_p) layers of the composite jacket, as shown in equation 9-21:

$$t_a + t_p = 0.1(\epsilon_{cu} - 0.004) \frac{Df'_{cc}}{f_{du}\epsilon_{du}} \quad (9-21)$$

If the properties of active and passive wraps are very different, a weighted average for f_{du} and ϵ_{du} should be used.

A simplified design approach may be used in which a confinement stress of 1.72 MPa (250 psi) is provided at a dilation strain of 0.004. This results in the following jacket thickness requirement to assure adequate displacement ductility to allow the retrofit to be designed using an R-factor of four in most typical columns:

$$t_a + t_p \geq \frac{215D}{E_j} \text{ (mm)} \quad (9-22a)$$

$$t_a + t_p \geq \frac{31D}{E_j} \text{ (in)} \quad (9-22b)$$

where E_j is the weighted average of the elastic moduli for the active and passive wraps (MPa or ksi units).

Shear Strength Enhancement – Following an approach similar to that used for steel jackets, the enhancement in column shear strength for fiber composite jackets is:

$$V_{sj} = \frac{\pi}{2} \left((t_a E_a + t_p E_p) \epsilon_p + T_a \right) D \cot \theta \quad (9-23)$$

where T_a is the active tensile force per unit height of the jacket due to active pressure, $T_a = f_a D/2$, and θ is the shear crack angle given by substituting E_j for E_s in equations 9-10 and 9-11.

Tests have shown that column retrofits designed assuming a maximum allowable passive strain due to shear (ϵ_p) = 0.006 and θ = 30 degrees, have ductile flexural response. A design example for a composite shell retrofit is given in example 9.3.

EXAMPLE 9.3: FIBER COMPOSITE SHELL RETROFIT

Given: a 6.1 m (20 ft) high single column pier that is 1.68 m (5.5 ft) in diameter. It is assumed to be rigidly connected to the footing. The dead load from the superstructure is 9.9 MN (2250 kips). The structure is located in a site where $F_v S_1 = 0.5$.

The main reinforcement in the column is 28 #42 (metric) (#14 cus) grade 40 reinforcing bars that are not lap spliced and are confined by #13 (#4 cus) hoops at 305 mm (12 in) spacing. Concrete cover is 50 mm (2 in) over the #13 (#4 cus) hoops. The concrete strength is assumed to be approximately 35 MPa (5000 psi) and the effective moment of inertia of the section is 0.194 m^4 (22.5 ft^4). Moment capacity, $M_n = 13.57 \text{ MNm}$.

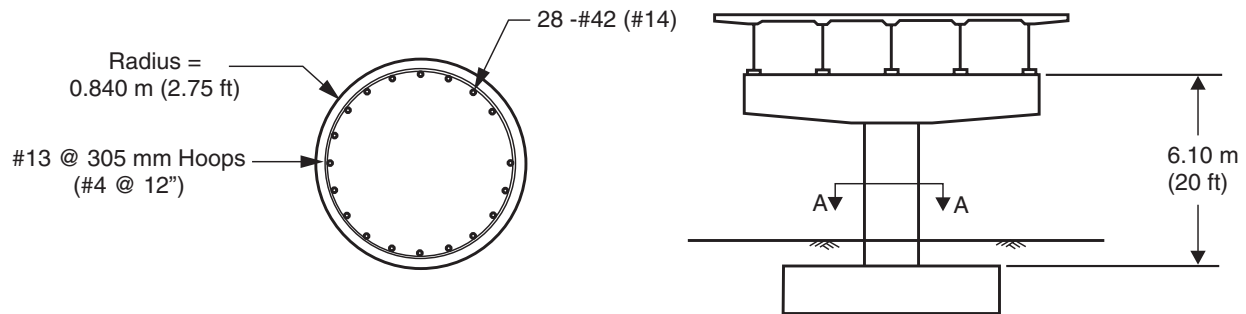
The column details are non-ductile and it is proposed to use a passive composite shell to retrofit the column. Calculate the thickness of the shell required for flexural confinement and check shear strength requirements. Assume $E_j = 42000 \text{ MPa}$.

STEP 1. SIMPLIFIED DYNAMIC ANALYSIS

$$\text{Stiffness } k_c = \frac{3E_{\text{eff}}}{L^3} = \frac{3(27800 \text{ MPa}) \cdot 0.194 \text{ m}^4}{6.10^3 \text{ m}^3} = 71.3 \text{ MN/m} \quad (4940 \text{ k/ft})$$

$$\text{Mass } m = \frac{W}{g} = \frac{9.90 \text{ MN}}{9.8 \text{ m/sec}^2} = 1.01 \text{ MNsec}^2/\text{m} \quad (69.2 \cdot \text{k-sec}^2/\text{ft})$$

$$\text{Period } T = 2\pi \sqrt{\frac{m}{k_c}} = 2\pi \sqrt{\frac{1.010 \text{ MN-sec}^2/\text{m}}{71.3 \text{ MN/m}}} = 0.748 \text{ sec}$$



Single Column Pier

$$S_a = \frac{F_v S_1}{T} = \frac{0.5}{0.748} = 0.668 g$$

$$V_{EQ} = S_a W = 0.668 \cdot (9.90 \text{ MN}) = 6.61 \text{ MN} \quad (1486 \text{ k})$$

$$M_{EQ} = V_{EQ} L = 6.61 \text{ MN} (6.10 \text{ m}) = 40.34 \text{ MNm} \quad (29,745 \text{ k/ft})$$

$$\Delta_{EQ} = \frac{V_{EQ}}{k_c} = \frac{6.61 \text{ MN}}{71.3 \text{ MN/m}} = 0.093 \text{ m} \quad (0.3 \text{ ft})$$

STEP 2. SIMPLIFIED PROCEDURE FOR FLEXURAL CONFINEMENT

$$t_p = \frac{215D}{E_j} = \frac{215 (1.68 \text{ m})}{42000 \text{ MPa}} = 0.0086 \text{ m} \quad (0.34 \text{ in}) \Rightarrow \text{minimum shell thickness} \quad (\text{Eq. 9-22a})$$

$$R_{eff} = \frac{M_{EQ}}{M_n} = \frac{40.34}{13.57} = 2.97 < 4 \Rightarrow \text{OK}$$

where M_n is derived from section analysis.

STEP 3. SHEAR STRENGTH ENHANCEMENT

$$V = \frac{1.4 M}{L} = \frac{1.4 (13.57 \text{ MN-m})}{6.10 \text{ m}} = 3.11 \text{ MN} \quad (699 \text{ k})$$

$V_c = \phi 0.8 A_g (0.083) \cdot 2\sqrt{f'_c} = 0.85(0.8) \cdot 2.21 \text{ m}^2 (0.083) \cdot 2\sqrt{35 \text{ MPa}} = 1.48 \text{ MN} \quad (333 \text{ k})$; i.e., concrete confined within the shell is 100 percent effective in resisting shear.

$$V_{sj} = \frac{V_p - V_c}{\phi} = \frac{3.11 \text{ MN} - 1.48 \text{ MN}}{0.85} = 1.922 \text{ MN} \quad (432 \text{ k})$$

Solving for t_a from formula 9-23:

$$t_a \geq \frac{2V_{sj}}{\pi E_i \epsilon_p D \cot \theta} = \frac{2(1.36 \text{ MN})}{3.142(42000 \text{ MPa})(0.006) \cdot 1.68 \text{ m}(1.0)} \\ = 0.003 \text{ m} \quad (0.08 \text{ in}) < 0.0086 \text{ m} \quad (0.34 \text{ in}) \Rightarrow \text{OK}$$

No additional shell thickness is required for shear strength enhancement, but the shell should be full height. The portion of shell above the plastic hinge zone may be reduced in thickness to reflect only shear requirements.

9.2.1.3(c). External Prestressing Steel

An improved form of confinement may be achieved by wrapping prestressing wire under tension around a column. Active pressure, rather than passive pressure, provides the lateral confining stresses needed to increase flexural ductility, although passive pressure will also add to the confinement. This procedure has successfully increased the flexural ductility of circular columns with lap splices at the critical section, but its effect on shear strength has not yet been quantified. It is, however, expected to be beneficial. An advantage of this technique is that it has little effect on the flexural strength and stiffness of the column. Reliable anchorage of the wire ends is essential for an effective field application.

Initial attempts to design a machine to wrap prestressing wire around a column proved not to be economical due to the size of the machine required to produce the desired tension in the strand. Another method of stressing uses standard 15 mm (0.6 inch) diameter prestressing strand that is anchored in special anchorages originally designed for prestressed water tanks. This method uses existing materials and equipment, and has been successfully tested in the laboratory (Lin et al., 1994). These anchors are shown in figure 9-14. Subsequent tests (Hawkins et al., 1999) showed that columns retrofitted with prestressing strand lose strength at dilation strains beyond 0.001 as a result of high prestress losses that occur due to stressing the strands around a typical column, and the penetration of the strand into the concrete during cyclic loading. This observation is used to set the strain limit in the design procedures that follow.

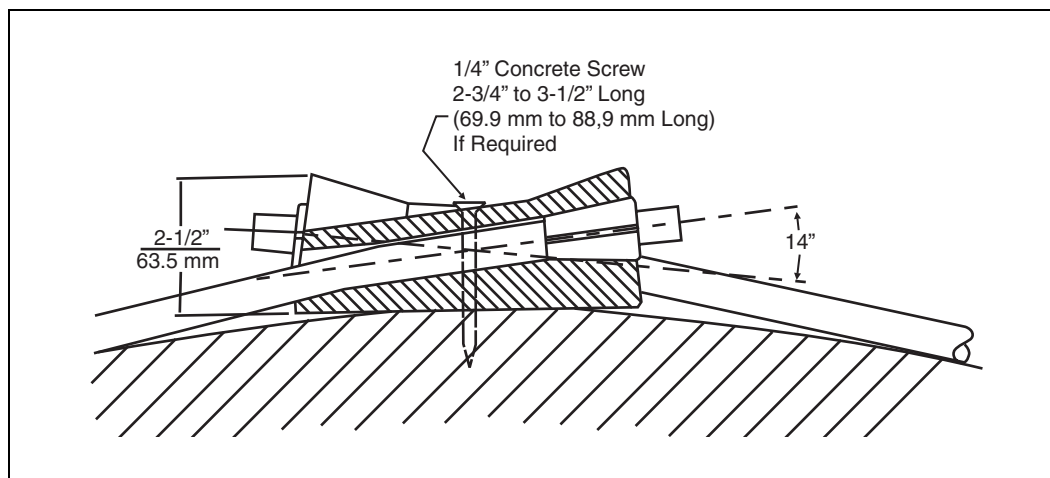


Figure 9-14. Anchorages for prestress strand retrofit.

Another method of stressing that has been developed and successfully tested involves placing unstressed strand around the column (Swanson, 1999). A hand-held machine is used to stress the strand by pulling a portion of the strand radially away from the column and inserting a steel wedge between the strand and the column, as shown in figure 9-15. This procedure is repeated around the circumference of the column until the strand is adequately stressed and provides a somewhat uniform confining stress. This stressing technique has the added advantage of minimizing prestress losses due to friction.

Threaded semicircular steel bars may be used instead of prestressing wire to achieve a similar effect. Originally designed to prevent the splitting of a concrete column under service conditions, these bars are placed around a column and tightened to produce a prestressing force to prevent nonductile column failure under cyclic loading (Lin et al., 1994). Similar improvements may be obtained from a system using semicircular threaded reinforcing bars tightened by threaded swage couplers, as shown in figure 9-16 (Coffman et al., 1991).



Figure 9-15. Prestressing retrofit by wedging between column and strand.

Steel on the outside of a column must be protected from corrosion. This can be done by encasing the wire with a concrete jacket of nominal thickness that stops short of adjacent members (footings or cap beams) to avoid increasing the flexural strength or stiffness of the column.

Since no data is available on the performance of rectangular or square columns using this technique, applications should be limited to circular columns at this time.

Performance of Lap Splices – The confinement stress required to prevent splice failure, f_ℓ , was discussed in section 9.2.1.3(a). The free body diagram of half of a circular column retrofitted by a wire wrap method is shown in figure 9-17. Equilibrium requires that

$$2 T = f_\ell D \quad (9-24)$$

and if $E_s = 200 \text{ GPa}$ (29,000 ksi):

$$\frac{2A_p}{s} (f_i + 200) = f_\ell D \quad (\text{MPa units}) \quad (9-25a)$$

$$\frac{2A_p}{s}(f_i + 29) = f_\ell D \quad (\text{ksi units}) \quad (9-25b)$$

where A_p is the cross-sectional area of wire equal to $0.785 d_p^2$, d_p is the diameter of wire, s is the spacing of wire, and f_i is the tensile stress in wire after losses (MPa, ksi).

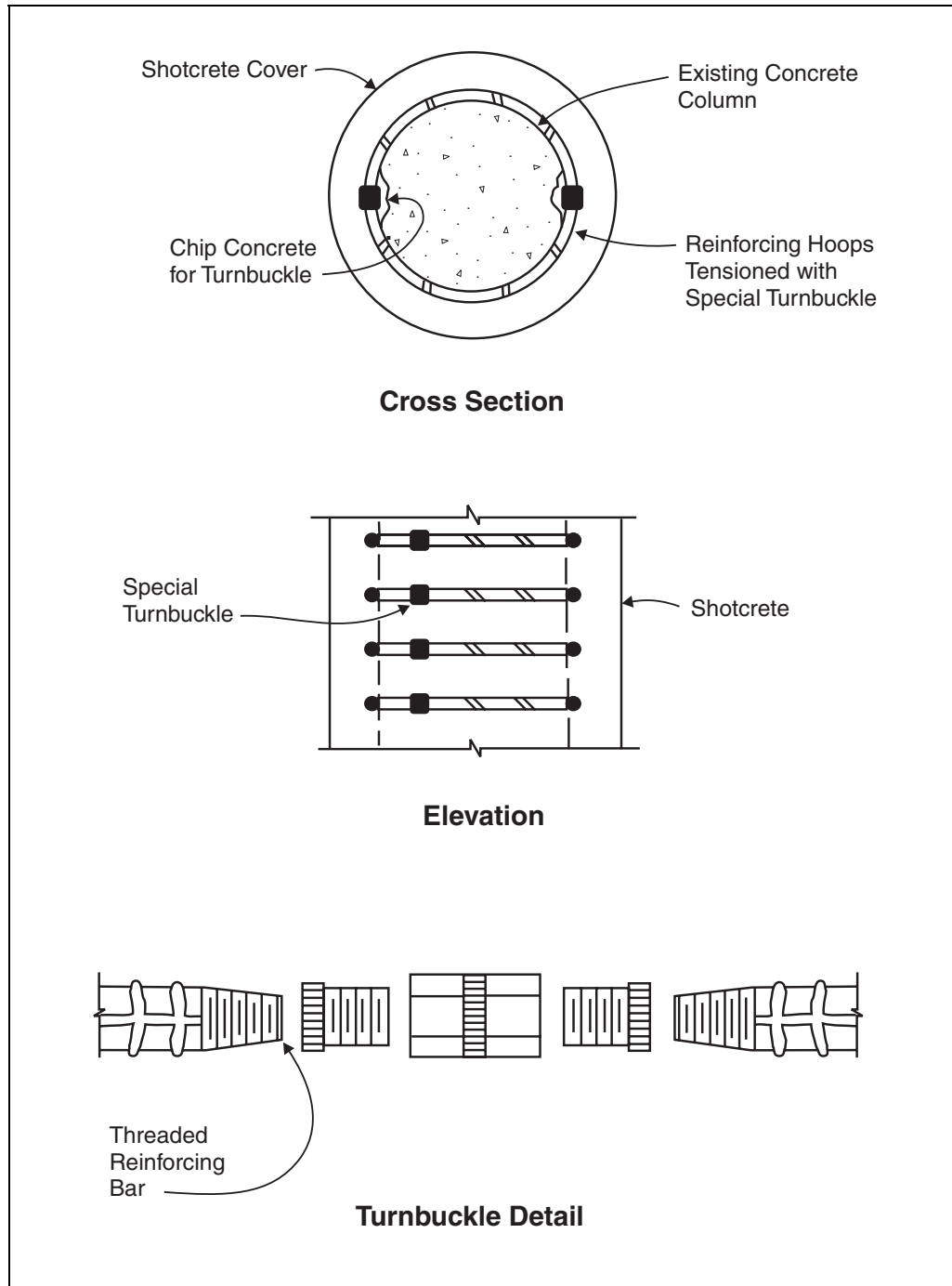
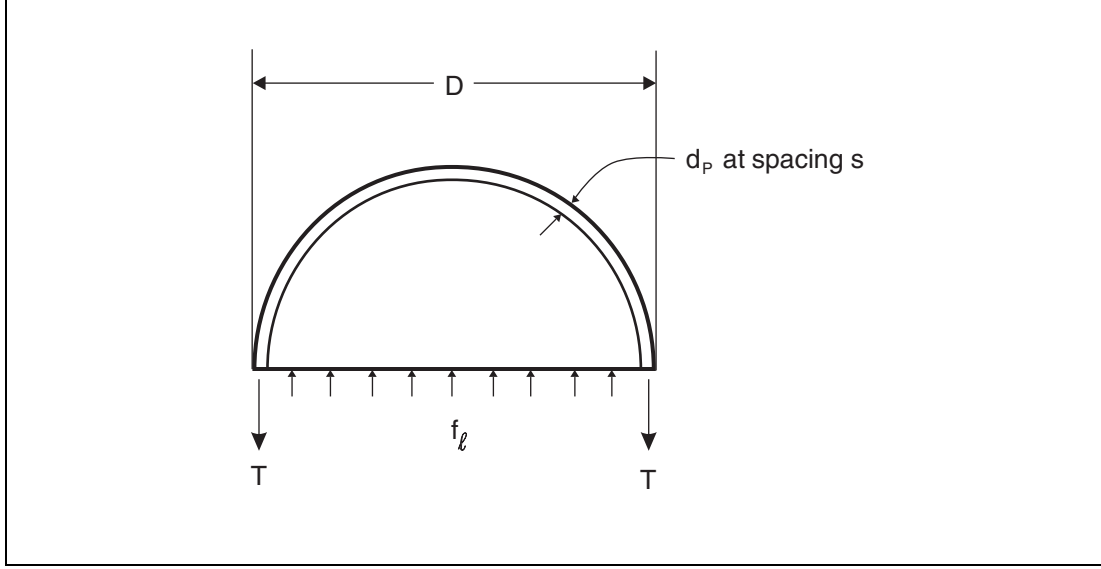


Figure 9-16. Semi-circular reinforcing bars with couplers.



after Priestley et al., 1992

Figure 9-17. Free body diagram of column retrofitting with external prestressing.

Solving equation 9-25 for the required spacing gives:

$$s \leq \frac{2A_p (f_i + 200)}{f_\ell D} \quad (\text{MPa units}) = \frac{2A_p (f_i + 29)}{f_\ell D} \quad (\text{ksi units}) \quad (9-26)$$

The required level of confinement, f_ℓ , can be determined from equation 9-1. Alternatively, the confinement stress can be taken as 2.07 MPa (300 psi), which will be adequate to prevent splice failure in most columns (Chai et al., 1991), and equation 9-26 then becomes:

$$s \leq \frac{A_p (f_i + 200)}{D} \quad \text{MPa units} = \frac{6.7A_p (f_i + 29)}{D} \quad (\text{ksi units}) \quad (9-27)$$

Strand spacing, s , should not exceed six times the diameter of the main reinforcing bar (Hawkins et al., 1999).

Flexural Confinement – Taking account of differences in the shape of the stress-strain curves for prestressing wire and mild structural steel, and the configuration of wire and strand versus that of a shell, equation 9-5 can be rewritten as:

$$\epsilon_{cu} = 0.004 + \frac{4A_p f_{pu} \epsilon_{su}}{Ds f'_{cc}} \quad (9-28)$$

where f_{pu} and ϵ_{su} are the ultimate design stress and strain, respectively, for prestressing wire, and f'_{cc} is as follows:

$$f'_{cc} = f'_c \left(-1.254 + 2.254 \sqrt{1 + \frac{15.88 A_p f_{pu}}{s D f'_c}} - \frac{4 A_p f_{pu}}{s D f'_c} \right) \quad (9-29)$$

Rewriting equation 9-28 leads to the following requirement for prestressed wire wraps:

$$\frac{A_p}{s} \geq \frac{D f'_{cc}}{4 f_{pu} \epsilon_{su}} (\epsilon_{cu} - 0.004) \quad (9-30)$$

Once the value of ϵ_{cu} at the target displacement has been determined from a moment-curvature curve and an inelastic static analysis, using the methods described above for steel shells, it will be possible to solve for A_p/s using an iterative approach. Assuming $\epsilon_{cu} = 0.002$, and $f'_{cc} = 1.7 f'_c$, will give a conservative initial value for A_p/s .

In the case of prestressing strand, the above design approach can be simplified by assuming a confinement stress, f_t , equal to 1.72 MPa (250 psi) and a passive steel strain of 0.004. This should be sufficient to keep the strand on the linear portion of the stress strain curve (i.e., $f_s = 0.8 f_{pu}$) provided moderate levels of active stress are used. This results in the following simplified design equations:

$$\frac{A_p}{s} \geq \frac{D}{0.92 f_{pu}} (\text{MPa units}) = \frac{D}{6.4 f_{pu}} (\text{ksi units}) \quad (9-31)$$

This simplified requirement for prestressed wire wraps will be adequate for most columns, although it may be overly conservative in some cases.

Shear Strength Enhancement – The shear strength provided by external prestressing wire may be determined in the same manner as conventional circular hoops or spirals. Therefore, the shear capacity contribution of this steel is given by equation 9-32:

$$V_{sp} = \frac{\pi}{2} \frac{A_{ps} (0.8 f_{pu}) D}{s} \cot \theta \quad (9-32)$$

A design example of a column wrap using external prestressing wire is given in example 9-4.

9.2.1.3(d). Concrete Jacketing

The addition of a jacket of reinforced concrete around an existing circular or rectangular column was discussed earlier in section 9.2.1.2(a). The application is straightforward, following the rules for reinforced concrete design. However, adding a concrete jacket requires holes to be drilled through the existing column and placement of supplemental ties through these holes. These ties must be adequately anchored on both sides of the existing column.

EXAMPLE 9.4: EXTERNAL PRESTRESS

Given: the single column pier in example 9-3. The column is 6.1 m (20 ft) high, and has a diameter of 1.68 m (5.5 ft). It is assumed to be rigidly connected to the footing. The dead load of the superstructure is 9.9 MN (2250 k). The structure is located in a site where $F_v S_1 = 0.5$.

The main reinforcement in the column is 28 #42 (metric) (#14 cus) grade 40 reinforcing bars that are not lap spliced and are confined by #13 hoops at 305 mm (12 in) spacing. The concrete cover over the #13 hoops is 50 mm (2 in). The concrete strength is assumed to be approximately 35 MPa (5000 psi) and the effective moment of inertia of the section is 0.194 m^4 (22.5 ft^4).

The column details are not ductile, and it is proposed to use a steel wire wrap to retrofit the column. Calculate the diameter and spacing of the wire using the simplified procedure for flexural confinement, and check shear strength requirements.

$$M_n = 13.75 \text{ MNm}$$

$$\text{Prestress strand } f_{pu} = 1862 \text{ MPa (270 ksi)}$$

STEP 1. SIMPLIFIED DYNAMIC ANALYSIS

$$k_c = \frac{3EI_{\text{eff}}}{L^3} = \frac{3(27800 \text{ MPa}) \cdot 0.194 \text{ m}^4}{6.10^3 \text{ m}^3} = 71.3 \text{ MN/m (4140 k/ft)}$$

$$\text{Mass: } m = \frac{W}{g} = \frac{9.90 \text{ MN}}{9.8 \text{ m/sec}^2} = 1.010 \text{ MNsec}^2/\text{m (69.2 k sec}^2/\text{ft)}$$

$$\text{Period: } T = 2\pi \sqrt{\frac{m}{k_c}} = 2\pi \sqrt{\frac{1.010 \text{ MN sec}^2/\text{m}}{71.3 \text{ MN/m}}} = 0.748 \text{ sec}$$

$$S_a = \frac{F_v S_1}{T} = \frac{0.5}{.748} = 0.668 \text{ g}$$

$$V_{EQ} = S_a W = 0.668 \cdot 9.90 \text{ MN} = 6.61 \text{ MN (1486 k)}$$

$$M_{EQ} = V_{EQ} L = 6.61 \text{ MN (6.10 m)} = 40.34 \text{ MNm (29,745 kft)}$$

$$\Delta_{EQ} = \frac{V_{EQ}}{k_c} = \frac{6.61 \text{ MN}}{71.3 \text{ MN/m}} = 0.093 \text{ m (0.3 ft)}$$

STEP 2. SIMPLIFIED PROCEDURE FOR FLEXURAL CONFINEMENT

$$\frac{A_p}{s} = \frac{D}{0.92 f_{pu}} = \frac{1.68}{0.92(1862)} = 0.00098 \text{ m}^2/\text{m} \quad (0.04 \text{ in}^2/\text{in}) \quad (\text{Eq. 9-31})$$

i.e., minimum wire wrap area per unit length is required, which is approximately a 12.7 mm strand at 75 pitch (0.5 in strand at 3" pitch).

$$R_{\text{eff}} = \frac{M_{\text{eq}}}{M_n} = \frac{40.34 \text{ MNm}}{13.57 \text{ MNm}} = 2.97 < 4 \Rightarrow \text{OK}$$

where M_n is derived from section analysis.

STEP 3. SHEAR STRENGTH ENHANCEMENT

$$V_P = \frac{1.4M_n}{L} = \frac{1.4(13.57 \text{ MNm})}{6.10 \text{ m}} = 3.11 \text{ MN} \quad (699 \text{ k})$$

$$V_c = \phi 0.8 A_g 0.083 \cdot 2\sqrt{f'_c} = 0.85(0.8) \cdot 2.21 \text{ m} (0.083) \cdot 2\sqrt{35 \text{ MN/m}^2 \text{ or MPa}} = 1.48 \text{ MN} \quad (333 \text{ k});$$

i.e., the concrete confined within the wire wrap is 100 percent effective in resisting shear.

$$V_{sj} = \frac{V_P - V_c}{\phi} = \frac{3.11 - 1.48}{0.85} = 1.92 \text{ MN} \quad (432 \text{ k})$$

Solving for $\frac{A_{ps}}{s}$ from equation 9-32:

$$\frac{A_{ps}}{s} \geq \frac{2V_{sj}}{\pi(0.8f_{pu})D \cot \theta} = \frac{2(1.92 \text{ MN})}{3.142(0.8)(1862 \text{ MPa})(1.68 \text{ m})(1.0)} = 0.000489 < 0.00098 \Rightarrow \text{OK}$$

No additional wire is required for shear strength enhancement, but wire wrap should be full height. Spacing of the wire wrap above the plastic hinge zone may be increased to reflect only the shear requirements.

Concrete jackets are usually constructed as overlays and may be of two types.

- Shotcrete overlays and mild steel reinforcement (Rodriguez and Park, 1992; Amari et al., 1994; Pardoen et al., 1998), and
- Fiber reinforced concrete overlays, comprised of a steel fiber mat wound around a column and infiltrated with slurry (Hawkins et al., 1999).

Concrete jackets have been used to force yielding away from the location of starter bar splices, and in such cases, the need to improve the performance of the lap-splice has been avoided.

Nevertheless, it is recommended that sufficient transverse reinforcement be provided in the concrete jacket to develop sufficient passive confinement to produce the pressures given by equation 9-1. Alternatively, a design pressure of 2.06 MPa (300 psi) can be used for typical columns. Flexural confinement and shear strength may be determined by methods similar to those used for design of new reinforced concrete members.

A concrete jacket will increase the flexural strength and stiffness of a column more than a steel jacket, composite or wire wrap, with potentially undesirable effects on bridge performance. These increases in strength and stiffness need to be included in the analytical model that is used to determine the effectiveness of any retrofit scheme using these jackets.

9.2.1.4. Supplemental Column Shear Walls

Infill shear walls are walls cast-in-place between the columns of a multi-column pier. They have been used successfully to increase transverse shear capacity, as shown in figure 9-18. These walls prevent the formation of plastic hinges in the columns during transverse loading, and will help overcome deficiencies in the flexural or shear strength of the pier cap. For single column piers, a buttress wall can be used on one side of the column. Strengthening in the longitudinal direction by this means is usually difficult, due to geometric constraints, but the need can often be avoided in relatively short bridges by relying on the abutments to carry the longitudinal earthquake forces.

To be effective, infill shear walls should be designed to act compositely with the existing members. This is usually done by providing a sufficient number of drilled and bonded dowels in the columns and bottom of the pier cap, so that shear is transferred at the interfaces through a shear friction mechanism. This may require the existing concrete surfaces to be roughened to minimize the number of dowels required. It may also be necessary to use a forming system that can be sealed so that concrete can be placed under pressure, in order to achieve a satisfactory joint along the underside of the cap beam. Small vent holes, on the order of 100 mm (4 in), through the existing cap may also be useful in this regard.

A footing, tied into the existing column footings, should be provided under the infill wall. The design should provide sufficient reinforcement to transfer all seismic forces, and should also consider the potential for differential settlement between the existing and new footings.

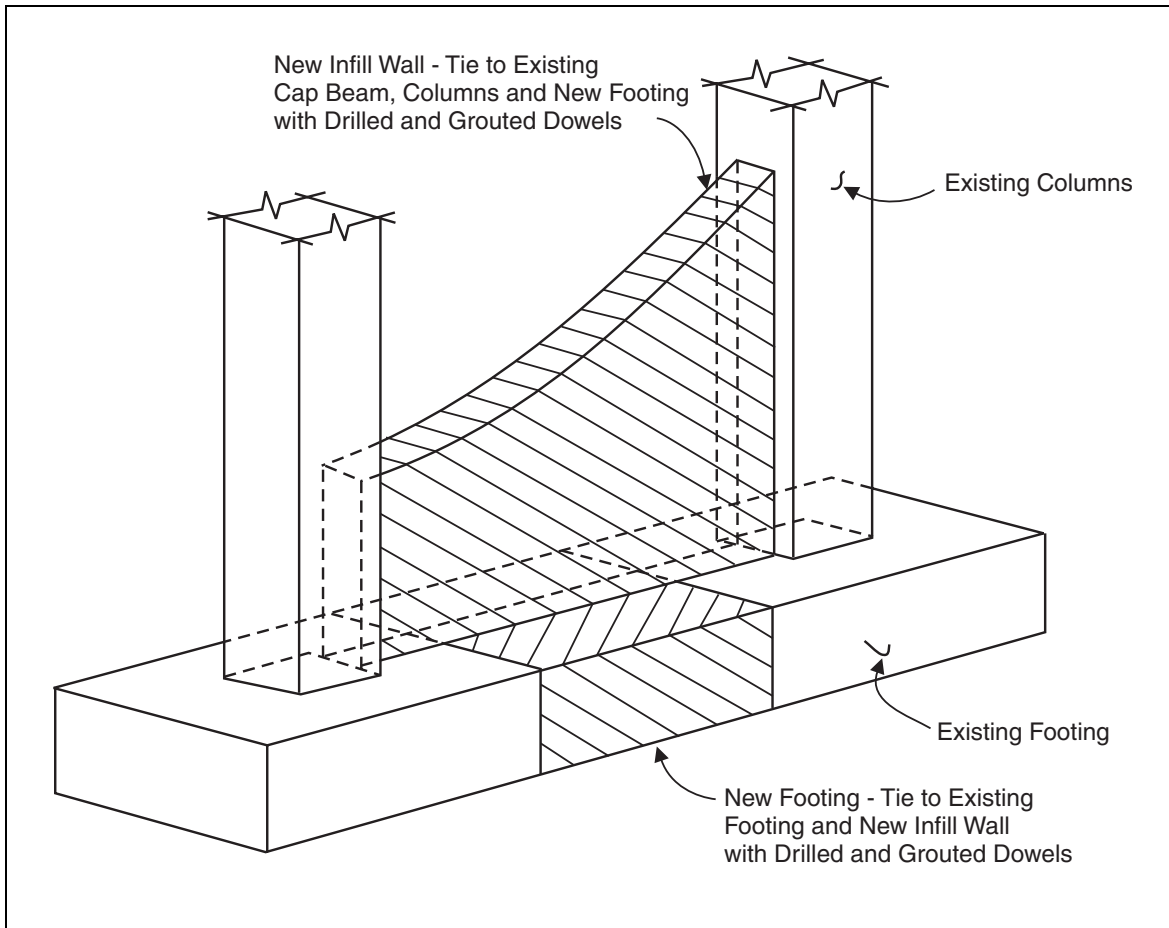


Figure 9-18. Infill shear wall in multi-column bents.

An infill wall constructed in this manner will also provide a small contribution to the longitudinal strength of the pier, which could be beneficial.

9.2.1.5. Preservation of the Vertical Load Capacity of Columns

Not all vertical load-carrying members in a bridge require strengthening or ductility improvement for lateral load, since these loads can be carried by adjacent members. However, it is necessary to ensure that the vertical load capacity of all members is preserved, at the displacements to which they will be subjected during an earthquake. Although a full retrofit of all columns would accomplish this result, it may also require that connecting elements, such as footings and pier caps, be strengthened as well.

To keep retrofitting costs to a minimum, some columns can be allowed to fail at splices or other weak points, provided their vertical load capacity is maintained. One retrofitting technique that achieves this purpose (called a 'Type P' retrofit), places a relatively thin layer of expansion joint material around the existing column before grout is placed between the column and a steel jacket (figure 9-19). The expansion joint material is flexible and will prevent flexural strengthening of the member through either composite action with the shell or enhanced performance of the

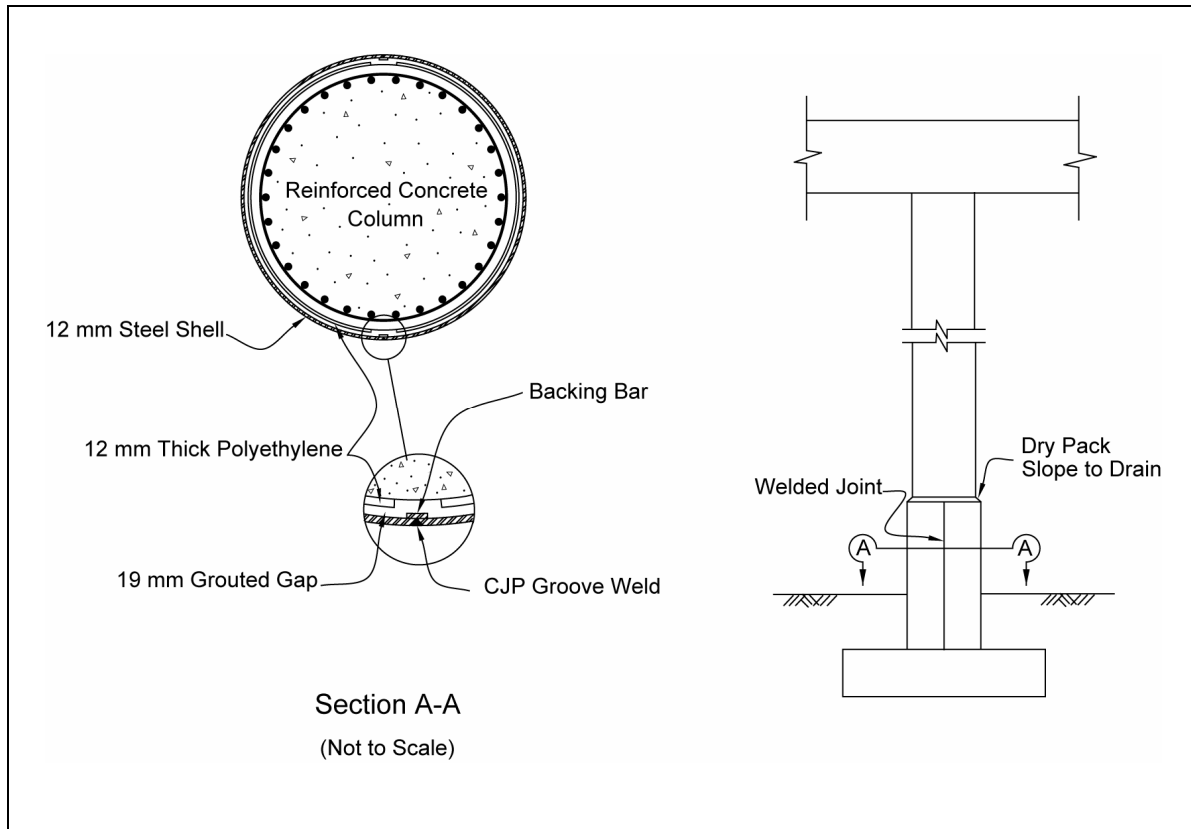


Figure 9-19. Steel shell retrofit for vertical capacity preservation.

confined concrete. As the column concrete fails, the resulting rubble will be retained within the steel shell and thus continue to support vertical load. The cost of this approach is typically only a fraction of the cost of a full column retrofit, particularly if the strengthening of footings and cap beams can be avoided.

9.2.1.6. Limitation of Column Forces

Instead of retrofitting columns to increase their capacity, an alternative approach is to reduce the forces to be resisted. This is a particularly useful approach when column strengthening or ductility improvement is impractical. Two methods for doing this are discussed below. Any method that uses a weakened section or ‘fuse’ to protect the substructure falls into this category.

9.2.1.6(a). Isolation Bearings

Isolation bearings can be used as a mechanism to limit inertial forces transmitted to the substructure. The bearings will change the dynamic properties of the bridge and add damping (section 8.3.2.2). The Sierra Point Overhead on US 101 near San Francisco was the first bridge in the U.S. to be retrofitted using this approach (figure 9-20). In this skewed, multi-span, steel beam bridge, the columns and footings were particularly weak and non-ductile. Isolation bearings were placed at the top of each column and at the abutment seats, to modify the response

and limit the forces that can be transferred to the columns. The result was a retrofit approach in which the columns did not require strengthening.

It is not always necessary to use custom-designed isolation bearings to limit the forces being transmitted to the substructure, nor is global response modification always required. Use of a standard sliding bearing at a vulnerable location, such as on top of a particularly stiff or brittle pier, could protect the pier from damage if the superstructure is continuous and can redistribute lateral loads to adjacent ductile supports.

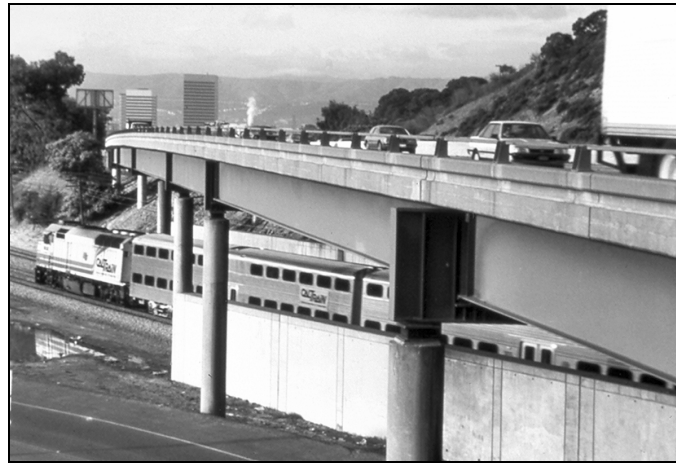


Figure 9-20. Sierra Point overhead, US 101, near San Francisco, California.

9.2.1.6(b). Flexural Strength Reduction

In certain cases, the flexural strength of a column can be reduced, in conjunction with ductility improvement, and thereby limit the shear forces transmitted to columns. This is because the ultimate shear demand on a column is directly proportional to the plastic moment that can be developed. Columns retrofitted according to section 9.2.1.3 may have sufficient capacity (as a result of a retrofit for flexure) to satisfy this shear demand. In some cases, it may not be practical or desirable to use column jacketing over the full height of the column – for example, when a large architectural column flare exists. Such flares are difficult to confine with a jacket, and it may be preferable to leave them in place for their architectural effect. If inadequate capacity exists to resist the shear demand, it may be possible to reduce the plastic moment by cutting longitudinal reinforcement near the base of the column; this will reduce the plastic shear demand. Because the ductility demand at the weakened section is likely to increase, it will also usually be necessary to provide some form of ductility improvement over the affected portion of the column. This part of the column is usually prismatic below the architectural flare and may even be below or near ground level.

A retrofit in which the primary column reinforcement is cut, allowing the column to act as a pin by rocking on steel bearing plates that are attached to a concrete retaining collar, is illustrated in figure 9-21.

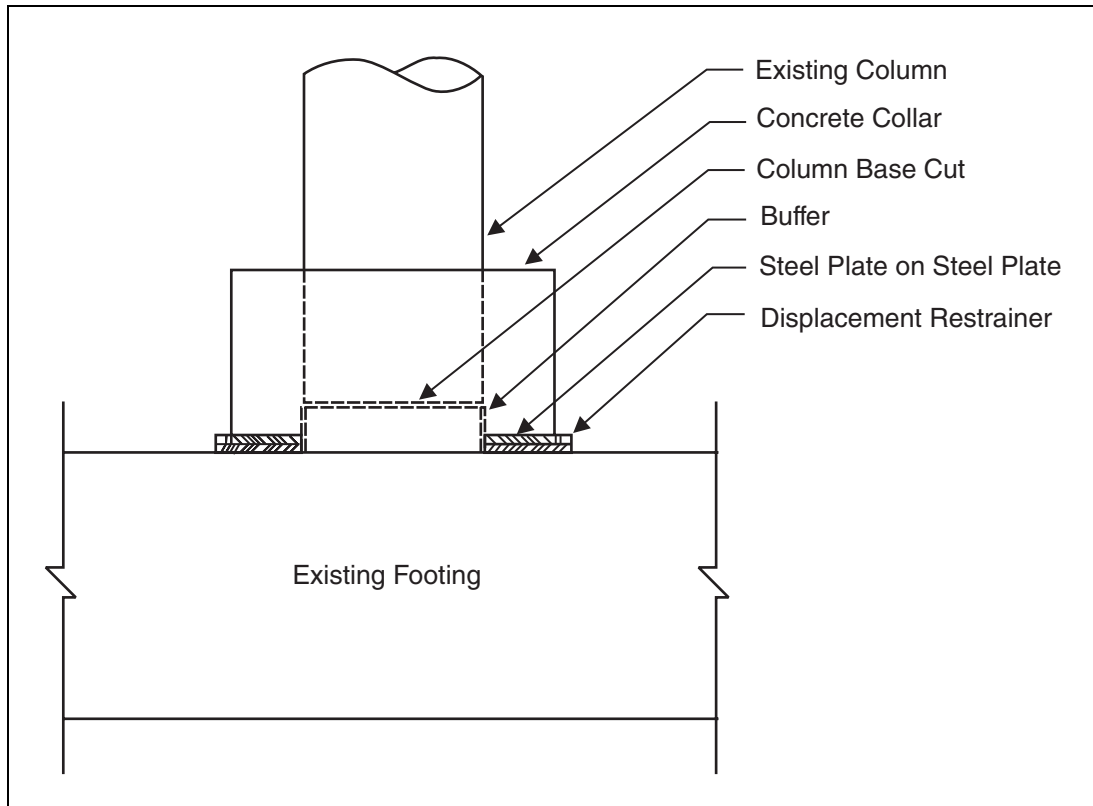


Figure 9-21. Column retrofit by flexural strength reduction.

9.2.2. STEEL COLUMNS, FRAMES AND COMPRESSION MEMBERS

Although steel is a ductile material, steel substructures and steel compression members are often vulnerable to damage during an earthquake due to inelastic buckling. Once local buckling occurs, steel can fracture due to low cycle fatigue. This type of behavior can cause a rapid loss in strength that will effectively limit the ductility of a steel member. Therefore, the retrofitting of steel compression members usually focuses on preventing or delaying inelastic buckling. The following sections describe retrofitting techniques that have been used or proposed for steel compression members.

9.2.2.1. Braced Frames

Although more common in building design, steel braced frames have been used as piers in many bridges. These frames rely on diagonal members subjected to both tension and compression to carry lateral load, and vertical members to carry gravity load. Seismic retrofitting may include strengthening of the steel members, or increasing the ductility of the frame.

The diagonal members in existing braced frames are usually not strong enough to resist earthquake loads elastically. When these members are subjected to compression loading, they will usually experience global or local inelastic buckling, which will reduce the overall ductility of the frame.

In the case of concentrically braced frames, the diagonals are usually not relied upon for compression. Therefore, only one set of diagonals, acting in tension, is considered effective in resisting lateral loads. Yielding of these members should be limited to prevent excessive permanent displacements of the frame, and to prevent tension diagonals from experiencing excessive buckling during the reverse cycle of loading. This may be done by strengthening the diagonal bracing, through either member replacement or adding supplemental diagonal members. An example of diagonal strengthening on a light steel structure is illustrated in figure 9-22. In designing such a retrofit, capacity design principles should be used to assure all other members and their connections behave elastically. The diagonal members may be designed in tension using a force-based approach. It is suggested that an R-factor of two be used, and that ultimate capacities be determined using the provisions of the *AASHTO LRFD Specifications* (AASHTO, 1998). Alternatively, a displacement-based approach using pushover analysis may be used if member elongation is limited to a reasonable level (e.g., on the order of one percent).

In the case of chevron bracing (K-bracing), diagonal members are designed to participate in both compression and tension. Earthquake loading will cause global or local inelastic buckling of the compression members if they are not designed to carry the loads elastically. Because member capacities that are sufficient to assure elastic behavior cannot generally be economically achieved, retrofits of these types of frames often seek to limit the force levels in the diagonal members by other means.

One example is the retrofit of the Richmond-San Rafael Bridge, a major structure spanning San Francisco Bay. Existing chevron braces in the bridge were replaced with eccentric braces that included a shear link (Itani, 1996). Vertical steel members were also strengthened. This retrofit was designed to increase the ductility of the pier, while forcing all yield to occur in the specially designed shear link. The existing pier and the proposed retrofit are shown in figure 9-23.

9.2.2.2. Built-up Compression Members

Steel bridge columns occasionally consist of members that are built-up from standard rolled shapes and plates. These members usually do not meet the criteria for compact sections and are prone to local inelastic buckling when plastic hinges form. Such buckling can lead to fracture of the steel due to low cycle fatigue and a corresponding decrease in the ductility capacity of the bent.

Steel columns of this type that can be retrofitted by the addition of steel plates are shown in the cross-section of figure 9-24 (Holombo et al., 1994). In addition to strengthening the column, these plates are intended to reduce local inelastic buckling of the section. Another method for retrofitting this column is to use an elliptical grouted steel shell, similar to that used for concrete columns, to prevent local inelastic buckling, as shown in figure 9-25.

Because many existing steel substructure members do not meet current design standards, it is often difficult to predict how they will behave under seismic loading conditions. When this is the case, laboratory testing involving cyclic loading should be considered to determine the behavior of as-built columns and to validate proposed retrofit concepts.

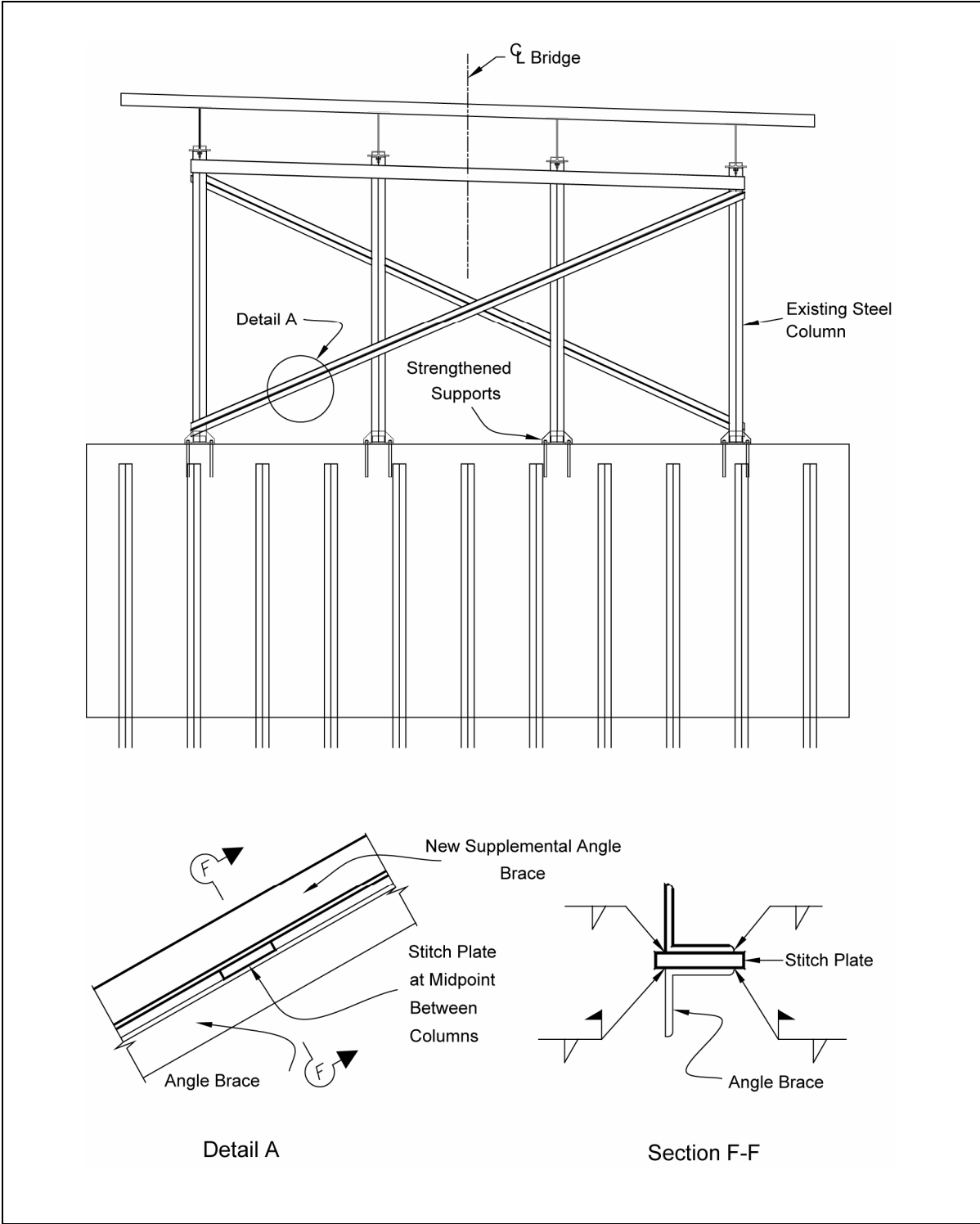


Figure 9-22. Retrofit of X-braced steel bent.

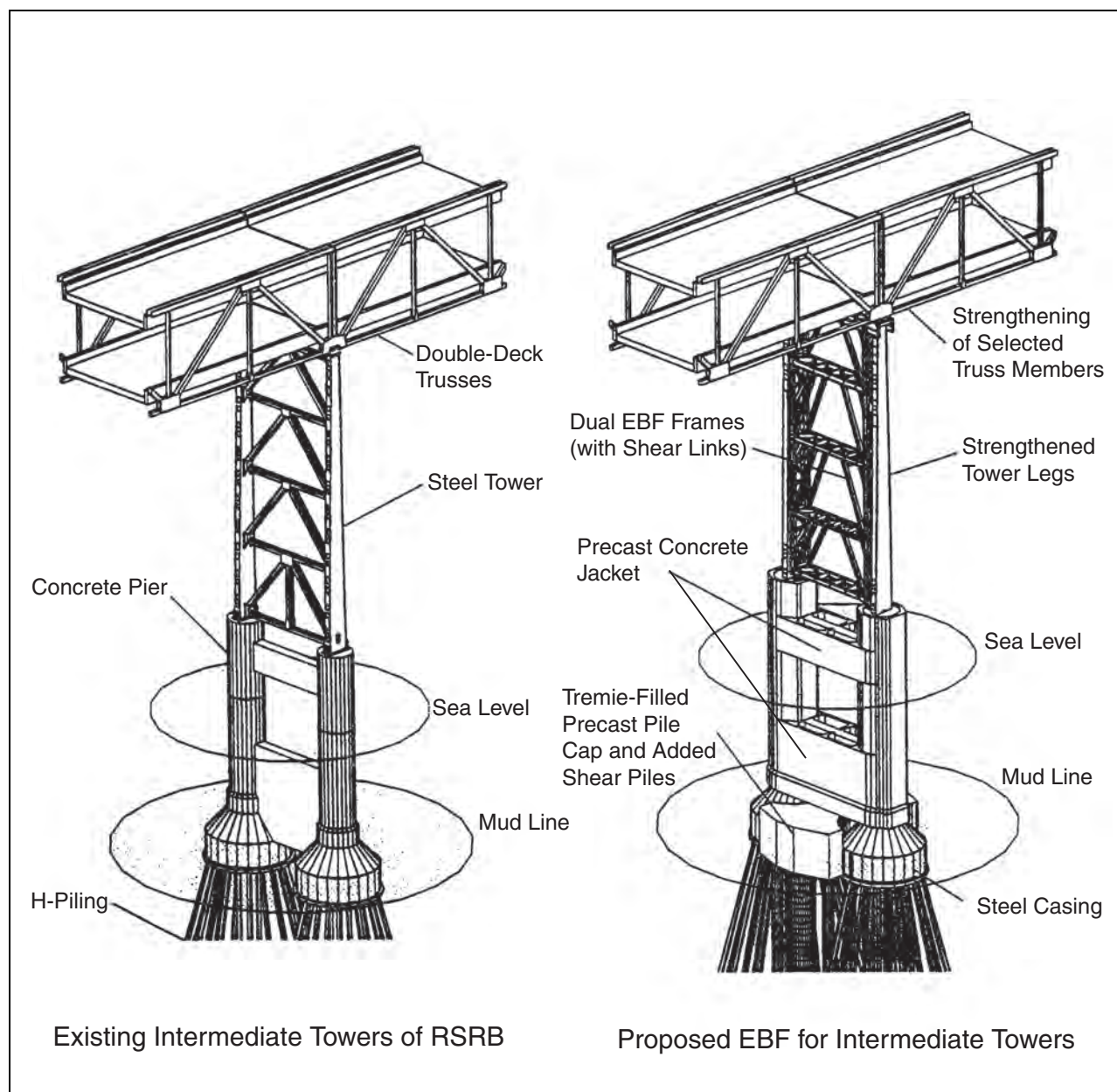


Figure 9-23. Richmond-San Rafael bridge bent retrofit.

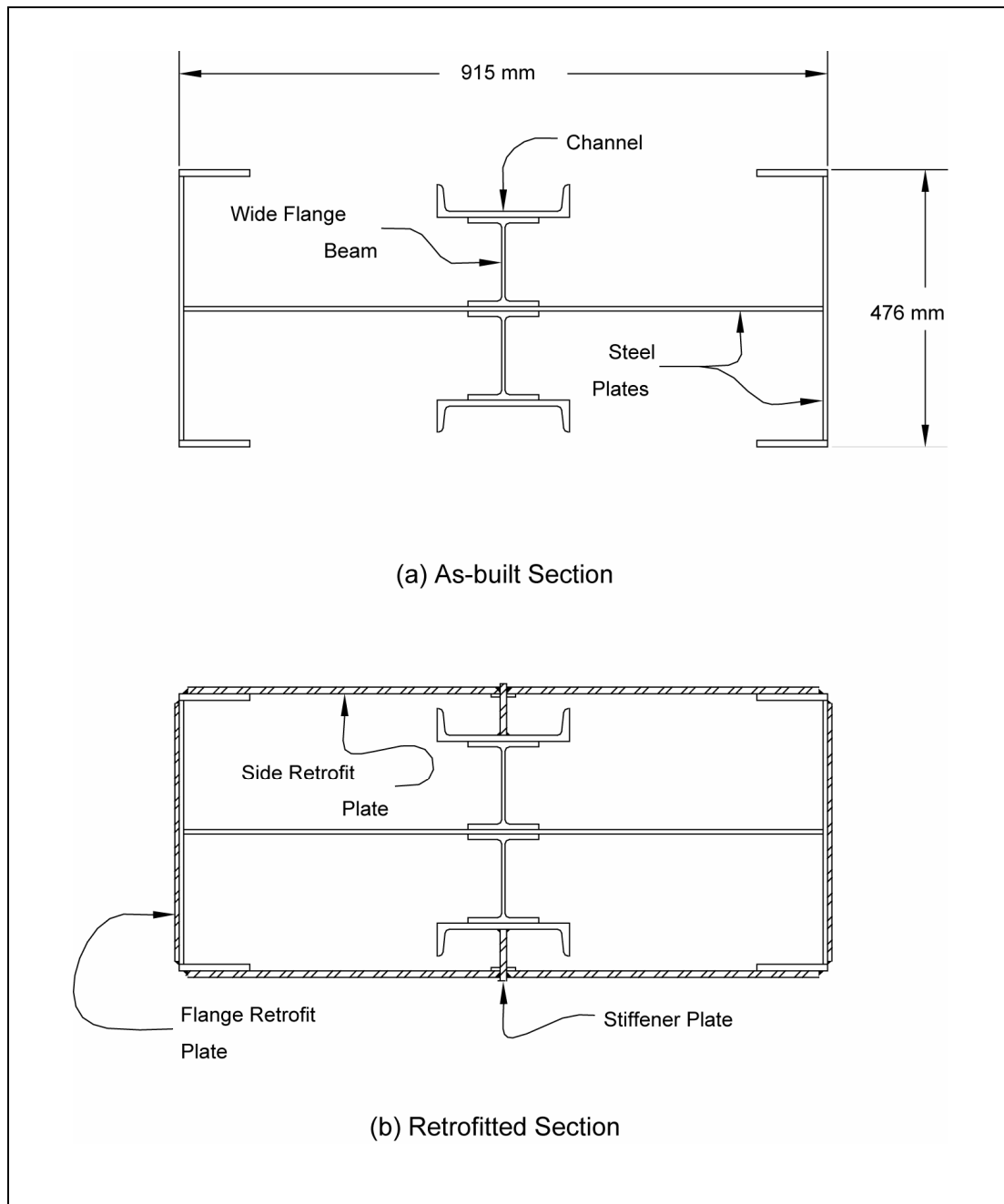


Figure 9-24. Built-up steel columns stiffened by plates.

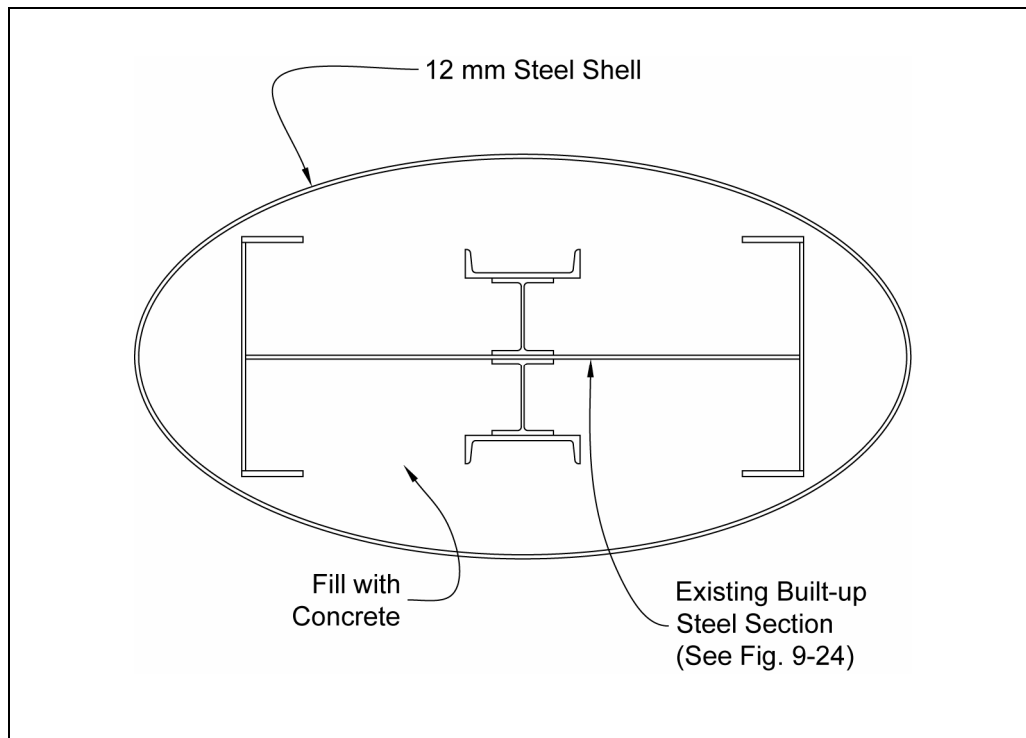


Figure 9-25. Built-up steel column retrofitted with steel shell.

In the case of single-column piers, the moment connection between the column and the footing may also require retrofitting, particularly if the column has been strengthened. This connection should be designed to behave elastically, based on capacity-design principles.

9.2.3. CONCRETE WALL PIERS

Concrete wall piers are very stiff and very strong in the transverse direction. In general, they will not require retrofitting in this direction, but the designer should make sure that the foundations are adequate for the lateral loads transmitted from the piers. These foundations should not experience displacements that could jeopardize the stability of the structure.

In the weak (longitudinal) direction, pier walls are typically treated like conventional reinforced concrete columns. However, even without retrofitting, walls often exhibit high ductility capacity in this direction because the axial concrete stresses are distributed over a larger area due to the large transverse width and low longitudinal reinforcement ratios. As a result, a force-based design is appropriate using R-factors of four or greater, even for walls with nominal levels of transverse reinforcement (Haroun et al., 1994; Abo-Shadi et al., 2000). Therefore, retrofitting of pier walls is frequently unnecessary unless inadequate starter bar splices are present within the potential plastic hinge zone. When they are present, the wall may be retrofitted by the placement of a steel plate over the height of the plastic hinge region of the pier (Haroun et al., 1994). Bolts, anchored by nuts and heavy steel and plate washers, are drilled through the pier at relatively close spacing to brace the steel plate. The bolts are placed so as not to interfere with the existing vertical reinforcing steel, as shown in figure 9-26.

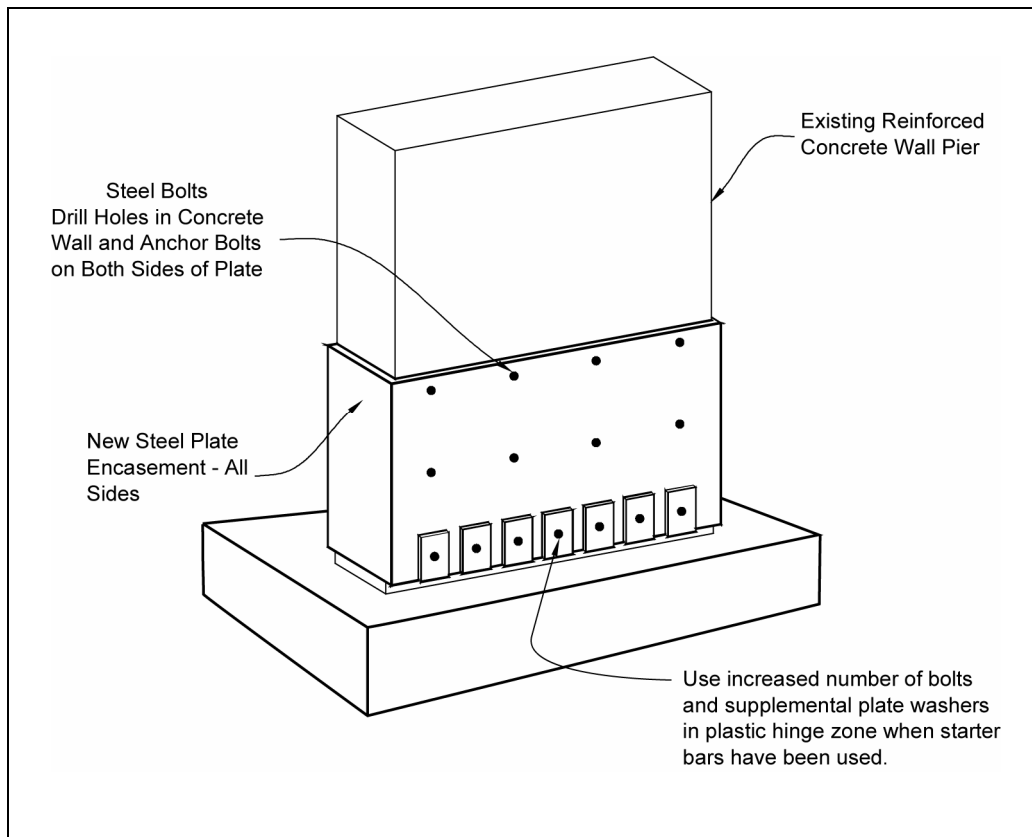


Figure 9-26. Retrofit for wall pier with starter bars.

9.3. RETROFIT MEASURES FOR CAP BEAMS AND COLUMN-TO-CAP BEAM JOINTS

The preferred location for plastic hinging is at the ends of columns. In the past, cap beams were designed without consideration for earthquake effects, and little if any positive moment reinforcement was provided in the cap beam adjacent to an exterior column. Negative moment reinforcement at this location may also be inadequate. This will lead to plastic hinging in the pier cap, which most probably will have only limited capacity for ductility and retrofitting the beam may be necessary. Cap beam retrofitting may also be necessary for unusual pier configurations, such as outrigger frames, 'C' frames, and double-deck bridges.

Retrofitting methods used for concrete cap beams must consider both the longitudinal and transverse response of the bridge, which is dependent on the configuration of the pier. Several typical configurations for multi-column piers are shown in figure 9-27.

Because cap beams are usually cast integrally with reinforced concrete columns, transverse loading will subject the cap beams to flexural and shear stresses. Column-to-cap beam joints will also be subjected to large stresses and are vulnerable to damage during an earthquake transverse to the bridge. Because existing cap beams and joints were not usually designed to behave in a ductile manner, the retrofit design must ensure that these elements are either capable

of accommodating the ductility demands placed on them, or are capable of elastically resisting the forces that will result from plastic hinging in the columns.

The longitudinal response of a pier with bearings, as shown in figure 9-27(a), does not usually result in significant cap beam stresses, although some torsion and weak axis bending will occur. This is because longitudinal moments at the tops of the columns are small. A similar situation exists in a cap beam that is integral with the superstructure when the columns are pinned at the top, as indicated in figure 9-27(d). Therefore, retrofit designs for these cap beams will generally be expected to resist stresses and strains resulting from transverse response only. An exception is for the cap beam of an outrigger pier, for which the longitudinal response of the bridge can cause significant weak-axis bending and shear in the beam.

Longitudinal response is most significant when the superstructure is integral with the pier cap and the columns are fixed at the top, as shown in figures 9-27(b) and (c). When the columns are located within the width of the superstructure, as in figure 9-27(b), the superstructure itself helps to resist the moments and shears generated at the tops of the columns (Priestley, 1993).

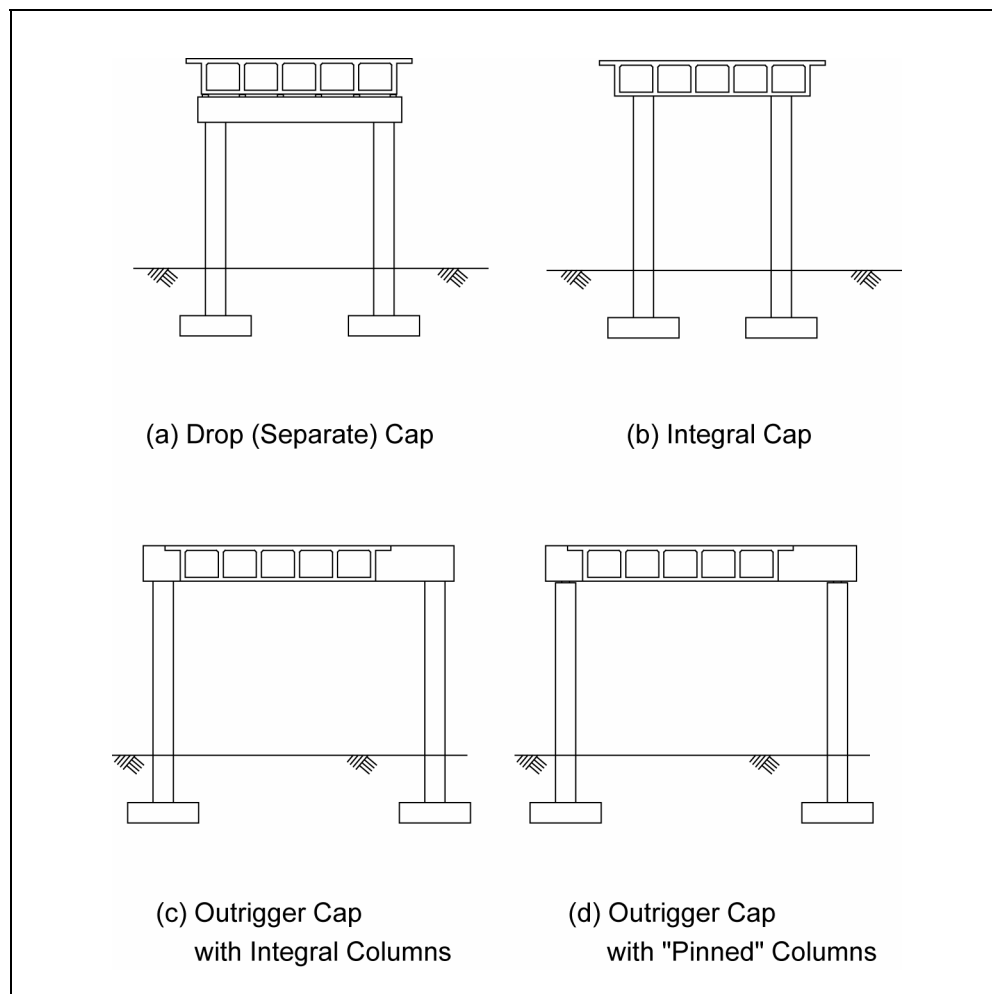


Figure 9-27. Typical cap beam configurations for boxgirder bridges.

Although research has shown that the pier cap can become overstressed and heavily cracked due to longitudinal response, a collapse mechanism is seldom formed in the cap and retrofitting will usually not be required unless a higher level of seismic performance is desired. However, when the pier cap is of an outrigger type, as shown in figure 9-27(c), the torsional and weak axis bending stresses in the cap and column-to-cap joint resulting from longitudinal response will be large. In this case, it is often necessary to strengthen the cap beam to resist these forces, as well as those resulting from transverse loading.

When cap beams can fail, the bridge is in danger of collapse and retrofitting the cap beams is essential. The following sections describe several methods for retrofitting concrete cap beams and column-to-cap beam joints.

9.3.1. PIER CAP REPLACEMENT

Total or partial pier cap replacement should be considered whenever column replacement is being contemplated.

9.3.1.1. Partial Replacement at a Joint

Because of the large amount of retrofitting required to make an outrigger cap-to-column joint seismically resistant, it is sometimes more practical to simply replace the joint. Design criteria are the same as for joints in new bridges. This method was widely used on knee joints in various San Francisco viaducts after the 1989 Loma Prieta earthquake. Many of these retrofits involved the replacement of existing columns or the construction of supergirders (see section 9.3.4) that made joint replacement necessary. These new joints must tie into existing or strengthened pier caps, which will require splicing into existing cap beam reinforcement. The remainder of the cap may also require strengthening by the methods discussed in section 9.3.2 and illustrated in figure 9-28.

9.3.1.2. Total Replacement

Total cap beam replacement is rare, but was used in San Francisco after the Loma Prieta earthquake where the decision to replace, rather than strengthen, was based on savings in time and cost. Significant shoring will be necessary if a cap beam is replaced and the bridge kept open to traffic.

9.3.2. PIER CAP STRENGTHENING

The flexural strength of a cap beam is usually less than that of the columns framing into it. This is frequently the case for positive moment in the cap beam (i.e., tension on the lower face) as a result of a small amount of bottom reinforcement anchored in the joint region. Negative moment capacity may also be insufficient to force plastic hinging into the columns, particularly when the top reinforcement is prematurely terminated. Both cases are a consequence of the design specifications used for older bridges, which were designed for full dead load but a reduced, or no, seismic load.

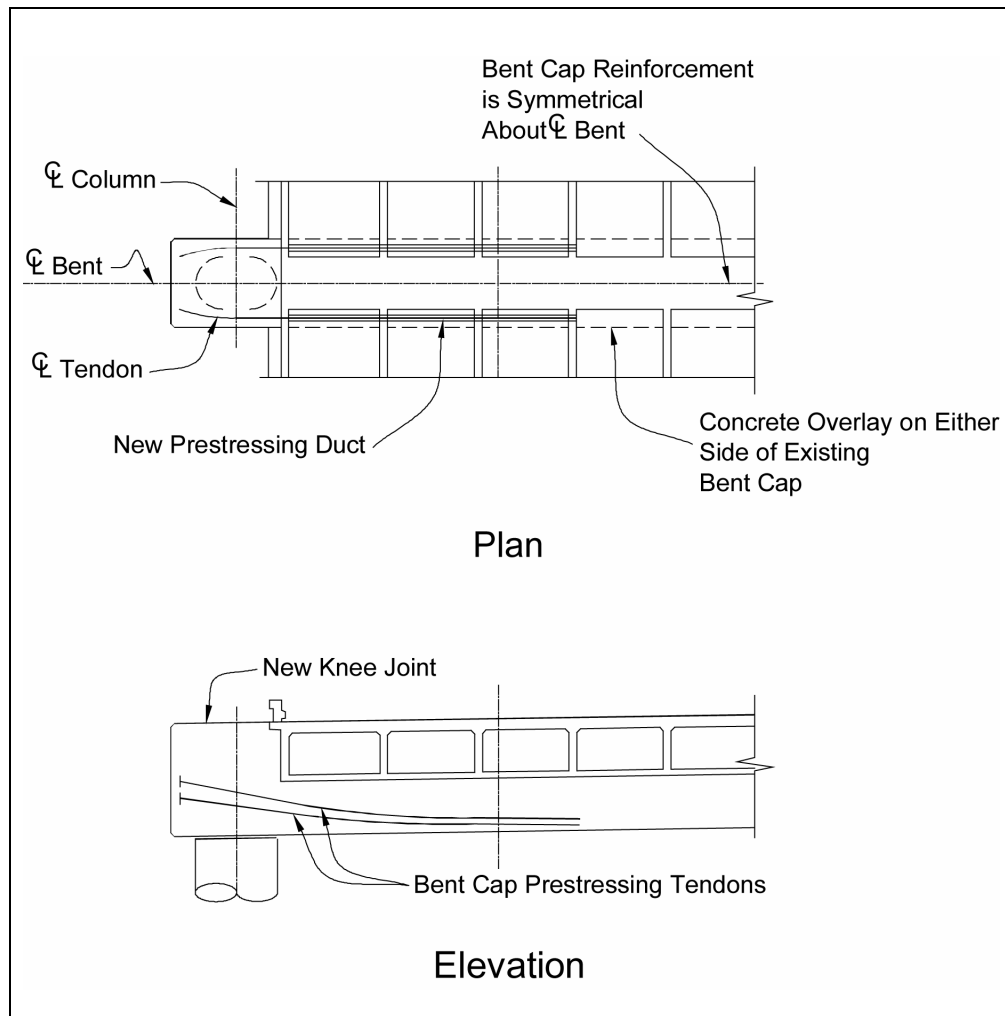
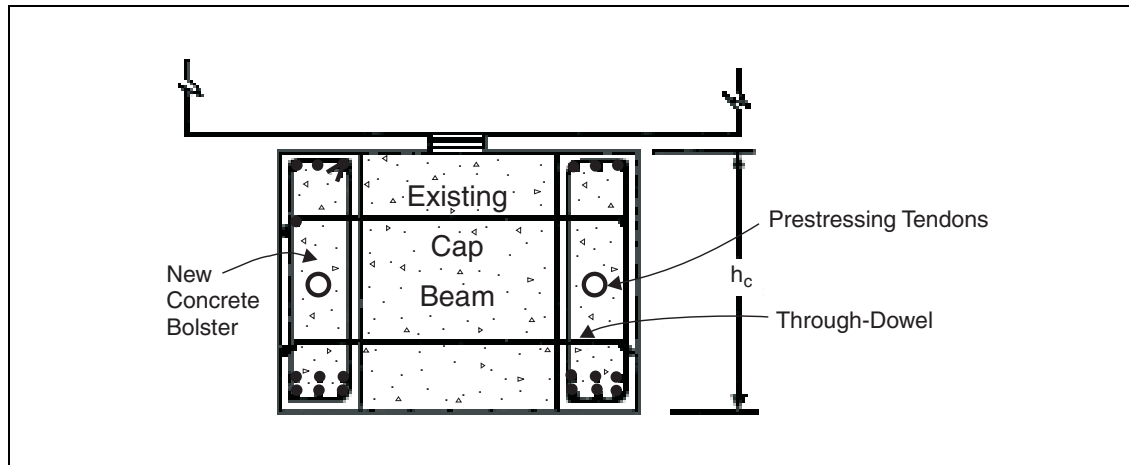


Figure 9-28. Pier cap strengthening.

There are at least two approaches to correcting these problems. One is to allow yielding to occur in the pier cap, but to make sure that the beam is capable of meeting the ductility demands placed upon it. This is often difficult to achieve, and will result in considerable damage to the cap beam that may be difficult to repair. It is generally preferable to adopt a second approach, in which the cap beam is strengthened in flexure to force plastic hinging into the columns. If necessary, the columns can then be retrofitted using one of the methods discussed earlier in this chapter. Capacity design principles are used to design the beam retrofit in the second approach.

In the case of a pier which uses bearings to support the superstructure (figure 9-27(a)), retrofitting can be done by adding reinforced or prestressed concrete bolsters to the sides of the cap beam, after roughening the interface, as shown in figure 9-29. Bolsters must act compositely with the existing bent cap to provide sufficient flexural and shear strength to prevent yielding of the cap. Because the column moment is transmitted into the existing cap, a sufficient number of dowels must be provided to transfer the moment capacity of the bolster into the existing cap at the face of the column. The number of required dowels is determined by calculating the force



after Priestley et al., 1992

Figure 9-29. Flexural and shear retrofit of free standing multi-column bents.

required to transfer the capacity of the bolster reinforcement across the vertical face of the existing cap by shear friction. For the bottom reinforcement, the vertical surface available for shear transfer may be taken as the lower half of the cap beam, taken between the centerline of the column and the midpoint between columns. Similarly, the capacity of top reinforcement in the bolster must be transferred across the corresponding upper half of the cap beam.

Prestressing the bolsters, either alone or in conjunction with additional reinforcing, will increase the flexural strength of a pier cap, as shown in figure 9-29. External prestressing may also be used, provided it is protected from corrosion. In both cases, the prestressing steel should be anchored at the end of the cap beam. It will not be necessary to transfer the capacity of the prestressing steel across the vertical interface of the existing cap beam.

Adding conventional stirrups within the bolsters, as shown in figure 9-29, may also increase the shear strength of the cap beam. Prestressing will also increase the shear capacity of the bolsters themselves. Shear design of a retrofitted bent cap should follow design procedures required for new bridges.

Prestressed bolsters were tested in the laboratory on part of a 30-year-old reinforced concrete frame, which had been salvaged from a bridge being demolished in upstate New York (figure 9-30 and Mander et al., 1996a). This retrofit also included an enlarged column-to-cap beam joint to improve the anchorage of existing reinforcing steel. The technique was effective in forcing plastic hinging to occur in the columns, which provided limited ductility for the frame as a whole. In lower seismic zones, this may be the only retrofitting that is required. Retrofitting columns, as discussed earlier in this chapter, could further enhance frame ductility for higher seismic zones.

The use of fiber composite materials has also been considered as a means of increasing the flexural and shear strength of a bent cap (Priestley et al., 1996). This method is more effective if the material can be wrapped completely around the cap (Pulido et al., 2002). Refer to ACI 440.2R-02 for guidance.

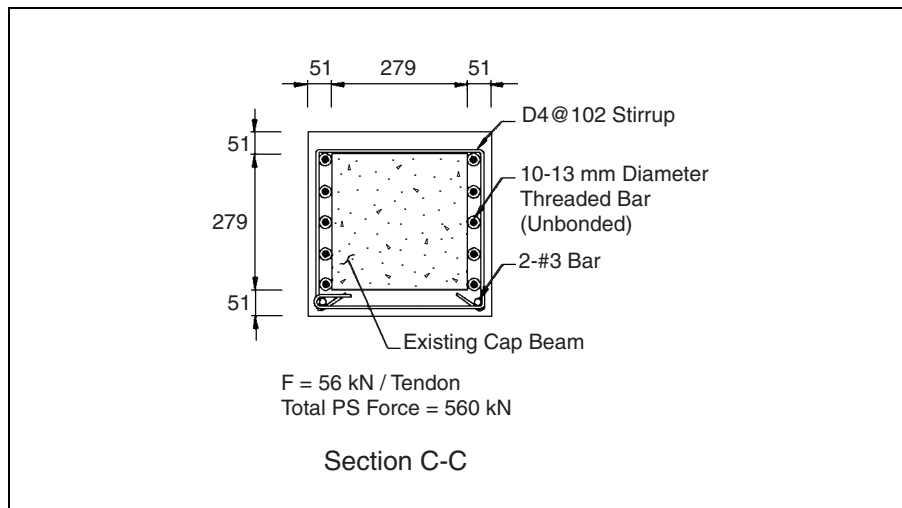
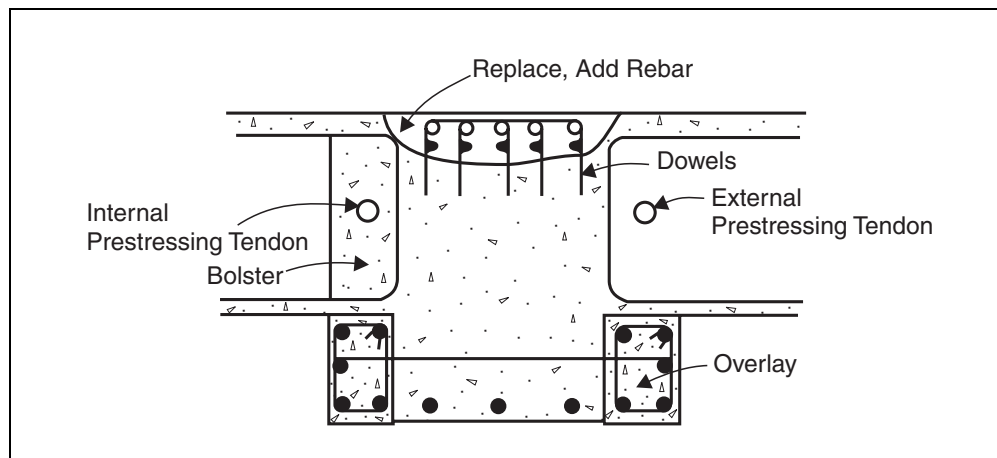


Figure 9-30. Pier cap retrofit tested at University at Buffalo.

Enhancing the flexural capacity of cap beams that are integral with the longitudinal girders is more difficult because of the geometric constraints presented by the existing girder stems on the sides of the cap. Reinforced bolsters may be added to the lower face of the cap beam to increase positive moment capacity, but it is more difficult to rectify inadequate negative moment capacity. Removing concrete from the top of the beam and adding additional reinforcement can increase this capacity, but this will require closure to traffic and most probably shoring of the cap beam to prevent failure under gravity loads. External prestressing placed in grouted galvanized ducts or conventional prestressing within bolsters placed between beam stems will generally be the most economical means for increasing both positive and negative moment capacity, provided elastic behavior in the cap can be assured through capacity design principles. This retrofit is shown in figure 9-31.



after Priestley et al., 1992

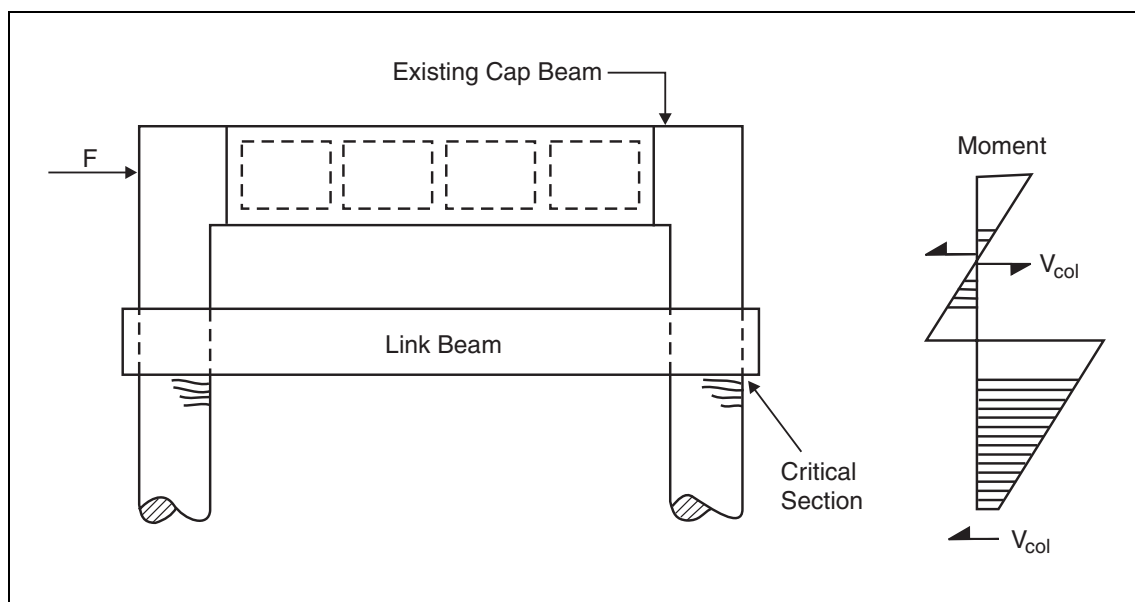
Figure 9-31. Flexural and shear retrofit of integral cap beams.

9.3.3. REDUCTION OF PIER CAP FORCES

It may be possible to reduce bent cap forces by using isolation bearings as force limiting devices, in a manner similar to that described earlier for columns. However, if the force reduction is not sufficient to prevent column yielding, it will not limit forces in the cap beam. An alternative method to alleviate cap beam problems is to construct a 'link beam' below the existing pier cap, as shown in figure 9-32.

The link beam is cast around the existing column and creates a new critical section in the column just below the link beam. This limits shear forces in the column to the plastic shear achieved in the portion of the column below the link beam. If the vertical distance between the link beam and existing cap beam is sufficiently small, then the moments in the section of the column between these two beams will also be small since they are a function of the plastic shear and the distance between the beams. Moment equilibrium at the column-to-cap beam joints then dictates that cap beam forces due to seismic actions are limited to relatively small values, and no further retrofit is needed. The link beam must be designed according to capacity design principles to ensure that plastic hinges form in the column, and not in the link beam.

Link beams can be very effective in retrofitting tall piers. Judicious choice of the position of the link beam will result in protection for the existing cap beams, coupled with a substantial increase in lateral strength and stiffness of the bent. The technique can also be used to advantage at ground level, by linking columns transversely or longitudinally to alleviate footing problems.



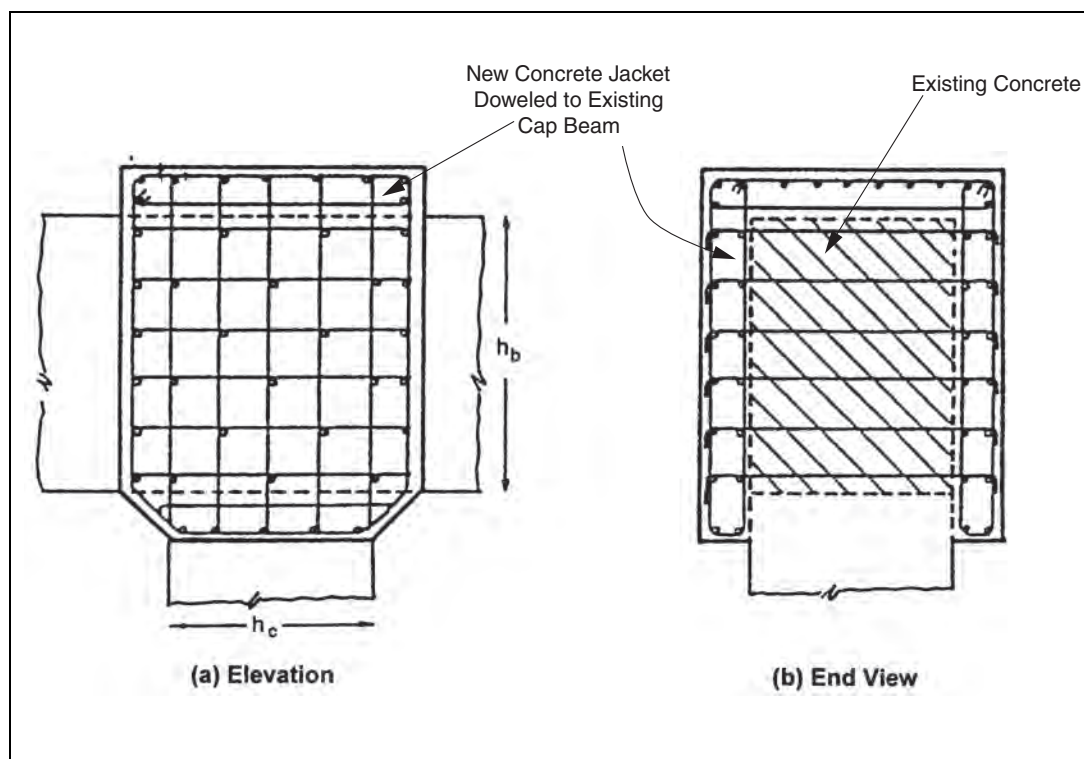
after Priestley et al., 1992

Figure 9-32. Horizontal link beams for pier cap force reduction.

The resulting location for column hinge formation must be checked for adequate ductility capacity. Shear forces in the columns will also increase due to the shorter column length below the link beam. Column retrofit measures, as described previously in this chapter, will need to be considered when the requirements for column ductility or the shear force demands become excessive as a result of adding the link beams.

9.3.4. STRENGTHENING OF COLUMN AND BEAM JOINTS

Inadequate shear strength is a common problem in column-to-cap beam joints in many older bridges. The anchorage of reinforcement within these joints and stresses resulting from torsion are also of concern. Techniques developed for the retrofit of several San Francisco double-deck viaducts following the 1989 Loma Prieta earthquake may also be applied to bridge piers of the types shown in figures 9-27(a) and 9-27(d). Generally, both vertical and horizontal shear reinforcement is needed in the joint. The most satisfactory solution will be the complete replacement of the joint, as described in section 9.3.1. This also enables deficiencies in the anchorage of column and beam reinforcement to be rectified. However, adequate performance could also be ensured by reinforced concrete jacketing, which is added to the sides of the joint region, as shown in figure 9-33.



after Priestley et al., 1992

Figure 9-33. Joint retrofit with external concrete jacket.

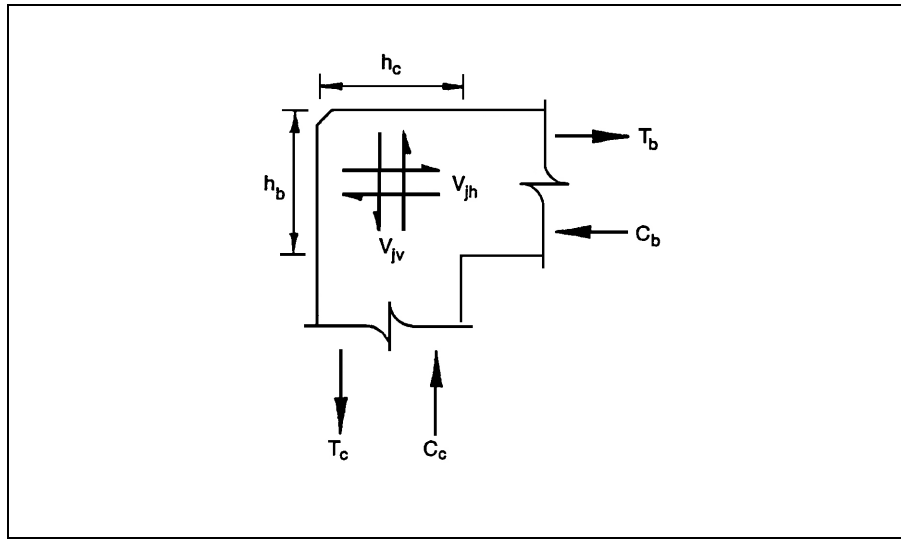
Since the shear resistance at the joint is provided by reinforcement external to the original joint, the new concrete jacket must be doweled into the existing concrete to transfer the shear force by friction. This is because shears develop within the original joint as a consequence of column

flexural actions, and these must be transferred across the joint by the external reinforcement. Referring to figure 9-34, the interface between new and old concrete is simultaneously subjected to friction forces in the vertical and horizontal directions. The shear forces are found from equilibrium with the flexural forces in the cap beam and column. Thus, in figure 9-34:

$$V_{jh} = T_b \quad (9-33)$$

and

$$V_{jv} \approx V_{jh} \cdot \frac{h_b}{h_c} \quad (9-34)$$



after Priestley et al., 1992

Figure 9-34. Free body diagram of shear forces on a knee joint.

Assuming that all joint shear resistance is provided by reinforcement in the new concrete on the side of the joint, the horizontal and vertical interface shear stresses will be:

$$v_{ih} \approx \frac{V_{jh}}{2h_b h_c} \quad (9-35)$$

and

$$v_{iv} \approx \frac{V_{jv}}{2h_b h_c} \quad (9-36)$$

where the two in the denominator is required because 50 percent of the shear is transmitted across each of the two interfaces between new and old concrete, one on each side of the joint. The maximum interface shear is the vector combination of v_{ih} and v_{iv} . That is:

$$v_i = \sqrt{v_{ih}^2 + v_{iv}^2} \quad (9-37)$$

Substituting V_{jh} and V_{jv} from equations 9-33 and 9-34 into equations 9-35 and 9-36, respectively, and further substituting into equation 9-37 yields:

$$v_i = \frac{V_{jh}}{2h_b h_c} \sqrt{1 + \left(\frac{h_b}{h_c}\right)^2} \quad (9-38)$$

A shear friction clamping stress equal to v_i must be provided across the interface, and it follows that the dowels must satisfy:

$$\frac{A_d f_y}{s^2} \geq v_i \quad (9-39)$$

where A_d is the area of the dowel bar, f_y is the yield stress of the dowel, and s is the spacing of dowels on a square grid.

Wherever possible, the jacket should extend over the top of and underneath (at the corners) the cap beam, as shown in figure 9-33, to improve the connection to the cap beam. It is also recommended that the interface friction stress given by equation 9-38 be limited to:

$$v_i \leq 0.2 f'_c \leq 6.9 \text{ MPa (1000 psi)} \quad (9-40)$$

where f'_c is based on the weaker of the existing and new concrete strengths. Increasing the size of the joint overlay will increase the effective bond lengths for existing column and cap beam reinforcement within the joint, thus mitigating anchorage problems.

It is noted that transverse prestressing reduces the need for horizontal shear reinforcement of the joint and should also improve the transfer of the vertical shear through the joint.

Steel jackets bonded to the sides of the joint and anchored to the bent cap are also an effective retrofit measure (Thewalt and Stojadinovic, 1995). This technique, which also includes column retrofitting to increase pier ductility, is illustrated in figure 9-35.

Column-to-cap beam joints that are integral with the superstructure are less likely to require retrofitting for longitudinal or transverse response. Despite the fact that these joints are subject to damage during an earthquake, this damage is unlikely to cause the collapse of the bridge (Priestley, 1993). When retrofitting is required to strengthen these joints for longitudinal response, transversely prestressed bolsters, as shown in figure 9-36, may be used.

9.3.5. SUPERGIRDERS

If an outrigger pier cap is integral with the superstructure, as shown in figure 9-27(c), the longitudinal response of the bridge produces flexural actions in the superstructure and torsion in

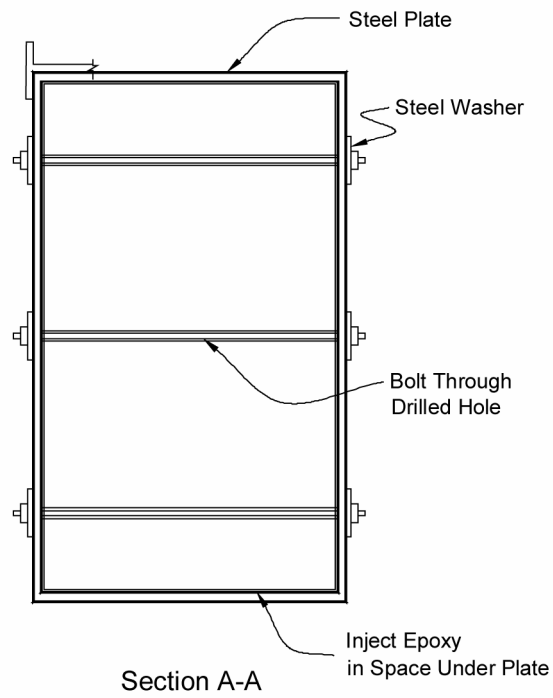
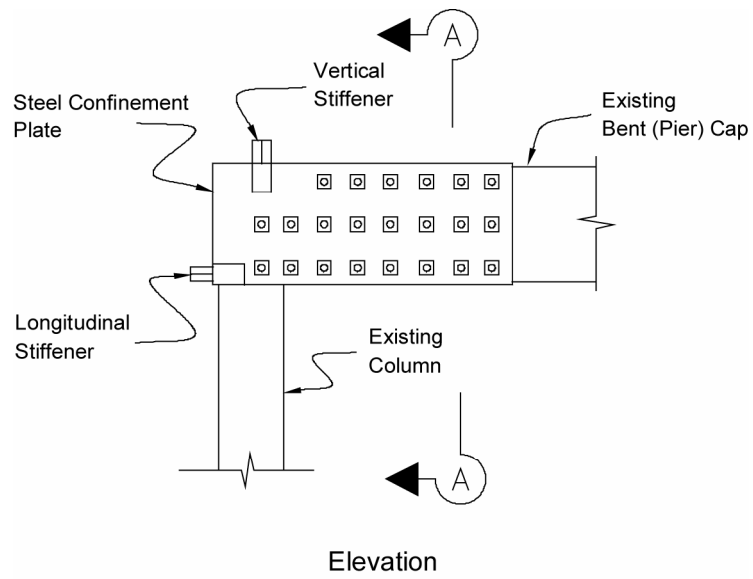


Figure 9-35. Knee joint retrofit with steel plates.

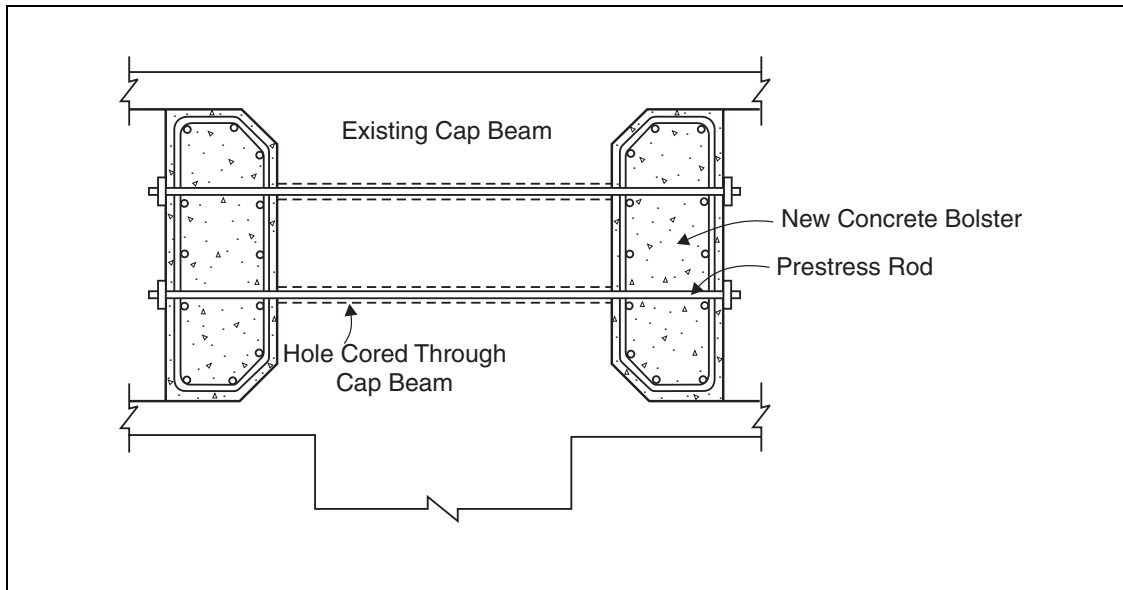


Figure 9-36. Retrofit of an integral cap beam joint for longitudinal loading.

the cap beam. These effects will not be significant in short bridges where superstructure displacements in the longitudinal direction are limited by the abutments. But in long, viaduct-type structures, comprising two or more segments, these effects will be important. In these cases, cap beam torsional moments will develop, equal to the column's longitudinal plastic moment capacity. Because of the torsional flexibility of the cap beam, this torsional moment is not uniformly distributed to the longitudinal beams in the superstructure. As a consequence, the moment demand on the beams closest to the columns will be highest, while beams near the bridge centerline will be subjected to very little moment. This effect is accentuated when torsional cracking of the cap beam occurs, since the torsional stiffness of a beam, after cracking, quickly reduces to about 10 percent of the uncracked value.

The retrofit of outrigger frames on several San Francisco double-deck viaducts involved the addition of an edge beam (termed a supergirder) in the plane of the columns from pier to pier to reduce the torsional effect, as shown in figure 9-37. Provided that the edge beam is sufficiently stiff and strong, inadequacies of cap beam torsional strength and superstructure flexural capacity become largely irrelevant, since satisfactory longitudinal response can be assured even when the cap beam has zero torsional capacity. Under these conditions, the design approach is to force plastic hinges into the column rather than the supergirder, since plastic hinges in the supergirder allow large rotations of the cap beam and can result in degradation of gravity load-carrying capacity. If the supergirder is protected against plastic rotation by a capacity design approach, torsional rotations of the cap beam will remain small, and will be dictated by rotational compatibility with the supergirder. Torsional cracking of the cap beam, if it occurs, reduces the torsional moment rather than increasing the torsional rotation.

Whereas the supergirder plays an important role in the longitudinal response of a long bridge, it is largely ineffective in the transverse direction. In this case, the cap beam is required to participate and simultaneously support gravity loads by beam action. Deficient cap beams may be retrofitted using one of the methods described earlier in this section.

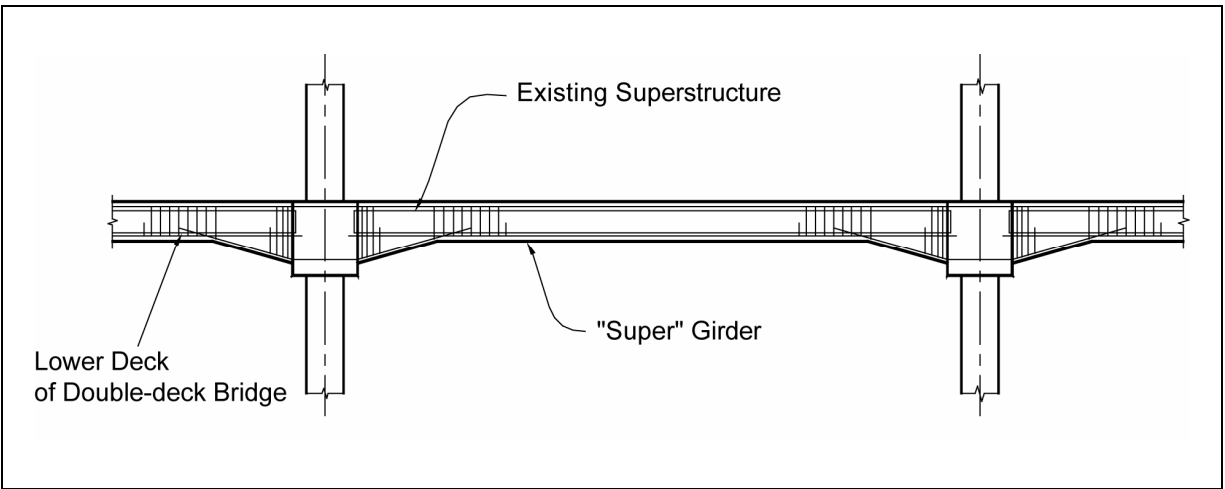


Figure 9-37. "Supergirders" added between piers to reduce torsion in pier caps.

CHAPTER 10: RETROFIT MEASURES FOR ABUTMENTS, FOOTINGS, AND FOUNDATIONS

10.1. GENERAL

Abutments, footings, and foundations connect a bridge to the earth. They are the means by which a bridge feels the effects of an earthquake. Most abutment, foundation and pier failures that occur during earthquakes can be attributed to the instability of the supporting soil due to liquefaction, lateral spreading, fault movement, or landslide. Very few bridges have collapsed due to structural failure of an abutment, piles or footings. Most failures have been soil failures. For this reason, and the fact that foundation retrofitting can often be very expensive, the designer should think twice before deciding to retrofit a foundation. It often makes more sense to tolerate a certain amount of abutment or foundation damage or movement, as long as the overall stability of the bridge is not compromised.

Nevertheless, there are instances when it may be desirable to retrofit abutments and foundations. For important bridges, immediate access to a bridge may be critical, and the potential for lateral movement of an abutment, or settlement of an abutment fill, may justify retrofitting. In addition, the use of restrainers to limit relative displacement at the abutment may result in much larger abutment forces than expected when the abutment was designed. Therefore, situations will exist in which abutment strengthening should be considered. Stiffening or strengthening an abutment can also provide an alternative load path for inertial forces, and thus reduce the load on other more critical components.

Footings that support columns may be structurally unable to resist the forces transmitted from those columns. This usually occurs when there is a lack of reinforcement in the top of the footing. Structural strengthening of the footing will be necessary to force plastic hinging into the column, which will be an important consideration if the columns are also to be retrofitted.

There are also instances where the capacity of pier foundations should be increased. This could be the case when movements of existing footings can result in overall instability of the pier. This becomes more likely when the piers are to be strengthened. Instability caused by liquefaction or lateral spreading can also occasionally be addressed by providing stronger foundations.

This chapter presents methods for abutment, footing and foundation retrofitting. Although many of these methods were proposed in the early 1980s, most were never implemented until after the 1989 Loma Prieta earthquake, when substructure retrofitting became commonplace.

10.2. RETROFIT MEASURES FOR ABUTMENTS

Retrofit measures depend to a large degree on the type of abutment. For seismic purposes, abutments may be divided into two types: seat-type abutments and integral abutments, as shown in figure 10-1.

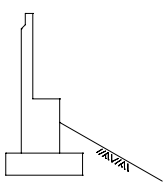
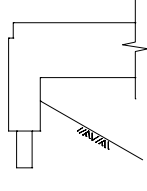
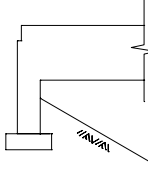
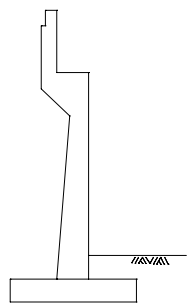
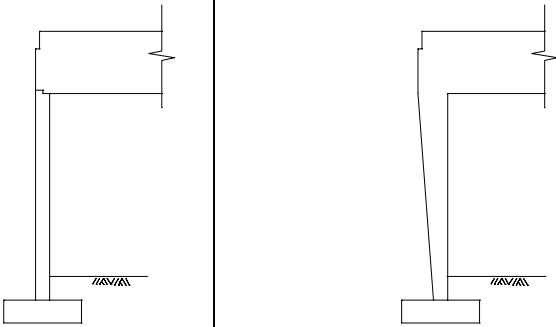
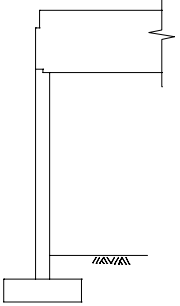
Seat-type Abutments	Integral Abutments	
 <p>Seat (Stub)</p>	 <p>Diaphragm (on piles)</p>	 <p>Diaphragm (on spread footings)</p>
 <p>Cantilever</p>	 <p>Rigid Frame</p>	
 <p>Strutted</p>		

Figure 10-1. Abutment types.

Seat-type abutments are probably the most common form. Even though significant longitudinal movement of the superstructure can occur at these abutments, loss of support does not usually result from this movement, unless the seat is particularly short or another supporting member, such as an adjacent pier, fails. In fact, unrestrained movement is often assumed in new design. Strengthening of seat-type abutments in both the longitudinal and transverse directions can, however, reduce forces on the piers in short-span bridges, and should be considered as part of an overall retrofit strategy.

Integral or diaphragm abutments are relatively stable during an earthquake. When earthquake loads are particularly large, the flexural and shear strength of the diaphragm wall may be an issue and strengthening may be necessary. As with seat-type abutments, strengthening should be considered as part of an overall retrofit strategy.

Abutments with high walls such as cantilever, strutted, or rigid frame abutments, that retain deep backfills, are likely to move outwards due to active pressure of the backfill. This can result in rotation of the bottom of the wall, causing cantilever and strutted abutment walls to become unstable and rigid frame abutments to become overstressed. Supplemental tiebacks may be required to prevent this type of failure. In these cases, the overall stability of the backfill, acting together with the abutment, must be considered.

The potential for settlement of the backfill often requires the use of approach slabs. These and other retrofit measures for abutments are discussed in the following sections.

10.2.1. APPROACH SLABS

Approach slabs, which are sometimes called settlement slabs, are intended to provide continuity between the bridge deck and the approach pavement, should the approach fill settle. An approach slab should be tied to the abutment to prevent it from pulling away and becoming ineffective. To minimize the discontinuity at the abutment, these slabs should have a minimum length of 3 m (10 ft). They are designed as simple span, reinforced concrete slabs spanning their full length.

Ties between the slab and the abutment should be capable of resisting the slab dead load, forces applied through friction between the slab and the abutment, and forces resulting from the spectral acceleration of the bridge in the longitudinal direction. That is:

$$F_D = (\mu + S_a) DL_s \quad (10-1)$$

where F_D is the design force, μ is the coefficient of friction between soil and concrete (~ 0.6), S_a is the spectral acceleration for longitudinal response (figure 1-8), and DL_s is the dead load of slab and any overlaying fill.

Note that this connection should be free to rotate so that moment will not be transferred to the abutment backwall as the approach fill settles.

At least two types of approach slabs have been used in the past. Figure 10-2 shows the type of slab commonly used in California. Its sole function is to provide limited access between the approach fill and the bridge abutment. If the anticipated fill settlements are large, consideration should be given to lengthening the slab to reduce rotational discontinuity that will occur at each end of the slab. Some form of traffic control will be required to construct this retrofit, but staged construction can be used to minimize disruption to traffic. Many other states use variations of this type.

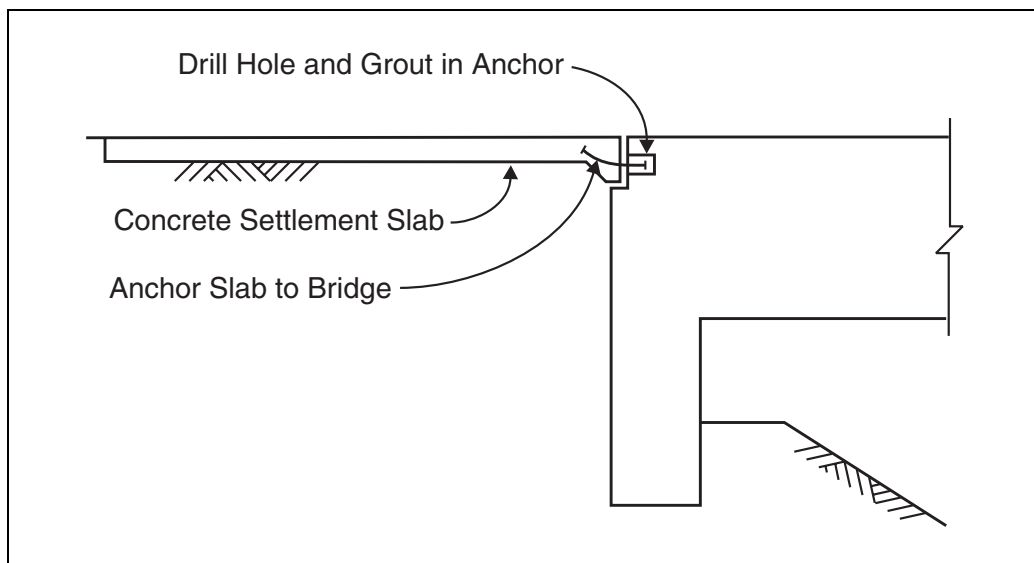


Figure 10-2. California style settlement slabs.

Another type of settlement slab is shown in figure 10-3. Because this slab is buried in the approach fill, it will deform and settle with the fill during an earthquake, providing a smooth ramp onto the bridge. It will also act as a friction slab and dissipate energy during an earthquake. It is therefore reasonable to assume some reduction in longitudinal design forces with these slabs, on the order of 10 to 20 percent. However, because these slabs are buried, they will be more difficult to construct under traffic than a California slab.

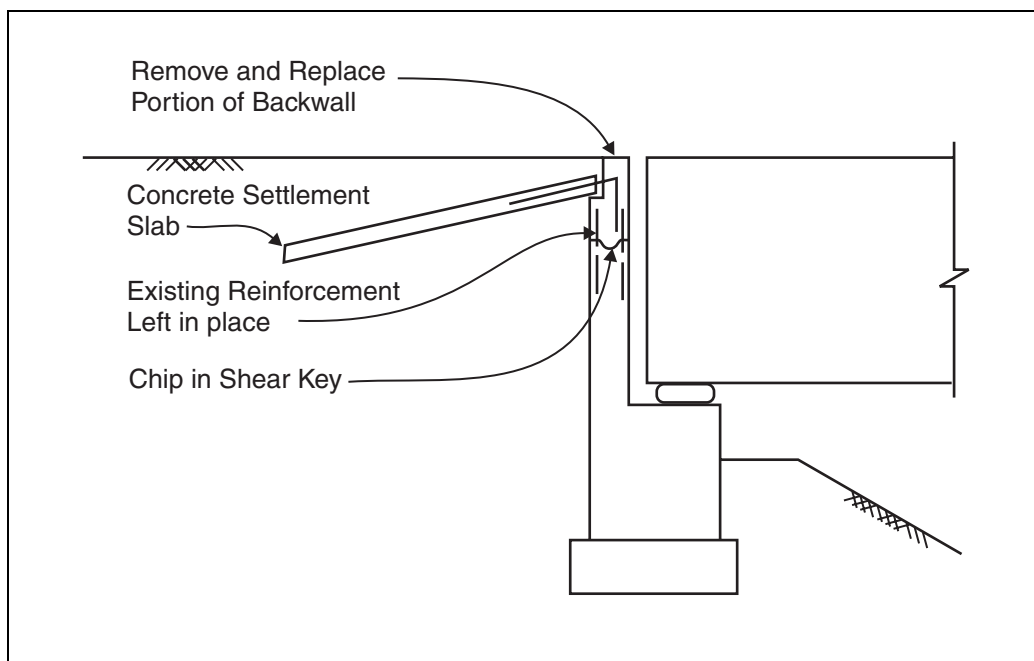


Figure 10-3. New Zealand style settlement slabs.

10.2.2. ANCHOR SLABS

Anchor slabs are used to increase the ability of abutments to carry both longitudinal and transverse loads, and are used to resist displacement in either of these directions. They can also serve as approach slabs, by providing access to the bridge following an earthquake. Anchor slabs are generally used on short, continuous bridges where the superstructure is capable of transferring loads away from the piers and into the abutments.

Two anchor slab designs are shown in figures 10-4 and 10-5. Both of these slabs take advantage of the passive resistance of the approach fill soils. The ‘waffle’ slab design in figure 10-4 provides a number of surfaces for passive resistance, in addition to the lateral resistance provided by the cast-in-drilled hole (CIDH) piles. It is recommended that the vertical stems in this design be spaced no closer than twice their depth, h , below the bottom of the horizontal slab. Passive resistance on the vertical surfaces can be assumed as:

$$p_p = 0.37h / 2.44 = 0.15h \text{ MPa} \quad (10-2a)$$

or
$$p_p = 7.7h / 8 = 0.96 h \text{ ksf} \quad (10-2b)$$

A standard 0.40 m (16 in) diameter CIDH pile can be assumed to have an ultimate lateral capacity of 178 KN (40 kips).

The CIDH pile anchor slab shown in figure 10-5 uses large diameter piles as the mechanism for lateral resistance. The vertical capacity of these piles is of no concern, so they need only to be deep enough to provide lateral stability. The stiffness and ultimate lateral capacity of large diameter piles is dependent on the type of soil and can be determined using the p-y curve approach (Reese and Allen, 1977). The slab acts as a beam on a continuous foundation, and computer programs are available to solve for design forces and displacements

Anchor slabs must be securely connected to the superstructure to be effective, and the connections must be strong enough to resist the forces determined from analysis. These forces can be substantial, and the bridge must be able to transfer them to the slab. This will often require the abutment diaphragm or backwall to be strengthened.

Because movement through the approach fill is necessary to develop the passive pressures needed for lateral resistance, these slabs dissipate a considerable amount of energy. This can be accounted for during analysis by increasing the equivalent viscous damping. Damping ratios of 10 percent can be assumed for systems that include these types of anchor slabs. This in turn reduces longitudinal design forces by approximately 20 percent, as compared to those obtained from five percent damped design spectra.

These retrofits will be disruptive to traffic, although staged construction can minimize this disruption. Problems can also develop during construction due to the excavation subsiding under the waffle slabs or into the holes drilled for CIDH piles. Concrete pours must be made against undisturbed soil, which requires excavations with near-vertical faces. In the past, pea gravel was used as a fill material behind bridge abutments. When encountered, this material cannot be

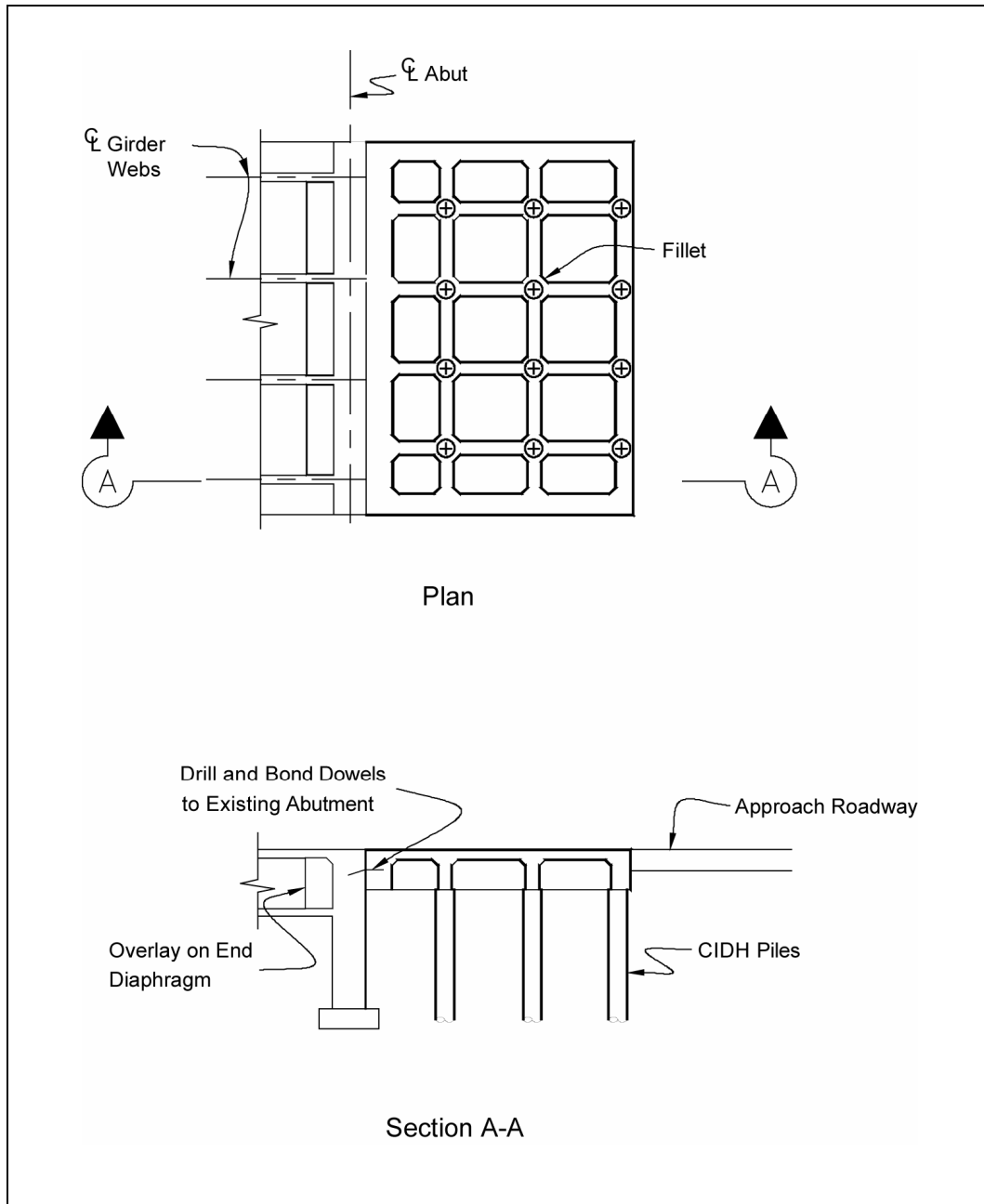


Figure 10-4. "Waffle" slabs.

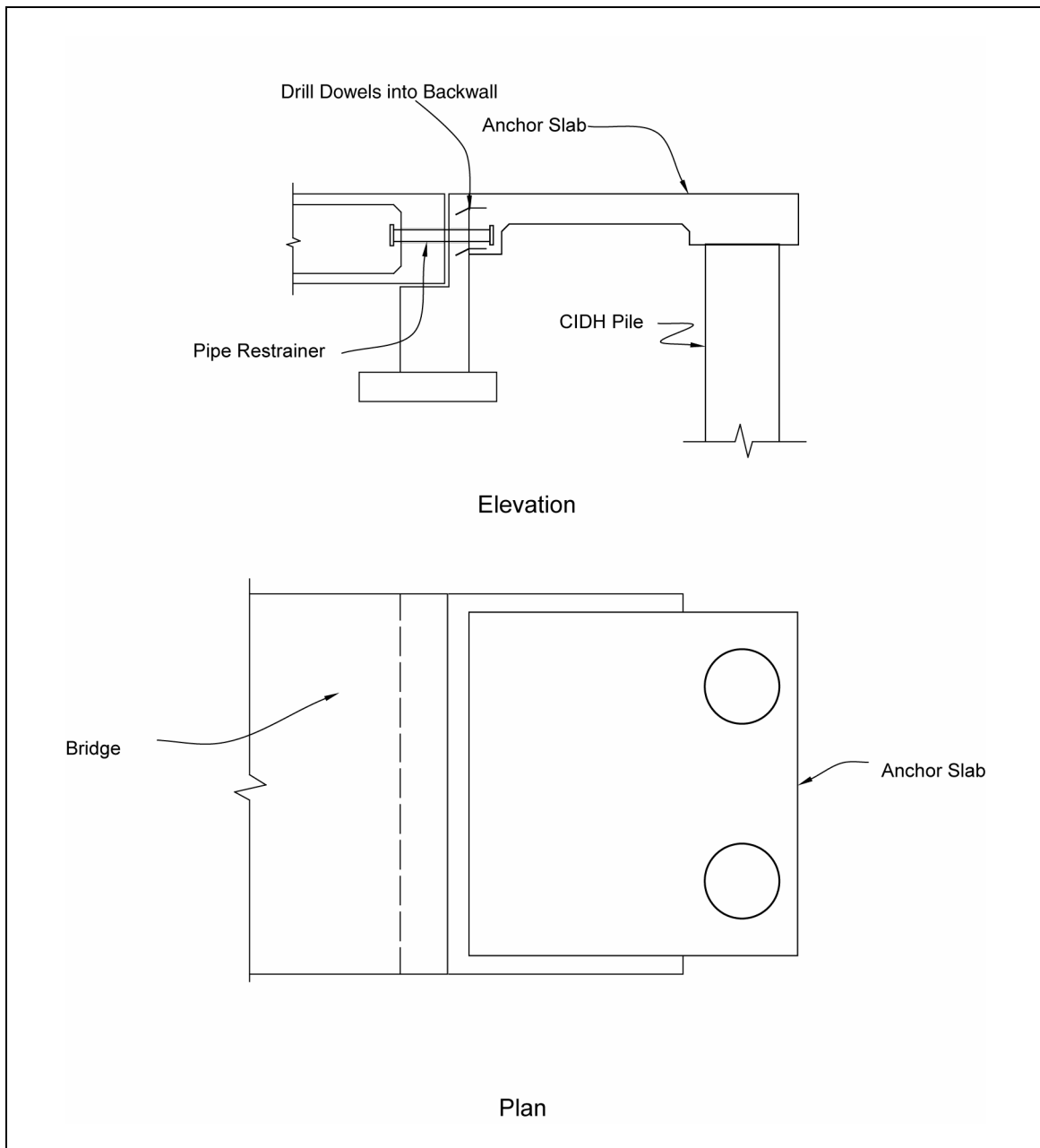


Figure 10-5. Anchor slabs with CIDH piles.

excavated with a vertical edge, which can cause the size of the excavation to become unacceptably large unless special precautions are taken to stabilize the fill, or it is removed and replaced.

10.2.3. DIAPHRAGM WALLS

It may be necessary to strengthen the end diaphragm of an integral abutment to prevent a shear or flexural failure. When an abutment is driven into an approach fill during an earthquake, large passive pressures on the back of the abutment wall are generated. This can result in structural failure of the wall that will, in turn, reduce the passive resistance at the back of the wall. If displacements are sufficiently large, support can be lost at the abutment, severely damaging the bridge and rendering it unusable. To avoid this type of failure, it may be necessary to strengthen the wall. This can be done by constructing a reinforced concrete overlay on the face of the abutment wall, as shown in figure 10-6. If the old and new concrete can be made to act as a composite member, then the entire section may be considered effective in resisting the forces generated by the passive soil pressure. To achieve composite action, the existing concrete surface should be roughened and the overlay must be connected to the existing backwall with a sufficient number of dowels to provide for shear transfer through friction at the interface between the existing and new concrete. In addition, flexural reinforcement in the overlay must be continuous or, as a minimum, adequately spliced.

This retrofit method is very disruptive to traffic, as well as to utilities that may be located on the back face of the wall. Staging is often difficult unless shoring is used. For these reasons, this method is easier to use when constructed on the front face of the wall, but construction may be limited on the front face due to restricted horizontal clearances under the bridge.

10.2.4. TRANSVERSE ABUTMENT SHEAR KEYS

Existing bearings and shear keys at seat-type abutments may be incapable of transferring transverse inertial forces from the superstructure to the abutments. While loss of support due to movement at the abutments may not be an issue, effective transfer of these forces can reduce forces on the piers and should be considered as part of an overall retrofit strategy. Two methods of strengthening the transverse shear transfer mechanism are shown in figures 10-7 and 10-8. Other methods are available. The goal of this approach is to design a transverse shear mechanism that remains essentially elastic (i.e., yielding is not permitted). The abutment must, itself, be able to resist the forces being transferred.

10.2.5. TRANSVERSE ABUTMENT ANCHORS

Other sources of transverse resistance at abutments include:

- Lateral capacity of piling,
- Passive soil pressure on wingwalls, and
- Friction on the bottom of a spread footing.

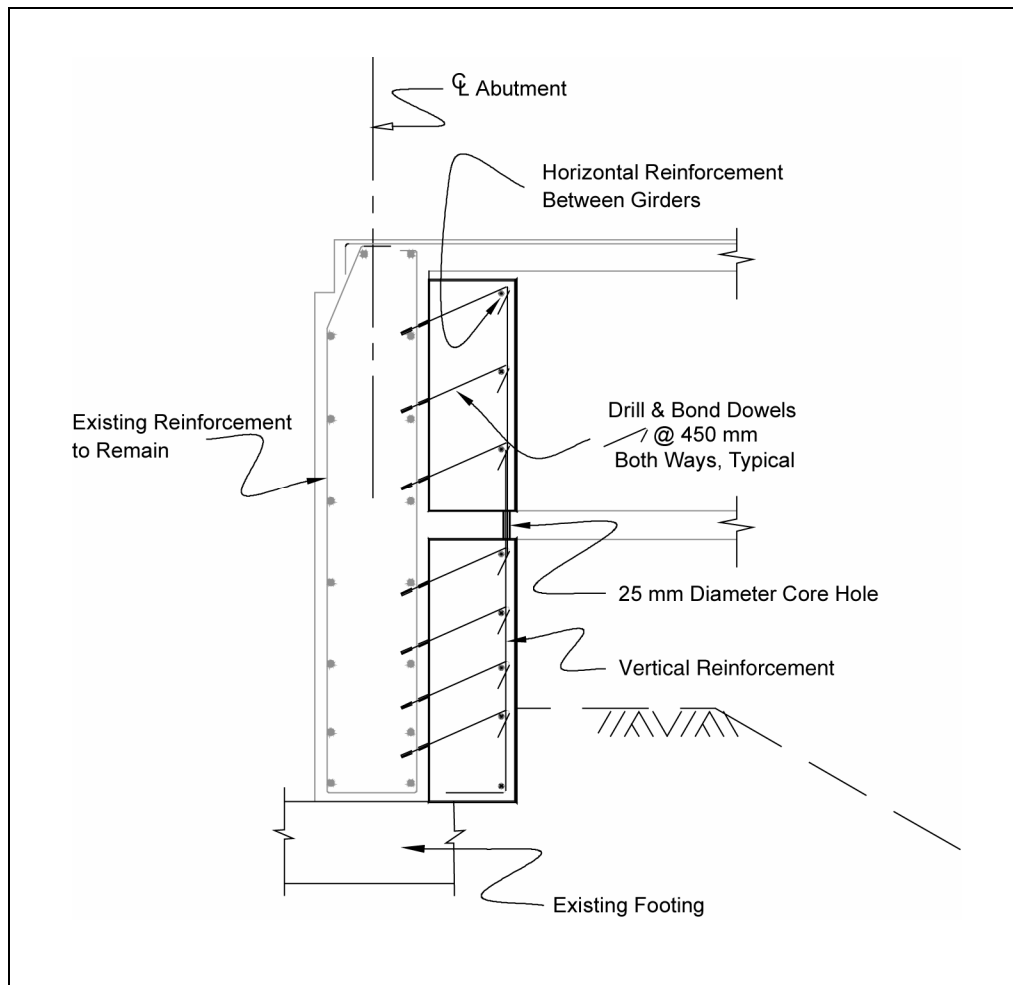


Figure 10-6. Diaphragm abutment overlay.

When these mechanisms are inadequate, the ability of the abutment to transfer transverse load into the approach embankments can be improved by retrofitting. In addition to the anchor slabs discussed in section 10.2.2, other methods are available as described in the following sections. In all cases, the displacement compatibility of the resisting mechanisms must be accounted for during design.

10.2.5.1. Soil Shear Keys

Soil shear keys are essentially short supplemental walls that project from the back face of the abutment wall into the fill, and resist load through passive soil pressure. An example is shown in figure 10-9. Construction of this type of retrofit can disrupt traffic and utilities, and the precautions discussed earlier should be applied here. To be fully effective, the minimum clear spacing between soil shear keys should be approximately equal to twice the distance they project into the fill. The passive pressure that can be developed is given by equation 10-2. When relying on passive pressure in the longitudinal direction, it is advisable to limit the resulting pressure to the value given by these equations.

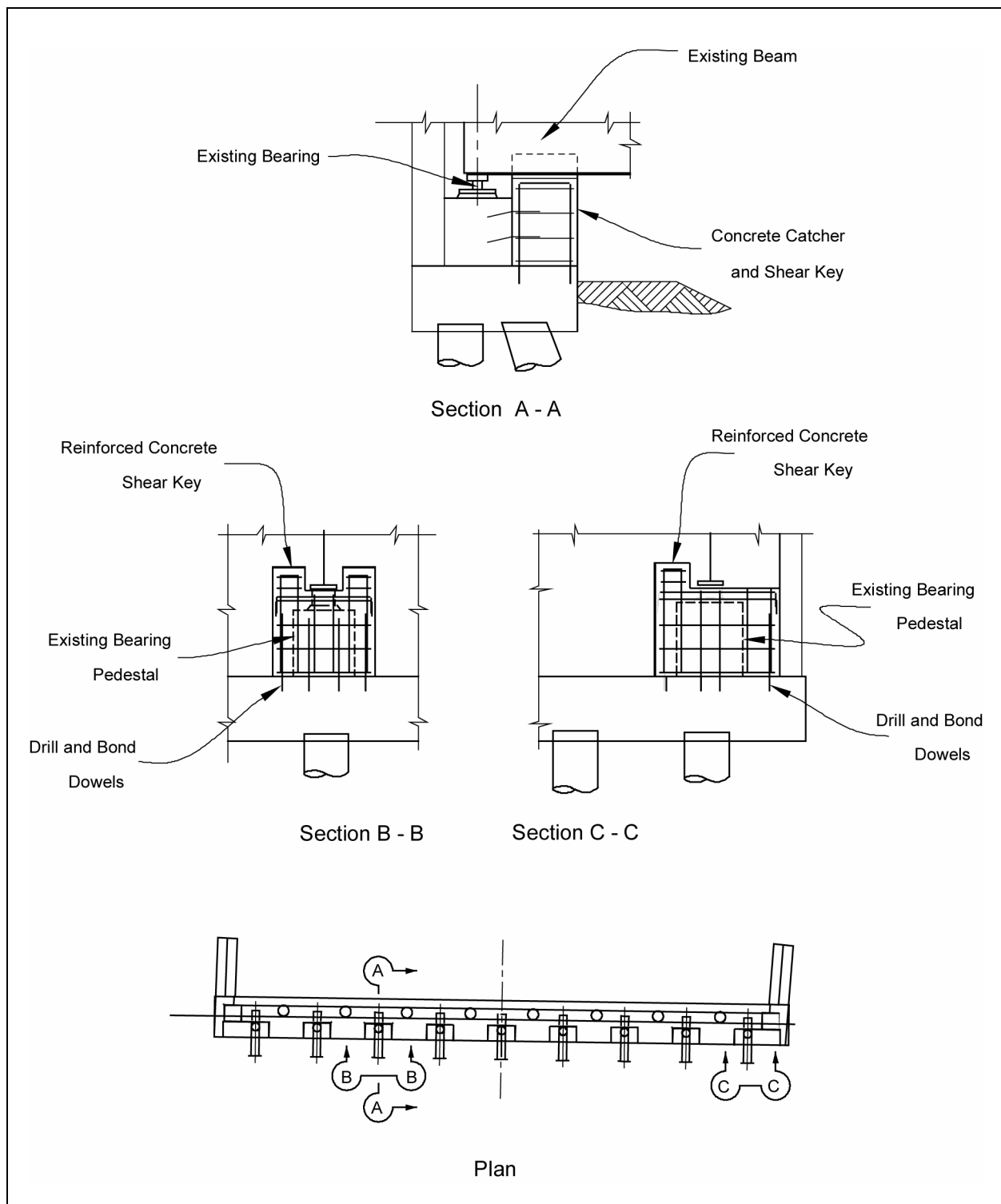


Figure 10-7. Concrete block abutment shear key.

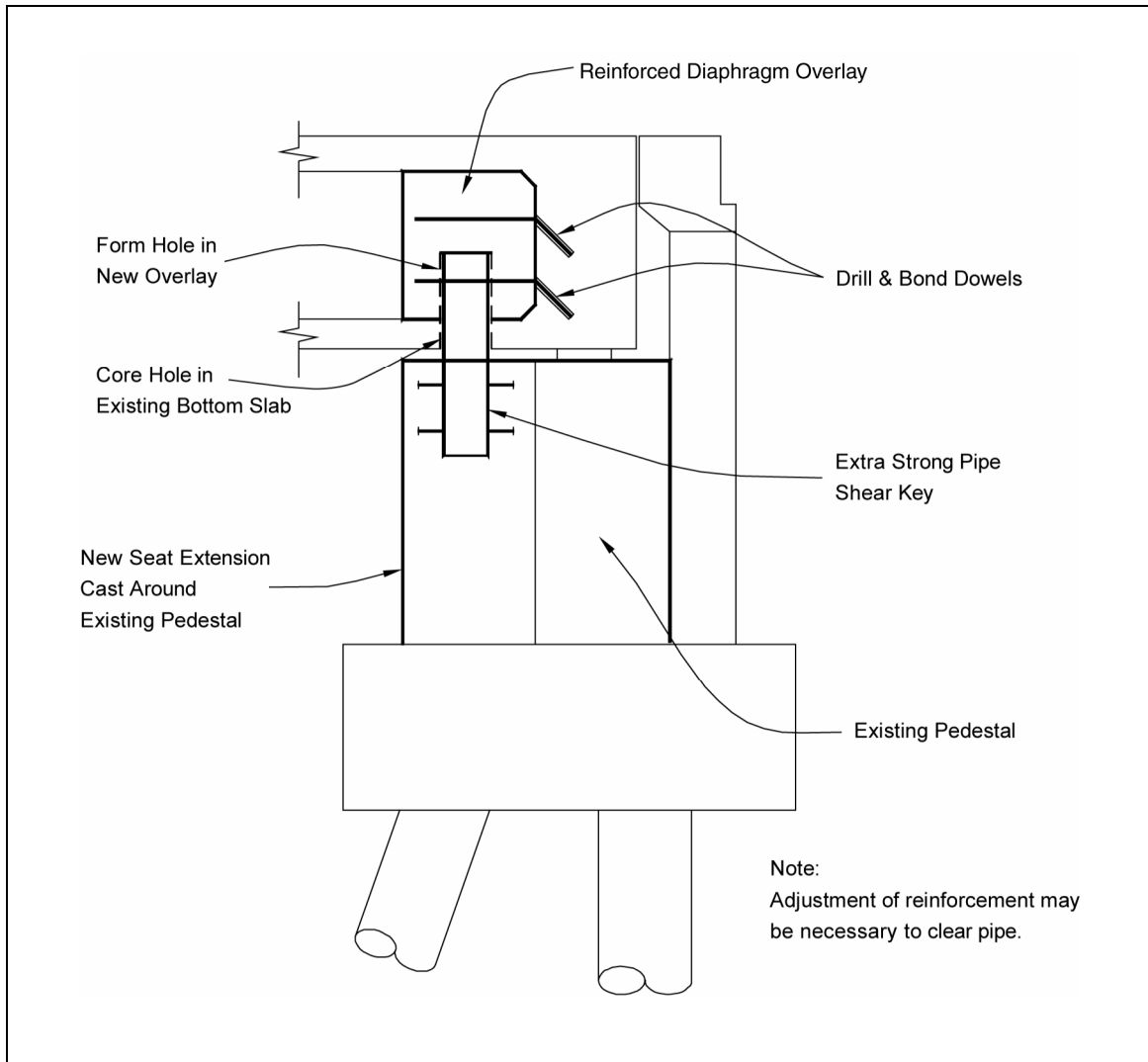


Figure 10-8. Pipe shear key at abutment.

These keys can be designed for limited ductility demands. An R-factor of two is acceptable for flexural design of the key, based on cantilever bending. The shear capacity should be designed for full passive pressure, to allow for the possibility of flexural overstrength and deviation from pure cantilever bending. The connection to the abutment wall should be capable of resisting the overstrength moment and shear capacity of the wall at this location. These keys will also introduce transverse bending moments and forces into the abutment wall, which may then require that the wall be strengthened.

10.2.5.2. Wingwall Strengthening

When the structural capacity of a wingwall limits its contribution to the transverse resistance of the abutment, structural strengthening of the wingwall is an option. This may be accomplished

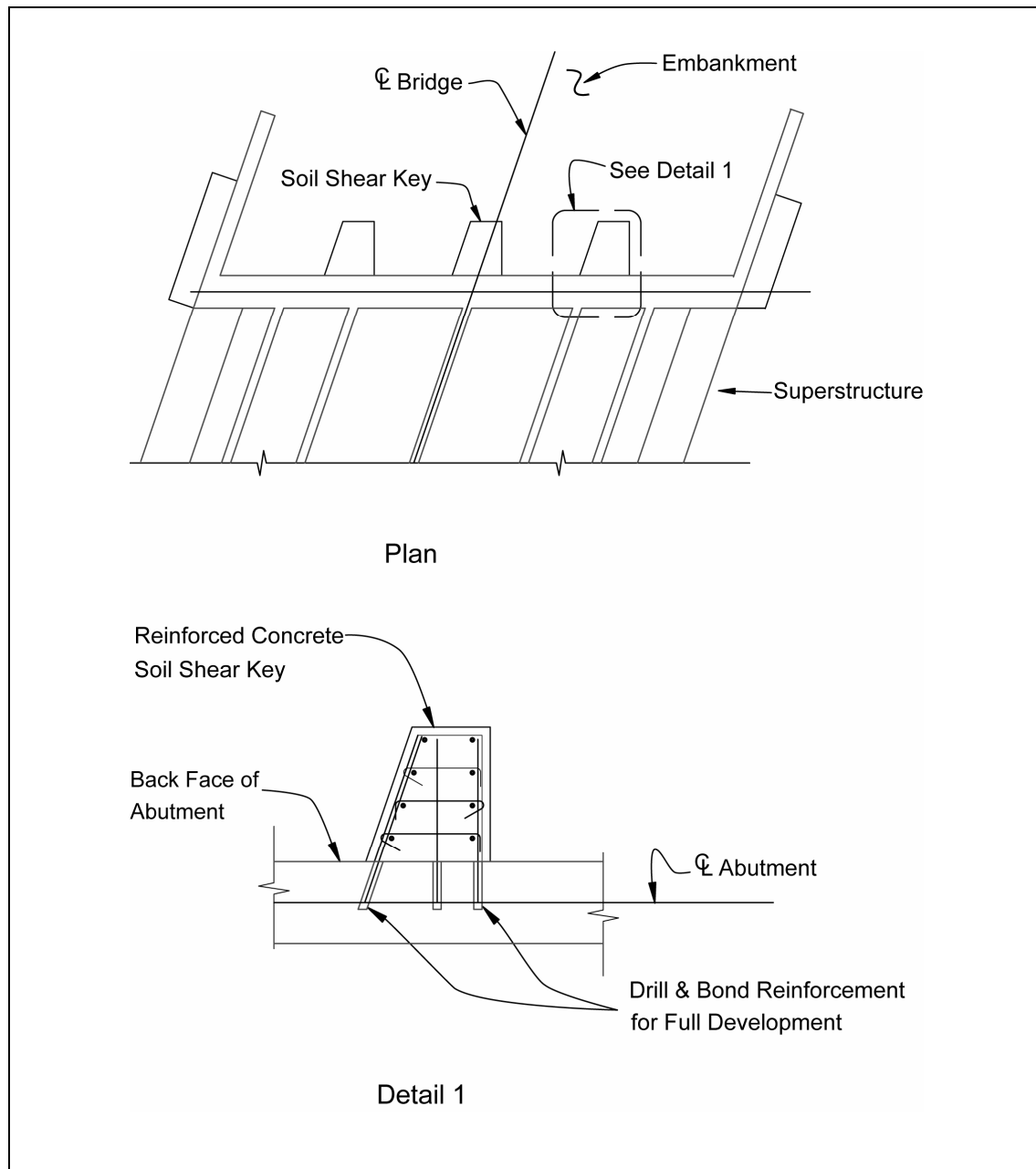


Figure 10-9. Abutment seismic shear walls.

by constructing composite concrete overlays on the wingwall, as shown in figure 10-10. The design criteria in this case are similar to those for supplementary shear keys discussed above.

Another method of increasing wingwall capacity that can be used in conjunction with wingwall strengthening is to place cross-ties between two wingwalls, as shown in figure 10-11. The cross-ties will help redistribute forces in the wingwalls, resulting in increased resistance to transverse loads. This method will cause disruption to traffic and utilities during construction.

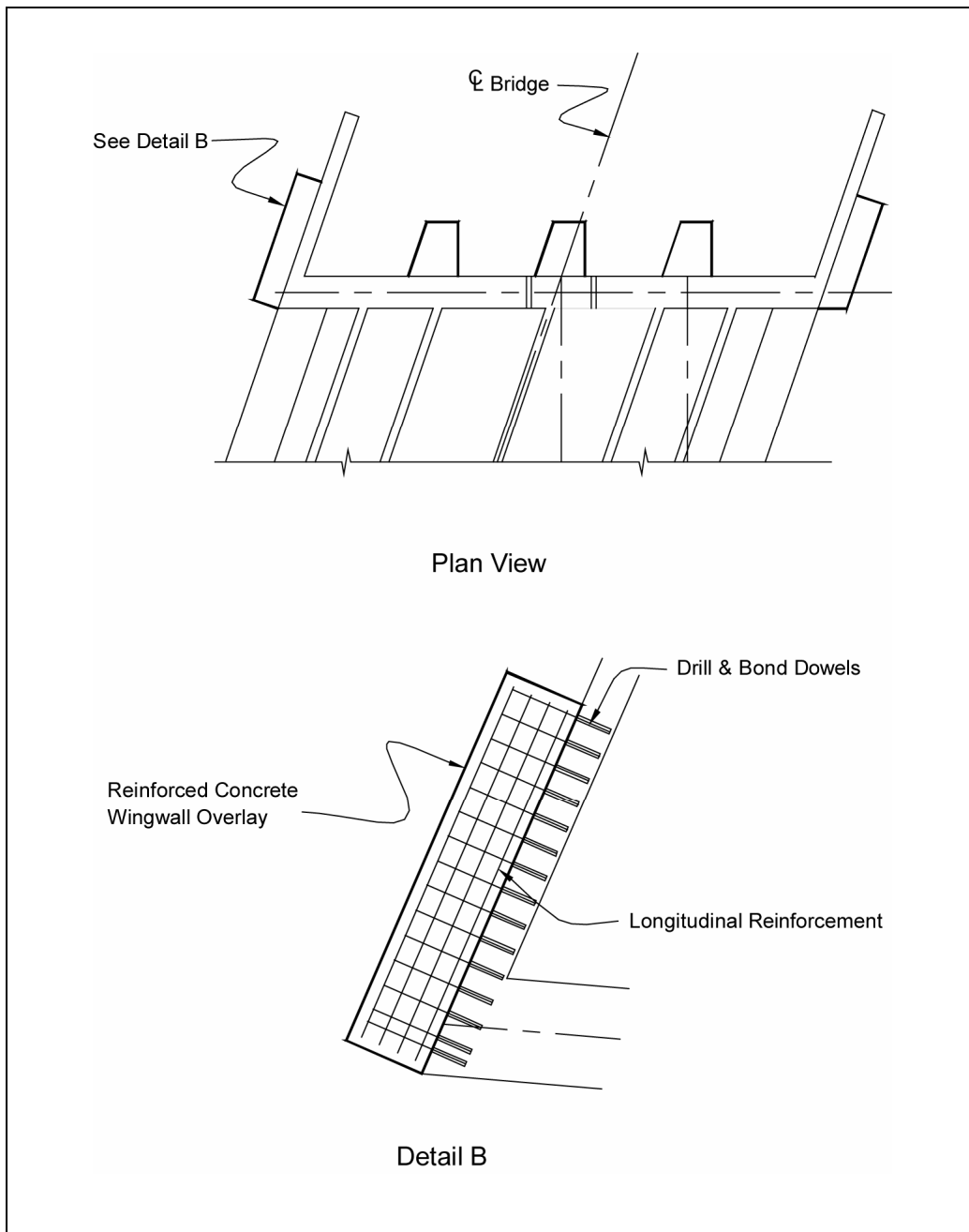


Figure 10-10. Wingwall overlay.

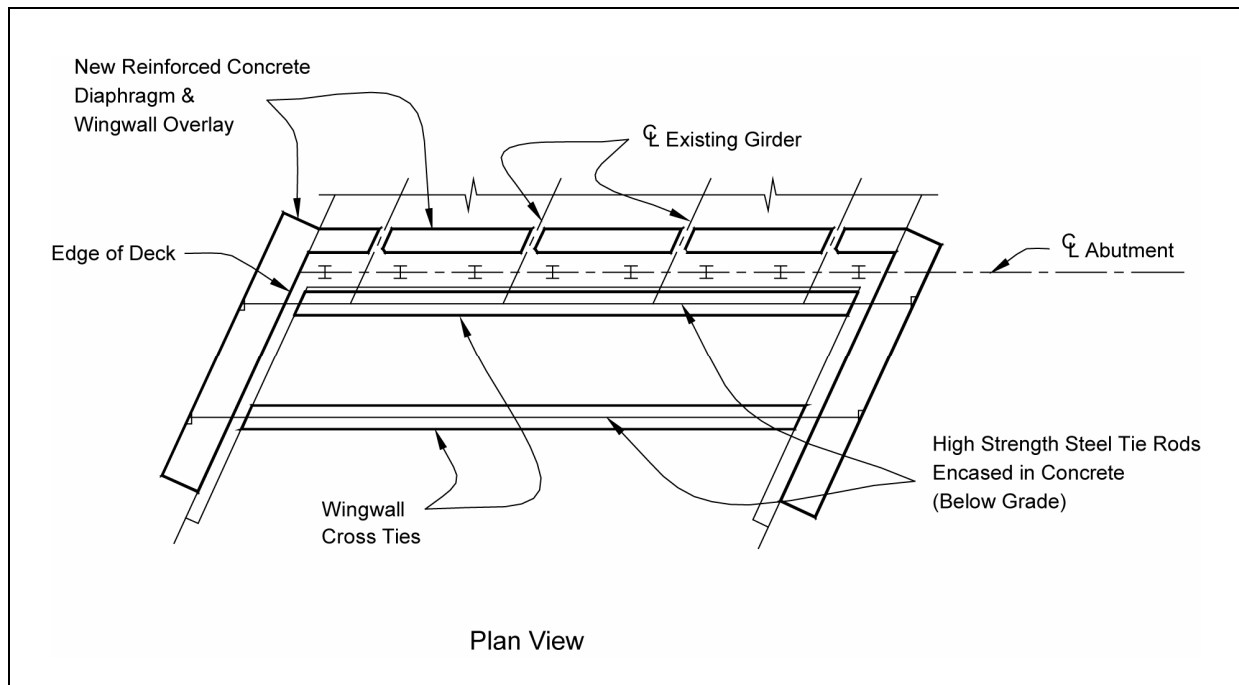


Figure 10-11. Wingwall cross-tie.

10.2.5.3. Cast-In-Drilled Hole Piles

A popular method for increasing the transverse capacity of abutments is to use supplemental large diameter CIDH piles at the edges of the abutment. These piles are usually designed to carry lateral load only, and their design therefore does not need to consider compression or uplift capacity. Lateral capacity can be determined using the p-y method discussed in section 6.2.2.2.

Because these piles are more effective for lateral loads when they have a fixed-head condition, it is often desirable to provide a moment-resistant connection at the abutment. This will not always be practical if the bridge must be free to accommodate large longitudinal temperature movements at the abutment. In the case of seat-type abutments, an extension of these piles can also be used as a transverse shear key. An example of this type of retrofit is shown in figure 10-12.

10.2.6. SOIL AND GRAVITY ANCHORS

Large horizontal displacements at the abutments may make the bridge inaccessible or, in some cases, result in bridge instability. Abutment displacements can be minimized by adding soil or gravity anchors. Various types of soil anchors may be used to transfer longitudinal loads into the approach embankments. These can resist inertial forces from the superstructure or they can stabilize the abutments and prevent rotation or sliding.

Various types of soil anchors have been used to retrofit abutments. Because the backfill may move during an earthquake, the anchors should extend a sufficient distance into the backfill to avoid being affected by this movement.

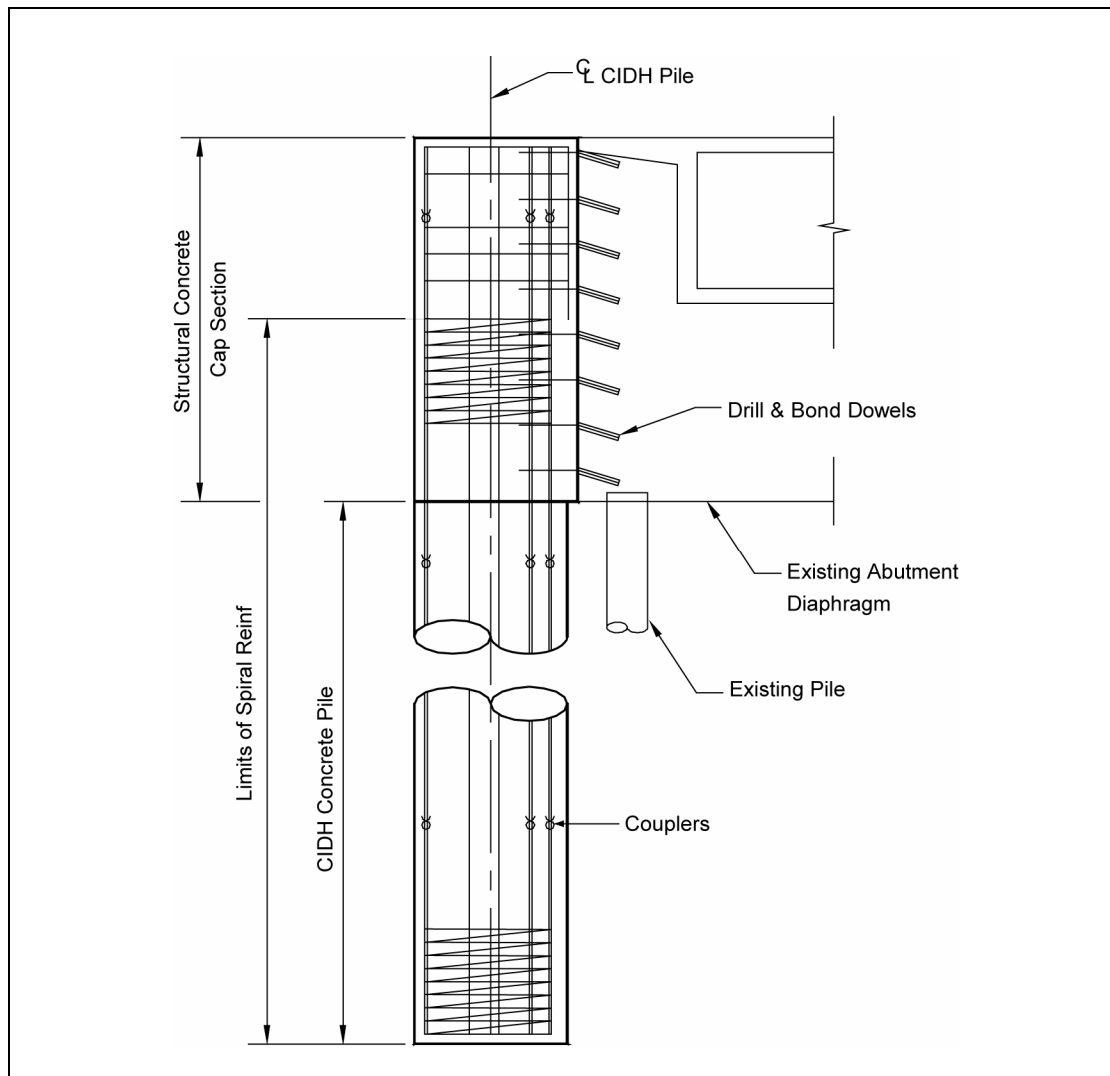


Figure 10-12. CIDH pile shear keys.

Gravity anchors, as shown in figure 10-13, consist of tie rods running between the superstructure or abutment and a 'dead man,' which may be a large diameter CIDH pile or a heavy beam buried in a trench some distance behind the abutment. This method is intended to provide longitudinal resistance against movement toward the mid-span of the bridge. Passive soil pressure and friction mechanisms on the dead man provide this resistance. The tie rods are usually embedded in a concrete trench to protect them from corrosion or other damage.

Soil anchors have been used for many years to stabilize retaining walls. Many of these systems are proprietary and require licenses for their use. Typically, a hole that is slightly inclined to the horizontal is drilled into the soil embankment. Prestressing rods or strands are placed in the hole and the hole is pressure-grouted. Anchorage for the strand is usually provided by a mechanical end-plate or toggle. Soil anchorage is provided through friction with the soil or formation of a grout bulb at the end of the hole. A portion of the steel rod is left unbonded so it can be prestressed. When it is stressed, it provides a test of the reliability of the anchor. If acceptable,

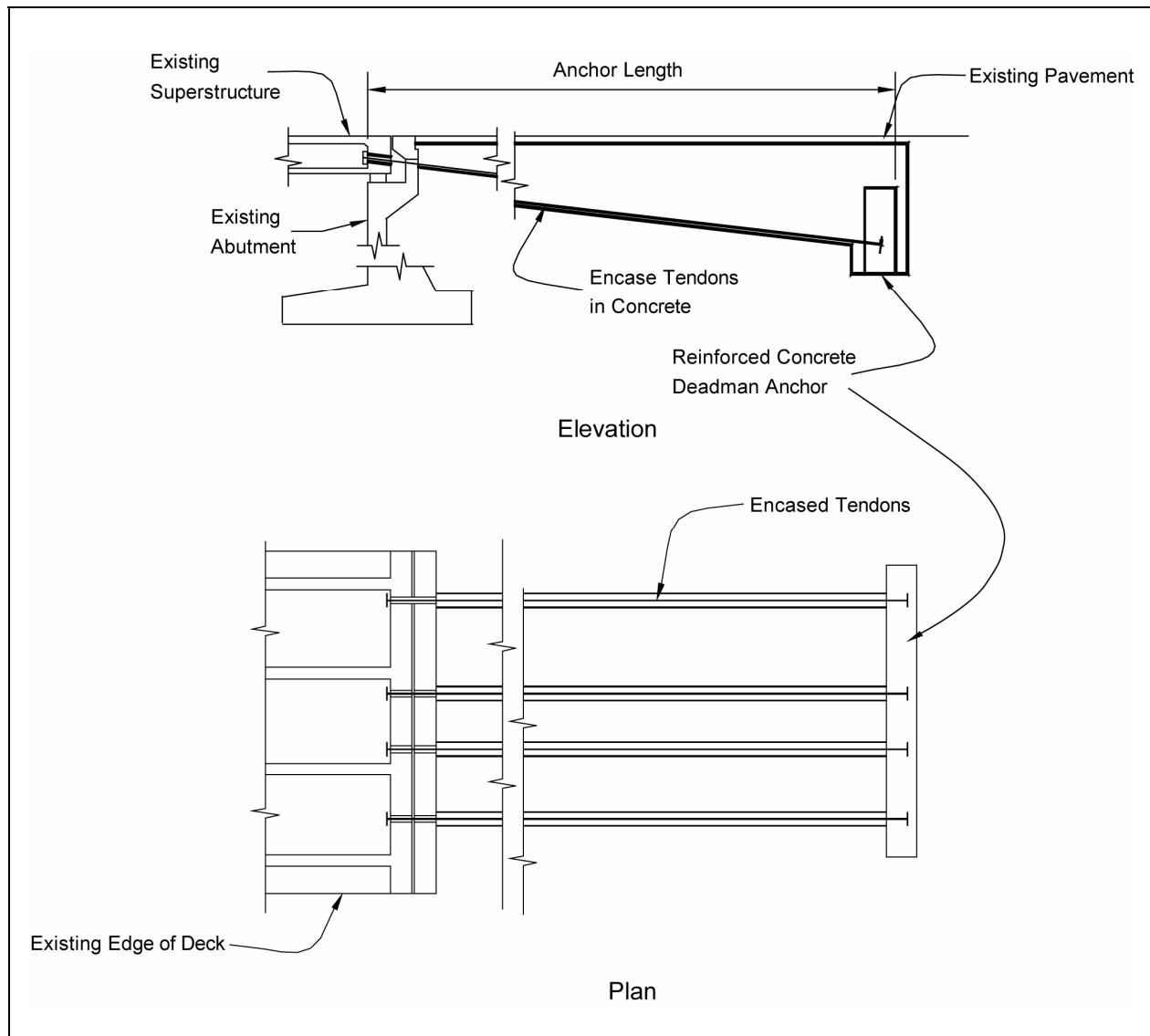


Figure 10-13. Gravity or “Deadman” anchors.

the steel is locked off at the face of the wall. The entire length of prestressing steel is then grouted to provide protection against corrosion. An abutment retrofit using soil anchors is shown in figure 10-14.

A modified friction slab anchor, as shown in figure 10-15, can be used in embankments with granular soils where little or no settlement is expected. In this case, flexible steel piles that can resist uplift are used to prevent vertical movement at the end of the slab. Because the slab is sloped at approximately 15 degrees to the horizontal, the soil under the slab is compressed as the wall is pulled toward the bridge. This generates friction between the slab and the soil, as well as increasing the shear strength of the soil under the slab, stabilizing it against failure. The slab, piles, and pile anchorages must be designed to resist the increased soil bearing forces. This method allows large tieback forces to be generated, resulting in tiebacks that are capable of resisting significant inertia forces from the superstructure.

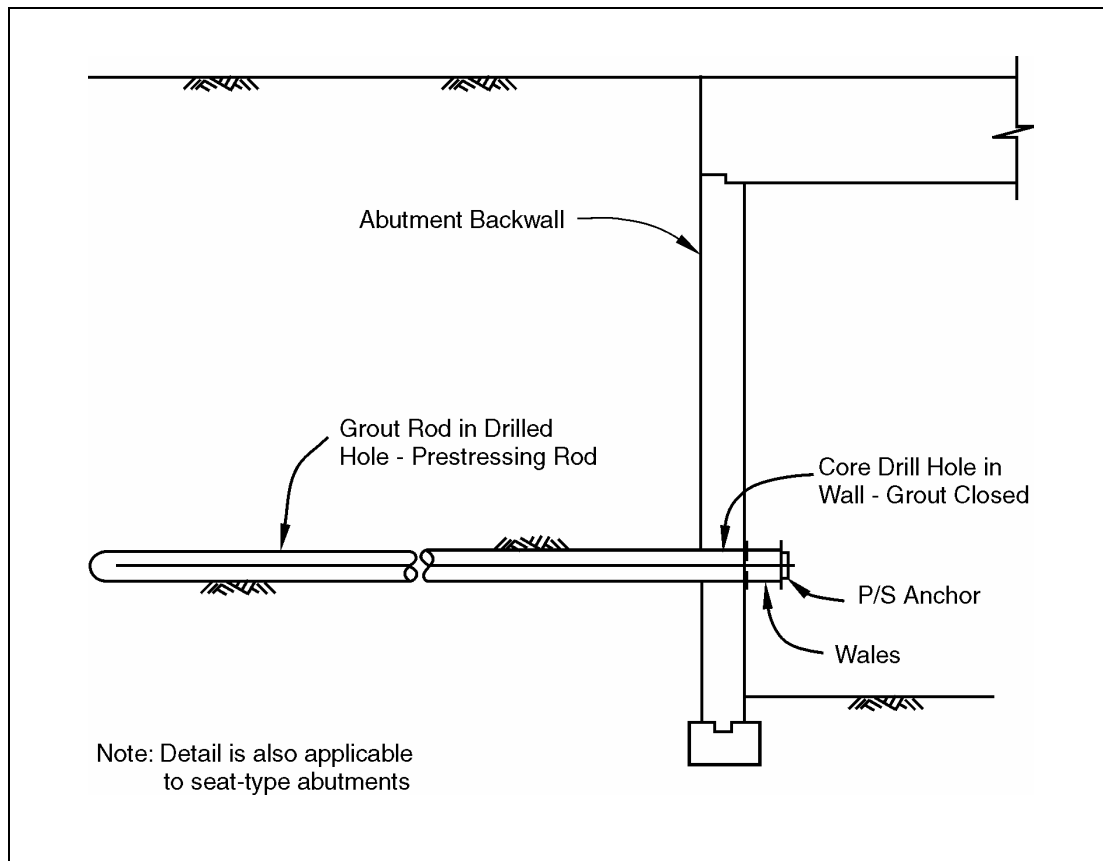


Figure 10-14. Abutment retrofit using soil anchors.

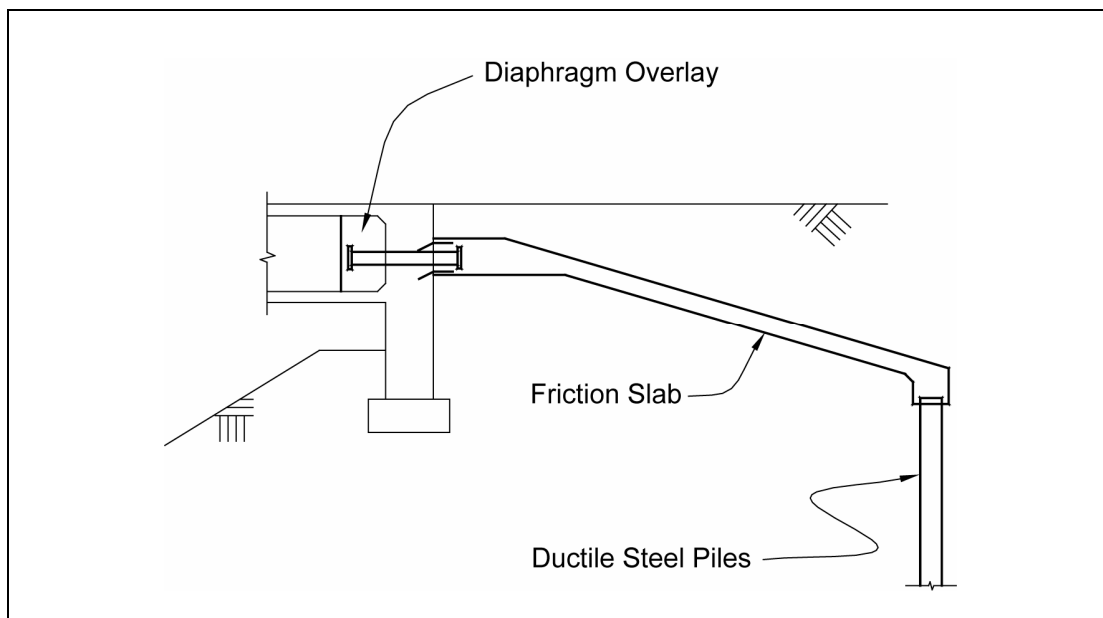


Figure 10-15. Modified abutment friction anchor.

The ultimate capacity of each of the above anchor types should be greater than or equal to the inertial forces transferred to the abutment from the superstructure, or the earth pressures acting against the abutment wall during the design earthquake.

10.3. RETROFIT MEASURES FOR FOOTINGS

This section discusses various approaches for retrofitting bridge footings. The approaches address structural deficiencies in footings as well as global deficiencies in bridge foundation capacity. As noted earlier, footing and foundation retrofitting is expensive, and a collapse resulting from structural failure in a footing or foundation is relatively rare. The cost of retrofitting footings must therefore be weighed against the consequences of not doing so. It is sometimes advisable to accept the risk of damage, unless there is a potential for loss of life.

10.3.1. FOOTING REPLACEMENT

Total footing replacement is an extreme measure, but was used on a number of bridges in San Francisco following the 1989 Loma Prieta earthquake. This type of retrofitting is usually necessary when columns are replaced, existing footings are inadequate and strengthening of the footing is not feasible due, in part, to the connections required between the new columns and the footing.

The structure must be supported during reconstruction of the foundation. This is further complicated if the bridge must continue to carry traffic during retrofitting. It is often necessary to drive new piles in this situation and if so, they must be driven with limited headroom under the existing superstructure and in the proximity of temporary supports. A discussion of piles used in bridge retrofitting is given in section 10.4.1.

10.3.2. STRENGTHENING OF FOOTINGS

Rocking of a spread footing or piled footing is not necessarily an undesirable response. If neither the column nor footing are ductile, rocking of the footing may provide a form of isolation that can prevent structural damage to the bridge. However, if rocking displacements are expected to be large or if failure of the footing is likely, retrofit will be necessary.

Overturning resistance may be improved by increasing the footing area, adding more piles (generally in conjunction with an increase in plan area), or by adding supplemental soil or rock anchors. The existing tensile capacity of the piles is often inadequate because of poor connections between the piles and footings, and the lack of continuous tensile reinforcement in the piles. Even if the pile's tensile capacity is adequate, the mobilization of this capacity will require vertical displacement of the pile and thus rocking of the footing. The designer should consider the rocking flexibility of the footing when performing seismic vulnerability analysis of the bridge, in order to assess the stability of the structure under seismic loads.

An increase in footing area is usually required if the stability of the footing itself is an issue. This is always accompanied by structural strengthening of the footing (figure 10-16).

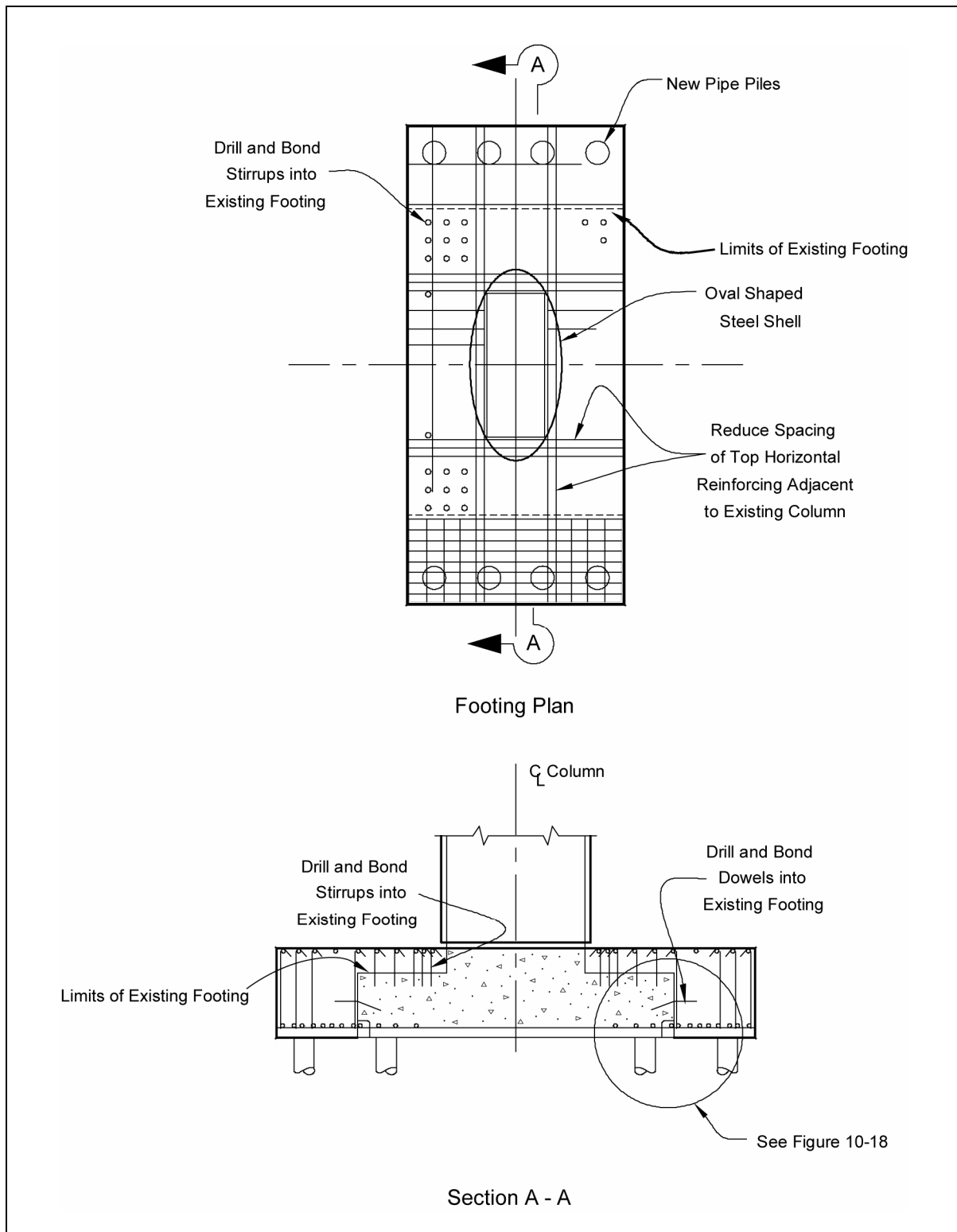


Figure 10-16. Global footing strengthening.

In many cases, the overall size of the footing is adequate, but the footings fail before the pier can develop its full plastic capacity. This is most often due to the absence of a top layer of reinforcement and vertical ties in existing footings. As a consequence, these footings have little negative moment capacity and diminished shear strength for resisting uplift forces. During an earthquake, this can result in flexural cracking in the footing or shear failure in the column-to-footing joint. There may also be a loss of anchorage for the longitudinal reinforcement in the column as a result of the damage to the footing. This failure mode results in a degradation of moment capacity, effectively creating a pinned condition at the column-to-footing connection. This can be a serious problem in single-column piers and is more likely to occur if the column is on a pile footing. These footings may be retrofitted with a concrete overlay, as shown in figure 10-17.

Although a concrete overlay can be easily designed to provide increased negative moment capacity in the footing, it is very difficult to add positive moment reinforcement. It is therefore desirable to use the existing positive moment reinforcing and rely on the added footing depth, provided by the overlay, to increase the positive moment capacity. If this is insufficient and the size of the footing must be increased, it will be necessary to splice the existing positive moment steel as illustrated in figure 10-18.

Alternatively, prestressing may be used to increase the positive moment capacity. This is done by drilling horizontal holes through the footings and adding new prestressing bars, as shown in figure 10-19. It should be noted that many existing footings were cast against undisturbed soil. Therefore, it is likely that footings will not have planar surfaces and will not conform exactly to the as-built plans. In this case, new anchor blocks will be required to accommodate the prestressing.

10.3.3. RETROFIT DESIGN OF FOOTINGS

Footing retrofits must be designed to prevent flexural, shear, and joint shear failure within the footing. Retrofit design is therefore similar in many ways to the design of new footings. Since it is often necessary to rely on resistance mechanisms that vary from those of new footings, the use of strut-and-tie models and yield line theory may be employed in addition to conventional beam theory. There are seven steps in the design of a footing retrofit:

Step 1. Determine footing design forces – Forces (moments and shears) are applied to the footing through the column. Unless the footing is assumed to be rock, these forces will be limited to the flexural capacity of the column at the level of applied axial load. Axial loads should include dead load and any additional axial load resulting from seismic response. The potential for flexural overstrength in the column must be considered. Increased moment capacity can result from material properties that are greater than nominal, confinement of the concrete, and strain hardening of the reinforcing steel. One method for determining moment overstrength capacity is to calculate the nominal moment capacity based on actual or estimated material strengths, and to apply a factor of 1.4 to account for the various overstrength factors. Therefore, the column overstrength is given by:

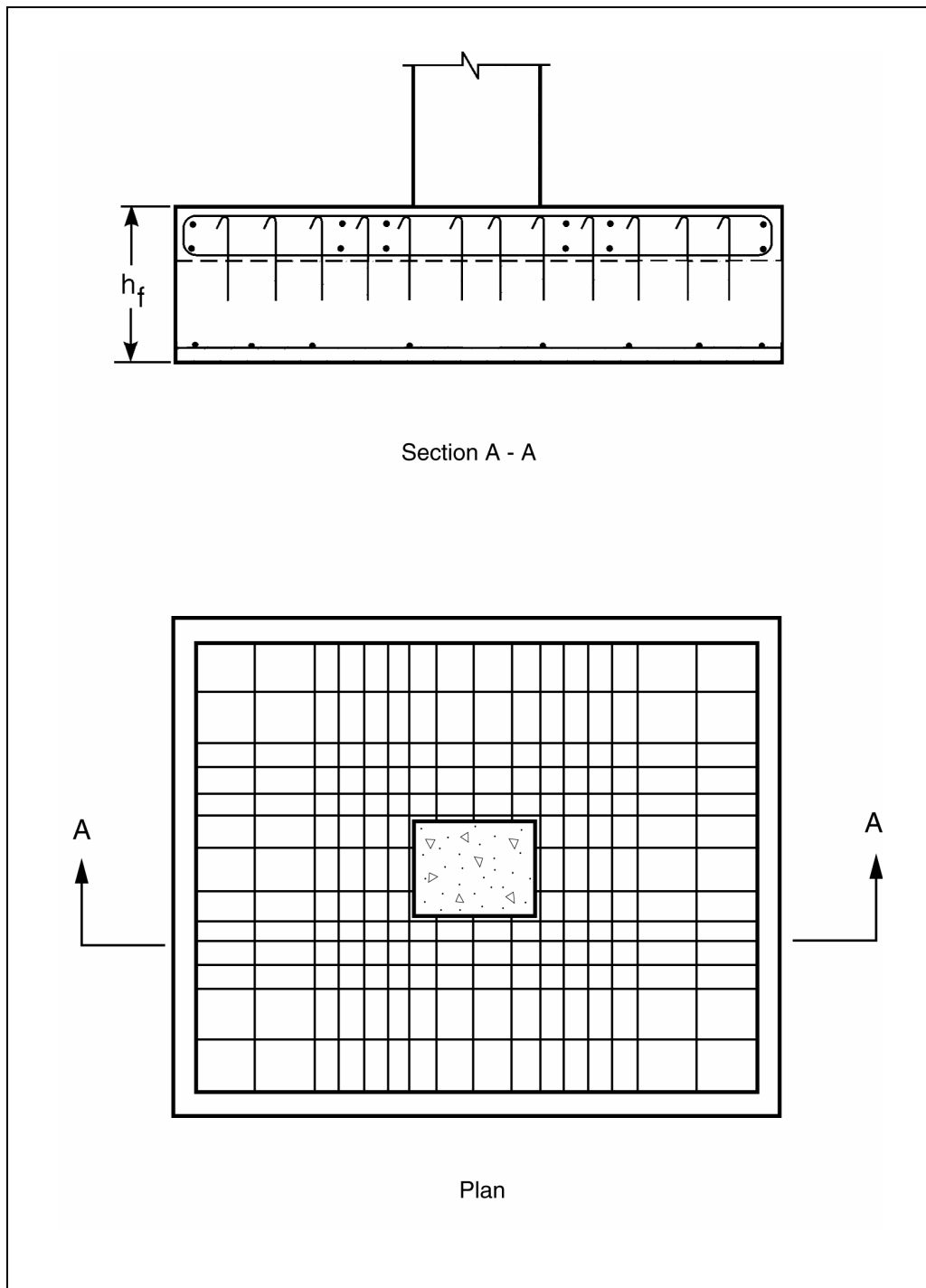


Figure 10-17. Footing retrofit with concrete overlay.

$$M_p = 1.4 M_n \quad (10-3)$$

Alternatively, a moment curvature analysis that accounts for concrete confinement and steel strain hardening can be used. If expected material strengths are used, the moment at the design displacement is increased by 15 percent to provide the overstrength moment. The moment applied to the footing need not be more than the unreduced moment obtained from a dynamic analysis of the bridge subjected to the design earthquake.

Step 2. Check the footing's overturning capacity – The overturning capacity of a spread footing is based on the ultimate bearing capacity of the soil, and on the ultimate tension and compression capacity of the piles in the case of a pile footing. If this capacity is exceeded, the stability of the footing, using a rocking analysis, should be checked. If the footing is stable against overturning and unacceptable permanent displacements in the footing can be avoided, it may not be necessary to increase the size of the footing, nor add additional piles or tie-down anchors. Rocking action may also reduce the forces in the column and the footing, eliminating or reducing the need for retrofitting these members.

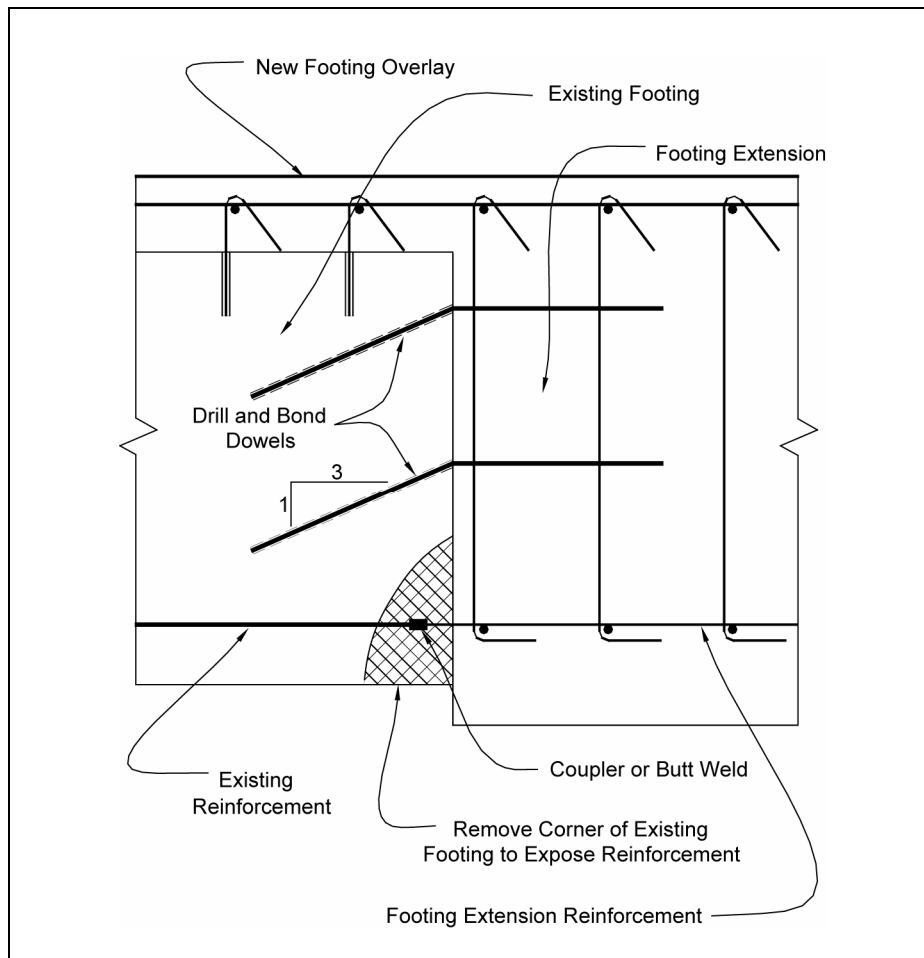


Figure 10-18. Bottom reinforcing splice detail.

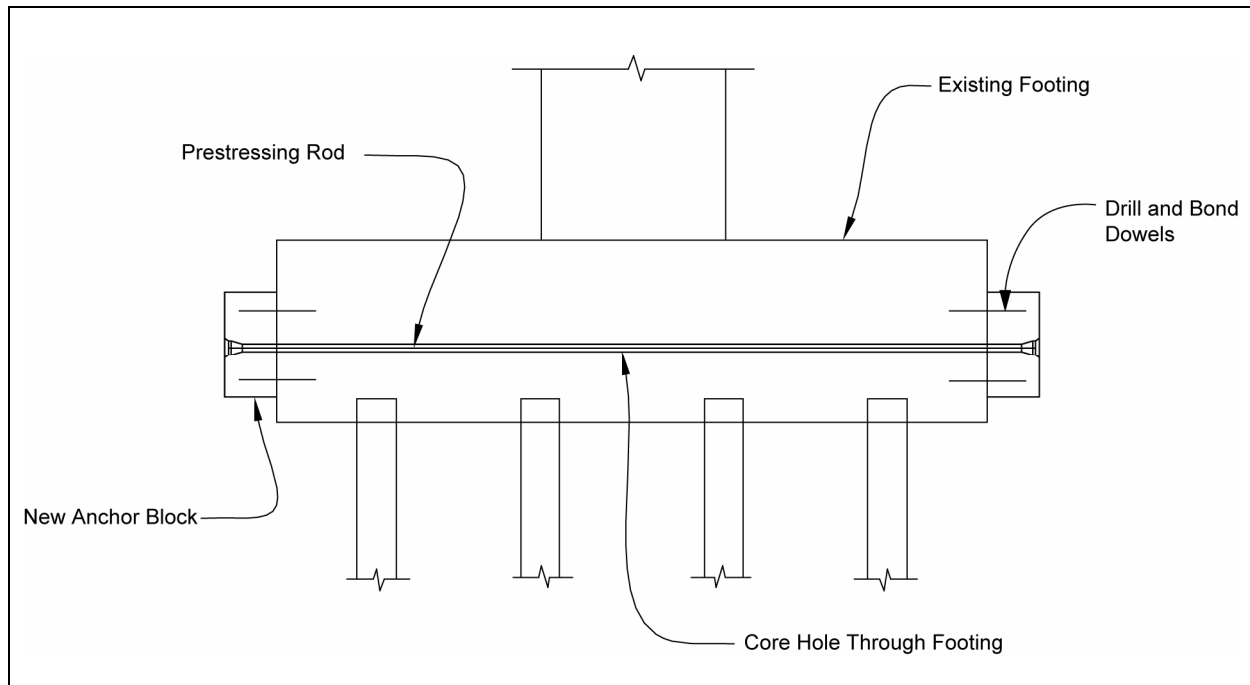


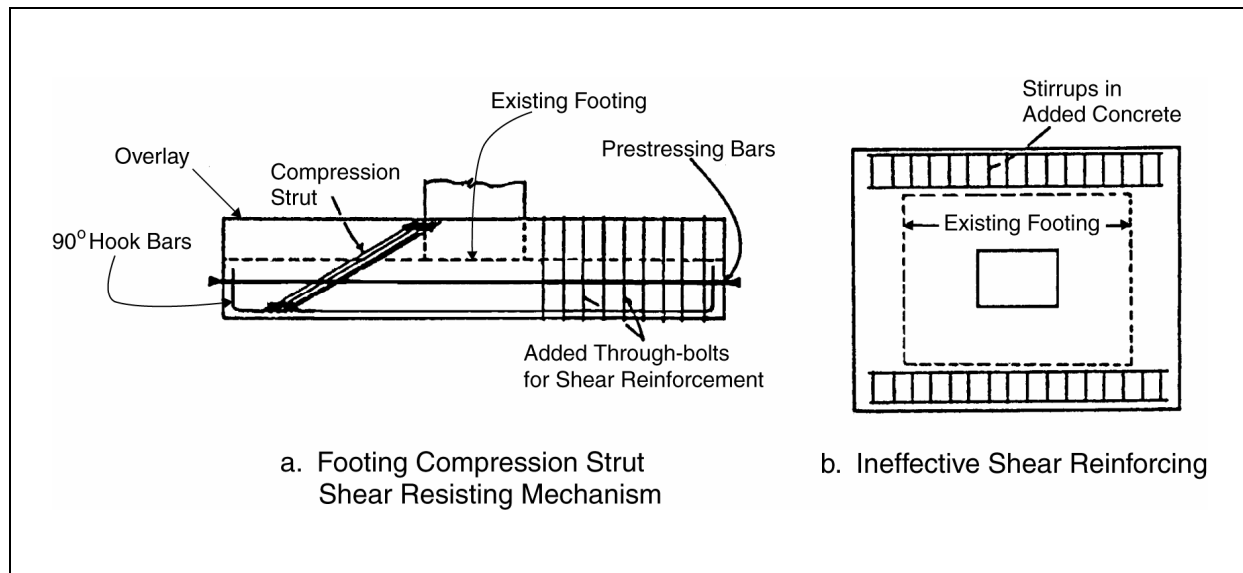
Figure 10-19. Footing strengthening by horizontal prestressing.

If an increase in footing size or the number of piles is necessary, follow conventional footing design procedures. Existing piles, which are carrying the dead load, may reach their ultimate capacity before the new piles. If this occurs, there may still be some capacity remaining in the footing as a whole. Therefore, existing piles can exceed their ultimate capacity as long as there is no excessive movement. If excessive movement can occur, the capacity of these piles should be ignored or limited. The same reasoning can be applied to the soil under spread footings.

Step 3. Design for shear – Shear strength deficiencies in footings are difficult to retrofit. In many existing footings, the shear between the column compressive stress resultant and the foundation or pile reaction may be carried by a diagonal compression strut. This, however, requires a dependable tie force in the bottom steel, which can be relied upon only if the bottom steel is anchored by a 90 degree hook, as shown in figure 10-20(a).

If the compression strut cannot be developed because either the bottom tensile reinforcement is inadequately anchored or the reinforcement has insufficient strength, the shear strength can be increased by:

1. Increasing the footing depth through the addition of a concrete overlay made composite with the existing footing, which will increase the shear capacity of the concrete.



after Priestley et al., 1992

Figure 10-20. Footing shear strength retrofitting.

2. Adding prestressing bars placed in holes drilled longitudinally through the footing, as recommended for increasing flexural strength, or
3. Placing additional reinforcement in vertical holes drilled into the footing, to act as additional shear reinforcement. Unless the bars pass through the footing and are anchored beyond the bottom layer of reinforcement, they will not be as effective as conventionally anchored shear reinforcement. Access to the underside of the footing is difficult, but is required to properly anchor this reinforcement. Vertical reinforcement in the overlay will be effective in resisting shear if there are two layers of reinforcement in the overlay. Vertical dowels that are anchored in drilled holes extending to the bottom layer of reinforcement but are not hooked around this reinforcement will have reduced effectiveness. In this case, it is recommended that they be considered to have 50 percent of the effectiveness of properly anchored stirrups (Priestley et al., 1996).

Note that the addition of shear reinforcement in a newly widened portion of a footing, as shown in figure 10-20(b), is unlikely to be effective because of its distance from the source of the shear force, which is primarily the resultant of the column's compression forces.

Step 4. Design for flexure – Even those footings with adequate tensile connections to piles will frequently be deficient in flexural strength, due to a lack of top reinforcing steel. Bottom steel may also be inadequate, particularly in wide footings where the reinforcing steel furthest from the column is likely to be ineffective.

Retrofitting to increase flexural strength may involve the addition of a reinforced concrete overlay connected by dowels to the existing footing, as shown in figures 10-16

and 10-17. The top reinforcement should be located so that more than half of it is within a distance of h_f from the column faces, where h_f is the depth of the retrofitted footing.

Increasing the depth of the footing will also increase the positive moment capacity due to the increased section depth. If this is still insufficient, horizontal prestressing, as noted earlier, can improve the positive moment capacity. This may be used alone or in conjunction with an overlay. Prestressing ducts should be kept as close as possible to the column.

Step 5. Design dowels for connecting existing and new concrete – Dowels between new and existing concrete should be capable of transferring the shear stress at the interface between existing and new concrete, using a shear friction approach and a coefficient of friction, μ , of 1.0. This assumes that the surface of the existing footing has been adequately roughened prior to casting the new concrete. The thickness of the overlay should be sufficient to develop the tensile capacity of the dowels, which are often hooked at the top end. If the dowels are also to be used to improve shear strength, they should pass through the full depth of the existing footing and be properly anchored at the bottom.

Step 6. Check column-to-footing joint shear – Experimental studies (Xiao et al., 1994; McLean et al., 1995) have shown that a principal mode of failure in existing footings is due to joint shear. Figure 10-21 presents a diagram illustrating the forces that generate joint shear. The vertical joint shear force, V_{jv} , can be calculated by subtracting the tensile forces in the piles, R_t , from the total tensile force in the column reinforcement, T_c ,

i.e.,
$$V_{jv} = T_c - R_t \quad (10-4)$$

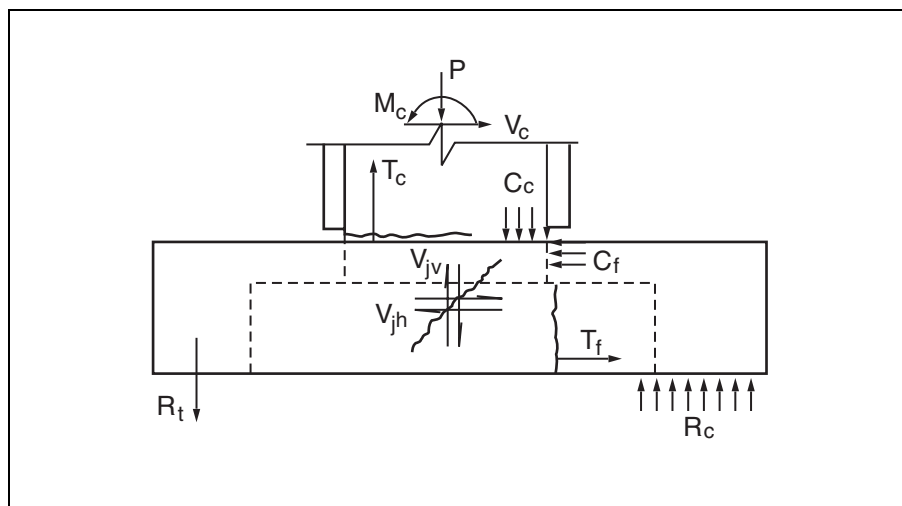


Figure 10-21. Footing joint shear forces.

The joint shear stress, v_{jv} , can be calculated from:

$$v_{jv} = \frac{V_{jv}}{b_{eff} d_f} \quad (10-5)$$

where b_{eff} is the $B_c + D_c$ for rectangular columns, B_c is the column width, D_c is the column depth, b_{eff} is $1.414 D$ for circular columns, D is the column diameter, and d_f is the depth of the retrofitted footing.

The effective axial compressive stress within the joint in the vertical direction is given by:

$$f_a = P / A_{eff} \quad (10-6)$$

where:

P = axial load (i.e., dead load + earthquake) at the base of the column, and
 A_{eff} = effective bearing area: $(B_c + d_f)(D_c + d_f)$ for rectangular columns, and
 $\pi (D + d_f)^2 / 4$ for circular columns.

Thus, the principle tensile stress in the joint region is given by:

$$f_t = -f_a/2 + \sqrt{(f_a/2)^2 + v_{jv}^2} \quad (10-7)$$

If $f_t < 0.42\sqrt{f'_c}$ MPa ($5\sqrt{f'_c}$ psi), no further design is required. Otherwise, proceed to the next step.

Step 7. Check the capacity of the footing overlay - When $f_t \geq 0.42\sqrt{f'_c}$ MPa ($5\sqrt{f'_c}$ psi), the ability of the overlay to participate in the resistance of joint shear stresses must be checked. The strut and tie model shown in figure 10-22 illustrates how the anchorage forces in the column tensile reinforcement are resisted. Two compression struts, one acting toward the interior of the column, C_{in} , and the other acting toward the exterior of the column, C_{ex} , act at the midpoint of the anchorage length, y_b , of the column reinforcement. The vertical component of C_{in} is balanced by the column compression block, but C_{ex} must be resisted by the footing overlay. The horizontal component of C_{ex} is resisted by membrane action, which stresses the horizontal reinforcement in the overlay. In addition, the overlay and the existing footing must be capable of resisting the vertical component of C_{ex} perpendicular to the overlay, as given by:

$$P_v = \cos (45) C_{ex} = 0.5T_c \quad (10-8)$$

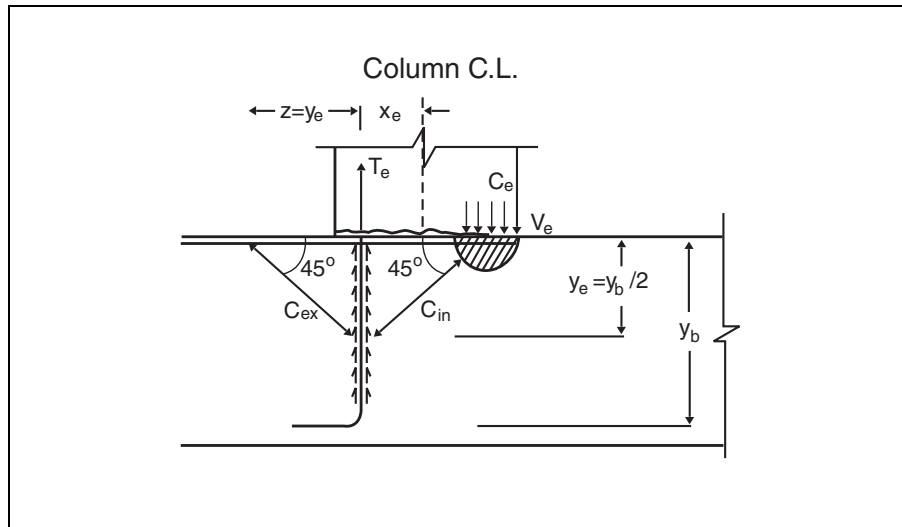


Figure 10-22. Strut and tie model for joint design.

The effective depth of an assumed concrete plate will be equal to the depth of the overlay plus the embedment of the dowels (i.e., this assumes a partial delamination plane at the bottom of the dowels). This results in both negative and positive bending forces in the assumed plate that is best resisted by two layers of horizontal reinforcing steel in the overlay. The ultimate capacity of the assumed plate to resist P_v can be determined using yield line theory. The computer program FT-YIELD, which employs a virtual work method, was developed for this purpose (Xiao et al., 1994). The assumed yield line pattern for a typical footing is shown in figure 10-23(a). If the plate assumes the displaced shape shown in figure 10-23(b), the virtual work done by P_v must be balanced by virtual work done by plate bending forces along the assumed plate fold lines. Increasing the thickness of the overlay, increasing the dowel embedment depth, or adding additional overlay reinforcement can increase the flexural capacity of the assumed plate.

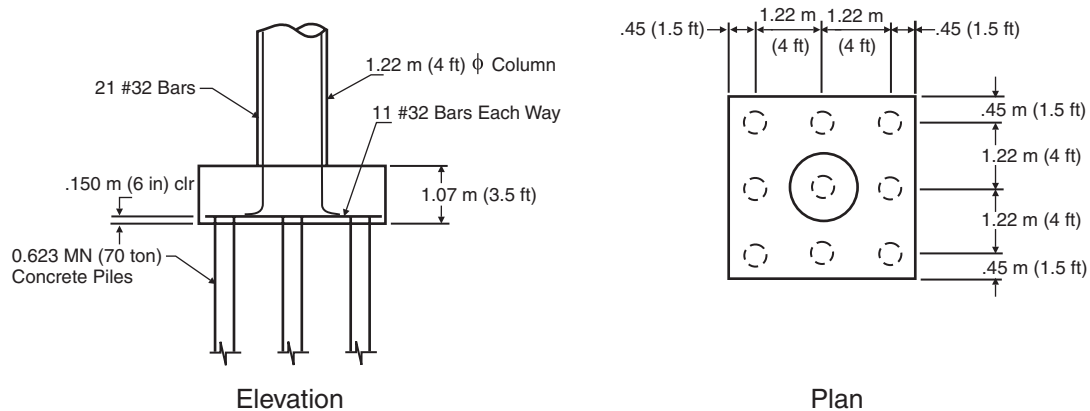
However, the simplest approach is to increase the overlay thickness until v_{jv} is less than $0.42\sqrt{f'_c}$ MPa ($5\sqrt{f'_c}$ psi), unless there is limited space available for doing this.

An example of a retrofit design of a bridge footing is presented in example 10-1.

EXAMPLE 10.1: RETROFIT DESIGN OF A FOOTING

The footing shown in the figure below supports a 1.22 m (4 ft) diameter reinforced concrete column with 21 # 32 (metric) (#10 cus) reinforcing bars grade 40. The column is fixed for moment into the footing. The footing does not have a top layer of reinforcement but it is supported on nine 0.381 m (1.25 ft) diameter concrete piles that are adequately connected to the footing to resist uplift forces.

Evaluate the capacity of the footing and design an appropriate overlay retrofit.



Assume the following data:

- $P_{DL} = 3.56 \text{ MN}$ (800 k)
- $P_{LL} = 1.56 \text{ MN}$ (350 k)
- $f'_c = 35 \text{ MPa}$ (5 ksi) (assumed existing strength and strength of new concrete)
- $P_{pile} = 0.623 \text{ MN}$ (70 tons) (design capacity)
- $P_{ultc} = 1.25 \text{ MN}$ (140 tons) (pile ultimate capacity in compression)
- $P_{ultt} = 0.623 \text{ MN}$ (70 tons) (pile ultimate capacity in tension)

STEP 1. DESIGN COLUMN MOMENTS USING CAPACITY DESIGN

- $M_n = 4.3 \text{ MN-m}$ (nominal moment capacity at dead load axial force, from interaction diagram in handbook, etc.)
- $M_p = 1.4 M_n = 1.4 (4.3 \text{ MN-m}) = 6.02 \text{ MN-m}$ (4437 k-ft)

STEP 2. EVALUATE FOOTING CAPACITY

$$N_{piles} = 9$$

$$S_{piles} = \frac{2 \times \#piles/row \times y^2}{c} = \frac{2(3) \cdot 1.22^2 \text{ m}^2}{1.22 \text{ m}} = 7.32 \text{ m} (24.02 \text{ ft})$$

$$P_{comp} = \frac{P_{DL}}{N_{piles}} + \frac{M_p}{S_{piles}} = \frac{3.56 \text{ MN}}{9} + \frac{6.02 \text{ MN-m}}{7.32 \text{ m}^3} = 1.22 \text{ MN/pile} < 1.25 \text{ MN} (140 \text{ tons}) \Rightarrow \text{OK}$$

$$P_{\text{ten}} = \frac{P_{\text{DL}}}{N_{\text{piles}}} - \frac{M_p}{S_{\text{piles}}} = \frac{3.56 \text{ MN}}{9} - \frac{6.02 \text{ MN/m}}{7.32 \text{ m}^3} = -0.427 \text{ MN tension}$$

$$P_{\text{ten}} < P_{\text{ultt}}$$

$$0.43 \text{ MN (48.3 tons)} > -0.623 \text{ MN (70 tons)} \Rightarrow \text{OK}$$

Therefore, the existing piles are adequate.

STEP 3. CHECK SHEAR CAPACITY OF EXISTING FOOTING

$$v_u = \frac{V_u}{bd} = \frac{3_{\text{piles}} (1.22 \text{ MN/pile})}{3.34 \cdot 0.915 \text{ m}^2} = 1.19 \text{ MPa (173 psi)}$$

$$V_c = \phi 0.168 \sqrt{f'_c} = 0.85 (0.168) \sqrt{35 \text{ MPa}} = 0.845 \text{ MPa (123 psi)}$$

$$V_c < V_u$$

$$= 0.845 \text{ MPa (123 psi)} < 1.193 \text{ MPa (173 psi)} \Rightarrow \text{NG (i.e., not satisfactory)}$$

Increase the depth of footing 0.305 m (1.0 ft) and add #16 (metric) stirrups at 0.305 m (12 in) spacing to accommodate the shear demand. Stirrups are assumed to be only 50 percent effective due to lack of proper anchorage.

$$v_u = 3_{\text{piles}} (1.22 \text{ MN/pile}) = 3.66 \text{ MN (822 k)}$$

$$v_u = v_c bd = 0.845 \text{ MPa (3.34 m)} 1.22 \text{ m} = 3.44 \text{ MN (778 k)}$$

$$s = 0.305 \text{ m}$$

$$V_s = \phi 0.5 \cdot A_b F_y \frac{d}{s} N_b = 0.85 (0.5) \cdot 0.0002 \text{ m}^2 (414) \text{ MPa} \frac{1.22 \text{ m}}{0.305 \text{ m}} (11 \text{ bars}) = 1.55 \text{ MN (348 k)}$$

$$V_c + V_s = 3.46 \text{ MN} + 1.55 \text{ MN} = 4.99 \text{ MN (1122 k)} > 3.66 \text{ MN (822 k)} \Rightarrow \text{OK}$$

Therefore, #16 stirrups @ 0.305 m (12 in) spacing are more than adequate for vertical shear.

STEP 4. CHECK MOMENT CAPACITY AND DESIGN TOP REINFORCEMENT FOR PILES IN TENSION

Distance from equivalent face of column to pile centerline.

$$X_{\text{pile}} = D - 0.5 (A_g)^{0.5}$$

$$x_{\text{pile}} = 1.22 - \frac{\sqrt{\pi(0.61^2)}}{2} = 1.22 - 0.54 = 0.68 \text{ m (2.23 ft)}$$

$$M_T = P_{ten} \text{ MN } (N_p) x_{pile_m} = \frac{0.43 \text{ MN}}{\text{pile}} (3_{piles}) 0.68 = 0.88 \text{ MN/m } (649 \text{ kft})$$

Try 8 #19 (metric) bars.

$$a = \frac{A_s f_y}{(.85 f'_c) b}$$

$$a = \frac{N_b \text{ bars } A_b \text{ m}^2 F_y \text{ MPa}}{(0.85 f'_c \text{ MPa}) b} = \frac{8 (0.000283 \text{ m}^2) 414 \text{ MPa}}{0.85 (35 \text{ MPa}) 3.34 \text{ m}} = 0.0094 \text{ m } (0.37 \text{ in})$$

$$M_u = \phi A_s f_y \left(d - \frac{a}{2} \right)$$

$$M_u = \phi N_b A_b F_y \left(d - \frac{a}{2} \right) \\ = 0.9 (8 \text{ bars}) 0.000283 \text{ m}^2 (414 \text{ MPa}) \left(1.287 - \frac{0.0094}{2} \right)$$

$$= 1.08 \text{ MN/m } (796 \text{ kft}) > 0.88 \text{ MN/m } \Rightarrow \text{OK}$$

$$M_u > M_t \quad \text{OK}$$

Check moment on compression side (#32 @ 0.3 m [1 ft] spacing)

$$M_C = P_{comp} N_p x_{pile} = 1.22 (3) \cdot 0.68 = 2.49 \text{ MN/m } (1835 \text{ kft})$$

$$a = \frac{A_s f_y}{(.85 f'_c) b} = \frac{11 \times .000818 \times 276}{3.34 \times 35 \times .85} = .025$$

$$M_u = \phi N_b A_b F_y \left(d - \frac{a}{2} \right) = 0.9 \cdot 11 \cdot 0.000818 \cdot 276 \cdot \left(1.22 - \frac{.025}{2} \right)$$

$$= 2.70 \text{ MN/m } (1990 \text{ k/ft}) > 2.49 \text{ MN/m } \Rightarrow \text{OK}$$

$$M_u > M_c \quad \text{OK}$$

STEP 5. CALCULATE HORIZONTAL SHEAR AT INTERFACE OF OVERLAY AND EXISTING FOOTING

Area of new concrete in footing

$$A = d_{ol}(b)$$

$$Q = A d_Q = 0.305 \text{ m} \cdot 3.34 \text{ m} \left(\frac{1.375 \text{ m}}{2} - \frac{0.305 \text{ m}}{2} \right) = 0.54 \text{ m}^3 (19.3 \text{ ft}^3)$$

$$I = \frac{bh^3}{12} = \frac{3.354 \text{ m} \cdot 1.372^3 \text{ m}^3}{12} = 0.528 \text{ m}^4 \quad (83.6 \text{ ft}^4)$$

$$v_h = \frac{V_u Q}{(I)b} = \frac{3.44 \text{ MN} \cdot 0.54 \text{ m}^3}{0.528 \text{ m}^4} \cdot \frac{1}{3.34 \text{ m}} = 1.06 \text{ MPa} \quad (154 \text{ psi})$$

$$v_{sf} = \frac{\phi \psi A_s F_y}{s^2} = \frac{0.85(1.0) \cdot 0.0002 \cdot 414}{0.305^2} = 0.757 \text{ MPa} \quad (110 \text{ psi}) \quad \text{NG}$$

$$V_{sf} < V_h \quad \text{NG}$$

Try #16 @ 0.250 m V_{sf} (0.82 ft) spacing (#16 and 35 MPa [5000 psi] concrete required to achieve anchorage in 0.3 m [1 ft] overlay)

$$v_{sf} = \frac{\phi \psi A_s F_y}{s^2} = \frac{(0.85) \cdot 1.0(0.000283 \text{ m}^2) \cdot 414 \text{ MPa}}{0.250^2} = 1.126 \text{ MPa} \quad (135 \text{ psi}) \quad \text{OK}$$

$$V_{sf} > V_h \quad \text{OK}$$

STEP 6. CHECK JOINT SHEAR

$$A_{\text{eff}} = \pi(D + d_f)^2 / 4 = \frac{3.1416 \cdot (1.22 \text{ m} + 1.22 \text{ m})^2}{4} = 4.68 \text{ m}^2 \quad (50.3 \text{ ft}^2) \quad (\text{Eq. 10-6})$$

$$b_{\text{eff}} = D\sqrt{2} = 1.414(1.22) = 1.73 \text{ m} \quad (5.67 \text{ ft})$$

$$T_{\text{col}} = A_s f_y$$

Assume grade 60 steel; therefore $f_y = 414 \text{ MPa}$

$$T_{\text{col}} = 15 \text{ bars} (0.000818 \text{ m}^2 \text{ bar}) \cdot 414 \text{ MPa} = 5.08 \text{ MN} \quad (1142 \text{ k}) \Rightarrow \text{if approximately 15 bars in tension}$$

$$V_{\text{JV}} = T_{\text{col}} - N_{\text{piles}} P_{\text{ten}} = 5.08 - 3 \cdot 0.43 = 3.79 \text{ MN} \quad (852 \text{ k}) \quad (\text{Eq. 10-4})$$

$$V_{\text{JV}} = \text{joint shear}$$

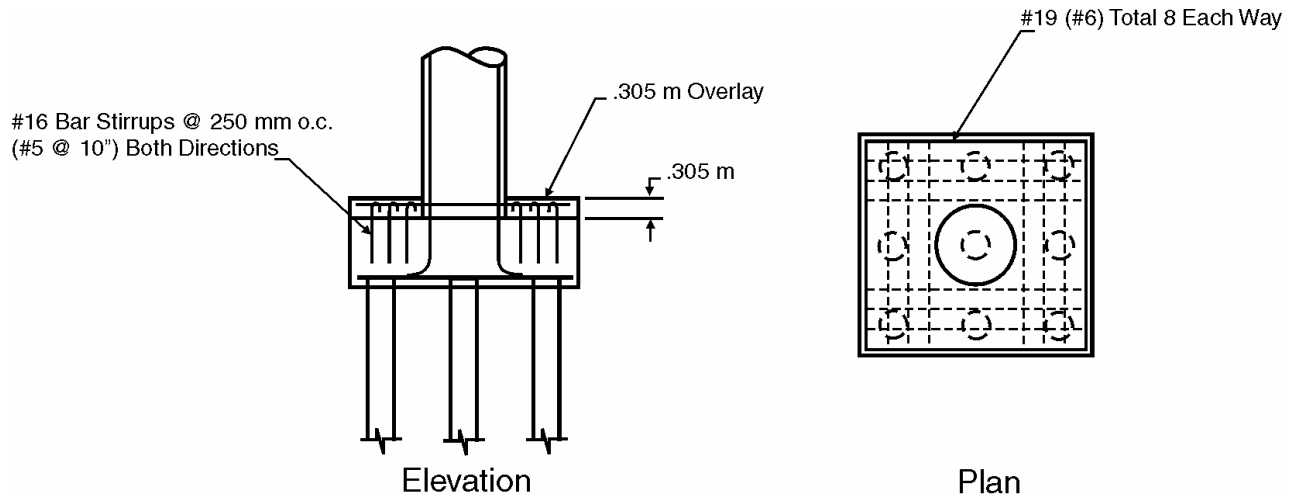
$$v_{\text{JV}} = \frac{V_{\text{JV}}}{b_{\text{eff}} d_f} = \frac{3.79 \text{ MN}}{1.73 \text{ m} (1.22 \text{ m})} = 1.80 \text{ MPa} \quad (261 \text{ psi}) \quad (\text{Eq. 10-5})$$

$$f_a = \frac{P_{\text{DL}}}{A_{\text{eff}}} = \frac{3.56 \text{ MN}}{4.68 \text{ m}^2} = 0.76 \text{ MPa} \quad (110 \text{ psi})$$

$$f_t = -f_a/2 + \sqrt{(f_a/2)^2 + v_{\text{JV}}^2} = -\frac{0.76 \text{ MPa}}{2} + \sqrt{\frac{(0.76 \text{ MPa})^2}{4} + (1.80 \text{ MPa})^2} = 1.46 \text{ MPa} \quad (212 \text{ psi}) \quad (\text{Eq. 10-7})$$

$$F_t = 0.42\sqrt{f'_c} = (0.42) \cdot \sqrt{35} = 2.48 \text{ MPa (360 psi)} > 1.46 \Rightarrow \text{OK}$$

Therefore, check of overlay capacity by yield line theory is not required. The following is a sketch of the footing retrofit.



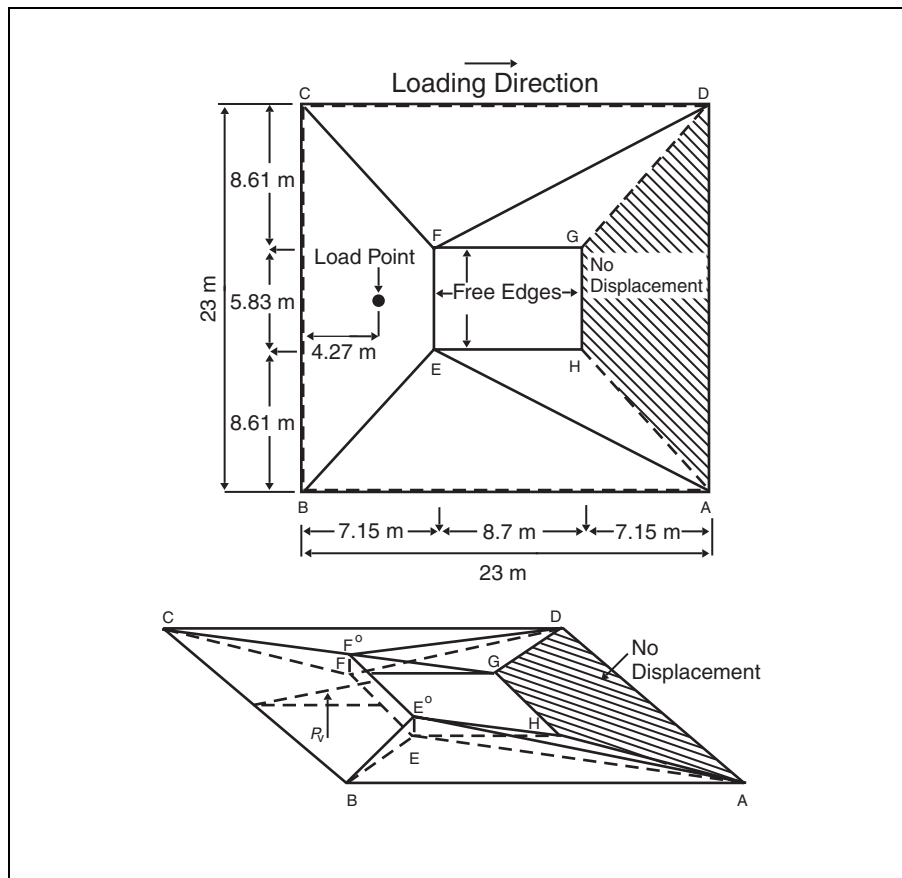


Figure 10-23. Yield line analysis of footing overlay.

10.3.4. LIMITING FORCES TRANSMITTED TO THE FOOTINGS

Link beams similar to those used to reduce moments in pier caps, as described in section 9.3.3, can be used to reduce the bending forces transmitted to the footings. Link beams are placed near the footing and can be constructed below grade against undisturbed soil. The design objective is to force a plastic hinge in the column just above the link beam. This limits the shear in the column below the link beam to the plastic shear that is generated in the column above the link beam. This, in turn, reduces the moment in the column below the link beam, which limits the moment transmitted to the foundation, and could therefore eliminate the need to retrofit the foundations. An example of such a retrofit is shown in figure 10-24.

10.4. RETROFIT MEASURES FOR PILES AND PILE-TO-FOOTING CONNECTIONS

During an earthquake, piles must carry compression, tension, and lateral loads. If they are inadequate for these loads, retrofitting is required. The most common method is to use supplemental piles.

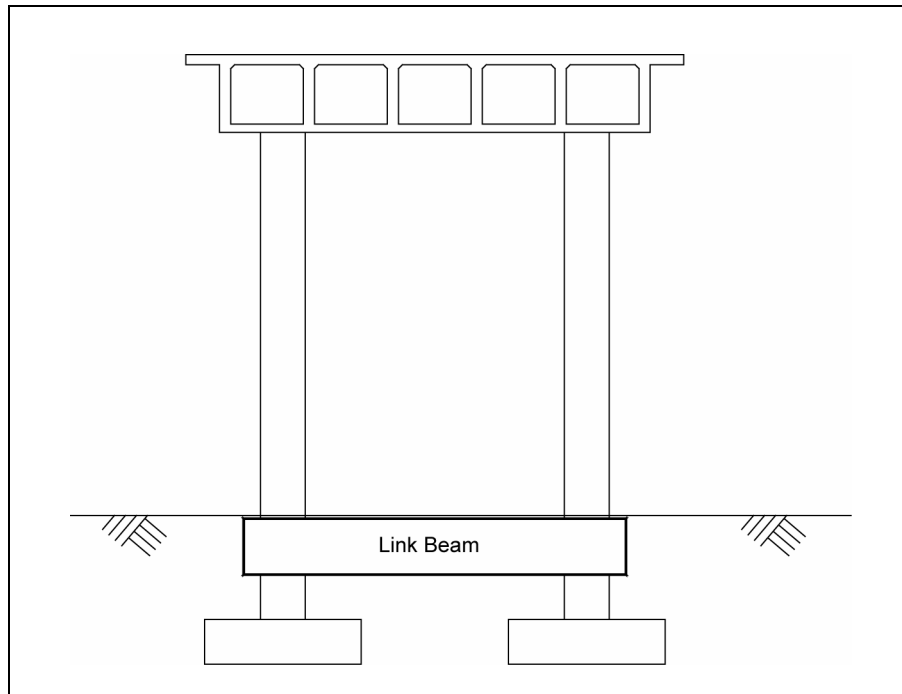


Figure 10-24. Footing link beam retrofit.

When piles are located in competent soils, their ultimate compression capacity is between two and four times the pile capacity based on allowable stress. If the soils are not competent, such as in a soft clay or sand susceptible to liquefaction, pile capacity will be limited by the structural capacity of the pile acting as a column. This may require supplemental piles that are stiffer and less likely to buckle. Supplemental piles will also limit the lateral displacements of the pile cap, reduce $P-\Delta$ effects, and increase the effectiveness of the existing piles.

The tensile capacity of piles is often limited by their connection to the footing. Timber piles have little or no capacity for resisting uplift forces. Standard connections for steel H piles are also inadequate for large tensile forces. The longitudinal reinforcing steel in reinforced concrete piles may be terminated too close to the top of the pile, resulting in insufficient tensile capacity of the pile. In each of these cases, and in others where pile uplift capacity is absent, it may be desirable to add hold-down anchors or supplemental tension piles.

The lateral capacity of piles in competent soil is generally not a problem. Such is not the case if lateral loads on the pile are exceptionally high or if the soil cannot provide adequate lateral support. In this case, supplemental piles with high lateral resistance can be added.

The following sections discuss considerations for the addition of piles as a seismic retrofitting approach, and details for seismic hold-down anchors.

10.4.1. PILE TYPE CONSIDERATIONS (NEW PILES)

It is often necessary to drive new piles when footing strengthening or replacement is required. Frequently, these piles must be driven under the existing superstructure, where there will be limited headroom. This requires that the piles be driven in short lengths and spliced at frequent intervals, effectively eliminating the use of precast concrete or timber piles. Steel H piles may be too flexible for some retrofitting projects, and they require complete butt-welding between sections to obtain moment continuity. Two types of piling that have received increased use for retrofitting are discussed below.

Steel pipe piles, often constructed with a cast-in-place concrete core, have been popular for retrofitting because they are relatively easily spliced with complete penetration butt welds. These piles come in 400-mm and 600-mm (16-in and 24-in) diameters and are stiffer than a steel H-pile of equal cross-sectional area. This makes them more efficient at resisting lateral loads, particularly if the surface soil is relatively weak. These shells can be driven with a closed bottom, or they can be driven with an open end and drilled out afterwards. The shells are usually filled with concrete and a reinforcing bar cage long enough to resist pile bending and axial forces. This allows the cage to be anchored at its top in new footing concrete, thus developing significant resistance to pile pullout. Drilling out the inside of steel shells results in loss of some skin friction.

CIDH piles with diameters between 400 mm and 2500 mm (16 in and 96 in) are also popular where site conditions allow. Equipment exists to allow small diameter piles of this type to be drilled with relatively little headroom. Large diameter shafts have considerable stiffness and are used where large axial or lateral loads must be developed in a relatively small horizontal area.

CIDH piles are easiest to construct if the hole is dry and not subject to caving in. If this is not the case, methods are available that will allow these piles to be installed under wet conditions or when cave-in is likely. These piles also have a reinforcing steel cage that is deep enough to resist axial forces and bending moments. If the soil is weak, the cage must extend deeper, which may require splicing of the longitudinal reinforcing when there is not enough headroom. The cage also provides a strong connection between the top of the pile and the new footing.

10.4.2. PILE TIE-DOWNS

For piles in tension (uplift), tie-downs can be added to an existing footing if overturning of the footing can occur. Several pile tie-down details have been developed and tested, such as that shown in figure 10-25. To be effective in providing sufficient tensile stiffness, tie-down anchors are usually prestressed, which also acts to proof-load the tie-down. The amount of prestressing is limited, however, by the compressive capacity of the remaining piles. This may allow significant rotation of the footing to take place before tie-downs are fully effective. These rotations must be checked against acceptable limits because large footing rotations can aggravate $P-\Delta$ effects in tall columns. For this reason, the use of tie-downs is often limited to footings with relatively short columns.

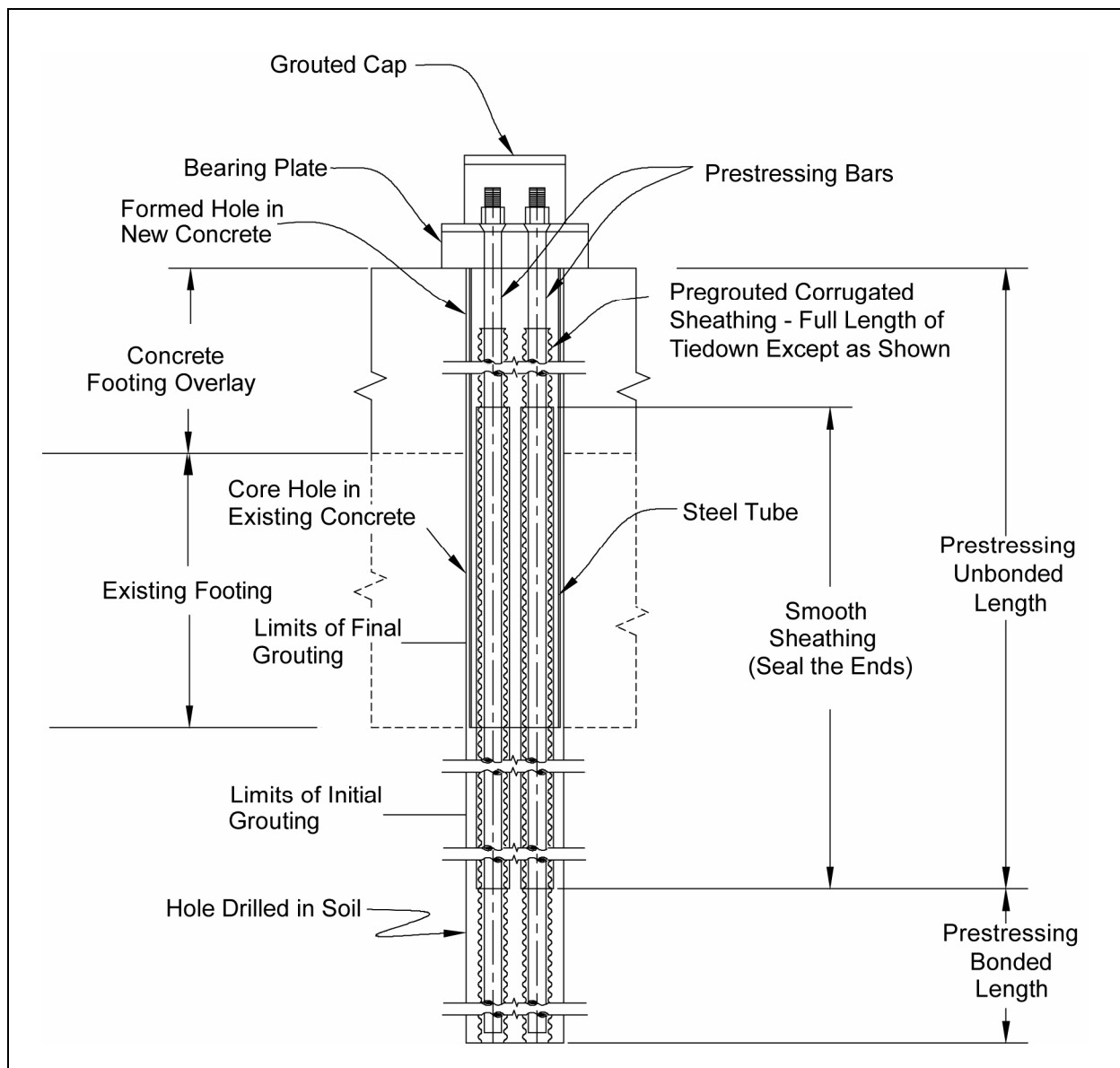


Figure 10-25. Prestressed tie-down anchor.

CHAPTER 11: RETROFIT MEASURES FOR BRIDGES ON HAZARDOUS SITES

11.1. GENERAL

A hazardous site is one that has the potential for extreme permanent displacement during an earthquake, leading to large forces and/or differential displacements in the structural members of a bridge. Such sites include bridges that cross or are immediately adjacent to:

- Active faults.
- Steep, unstable slopes.
- Liquefiable sands or silty sands.

This chapter discusses issues and approaches to be considered when retrofitting a bridge on such a site.

11.2. BRIDGES ACROSS OR NEAR ACTIVE FAULTS

Bridges crossing or immediately adjacent to active faults may be subjected to large differential displacements between adjacent piers and/or abutments due to surface faulting. Although the probability of this occurring at a given location during the life of a bridge will be low, the possibility should be considered when choosing retrofit measures for the bridge.

Methods for determining the likelihood of surface fault rupture are discussed in chapter 3. A conservative design approach should be adopted if surface faulting is possible. For example, adding extra confinement in the plastic hinge zones of the substructure might be used to provide the maximum displacement capacity.

If a bridge is a series of simply supported spans, the relative merits of making the structure continuous should be carefully evaluated. This may require increases in the section modulus at the ends of the simple beams due to the creation of negative moments. On the other hand, simple spans can tolerate large relative movements, but it will be difficult to ensure that the spans do not become unseated. To minimize this risk, very generous support lengths should be provided.

The additional redundancy in continuous superstructures that are integral with their substructures will reduce the probability of total collapse. There is, however, a practical limit to the amount of relative displacement across a fault that can be accommodated in a monolithic structure. One alternative is to support a continuous superstructure on elastomeric bearings at each pier and abutment. These bearings can accommodate relatively large displacements and still provide an elastic restoring force to the superstructure. Restrainers may also be provided if gross movements are expected. Note that acceleration records from recent earthquakes indicate

vertical accelerations in excess of 1.0 g in the near-field of the fault. In these situations, integral construction is preferred, but if elastomeric bearings are used, vertical restrainers should be provided to limit the uplift.

11.3. BRIDGES ON OR NEAR UNSTABLE SLOPES

Many bridges in mountainous regions cross steep-sided valleys. Detailed geotechnical investigations should be made to evaluate the potential for slope instability under seismic conditions.

For major structures, these investigations should include geological and geomorphic studies, including expert study of aerial photographs for evidence of bank movement during recent earthquakes, as well as material testing and extensive bore hole and trenching investigations to check for unstable layers and vertical fissures. Particular attention should be paid to drainage to prevent infiltration of surface water and increased porewater pressures in potential failure regions. Special studies should be made to investigate the practicality of increasing the factor of safety against slope failure by such means as unloading the banks by removal of overburden. For important structures, it may be advisable to move the abutments back from the top of the slope, and reconstruct each end span accordingly. It may also be prudent to tie back footings located on the bank, with rock anchors or other techniques.

Methods for evaluating the potential for earthquake-induced slope stability and the magnitude of slope deformations, together with suggested retrofit measures to improve slope stability, are described in more detail in Part 2 of this manual.

11.4. BRIDGES ON LIQUEFIABLE SOILS

The vulnerability of bridges to liquefaction-induced ground failure has been clearly demonstrated in past earthquakes (1964 Niigata, 1964 Alaska, 1990 Luzon, 1991 Costa Rica, 1995 Kobe).

Based on past experience, three liquefaction-related hazards should to be considered:

1. Flow slides (large translational or rotational movements) mobilized by existing static stresses.
2. Limited cyclic or permanent lateral spreads (displacements) triggered and sustained by the earthquake's ground motion.
3. Post-liquefaction ground settlement.

Each of these hazards can cause major structural damage (figure 11-1) and should be considered during the development of a bridge retrofit plan. Damage modes include:

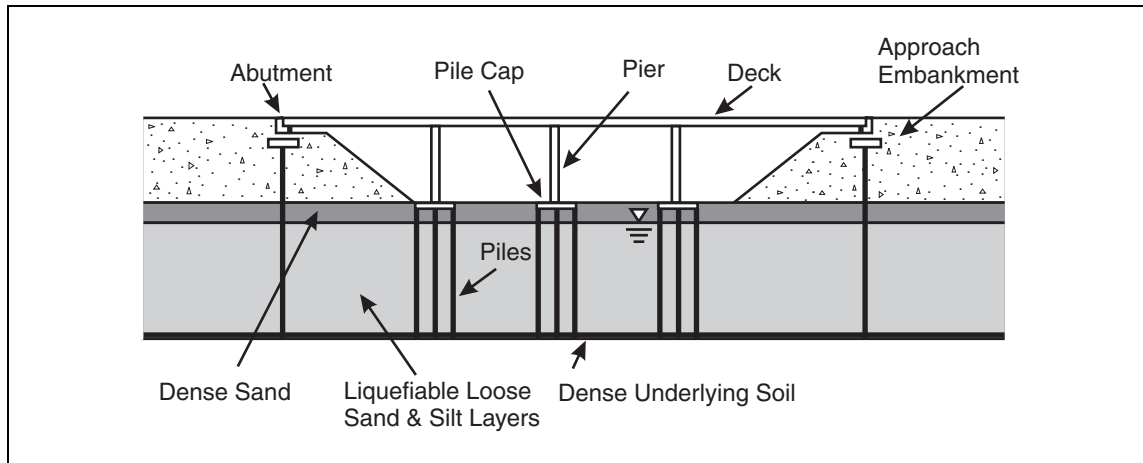


Figure 11-1. Elevation view of a representative bridge on a liquefiable stratum.

- Lateral deformation of abutments and piers due to liquefaction-induced flow or lateral spreads, leading to pile damage and potential span collapse.
- Differential ground lurching between adjacent piers with the potential for span collapse.
- Differential settlement of footings and abutments leading to damage in continuous superstructures and pile damage due to downdrag.
- Loss of pile stiffness and capacity leading to structural damage during shaking.

Methods to assess the potential for liquefaction at a bridge site are discussed in chapter 3, together with recommended procedures to estimate post-liquefaction settlement. Refer to appendix B (figure B-1) for evaluation of liquefaction potential. The calculation of the amount of lateral ground deformation to be expected in the free-field (i.e., in the absence of a bridge) is also described in chapter 3. Since this calculation involves considerable uncertainty, and is the subject of ongoing research, current practice uses the Newmark sliding block approach on an assumed dominant failure plane within the liquefied zone. Free-field displacements are defined by an estimated lateral displacement on a failure surface, with the displacement linearly distributed over the failure zone, as shown in figure 11-2.

Mitigation methods should be considered when any of the above damage modes are likely to occur. Aside from relocating the bridge to a less vulnerable site, two basic options are available:

1. Structural retrofit to accommodate the predicted liquefaction and related ground displacement demands. This requires an analysis of the soil-structure interaction (SSI) to determine if the deformation and load capacity of the existing foundation system can accommodate the ground deformation demands without collapse, or can meet other prescribed performance criteria. If it is inadequate, mitigation methods to strengthen the foundation should be evaluated, and costs compared to the ground modification option described below. Evaluation methods that may be used in this approach are discussed in section 11.4.1.

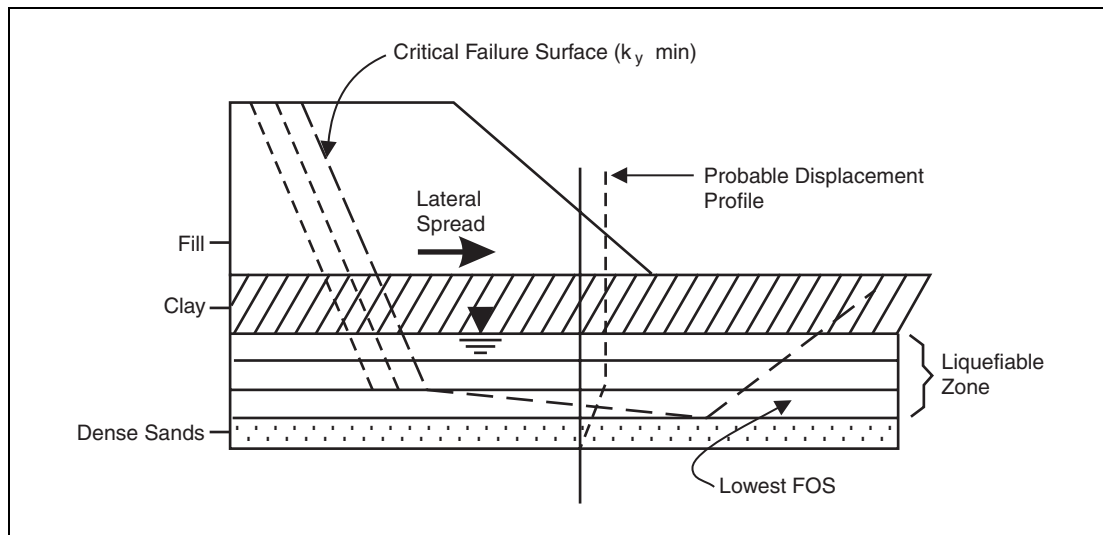


Figure 11-2. Pseudo-static stability analysis.

2. Site remediation to stabilize the soil and prevent or inhibit liquefaction, and minimize ground displacement demands. Remediation methods include:

- In-situ densification of liquefiable soils in zones surrounding bridge piers, and underneath the toe of approach fills; this will reduce ground deformations to tolerable levels.
- Deep soil mixing using cement, which creates stabilizing zones in the soil similar to those developed by ground densification techniques.
- Dewatering, installation of gravel drains or permeation grouting, and similar techniques.

A summary of ground improvement methods for liquefaction remediation at existing bridges is given in table 11-1. Overviews of the state-of-practice are documented in several publications (ASCE, 1997; Andrus and Chung, 1995). A comprehensive report on ground remediation measures for liquefaction at existing bridge sites has also been developed (Cooke and Mitchell, 1999).

In-situ densification, using either the vibro-replacement technique or compaction grouting, is the most widely used ground remediation techniques for both new and existing bridges.

11.4.1. STRUCTURAL RETROFITTING OF PILED FOUNDATIONS

An initial assessment should be made to see if the shear and moment capacity of pile foundations is sufficient to prevent collapse of the bridge under the displacement demands imposed on the foundation system. This is done by using analytical results that give the magnitude of the lateral

Table 11-1. Summary of ground improvement methods for liquefaction remediation at existing bridges

Method	Principle	Suitable Soil Types	Treated Soil Properties	Relative Costs	Abutment Applicability*		Pier Applicability*	Comments
					Stub	Full-Height/Wingwalls		
Compaction Grout	Highly viscous grout acts as spherical hydraulic jack when pumped under high pressure resulting in densification.	Compressible soils with some fines	Increased D_r SPT: $(N_1)_{60}$ 25 to 30 CPT: $q_d = 80$ to 150 tsf (Kg/cm ²)	Low material cost; high injection cost.	1. High. Treat anywhere between abutment and embankment toe; treat under and around abutment if excessive settlement expected. 2. High. Treat around pile groups.	1. Generally high. Treat under and around footing. 2. High. Treat around pile groups.	High for solid wall, multi-column, and hammerhead piers. High to moderate for circular single-column piers. 1. Treat under and around footing. 2. Treat around pile groups.	Must control heave and/or hydraulic fracture of soil. Particulate and chemical grouting: verify size and strength of grouted soil mass. Jet grouting: stage work to limit settlements. Evaluate potential damage to piles from jetting pressure.
Particulate Grouting	Penetration grouting: fill soil pores with cement, soil and/or clay.	Clean, medium to coarse sand and gravel	Cement-grouted soil: high strength	Lowest of grouting systems				
Chemical Grouting	Solutions of two or more chemicals react in soil pores to form a gel or solid precipitate.	Silts and sands	Low to high strength	High to very high				
Jet Grouting	High speed jets at depth excavate, inject and mix stabilizer with soil to form column or panels.	Sands, silts and clays	Solidified columns and walls	High				
Vibratory Probe	Densification by vibration, liquefaction-induced settlement underwater.	Sand (< 15% passing No. 200 sieve)	D_r : up to 80+% Ineffective in some sands.	Moderate	1. Moderate for lateral spreading; low for settlement. Treat at embankment toe to reduce risk of construction settlement. 2. Low. Treating around piles difficult due to access problems.	1. Low. Potential for excessive settlement and vibrations of bridge. Overhead clearance limitations. 2. Low. Treating around piles difficult due to access problems.	1. Low. Potential for excessive settlement and vibrations of bridge. Overhead clearance limitations. 2. Moderate to high. Treat around pile groups.	Overhead clearance limitations will restrict use. Monitor bridge for excessive vibrations. Construction in water requires special procedures.
Vibro-Compaction	Densification by vibration and compaction of backfill at depth.	Sand (< 20% passing No. 200 sieve)	D_r : up to 85+% SPT: $(N_1)_{60}$ 25 to 30 CPT: $q_d = 80$ to 150 tsf (Kg/cm ²)	Moderate				

(continued)

Table 11-1. (continued) Summary of ground improvement methods for liquefaction remediation at existing bridges

Method	Principle	Suitable Soil Types	Treated Soil Properties	Relative Costs	Abutment Applicability*		Pier Applicability*	Comments
					Stub	Full-Height/Wingwalls		
Vibro-replacement/ Stone Columns	Densely compacted gravel columns provide densification, reinforcement, and drainage	Sands and silts	Increased D_r , $SPT: (N_1)_{60}$ 25 to 30 CPT: $q_d = 80$ to 150 tsf (Kg/cm ²)	Moderate to high				
Surcharge/ Buttress Fill	Weight of surcharge increases liquefaction resistance by increasing effective stresses. Buttress fill increases stability by reducing overturning moment and increasing resisting moment.	Any soil surface provided it will be stable	Increase in strength	Low	1. High for slope stability and low for settlement. Place at embankment toe. 2. Low. Ineffective in increasing soil stresses at piles.	1 & 2. Moderate. Place buttress fill in front of wall.	1 & 2. Moderate to low. Place surcharge around pier.	Need large area. Evaluate loads and settlement imposed on bridge.
Drains: Gravel Sand Wick	Relief of excess pore water pressure to prevent liquefaction. Intercept and dissipate excess pore water pressure plumes from adjacent liquefied soil.	Sands, Silt	Improved drainage	Low to moderate	1 & 2. Moderate. Install drains around zone improved by other method(s).	1 & 2. Moderate. Install drains around zone improved by other method(s).	1 & 2. Moderate. Install drains around zone improved by other method(s).	Topography and space limitations may restrict use.
Mini-Piles	Provide piles to carry loads through liquefiable soils to firm stratum.	All soils	-	High	1 & 2. High to moderate.	1 & 2. High to moderate.	1 & 2. High to moderate.	Must provide means of tying mini-piles into existing foundation.
Note: * Item No. 1 indicates applicability of improvement method for foundations over or in liquefiable soils. Item No. 2 indicates applicability for pile (or drilled shaft) foundations extending through liquefiable soils.								

Cooke and Mitchell, 1999

deformations in a liquefied layer (normally the layer with the lowest factor of safety against liquefaction) and the geometry of the most likely failure surfaces based on Newmark analyses.

These analyses assume that the effects of ground displacement can be uncoupled from the effects of structural inertial loading. In most cases this is a reasonable assumption, because peak vibration response is likely to occur in advance of maximum ground displacement, and maximum values of displacement-induced moment and shear will generally occur at deeper depths than the depths at which maximum moments and shears occur due to structural inertial loading.

The magnitude of moments and shears induced in pile foundations by ground displacements may be computed using soil-pile interaction computer programs such as LPILE (Wang and Reese, 1998), where the assumed displacement field is applied to interface springs using p-y curves. Many examples of such analyses are described in the literature¹. In the liquefied zone, the soil is normally treated as being soft and cohesive. When calculating the characteristics of the lateral springs (i.e., the p-y curves), the maximum soil cohesion is assumed equal to the residual strength of the liquefied soil. In some cases, large ground deformations may slide past the foundation system, exerting full passive pressures in the process (Berrill et al., 1997).

A refinement of the above approach is to consider the reinforcement or ‘pinning’ effect that a pile or pile group may have on lateral displacements. This is done by representing the pile shear forces at the location of the failure plane as an equivalent shear strength in the calculation of yield accelerations used in the Newmark analyses. This becomes an iterative approach, since shear forces are a function of displacements, which in turn are reduced as the shear forces increase.

The impact of lateral spread on an existing pile foundation depends on a number of geotechnical factors, such as the thickness of the crustal layer overlying the liquefied zone, the thickness of the liquefied layer, and the magnitude of lateral displacement. Pinning action becomes less effective as the thickness of liquefied soil increases. A simplified analysis using this technique is described below.

If the pile foundations cannot tolerate the displacement demands, one option is to install additional piles to increase the pinning action and reduce the displacement demands. In such a case, the footing will need to be extended and possibly overlaid. Another option is to use pinch piles, driven through the liquefiable layer and failure surface, to provide additional pinning action. The former option is particularly relevant if additional piles are required to resist high overturning moments or minimize downdrag effects. Before deciding on this approach, the cost of additional piles and extended footings should be compared with the cost of ground remediation as described in section 11.4.2.

11.4.1.1. Simplified Analysis

A simplified analytical method for designing the foundations of new bridges is described in ATC/MCEER 2003 and is applicable to existing foundations. It involves four basic elements:

¹ Jakura and Abghari (1994); O’Rourke et al. (1994); Soydemir et al. (1997); Ishihara and Cubrinovski (1998).

1. A pseudo-static stability analysis to establish seismic coefficients that cause yield.
2. Newmark sliding block analysis.
3. Calculation of foundation forces due to soil movement in the liquefied zone.
4. Determination of plastic hinge mechanisms that are likely to develop in the foundations.

The rationale behind this approach is to determine the likely magnitude of lateral soil movement, and to evaluate the ability of the pile foundation and the bridge above, to accommodate this movement.

Allowing a plastic mechanism to form in the foundation, under the action of lateral spreading, is tantamount to accepting substantial damage in the foundation. This is a departure from the design philosophy of most seismic codes where plastic hinging is only acceptable if it occurs above the ground where it can be inspected and repaired. This exception is reasonable because it is unlikely that a plastic hinge in the foundation will lead to overall structural collapse. This is because lateral spreading is essentially a displacement-controlled process. Thus, the estimated soil displacements represent a limit on the structure displacement, while excluding the phenomena of buckling of the piles or shafts below grade and the continued displacement that could be produced by large $P-\Delta$ effects. Buckling should be checked and methods that include the residual resistance of the soil should be used. A method for checking buckling is described in O'Rourke et al. (1994).

A flowchart for estimating lateral spreading is given in figure 11-3 and the methodology is described below. This approach also allows the benefits of passive piles or pin piles to be determined. The steps involved are as follows:

Step 1. Identify the soil layers that are likely to liquefy.

Step 2. Conduct a stability analysis to determine the likelihood of soil movements and the extent of such movements.

This includes finding the depths of soil likely to move and the extent of the soil block that is likely to fail. The effect of these movements on the bridge can then be determined by considering the proximity of the failure block to the foundation system.

Step 3. Estimate the maximum lateral spread displacement of the soil.

This may be done using Newmark displacement charts, or by conducting a site-specific Newmark time history analysis.

Step 4. Decide whether the soil will continue to flow around the footing and/or piles or whether they will move with the soil.

This assessment requires a comparison between the estimated passive soil forces that can be exerted on the foundation and the ultimate resistance that can be developed by the bridge. In cases where a crust of non-liquefied material exists at the ground surface,

the structural resistance of the bridge may be less than the displacement-induced passive forces. If so, the substructure is then likely to move with the soil. In many situations, it will be immediately obvious which condition is more likely to occur.

Step 5. Design the foundation to withstand the passive pressures created by the flowing soil.

Step 6. Evaluate the adequacy of the bridge at the maximum expected displacement if analysis indicates that the foundation is likely to move with the soil.

The implication of this assessment is that, for relatively large ground movements, soil displacements are likely to cause similar movements of the foundation. In this context, 'large' is assessed relative to the structural resistance at yield. The resulting movement of the foundation may produce substantial plasticity or hinge zones in the piles, and may induce large reactions in the superstructure.

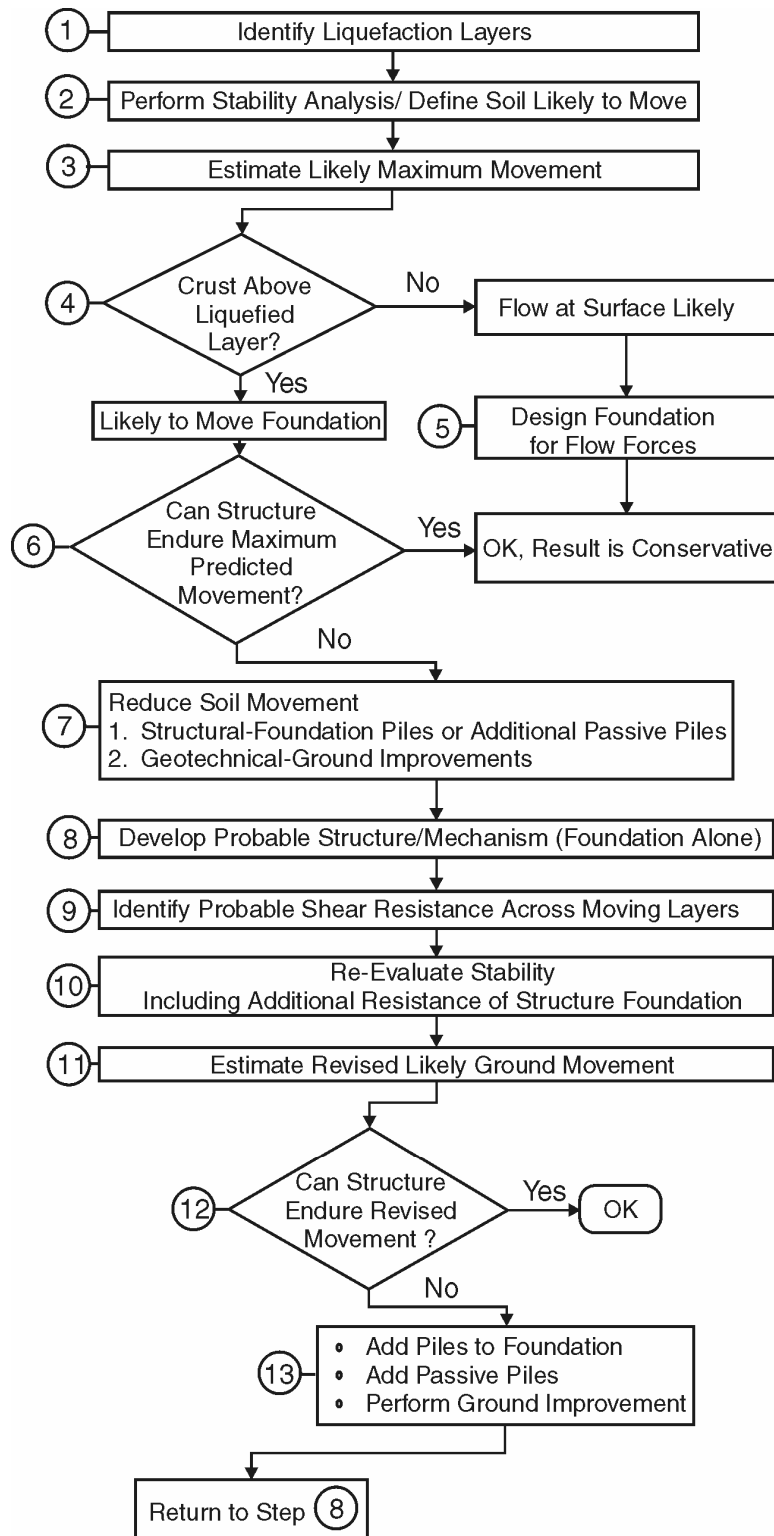
Step 7. Limit the pile and substructure forces to values less than yield if the deformations determined in Step 6 are unacceptable.

This can be done by either of two methods. The first is to retrofit the foundations to resist the forces that accompany passive flow of the soil around them. The second is to limit ground movement by providing either soil or structural remediation. Structural remediation makes use of the pinning or dowel action that piles and foundation shafts contribute when they cross the potential failure plane of the moving soil mass. This can be very effective in reducing the magnitude of the lateral movement.

Step 8. Determine the plastic mechanism that is likely to develop in the presence of spreading. This should be done in a rational manner. Due to the number of uncertainties in the process, precision in the calculation of the various mechanisms may not be justified and may not produce more accurate results. Simplified approximations for the lateral capacity of various mechanisms may be adequate.

Such approximations could be based on hinge development in the stable soil zones at two pile diameters above and below the liquefiable layer. The maximum pile shear could then be assumed equal to $2M_p/L$, where M_p is the plastic moment and L is the distance between hinges. Note that this assumes the load transfer in the liquefied zone is negligible. The lateral shear that produces the plastic mechanism can be adjusted downward to account for the influence of the $P-\Delta$ effect. Figure 11-4 illustrates first-order corrections for $P-\Delta$ effects.

A more precise method of determining the plastic hinge mechanism would be to ensure compatibility of deformations between the soil and piles, as in the computer program LPILE. Another refinement is to account for the plastic deformations in the piles themselves, as in the program BSTRUCT (O'Rourke et al., 1994).



ATC/MCEER, 2003

Figure 11-3. Design flowchart.

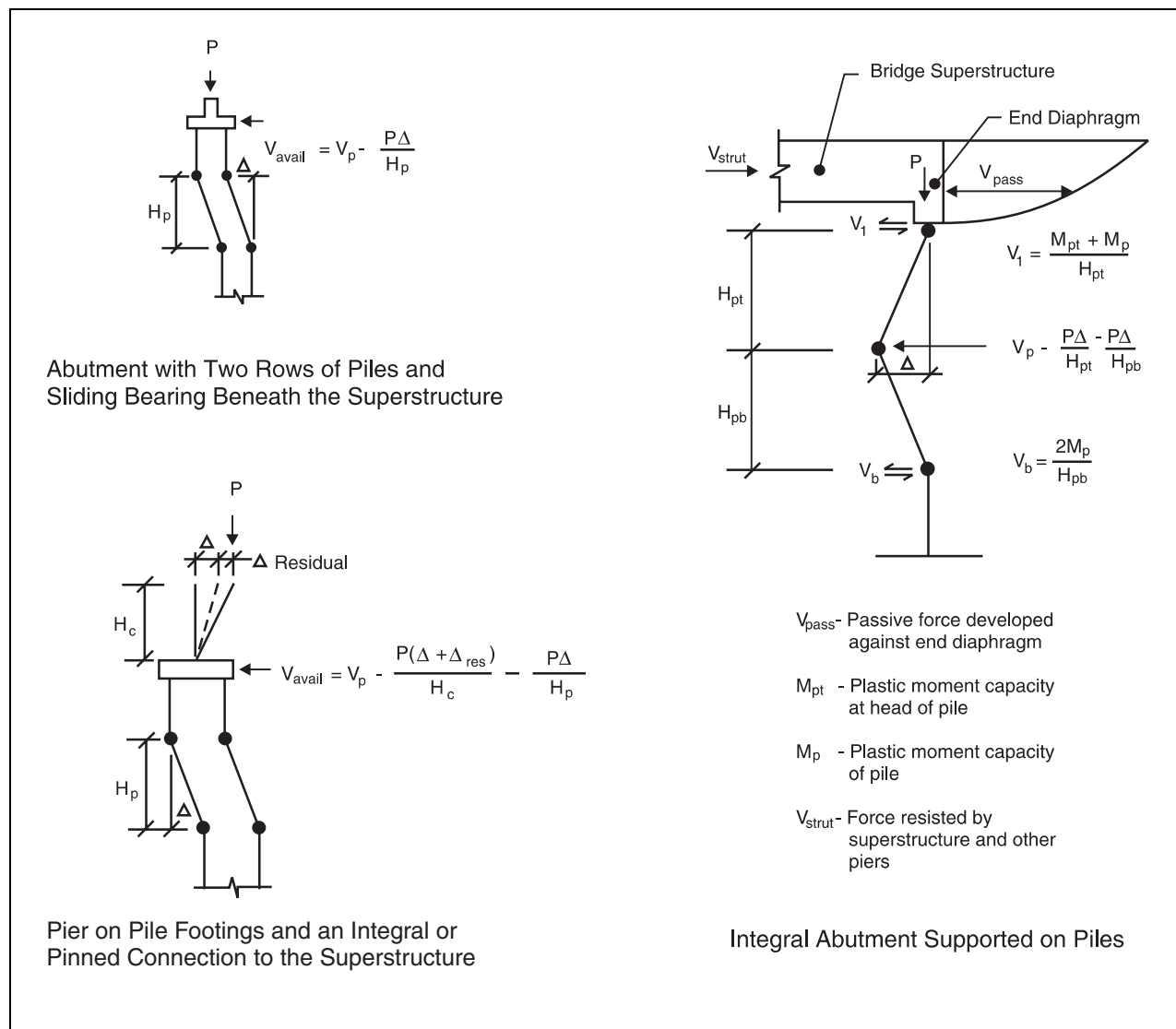


Figure 11-4. Corrections for P-Δ effects in piles with plastic hinges.

Step 9. Evaluate the foundation system for a displacement field that represents the likely deformations due to lateral spreading. From this analysis, an estimate of the likely shear resistance that the foundation can provide is determined, which can then be included in the stability analysis.

Step 10. Re-evaluate the stability of the soil block taking into account the additional resistance provided by the piles.

Steps 11 and 12. Recalculate the overall displacement using the revised resistance levels. Once a realistic displacement is calculated, the foundation and structural system can be analyzed for this movement. It is at this point that larger displacements than those

normally allowed in substructure design can be used. This implies that large plastic rotations are allowed to occur in the foundation under these conditions.

Step 13. If the response of the bridge is acceptable, then the retrofit design is complete, but if not determine if the behavior can be improved by providing additional piles or shafts.

Note that the additional piles do not need to connect to the footing. Alternatively, ground improvement approaches may be considered, such as stone columns. The selection of structural or geotechnical remediation methods is based on the relative economics of the system being used.

This process is repeated by returning to Step 8 and modifying the available resistance until the slope is stabilized.

11.4.2. SITE REMEDIATION USING GROUND IMPROVEMENT

To prevent or inhibit liquefaction and reduce lateral ground deformation to acceptable levels, site remediation such as ground densification is commonly used in selected liquefiable soil zones.

The most widely used densification method is the vibro-replacement technique, which has been shown to be effective in past earthquakes (Mitchell et al., 1995). This method involves the repeated insertion and withdrawal of a large vibrating probe into the soil to a desired depth of densification, as shown in figure 11-5. As vibration-induced liquefaction occurs, crushed stone backfill is placed around the vibrator, leading to the development of a stone column that is approximately 1 m (3 ft) in diameter. The stone column increases the effectiveness of vibration transmission, and facilitates drainage of excess pore water pressures as densification occurs. The

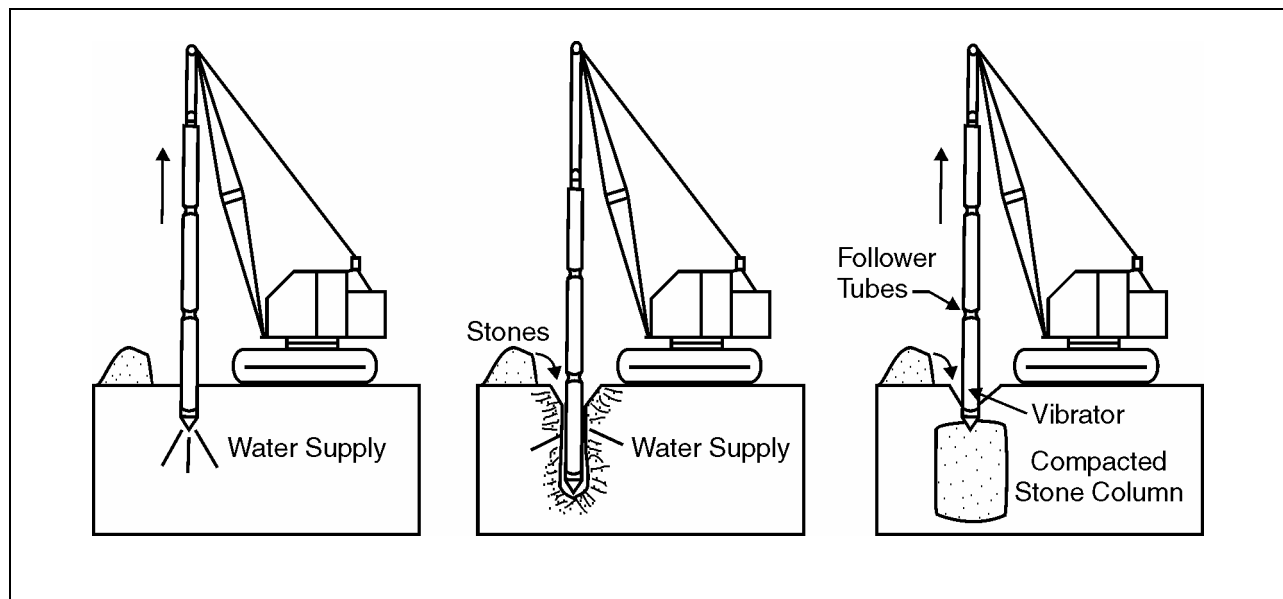


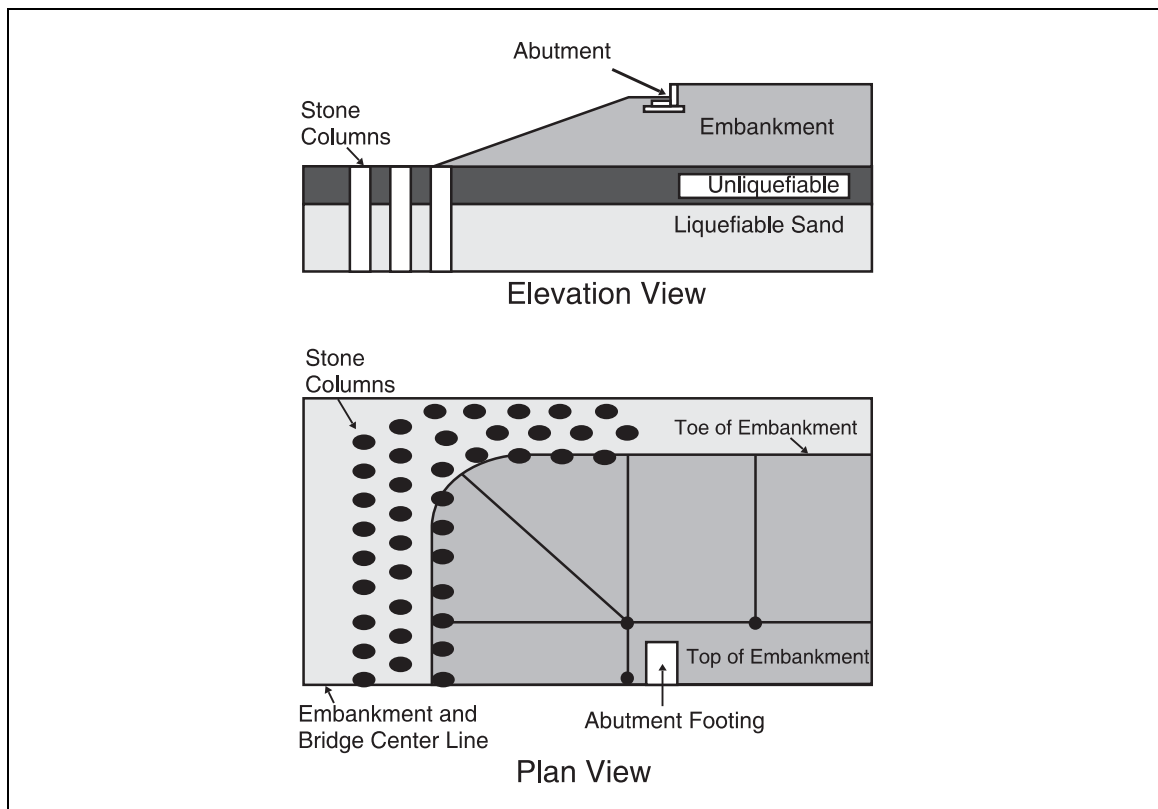
Figure 11-5. Vibro-replacement equipment and process.

procedure is repeated at a grid spacing of 2.4 to 3.7 m (8 to 12 ft) to form a densified zone. Relative densities of the order of 80 percent can be achieved by this method.

Vibro-replacement is effective if the sands to be densified contain less than 15 to 20 percent fines. In addition, the use of wick drains placed at the midpoints of stone column grid points will aid drainage and can potentially help densify sandy silts (Luehring et al., 1998). Details on design approaches and equipment applications can be found in many publications².

A representative application of vibro-replacement is shown in figure 11-6, where a densified stone column buttress has been constructed at the toe of an embankment. The effect of the buttress is to increase values of the lateral yield acceleration computed using the Newmark approach to evaluate embankment stability. This, in turn, reduces lateral spreading. Hence, the buttress width is determined based on acceptable displacement-performance criteria for bridge piles located in the failure zone. An example of this approach is described by Egan et al. (1992).

A further application is shown in figure 11-7, where a densified soil zone has been placed around a pile-supported bridge pier. The placement of such a zone (normally within a radius of 150 to 200 percent of the thickness of the liquefiable layer) would be used to eliminate post-liquefaction downdrag on the piles, and the potential effects of cyclic ground lurch.

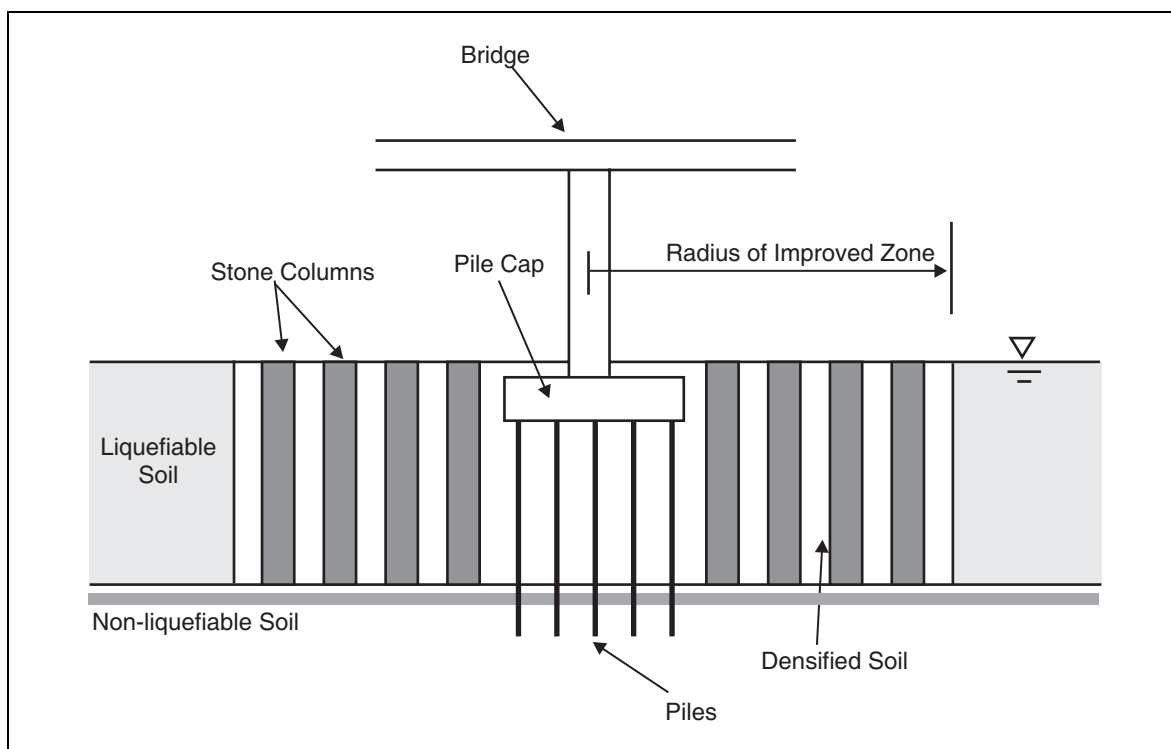


Cooke and Mitchell, 1999

Figure 11-6. Vibro-system (stone column) treatment at toe of approach embankment.

² Baez (1995), Baez and Martin (1995), Hayden and Baez (1994); Martin (1998b)

For sites where vibratory techniques may be impractical, compaction grouting can be used. Shown schematically in figure 11-8, compaction grouting involves pumping a stiff mix of soil, cement, and water into the ground under high pressure to compress or densify the soil. A very stiff soil-cement and water mixture is injected into the soil forming a grout bulb, which displaces and potentially densifies the surrounding ground, without penetrating the soil pores. A grid or network of grout columns that is formed by grouting from the bottom up, results in improved liquefaction resistance over the required surface area, similar to a network of stone columns (Boulanger and Hayden 1995). A theoretical study of the mechanics of ground improvement in sands (Mace and Martin, 2000) has shown that increased liquefaction resistance arises primarily from increased lateral stresses rather than from densification. Consequently, increases in liquefaction strength are best measured using cone penetration test (CPT) correlations (Salgado et al., 1997). In this respect, some uncertainties still remain as to the permanence of increases in the lateral stress.



Jackura and Abghari, 1994

Figure 11-7. Vibro-system (stone column) treatment around a pile-supported bridge pier.

11.4.3. SUPERSTRUCTURE IMPROVEMENTS

In addition to site stabilization, retrofitting the superstructure will often be necessary to improve its tolerance for large differential displacements. Required strengthening methods will depend on the configuration of the structure and the components most susceptible to damage. These will usually involve tying superstructure sections together and providing a positive connection between the superstructure, piers and abutments. In some cases, column retrofitting may also be

required. Attempts to stabilize the abutments through the use of anchors would probably not be very effective. Because abutment tilting usually does not result in collapse, this type of failure is not considered to be critical. The use of settlement slabs may be in order, however, if immediate access to the bridge is important.

Longitudinal restrainers should be provided at all bearings to prevent a loss of support. If the superstructure is not tied to its piers, foundation movements may pull the support out from under the bearings, as shown in figure 11-9. It would be preferable to fail the column in flexure rather than have the span fall off the pier.

Transverse and vertical restrainers at expansion joints tend to prevent the superstructure from buckling (sideways) and should be used along with longitudinal restrainers. When expansion joints occur at the piers, these restrainers should provide a positive tie to the substructure.

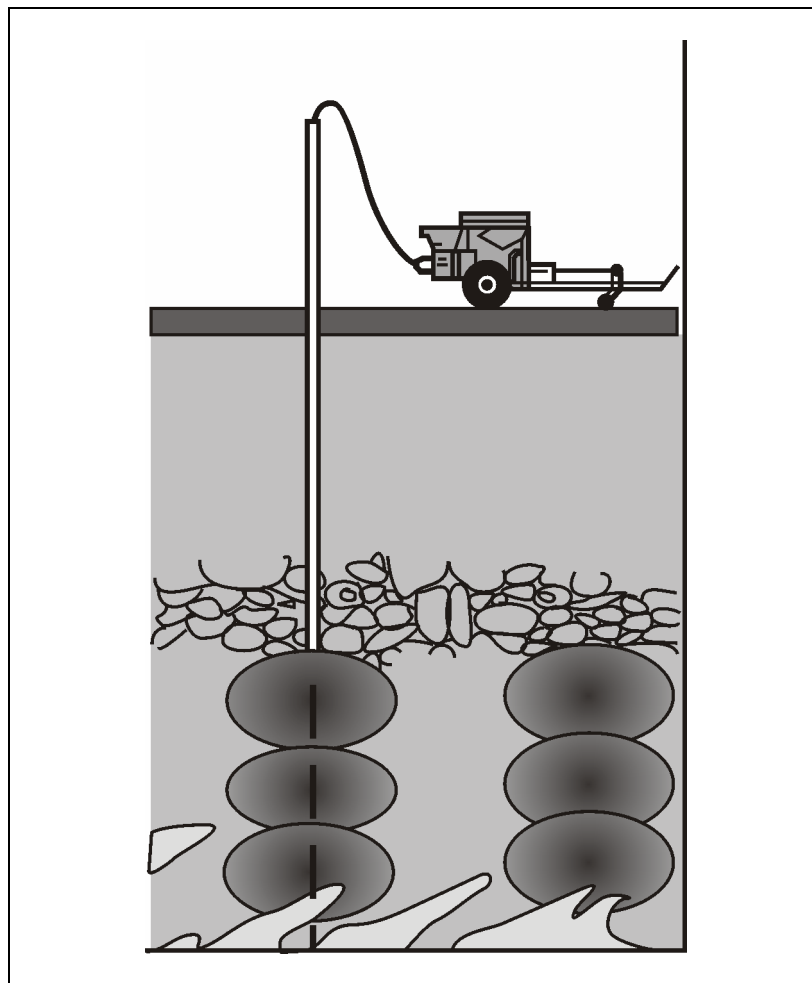


Figure 11-8. Compaction grout bulb construction.

The superstructure should be anchored to the pier, and the design load in the anchors should be greater than the capacity of the pier. Care should be taken to provide a sufficient gap in the restrainers so that normal temperature movement or moderate earthquakes will not result in a column failure.

Because ductile failures of the piers are required to accommodate large movements, pier retrofitting may be necessary to ensure that a brittle failure does not occur. Suitable methods for retrofitting piers, joints, and foundations are described in chapters 9 and 10.

An alternative to adding ductility is to increase the stiffness of the structure so as to uncouple it from the long period motions associated with liquefiable layers. Stiffening may be accomplished by improving the lateral resistance of the foundations, adding infill walls between columns, or even increasing the number of substructure units. These measures will be costly, but may be justified for critical bridges.

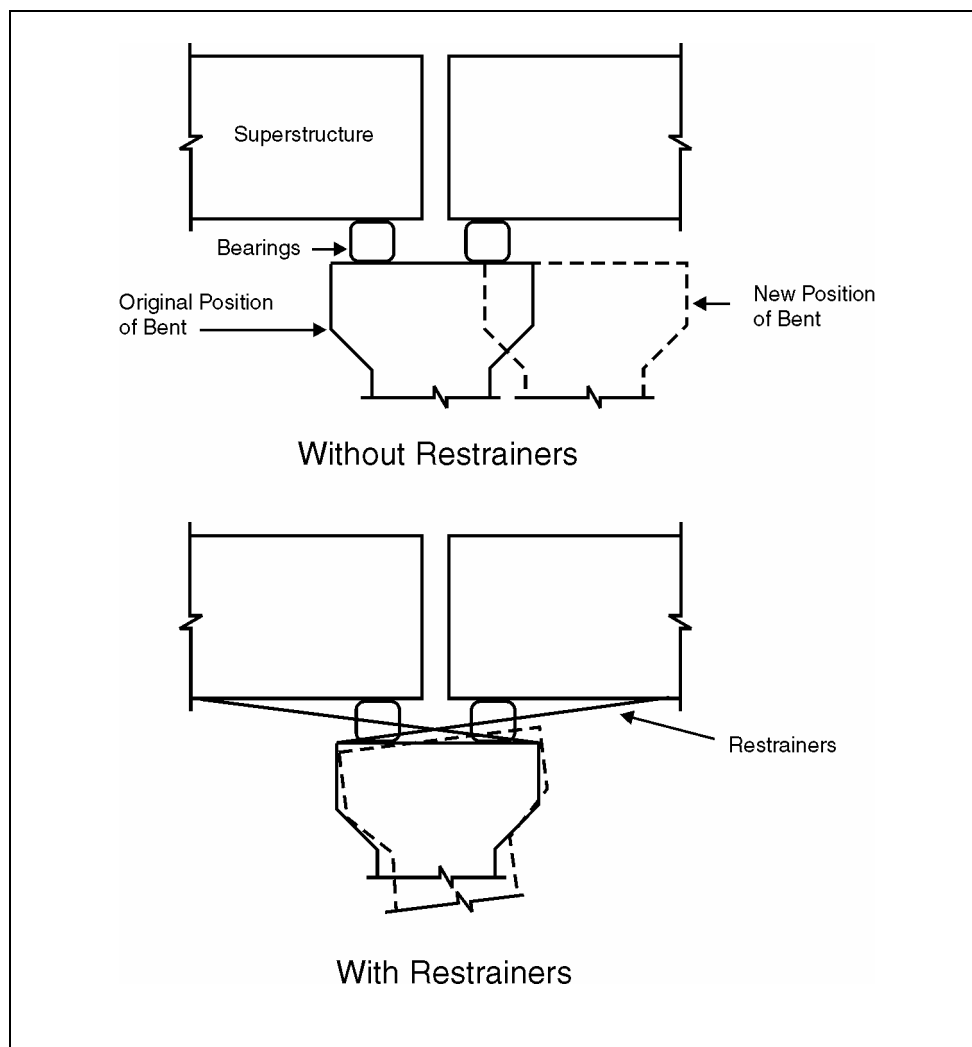


Figure 11-9. Effect of restrainers at bent during liquefaction failure.

APPENDIX A: GUIDELINES FOR CONDUCTING SITE-SPECIFIC GEOTECHNICAL INVESTIGATIONS AND DYNAMIC SITE RESPONSE ANALYSES

As indicated in section 2.4 and table 2-4, site coefficients F_a and F_v are not provided for Site Class F soils. Instead, site-specific geotechnical investigations and dynamic site response analyses are required for these soils. Guidelines are given below for conducting site-specific investigations and site response analyses for Site Class F soils. These guidelines are also applicable if it is desired to conduct site response analyses for other soil types. Additional guidance on topics addressed below is presented in CSABAC (1999).

A.1. SITE-SPECIFIC GEOTECHNICAL INVESTIGATION

For purposes of obtaining data to conduct a site response analysis, site-specific geotechnical investigations should include borings with sampling, standard penetration tests (SPTs), cone penetrometer tests (CPTs), and/or other subsurface investigative techniques and laboratory soil testing to establish the soil types, properties, layering and the depth to rock or rock-like material. Shear wave velocities should be measured in all soil layers unless they can be confidently estimated from shear wave velocity data for similar soils in the same area.

A.2. DYNAMIC SITE RESPONSE ANALYSIS

Components of a dynamic site response analysis include modeling the soil profile; selecting rock motions as input to the soil profile; and conducting site response analysis and interpreting results.

A.2.1. MODELING THE SOIL PROFILE

Typically, a one-dimensional soil column extending from the ground surface to bedrock is adequate to capture first-order site response characteristics. However, two- or three-dimensional models may be considered for critical projects when two- or three-dimensional wave propagation effects may be significant (e.g., in basins). The soil layers in a one-dimensional model are characterized by their total unit weights, shear wave velocities from which low-strain (maximum) shear moduli may be obtained, and by relationships defining the nonlinear shear stress-strain relationships of the soils. The required relationships for analysis are often in the form of curves that describe the variation of shear modulus with shear strain (modulus reduction curves) and by curves that describe the variation of damping with shear strain (damping curves). In a two- or three-dimensional model, compression wave velocities or moduli, or Poisson's ratios, are also required. In an analysis to estimate the effects of liquefaction on soil site response, the nonlinear soil model must also incorporate the buildup of soil pore water pressures and the consequent reduction in soil stiffness and strength. Typically, modulus reduction curves and damping curves are selected on the basis of published relationships for similar soils¹. Site-

¹ Seed and Idriss, 1970; Seed et al., 1986; Sun et al., 1988; Vucetic and Dobry, 1991; Electric Power Research Institute, 1993; Kramer, 1996

specific laboratory dynamic tests on soil samples to establish nonlinear soil characteristics can be considered where published relationships are judged to be inadequate for the types of soils present at the site. The uncertainty in soil properties should be estimated, especially in the selected maximum shear moduli and modulus reduction and damping curves.

A.2.2. SELECTING INPUT ROCK MOTION

Acceleration time histories that are representative of horizontal rock motions at the site are required as input to the soil model. Unless a site-specific analysis is carried out to develop the design rock response spectrum at the site, the design rock spectrum for Site Class B rock can be defined using the general procedure described in section 2.5. For hard rock (Site Class A), the spectrum may be adjusted using the site factors in table 2-4. For profiles having great depths of soil above Site Class A or B rock, consideration can be given to defining the base of the soil profile and the input rock motions at a depth at which soft rock or very stiff soil of Site Class C is encountered. In such cases, the design rock response spectrum may be taken as the spectrum for Site Class C defined using the site factors in table 2-4.

Several acceleration time histories, usually four or more, recorded during earthquakes having magnitudes and distances that significantly contribute to the site seismic hazard should be selected for analysis. The USGS results for deaggregation of seismic hazard (website address: <http://eqhazmaps.usgs.gov>) can be used to evaluate the dominant magnitudes and distances contributing to the hazard. Prior to analysis, each time history should be scaled so that its spectrum is at the approximate level of the design rock response spectrum in the range of periods of structural significance. The average of the response spectra of the suite of scaled input time histories should be approximately at the level of the design rock response spectrum in the period range of interest. Because rock response spectra are defined at the ground surface rather than at depth below a soil deposit, the rock time histories should be input in the analysis as rock outcrop motions rather than at the soil-rock interface.

A.2.3. SITE RESPONSE ANALYSIS AND RESULTS INTERPRETATION

Analytical methods may be linear, using equivalent linearized properties, or explicitly nonlinear. Frequently used computer programs for one-dimensional analysis include the equivalent linear program SHAKE (Idriss and Sun, 1992) and various nonlinear programs (DESR-2 (Lee and Finn, 1978), MARDES (Chang et al., 1991), SUMDES (Li et al., 1992), D-MOD (Matasovic, 1993), TESS (Pyke, 1992), and DESRA-MUSC (Qiu, 1998)). If the soil response is highly nonlinear (e.g., high acceleration levels and soft clay soils), nonlinear programs are generally preferable to equivalent linear programs. For analysis of liquefaction effects on site response, computer programs incorporating pore water pressure development (effective stress analyses) must be used (e.g., DESRA-2, SUMDES, D-MOD, TESS and DESRA-MUSC). Response spectra of output motions at the ground surface should be calculated and the ratios of response spectra of ground surface motions to input rock outcrop motions should be calculated. Typically, an average of the response spectral ratio curves is obtained and multiplied by the design rock response spectrum to obtain the design soil response spectrum. Sensitivity analyses to evaluate effects of soil property uncertainties should be conducted and considered in developing the design response spectrum.

APPENDIX B: EVALUATION OF GEOTECHNICAL HAZARDS

B.1. GENERAL

This appendix describes procedures for the evaluation of seismically-induced geotechnical hazards, which include soil liquefaction, soil settlement, surface fault rupture, and flooding. Slope failures (landslides and rockfalls) are treated in Part 2 of this manual. Hazard evaluation should be carried out by engineers and earth scientists (e.g. geotechnical engineers, geologists, and seismologists) who have expert knowledge of the hazard and experience with its evaluation.

B.2. EVALUATION OF SOIL LIQUEFACTION HAZARD

Procedures given in this appendix for the assessment of liquefaction are based in part on three major source documents:

- Proceedings of the 1996 NCEER Workshop (now MCEER) on evaluating liquefaction resistance (Youd and Idriss, 1997; Youd et al., 2001).
- Recommended LRFD guidelines for the seismic design of highway bridges (ATC/MCEER, 2003).
- Procedures for implementing guidelines for analyzing and mitigating liquefaction in California (SCEC, 1999).

B.2.1. FIELD EXPLORATION FOR LIQUEFACTION HAZARD ASSESSMENT

A number of factors must be considered during the planning and conduct of the field exploration phase of the liquefaction investigation. These include:

- Location of liquefiable soils.
- Location of groundwater level.
- Depth of liquefaction.

These factors are discussed below.

B.2.1.1. Location of Liquefiable Soils

During the field investigation, the limits of unconsolidated deposits with liquefaction potential should be mapped within and beyond the footprint of the bridge. Typically, this will involve an investigation at each pier location and at a sufficient number of locations away from the approach fill to establish the spatial variability of the material. The investigation should establish

the thickness and consistency of liquefiable deposits from the ground surface to the depth at which liquefaction is not expected to occur. The ‘zone of influence’ where liquefaction could affect a bridge approach fill will generally be located within a 2H:1V (horizontal to vertical) projection from the bottom of the approach fill.

B.2.1.2. Location of Groundwater Level

The permanent groundwater level should be established during the exploration program. Shallow groundwater may exist for a variety of reasons, some of which are of natural and some of man-made origin. Groundwater may be shallow because the ground surface is only slightly above the elevation of the ocean, a nearby lake or reservoir, or the sill of a basin. Another concern is man-made lakes and reservoirs that may create a shallow groundwater table in young sediments that were previously unsaturated. If uncertainty exists in the location of the groundwater level, piezometers should be installed during the exploration program. The location of the groundwater level should be monitored in the piezometers over a sufficient duration to establish seasonal fluctuations that may be due to rainfall, river runoff, or irrigation.

Usually, soils located below the groundwater level are fully saturated. However, at locations where fluctuations in groundwater occur, soil can be in a less-than-fully saturated condition. The liquefaction resistance of the soil is affected by the degree of saturation, with the resistance increasing significantly as the degree of saturation decreases. If the groundwater level fluctuates due to tidal action or seasonal river fluctuations, then the zone of fluctuation will often have a lower degree of saturation, making the soil more resistant to liquefaction. Unless the seasonal fluctuation is in place for an extended period of time, say weeks at a higher level, it is usually acceptable to use a long-term groundwater level as a basis for design.

B.2.1.3. Depth of Liquefaction

Field exploration should be conducted to the maximum depth of liquefiable soil. A depth of about 15 m (50 ft) has often been used as the depth of analysis for the evaluation of liquefaction. However, the EERI Monograph (Seed and Idriss, 1982) does not recommend a minimum depth for evaluation, but notes 12 m (40 ft) as a depth to which some of the numerical quantities in the ‘simplified procedure’ can be estimated reasonably. Liquefaction has been known to occur during earthquakes at depths greater than 15 m (50 ft) given the proper conditions such as low-density granular soils, presence of groundwater, and sufficient cycles of earthquake ground motion. For example, liquefaction occurred to depths in excess of 25 m (80 ft) during the 1964 Alaska earthquake.

For this reason it is recommended that a minimum depth of 25 m (80 ft) below the existing ground surface or lowest proposed finished grade (whichever is lower) be investigated for liquefaction potential. For deep foundations (e.g. shafts or piles), the depth of investigation should extend to a depth that is a minimum of 6 m (20 ft) below the lowest expected foundation level (e.g. shaft bottom or pile tip) or 25 m (80 ft) below the existing ground surface or lowest proposed finished grade, whichever is deeper. However, an investigation need not extend below a depth at which geologic deposits that are clearly non-liquefiable are present.

If, during the investigation, the indices to evaluate liquefaction indicate that the potential for liquefaction may extend to a greater depth, the exploration should be continued until a significant thickness (e.g., at least 3 m (10 ft) if possible) of non-liquefiable soils is encountered.

B.2.1.4. Field Exploration Methods

Two field exploration methods are normally used during the evaluation of liquefaction potential: the Standard Penetration Test (SPT) method, and the Cone Penetrometer Test (CPT) method. Other methods should be used as required. For example, the measurement of shear wave velocities or the use of the Becker Hammer Test (BHT) method may be useful in some assessments of liquefaction potential (section B.2.2.1). A geologic reconnaissance and review of the available geotechnical information for the site should supplement any field investigation.

B.2.1.4(a). SPT Method

Procedures for evaluating liquefaction potential using SPT methods are described in detail by Youd and Idriss (1997), Youd et al. (2001) and SCEC (1999). These procedures include consideration of correction factors for drilling method, hole diameter, drive-rod length, sampler type, energy delivery, and spatial frequency of tests.

Information presented in Youd and Idriss (1997), Youd et al. (2001) and SCEC (1999) indicate that the results of SPT explorations are affected by small changes in measurement method. Therefore, it is critical for these tests that standard procedures are followed and that all information regarding the test method and equipment used during field work be recorded. The energy of the SPT hammer system should also be established for the equipment, as this energy directly affects the determination of liquefaction potential. The variation in hammer energy can be as much as a factor of 2, which can easily cause a liquefiable site to be identified as being non-liquefiable, if a correct hammer calibration factor is not introduced.

Primarily because of their inherent variability, sensitivity to test procedure, and uncertainty, SPT N-values have the potential to provide misleading assessments of liquefaction hazard, if the tests are not performed carefully. The engineer who wishes to use the results of SPT N-values to estimate liquefaction potential should become familiar with the details of SPT sampling as given in ASTM D 1586 (ASTM, 1998) and the recommendations in SCEC (1999) in order to avoid, or at least reduce, some of the major sources of error.

B.2.1.4(b). CPT Method

The CPT method is gaining recognition as the preferred method of evaluating liquefaction potential in many locations. Methods for assessing liquefaction potential from CPT results are given in Youd and Idriss (1997) and Youd et al. (2001). The primary advantages of the CPT method are:

- It provides an almost continuous penetration resistance profile that can be used for stratigraphic interpretation, which is particularly important in determining the potential for lateral spreading, lateral flows, and significant differential post-liquefaction settlements.

- Repeatability of the test is very good.
- Test is fast and economical compared to drilling and laboratory testing of soil samples.

The limitations of the method are:

- It does not routinely provide soil samples for laboratory tests.
- It provides approximate, interpreted soil behavior types and not the actual soil types according to ASTM Test Methods D 2488 (Visual Classification) or D 2487 (USCS Classification) [ASTM, 1998].
- Tests cannot be performed in gravelly soils and sometimes the presence of hard/dense crusts or layers at shallow depths makes penetration to desired depths difficult.

The CPT method should be performed in accordance with ASTM D 5778 (ASTM, 2003). Unless site-specific experience is available on the correlation of CPT resistance and soil type, it is recommended that at least one boring be drilled to confirm soil types and obtain samples for laboratory testing.

B.2.2. EVALUATION OF LIQUEFACTION POTENTIAL

Two basic procedures are used to evaluate the potential for liquefaction at a site. These are:

- Simplified procedure that is based on empirical correlations to observations of liquefaction.
- More rigorous numerical modeling.

The decision between the two procedures should be made after careful review of conditions at the site and the risks associated with liquefaction, and with the concurrence of the owner.

For most projects, the simplified procedure will be acceptable. However, for some projects, more rigorous modeling using equivalent linear and nonlinear computer codes may be appropriate. Conditions warranting the use of more rigorous methods include:

- Sites where liquefiable soils extend to depths greater than 25 m (80 ft).
- Sites that have significant interlayering, particularly where interlayers comprise highly permeable soils or soft clay layers.
- Sites where the cost of ground remediation methods to mitigate liquefaction is great.

Results of most site-specific ground response analyses result in lower estimates for ground acceleration and shearing stresses within the soil profile, because the energy dissipative mechanisms occurring during liquefaction are explicitly considered in this approach.

B.2.2.1. Simplified Procedure

The most basic procedure used in engineering practice for assessment of site liquefaction potential is that of the ‘Simplified Procedure’¹. The procedure compares the cyclic resistance ratio (CRR, the cyclic stress ratio required to induce liquefaction for a cohesionless soil stratum at a given depth) with the earthquake-induced cyclic stress ratio (CSR) at that depth from a specified design earthquake (defined by a peak ground surface acceleration and an associated earthquake magnitude). CRR and CSR are ratios of cyclic shear stress to initial (pre-earthquake) effective overburden pressure on a horizontal plane at a given depth in the soil deposit.

B.2.2.1(a). Cyclic Resistance Ratio, CRR

CRR from SPT Blowcount Data: Values of CRR for the Simplified Procedure were originally established from databases for sites that did or did not liquefy during past earthquakes and where values of the normalized SPT value, $(N_1)_{60}$, could be correlated with liquefied strata. The current version of the baseline chart defining values of CRR as a function of $(N_1)_{60}$ for magnitude 7.5 earthquakes is shown in figure B-1. This chart was established by a consensus at the 1996 MCEER Workshop (Youd and Idriss, 1997; Youd et al., 2001). The determination of CRR must consider the fines content of the soil, the energy of the hammer, the effective overburden pressure, and the magnitude of the earthquake (Youd and Idriss 1997; Youd et al., 2001).

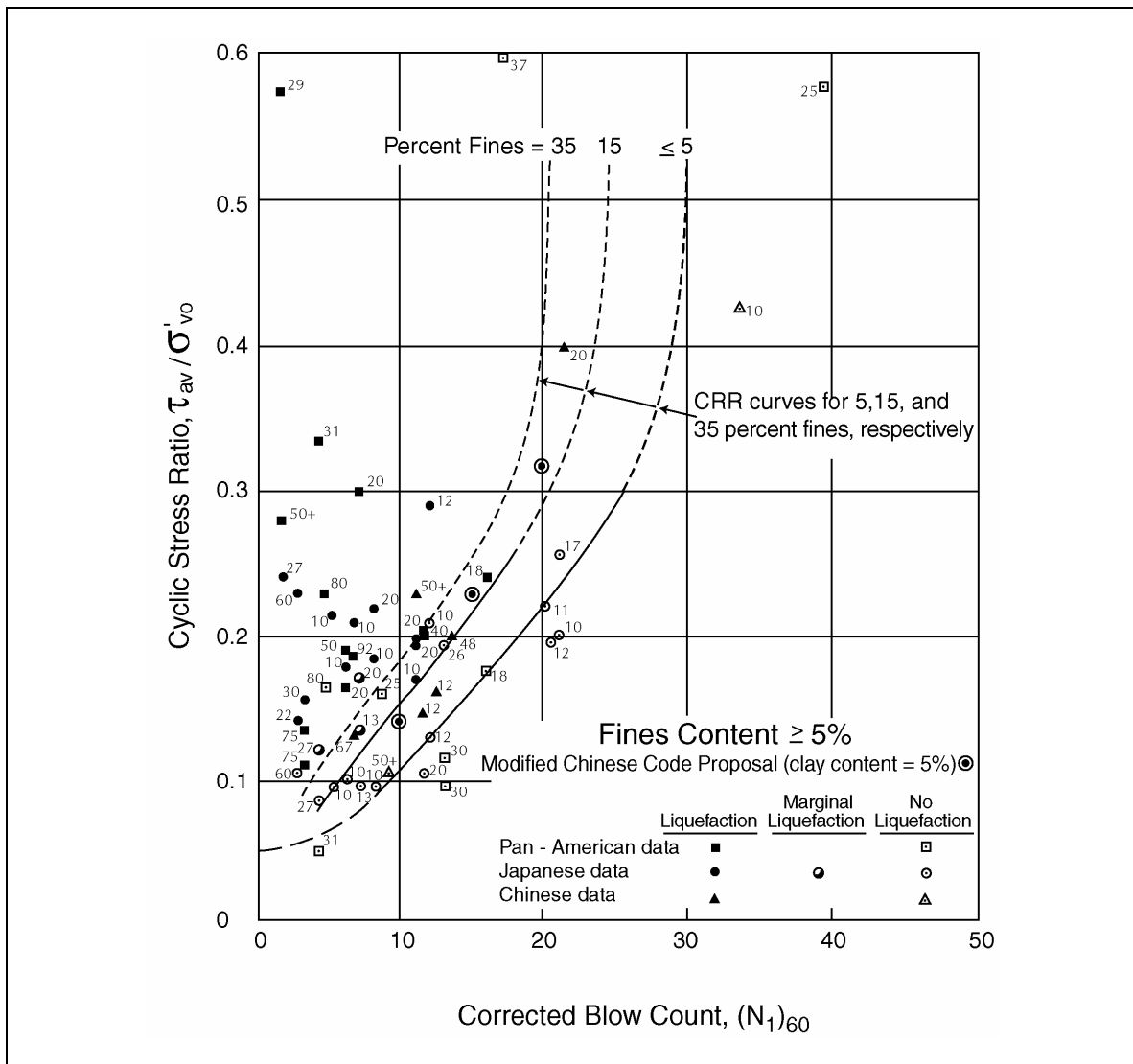
The effect of the earthquake magnitude on CRR (i.e. the effect of magnitude on the ordinates of figure B-1) was re-evaluated during the 1996 MCEER Workshop (Youd and Idriss, 1997; Youd et al., 2001). The resulting range of magnitude scaling factors is shown in figure B-2. It is recommended that the factors defined by the curve at the lower-bound of the recommended range (cross-hatched area) in figure B-2 be used unless different factors can be adequately justified. Note that for magnitudes greater than 7.5, the corresponding recommended curve is the second highest curve shown in figure B-2.

Adjustments for changes in water table and overburden condition should be made during the simplified analyses. The following provides guidance when making these adjustments.

- Overburden Corrections for Differing Water Table Conditions To perform analyses of liquefaction potential, liquefaction settlement, seismically induced settlement, and lateral spreading, it is necessary to develop a profile of SPT blowcounts that have been normalized using the effective overburden pressure. Normalization factors are presented in Youd and Idriss (1997) and Youd et al. (2001).

This normalization should be performed using the effective stress profile that existed at the time the SPT testing was performed. These normalized values are then held constant throughout the remainder of the analyses, regardless of whether or not the analyses are performed using higher or lower water-table conditions. Although the possibility exists that softening effects due to soil moistening can influence SPT results if the water table

¹Seed and Idriss (1982), Seed et al. (1983) and (1985), Seed and De Alba (1986), Seed and Harder (1990), Youd and Idriss (1997) and Youd et al. (2001)

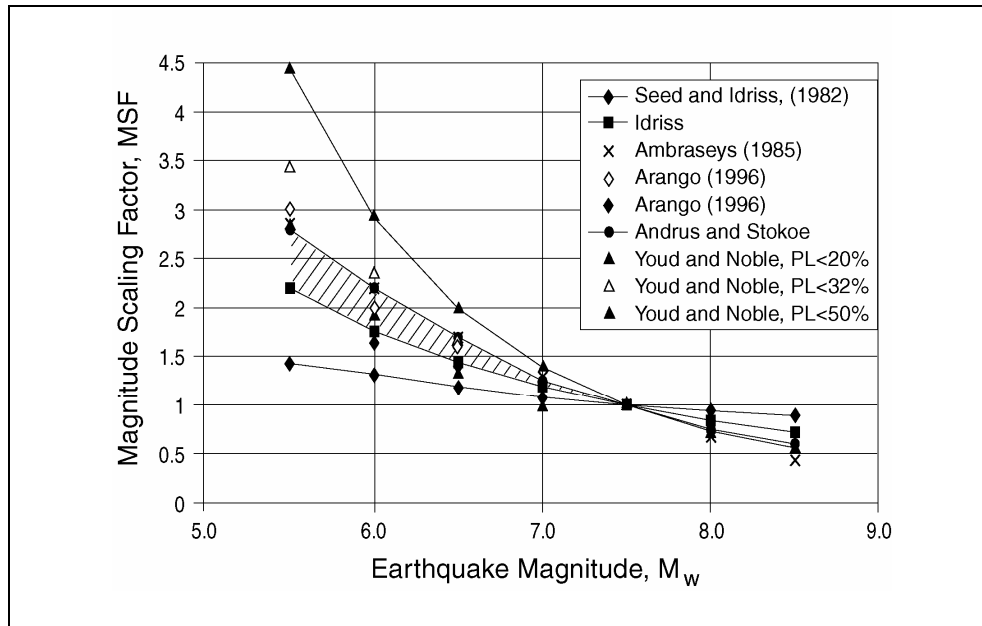


after Youd and Idriss, 1997; Youd et al., 2001

Figure B-1. Simplified base curve recommended for determination of CRR from SPT data for magnitude 7.5 along with empirical liquefaction data.

fluctuates, it is commonly assumed that the only effect that changes in the water table have on the results is due to changes in the effective overburden stress.

- Overburden Corrections for Differing Fill Conditions Approach fills, and other increases in overburden pressure, should be handled similarly to that described above for changes in groundwater location. It is necessary to develop a profile of SPT blowcounts that have been normalized using the effective overburden pressure existing before the fill is placed. These normalized values are then held constant throughout the remainder of the analyses, regardless of whether or not the analyses are performed using a higher fill condition.



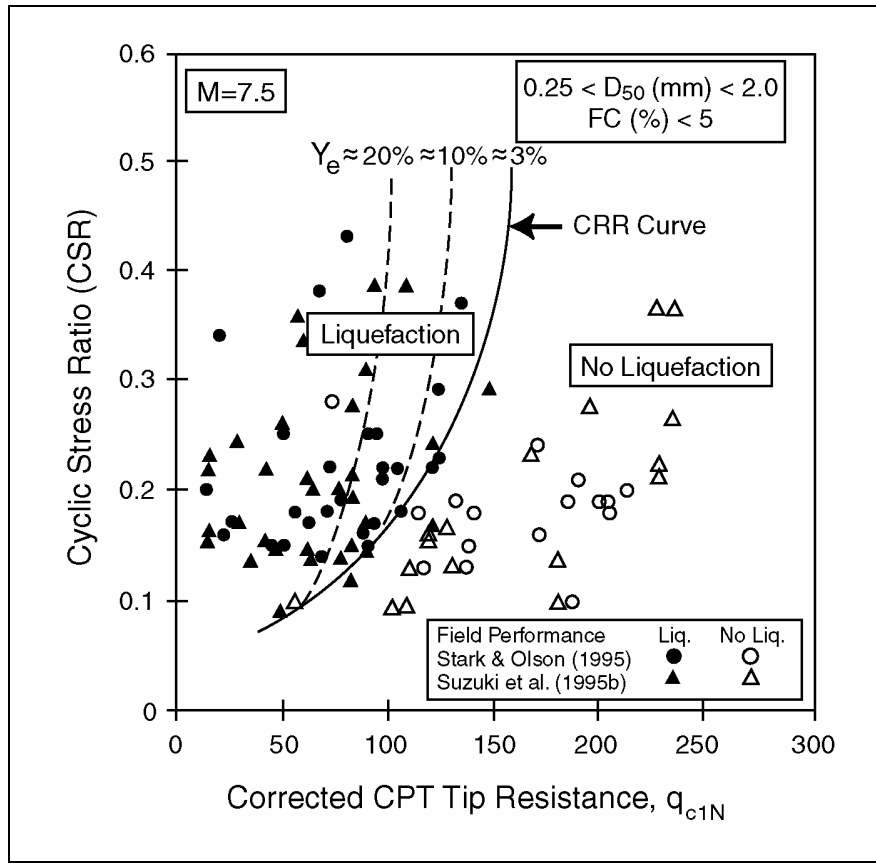
after Youd and Idriss, 1997; Youd et al., 2001

Figure B-2. Magnitude scaling factors derived by various investigators.

CRR from CPT Data: Figure B-3 shows the Robertson and Wride chart (Youd and Idriss, 1997) for determining liquefaction strength (CRR) for clean sands (fines content, FC, less than or equal to 5 percent) from CPT data. The chart, which is only valid for magnitude 7.5 earthquakes, shows calculated cyclic stress ratios plotted as a function of corrected and normalized CPT resistance q_{CIN} , from sites where liquefaction effects were or were not observed following past earthquakes. A curve separates regions of the plot with data indicative of liquefaction from regions indicative of non-liquefaction. Dashed curves showing approximate cyclic shear strain potential as a function of q_{CIN} are shown to emphasize that cyclic shear strain and ground deformation potential of liquefied soils decrease as penetration resistance increases.

As for the SPT method, the determination of CRR using the CPT method must account for fines content of the soil, the effective overburden pressure, and the magnitude of the earthquake. Factors to account for fines content and effective overburden pressure are presented in Youd and Idriss (1997) and Youd et al. (2001). Comments given above regarding use of normalized (for effective overburden pressure) SPT blowcounts in analyses are valid for use of normalized CPT data. Magnitude scaling factors for CRR are recommended to be the same for SPT and CPT and are shown in figure B-2.

CRR from other Types of Data: The CRR can also be obtained using shear wave velocity data and Becker Hammer Test (BHT) data, as discussed in Youd and Idriss (1997) and Youd et al. (2001). These procedures are potentially useful especially for gravelly soils, because of the difficulty of obtaining meaningful SPT blowcounts or CPT resistances in gravelly soils (due to the large size [relative to sand] of gravel particles in comparison to the diameter of the SPT sampler and the cone penetrometer).



after Youd and Idriss, 1977

Figure B-3. Robertson and Wride chart.

B.2.2.1(b). Cyclic Stress Ratio, CSR

For estimating values of the earthquake-induced cyclic shearing stress ratio, CSR, the MCEER workshop (Youd and Idriss, 1997; Youd et al., 2001) recommended essentially no change to the original simplified procedure (Seed and Idriss, 1971), where a mean soil flexibility factor, r_d , (figure B-4) is used to define the reduction in CSR with depth. Idriss (1999) proposed a quantification of r_d as a function of earthquake magnitude that differs from the r_d chart in figure B-4. As an alternative to using r_d charts, a site-specific response analysis of the ground motions can be performed, as discussed in section B.2.2.2.

With the Simplified Procedure, CSR is calculated using the following equation:

$$CSR = (\tau_{av}/\sigma'_{vo}) = 0.65(a_{max}/g)(\sigma_{vo}/\sigma'_{vo})r_d \quad (B-1)$$

where τ_{av}/σ'_{vo} is the average earthquake induced shearing stress divided by the effective overburden stress, a_{max} is the peak ground acceleration in units of g (acceleration due to gravity), σ_{vo}/σ'_{vo} is the ratio of total overburden stress to effective overburden stress, and r_d is a soil flexibility factor.

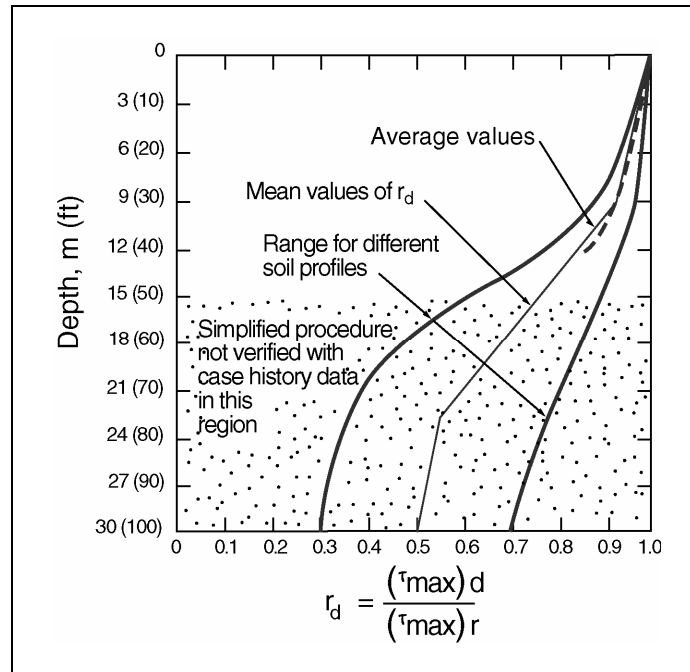


Figure B-4. Soil flexibility factor (r_d) versus depth curves developed by Seed and Idriss (1971) with added mean value lines.

B.2.2.1(c). Liquefaction Potential

After values of CRR and CSR are established for a soil stratum at a given depth, the factor of safety against liquefaction (i.e. $FS = CRR/CSR$) can be computed. The ratio of CRR to CSR should be greater than 1.0 to preclude the development of liquefaction. As the ratio drops below 1.0, the potential for liquefaction increases. Even when the ratio of CRR to CSR is as high as 1.5, increases in pore water pressure can occur. The potential consequences of these increases should be considered during design.

B.2.2.2. Numerical Modeling Methods

For important projects, the use of equivalent linear or nonlinear site-specific, one-dimensional ground response analyses may be warranted to assess the liquefaction potential at a site. For these analyses, acceleration time histories representative of the seismic hazard at the site are used to define input ground motions at a hypothetical outcrop of an appropriate rock or firm-ground interface at depth.

One common approach to numerical modeling is to use the equivalent linear total stress computer program SHAKE (Idriss and Sun, 1992) to determine maximum earthquake-induced shearing stresses at depth for use with the simplified procedure described above, in lieu of using equation B-1. Note that, as in equation B-1, a factor of 0.65 should still be applied to maximum values of CSR obtained using SHAKE to obtain average values of CSR for comparison with

CRR values. Another alternative involves the use of nonlinear effective stress methods to directly determine developed pore water pressures.

In general, equivalent linear analyses are considered to have reduced reliability as ground shaking levels increase to values greater than about 0.4g in the case of softer soils, or where maximum shearing strain amplitudes exceed 1 to 2 percent. For these cases, true nonlinear effective stress site response programs should be used, where nonlinear shear stress-shear strain models (including failure criteria) can replicate the hysteretic, degrading soil response and pore pressure development over the full time history of earthquake loading. The computer program DESRA 2, originally developed by Lee and Finn (1978), was perhaps the first widely recognized nonlinear, effective stress, one-dimensional site response program. Since the development of DESRA 2, a number of other nonlinear, effective stress, one-dimensional programs have been developed, including D-MOD (Matasovic, 1993), SUMDES (Li et al., 1992), TESS (Pyke, 1992) and DESRA-MUSC (Martin and Qiu, 2000).

B.2.3. LIQUEFACTION HAZARDS ASSESSMENT

Results of the liquefaction assessment are used to evaluate the potential severity of three liquefaction-related hazards to the bridge:

1. Flow failures, which involve large translational or rotational slope failures mobilized by existing static stresses (i.e., the site static factor of safety drops below 1.0 due to low strengths of liquefied soil layers).
2. Limited lateral spreads, which involve a progressive accumulation of deformations during ground shaking with eventual deformations that can range from a fraction of a meter to several meters.
3. Ground settlement.

The potential for these hazards can be determined initially on the basis of the factor of safety calculated from the ratio of CRR to CSR. If the ratio is less than 1.3, the hazard should be evaluated following guidelines given below. No single factor of safety value constitutes an appropriate criterion in all situations, and considerable judgment is needed in weighing the many factors involved in a decision as to whether to perform additional analyses. These factors include:

- The type of structure and its vulnerability to damage. Structural mitigation solutions may be more economical than ground remediation.
- Levels of risk accepted by the owner regarding design for life safety, limited structural damage, or essentially no damage.
- Damage potential associated with the particular liquefaction hazards. Flow failures or major lateral spreads pose more damage potential than differential settlement. Hence, factors of safety could be adjusted accordingly.

- Damage potential associated with design earthquake magnitude. A magnitude 7.5 event is potentially far more damaging than a 6.5 event.
- Damage potential associated with SPT values, i.e. low blowcounts are indicative of a greater cyclic strain potential than higher blowcounts.
- Uncertainty in SPT- or CPT- derived liquefaction strengths used for evaluations. Note that a change in silt content from 5 to 15 percent could change a factor of safety from say 1.0 to 1.25 (see figure B-1).
- For high levels of design ground motion, factors of safety may be indeterminate. For example, if $(N_1)_{60} = 20$, $M = 7.5$ and fines content = 35 percent, liquefaction strengths cannot be accurately defined due to the vertical asymptote on the empirical CRR curve (figure B-1).

Factors of safety of about 1.1 may be acceptable for some locations, where the potential for lateral spreading is very low and differential settlement is the hazard of concern. On the other hand, factors of safety of 1.3 may be more appropriate for assessing hazards related to flow failure potential or loss of foundation-bearing capacity. The final choice of an appropriate factor of safety must reflect the particular conditions associated with a specific site and the vulnerability of site related structures.

Sections B.2.3.1 and B.2.3.2 describe an evaluation methodology for liquefaction-induced flow failures and lateral spreading, respectively. Methodology for the evaluation of liquefaction-induced settlement is described in section B.3, which also provides a methodology for estimating settlements of dry or unsaturated soils.

B.2.3.1. Flow Failures

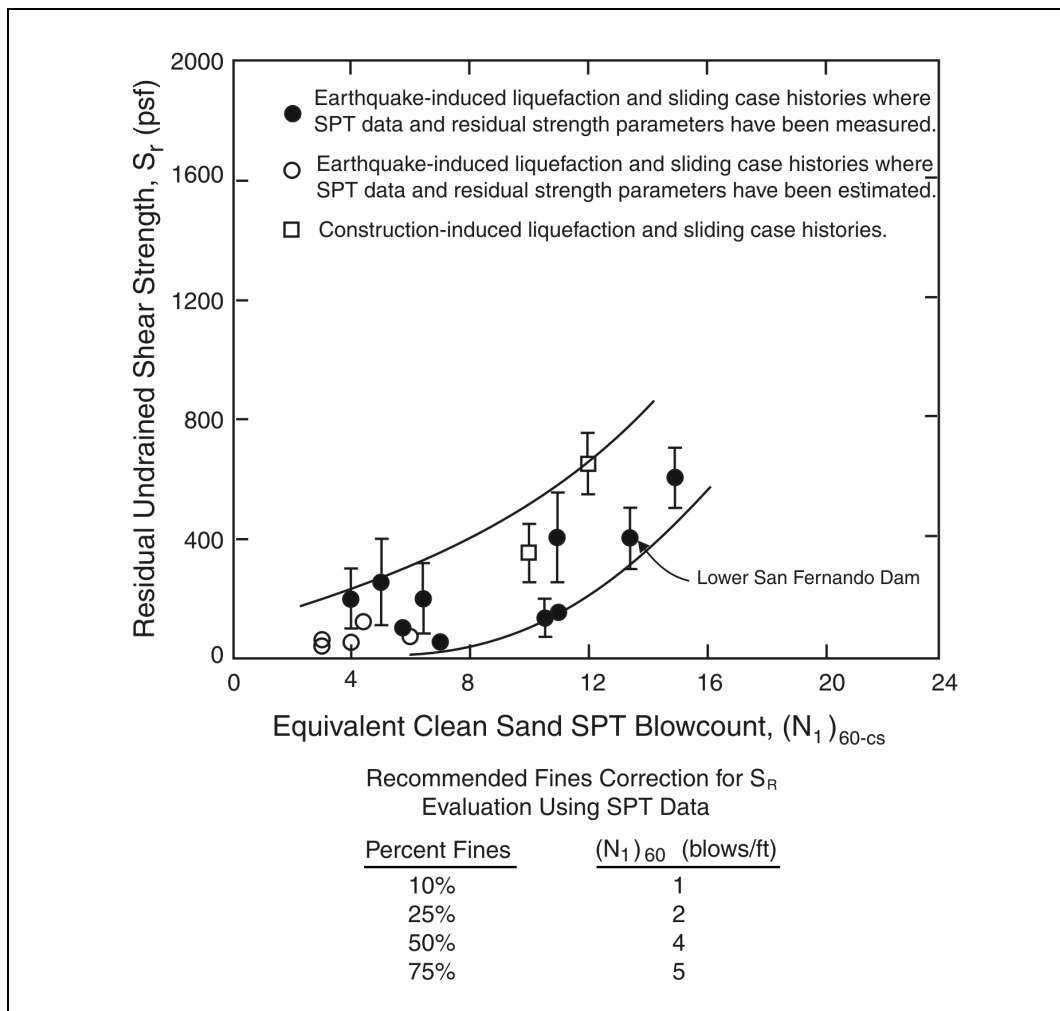
Flow failures are the most catastrophic form of ground failure that may be triggered when liquefaction occurs. These large translational or rotational flow failures are produced by existing static stresses when average shearing stresses on potential failure surfaces exceed the average residual strength of the liquefied soil.

To assess the potential for flow failure, the static strength properties of the soil in a liquefied layer are replaced with the residual strength of liquefied soil. A widely used correlation to estimate residual strength is given in figure B-5. A conventional slope stability check is then conducted. No seismic coefficient is used during this evaluation, thus representing conditions after completion of earthquake shaking. The resulting factor of safety defines the potential for flow failures. If the factor of safety is less than 1.0, lateral flow is predicted.

The estimation of deformation associated with lateral flow cannot be easily made. The deformations can be on the order of tens of meters, depending on the geometry of the flowing ground and the types and layering of soil. In the absence of reliable methods for predicting deformations, it is usually necessary to assume that the soil will undergo unlimited

deformations. If the loads imposed by these movements exceed those that can be tolerated by the structure, some type of ground remediation will likely be required. This situation should be brought to the attention of the owner and a strategy for dealing with the flow problem agreed upon.

Valuable commentary on the lateral flow problem may be found in several publications². The topic of post-liquefaction shear strength of granular soils was also the subject of an NSF-sponsored MCEER workshop at the University of Illinois in 1997 (Stark et al., 1998). The complexities of the problem have also been illustrated in centrifuge tests³.



after Seed and Harder, 1990

Figure B-5. Relationship between residual strength (S_r) and corrected 'clean sand' SPT blowcount $(N_1)_{60}$ from case histories.

² NRC (1985), Seed (1987), Seed and Harder, (1990), Dobry (1995), and Kramer (1996)

³ Arulandan and Zeng (1994), Fiegel and Kutter (1994)

The most difficult determination in the lateral flow problem is the determination of the residual strength of the soil. The most common procedure for evaluating the residual strength involves an empirical correlation between SPT blowcounts and apparent residual strength, back-calculated from observed flow slides. This relationship is shown in figure B-5. Mean or lower-bound values in the data range shown are often adopted. Some experimental work suggests that residual strength is related to confining pressure (Stark and Mesri, 1992). Steady state undrained shear strength concepts based on laboratory tests have also been used to estimate post liquefaction residual strengths⁴. Due to the difficulties of test interpretation and corrections for sample disturbance, the empirically based correlations are normally used rather than laboratory tests.

B.2.3.2. Lateral Spreading

The degradation in undrained shearing resistance arising from liquefaction can lead to limited lateral spreads induced by earthquake inertial loading. Such spreads can occur on gently sloping ground or where nearby drainage or stream channels can lead to static shearing stress biases on essentially horizontal ground (Youd, 1995).

The lateral spreading mechanism is a complex process involving the post-liquefaction strength of the soil, coupled with the additional complexities of potential pore water pressure redistribution and the nature of earthquake loading on the sliding mass. At larger cyclic shearing strains, the effects of dilation can also significantly increase post-liquefaction undrained shearing resistance of the liquefied soil. Incremental permanent deformations will still accumulate during portions of the earthquake load cycles when low residual resistance is available. Such low resistance will continue even while large permanent shearing deformations accumulate through a ratcheting effect. These effects have recently been demonstrated in centrifuge tests to study liquefaction-induced lateral spreads, as described by Balakrishnan et al. (1998). Once earthquake shaking has ceased, the effects of dilation under static loading can mitigate the potential for a flow slide.

Four approaches can be used to assess the magnitude of deformations from lateral spreading as follows:

1. Youd et al. empirical approach.
2. Newmark time history analyses.
3. Simplified Newmark charts.
4. Numerical modelling.

Each method is described in the following sections.

⁴ Poulos et al., 1985, and Kramer, 1996

B.2.3.2.1. Youd et al. Empirical Approach

Using regression analyses and a large database of lateral spread case histories from past earthquakes, Bartlett and Youd (1992) developed empirical equations relating lateral-spread displacements to a number of site and earthquake parameters. A refined version of this approach was presented by Youd et al. (2002). Generally, this approach should be used only for screening of the potential for lateral spreading, as the uncertainty associated with this method of estimating displacement is generally assumed to be too large for bridge design.

The Youd et al. empirical approach uses a variety of earthquake and site parameters, including earthquake magnitude, geometry, and soil grain size in an empirical equation to estimate displacement. Two cases, a sloping ground model and a free-face model, are used. This prediction method is the least reliable in the small displacement range with the level of accuracy probably no better than 1 meter. However, it does allow a relatively straightforward screening to be accomplished to identify the potential severity of lateral spreads.

B.2.3.2.2. Newmark Time History Analyses

The simplest of the numerical methods is the so-called Newmark sliding block analysis⁵ where deformation is assumed to occur on a well-defined failure plane and the sliding mass is assumed to be a rigid block. This approach requires:

1. An initial pseudo-static stability analysis to determine the critical failure surface and associated yield acceleration coefficient (k_y) corresponding to a factor of safety of 1.0.
2. A design earthquake acceleration record at the base of the sliding mass.

Cumulative displacements of the sliding mass generated when accelerations exceed the yield acceleration are computed using computer programs such as described by Houston et al. (1987). These methods are most appropriate when local site effects modify the ground motion as it propagates through the soil profile and when the database for the chart method described below is not adequate. This latter consideration generally involves sites where the source mechanism will be from a magnitude 8 or higher earthquake.

The Newmark method has been used extensively to study earthquake-induced displacements in dams (e.g., Makdisi and Seed, 1978) and natural slopes (e.g., Jibson, 1993). This approach involves the double integration of earthquake records above the yield acceleration. The yield acceleration (k_y) is determined by finding the seismic coefficient that causes the factor of safety in a slope stability assessment to be 1.0. During the stability analyses, the liquefied layer is modeled with the residual strength of the soil. Other layers with partial buildup in porewater pressure can also be degraded in strength for the evaluation.

The earthquake records must be selected from the available catalogue of records, such that they are representative of the source mechanism, magnitude, and distance for the site. A minimum of three records from three independent earthquakes should be selected for the Newmark analyses.

⁵ Newmark, 1965, and Kramer, 1996

Often it is necessary to modify these records for local site effects, as the ground motion propagates through soil to the base of the sliding block.

A number of uncertainties are inherent in the approach due to the assumptions involved. In particular, for liquefaction-induced lateral spreads, uncertainties include:

- The point in the time history when cyclic strength degradation or liquefaction is triggered.
- The magnitude of the apparent post-liquefaction residual resistance as discussed above.
- The influence of the thickness of liquefied soil on displacement.
- Changes in values of yield acceleration (k_y) as deformations accumulate.
- The influence of a non-rigid sliding mass.
- The influence of ground motion incoherence over the length of the sliding mass.

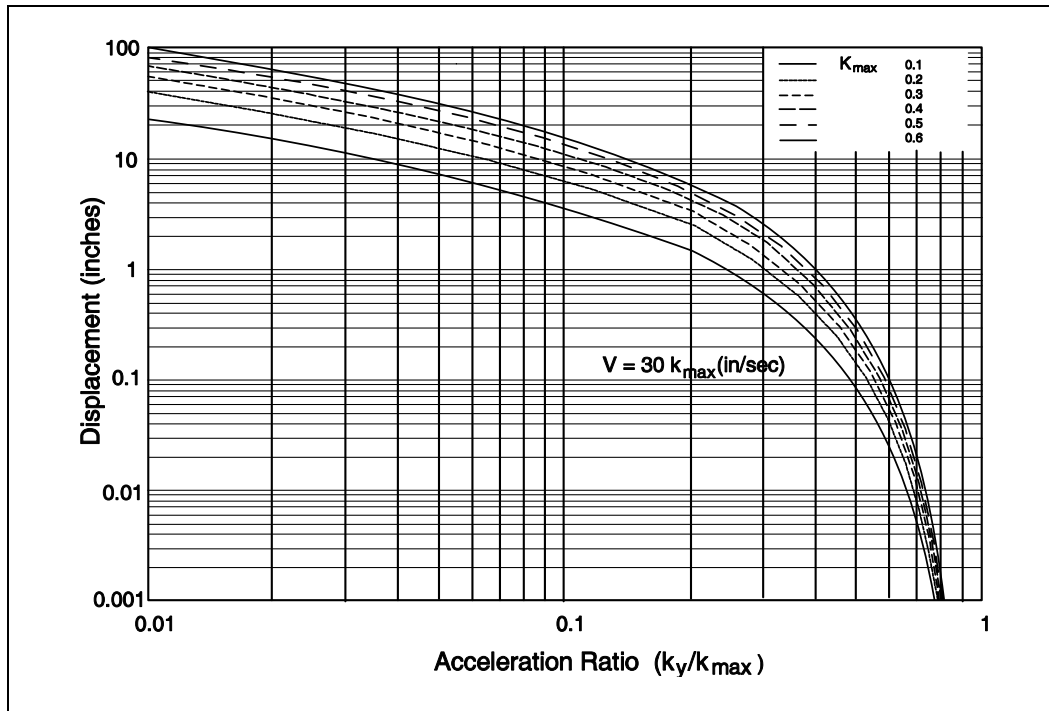
B.2.3.2.3. Simplified Newmark Charts

Charts have been developed by a number of individuals⁶ using large databases of earthquake records and the Newmark Time History Analysis method. These charts allow deformations during seismic loading to be estimated using relationships between the acceleration ratio (i.e. ratio of yield acceleration (k_y) to the peak ground acceleration (k_{max}) occurring at the base of the sliding mass) to ground displacement. The Martin and Qiu (1994) charts are recommended for most cases, as they include both peak ground acceleration and peak ground velocity as regression parameters. Figures B-6 and B-7 show the relationships developed by Martin and Qiu (1994).

The Franklin and Chang (1977) procedure, which was given in earlier editions of the AASHTO Specifications, is now thought to overestimate displacements, partly because it was developed by bounding all data and partly because the database had some records that produced unusually large displacements. The Hynes and Franklin (1984) charts used the same database as did Martin and Qiu, and therefore the mean values from the Hynes and Franklin chart are normally similar to the values estimated by the Martin and Qiu method. The Wong and Whitman (1982) chart provides the smallest estimate of displacements, and appears to be unconservative in some cases.

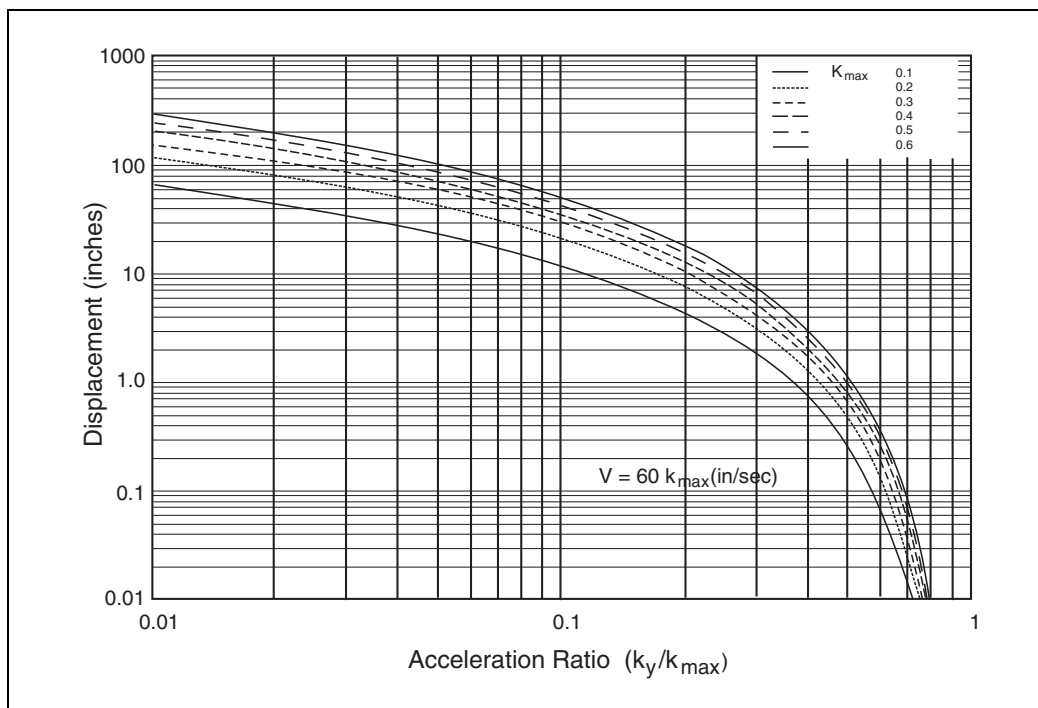
To use these charts, the yield acceleration is determined by finding the seismic coefficient that causes the factor of safety in a slope stability assessment to be 1.0. As noted for the Newmark Time History Analyses, the liquefied layer is modeled with the residual strength of the soil.

⁶ Franklin and Chang, 1977, Hynes and Franklin, 1984, Wong and Whitman, 1982, and Martin and Qiu, 1994



after Martin and Qiu, 1994

Figure B-6. Simplified displacement chart for velocity-acceleration ratio of 30.



after Martin and Qiu, 1994

Figure B-7. Simplified displacement chart for velocity-acceleration ratio of 60.

Other layers with partial buildup in pore water pressure can also be degraded in strength during the evaluation. With the yield acceleration (k_y) and the peak ground acceleration at the base of the failure surface (k_{max}), it is a simple matter to enter the chart and determine the estimated amount of displacement.

These simplified chart methods are limited by the database used in their development. Typically few records greater than magnitude 7.5 were available for analysis and therefore, use of the methods for larger magnitudes must be done with caution. Other limitations are similar to those presented for the Newmark Time History Analyses.

B.2.3.2.4. Numerical Modeling

The most rigorous approach to assessing liquefaction-induced lateral spread or slope deformations entails the use of dynamic finite element / finite difference programs coupled with effective stress-based soil constitutive models. However, the use of such programs is normally beyond the scope of routine bridge design projects. Finn (1991) gives a summary of such approaches, and a recent case history has been described by Elgamal et al. (1998). Various two-dimensional, nonlinear computer programs have been used to perform these analyses. For realistic modeling, these programs must be able to account for large displacements, nonlinear soil properties, and changes in effective stress during seismic modeling. One computer program seeing increasing use for this type of modeling is FLAC⁷. This program has been used on a number of bridge-related projects, including the Alaska Way Viaduct in downtown Seattle, Washington.

As with any rigorous modeling method, considerable experience and judgment are required when using a program such as FLAC. Good practice when using these methods is to compare their output to results obtained from empirically-based simplified methods or to laboratory experimental data, such as those produced in the centrifuge.

If lateral spreading is anticipated at a site, the geotechnical engineer should meet with the owner and decide what approach offers the most appropriate method of estimating the magnitude of lateral spread.

B.3. EVALUATION OF SOIL SETTLEMENT HAZARD

Another consequence of liquefaction resulting from an earthquake is the post-earthquake volumetric strain caused by the dissipation of excess pore water pressures generated in saturated granular soils by the earthquake shaking. The volumetric strain, in the absence of lateral flow or spreading, results in settlement. Liquefaction-induced settlement could lead to collapse or partial collapse of a structure, especially if there is significant differential settlement between adjacent structural elements. Even without collapse, significant settlement could result in damage or render the bridge deck impassable to traffic.

⁷ Itasca, 1998, Wang and Makdisi, 1999

In addition to the settlement of saturated soil deposits, the settlement of dry or unsaturated granular deposits due to earthquake shaking should also be considered in estimating the total seismically induced settlements.

The Tokimatsu and Seed (1987) methodology for saturated and dry/unsaturated sands is the most common procedure currently used to estimate the magnitude of settlement. Figure B-8 shows the relationship between the cyclic stress ratio (τ_{av}/σ'_o) and volumetric strain for saturated clean sands for different values of $(N_1)_{60}$. It is noted that the settlement estimates are valid only for level-ground sites that have no potential for lateral spreading. If lateral spreading is likely at a site and is not mitigated, the settlement estimates using the Tokimatsu and Seed method will likely be less than the actual values.

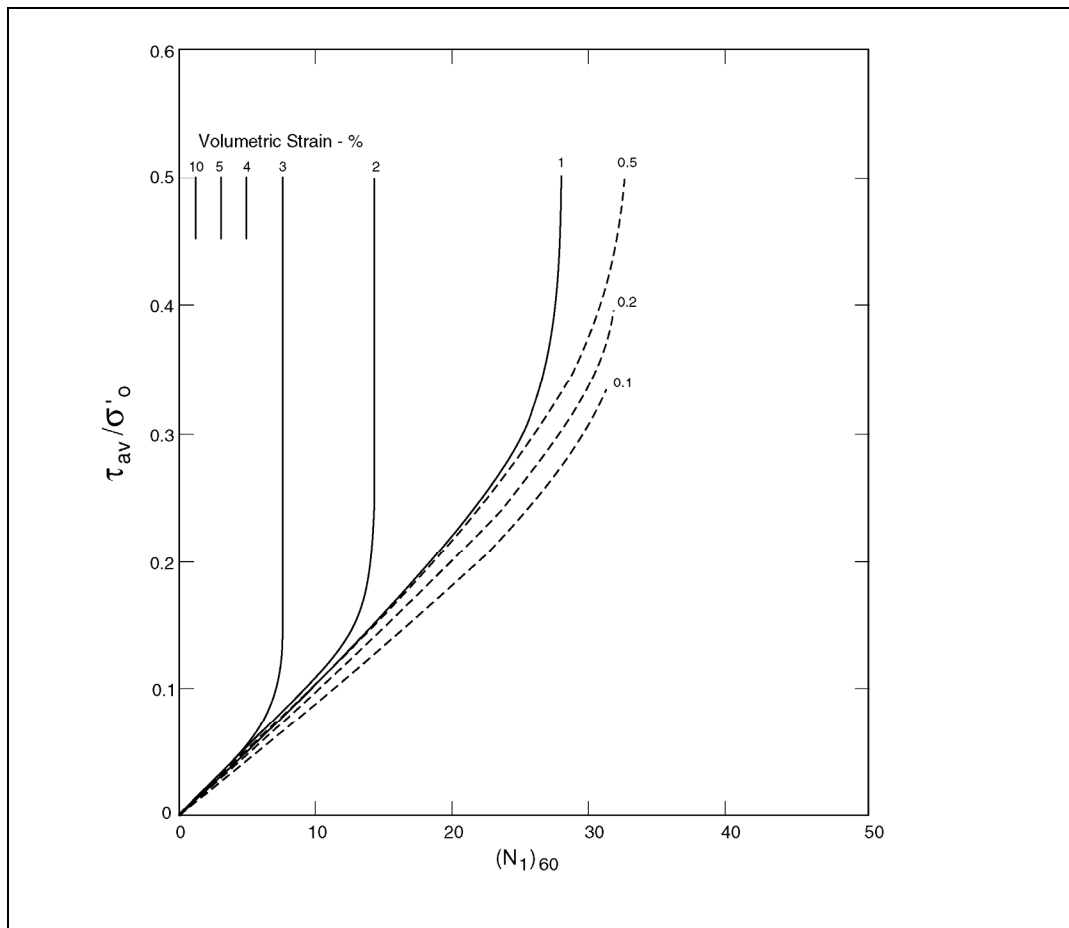
The settlement of saturated silty sand and silt requires adjustments to the cyclic strength for fines content. Ishihara (1993) recommends increasing the cyclic shear strength of the soils if the Plasticity Index (PI) of the fines is greater than 10. This increases the factor of safety against liquefaction and decreases the seismically-induced settlement estimated using the Ishihara and Yoshimine procedure. Field data suggest that use of the Tokimatsu and Seed procedure without correcting the SPT values for fines content could result in an overestimation of seismically-induced settlements⁸. The use of an appropriate fines-content correction will depend on whether the soil is dry/unsaturated or saturated and, if saturated, whether it is completely liquefied (i.e. post-liquefaction), on the verge of becoming liquefied (initial liquefaction), or not liquefied. SCEC (1999) suggests that for 15 percent fines, the SPT correction value ranges from 3 to 5 and for 35 percent fines it ranges from 5 to 9.

Although the Tokimatsu and Seed procedure for estimating seismically-induced settlements in saturated sand is applicable for most level-ground cases, caution is required when using this method for stratified subsurface conditions. Martin et al. (1991) demonstrated that for stratified soil systems, the SPT-based method of liquefaction evaluation⁹ could over-predict (conservative) or under-predict (unconservative) excess pore water pressures developed in a soil layer depending on the location of the soil layer in the stratified system. Given the appropriate boundary conditions, Martin et al. (1991) shows that thin, dense layers of soils could liquefy if sandwiched between liquefiable layers. The estimated settlement using the Tokimatsu and Seed procedure (which is based on the SPT values and excess pore pressures generated in the individual sand layers) may therefore be over-predicted or under-predicted.

The Tokimatsu and Seed (1987) method can be used to estimate settlement in layered deposits of saturated granular soils by accounting for settlement of non-liquefiable layers. One approach to estimate the settlement of such a non-liquefiable soil layer is to use figure B-8, in combination with figure B-9, to determine if the layer will be affected by the layer below. If $H_b \leq H_c$ (see figure B-9), then the settlement of the layer should be estimated by assuming settlement in the non-liquefiable layer (H_b) will be approximately 1.0 percent, provided that the non-liquefiable layer meets all of the following criteria:

⁸ O'Rourke et al., 1991; Egan and Wang, 1991

⁹ Seed et al. (1983) and (1985)



after Tokimatsu and Seed, 1987

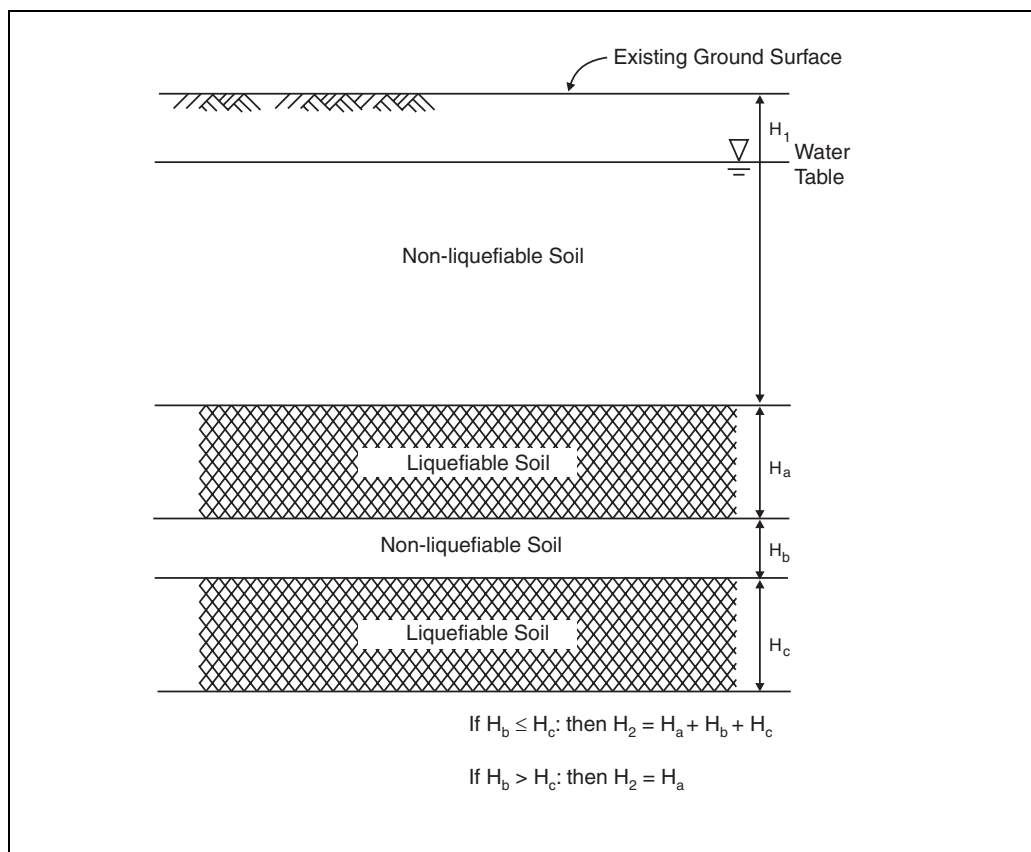
Figure B-8. Relationship between cyclic stress ratio, blowcount $(N_1)_{60}$, and volumetric strain for saturated clean sands and magnitude 7.5.

- Thickness of the layer is less than or equal to 1.5 m (5 ft).
- Corrected SPT value $(N_1)_{60}$ is less than 30 or CPT tip resistance (q_{c1N}) normalized to 100 kPa (15 psi) is less than 160.
- Soil type is sand or silty sand with fines content less than or equal to 35 percent.
- Magnitude of design earthquake is greater than or equal to 7.0.

The logic for using these four criteria is that the migration of pore water pressure into, and subsequent settlement of, the non-liquefiable layer depends on factors such as the thickness, density (SPT or CPT tip value), permeability (soil type) of the layer, and the duration of earthquake shaking (magnitude). It is noted that these criteria are only guidelines to allow the designer to be aware of the potential settlement contributions from certain non-liquefiable soil layers present in a layered system.

Loose cohesionless soil above the water table (dry or unsaturated soils) will tend to densify during the period of earthquake ground shaking. This potential should be considered when evaluating the potential for differential displacement between the bridge abutment and the closest central pier or between central piers in a multiple span bridge. These settlements are additive to the settlements of soils below the water table discussed above (assuming settlement-susceptible soils are located beneath foundation depths).

Procedures described by Tokimatsu and Seed (1987) can be used to estimate the amount of settlement of dry or unsaturated sand. The Tokimatsu and Seed procedure for estimating seismically-induced settlements in these soils requires that the settlement estimates be multiplied by a factor of 2.0 to account for the effect of multidirectional shaking, as discussed by Tokimatsu and Seed (1987).



after Isihara, 1985

Figure B-9. Schematic diagram for determination of H_1 and H_2 .

B.4. EVALUATION OF SURFACE FAULT RUPTURE HAZARD

After a site has been evaluated by the screening criteria presented in chapter 3 and either there is insufficient information to rule out a surface fault rupture hazard, or there is seismic, geomorphic, and/or geologic data that suggests active fault(s) might be present at or near the site, the following information is required to refine definition of the hazard:

1. The location of fault traces (if any) with respect to the site.
2. The timing of most recent slip activity on the fault.
3. The ground rupture characteristics for a design earthquake on the fault (e.g. type of faulting (figure B-10), amount of slip and distribution into strike-slip and dip-slip components, and width of the zone of ground deformation).

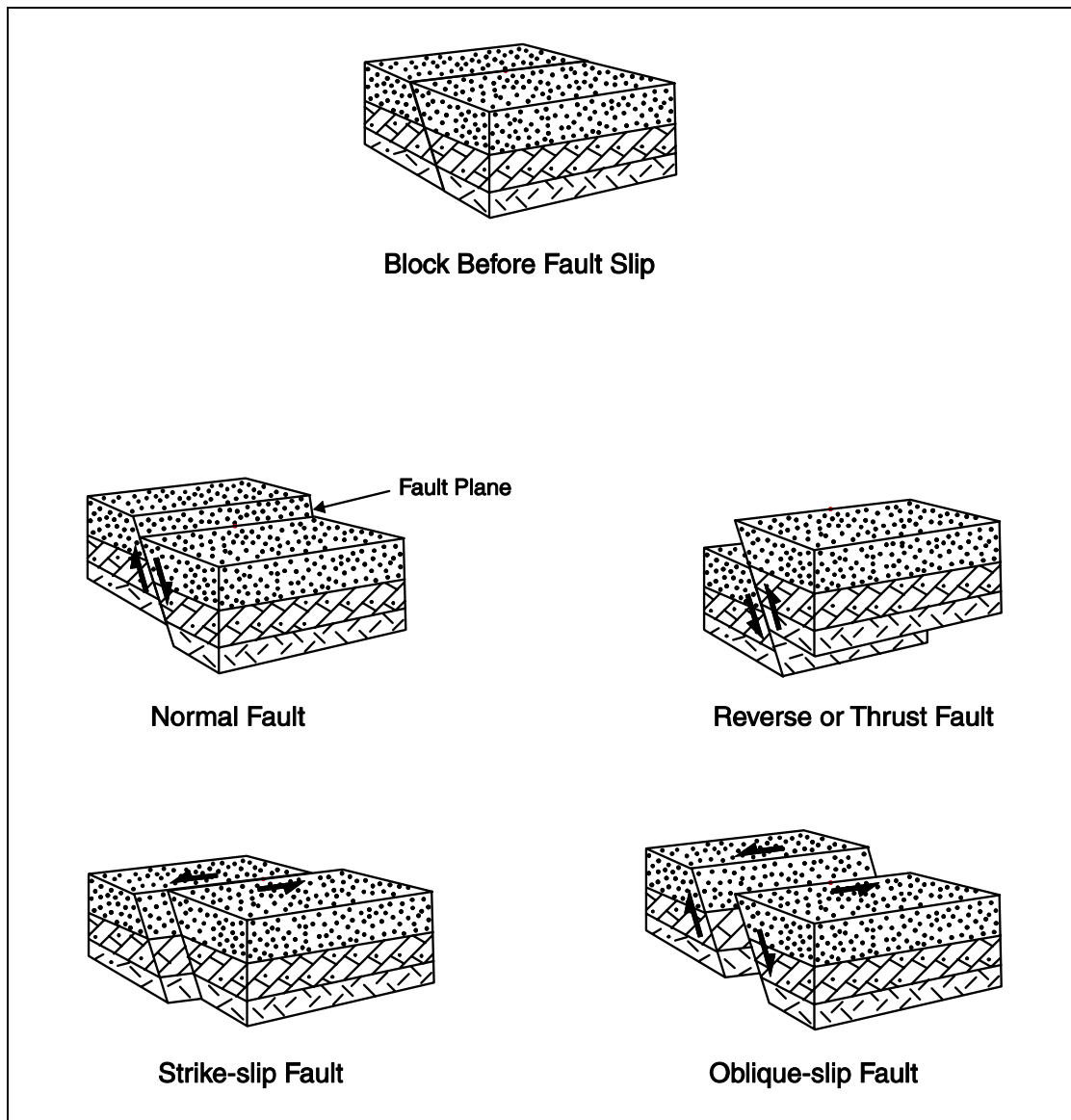


Figure B-10. Types of earthquake faults.

B.4.1. FAULT LOCATION

There are several steps that can be taken to confirm and define the location of faults. Further assessments are not required if it can be shown, on the basis of the procedures outlined below, that there are no faults passing beneath the site.

B.4.1.1. Interpretation of Aerial Photographs

Aerial photographs can be an excellent supplementary resource to geologic and topographic maps of the site and vicinity for identifying faults. Older photographs are particularly useful if they depict the site and/or its environs prior to development activities that would have altered or destroyed landforms that indicate the presence of faults. For many parts of the country, stereo photographic coverage is available as far back as the 1920s or 1930s. Aerial photographs are usually available from several sources including private companies and from various governmental agencies including the U.S. Geological Survey (USGS), U.S. Department of Agriculture (Soil Conservation Service), Bureau of Land Management, and the Forest Service. The USGS maintains the repository for federal photographic resources at its EROS Data Center, Sioux Falls, South Dakota 57198.

B.4.1.2. Contacting Knowledgeable Geologists

Geologists and other earth scientists familiar with geologic and tectonic conditions in the site vicinity may be willing to share their knowledge. These geologists might work for governmental agencies (federal, state, and local), teach and conduct research at nearby colleges and universities, or practice as consultants.

B.4.1.3. Ground Reconnaissance of Site and Vicinity

A walk-down of the site and its vicinity should be conducted to observe unusual topographic conditions and evaluate any geologic relationships visible in cuts, channels, or other exposures. Features requiring a field assessment might have been previously identified during the geologic and topographic map review, aerial photographic interpretation, and/or during conversations with geologists.

B.4.1.4. Surface Exploration

Faults obscured by overburden soils, site grading, and/or structures can potentially be located by one or more techniques. Geophysical techniques such as seismic refraction surveying provide a remote means of identifying the location of steps in a buried bedrock surface and the juxtaposition of earth materials with different elastic properties. Geophysical surveys require specialized equipment and expertise, and their results may sometimes be difficult to interpret. Trenching investigations are commonly used to expose subsurface conditions to a depth of 4.5 to 6 m (15 to 20 feet). While expensive, trenches have the potential to locate faults precisely and provide exposures for assessing their slip geometry and slip history. Borings can also be used to assess the nature of subsurface materials and to identify discontinuities in material type or elevation that might indicate the presence of faults.

B.4.2. FAULT ACTIVITY

If it is determined that faults pass beneath the site, it is essential to assess their activity by determining the timing of the most recent slip(s) as discussed below. If it is determined, based on the procedures outlined below, that the faults are not active faults (see section 3.4.2), further assessments are not required.

B.4.2.1. Assess Fault Relationship to Young Deposits/Surfaces

The most definitive assessment of the recent history of fault slip can be made in natural or artificial exposures of the fault where it is in contact with earth materials and/or surfaces of Quaternary age (last 1.8 million years). Deposits might include native soils, glacial sediments like till and loess, alluvium, colluvium, beach and dune sands, and other poorly consolidated surficial materials. Surfaces might include marine, lake, and stream terraces, and other erosional and depositional surfaces. A variety of age-dating techniques, including radiocarbon analysis and soil profile development, can be used to estimate the timing of the most recent fault slip.

B.4.2.2. Evaluate Local Seismicity

If stratigraphic data are not available for assessment of fault activity, historical seismicity patterns might provide useful information. Maps and up-to-date plots depicting historical seismicity surrounding the site and vicinity can be obtained from the USGS at its National Earthquake Information Center in Golden, Colorado. Additional seismicity information may be obtained from state geologic agencies and from colleges and universities that maintain a network of seismographs (e.g. California Institute of Technology, University of California, Berkeley, University of Nevada, Reno, University of Washington, and the Multidisciplinary Center for Earthquake Engineering Research, Buffalo, New York). If the fault(s) that pass beneath the site are spatially associated with historical seismicity, and particularly if the seismicity and fault trends are coincident, the faults should probably be considered active.

B.4.2.3. Evaluate Structural Relationships

In the absence of both stratigraphic and seismological data, an assessment of the geometric/structural relationships between faults at the site and faults of known activity in the region could be useful. Although less definitive than the two prior criteria, the probability that the site fault is active increases if it is structurally associated with another active fault, and if it is favorably oriented relative to stresses in the current tectonic environment.

B.4.3. FAULT RUPTURE CHARACTERISTICS

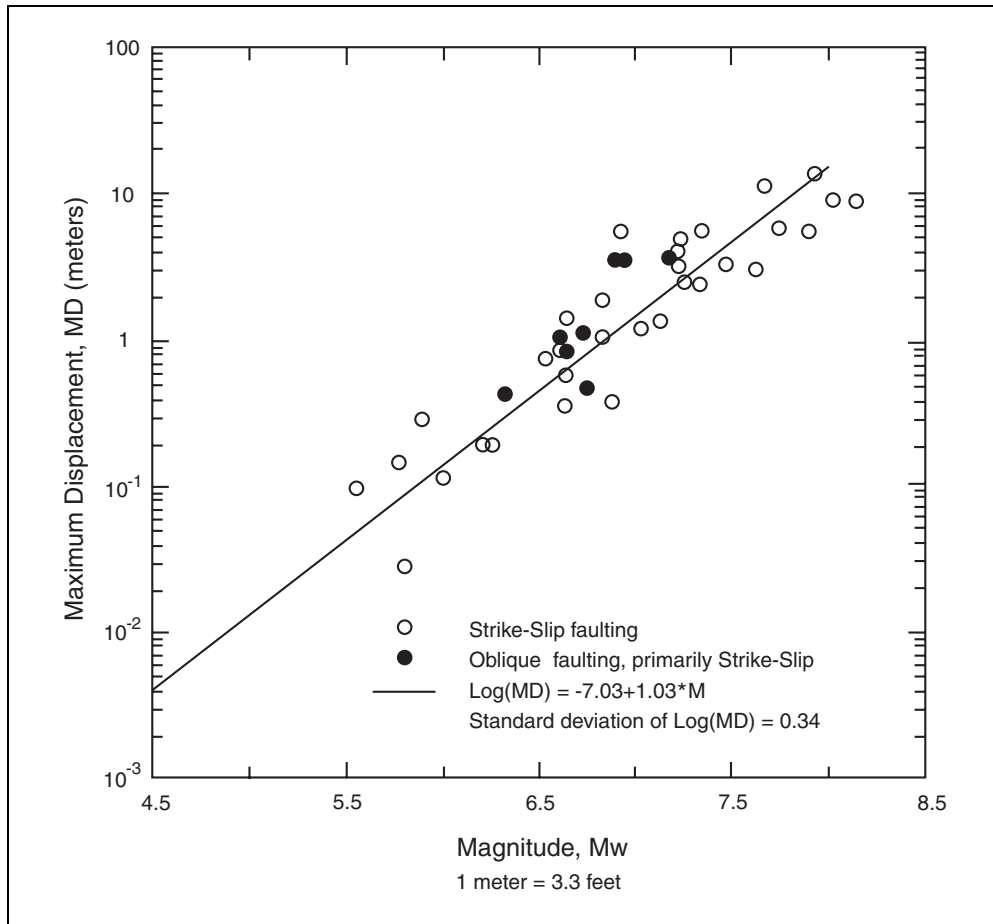
If the evaluation indicates one or more active faults are present beneath the site, the characteristics of future slip on the faults can be estimated. Several methods can be used to estimate the size of future fault displacements. These include:

1. Observations of the amount of displacement during past surface-faulting earthquakes.
2. Empirical relations that relate displacement to earthquake magnitude or to fault rupture length.
3. Calculated values based on the cumulative fault displacement or fault slip rate.

The most reliable displacement assessments are based on past events. Observations of historical surface ruptures and geologic evidence of paleoseismic events provide the most useful indication of the location, nature, and size of future events. Where the geologic conditions do not permit a direct assessment of the size of past fault ruptures, the amount of displacement must be estimated using indirect methods. Empirical relations between displacement and earthquake magnitude based on historical surface-faulting earthquakes (e.g. Wells and Coppersmith, 1994) provide a convenient means for assessing the amount of fault displacement. An example of such a relationship is shown in figure B-11. In this example, maximum displacement along the length of a fault rupture is correlated with earthquake magnitude. Maximum displacement typically occurs along a very limited section of the fault rupture length. Relationships are also available for the average displacement along the rupture length. Data from well-documented historical earthquakes indicate that the ratio of the average displacement to the maximum displacement ranges between 0.2 and 0.8 and averages 0.5 (Wells and Coppersmith, 1994). Other methods for calculating the average size of past displacements include dividing the cumulative displacement by the number of events that produced the displacement, and multiplying the geologic slip rate by the recurrence interval.

Predicting the width of the zone and the distribution of slip across the zone of surface deformation associated with a surface faulting event is more difficult than predicting the total displacement. The best means for assessing the width of faulting is site-specific trenching that crosses the entire zone. Historical records indicate that the width of the zone of deformation is highly variable along the length of a fault. No empirical relationships having general applicability have been developed that relate the size of the earthquake or the amount of displacement on the primary fault trace to the width of the zone or to the amount of secondary deformation. The historical record indicates, and fault modeling shows, that the width of the zone of deformation and the amount of secondary deformation tend to vary as a function of the dip of the fault and the sense of slip. Steeply dipping faults, such as vertical strike-slip faults, tend to have narrower zones of surface deformation than shallow-dipping faults. For dipping faults, the zone of deformation is generally much wider on the hanging wall side than on the foot wall side. Low-angle reverse faults (thrust faults) tend to have the widest zones of deformation.

Probabilistic methods for assessing the hazard of fault rupture have been developed that are similar to the probabilistic seismic hazard analysis (PSHA) methods used to assess earthquake ground motions (e.g. Coppersmith and Youngs, 1990, 2000). A PSHA for fault rupture defines the likelihood that various amounts of displacement will be exceeded at a site during a specified time period. For critical bridges, such analyses could be considered to assess whether the likelihood of surface fault rupture is high enough to warrant design for the hazard and to aid in quantifying design values of displacement.



after Wells and Coppersmith, 1994

Figure B-11. Relationship between maximum surface fault displacement and earthquake moment magnitude for strike-slip faulting.

B.5. EVALUATION OF FLOODING HAZARD

If a bridge site has the potential for earthquake-induced flooding based on the initial screening described in section 3.5.2, then further evaluations should be directed at assessing the potential for, and severity, consequences, and likelihood of the hazard. The evaluation of the potential for landslides into, or within, a body of water uses methodologies described for evaluating liquefaction hazards (section B.2 of this appendix) and landslide hazards (chapter 3 of Part 2 of this manual).

Evaluation of the height of waves that could be produced by a tsunami, seiche, or landslide requires special expertise in fields such as fluid dynamics and coastal engineering as well as seismological, geophysical, and earthquake engineering expertise in characterizing the earthquakes and ground shaking that cause these phenomena. Similarly, geological, seismological, and geophysical expertise is required to assess tectonic movements such as uplift or tilting that could cause flooding. Such studies of hazard potential and severity should be considered unless it can be concluded that the effects of flooding on the bridge are tolerable.

considering the performance objective, or the probability of occurrence of the hazard is sufficiently low that the risk can be accepted.

If a bridge has possible exposure to flooding from failure of a dam or other water retention structure, the agencies having jurisdiction over these facilities should be contacted to determine whether the structure has been evaluated or designed for appropriate ground shaking using modern seismic analysis and design methods. The potential effects of the flooding at the site should also be evaluated.

APPENDIX C: FRAGILITY CURVE THEORY

For a given bridge, it is not possible to precisely determine the level of ground shaking necessary to cause a target level of response or damage state to be achieved. In addition to assuming material properties and certain other structural attributes that affect the overall *capacity* of a bridge, such a deterministic assessment requires certain assumptions to be made about the ground motion and site conditions. These are both factors that also affect seismic *demand*. Naturally, values of these parameters are not exact. Instead, they invariably have a measure of both randomness and uncertainty associated with them. An increasingly popular way of characterizing the probabilistic nature of these phenomena is through the use of so-called *fragility curves*¹.

Figure C-1 shows how the inherent uncertainty and randomness of bridge capacity versus ground motion demand can be used to establish fragility curves. The pushover capacity of a bridge has been superimposed on the acceleration-displacement spectra in this figure. In a deterministic analysis, the intersection of the two curves gives the expected level of performance. However, probability distributions are drawn over both the capacity and demand curves to indicate the associated uncertainty and randomness of performance. From this graph, it is evident there is a wide range of possible performance outcomes. In other words, there is not a unique outcome.

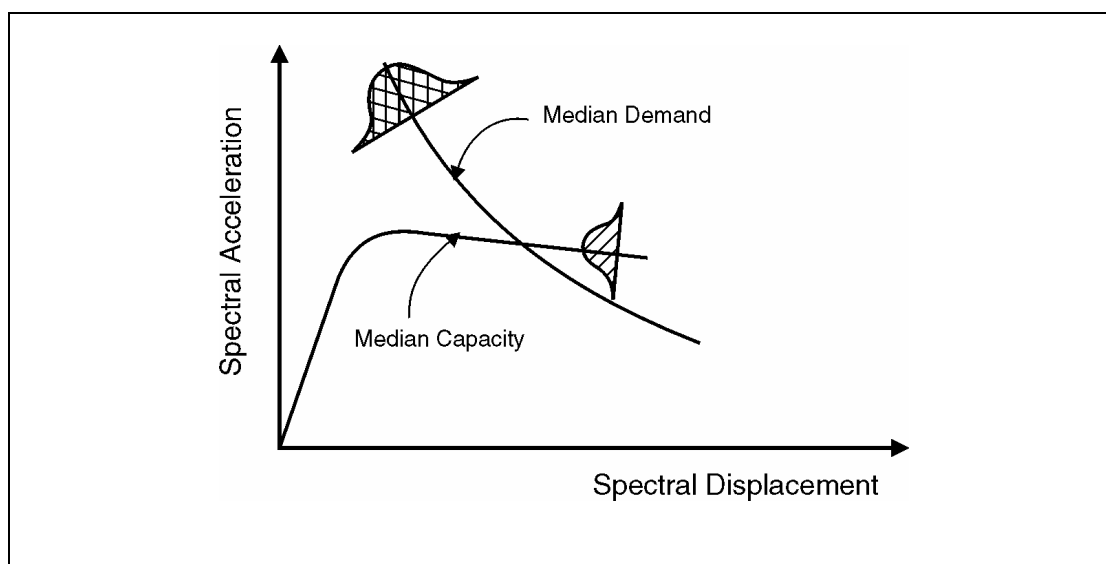


Figure C-1. Capacity-demand acceleration-displacement spectra showing randomness and/or uncertainty in structural behavior and ground motion response.

If structural capacity and seismic demand are random variables that roughly conform to either a normal or log-normal distribution, then by following the *central limit theorem*, it can be shown that the composite performance outcome will be log-normally distributed. Therefore, the

¹ Ayyub and McCuen, 1997; Benjamin and Cornell, 1970

probabilistic distribution is expressed in the form of a so-called fragility curve given by log-normal cumulative probability density function. Fortunately, only two parameters are needed to define such a curve: a median value (the 50th percentile) and a normalized logarithmic standard deviation.

Figure C-2 presents the form of a normalized fragility curve for bridges. The cumulative probability function is given by:

$$F(S_a) = \Phi \left[\frac{1}{\beta_c} \ln \left(\frac{S_a}{A_i} \right) \right] \quad (C-1)$$

where S_a is the spectral acceleration at a period $T = 1.0$ sec, A_i is the median spectral acceleration necessary to cause the i^{th} damage state to occur, and β_c is the normalized composite log-normal deviation which incorporates aspects of uncertainty and randomness for both capacity and demand. This parameter is sometimes referred to as either the *coefficient of variation* or the *coefficient of dispersion*. It has been calibrated theoretically by several researchers², and validated against experiential fragility curves obtained from the 1989 Loma Prieta and 1994 Northridge earthquakes (Basoz and Mander, 1999). Based on these investigations, it is recommended that $\beta_c = 0.6$, and Φ is the standard log-normal cumulative distribution function.

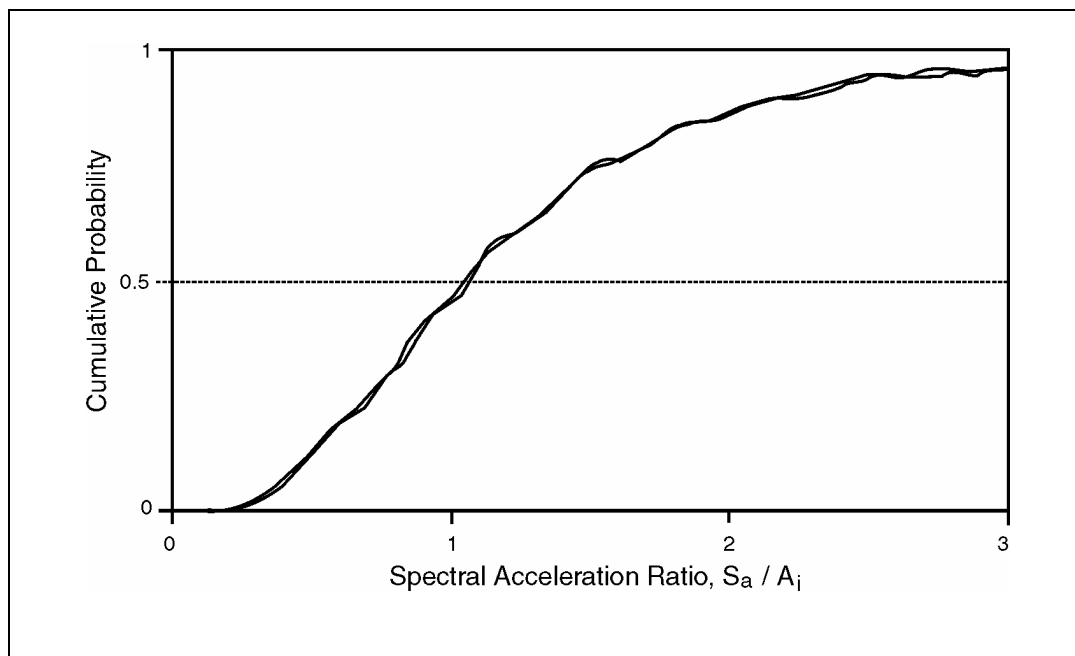


Figure C-2. A normalized fragility curve based on a lognormal probability distribution with a coefficient of dispersion $\beta_c = 0.6$.

² Pekcan (1998); Dutta and Mander (1998); Dutta (1999)

Unfortunately, evaluating the cumulative distribution function is not trivial, as considerable numerical integration is usually necessary. However, the fragility curve can be established using intrinsic functions found in most computer software for spreadsheet calculations. For example, LOGNORMDIST(S_a , $\ln(A_i)$, β_c) is a function which returns the cumulative normal distribution of S_a , where $\ln(S_a)$ is normally distributed with mean $\ln(A_i)$ and standard deviation β_c .

As an alternative to using standard spreadsheet software, equation (C-1) can be evaluated using the following approximation:

$$P[D > DS_i | S_a] = \frac{1}{1 + \left(\frac{S_a}{A_i} \right)^{\frac{-1.7}{\beta_c}}} \quad (C-2)$$

where $P[D > DS_i | S_a]$ is the probability of being in damage state D that is equal to or greater than DS_i for a given spectral acceleration S_a at a structural period $T = 1.0$ sec, and DS_i is the i^{th} damage state described as follows:

- DS_1 = no damage (pre-yield),
- DS_2 = slight damage,
- DS_3 = moderate damage,
- DS_4 = extensive damage,
- DS_5 = collapse,

and all other terms are defined as above.

APPENDIX D: CAPACITY/DEMAND RATIOS FOR BRIDGE MEMBERS AND COMPONENTS

D.1. GENERAL

Capacity/demand (C/D) ratios are used to quantify the likely performance of a bridge during an earthquake and can be thought of as that fraction of the design earthquake which will cause a member or component to be damaged. The consequences of this damage must then be assessed in terms of its effect on the stability and usability of the bridge following an earthquake.

This appendix presents a methodology for calculating C/D ratios for various member and component limit states based on a combination of analysis, testing, and engineering judgment. Eleven ratios are defined in four categories as follows:

1. Support length and restrainer C/D ratios:

- r_{ad} displacement C/D ratio for abutment
- r_{bd} displacement C/D ratio for bearing seat or expansion joint
- r_{bf} force C/D ratio for bearing or expansion joint restrainer

2. Column C/D ratios:

- r_{ca} anchorage length C/D ratio for column longitudinal reinforcement
- r_{cc} confinement C/D ratio for column transverse reinforcement
- r_{cs} splice length C/D ratio for column longitudinal reinforcement
- r_{cv} shear force C/D ratio for column
- r_{ec} bending moment C/D ratio for column

3. Footing C/D ratios:

- r_{ef} bending moment C/D ratio for footing
- r_{fr} rotation C/D ratio for footing

4. Soil C/D ratio:

- r_{sl} acceleration C/D ratio for liquefaction potential

The relative magnitudes of these ratios may be used to sequentially upgrade a deficient bridge.

D.2. MINIMUM BEARING OR RESTRAINER FORCE DEMANDS

When determining the minimum bearing or restrainer force demands for the evaluation of an existing bridge, the minimum equivalent horizontal force given in section 5.2 should be used. This minimum is either 10 percent or 25 percent of the tributary dead load as described in section 5.2.

Bearing or restrainer force demands are generally obtained from an analysis of the bridge. However, bearing or restrainer forces derived from an elastic analysis do not include the effects of nonlinear response of the structure or variations in motions at the supports due to traveling surface waves. Because a linear analysis of a bridge often results in relatively low bearing or restrainer forces, minimum force demands are specified to account for uncertainties in the analysis and to identify bearings that have unreasonably low force capacities. These minimum forces are intended for evaluation and should not be confused with minimum design forces for bearing restrainers. Different minimum forces for evaluation and design are consistent with other requirements of this manual in which evaluation and design are treated differently. Minimum force demands are not applicable to devices specifically designed to limit the transfer of forces.

The engineer performing the evaluation may use simplified methods to determine the portion of the minimum equivalent horizontal force carried by the bearings and restrainers. As an example, the minimum equivalent horizontal force may be distributed to each horizontal force-resisting element based on the portion of the total dead load included within the plan area of the bridge bounded by imaginary lines midway between adjacent horizontal force-resisting elements. When the ultimate force capacity of a ductile horizontal force-resisting element is insufficient to resist its share of the minimum equivalent horizontal force, then the excess of that force should be distributed to adjacent bearings or restrainers.

D.3. MINIMUM SUPPORT LENGTHS

The supports at the abutments, columns, and expansion joints must be of sufficient length to accommodate anticipated relative displacements. Minimum support lengths are specified because an elastic analysis does not account for the effects of nonlinear response of the structure or variation in motions at the support due to traveling surface waves.

Minimum support lengths, $N(d)$, for bearing seats supporting the unrestrained expansion ends of girders, as shown by the dimension N in figure D-1, are used to calculate bearing displacement C/D ratios, r_{bd} by Method 1, as described in section D.4. These support lengths are measured normal to the face of abutment, pier, or mid-span joint. The values for minimum support length are given by the equations below:

$$N(d) = \left[100 + 1.7L + 7.0H + 50\sqrt{H} \sqrt{1 + \left(2 \frac{B}{L} \right)^2} \right] \frac{(1 + 1.25F_v S_1)}{\cos \alpha} \quad (D-1a)$$

where:

- $N(d)$ is the minimum seat width (mm),
- L is the distance between joints, or $(L_1 + L_2)$ for a hinge seat within a span (m),
- H is the tallest pier between the joints (m), and
- B is the width of the superstructure (m).

Or, in customary units:

$$N(d) = \left[4.0 + 0.02L + 0.08H + 1.1\sqrt{H} \sqrt{1 + \left(2\frac{B}{L} \right)^2} \right] \frac{(1 + 1.25F_v S_1)}{\cos \alpha} \quad (D-1b)$$

where:

$N(d)$ is the minimum seat width (in),

L is the distance between joints, or $(L_1 + L_2)$ for a hinge seat within a span (ft),

H is the tallest pier between the joints (ft), and

B is the width of the superstructure (ft).

In both equations, α is the angle of skew (zero for a right bridge). The ratio of B/L need not be taken greater than $3/8$.

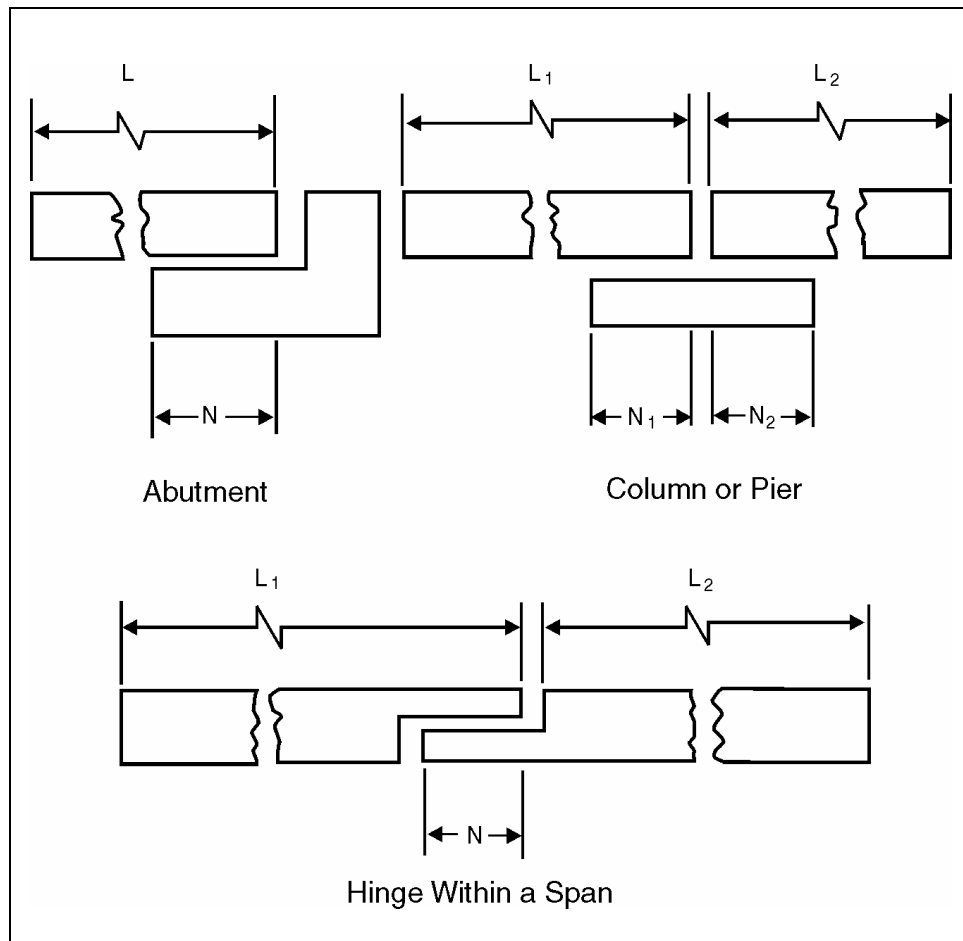


Figure D-1. Minimum support length requirements.

D.4. CAPACITY/DEMAND RATIOS FOR EXPANSION JOINTS AND BEARINGS

D.4.1. GENERAL

Bridge superstructures are often constructed with intermediate expansion joints to accommodate anticipated superstructure movements, such as those caused by temperature variation or to allow for the use of incompatible materials. Joints necessitate the use of bearings, which provide for rotational and/or translational movement. During earthquakes, bridge bearings have proven to be one of the most vulnerable of all bridge components.

In major earthquakes, the loss of support at bearings has been responsible for several bridge failures. Although many of these failures resulted from permanent ground displacements, several were caused by vibration effects alone. Some recent examples of earthquakes in which bridge collapse resulted from bearing failure include the Loma Prieta, California, earthquake of 1989, and the Scotts Mills earthquake in Oregon of 1993, and the Kobe, Japan, earthquake in 1995¹. Even relatively minor earthquakes have caused failure of anchor bolts, keeper bar welds, and concrete shear keys. In many of these cases, the collapse of the superstructure was believed imminent and would have occurred had the ground motion been slightly more intense or longer in duration.

The dynamic behavior of bridge bearings is often very nonlinear and difficult to analyze using conventional linear-elastic analysis techniques. Elastic bearing forces obtained from a conventional analysis are likely to be lower than those actually experienced by bearings during an earthquake. This is because bearings, which are non-ductile components, often do not resist loads simultaneously. This has been demonstrated in past earthquakes by the failure of anchor bolts or keeper bars in some, but not all, of the bearings at a support. In addition, the yielding of ductile members, such as columns, can transfer load to the bearings. This phenomenon has been observed in the results from nonlinear analytical case studies of several bridge structures. For these reasons, it is necessary to increase elastic analysis force results when evaluating the force demand on non-ductile motion-restraining components.

In the case of differential horizontal displacements at expansion joints during earthquakes, elastic response spectrum analysis results yield displacements that are often below those intuitively expected based on observed bridge behavior during past earthquakes. In addition to the nonlinear behavior of expansion joints, possible independent movement of different parts of the substructure and out-of-phase movement of abutments and columns resulting from traveling surface-wave motions also tend to result in larger displacements. As noted in the previous section, minimum support lengths are required in the *AASHTO Specifications* to allow for this possibility. These support lengths are useful in evaluating the girder seats of existing bridges at unrestrained expansion joints.

When retrofitting expansion joints, however, it is often difficult or impossible to increase the existing support length. In these cases, longitudinal restrainers or other displacement-limiting devices may be the only feasible means of preventing a loss of support at the bearings. To

¹ Fung et al., 1971; Imbsen, 1981; Governor's Board of Inquiry, 1990; EERI, 1993

evaluate the effectiveness of these devices in reducing displacements, it is necessary to more accurately analyze the movement at bearings. To obtain a reasonable estimate of the actual displacements, a multi-mode spectral method of analysis including the effect of foundation flexibility should be performed.

When evaluating the effect of seismic displacements, it is necessary to remember that the entire seat width will not be available during an earthquake. Shortening of the bridge superstructure due to shrinkage, temperature, or creep may reduce the effective support width. In addition, the pounding of adjacent superstructure sections during strong seismic shaking is likely to cause localized damage of the expansion joints. This damage will involve crushing of concrete and a probable loss of concrete cover, which will further reduce the available seat width. This is shown schematically in figure D-2.

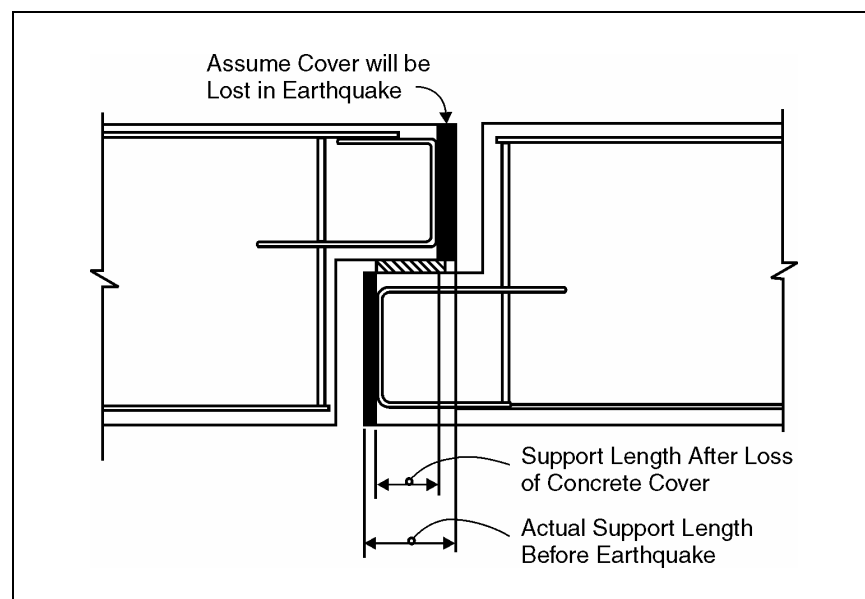


Figure D-2. Effective seat width.

A bridge with a sloping vertical alignment may have a tendency to shift downhill during an earthquake, leaving some expansion joints closed and others open. This same tendency to move downhill may also result from other causes, such as temperature movement, traffic vibrations, and vehicle braking forces. This latter phenomenon should also be considered in determining the available support length.

In determining the force capacity of bearings, consideration should be given to the following shortcomings of bridge bearings:

- Grout pads under bearing masonry plates have traditionally given trouble during and after construction and have been one of the main sources of trouble in minor earthquakes. Failure of a grout pad will allow the bearing assembly to move, subjecting the anchor bolts to combined bending and shear.

- Anchor bolts which pass through an elastomeric bearing pad will be subjected to combined bending and shear.
- Anchor bolts are frequently installed with threads that extend below the top surface of the pier or abutment seat. This gives a reduced area for shear and may reduce the flexural capacity of the bolt due to notch sensitivity at the root of the threads leading to brittle fracture.
- Anchor bolts may have insufficient uplift capacity unless provided with an embedded anchor plate.
- Anchor bolts may be too close to the edge of the bearing seat and may break through the concrete when subjected to horizontal loads.
- All of the bearings supporting one end of a span do not resist horizontal forces equally or even simultaneously. Because keeper bars or other devices are not set with exactly the same clearances, the bearings will not be equally effective in resisting load. It is quite common for bearings on the same support line to be damaged to different degrees during an earthquake.
- Bridge bearings may not be what they are represented to be on "as-built" plans or maintenance records. Adjustments to keeper bars and other details are occasionally made after construction is completed. The details and workmanship in such cases may be inferior to the original construction.

D.4.2. DISPLACEMENT CAPACITY/DEMAND RATIOS

The displacement C/D ratios, r_{bd} should be calculated for restrained and unrestrained expansion joints and for bearings at which movement can occur due to the absence of fixity in a horizontal direction. The displacement C/D ratio is the lesser of the values calculated using the following two methods, except in the case where displacement-limiting devices such as restrainers are provided. In that case, Method 2 should be used.

Method 1:

$$r_{bd} = \frac{N(c)}{N(d)} \quad (D-2)$$

where $N(c)$ is the actual support length provided, measured normal to the expansion joint or bearing line, and $N(d)$ is the minimum support length defined in section D.3.

Method 2:

$$r_{bd} = \frac{\Delta_s(c) - \Delta(d)}{\Delta_{eq}(d)} \quad (D-3)$$

where:

$\Delta_s(c)$ is the available capacity of the expansion joint or bearing for movement;
for structures in SRC D, cover concrete should not be included in determining the

- allowable movement,
- $\Delta_i(d)$ is the maximum possible movement resulting from temperature, shrinkage, and creep shortening (if field measurements of available capacity in older bridges are used for $\Delta_s(c)$, then only temperature effects need to be considered here), and
- $\Delta_{eq}(d)$ is the maximum calculated relative displacement due to earthquake loading for the load cases described in section 7.4.

D.4.3. FORCE CAPACITY/DEMAND RATIOS

The force C/D ratio for bearings and expansion joint restrainers are evaluated as follows:

$$r_{bf} = \frac{V_b(c)}{V_b(d)} \quad (D-4)$$

where $V_b(c)$ is the nominal ultimate capacity of the component in the direction under consideration, and $V_b(d)$ is the seismic force acting on the component. This force is the elastic force determined from an analysis in accordance with section 7.4, multiplied by 1.25. The minimum bearing force demand, as specified in section D.2, is used when an analysis is not performed, or when it exceeds the force demand obtained from an analysis.

D.5. CAPACITY/DEMAND RATIOS FOR REINFORCED CONCRETE COLUMNS, WALLS, AND FOOTINGS

It is expected that reinforced concrete columns, walls, and even footings may yield and form plastic hinges during a strong earthquake. The interaction between these components will determine the probable mode of failure. To evaluate these components, it is first necessary to determine the location of potential plastic hinges. Plastic hinges form at locations of peak bending moment and are therefore likely to occur in the end regions of columns or within a footing near the column face. An effect similar to a plastic hinge may also develop due to yielding of the soil or pilings. Walls, which are defined as supports having a height-to-width ratio of 2.5 or less in the strong direction, may develop plastic hinges in the end regions about the strong, as well as the weak, axes.

Once potential plastic hinges have been located, it is necessary to investigate the potential modes of column and/or footing failure associated with the location and type of plastic hinging. A ductility indicator is used to account for the ability of the columns and/or footings to resist certain modes of failure controlled by the amount of yielding. The ultimate moment capacity / elastic moment demand ratios are multiplied by ductility indicators to enable elastic analysis results to be used for determining the C/D ratios of components subject to yielding.

The following procedure should be used to determine the C/D ratio for columns, walls, and footings as illustrated in the flowchart in figure D-3. This procedure includes a systematic method for locating plastic hinges and evaluating the capacity of the columns and / or footings to due to plastic hinging. Sections D.5.1 through D.5.5 describe detailed procedures for investigating different column and/or footing failure modes sometimes associated with plastic hinging.

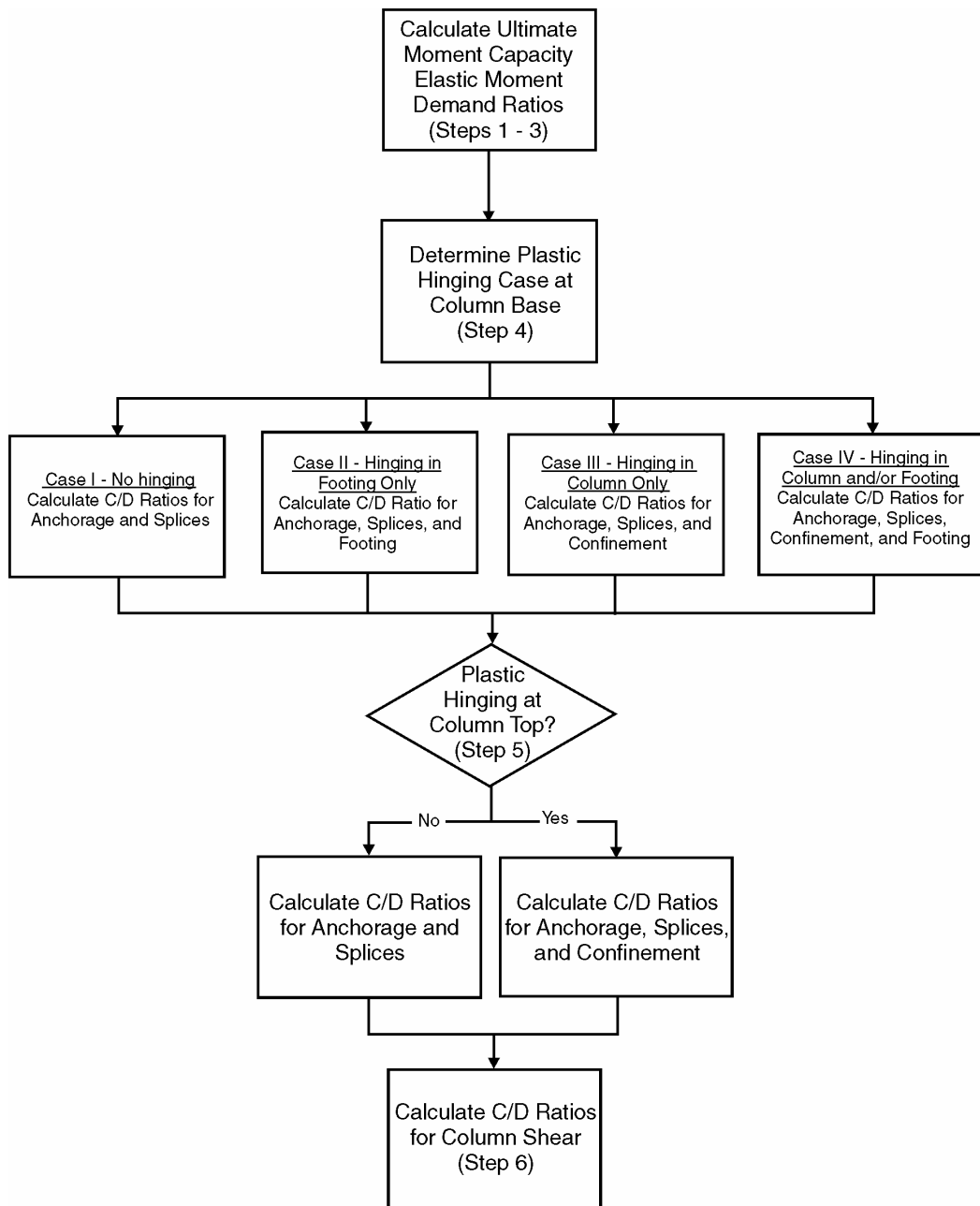


Figure D-3. Procedures for determining capacity/demand ratios for columns, piers and footings.

Step 1: Determine the elastic moment demands at both ends of the column or wall for the seismic load cases described in section 7.4. Moment demands for both the columns and footings should be determined. The elastic moment demand may be taken as the sum of the absolute values of the earthquake and dead load moments.

Step 2: Calculate nominal ultimate moment capacities for both the column and the footing at axial loads equal to the dead load plus or minus the seismic axial load resulting from plastic hinging in the columns, walls, or footings as discussed in Article 7.2.2 of the *AASHTO Standard Specifications* (AASHTO, 2002).

Step 3: Calculate the set of moment C/D ratios (nominal ultimate moment capacity / elastic moment demand), r_{ec} and r_{ef} , for each combination of capacity and demand, assuming first that the column will yield and the footing will remain elastic, and second that the footing will yield and the column will remain elastic.

Step 4: Calculate the C/D ratios for the anchorage of longitudinal reinforcement, splices in the longitudinal reinforcement, and/or transverse confinement reinforcement at the base of the column, and/or footing rotation or yielding for the most severe possible cases of plastic hinging as indicated by each set of r_{ec} and r_{ef} . The following cases describe the C/D ratios that should be investigated based on the location and extent of plastic hinging.

- Case I: Both r_{ec} and r_{ef} exceed 0.8 It may be assumed that neither the footing nor the column will yield sufficiently to require an evaluation of their ability to withstand plastic hinging. In this case, only the column C/D ratios for anchorage of longitudinal reinforcement (section D.5.1) and splices in longitudinal reinforcement (section D.5.2) need to be calculated.
- Case II: r_{ef} is less than 0.8 and r_{ec} either exceeds 0.8 or exceeds r_{ef} by 25 percent The footing will require an evaluation of its ability to rotate and/or yield unless an anchorage or splice failure will occur and prevent footing rotation. Anchorage or splice failures may be assumed when either the C/D ratio for anchorage of longitudinal reinforcement (section D.5.1) or for splices in longitudinal reinforcement (section D.5.2) is less than 80 percent of r_{ef} . When this is not the case, only the C/D ratio for rotation and/or yielding of the footing should be calculated.
- Case III: r_{ec} is less than 0.8 and r_{ef} either exceeds 0.8 or exceeds r_{ec} by 25 percent It may be assumed that only the column will yield sufficiently to require an evaluation of its ability to withstand plastic hinging. In this case, the column C/D ratios should be calculated for anchorage of longitudinal reinforcement (section D.5.1), splices in longitudinal reinforcement (section D.5.2), and column transverse confinement (section D.5.4).
- Case IV: r_{ec} and r_{ef} are both less than 0.8 and within 25 percent of one another It may be assumed that both the column and footing have the potential to yield sufficiently to require further evaluation. Since yielding of the footing will be prevented by a column failure prior to column yield, column C/D ratios for anchorage of longitudinal

reinforcement (section D.5.1), splices of longitudinal reinforcement (section D.5.2), and column transverse confinement (section D.5.4) should be calculated first. When all of these C/D ratios exceed 80 percent of r_{ef} , then the C/D ratio for rotation and/or yielding of the footing (section D.5.5) should also be calculated.

Step 5: Calculate the column C/D ratios for anchorage of longitudinal reinforcement (section D.5.1) and splices in longitudinal reinforcement (section D.5.2) at the top of the column. If the moment C/D ratio, r_{ec} , of the column is less than 0.8, the C/D ratio for column transverse confinement (section D.5.4) should also be calculated.

Step 6: Calculate the column C/D ratios for column shear (section D.5.3).

C/D ratios for anchorage of longitudinal reinforcement (r_{ca}), longitudinal reinforcement splice lengths (r_{cs}), column shear capacity (r_{cv}), column confinement reinforcement (r_{cc}), and rotation and/or yielding of the footing (r_{fr}) are dependent on the amount of flexural yielding in the column or footing. In columns with poorly detailed transverse reinforcement, one of the most critical consequences of flexural yielding is the spalling of cover concrete. Such spalling is followed by a rapid degradation in the effectiveness of the transverse steel that can lead to column failure. The procedure for calculating C/D ratios for column confinement reinforcement is based on the assumption that spalling will begin at a ductility indicator of 2. The effectiveness of poorly detailed transverse reinforcement is assumed to begin to degrade at the onset of spalling. This type of transverse reinforcement is considered totally ineffective beyond a ductility indicator of 5. Figure D-4 shows the relationship between the ductility indicator and the effectiveness factor, k_3 , for poorly detailed transverse reinforcement. The effectiveness factor gives the decimal fraction of the transverse steel reinforcing that can be considered effective.

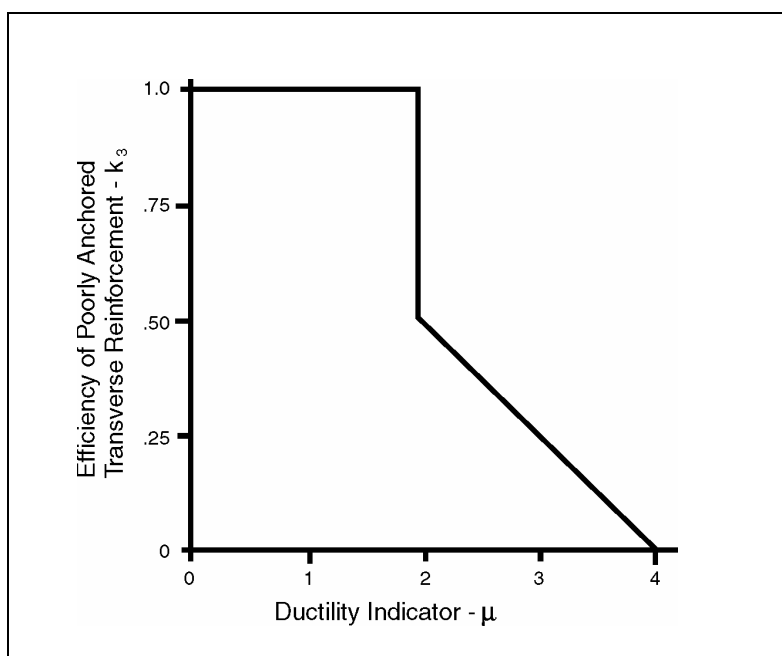


Figure D-4. Effectiveness of poorly anchored transverse reinforcement as a function of ductility indicator.

Commentary

Reinforced concrete columns or walls and the footings to which they are attached form a group of interacting components that are among the most vulnerable to earthquake damage. During high levels of ground shaking, it is likely that one of these components will be subjected to yielding. Because of the interaction between yielding in one component and the response of the remaining components, the columns, walls, and footings should be considered as a group. The weakest of these components will determine the type of failure that is likely to occur.

In quantitatively evaluating the strength of the columns and walls, four failure modes should be considered. These are: pullout of main reinforcement, splice failures in the main reinforcement, sudden shear failure, and loss of flexural capacity due to insufficient confinement. Each of these failure modes is a function of the level of column yielding that takes place in the column and depends on the amount of transverse confinement of the main longitudinal reinforcing steel. Although some useful research has been performed with respect to the behavior of bridge columns under cyclic loading, the state-of-the-art is such that column evaluation must rely heavily on engineering judgment, especially in the case of existing columns which may have vulnerable details.² The methods proposed for evaluating the C/D ratios are based on the latest research related to the behavior of reinforced-concrete columns, but still reflect considerable judgment on the part of the researchers.

Most existing bridge columns not only have an insufficient quantity of transverse reinforcing steel, but the details with regard to the placement of this steel make it less effective than new construction in resisting cyclic column loading. Evaluation of the effectiveness of this reinforcement is necessary if a reasonably accurate analysis of seismic capacity is to be made.

The effectiveness of this steel will be greatly reduced when the concrete cover in the vicinity of the plastic hinge spalls. Transverse steel in the region of spalling will then be partly exposed, which will greatly reduce anchorage. To some extent, the reduction of efficiency of lap splices in transverse reinforcement depends on the degree of spalling. It is assumed that spalling of cover concrete will commence at a ductility indicator of approximately 2 and, at this ductility indicator, the efficiency of the lap splice drops to approximately 50 percent. At higher ductility indicators, a greater amount of spalling of the cover concrete is assumed, and the efficiency of a lap splice is assumed to be reduced linearly, eventually reaching zero at a ductility indicator of approximately 4. These estimates of the efficiency of lap splices in transverse steel are based mostly on engineering judgment, although observed column behavior during past earthquakes lends support to the conclusions drawn.

When a column failure occurs due to insufficient transverse reinforcement in any of the four potential failure modes, it is likely that poorly anchored transverse reinforcement will unravel and become totally ineffective. Therefore, this reinforcement should not be considered in calculating C/D ratios for the remaining indicators above the level where the initial column failure occurred.

² Priestley and Park, 1979; Jirsa, 1979

D.5.1. ANCHORAGE OF LONGITUDINAL REINFORCEMENT

A sudden loss of flexural strength can occur if longitudinal reinforcement is not adequately anchored. The following terms are used to calculate the C/D ratio for anchorage of longitudinal reinforcement, r_{ca} :

$L_a(c)$ is the effective anchorage length of longitudinal reinforcement as shown in figure D-5, and $L_a(d)$ is the required effective anchorage length of longitudinal reinforcement.

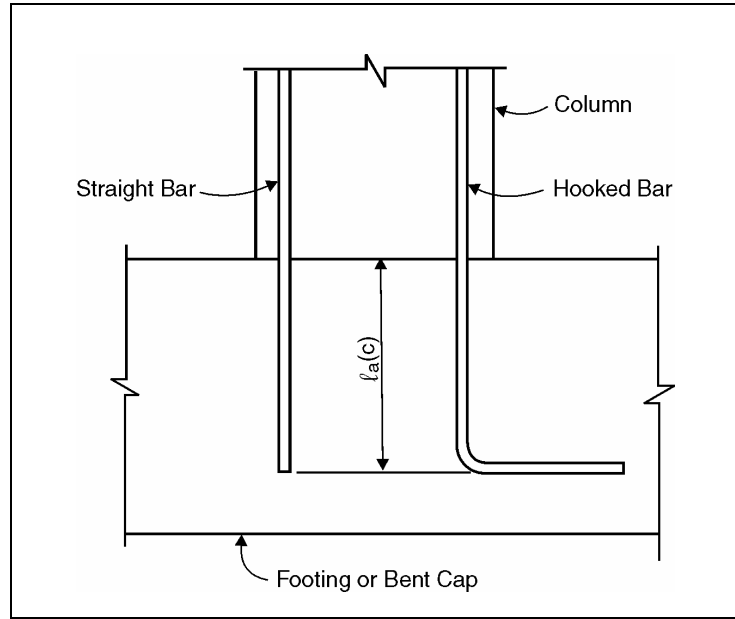


Figure D-5. Effective anchorage length of longitudinal reinforcement.

For straight anchorage, the effective anchorage length, in mm or in, is given by:

$$L_a(d) = \frac{(2.626)k_s d_b}{(1 + 2.5c/d_b + k_{tr})\sqrt{f'_c}} \geq 30 \geq d_b \quad (\text{mm, kPa}) \quad (\text{D-5a})$$

$$= \frac{k_s d_b}{(1 + 2.5c/d_b + k_{tr})\sqrt{f'_c}} \geq 30 d_b \quad (\text{in, psi}) \quad (\text{D-5b})$$

where:

k_s = constant for reinforcing steel with a yield stress of f_y (kPa or psi), i.e.,

$$\frac{(f_y - 75,845)}{33.1} \text{ kPa or } \frac{(f_y - 11,000)}{4.8} \text{ psi,}$$

d_b = nominal bar diameter (mm or in),

f'_c = concrete compression strength (kPa or psi),

c = lesser of the clear cover over the bar, or half the clear spacing between adjacent bars,

$$k_{tr} = \frac{(A_{tr}(c)f_{yt})}{(4137 sd_b)} \leq 2.5 \text{ (mm, kPa) or } \frac{(A_{tr}(c)f_{yt})}{(600 sd_b)} \leq 2.5 \text{ (in, psi),} \quad (D-6)$$

$A_{tr}(c)$ = area of transverse reinforcing normal to potential splitting cracks (when splitting will occur between several bars in a row, $A_{tr}(c)$ is the total of the transverse steel crossing the potential crack divided by the number of longitudinal bars in the row),

f_{yt} = yield stress of transverse reinforcement (kPa or psi), and

s = spacing of transverse reinforcement (mm or in).

Note that the value for c/d_b should not be taken more than 2.5.

For anchorage with 90° standard hooks, the effective anchorage length, in mm, is:

$$L_a(d) = 1200k_m d_b \left(\frac{(2.626)f_y}{60000 \sqrt{f'_c}} \right) > 15 d_b \quad (\text{mm, kPa}) \quad (D-7a)$$

$$L_a(d) = 1200k_m d_b \left(\frac{f_y}{60000 \sqrt{f'_c}} \right) > 15 d_b \quad (\text{in, psi}) \quad (D-7b)$$

where k_m is 0.7 for #11 bars or smaller, when the side cover (normal to plane of the hook) is not less than 63 mm (2.5 in), and the cover on the bar extension beyond the hook is not less than 50 mm (2 in), and 1.0 for all other cases.

The procedure for calculating the C/D ratio for the anchorage of the longitudinal reinforcement, r_{ca} , is shown in figure D-6. Methods for calculating r_{ca} will depend on the adequacy of the effective anchorage length provided and the reinforcing details at the anchorage. These methods are described in the two cases that follow.

Case A: If the effective development length provided is insufficient ($l_a(c) < l_a(d)$), then the C/D ratio for anchorage of the longitudinal reinforcement r_{ca} is given by:

$$r_{ca} = \frac{L_a(c)}{L_a(d)} r_{ec} \quad (D-8)$$

Case B: If the effective development length is sufficient ($L_a(c) \geq L_a(d)$), the C/D ratio will depend on the reinforcing details at the anchorage. The six possible details and corresponding methods for calculating the C/D ratios are as follows:

- Detail 1: When no flexural tensile reinforcement is present in the top of the footing and column bar development is by straight anchorage, i.e., no hooks are present at the bottom of the footings,

$$r_{ca} = r_{ef} \quad (D-9)$$

unless 1.25 times the soil overburden and/or pile anchorage is insufficient to overcome the negative moment capacity of the footing based on the modulus of rupture of the concrete, in which case, $r_{ca} = 1.0$. This negative moment capacity will be used to calculate r_{ef} for this and the following two detail types.

- Detail 2: when no flexural tensile reinforcement is present in the top of the footing and the column bars are anchored with 90° or greater standard hooks, turned away from the column towards the edges of the footing,

$$r_{ca} = 1.3 r_{ef} \leq 1.0 \quad (D-10)$$

- Detail 3: When no flexural tensile reinforcement is present in the top of the footing and the column bars are anchored with 90° or greater standard hooks turned toward the vertical centerline of the column,

$$r_{ca} = 2r_{ef} \leq 1.0 \quad (D-11)$$

- Detail 4: When the top of the footing contains adequately anchored flexural tensile reinforcement so that r_{ef} can be reliably computed from the flexural strength of the top reinforced footing section, and the column bar development is by straight anchorage only,

$$r_{ca} = 1.5 r_{ef} \leq 1.0 \quad (D-12)$$

unless soil overburden and/or pile anchorage is insufficient to overcome the negative moment capacity of the footing, in which case $r_{ca} = 1.0$.

- Detail 5: When the top of the footing contains adequately anchored flexural reinforcement, as for the above detail, and the column bars have been provided with 90° standard hooks, the C/D ratio for anchorage should be taken as 1.0.
- Detail 6: When the anchorage is in a bent cap, the C/D ratios for anchorage should also be taken as 1.0.

Commentary

The pullout of longitudinal reinforcement can occur at the footings or at the bent cap. This may result either due to an inadequate anchorage length or as a result of bond degradation due to flexural or shear cracking of the concrete in the footing or cap. In either case, a sudden loss of flexural capacity may result.

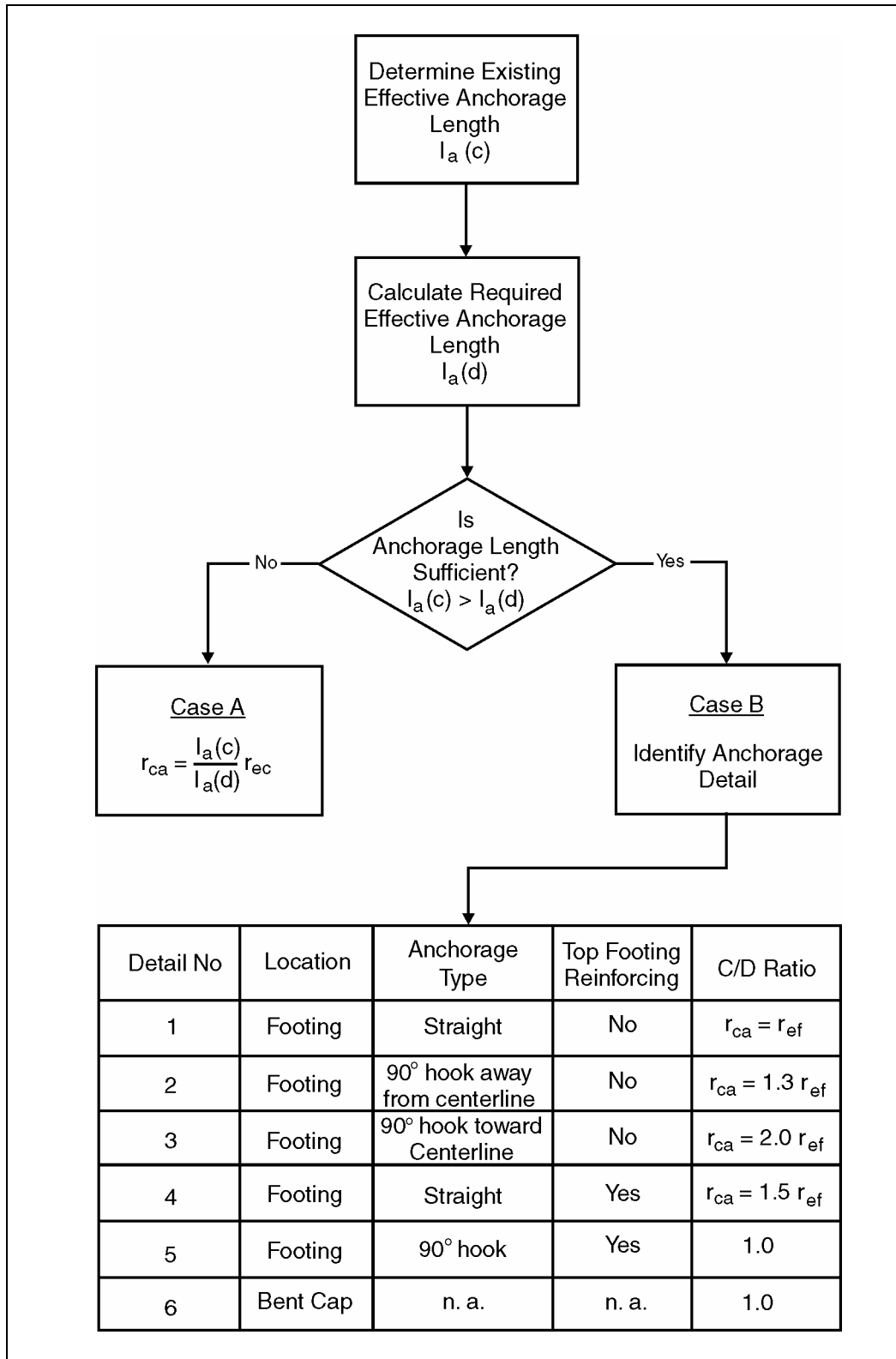


Figure D-6. Procedure for determining capacity/demand ratios for anchorage of longitudinal reinforcement.

If inadequate anchorage length is provided for the reinforcing steel, the ultimate capacity of the steel cannot be developed and failure will occur below the ultimate moment capacity of the column.

If anchorage failure results from bond degradation that accompanies the flexural cracking of footing concrete, the load level at which failure occurs will depend on the amount of yield in the footing. This is accounted for by multiplying the moment C/D ratio for the footing, r_{ef} , by a ductility indicator. Since most existing footings are not reinforced to resist flexural cracking resulting from footing uplift, failure may occur as a result of the negative moments developed in the footing due to overturning. Usually this will not be a problem in spread footings, since they are not sufficiently restrained by the soil overburden to develop high tensile stresses in the concrete. On the other hand, pile footings are usually anchored, although only nominally, to the piles. This will allow high tensile stresses to be developed due to overturning of the footing and the resulting flexural cracking of the concrete could cause anchorage failures.

The ductility indicator that is applied to the footing moment C/D ratio to evaluate anchorage failure due to flexural cracking in a footing depends on the details of the anchorage and the extent to which flexural cracking will occur. Straight anchorage in a footing without a top layer of reinforcement may fail rather suddenly when flexural cracking occurs, and therefore a ductility indicator of 1.0 is used. Failure will be delayed somewhat when anchored bars are hooked. When the hooks are bent away from the centerline of the column, the concrete in the vicinity of the hook may eventually be subjected to flexural cracking, and therefore a ductility indicator of 1.3 is specified. A greater ductility indicator is allowed when hooks project toward the centerline of the column because concrete in the vicinity of the hook will be in compression, which will tend to mitigate an anchorage failure when nonstandard hooks are present, the required anchorage length will be determined by interpolating between equation D-5 and D-7, based on the ratio of the actual length of the hook extension to the length of a standard hook extension.

When a top layer of footing flexural reinforcement is provided, flexural cracking may occur if the reinforcement is inadequate, but will progress more slowly and allow a larger ductility demand indicator to be used. When straight anchorage is provided, anchorage failure may still occur, although the ductility indicator related to this detail is specified as 1.5. If hooks are provided, the performance of the splice is assumed to be dependent on the nominal adequacy of the anchorage.

It must be stressed again that the procedures for evaluating loss of anchorage in a footing are based largely on engineering judgment.

This type of failure can also occur in pier shafts if bars are not extended below the level of fixity a sufficient distance to develop the ultimate stress in the reinforcement. Similarly, if splices occur in a pier shaft, sufficient confinement of the shaft must exist within the area of potential yielding to provide for a transfer of stresses in the reinforcing steel.

Development lengths used to evaluate columns for retrofitting were determined by research carried out at the University of Texas (Orangun et al., 1975) The failure hypothesis presented as

a result of this research assumes that the radial component of reactions on the lugs of an anchored bar will produce stresses analogous to bursting stresses on a thick-walled hollow-concrete cylinder as shown in figure D-7. The resistance to bursting is a function of the wall thickness of the hypothetical concrete cylinder taken as the lesser of the clear bar cover or half the clear bar spacing. In addition, bursting will be prevented by transverse reinforcement crossing a potential splitting crack in the hypothetical cylinder wall. In some cases, the proposed equation for development lengths will result in lengths significantly below those specified by previous design codes. In the case where the clear bar cover is much larger than half the clear bar spacing, the confining effect of this large cover may be considered by assuming the cover to be equivalent to transverse steel of equal tensile strength.

In circular columns, potential splitting cracks may occur between adjacent bars, resulting in all bars failing in anchorage as a group and pulling out of the footings as a plug. In this case, the amount of transverse steel, $A_{tc}(c)$, can be assumed to be twice the cross-sectional area of a single hoop divided by half the number of anchored bars. A similar group anchorage failure can occur with columns having cross-sections of different shapes.

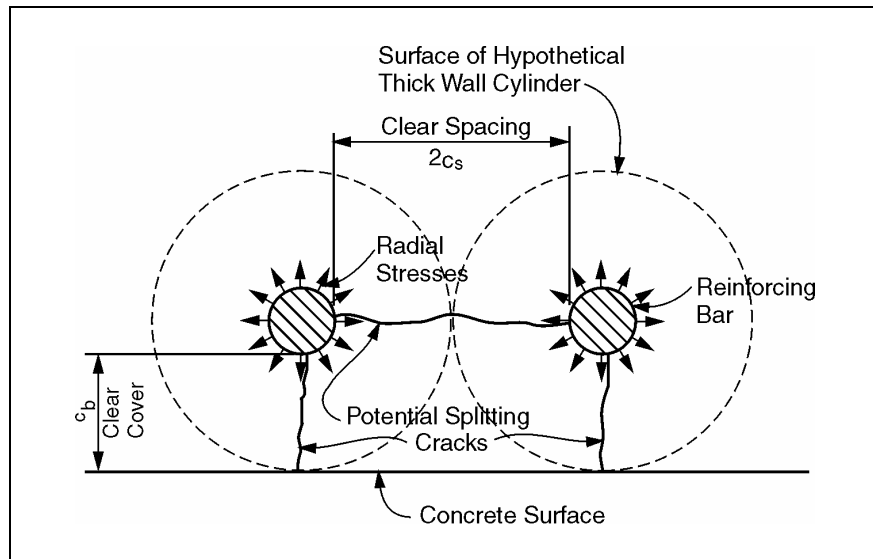


Figure D-7. Radial stresses developed due to bar anchorage.

D.5.2. SPLICES IN LONGITUDINAL REINFORCEMENT

Columns that have longitudinal reinforcement spliced near or within a zone of flexural yielding may be subject to a rapid loss of flexural strength at the splice unless sufficient closely spaced transverse reinforcement is provided. The minimum area of transverse reinforcement required to prevent a rapid splice failure due to reversed loading below the yield strength of the spliced bars is given by:

$$A_{tr}(d) = \frac{s f_y}{L_s f_{yt}} A_b \quad (D-13)$$

where s is the spacing of transverse reinforcement, L_s is the splice length, f_y is the yield stress of the longitudinal reinforcement, f_{yt} is the yield stress of the transverse reinforcement, and A_b is area of the spliced bar.

If the clear spacing between spliced bars is greater than or equal to $4d_b$, where d_b is the diameter of the spliced reinforcement, $A_{tr}(c)$ will be the cross-sectional area of the confining hoop. If the clear spacing is less than $4d_b$, then $A_{tr}(c)$ will be the area of the transverse bars crossing the potential splitting crack along a row of spliced bars divided by the number of splices. Extra splice length by itself does not significantly improve the inelastic response of splices, but splice lengths should not be less than $4885 d_b / \sqrt{f'_c}$ mm ($1860 d_b / \sqrt{f'_c}$ in).

The procedure for calculating the seismic C/D ratio for splices in longitudinal reinforcement, r , is shown in figure D-8. This C/D ratio should be determined only when splices occur within locations potentially subject to column flexural yielding unless minimum splice lengths are not provided. This includes splices located outside the center half of columns with height-to-depth ratios greater than 3 and all splices located within columns with height-to-depth ratios less than or equal to 3. The following two cases will apply to these splices.

Case A: When splice length, transverse reinforcement amount, or transverse reinforcement spacing is inadequate [$L_s < 4885 d_b / \sqrt{f'_c}$ mm ($1860 d_b / \sqrt{f'_c}$ in); $A_{tr}(c) < A_{tr}(d)$; or $s > 150$ mm (6 in)], then the C/D ratio for splices in longitudinal reinforcement, r_{cs} , is given by:

$$r_{cs} = \frac{A_{tr}(c)}{A_{tr}(d)} \left(\frac{\left(\frac{150}{s} \right) L_s}{\left(\frac{4885}{\sqrt{f'_c}} \right) d_b} \right) r_{ec} \leq \frac{A_{tr}(c)}{A_{tr}(d)} r_{ec} \text{ (mm and kPa)} \quad (D-14a)$$

$$r_{cs} = \frac{A_{tr}(c)}{A_{tr}(d)} \left(\frac{\left(\frac{6}{s} \right) L_s}{\left(\frac{1860}{\sqrt{f'_c}} \right) d_b} \right) r_{ec} \leq \frac{A_{tr}(c)}{A_{tr}(d)} r_{ec} \text{ (in and kips)} \quad (D-14b)$$

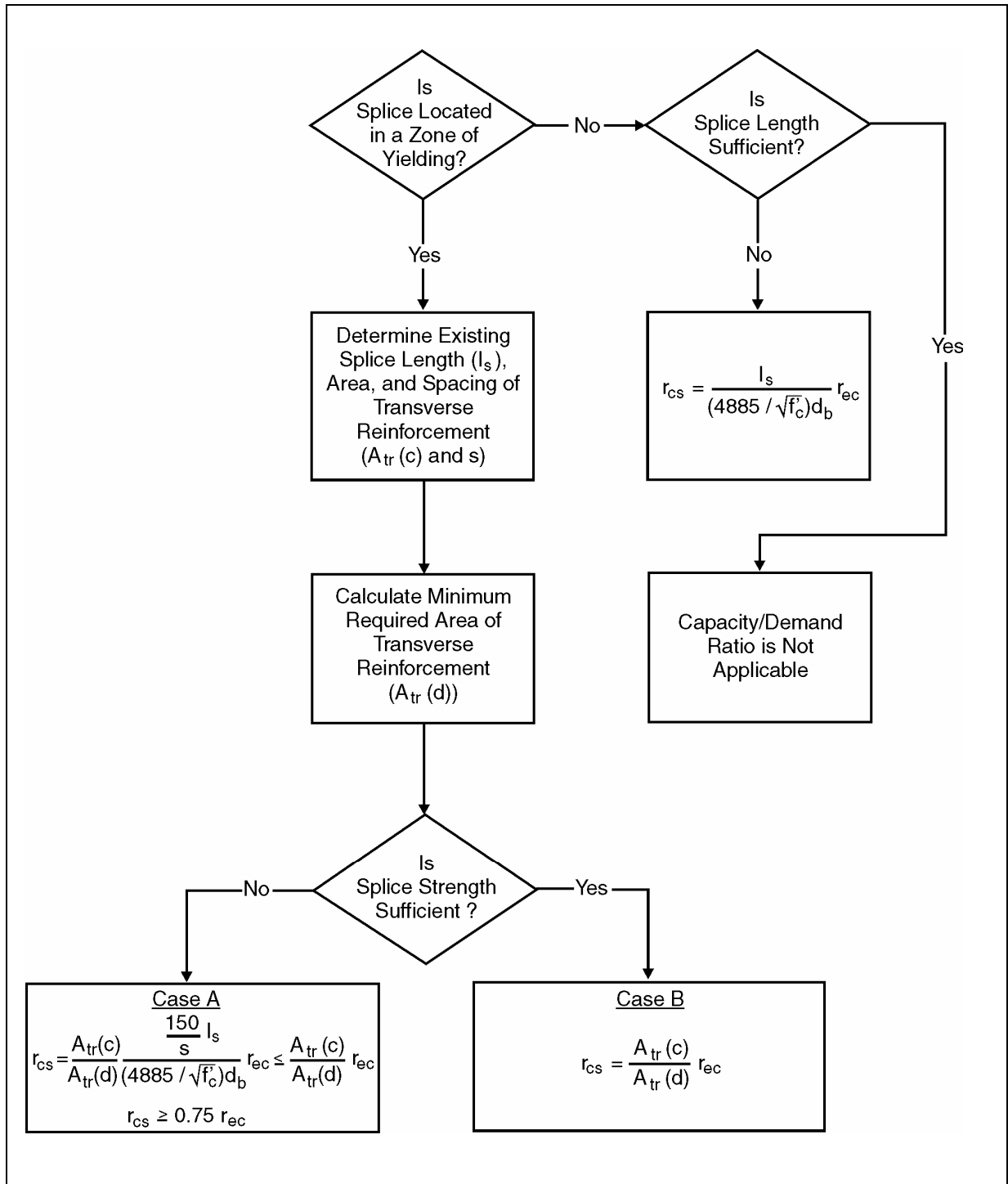


Figure D-8. Procedure for determining capacity/demand ratios for splices in longitudinal reinforcement (mm and kPa).

where the ratio $150/s$ ($6/s$) should not be taken larger than 1 and $4885/d_b/\sqrt{f'_c}$ ($1860/d_b/\sqrt{f'_c}$) should not be taken less than 30. The C/D ratio for splices, r_{cs} , need not be taken as less than $0.75r_{ec}$ when the minimum splice length is provided.

Case B: When the splice is sufficient [$L_s > 4885 d_b/\sqrt{f'_c}$ mm ($1860 d_b/\sqrt{f'_c}$) in]; $A_{tr}(c) \geq (d)$; and $s \leq 150$ mm (6 in)], then the C/D ratio for splices in longitudinal reinforcement, r_{cs} is given by:

$$r_{cs} = \frac{A_{tr}(c)}{A_{tr}(d)} r_{ec} \leq 2r_{ec} \quad (D-15)$$

Commentary

Stress is transferred between spliced bars by the longitudinal component of diagonal compressive stresses that are developed in the concrete between the bars. The transverse component of this concrete stress acts against the spliced bars and may cause a longitudinal split to form in the concrete between the bars unless sufficient reinforcement is provided across the potential splitting surface. Splitting cracks may also develop between adjacent sets of spliced bars if sufficient spacing is not provided between bars. In the absence of sufficient reinforcement, failure will be initiated by splitting at the ends of the splice. This splitting will propagate along the splice under progressive cyclic reversed loading, eventually causing the splice to "unzip." Therefore, additional splice length will not necessarily prevent failure. The key to preventing a splice failure in a bridge column is the presence of sufficient, closely spaced transverse reinforcement that will prevent the initiation of splitting. It is necessary, however, to provide a minimum splice length.

The provisions for evaluating the potential for a splice failure are based on the results of experimental research conducted at Cornell University and the University of Canterbury, New Zealand³. The research has been directed primarily at splices in building columns, which are typically subjected to stress reversals slightly below yield stress. This research was successful in identifying the amount and maximum spacing of transverse reinforcement required to prevent a splice failure under these loading conditions. In addition, minimum splice lengths were determined based on concrete strength.

For the case where splices could be expected to yield, as might be the case in the zones of maximum moment in a bridge column, testing showed that rapid degradation in the stiffness and strength of the splice would occur when transverse reinforcement equal to or less than that required for unyielding splices was provided. Further testing indicated, however, that an improvement in splice performance resulted when additional transverse reinforcement was used. If approximately twice the transverse reinforcement required for the unyielding case was used, splices were shown to be capable of withstanding reversed loading with displacement ductilities as high as six in some cases, although at these extreme ductilities, tensile fracture of the spliced bars occurred. Other tests did not result in bar fracture, but indicated strength losses at somewhat lower ductility demands. In evaluating splice performance for the yielding case a conservative

³ Sivakuman et al., 1983; Lukose et al., 1982; Paulay et al., 1981

estimate of the maximum allowable ductility is proposed in the guidelines. This is because of the small amount of testing done for the yielding case and the poor transverse reinforcing anchorage details typical of most existing bridge columns. Based on judgment, the allowable ductility was assumed to be linearly related to the amount of transverse reinforcement in excess of that required for the non-yielding case.

When spliced bars are not stressed beyond 75 percent of the yield capacity, the splice will not degrade when subjected to reversed loading. Therefore, the C/D ratio for splices should not be less than $0.75 r_{ec}$ when sufficient splice length is provided.

D.5.3. COLUMN SHEAR

Column shear failure will occur when shear demand exceeds shear capacity. This may occur prior to flexural yielding or during flexural yielding due to the degradation of shear capacity. The following terms are used to calculate the C/D ratio for column shear, r_{cv} :

- $V_u(d)$ = the maximum column shear force resulting from plastic hinging at both the top and bottom of the column (if both ends are fixed or at one end if the other end is pinned) due to yielding in the column or footing ($V_u(d) = 1.3 \Sigma M_u/L_c$), or due to an anchorage or splice failure in the column, whichever occurs first (see Note 1 below),
- $V_e(d)$ = maximum calculated elastic shear force,
- $V_i(c)$ = initial shear resistance of the undamaged column (includes the resistance of the gross concrete section and the transverse steel, see Note 2 below), and
- $V_f(c)$ = final shear resistance of the damaged column (includes the resistance of the concrete core of the column and only that transverse steel which is effectively anchored). When the axial stress is greater than or equal to $0.10 f'_c$, an allowable shear stress of $5.2 \sqrt{f'_c}$ kPa ($2 \sqrt{f'_c}$ psi) may be assumed for the core of the concrete column; otherwise use a value of zero.

Note 1: Procedures for calculating shear forces resulting from column hinging are given in Article 7.2.2 of the AASHTO Standard Specifications (AASHTO, 2002). These procedures may be extended to consider nominal moment capacities of the footings or a reduced column nominal moment capacity due to an anchorage or splice failure below the nominal ultimate column moment. The shear force associated with a pinned end should also be included. Few pin connections are frictionless, which will cause a shear demand during member rotation.

Note 2: The shear resistance of concrete columns is calculated using the provisions of Article 8.16.6 of Division I of the AASHTO Standard Specifications⁴, or Article 5.8 of the LRFD Specifications (AASHTO 1998), except that capacity reduction factors are not used, i.e., $\phi = 1.0$.

The procedure for calculating the C/D ratio for column shear is shown in figure D-9.

⁴ This reference is to Art. 8.16.6 in Division I of the AASHTO Standard Specifications for Highway Bridges, not Division I-A of the same Specifications.

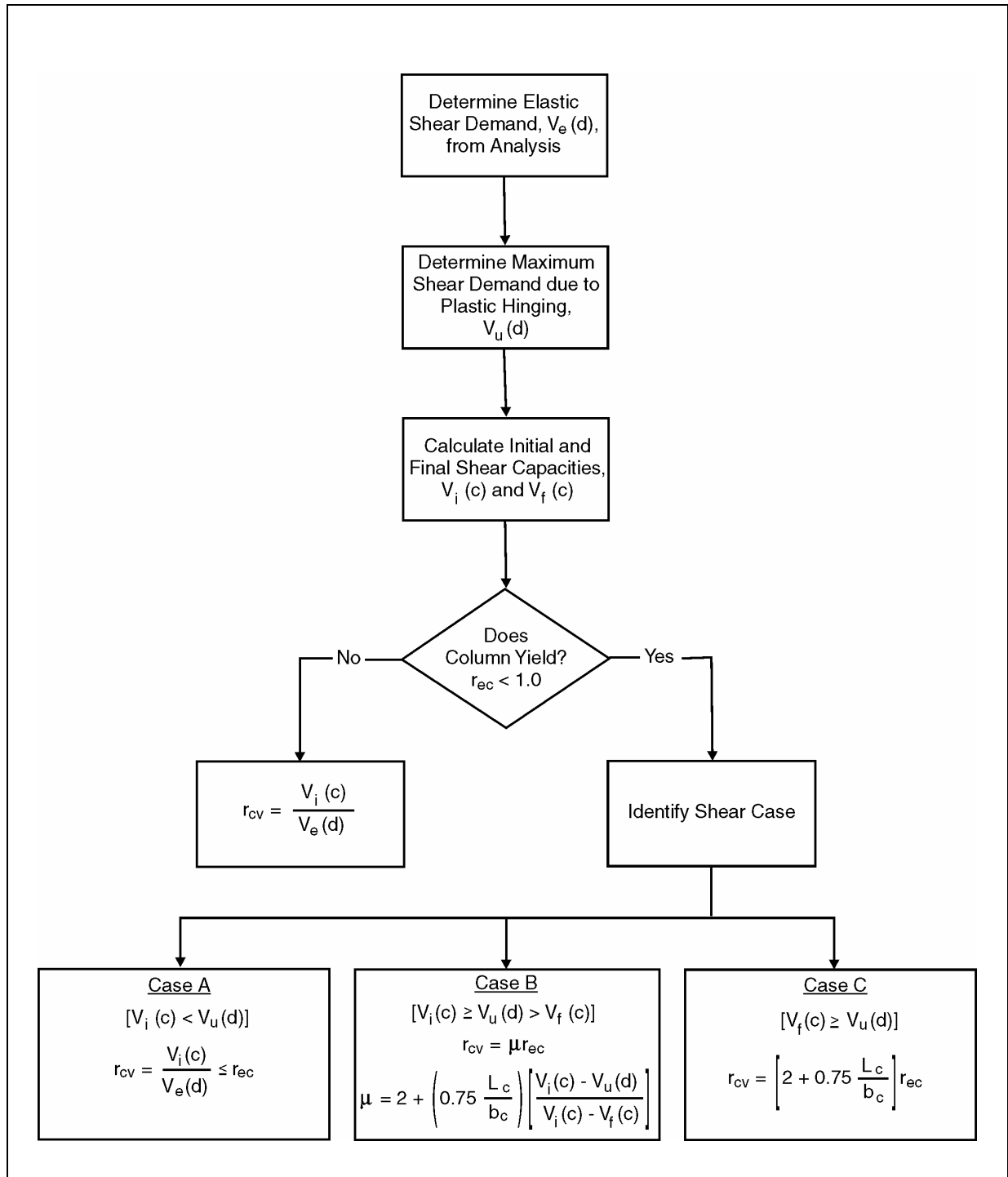


Figure D-9. Procedure for determining capacity/demand ratios for column shear.

When columns do not experience flexural yielding ($r_{ec} \geq 1.0$), the C/D ratio for column shear should be calculated using the initial shear capacity, $V_i(c)$, and the elastic shear demand, $V_e(d)$. In columns subject to yielding ($r_{ec} < 1.0$), the C/D ratio for column shear, r_{cv} is calculated according to the procedure outlined in figure D-9. Each of three possible cases are described below.

Case A: If the initial shear resistance of the undamaged column is insufficient to withstand the maximum shear force due to plastic hinging, [$V_i(c) < V_u(d)$], a brittle shear failure may occur prior to formation of a plastic hinge and the C/D ratio, r_{cv} must be calculated using elastic shear demands, i.e.,

$$r_{cv} = \frac{V_i(c)}{V_e(d)} \leq r_{ec} \quad (D-16)$$

Case B: If the initial shear resistance of the column is sufficient to withstand the maximum shear force due to plastic hinging, but the final shear resistance of the column is not, [$V_i(c) \geq V_u(d) > V_f(c)$], then the C/D ratio for column shear will depend on the amount of flexural yielding, which will cause a degradation in shear capacity from $V_i(c)$ to $V_u(d)$. The C/D ratio is given by:

$$r_{cv} = \mu r_{ec} \quad (D-17)$$

where:

$$\mu = 2 + \left(0.75 \frac{L_c}{b_c} \right) \frac{V_i(c) - V_u(d)}{V_i(c) - V_f(c)}, \quad (D-18)$$

L_c = the height of the column, and

b_c = the width of the column in the direction of shear.

The column height-to-width ratio should not be taken to be greater than 4 in equation D-18.

Case C: If the final shear resistance of the column is sufficient to withstand the maximum shear force due to plastic hinging, [$V_f(c) > V_u(d)$], then the C/D ratio for column shear is given by:

$$r_{cv} = \left(2 + 0.75 \frac{L_c}{b_c} \right) r_{ec} \quad (D-19)$$

where the terms are defined above. As with Case B, the column height-to-width ratio should not be taken to be greater than 4.

Commentary

Column shear failure is critical because it results in a comparatively sudden loss of shear strength. when this occurs, the resulting excessive deformations may cause disintegration of the column and the loss of vertical support. This happened to the Route 5 (Truck Lane) / 405

Separation (California Bridge No.53-1548) during the San Fernando earthquake. Several other bridges in the San Fernando earthquake were in various stages of this type of failure and probably would have collapsed had the intensity of the ground motion been higher or longer in duration.

The method proposed for evaluating a column for shear failure is based on engineering judgment and assumes an idealized model of column behavior. This method may be visualized by examining the assumed relationship between shear capacity and shear demand as shown in figure D-10. Three possible cases are considered in evaluating C/D ratios for column shear. Case A occurs when the column cannot achieve flexural yielding because of a low initial shear capacity. In this case, column C/D ratios for shear are calculated by dividing the initial shear capacity of the column by the elastic shear demand. This is possible because the initial shear strength of the column is not expected to degrade in the absence of plastic hinging, although a brittle shear failure can be expected when the initial shear capacity is exceeded. Case B will result when a shear failure is expected to occur due to shear capacity degradation resulting from plastic hinging of the column. In this case, column C/D ratios for shear are calculated by multiplying the column moment C/D ratio, r_{ec} , by the ductility indicator corresponding to the amount of yielding at which the column shear demand is assumed to exceed the column shear capacity. Case C is assumed when the degradation in column shear capacity is not expected to result in a shear failure. In this case, the column C/D ratio for shear will be calculated by multiplying the column moment C/D ratio by the ductility indicator corresponding to an assumed maximum allowable level of flexural yielding.

The assumed relationship between shear demand and shear capacity in reinforced concrete columns is used to identify which of the three cases applies and to determine the ductility indicator for Case B. Both demand and capacity are assumed to be dependent on the level of flexural yielding as measured by the ductility indicator.

The relationship between column shear demand and the ductility indicator is based on the observation that column behavior will be linear-elastic at a ductility indicator of 1.0 or less. At a ductility indicator above 1.0, the shear demand is assumed to be constant and may be determined from statics assuming that, where possible, plastic hinges have formed in the column end regions. The moments developed in the plastic hinges are assumed to be the maximum ultimate column moments adjusted for the possibility of overstrength. Actual shear demands at a ductility indicator above 1.0 will vary due to variation in the column axial load, strain hardening of the column flexural reinforcement, degradation of column ultimate moment capacity, failure of the column to form plastic hinges at both ends simultaneously, and other factors. The proposed model of shear demand was selected because it provides a simple yet conservative method for relating shear demand to flexural yielding.

The assumed relationship between shear capacity and flexural yielding, as measured by a ductility indicator, is based on observations of column shear behavior during experimental investigations and past earthquakes. These observations have established a qualitative relationship between shear capacity and flexural yielding, but the quantification of this relationship, as proposed in the guidelines, is based largely on the judgment of specialists in reinforced concrete column behavior.

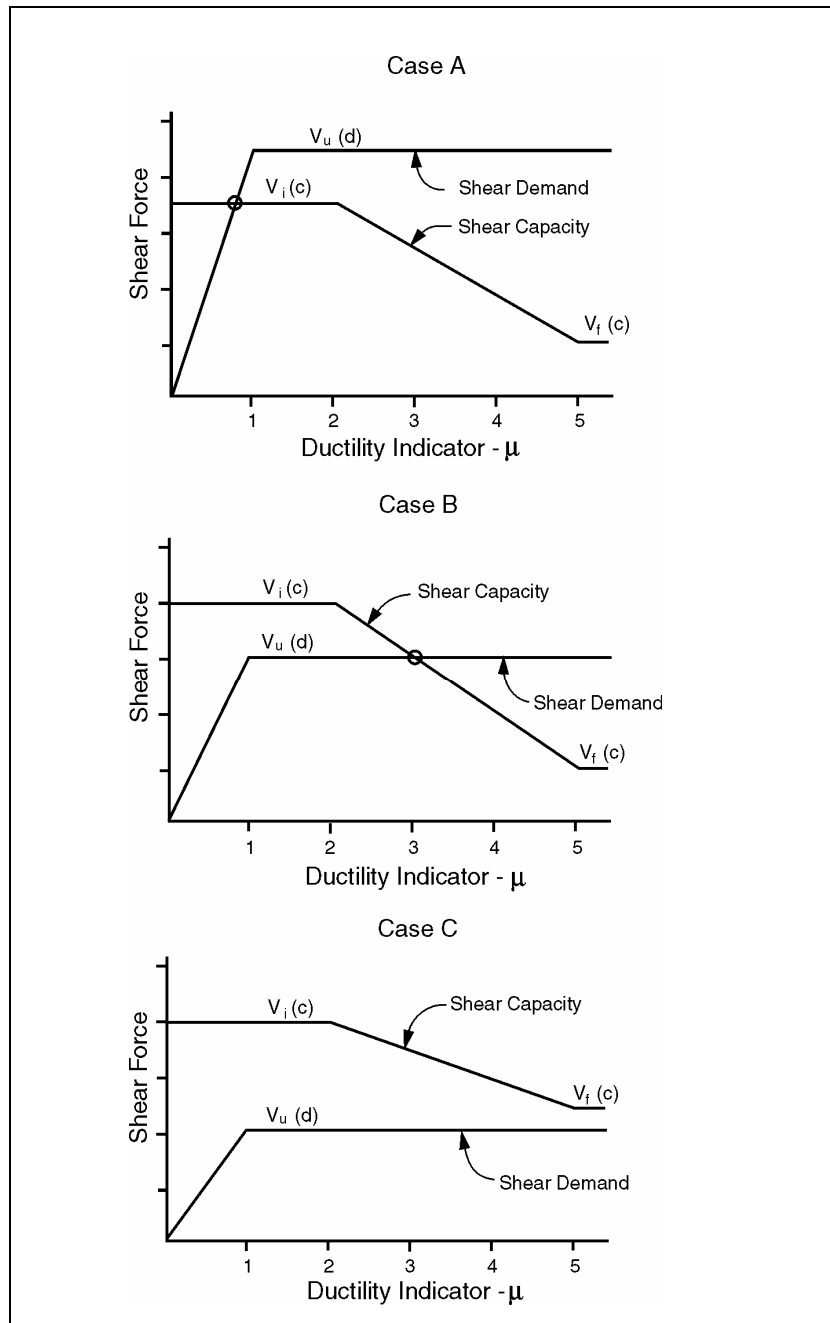


Figure D-10. Resolution of shear demand and shear capacity.

Writers of design codes have found it convenient to subdivide the shear capacity of reinforced concrete columns into two parts. The first part is the resistance provided by shear reinforcement, such as hoops or spirals. The assumed resistance provided by the reinforcement has been derived from a logical model of shear behavior that is based on a truss analogy.

The shear resistance of the concrete portion of the column is assumed to provide the second part of the total column shear capacity. However, attributing all shear resistance other than that provided by shear reinforcement to the concrete portion of the column is an oversimplification of what actually occurs. This shear resistance in reality is composed of shear resistance of concrete within the zone of flexural compression stress, dowel action of the flexural reinforcement, and aggregate interlock along diagonal cracks. In present design codes, these mechanisms of shear resistance are usually lumped into a single empirically derived effective shear stress that conservatively approximates the actual shear capacity not provided by shear reinforcement. This simplified approach is usually adequate when designing for static loads, since the mechanisms of shear resistance will remain intact at these load levels. Such an approach is probably also adequate for low levels of seismic loading that will not result in excessive flexural yielding of the columns.

The sum of the shear resistance provided by shear reinforcement and the concrete portion of the column is termed the initial shear capacity in this manual. It is assumed that the initial shear capacity will not be significantly affected prior to the commencement of spalling of the cover concrete and, therefore, column shear capacity is assumed constant at a ductility indicator of 2 or less.

With reversed cyclic loading beyond the elastic limit, many of the mechanisms of shear resistance will begin to break down. This breakdown in shear resistance, which is assumed to commence at a ductility indicator of 2, is more rapid in columns with a low height-to-width ratio because shear demands are typically higher than in more slender columns. For this reason, this manual considers height-to-width ratios when evaluating columns for a Case B or Case C shear failure.

Shear reinforcement will not be seriously affected by moderate flexural yielding provided it is adequately anchored into the core of the column. However, many existing columns were built prior to 1973, when transverse reinforcement anchorage requirements were first included in the *AASHTO Specifications*. Reinforcement that is not adequately anchored into the core of the column will be subject to a rapid loss of effectiveness when cover concrete spalls.

Reversed cyclic flexural yielding will usually have a detrimental effect on the shear resistance of the column that is not provided by shear reinforcement. Flexural and diagonal cracks may open under loading in one direction and never close on subsequent stress reversals. The mechanism of aggregate interlock will be affected as small transverse movements occur along these crack interfaces. The shear resistance due to the doweling action of flexural reinforcement will also be reduced as the concrete cover spalls and transverse confinement either fails or yields.

Some experimental research has shown that this degradation of the concrete shear resistance seems to be mitigated by increased column axial loads. Although the relationship between axial load and concrete shear resistance under reversed cyclic loading has not been precisely quantified, many researchers have suggested that the concrete shear resistance be ignored in columns with an average axial stress below $0.10 \sqrt{f'_c}$, and considered totally effective for columns with greater average stresses. While this is a rather crude treatment of axial load effects,

it has been used in other seismic design provisions and is therefore adopted in this manual until a more precise relationship can be derived.

For purposes of simplicity, it is assumed that a linear degradation of shear capacity will occur between a ductility indicator of 2 and a ductility indicator based on the maximum allowed level of flexural yielding. At the maximum level of yielding, the column shear capacity, termed the "final shear capacity" in this manual, will be assumed to consist of the shear resistance provided by adequately anchored shear reinforcement and the effective concrete shear resistance based on the magnitude of the axial loads. This method seems appropriate until research establishes a more precise relationship between shear capacity degradation and flexural yielding.

D.5.4. TRANSVERSE CONFINEMENT REINFORCEMENT

Inadequate transverse confinement reinforcement in the plastic hinge region of a column will cause a rapid loss of flexural capacity due to buckling of the main reinforcement and crushing of the concrete in compression. The following equation may be used to calculate the C/D ratio for transverse confinement, r_{cc} :

$$r_{cc} = \mu r_{ec} \quad (D-20)$$

where:

$$\mu = 2 + 4 \left(\frac{k_1 + k_2}{2} \right) k_3, \quad (D-21)$$

$$K_1 = \frac{\rho(c)}{\rho(d) \left(0.5 + \frac{1.25 P_c}{f'_c A_g} \right)} \leq 1, \quad (D-22)$$

$k_2 = 6d_b/s \leq 1$ or $0.2 b_{min}/s \leq 1$, whichever is smaller,

$k_3 =$ effectiveness of transverse bar anchorage. This will be 1.0 unless transverse bars are poorly anchored, in which case figure D-4 shall be used to determine k_3 . Note that when this is the case, an iterative solution of equation D-21 will be required,

$\rho(c) =$ volumetric ratio of existing transverse reinforcement,

$\rho(d) =$ required volumetric ratio of transverse reinforcement determined in accordance with the provisions of Article 7.6 of the AASHTO Standard Specifications (AASHTO, 2002), or Article 5.10.11 of the AASHTO LRFD Specifications (AASHTO 1998),

$P_c =$ axial compressive load on the column,

$f'_c =$ compressive strength of the concrete,

$A_g =$ gross area of column,

$s =$ spacing of transverse steel,

$d_b =$ diameter of longitudinal reinforcement, and

$b_{min} =$ minimum width of the column cross-section.

Commentary

Transverse confinement reinforcement is required to prevent strength degradation in a column subjected to reversed cycles of flexural yielding. Degradation is prevented because confinement increases the capability of the concrete core to develop significant stress at high compressive strains and prevents buckling of longitudinal compressive reinforcement by providing lateral restraint for the reinforcing bars. The degree to which degradation will be prevented is dependent on the amount and spacing of transverse reinforcing and the adequacy of the anchorage of this reinforcing.

Current requirements for transverse confinement used in the *AASHTO Specifications* were developed by calculating the amount of reinforcement required to prevent a loss of axial strength in a reinforced concrete column due to the loss of cover concrete. Although this approach is simple and will result in column designs that can withstand high ductility demands, it is based on an inappropriate criteria for column performance and is of limited use for evaluating existing columns.

A more rational approach to calculating the effect of confinement was initially suggested by Priestley and Park (1979). This approach uses the calculated moment curvature relationships of a concrete column based on the assumed stress strain behavior of reinforcing steel and concrete at various levels of confinement. The available curvature ductility of a column would be assumed at a curvature that corresponds to a predetermined reduction (e.g. 80 percent) in the column moment capacity. This approach was subsequently used to develop the transverse confinement requirements for the New Zealand Concrete Design Code: NZS 3101 (Standards Association of New Zealand, 1982). The confinement provisions of NZS 3101 are based on the confinement requirements used in the *AASHTO Specifications* modified to account for the effect of axial load level. For low axial loads, NZS 3101 results in as much as a 50 percent savings over the amount of confinement reinforcing required by the *AASHTO Specifications*. The New Zealand code requires that maximum spacing of transverse steel for adequate concrete confinement be 20 percent of the minimum cross-section dimension or 6 times the longitudinal bar diameter, whichever is less. Testing of near full-scale columns demonstrated the validity of the New Zealand transverse confinement requirements (Park et al., 1980).

Despite the work mentioned in the previous paragraphs, the evaluation of transverse confinement in existing columns must be tempered with judgment based on experience gained from past earthquakes. It is assumed that spalling of cover concrete commences at a ductility indicator of 2 and that even poorly confined columns can withstand yielding up to this level because the cover concrete provides some confinement. Columns with transverse reinforcement complying with the New Zealand code are assumed to be capable of withstanding cyclic yielding corresponding to a ductility indicator of 6. Most existing columns have deficiencies in transverse reinforcement and are assumed to be able to withstand a limited level of yielding corresponding to a ductility indicator between 2 and 6. The equation developed to determine the appropriate ductility indicator uses three factors for assessing the relative effectiveness of transverse reinforcement. These factors are intended to account for reduction in the efficiency of confinement due to deficiencies in the amount, spacing, and anchorage of reinforcement. Factors for amount and spacing are averaged because they affect the efficiency of confinement in parallel but separate

ways. A product of these factors would yield results that are too conservative. Deficiencies in anchorage, however, will effect the overall efficiency of transverse reinforcement and therefore the factor for anchorage is multiplied by the average of the first two factors to obtain the overall confinement efficiency. Although this approach is based largely on engineering judgment, it will allow for a reasonably accurate evaluation of the C/D ratio for transverse confinement.

D.5.5. FOOTING ROTATION AND/OR YIELDING

Column footings may rotate and/or yield before columns can yield. This can occur due to any one of several failure modes. The amount of rotation and/or yielding allowed in the footing will depend on the mode of failure. The seismic C/D ratio for these types of footing failures, r_{fr} , are calculated as follows:

$$r_{fr} = \mu r_{ef} \quad (D-23)$$

where μ the ductility indicator, is taken from table D-1 and depends on the type of footing and mode of failure. See the commentary below for a discussion on the method for calculating the nominal ultimate capacity of the footing.

Table D-1. Footing ductility indicators.

Type of Footing	Factor Limiting the Capacity	μ
Spread Footing	Soil Bearing Failure	4
	Reinforcing Steel Yielding in the Footing	4
	Concrete shear or Tension in the Footing	1
Pile Footing	Pile overload (Compression or Tension)	3
	Reinforcing Steel Yielding in the Footing	4
	Pile Pullout at Footing	2
	Concrete Shear or Tension in the Footing	1
	Flexural Failure of Piling	4
	Shear Failure of Piling	1

Commentary

Footing failures may be classified in one of two ways. The first type of failure involves large displacements of the foundation material resulting from instabilities generated within the soil by the earthquake ground motion. Liquefaction or slope instability would fall into this category. More discussion of these types of failures is included in section D.7.

The second type of failure, which will be discussed in this section, involves the yielding or rupture of foundation elements due to excessive seismic forces transmitted from the structure itself. This would include steel and/or concrete failure, bearing failure of the soil, footing failure due to sliding or overturning, and pile failure. These failures may result in ductile behavior or in sudden brittle failure.

Ductile yielding in the footing is avoided in the design of new bridges because of the difficulties involved in inspecting and repairing foundations. Such yielding results in structural damage, but will not usually result in structure collapse unless yielding is particularly extensive. Therefore, in the case of existing structures, the prospects of yielding in the footings is generally not sufficient grounds to justify seismic retrofitting. In fact, from the standpoint of preventing collapse, footing yielding may have a beneficial effect, since it can limit shear and flexure in the columns and thus decrease the chances of a brittle column failure.

A sudden brittle failure of the footing, on the other hand, could have serious consequences in terms of the ability of the structure to remain standing. The chances of total collapse will depend on the configuration of the structure and the nature of the footing failure. For example, the sudden loss of flexural capacity in the footings supporting a multi-column bent would probably not result in a structure collapse, since the bent would remain stable. However, similar failure in a structure with single-column bents would be much more serious. Structure collapse due to a sliding failure of the footing is difficult to imagine unless the movement is extensive and the structure is discontinuous and supported on narrow bearing seats. In summary, therefore, structures with single-column bents are most threatened by a footing failure.

In evaluating a structure, it is important to determine the capacity of the footings even if footing failure will not result in the collapse of the bridge. Footing failure modes will depend, to a certain extent, on the type of footing that is being examined. The following sections contain recommended procedures for determining the capacities of the two major types of footings used in bridge construction: spread and pile footings.

Spread Footings. The capacity of the footing to resist the loads transmitted from the column or pier should be determined. There is an interaction between vertical load and moment capacity, which may be governed by the following types of footing failures, as shown in figure D-11:

- Tilting of the footing due to a soil bearing failure.
- Flexural yielding of footing reinforcing.
- Concrete shear failure of the footing.
- Bond failure of the main column steel.

The last two failure modes could have serious consequences that, in some cases, could potentially result in a structure collapse. Bond failure will be the most critical and should be evaluated based on the strength of the anchorage of the column main reinforcement in the footing, as discussed in section D.5.1. Insufficient anchorage indicates that the yield capacity of the reinforcing cannot be developed and that failure will occur before the column reaches its ultimate capacity. A reduction in the effectiveness of the anchorage due to flexural cracking of the footing is usually not a problem for unanchored spread footings because the tensile strength of the concrete is usually sufficient to prevent cracking.

A concrete shear failure in the footing could be serious because it could result in a fairly sudden loss of overturning resistance. In determining the possibility of a shear failure, the shear capacity at the critical section determined according to the *AASHTO Specifications* should be sufficient to resist a uniform pressure equal to 1.3 times the ultimate soil bearing capacity.

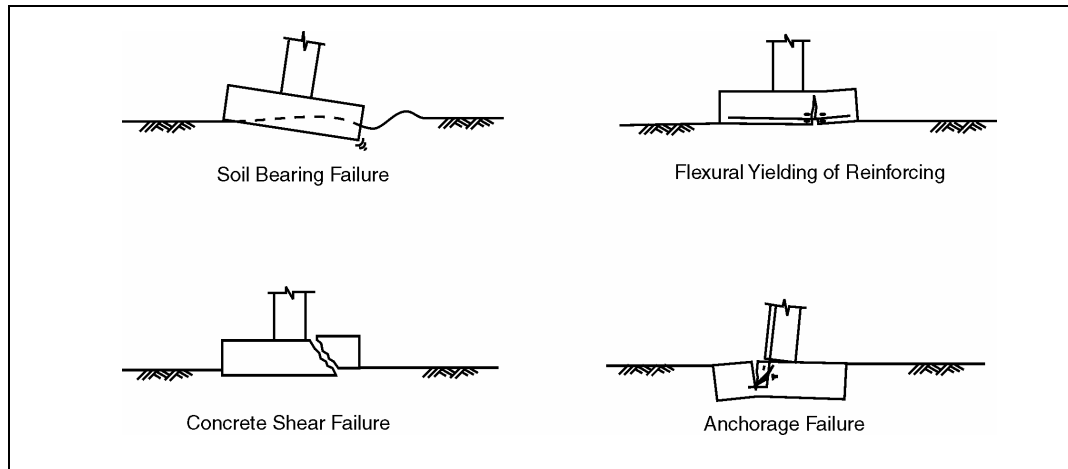


Figure D-11. Modes of failure for spread footings.

Flexural yielding of the footing is also possible, but will not result in a rapid loss of overturning resistance as is the case with shear failure. Flexural capacity should be checked at the critical section according to the *AASHTO Specifications*. This capacity should be sufficient to resist uniform footing pressures of 1.3 times the ultimate soil bearing capacity. Flexural yielding of the footing will cause the column shear force to be limited in order to satisfy static equilibrium.

If neither shear nor flexural failure will occur in the footing, then the footing capacity will be governed by a soil bearing failure. The interaction between axial force and moments at the yield capacity of the footing may be calculated by assuming various areas of the footing to be loaded with a uniform pressure equal to the ultimate soil pressure. This will produce an interaction surface that will indicate the possibility of bearing failure only at the locations where this surface falls within the column interaction surface factored for overstrength. Ultimate soil bearing pressures can generally be taken at three times the design allowable value. The actual ultimate capacity should be provided by the geotechnical engineer.

This mode of "failure" is considered acceptable by Caltrans because it generally does not lead to structure collapse. Retrofitting would only be considered if the structure was required to perform to a higher level, i.e., to meet certain functionality criteria immediately following an earthquake.

Pile Footings. Possible failure modes for pile footings are shown in figure D-12 and may be classified as follows:

- Tilting of the footing due to uplift or compression failures in the piling.
- Pullout of a pile from the footing.

- Flexural yielding of footing reinforcing.
- Concrete shear failure of the footing.
- Bond failure of the main column steel.
- Flexural or shear failure of the piling.

Unlike spread footings, the tensile stress in the concrete of footings unreinforced for uplift may be insufficient to prevent flexural cracking of the footing and a subsequent loss of column-steel anchorage. This type of failure is accounted for in section D.5.1.

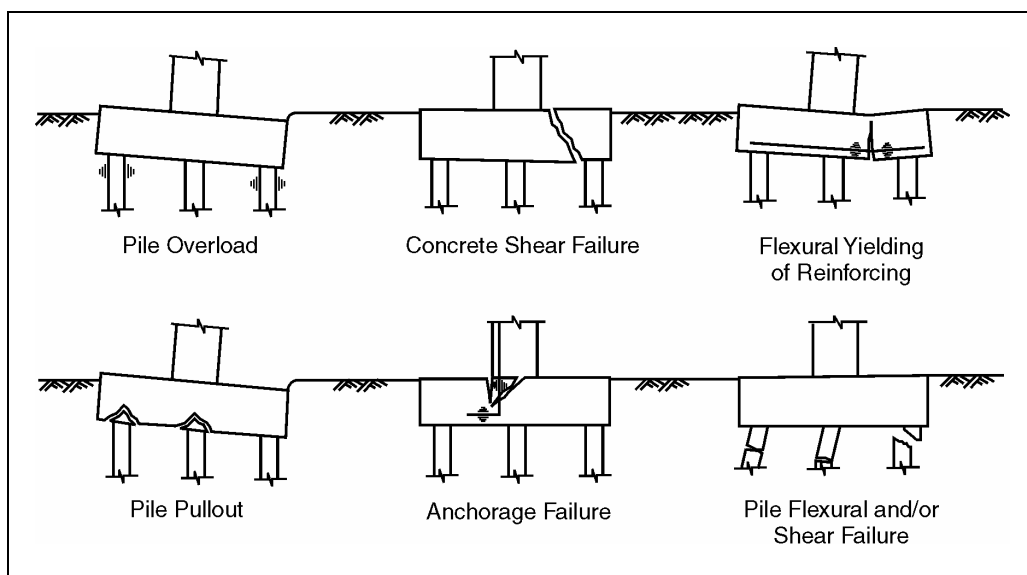


Figure D-12. Modes of failure for pile footings.

A concrete shear failure in the footing could be serious because it could result in a fairly sudden loss of overturning resistance. In determining the possibility of a shear failure, the shear capacity at the critical section determined according to the *AASHTO Specifications* should be sufficient to resist the shear produced by 1.3 times the ultimate capacity of the piles.

A flexural failure of the footing is also possible, but will not result in a rapid loss of overturning resistance as is the case with shear failure. Flexural capacity should be checked at the critical section according to the *AASHTO Specifications*. This capacity should be sufficient to resist the moment produced by the piles acting at 1.3 times their ultimate capacity. Flexural yielding of the footing will cause the column shear force to be limited in order to satisfy static equilibrium.

If neither shear nor flexural failure will occur in the footing, then the footing capacity will be governed by pile failure. The interaction surface for axial force and moments at the yield capacity of the footing may be produced by assuming the ultimate compression or uplift in various combinations of piles. Pile uplift may be limited by pullout of the pile from the footing

or by the pile withdrawal force. In the case where piles will pull out of the footing, a lower ductility indicator is proposed because of the more brittle nature of this type of failure. Ultimate pile compression capacity for friction piles can generally be taken at four times the design allowable capacity. The actual capacity should be provided by the geotechnical engineers.

This mode of 'failure' is considered acceptable by Caltrans because it generally does not lead to structure collapse. Retrofitting would only be considered if the structure was required to perform to a higher level, i.e., to meet certain functionality criteria immediately following an earthquake.

Geotechnical specialists should be consulted for the ultimate capacity of the soils, especially with respect to the uplift capacity. At poor soil sites, the potential degradation of soil strength should be evaluated. The soil capacities can then be compared with the capacities of the connection details and the pile members based on the pile type and the expected failure mode, i.e., pile overload or pile pullout at the footings.

D.6. CAPACITY/DEMAND RATIOS FOR ABUTMENTS

Failure of abutments during earthquakes usually involves tilting or shifting of the abutment, either due to inertia forces transmitted from the bridge superstructure or to seismically induced earth pressures. Usually these types of failures alone do not result in collapse or impairment of the ability of the structure to carry emergency traffic loadings. However, these failures often result in loss of access, which can be critical in certain important structures.

Large horizontal movement at the abutments is often the cause of large approach fill settlements that can prevent access to the bridge. Therefore, when required, abutment C/D ratios are based on the horizontal abutment displacement. The displacement demand, $D(d)$, will be the elastic displacements at the abutments obtained by properly modelling the abutment stiffness. The displacement capacity, $D(c)$, is taken as 75 mm (3 in) in the transverse direction and 150 mm (6 in) in the longitudinal direction, unless determined otherwise by a more detailed evaluation. Therefore:

$$r_{ad} = \frac{D(c)}{D(d)} \quad (D-24)$$

Commentary

Abutment displacement capacities are limited to those that are likely to cause problems with accessibility to the bridge. Based on experience from past earthquakes, displacement capacities of 75 mm (3 in) in the transverse direction and 150 mm (6 in) in the longitudinal direction were chosen. These values are based largely on engineering judgment and are likely to be modified as more experience is gained.

D.7. CAPACITY/DEMAND RATIOS FOR LIQUEFACTION INDUCED FOUNDATION FAILURE

Many foundation failures that occur during earthquakes are the result of loss of foundation support due to liquefaction. A C/D ratio should be calculated when the preliminary screening indicates the potential exists for major or severe liquefaction-related foundation damage. To determine the C/d ratio for liquefaction failure, r_{sl} a two-stage procedure is necessary. First, the depth and areal extent of soil liquefaction required for foundation failure and associated damage must be assessed. Second, the level of seismic shaking that will produce liquefaction of the above foundation soils must be evaluated. The C/D ratio is obtained by dividing the effective peak ground acceleration at which liquefaction failure is likely to occur by the design acceleration coefficient:

$$r_{sl} = \frac{A_L(c)}{A_L(d)} \quad (D-25)$$

where $A_L(c)$ is the effective peak ground acceleration at which liquefaction failures are likely to occur, $A_L(d)$ is the effective acceleration coefficient for the site equal to $0.4 S_s/g$, and S_s is the 'short-period' spectral acceleration defined in section 1.5.1.

Although a great deal of work has been done with respect to determining earthquake-induced liquefaction potential of soils, the parameter $A_L(c)$ is difficult to determine precisely. Selection of a realistic value for $A_L(c)$ will require considerable engineering judgment. For example, whereas a sand seam may liquefy, its influence on a pile foundation may be minimal. Significant lateral foundation displacement leading to damage may require a 3 m (10 ft) depth of liquefied soil to occur near the pile head followed by continued ground shaking.

The amount of movement at a given site due to soil liquefaction is a function of the intensity and duration of shaking, the extent of liquefaction, and also the relative density of the soil, which controls post-liquefaction undrained or residual strength. In addition, different bridges will be able to sustain different amounts of movement. Therefore, when determining $A_L(c)$, both the site and the bridge characteristics must be taken into consideration.

The references to bridge-related liquefaction failures noted in the commentary may be of assistance in evaluating this problem, as well as references related to assessing liquefaction potential of soils. Finally, it is recommended that geotechnical specialists participate in the determination of $A_L(c)$ at a specific bridge site and assist in the evaluation of the subsequent foundation displacement and damage potential.

Commentary

Bridge failures resulting from seismic activity have often been classified as failures resulting from permanent displacement of the foundations or from structural failures arising from dynamic loading. The majority of severe seismic bridge failures have resulted from liquefaction-induced permanent displacement of the foundation systems. Despite this fact, the emphasis in both

research and design has been on preventing structural failures. This perhaps reflects the problem that foundation failures are difficult to treat quantitatively, whereas structural response is more amenable to analysis and generally represents a preventable type of failure.

Designers have generally approached the problem of liquefaction by attempting to select bridge sites at which such failures are unlikely. In many cases, however, the use of such sites is unavoidable. In the case of existing bridges, vulnerable sites may have been used without a full understanding of the consequences. Designers faced with improving the earthquake resistance of such bridges should take advantage of knowledge gained from the performance of bridges in past earthquakes to identify collapse mechanisms and evaluation procedures.

A qualitative description of mechanisms of foundation failure or displacement arising from liquefaction is provided in chapter 3 and appendix B. Bridge failures in recent Alaskan and Japanese earthquakes are probably the best documented examples⁵. In many other earthquakes where bridge damage has been reported as a result of liquefaction, modes of foundation failure have been similar to the Japanese and Alaskan earthquake case histories. Multispan bridges with unrestrained simply supported spans have usually suffered the most damage.

Foundation conditions which are susceptible to liquefaction are common to bridges that cross waterways where foundation soils have been deposited over the years by flowing water. These soils are often loose, saturated cohesionless deposits, and are most susceptible to liquefaction. It is noteworthy that liquefaction is a combination of earthquake intensity and duration. In the 1964 Alaskan earthquake, it is estimated that maximum ground accelerations as low as 0.1g to 0.2g were responsible for the extensive and widespread bridge foundation failures (Ross et al., 1973). The duration of strong shaking was rather long, however, lasting more than 90 seconds. Therefore, bridge sites located some distance from a major fault could still be subjected to liquefaction failure if the necessary soil conditions are present.

Methods for assessing the liquefaction potential of site soils are provided in Appendix B. Two basic approaches are typically used, namely empirical methods based on blowcount correlations for sites that have not liquefied, and analytical techniques based on the laboratory determination of liquefaction strengths and dynamic site-response analyses. A rough indication of the potential for liquefaction may be obtained by making use of empirical correlations between earthquake magnitude and epicenter distance, as described in chapter 3.

D.8. SUMMARY

This appendix presented a methodology for determining the capacity/demand ratios for displacements and forces for a number of bridge components, including expansion joints and bearings, reinforced concrete columns and walls, and foundations. A summary of these C/D ratios is given in table D-2, where they listed according to member or component.

⁵ Ross et al., 1973; Iwasaki et al., 1972

Table D-2. List of capacity/demand ratios.

Notation	Definition	Equation	Page
SUPPORT LENGTH and RESTRAINER C/D RATIOS			
r_{ad}	Displacement C/D ratio for abutment	D-24	
r_{bd}	Displacement C/D ratio for bearing seat or expansion joint	D-2, D-3	
r_{bf}	Force C/D ratio for bearing or expansion joint restrainer	D-4	
COLUMN C/D RATIOS			
r_{ca}	Anchorage length C/D ratio for column longitudinal reinforcement	D-8 through D-12	
r_{cc}	Confinement C/D ratio for column transverse reinforcement	D-20	
r_{cs}	Splice length C/D ratio for column longitudinal reinforcement	D-14, D-15	
r_{cv}	Shear force C/D ratio for column	D-16 through D-19	
r_{ec}	Bending moment C/D ratio for column	(Section D.5, Steps 1-4)	
FOOTING C/D RATIOS			
r_{ef}	Bending moment C/D ratio for footing	(Section D.5, Steps 1-4)	
r_{fr}	Rotation C/D ratio for footing	D-23	
SOIL C/D RATIO			
r_{sl}	Acceleration C/D ratio for liquefaction potential	D-25	

APPENDIX E: EXAMPLE PROBLEM 5.1: COMPONENT CAPACITY/DEMAND EVALUATION OF A 4-SPAN, REINFORCED CONCRETE BOX GIRDER BRIDGE

E.1. INTRODUCTION

This example problem illustrates how some of the recommendations of this Manual are applied to a reinforced concrete box girder bridge. In particular, the Seismic Rating of the bridge is calculated using the indices method for the Vulnerability Rating, as described in section 4.2. In addition, a detailed evaluation of the bridge is performed using the Component Capacity/Demand Method described in section 5.4 (Method C). This evaluation is then used to identify and evaluate potential seismic retrofitting measures.

E.2. DESCRIPTION OF THE EXAMPLE BRIDGE

The bridge to be examined is a typical freeway overcrossing of the type that was being constructed in California prior to improved seismic design provisions. It carries a major city street over an urban freeway in the region and is classified as ‘essential’. It has an anticipated service life of 55 years (ASL 3, table 1-1). Soils are Site Class C (table 1-3). The short and long-period spectral accelerations for the site are 1.00 and 0.40 respectively for the upper level event. The Seismic Retrofit Category (SRC) is D (section 1.6).

The superstructure is a concrete box girder. One portion of this bridge is prestressed and the other is conventionally reinforced. An in-span expansion joint is located between the prestressed and reinforced sections. The 143 meter (470 foot) long superstructure is divided into four spans, which are continuous over three 2-column bents as shown in figure E-1. The diaphragm type abutments are cast monolithically with the superstructure and the entire structure is supported on spread footings.

As is the case with most existing bridges of this vintage and type, the expansion joint is unrestrained and supported on a relatively narrow bearing seat. The details of the expansion joint are shown in figure E-2. Concrete columns are confined by steel hoops, which are inadequate for seismic resistance. At two of the bents, column steel is spliced within a zone of potential plastic hinging. The column details are shown in figure E-3.

E.3. SEISMIC RATING

A seismic rating system is used to identify those bridges that are in greatest need of retrofitting. This process is sometimes called preliminary screening because it quickly identifies structures that are at risk and deserve closer examination. In practice, all bridges in a region should be rated and the results compared in order to develop a prioritized list of bridges requiring detailed evaluation.

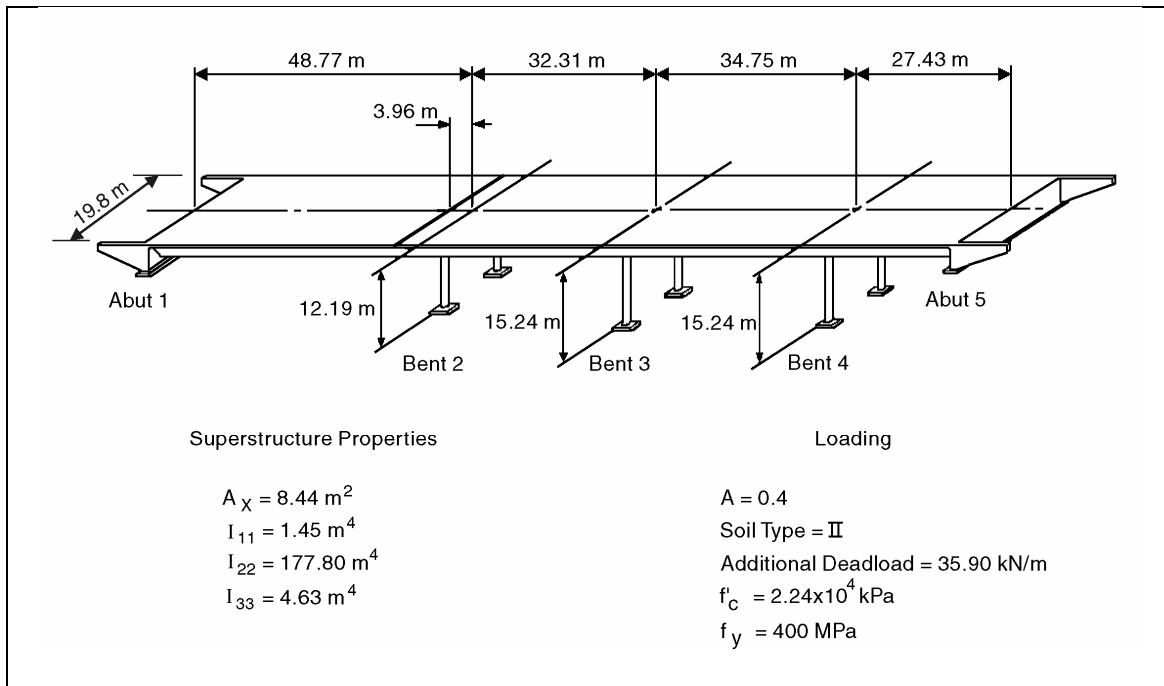


Figure E-1. Example bridge.

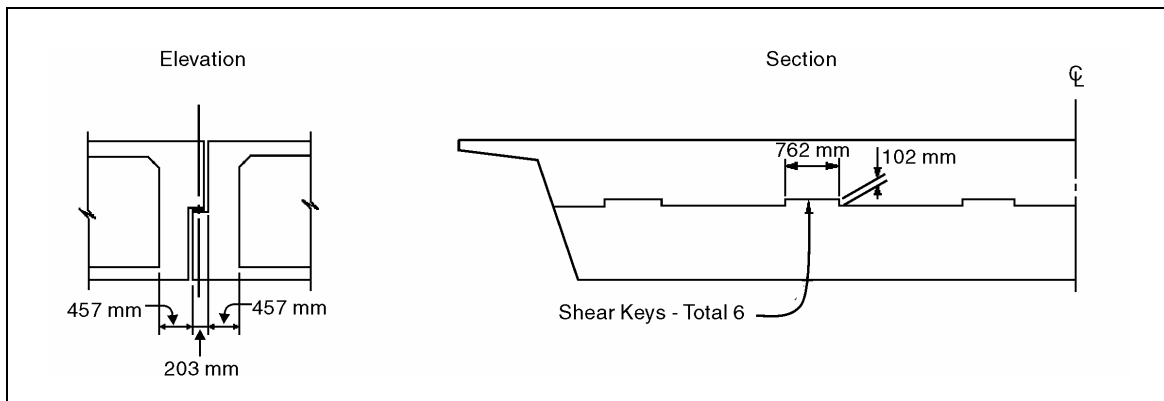


Figure E-2. Expansion joint detail.

As described in section 4.2, this rating system requires the calculation of a priority index for each bridge. This index is based on an assessment of bridge rank, importance, non-seismic deficiencies, and other factors such as network redundancy, political, and economic considerations. One of the critical elements in this calculation is the bridge rank (R), which is obtained from the vulnerability rating of the structure (V) and the seismic hazard rating of the site (E), as follows (equation 4-2):

$$R = V E$$

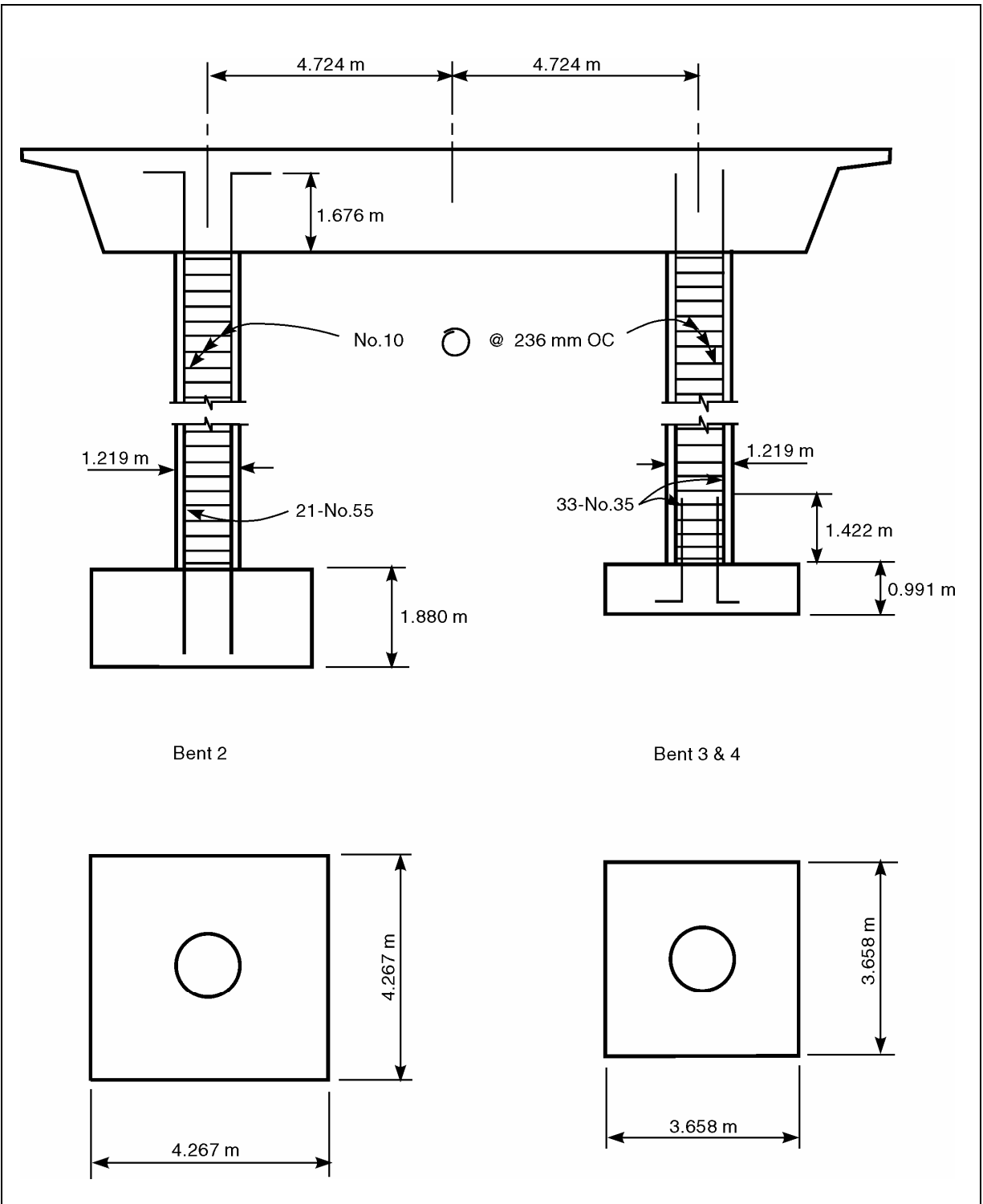


Figure E-3. Column details.

Both of these ratings are determined for the example bridge in the following sections.

E.3.1. VULNERABILITY RATING, V

The procedure suggested in section 4.2.1.1 is used to calculate the vulnerability rating. Because the structure is classified as SRC D, all components will be considered.

A. Bearings

Step 1: Because the bridge superstructure is discontinuous at the expansion joint, the bridge does not have satisfactory bearing details.

Step 2: Although the concrete shear keys are subject to failure, the bearing seat is continuous in the transverse direction and therefore not subject to a serious failure resulting from transverse movement; i.e., $V_T = 5$.

Step 3: In the longitudinal direction, calculate the minimum required support length at the hinge seat. Given:

$$\begin{aligned} L &= L_1 + L_2 = 143 \text{ m (470 ft)} \\ H &= (12.2 + 0) \div 2 = 6.1 \text{ m (20 ft)} \\ B &= 19.8 \text{ m (65 ft)} \\ S_1 &= 0.40 \\ F_v &= 1.4 \text{ (Site Class C, table 1-4(b))} \\ S_{D1} &= F_v S_1 = 0.56 \\ \alpha &= 0^\circ \text{ (no skew)} \end{aligned}$$

Then from equation 5-1a:

$$\begin{aligned} N(d) &= \left[100 + 1.7L + 7.0H + 50\sqrt{H} \sqrt{1 + \left(2 \frac{B}{L} \right)^2} \right] \frac{(1 + 1.25S_{D1})}{\cos \alpha} \\ &= [100 + 243 + 43 + 128] 1.70 \\ &= 874 \text{ mm} \end{aligned}$$

$$\text{and } \frac{N(c)}{N(d)} = \frac{203}{874} = 0.23 < 0.50$$

Since $0.5 N_D > N_c$,

Therefore, $V_L = 10$ and the overall rating for connections, bearings, and seatwidths:

$$\begin{aligned} V_1 &= \text{maximum of } V_L \text{ and } V_T \\ &= 10 \end{aligned}$$

B. Columns, Piers, and Footing

Step 1: Does not apply

Step 2: Does not apply

Step 3: Does not apply

Step 4: Calculate the value for Q, for the shortest and most heavily reinforced columns which are the columns in bent 2.

$$\begin{aligned} Q &= 13 - 6 \left(\frac{L_c}{P_s F_{b_{\max}}} \right) \\ &= 13 - 6 \left(\frac{12.19}{4.6(2)(1.219)} \right) \\ &= 6.5 \end{aligned}$$

Because the support skew is less than 20^0 , the maximum reduction that can be taken is 2 (table 4-1), i.e.:

$$CVR = Q - 2 = 6.5 - 2 = 4.5 \approx 5$$

Step 5: Does not apply

Step 6: Does not apply

Therefore column vulnerability rating, $CVR = 5$

C. Abutments

Step 1: Does not apply

Step 2: Does not apply because the freeway passing under the bridge is in a cut.

Step 3: Does not apply

Therefore abutment vulnerability rating, $AVR = 0$

D. Liquefaction

Step 1: The soil at the site is dense to very dense unsaturated sand and gravel. Therefore, the site has a low susceptibility to liquefaction.

Step 2: Low liquefaction-related damage is likely.

Step 3: Does not apply

Step 4: Does not apply

Step 5: Does not apply

Step 6: Therefore liquefaction vulnerability rating, $LVR = 0$

E. Vulnerability Rating for Components Other Than Bearings, V_2

$$\begin{aligned} V_2 &= CVR + AVR + LVR \\ &= 5 + 0 + 0 = 5 \end{aligned} \quad (\text{Eq. 4-4})$$

F. Overall Bridge Vulnerability (V)

The overall bridge vulnerability rating is the maximum of V_1 and V_2 , i.e.:

$$V = 10.$$

E.3.2. SEISMIC HAZARD RATING, E

The seismic hazard rating, E , is determined by the seismic coefficient at 1.0 sec period (S_{D1}) as defined in equation 4-8. Thus:

$$\begin{aligned} E &= 10 S_{D1} \\ &= 10 (0.56) \\ &= 5.6 \end{aligned}$$

E.3.3. BRIDGE RANK, R

Bridge rank is given by:

$$\begin{aligned} R &= V E \\ &= 10 (5.6) \\ &= 56 \end{aligned} \quad (\text{Eq. 4-2})$$

E.3.4. PRIORITY INDEX

A priority index is assigned once all of the bridges are listed in order of their bridge rank, R . This process will require considerable judgment since this prioritized list must also take into account such factors as structure importance, non-seismic deficiencies, remaining useful life, network redundancy and the like.

E.4. DETAILED EVALUATION

The existing bridge is evaluated in detail to identify structural weaknesses and potential retrofitting measures. The Component Capacity/Demand method is used for this evaluation (Method C, section 5.4).

E.4.1. CAPACITY/DEMAND RATIOS - EXISTING BRIDGE

Capacity/Demand ratios are calculated for the applicable components shown in table 5-2.

Analysis Procedure (Section 5.4.2)

A multi-modal spectral analysis, is used to calculate the elastic demands on the bridge. Although any one of a number of computer programs can be used for such an analysis, the SEISAB computer program was used for this problem. SEISAB is a user-oriented program specifically developed for the seismic analysis of bridges and the implementation of the seismic design provisions in Division I-A of the AASHTO Standard Specifications (AASHTO 2002). It may also be used in accordance with the AASHTO LRFD Specifications (AASHTO 1998). The program automatically combines orthogonal elastic forces as described in section 7.4.2. Foundation stiffnesses at the abutments were selected using the procedure outlined in chapter 6. The following pages include the input coding and the applicable portion of the output from this program for the example bridge. It will be seen that the version of SEISAB used for this analysis does not permit the direct input of S_1 and F_v . Instead an Acceleration Coefficient $A = 0.4$ is used and Soil Type II ($S=1.2$) is specified. The product $AS (= 0.48)$ is then approximately the same as the $F_v S_1$ product of 0.56. Output from SEISAB is consistent with the input, which means that in this case the units are kilonewtons and meters. Forces and moments should be interpreted according to the convention shown in figures E-4 and E-5.

Minimum Bearing Force Demands (Appendix D.2)

The minimum force demand for the transverse shear key at the expansion joint is calculated by considering the equivalent static load to be acting only on the suspended portion of the first span.

$$\text{Superstructure Weight} = 8.44 (23.56) + 35.90 = 234.7 \text{ kN/m}$$

$$\text{Minimum Force Demand} = 0.25(234.7)(44.81 \div 2) = 1,315 \text{ kN}$$

Minimum Support Length (Appendix D.3)

$$N(d) = [100 + 1.7(143) + 7(6.10) + 50(2.56)] 1.70 = 874 \text{ mm}$$

Capacity/Demand Ratio at the Expansion Joints and Bearings (Appendix D.4)

Displacement C/D Ratio (Appendix D.4.2) - Expansion joint

Method 1:

$$\begin{aligned} N(c) &= 203 \text{ mm} \\ r_{bd} &= \frac{N(c)}{N(d)} = \frac{203}{874} = 0.23 \end{aligned}$$

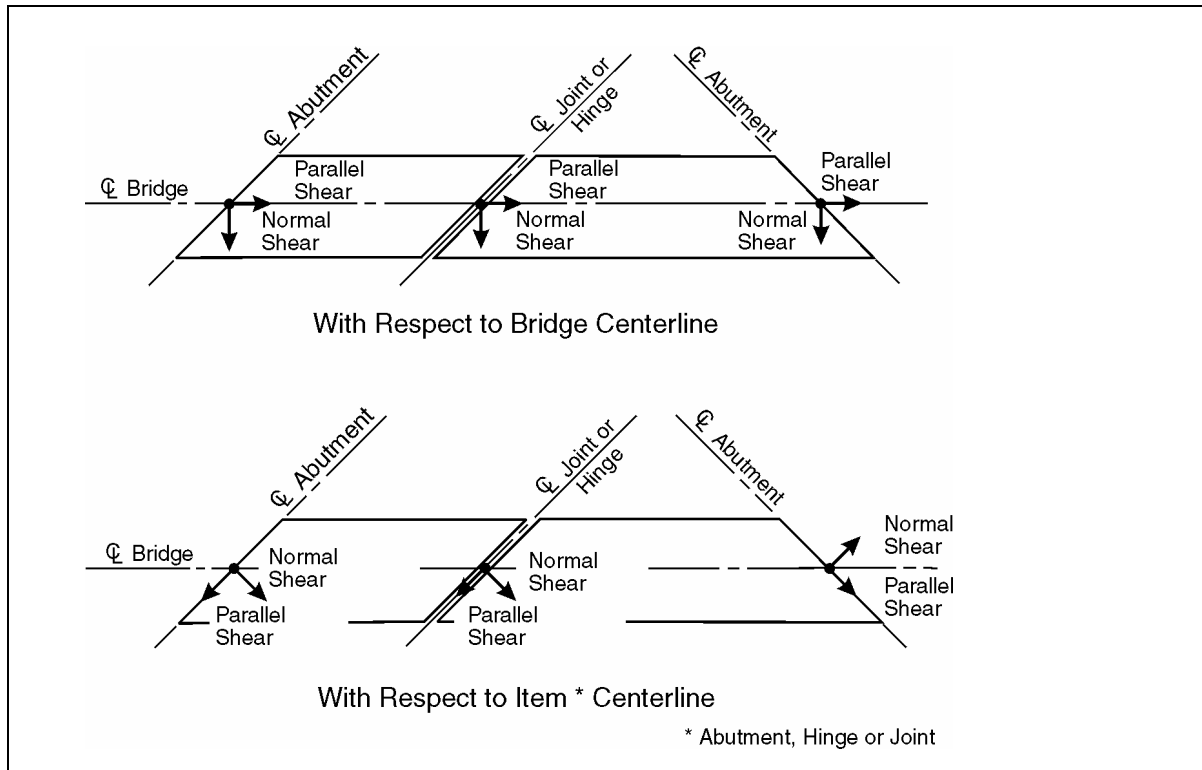


Figure E-4. Positive sign convention for abutment, hinge and joint forces.

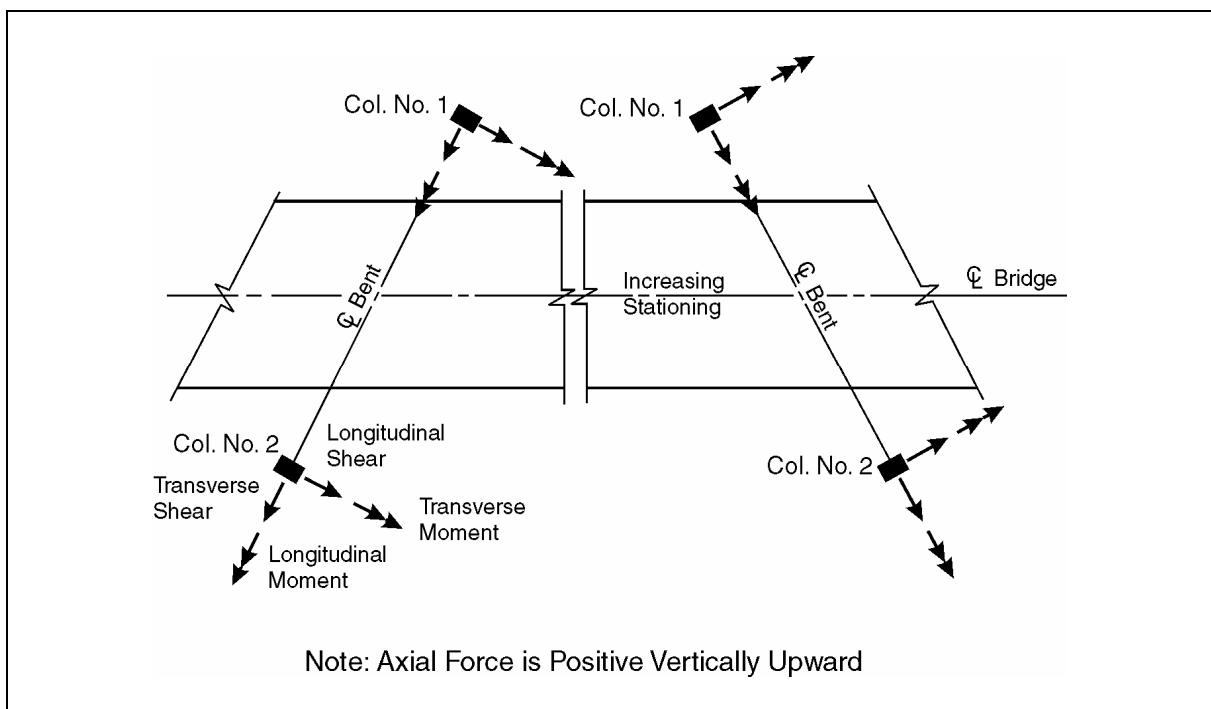


Figure E-5. Positive sign convention for column forces and moments.

Method 2:

Assume that of the 203 mm of total seat length, 76 mm may be considered ineffective because it is the cover on the expansion joint reinforcement.

$$\Delta_s(c) = 203 - 76 = 127 \text{ mm}$$

$$\Delta_i(d) = 84 \text{ mm (temperature, other environmental effects)}$$

$$\Delta_{eq}(d) = 135 \text{ mm (from computer output)}$$

$$r_{bd} = (127 - 84) \div 135 = 0.32$$

```

C *****
C #
C # WORKED EXAMPLE #
C # RESPONSE SPECTRUM ANALYSIS OF THE EXISTING BRIDGE - F'c = 2.2408E+04 KPa #
C #
C *****
C
SEISAB 'WORKED EXAMPLE - NO RETROFITTING'
RESPONSE SPECTRUM ANALYSIS
C
C --- ALIGNMENT DATA ---
ALIGNMENT
STATION 0.00
COORDINATES N 0.00 E 0.00
BEARING N 0 35 27 E
C
C --- SPAN DATA ---
SPANS
LENGTHS /48.590/ /32.310/ /34.750/ /27.010/
AREAS /8.4400/ /8.4400/ /8.4400/ /8.4400/
I11 /1.4500/ /1.4500/ /1.4500/ /1.4500/
I22 /177.80/ /177.80/ /177.80/ /177.80/
I33 /4.6300/ /4.6300/ /4.6300/ /4.6300/
DENSITY /23.563/ /23.563/ /23.563/ /23.563/
E /2.2408E+07/ /2.2408E+07/ /2.2408E+07/ /2.2408E+07/
WEIGHT /35.900/ /35.900/ /35.900/ /35.900/
C
C --- DESCRIBE DATA BLOCK ---
C
DESCRIBE
C
C ** INDIVIDUAL COLUMN PROPERTIES **
COLUMN 'Type 1' "4 FT. ROUND COLUMN"
AREA 1.1710
I11 0.21700
I22 0.10800
I33 0.10800
DENSITY 23.563
E 2.2408E+07
C
C ** WALL PROPERTIES ***
WALL 'Type 1' "ABUTMENT 1 BACKWALL"
AREA 13.006
I11 2.5200
I22 0.63000
I33 315.89
DENSITY 23.563
E 2.2408E+07
WALL 'Type 2' "ABUTMENT 5 BACKWALL"
AREA 13.285
I11 2.5600
I22 0.64000
I33 333.16
DENSITY 23.563
E 2.2408E+07
C
C ** BENT CAP PROPERTIES **
CAP 'Type 1'
AREA 2.7220

```

```

111 889.00
122 889.00
133 0.88900
DENSITY 23.563
E 2.2408E+07
C
C --- ABUTMENT DATA ---
ABUTMENT STATION 0.00
BEARING -
S 85 38 0 W -
N 78 30 0 W
ELEV TOP 418.11 AT ABUT 1
ELEV WALL BOTTOM 415.12 AT ABUT 1
ELEV TOP 427.62 AT ABUT 5
ELEV WALL BOTTOM 424.60 AT ABUT 5
CONNECTION PIN AT ABUT 1 5
WALL 'Type 1' AT ABUTMENT 1
WALL 'Type 2' AT ABUTMENT 5
C
C --- BENT DATA ---
BENT
BEARING N 89 36 58 W, N 89 36 58 W, N 79 52 0 W
ELEVATION TOP 421.53, 423.66, 425.96
ELEVATION BOTTOM 408.01, 408.01, 410.14
CAP 'Type 1' AT BENT 2 3 4
COLUMN SKEVED LAYOUT 'Type 1' 9.4500 'Type 1' AT BENT 2 3
COLUMN SKEVED LAYOUT 'Type 1' 9.5700 'Type 1' AT BENT 4
C
C --- EXPANSION JOINT DATA ---
HINGE
AT 1 44.620 $ Data for Hinge 1
BEARING N 89 36 58 W
C
C --- FOUNDATION STIFFNESSES ---
FOUNDATION
AT ABUTMENT 1
SPRING CONSTANTS
KF1F1 980710.0
KF2F2 291878.0
KN1N1 1.356E+12
KN2R2 1.356E+12
KN3R3 1.356E+12
AT ABUTMENT 5
SPRING CONSTANTS
KF1F1 77348.0
KF2F2 291878.0
KN1N1 1.356E+12
KN2R2 1.356E+12
KN3R3 1.356E+12
C
C --- LOAD DATA ---
LOADS
RESPONSE SPECTRUM
ATCS CURVE
SOIL TYPE 11
ACCELERATION COEFFICIENT 0.40000
GRAVITY 9.8070
DAMPING COEFFICIENT 0.050000
FINISH

```

WORKED EXAMPLE - NO RETROFITTING

RESPONSE SPECTRUM RESULTS

VIBRATION CHARACTERISTICS

MODE	PERIOD	CS	PARTICIPATION FACTORS			% OF TOTAL MASS		
			Long	Vert	Tran	Long	Vert	Tran
1	1.359	0.47	-0.494	-0.001	-53.394	0.006	0.000	71.101
2	0.937	0.60	52.104	-2.628	2.259	67.711	0.172	71.228
3	0.687	0.74	-12.650	27.806	0.111	71.702	19.454	71.228
4	0.375	1.00	-3.621	0.736	15.299	72.030	19.468	77.065
5	0.324	1.00	-12.841	-1.988	0.778	76.142	19.566	77.080
6	0.315	1.00	28.320	11.245	-1.069	96.144	22.720	77.109
7	0.268	1.00	-4.011	-18.588	0.061	96.546	31.337	77.109
8	0.242	1.00	-2.957	-42.741	0.055	96.764	76.895	77.109
9	0.210	1.00	1.934	6.908	-0.155	96.857	78.085	77.110
10	0.153	1.00	4.505	-22.219	-0.373	97.363	90.398	77.113
11	0.147	1.00	0.468	0.411	-0.278	97.369	90.402	77.115
12	0.124	1.00	0.890	-2.352	-0.949	97.388	90.540	77.137

ABUTMENT CQC DISPLACEMENTS

ITEM	LCLEFT FACE....	RIGHT FACE....		...OPENING/CLSNG...	
		LNGTUDNL	TRNSVRSE	LNGTUDNL	TRNSVRSE	LNGTUDNL	TRNSVRSE
ABU 1	1	0.009	0.001	0.009	0.001	0.000	0.000
	2	0.000	0.000	0.000	0.000	0.000	0.000
	3	0.009	0.001	0.009	0.001	0.000	0.000
	4	0.003	0.000	0.003	0.000	0.000	0.000
ABU 5	1	0.117	0.023	0.117	0.023	0.000	0.000
	2	0.006	0.001	0.006	0.001	0.000	0.000
	3	0.119	0.023	0.119	0.023	0.000	0.000
	4	0.041	0.008	0.041	0.008	0.000	0.000

SPAN HINGE CQC DISPLACEMENTS

ITEM	LCLEFT FACE....	RIGHT FACE....		...OPENING/CLSNG...	
		LNGTUDNL	TRNSVRSE	LNGTUDNL	TRNSVRSE	LNGTUDNL	TRNSVRSE
S 1 H1	1	0.024	0.012	0.130	0.012	0.133	0.000
	2	0.001	0.317	0.006	0.317	0.007	0.000
	3	0.025	0.107	0.132	0.107	0.135	0.000
	4	0.008	0.320	0.045	0.320	0.047	0.000

*** LOAD CASE/COMB	DESCRIPTION
1	Longitudinal
2	Transverse
3	1.0*Long + 0.3*Trans
4	0.3*Long + 1.0*Trans

WORKED EXAMPLE - NO RETROFITTING

CRC COLUMN FORCES

	LONGITUDNL....	TRANSVRSE....				
CL	LOC	LC	SHEAR	MOMENT	SHEAR	MOMENT	AXIAL	TORSION
BNT 2								
1	BOT	1	1468.1	10097.	112.1	749.	1179.3	68.7
		2	168.7	1132.	3427.3	23469.	4751.2	461.0
		3	1518.7	10436.	1140.3	7790.	2604.7	207.0
		4	609.1	4161.	3460.9	23693.	5105.0	481.6
1	TOP	1	1394.3	9335.	100.8	710.	1176.4	68.7
		2	162.9	1116.	3345.8	22406.	4750.5	461.0
		3	1443.1	9670.	1104.6	7432.	2601.6	207.0
		4	581.2	3916.	3376.0	22619.	5103.4	481.6
2	BOT	1	1420.0	9776.	138.5	876.	1273.4	68.9
		2	199.9	1349.	3426.6	23466.	4732.7	461.0
		3	1480.0	10180.	1166.5	7915.	2693.2	207.2
		4	625.9	4281.	3468.2	23728.	5114.7	481.7
2	TOP	1	1348.5	9020.	129.6	950.	1270.7	68.9
		2	191.6	1305.	3345.1	22400.	4732.0	461.0
		3	1406.0	9412.	1133.1	7670.	2690.3	207.2
		4	596.2	4011.	3384.0	22685.	5113.2	481.7
BNT 3								
1	BOT	1	1027.9	7938.	33.1	256.	618.5	53.6
		2	108.7	845.	1512.0	11914.	2393.9	408.9
		3	1060.6	8191.	486.7	3830.	1336.6	176.3
		4	417.1	3227.	1522.0	11991.	2579.5	425.0
1	TOP	1	940.1	7573.	23.6	204.	617.4	53.6
		2	103.3	821.	1446.9	11319.	2393.4	408.9
		3	971.1	7819.	457.7	3600.	1335.4	176.3
		4	385.4	3092.	1454.0	11380.	2578.6	425.0
2	BOT	1	998.3	7710.	53.3	370.	693.3	53.7
		2	138.3	1068.	1511.1	11910.	2364.3	408.9
		3	1039.8	8030.	506.6	3943.	1402.6	176.4
		4	437.8	3381.	1527.1	12021.	2572.3	425.0
2	TOP	1	913.0	7353.	46.8	419.	692.3	53.7
		2	130.6	1045.	1446.0	11310.	2363.8	408.9
		3	952.1	7667.	480.6	3813.	1401.4	176.4
		4	404.5	3251.	1460.1	11436.	2571.5	425.0
BNT 4								
1	BOT	1	1004.2	7808.	33.2	281.	822.4	42.8
		2	44.5	348.	653.3	5191.	1073.1	431.0
		3	1017.6	7913.	229.2	1838.	1144.4	172.1
		4	345.7	2690.	663.3	5275.	1319.9	443.9
1	TOP	1	915.2	7487.	22.5	174.	821.9	42.8
		2	40.5	329.	619.4	4914.	1072.9	431.0
		3	927.4	7586.	208.3	1648.	1143.8	172.1
		4	315.0	2575.	626.1	4966.	1319.4	443.9
2	BOT	1	980.6	7624.	61.5	436.	433.4	42.9
		2	252.8	1992.	652.4	5186.	1042.1	431.0
		3	1056.4	8222.	257.3	1992.	746.0	172.2
		4	547.0	4280.	670.9	5317.	1172.1	443.9
2	TOP	1	893.7	7311.	52.9	478.	432.8	42.9
		2	240.8	1927.	618.5	4905.	1041.8	431.0
		3	965.9	7889.	238.5	1949.	745.3	172.2
		4	508.9	4120.	634.4	5048.	1171.7	443.9

WORKED EXAMPLE - NO RETROFITTING

ABUTMENT CQC FORCES

ITEM	LC	VERT SHEAR	W/R TO BRIDGE C.L.		W/R TO ITEM C.L.	
			LONGITUDNL	TRANSVERSE	NORMAL	PARALLEL
ABU 1	1	3527.3	9082.2	268.9	9066.4	599.2
	2	135.9	370.4	1286.7	387.3	1281.8
	3	3568.1	9193.3	654.9	9182.5	983.7
	4	1194.1	3095.1	1367.4	3107.2	1461.5
ABU 5	1	1045.1	9289.9	1001.8	9253.2	1298.0
	2	102.5	709.5	2901.8	445.8	2953.9
	3	1075.9	9502.8	1872.4	9386.9	2184.1
	4	416.1	3496.4	3202.4	3221.8	3343.2

SPAN HINGE CQC FORCES

ITEM	LC	VERT SHEAR	W/R TO BRIDGE C.L.		W/R TO ITEM C.L.	
			LONGITUDNL	TRANSVERSE	NORMAL	PARALLEL
S 1 H1	1	1789.9	0.0	366.6	1.3	366.6
	2	49.8	0.0	2816.0	10.2	2816.0
	3	1804.9	0.0	1211.4	4.4	1211.4
	4	566.7	0.0	2926.0	10.6	2926.0

*** LOAD CASE/COMB	DESCRIPTION
1	Longitudinal
2	Transverse
3	1.0*Long + 0.3*Trans
4	0.3*Long + 1.0*Trans

Shear Force C/D Ratio (Appendix D.4.3)

$$V_b(d) = 2926 \times 1.25 = 3658 \text{ kN} > 1,315 \text{ kN}$$

$$V_b(c) = 6 \times 12 \times \frac{100}{10^6} 1 \times 400 \times 10^3 = 2,880 \text{ kN}$$

$V_b(c)$ is the shear resistance provided by six, 762 mm long shear keys with twelve No. 4 bars in each key.

$$r_{bf} = \frac{2880}{3658} = 0.79$$

Capacity/Demand Ratios at Columns, Piers, and Footings (Appendix D.5)

Step 1: Elastic Moment Demands

The elastic moment demands are calculated by combining the moments about the principal axes of the columns to obtain the maximum moments. In most cases, Load Case 2 has the highest demands. Dead load moments, which are also included in the calculations, have been obtained from a separate analysis. Moments at the base of the footing were obtained by adding the moment created by the shear at the top of the footing to the moment at the top of the footing. Elastic moments of highest demands are summarized in table E-1.

Table E-1. Maximum elastic moment demands (kN m).

Location	Component	Trans. Moment		Long. Moment		Elastic Moment Demand
		EQ	DL	EQ	DL	
B-2 (C-2) Top	Column	22,685	1,786	4,011	107	24,815
B-2 (C-2) Bottom	Column	23,728	895	4,281	14	24,995
B-2 (C-2) Bottom	Footing	30,248	1,268	5,458	27	31,990
B-3 (C-2) Top	Column	11,436	1,243	3,251	228	13,148
B-3 (C-2) Bottom	Column	12,021	619	3,381	168	13,129
B-3 (C-2) Bottom	Footing	13,534	737	3,815	193	14,823
B-4 (C-2) Top	Column	1,949	1,315	7,889	33	8,568
B-4 (C-2) Bottom	Column	1,992	660	8,222	68	8,704
B-4 (C-2) Bottom	Footing	2,247	784	9,269	74	9,822

Step 2: Ultimate Moment Capacities

Ultimate moment capacities for the columns are obtained from the computer generated column interaction diagrams shown in figures E-6 and E-7. Ultimate moment capacities for the footing are obtained from interaction diagrams for the footings, which are also shown in figures E-6 and E-7. Ordinates for the footing interaction diagram for bent 2 are calculated in figure E-8. Interaction diagrams for the footings at bents 3 and 4 are similar.

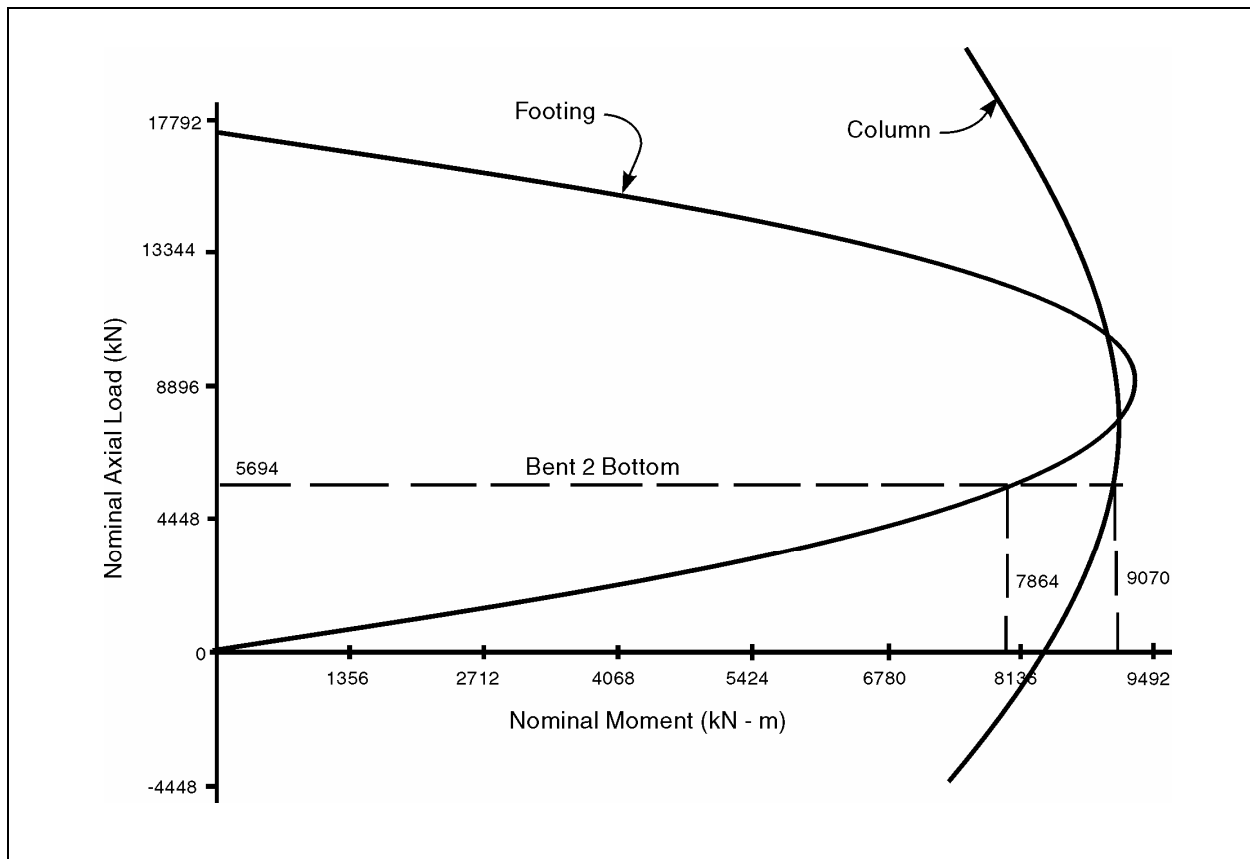


Figure E-6. Bent 2 column and footing interaction diagrams.

Because the elastic moment demands are primarily in the plane of the bent, moment capacities will be calculated for bending in this plane. This requires a consideration of the variation in axial load due to bent overturning as outlined in the iterative procedure presented in article 4.8.2 of Division I-A of the AASHTO Standard Specifications (AASHTO, 2002). The steps of this procedure are as follows.

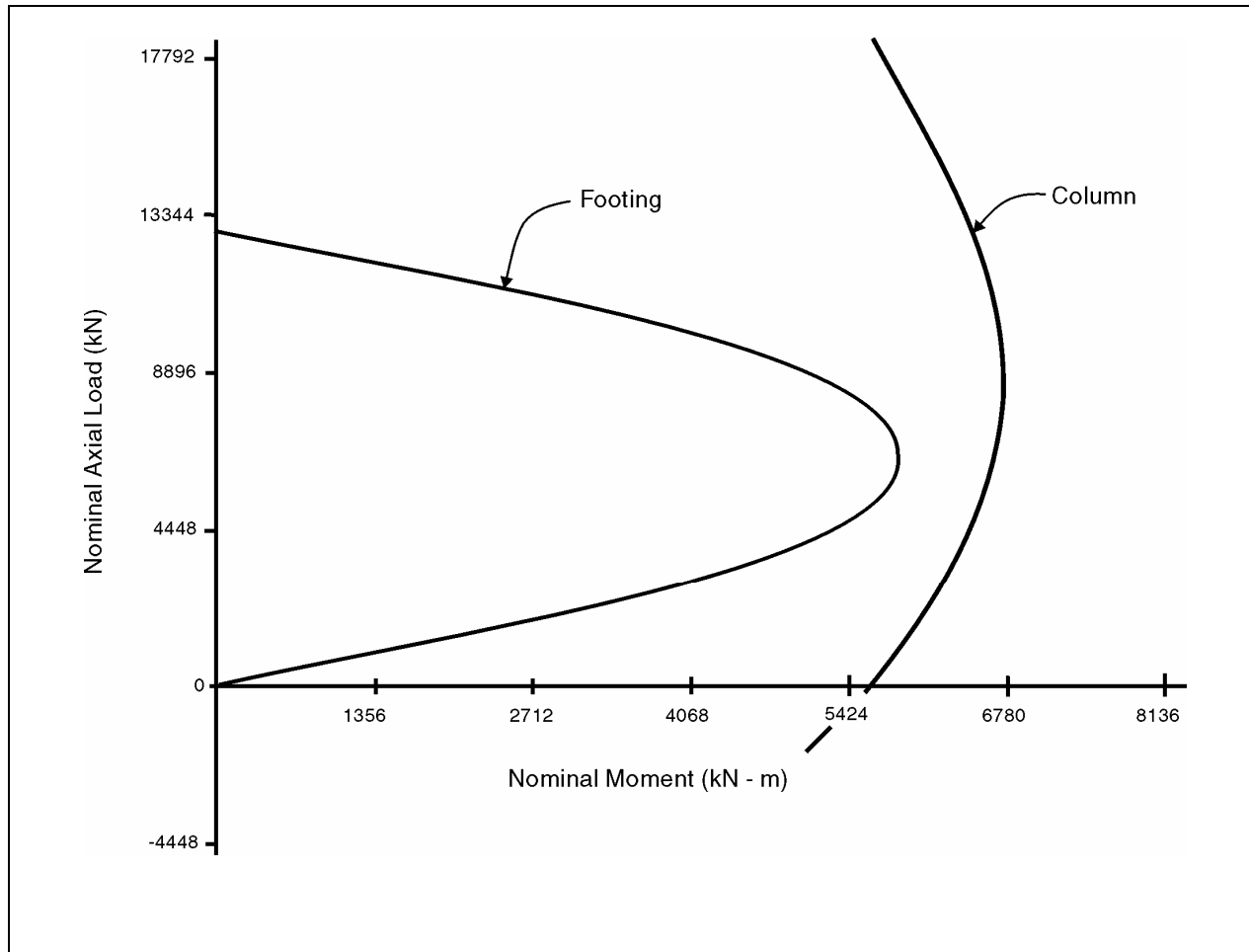


Figure E-7. Bents 3 and 4 column and footing interaction diagrams.

Step 2.1 Overstrength Moment Capacities at Axial Load Corresponding to Dead Load

Table E-2 summarizes the overstrength column and footing moment capacities taken from the interaction diagrams. An example for the bottom of bent 2 is shown in figure E-8. Bents 3 and 4 have identical capacities.

Table E-2. Column and footing overstrength moments.

Bent	End	Axial Force Due to Dead Load	1.3 M _u	
			Column	Footing
2	Top	5,293	11,796	-
2	Bottom	5,694	11,796	10,223
3 & 4	Top	4,270	8,379	-
3 & 4	Bottom	4,715	8,528	7,213

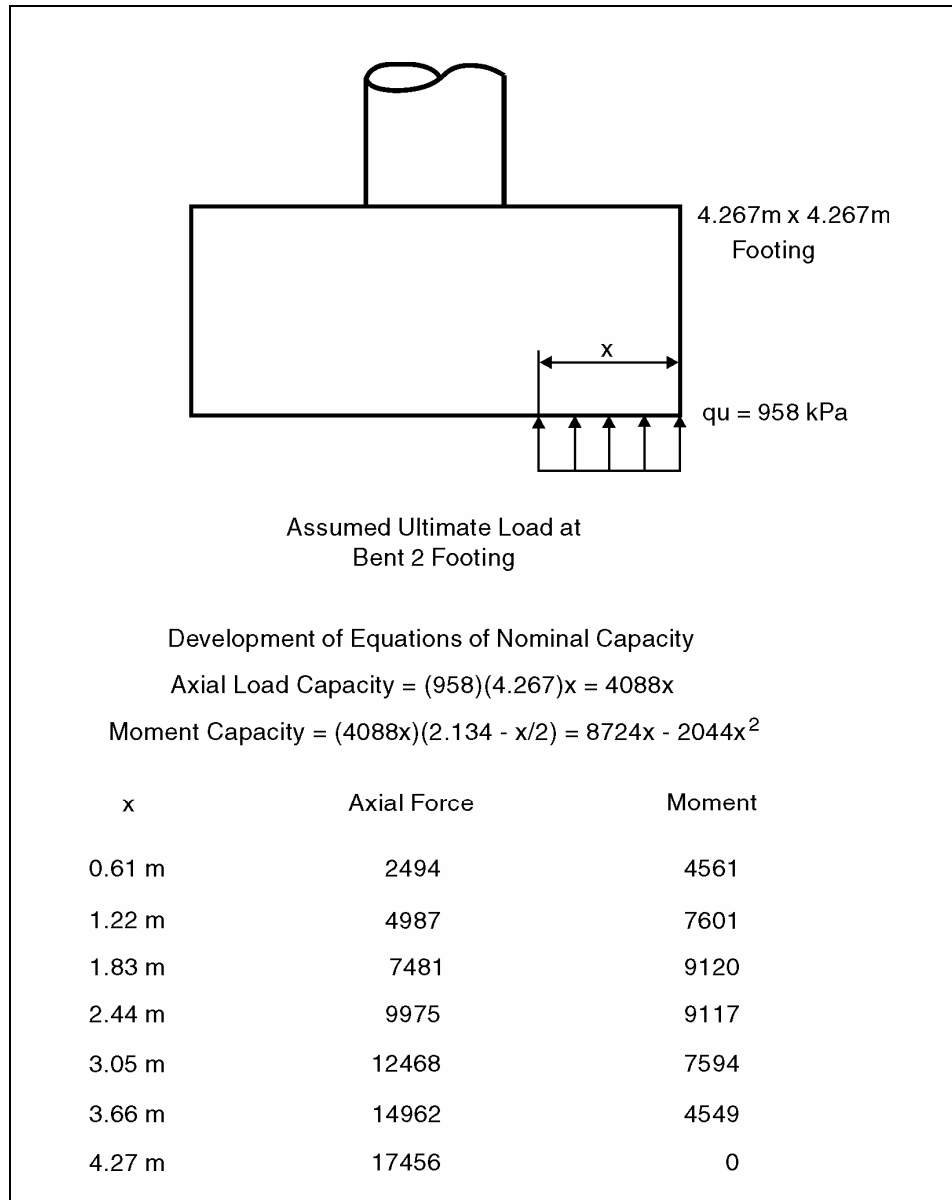


Figure E-8. Development of footing interaction diagram at bent 2.

Step 2.2 Column Shear Forces*

$$\text{Bent 2: } V_u = (11769 + 10223) \div 14.08 = 1,562 \text{ kN}$$

$$\text{Bent 3 \& 4: } V_u = (8379 + 7213) \div 16.25 = 960 \text{ kN}$$

* Because the ultimate moment is less at the footing than at the column base, the footing moments and the distance between the superstructure soffit and the base of the footing are used to calculate column shears.

Step 2.3 Axial Forces Due to Overturning in the Transverse Direction

$$\text{Bent 2: Axial Force} = 2(1562)(14.08) \div 9.45 = + 4,655$$

$$\text{Bent 3 \& 4: Axial Force} = 2(960)(16.25) \div 9.45 = + 3,302$$

Step 2.4 Revised Overstrength Moment Capacities

The axial loads due to overturning calculated in Step 3 are used to obtain new overstrength moment capacities from the interaction diagrams. Table E-3 summarizes these revised moment capacities.

These moment capacities are used to calculate revised shear forces at the bent.

$$\text{Bent 2: Shear} = (11036 + 2088) \div 14.08 + (11796 + 11674) \div 14.08 = 2,599 \text{ kN}$$

$$\text{Bents 3 \& 4: Shear} = (6996 + 2996) \div 16.25 + (8786 + 7132) \div 16.25 = 1,594 \text{ kN}$$

These bent shears are not within 10 percent of the bent shears (twice the column shear) calculated in Step 2. Therefore the axial forces due to overturning must be recalculated.

$$\text{Bent 2: Axial Force} = 2599(14.08) \div 9.45 = 3,872 \text{ kN}$$

$$\text{Bent 3 \& 4: Axial Force} = 1594(16.25) \div 9.45 = 2,741 \text{ kN}$$

These axial loads are used to recalculate the overstrength moments, which are summarized in table E-4.

Table E-3. Revised column and footing overstrength moments (iteration 1).

Bent	End	Axial Force Due to Dead Load + Overturning	1.3 M _u	
			Column	Footing
2	Top	638	11,036	-
2	Top	9,948	11,796	-
2	Bottom	1,039	11,145	2,088
2	Bottom	10,349	11,741	11,674
3 & 4	Top	968	6,996	-
3 & 4	Top	7,572	8,786	-
3 & 4	Bottom	1,413	7,769	2,996
3 & 4	Bottom	8,017	8,813	7,132

Table E-4. Revised column and footing overstrength moments (iteration 2).

Bent	End	Axial Force Due to Dead Load + Overturning	1.3 M _u	
			Column	Footing
2	Top	1,421	11,240	-
2	Top	9,165	11,836	-
2	Bottom	1,822	11,321	3,715
2	Bottom	9,566	11,823	11,972
3 & 4	Top	1,529	7,728	-
3 & 4	Top	7,011	8,759	-
3 & 4	Bottom	1,974	7,850	3,864
3 & 4	Bottom	7,456	8,786	7,389

New shear forces at the bents are calculated using these moments.

$$\text{Bent 2: Shear} = (11240 + 3715) \div 14.08 + (11836 + 11972) \div 14.08 = 2,753 \text{ kN}$$

$$\text{Bents 3 \& 4: Shear} = (7728 + 3864) \div 16.25 + (8759 + 7389) \div 16.25 = 1,707 \text{ kN}$$

The bent shears are now within 10 percent of the previously calculated shears and therefore no further iteration is needed.

Step 3: Ultimate Moment Capacity/Elastic Moment Demand Ratios

The most critical combinations of the unfactored nominal ultimate moment capacities (M_u) and elastic moment demands are used to calculate r_{ec} and r_{ef} at each bent. Values of r_{ec} and r_{ef} are summarized in table E-5.

Table E-5. Ultimate moment capacity/elastic moment demand ratios.

Bent	End	Axial Load	Column			Footing		
			Demand	Capacity	r_{ec}	Demand	Capacity	r_{ef}
2	Top	Min.	24,815	8,650	0.35	-	-	
2	Top	Max.	24,815	9,111	0.37	-	-	
2	Bottom	Min.	24,995	8,704	0.35	31,990	2,861	0.09
2	Bottom	Max.	24,995	9,098	0.36	31,990	9,206	0.29
3	Top	Min.	13,148	5,938	0.45			
3	Top	Max.	13,148	6,738	0.51			
3	Bottom	Min.	13,129	6,033	0.46	14,823	2,969	0.20
3	Bottom	Max.	13,129	6,752	0.51	14,823	5,681	0.38
4	Top	Min.	8,568	5,938	0.69			
4	Top	Max.	8,568	6,738	0.79			
4	Bottom	Min.	8,704	6,033	0.69	9,822	2,969	0.30
4	Bottom	Max.	8,704	6,752	0.76	9,822	5,681	0.58

Step 4: Calculate C/D Ratios for Possible Plastic Hinging Cases at the Bottom of the Columns

Bent 2 - Case II ($r_{ec} = 0.35$ and $r_{ef} = 0.09$):

1. Anchorage (appendix D.5.1) - Straight anchorage

$$l_a(c) = 1880 - 76 = 1,804 \text{ mm}$$

For anchorage in the footing, assume the large cover (1575 mm) has a confining effect equal to transverse steel with equivalent tensile strength. In this case, twice the area of the cover divided by half the number of longitudinal bars is considered.

$$\text{Concrete tensile strength} = 19.69\sqrt{f'_c} = 2947 \text{ kPa}$$

$$k_{tr} = 2947(1575)(2)/[21 \div 2)(4137)(55)] = 3.89 > 2.5$$

$$\ell_a(d) = \frac{((400 \times 10^3 - 75842) \div 33.1) 55}{\left(\sqrt{2.24 \times 10^4}\right) / 2.63 (1 + 2.5(55 \div 55) + 2.5)} = 1,578 \text{ mm}$$

Therefore, Case B applies. Calculate the negative moment capacity of the footing using a concrete tensile strength of 2,947 kPa ($19.69\sqrt{f'_c}$).

$$\begin{aligned}\text{Negative Moment Capacity} &= 2947(4.267(1.88)^2 \div 6) \\ &= 7,407 \text{ kN m}\end{aligned}$$

This capacity is sufficient to resist the weight of the overburden. Therefore:

$$r_{ca} = 1.0$$

2. Splices (appendix D.5.2) - Does not apply
3. Footing Rotation (appendix D.5.5)

Because anchorage or splice failures will not prevent footing rotation:

$$r_{fr} = \mu r_{ef} = 4(0.09) = 0.36$$

Bent 2 - Case II ($r_{ec} = 0.36$ and $r_{ef} = 0.29$):

1. Anchorage - Same as before

$$r_{ca} = 1.0$$

2. Splices - Does not apply
3. Footing Rotation

$$r_{fr} = \mu r_{ef} = 4(0.29) = 1.16$$

Bent 3 - Case II (Two possible combinations of r_{ec} and r_{ef} must be investigated: $r_{ec} = 0.46$ and $r_{ef} = 0.20$ plus $r_{ec} = 0.51$ and $r_{ef} = 0.38$).

1. Anchorage - Hooked Anchorage

$$l_a(c) = 838 \text{ mm}$$

$$l_a(d) = 0.7(1200)(35) \div (\sqrt{2.24 \times 10^4} / 2.63) = 517 \text{ mm}$$

Case B applies.

$$\begin{aligned}\text{Negative Moment Capacity} &= 2947(3.658(0.991)^2 \div 6) \\ &= 1,764 \text{ kN m}\end{aligned}$$

Because this capacity is sufficient to resist the weight of the overburden,

$$r_{ca} = 1.0$$

2. Splices (appendix D.5.2)

Because the clear spacing between splices = 38 mm < 4(35)

$$A_{tr}(c) = 2(100)/(33 \div 2) = 12.1$$

$$A_{tr}(d) = \frac{236}{1422} 1000 = 166$$

$$l_s = 1422 > \left(\frac{4885}{\sqrt{f_c}} \right) d_b 2 = 1,144$$

Therefore, Case A applies.

$$r_{cs} = 0.75 (0.46) = 0.35$$

$$r_{cs} = 0.75 (0.51) = 0.38$$

Notice that the minimum value for r_{cs} controls.

3. Footing

$$0.8 r_{ef} = 0.8(0.38) = 0.30 < 0.38$$

$$0.8 r_{ef} = 0.8(0.20) = 0.16 < 0.35$$

Therefore a splice failure cannot be assumed to prevent footing rotation. The minimum C/D ratio for the footing is given by

$$r_{fr} = 4(0.20) = 0.80$$

Bent 4 - Case II ($r_{ec} = 0.69$ and $r_{ef} = 0.30$):

1. Anchorage - Same as bent 3

$$r_{ca} = 1.0$$

2. Splices

$$r_{cs} = 0.75 (0.69) = 0.52$$

3. Footing

$$0.8 r_{ef} = 0.8(0.30) = 0.24 < 0.52$$

Bent 4 - Case II ($r_{ec} = 0.76$ and $r_{ef} = 0.58$):

1. Anchorage

$$r_{ca} = 1.0$$

2. Splices

$$r_{cs} = 0.75 (0.76) = 0.57$$

3. Footing

$$0.8 r_{ef} = 0.8(0.58) = 0.46 < 0.57$$

Therefore, a splice failure cannot be assumed to prevent footing rotation. The minimum C/D ratio for the footing is given by:

$$r_{fr} = 4(0.30) = 1.20$$

Step 5: Calculate C/D Ratio at the Top of the Column

Bent 2

1. Anchorage

$$l_a(c) = 1,676 \text{ mm}$$

$$l_a(d) = 1200 (55) \div \sqrt{2.24 \times 10^4} / 2.63 = 1160 \text{ mm}$$

Therefore Case B applies:

$$r_{ca} = 1.0$$

2. Splices - Does not apply

3. Confinement (appendix D.5.4)

$$\rho(c) = 100(\pi)(1118) \div [\pi(610)^2(236)] = 0.0013$$

$$\rho(d) = 0.45 \left(\frac{\pi(610)^2}{\pi(559)^2} - 1 \right) \frac{2.24 \times 10^4}{4 \times 10^5} = 0.0048$$

$$\frac{P_c}{f'_c A_g} = \frac{9165}{(2.24 \times 10^4) \pi (610)^2 / (1000)^2} = 0.35$$

$$k_1 = \frac{0.0013}{0.0048 (0.5 + 1.25(0.35))} = 0.29$$

$$k_2 = \frac{0.2}{(305 \div 1219)} = 0.8$$

Because transverse steel is poorly anchored, an iterative solution for μ is required.

Try $k_3 = 0.35$ (corresponds to $\mu = 2.7$)

$$\mu = 2 + 4 \left(\frac{0.29 + 0.80}{2} \right) 0.35 = 2.8 \quad \text{ok}$$

$$r_{cc} = \mu r_{ec} = 2.8(0.35) = 0.98$$

Bent 3

1. Anchorage

$$l_a(c) = 1,676 \text{ mm}$$

$$l_a(d) = \frac{((400 \times 10^3 - 75842) \div 33.1) 35}{(\sqrt{2.24 \times 10^4 / 2.63}) (1 + 2.5 \frac{36}{35})} = 1,687 \text{ mm}$$

Case A applies

$$r_{ca} = \frac{1676}{1687} (0.45) = 0.45$$

2. Splices - Does not apply

3. Confinement

$$k_1 = \frac{0.0013}{0.0048 (0.5 + 1.25(0.270))} = 0.32$$

$$k_2 = \frac{6}{305/35} = 0.69$$

Try $k_3 = 0.35$ (corresponds to $\mu = 2.7$)

$$\mu = 2 + 4 \left(\frac{0.32 + 0.69}{2} \right) 0.35 = 2.7 \quad \text{ok}$$

$$r_{cc} = 2.7 (0.45) = 1.22$$

Bent 4

1. Anchorage

$$r_{ca} = \frac{1676}{1687} (0.69) = 0.69$$

2. Splices - Does not apply

3. Confinement

$$r_{cc} = 2.7(0.69) = 1.86$$

Step 6: Calculate C/D Ratios for Column Shear (appendix D.5.3)

Bent 2 - Transverse bending - Footing rotation will govern the maximum shear.

Therefore use the nominal footing overstrength moment plus an effective length measured to the base of the footing.

$$V_u(d) = \frac{11836 + 11972}{14.08} = 1,691 \text{ kN}$$

$$V_c(d) = 3468 + 198 = 3,666 \text{ kN}$$

$$\begin{aligned} V_i(c) &= v_c db + \frac{A_{tr} f_{yt} d}{s} \\ &= \frac{787(1059)(1219)}{(1000)^2} + \frac{(2 \times 100)(4 \times 10^5)(1059)}{236(1000)^2} \\ &= 1,375 \text{ kN} \end{aligned}$$

Because column axial stress may fall below $0.10f'_c$ and transverse steel is ineffective:

$$V_f(c) = 0$$

Therefore, Case A applies; i.e.:

$$r_{cv} = \frac{1375}{3666} = 0.38 > 0.36 \text{ (the value of } r_{ec})$$

$$r_{cv} = 0.36$$

Bent 3 - An anchorage failure at the top of the column and rotation of the footing at the bottom of the column will limit the maximum shear.

$$V_u(d) = \frac{(1676/1687) 8759 + 7389}{16.25} = 990 \text{ kN}$$

$$V_e(d) = 1527 + 119 = 1,646 \text{ kN}$$

$$V_i(c) = 1,375 \text{ kN}$$

$$V_f(c) = 0$$

Therefore, Case B applies; i.e.

$$\mu = 2 + (0.75)(4) \left(\frac{1375 - 990}{1375 - 0} \right) = 2.8$$

$$r_{cv} = 2.8(0.45) = 1.26$$

Bent 4

$$r_{ec} = 0.69$$

$$V_e(d) = 671 + 125 = 796 \text{ kN}$$

$$\mu = 2.8$$

$$r_{cv} = 2.8 (0.69) = 1.93$$

Capacity/Demand Ratio for Abutments (Appendix D.6)

Abutment C/D ratios are based on the displacements from the analysis.

Transverse Displacement

$$d(c) = 75 \text{ mm}$$

Abutment 1:

$$d(d) = 1 \text{ mm}$$

$$r_{ad} = \frac{75}{1} = 75$$

Abutment 5:

$$d(d) = 23$$

$$r_{ad} = \frac{75}{23} = 3.3$$

Longitudinal Displacement

$$d(c) = 150 \text{ mm}$$

Abutment 1:

$$\begin{aligned} d(d) &= 9 \text{ mm} \\ r_{ad} &= \frac{150}{9} = 16.7 \end{aligned}$$

Abutment 5:

$$\begin{aligned} d(d) &= 119 \text{ mm} \\ r_{ad} &= \frac{150}{119} = 1.26 \end{aligned}$$

Capacity/Demand Ratio for Liquefaction (Appendix D.7)

Because the preliminary screening (Seismic Rating System) indicated that the likelihood of liquefaction-related damage was low, a C/D ratio for liquefaction is not determined.

E.4.2. IDENTIFICATION AND ASSESSMENT OF POTENTIAL RETROFIT MEASURES

Table E-6 summarizes the C/D ratios that are less than 1.0 for the bridge.

Table E-6. Capacity/demand ratios for the as-built bridge.

Component	Notation	C/D Ratios for As-Built Bridge
Expansion Joint	r_{bd}	0.23
	r_{bf}	0.79
Bent 2 (Overall)	r_{cv}	0.36
Bent 2 (Bottom)	r_{fr}	0.36
Bent 3 (Bottom)	r_{fr}	0.80
Bent 3 (Top)	r_{ca}	0.45
Bent 4 (Top)	r_{ca}	0.69

The expansion joint displacement is critical because it has the lowest C/D ratio and may result in a partial collapse of the bridge. This may be economically corrected by retrofitting the joint with longitudinal expansion joint restrainers. Because the transverse shear keys are also inadequate as indicated by the C/D ratio for bearing force, transverse pipe restrainers should also be included in the retrofit.

A potentially serious failure is indicated by the C/D ratio for shear in bent 2. Shear failure could be sudden and result in rapid disintegration of the column's ability to support axial load. The seriousness of this particular failure is compounded because the column is located adjacent to the

expansion joint, which increases the probability of a partial collapse. Therefore, the consequences of a shear failure in bent 2 are unacceptable and this deficiency should be corrected. Because this failure mode is caused by forces transverse to the centerline of the bridge, an infill shear wall at bent 2 would be a relatively economical way to retrofit the bridge. This type of retrofit would also reduce the potential for a rotational failure of the footing at bent 2.

The next lowest C/D ratio occurs at the column steel anchorage in bent 3. There are several factors that make this potential failure of less concern. The primary effect of anchorage loss will be a reduction in the flexural strength at the top of the column. But because the bent is redundant, this will not result in the formation of a collapse mechanism. Therefore, this kind of failure in itself is not considered unacceptable. However, the rotation failure of the footing at bent 3 would threaten the stability of this bent, particularly when combined with the possibility of anchorage failure. But as noted, if the bent is stiffened with an infill shear wall, the likelihood of this happening is greatly reduced and additional retrofitting is not proposed.

The top column steel anchorage of bent 4 has a C/D ratio (r_{ca}) of 0.69. Since the C/D ratio of footing rotation ($r_{fr} = 1.20$) is larger than 1.0, failure of steel anchorage would not cause a collapse mechanism to occur, and is considered an acceptable failure. Therefore, it is not proposed to retrofit bent 4.

Because the infill shear wall at bent 2 would significantly affect the dynamic response of the structure, another analysis is required. Computer input and output files for the retrofitted bridge are included on the following pages. An abbreviated reevaluation of the C/D ratios for the most critical components in the retrofitted bridge shows that the C/D ratios at bent 3 are greatly improved by the modified response.

Capacity/Demand Ratio at the Retrofitted Expansion Joint

Displacement C/D Ratio

Method 2:

$$\begin{aligned}\Delta_s(c) &= 127 \text{ mm} \\ \Delta_i(d) &= 84 \text{ mm} \\ \Delta_{eq}(d) &= 24 \text{ mm} \\ r_{bd} &= \frac{(127 - 84)}{24} = 1.79 > 1 \text{ ok}\end{aligned}$$

Capacity/Demand Ratios at the Columns, Piers, and Footing

Bent 3 (Bottom)

$$\begin{aligned}r_{ef} &\approx 2969 \div 6052 = 0.49 \\ r_{fr} &= 4(0.49) = 1.96 \text{ ok}\end{aligned}$$

Bent 3 (Top)

$$r_{ec} \approx 5938 \div 5058 = 1.17 \quad \text{ok}$$

$$r_{ca} = \frac{1676}{1687}(1.17) = 1.16 \quad \text{ok}$$

```

C *****
C *
C *          WORKED EXAMPLE
C * RESPONSE SPECTRUM ANALYSIS OF THE EXISTING BRIDGE - F'c = 2.2408E+04 KPa
C *
C *****
C
SEISAB 'WORKED EXAMPLE - RETROFITTED'
RESPONSE SPECTRUM ANALYSIS
C
C --- ALIGNMENT DATA ---
ALIGNMENT
STATION 0.00
COORDINATES N 0.00 E 0.00
BEARING N 0 35 27 E
C
C --- SPAN DATA ---
C
SPANS
LENGTHS /48.590/ /32.310/ /34.750/ /27.010/
AREAS /8.4400/ /8.4400/ /8.4400/ /8.4400/
I11 /1.4500/ /1.4500/ /1.4500/ /1.4500/
I22 /177.80/ /177.80/ /177.80/ /177.80/
I33 /4.6300/ /4.6300/ /4.6300/ /4.6300/
DENSITY /23.563/ /23.563/ /23.563/ /23.563/
E /2.2408E+07/ /2.2408E+07/ /2.2408E+07/ /2.2408E+07/
WEIGHT /35.900/ /35.900/ /35.900/ /35.900/
C
C --- DESCRIBE DATA BLOCK ---
C
DESCRIBE
C
C ** INDIVIDUAL COLUMN PROPERTIES **
C
COLUMN 'Type 1' "4FT. ROUND COLUMN"
AREA 1.1710
I11 0.21700
I22 0.10800
I33 0.10800
DENSITY 23.563
E 2.2408E+07
COLUMN 'INFILL'
AREA 4.757
I11 0.518
I22 0.236
I33 61.582
DENSITY 23.563
E 2.2408E+07
C
C ** RESTRAINER PROPERTIES **
C
RESTRAINER 'Type 1' "CALIFORNIA CABLE RESTRAINER"
LENGTH 2.438
AREA 0.002
E 1.24E+08
C
C ** WALL PROPERTIES **
C
WALL 'Type 1' "ABUTMENT 1 BACKWALL"

```

```

        AREA 13.006
        I11 2.5200
        I22 0.63000
        I33 315.89
        DENSITY 23.563
        E 2.2408E+07
WALL 'Type 2' "ABUTMENT 5 BACKWALL"
        AREA 13.285
        I11 2.5600
        I22 0.64000
        I33 333.16
        DENSITY 23.563
        E 2.2408E+07
C
C ** BENT CAP PROPERTIES **
C
        CAP 'Type 1'
        AREA 2.7220
        I11 889.00
        I22 889.00
        I33 0.88900
        DENSITY 23.563
        E 2.2408E+07
C
C --- ABUTMENT DATA ---
C
        ABUTMENT STATION 0.00
        BEARING -
            S 85 38 0 W -
            N 78 30 0 W
        ELEV TOP 418.11 AT ABUT 1
        ELEV WALL BOTTOM 415.12 AT ABUT 1
        ELEV TOP 427.62 AT ABUT 5
        ELEV WALL BOTTOM 424.60 AT ABUT 5
        CONNECTION PIN AT ABUT 1 5
        WALL 'Type 1' AT ABUTMENT 1
        WALL 'Type 2' AT ABUTMENT 5
C
C ---- BENT DATA ----
C
        BENT
        BEARING N 89 36 58 W, N 89 36 58 W, N 79 52 0 W
        ELEVATION TOP 421.53, 423.66, 425.96
        ELEVATION BOTTOM 408.01, 408.01, 410.14
        CAP 'Type 1' AT BENT 2 3 4
        COLUMN 'INFILL' AT BENT 2
        COLUMN SKEVED LAYOUT 'Type 1' 9.4500 'Type 1' AT BENT 3
        COLUMN SKEVED LAYOUT 'Type 1' 9.5700 'Type 1' AT BENT 4
C
C --- EXPANSION JOINT DATA ---
C
        HINGE
            AT 1 44.620 $ Data for Hinge 1
            BEARING N 89 36 58 W
            RESTRAINER NORMAL LAYOUT 'Type 1' 2.286, 7.62, 2.286 'Type 1' AT 1
C
C --- FOUNDATION STIFFNESSES ---
        FOUNDATION
            AT ABUTMENT 1
            SPRING CONSTANTS

```

```

KF1F1 980710.0
KF2F2 291878.0
KM1M1 1.356E+12
KM2M2 1.356E+12
KM3M3 1.356E+12
AT ABUTMENT 5
  SPRING CONSTANTS
    KF1F1 77348.0
    KF2F2 291878.0
    KM1M1 1.356E+12
    KM2M2 1.356E+12
    KM3M3 1.356E+12
C
C --- LOAD DATA ---
C
  LOADS
    RESPONSE SPECTRUM
      ATC5 CURVE
        SOIL TYPE 11
        ACCELERATION COEFFICIENT 0.40000
        GRAVITY 9.8070
        DAMPING COEFFICIENT 0.050000
FINISH

```

WORKED EXAMPLE - RETROFITTED

RESPONSE SPECTRUM RESULTS

VIBRATION CHARACTERISTICS

MODE	PERIOD	CS	PARTICIPATION FACTORS			% OF TOTAL MASS		
			Long	Vert	Tran	Long	Vert	Tran
1	0.727	0.71	-44.508	22.031	-3.565	49.360	12.094	0.317
2	0.539	0.87	39.793	17.654	7.838	88.816	19.859	1.848
3	0.444	0.99	10.037	1.221	-44.675	91.326	19.897	51.578
4	0.320	1.00	1.213	1.431	0.270	91.362	19.948	51.580
5	0.267	1.00	3.269	16.783	-0.185	91.628	26.966	51.581
6	0.242	1.00	4.808	43.297	-0.192	92.204	73.576	51.582
7	0.227	1.00	12.317	2.492	-1.797	95.984	73.831	51.662
8	0.197	1.00	-4.682	-1.764	0.881	96.531	73.909	51.681
9	0.159	1.00	2.036	0.160	30.945	96.634	73.909	75.542
10	0.147	1.00	-0.275	-0.995	0.923	96.636	73.934	75.564
11	0.131	1.00	-5.077	17.580	0.819	97.278	81.635	75.580
12	0.121	1.00	2.717	-5.041	0.418	97.462	82.268	75.585

ABUTMENT CRC DISPLACEMENTS

	LEFT FACE....	RIGHT FACE....		...OPWNG/CLSNG...	
ITEM	LC	LNGTUDNL	TRNSVRSE	LNGTUDNL	TRNSVRSE	LNGTUDNL	TRNSVRSE
ABU 1	1	0.013	0.001	0.013	0.001	0.000	0.000
	2	0.002	0.000	0.002	0.000	0.000	0.000
	3	0.014	0.001	0.014	0.001	0.000	0.000
	4	0.006	0.001	0.006	0.001	0.000	0.000
ABU 5	1	0.059	0.011	0.059	0.011	0.000	0.000
	2	0.008	0.002	0.008	0.002	0.000	0.000
	3	0.061	0.012	0.061	0.012	0.000	0.000
	4	0.026	0.005	0.026	0.005	0.000	0.000

SPAN HINGE CRC DISPLACEMENTS

	LEFT FACE....	RIGHT FACE....		...OPWNG/CLSNG...	
ITEM	LC	LNGTUDNL	TRNSVRSE	LNGTUDNL	TRNSVRSE	LNGTUDNL	TRNSVRSE
S I H1	1	0.045	0.001	0.063	0.001	0.023	0.000
	2	0.005	0.006	0.009	0.006	0.004	0.000
	3	0.047	0.003	0.065	0.003	0.024	0.000
	4	0.019	0.006	0.028	0.006	0.011	0.000

*** LOAD CASE/COMB	DESCRIPTION
1	Longitudinal
2	Transverse
3	1.0*Long + 0.3*Trans
4	0.3*Long + 1.0*Trans

WORKED EXAMPLE - RETROFITTED

CQC COLUMN FORCES

		LNGITUDNL....	TRANSVRSE....			
CL	LOC	LC	SHEAR	MOMENT	SHEAR	MOMENT	AXIAL	TORSION
BNT 2								
1	BOT	1	1695.9	11124.	2294.7	30816.	4708.4	167.4
		2	212.3	1448.	13045.0	174563.	680.9	628.8
		3	1759.6	11559.	6208.2	83185.	4912.7	356.0
		4	721.1	4786.	13733.5	183808.	2093.4	679.0
1	TOP	1	1419.5	10278.	2282.3	308.	4704.1	167.4
		2	151.7	1084.	12838.0	664.	680.2	628.8
		3	1465.0	10603.	6133.7	507.	4908.2	356.0
		4	577.6	4167.	13522.7	756.	2091.4	679.0
BNT 3								
1	BOT	1	518.1	3936.	114.7	861.	651.8	36.1
		2	70.1	514.	458.8	3371.	744.4	111.7
		3	539.1	4090.	252.3	1873.	875.1	69.7
		4	225.5	1695.	493.2	3629.	939.9	122.6
1	TOP	1	427.3	3573.	79.8	701.	649.7	36.1
		2	54.4	471.	297.6	2740.	743.0	111.7
		3	443.6	3714.	169.1	1523.	872.6	69.7
		4	182.6	1543.	321.6	2950.	937.9	122.6
2	BOT	1	502.5	3818.	127.6	930.	759.1	36.2
		2	106.2	772.	450.8	3330.	497.9	111.7
		3	534.3	4049.	262.9	1929.	908.4	69.7
		4	256.9	1918.	489.1	3609.	725.6	122.6
2	TOP	1	414.2	3463.	92.7	833.	757.1	36.2
		2	74.0	668.	291.2	2667.	497.0	111.7
		3	436.4	3663.	180.1	1633.	906.2	69.7
		4	198.3	1707.	319.0	2917.	724.1	122.6
BNT 4								
1	BOT	1	518.5	3955.	86.3	638.	396.8	35.8
		2	71.8	535.	382.9	2837.	570.9	161.6
		3	540.0	4116.	201.1	1489.	568.1	84.3
		4	227.4	1722.	408.8	3028.	690.0	172.4
1	TOP	1	427.3	3638.	56.4	527.	396.0	35.8
		2	53.7	477.	242.8	2267.	569.9	161.6
		3	443.4	3781.	129.2	1207.	567.0	84.3
		4	181.9	1568.	259.7	2425.	688.7	172.4
2	BOT	1	515.9	3936.	83.8	624.	198.6	35.8
		2	95.4	719.	383.2	2839.	580.5	161.6
		3	544.5	4152.	198.8	1476.	372.8	84.3
		4	250.1	1900.	408.4	3026.	640.1	172.4
2	TOP	1	425.2	3620.	53.6	499.	197.6	35.8
		2	67.8	604.	243.1	2271.	579.4	161.6
		3	445.5	3801.	126.5	1180.	371.4	84.3
		4	195.4	1689.	259.1	2420.	638.7	172.4

*** LOAD CASE/COMB	DESCRIPTION
1	Longitudinal
2	Transverse
3	1.0*Long + 0.3*Trans
4	0.3*Long + 1.0*Trans

WORKED EXAMPLE - RETROFITTED

ABUTMENT CQC FORCES

ITEM	LC	VERT SHEAR	W/R TO BRIDGE C.L.		W/R TO ITEM C.L.	
			LONGITUDNL	TRANSVERSE	NORMAL	PARALLEL
ABU 1	1	5298.8	12691.7	292.5	12661.0	928.9
	2	1108.9	2448.9	2509.3	2407.5	2549.0
	3	5631.5	13426.3	1045.2	13383.3	1693.6
	4	2698.5	6256.4	2597.0	6205.8	2827.6
ABU 5	1	580.6	4499.1	2213.0	4612.6	1965.4
	2	152.3	2073.8	8645.8	658.5	8866.6
	3	626.3	5121.2	4806.7	4810.2	4625.4
	4	326.5	3423.5	9309.7	2042.3	9456.2

SPAN HINGE CQC FORCES

ITEM	LC	VERT SHEAR	W/R TO BRIDGE C.L.		W/R TO ITEM C.L.	
			LONGITUDNL	TRANSVERSE	NORMAL	PARALLEL
S 1 HI	1	4409.9	9404.6	283.8	9404.5	287.1
	2	541.4	1829.6	4216.7	1829.2	4216.9
	3	4572.3	9953.5	1548.8	9953.2	1552.2
	4	1864.3	4650.9	4301.9	4650.6	4303.0

SPAN HINGE RESTRAINER CQC FORCES

RES	LC	AXIAL
SPN 1 - JNT 1		
1	1	2489.5
	2	993.6
	3	2787.5
	4	1740.5
2	1	2435.0
	2	649.9
	3	2630.0
	4	1380.4
3	1	2276.7
	2	952.1
	3	2562.3
	4	1635.1
4	1	2236.9
	2	1327.4
	3	2635.1
	4	1998.5

*** LOAD CASE/COMB	DESCRIPTION
1	Longitudinal
2	Transverse
3	1.0*Long + 0.3*Trans
4	0.3*Long + 1.0*Trans

APPENDIX F: EXAMPLE PROBLEM 5.2: COMPONENT CAPACITY-DEMAND EVALUATION OF A MULTISPAN SIMPLY-SUPPORTED STEEL GIRDER BRIDGE

F.1. INTRODUCTION

This example problem illustrates the evaluation of a multiple span, simply-supported steel girder bridge using the Component Capacity-Demand method described in section 5.4 (Method C). Two cases are analyzed for the bridge: Case 1 assumes the bridge is located where the long-period spectral acceleration for the upper level earthquake (S_1) is 0.16g, and Case 2 assumes this acceleration is 0.26g.

F.2. DESCRIPTION OF THE EXAMPLE BRIDGE

The example bridge is part of the L.R. 767-5 bridge over L.R. 22019 in Dauphin County, Pennsylvania. The bridge contains several simple steel beam spans and several continuous spans. A plan and elevation of the portion of the bridge studied in this example is shown in figure F-1. Pier 2 is evaluated in detail in this example, and is shown in figure F-2.

The bridge was built in 1968 and rehabilitated 10 years ago to give an anticipated service life of at least 50 years. It is considered to be an essential bridge. The bearings are of the steel rocker type. Two 32 mm anchor bolts per bearing are used to connect the bearing shoes to the bent cap. Both piers 1 and 2 are founded on rock.

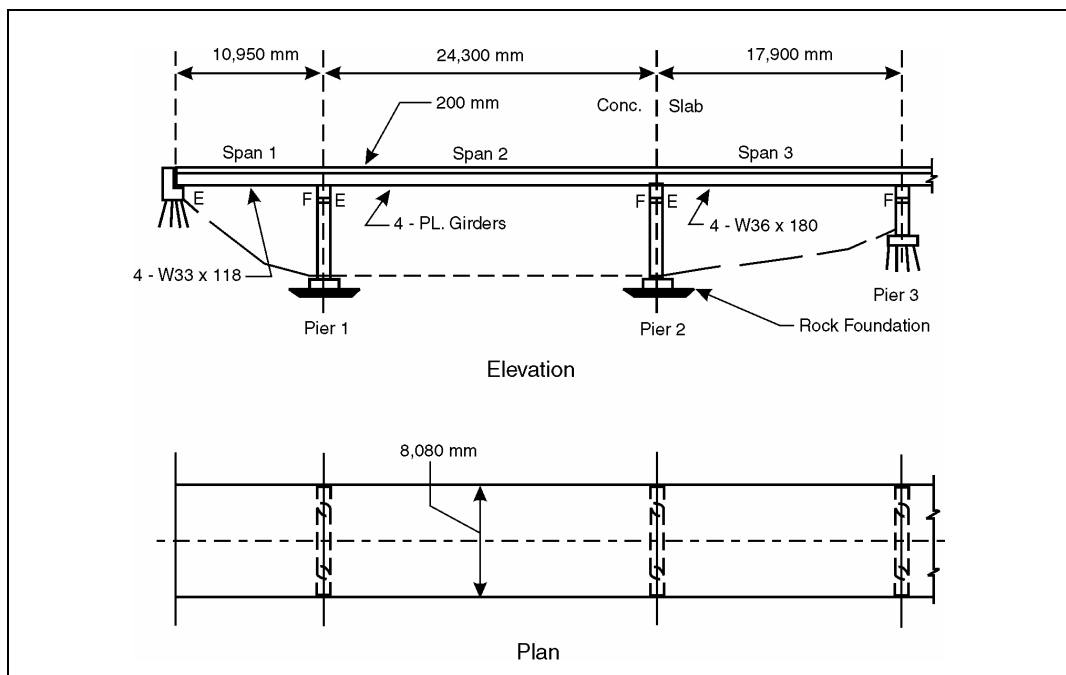


Figure F-1. Plan and elevation of example bridge.

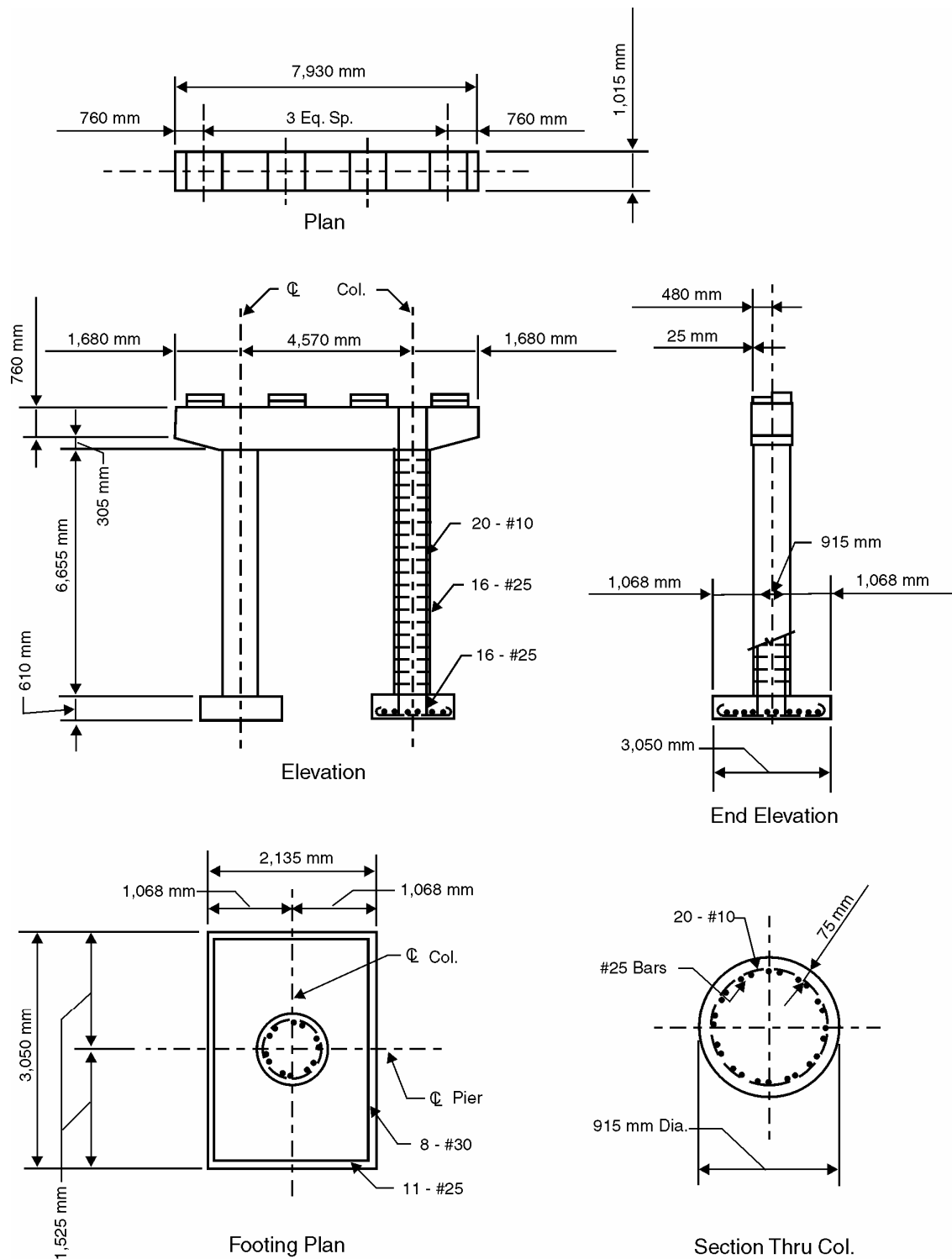


Figure F-2. Pier 2 bent details.

F.3. BRIDGE EVALUATION

F.3.1. SEISMIC RETROFIT CATEGORIES

Based on the estimated 50-year service life, the Service Life Category is ASL 3 (table 1-1). Since the bridge is ‘essential’, the performance level is PL2 (table 1-2), for the upper earthquake level. The Site Class is B, for which $F_v = 1.0$ (table 1-4(b)). The Seismic Retrofit Category is determined using the procedure given in section 1.6, and the results are summarized in table F-1.

F.3.2. COMPONENTS FOR CAPACITY/DEMAND RATIO EVALUATION

Case 1

Based on table 5-2 the components that must be evaluated are the bearings (support length and forces) and the potential for liquefaction.

Case 2

Based on table 5-2, the components that must be evaluated include the bearings (support length and forces), the reinforced concrete column bents and their footings (anchorage, splices, shear, and confinement), and the potential for liquefaction.

Table F-1. Seismic retrofit categories for upper level earthquake ($F_v=1.0$, PL2).

Case	Long-Period Spectral Acceleration, Upper Level Earthquake, S_1	Seismic Coefficient $S_{D1} = F_v S_1$	Seismic Hazard Level SHL (table 1-5)	Seismic Retrofit Category SRC (table 1-6)
1	0.16	0.16	II	B
2	0.26	0.26	III	C

F.3.3. ANALYSIS PROCEDURE

Case 1

Based on table 1-9, analysis is not required for this case. Minimum capacity checks are performed instead.

Case 2

Based on table 1-9 and recommendations in section 5.1.1, Method C is chosen (Component Capacity-Demand Method) and since the bridge is regular, the Uniform Load Method is used to obtain elastic demands.

F.3.4. UNIFORM LOAD METHOD FOR CASE 2

F.3.4.1. Structural Data - Pier 2

Column diameter	D	=	915 mm
Column area	A	=	$660 \times 10^3 \text{ mm}^2$
Column moment of inertia	I	=	$34.5 \times 10^9 \text{ mm}^4$
Bent cap area	A_c	=	$1,100 \times 10^3 \text{ mm}^2$
Bent cap moment of inertia	I_c	=	$103 \times 10^9 \text{ mm}^4$
Modulus of elasticity	E	=	$26 \times 10^3 \text{ MPa}$
Weight of span 2	W_{sp2}	=	1,920 kN
Average weight of spans 2+3	$W_{sp2,3}$	=	1,530 kN

F.3.4.2. Longitudinal Earthquake Loading

The expansion rocker bearings provide very little resistance to longitudinal movements and most of the longitudinal load will be transferred to the fixed end of the span. Span 2 will most likely move as a rigid body and its movement will be resisted by the longitudinal stiffness of pier 2. The weight distribution along the span is uniform and, if the response of each simple span is assumed to be independent of the other spans, the natural period in the longitudinal direction may be computed as follows:

Longitudinal Stiffness of Bent 2 Acting as a Cantilever:

$$K_L = (2) \frac{3EI}{H_L^3} = (2) \frac{(3)(26 \times 10^3 \text{ MPa})(34.5 \times 10^9 \text{ mm}^4)}{(7,700 \text{ mm})^3} = 11.8 \text{ kN/mm}$$

Note that uncracked section properties are used due to an anticipated overdesign of the columns.

Fundamental Period of Pier 2 in the Longitudinal Direction:

$$T_L = 2\pi \sqrt{\frac{W_L}{K_L g}} = 2\pi \sqrt{\frac{1,920 \text{ kN}}{(11.8 \text{ kN/mm})(9,810 \text{ mm/sec}^2)}} = 0.81 \text{ sec}$$

Seismic Coefficient (figure 1-8):

$$C_s = S_{D1}/T$$

Thus

$$C_s = 0.16/0.81 = 0.20 \text{ for Case 1 } (S_{D1} = 0.16)$$

$$C_s = 0.26/0.81 = 0.32 \text{ for Case 2 } (S_{D1} = 0.26)$$

F.3.4.3. Transverse Earthquake Loading

Since the superstructure comprises several simple spans sitting on rocker type bearings, the in-plane continuity effect of the spans is neglected. Thus the natural period of pier 2 in the transverse direction is computed as a stand-alone pier based on the stiffness of the pier and the tributary mass of the superstructure from spans 2 and 3.

Transverse Stiffness of Pier 2 Acting Alone:

The transverse stiffness of pier 2 was obtained from a plane frame model of analysis by computing the horizontal displacement of the cap due to a unit horizontal load and then taking its inverse.

$$K_T = 54 \text{ kN/mm}$$

The transverse stiffness of the bent may also be approximated by assuming a rigid cap and fixed end conditions:

$$K_T' = (2) \frac{12 EI}{H_T^3} = (2) \frac{(12)(26 \times 10^3 \text{ MPa})(34.5 \times 10^9 \text{ mm}^4)}{(7,200 \text{ mm})^3} = 58 \text{ kN/mm}$$

which yields a value about 9 percent higher.

Fundamental Period of Pier 2 in the Transverse Direction:

$$T_T = 2 \pi \sqrt{\frac{W_T}{K_T g}} = 2 \pi \sqrt{\frac{1.53 \text{ kN}}{(54 \text{ kN/mm})(9,810 \text{ mm/sec}^2)}} = 0.34 \text{ sec}$$

Seismic Coefficient (figure 1-8):

$$C_s = S_{D1}/T$$

$$\begin{aligned} \text{Thus } C_s &= 0.16/0.34 = 0.47 \text{ for Case 1 } (S_{D1} = 0.16) \\ C_s &= 0.26/0.34 = 0.76 \text{ for Case 2 } (S_{D1} = 0.26) \end{aligned}$$

F.4. CAPACITY/DEMAND RATIO FOR BEARINGS FOR CASE 1

F.4.1. DISPLACEMENT CAPACITY/DEMAND RATIO (CASE 1)

The available support length is:

$$N(c) = 430 \text{ mm (This is the length from the end of the girder to the edge of the cap.)}$$

The minimum support length using equation 5-1a, for Case 1 ($S_{D1} = 0.16$) is given by:

$$N(d) = (100 + 41 + 53 + 166) 1.2 = 432 \text{ mm}$$

The displacement capacity/demand ratio is:

$$r_{bd} = \frac{N(c)}{N(d)} = \frac{430}{432} = 1.0 \text{ *****}$$

F.4.2. FORCE CAPACITY/DEMAND RATIO (CASE 1)

Bearing failure may be caused by shearing of the anchor bolts, sliding along the rotation pin in the transverse direction, or shifting over the rotation pin in the longitudinal direction.

Shearing of Anchor Bolts

The shear capacity of the anchor bolts is:

$$V_b(c) = (2)(4)(800 \text{ mm}^2)(186 \text{ MPa}) = 1,200 \text{ kN}$$

The minimum bearing force demand is 25 percent of the dead load:

$$V_b(d) = (0.25)(1,920 \text{ kN}) = 480 \text{ kN}$$

The anchor bolts C/D ratio is:

$$r_{bf} = \frac{V_b(c)}{V_b(d)} = \frac{1,200}{480} = 2.5 \text{ *****}$$

Sliding of Bearing Along the Rotation Pin

If a coefficient of friction of 0.25 is assumed, the C/D ratio is given by:

$$r_{bf} = \frac{V_b(c)}{V_b(d)} = \frac{0.25}{0.47} = 2.5 \text{ *****}$$

F.5. POTENTIAL FOR LIQUEFACTION IN CASE 1

Since pier 2 is founded on rock, there is no potential for liquefaction.

Thus, the governing force C/D ratio is 0.53 for Case 1.

F.6. CAPACITY/DEMAND RATIO FOR BEARINGS FOR CASE 2

The rocker type bearings are vulnerable to earthquakes and they may suffer damage even during a moderate earthquake.

F.6.1. DISPLACEMENT CAPACITY/DEMAND RATIO (CASE 2)

Method 1

The available support length is:

$$N(c) = 430 \text{ mm} \quad (\text{This is the length from the end of the girder to the edge of the cap.})$$

The minimum support length using equation 5-1a, for Case 2 ($S_{D1} = 0.26$) is:

$$N(d) = (100 + 41 + 53 + 166) 1.325 = 477 \text{ mm}$$

The displacement C/D ratio is:

$$r_{bd} = \frac{N(c)}{N(d)} = \frac{430}{477} \approx 0.9 \text{ *****}$$

Method 2

The available capacity of the expansion bearing for movement is:

$$\Delta_s(c) = 430 \text{ mm}$$

The maximum possible movement resulting from temperature changes is:

$$\Delta_i(d) = (11.7 \times 10^{-6})(42^\circ\text{C})(24,300 \text{ mm}) = 1 \text{ mm}$$

The maximum calculated relative displacement in the longitudinal direction for Case 2 ($S_{D1} = 0.32$) is:

$$\Delta_{eq}(d) \approx (2)(0.32)(1,920 \text{ kN})/(11.8 \text{ kN/mm}) = 104 \text{ mm}$$

This is conservatively estimated by assuming completely out-of-phase motion at the two adjacent piers; i.e., $\Delta_{eq}(d)$ has been increased by a factor of 2.

The displacement C/D ratio is:

$$r_{bd} = \frac{\Delta_s(c) - \Delta_i(d)}{\Delta_{eq}(d)} = \frac{430 - 1}{104} = 4.0 > 1.0 \text{ *****}$$

Thus, the lowest displacement C/D ratio is 0.9 by Method 1, but may be replaced by the more realistic result from Method 2, to obtain the governing value (4.0).

F.6.2. FORCE CAPACITY/DEMAND RATIO (CASE 2)

Bearing failure may be caused by shearing of the anchor bolts, sliding along the rotation pin in the transverse direction, or shifting over the rotation pin in the longitudinal direction.

Shearing of Anchor Bolts

The longitudinal seismic force demand per anchor bolt for $C_s = 0.32$ is:

$$V_{b(d)_l} = (1.25)(0.32)(1,920 \text{ kN})/8 = 96 \text{ kN}$$

The transverse seismic force demand per anchor bolt for $C_s = 0.76$ is:

$$V_{b(d)_t} = (1.25)(0.76)(1,530 \text{ kN})/16 = 91 \text{ kN}$$

The combined seismic force demand per anchor bolt for this case is:

$$V_{b(d)_c} = \sqrt{(96)^2 + [(0.3)(91)]^2} = 100 \text{ kN} \text{ *****}$$

The anchor bolt C/D ratio is:

$$r_{bf} = \frac{V_{b(c)}}{V_{b(d)_c}} = \frac{150}{100} = 1.5 \text{ *****}$$

Sliding of Bearing Along the Rotation Pin

If a coefficient of friction of 0.25 is assumed the C/D ratio is given by:

$$r_{bf} = \frac{V_{b(c)}}{V_{b(d)}} = \frac{0.25}{0.76} = 0.33 \text{ *****}$$

Thus, the governing force C/D ratio is 0.33 for Case 2.

F.7. CAPACITY/DEMAND RATIOS FOR PIER 2 FOR CASE 2

The C/D ratio computations for pier 2 are shown in the following pages. The computations include derivation of the column interaction surface, the footing interaction surface in the transverse and the longitudinal direction (see figures F-3, F-4, and F-5), plastic hinge analysis for the transverse direction, seismic elastic load analysis, ultimate moment capacity calculations based on seismic axial loads, and a C/D ratio evaluation for the bent.

Note that these results have been computed using SEISAB, which does not allow the direct input of S_{D1} , nor does it use the spectral shape specified in figure 1-8. Instead an Acceleration Coefficient, A , is used and the seismic coefficient is calculated using $C_s = 1.2 AS/T^{2/3}$ for the spectral shape. For rock, $S = 1$ and therefore C_s at $T = 1.0 \text{ sec} = 1.2 A$. Hence values of $A = 0.1$

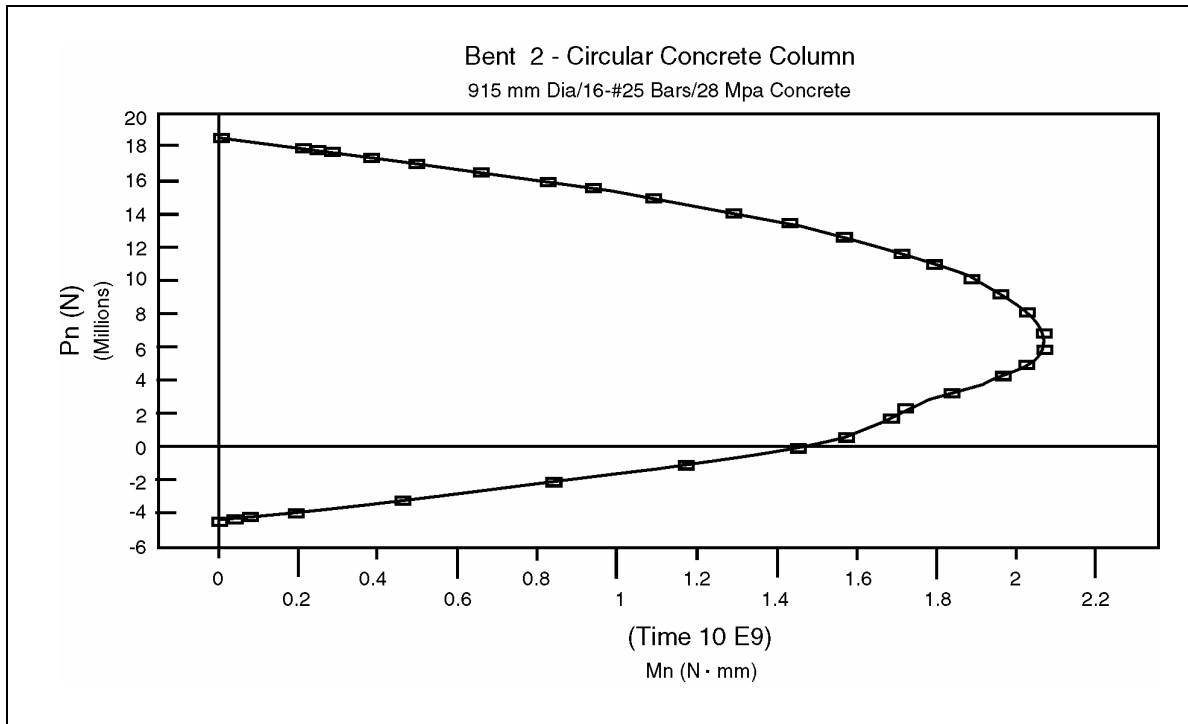


Figure F-3. Column interaction diagram.

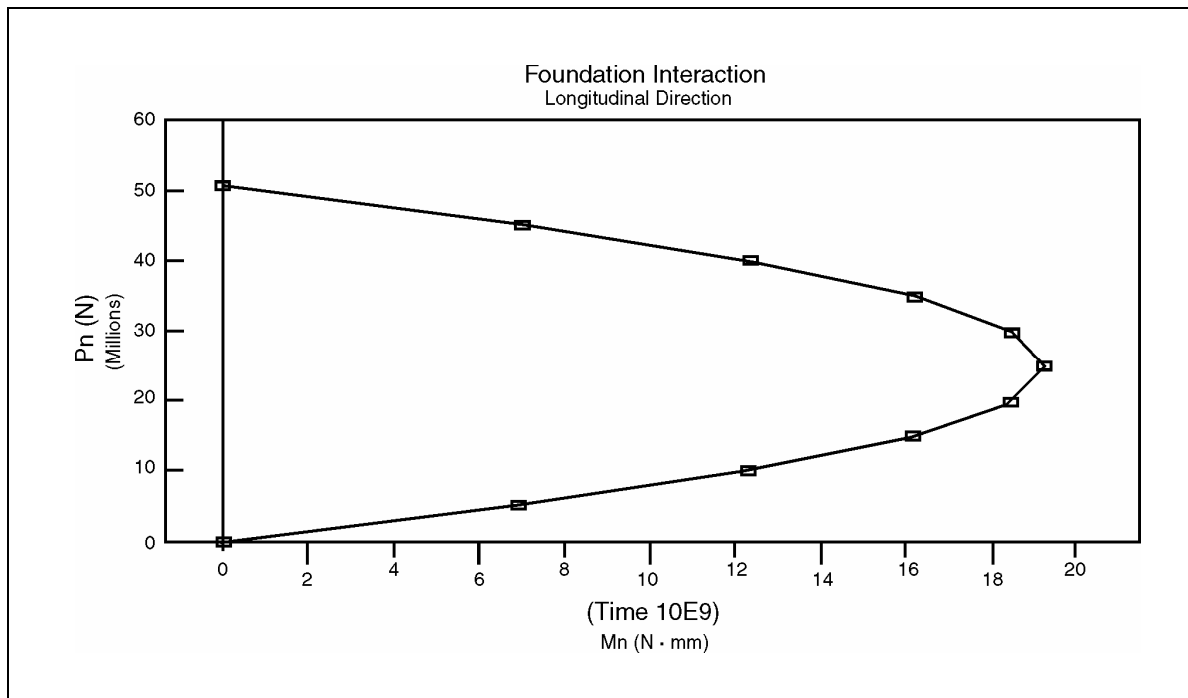


Figure F-4. Foundation interaction diagram.

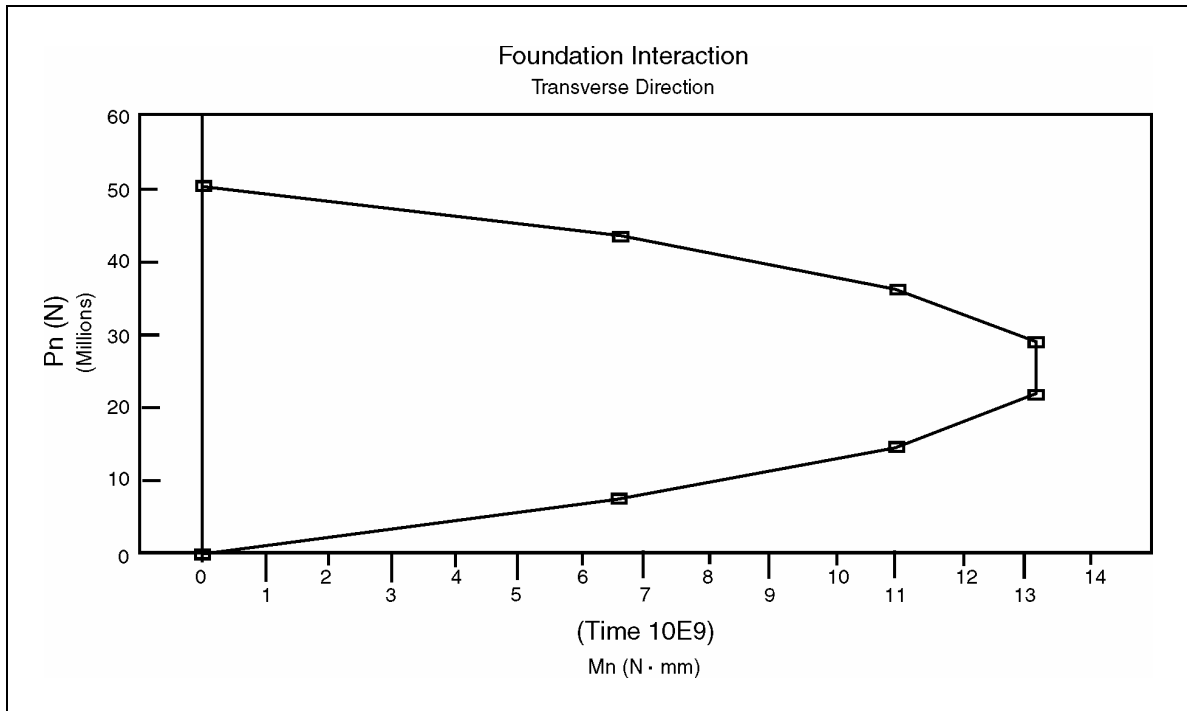


Figure F-5. Foundation interaction diagram - transverse direction.

and 0.2, give seismic coefficients very close to the S_{DI} values of 0.16 and 0.26 respectively. Thus values of $A = 0.1$ and 0.2 have been used to obtain the attached output.

The plastic hinge analysis in the transverse direction shows that the capacity of the bent is limited by uplift of the column footing sitting on rock foundation, before any hinge mechanism can form. Low axial compression load in a column can significantly reduce the C/D ratio at the base of the footing since the resistance to rotation provided by the foundation rock is dependent on the existence of compression stresses at the interface.

In the longitudinal direction, the acceleration coefficient (A) of 0.1 yields C/D ratios of greater than 1.0. When A is 0.2, C/D ratios less than 1.0 are obtained. The limiting factor is also the resistance to rotation provided by the foundation rock. This condition is caused by the relatively large moment arm to foundation width ratio. Thus, for an acceleration coefficient of 0.2, the assumption of column base fixity used in the computation of the natural period is not adequate. A partial column base fixity assumption would be more appropriate for both the longitudinal and the transverse direction. This would increase the fundamental periods, lower the seismic demand, and further increase the column C/D ratios. For all cases, the seismic elastic loads are relatively low. Due to the limited capacity for uplift and rotation provided by the foundation rock, flexural yielding of the columns is not expected. Thus, the assumption of uncracked column section properties used is applicable in this case. In addition, only the C/D ratios for anchorage, splices of longitudinal reinforcement, and column shear need to be evaluated (see figure D-3). The anchorage of the reinforcing bars is satisfactory. The minimum splice length for the longitudinal reinforcement is provided; however, the C/D ratio for the splices is less than $0.75 r_{ec}$ and therefore a value of $0.75 r_{ec}$ is applicable. Also, since the columns do not yield, the

C/D ratio for column shear is given by the ratio of initial shear resistance of the undamaged column to the maximum calculated elastic shear force, which is greater than 1.0.

F.8. POTENTIAL FOR LIQUEFACTION IN CASE 2

Since pier 2 is founded on rock, there is no potential for liquefaction.

WORKED EXAMPLE PROBLEM 2, CASE II
CAPACITY/DEMAND RATIO CALCULATION WORKSHEET FOR BENT 2

DEAD LOAD FORCES AND BENT GEOMETRY

DEAD LOAD AXIAL FORCES

@ TOP OF COLUMN:	$866 \times 10^3 \text{ N}$
@ BOTTOM OF COLUMN:	$978 \times 10^3 \text{ N}$
@ BASE OF FOOTING	$1085 \times 10^3 \text{ N}$

BENT GEOMETRY

COLUMN HEIGHT	6655 mm
COLUMN SPACING	4570 mm
COLUMN TOP TO C.G. OF SUPERSTRUCTURE	3050 mm
FOOTING DEPTH	610 mm

INTERACTION DIAGRAMS FOR THE COLUMN AND THE FOOTING

COLUMN INTERACTION DIAGRAM

$P_n \text{ (N} \times 10^3\text{)}$	$M_n \text{ (N.mm} \times 10^3\text{)}$
18584	0
17735	205531
17669	237959
17568	276372
17302	376154
16973	495056
16499	655684
15968	821891
15580	934981
15010	1088461
14198	1281265
13486	1428294
12730	1563952
11774	1708812
11108	1793233
10256	1883542
9379	1956146
8266	2023423
7088	2065866
6114	2068055
5190	2023481
4437	1967479
3385	1835830
2502	1717142
1802	1685934
681	1571139
0	1454484
-1002	1171526
-2045	842134
-3164	461098
-3892	191738
-4164	77660
-4261	35062
-4339	0

FOOTING INTERACTION DIAGRAM

TRANSVERSE DIRECTION

$P_n \text{ (N} \times 10^3\text{)}$	$M_n \text{ (N.mm} \times 10^3\text{)}$
0	0
7209	6590160
14418	10983600
21627	13180320
28836	13180320
36045	10983600
43254	6590160
50463	0

LONGITUDINAL DIRECTION

$P_n \text{ (N} \times 10^3\text{)}$	$M_n \text{ (N.mm} \times 10^3\text{)}$
0	0
5046	6919668
10093	12301632
15139	16145892
20185	18452448
25232	19221300
30278	18452448
35324	16145892
40370	12301632
45417	6919668
50463	0

WORKED EXAMPLE PROBLEM 2, CASE II
CAPACITY/DEMAND RATIO CALCULATION WORKSHEET FOR BENT 2

PLASTIC HINGE ANALYSIS FOR THE TRANSVERSE DIRECTION

OVERSTRENGTH MOMENT CAPACITY

1. OVERSTRENGTH MOMENT CAPACITY AT DEAD LOAD AXIAL LOADS

	DL AXIAL LOAD (N * 10 ³)	Mn (N.mm * 10 ³)	1.3*Mn (N.mm * 10 ³)
TOP OF COLUMN	866	1590083	2067108 HINGE
BOTTOM OF COLUMN	978	1601524	2081982
BASE OF FOOTING	1085	1145422	1489049 HINGE

2. TOTAL COLUMN SHEAR FORCE

$$V_u = 978 \times 10^3 \text{ N}$$

$$V_u = 768 \times 10^3 \text{ N} \quad \text{<-----ADJUSTED TO AVOID FOOTING UPLIFT, ASSUMING NO TENSION CAPACITY BETWEEN FOOTING AND ROCK.}$$

3. COLUMN AXIAL FORCE DUE TO OVERTURNING

$$\text{AXIAL FORCE} = 1556 \times 10^3 \text{ N} \quad > 1085 \text{ N} \times 10^3 = \text{DEAD LOAD AT BASE OF FOOTING}$$

$$\text{AXIAL FORCE} = 1082 \times 10^3 \text{ N} \quad \text{<-----ADJUSTED TO AVOID FOOTING UPLIFT}$$

REVISED OVERSTRENGTH MOMENT CAPACITY

1. OVERSTRENGTH MOMENT CAPACITY AT DEAD LOAD AXIAL LOADS PLUS OVERTURNING

	DL +/- OVERTURN (N * 10 ³)	Mn (N.mm * 10 ³)	1.3*Mn (N.mm * 10 ³)
TOP OF COLUMN (+)	1948	1692459	2200197 HINGE
TOP OF COLUMN (-)	-216	1393589	1811666 HINGE
BOTTOM OF COLUMN (+)	2060	1697441	2206674 HINGE
BOTTOM OF COLUMN (-)	-104	1425139	1852680
BASE OF FOOTING (+)	2167	2211811	2875354
BASE OF FOOTING (-)	0	0	0 HINGE

2. TOTAL COLUMN SHEAR FORCE

$$V_u = 933 \times 10^3 \text{ N WITHIN 10\% OF PREVIOUS } V_u$$

3. AXIAL FORCE DUE TO OVERTURNING

$$\text{AXIAL FORCE} = 1500 \times 10^3 \text{ N} > 1085 \times 10^3 \text{ N} = \text{DEAD LOAD AT BASE OF FOOTING}$$

FOOTING UPLIFT OCCURS FIRST.

NOTE: FOOTING UPLIFT GOVERNS AND THERE IS NO HINGE MECHANISM.

WORKED EXAMPLE PROBLEM 2, CASE II
CAPACITY/DEMAND RATIO CALCULATION WORKSHEET FOR BENT 2

CALCULATED SEISMIC AXIAL LOADS

TRANSVERSE DIRECTION

FOR A=0.1

TOP OF COLUMN (+)	$500 \times 10^3 \text{ N}$
TOP OF COLUMN (-)	$-500 \times 10^3 \text{ N}$
BOTTOM OF COLUMN (+)	$500 \times 10^3 \text{ N}$
BOTTOM OF COLUMN (-)	$-500 \times 10^3 \text{ N}$
BASE OF FOOTING (+)	$500 \times 10^3 \text{ N}$
BASE OF FOOTING (-)	$-500 \times 10^3 \text{ N}$

FOR A=0.2

TOP OF COLUMN (+)	$1000 \times 10^3 \text{ N}$
TOP OF COLUMN (-)	$-1000 \times 10^3 \text{ N}$
BOTTOM OF COLUMN (+)	$1000 \times 10^3 \text{ N}$
BOTTOM OF COLUMN (-)	$-1000 \times 10^3 \text{ N}$
BASE OF FOOTING (+)	$1000 \times 10^3 \text{ N}$
BASE OF FOOTING (-)	$-1000 \times 10^3 \text{ N}$

LONGITUDINAL DIRECTION

FOR A=0.1 AND A=0.2

TOP OF COLUMN (+)	$0 \times 10^3 \text{ N}$
TOP OF COLUMN (-)	$0 \times 10^3 \text{ N}$
BOTTOM OF COLUMN (+)	$0 \times 10^3 \text{ N}$
BOTTOM OF COLUMN (-)	$0 \times 10^3 \text{ N}$
BASE OF FOOTING (+)	$0 \times 10^3 \text{ N}$
BASE OF FOOTING (-)	$0 \times 10^3 \text{ N}$

WORKED EXAMPLE PROBLEM 2, CASE II
CAPACITY/DEMAND RATIO CALCULATION WORKSHEET FOR BENT 2

ULTIMATE MOMENT CAPACITY AT DEAD LOAD AXIAL FORCES PLUS THE SEISMIC AXIAL LOADS

TRANSVERSE DIRECTION

FOR A=0.1

	DL +/- EQ (N * 10 ³)	Mn (N.mm * 10 ³)
TOP OF COLUMN (+)	1366	1641297
TOP OF COLUMN (-)	366	1517213
BOTTOM OF COLUMN (+)	1478	1652739
BOTTOM OF COLUMN (-)	478	1536333
BASE OF FOOTING (+)	1585	1637202
BASE OF FOOTING (-)	585	616630

FOR A=0.2

	DL +/- EQ (N * 10 ³)	Mn (N.mm * 10 ³)
TOP OF COLUMN (+)	1366	1688798
TOP OF COLUMN (-)	-134	1416776
BOTTOM OF COLUMN (+)	1978	1693780
BOTTOM OF COLUMN (-)	-22	1448325
BASE OF FOOTING (+)	2085	2131639
BASE OF FOOTING (-)	85	90496

LONGITUDINAL DIRECTION

FOR A=0.1 AND A=0.2

	DL AXIAL FORCE (N * 10 ³)	Mn (N.mm * 10 ³)
TOP OF COLUMN (+)	866	1590083
TOP OF COLUMN (-)	866	1590083
BOTTOM OF COLUMN (+)	978	1601524
BOTTOM OF COLUMN (-)	978	1601524
BASE OF FOOTING (+)	1085	1617427
BASE OF FOOTING (-)	1085	1617427

WORKED EXAMPLE PROBLEM 2, CASE II
CAPACITY/DEMAND RATIO CALCULATION WORKSHEET FOR BENT 2

SUMMARY OF MAXIMUM ELASTIC MOMENT DEMANDS

A=0.1

LOADING	LOCATION	COMPONENT	LONG. MOMENT (N * 10 ³)		TRANSEVERSE MOMENT (N.mm * 10 ³)		TOTAL MOMENT (N.mm * 10 ³) DEMAND
			EQ	DL	EQ	DL	
CASE 1	TOP	COLUMN	1110	0	198478	197323	520736
	BOTTOM	COLUMN	4291	0	214343	98485	1344385
	BASE	FOOTING	4560	0	249328	123536	1438678
CASE 2	TOP	COLUMN	333	0	661592	197323	864894
	BOTTOM	COLUMN	1287	0	714476	98485	902642
	BASE	FOOTING	1368	0	831092	123536	1041674

A=0.2

LOADING	LOCATION	COMPONENT	LONG. MOMENT (N * 10 ³)		TRANSEVERSE MOMENT (N.mm * 10 ³)		TOTAL MOMENT (N.mm * 10 ³) DEMAND
			EQ	DL	EQ	DL	
CASE 1	TOP	COLUMN	2221	0	396955	197323	900665
	BOTTOM	COLUMN	8582	0	428686	98485	2667574
	BASE	FOOTING	9120	0	498655	123536	2847839
CASE 2	TOP	COLUMN	666	0	1323185	197323	1534004
	BOTTOM	COLUMN	2574	0	1428953	98485	1717117
	BASE	FOOTING	2736	0	1662185	123536	1970755

WORKED EXAMPLE PROBLEM 2, CASE II
CAPACITY/DEMAND RATIO CALCULATION WORKSHEET FOR BENT 2

ULTIMATE MOMENT CAPACITY/ELASTIC MOMENT DEMAND RATIOS

A=0.1

		LONGITUDINAL DIRECTION 100% + TRANSVERSE DIRECTION 30% (N.mm * 10 ³)		
LOAD	LOCATION	ELASTIC	NOMINAL	CAPACITY/DEMAND
CASE		DEMAND	CAPACITY	RATIO
1	TOP OF COLUMN (+)	520736	1590083	3.05 rec
1	TOP OF COLUMN (-)	520736	1590083	3.05 rec
1	BOTTOM OF COLUMN (+)	1344385	1601524	1.19 rec
1	BOTTOM OF COLUMN (-)	1344385	1601524	1.19 rec
1	BASE OF FOOTING (+)	1438678	1617427	1.12 ref
1	BASE OF FOOTING (-)	1438678	1617427	1.12 ref

		TRANSVERSE DIRECTION 100% + LONGITUDINAL DIRECTION 30% (N.mm * 10 ³)		
LOAD	LOCATION	ELASTIC	NOMINAL	CAPACITY/DEMAND
CASE		DEMAND	CAPACITY	RATIO
2	TOP OF COLUMN (+)	864894	1641297	1.90 rec
2	TOP OF COLUMN (-)	864894	1517213	1.75 rec
2	BOTTOM OF COLUMN (+)	902642	1652739	1.83 rec
2	BOTTOM OF COLUMN (-)	902642	1536333	1.70 rec
2	BASE OF FOOTING (+)	1041674	1637202	1.57 ref
2	BASE OF FOOTING (-)	1041674	616630	0.59 ref

A=0.2

		LONGITUDINAL DIRECTION 100% + TRANSVERSE DIRECTION 30% (N.mm * 10 ³)		
LOAD	LOCATION	ELASTIC	NOMINAL	CAPACITY/DEMAND
CASE		DEMAND	CAPACITY	RATIO
1	TOP OF COLUMN (+)	900669	1590083	1.77 rec
1	TOP OF COLUMN (-)	900669	1590083	1.77 rec
1	BOTTOM OF COLUMN (+)	2667577	1601524	0.60 rec
1	BOTTOM OF COLUMN (-)	2667577	1601524	0.60 rec
1	BASE OF FOOTING (+)	2847844	1617427	0.57 ref
1	BASE OF FOOTING (-)	2847844	1617427	0.57 ref

		TRANSVERSE DIRECTION 100% + LONGITUDINAL DIRECTION 30% (N.mm * 10 ³)		
LOAD	LOCATION	ELASTIC	NOMINAL	CAPACITY/DEMAND
CASE		DEMAND	CAPACITY	RATIO
2	TOP OF COLUMN (+)	1534002	1688798	1.10 rec
2	TOP OF COLUMN (-)	1534002	1416776	0.92 rec
2	BOTTOM OF COLUMN (+)	1717116	1693780	0.99 rec
2	BOTTOM OF COLUMN (-)	1717116	1448325	0.84 rec
2	BASE OF FOOTING (+)	1970756	2131639	1.08 ref
2	BASE OF FOOTING (-)	1970756	90496	0.05 ref

WORKED EXAMPLE PROBLEM 2, CASE II
CAPACITY/DEMAND RATIO CALCULATION WORKSHEET FOR BENT 2

CAPACITY/DEMAND RATIO OF ANCHORAGE REINFORCEMENT

AT THE BOTTOM OF THE COLUMN

#25 BAR - 90 DEGREE HOOK

$K_m = 0.7$
 $d_b = 25 \text{ mm}$
 $f_c' = 28 \text{ MPa}$
 $f_y = 414 \text{ MPa}$
 $l_a(c) = 502 \text{ mm}$

$l_a(d) = 337 \text{ mm}$
 $l_a(d) = 381 \text{ mm}$
 $l_a(d) = 381 \text{ mm}$ USED

$502 \text{ mm} > 381 \text{ mm}$
 $l_a(c) > l_a(d)$

CASE 8 APPLIES

NO TOP REINFORCING BARS AT TOP OF FOOTING
AND HOOK OUTWARDS

DETAIL 2 APPLIES

$rca = 1.3 \text{ ref } \leq 1.0$

AT THE TOP OF THE COLUMN

#25 BAR - STRAIGHT

$K_s = 10208.33$
 $K_{tr} = 0$
 $d_b = 25 \text{ mm}$
 $f_c' = 28 \text{ MPa}$
 $f_y = 414 \text{ MPa}$
 $C = 76 \text{ mm}$
 $l_a(c) = 914 \text{ mm}$

$l_a(d) = 482 \text{ mm}$
 $l_a(d) = 762 \text{ mm}$
 $l_a(d) = 762 \text{ mm}$ USED

$914 \text{ mm} > 762 \text{ mm}$
 $l_a(c) > l_a(d)$

CASE 8 APPLIES

DETAIL 6 APPLIES

$rca = 1.0$

WORKED EXAMPLE PROBLEM 2, CASE II
CAPACITY/DEMAND RATIO CALCULATION WORKSHEET FOR BENT 2

CAPACITY/DEMAND RATIO FOR COLUMN SHEAR

SINCE THE COLUMNS DO NOT YIELD, THE CAPACITY/DEMAND RATIO
CAN BE CALCULATED AS FOLLOWS:

1. ELASTIC SHEAR DEMAND

	LONG	TRANS	CASE 1	CASE 2	
A=0.1	135	191	146	196	(N * 10 ³)
A=0.2	269	383	293	391	(N * 10 ³)
Ve(d) =	196 N * 10 ³ A=0.1				
Ve(d) =	391 N * 10 ³ A=0.2				

2. INITIAL SHEAR CAPACITY

fc' =	28 MPa
fy =	414 MPa
Ag =	656708 mm ²
d =	737 mm
S =	305 mm
Atr =	258 mm ²
Vi(c) =	831 N * 10 ³

3. CAPACITY/DEMAND RATIO FOR COLUMN SHEAR

rcv =	4.25	A=0.1
rcv =	2.12	A=0.2

CAPACITY/DEMAND RATIO FOR SPLICE

s =	305 mm
ls =	838 mm
fc' =	28 MPa
fy =	414 MPa
fyt =	276 MPa
db =	25 mm
Ab =	510 mm ²
Atr(d) =	278 mm ²

SINCE THE CLEAR SPACING BETWEEN SPLICES 114 mm > 4db = 102 mm:
Atr(c) = 129 mm²

Atr(c) < Atr(d), CASE A APPLIES.

r_{cs} = 0.00 rec <= 0.46 rec

SINCE ls=838 mm IS GREATER THAN MINIMUM SPLICE LENGTH 763 mm:

r_{cs} = 0.75 rec CONTROLS

Glossary

Anticipated Service Life (ASL) – An estimate of the remaining life of a bridge based on current age, structural condition, specification used for design, and capacity to handle current and future traffic. The ASL may be taken as the expected life of a *new* bridge (75 years, AASHTO 1998) less the age of the bridge under consideration.

Arching – One of the mechanisms by which a bridge deck distributes lateral loads to the abutments, by acting as an arch in the plane of the deck spanning from one abutment to the other. If expansion joints occur within the superstructure, arching action cannot develop until all of these joints are closed.

Bolster – A structural addition to the face of a cap beam or abutment seat that extends the support length for the superstructure. Bolsters are usually dowelled to beam or seat to assist the transfer of forces and moments across the interface. In some cases a bolster may be used as an overlay. See Overlay.

Bridge Rank – A numerical index which indicates the seismic vulnerability of a bridge. It is based on the structural vulnerability of the bridge (seismic deficiencies) and the site hazard. The rating ranges from 0 to 100; the higher the number the greater the vulnerability.

Bumper Block – A steel bracket attached to the underside of a steel stringer that will restrict longitudinal movement of the bridge superstructure in the event of excessive motion. The superstructure will be free to move until the block impacts the abutment.

Capacity / Demand (C/D) Ratio – The ratio of the capacity of a member (or bridge system) to the seismic demand on that member (or bridge system). Ratios less than 1.0 indicate members or systems needing consideration for retrofitting. In this Manual, C/D ratios are developed for bending moments, shear and axial forces, displacements, and rotations.

Capacity Protected Design – A design methodology that protects selected components and/or members of a bridge from excessive seismic forces by the yielding of adjacent components and/or members. For example, the maximum shear that can be transmitted to a footing by a column is determined by the flexural capacity of the column, i.e., the column's yield strength. In other words, the footing is protected by the capacity of the column, and need only be designed for the forces that can be transmitted by the column when at yield (including the effect of any overstrength in the column). See Capacity Protected Element.

Capacity Protected Element – An element of a bridge that is protected from excessive seismic forces by the yielding of an adjacent element in the same load path. See Capacity Protected Design.

Capacity Spectrum Design – A design procedure that combines demand and capacity analyses in one step, usually through the use of a capacity spectrum which plots spectral acceleration against spectral displacement (e.g., total base shear against structure displacement).

Central and Eastern United States – The Central and Eastern U.S. is generally considered to be those states east of the Rocky Mountains.

Collateral Seismic Hazard – A seismic hazard other than direct ground shaking e.g. ground failure (slumping, settlement), liquefaction, fault rupture, landslide and the like.

Complete Quadratic Combination (CQC) – A statistical rule for combining individual modal responses of a bridge subject to earthquake loads so as to obtain the maximum response to be used for design. See Multimode Spectral Analysis Method.

Design Strength – This is the strength of a member after making allowance for approximations in calculations and variations in material strengths, workmanship, and dimensions. Each of these factors may be within tolerable limits but in combination may result in a capacity that is less than the nominal strength. A strength reduction factor, which is always less than unity, is used to relate the design strength to the nominal strength.

Dowel – A short bar of steel used to assist the transfer of shear between a structural overlay or bolster and an existing concrete member.

Ductile Elements – Members or components of a bridge that are expected to undergo significant inelastic deformations while maintaining their strength and stability.

Energy Dissipation Device – A mechanical device that dissipates energy during an earthquake and limits bridge movements to acceptable levels. Energy is typically dissipated by plastically deforming a metal such as lead or steel, employing friction, or moving a viscous fluid through an orifice.

Essential Bridge – A bridge that is needed to continue functioning immediately after an earthquake, or one which crosses a route that is expected to remain open immediately following an earthquake. Any bridge not classified as *essential* is said to be a *standard* bridge.

Exempt Bridge – A bridge may be exempt from retrofitting if it is located in the lowest seismic zone, or has limited remaining useful life. Temporary bridges and those closed to traffic, may also be exempt.

Expected Damage Method - One of three methods used to determine the seismic vulnerability rating of a bridge in the screening and prioritization of bridges for retrofitting. This method compares the severity of expected damage for each bridge in the inventory, for the same earthquake. Severity of damage is measured either by the damage state(s) sustained or by the estimated direct economic losses.

Expected Strength – This is the strength of a member or component after making allowance for the fact that actual material strengths are generally greater than the specified strengths. For example, the yield strength of steel may be 20 percent higher than the specified strength, and concrete strength may be 30 percent higher the specified strength, or even greater with age and/or confinement. Expected strengths can be found from routine testing of material samples taken from existing bridges, but if these are not available, they are based on previous experience

with the same materials in other bridges. An expected strength factor (ϕ_e) is used to relate the expected strength to the nominal strength, where ϕ_e is always greater than unity.

Fragility Curve – A graph that indicates the probability of a bridge sustaining a particular degree of damage when subject to a given level of ground shaking.

Indices Method – One of three methods used to determine the seismic vulnerability rating of a bridge in the screening and prioritization of bridges for retrofitting. Indices for both structure vulnerability and hazard level range from 0 to 10, and their product is used to give the Bridge Rank. These indices are based on conservative, semi-empirical rules. See Bridge Rank.

Lateral Ground Movement – This seismically induced movement is a permanent offset in the ground and usually occurs due to one or more of the collateral hazards. See Collateral Seismic Hazards, and Liquefaction-Induced Lateral Flow.

Liquefaction – A seismically induced loss of shear strength in loose, cohesionless soil that results from a build-up of pore water pressure in the soil as it tries to consolidate during strong ground shaking.

Liquefaction-Induced Lateral Flow – A lateral displacement of a relatively flat slope that occurs under the combination of gravity load and excess pore water pressure due to liquefaction. This flow can occur without earthquake inertial loading and often continues well after the cessation of ground shaking.

Lower Level Earthquake Ground Motion – A small earthquake that has a reasonable probability of occurrence within the life of the bridge (assumed to be 75 years). This ground motion may also be called the frequent earthquake, the expected earthquake (NCHRP 12-49 - ATC/MCEER 2003), or the functional evaluation earthquake (FEE) (Caltrans *Seismic Design Methodology* (Caltrans 1999)). Rather than assign a probability of occurrence, it is common practice to use a probability of exceedance to characterize the motion. Accordingly, the lower level motion has a relatively high probability of exceedance within the life of a bridge and a figure of 50 percent is recommended for retrofit design, which corresponds to a return period of about 100 years.

Minimum Seat Width – The minimum prescribed width of a beam seat that must be provided to avoid loss of support to the superstructure.

Multi-mode Spectral Analysis Method – A linear dynamic analysis of a two- or three-dimensional model of a bridge, that is used when more than one mode of vibration contributes significantly to the dynamic response of the bridge. The method gives peak design values for moment, shear, and displacement by combining modal maxima. See CQC Method and SRSS Method.

Network Redundancy - A measure of route availability that considers the presence of alternate routes and detour lengths. Network redundancy is used in the prioritization of bridges for retrofitting (along with Bridge Rank), and for defining bridge importance.

Nominal strength – This strength is obtained from failure theory for a section of the member or component and is based on assumed section geometry and specified material strengths. Material resistance factors are taken as 1.0 for the calculation of this strength. Other strength levels are usually referenced to the nominal strength.

Overlay – A reinforced concrete slab added to the face of an existing structural element to increase its strength or stiffness, such as a footing overlay. Overlays are usually dowelled to the existing element to assist transfer of forces and moments across the interface. In some cases an overlay may be used as a bolster. See Bolster.

Overstrength – The strength of a member that takes into account all possible factors contributing to an increase in strength above the nominal value. These include but are not limited to: steel strength higher than the specified yield strength; additional steel strength due to strain hardening at large deformations; concrete strength higher than specified; section sizes larger than assumed; axial compression in flexural members due to lateral restraint; additional reinforcement placed for construction purposes and not accounted for in design; and conservative assumptions made in the derivation of the equations for nominal strength. An overstrength factor (ϕ_o), is used to relate the *overstrength* to the *nominal strength*, and is always greater than unity.

Performance-Based Design – A design philosophy that explicitly provides for different levels of bridge performance for earthquakes of different sizes, according to the importance of the bridge and its anticipated service life.

Performance Level (PL) or Performance Criteria – A level of performance, expressed in terms of post-earthquake service and damage, that is expected to be achieved during and immediately following an earthquake of a specified size.

Plastic Hinge – The region of a structural member, which undergoes flexural yielding and plastic rotation without loss of strength or stability.

Probability of Exceedance – The likelihood that an earthquake, larger than the one under consideration, will occur within a specific time frame, usually taken to be the life of a bridge. This same likelihood can also be described by an annual probability of occurrence, or a return period expressed in years.

R-Factor (Response Modification Factor) – Factors used to modify the element demands from an elastic analysis to account for ductile behavior and obtain design demands.

Reference Bridge – A bridge that is a ‘long’ structure with no appreciable three-dimensional effects present; used for creating bridge fragility curves.

Restrainer – A cable or steel rod used to limit the relative displacement at a movement joint in a bridge superstructure to decrease the likelihood of the superstructure becoming unseated at that joint during an earthquake.

Retrofit Priority – The priority assigned to a bridge for detailed evaluation and possible retrofitting, based on bridge rank and such qualitative factors as importance, network

redundancy, non-seismic deficiencies, remaining useful life, and relevant socio-economic issues. See Bridge Rank.

Seismic Hazard Level (SHL) – Used to describe the severity of the seismic and geotechnical hazard at a bridge site for the purpose of detailed evaluation and retrofitting. Four levels are defined in this Manual based on the short- and long-period spectral accelerations (S_s and S_1) for the upper level earthquake and corresponding site factors.

Seismic Hazard Rating (E) – Used to describe the severity of the seismic and geotechnical hazard at a bridge site for the purpose of screening and prioritization. The rating is based on the long-period spectral acceleration (S_1) for the upper level earthquake and the corresponding site factor, and ranges from low (0) to high (10). See Bridge Rank.

Seismic Isolator – A mechanical device that uncouples a bridge from earthquake ground motions by adding flexibility and lengthening the period of vibration. Seismic forces are reduced due to the longer period, but isolator displacements may be very large. To limit these displacements, energy dissipation devices are sometimes used in parallel with seismic isolators. Typical isolators include elastomeric and sliding systems. See Energy Dissipation Devices.

Seismic Retrofitting Category (SRC) – Used to recommend minimum screening requirements, evaluation methods and retrofitting measures for deficient bridges. Four categories are defined in this Manual, which are determined by the anticipated service life, importance, and the seismic and geotechnical hazards at the site.

Seismic Risk Assessment Method - One of three methods that may be used to determine the seismic vulnerability rating of a bridge. Explicit analysis of a highway network is performed for a given hazard level and the resulting damage states used to estimate system performance as measured by traffic flow (e.g., increased travel times). Sensitivity of this performance to bridge condition is subsequently used to determine bridge retrofit needs and priorities.

Shock Transmission Unit (STU) – A device installed across a movement joint in a superstructure that allows very slow movement to occur, such as that caused by temperature change, but ‘locks up’ under rapid motion. An STU is typically composed of a piston and cylinder filled with a viscous fluid.

Site Class – Used to classify a site according to the properties of the soil as measured by shear wave velocities, blow counts, layer depths and thicknesses.

Site Factors – Two site factors are defined: F_a and F_v . F_a is determined by the site class and the short-period spectral acceleration (S_s) for the upper level earthquake. F_v is determined by the site class and the long-period spectral acceleration (S_1) for the upper level earthquake. These factors are used to account for soil amplification of bedrock ground motions when determining the design response spectrum at the surface.

Square Root of the Sum of the Squares (SRSS) Combination – This classical statistical combination rule is used in three ways in this Manual: (1) for the combination of individual modal responses to obtain design maxima in a multimode spectral analysis; (2) for the combination of forces resulting from two or three orthogonal ground motion components; and

(3) for establishing orthogonal moments in the biaxial design of a column. See Multimode Spectral Analysis Method.

Starter Bar – Reinforcing steel that extends from a footing a short distance into a column. The main longitudinal reinforcing steel in the column is then lapped (spliced) with these starter bars. Lapping or splicing rebar in plastic hinge zones is not recommended and is a common seismic deficiency in many older bridges. It is another name for a footing dowel.

STRAHNET – The defense highway network. This network is a subset of the National Highway System and provides connecting routes to military installations, industries and resources.

Uniform Risk – Used to describe the methodology for characterizing the seismic hazard in the United States. In this approach, the same probability of exceedance (return period) is used from one region to another to specify the hazard. In a country where the seismicity varies from low to high, this approach is considered to be more rational than using the maximum historical event for each region, which may have a very low probability of occurrence.

Upper Level Earthquake Ground Motion – A large earthquake that has a finite, but remote, probability of occurrence within the life of the bridge. This ground motion may also be called the *rare earthquake*, *maximum considered earthquake (MCE)* (NCHRP 12-49 - ATC/MCEER 2003) or the *safety evaluation earthquake (SEE)* (Caltrans *Seismic Design Methodology* (Caltrans 1999)). In this manual, the upper level motion has a 7 percent probability of exceedance in 75 years, which corresponds to a return period of about 1,000 years.

Vulnerability Rating (V) – Used to describe the severity of the seismic deficiencies in a bridge for the purpose of screening and prioritization. The rating is based on structural and geotechnical deficiencies and ranges from low (0) to high (10). See Bridge Rank.

REFERENCES

- Abo-Shadi, N., Saiidi, M., and Sanders, D., 2000, *Seismic Response of Reinforced Concrete Pier Walls in the Weak Direction*, Technical Report MCEER 00-0006, Multidisciplinary Center for Earthquake Engineering Research, University at Buffalo.
- Abrahamson, N.A., 1985, *Estimation of Seismic Wave Coherency and Rupture Velocity Using the SMART 1 Strong Motion Array Recordings*, Report EERC/UCB/85-02, Earthquake Engineering Research Center.
- Abrahamson, N.A., 1992, *Spatial Variation of Earthquake Ground Motion for Application to Soil-Interaction*, TR-100463, Electric Power Research Institute.
- Abrahamson, N.A., 1993, *Non-stationary Spectral Matching Program: RSPMATCH* (unpublished).
- Abrahamson, N.A. and Silva, W.J., 1997, "Empirical Response Spectral Attenuation Relations for Shallow Crustal Earthquakes," *Seismological Research Letters*, Volume 68, Number 1, pp. 94-127.
- Abrahamson, N.A., Schneider, J.F., and Stepp, J.C., 1991, "Empirical Spatial Coherency Functions for Application to Soil-Structures Interaction Analyses, *Earthquake Spectra*, Volume 7, pp. 1-27.
- Aiken, I.D., Nims, D.K., Whittaker, A.S. and Kelley, J.M., 1993, "Testing of Passive Energy Dissipation Systems," *Earthquake Spectra*, August, 1993, pp. 335-370.
- Akimoto, T., Hakajima, H. and Kogure, F., 1990, "Seismic Strengthening of Reinforced Concrete Bridge Piers on Metropolitan Expressway," *First U.S.-Japan Workshop on Seismic Retrofit of Bridges*, Tsukuba Science City, Japan, December 17-18, 1990, pp. 280-298.
- Alfawakhiri, F. and Bruneau, M., 2000, "Flexibility of Superstructures and Supports in the Seismic Analysis of Simple Bridges," *Journal of Earthquake Engineering and Structural Dynamics*, Volume 29, Number 5, pp. 711-729.
- Amari, K., Hanno, H., Otsuka, K. and Fujimoto, Y., 1994, "Seismic Reinforcement of Existing Reinforced Concrete Piers," *Second U.S.-Japan Workshop on Seismic Retrofit of Bridges*, Public Works Research Institute (Japan) and Federal Highway Administration, January 20-21.
- AASHTO, 1983 *Guide Specifications for the Seismic Design of Highway Bridges*, American Association of State Highway and Transportation Officials, Washington, DC, 106 pp.
- AASHTO, 1998, *LRFD Bridge Design Specifications*, Second Edition, American Association of State Highway and Transportation Officials, Washington, DC.

AASHTO, 1999, *Guide Specifications for Seismic Isolation Design*, Second Edition, American Association of State Highway and Transportation Officials, Washington, DC.

AASHTO, 2002, *Standard Specifications for Highway Bridges, Division I-A: Seismic Design*, 17th Edition, American Association of State Highway and Transportation Officials, Washington, DC.

American Concrete Institute (ACI), 2002, *Design and Construction of Externally Bonded FRP Systems for Strengthening Concrete Structures*, ACI 440, 2R-02, 45 p.

American Society of Civil Engineers (ASCE), 1997, *Ground Improvement, Ground Reinforcement, Ground Treatment, Developments 1987 – 1997*, Geotechnical Special Publication No. 69, ASCE, New York, 616 pp.

American Society for Testing and Materials (ASTM), 1998, *Soil and Rock*, American Society for Testing and Materials, v. 4.08, March.

American Society for Testing and Materials (ASTM), 2003, *Standard Test Method for Performing Electronic Friction Cone and Piezocone Penetration Testing of Soils*, D5778-95(2000), ASTM International.

Andrus, R.D. and Chung, R.M., 1995, *Ground Improvement Techniques for Liquefaction Remediation Near Existing Lifelines*, Report NISTIR 5714, National Institute of Standards and Technology, Gaithersburg, MD, 74 pp.

Applied Technology Council (ATC), 1983, *Seismic Retrofitting Guidelines for Highway Bridges*, Report ATC-6-2, Redwood City, California.

Applied Technology Council (ATC), 1996, *Improved Seismic Design Criteria for California Bridges: Provisional Recommendations*, Report ATC-32, Redwood City, California.

ATC/MCEER, 1998, *Major LRFD Seismic Design Criteria Issues*, NCHRP 12-49 Interim Report, Multidisciplinary Center for Earthquake Engineering Research/Applied Technology Council Joint Venture.

ATC/MCEER, 2003, *Recommended LRFD Guidelines for the Seismic Design of Highway Bridges, Specifications and Commentary*, Applied Technology Council/Multidisciplinary Center for Earthquake Engineering Research Joint Venture, MCEER-ATC 49.

Aquino, W., Hawkins, N.M. and Lange, D.A., 2004, “Moisture Distribution in Partially Enclosed Concrete,” *ACI Materials Journal*, July/August.

Arulanandan, K. and Zeng, X., 1994, “Mechanism of Flow Slide-Experimental Results of Model No. 6,” *Proceedings of International Conference on Verification of Numerical Procedures for the Analysis of Soil Liquefaction Problems*, Arulanandan and Scott (eds.), Davis, California, October 17-20, Volume 2, A. A. Balkema, Rotterdam, The Netherlands, pp. 1543-1551.

Ayyub, B.M. and McCuen, R.H., 1997, *Probability, Statistics and Reliability for Engineers*, CRC Press, Boca Raton, FL.

Baez, J.I., 1995, *A Design Model for the Reduction of Soil Liquefaction by Vibro-Stone Columns*, Ph.D. Thesis, University of Southern California.

Baez, J.I., and Martin, G.R., 1995, "Permeability and Shear Wave Velocity to Vibro Replacement Stone Columns," *Soil Improvement for Earthquake Hazard Mitigation*, Geotechnical Special Publication No. 49, ASCE, pp. 66-81.

Balakrishnan, A., Kutter, B.L., and Idriss, I.M., 1998, "Remediation and Apparent Shear Strength of Lateral Spreading Centrifuge Models," *Proceedings of the Fifth Caltrans Seismic Research Workshop*, Sacramento, California, June.

Bartlett, S.F. and Youd, T.L., 1992, *Empirical Analysis of Horizontal Ground Displacement Generated by Liquefaction Induced Lateral Spreads*, Technical Report NCEER 92-0021, National Center for Earthquake Engineering Research, University at Buffalo.

Basoz, N., and A.S. Kiremidjian, 1997, *Evaluation of Bridge Damage Data from the Loma Prieta and Northridge, CA Earthquakes*, Technical Report No. 127, John A. Blume Earthquake Engineering Center, Civil Engineering Department, Stanford University, Stanford, California (also Multidisciplinary Center for Earthquake Engineering Research Technical Report 98-0004).

Basoz, N., and Mander, J.B., 1999, *Enhancement of the Highway Transportation Lifeline Module in HAZUS*, Final Pre-Publication Draft (#7) prepared for the National Institute of Building Sciences, March 31.

Bergman, D.M. and Hanson, R.D., 1993, "Viscoelastic Mechanical Damping Devices Tested at Real Earthquake Displacements," *Earthquake Spectra*, August 1993, pp. 389-418.

Benjamin, J.R. and Cornell, C.A., 1970, *Probability, Statistics and Decision for Civil Engineers*, McGraw Hill, NY, 684 pp.

Berrill, J.B., Christensen, S.A., Keenan, R.J., Okada, W., and Pettinga, J.R., 1997, "Lateral-spreading Loads on a Piled Bridge Foundation," *Seismic Behavior of Ground and Geotechnical Structures, Proceedings, Special Technical Session on Earthquake Geotechnical Engineering*, 14th ICSMFE, A. A. Balkema, Rotterdam, pp. 173-183.

Bolt, B.A., and Gregor, N.J., 1993, *Synthesized Strong Ground Motions for the Seismic Condition Assessment of the Eastern Portion of the San Francisco Bay Bridge*, Report UCB/EERC-93.12, Earthquake Engineering Research Center, University of California, Berkeley, California.

Bonilla, M.G., 1970, "Surface Faulting and Related Effects," *Earthquake Engineering*, Prentice Hall, New York, pp. 47-74.

Boulanger, R.W. and Hayden, R.F., 1995, "Aspects of Compaction Grouting of Liquefiable Soils," *Journal of Geotechnical Engineering*, Volume 1121, Number 12, pp. 844-855.

Bozorgnia, Y., Campbell, K. and Niazi, M., 1999, "Vertical Ground Motion: Characteristics, Relationships with Horizontal Components, and Building Code Implications," *Proceedings of SMIP Seminar on Utilization of Strong-Motion Data*, San Francisco, CA, California Strong Motion Instrumentation Program, Division of Mines and Geology, p. 23-49.

Brown, D.A., Morrison, C. and Reese, L.C., 1988, "Lateral Load Behavior of a Pile Group in Sand," *Journal of Geotechnical Engineering*, ASCE, Volume 114, Number 11.

Buckle, I.G., 1991, "Screening Procedures for the Retrofit of Bridges," *Proceedings of the Third U.S. Conference on Lifeline Earthquake Engineering*, ASCE, Monograph Number 4, Technical Council on Lifeline Earthquake Engineering, pp. 156-165.

Buckle, I.G., 1994, *The Northridge, California Earthquake of January 17, 1994: Performance of Highway Bridges*, Technical Report NCEER-94-0008, National Center for Earthquake Engineering Research, University at Buffalo.

Buckle, I.G., 2003, "Application of Response Modification Technologies to the Seismic Design of Bridges" *Proceedings of the Seminar on Response Modification Technologies for Performance-Based Design*, Report ATC-17-2, Applied Technology Council, Redwood City CA.

Buckle, I.G. and Friedland, I.M., 1995, "Improved Screening Procedures for the Seismic Retrofitting of Highway Bridges," *Fourth International Bridge Engineering Conference*, Transportation Research Board, San Francisco.

BSSC, 1994, *NEHRP Recommended Provisions for Seismic Regulations for New Buildings: Part I Provisions; Part II Commentary*, Report FEMA 222A and 223A, Building Seismic Safety Council, Washington, DC.

BSSC, 1998, *NEHRP Recommended Provisions for Seismic Regulations for New Buildings and Other Structures: Part I, Provisions; Part II Commentary*, Report FEMA 302 and 303, Building Seismic Safety Council, Washington, DC.

Button, M.R., Cronin, C.J. and Mayes, R.L., 1999, *Effect of Vertical Ground Motions on the Structural Response of Highway Bridges*, Technical Report MCEER-99-0007, Multidisciplinary Center for Earthquake Engineering Research, University at Buffalo.

Caltrans, 1989, *Bridge Design Aids - Equivalent Static Analysis of Restrainers*, California Department of Transportation, Sacramento, California, pp 14-11 to 14-25.

Caltrans, 1990, "Competing Against Time," *Report to Governor George Deukmejian by the Governor's Board of Inquiry on the 1989 Loma Prieta Earthquake*, Department of General Services, North Highlands, California.

Caltrans, 1995, *Standard Specifications*, California Department of Transportation, Sacramento, California.

Caltrans, 1996, *Earthquake Retrofit Guidelines for Bridges*, Memo to Designers 20-4, California Department of Transportation, Sacramento, California.

Caltrans, 1999, *Seismic Design Methodology*, Memo to Designers 20-1, California Department of Transportation, Sacramento, California, 14 pp.

Caltrans Seismic Advisory Board Ad Hoc Committee on Soil-Foundation-Structure Interaction (CSABAC), 1999, *Seismic Soil-Foundation-Structure Interaction: Final Report*, prepared for California Department of Transportation, February.

Campbell, K., 1997, "Empirical Near-Source Attenuation Relationships for Horizontal and Vertical Components of Peak Ground Acceleration, Peak Ground Velocity, and Pseudo-absolute Acceleration Response Spectra," *Seismological Research Letters*, Volume 68, Number 1, pp. 154-179.

Campbell, K. and Bozorgnia, Y., 2000a, *Vertical Ground Motion: Characteristics, Relationship with Horizontal Component, and Building Code Implications*, prepared for California Division of Mines and Geology, Strong Motion Instrumentation Program, under Contract No. 1097-606.

Campbell, K. and Bozorgnia, Y., 2000b, "New Empirical Models for Predicting Near-Source Horizontal, Vertical and v/h Response Spectra: Implications for Design," *Proceedings of the Sixth International Conference on Seismic Zonation*, Earthquake Engineering Research Institute, Palm Springs, CA.

Chai, Y.H., Priestley, M.J.N., and Seible, F., 1991, *Flexural Retrofit of Circular Reinforced Concrete Bridge Columns by Steel Jackets*, Report Number SSRP-91/06, Department of Applied Mechanics and Engineering Sciences, University of California, San Diego.

Chai, Y.H., Priestley, M.J.N., and Seible, F., 1992, "Retrofit of Bridge Columns for Enhanced Seismic Performance," *Seismic Assessment and Retrofit of Bridges*, Report Number SSRP-91/03, Department of Applied Mechanics and Engineering Sciences, University of California, San Diego.

Chang, C.-Y., Mok, C.M., Power, M.S., and Tang, Y.K., 1991, *Analysis of Ground Response at Lotung Large-Scale Soil-Structure Interaction Experiment Site*, Report Number NP-7306-SL, Electric Power Research Institute, Palo Alto, California.

Cheng, C-T. and Mander, J.B., 1997, *Seismic Design of Bridge Columns Based on Control and Repairability of Damage*, Report MCEER-97-0013, Multidisciplinary Center for Earthquake Engineering Research, University at Buffalo.

- Cheng, C-T., Mander, J.D., and Dutta, A., 1999, *New Retrofit Paradigms for Seismic Resistant Bridge Columns*, Unpublished Technical Report, Multidisciplinary Center for Earthquake Engineering Research, University Buffalo.
- Chiou, B.S-J., Silva, W., and Power, M.S., 2002, "Vertical to Horizontal Spectral Ratios for Seismic Design and Retrofit of Bridges in Western and Eastern United States," Poster Session, Third National Seismic Conference and Workshop on Bridges and Highways, Portland, Oregon.
- Coffman, H.L., Marsh, M.L. and Brown, C.B., 1991, *Seismic Durability of Retrofitted R.C. Columns*, Washington State Department of Transportation, 1991.
- Constantinou, M.C., Kartoum, A., Reinhorn, A.M. and Bradford, P., 1992, "Sliding Isolation System for Bridges: Experimental Study," *Earthquake Spectra*, Volume 8, Number 30, pp. 321-344.
- Cooke, H.G., and Mitchell, J.K., 1999, *Guide to Remedial Measures for Liquefaction Mitigation at Existing Highway Bridge Sites*, Technical Report MCEER-99-0015, Multidisciplinary Center for Earthquake Engineering Research, University at Buffalo, 176 pp.
- Coppersmith, K.J. and Youngs, R.R., 1990, "Earthquakes and Tectonics," *Demonstration of a Risk-Based Approach to High-Level Nuclear Waste Repository Evaluation*, Report EPRI NP-7057, Electric Power Research Institute, Palo Alto, CA.
- Coppersmith, K.J., and Youngs, R.R., 2000, "Data Needs for Probabilistic Fault Displacement Hazard Analysis," *Journal of Geodynamics*, Volume 29, pp. 329-343.
- Darwish, I., Saiidi, M. and Sanders, D., 1995, "Seismic Retrofit of R/C Bridge Columns with Inadequate Bar Anchorage in Footings," *Proceedings, National Seismic Conference on Bridges and Highways*, San Diego, California, Federal Highway Administration and California Department of Transportation, December.
- Das, B.M., 1999, *Principles of Foundation Engineering Plus*, Kent Publishing Co., Fourth Edition.
- Der Kiureghan, A., 1981, "A Response Spectrum Method for Random Vibration Analysis of MDF Systems," *Earthquake Engineering and Structural Dynamics*, Volume 9, pp. 419-435.
- DesRoches, R., and Fenves, G.L., 1998, *Design Procedures for Hinge Restrainers and Hinge Seat Width for Multiple-Frame Bridges*, Technical Report MCEER-98-0013, Multidisciplinary Center for Earthquake Engineering Research, University at Buffalo.
- Dobry, R., 1995, "Liquefaction and Deformation of Soils and Foundations Under Seismic Conditions," State-of-the-Art Paper, S. Prakash (ed.), *Proceedings, Third Intl. Conf. on Recent Advances in Geotechnical Earthquake Engineering and Soil Dynamics*, St. Louis, MO, April 2-7, Volume III, pp. 1465-1490.

Dobry, R., Borchardt, R.D., Crouse, C.B., Idriss, I.M., Joyner, W.B., Power, M.S., Rinne, E.E., and Seed, R.B., 2000, "New Site Coefficients and Site Classification System Used in Recent Building Seismic Code Provisions," *Earthquake Spectra*, Volume 16, Number 1, pp. 41-67.

Dutta, A., 1999, *On Energy-based Seismic Analysis and Design of Highway Bridges*, Ph.D. Dissertation, State University of New York at Buffalo, Buffalo, NY.

Dutta, A., and Mander, J.B., 1998, "Seismic Fragility Analysis of Highway Bridges," *INCEDE-MCEER Center-to-center Workshop on Earthquake Engineering, Frontiers in Transportation Systems*, Tokyo, Japan, June.

Dutta, A., Kokorina, T. and Mander, J.B., 1999, *Experimental Study on the Seismic Design and Retrofit of Bridge Columns Including Axial Load Effects*, Technical Report MCEER-99-0003, Multidisciplinary Center for Earthquake Engineering Research, University at Buffalo.

Earthquake Engineering Research Institute (EERI), 1993, *The Scotts Mills Earthquake of March 25, 1993*, EERI Special Earthquake Reconnaissance Report, May.

Egan, J.A. and Wang, Z-L., 1991, "Liquefaction-Related Ground Deformation and Effects on Facilities at Treasure Island, San Francisco, During the 17 October 1989 Loma Prieta Earthquake," *Proceedings of the 3rd Japan-U.S. Workshop on Earthquake Resistant Design of Lifeline Facilities and Countermeasures for Soil Liquefaction*, San Francisco, California, December 17-19.

Egan, J.A., Hayden, R.F., Scheibel, L.L., Otus, M. and Servanti, G.M., 1992, "Seismic Repair at Seventh Street Marine Terminal," *Proceedings of the ASCE Grouting, Soil Improvement and Geosynthetics Conference*, Geotechnical Special Publication Number 30, Volume 2, pp. 867-878.

Electric Power Research Institute, 1993, *Guidelines for Determining Design Basis Ground Motions*, Report No. EPRI TR-102293, Electric Power Research Center, Palo Alto, California.

Elgamal, A.W., Dobry, R., Parra, E. and Yang, Z., 1998, "Soil Dilation and Shear Deformations During Liquefaction," *Proceedings 4th Intl. Conf. on Case Histories in Geotechnical Engineering*, S. Prakash (ed.), St. Louis, MO, March 8-15.

Elms, D.G. and Martin, G.R., 1979, "Factors Involved in the Seismic Design of Bridge Abutments," *Proceedings of a Workshop on Earthquake Resistance of Highway Bridges*, Applied Technology Council, Report No. ATC-6-1.

Federal Highway Administration (FHWA), 1981, *Seismic Design Guides for Highway Bridges*, FHWA-RD-81-081, Washington, DC.

Federal Highway Administration (FHWA), 1983, *Seismic Retrofitting Guidelines for Highway Bridges*, FHWA-RD-83-007, Washington, DC.

Federal Highway Administration (FHWA), 1987, *Seismic Design and Retrofit Manual*, FHWA-IP-87-6, Washington, DC.

Federal Highway Administration (FHWA), 1995, *Seismic Retrofitting Manual for Highway Bridges*, Publication No. FHWA-RD-94-052, Department of Transportation, McLean, Virginia.

Fehling, E., Pauli, W. and Bouwkamp, J.G., 1992, "Use of Vertical Shear-Links in Eccentrically Braced Frames," *Proceedings of the 10th World Conference on Earthquake Engineering*, Volume 8, A.A. Balkema, Rotterdam, The Netherlands, pp. 4475-4479.

Fiegel, G.L. and Kutter, B.L., 1994, "Liquefaction-Induced Lateral Spreading of Mildly Sloping Ground," *Journal of Geotechnical Engineering*, ASCE, Volume 120, Number 12, December, pp. 2236-2243.

Finn, W.D.L., 1991, "Assessment of Liquefaction Potential and Post Liquefaction Behavior of Earth Structures: Developments 1981-1991," State-of-the-Art Paper, *Proc. of the Second Intl. Conf. on Recent Advances in Geotechnical Earthquake Engineering and Soil Dynamics*, S. Prakash (ed.), St. Louis, MO, March 11-15, Volume II, pp. 1833-1850.

Frankel, A.D. and Leyendecker, E.V., 2001, *Seismic Hazard Curves and Uniform Hazard Response Spectra for the United States*, Open File Report 01-436, U.S. Geological Survey, CD-ROM.

Frankel, A., Mueller, C., Barnhard, T., Perkins, D., Leyendecker, E.V., Dickman, N., Hanson, S., and Hopper, M., 1996, *National Seismic Hazard Maps*, U.S. Geological Survey Open-File Report 96-532, June.

Frankel, A., Mueller, C., Barnhard, T., Perkins, D., Leyendecker, E.V., Dickman, N., Hanson, S., and Hopper, M., 1997a, *Seismic Hazard Maps for the Conterminous United States*, U.S. Geological Survey Open-File Report 97-131, 12 maps.

Frankel, A., Mueller, C., Barnhard, T., Perkins, D., Leyendecker, E.V., Dickman, N., Hanson, S., and Hopper, M., 1997b, *Seismic Hazard Maps for California, Nevada, and Western Arizona/Utah*, U.S. Geological Survey Open-File Report 97-130, 12 maps.

Frankel, A., Harmsen, S., Mueller, C., Barnard, T., Leyendecker, E.V., Perkins, D., Hanson, S., Dickman, N., and Hopper, M., 1997c, "U.S. Geological Survey National Seismic Hazard Maps: Uniform Hazard Spectra, Deaggregation, and Uncertainty," *Proceedings of the FHWA/NCEER Workshop on the National Representation of Seismic Ground Motion for New and Existing Highway Facilities*, Technical Report NCEER-97-0010, National Center for Earthquake Engineering Research, University at Buffalo, pp. 39-73.

Frankel, A.D., Mueller, C.S., Barnhard, T.P., Leyendecker, E.V., Wesson, R.L., Harmsen, S.C., Klein, F.W., Perkins, D.M., Dickman, N.C., Hanson, S.L., and Hooper, M.G., 2000, "USGS National Seismic Hazard Maps," *Earthquake Spectra*, Volume 16, Number 1, pp. 1-19.

- Franklin, A.G. and Chang, F.K., 1977, *Earthquake Resistance of Earth and Rock-Fill Dams; Permanent Displacements of Earth Embankments by Newmark Sliding Block Analysis*, Miscellaneous Paper S-71-17, Report 5, U.S. Army Waterways Experiment Station, CE, Vicksburg, MS.
- Fung, G.G., LeBeau, R.J., Klein, E.E., Belvedere, J., and Goldschmidt, A. F., 1971, *Field Investigation of Bridge Damage in the San Fernando Earthquake*, State of California, Division of Highways, Bridge Department.
- Fyfe, E.R., 1994, "The High Strength FIBERWRAP System for Retrofitting Bridge and Other Structure Columns," *Proceedings of the Third Annual Seismic Research Workshop*, California Department of Transportation, Division of Structures, Sacramento, California.
- Gadre, A., 1997, *Lateral Response of Pile-Cap Foundation Systems and Seat-Type Bridge Abutments in Dry Sand*, Ph.D. Dissertation, Dept. of Civil Engineering, Rensselaer Polytechnic Institute.
- Gasparini, D., and Vanmarcke, E.H., 1976, *SMIQKE: A Program for Artificial Motion Generation*, Department of Civil Engineering, Massachusetts Institute of Technology, Cambridge.
- Gazetas, G., 1991, "Foundation Vibrations," *Foundation Engineering Handbook*, Second Edition, edited by Hsai-Yang Fang, Van Nostrand Reinhold.
- Gazetas, G. and Mylonakis, G., 1998, "Seismic Soil-Structure Interaction: New Evidence and Emerging Issues," *Proceedings of an ASCE Specialty Conference on Geotechnical Earthquake Engineering and Soil Dynamics III*, Seattle, August 3-6, ASCE Special Publication No. 75, pp. 1119-1174.
- Gazetas, G. and Mylonakis, G., 2001, "Soil Structure Interaction Effects on Elastic and Inelastic Structures," *4th International Conference on Recent Advances in Geotechnical Earthquake Engineering and Soil Dynamics*, San Diego, March.
- Gohl, W.B., 1993, "Response of Pile Foundations to Earthquake Shaking – General Aspects of Behavior and Design Methodologies," *Seismic Soil/Structure Interaction Seminar*, Canadian Society for Civil Engineering/Vancouver Structural Engineers Group, Vancouver, May.
- Governors Board of Inquiry, 1990, *Competing Against Time*, Report on the 1989 Loma Prieta Earthquake, May.
- Grigorian, C.E., Yang, T.S. and Popov, E.P., 1993, "Slotted Bolted Connection Energy Dissipators," *Earthquake Spectra*, August, 1993, pp. 491-504.
- Gulkan, P. and Sozen, M., 1974, "Inelastic Response of Reinforced Concrete Structures to Earthquake Motions," *ACI Journal*, December.

Hall, J.F. and Scott, R.F., 1995, *Evaluation of Bridge Damage in the 1990 Luzon and 1991 Costa Rica Earthquakes*, Southern California Earthquake Center, University of Southern California.

Hamburger, R.O. and Hunt, R.J., 1997, "Development of the 1997 NEHRP Provisions Ground Motion Maps and Design Provisions" *Proceedings of the FHWA/NCEER Workshop on the National Representation of Seismic Ground Motion for New and Existing Highway Facilities* National Center for Earthquake Engineering Research, University at Buffalo, Technical Report NCEER-97-0010, pp. 75-92.

Hanson, K.L., Kelson, K.I., Angell, M.A., and Lettis, W.R., 1999, *Techniques for Identifying Faults and Determining their Origins*, Report NUREG/CR-5503, Office of Nuclear Regulatory Research, U.S. Nuclear Regulatory Commission, Washington, DC.

Hao, H., Olivera, C.S., and Penzien, J., 1989, "Multiple-Station Ground Motion Processing and Simulation Based on SMART-1 Array Data," *Nuclear Engineering and Design*, Volume 111, pp. 293-310.

Haroun, M.A., Pardoen, G.C. and Shepard, R., 1994, "Seismic Strengthening of Reinforced Concrete Bridge Pier Walls Designed to Old Standards," *Second U.S.-Japan Workshop on Seismic Retrofit of Bridges*, Public Works Research Institute Japan and Federal Highway Administration, January 20-21.

Hawkins, N.M., 2000, "Seismic Strengthening of Inadequate Length Lap Splices," *12th World Conference on Earthquake Engineering*, January 30-February 4, 2000, New Zealand Society for Earthquake Engineering: Upper Hutt, New Zealand, Paper #1755.

Hawkins, N.M., Kaspar, I.I., and Karshenas, M., 1999, "Seismic Retrofit of Poplar Street Interchange in East St. Louis," *Structures Congress*, ASCE, April, 1999.

Hayden, R.F., and Baez, J.I., 1994, "State of Practice for Liquefaction Mitigation in North America," *Proceedings of the International Workshop on Remedial Treatment of Liquefiable Soils*, Tsukuba, Japan, July 4-6.

HAZUS, 1997, *Earthquake Loss Estimation Methodology*, Technical Manual, Prepared by the National Institute of Building Sciences for Federal Emergency Management Agency.

HITEC, 1998a, *Evaluation Findings for FIP-Energy Absorption Systems L.L.C. Slider Bearings*, CERF Report, HITEC 98-05, Highway Innovative Technology Evaluation Center, Washington, DC.

HITEC, 1998b, *Evaluation Findings for Dynamic Isolation Systems Inc. Elastomeric Bearings*, CERF Report, HITEC 98-06, Highway Innovative Technology Evaluation Center, Washington, DC.

HITEC, 1998c, *Evaluation Findings for Earthquake Protection Systems Inc. Friction Pendulum Bearings*, CERF Report, HITEC 98-07, Highway Innovative Technology Evaluation Center, Washington, DC.

HITEC, 1998d, *Evaluation Findings for R.J. Watson Inc. Sliding Isolation Bearings*, CERF Report, HITEC 98-08, Highway Innovative Technology Evaluation Center, Washington, DC.

HITEC, 1998e, *Evaluation Findings for Tekton Inc. Roller Bearings*, CERF Report, HITEC 98-09, Highway Innovative Technology Evaluation Center, Washington, DC.

HITEC, 1998f, *Evaluation Findings for Tekton Inc. Steel Rubber Bearings*, CERF Report, HITEC 98-10, Highway Innovative Technology Evaluation Center, Washington, DC.

HITEC, 1998g, *Evaluation Findings for Scougal Rubber Corporation High Damping Rubber Bearings*, CERF Report, HITEC 98-11, Highway Innovative Technology Evaluation Center, Washington, DC.

HITEC, 1998h, *Evaluation Findings for Skellerup Base Isolation Elastomeric Bearings*, CERF Report, HITEC 98-12, Highway Innovative Technology Evaluation Center, Washington, DC.

HITEC, 1999a, *Summary of Evaluation Findings for the Testing of Seismic Isolation and Energy Dissipating Devices*, CERF Report, #40404, Highway Innovative Technology Evaluation Center, Washington, DC.

HITEC, 1999b, *Evaluation Findings for Enidine Inc. Viscous Damper*, CERF Report, HITEC 99-02, Highway Innovative Technology Evaluation Center, Washington, DC.

HITEC, 1999c, *Evaluation Findings for Taylor Devices Fluid Viscous Damper*, CERF Report, HITEC 99-03, Highway Innovative Technology Evaluation Center, Washington, DC.

HITEC, 1999d, *Evaluation Findings for Oiles Multiple Viscous Shear Damper (MS-Damper)*, CERF Report, HITEC 99-04, Highway Innovative Technology Evaluation Center, Washington, DC.

Hoit, M.I. and McVay, M.C., 1996, *FLPIER Users Manual*, University of Florida, Gainesville.

Holombo, J., MacCrae G., Priestley, M.J.N. and Seible, F., 1994, "Seismic Retrofitting of Steel Bridge Columns," *Proceedings of the Third Annual Seismic Research Workshop*, California Department of Transportation, Division of Structures, Sacramento, California.

Housner, G., 1990, *Competing Against Time*, Report to Governor George Deukmejian from Governor's Board of Inquiry on the 1989 Loma Prieta Earthquake, Department of General Services, North Highlands, California.

Houston, S.L., Houston, W.N. and Padilla, J.M., 1987, "Microcomputer-Aided Evaluation of Earthquake-Induced Permanent Slope Displacements," *Microcomputers in Civil Engineering*, Volume 2, pp. 207-222.

Hudson, M., Idriss, I.M., and Beikae, M., 1994, *User's Manual for QUAD4M, A Computer Program to Evaluate the Seismic Response of Soil Structures Using Finite Element Procedures and Incorporating a Compliant Base*, Center for Geotechnical Modeling, University of California, Davis.

Hynes, M.E. and Franklin, A.G., 1984, *Rationalizing the Seismic Coefficient Method*, Miscellaneous Paper GL-84-13, U.S. Army Waterways Experiment Station, Vicksburg, MS, July, 21 pp.

Idriss, I.M., 1993, *Procedures for Selecting Earthquake Ground Motions at Rock Sites*, Report No. NIST GCR 93-625, National Institute of Standards and Technology, Gaithersburg, Maryland.

Idriss, I.M., 1999, "Evaluation of CPT Liquefaction Analysis Methods Against Inclinator Data from Moss Landing," *Proceedings of the Seventh US-Japan Workshop on Earthquake Resistant Design of Lifeline Facilities and Countermeasures Against Soil Liquefaction*, Seattle, Washington, August 15-17, O'Rourke, Thomas D, et al., eds., Multidisciplinary Center for Earthquake Engineering Research, University at Buffalo, pp. 35-53.

Idriss, I.M., and Sun, J.I., 1992, *User's Manual for SHAKE91*, Center for Geotechnical Modeling, Department of Civil and Environmental Engineering, University of California, Davis, California, 13 pp. (plus Appendices).

Imbsen, R.A., 1981, *Highway Structure Damage Caused by the Trinidad-Offshore California Earthquake of November 8, 1980*, Report No. FHWA/RD-82017, FHWA, Washington, DC, December.

Ingham, J., Priestley, M.J.N. and Seible, F., 1993, "Shear Strength of Knee Joints," *Proceedings of the Second Annual Seismic Research Workshop*, California Department of Transportation, Division of Structures, Sacramento, California.

International Code Council, Inc. (ICC), 2000, *International Building Code: Building Officials and Code Administrators International, Inc.*, International Conference of Building Officials, and Southern Building Code Congress International, Inc., Birmingham, Alabama.

ICBO, 1997, *Uniform Building Code, Volume 2, Structural Engineering Design Provisions*, International Conference of Building Officials.

Ishihara, K., 1985, "Stability of Natural Deposits During Earthquakes," *Proceedings, 11th International Conference on Soil Mechanics and Foundation Engineering*, San Francisco, CA, Volume 1, p. 321-376.

Ishihara, K., 1993, "Liquefaction and Flow Failure During Earthquakes," 33rd Rankine Lecture, *Geotechnique*, Volume 43, Number. 3.

Ishihara, K., and Cubrinovski, M., 1998, "Problems Associated with Liquefaction and Lateral Spreading During Earthquakes," *Geotechnical Earthquake Engineering and Soil Dynamic III*, ASCE, Geotechnical Special Publication Number 75, Volume 1, pp. 301-312.

Itani, A., 1996, "Cyclic Behavior of Shear Links in Retrofitted Richmond-San Rafael Bridge Towers," *Third U.S.-Japan Workshop on Seismic Retrofit of Bridges*, Tsukuba Science City, Japan, December 10-11, pp. 261-268.

ITASCA, 1998, *FLAC, Fast Lagrangian Analysis of Continua, Version 3.40 User's Guide*, Itasca Consulting Group, Inc., Minneapolis, Minnesota.

Iwasaki, T., Penzien, J., and Clough, R., 1972, *Literature Survey-Seismic Effects on Highway Bridges*, Report No. 72-11, Earthquake Engineering Research Center, University of California, Berkeley, November.

Jackura, K. A., and Abghari, A., 1994, "Mitigation of Liquefaction Hazards at Three California Bridge Sites," *Proceedings, 5th U.S.-Japan Workshop on Earthquake Resistant Design of Lifeline Facilities and Countermeasures Against Soil Liquefaction*, Technical Report NCEER-94-0026, National Center for Earthquake Engineering Research, University at Buffalo, pp. 495-513.

Jibson, R.W., 1993, *Predicting Earthquake-Induced Landslide Displacements Using Newmark's Sliding Block Analysis*, Transportation Research Record 1411, National Research Council, 17 pp.

Jin, L., Saadatmanesh, H. and Ehsani, M.R., 1994, "Seismic Retrofit of Existing Reinforced Concrete Columns by Glass-Fiber Composites," *Infrastructure: New Materials and Methods of Repair, Proceedings of the Third Materials Engineering Conference*, San Diego, California, Materials Engineering Division of the American Society of Civil Engineers, November 13-16, pp. 758-763.

Jirsa, J., 1979, "Applicability to Bridges of Experimental Seismic Test Results Performed on Subassemblages of Buildings," *Proceedings of a Workshop on Earthquake Resistance of Highway Bridges*, Applied Technology Center, Report No. ATC-6-1, November, pp. 547-565.

Kasai, K. and Popov, E.P., 1986, "Cyclic Web Buckling Control for Shear Link Beams," *Journal of Structural Engineering*, ASCE, Volume 112, Number 3, pp. 505-523.

Kim, J.H and Mander, J.B., 1999, *Truss Modeling of Reinforced Concrete Shear-Flexure Behavior*, Technical Report MCEER-99-0005, Multidisciplinary Center for Earthquake Engineering Research, University at Buffalo.

Klein, F., Frankel, A., Mueller, C., Wesson, R., and Okubo, P., 1999, *Seismic Hazard Maps for Hawaii*, U.S. Geological Survey Geologic Investigations Series, <http://geohazards.cr.usgs.gov/eq/>.

Kramer, S.L., 1996, *Geotechnical Earthquake Engineering*, Prentice Hall, New Jersey.

Lam, I.P., 1994, "Soil-Structure Interaction Related to Piles and Footings," *Proceedings, Second International Workshop in Queenstown*, New Zealand, Aug. 9-12.

Lam, I.P., 2000 *Approach to Evaluate Moment Capacity of Pile Footing in Retrofit Projects*, unpublished draft technical report to the Multidisciplinary Center for Earthquake Engineering Research, University at Buffalo.

Lam, I.P., and Law, H., 2000, *Soil Structure Interaction of Bridges for Seismic Analysis*, Technical Report MCEER-00-0008, Multidisciplinary Center for Earthquake Engineering Research, University at Buffalo.

Lam, I.P. and Martin, G.R., 1986, *Seismic Design of Highway Bridge Foundations*, Volume 2, Report No. FHWA/RD-86/102, Federal Highway Administration, McLean, Virginia.

Lam, I.P., Kapuskar, M. and Chandhuri, 1998, *Modeling of Pile Footings and Drilled Shafts for Seismic Design*, Technical Report MCEER-98-0018, Multidisciplinary Center for Earthquake Engineering, University at Buffalo.

Lam, I.P., Martin, G.R., and Imbsen, R., 1991, "Modeling Bridge Foundations for Seismic Design and Retrofitting," *Transportation Research Record*, 1290.

Lee, M.K.W., and Finn, W.D.L., 1978, DESRA-2, "Dynamic Effective Stress Response Analysis of Soil Deposits with Energy Transmitting Boundary Including Assessment of Liquefaction Potential," *Soil Mechanics Series*, Number 36, Department of Civil Engineering, University of British Columbia, Vancouver, Canada, 60 pp.

Leyendecker, E.V., Frankel, A.D., and Rukstales, K.S., 2000a, "Seismic Design Parameters for Use with the 2000 International Building Code, 2000 International Residential Code," *1997 NEHRP Seismic Design Provisions, and 1997 NEHRP Rehabilitation Guidelines*: CD-ROM Published by the U.S. Geological Survey in Cooperation with the Federal Engineering Management Agency and the Building Seismic Safety Council.

Leyendecker, E.V., Hunt, R.J., Frankel, A.D., and Rukstales, K.S., 2000b, "Development of Maximum Considered Earthquake Ground Motion Maps" *Earthquake Spectra*, Volume 16, Number 1, pp. 21-40.

Li, X.S., Wang, Z.L., and Shen, C.K., 1992, *SUMDES, A Nonlinear Procedure for Response Analysis of Horizontally-layered Sites Subjected to Multi-directional Earthquake Loading*, Department of Civil Engineering, University of California, Davis.

- Lilhanand, K., and Tseng, W.S., 1988, "Development and Application of Realistic Earthquake Time Histories Compatible with Multiple-damping Design Spectra," *Proceedings of the 9th World Conference on Earthquake Engineering*, Tokyo-Kyoto, Japan, August 2-9.
- Lin, Y., Gamble, W.L. and Hawkins, N.M., 1994, *Report to ILLDOT for Testing of Bridge Piers, Poplar Street Bridge Approaches*, East St. Louis, IL, Department of Civil Engineering, University of Illinois at Urbana-Champaign.
- Lowes, L.N. and Moehle, J.P., 1994, "Shear Strength of Knee Joints," *Proceedings of the Third Annual Seismic Research Workshop*, California Department of Transportation, Division of Structures, Sacramento, California.
- Luehring, R., Dewey, B., Mejia, L., Stevens, M. and Baez, J., 1998, "Liquefaction Mitigation of Silty Dam Foundation Using Vibro-Stone Columns and Drainage Wicks – A Test Section Case History at Salmon Lake Dam," *Proceedings of the 1998 Annual Conference Association of State Dam Safety Officials*, Las Vegas, Nevada.
- Lukose, K., Gergely, P., and White, R.N., 1982, "Behavior of Reinforced Concrete Lapped Splices for Inelastic Cyclic Loading," *ACI Journal*, September-October.
- Lysmer, J., Udaka, T., Tsai, C.-F., and Seed, H.B., 1975, *FLUSH – A Computer Program for Approximate 3-D Analysis of Soil-structure Interaction Problems*, Report No. EERC 75-30, Earthquake Engineering Research Center, University of California, Berkeley.
- Mace, N., and Martin, G. R., 2000, *An Investigation of Compaction Grouting for Liquefaction Mitigation*, Unpublished Report, Multidisciplinary Center for Earthquake Engineering Research, University at Buffalo.
- Makdisi, F.I. and Seed, H.B., 1978, "Simplified Procedure for Estimating Dam and Embankment Earthquake-Induced Deformations," *Journal of Geotechnical Engineering*, ASCE, Volume 104, Number 7, pp. 849-867.
- Malley, J.O. and Popov, E.P., 1983, *Design Considerations for Shear Links in Eccentrically Braced Frames*, Report No. UBC/EERC 83-24, Earthquake Engineering Research Center, University of California, Berkeley, California.
- Mander, J.B., Priestley, M.J.N., and Park, R., 1988, "Theoretical Stress-Strain Model for Confined Concrete," *Journal of Structural Engineering*, Volume 114, Number 8, August, pp. 1804-1826.
- Mander, J.B., Mahmoodzadegan, B., Bhadra, S. and Chen, S.S., 1996a, *Seismic Evaluation of a 30-Year Old Non-Ductile Highway Bridge Pier and Its Retrofit*, Technical Report NCEER-96-0008, National Center for Earthquake Engineering Research, University at Buffalo.

Mander, J.B., Kim, J.H., and Ligozio, C.A., 1996b, *Seismic Performance of a Model Reinforced Concrete Bridge Pier Before and After Retrofit*, Technical Report NCEER-96-0009, National Center for Earthquake Engineering Research, University at Buffalo.

Mander, J.B., Kim, D-K, Chen, S.S., and Premus, G.J., 1996c, *Response of Steel Bridge Bearings to Reversed Cyclic Loading*, Technical Report NCEER-96-0014, National Center for Earthquake Engineering Research, University at Buffalo.

Mander, J.B., Dutta, A. and Goel, P., 1998a, *Capacity Design of Bridge Piers and the Analysis of Overstrength*, Technical Report MCEER-98-0003, Multidisciplinary Center for Earthquake Engineering Research, University at Buffalo, June.

Mander, J.B., Dutta, A. and Kim, J.H., 1998b *Fatigue Analysis of Unconfined Concrete Columns*, Technical Report MCEER-98-0009, Multidisciplinary Center for Earthquake Engineering Research, University at Buffalo, September.

Martin, G.R., 1998a, *Design Recommendations, Site Response and Liquefaction*, Unpublished Technical Report, Multidisciplinary Center for Earthquake Engineering Research, University at Buffalo.

Martin, G. R., 1998b, *Development of Liquefaction Mitigation Methodologies: Ground Densification Methods*, Unpublished Technical Report, National Center for Earthquake Engineering Research, University at Buffalo.

Martin, G.R., and Dobry, R., 1994, "Earthquake Site Response and Seismic Code Provisions," *NCEER Bulletin*, Volume 8, Number 4, October, pp. 1-6.

Martin, G.R., and Lam, I.P., 1995, "Seismic Design of Pile Foundations: Structural and Geotechnical Issues," *Proceedings, Third International Conference on Recent Advances in Geotechnical Earthquake Engineering and Soil Dynamics*, St. Louis, Volume 3, pp. 1491-1515.

Martin, G.R., and Lam, I.P., 2000, "Earthquake Resistant Design of Foundations: Retrofit of Existing Foundations," *Proceedings, GeoEng 2000 Conference*, Melbourne, Australia, November 19-24.

Martin, G.R. and Qiu, P., 1994, *Effects of Liquefaction on Vulnerability Assessment*, Unpublished Year One Research Report, National Center for Earthquake Engineering Research, University at Buffalo.

Martin, G.R. and Qiu, P., 2000, *Site Liquefaction Evaluation: The Application of Effective Stress Site Response Analyses*, Unpublished Research Report, Task Number 106-E-3.1 (A), Multidisciplinary Center for Earthquake Engineering Research, University at Buffalo.

Martin, G.R., Tsai, C-F., and Arulmoli, K., 1991, "A Practical Assessment of Liquefaction Effects and Remediation Needs," *Proceedings, 2nd International Conference on Recent Advances in Geotechnical Earthquake Engineering and Soil Dynamics*, St. Louis, Missouri, March 11-15.

Matasovic, N., 1993, *Seismic Response of Composite Horizontally-layered Soil Deposits*, Ph.D. Dissertation, Civil and Environmental Engineering Department, University of California, Los Angeles, 452 pp.

Matlock, H., 1970, "Correlations for Design of Laterally Loaded Piles in Soft Clay," 2nd *Offshore Technology Conference*, Houston, Volume 1, pp. 579-594.

Matlock, H., Foo, S.H.C., and Bryant, L.M., 1978, "Simulation of Lateral Pile Behavior Under Earthquake Motion," *Proceedings, Earthquake Engineering and Soil Dynamics*, ASCE Specialty Conference, Pasadena, California, pp. 601-619.

Matlock, H., Martin, G.R., Lam, I.P. and Tsai, C.F., 1981, "Soil-Pile Interaction in Liquefiable Cohesionless Soils During Earthquake Loading," *Proceedings, International Conference on Recent Advances in Geotechnical Earthquake Engineering and Soil Dynamics*, St. Louis, Missouri, Volume 2, April 1981.

Matsuda, T., Sato, T., Fujiwara, H. and Higashida, Y., 1990, "Effect of Carbon Fiber Reinforcement as a Strengthening Measure for Reinforced Concrete Bridge Piers," *First U.S.-Japan Workshop on Seismic Retrofit of Bridges*, Tsukuba Science City, Japan, December 17-18, pp. 356-374.

McCalpin, J.P., 1996, editor, *Paleoseismology*, Academic Press, 588 pp.

McLean, D.I., Saunders, T.D. and Hahnenkratt, H.H., 1995, *Seismic Evaluation and Retrofit of Bridge Substructures with Spread and Pile-Supported Foundations*, Report No. WA-RD 382.1, Washington State Department of Transportation, Olympia, Washington.

McVay, M., Casper, R. and Shang, Te-I, 1995, "Lateral Response of Three-Row Groups in Loose to Dense Sands at 3D and 5D Pile Spacing," *Journal of Geotechnical Engineering*, ASCE, Volume 121, Number 5.

Mitchell, J.K., Baxter, C.D.P., and Munson, T.C., 1995, "Performance of Improved Ground During Earthquakes," *Soil Improvement for Liquefaction Hazard Mitigation*, ASCE Geotechnical Special Publication No. 49, pp. 1-36.

Mitchell, J.K., Cooke, H.G., and Schaeffer, J.A., 1998, "Design Considerations in Ground Improvement for Seismic Risk Mitigation," *Proceedings, Geotechnical Earthquake Engineering and Soil Dynamics III*, Volume I, ASCE Geotechnical Special Publication No. 75, pp. 580-613.

Murchison, J.M. and O'Neill, M.W. (1984), "Evaluation of p-y Relationships in Cohesionless Soils," *Analysis and Design of Pile Foundations*, ASCE, New York, pp. 174-191.

Mylonakis, G., Gazetas, G., Nikolaou, A., and Chauncey, A., 2002, *Development of Analysis and Design Procedures for Spread Footings*, Technical Report MCEER-02-0003, Multidisciplinary Center for Earthquake Engineering Research, University at Buffalo.

Nakashima, M., 1994, "Energy Dissipation Behavior of Shear Panels Made of Low Yield Steel," *Earthquake Engineering and Structural Dynamics*, Volume 23, Number 12, pp. 1299-1313.

NCHRP, 2001, *Comprehensive Specification for the Seismic Design of Bridges – Third Draft Specifications and Commentary*, National Cooperative Highway Research Program, Transportation Research Board, Washington, DC, March.

NCHRP, 2002, *Comprehensive Specification for the Seismic Design of Bridges*, Report 472, National Cooperative Highway Research Program, Transportation Research Board, Washington, DC, 47 pp.

NEHRP, 1997a, 1997b, *National Earthquake Hazard Reduction Program Guidelines and Commentary for the Seismic Rehabilitation of Buildings*, Developed for the Building Seismic Safety Council for the Federal Emergency Management Agency, FEMA 273 and 274.

NRC, 1985, *Liquefaction of Soils During Earthquakes*, Committee on Earthquake Engineering, National Research Council, Report No. CETS-EE-001, Washington, DC.

Newmark, N.M., 1965, "Effects of Earthquakes on Dams and Embankments," *Geotechnique*, Volume 15, Number 2, pp. 139-160.

Newmark, N.M. and Rosenblueth, E., 1979, *Fundamentals of Earthquake Engineering*, Prentice Hall, Englewood Cliffs, N.J. pp. 308-312.

Newmark, N.M., and Hall, W.J., 1982, *Earthquake Spectra and Design*, Earthquake Engineering Research Institute.

Novak, M., 1991, "Piles Under Dynamic Loads," *Proceeding, Second International Conference on Recent Advances on Geotechnical Earthquake Engineering and Soil Dynamics*, Rolla, Missouri, Volume 3, pp. 2433-2456.

O'Rourke, T. D., Gowdy, T. E., Stewart, H. E., and Pease, J. W., 1991, "Lifeline Performance and Ground Deformation in the Marina During 1989 Loma Prieta Earthquake," *Proceedings of the 3rd Japan-U.S. Workshop on Earthquake Resistant Design of Lifeline Facilities and Countermeasures for Soil Liquefaction*, San Francisco, California, December 17-19, Technical Report NCEER-91-0001, National Center for Earthquake Engineering Research, University at Buffalo.

O'Rourke, T. D., Meyersohn, W. D., Shiba, Y. and Chaudhuri, D., 1994, "Evaluation of Pile Response to Liquefaction-Induced Lateral Spread," *Proceedings, 5th U.S.-Japan Workshop on Earthquake Resistant Design of Lifeline Facilities and Countermeasures Against Soil Liquefaction*, Technical Report NCEER-94-0026, National Center for Earthquake Engineering Research, University at Buffalo, pp. 457-478.

Ogata, N., Maeda, Y., Murayama, A., Andoh, H., Kobatake, Y. and Ohno, S., 1993, "Earthquake Resistant Capacity of RC Pier Retrofitted with Carbon Fibre," *Proceedings of the Ninth U.S.-Japan Bridge Engineering Workshop*, Tsukuba Science City, Japan, May 10-11, Technical Memorandum of PWRI No. 3230, Public Works Research Institute, pp. 385-399.

Orangun, C.O., Jirsa, J., and Breen, J.E., 1975, *The Strength of Anchor Bars: A Re-evaluation of Test Data on Development Length and Splices*, Research Report 154-3F, University of Texas at Austin, January.

Pardoen, G.C., Kazanjy, R.P., Shahi, S.B. and Navalpakkam, S., 1998, "Experimental Verification of Shotcrete Jacket, Retrofitted Bridge Columns," *Proceedings of the Fifth Annual Seismic Research Workshop*, California Department of Transportation, Division of Structures, Sacramento, California.

Park, R. and Paulay, T., 1975, *Reinforced Concrete Structures*, John Wiley & Sons, New York, 769 pp.

Park, R., Priestley, M.J.N., Gill, W.D., and Potangaroa, R.T., 1980, "Ductility and Strength of Reinforced Concrete Columns with Spirals or Hoops Under Seismic Loading," *Proceedings of the Seventh World Conference on Earthquake Engineering*, Istanbul, Turkey, September 8-13.

Paulay, T. and Priestley, M.J.N., 1991, *Seismic Design of Reinforced Concrete and Masonry Buildings*, John Wiley & Sons, New York, 744 pp.

Paulay, T., Zanza, M., and Scarpas, A., 1981, *Lapped Splices in Bridge Piers and in Columns of Earthquake-Resisting Reinforced Concrete Frames*, Research Report 81-6, Department of Civil Engineering, University of Canterbury, Christchurch, New Zealand, August.

Pecker, A. and Pender, M., 2000, "Earthquake Resistant Design of Foundations: New Construction," *Proceedings, GeoEng 2000 Conference*, Melbourne, Australia, November 19-24.

Pekcan, G., 1998, *Design of Seismic Energy Dissipation Systems for Concrete and Steel Structures*, Ph.D. Dissertation, Department of Civil, Structural and Environmental Engineering, University at Buffalo.

Pender, M.J., 1993, "Aseismic Pile Foundation Design and Analysis," *Bulletin of the New Zealand National Society for Earthquake Engineering*, Volume 26, Number 1, pp. 49-160.

Petersen, M., Bryant, W., Cramer, C., Cao, T., Reichle, M., Frankel, A., Lienkaemper, J., McCrory, P., and Schwartz, D., 1996, *Probabilistic Seismic Hazard Assessment for the State of California*, California Department of Conservation, Division of Mines and Geology Open-File Report 96-08, U.S. Geological Survey Open-File Report 96-706.

Poulos, S.J., Castro, G. and France, W., 1985, "Liquefaction Evaluation Procedure," *Journal of Geotechnical Engineering*, ASCE, Volume 111, Number 6, pp. 772-792.

Power, M.S., and Chiou, S.-J., 2000, *National Representation of Seismic Ground Motion for New and Existing Highway Facilities*, Unpublished Report, Multidisciplinary Center for Earthquake Engineering Research, University at Buffalo.

Power, M.S., Chiou, S.-J., Rosidi, D., and Mayes, R.L., 1997, "Background Information for Issue A: Should New USGS Maps Provide a Basis for the National Seismic Hazard Portrayal for Highway Facilities? If So, How Should They be Implemented in Terms of Design Values?," *Proceedings of the FHWA/NCEER Workshop on the National Representation of Seismic Ground Motion for New and Existing Highway Facilities*, Burlingame, California, May 29-30, Technical Report NCEER-97-0010, National Center for Earthquake Engineering Research, University at Buffalo.

Power, M.S., Mayes, R.L., and Friedland, I.M., 1998, "National Representation of Seismic Ground Motion for New and Existing Highway Facilities," *Proceedings of Sixth National Conference on Earthquake Engineering*, Earthquake Engineering Research Institute, May 31-June 4, Seattle, Washington.

Priestley, M.J.N., 1993, *Assessment and Design of Joints for Single-Level Bridges with Circular Columns*, Report No. SSRP-93/02, Department of Applied Mechanics and Engineering Sciences, University of California, San Diego.

Priestley, M.J.N., and Park, R., 1979, "Seismic Resistance of Reinforced Concrete Bridge Columns," *Proceedings of a Workshop on Earthquake Resistance of Highway Bridges*, Applied Technology Council, Report No. ATC-6-1, November, pp. 254-283.

Priestley, M.J.N. and Seible, F., 1991, *Seismic Assessment and Retrofit of Bridges*, Research Report SSRP-91/03, Department of Applied Mechanics and Engineering Sciences, University of California, San Diego.

Priestley, M.J.N., Seible, F. and Chai, R., 1992, *Design Guidelines for Assessment Retrofit and Repair of Bridges for Seismic Performance*, Report SSRP-92/01, Department of Applied Mechanics and Engineering Sciences, University of California, San Diego, 1992.

Priestley, M.J.N., Seible, F. and Fyfe, E., 1994, *Column Seismic Retrofit Using Fiberglass/Epoxy Jackets*, Hexcel Fyfe Co., San Diego.

Priestley, M.J.N., Seible, F. and Calvi, G.M., 1996, *Seismic Design and Retrofit of Bridges*, John Wiley & Sons, Inc., New York, New York.

Pulido, C., Saiidi, M., Sanders, D. and Itani, A., 2002, "Experimental Validation and Analysis of CFRP Retrofit of A Two-Column Bent," *Proceedings, Third International Conference on Composites in Infrastructure*, San Francisco, California, June, Paper No. 077, 9 pp.

Pyke, R.M., 1992, *TESS: A Computer Program for Nonlinear Ground Response Analyses*, TAGA Engin. Systems & Software, Lafayette, California.

Qiu, P., 1998, *Earthquake-induced Nonlinear Ground Deformation Analyses*, Ph.D. dissertation, University of Southern California, Los Angeles.

Randall, M.J., Saiidi, M.S., Maragakis, E.M. and Isakovic, T., 1999, *Restraint Design Procedures for Multi-Span Simply-Supported Bridges*, Technical Report MCEER-99-0011, Multidisciplinary Center for Earthquake Engineering Research, University at Buffalo.

Reese, L.C., and Allen, J.D., 1977, *Drilled Shaft Design and Construction Guidelines Manual – Volume II – Structural Analysis and Design for Lateral Loading*, U.S. Dept. of Transportation, Federal Highway Administration, Washington, DC.

Reese, L.C., Cox, W.R. and Koop, F.D., 1974, “Analysis of Laterally Loaded Piles in Sand,” *6th Offshore Technology Conference*, Houston, Volume 2, pp. 473-483.

Reese, L.C., Wang, S-T, Arrellaga, J.A. and J. Hendrix, 1997, *Computer Program LPILE Plus*, Ensoft, Inc., Austin, Texas.

Richter, P.J., Nims, D.K., Kelley, J.M. and Kallenbach, R.M., 1990, “The EDR-Energy Dissipating Restraint, A New Device for Mitigating Seismic Effects,” *Proceedings of the 1990 Structural Engineer’s Association of California Convention at Lake Tahoe*, September.

Riemer, M.F., Lok, T.M., and Mitchell, J.K., 1996, “Evaluating Effectiveness of Liquefaction Remediation Measures for Bridges,” *Proceedings, 6th U.S.-Japan Workshop on Earthquake Resistant Design of Lifeline Facilities and Countermeasures Against Soil Liquefaction*, Technical Report NCEER-96-0006, National Center for Earthquake Engineering Research, University at Buffalo.

Rinne, E.E., 1994, “Development of New Site Coefficients for Building Codes,” *Proceedings, Fifth U.S. National Conference on Earthquake Engineering*, July 10-14, Volume III, pp. 69-78.

Roberts, J.E., 1998, “Seismic Design Philosophy for California Bridges,” *Proceedings of the Structural Engineers World Congress*, San Francisco, California.

Robinson, R.R., Longinow, A., and Chu, K.H., 1979, *Seismic Retrofit Measures for Highway Bridges*, Volumes I and II, Federal Highway Administration, Department of Transportation, Washington, DC.

Rodriguez, M. and Park, R., 1992, *Seismic Load Tests on Reinforced Concrete Columns Strengthened by Jacketing*, University of Canterbury, Department of Civil Engineering, Christchurch, New Zealand.

Ross, G.A., Seed, H.B. and Migliaccio, R.R., 1973, “Performance of Highway Bridge Foundations,” *The Great Alaska Earthquake of 1964-Engineering*, Committee on the Alaska Earthquake of the Division of Earth Sciences, National Research Council, National Academy of Sciences, Washington, DC.

Ross, G.A., Seed, H.B., and Migliaccio, R.R., 1973, "Performance of Highway Bridge Foundations," *The Great Alaska Earthquake of 1964-Engineering*, Committee on the Alaska Earthquake of the Division of Earth Sciences, National Research Council, National Academy of Sciences, Washington, DC.

Sadigh, K., Chang, C.-Y., Abrahamson, N.A., Chiou, S.J. and Power, M.S., 1993, "Specification of Long-period Ground Motions: Updated Attenuation Relationships for Rock Site Conditions and Adjustment Factors for Near-fault Effects," *Proceedings of the Applied Technology Council Seminar on Seismic Isolation, Passive Energy Dissipation, and Active Control*, ATC-17-1, March 11-12, San Francisco, California, pp. 59-70.

Salgado, R., Boulanger, R.W., and Mitchell, J.V., 1997, "Lateral Stress Effects on CPT Liquefaction Resistance Correlations," *Journal of Geotechnical and Geoenvironmental Engineering*, ASCE, August.

Sarraf, M. and Bruneau, M., 1998a, "Ductile Seismic Retrofit of Steel Deck-Truss Bridges. I: Strategy and Modeling," *Journal of Structural Engineering*, November.

Sarraf, M. and Bruneau, M., 1998b, "Ductile Seismic Retrofit of Steel Deck-Truss Bridges. II: Design Applications," *Journal of Structural Engineering*, November.

Seed, H.B., 1987, "Design Problems in Soil Liquefaction," *Journal of the Geotechnical Engineering Division*, ASCE, Volume 113, Number 8, August.

Seed, H.B. and DeAlba, P., 1986, "Use of SPT and CPT Tests for Evaluating the Liquefaction Resistance of Sands," *Use of In Situ Tests in Geotechnical Engineering*, Clemence, S.P., editor, New York, ASCE Geotechnical Special Publication No. 6, pp. 281-302.

Seed, R.B. and Harder, L.F., Jr., 1990, "SPT-Based Analysis of Cyclic Pore Pressure Generation and Undrained Residual Strength," *Proceedings, H. Bolton Seed Memorial Symposium*, BiTech Publishers, Ltd., pp. 351-376.

Seed, H.B., and Idriss, I.M., 1970, *Soil Moduli and Damping Factors for Dynamic Response Analyses*, Report No. EERC 70-10, University of California, Berkeley, Earthquake Engineering Research Center.

Seed, H.B., and Idriss, I.M., 1971, "Simplified Procedure for Evaluating Soil Liquefaction Potential," *Journal of the Soil Mechanics and Foundations Division*, American Society of Civil Engineers, Volume 97, Number SM9, September, pp. 1249-1273.

Seed, H.B., and Idriss, I.M., 1982, *Ground Motions and Soil Liquefaction During Earthquakes*, Earthquake Engineering Research Institute, Oakland, California, Monograph Series, 134 pp.

Seed, H.B., Idriss, I.M., and Arango, I., 1983, "Evaluation of Liquefaction Potential Using Field Performance Data," *Journal of the Geotechnical Engineering Division*, ASCE, Volume 109, Number 3, March.

Seed, H.B., Tokimatsu, K., Harder, L.F., and Chung, R.M., 1985, "Influence of SPT Procedures in Soil Liquefaction Resistance Evaluations," *Journal of the Geotechnical Engineering Division*, ASCE, Volume 111, Number 12, December.

Seed, H.B., Wong, R.T., Idriss, I.M. and Tokimatsu, K., 1986, "Moduli and Damping Factors for Dynamic Analyses of Cohesionless Soils," *Journal of Geotechnical Engineering*, ASCE, Volume 112, Number GT1, pp. 1016-1032.

Seible, F. and Priestley, M.J.N., 1993, "Retrofit of Rectangular Flexural Columns with Composite Fiber Jackets," *Proceedings of the Second Annual Seismic Research Workshop*, California Department of Transportation, Division of Structures, Sacramento, California.

Seible, F., Hegemier, G.A., Priestley, M.J.N. and Innamorato, D., 1995, "Developments in Bridge Column Jacketing using Advanced Composites," *Proceedings, National Seismic Conference on Bridges and Highways*, San Diego, California, Federal Highway Administration and California Department of Transportation, December.

Seible, F., Hegemier, G.A., Priestley, M.J.N., Innamorato, D. and Ho, F., 1995, *Carbon Fiber Jacket Retrofit Test of Rectangular Flexural Column with Lap Spliced Reinforcement*," Advanced Composites Technology Transfer Consortium Report No. ACTT-95/04, University of California, San Diego.

Selna, L.G., and Malvar, L.J., 1987, *Full Scale Testing of Retrofit Devices Used for Reinforced Concrete Bridges*," Report No. 87-01, University of California Earthquake Engineering Structural Laboratory, Los Angeles, California.

Shinozuka, M., Saxena, V., and Deodatis, G., 2000, *Effect of Spatial Variation of Ground Motion on Highway Structures*, Technical Report MCEER-00-0013, Multidisciplinary Center for Earthquake Engineering Research, University at Buffalo.

Silva, W., 1997, "Characteristics of Vertical Strong Ground Motions for Applications to Engineering Design," *Proceedings of the FHWA/NCEER Workshop on the National Representation of Seismic Ground Motions for New and Existing Highway Facilities*, San Francisco, California, May 29-30, Technical Report NCEER-97-0010, National Center for Earthquake Engineering Research, University at Buffalo, pp. 205-252.

Silva, W., and Lee, K., 1987, "WES RASCAL Code for Synthesizing Earthquake Ground Motions," *State-of-the-Art for Assessing Earthquake Hazards in the United States*, Report 24, U.S. Army Corps of Engineers Waterways Experiment Station, Miscellaneous Paper 5-73-1.

Sivakuman, B., Gergely, P., and White, R.N., 1983, "Suggestions for the Design of R/C Lapped Splices for Seismic Loading," *Concrete International: Design and Construction*, February.

Somerville, P.G., 2003, "Magnitude Scaling of the Near Fault Rupture Directivity Pulse," *Physics of the Earth and Planetary Interiors*, Volume 137, p. 201-212.

Somerville, P.G., 1997, "The Characteristics and Quantification of Near Fault Ground Motions," *Proceedings of the FHWA/NCEER Workshop on National Representation of Seismic Ground Motion for New and Existing Highway Facilities*, San Francisco, California, May 29-30, Technical Report NCEER-97-0010, National Center for Earthquake Engineering Research, University at Buffalo.

Somerville, P., Smith, N.F., Graves, R.W., and Abrahamson, N.A., 1997, "Modification of Empirical Strong Ground Motion Attenuation Relations to Include the Amplitude and Duration Effects of Rupture Directivity," *Seismological Research Letters*, Volume 68, pp. 199-222.

Somerville, P., Krawinkler, H., and Alavi, B., 2000, *Development of Improved Ground Motion Representation and Design Procedures for Near-fault Ground Motion*, California Strong Motion Instrumentation Program, California Division of Mines and Geology, Data Utilization Report, Contract 1097-601.

SCEC, 1999, *Recommended Procedures for Implementation of DMG Special Publication 117, Guidelines for Analyzing and Mitigating Liquefaction Hazards in California*, Southern California Earthquake Center, University of Southern California, March, 63 pp.

Sowers, J.M., Noller, J.S., and Lettis, W.R., 1998, *Dating and Earthquakes: Review of Quaternary Geochronology and Its Application to Paleoseismology*, Report NUREG/CR-5562, Office of Nuclear Regulatory Research, U.S. Nuclear Regulatory Commission, Washington, DC.

Soydemir, C., Zoli, T., LaPlante, K., Kraemer, S., Davidson, W. and McCabe, R., 1997, "Seismic Design of Central Artery Bridges Across Charles River in Boston: Geotechnical/Substructure Aspects," *NCEER Post-Liquefaction Ground Deformation Workshop*, University of Southern California, August.

Standards Association of New Zealand, 1982, *Code of Practice for the Design of Concrete Structures*, NZS 3101.

Stark, T.D. and Mesri, G., 1992, "Undrained Shear Strength of Liquefied Sands for Stability Analyses," *Journal of the Geotechnical Engineering Division*, ASCE, Volume 118, Number 11, November, pp. 1727-1747.

Stark, T.D., Olson, S.M., Kramer, S.L., and Youd, T.L., 1998, "Shear Strength of Liquefied Soil," *Proceedings, 1998 ASCE Specialty Conference on Geotechnical Earthquake Engineering and Soil Dynamics*, Seattle, WA, August 3-6.

Steckel, G.L., Hawkins, G.F. and Bauer, J.L., 1998, "Long Term Durability Testing of Composite Materials," *Proceedings of the Fifth Annual Seismic Research Workshop*, California Department of Transportation, Division of Structures, Sacramento, California.

Sun, J.I., Golesorkhi, R., and Seed, H.B., 1988, *Dynamic Moduli and Damping Ratios for Cohesive Soils*, Report No. UBC/EERC-88/15, University of California, Berkeley, Earthquake Engineering Research Center.

Sun, Z., Seible, F. and Priestley, M.J.N., 1993, *Flexural Retrofit of Rectangular Reinforced Concrete Bridge Columns by Steel Jacketing*, Report No. SSRP-93/01, Department of Applied Mechanics and Engineering Sciences, University of California, San Diego.

Swanson, Dave, 1999, Personal Communication.

Taylor, P.W., and Williams, B.C., 1979, "Foundations for Capacity Designed Structures," *Bulletin of the New Zealand National Society for Earthquake Engineering*, Volume 12, Number 2, pp. 101-113.

Taylor, P.W., Barlett, P.E., and Wiessing, P.R., 1981, "Foundation Rocking under Earthquake Loading," *Proceedings of the Tenth International Conference on Soil Mechanics and Foundation Engineering*, Volume 3, pp. 33-322.

Terzaghi, K., 1955, "Evaluation of Coefficients of Subgrade Reaction," *Geotechnique*, Volume 5, Number 4, pp. 297-326.

Thewalt, C.R. and Stojadinovic, B., 1993, "Behavior of Bridge Outriggers: Summary of Test Results," *Proceedings of the Second Annual Seismic Research Workshop*, California Department of Transportation, Division of Structures, Sacramento, California.

Thewalt, C.R. and Stojadinovic, B., 1995, "Outrigger Knee Joint Seismic Upgrade Design Procedure," *Proceedings, National Seismic Conference on Bridges and Highways*, San Diego, California, Federal Highway Administration and California Department of Transportation, December.

Tokimatsu, K. and Seed, H.B., 1987, "Evaluation of Settlements in Sands Due to Earthquake Shaking," *Journal of the Geotechnical Engineering Division*, ASCE, Volume 113, Number 8, pp. 861-878.

Tokimatsu, K. and Asaka, Y., 1998, "Effects of Liquefaction-Induced Ground Displacements on Pile Performance in the 1995 Hyogoken-Nambu Earthquake," *Special Issue of Soils and Foundation*, pp. 163-177.

Trochalakis, P., 1996, *Design of Seismic Restrainers for In-Span Hinges*, Report No. WA-RD 387.1, Research Project T9903, Task 41, Washington State Transportation Center, University of Washington, Seattle, Washington.

Tsai, K.C., Chen, H.W., Hong, C.P. and Su, Y.F., 1993, "Design of Steel Triangular Plate Energy Absorbers for Seismic-Resistant Construction," *Earthquake Spectra*, Volume 9, Number 3, pp. 505-528.

U.S. Army Corps of Engineers, 2003, *Time-History Dynamic Analysis of Concrete Hydraulic Structures*, USACE Engineer Manual EM1110-2-6051.

U.S. Geological Survey, Building Seismic Safety Council, and Federal Engineering Management Agency, 1998, *Maps of Maximum Considered Earthquake Ground Motion for the United States*, prepared for USGS/BSSC Project 97.

Vucetic, M., and Dobry, R., 1991, "Effect of Soil Plasticity on Cyclic Response," *Journal of Geotechnical Engineering*, ASCE, Volume 117, Number 1, pp. 89-107.

Wang, S.T., and Reese, L.C., 1998, "Densified Pile Foundations in Liquefied Soils," *Geotechnical Earthquake Engineering and Soil Dynamics III*, ASCE Geotechnical Special Publication No. 75, Volume 2, pp. 1331-1343.

Wang, Z.L., and Makdisi, F.I., 1999, "Implementing a Bounding Surface Hypoplasticity Model for Sand into the FLAC Program," *Proceedings of the International Symposium on Numerical Modeling in Geomechanics*, Minnesota, September, pp. 483-490.

Wells, D.L., and Coppersmith, K.J., 1994, "Empirical Relationships Among Magnitude, Rupture Length, Rupture Area, and Surface Displacement," *Bulletin of the Seismological Society of America*, Volume 84, pp. 974-1002.

Wendichansky, D.A., Chen, S.S. and Mander, J.B., 1998, *Experimental Investigation of the Dynamic Response of Two Bridges Before and After Retrofitting with Elastomeric Bearings*, Technical Report NCEER-98-0012, Multidisciplinary Center for Earthquake Engineering Research, University at Buffalo.

Werner, S.D., Taylor, C.E., Moore, J.E., Walton, J.S., and Cho, S., 2000, *A Risk-based Methodology for Assessing the Seismic Performance of Highway Systems*, Technical Report MCEER-00-0014, Multidisciplinary Center Earthquake Engineering Research, University at Buffalo, 265 pp.

Wesson, R.L., Frankel, A.D., Mueller, C.S., and Harmsen, S.C., 1999a, *Probabilistic Seismic Hazard Maps of Alaska*, U.S. Geological Survey Open-File Report 99-36.

Wesson, R.L., Frankel, A.D., Mueller, C.S., and Harmsen, S.C., 1999b, *Seismic Hazard Maps for Alaska and the Aleutian Islands*, U.S. Geological Survey Geologic Investigation Series, map I-2679.

Whittaker, A., Bertero, V.V. and Alonso, J., 1989, *Earthquake Simulator Testing of Steel Plate Added Damping and Stiffness Elements*, UBC/EERC Report 89/02, Earthquake Engineering Research Center, University of California, Berkeley, California.

Wilson, D.W., Boulanger, R.W., and Kutter, B.L., 1999, "Lateral Resistance of Piles in Liquefying Sand," *Proceedings, Analysis, Design, Construction, and Testing of Deep Foundations*, Offshore Technology Research Center 1999 Conference, ASCE Geotechnical Special Publication No. 88, pp. 165-179.

Wipf, T.J., Klaiber, F.W. and Russo, F.M., 1997, *Evaluation of Seismic Retrofit Methods for Reinforced Concrete Bridge Columns*, Technical Report NCEER-97-0016, National Center for Earthquake Engineering Research, University at Buffalo.

Wong, C.P. and Whitman, R.V., 1982, *Seismic Analysis and Improved Seismic Design Procedure for Gravity Retaining Walls*, Research Report 82-83, Department of Civil Engineering, Massachusetts Institute of Technology, Cambridge, MA.

Xiao, Y, Priestley, M.J.N. and Seible, F., 1994, "Experimental Results and Design Recommendations from Bridge Footing Research Program," *Proceedings of the Third Annual Seismic Research Workshop*, California Department of Transportation, Sacramento, California.

Xiao, Y., Martin, G.R., Yin, Z, and Ma, R., 1995, *Bridge Column Retrofit Using Snap-Tite Composite Jacketing for Improved Seismic Performance*, Structural Engineering Research Report No. USC-SERR 95/02, Department of Civil Engineering, University of Southern California.

Yashinsky, M., 1997, "Caltrans' Bridge Restraint Retrofit Program," *Second U.S.-Japan Workshop on Seismic Retrofit of Bridges*, Report No. UCB/EERC-97/09, University of California at Berkeley.

Youd, T. L., 1992, "Liquefaction, Ground Failure and Consequent Damage During the April 22, 1991, Costa Rica Earthquake," *Proceedings, U.S.-Costa Rica Workshop on the Costa Rica Earthquakes of 1990-1991, Effects on Soils and Structures*, EERI Pub. No. 93-A, Earthquake Engineering Research Institute, Oakland, CA, pp. 73-95.

Youd, T. L., 1993, *Liquefaction-Induced Damage to Bridges*, Transportation Research Record No. 14311, Transportation Research Board, National Academy Press, Washington, DC., pp. 35-41.

Youd, T.L., 1995, "Liquefaction-Induced Lateral Ground Displacement," State-of-the-Art Paper, *Proceedings, Third Intl. Conf. on Recent Advances in Geotechnical Earthquake Engineering and Soil Dynamics*, S. Prakash (ed.), St. Louis, MO, April 2-7, Volume II, pp. 911-925.

Youd, T.L., 1998, *Screening Guide for Rapid Assessment of Liquefaction Hazard at Highway Bridge Sites*, Technical Report MCEER-98-0005, Multidisciplinary Center for Earthquake Engineering Research, University at Buffalo.

Youd, T. L. and Idriss, I.M., editors, 1997, *Proceedings of the NCEER Workshop on Evaluation of Liquefaction Resistance of Soils*, Salt Lake City, UT, January 5-6, 1996, Technical Report NCEER-97-0022, National Center for Earthquake Engineering Research, University at Buffalo.

Youd, T.L. and Perkins, D.M., 1978, "Mapping of Liquefaction-Induced Ground Failure Potential," *Journal of the Geotechnical Engineering Division*, American Society of Civil Engineers, Volume 104, Number 4, April, pp. 433-446.

Youd, T.L., Idriss, I.M., Andrus, R.D., Arango, I., Castro, G., Christian, J.T., Dobry, R., Finn, W. D.L., Harder, L.F. Jr., Hynes, M.E., Ishihara, K., Koester, J.P., Liao, S.S.C., Marcuson, W.F., III, Martin, G.R., Mitchell, J.K., Moriwaki, Y., Power, M.S., Robertson, P.K., Seed, R.B., and Stokoe, K.H., II, 2001, "Liquefaction Resistance of Soils: Summary Report from the 1996 NCEER and 1998 NCEER/NSF Workshops on Evaluation of Liquefaction Resistance of Soils," *Journal of Geotechnical Geoenvironmental Engineering*, ASCE, Volume 127, No. 10, p. 817-833.

Youd, T.L., Hansen, C.M., and Bartlett, S.F., 2002, "Revised Multilinear Regression Equations for Prediction of Lateral Spread Displacement," *Journal of Geotechnical and Geoenvironmental Engineering*, ASCE, Volume 128, No. 12, p. 1007-1017.

Zahrai, S.M. and Bruneau, M., 1998, "Impact of Diaphragms on Seismic Response of Straight Slab-on-Girder Steel Bridges," *Journal of Structural Engineering*, August.

Zahrai, S.M. and Bruneau, M., 1999, "Ductile End-Diaphragms for Seismic Retrofit of Slab-on-Girder Steel Bridges," *Journal of Structural Engineering*, January.

Zayati, F., Mahin, S. and Mazzoni, S., 1993, "Evaluation of a Seismic Retrofit Concept for Double Deck Viaduct," *Proceedings of the Second Annual Seismic Research Workshop*, California Department of Transportation, Division of Structures, Sacramento, California.



EARTHQUAKE ENGINEERING TO EXTREME EVENTS

University at Buffalo, The State University of New York

Red Jacket Quadrangle ▪ Buffalo, New York 14261

Phone: (716) 645-3391 ▪ Fax: (716) 645-3399

E-mail: mceer@buffalo.edu ▪ WWW Site <http://mceer.buffalo.edu>



University at Buffalo *The State University of New York*